LAWRENCE
LIVERMORE
NATIONAL
LABORATORY

LLNL-TH-764287

The Origin of Agglomerates and their Role in Forming Near-Surface Glassy Fallout

L. A. Lewis

December 17, 2018

Disclaimer

This work performed under the auspices of the U.S. Department of Energy by Lawrence Livermore National Laboratory under Contract DE-AC52-07NA27344.

The Origin of Agglomerates and their Role in Forming Near-Surface Glassy Fallout

by

Laurence Abed Lewis

A dissertation submitted in partial satisfaction of the

requirements for the degree of

Doctor of Philosophy

in

Engineering – Nuclear Engineering

in the

Graduate Division

of the

University of California, Berkeley

Committee in charge:

Professor Eric B. Norman, Chair
Professor Karl Van Bibber
Professor Paul Renne
Kim B. Knight

Fall 2018

The Origin of Agglomerates and their Role in Forming Near-Surface Glassy Fallout

Abstract

The Origin of Agglomerates and their Role in Forming Near-Surface Glassy Fallout

by

Laurence Abed Lewis

Doctor of Philosophy in Engineering – Nuclear Engineering

University of California, Berkeley

Professor Eric B. Norman, Chair

One of the primary goals of fallout formation models is to predict the activity-size distribution of the resulting fallout. However, these models rely heavily on empirical data from a limited set of testing environments. Furthermore, fallout formation is known to be sensitive to the emplacement environment, particularly in the case when the fireball incorporates larges masses of surrounding material, as in the near-surface burst. The fidelity of these models in new and untested environments is not well constrained. As a result, there is a need to better understand the processes that control fallout formation. In near-surface bursts, the two primary processes that control radionuclide incorporation and the size distribution in fallout are condensation of species from the bomb vapor phase onto melts and agglomeration of melts to form larger melts.

Historically, fallout formation models have ignored agglomeration in predicting both the activity-size and size distribution of fallout. However, attempts at building thermodynamic models of radionuclide fractionation in the fireball show poor agreement with experimental data. Many have hypothesized that this disagreement is due to agglomeration—the collision and accretion of smaller parcels of melt with larger parcels of melt, both of which have incorporated relatively different amounts of radionuclides and when the whole object is dissolved and analyzed, leads to a mixing effect between the two objects. Furthermore, fallout in surface tests is known to form by several different mechanisms, including a small particle population known to form as "primary condensates", that is, primarily derived from the vapor phase of fireball, which includes high concentrations of vaporized device material and likely some concentration of vaporized soil. Primary condensates have been observed to form up to diameters of 20 μm, within the range of the diameter of some observed agglomerates. As a result, it is also possible that some agglomerates observed in glassy fallout could be derived primarily from the fireball's vapor term, instead of being composed primarily of a mixture of the surrounding soil, as has been previously observed in aerodynamic glassy fallout.

Agglomerates are readily observed adhered to the exteriors of whole samples and agglomerates incorporated into samples are observable in sample cross-sections due to a distinct

compositional interface between agglomerates and hosts. To determine the likely origin and role agglomerates play in forming aerodynamic glassy fallout, agglomerates and their host objects (the larger objects agglomerates are attached to) were studied starting with an initial population of 49 glassy fallout samples collected a similar distance from ground zero from a historic U-fueled U.S. nuclear test. After polishing to expose an internal cross-section, host objects and agglomerates in a subset of samples were characterized for major element composition using energy-dispersive X-ray spectroscopy (EDS) and for their U isotope ratios using secondary ion mass spectrometry (SIMS). Using these techniques, two datasets were collected. First, EDS analyses were used to characterize the major element composition across entire host objects (in 37 samples) and agglomerates (53 agglomerates in 15 samples) to compare the compositions between the two populations to determine if agglomerates are likely derived from similar melts relative to host objects. Second, EDS raster analyses were used to characterize the major element compositions within/adjacent to SIMS analysis craters to combine the U isotope ratio and major element composition and determine if agglomerates incorporated distinctly different amounts of radionuclides from the vapor phase in the fireball than hosts. These data sets were analyzed separately using two multivariate techniques: principal components analysis (PCA) and multidimensional scaling (MDS). PCA was used to determine the greatest sources of variance in the dataset and correlations amongst different major elements and the $^{235}U/^{238}U$ ratio. MDS was used to determine the compositional similarity between agglomerates and their host objects. Finally, quantified EDS maps and NanoSIMS rasters over compositional interfaces were used to determine the major element and U isotopic behavior across the different types of compositional interfaces observed between agglomerates and host objects in glassy fallout from this test.

The size and frequency of agglomerates observed in samples occupies between 0 and 20% of a sample's exposed cross-section, with samples exhibiting as few as 0 and as many as 57 agglomerates, ranging in diameter from 5 to 855 μm. However, the majority of samples have fewer than 20 agglomerates that occupy <10% of the exposed sample's cross-section. Major element compositions of agglomerates are observed to be a subset of the range of major element compositions measured in the host objects, suggesting they were more throughly melted and are well-mixed, in contrast to host objects which often contain partially-melted/unmelted mineral compositions. Both agglomerates and hosts are bounded by compositions measured in unmelted soil, suggesting both the major element composition of both are controlled by the soil incorporated into the fireball. Furthermore, major element homogeneity is strongly correlated with U isotopic homogeneity, indicating bulk mixing is responsible for distributing anthropogenic U throughout the volume of melts and suggesting that agglomerates, which are more compositionally homogeneous than hosts, are also more uniform with respect to their U isotope composition than host objects. Major element compositions from EDS analyses show that agglomerates tend to have similar compositions to hosts, particularly to the hosts they are attached to. Specifically, 81% of agglomerates were measured to have more similar major element compositions to their hosts than 50% of all other characterized agglomerates and hosts. Combined U isotopic and major element compositions show that agglomerates tend to be approximately as similar to their hosts

when including U isotopic compositions. Specifically, 83% of agglomerates fall within the 50th percentile in terms of similarity to their hosts when compared to all other characterized agglomerates and hosts. Finally, two types of compositional interfaces are observed: an interface that tends to be enriched in CaO, MgO, FeO, and ^{235}U ("CaMgFe interfaces"), which has been studied previously in the literature, and a compositional interface that tends to only be enriched in SiO_2 ("Si interfaces"), which has not been noted in previous studies of fallout.

The variation of the major element and U isotopic composition between samples suggest a highly heterogeneous fireball environment and starting melts. However, the compositional similarity between agglomerates and their hosts suggest individual glassy fallout samples forming and agglomeration occurring in localized regions within the fireball. Because agglomerates are more likely to have similar compositions to their hosts, they most likely formed from similar parcels of melt, which either homogenized locally within the fireball or did not travel far during the fallout formation process, starting once they were swept into the fireball, then incorporated radionuclides from the fireball's vapor term, experienced agglomeration, and then exiting the fireball and quenching. Furthermore, given that agglomerates and host objects incorporated similar amounts of species anthropogenic U from the vapor phase, they likely experienced similar fireball environments (*i.e.*, were swept into the fireball at a similar time and temperature). While some samples are observed to be formed from a relatively large number of agglomerates (occupying at most $\approx$20% of the exposed cross-section of the sample) the trend towards compositional similarity between agglomerates and their hosts suggests the observed agglomerates do not appreciably alter the overall major element and U isotopic composition of samples. However, there are outliers. Several $\sim$20 μm scale agglomerates in one sample are observed to be enriched in SiO_2 and highly enriched in ^{235}U relative to their host object and the statistical medians of the host population and combined agglomerate and host population. These agglomerates are possible candidates for being formed primarily from the vapor phase. However, their size and frequency are too small to appreciably alter the composition of the sample.

To IDH

Contents

List of Figures

List of Tables

Acknowledgments

I owe my deepest debt of gratitude to Ian D. Hutcheon. He gave me my start at LLNL and set me on this path. He showed me what a scientist should be: meticulous, methodical, thorough, and determined. But I also admired his kindness, humility, humor, and his passion for mentoring. I can never fully express the debt I owe to him and how he made the most impossible, infuriating days with the 3f feel possible and just downright fun. He is always what I have aspired to be as a scientist.

I also owe an enormous debt to Stanley G. Prussin. As my Berkeley advisor, he showed me what it means to truly *know* something. His interrogative demeanor and contentious group meetings were legendary, but so was his gentle nature and advocacy for his students. His graduates are known for their high caliber, quality, and for embodying Stan's scientific integrity and willingness to constantly question methods and data. It is a caliber that I strive for everyday.

After Ian and Stan passed, Kim Knight tried to fill their impossibly large shoes. She put up with me through thick and thin, which I know was not easy. She is tenacious, dedicated, thorough, extremely competent, and worked herself sick mentoring myself and others through grad school. She spent months learning the ins and outs of my work so she could critique my research. She never compromised on quality, reading two, three, four drafts of each chapter before ultimately signing off on my dissertation. Her bar is incredibly high and I truly never thought I would reach it. She made the best out of a terrible and tragic situation and I gained more from my relationship with her than I can truly express here. What speaks most highly of her, however, is how patient and understanding she was with me and how unwaveringly she advocated for me through everything. I finished this dissertation and research project largely thanks to her and I am not sure that I will ever be able to fully express how grateful I am. Thank you, Kim.

I also thank the rest of my committee, Rick Norman, Karl van Bibber, and Paul Renne, for not only committing to read and critique my dissertation, but not even flinching after finding out how long it was. They are extremely busy and accomplished scientists, and I truly appreciate the time, advice, and insight they donated to a dissertation that was in the works for a very long time. I extend a special thank you to Rick Norman, who graciously and unquestioningly stepped in as committee chair after Stan passed. He taught the first class I ever took at Berkeley and I am honored that his signature is on this dissertation.

Throughout this process Jenny Matzel has been nothing short of incredible. Her downright brilliance, work ethic, patience, photographic memory, ridiculously thorough and organized notes, and ability to just know how things work has been absolutely invaluable when trying to operate the 3f, the NanoSIMS, L'IMAGE, and pretty much any other instrument or problem I have come across at the lab since 2009. I am absolutely convinced I would be at least another year from graduating if it was not for her willingness to drop everything and help, listen, and provide incredibly thoughtful critiques of my research and writing and she has done so consistently and unwaveringly since the first day we started working together.

While Brett was mostly involved with shepherding me along in the dissertation writing, he has been an indispensable steadying and calming sounding board. His advice has always been insightful, meaningful, and delivered with tact and I was absolutely lucky to have him in the room when I was struggling to interpret and write up a lot of the results in the later chapters.

My office mates, David Weisz and Marc Fitzgerald had to put up with a lot, and they deserve a lot of credit for that. We shared a small, windowless space and usually got along well. Towards the end, headphones were used liberally, but trips to the snack shack, Tin Thai, Starbucks, or anywhere that got us out of our office helped relieve any pent up grad school angst.

I need to thank Peter Weber, the SIMS whisperer, for generously donating his time during the week and on the weekends to help me set up, troubleshoot, and run the NanoSIMS and the 3f, interpret SIMS data, and for talking out the pros and cons and his own experience of taking different career paths with me in between SIMS runs.

I also thank Mindy Zimmer, Will Kinman, Todd Williamson, and Chloë Bonamici for taking the time to collect beautiful uranium isotopic measurements of these samples using LANL's IMS-1280. The data Mindy and Will collected and I worked with Todd and Chloë to collect are used liberally in this dissertation and helped build the substantial data set of uranium isotope measurements we have for these samples. And every single time I visited LANL they were beyond kind, hospitable, and just downright great people to spend time with. I owe a special thank you to Todd for donating a huge three week block of time to me in 2015. It is greatly appreciated.

Lastly, I cannot express how much my mom's unwavering love meant to me during this process and how instrumental it was in helping me graduate. Thank you, mom.

Chapter 1

Introduction

The effects of nuclear weapons have been recognized since the Trinity test in 1945, and studied in depth since the U.S. began an extensive nuclear testing campaign in 1951. In a nuclear test, the prompt release of neutrons and γ-rays, which are mostly captured within the device, and the rapid deposition and absorption of highly energetic fission products and γ-rays into the surrounding device creates temperatures on the order of millions of Kelvin, vaporizing and ionizing the device and other surrounding material [1]. This high pressure, high temperature plasma constitutes the initial fireball and rapidly expands, vaporizing air and other material as the fireball grows, forming a dense shock front that propagates outward faster than the fireball's diameter increases [1, 2]. Combinations of prompt effects can have an enormously destructive impact on the surrounding environment. The weapon effect with the longest-lasting impact, however, is the formation and spread of fallout following a nuclear explosion, which consists of residual and induced radioactivity that spreads post-detonation into the environment.

Fallout from nuclear explosions consists of "early" or "local" fallout, which deposits near and downwind from ground zero shortly after the explosion (defined as particles that settle within the first 24 hours) and "global" or "delayed" fallout, which consists of sub-micron particles that deposit in the atmosphere and settles over great distances in very low concentrations [2]. The sources of the radioactivity in fallout are fission products, U or Pu fuel that escaped fission ("unfissioned" or "residual" fuel), and activation species induced in weapon debris or any surrounding material [2]. These radionuclides are spread by the considerable air currents and the rapidly expanding and rising fireball [2].

Fallout formation has been studied and modeled to understand how radionuclides partition into fallout particles of different sizes and how these particles may move in the surrounding environment following a detonation to understand health hazards and inform responses for the military, public, and the environment both close to and far from ground zero [3]. While fallout formation models were originally created for the purpose of military and civil defense, the threat of nuclear terrorism in urban environments is now pervasive. To best inform the public and first responders about how to respond to the hazards fallout poses in such a catastrophic scenario requires the adaptation of formation models to predicting

the formation and distribution of radioactivity in previously untested environments. In addition, an ability to predict basic chemical and physical properties for fallout in untested environments is necessary for post-detonation nuclear forensics. The fidelity of these historic fallout formation models in new and untested environments is not well constrained given the limited historic testing environments and the sensitivity of fallout formation to the surrounding materials available to be incorporated into the fireball [4]. While fallout formation models have been refined over decades, they remain highly empirical and rely on historic testing data from a limited set of testing environments. Specifically, detonations were largely conducted in atmospheric, marine, or desert environments [5]. These historic data show that fallout formation is sensitive not only to the height of detonation (affecting the timing and mass of environmental material incorporation into the fireball), but also to the composition of the surrounding lithology [5]. This dissertation pursues new research into understanding fundamental processes affecting environment-bomb vapor interactions.

1.1 Historical and modern motivations for studying fallout

In the nuclear testing era, fallout was primarily studied to understand the residual effects of nuclear explosions close to ground zero. Studies focused on understanding the transport and deposition of radioactivity post-detonation (*e.g.*, [6, 7]). To this end, authors characterized fallout patterns, and the radiological, physical, and chemical properties of fallout [6]. Defense researchers developed models for the formation and spread of fallout, using empirical data to predict how radionuclides would partition in fallout and hydrodynamic physics to predict other nuclear weapon effects and how fallout particles would be dispersed in different detonation environments [8]. These preliminary studies created the foundation for semi-empirical models attempting to predict fallout chemistry and transport, and ultimately, fallout formation.

Recently, there has been a renewed interest in studying fallout produced in atmospheric detonations (discussed below in Section 1.4). Samples from surface detonations are readily available: trinitite, or irregularly-shaped fallout produced in the Trinity test can be readily purchased from mineral dealers. Atmospheric and near-surface detonations also represent a plausible detonation scenario in the case of a nuclear attack by both state and non-state actors [9]. In addition, detonations near the Earth's surface represent the greatest fallout hazard because they can activate and disperse radioactivity in many thousands of tons of environmental material for each kT of yield, and distribute it both locally and globally [10]. Finally, surface bursts are particularly interesting phenomenologically: their formation processes remain the most poorly understood and the fallout patterns the most difficult to predict because of the complex coupling between the device, the ground, and air. Because of the these different interactions and the wide range of material that can be incorporated into the fireball, near-surface detonations also produce the most diverse morphologies and

sizes of fallout [4, 11].

Most recent studies of fallout have been analytical.[1] Given modern analytical techniques, which provide the ability to characterize fallout on a scale and with an accuracy and precision far exceeding the technology available in the 1950s–1970s, researchers have begun to re-investigate fallout to better understand the high temperature, complex environment present in the fireball. With advances in computational power, researchers are also interested in better understanding fallout formation to create predictive models more reliant on first-principles, which may more accurately predict how fallout may form in new and untested environments (most notably Moresco (2012) [12]). Such models may better represent how radionuclides will contaminate the environment, which can inform health and safety procedures or emergency responders following a detonation. In addition, a better understanding of weapons effects or radionuclide chemistry in the fireball will also help inform nuclear forensics investigators on which samples to collect, how best to analyze them, and possible interpretations for their results.

1.2 Fallout formation

How fallout forms, how much debris is produced, and its chemical and isotopic characteristics are highly dependent on the detonation environment [4, 13]. For example, in air burst debris, where the device was detonated high in the atmosphere, the total mass of fallout formed is small. Fallout samples collected on air filter several hours post-detonation tend to have modal diameters on the order of hundreds of nanometers, mean diameters on the order of microns, are spherical, highly radioactive and are composed primarily of Fe oxide, Al oxide, Pu, and/or U, resembling recondensed device debris [4, 14, 15]. In contrast, during a detonation near the Earth's surface, the fireball may interact with and incorporate large amounts of inert environmental material or man-made structures, such as soil or a detonation platform. As a result, the amount of fallout and its size distribution tends to become much wider (mean diameter may only be tens to hundreds of microns, but dimensions may range from hundreds of nanometers to centimeters in diameter, depending on the amount and size distribution of the incorporated surrounding material) and the total mass of fallout generated is greater. Fallout generated in surface detonations are largely representative of the surrounding lithology[2] and its specific activity can be 10^4–10^7 times lower than airburst debris (Table 1.1) [4, 10, 17–19].

Estimates for the amount of fallout produced in surface bursts varies widely (Table 1.1). Key estimates are contained in Izrael (2002), the National Research Council (1985), Miller (1960), and Freiling (1962) [10, 11, 20, 21]. The 100–120 tons per kiloton (T/kT) estimate

[1] The work of Izrael (2002) is the notable exception. First translated to English in 2002, he has best synthesized the English and Russian historic work on fallout and contributed several careful calculations on fallout formation phenomena that are now considered a benchmark study in the fallout literature [10].

[2] excluding C, which usually is present as a carbonate, and decomposes at low temperatures into CO_2 [16].

from the National Research Council is the total mass of melt produced per kT of device yield; they then estimate only half this melt would leave the crater, so only half the 100–120 T/kT of melt would be available for fallout formation [11]. Miller uses scaling laws presented in *The Effects of Nuclear Weapons* and a uniform soil density of 1.76 g/cm^3 to estimate the total mass of soil thrown out of a crater in a surface detonation [2, 20]. This ignores material brought into from outside the crater by the strong afterwinds. Finally, the Freiling estimate comes from the Rainier shot, a nuclear test that was detonated 800 feet in an underground tunnel with a yield of 1.7 kT. Similar to the National Research Council, to estimate the amount of soil vaporized and melted from a device placed directly on the Earth's surface, the data have been divided by two [21]. In addition, multiple fallout morphologies are observed because the fireball may entrain surrounding material into the plasma as a vapor, melt, or solid.

Table 1.1: Estimates for the amount of fallout produced in surface bursts as a function of phase (solid, melt, or vapor) when the material initially interacts with the fireball. The estimates have units of metric tons per kiloton of device yield.

Study	Solid (T/kT yield)	Melt (T/kT yield)	Vapor (T/kT yield)	Total (T/kT yield)
Izrael [10]	5000	155–198.5	1.5–25	5155–5200
National Research Council [11]	5000	100–120	60	5160–5180
Miller [20]	-	-	-	5030
Freiling [21]	-	250	0.4	-

Fallout from air bursts

In the simplest detonation scenario, the high-altitude air burst, the fireball never makes contact with the Earth or any surrounding structures. Vaporized device debris only interacts with itself (the device casing, fission products, and unfissioned fuel), entrained air, and possibly molten or vaporized dust and or other particulates to produce fallout [14]. As the fireball cools below several thousand K, two primary processes occur: **condensation** (vapor-liquid or vapor-solid collisions) and **agglomeration** (liquid-liquid collisions). In an air burst, these two processes are predominantly responsible for the resulting activity-size distribution of the fallout (how activity is distributed among fallout of different sizes) and the size distribution in fallout, respectively [12].

As the fireball cools below several thousand K, vaporized species begin to condense onto available surfaces, such as entrained solid or molten dust particulates, driven to condensation by the difference in Gibbs free energy between the vapor and liquid states [22]. Absent any condensing surfaces (*i.e.*, material in the liquid or solid phase) this would have to happen "spontaneously". That is, given a high enough supersaturation of a vaporized species in a small enough volume, there is a probability many atoms in the gas phase will collide and form small, stable embryonic droplets that remain intact and act as a condensing surface

for other vaporized species, a process known as homogeneous nucleation [22]. However, and more likely, entrained dust or other particulates are entrained in the fireball and act as condensation sites, which reduces the supersaturation levels required to allow a species to condense This rapidly enhances the phase transformation to a liquid as the temperature drops, a process known as heterogeneous nucleation [22, 23].

The timing of a particular elemental or molecular species condensing is predominantly controlled by the chemical or molecular volatility of the species, as well as the relevant vaporization/condensation temperature. Variations in relative volatility lead to different fission product mass chains preferentially partitioning into fallout at different times, a phenomenon known as chemical fractionation [5, 24].

Once in the liquid phase, fallout droplets may collide due to the turbulent motion in the fireball. These collisions may simply be glancing, resulting in no change in particle mass, may break up melts into smaller particles, or may cause the objects to coalesce into a single, larger particle, a process known as agglomeration (also called coagulation or coalescence by other authors) [25]. This continuous process of condensation and agglomeration continues until the fireball drops below the melting point of the molten particles and/or the particles exit the fireball, after which they are deposited globally as fallout [24]. Fallout collected from these tests are often called "primary" condensates because they better resemble condensed device debris [4, 24].

The two mechanisms of condensation and agglomeration form the modern basis for understanding fallout formation in other, more complicated detonation scenarios [24]. Using only the theory of agglomeration, Stewart (1956), and later Nathans et al. (1970), were able to successfully model and match the observed shape of size distribution of fallout from air burst debris [14, 25, 26]. Both neglected condensation as a process that significantly contributed to the growth of primary condensates, but instead focused on the agglomeration of colliding molten fallout particles. Their theories were able to reproduce the observed shape of the size distribution of these particles collected from air filters collected several hours post-detonation, which are well-described by a log-normal distribution (Fig. 1.1) [12, 14, 24, 25]. However, by neglecting condensation, they always underestimated the mean diameter of the particles. Recently, Moresco (2012) showed that by assuming a continuous process of condensation before, during, and after agglomeration takes place, size distributions could be more accurately reproduced (*i.e.*, after the particles solidify and can no longer agglomerate, they still grow by condensing material on their surfaces) [12].

Fallout from surface bursts

In the case of a surface burst, where the fireball of the detonation directly interacts with proximate environmental material (such as silicate soil), the situation becomes more complex. As surrounding material absorbs the energy of the blast, it may become incorporated into the fireball in a vaporized, molten, or solid state. In the latter two cases, the entrained material can act as a condensing surface for vaporized device material. Condensation and agglomeration of device material may no longer serve as primary controls on the formation

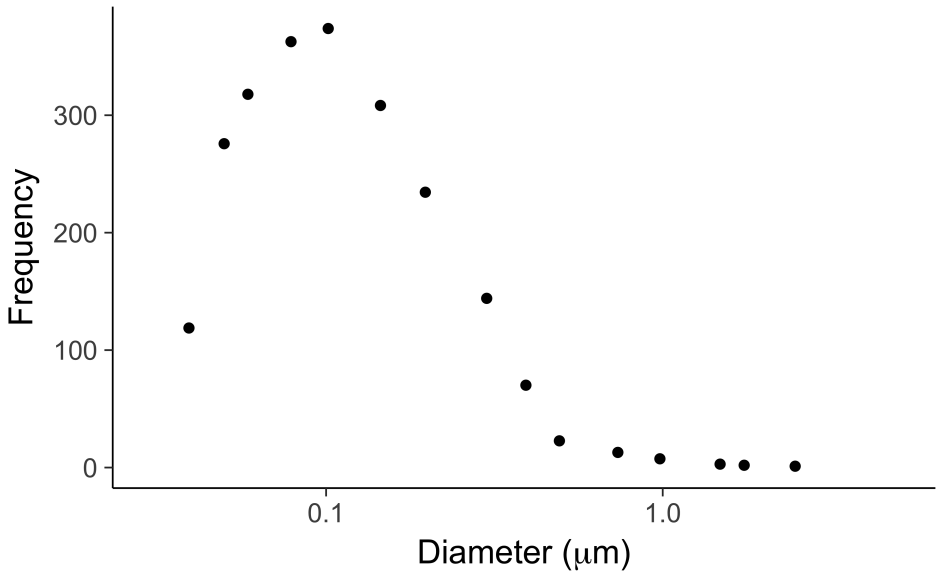

Figure 1.1: Observed size distribution from air-filter collections of debris from an air burst. Note the log x-axis and the approximately log-normal distribution, which is typical for published observations of air burst fallout. This size distribution is from a 200 kT air burst and samples were collected 4 hours post-detonation from the stem of the debris cloud [14]. Data for the plot were extracted from Fig. 9 in Nathans et al. (1970) [14].

of fallout. Instead, the size and activity distribution of the debris is affected by the time-varying incorporation of environmental material of some size distribution. The addition of the environmental material also has the added effect of significantly altering the cooling rate, growth rate, and size of the fireball [10]. Molten soil incorporated into the fireball is often called the "carrier material" or "inert material", as it is thought to act as a condensing surface for vaporized radionuclides. These radionuclides subsequently diffuse or physically mix into (if molten), eventually becoming incorporated into the fallout carrier material matrix once the molten soil quenched, or, if the carrier is solid, simply coating the exterior [21].

Fallout formed in surface bursts tends to have major element compositions largely representative of the surrounding lithology or structural material, with fission products, unfissioned fuel, and activation products present in trace quantities [27, 28]. Not only is fallout from surface bursts representative of the surrounding local material, it also appears to be *strongly influenced* by it—with the parameters of the size distribution of fallout (*i.e.*, the mean size and standard deviation) generated in surface bursts being dependent on the size of the soil, coral, or rocks in the immediate vicinity [25, 27]. For example, several studies of size distributions of fallout generated from near-surface bursts over silicate soil have indicated $\sim$100 μm for the mean particle diameter of fallout deposited close to ground zero versus $\sim$150 μm for bursts over coral, such as on a Pacific island [10, 27]. However, some device material may interact little with the surrounding material, and instead remain in the fireball and be

injected into the stratosphere to spread globally. As a result, debris from surface bursts may represent two or more chemically-distinct populations, each of which underwent different formation processes, and so appear as the convolution as multiple log-normal distributions when samples are collected from the ground, early fireball, and atmosphere. This is often referred to as the "Heft distribution" of fallout, named for the author that first hypothesized it (Fig. 1.2) [27].

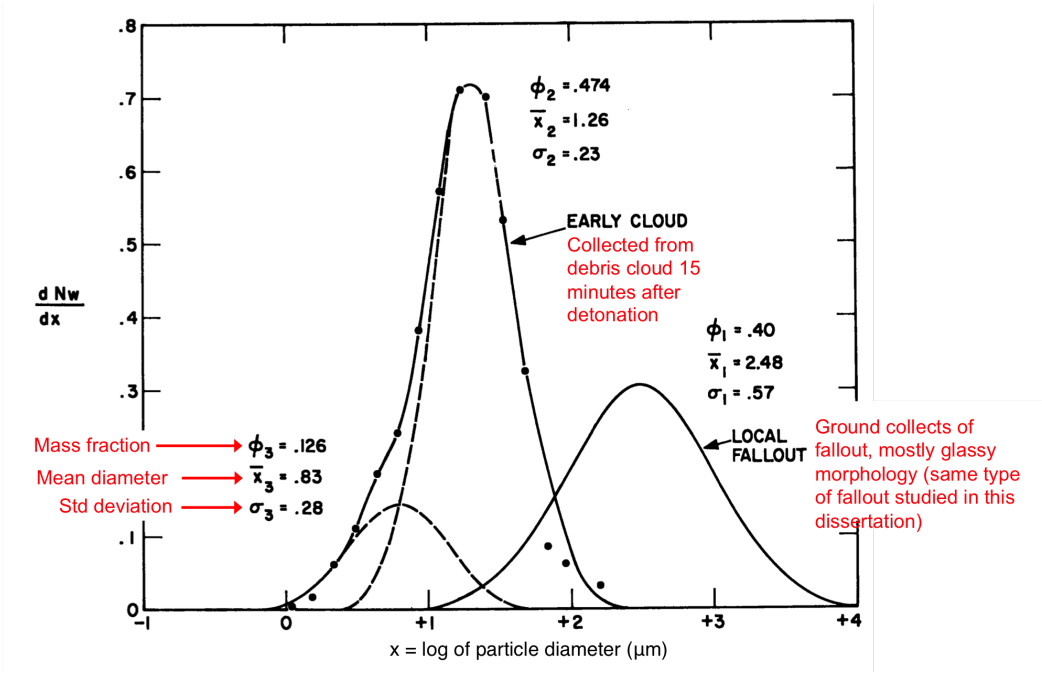

Figure 1.2: Size distribution (determined by mass) from a surface burst after Heft (1970) [27]. The x-axis has units of log of particle diameter in μm. The y-axis shows the relative weight each of the size fractions less than approximately 200 μm (each data point), which was used to determine the relative abundance of each of the size fractions in the "early cloud" log-normal distribution. Each point corresponds to a size fraction of fallout particles collected from air filter samples. The "local fallout" log-normal distribution is from ground collections from the same test and does not include data points, but only a curve representing the observed distribution. The existence of three distinct particle populations (specifically the population at the smallest size fraction, characterized by parameters ϕ_3, $\bar{x}_3$, and σ_3) was confirmed using both specific activity data and size distribution data [27]. This convolution of multiple log-normal distributions from fallout collections is known as the "Heft distribution," and is the basis for conventional fallout formation models and understanding of the formation of fallout size distributions. Local fallout is the population most influenced by the surrounding environment and has most intimately interacted with it.

In detonations over silicate soil, local fallout tends to be glassy (from the melting, mixing, and quenching of silicate minerals) and exhibits a range of morphologies. Irregularly-shaped fused fallout may appear largely melted only one side, with unmelted soil and rocks adhered to the bottom (suggesting one side was more thoroughly heated), as well as nearly-spherical and highly-symmetric glassy fallout, suggesting solidification while aloft (Fig. 1.3).

Irregularly-shaped fallout containing both glassy (one on side) and unmelted (on the other side) morphologies is colloquially known as "ground glass" as it appears to not have fully interacted with the fireball [29, 30]. In contrast, highly-symmetric glassy fallout, also known as aerodynamic glassy fallout, tends to appear glassy throughout, often containing vesicles and relict minerals. These material are likely soil that was nearly completely melted in the fireball and quenched while aloft before falling back to Earth [30, 31]. Ground glass from the Trinity detonation is frequently studied because it is readily available from mineral dealers. However, aerodynamic glassy fallout is of interest because it is more likely to have significantly and intimately interacted with the fireball and anthropogenic material, and often shows higher activity (usually by an order-of-magnitude or more) than ground glass [32–34].

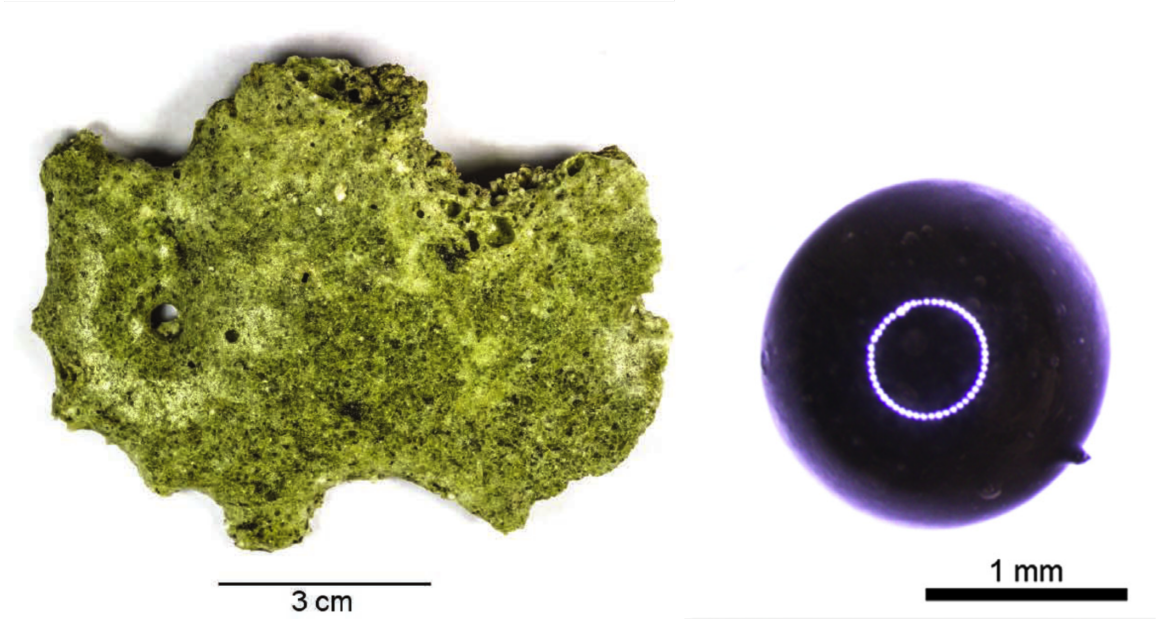

Figure 1.3: Typical pieces of ground glass (left) and aerodynamic glassy fallout (right). Note the change in scale bars between the two. Both are reflected light images. Ground glass is an example of trinitite from Eby et al. (2015) [35]. The bright, circular feature in the center of the aerodynamic glassy fallout is an artifact of the reflection of the ring light from the optical microscope, highlighting how symmetric and spherical these objects are.

Glassy fallout often preserves evidence for the collision and agglomeration of molten parcels of melt (Fig. 1.4). Despite agglomeration largely controlling the ultimate size distribution in air burst debris, it is not known to what extent this process controls the ultimate size distribution of fallout and impacts the incorporation of anthropogenic material into fallout.

Figure 1.4: Optical micrograph of agglomerated objects adhered to the exterior of sample FLD14, a piece of aerodynamic glassy fallout studied in this dissertation. The bright, circular feature in the center of FLD14 is an artifact of the reflection of the ring light from the optical microscope, highlighting the symmetry of the sample.

1.3 Chemical fractionation

One of the most studied phenomena in fallout formation is chemical fractionation [1, 5, 13, 15, 19, 24, 27, 36–42]. Chemical fractionation is any chemical process that causes "alteration of the radionuclide composition occurring between the time of detonation and the time of radiochemical analysis which causes the debris sample to be non-representative of the detonation product taken as a whole" [18]. Condensation, being dependent on the volatility of the condensing species, is such a process and is primarily responsible for variations in the activity-size distribution of fallout, and therefore how radioactivity spreads post-detonation – a primary motivation for studying fallout [15, 24].[3] As a result, in contrast to agglomeration, the role of condensation in fallout formation has historically been of much greater interest. The chemical fractionation of fission products, activation products, and actinides, have been examined in different testing environments [5, 21, 24]. Researchers have conducted fractionation studies in dozens of detonations (see [5, 21, 24] for comprehensive discussions) and built several models around condensation (see [20, 43]) to explain the chemical fractionation of radionuclides in fallout debris in air, tower, ocean, and surface bursts.

The primary cause of chemical fractionation in nuclear events is differences in volatility between different species condensing from the vapor phase of a rapidly cooling system. Because the speciation of radionuclides and the oxygenation of the fireball is not well understood, empirical data have been used to interpret (and subsequently predict) how a particular

[3]Other factors may affect fractionation, such as the speciation of the condensing material (discussed in Section 1.4) and the chemistry of the matrix that species are condensing onto (whether they are solid or liquid, metallic or silicate, crystalline or amorphous, etc.), etc. Oe notable exception is that the degree of fractionation appears to be relatively invariant with yield [18, 43].

species behaves in a detonation. Historically, radionuclides were classified in three ways as it relates to fractionation: those that are "volatile-behaving", "refractory-behaving", and those that exhibit "intermediate volatility" [5]. Volatile-behaving species are those found to be enriched in smaller fallout particles, many of which do not fall out close to ground zero, but instead may be injected into the atmosphere by the nuclear event [24]. These species tend to have lower condensation temperatures (on the order of hundreds of K, assuming oxides) or do not condense at all (*e.g.*, ^{89}Kr). This enrichment of volatile-behaving species in smaller fallout particles creates a corresponding relative enrichment in larger fallout particles of so-called refractory-behaving species, which often condense at temperatures on the order of several thousand K [20]. These species will condense onto and mix into melts earlier and therefore have the opportunity to form larger fallout particles and deposit closer to ground zero.

One complicating factor in understanding chemical fractionation due to differing volatilities is the rapid decay of many species. Radionuclides may quickly decay into species of differing volatility while the fireball is still cooling. As a result, when measured hours or days post-detonation, the end member (or the unstable long-lived parent) of the mass chain is observed to be enriched or depleted, but that may depend on the volatility of some parent radionuclide several decays removed from that end member. For example, in air bursts, the 89 mass chain is observed to be the most volatile, due to the high independent yield and relatively long half-life (on the scale of fireball cooling) of the ^{89}Kr precursor ($t_{1/2}$=3.15 min), even though ^{89}Sr, which has a high condensation temperature, is the isobar measured in the laboratory. Therefore, entire fission product mass chains are referred to as being "volatile", "refractory", or of "intermediate volatility" [39].[4] Radionuclides exhibiting the greatest degree of fractionation are those that have Kr and Xe precursors, such as those with A=89, 90, and 137 (whose mass chains terminate with ^{89}Sr, ^{90}Sr, and ^{137}Cs, respectively) [37, 45]. Contrast this with the 95 mass chain, which is predominantly produced as ^{95}Sr, and assuming a SrO species, has a condensation temperature ∼3200 K, exceeding even the boiling point of quartz by some 700 K [46].

While both air bursts and surface bursts have been observed to exhibit chemical fractionation, most fallout from air bursts show a smaller degree of fractionation relative to surface bursts [18]. In addition, because of the large mass of fallout produced in a surface burst, and the ease with which it can be studied (*i.e.*, much of it is macroscopic), chemical fractionation models have primarily focused on reproducing chemical fractionation effects in fallout from surface bursts. These models of fractionation in surface bursts are unable to fully reproduce the observed fractionation from first principles, however, leading some authors to suggest that the agglomeration of small fallout particles with larger fallout particles, which is ignored and unaccounted for in surface burst fractionation models, may cause the deviation [5].

[4]Recently, Cassata et al. (2014) have been able to determine the relative volatility behavior of individual isotopes in a mass chain [44].

Modeling fractionation

Researchers have attempted to build predictive models of fallout chemistry and chemical fractionation using thermodynamics, empirical data on radionuclide volatility behavior, and, later, diffusion theory [3, 20, 23, 47]. Fundamentally, fractionation behavior is the result of several processes, which occur "rapidly and reversibly" in the vapor and liquid phase in the fireball: (1) Brownian motion of a vaporized species through the vapor phase until it collides with a molten particle, (2) condensation on some surface, and (3) diffusion into the particle's interior (if still molten) (Fig. 1.5) [43]. While early theories began with fundamental, first-principles calculations of vapor pressures and condensation behavior, this ultimately proved too unwieldy because computational power and experimental data at the time were insufficient. Eventually, most historical approaches settled on a simple, radial power approach, sufficient for "rule-of-thumb" fractionation estimates to capture the fundamental predictions of the more complicated models [23]. These approaches have two primary assumptions:

1. Fallout is macroscopically homogeneous, spherical, and has a log-normal size distribution (or a convolution of multiple log-normal distributions, following [27]), whose parameters are determined by conditions of the nuclear detonation (calculated using empirical scaling laws and data).

2. Radionuclides distribute themselves within these particles as some function of radius. That is, volatile mass chains will be surface-distributed ($\propto r^2$) and refractory mass chains will be volume-distributed ($\propto r^3$). How different mass chains behave is determined empirically.

Miller's thermodynamic model

Miller's fractionation model was the first quasi-fundamental modeled approach to estimate how radionuclides partition in surface bursts [20, 21, 48]. It assumes a simplified picture of condensation that occurs in two phases.[5] In the first phase, the idealized and chemically-inert carrier material (as in the case of silicate soil) is molten.[6]

Assuming Raoult's Law (which states the partial vapor pressure of an ideal substance in a mixture is the vapor pressure of the pure substance multiplied by its mole fraction) and using empirical fireball cooling equations, Miller's model calculates the equilibrium vapor

[5]It also assumes a log-normal size distribution of spherical, homogeneous particles and that condensation begins when the most refractory species can sustain a macroscopic liquid, beginning ≈4000 K, as determined by empirical fireball cooling equations, known as the Hillendahl equations [2].

[6]This idealized carrier material is assumed to be the alkali aluminosilicate anorthoclase, an alkali feldspar: $Na_2O{\cdot}Al_2O_3{\cdot}6SiO_2$ [21]. In addition, for this idealized soil, his model assumes 50% of the gross activity is in particles smaller than 100 μm and 1% is in particles greater than 1 cm.

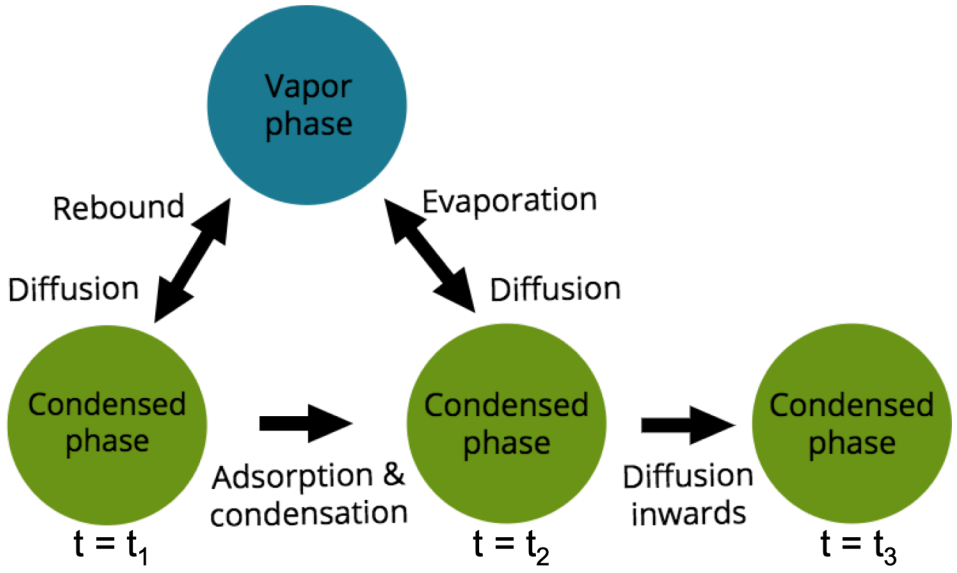

Figure 1.5: Schematic of vapor and condensed phase processes, adapted from [5]. Incorporating vaporized species into molten material involves multiple, reversible stochastic processes, such as: (1) diffusion through the vapor phase until colliding with a molten particle (at time t_1), (2) some probability of condensing or rebounding from that particle, (3) if condensed, some probability of diffusing inward or evaporating from that particle (which may be allowed to occur at some later time t_2), and finally (4) diffusing and mixing inward (which may be allowed to occur at some later time t_3).

pressure of each radionuclide as the fireball cools. The concentrations of each radionuclide in the vapor phase and liquid phase are then determined at a given temperature.[7]

The second phase of condensation begins once the idealized soil drops below its hypothetical melting point of 1673 K. As the fireball temperature drops, more volatile nuclides with condensation temperatures below 1673 K may condense and distribute on the surface of particles, while the more refractory radionuclides are assumed to be trapped within. Refractory species and species of intermediate volatility will continue to condense onto the surface of particles, as many have non-zero and non-trivial equilibrium vapor pressures around 1673 K.

This approach is often referred to as the "go/no go" fractionation model, where radionuclides are "frozen out" based on the melting point of the surrounding soil and the cooling rate of the fireball (Fig. 1.6). The model assumes that fractionation is then from two sources: larger particles falling out of the cloud based on their mass, and the freezing out of volatile species from condensing volumetrically, leading to them dispersing their activities as function of a fallout particle's surface area ($\propto r^2$).

Conceptually, Miller's model explains empirical observations of both the physical sep-

[7]Miller justifies using Raoult's Law here because fission products are of low concentration both in the condensed and vapor phase, so Miller assumes they can be treated independently and do not interact with on another or alter the silicate melt once they condense.

aration (local vs. global fallout) and the chemical separation (based on mass chain) of radionuclides. Unfortunately, this model has limited practical utility, in that the required thermodynamic data to calculate the equilibrium vapor pressures as a function of temperature are sparse and contain high uncertainties, particularly at higher temperatures.

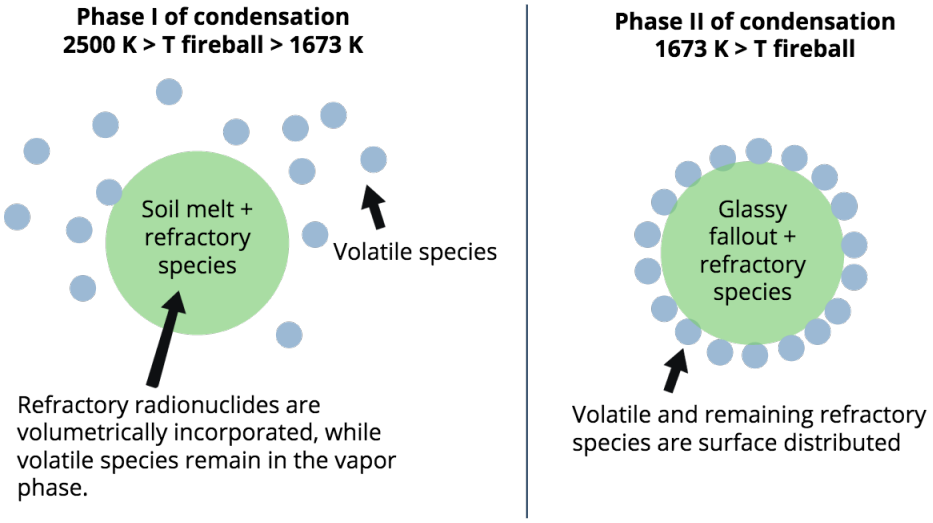

Figure 1.6: Schematic of Miller's "go/no go" thermodynamic fractionation model for silicate bursts [20, 48]. The first phase of condensation is assumed to begin at 2500 K, the approximate boiling point of SiO_2, the most refractory mineral in the idealized soil composition, and end at 1673 K. After, the molten soil quenches and the second phase of condensation begins, allowing more volatile species and other non-volatile species to deposit on the surface.

Norman and Winchell's diffusion-limited model

Norman and Winchell modified Miller's model specifically for a silicate carrier material [43, 49]. Instead of assuming a "freezing out" of radionuclides, this model assumes that the dissolution of fission products into silicate melts is limited by diffusion due to the high viscosity of molten silicates at temperatures well above their liquidus temperature. A species that condenses on a silicate melt above 1673 K would not be assumed to be instantaneously and volumetrically dispersed within a melt (as is the case in Miller's model), but would condense on the surface and subsequently diffuse inwards. If condensing at high enough a temperature, the species would quickly distribute itself volumetrically. However, at lower temperatures and if the viscosity of the melt were high enough, the species would not diffuse far inwards, so the apparent surface concentration appears much higher than if volumetrically dispersed, preventing other identical species from condensing as soon as Miller's model predicts. This model also relies on calculations of the equilibrium vapor pressure of radionuclides, but uses Henry's Law, which relies on a gas' partial pressure above a solution to calculate its solubility

in the solution, and the apparent surface concentration of the species of interest instead of Raoult's Law.

Norman and Winchell's model is a better fit (but is still relatively poor) to chemical fractionation data observed in surface bursts, particularly for larger fallout glasses (hundreds of μm to mm scale), which experimental data show and the diffusion-limited predict would exhibit less fractionation than Miller's model predicts [50]. While the diffusion-limited model underpredicts fractionation at smaller particle sizes and overpredicts fractionation at larger particle sizes, it does match the generally observed trend (Fig. 1.7).

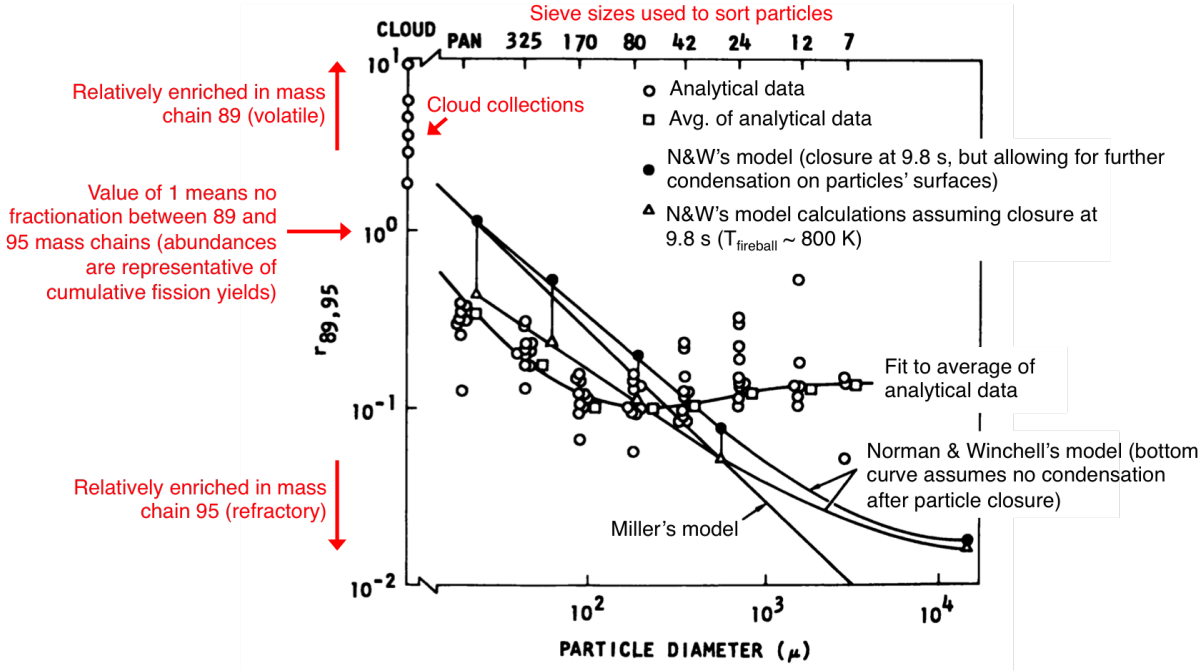

Figure 1.7: Experimental data from Crocker et al. (1965) of fractionation measurements from the surface detonation Small Boy overlaid with model predictions [47, 50]. The plot shows fractionation of mass chain 89 (considered volatile) from mass chain 95 (considered refractory) as a function of fallout size. The 95 mass chain is selected as the prototypical refractory mass chain and used in the denominator because the concentration of ^{95}Zr is observed to be approximately constant across the range of fallout dimensions, so variations in $r_{89,95}$ is primarily due to differences in the ^{89}Sr concentration [4]. A $r_{89,95}$ value of 1 indicates no fractionation between these two mass chains and that they are representative of the cumulative yields expected from fission. These data are plotted as a function of particle size (circles are analytical data, squares are averages), overlaid with predictions assuming refractories become volumetrically-distributed (assumptions from Miller's model) and the diffusion-limited approach from Norman and Winchell. While the diffusion-limited model matches the trend of the data, it is a poor fit. Freiling has speculated that this could be due to agglomerative effects, which both models ignore [23].

Model Limitations

Early models were used primarily for "rule-of-thumb estimates" and as a "stop-gap until better models or more extensive information" became available [23]. These models do a relatively good job of matching observations of fractionation, particularly in air burst debris, despite being largely empirical [23]. However, due to the heavy reliance on historical testing data from a limited set of testing environments (primarily the Nevada National Security Site and the Pacific Proving Grounds) the fidelity of these models to new and untested detonation environments is unknown.

Even in previously tested environments, fallout formation in surface bursts are the least predictable phenomena, primarily because of the complex effects of the carrier material, agglomeration, including the sensitivity of height-of-burst to fallout formation [23]. Take the example shown in Fig. 1.7, which shows that larger glassy fallout samples are observed to be less depleted in volatile species than either Miller's or Norman and Winchell's model predicts. Freiling has speculated the observed discrepancies at larger particle sizes could be due to the agglomeration of smaller particles (relatively enriched in volatile species) with larger particles (relatively depleted in volatile species) prior to quenching, which all models ignore because the effect of agglomeration has not been extensively studied experimentally [23]. The inability to account for agglomeration in these models is a serious weakness noted by several authors and one of the motivations for this dissertation [5].

Another example of the limitations of historical models is explaining the contrasting volatility behavior of U in air burst compared to surface burst debris. In air burst debris, U behaves with intermediate volatility, being relatively enriched in smaller particles collected on air filters, in contrast to Pu, which behaves as a highly refractory species, with compositions in the largest particles being essentially representative of those from the device [5, 47]. Pu maintains this refractory behavior in surface burst debris, while U does not [5]. Once detonations incorporate significant amounts of environmental material, depending on the environment and detonation conditions, U is observed to alter its fractionation behavior [47]. In high-yield bursts over coral, U is observed to behave as a strong refractory (it is considered to follow the 95 mass chain and Pu in its fractionation behavior) [47]. However, in bursts over silicate soils, U tends to become more refractory, but still fractionates appreciably from ^{95}Zr and ^{239}Pu [47].[8] This behavior is not predicted or explained by fallout formation models, and is only taken into account by relying on empirical datasets from historic U.S. tests.

1.4 Contemporary fallout research

Recent studies have sought to better the understand fallout formation processes by using advanced bulk and spatially-resolved analytical techniques to characterize fallout. These

[8] In the laboratory, the fractionation of behavior of U is determined by measuring the concentration of ^{239}Np in fallout, as ^{239}U has a half-life of ∼23.5 min.

studies not only serve to reveal new insights into evolution and environment of the rapidly-evolving nuclear fireball, but may be used to build better models to predict how fallout forms and how different materials such as fission products and other device debris will fractionate in untested environments.

Since 2000, there has been a flurry of experimental research on glassy fallout, primarily using debris from Trinity event. Researchers have primarily sought to collect new data to address:

- What are the timescales relevant to fallout formation?
- How is anthropogenic material distributed in fallout?
- What were the oxidation conditions of the fireball?
- What controls how anthropogenic material is distributed in fallout?

Modern advancements in analytical techniques can reveal chemical and isotopic information in fallout that simply were not an option for historical studies. Many new studies have used multiple techniques in concert, often combining technologies regularly applied in the fields of geochemistry, cosmochemistry, radiation detection, and materials sciences, including:

- High-resolution bulk counting techniques (γ-spectroscopy, α-spectroscopy, and β counting) to measure the decay of fission products, activation products, and actinides
- Electron microscopy to characterize morphologies, textures, and chemical mixing patterns
- X-ray spectroscopy to measure major element compositions of both fallout and soil from the detonation sites
- Bulk and spatially-resolved mass spectrometric techniques to characterize isotope ratios, and distributions and concentrations of major and trace elements

Glassy fallout has been characterized using radiation detection (*e.g.*, [28, 51–53]), then including spatially-resolved methods such as scanning electron microscopy (SEM) and X-ray spectroscopy techniques (energy-dispersive X-ray spectroscopy (EDS) and wavelength-dispersive X-ray spectroscopy (WDS)) to identify and characterize inclusions (*e.g.*, [30, 54, 55]), and spatially-resolved mass spectrometry to measure isotope ratios (*e.g.*, [56]). Several studies have compared major element compositions and relict/partially-melted minerals in fallout to the surrounding sediment from the test location to better understand the molten mixing processes in both aerodynamic (*e.g.*, [30, 35, 57]) and ground glass samples (*e.g.*, [30, 35, 58]). Researchers have also sought to characterize activity distributions in both ground glass and aerodynamic glassy fallout using autoradiography to determine spatial distributions

(*e.g.*, [55, 58–60]) and spatially-resolved mass spectrometry (*i.e.*, secondary ion mass spectrometry (SIMS) and laser ablation inductively-coupled mass spectrometry (LA-ICPMS)) to measure and correlate the distributions of specific radionuclides, stable fissionogenic isotopes, and major and trace elements (*e.g.*, [58, 60–68]). Some of the spatial studies have led to hypotheses of why certain major elements are co-located with unfissioned fuel (see [66–68]) and how some anthropogenic material is incorporated (see [67, 68]). Finally, studies of bulk samples of fallout have also been revealing, constraining the oxidation environment in the fireball (*i.e.*, [44, 69]), showing that aerodynamic glassy fallout quenches within seconds (see [44]), and that different pieces of aerodynamic glassy fallout incorporate vastly different amounts of unfissioned fuel, despite being compositionally and morphologically similar (see [57]).

While many recent studies have expanded the understanding of how fallout forms and the conditions within the fireball, much still remains unknown about fallout formation in surface bursts. In particular, deviation between empirical data and fractionation models due to the relative enrichment of glassy fallout objects with diameters greater than several hundred microns noted in Figure 1.7 remains unexplained. While agglomeration has been hypothesized to be the cause of this deviation, no recent studies have sought to explore if agglomerates have a significant role in forming glassy fallout and whether characterizations of agglomerates support this hypothesis.

Recent observations of Trinity from trinitite

Forensics-motivated characterization of trinitite began appearing in the literature as early as 1995 when Atkatz and Bragg used γ-spectroscopy to estimate the yield of Trinity using the decay of ^{137}Cs and simple assumptions about chemical fractionation of it relative to other fission products within the fireball [51]. Results (they estimated a 13 kT yield for Trinity) were within the range of non-nuclear estimates of Trinity's yield (*e.g.*, seismographic, air pressure measurements, etc.) of 5-15 kT [70]. However, a different trinitite sample used later by Schlauf et al. (1997) had a ^{137}Cs specific activity more than two orders of magnitude greater than the sample used by Atkatz and Bragg, leading to a calculated Trinity yield of approximately 60 kT [52]. (The reported yield was $\approx$20 kT [71].) These studies illustrate the difficulties presented by chemical fractionation and other fallout formation processes to nuclear forensics, and have also helped spurn a new generation of researchers to analyze these materials to better understand fallout formation processes.

About a decade later, Parekh et al. (2006) sought to estimate the enrichment of Trinity's Pu core and determine what other radionuclides were measurable in trinitite using a variety of radiation detection techniques [28]. They presented bulk characterization of several trinitite samples using α-spectrometry, γ-spectrometry, and β counting techniques [28]. They measured the specific activities of several fission products, activation products, naturally-occurring radionuclides, and Pu isotopes, observing chemical fractionation between the different samples, an enrichment in the specific activity of ^{238}U relative to local soil (they assume from the device's tamper), and estimated the enrichment of ^{239}Pu and ^{240}Pu. As

researchers began to understand that these materials were a heterogeneous mixtures of environment and device, it became recognized that using spatially-resolved analytical techniques could reveal characteristics not accessible using bulk techniques.

Initially, authors used non-destructive spatially-resolved techniques such SEM and EDS to interrogate trinitite at higher spatial resolutions [30, 54]. Authors noted that some glassy regions were enriched in materials such as Cu, hypothesized to be anthropogenic, and discovered and characterized metallic-appearing inclusions [30, 54].[9] These inclusions separately contained Pb, W, Ta, and Ga, hypothesized to be sourced from the device and device support structure.

Soon after, researchers sought to use isotope ratios to establish the geographic provenance of Pb used in Trinity [62]. Hypothesizing that Pb co-located with Cu could be assumed to be anthropogenic Pb (following the observations of [30]), Bellucci et al. (2013) used LA-ICPMS to measure Pb isotope ratios in the glassy portions of trinitite samples (their spatial resolution appears to be $\approx$100 μm). By comparing their measured Pb ratios with published Pb ratio data from Pb mines around the world, they concluded that Pb for the Trinity device came from a Pb mine in Canada. Following this study in 2016, they sought to bolster their earlier analysis by directly measuring the Pb isotope ratios of a Pb inclusion in trinitite using SIMS, finding ratios that were consistent with their earlier measurements from LA-ICPMS in the glassy portions of trinitite [56].

The above studies used nuclear forensics as a motivation to study glassy fallout debris, but showed that the debris is primarily a mixture of environmental materials. More recent works have studied glassy fallout not for their forensic value, which may rely on unverifiable speculation about device components and design, but for what can be learned about the conditions within the fireball and to better understand how device vapor becomes distributed within fallout and what controls or affects these distributions.

Oxidation conditions

Understanding whether the fireball acts as an oxygen-starved or oxygen-rich environment can be used to infer the chemical speciation of vaporized radionuclides as the fireball cools and predict when, and in what oxidation state, different vaporized species will condense onto and begin mixing into silicate melts. Analytical data on the oxygen fugacity of the fireball could be used to explain the co-locations of different elements with material from the device based on chemistry or volatility arguments. Furthermore, it may explain the unresolved discrepancy as to why U appears to behave with intermediate-volatility in an air burst and a strong refractory in a surface burst. If surface detonations have a considerably different oxygen environment in the fireball compared to air bursts, U speciation could also be different, leading U to perhaps condense earlier, along with other refractories such as Pu and the radionuclides in mass chain 95.

[9] These inclusions appear embedded in the glass as small, fairly circular impact features that reside in and near vesicles in trinitite thin sections.

Historical models assume an oxidizing environment and treat fission products as oxides both in the gas phase and once condensed onto the surface of the silicate melt [10, 20, 29, 72]. However, the rates and degrees of oxidation of condensing materials has historically been an open question. In the case where multiple oxides exist, authors usually opt for the more reduced form, relying on the argument that as the temperature of the fireball drops to where molecules can form, species are much more likely to collide with single atoms of O than multiple atoms of O [5, 73]. Recent observations have begun to challenge this assumption.

Early research into oxidation conditions in trinitite sought to draw comparisons to tektites, which are glassy, highly-symmetrical debris created by meteorites impact-melting soil as they crash into Earth [74]. In the study, the authors measured the majority of Fe in aerodynamic glassy fallout produced in the Trinity test as Fe(II) (Fe(III)/Fe(II)$\approx$0.1) [74]. Recent X-ray absorption near-edge spectroscopy (XANES, which can be used to measure both the speciation and coordination of elements in bulk material) measurements of trinitite have bolstered those findings. It was observed that soil fused to bottom of trinitite (the sandy side) contain a combination of Fe(II) and Fe(III), but measured the glassy portions to primarily contain Fe(II), suggesting much of the Fe in the soil was reduced [75].

A single oxygenation environment may be too simplistic, however. Authors have reported both "quenched magnetite" and metallic Fe, Pb, W, Ta, and Ga features in trinitite [30, 54, 76]. If these inclusions are derived from the device, this suggests that the oxygenation conditions vary considerably over short distances, and can be quite reducing. Sheffer and Dyar continued this line of inquiry with Mössbauer spectroscopic studies, showing that the majority of Fe in trinitite had been reduced to Fe(II) [77].

This Fe reduction phenomena is not unique to fallout or tektites, also appearing in studies of fulgurites, which are melt glasses produced by lightning strikes [74, 76, 78]. In addition to Mössbauer spectroscopic studies of trinitite fulgurites, Sheffer conducted thermodynamic modeling studies of the reduction of Fe(III) to Fe(II) in tektites and fulgurites, which suggested that the mechanism for this reduction is the non-equilibrium rapid quenching of the molten silicates, preventing Fe_2O_3 from forming [78]. While the modeling in Sheffer (2007) suggests a non-equilibrium rapid quenching as mechanism for reduction, the fireball likely interacted with a large quantity of metallic Fe (steel, etc.). How this material affects the ultimate speciation of Fe measured in glassy fallout is unclear, although several authors have speculated it acts as a buffer for other elements, preventing them from oxidizing (discussed below) [44, 69].

Recently, researchers have sought to expand on historical observations of Fe speciation with speciation measurements of other elements. In particular, they have sought to characterize the oxidation state of species that were vaporized in the fireball and are unquestionably anthropogenic, such as fission products and residual fuel, and attempted to infer the oxidation state of these species while they were still in the fireball. Cassata et al. (2014) demonstrated that fissiogenic Xe could be used to infer the speciation of direct fission products while they were within the fireball [44]. Using noble gas mass spectrometry, they analyzed fissiongenic Xe isotopes trapped in whole pieces of glassy fallout produced in a Pu-fueled test [44]. These stable Xe species are created primarily from the decay of the fissiongenic isotopes Sb, Sn,

Te, or I in the 131, 132, 134, and 136 mass chains. Most of the half-lives of the species in these mass chains are long compared to fireball cooling timescales. As a result, by analyzing different ratios of the Xe end-products, Cassata et al. (2014) were able to determine how Sb, Sn, and Te fractionated relative to each other in the fireball (assuming I and Xe are non-condensing and immiscible pure volatiles), and the timescales for closure of the surface of glassy fallout (discussed in the next section). Given the condensation temperatures of different forms of Sb, Sn, and Te, (*e.g.*, Te, TeO, TeO_2) the results are more consistent with a reducing environment than an oxygen-rich environment, which they hypothesize may due to the substantial amount of metallic Fe likely present in a device assembly. While this was the first study to characterize the speciation of material that wholly existed as bomb vapor, they were unable to determine whether the species were reduced while in the vapor phase or once they were incorporated into the silicate melt. Furthermore, this study could not quantify the degree to which species were reduced, as some of the Fe studies did above.

Pacold et al. (2016) directly measured the oxidation states of U, Pu, and Fe present in glassy fallout from three different tests (one U-fueled test and two tests that contained both Pu and U) using XANES [44, 69]. While Fe in umelted soil is likely predominantly Fe(III), Fe in the fallout from all three tests had a measured oxidation state near 2, suggesting that the fireball incorporated large amounts of Fe(II) and/or Fe(III) was reduced to Fe(II) during fallout formation. In contrast, there was a discrepancy when measuring the U oxidation from the test containing only U compared to the U and Pu tests. While all studied debris contained a combination of U(IV) and U(VI), the U in fallout from the U fueled test was nearly 60% U(VI) (having a measured oxidation state of 5.7). In the other two tests, U and Pu were more reduced towards their IV states (with measured oxidation states for U of 4.6 and 4.7). Like Cassata et al. (2014), Pacold et al. (2016) hypothesizes that metallic Fe likely present in these devices and the surrounding support structures ultimately played a role in U speciation, acting as a buffer for U. They also suggested cooling timescales may be another possible factor affecting these species' redox behavior. However, measuring both the most reduced Fe and the most oxidized U in fallout from the U-fueled test suggests that "melt glass redox chemistry varies widely depending on test conditions" and that "a single oxygen fugacity and redox equilibrium do not apply to melt glasses from nuclear weapons testing" [69]. If U speciation can vary widely over short distances and a fireball can exhibit multiple oxygen fugacities, this suggests that U can also exhibit multiple chemical behaviors, as a vapor and likely also once incorporated into the silicate melt, depending on local conditions in the fireball.

Timescales for fallout formation in surface detonations

Measuring the timescales for fallout formation can give insights into fireball, which historically come from using empirical fits of luminosity measurements of the fireball's exterior. Understanding these timescales can constrain possible physical and chemical processes that can occur within the fireball, such the timescales over which condensation and agglomeration are active or how long the surface of fallout remains molten, allowing vaporized species to

condense and diffuse inward. In addition, fireball temperature measurements primarily come from luminosity measurements of its exterior, and measuring fallout formation timescales can reveal how rapidly the interior of the fireball is cooling.

Most theoretical estimates for the timescales of fallout formation come from using empirical fits to luminosity measurements of the fireball [2, 10]. Because of the heavy absorption of radiation by air far in front of the shock front (rendering the fireball opaque), at times up to 10 ms the fireball temperature is calculated from the velocity of the shock wave, which is directly related to the rate of fireball expansion. For a 20 kT air burst, these temperatures are in excess of 4000 K [2]. As the temperature of the shock front drops below 3200 K, it radiates photons less readily, and becomes more transparent to the radiation emitted by the much hotter, much smaller, approximately isothermal sphere behind it. This transition is referred to as shock "breakaway", occurring around 10 ms (again, scaled to a 20 kT air burst). Because the hotter fireball is now visible, the apparent fireball temperature rises, reaching the "time of second maximum" at around 8000 K and 200 ms. (This rise in temperature is not actually occurring, it is an artifact of using optical methods outside the fireball to measure the fireball temperature.) After reaching this apparent second maximum, the fireball cools rapidly through radiative emission and incorporating cooler air (going approximately as $T \propto 1/\sqrt{t}$) [10]. The surface of the fireball drops to 1673 K (Miller's melting point for siliceous soil) in 2-4 s [2].

This thermal profile describes the cooling visible at the surface of the fireball, not within the fireball, and for an air burst, not a surface burst. An empirically-derived scaling equation, known as Hillendahl's equation, is instead applied to calculate the cooling rate for fireballs of different yields after the time of second maximum:

$$-\frac{dT}{dt} \approxeq 3 \times 10^{-11} W^{-0.3} T^4, \tag{1.1}$$

where W is the yield in kT, T is the temperature in kT and $-\frac{dT}{dt}$ is in K/s [5]. This scaling law, commonly applied by many studies across the literature, was calculated from observations of MT-scale air bursts and relies on data that do not extend below 2000 K, when the entrainment of cooler air becomes an important source of cooling, altering the cooling rate compared to radiative emission alone. There have been attempts to calculate the temperature inside the fireball due to entrainment of cooler air, most notably by Störebo (still for an air burst, not a surface burst)[79]. However, the velocity of the incorporated air is not known, so is presented for values ranging from 1 to 10 m/s.

Izrael (2002) expanded on Hillendahl's and Störebo's work, attempting to calculate fireball cooling for kT surface bursts [10]. He relies on Störebo's calculations for 3 m/s air entrainment and also accounts for additional effects caused by the incorporation of soil into the fireball, such as how the soil's heat capacity, enthalpy of vaporization and fusion, and dissociation energy affect fireball cooling rates [10]. He estimates that overall, the incorporation of soil slightly decreases the temperature of the fireball and that surface bursts cool much like air bursts until they drop below ∼2000 K, when effects such as the effect of vaporized soil condensing (releasing its latent heat of vaporization) or molten soil quenching

(releasing its latent heat of fusion) slightly lengthen the amount of time (between 0.6 and 1.6 s) it takes for the fireball to cool beyond the melting temperature of the surrounding soil as if it were an air burst (Fig. 1.8).

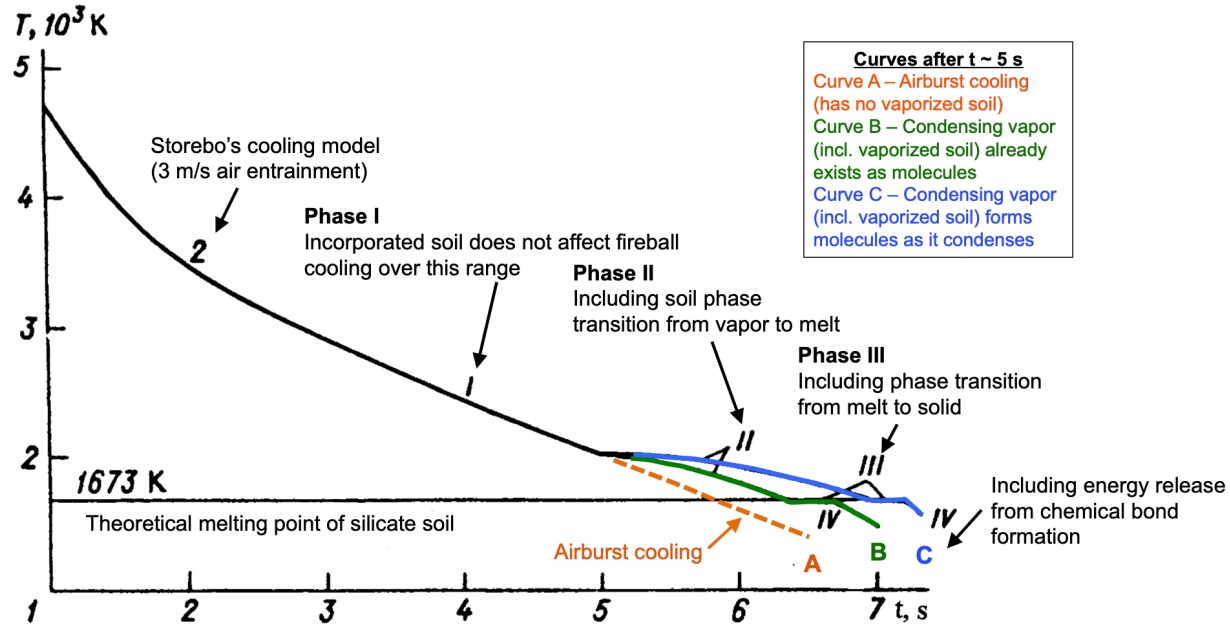

Figure 1.8: Calculations of fireball cooling for a 20 kT surface burst by Izrael after the time of second maximum [10]. The y-axis shows temperature in thousands of K and the x-axis shows time in seconds. The time axis starts at $t = 1$ s. For cooling at early times, Izrael adopts Störebo's fireball cooling calculation for an air burst, assuming air entrainment at 3 m/s. Izrael includes the cooling effect of the addition of soil during Phase I (from ≈3-5 s), finding that it does not cool the fireball significantly from including no soil at all, so the surface burst and air burst cool similarly in this regime. At t≈5 s (Phase II), a lag in cooling is predicted from the vaporized soil releasing energy into the fireball as it condenses. During Phase III, another lag in cooling is predicted from the molten soil releasing energy into the fireball as it quenches. The orange dashed line (curve A) is the calculated cooling curve from an air burst. Curves B and C (green and blue solid lines, respectively) differ in that Curve C assumes that chemical bonds are formed as the vapor condenses, releasing more energy into the fireball, adding to the cooling time delay. Curve B assumes the condensing vapor already exists as molecules. Adapted from [10].

Izrael also includes calculations for the additional time it would take for molten particles to reach the ambient fireball temperature, which is delayed to conduction of heat into the particles [10]. He calculates a delay of 0.035 s for fallout ∼1 mm in diameter, and 0.14 s for fallout ∼2 mm in diameter, the size of many of the studied fallout samples, including those used in this study, Lewis et al. (2015) [60], Weisz et al. (2017) [67], Eppich et al. (2014) [57], and Cassata et al. (2014) [44]. Combining the time delay from both of these effects, by Izrael's estimates, the interior of 1 mm diameter molten particles in a 20 kT surface burst should reach their liquidus temperature of 1673 K between 0.6 to 1.6 s *after* an air burst reaches the same temperature (∼4.4 s), or approximately between 5 and 6 s after detonation.

This clearly will be different for tests of different yields, and in detonation environments with soil of a different composition, etc.

In Cassata et al.'s 2014 study of Xe isotopes in fallout (discussed above), they were able to uniquely constrain the time at which each sample's surface became impervious to further mass transfer [44]. Constraints on time of closure ranged from 0 ± 0.1 s to 2.9 ± 1.1 s (1σ). These measurements are within an order-of-magnitude (but shorter than) Izrael's quenching timescales.

Weisz took an independent approach for calculating fallout formation timescales using diffusion theory [68]. He observed compositional interfaces at points of contact between small spherical glassy objects attached to the exterior of millimeter-scale aerodynamic pieces of glassy fallout (*i.e.*, agglomerates attached to host glasses). Using SIMS and X-ray spectroscopy, he determined these interfaces were consistently enriched in ^{235}U, Ca, Fe, and Mg, and preserved as the agglomerate collides and coalesces with the host glass. By extracting parameters from Gaussian fits to diffusion profiles across these compositional interfaces, he was able to extract estimates for the time and temperature at which the agglomerate attached to the host.[10] For the cooling of vapor from a 1 kT yield detonation (he also gives time and temperature for 0.1 and 10 kT yields), Weisz estimates the agglomerate attached at approximately 1 ± 0.5 s (1σ) and at a temperature of 2100 ± 150 K (1σ).[11,12] At this time and temperature, the fireball is cooling rapidly, but the particles are still molten, yet quite viscous (likely why the agglomerates retained their spherical shape and were not fully incorporated into the host glass, but instead only attached on the outside). Cassata et al. (2014) estimates their samples closed to mass transport between 0 and 3 s, which would put the temperature of their fallout glasses somewhere near 1673 K at the times the molten agglomerates attached to Weisz's still molten host glasses [44]. Therefore, samples from the Pu-fueled test studied in Cassata et al. (2014) may have cooled more quickly than samples from the U-fueled test studied in Weisz (2016).

Cassata et al. (2014) and Weisz (2016) are the first direct (and independent) experimental measurements of fallout formation timescales, and they are consistent with, but shorter than, Izrael's estimates for fallout formation for a 20 kT surface burst. While subject to unknown yields, detonation conditions, and some experimental uncertainty, in addition to many scenarios that could lead to glassy fallout experiencing vastly different times and temperatures in the fireball (such as different times of being swept up, being near the surface vs. in the fireball's center, etc.), collectively, these results suggest that millimeter-scale aerodynamic fallout quenches on the order of seconds for detonations in the 1-20 kT range.

Most recently, Bonamici et al. (2017) used electron probe microanalysis (EPMA) to fit diffusion profiles in samples from Trinity, where the device's yield is known to be $\sim$20 kT [66, 71]. They focused samples where different molten phases had come into contact and

[10] see Table 5.4 on page 164 in [68].

[11] Diffusion profiles in different samples have different widths, but the time/temperature calculations and their uncertainties are all near these values.

[12] The uncertainties in these values are dominated by the uncertainties in U diffusivity data in silicate melts, which fundamentally limit the precision of this approach.

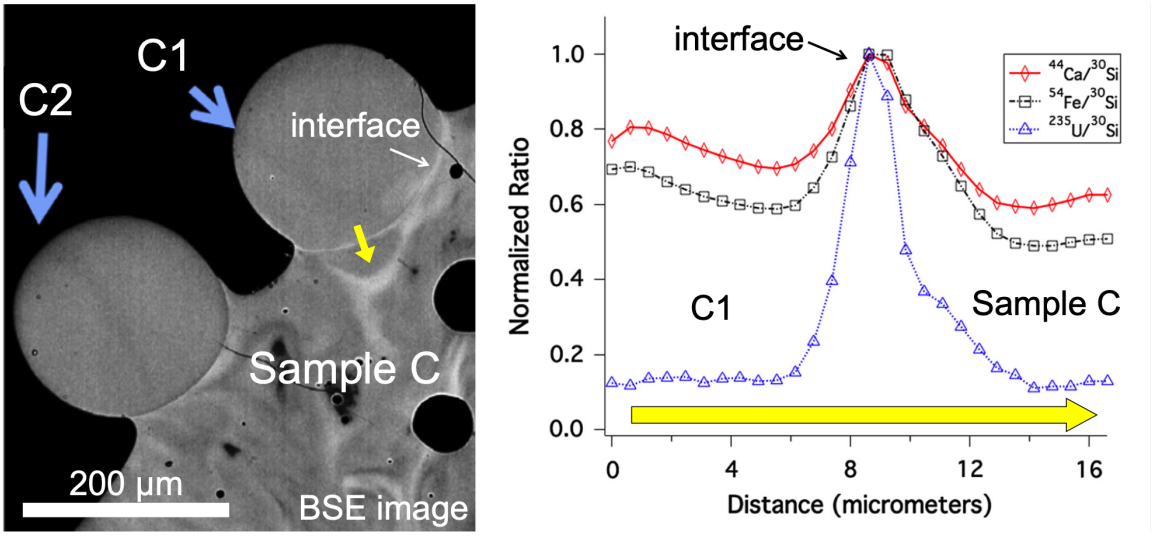

Figure 1.9: Enrichment of ^{235}U, Ca, Fe at the compositional interface between an agglomerate and host object. Image on left is a backscatter electron micrograph of agglomerates C1 and C2 attached to sample C from [67]. The compositional interface of C1 is visible as a bright line separating C1 from Sample C. Plot on right shows the normalized isotope ratios of ^{44}Ca/^{30}Si, ^{54}Fe/^{30}Si, and ^{235}U/^{30}Si as measured by SIMS and normalized by their maximum values showing the traverse across the compositional interface of C1 (marked by the yellow arrow in the image). ^{30}Si is used as the denominator in these isotope ratios as Si is relatively invariant across these compositional interfaces [67]. The peak occurs at the compositional interface between C1 and Sample C. In the plot, the agglomerate C1 is on the left of the peak and sample C is on the right of the peak.

evidence for diffusion is observed across the boundary between them [66]. By assuming binary diffusion of Si from one melt into the other (the observed difference in SiO_2 concentration was between 4-12 wt.%) they calculated temperature ranges and times over which these melts were in contact. The best fit parameters from six profiles in four different samples indicate similar peak temperatures between 2000-2100 K and cooling times ranging between 3-6 s. This range in cooling times is also in line with both Izrael's estimates and Hillendahl's empirical scaling laws [2].

One limitation of the approaches presented by Weisz (2016) and Bonamici et al. (2017) are their assumption that only diffusion occurs. Mixing patterns in fallout show extensive evidence for convection (see [30, 60]), however, which would almost certainly broaden diffusion profiles. To what extent is unknown, but it is likely these profiles overestimate, to some degree, the time and temperature of contact.

Distribution of anthropogenic material in fallout

Measuring how anthropogenic material, such as unfissioned fuel, is distributed in fallout can reveal the chemical behavior of these species, how and when these species are incorporated into fallout, and provide clues about the emplacement environment prior to the nuclear

event. Despite historic studies qualitatively and broadly describing the distribution of radioactivity in fallout using autoradiographs as well as recent studies presenting qualitative characterizations of mixing patterns of major elements using non-destructive methods such as EDS X-ray mapping, only recently have studies attempted to correlate the two distributions quantitatively.

Historic and recent studies reveal that glassy fallout is an inhomogeneous, vitrified mixture of the surrounding environment with anthropogenic material present in trace concentrations [28, 30]. In the case of trinitite ground glass, authors note that ground glass was a highly vesicular and heterogeneous mixture common rock-forming minerals found around the White Sands site, such as quartz, potassium feldspar, calcite, and plagioclase [30]. In contrast, aerodynamic glassy fallout from Trinity is observed to be largely glassy throughout, with fewer relict mineral phases, less vesicularity, but still an inhomogeneous mixture of soil that had melted and quenched. Flow-banding mixing patterns on the scale of 10-100 μm scale are seen, and many partially-melted quartz grains have diffuse boundaries [30]. Autoradiographs largely show either a fairly uniform volumetric incorporation (in aerodynamic glasses) or surface coatings of activity (in ground glass), bolstering Miller's "open/closed" condensation theory, which more or less remained the standard until Norman and Winchell modified this with their diffusion-limited theory [3, 4]. Recent attempts to clarify how activity is distributed in trinitite using autoradiography report it is dominant in the glassy phases towards the surface or as a coating, suggesting activity can only be volumetrically-distributed in materials that were either molten or vaporized in the fireball [59].

The extent of these inhomogeneities and how anthropogenic species from the device distributed themselves among the major elements derived from the carrier material (such as soil) remained relatively unstudied until the 2000s. Mass spectrometric techniques with higher sensitivity and spatial resolution, such as SIMS and LA-ICPMS, have enabled characterization and quantification of the degree of mixing between device debris and different major elements in the glassy phase.

Fahey et al. (2010) were the first to use spatially-resolved mass spectrometry (SIMS) to directly measure Pu, U, and Pb isotopes in a thin section of trinitite [58]. By combining isotopic maps from SIMS with X-ray mapping of the major elements in the glass, their study revealed a co-location between device-derived Pu and U and environment-derived Ca, a major constituent of both trinitite and White Sands soil (Fig. 1.10). (By measuring spatially-correlated non-natural Pb ratios, they also concluded observed U was device-derived, not soil-derived.) One short coming of this study (and all other studies conducting *in situ* measurements of Pu using mass spectrometry) is that they rely on the intensity of the Pu signal as a proxy for Pu abundance, uncorrected for instrumental mass bias because there is no commercially available Pu-bearing glass standard. This and other studies that measure Pu isotope ratios assume the instrumental mass bias between different Pu isotope ratios is small (it is typically <1% in U isotopes, so likely would be similar in Pu), but count rates can vary considerably between analyses and are highly dependent on instrumental conditions, sample roughness, and even ambient temperature. Some studies have used literature values for the relative ionization rate of U and Pu to estimate the Pu abundance (*i.e.*,[66]), while

others have demonstrated that the activity shown in autoradiographs of fallout from Trinity is dominated by activity from Pu, and justify using qualitative maps of radioactivity instead of in situ isotopic measurements [80].

Fahey et al. (2010) and other author's findings (*e.g.*, [55, 66, 81]) of Pu and Ca co-location (which has recently been expanded to correlations between Pu and Ca, Mg, and Fe by Wallace et al. (2013) have led several authors to develop new theories about how anthropogenic material becomes incorporated into glassy fallout (discussed below) [61]. Wallace et al. (2013) sought to replicate and expand on Fahey's observations of correlations between anthropogenic material and environmentally-derived material in trinitite [61]. They combined autoradiography, electron microscopy, and LA-ICP-MS to attempt to correlate ^{239}Pu, ^{238}U, ^{137}Cs, Fe, and Ca in the glassy portions of trinitite, concentrated in the uppermost layers of their samples [61]. However, their study suffered from a small number of measurements and the presented correlations are not strong.

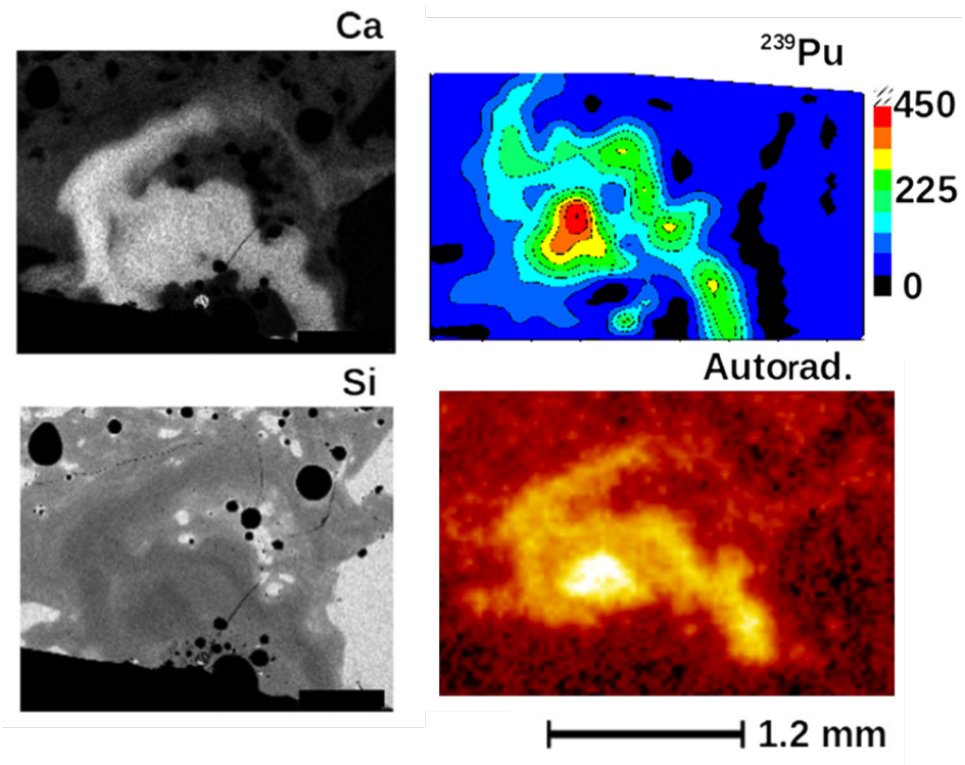

Figure 1.10: Compositional maps of Ca and Si, ^{239}Pu SIMS ion image, and autoradiograph showing co-location of Pu, radioactivity, and Ca in a thin section of trinitite from [58]. In the compositional maps and autoradiograph, higher brightness indicates higher intensity and the scale in the Pu ion images indicates number of counts. The autoradiograph primarily reveals α activity in the sample (assumed to be dominated by the α decay of ^{239}Pu). The black circular features in the Ca and Si maps are vesicles and the black region towards the bottom of the Ca and Si maps is epoxy.

Bellucci et al. (2014) measured both major elements (using EPMA) and trace elements

(using LA-ICPMS) in trinitite thin sections to expand on the findings in Wallace et al. (2013) by applying a multivariate approach to the data [63]. Using PCA, they attempted to understand the correlation between major and trace elements to delineate what minerals phases had mixed in the glassy regions of trinitite and determine what elements were correlated with material from the device and tower. While they were able to use major element correlations to delineate between different dominant soil contributions (*e.g.*, correlations of K, Al, and Si suggesting a potassium feldspar contribution), a shortcoming of this study is too few analyses and too many variables for a strong PCA analysis. PCA is most effective when the number of analyses is much greater than the number of variables. In their study, they present 119 analyses (from 13 different samples) with 40 variables, and they do not demonstrate that this number of analyses and variables builds a sufficiently stable model (see Chapter 6). Regardless, their interpretations are consistent with their previous findings, observing correlations between metals (Co, Cu, Cr, and Pb – similar to the inclusions noted in [30, 54]) and two separate correlations of U: one with elements typically found in zircon, monazite, and apatite (interpreted as the natural U contribution from soil) and one associated with Cu, Co, and Cr (interpreted as anthropogenic U) [54].

Lewis et al. (2015) performed the first spatially-resolved mass spectrometric study in aerodynamic glassy fallout from a U-fueled event [60]. Until 2012, spatially-resolved isotopic studies had only been performed in ground glass from Trinity. It was not known how, for example, U fuel would distribute compared to Pu fuel, if U would be correlated with the same major elements as Pu, and how these distributions would be different in aerodynamic glassy fallout versus ground glass. Using SIMS to perform traverses across samples, they measured the U isotope composition of approximately 200 regions (10–30 μm in diameter) in five aerodynamic glassy fallout samples (1-2 mm diameter) from a U-fueled test. They found the $^{235}U/^{238}U$ ratio to be greater than natural (>0.00725) in every analysis, implying that U was likely volumetrically distributed throughout the glasses [60].[13] The $^{235}U/^{238}U$ ratio spanned nearly three orders of magnitude, ranging from $0.02 < ^{235}U/^{238}U < 11.8$, or $2\% < \text{atom}\%\ ^{235}U < 92\%$. Minor U isotope ratios, $^{234}U/^{238}U$ and $^{236}U/^{238}U$, exhibited strong correlations with the $^{235}U/^{238}U$ ratio ($R^2 = 0.99$). Finally, some of their analyses also included U concentration measurements, which spanned from 5–20 ppm (soil proximate to this test has U concentrations between 2.7–4.8 ppm, see [57]), and were approximately correlated with the $^{235}U/^{238}U$ ($R^2 = 0.77$), implying that higher concentrations are simply the addition of fuel from the device.

Combining the U isotope data with X-ray mapping and autoradiography, Lewis et al. (2015) did not find a consistent co-location of unfissioned fuel with Ca, in contrast to measurements of Pu and Ca in trinitite. In two of their samples, the samples could be generally be divided into two compositional regions: one enriched in Ca and one depleted in Ca. The $^{235}U/^{238}U$ ratio exhibited an enrichment and depletion depending on which region was ana-

[13] The glasses did contain several high SiO_2 regions, which were not measured with SIMS. Wallace et al. (2013) and Bonamici et al. (2017) found such features to contain no radioactive component in their samples from Trinity [61, 66].

lyzed. However, in one sample, $^{235}U/^{238}U$ in the Ca-rich region was enriched relative to the Ca-poor region (Fig. 1.11) and in the another sample, $^{235}U/^{238}U$ was depleted in the Ca-rich region relative to the Ca-poor region. In one sample, Ca was positively associated with $^{235}U/^{238}U$, and in the other, Ca was negatively associated with $^{235}U/^{238}U$. This bi-modal behavior was exhibited in the autoradiograph as well – being correlated with the regions most enriched $^{235}U/^{238}U$. Because the samples exhibited this partitioned behavior in major element composition, unfissioned fuel, and total activity, Lewis et al. (2015) concluded that these samples were formed by the collision and agglomeration of two parcels of melt with different composition, which had also incorporated different amounts unfissioned fuel and radionuclides. These two parcels did not have an opportunity to thoroughly mix before quenching, preserving these textures.

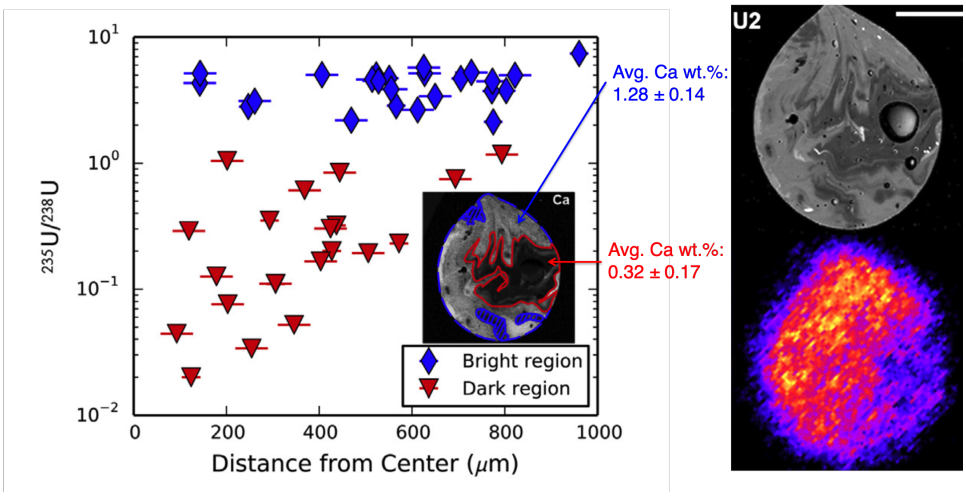

Figure 1.11: Co-location of U isotopic enrichment with Ca concentration and gross radioactivity from [60]. Plot on left shows the $^{235}U/^{238}U$ ratio as a function of distance from the spherule's center on sample U2. Note the logarithmic y-axis. Data are separated into SIMS measurements taken in the bright and dark regions of using the Ca X-ray compositional map in the inset. The higher Ca region is the bright region and is bounded by the dashed blue and solid red lines while the dark region contains less Ca is bounded by the solid red line and show a bimodal distribution. Regions denoted with hash marks within the bright region were excluded from this data subset. Uncertainties are 2σ. On the right are BSE (top; scale bar is 500 μm) and autoradiography (bottom; brighter indicates more activity).

Eppich et al. (2014) studied fallout from the same U-fueled event, but performed bulk isotopic and elemental analyses [57]. They dissolved 28 entire samples of aerodynamic glassy fallout and analyzed them for major elements, trace elements, and isotopes of U (along with its several isotopes of its decay daughters) [57]. Again, in contrast to Trinity and consistent with observations in Lewis et al. (2015), there was no observable correlation between unfissioned U fuel and Ca in samples from this U-fueled test [60]. In fact, there was a weak inverse correlation between $^{235}U/^{238}U$ and Ca (R^2=0.47), and no observable correlation between U and Ca concentrations. Finally, they observed similar isotope ratios to Lewis et

al. (2015), but their observations spanned a smaller range, between $2.3 < {}^{235}U/{}^{238}U < 7.7$, bolstering the argument that anthropogenic material is likely volumetrically distributed in these glasses.

Holliday et al. (2017) also reported spatially-resolved observations (autoradiography and SEM/EDS) from a Pu-fueled device. In polished samples of aerodynamic glassy fallout, they report finding correlations between Pu (inferred from autoradiography), Ca, Mg, and Fe (from compositional X-ray maps) observed in samples from Trinity [55].

How anthropogenic material is incorporated into fallout

Miller's "go/no go" condensation model and Norman and Winchell's diffusion-limited theory remain the primary sources of understanding how radionuclides will distribute in fallout. That is, refractory material from the vapor phase will tend to disperse volumetrically and volatile species in the vapor phase will tend to coat the exterior and will frequently exhibit a strong radial concentration gradient from the surface inwards (just as Norman and Winchell's fallout glass with diffuse coating of Fe and Pb did) [43]. However, these theories do not explain the observation of Weisz (2016) of associations between U, Ca, Mg, and Fe at compositional interfaces or in samples from Trinity and the Pu-fueled test from Holliday et al. (2017) between Pu, Ca, Mg, and Fe [55, 67].

The observation of Weisz (2016) of the co-location of U, Ca, Mg, and Fe at compositional interfaces between two collided and agglomerated objects offers the only analytical evidence for another way anthropogenic material can be incorporated into fallout, possibly being a late-stage deposition layer from the vapor phase [67]. The interfaces are typically <10 μm wide and $\sim$100 μm across and tend to occur infrequently in fallout samples collected from this test. The frequency of these interfaces and the amount material located at them represent an extremely small total fraction of glassy fallout's volume. Accordingly, the contribution they make to the volumetric incorporation of unfissioned fuel is likely small.

There have been proposals or observations to explain the volumetric incorporation of unfissioned fuel observed in aerodynamic glassy fallout [57, 60]. Eby et al. (2015) and others studying aerodynamic glassy fallout (*e.g.*, [35, 60, 67]) have noted millimeter-scale flow-banding patterns when these glasses are polished to expose their interiors and examined under electron microscopy, indicating physical mixing of bulk molten material on the scale of many of these glasses' diameters [30]. In silicate melts, mass transport can occur through two processes: diffusion or bulk convective flow [82]. If diffusion length scales are insufficient, this millimeter-scale mixing of molten material could help distribute radionuclides that condense on the surface into the molten particle's center. In the case of Trinity and other Pu-fueled devices, Pu appears primarily associated with Ca, Fe, and Mg.

The correlation of Pu with Ca, Mg, and Fe in Trinity and the other Pu-fueled test occurs not only at interfaces between agglomerated and host objects, but throughout the sample. The initial observation of Fahey et al. (2010) of Pu and Ca co-location in trinitite has led many researchers to attempt to establish a correlation, not just a co-location, between Pu and Ca (and later Mg and Fe), but the trends have not been particularly strong [61, 65].

Others have sought to use the relationship between these major elements and unfissioned fuel in fallout as a theoretical basis to further our understanding about fallout formation, leading to two recent proposals:

- That Pu and Ca (along with Mg and Fe) co-condensed from the vapor state into the melt [66].
- The incorporation of Pu (and other anthropogenic species) is controlled by the viscosity of the melt, and melts high in Ca, Mg, and Fe tend to have lower viscosity at a given temperature than the other glassy phase compositions [55].

Bonamici et al. (2017) observed that Pu is solely co-located with a glass composition described as a "CaMgFe" glass in their samples of fallout from Trinity [66]. Using autoradiography, SIMS for Pu isotopics, and EPMA for major elements in Trinity fallout, Bonamici et al. (2017) observed that the majority of radioactivity (and therefore Pu) is contained in what they call a "CaMgFe" silicate glass, which is the "volumetrically dominant glass phase" in their samples [66].[14] The other glassy phases comprising their samples: a silica-rich glassy phase, alkali-rich glassy phase (feldspathic), and Ca-rich glassy phase show little to no radioactivity.

They interpret the association of Pu and the CaMgFe glass to result from Pu and the CaMgFe glass having both been vaporized and co-condensed onto the other glassy phases, which were simply melted. In addition, they propose that this co-condensation is controlled by volatility, arguing that as pure elements, Ca, Mg, and Fe are more refractory than Na, K, and Si, and should condense with Pu, a known refractory in both air and surface bursts [5]. However, Al is the most refractory elemental species present as a major element in their samples, but they note that Al often displays a large enrichment in the CaMgFe glassy phase relative to sediment. Bonamici et al. acknowledge that their co-condensation hypothesis is contentious. It goes against decades of understanding of fallout formation, countering historic observations (*e.g.*, [14, 27]) and calculations (*e.g.*, [25]) that condensation alone leads to particles with maximum diameter of $\sim$20 μm. It is also counter to recent attempts to model the fallout formation processes in air bursts, which match historic observations well [12]. Bonamici et al. (2017) argue that these models assume homogeneous nucleation in a clean plasma and do not account for the presence of a significant amount of molten material that acts heterogeneous nucleation sites, which may greatly enhance condensation behavior. This argument relies on several works modeling the formation of spherules in asteroid impacts (*e.g.*, [83]). However, it is unclear if fallout formation in a nuclear detonation can be explained using models for spherule formation in asteroid impacts.

In contrast, Holliday et al. (2017) proposes that melt viscosity controls Pu incorporation [55]. In their samples from a Pu-fueled test, they observed Pu activity primarily in regions

[14]While they present their samples as being aerodynamic glassy fallout and some samples do show a degree of sphericity and symmetry. However, the exposed cross-section appears highly vesicular and appear to contain a large amount of unmelted minerals. As such, several samples appear to be closer to trinitite ground glass than aerodynamic glassy fallout in type.

with a "mafic" (approximately 45 wt.% SiO_2, 25 wt.% CaO, 15 wt.% Al_2O_3, 10 wt.% MgO, and 5 wt.% FeO) composition but absent in the two other glassy regions: one with a "felsic" composition (approximately 60 wt.% SiO_2, 20 wt.% Al_2O_3, 10 wt.% K_2O, and 5 wt.% Na_2O), and one of nearly pure SiO_2. While their observations are consistent with Pu being associated with Ca, Mg, and Fe, they also report Fe or Mg inclusions with no Pu associated. This is counter to volatility-controlled processes that would lead to Pu always being associated with any large enrichment in Ca, Fe, or Mg. They instead propose a viscosity-controlled process, calculating the viscosity as a function of temperature for the three compositional regions. At most temperatures, the viscosity of the mafic phase is ≈3-4 orders-of-magnitude below the felsic phase and ≈7-8 orders-of-magnitude below pure SiO_2 [55]. As such, how unfissioned fuel is incorporated into the bulk of melts and why Pu tends to be associated with Ca, Mg, and Fe in glassy fallout remains unsettled and requires further exploration and study.

1.5 This study

Agglomeration, despite being commonly observed in both historical and current research of fallout in surface bursts, remains largely unstudied. In air burst debris, models suggest that agglomeration largely controls the shape of the size distribution. Agglomeration's impact on chemical fractionation has not been investigated (possibly because chemical fractionation in air bursts is small relative to surface burst debris [18]), and in surface bursts, the role of agglomeration in forming and altering fallout is ignored [5]. Authors have cited this as one of the major weaknesses in fallout formation models and hypothesized agglomerative effects could be responsible for the large deviations between modeled and observed chemical fractionation predictions at larger fallout dimensions [3, 5]. In surface bursts, it remains unclear if agglomerates contain a significantly different radionuclide inventory than their host objects. In addition, it is unknown if agglomerates comprise a large enough volume within samples to possibly alter the overall radionuclide or major element composition of millimeter-scale glassy fallout samples.

In air burst debris, agglomeration is known to create larger particles than expected, with particles larger than 1 μm frequently appearing as multiple particles adhered to each other [14, 36]. In surface bursts, because of the much higher material density when large masses of carrier material are introduced into the fireball, agglomerative effects should be more pronounced. In particular, there is a need to study the frequency, size, and location of agglomerates, and to characterize their major element and radionuclide compositions to determine whether they are likely sourced from similar melts and whether they incorporated similar amounts of radionuclides from the fireball vapor term as host objects. Such behavior could potentially affect the overall radionuclide composition of aerodynamic glassy fallout samples.

The frequency of observed agglomerates is of interest because if agglomeration and agglomerates greatly alter fractionation and the size distribution in aerodynamic glassy fallout, it would be because it occurs often and agglomerates therefore should make up some signifi-

cant volume of glassy fallout. The dimension of agglomerates also matters. If some agglomerates were formed through a fundamentally different mechanism (*i.e.*, primarily constituted from the condensing vapor term instead of molten material onto which relatively little vapor phase material condensed onto and mixed into), they are likely to occur at smaller dimensions ($\lesssim$20 μm), the approximately maximum dimension of observed fallout particles from airburst debris [14]. Observing the location of agglomerates is also useful. Agglomerates are observed attached to the exterior of glassy fallout samples. Samples polished to expose an interior cross-section have been found to also contain agglomerates at the surface of samples [68]. Agglomerates attached to the exterior of samples must have accreted and coalesced with the host when both were close to closure, relatively late in time and at relatively low temperatures (Fig. 1.8). In contrast, agglomerates fully incorporated to the interior of samples must have accreted with the host object at comparatively early times, when the host was still molten enough and low enough in viscosity to envelop the agglomerate. Given that chemical fractionation is a time, temperature, and species dependent process, comparing the major element and radionuclide composition amongst agglomerates located in different regions of the sample (*i.e.*, attached to the exterior, at the surface, or fully incorporated into the host object) will allow a comparison between agglomerates to determine if there is a persistent difference between the major element composition and U isotope composition between agglomerates located in different regions of a sample.

Finally, characterization of agglomerates will serve to bolster or refute the claim made by Glesston 1966 (in Russian, but summarized by Izrael [10]) that once entrained, material does not move very far in the fireball before it exits and quenches. Specifically, Glesston states that the distance parcels of melt travel in the fireball before quenching is small (see Izrael, Ch 1, p. 10) [10]. Izrael uses this claim to justify the assumption of neglecting turbulence and other motion and calculating formation using Brownian motion alone. This hypothesis would predict that molten materials that agglomerated would experience similar vapor environments, and thus likely incorporate similar amounts of material from the vapor term (still being dependent on the curvature of the parcel of melt, the miscibility of vaporized species onto the melt, the composition of the different melts, etc.).

Goals of this study

The goal of this study is to characterize and compare the major element and U isotopic composition of agglomerates and the objects they are attached to (the hosts) to determine if (a) the frequency and size of agglomerates is significant enough to appreciably alter the major element or radionuclide composition of millimeter-scale glassy fallout samples, (b) if agglomerates and hosts are likely derived from similar starting melts, and therefore, are likely formed in a similar manner to hosts, and (c) if they have consistently incorporated a significantly different amount of enriched U from the vapor term of the fireball, suggesting they experienced a significantly different fireball environment prior to agglomerating.

Small agglomerates may be created in several ways. First, they may originate as smaller parcels of melt that were lofted into the fireball sooner and had more intimate and longer

contact with the fireball, leading to a greater incorporation of material from the vapor term. If this were the case, and based on their smaller radii and higher surface area to volume ratio, they may show evidence having been more thoroughly heated and could possibly exhibit some volatile loss (measured through a relative depletion in the alkali oxides) and/or have more thoroughly mixed material in the vapor phase compared to larger objects. In addition, if U behaves with intermediate volatility in silicate surface bursts (as empirical data indicates), U would exhibit some enrichment in smaller agglomerates relative to the larger host objects they are attached to [47]. If smaller melts were lofted into the fireball sooner, they should have incorporated more U than larger glasses due to longer residence times in the fireball. Finally, following Glesston (1966), if the mean free path of melts is small while in the fireball, agglomerates would likely experience a similar fireball environment to their hosts, and therefore exhibit similar U isotope ratios [10].

Smaller agglomerates may also be formed by the break-up of larger parcels of melt. This can and should be expected given the turbulent currents these melts are expected to experience, which could shear larger particles into smaller particles, depending on their surface tension. In addition, many collisions between melts and solids in the fireball will not result in agglomeration, but could either result in no mass transfer or the break up of melts. If smaller agglomerates are formed in this way, particularly late in the fallout formation process, there should be little no difference in major element composition or U isotope ratio between agglomerates and hosts.

Thesis of this study

Agglomerates are likely formed through several different mechanisms: the melting of smaller soil grains, the breakup of larger melts due to fireball turbulence, and the condensation of primarily vapor phase material within the fireball. As a result, characterizing many agglomerates will likely show evidence for agglomerates formed through all of these mechanisms. Agglomerates formed from smaller size fractions of soil may have been lofted into the fireball earlier and therefore show some evidence for volatile loss or a persistently different composition than hosts formed from melts derived from larger size fraction soils and may incorporate more U from the fireball than hosts due to longer residence times in the fireball. Agglomerates formed from the breakup of larger melts will likely shown no significant differences in major element or U isotopic composition, unless they were formed from the mixture of molten soils of significantly different major element composition or incorporated U from a different part of the fireball which had a significantly different U content in the vapor phase prior to breaking up, colliding, and agglomerating with the host glass. Finally, agglomerates formed through a fundamentally process, such as condensation of primarily vapor phase material, should be rich in anthropogenic materials in addition to radionuclides, such as likely materials that may comprise the casing of a nuclear device such as Fe and Al, and enriched in unfissioned fuel relative to host glasses. Finally, the statement in Glesston (1966) regarding the mean free path of parcels of melt in the fireball is counterintuitive given the rapid expansion of the fireball, the expected high degrees of turbulence, and the timescale for cooling

(∼s), so agglomerates that have frequently incorporated a different amount of material from the vapor phase (*i.e.*, anthropogenic U) should be observed with some frequency [10].

In addition, given the relatively low frequency of observed agglomerates in recent studies (*e.g.*, [60, 68]) and in tektites, the natural analogues to glassy fallout formed when meteorites collide with the Earth, impact-melting large masses of soil (*e.g.*, [76]), agglomerates will likely not volumetrically comprise a large enough fraction of a fallout glass to appreciably alter either the major element or radiochemical composition of an entire sample when considered as a whole (*i.e.*, the measured major element or U isotopic composition of a bulk dissolved and analyzed glassy fallout sample).[15]

Scope of this study

This study characterizes agglomerates and host objects starting from an initial sample suite of 49 glassy fallout samples from a single, historic nuclear test whose fuel was highly enriched U. While previous studies of fallout from this test have focused on millimeter-scale fallout ([57, 60, 67–69, 84]), the samples studied here were selected from a range of sizes, from approximately 250 μm up to nearly 1 cm in dimension.

These 49 samples are characterized using optical microscopy, electron microscopy, and autoradiography before being downselected to characterize the hosts and agglomerates in a subset of samples. Of the 49 samples, 32 are downselected and characterized with elemental X-ray maps to identify agglomerates for further study. In 18 of these samples, the size, location, and frequency of agglomerates is measured. In 37 samples, the host composition is characterized using energy-dispersive X-ray spectroscopy (EDS) to determine the range of compositions spanned by the hosts. To compare these host compositions to agglomerates, the major element composition of 58 agglomerates in 15 samples is also characterized. To compare the U isotopic composition between hosts and agglomerates, U isotope ratios were measured in 18 host objects and 36 agglomerates in 13 samples using secondary ion mass spectrometry (SIMS). These analyses analyze microvolumes of material, having a spatial resolution of 10-30 μm, allowing for the characterization of U isotope ratios within small agglomerates. For this dataset, recent SIMS data from [60] and [67] in agglomerates and hosts was also used.

The major element composition of the SIMS analyses regions were measured using EDS rasters within/around the SIMS analysis to form a combined U/major element dataset. Due to the large number of elements measured, to compare agglomerates and hosts, these two datasets (the major element and U/major element dataset) were analyzed using the multivariate techniques of principal components analysis (PCA) and multidimensional scaling (MDS). PCA allows for the 2D visualization of many dimensional space and reveals correlations amongst different variables (major elements) that creates the variance in the compositional dataset. This technique is used to visualize not only correlations between

[15]This hypothesis comes from observations of whole glassy fallout pieces and earlier studies from Lewis et al. (2015) and Weisz (2016), that commonly do have smaller spherules attached to their exterior, but the size these spherules is typically small compared to the volume of the larger host glass [60, 67].

major elements but explore correlations between major elements and U isotopic enrichment, as has been repeatedly documented in the case of Pu's correlation with Ca, Mg, and Fe in fallout glass samples from Trinity [55, 66, 80]. Furthermore, PCA is used to compare the major element and U isotope/major element composition of hosts and agglomerates to determine whether agglomerates could plausibly be derived from a different starting material than hosts.

Multidimensional scaling is used to compare the similarity of entire objects (using the median composition of the agglomerates and hosts calculated from each of the two datasets) to determine how similar agglomerates are to hosts as a population. While multidimensional scaling is a model that projects the similarities of agglomerates from $\mathbf{R}^n$ down to two or three dimensions, the exact measure of similarity (the Euclidean distance in multivariate space) is used to calculate the compositional and U isotopic/compositional similarity directly to the hosts they are attached to, revealing how similar agglomerates are to *their* host objects considering only their major element composition and then their U isotopic/major element composition. This analyses highlights whether agglomerates and host objects in the same samples were likely formed from similar starting melts (through similarity analysis using only the major element composition dataset) and incorporated similar amounts of enriched U from the vapor term in the fireball (through a similarity analysis using the combined major element/U isotopic dataset).

Finally, to compare different agglomerates, the behavior of major elements across the different compositional interfaces identified between hosts and agglomerates was characterized using high resolution quantified EDS compositional maps and isotope ratio raster images from SIMS. These data are used to better understand the ambient environment in the fireball as agglomeration occurred and discuss possible formation hypotheses for the different types of compositional interfaces observed.

Outline of this study

Chapter 2 presents an initial characterization and survey of the 49 glassy fallout samples. It shows optical micrographs, electron micrographs, and autoradiographs for all 49 samples and highlights representative and unique features amongst the sample set. It presents the analytical plan, showing how samples were downselected and the subsequent analyses performed. It also discusses the representativeness of the downselected samples to the sample suite as a whole for both the samples downselected for further characterization with EDS and those downselected for further characterization by SIMS and EDS techniques.

Chapter 3 discusses agglomerates, how they are defined and how they are identified using different compositional interfaces, showing representative examples of agglomerates located in different regions of samples. The results from measuring the size, location, and frequency of agglomerates in 18 samples are given, showing how much area agglomerates occupy relative to host objects, the measured size distribution of identified agglomerates. Finally, detail as to how representative the agglomerates downselected for further characterization are relative to the agglomerates identified in the 18 samples is provided.

Chapter 4 discusses compositional measurements of fallout using EDS. The chapter details how EDS spectra are collected, processed, and quantified, and shows how compositional measurements across host objects and agglomerates were performed. It then discusses the collection of compositional measurements across 37 hosts ($n = 3,698$), comparing these results to bulk analyses of entirely dissolved and analyzed fallout samples, and the EDS measurements within 58 agglomerates from 15 samples ($n = 679$). Host object and agglomerate compositions are compared to compositions measured in unmelted soil collected proximate to ground zero and discusses the sources of variation and major element trends using bivariate plots. The chapter concludes by searching for volatile loss (through systematic depletions in alkali oxide compositions) in agglomerates and host objects based on their surface area to volume ratio.

Chapter 5 discusses the U isotopic measurements in fallout using SIMS. It discusses SIMS and mass spectrometry as a method, the different SIMS analytical campaigns spanning from 2012–2017, the different isotope ratios measured, and how the SIMS data are standardized to compare isotopic data between instruments collected over a five year span. A section is also dedicated to rastered isotope ratio images collected using the NanoSIMS (*e.g.*, a $^{235}U/^{30}Si$) of a 15 μm $\times$ 15 μm region in fallout). The collection of U isotope ratios is discussed, showing the full range of the $^{235}U/^{238}U$ ratio measured in fallout from this test. Next these data were separated into isotope ratio measurements performed in host objects and agglomerates and the statistics of the two populations are compared. Furthermore, the deviation of the U isotopic enrichment of the agglomerates relative to *their* hosts is presented to determine whether agglomerates statistically incorporated more or less enriched U than *their* host objects.

Chapter 6 then uses Principal Components Analysis to determine and analyze the major sources of variance in the dataset. It shows first how the compositions of the hosts, agglomerates, and unmelted soil compare, then uses the second combined U isotope/major element dataset to search for correlations between U isotope ratios and major elements. It highlights and discusses major element and U isotope outliers, showcasing how these affect perceived trends in the dataset. Similar to the previous two chapters, it highlights how the combined U isotope ratio/major element composition of agglomerates compares to their hosts, drawing conclusions about how similar agglomerates are to their hosts when considering the U isotope and major element composition from these analyzed regions collectively.

Chapter 7 uses the concept of compositional similarity (based on the Euclidean distance between objects in multidimensional compositional space, shorter distances implying objects are more similar) to compare the major element and combined U isotope ratio/major element composition of agglomerates and hosts (using the statistical median compositions as representing an entire agglomerate or host). These data are used to generate a 2D projection of all analyzed objects simultaneously using a method known as Multidimensional Scaling to show a single plot how the composition of agglomerates and hosts compare. Then, instead of applying on an approximate model, the exact Euclidean distance is between agglomerates and *their* host objects is calculated to show how similar agglomerates are to their particular hosts.

Chapter 8 uses high resolution EDS maps to characterize the behavior of major elements across the two different types of compositional interfaces identified in this study. One type, so-called in this dissertation "CaMgFe interfaces" was previously studied in detail by [68], who presents a possible scenario that leads to its formation. The other type, called "Si interfaces" here, have not been previously noted in the literature. These interfaces are analyzed in greater detail and a hypothesis about the environment in which they formed is presented by comparing glassy fallout to potential natural analogues known as chondrites.

Chapter 9 shows ion and isotope ratio images from NanoSIMS analyses over both CaMgFe and Si compositional interfaces. The NanoSIMS analyses over CaMgFe interfaces collected for this study are compared to the results of previous studies and the U isotopic behavior and the $^{235+238}U/^{30}Si$ and $^{235+238}U/^{42}Ca$ behavior across Si interfaces is presented and analyzed to determine the possible condensation conditions within the fireball when Si interfaces formed.

Chapter 10 summarizes the results from Chapters 2-9 and presents limitations of this study, hypotheses and future questions posed by this study, and possible avenues of future work that will lead to a more improved understanding of agglomeration and its role in fallout formation.

Chapter 2

Initial Characterization and Survey of Samples

2.1 Chapter overview

This study characterizes aerodynamic glassy fallout samples from an historic uranium-fueled U.S. nuclear test. Fallout from this event has been previously studied, but this study includes a greater range of sizes and morphologies previous studies, including a large number of agglomerates. Starting from 49 samples, which span in dimension ∼250 μm–7 mm, 37 samples were analyzed with EDS and 18 samples were analyzed with SIMS and EDS.

Previous studies have shown that compositional textures within samples preserve evidence of agglomeration. The compositional interfaces imply agglomerates are distinct objects, with their own major element compositions, U isotope compositions, and histories within the fireball prior to agglomeration with the host. By studying agglomerates, this study expands the dimensions of analyzed glassy fallout samples characterized by modern techniques to as low as 17 μm.

2.2 Previous characterization studies

Fallout from this same test has previously been analyzed by Eppich et al. (2014), Lewis et al. (2015), Weisz et al. (2017, 2018), and others, as discussed in Chapter 1. These studies characterized glassy fallout samples with diameters ∼1 mm exhibiting "aerodynamic" morphologies, (*i.e.*, highly symmetric, often being oblong or nearly-spherical glassy materials).

Previous studies have been limited to a narrow size range, and either dissolved whole samples or used spatially-resolved techniques to characterize a limited number of samples. Despite focusing on limited size ranges, previous observations have nonetheless advanced the understanding of fallout formation, timescales of closure, and chemical speciation in the fireball. Collections of glassy fallout from this test expand previous studies, and contain samples ranging in dimension from 250 μm to nearly 1 cm in scale.

Eppich et al. (2014) performed bulk dissolution of 22 glassy fallout samples ranging in mass from 7.1 to 35.6 mg and reported measurements major and trace element concentrations, as well as isotope ratios of U, Th, and Pa. They reported a wide range in measured U isotope ratios, from $^{235}U/^{238}U = 2.321 \pm 0.003$ to 7.725 ± 0.008. The morphologies of their samples were broadly characterized as either being quasi-spherical or oblong. Their study found no bulk compositional difference between the two morphologies, however they noted that their oblong samples exhibited a higher frequency of agglomeration on their surface compared to the quasi-spherical samples. These observations suggested that agglomerates and their hosts are neither chemically nor isotopically distinct.

Looking at similar samples, Lewis et al. (2015) used spatially-resolved analytical techniques to characterize the U isotope heterogeneity and major element composition within individual pieces of glassy fallout [60]. The five samples of glassy fallout from this study (samples U1A, U1B, U2, U3, and U4) were quasi-spherical in morphology and ranged in mass from 2.5 to 14.8 mg (Table 2.1). SIMS measurements within these five samples showed that the $^{235}U/^{238}U$ ratio spans nearly three orders of magnitude between the samples ($0.02 < ^{235}U/^{238}U < 11.81$) and greater than a factor of 350 within a single sample ($0.02 < ^{235}U/^{238}U < 7.41$). In the suite of five samples, three trends were noted: in two samples, U isotopes were generally homogeneously distributed; in two samples U isotopes were co-located with distinct compositional regions; in the final sample U isotopes were heterogeneously distributed with no apparent trend in major element composition. Although intriguing, the prevalence of these isotopic and compositional trends in fallout remains unknown. This was the first study of its kind, but was limited by a small sample set, uniform morphology, and limited range in sample dimensions.

In a further spatially-resolved study, Weisz et al. (2017) characterized the U isotope ratio and major element behavior between agglomerates and host glasses in four samples of glassy fallout from the same event (samples AA.B, AE.C, AG.D, and AH.E; Table 2.1). The Weisz samples were oblong glasses selected because they exhibited small agglomerates adhered to their surfaces. The study found that these agglomerates retain a distinct compositional interface between themselves and the host objects they are attached to. Seven of the nine characterized interfaces were enriched in $^{235}U/^{30}Si$ (used as a proxy for U concentration), ^{235}U, and the major elements Fe, Ca, Mg, Na, and K. They interpreted these interfaces as a late-stage deposition layer from the vapor phase of the fireball that occurred just prior to agglomeration. This indicates that the agglomerates and their host glasses retain their distinct major element and isotopic compositions, preserving individual thermal and chemical histories related to interactions with the fireball. This study, albeit of a limited sample set, was the first to observe these interfaces. While the study focused on interface enrichments, it did not compare host and agglomerate compositions, and therefore leaves unanswered how different the U isotopic and major element compositions are between the host object and agglomerate populations.

Historic studies of fallout documented occurrences of different types of glassy fallout, but primarily focused on fallout with limited dimensions and morphologies. Agglomerates appear to be a common feature in fallout from near-surface tests. Recent spatially-resolved

studies of glassy fallout suggest agglomerates and hosts retain their distinct compositions, which may be linked to their individual fireball histories. In addition, agglomerates provide access to a much smaller size range of fallout, allowing for a fuller picture of activity-size relationships than has been characterized in recent studies. The studies described above pose new questions, including:

- What is the prevalence and frequency of agglomerates in samples of different sizes?
- Is there evidence for agglomeration in the interiors of samples, or is this feature limited to sample surfaces?
- If agglomerates are preserved within samples, how do their compositional interfaces, size, and frequency compare to exterior agglomerates?
- Are agglomerates and hosts formed by similar processes?
- Have agglomerates and hosts incorporated similar amounts of material from the vapor phase of the fireball?

To address these questions, a larger and more diverse sample set was selected for this study (49 samples). One part of this sample suite includes samples from the Lewis and Weisz studies [60, 67]. Others are previously uncharacterized. Collectively, these samples and data will form a basis for a better understanding of the bulk incorporation of anthropogenic material into fallout by studying the source, frequency, and role of agglomeration in forming in fallout.

2.3 Sample suite and down-selection

The samples for this study comprise a population of 49 pieces of glassy fallout collected near a U-fueled near-surface nuclear test. All 49 samples were imaged using using backscatter optical microscopy, electron microscopy, and autoradiography (Figs. 2.12-2.19). Of the 49, five are samples that were also previously characterized using secondary ion mass spectrometry (SIMS), scanning electron microscopy (SEM), and electron probe microanalysis/wavelength-dispersive x-ray spectroscopy (EPMA/WDS) by Lewis et al. 2015 (samples U1A, U1B, U2, U3, and U4; [60]), four were characterized by Weisz et al. 2017 (samples AA.B, AE.C, AG.D, and AH.E; [67]) in their study of interfaces between glassy objects attached to hosts. Forty additional samples were selected from sieved fallout collections for this study.

Thirty-seven samples were downselected for further study and their chemical composition measured using energy-dispersive x-ray spectroscopy (EDS). Compositional and textural evidence for agglomeration was identified across the population. Agglomerates are observed in this sample suite adhered to the exterior of hosts, at the surface of hosts, and fully incorporated into hosts. Chemical compositions of 53 agglomerates were also characterized by EDS in 15 samples. To quantify and compare the U composition of hosts and agglomerates, 18

samples characterized by EDS were also characterized by SIMS. Within the set characterized by SIMS, 37 agglomerates in 13 samples were characterized for their U isotope composition. Figure 2.1 shows the selection of characterized samples, hosts, and agglomerates for EDS and SIMS analyses; Table 2.1 lists the studied samples and how they were characterized.

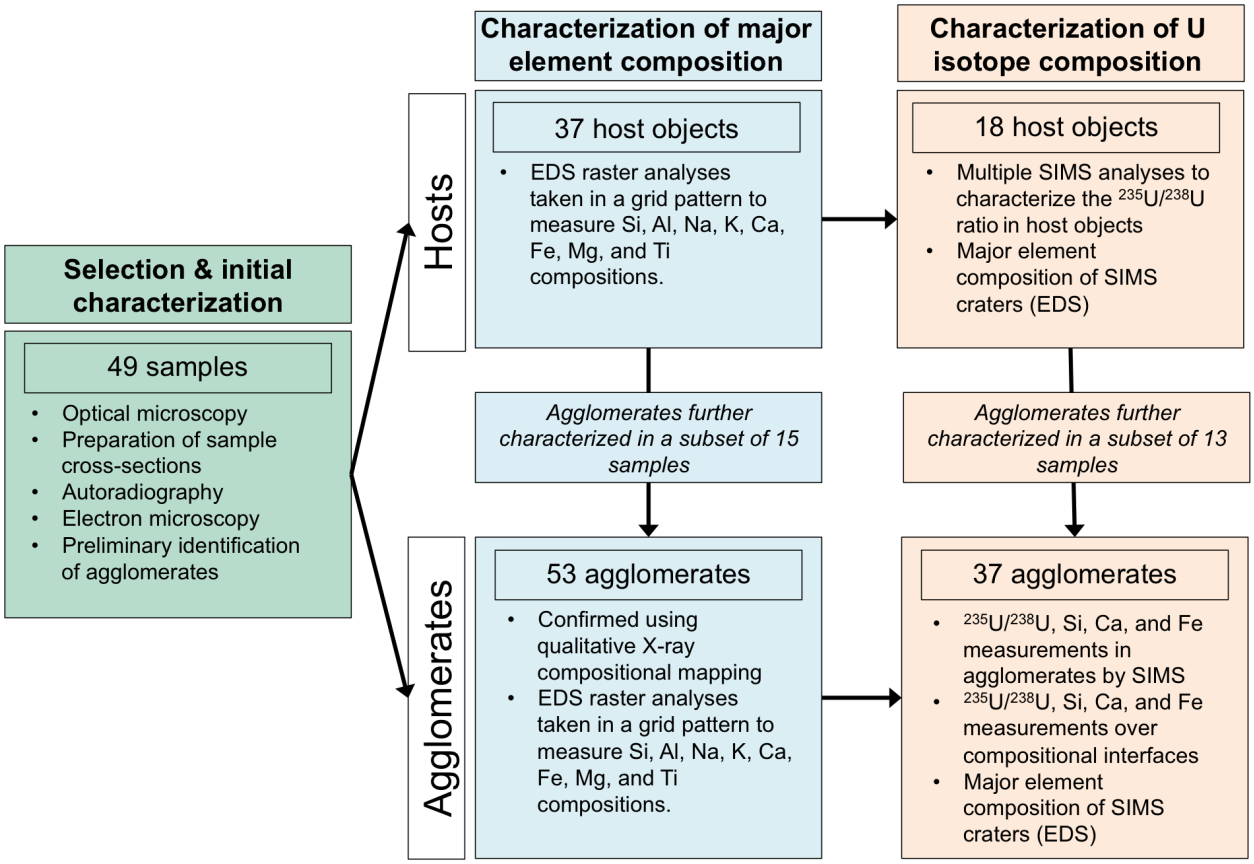

Figure 2.1: Initial characterization and down-selection of hosts objects and agglomerates for further analyses. Samples were characterized by a variety of methods including EDS (for major elements), SIMS (for $^{235}U/^{238}U$, $^{235}U/^{30}Si$, and $^{235}U/^{42}Ca$), and X-ray compositional mapping. For methods used to characterize each sample, see Table 2.1.

Table 2.1: Table of sample IDs, basic physical properties, peak activity (shown as the max pixel value from a 16 bit autoradiograph image; see Section 2.7), and analyses performed. Samples are sorted by their cross-sectional area. The * and ** superscripts denote samples also characterized by Weisz et al. (2017) and Lewis et al. (2015), respectively. Samples that were not massed prior to polishing are denoted with a "n.m." in the Mass column.

Sample ID	Mass (mg)	Cross-Sectional Area (μm^2)	Equiv. Diameter (mm)	Peak Activity (max pixel val.)	Host EDS Meas.	X-ray Compositional Maps	Host SIMS Meas.
FLD9	193.2	4.15E+07	7.27	56118	X	X	
FLD13	68.7	1.72E+07	4.68	44066	X	X	
FLD11	105.2	1.56E+07	4.46	53133	X		

FLD10	92.2	1.52E+07	4.40	47532	X	X	X
FLD12	45.6	8.07E+06	3.21	53443	X	X	
FLD14	27.9	6.54E+06	2.89	39243	X	X	X
AA.B*	16.5	6.24E+06	2.82	39243	X	X	X
FLD15	20.9	4.72E+06	2.45	43517	X	X	X
AG.D*	12.0	4.56E+06	2.41	51887	X	X	X
FLD7	n.m.	4.54E+06	2.40	52560			
U3**	14.8	4.41E+06	2.37	39050	X	X	X
FLD1	n.m.	4.20E+06	2.31	47031			
AH.E*	9.4	4.15E+06	2.30	50434	X		X
U4**	14.4	3.90E+06	2.23	45444	X	X	X
AE.C*	11.2	3.88E+06	2.22	44851	X	X	X
FLD17	11.6	3.88E+06	2.22	41302	X	X	X
FLD16	13.8	3.65E+06	2.16	49855	X	X	X
FLD20	13.9	3.36E+06	2.07	43464	X	X	X
FLD23	5.8	2.91E+06	1.92	38461	X	X	X
FLD18	11.7	2.61E+06	1.82	41580	X	X	X
CD	n.m.	2.60E+06	1.82	59381	X	X	
FLD21	6.6	2.50E+06	1.78	35256	X	X	
CC	n.m.	2.43E+06	1.76	65535	X	X	
U1A**	n.m.	1.97E+06	1.58	31230	X	X	X
U2**	4.5	1.86E+06	1.54	42067	X	X	X
FLD3.1	n.m.	1.83E+06	1.53	55464	X	X	
FLD3.3	n.m.	1.80E+06	1.51	47578	X		
FLD28	4.2	1.80E+06	1.51	39174		X	
FLD4.2	n.m.	1.73E+06	1.48	52523	X	X	
FLD4.3	n.m.	1.70E+06	1.47	54624	X	X	X
FLD4.1	n.m.	1.67E+06	1.46	41397	X	X	
FLD4.4	n.m.	1.58E+06	1.42	41422	X	X	
FLD3.2	n.m.	1.53E+06	1.40	32420	X		
FLD25	4.1	1.51E+06	1.39	32084	X	X	
U1B**	2.5	1.41E+06	1.34	46372	X	X	X
FLD2	n.m.	1.28E+06	1.28	32260			
FLD6.7	n.m.	9.55E+05	1.10	36787			
FLD5.3	n.m.	9.47E+05	1.10	35579	X		
FLD5.2	n.m.	9.45E+05	1.10	43533	X		
FLD5.5	n.m.	8.04E+05	1.01	44324	X	X	
FLD5.1	n.m.	7.74E+05	0.99	44539	X		
FLD5.4	n.m.	7.00E+05	0.94	41430	X	X	
FLD6.2	n.m.	6.43E+05	0.90	34703			
FLD6.8	n.m.	5.71E+05	0.85	29007			
FLD6.5	n.m.	1.88E+05	0.49	19199		X	
FLD6.3	n.m.	1.67E+05	0.46	25905		X	
FLD6.4	n.m.	1.44E+05	0.43	21014			
FLD6.6	n.m.	1.01E+05	0.36	23233			
FLD6.1	n.m.	6.21E+04	0.28	23025			

2.4 Sample collection and selection

All samples for this study, including those used in previous studies (*e.g.*, [60, 67]) were collected along the path of the fallout plume of an historic nuclear test. The collects were obtained from the upper 10 cm of sediment [57]. The collects of bulk soil and fallout were then sieved by size. These size-sorted mixtures of soil and fallout were then inspected under an optical microscope to manually separate fallout glasses from the soils. Fallout glasses are easily identified in soil collections by their vitreous luster and smooth morphologies. The

Figure 2.2: Photograph of typical sediment from near ground zero. The sediment includes fine clays and minerals as well as larger, centimeter-scale gravels and volcanic clasts. The dark, glossy objects visible in the image are fallout glasses. The blue object in the bottom left of the image is the cap of a Sharpie pen, shown for scale. In this image, irregularly-shaped fallout glasses tend to be larger than the more symmetric fallout glasses (such as those to the right of the pen cap).

sediments proximate to this test contain abundant volcanic lithics and the dominate minerals include quartz and feldspars (Fig. 2.2) [57].

Sample selection was motivated by several criteria. Samples U1A–U4 were five samples selected at random from two similar size fractions (selection described further in Lewis et al. (2015)). Samples AA.B, AE.C, AG.D, and AH.E were selected for this study primarily because they contain agglomerates and to build on prior work characterizing both the agglomerates and hosts with SIMS, SEM/EDS, and EPMA (previously studied by Weisz (2016) and Weisz et al. (2017)). The remaining 40 samples were selected from different size fractions to diversify the studied fallout population. With this population, glassy fallout ranging in equivalent diameter from 0.28 to 7.27 mm are included, with morphologies ranging from symmetric and near-spherical to highly asymmetric. These additional samples were chosen at random without regard to the presence or absence external agglomerates. Finally, several of the new samples were selected based on their relatively high specific activity, which is discussed more in Section 2.7. Measured masses range from 2.5 to 193.2 mg (Table 2.1), though several samples were not massed before being prepared for further analysis. Estimates of their masses is calculated from their exposed cross-sectional areas and discussed in the next section.

The optical images of the unpolished samples exhibit a range of morphologies, symmetry, and texture. Most samples are light to dark green in color, except for sample FLD25 (Fig. 2.5), which varies from translucent to a lightly opaque grey. The two previously studied

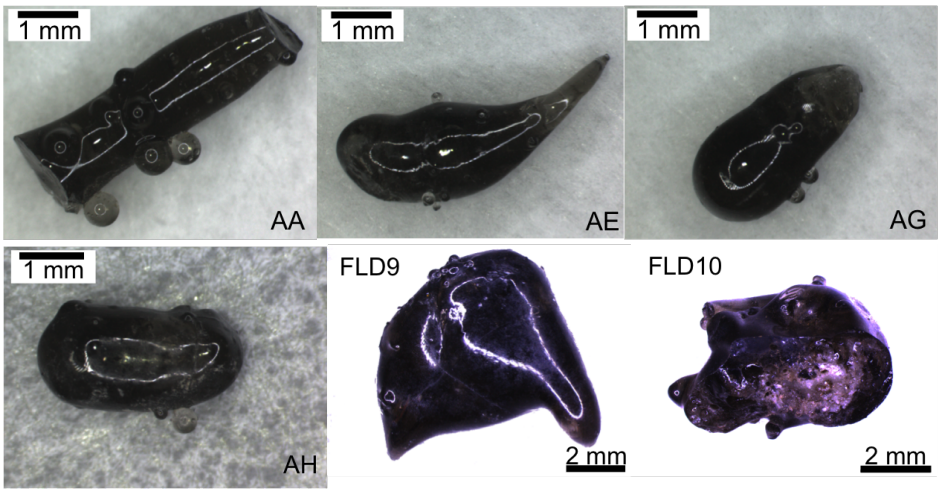

Figure 2.3: Optical micrographs of intact glassy fallout samples. Top image shows samples AA.B, AE.C, and AG.D and bottom image shows samples AH.E, FLD9, and FLD10. These samples are elongated and all exhibit some agglomerates preserved on their exteriors. Sample FLD10 is distinct because of the lighter rocky region at its surface. FLD9 is the largest studied sample at over 7 mm in length.

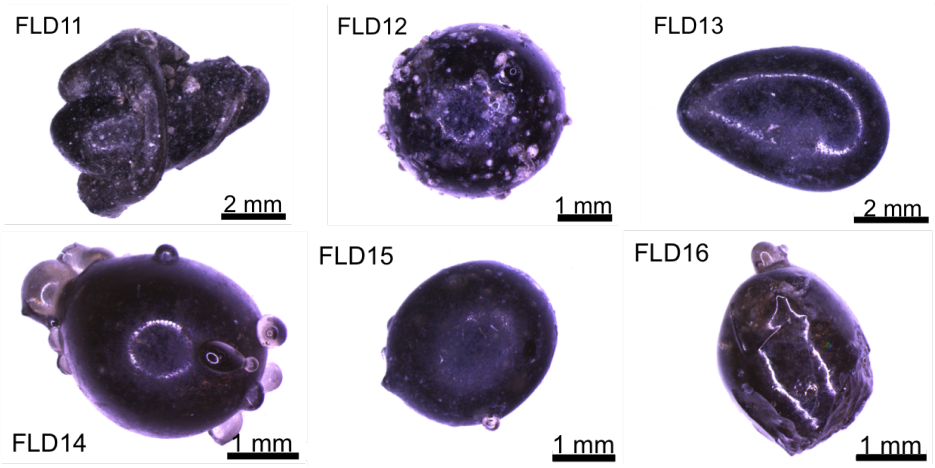

Figure 2.4: Optical micrographs of intact glassy fallout samples. Top image shows samples FLD11, FLD12, and FLD13 and bottom image shows samples FLD14, FLD15, and FLD16. FLD11 preserves evidence of the collision of multiple melts of similar dimension. FLD12 is notable for the preservation of unmelted dust and minerals surrounding its exterior.

morphologies, nearly-spherical and oblong are well represented (*e.g.*, samples AA.B, AE.C, AG.D, AH.E and samples FLD20, FLD28, U1A, U1B, U3, and U4, respectively). These samples, and most others, exhibit smooth exteriors. Counter examples include samples FLD10, which has an exposed rocky center (Fig. 2.20) and FLD16, which may have been cleaved from a larger piece of fallout glass (the cleaved surface visible at the bottom of FLD16

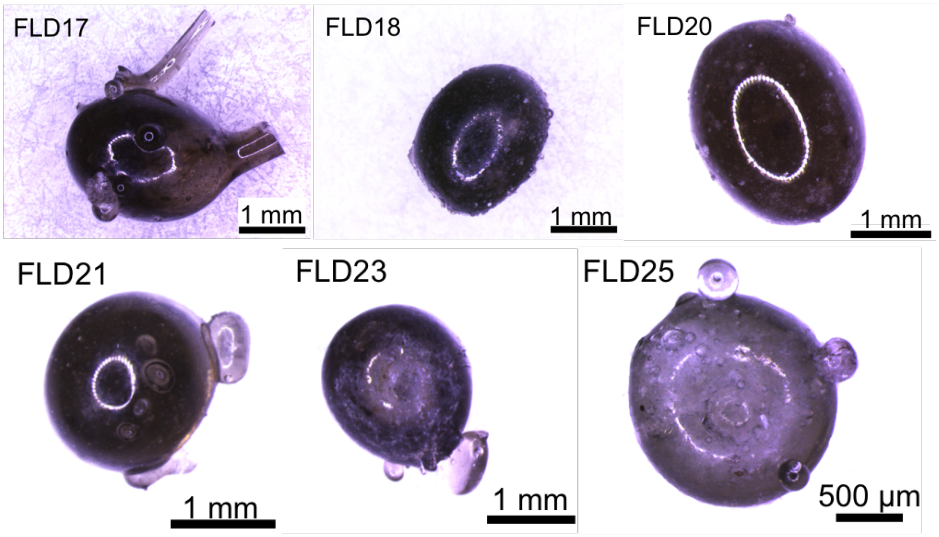

Figure 2.5: Optical micrographs of glassy fallout samples. Top image shows samples FLD17, FLD18, and FLD20, and U1A and bottom image shows samples FLD21, FLD23, and FLD25. These samples preserve agglomerates at their exterior. Sample FLD25 is much lighter in color (appearing grey) than the other samples (which tend to be darker and green hued). The surface of FLD18 is distinct as it appears matte instead of glossy (see also sample FLD15 in Fig. 2.4).

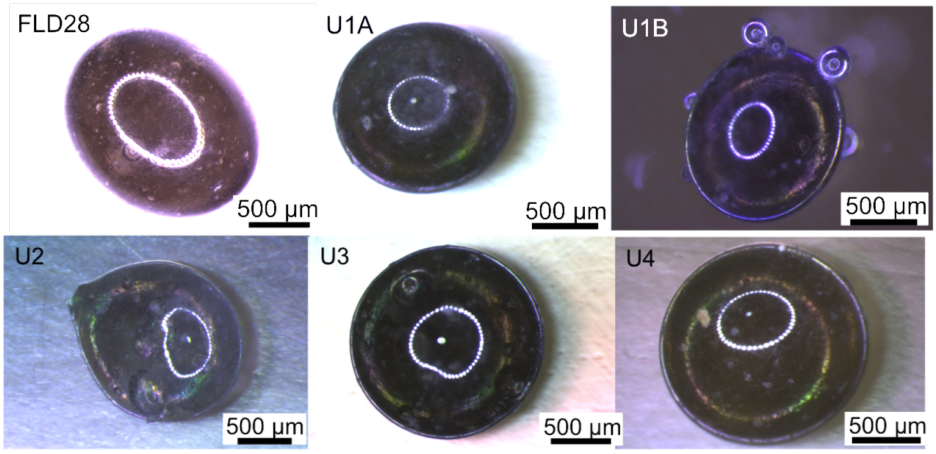

Figure 2.6: Optical micrographs of glassy fallout samples. Top image shows samples FLD28, U1A, and U1B and bottom image shows samples U2, U3, and U4. These samples are highly reflective and symmetric, as evidenced by the reflection of the optical microscope's ring lights visible on the surface of each sample.

in Fig. 2.4). The majority of samples have glossy exteriors with vitreous luster except for samples FLD11 and FLD12 (Fig. 2.3) where unmelted dust and minerals surround their exterior, dulling the surface, and samples FLD13, FLD15, and FLD18 (Figs. 2.4 and 2.5), where the surfaces are matte. Most samples have vesicles visible beneath their surfaces, and

several samples have dimpled centers (*e.g.*, samples FLD13, FLD23, and FLD25). Sample FLD13 is relatively flat, so the dimpled surface may be caused by the sample rotating while molten (axis of rotation being into the page), moving mass from the center toward the sample edges, flattening the sample and causing the dimpling. In contrast, the dimple in sample FLD23 is likely due to a large void at its center visible in its cross-section (Fig. 2.16). Similarly, sample FLD17 also has a large void observable in cross-section, but exhibited no surface dimpling on its exterior (contrast FLD17 in Figs. 2.5 and Fig. 2.15).

Most unpolished samples preserve visible agglomerates on their exteriors. Agglomerates on samples appear to have formed as distinct parcels of melt that collided with the larger, primary melt ("the host") just prior to quenching (Fig. 2.7). Most exterior agglomerates are nearly spherical, suggesting they solidified while still aloft and were close to solidification upon impacting the host melt (as many of the host objects are oblong). However, some agglomerates are oblong (*e.g.*, the agglomerates visible in the top right and bottom right of samples FLD21 and FLD23 in Figure 2.5) and some exhibit highly elongated, stretched features (*e.g.*, the two tail-like glassy features visible at the top and the right of sample FLD17 in Figure 2.5). In this sample population, agglomerates tend to be much smaller than their host object. One exception includes sample FLD11, which preserves the collision and accretion of least two similarly-sized melts, which have wrapped around one another (Figure 2.4).

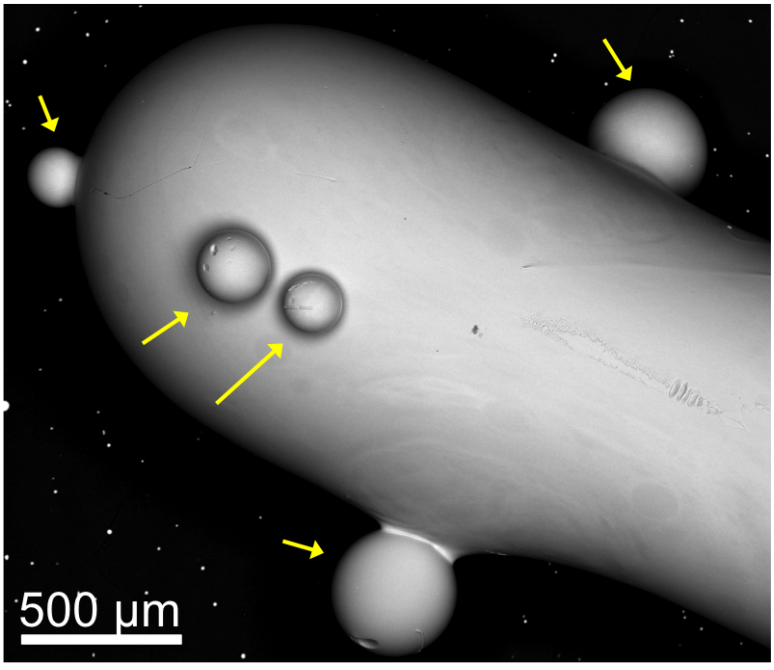

Figure 2.7: Backscatter electron image of unpolished aerodynamic fallout glass associated with the samples of this study. Agglomerates, or accretion features, are readily visible and denoted with yellow arrows. Image provided by J. Wilkinson. Sample was not included in this study.

Further characterization of the sample suite required the fallout glasses to be polished flat. Whole pieces of fallout were mounted in epoxy, which was then allowed to cure overnight in an 80°C oven. Next, to expose the interior of the samples at their approximate mid-plane, the mounted samples were successively polished with 240, 320, 400, 600, and then 800 grit sand paper. Final polishing used diamond polish pastes with average particle diameters of 6, 3, and 1 μm. In between each polishing step, samples were sonicated for 5 minutes and rinsed with ethanol to remove residual grit or polishing paste from the previous polishing step. After polishing, samples were placed in an an 80°C oven to drive off residual water.

Polished samples were sputter-coated with ~10 nm of carbon to conduct and dissipate excess charge during SEM and SIMS analyses (Fig. 2.8). Carbon is used as a conductive coating because its only characteristic X-ray, the 0.277 keV K_α X-ray, is low energy, so does not generally interfere with quantifying major elements of interest by EDS. Carbon does slightly interfere with the O 0.525 keV K_α X-ray (which is not used for quantification in this study), but the Na K_α X-ray is higher in energy (1.041 keV) and is resolved. While all conductive coatings attenuate X-rays to some degree, a carbon coating is the least attenuating, and at accelerating voltages above 10 keV and coating thicknesses below 15 nm it has a negligible effect on accuracy when quantifying chemical compositions [85].

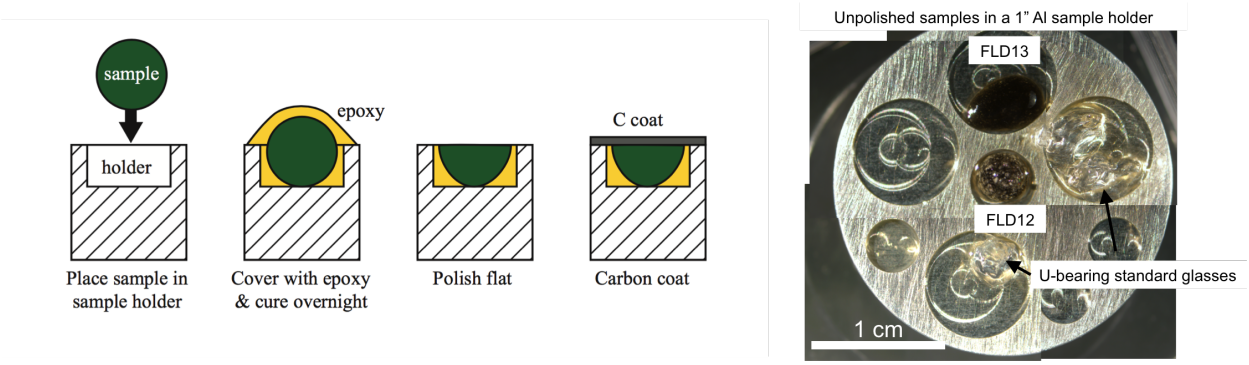

Figure 2.8: Schematic of mounting a sample in epoxy, polishing it to its approximate mid-plane, and coating it with a conductive layer of carbon (left). Sample holders are made of stainless steel or aluminum (photograph at right). The example image of a sample holder contains two unpolished samples, FLD12 and FLD13, and three unpolished U-bearing standard glasses that have been covered with epoxy and the epoxy cured overnight (the second step in the schematic on the left). The other machined holes are filled with epoxy but contain no samples or standards.

2.5 Physical characteristics

Samples massed prior to polishing range from 2.5 to 193.2 mg, but the lower limit of the mass range is likely even lower, as not all samples in the suite of 49 were massed prior to polishing. For example, sample FLD6.1 has the smallest exposed cross sectional area (6.21×10^4 μm^2) approximately 20 times lower than sample U1.B (2.5 mg, 1.41×10^6 μm^2). Assuming identical

densities and that their exposed cross-sections are through their mid-planes, sample FLD6.1 would have had an unpolished mass of approximately 0.5 mg.

The sample suite spans a large range of dimensions, best characterized through their cross-sectional areas. Cross-sectional areas were measured by tracing around electron micrographs of samples using ImageJ image processing software, with the scales adjusted individually for each image [86]. As a basis for inter-sample comparison, the equivalent diameter is used. By measuring the cross-sectional area (A) and approximating the samples as spheres, the radius (r) is calculated by solving for r in $A = \pi r^2$.

Using cross-sectional areas to calculate equivalent diameters of unpolished samples may not be a highly robust assumption. Cross-sections may not be polished to the exact mid-plane, and while these objects are generally symmetric, several samples are observed to be oblong (Figs. 2.3–2.6), so the orientation they were mounted into the epoxy matters. Not all of the glassy fallout samples exhibited highly symmetric shapes and smooth, glassy surfaces. For example, FLD3.2 (Fig. 2.17) and FLD10 (Fig. 2.13) contain large unmelted soil-like regions that indicate either they only experienced partial melting or they were partially coated with molten environmental material. The center regions of FLD9 and FLD11 (Fig 2.13) are highly vesiculated and are texturally similar to the center of FLD10.

Equivalent diameters are listed in Table 2.1. The largest sample, FLD9, has an equivalent diameter of 7.3 mm, while sample FLD6.1 has a diameter of just 0.3 mm (Fig. 2.9). Based on the measured mass data and using equivalent diameters to approximate sample volumes, samples exhibit fairly uniform densities, despite the variation in the frequency and size of voids (see optical images of polished samples in Figs. 2.12–2.19). The mean and standard deviation of the estimated densities (calculated from 23 samples, see Table 2.1) are 2.2 ± 0.6 g/cm^3 (1σ; ranging from 0.96 to 3.69 g/cm^3). These density estimates are similar to those observed in the sediments collected along with the fallout samples [57]. The sample with the lowest estimated density (FLD9, 0.96 g/cm^3) is also the largest sample and exhibits many exposed voids in cross-section. The sample with the next lowest density (FLD13, 1.28 g/cm^3) has few exposed voids. Sample FLD18 has the highest calculated density (3.69 g/cm^3) and also exhibits few voids in its cross-section.

2.6 Scanning electron microscopy

In scanning electron microscopy (SEM), the primary electron beam is scanned or rastered over the sample. The software forms an image by detecting electrons emitted from different interactions between the primary electron beam and the sample as a function of position. Generally, two types of electron emissions are detected: secondary electrons that best characterize the topography of a sample surface, and backscattered electrons that can be used to form qualitative images where differences in brightness reflect differences in the average composition of a sample.

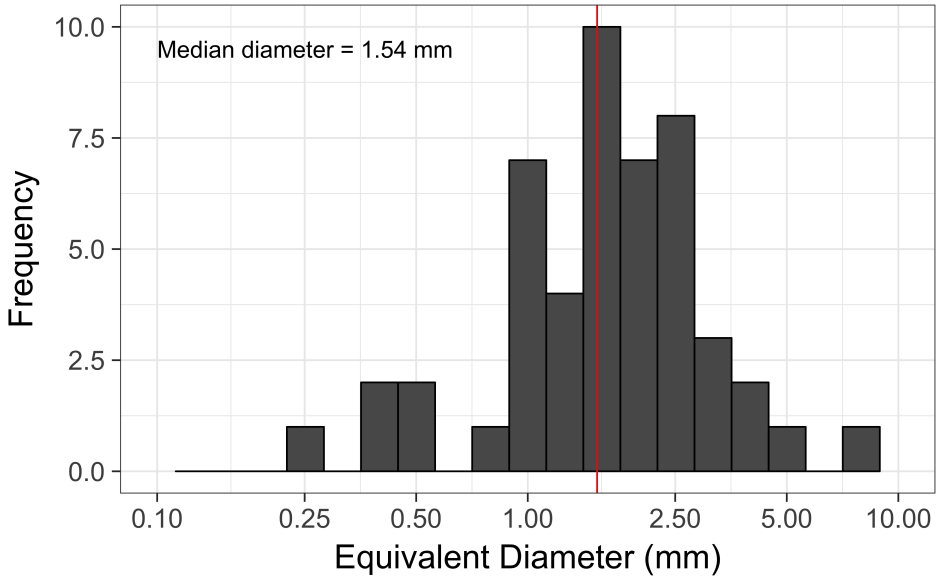

Figure 2.9: Log histogram of samples' equivalent diameters, calculated assuming the exposed cross-sectional area of the polished samples is circular. The vertical red line indicates the median diameter of the sample set. Due to the log x-axis, the histograms are of unequal width—there are 21 bins between 0.1 and 10 mm.

Secondary electron imaging

Secondary electrons are valence electrons that have received enough kinetic energy from inelastic scattering with the primary electron beam to be ejected from their bound orbits and leave the sample. They have low characteristics kinetic energies, on of the order of a few eV [87]. Because electrons quickly down-scatter in energy as they move through solid samples and require several eV of kinetic energy to overcome the material's work function and escape the sample surface, secondary electrons are only able to escape from the top few nanometers from the sample surface ($\sim$1 nm for metals and $\sim$10 nm for insulators) [87]. As a result, images formed from secondary electron emission emphasize the surface characteristics (morphology) of a sample.

Secondary electrons are detected with a scintillator-photomultiplier detector. Due to the low energies of secondary electrons, they are easily manipulated by small electric and magnetic fields, so the detector is placed on the side of the analysis chamber, surrounded by a mesh Faraday cage. The Faraday cage has a small applied bias to guide secondary electrons to it, but once secondary electrons pass the Faraday cage, they are accelerated to high energies by the large bias placed on the secondary electron detector, which allows the electrons to scintillate the detector material effectively [87]. The Faraday cage ensures the large bias on the detector does not affect the primary beam electrons or backscattered electrons.

Secondary electron images provide limited information for polished samples, primarily highlighting vesicles and cracks. In this study, secondary electron images are used to assess

damage to a sample's conductive coating and image unpolished samples.

Backscattered electron imaging

Backscattered electrons are primary beam electrons that enter the sample and are ejected back out from the sample with typically high energies, up to the energy of the primary beam (15 keV). Because of their high energy, backscattered electrons can be emitted from deeper in the sample, up to 100 times deeper than SE electrons (up to ∼100 nm for metals and ∼1 μm for insulators) [87]. Generally, backscattered electrons are ejected from the sample by multiple large-angle elastic scattering events of primary beam electrons off of nuclei. Nuclei with higher atomic number (Z) have stronger electric fields, which produce large-angle scattering events with primary beam electrons more frequently, increasing backscatter electron emission. The fraction of backscattered electrons relative the number of primary beam electrons goes approximately as $\ln(\bar{Z})$ (ranging from less than 0.1 for $\bar{Z} < 10$ to about 0.5 for $\bar{Z} > 90$). Different compositional regions can be distinguished with backscattered electron images if the differences in $\bar{Z}$ are large enough [87].

In this study, backscattered electron images are most frequently used to qualitatively characterize the gross compositional heterogeneity in polished sample cross-sections prior to compositional X-ray mapping of down-selected samples. Collection of a backscattered electron image takes seconds, while compositional X-ray maps may takes tens of hours to obtain statistically significant counts of characteristic X-rays per pixel (described below).

Because both secondary electrons and backscattered electrons are emitted with a cosine distribution from the sample surface, the greatest flux of both types of electrons is anti-parallel to the direction of the primary electron beam [87]. Because the secondary electron detector is placed on the side of the analysis chamber in the SEM used in this study (see below), this reserves the region above the sample for the backscattered electron detector, which is an annular semiconductor detector that snaps over the aperture of the primary beam optics system. As backscattered electrons enter the semiconductor, they dissipate their kinetic energy in scattering events with electrons in the semiconductor, many of which gain enough kinetic energy to move into the conduction band (3.76 eV band gap for Si), creating an electron-hole pair. Applied biases on either side of the detector collect the electrons and holes, creating a detectable signal, which is converted to a voltage, amplified, shaped, and processed by software's electronics and used to determine the intensity in each pixel in the image.

SEM operating conditions

An FEI Inspect-F Scanning Electron Microscope (SEM) is used for SE imaging, BSE imaging, and EDS measurements (both single analyses and compositional maps). The SEM is equipped with a semiconductor backscatter detector and scintillating secondary electron detector. Unless otherwise noted, all images were captured using an accelerating voltage of 15 kV and a spot size of 5.0 (∼1 nA primary e^- beam current). Pictures of larger samples

(>2.5 mm in diameter) were stitched together from several individual images collected using the same operating conditions.

2.7 Autoradiography

An autoradiograph predominantly records the distribution of β activity and near-surface α activity [60, 88]. However, given the low specific activity of U (present at ∼10 ppm in these samples), these radiographs are dominated by the β^- activity of long-lived fission and activation products [57]. ^{90}Sr and ^{137}Cs are the dominant sources of β^- activity in decades-old fallout and are likely the main contributors to the activities shown in Figure 2.10. As an example, note four U-bearing glass standards with no appreciable β-emitting radionuclides (with concentrations of approximately 50 ppm U and variable ^{235}U enrichment) highlighted with red circles in the autoradiograph (Fig. 2.10). The autoradiograph records no significant radioactivity in these synthetic glass standards.

To create the autoradiograph in Figure 2.10, the samples were placed onto a Fujifilm BAS-SR photo-phosphor imaging plate (IP) for 10 days inside a light-blocking tent. The IPs have a spatial resolution ∼50 μm. Because the linearity of the response of the film is not known, all 49 samples were imaged together on the same plate to allow for relative, qualitative comparisons of the activity distributions. After 10 days, the samples were removed from the film and the film was digitized using a GE Typhoon 7000 laser scanner with the photomultiplier tubes (PMTs) set to a voltage of 750 V, which scanned the plates with a resolution of 25 μm/pixel. The scanner reads the image plates at a higher resolution than the IP spatial resolution to ensure no information is lost when digitizing the film. The digitized images of the autoradiographs are output as images with a 16-bit depth, yielding a maximum pixel value of 65,535. After the first scan of the autoradiograph, the image contained several saturated pixels in samples with relatively high specific activity. Because the image on the IP is not completely removed by a single scan with laser scanner, another scan was performed using the same resolution and PMT voltage, which produced the autoradiograph shown in Figure 2.10, which contains no completely saturated pixels [88]. Autoradiographs are then processed with ImageJ image processing software [86].

In Figure 2.11, the peak pixel value within a sample is used as a proxy of a sample's overall activity. Mean pixel values are not presented because vesicles, heterogeneity of the distribution of activity, and diffusivity of the β particles prevent meaningful comparison. Larger samples appear more intense (darker) in the autoradiograph because the β particles have a relatively long mean free path (∼1 cm in silicate glasses), so there is little self-shielding. As a result, in semi-log space, maximum pixel intensity plotted as a function of equivalent diameter shows an approximately linear trend.

Despite the trend of larger samples appearing more intense simply due to greater mass, samples of similar dimension often exhibit greatly different activities. As examples, contrast sample U1A from U1B, sample FLD5.3 from FLD5.1, FLD5.2, FLD5.4, and FLD5.5, and FLD4.3 and FLD4.4 from FLD4.1 and FLD4.2 in Figure 2.10. Furthermore, several samples

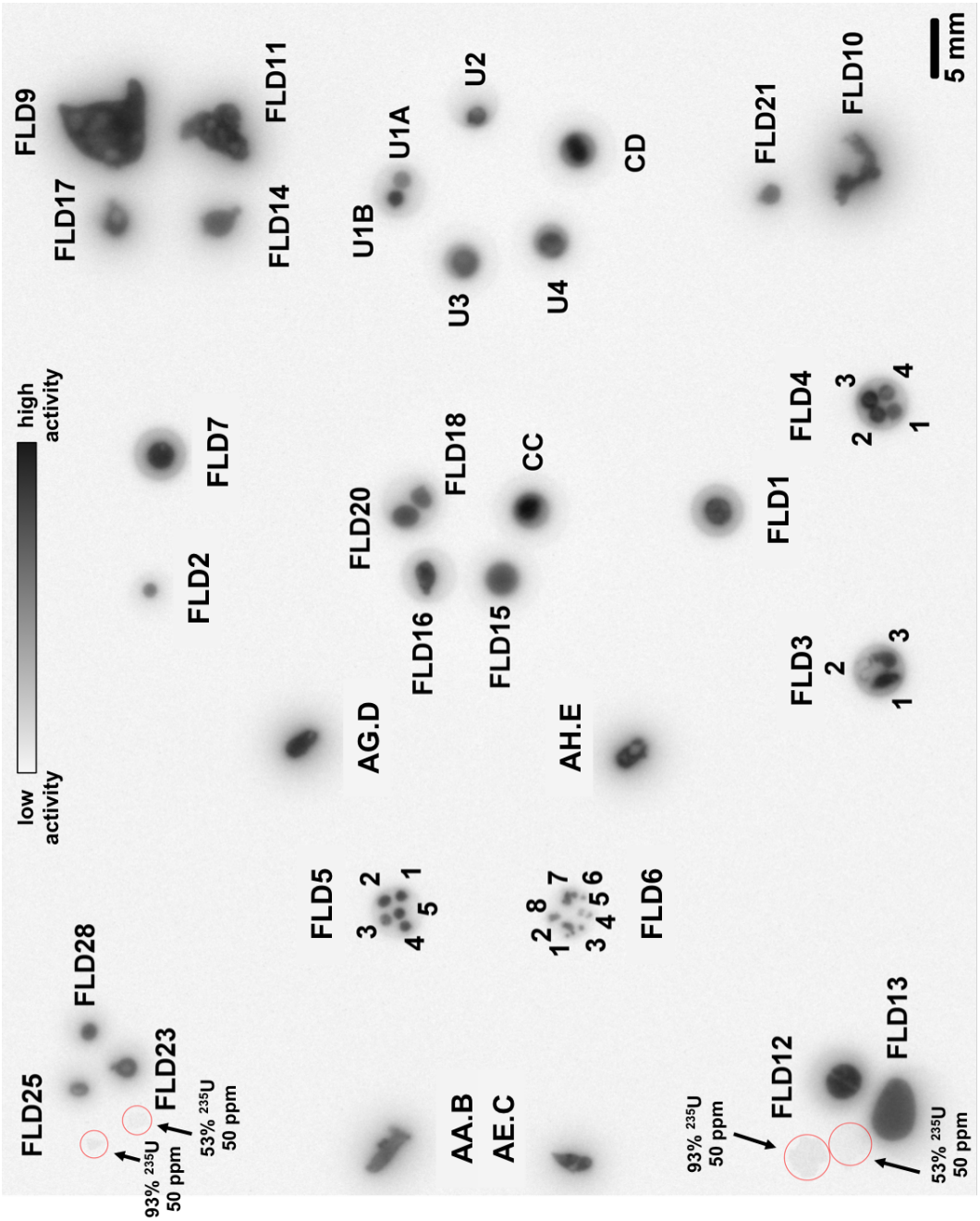

Figure 2.10: Autoradiograph of all 49 samples taken as a single exposure. Red circles denote four U-bearing glass standards, illustrating the radiograph is dominated by β^- activity in the fallout samples relative to the U (and other alpha-emitters) present at ≈10 ppm. The ^{235}U enrichment and U concentration for each of the standard glasses is noted.

exhibit high activity given their exposed cross-sectional area, such as (in decreasing order): CC, CD, FLD3.1, FLD4.3, and FLD4.2 (Fig. 2.11).

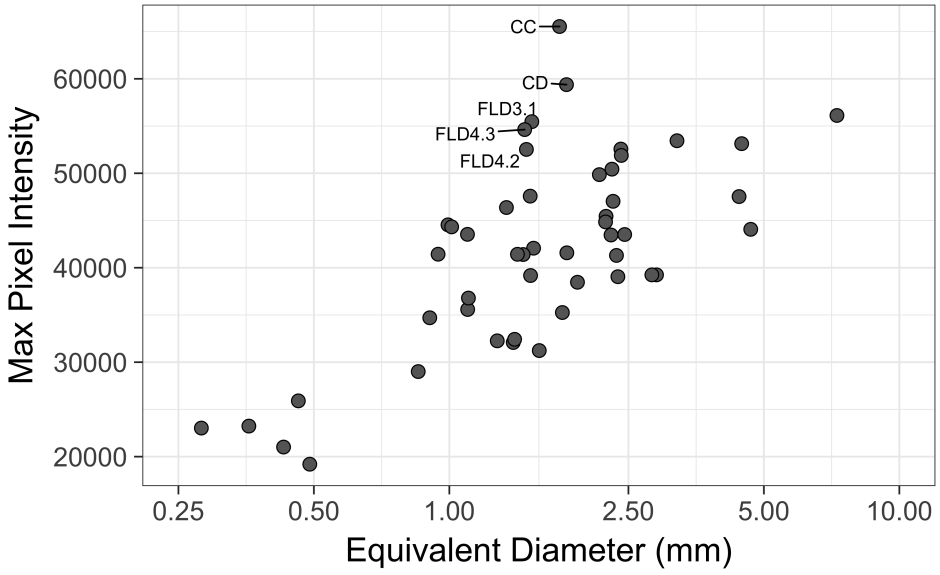

Figure 2.11: Maximum pixel value of the samples' autoradiographs as a function of their equivalent diameter (note the log x-axis), including vesicles and any unmelted regions in the samples. There is an approximately linear trend with sample size, likely due to a corresponding increase in sample thickness and the relatively long mean free path of the β particles in silicate glasses. The five samples that deviate from the approximately linear trend in semi-log space are marked.

All samples contain some activity, indicating all glasses incorporated bomb vapor and radionuclides from the vapor phase, but to varying degrees. Furthermore, the activity distributions *within* individual samples varies considerably. Qualitatively, individual samples within the sample suite exhibit both homogeneous and heterogeneous activity distributions. The likely causes of heterogeneous activity distributions is discussed in Section 2.8, where individual samples autoradiographs are compared to their optical and backscatter electron microscopy images.

2.8 Composite Images

Figures 2.12–2.19 show reflected light optical micrographs, BSE images, and false color autoradiographs for the polished cross-sections of all 49 samples. The optical micrographs highlight vesicles and cracks within the samples but otherwise reveal few topological features due to the high degree of polish required for SIMS and SEM analyses. Traverses of SIMS analyses are visible in the optical images of samples U1B, U2, and U3 as series of equally spaced analysis craters traversing the sample cross-section in a straight line (Fig. 2.19). BSE

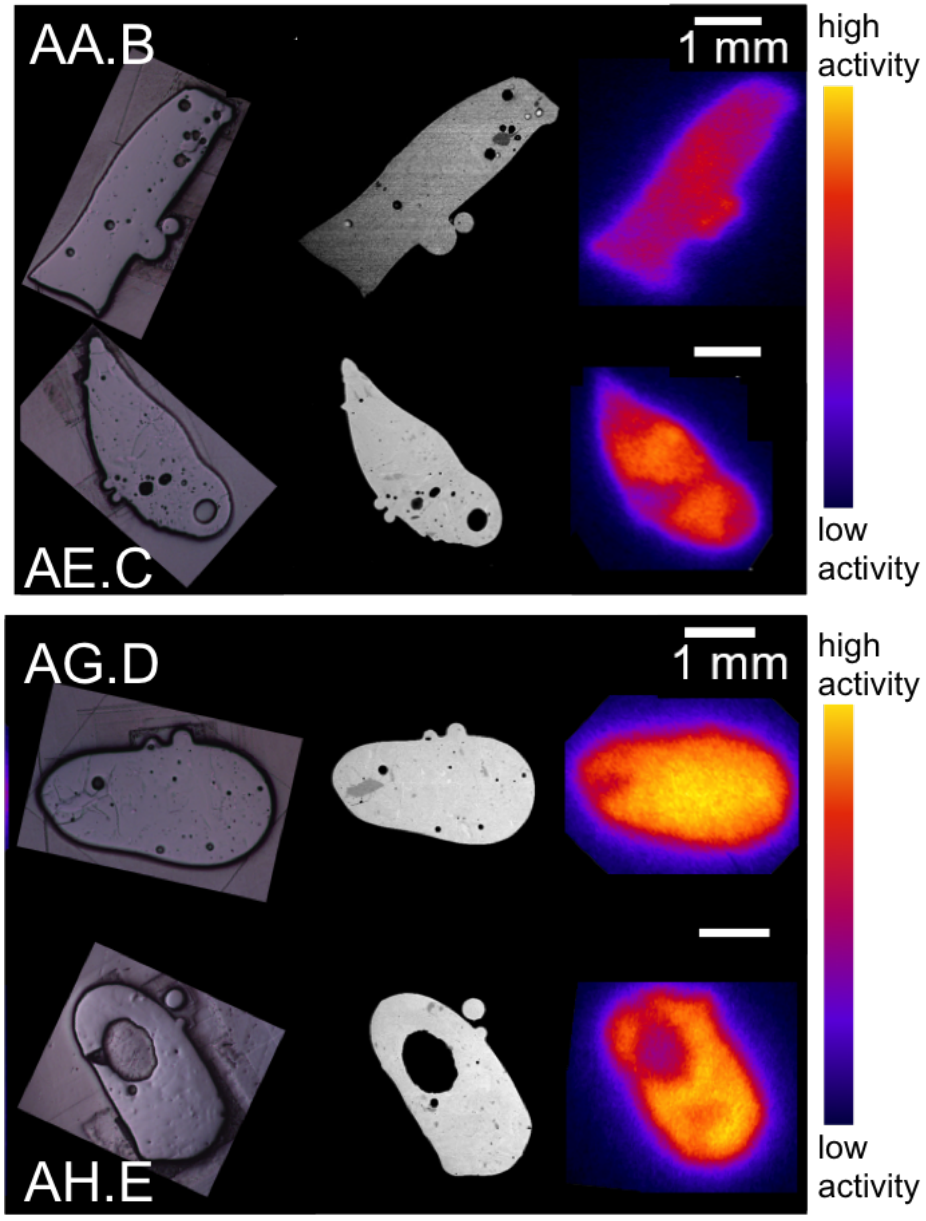

Figure 2.12: Optical micrographs, backscatter electron micrographs, and false color autoradiographs of samples AA.B, AE.C, AG.D, and AH.E (previously analyzed by Weisz et al. (2017)). These samples all contain evidence for exterior agglomerates. Sample AE.C has a highly heterogeneous activity distribution while the activity distribution in AG.D is fairly uniform except in the high silica region on the left hand side of the sample (dark grey shade). Sample AH.E contains a large void space near the center.

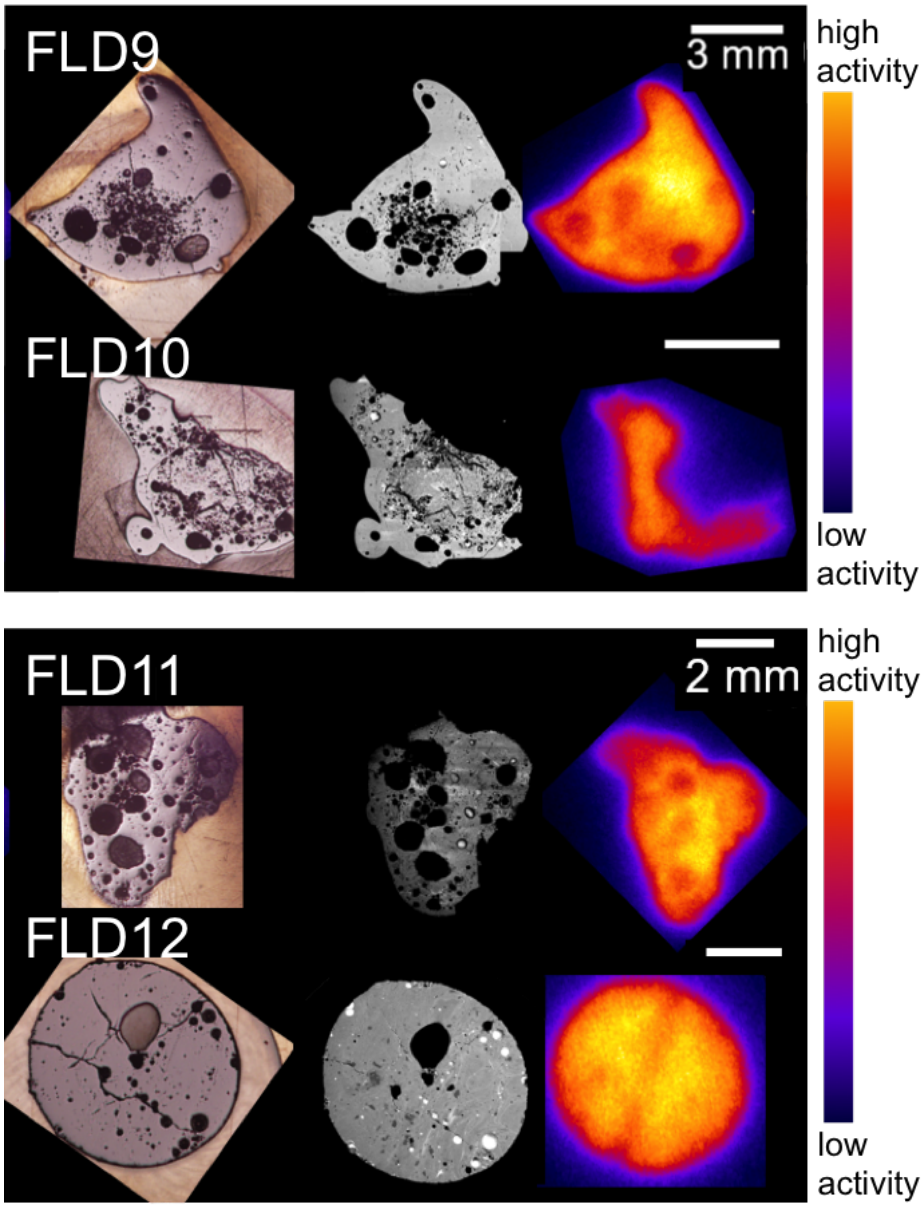

Figure 2.13: Optical micrographs, backscatter electron micrographs, and false color autoradiographs of samples FLD9, FLD10, FLD11, and FLD12. Samples FLD9, FLD10, and FLD11 are highly vesiculated and have irregular morphologies. A linear area of low activity in sample FLD12 the passes through the large center vesicle. Sample FLD10 has a large region that shows little to no radioactivity, corresponding to unmelted or partially-melted rock. The top right of sample FLD11 appears lower in activity due to partial coverage by epoxy.

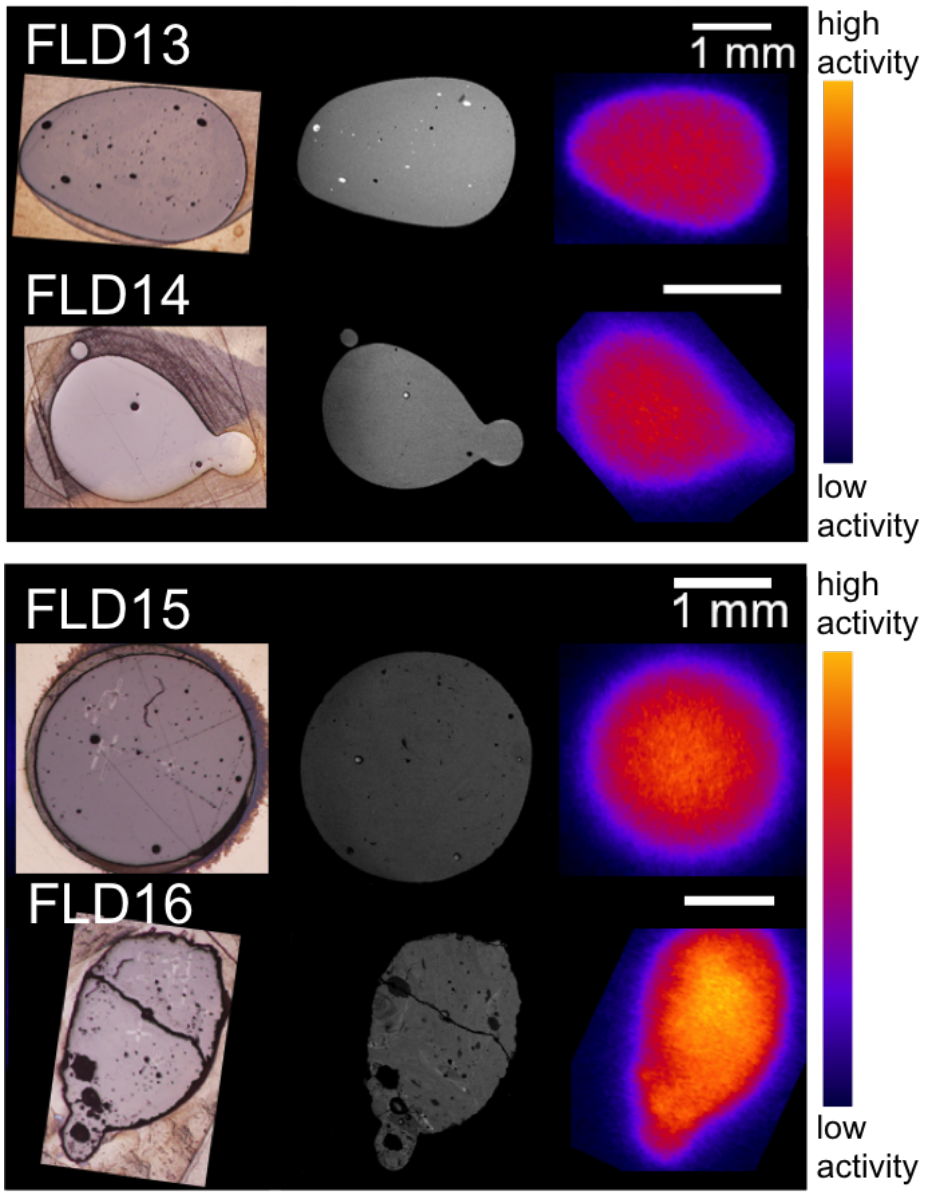

Figure 2.14: Optical micrographs, backscatter electron micrographs, and false color autoradiographs of samples FLD13, FLD14, FLD15, and FLD16. Samples FLD13, FLD14, and FLD15 have few vesicles and highly symmetric, smooth surfaces and homogeneous activity distributions. FLD16 retains irregular edges and several voids near one edge of the sample.

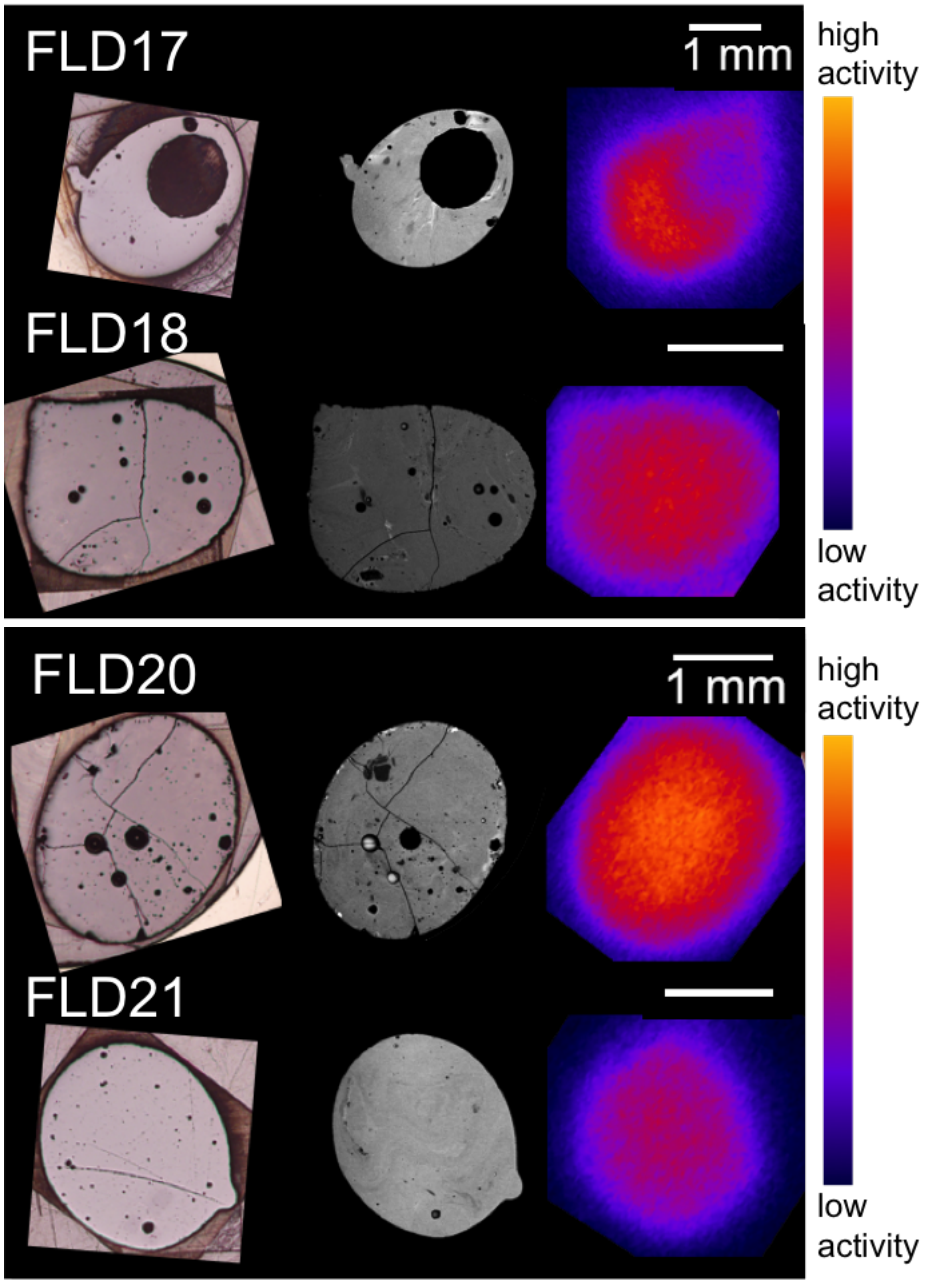

Figure 2.15: Optical micrographs, backscatter electron micrographs, and false color autoradiographs of samples FLD17, FLD18, FLD20, and FLD21. Sample FLD17 has a large void near its center, while samples FLD18, FLD20, and FLD21 have fewer, smaller voids distributed throughout their cross-section.

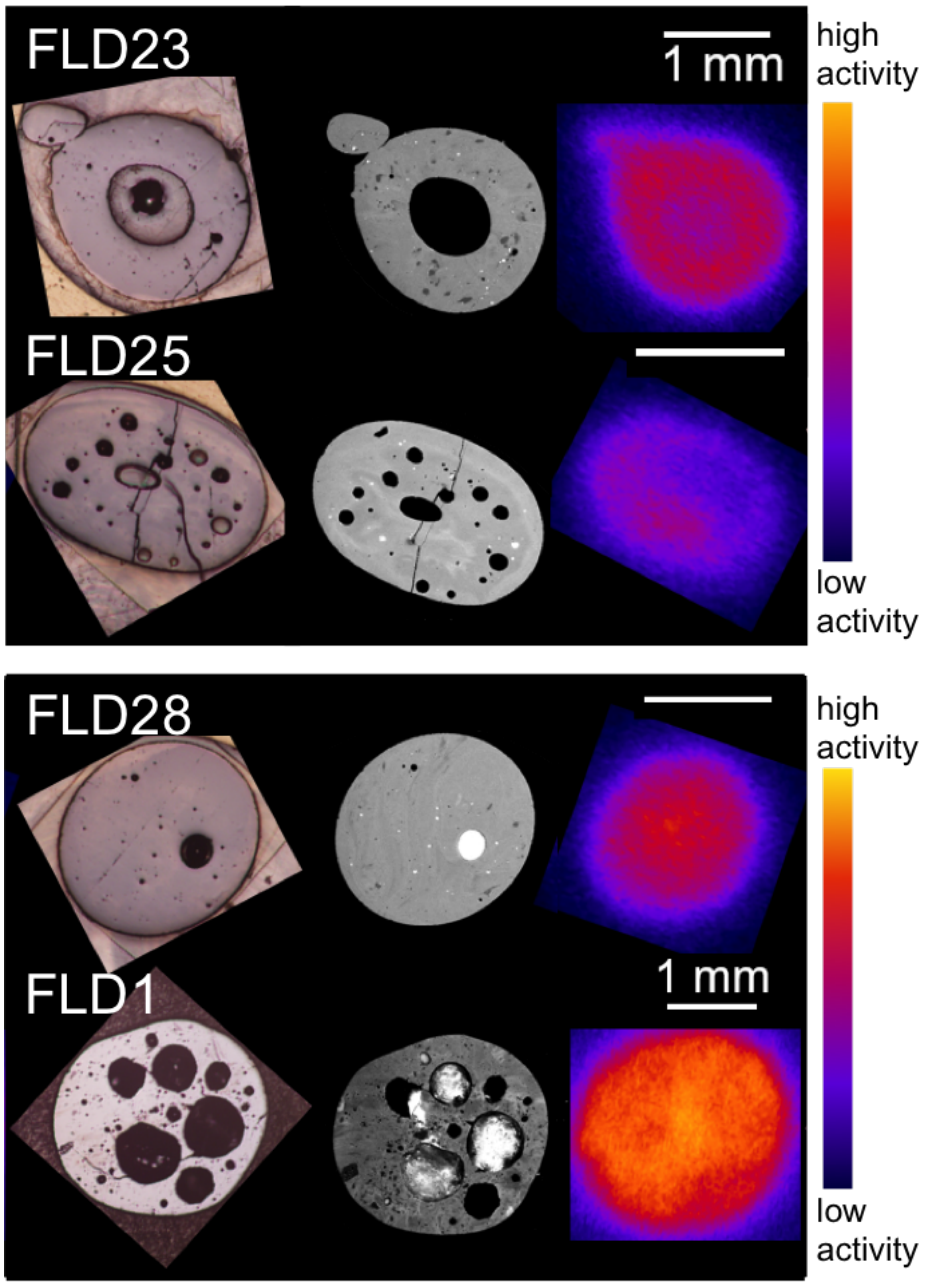

Figure 2.16: Optical micrographs, backscatter electron micrographs, and false color autoradiographs of samples FLD23, FLD25, FLD28 and FLD1. Sample FLD25 is the sample previously noted for its light, grey color and is relatively low in activity. Sample FLD23 has a large void at its center. In contrast, FLD21 has many large voids distributed throughout its cross-section. The bright regions in the BSE images of the void regions of FLD28 and FLD1 are due to charge build up during the SEM imaging.

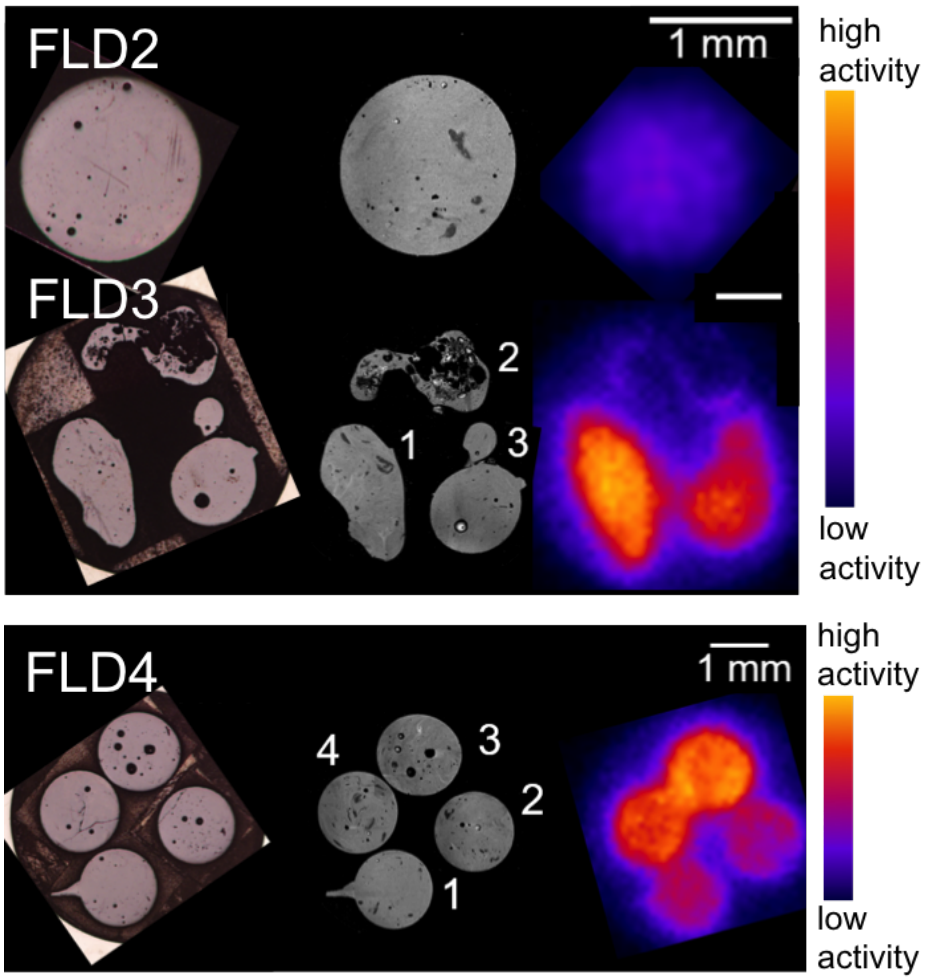

Figure 2.17: Optical micrographs, backscatter electron micrographs, and false color autoradiographs of samples FLD2–FLD4. The BSE image contrast for the three FLD3 samples (FLD3.1, FLD3.2, and FLD3.3) are comparable because they are in a single holder. Similarly, the backscatter contrast for the four FLD4 samples (FLD4.1, FLD4.2, FLD4.3, and FLD4.4) are comparable. Sample FLD3.2 contains a low to no activity region corresponding to a large, rocky area that is likely unmelted.

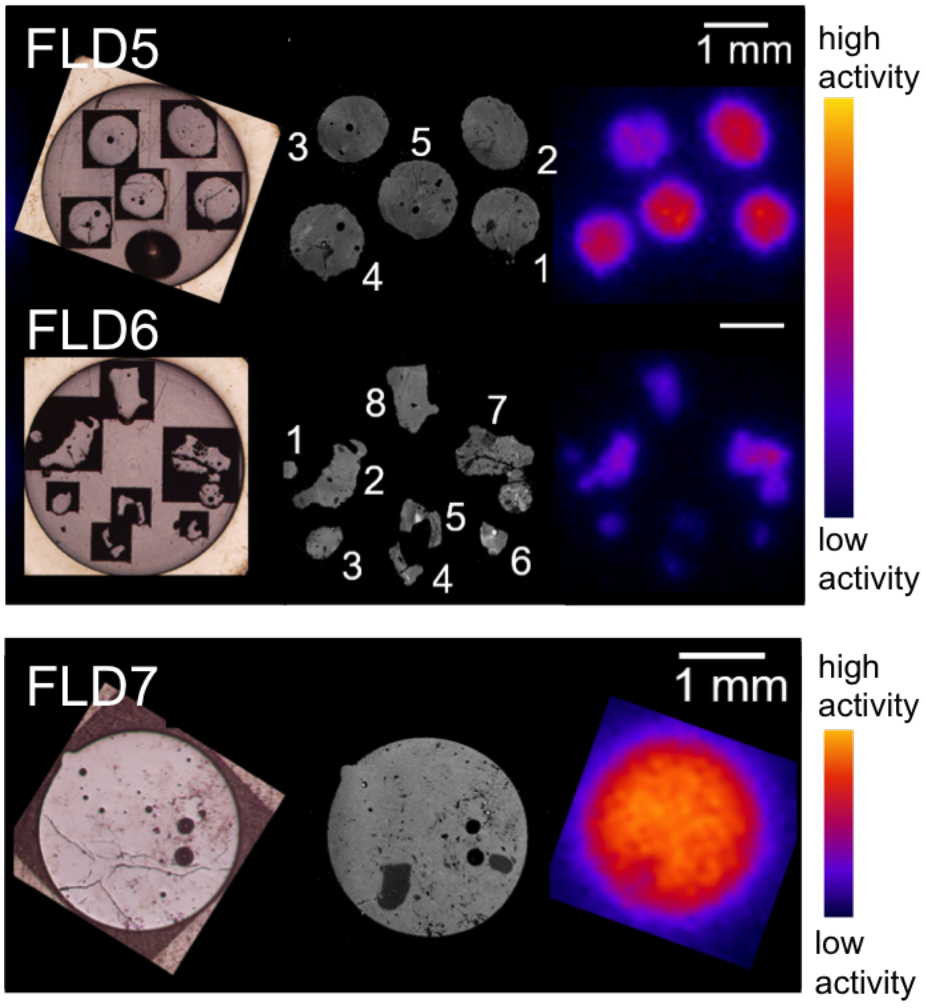

Figure 2.18: Optical micrographs, backscatter electron micrographs, and false color autoradiographs of samples FLD5, FLD6, and FLD7. The BSE image contrast for the five FLD5 samples are comparable because they are in a single holder. Similarly, the BSE image contrast for the six FLD6 samples are comparable. The FLD5 samples are approximate spheres while the FLD6 samples, the smallest individual samples characterized in this study, are irregularly shaped, except for FLD6.1, the smallest sample characterized.

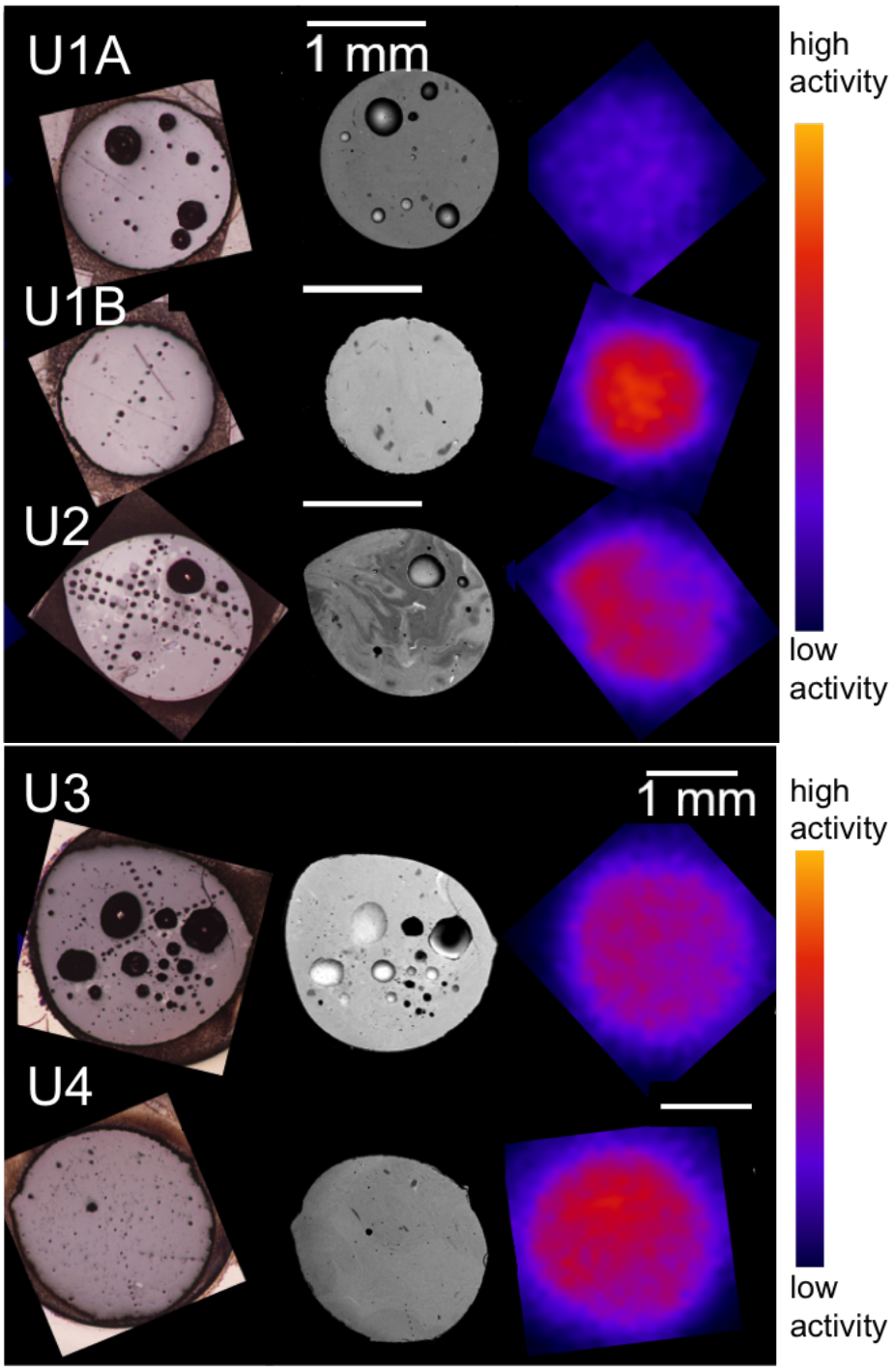

Figure 2.19: Optical micrographs, backscatter electron micrographs, and false color autoradiographs of samples U1A–U4. Traverses of SIMS analyses are visible as artifacts in the optical images. These samples were previously analyzed and are further described in Lewis et al. (2015).

images of samples highlight major element compositional variation. The brightness and contrast of the BSE images have been independently adjusted to highlight these compositional variations, so absolute inter-sample comparison of BSE images is not meaningful, even for samples in the same image, such as FLD3.1–FLD3.3, FLD4.1–FLD4.4, FLD5.1–FLD5.5, and FLD6.1–FLD6.8 (Figs. 2.17 and 2.18). Black, round features within samples are vesicles or voids, while dark grey, regularly-shaped regions are generally unmelted or partially-melted quartz grains, as evidenced by these regions incorporating little to no radioactivity, such as the dark polygonal region visible in the left region of the BSE image of sample AG.D and near the bottom of the BSE image of sample FLD7 (Figs. 2.12 and 2.18).

Comparison of the sample autoradiographs with their optical and backscattered electron micrographs show that some samples have active regions that are glassy and exhibit advective mixing patterns such as flow-banding, whereas the inactive regions are frequently rocky and/or vesicular. Two examples are samples FLD3.2 and FLD10 (Figs 2.17 and 2.13), which exhibit activity only in the glassy portion of their exposed cross section. To form such textures, active parcels of melt may have agglomerated onto the unmelted carrier materials. In these two samples, the glassy regions occur primarily at the periphery, so alternatively it is possible that heating from the fireball was sufficient to only partially melt the rock, and that only melted regions incorporated significant bomb vapor (Fig. 2.20). Autoradiography alone cannot distinguish between these two hypotheses.

At the smaller size scale ($\sim$100 μm), samples AA.B and AE.C have agglomerates attached to their exterior that exhibit differing activities (both higher and lower with respect to their hosts; Fig. 2.12). Previous study of these samples did not include autoradiography and these new data suggest that the agglomerates and hosts incorporated different amounts of fissionogenic radionuclides from the vapor phase. These examples are visible in the autoradiograph because the agglomerates are attached to the exterior of samples and can be distinguished based on morphology alone. The spatial resolution of the autoradiograph (50 μm/px) and the small physical size of many agglomerates prevent directly identifying smaller agglomerates with differing amounts of activity than the host sample. In Chapter 3, other methods including compositional X-ray mapping will be used to identify these smaller and/or interior agglomerates without knowing their activity relative to the host.

Homogeneous samples (*e.g.*, FLD13, FLD15, FLD20, and FLD4.1) tend to have few voids in their exposed cross section and appear compositionally quasi-uniform in their backscattered electron images (Figs. 2.14, 2.15, and 2.17). By comparing backscatter electron images to their autoradiographs, heterogeneous activity distributions generally correspond to large voids in exposed cross-sections (*e.g.*, AH.E, FLD9, FLD11, FLD17, and FLD23; Figs. 2.12, 2.13, 2.15, and 2.16) or large lower Z regions (later to confirmed to primarily be SiO_2 regions that were likely quartz grains that remained unmelted or were only partially melted). Examples include samples AG and FLD7 (Figs. 2.12 and 2.18).

Generally, samples that are homogeneous in the autoradiograph are compositionally homogeneous (see BSE images of samples FLD13, FLD14, and FLD15 in Figure 2.14). Heterogeneous activity distributions primarily correspond with voids or unmelted/partially-melted mineral regions in samples (examples include samples AG.D and FLD17 in Figs. 2.12 and

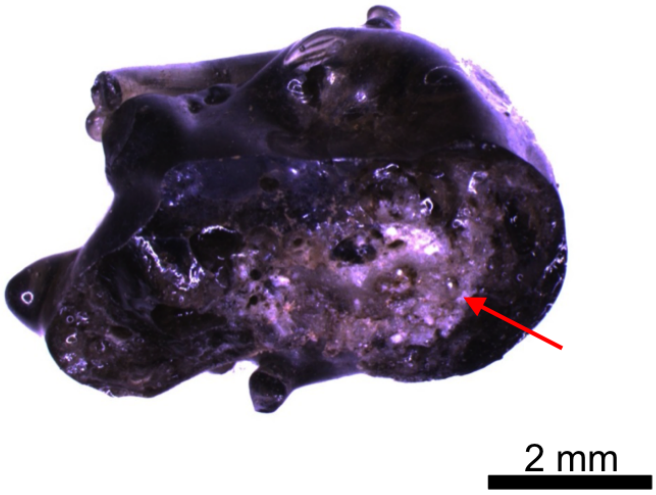

Figure 2.20: Sample FLD10 before polishing. Note the dark green, glassy exterior and lighter-colored, rocky interior (denoted with the arrow).

2.15, respectively). In some samples, activity distributions are co-located with compositionally distinct regions, including samples U2 and U4, consistent with observations originally discussed in Lewis et al. (2015). In Lewis et al (2015), these activity distributions were correlated with differing U content, which they concluded was due to the collision and accretion of melts of differing composition. While the radiography primarily records β emission, which serves as a qualitative proxy for the incorporation of bomb vapor, the relationship between the incorporation of anthropogenic U and chemical composition will be further investigated in Chapter 6.

There are several samples whose heterogeneous activity distributions are correlated with chemical composition, based qualitatively on differences in apparent brightness in their backscatter electron images (*e.g.*, FLD25, FLD4.2, FLD4.3, FLD4.4, U2, and U4; Figs. 2.12, 2.16, 2.17, and 2.19), revealing that bomb vapor was heterogeneously incorporated within several samples. In samples U2 and U4, SIMS analyses revealed that these regions of different activity also contained different U isotope compositions, indicating some of the compositional heterogeneities correlated with activity distributions are likely due to agglomeration of melts that interacted to different degrees with the bomb vapor prior to colliding in the fireball.

2.9 Sample down-selection and further characterization

The methods and analyses in this chapter provide information about the physical characteristics of these samples and the general characteristics about the sample population studied here. BSE images, in particular, highlight widespread occurrence of chemical heterogeneity. Further element-specific techniques are necessary to semi-quantitatively or quantitatively determine which elements responsible for these observed compositional variations. The BSE images also show that agglomerates attached to the exterior of samples preserve evidence of distinct compositional interfaces with the host objects. In order to confirm the composition of these interfaces and the relative and enrichment depletion of major elements at these interfaces, semi-quantitative X-ray mapping is used. X-ray mapping can also be used to locate and confirm the existence of other agglomerates within sample interiors that are not otherwise visible in BSE or optical images.

The autoradiography results reveal that many samples contain heterogeneous activity distributions. However, this technique has limited spatial resolution (50 μm/pixel) and is insufficient to characterize and compare activity-compositional relationships *within* the samples and with observed agglomeration textures. Mass spectrometry is therefore needed to measure the $^{235}U/^{238}U$ ratios within hosts and agglomerates. Here, U isotope data is used as a proxy to determine the differing degrees to which the hosts and agglomerates incorporate radionuclides such as U from the vapor phase. These data will elucidate formation processes and fireball histories of agglomerates relative to hosts.

EDS and SIMS are time-intensive methods optimized for small scale analyses ($\sim$10s–100s of microns). Accordingly, following the initial characterization and screening of the entire sample set, samples were down-selected for additional analyses (compositional X-ray mapping, characterization of major element composition using EDS, characterization of U isotope ratios using SIMS; Chapters 3–5). Samples were down-selected to best represent the sizes and morphologies present in the initial population of 49 glassy fallout samples. Select host glasses with diameters $\sim$0.1–1 mm were selected to allow comparison with much of the other data collected on fallout from this test (see Eppich et al. (2014) [57]). Similarly, samples with prior SIMS analyses were included to expand on previous characterizations presented in [60, 67, 68]. Table 2.1 denotes these samples; Figure 2.21 shows a histogram of their equivalent diameters plotted with the initial sample suite.

Figures 2.21 and 2.22 show the histogram of equivalent diameters of all 49 glassy fallout samples overlaid with the sample populations downselected for EDS analyses and EDS and SIMS analyses, respectively. These figures serve to show that both downselected populations are representative of the distribution of dimensions of the initial population of 49 samples. Of samples down-selected for EDS analyses, samples were further down-selected to measure their U isotope ratio compositions using SIMS. Table 2.1 denotes these samples; Fig. 2.22 shows a histogram of their equivalent diameters plotted with the initial sample suite.

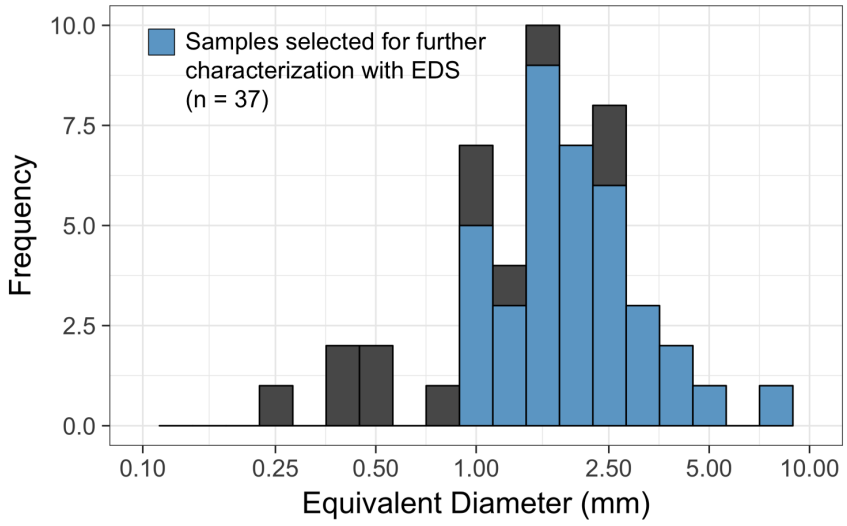

Figure 2.21: Histogram of the equivalent diameters of the initial suite of 49 glassy fallout samples (from Fig. 2.9) overlaid with samples downselected for further characterization by EDS (37 samples). Down-selected samples are approximately representative of the initial population of 49 samples.

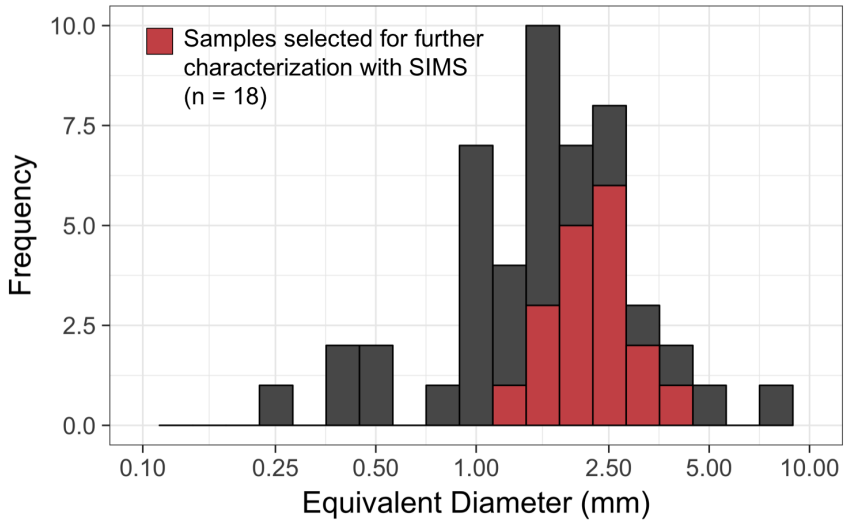

Figure 2.22: Histogram of the equivalent diameters of the initial suite of 49 glassy fallout samples (from Fig. 2.9) overlaid with samples downselected for further characterization by SIMS (18 samples). Downselected samples are approximately representative of the initial population of 49 samples.

2.10 Chapter summary

This chapter introduced the initial suite of 49 samples chosen for study (Table 2.1). While previous studies of fallout from this test have focused on millimeter-scale fallout, the samples

studied here were selected from a range of sizes, from approximately 250 μm up to nearly 1 cm in dimension. This population also captured fallout morphologies beyond nearly-spherical or oblong-shaped glasses, including more irregularly-shaped samples. Optical images of unpolished samples frequently show agglomerates attached to the exteriors of samples, regardless of morphology. In cross-section, agglomerates adhered to the exterior of samples are frequently observed in optical and BSE images.

Chemical heterogeneity is observed between samples, from relatively homogeneous to extremely heterogeneous, as evidenced by their BSE images (Figs. 2.12–2.19). Many samples contain large unmelted and partially-melted regions (as in the case of samples FLD10 and FLD3.2; Figs. 2.13 and 2.17). Autoradiographs of the samples highlight radionuclide incorporation from the bomb vapor and show a range in activity not only between samples, but within individual samples. In addition, agglomerates attached to their exterior of some samples contain different amounts of activity than the host samples they are attached to (*e.g.*, samples AA.B and AE.C; Fig. 2.12).

This chapter surveyed an initial suite of 49 samples using optical microscopy, electron microscopy, and autoradiography. Samples were then down-selected (Fig. 2.1) for additional characterization, ensuring the down-selected populations were representative of the initial sample suite by including samples covering the observed range of dimensions, chemical heterogeneity, total activity, and distribution of activity. Samples analyzed previously in with SIMS (from Lewis et al. (2015) and Weisz (2016)) were included in the down-selection.

While many agglomerates attached to the exterior of samples are readily identified by their morphology using BSE and optical imaging of polished sample cross-sections, agglomerates may also be fully incorporated into some samples and therefore difficult to identify. To identify the preserved population of agglomerates associated with these samples, X-ray compositional maps are needed. It is expected that X-ray compositional maps of entire samples will reveal more agglomerates than can be identified with BSE images alone. It is suspected that these agglomerates will not only be attached at the exterior of samples, but fully incorporated into some samples. If so, this suggests the host and agglomerate collided while the host was relatively molten and provide insight into the time and temperature of agglomeration.

Identifying agglomerates, counting their frequency, size, location of attachment (attached, surface, interior), and down-selected agglomerates for characterization by EDS and EDS and SIMS is discussed in the next chapter. In these down-selected samples, agglomerates will be identified and characterized and their major element and U isotope composition measured and compared to their hosts to better constrain the source and role of agglomerates in fallout formation.

Chapter 3

Agglomerates

3.1 Chapter overview

Agglomerates are distinct parcels of melt that collided with the larger primary or "host" melt in the fireball prior to quenching. They are commonly observed adhered to the exteriors of intact fallout glasses. In initial studies, agglomerates have been shown to preserve a compositional interface between themselves and the host, suggesting no mass transfer between the objects occurred [67, 68, 84]. Therefore, at least some agglomerates preserve their compositions, activity, and mixing patterns relative to the host. These objects are frequently much smaller than their host glasses (∼10-100s of μm), providing access to size fractions in historic fallout previously associated with larger fallout glass populations.

Due to their morphology, agglomerates attached to the exterior of samples are readily identified in BSE and optical images of fallout glasses in cross-section (Chapter 2). However, agglomeration during fallout formation is likely a continuous process, so long as the hosts remain molten. Accordingly, agglomerate textures may also be observed *within* hosts, representing earlier agglomeration events relative to exterior agglomerates.

In this chapter, compositional X-ray maps are used to definitively identify agglomerates preserved within host glasses. These X-ray maps reveal that, in addition to being adhered to the exterior of host objects ("exterior agglomerates"), agglomerates are also frequently preserved *within* samples. Agglomerates within samples are either bounded by a compositional interface and the sample surface (a "surface agglomerate"), or fully incorporated into the host and being fully bounded by a compositional interface (an "interior agglomerate") (Figure 3.1). BSE images were used to identify compositional interfaces between external agglomerates and hosts in Weisz et al. (2017). The broader study presented here finds that compositional interfaces of these objects are not always enriched high Z elements such as Ca, Mg, and Fe. Instead, surface and interior agglomerates more frequently exhibit a compositional interface only enriched in Si, which are difficult to definitively identify using BSE images alone because the average enrichment of Si interfaces relative to the host composition is only ∼10%, a relatively small change in composition relative to surrounding glassy regions

of the host or agglomerate.

Counting the size and frequency of these agglomerates in several samples shows that surface agglomerates occur most frequently in the population of exterior, surface, and interior agglomerates. Furthermore, agglomerates are observed to comprise up to ∼20% of the total exposed cross-sectional area of sample, with individual samples preserving between 0 and 58 identified agglomerates. In subsequent chapters, agglomerates are down-selected for further characterization with EDS and/or SIMS, with a subset chosen to span the range of observed sizes, attachment locations, and different observed compositional interfaces.

3.2 Defining and identifying agglomerates

Agglomerates are defined in this dissertation as smaller melts ("the agglomerate") that collided with a larger melt ("the host"). The combined melt then quickly quenches, preventing the two melts from mixing and the homogenizing. Exterior agglomerates are easily identified by their spherical or highly symmetric morphology when adhered to the exterior of fallout glasses and were first noted in historic studies of glassy fallout (Figure 2.7) [13]. These objects have also been observed and studied to some degree in tektites, where they are commonly referred to as collision or accretion features [76, 89–91]. However, agglomerates in the fallout studied in this dissertation not only appear attached to the exterior of samples, but also incorporated into their hosts, where they may be bound by the sample surface and a compositional interface separating them from the host. They also may occur fully subsumed into hosts and remain identifiable due to the preservation of compositional interface between themselves and the host.

In cross-section, preserved agglomerates retain a distinct compositional interface separating them from the host, which indicates that there has likely been little to no mass transfer between the two objects [68]. These compositional interfaces enable unambiguous identification of agglomerates, and are used as the criterion for identifying preserved agglomerates in this study. Interface-based identification of agglomerates is often supported by near-circular or semi-circular morphologies of the agglomerate as well as distinct compositions and/or mixing patterns within the agglomerate. Note, however, this approach to identifying agglomerates cannot identify agglomerates lacking compositional interfaces. One exception are some of the agglomerates counted in U4 (U4.1 and U4.3), which exhibit no measurable compositional change at the interface between themselves and the host. Instead, they exhibit circular and semi-circular shapes, distinct major element composition, and, as measured by SIMS and reported in Lewis et. al (2015), distinct enrichments in ^{235}U [60]. This implies these melts were distinct and separate in the fireball, each incorporating different amounts of U from the ambient environment, but agglomerated with the molten host while comparatively cool (preserving the circular shapes of the agglomerates) and quickly quenched. This prevented significant mass transfer between the two melts, either through diffusion or bulk mixing. Sample U2 also exhibits an approximately bimodal composition with a bimodal ^{235}U enrichment and no compositional interface between the two regions (Figure 1.11). When the

melts collided they must have been relatively molten, allowing partial mixing. As neither melt is much greater in area than the other, one cannot be definitively identified as the "host" and the other the "agglomerate", though agglomeration clearly occurred. One of these melts contains greater α/β^- radioactivity and enrichment in ^{235}U relative to the other, preserving their distinctive radionuclide compositions they acquired from the bomb vapor prior to agglomeration.

Weisz (2016) first noted the preservation of a compositional interface at agglomerate-host boundaries [67]. In Weisz (2016), most of the studied compositional interfaces were of agglomerates adhered to the exteriors of samples. These interfaces tend to be chemically enriched in Ca, Fe, and Mg, and isotopically enriched in ^{235}U, and chemically depleted in Al and Ti (Figure 1.9, Table 3.1). The compositional interface completely separating the agglomerate from the host implies that mass transfer between the two objects did not occur. In the limited sample set of Weisz (2016), the agglomerates also exhibited distinct compositions and mixing patterns from the host object. These results suggest agglomerates may also preserve a distinct radionuclide content from the host, providing a way to distinguish and constrain how different their formation processes may be from the host.

For the purpose of identifying agglomerates in this dissertation, objects were counted as agglomerates if and only if they were fully-enclosed by a well-defined compositional interface and exhibited a rounded shape. Figure 3.1 illustrates the nomenclature used in this dissertation and Figures 3.2–3.5 show examples of agglomerates in samples identified using the above criteria.

3.3 Attachment locations

Agglomerates are observed attached to the exterior of samples, residing at the surface of a sample (where they are bound by a compositional interface and the sample surface), or completely incorporated into a sample where they are completely bound by a compositional interface (exterior, surface, and interior agglomerates, respectively; Figure 3.1).

The transition from an "exterior" agglomerate to a "surface" agglomerate is continuous, as agglomerates vary from completely attached at the exterior (as those appearing in Figure 2.7), maintaining their spherical shapes, to slightly deforming the surface of the host melt upon impact, to greatly deforming the molten surface of the host melt. To distinguish between these objects, in this dissertation, an "exterior" agglomerate is defined as an agglomerate with 50% of its cross-sectional area above the boundary of the surface of the host if it were extrapolated over where the agglomerate is attached. A surface agglomerate is defined as one with less than 50% of its cross-sectional area above the boundary of the surface of host, but still bounded by the sample surface and its compositional interface with the host. Finally, an interior agglomerate is defined as an agglomerate completely encircled by a compositional interface (a schematic of these different agglomerate definitions is shown in Figure 3.1).

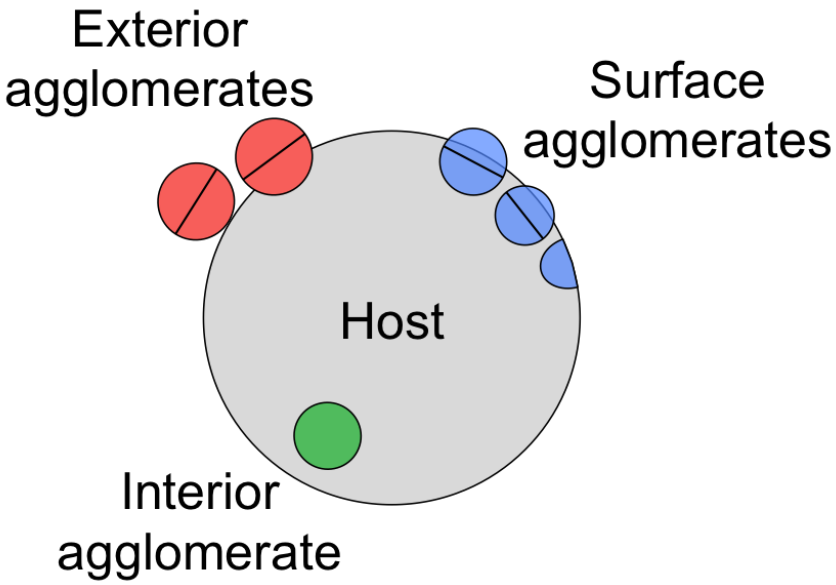

Figure 3.1: The assigned agglomerate nomenclature are defined in this dissertation, based on agglomeration attachment location. The horizontal line denotes 50% of the agglomerate's cross-sectional area, which is used to distinguish between "exterior" and "surface" agglomerates. Agglomerates with greater than 50% of their cross-sectional area outside the host are classified as exterior agglomerates.

3.4 The source of compositional interfaces enriched in Ca, Mg, Fe, and ^{235}U

Weisz studied compositional interfaces of exterior agglomerates enriched in Fe, Ca, Mg, and ^{235}U (called "CaMgFe interfaces" herein). These interfaces are likely not the primary source of uranium enrichment observed in all U isotopic measurements of these glassy fallout samples, because these agglomerates fuse to the host when both melts are highly viscous, so anthropogenic U has little time to be incorporated volumetrically [57, 60, 67]. Table 3.1 shows how frequently each species was enriched and depleted at the interfaces they studied [68]. The enrichment of these species was interpreted by Weisz as a vapor deposition layer that coated the agglomerates and was preserved as the agglomerates fused to the samples near the quenching temperature [67]. Most agglomerates fused to the exterior of samples and several agglomerates that reside at the surface of samples show this type of CaMgFe enrichment and Al depletion behavior (Figure 3.6 shows an example of the enrichment of Ca and Fe and depletion of Al across the interface of an exterior agglomerate studied in this dissertation).

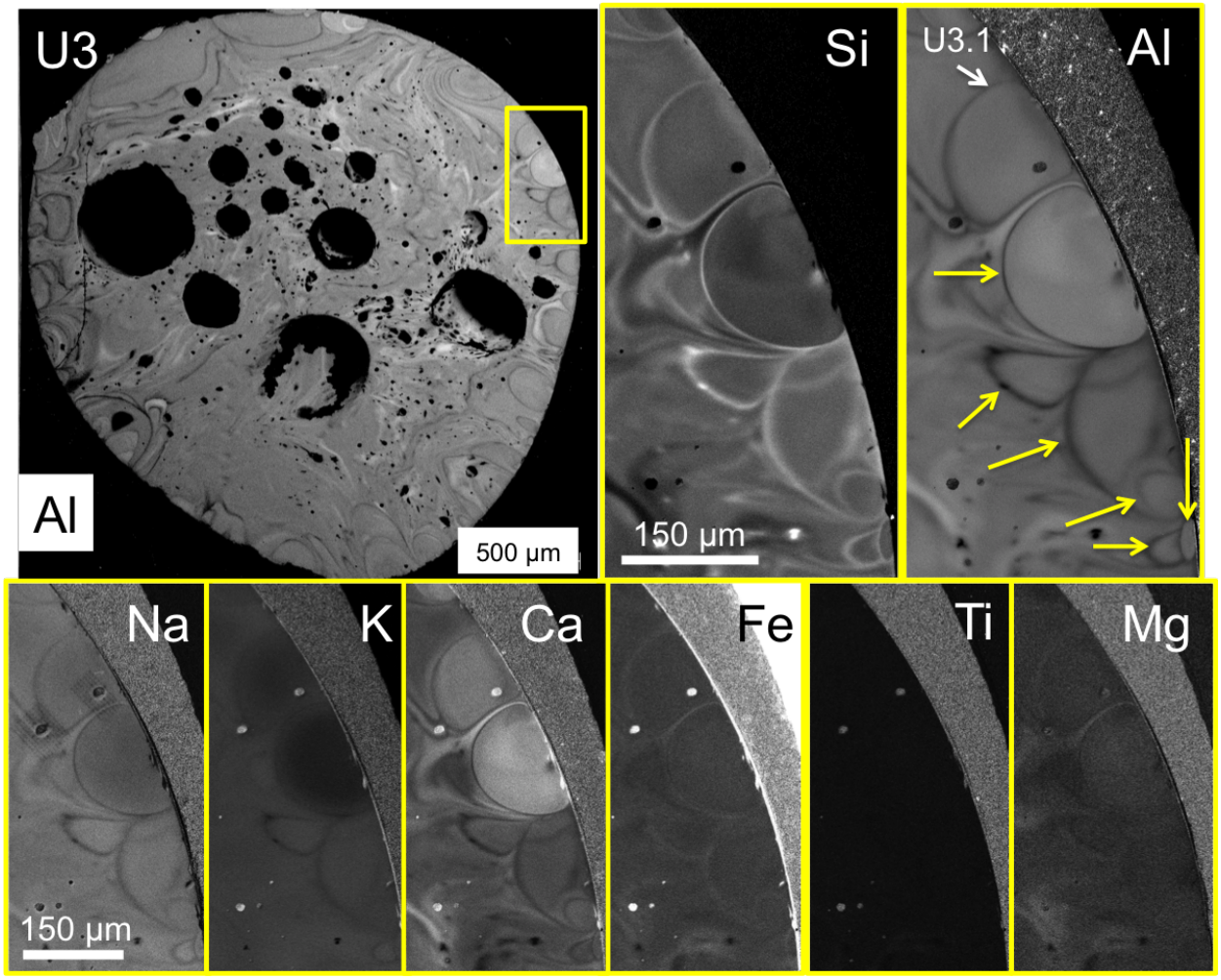

Figure 3.2: X-ray compositional maps of sample U3 for all elements showing surface agglomerates and interior agglomerates. The Si enrichment and Al depletion features are preserved at the compositional interface between agglomerates and hosts. The frequency of agglomerated objects is illustrated not just in the inset region, but generally surrounding sample U3. Arrows in the magnified Al map (top right panel) mark these agglomerates. U3.1, a surface agglomerate characterized using both EDS and SIMS, is marked in the magnified Al map in the top right panel. Maps have been independently adjusted in contrast and brightness to bring out relative compositional variation.

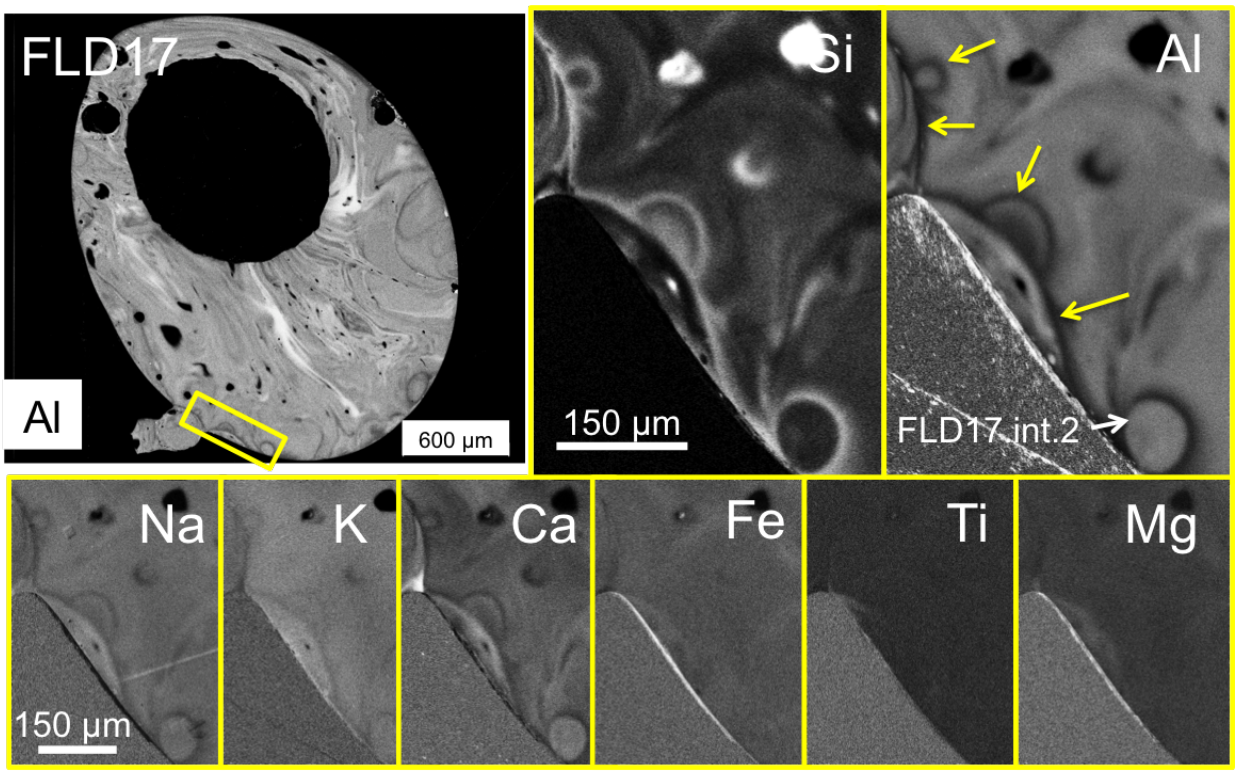

Figure 3.3: X-ray compositional map of sample FLD17 for all elements in an area preserving both surface agglomerates and interior agglomerates. The Al depletion at the compositional interface between agglomerates and hosts is a consistent feature. Arrows in the magnified Al map (top right panel) mark these agglomerates. FLD17.int.2, an interior agglomerate characterized using both EDS and SIMS, is marked in the magnified Al map in the top right panel.Maps have been independently adjusted in contrast and brightness to bring out relative compositional variation.

3.5 A new type of compositional interface

CaMgFe interfaces appear to almost always be depleted in Al (Table 3.1). As a result, Al compositional maps are used in this dissertation to identify compositional interfaces, and therefore, agglomerates partially or fully incorporated into samples. The operating conditions used to collect X-ray compositional maps of whole samples are described in Chapter 4. Al compositional maps of entire samples revealed more objects exhibiting interfaces with these relative enrichments and depletions are visible *within* host glasses, not just with agglomerates adhered to the exterior or residing at the surface (examples of interior compared to surface agglomerates are shown in Figure 3.7). The difference here, perhaps, is that the host glass was simply more molten, deforming upon impact with the agglomerate, which still retained its circular morphology. In addition, while the interfaces studied by Weisz were readily identified using backscatter electron images (due to the enrichment in Fe and Ca relative to the surrounding glass they appear brighter in BSE images), many of the agglom-

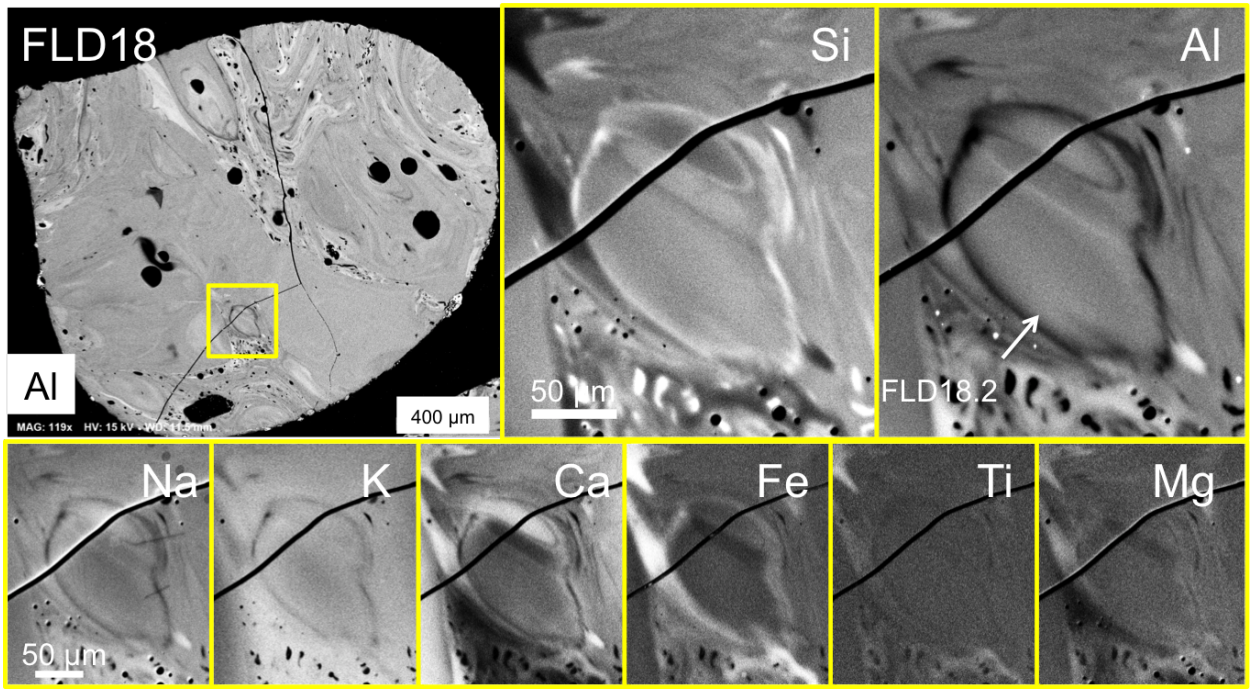

Figure 3.4: Compositional map of sample FLD18 for all elements showing an interior agglomerate (FLD18.2). An Si enrichment and Al depletion is preserved at the compositional interface between agglomerate and host. Maps have been independently adjusted in contrast and brightness to bring out relative compositional variation.

erates observed in Al compositional maps were not clearly visible in BSE images, implying they do not exhibit the same enrichments in minor elements.

After compositional interfaces were identified with Al compositional maps, their enrichment was confirmed using compositional X-ray maps of other major elements. These compositional X-ray maps reveal that compositional interfaces do not always exhibit enrichments in Fe, Ca, Mg, and ^{235}U, but are still depleted in Al. When enrichments in these species are absent, the Al depletion is typically accompanied by a Si enrichment (herein referred to as an "Si" interface). Examples of agglomerates exhibiting these interfaces are shown in Figs. 3.2, 3.3, 3.4, 3.5, and 3.7. The relative frequency of Si and CaMgFe interfaces and where they are found (bounding exterior, surface, or interior agglomerates) is discussed in the next section.

3.6 The frequency of agglomerates

Compositional X-ray maps were used to identify agglomerates ($n = 233$) in 18 samples to determine their frequency, size, and attachment location. The agglomerates occupy a minimum of 0% of the exposed cross-sectional area (U2 had no identified agglomerates) to

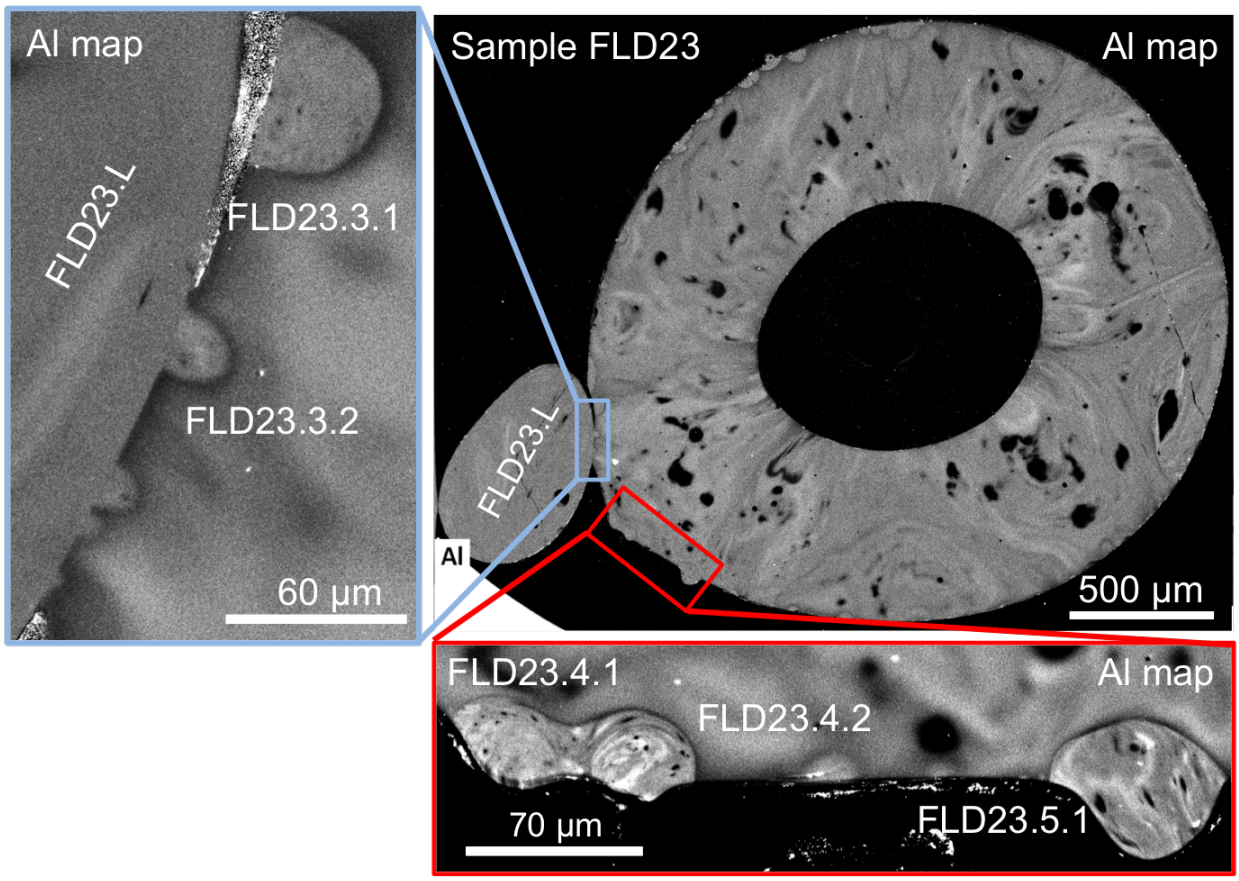

Figure 3.5: Al composition map of sample FLD23 showing surface agglomerates, some of which are shown in the insets. FLD23 also includes an agglomerate attached at the exterior (FLD23.L), visible on the left hand side of the Al map. The black region in the center of the Al map of FLD23 is a void and the black regions throughout the sample are likely partially-melted quartz grains. Al maps have been independently adjusted to highlight compositional variation.

20.5% of the exposed cross-sectional area in the sample (sample U4). No correlation with sample size is observed, suggesting that larger samples are not necessarily comprised of more agglomerates (Figure 3.8).

More preserved agglomerates in a sample does not necessarily imply a greater contribution of the agglomerates to the total exposed cross-section (Figure 3.9). Figure 3.9 shows the total sum of agglomerate area as a function of the number of identified agglomerates suggests two trends. Some samples preserve many small agglomerates whose cumulative area sums to a large fraction of the total sample area (the trend with samples CD, FLD18, FLD23, CC, and U3). Other samples retain few, but comparatively large agglomerates (relative to the total sample size), such as FLD14, FLD5.4, and U4. For example, in one sample U3, 56 agglomerates occupy only 14.5% of the total area (examples of agglomerates in U3 are shown in Figure 3.2), while in sample FLD14, four agglomerates occupy 10.9% of the total

Table 3.1: Observed enrichment and depletion of major elements, the $^{235}U/^{30}Si$ ratio and $^{235}U/^{238}U$ ratio at 9 interfaces (11 total interface scans: two scans were conducted across agglomerate C1 and C3) in 5 samples from Weisz [68]. This table summarizes Table 4.1 and Figures 4.17–4.26 from [68]. Interface compositions are considered enriched if a point within 1 μm of the interface peak identified by Weisz (2016) is greater than the mean of concentrations or ratios between 1 and 3 μm on both sides of that interface.

Element	Interface behavior
Si	Enriched in 5 of 11 interface scans
Al	**Depleted** in 10 of 11 interface scans
Na	Enriched in 3 of 11 interface scans
K	**Depleted** in 7 of 11 interface scans
Ca	Enriched in 11 of 11 interface scans
Fe	Enriched in 11 of 11 interface scans
Ti	**Depleted** in 6 of 11 interface scans
Mg	Enriched in 9 of 11 interface scans
$^{235}U/^{30}Si$	Enriched in 5 of 9 interface scans
$^{235}U/^{238}U$	Enriched in 6 of 9 interface scans

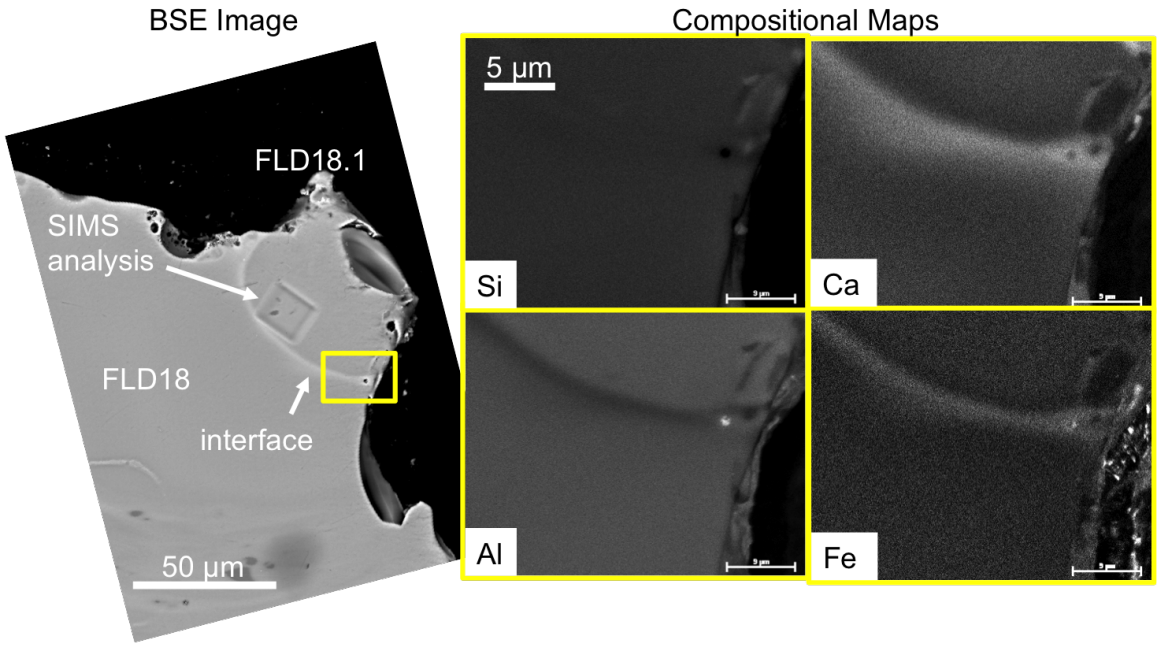

Figure 3.6: BSE image of agglomerate FLD18.1 (left) and X-ray compositional maps showing no relative change in Si across the interface, a depletion of Al across the interface, and characteristic enrichments of Ca and Fe across the interface. (The map for Mg is not shown, but it is also enriched at this interface.)

exposed area. These observations suggest that agglomerates themselves vary widely in size and contribute highly variable amounts to the overall sample. Nevertheless, in all cases,

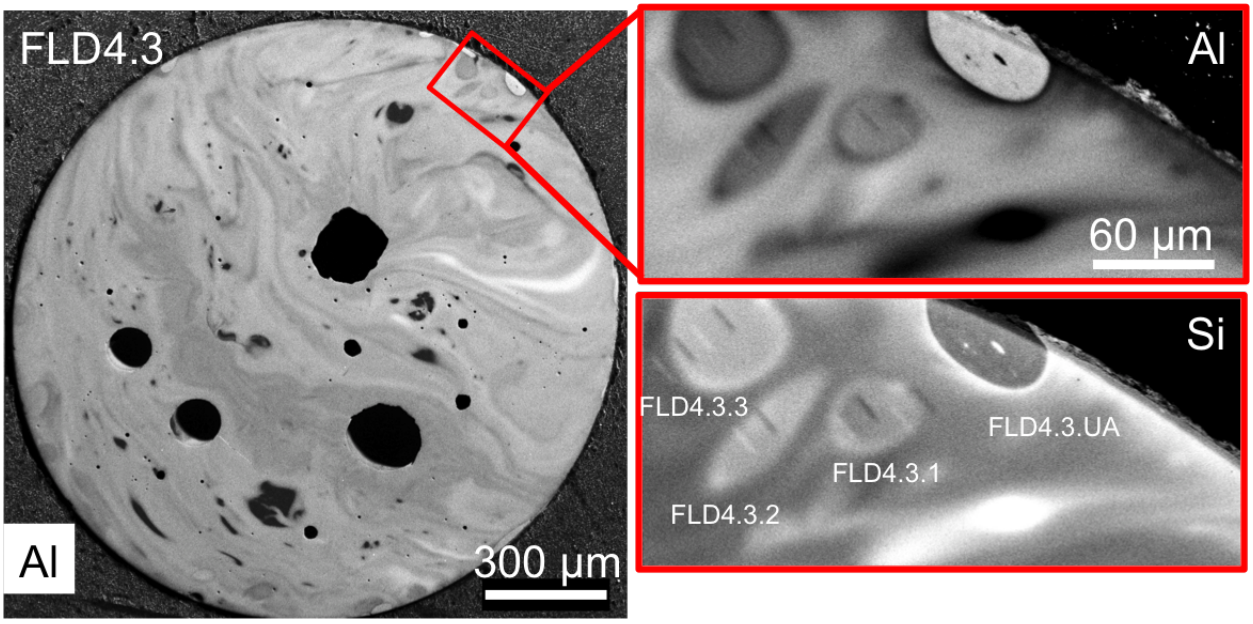

Figure 3.7: Al and Si X-ray compositional map of sample FLD4.3 showing interior agglomerates, magnified shown in the insets. In the top of the inset, an agglomerate residing at the surface is also visible (FLD4.3.UA). SIMS analytical regions are visible in the insets as square features in the agglomerates and overlapping compositional interfaces. Agglomerates are labeled in the Si inset.

the area occupied by the host is much greater than the total sum area occupied by the agglomerates. The median total area occupied by agglomerates in these 18 samples is 5.7%, revealing that in all samples the host is volumetrically dominant, likely a general trend in fallout glasses.

Figure 3.10 shows a histogram of the equivalent diameter of agglomerates, colored by their location of attachment. Plotting the sizes of all the identified agglomerates and their location of attachment shows that by far, surface agglomerates occur most frequently, with 85% of identified agglomerates being surface agglomerates (199 of 233 identified agglomerates). Interior agglomerates are the next most abundant, accounting for 11% of the identified agglomerates (26 of the 233 identified agglomerates). Finally, while most easily identified and first noted in the literature, exterior agglomerates account for the least frequently occurring fraction of identified agglomerates in the 18 samples with 7 exterior agglomerates (5% of the population).

Note that sampling and sample preparation bias may explain in part the low number of identified exterior agglomerates. First, the counted samples are largely spheroidal in shape, while Eppich et al. (2014) noted an increased frequency of exterior agglomerates in oblong, elongated-shaped fallout glasses. Furthermore, characterized samples were mounted and polished to expose their cross-section, which exposes a large interior area of the fallout glass at the expense of the fallout sample's surface area. A more exhaustive study would count

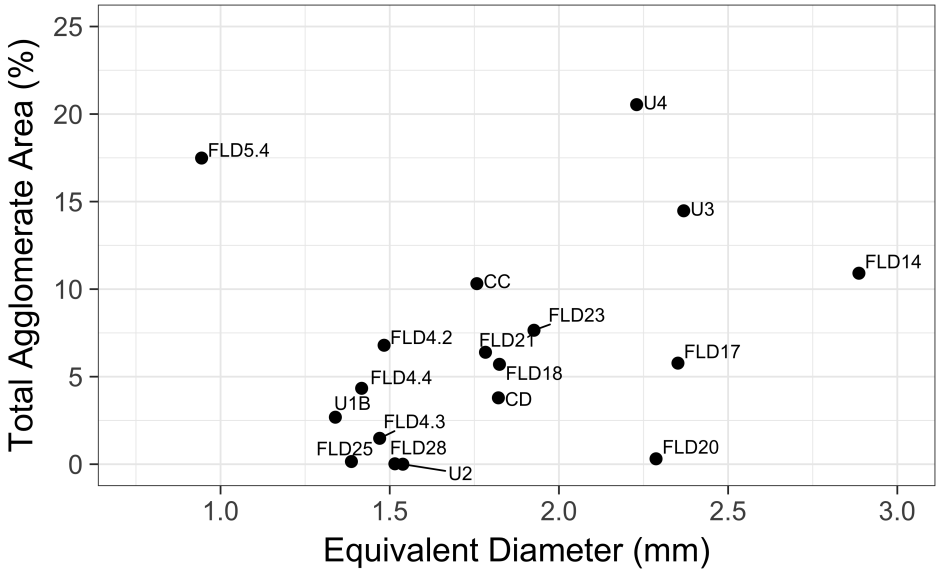

Figure 3.8: The cumulative sum of agglomerate cross-sectional areas (as a percent of the total sample area) as a function of the equivalent diameter of a sample (including both the host and agglomerates). There is a general lack of a correlation, demonstrating that larger samples are not necessarily comprised of more agglomerates. Data are tabulated in Appendix A.1.

exterior agglomerates prior to mounting and polishing these samples to their mid-plane.

The range in size of identified agglomerates in these 18 samples spans three orders-of-magnitude, from a surface agglomerate 5 μm in diameter in sample FLD18 to an exterior agglomerate in FLD14 with a diameter of 860 μm.[1] Agglomerates of order 10 μm in diameter were easily resolvable using these approaches, but these counts are likely biased towards sizes larger than 5–10 μm, as the ability to distinguish smaller agglomerates is limited by the resolution of the compositional map. Collectively, the distribution of agglomerate diameters appears quasi-log-normal, having a mean of 92 $\pm$ 108 μm (the median diameter is 48 μm). The large standard deviation is due to the large range in diameters of identified agglomerates, which also makes it difficult to statistically compare the relative sizes of surface, interior, and exterior agglomerates.

Exterior agglomerate diameters range from 60 μm to 855 μm, while interior and surface agglomerates range from 20 μm to 335 μm and 5 μm to 553 μm, respectively. The identified exterior agglomerates generally have larger diameters relative to surface and interior agglomerates. Because the location of attachment is dependent on the viscosity of the host melt, and therefore the temperature of the host melt (as well as the impact velocity) and time after detonation, it is possible that surface and interior agglomerates tend to be smaller in

[1]This only includes agglomerates identified using the X-ray maps. The range of agglomerates downselected for further characterization spans a different range of equivalent diameters, spanning from 17 μm in sample FLD4.3 to 1,089 μm in sample FLD10.

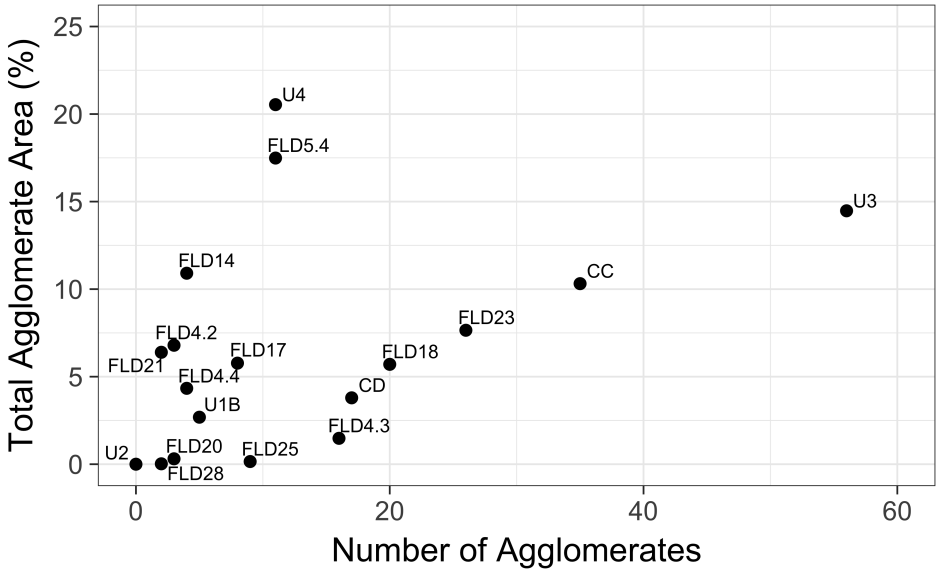

Figure 3.9: The cumulative sum of agglomerate cross-sectional areas (as a percent of the total sample area) as a function of the number of identified agglomerates in 18 samples. Two general trends are present: samples that have many agglomerates that cumulatively sum to account for a large percentage of the sample's exposed cross-sectional area (*e.g.*, samples FLD18, FLD23, CC, and U3), and samples that have few, relatively large agglomerates accounting for a large proportion of the total exposed cross-sectional area (e.g., samples FLD14, FLD5.4, and U4). The median total area occupied agglomerates in a sample is 5.7% and the median number of agglomerates identified in a sample is 8.5. Data are tabulated in Appendix A.1.

diameter because at earlier times and/or hotter temperatures, the surface tension of a melt is lower, allowing them to break apart into smaller melts more easily. If so, breakup may play a key role in the formation of smaller parcels of melt prior to ultimately agglomerating with and incorporating into host melts.

The frequency of Si and CaMgFe interfaces

Si interfaces are more abundant than CaMgFe interfaces. Of the 233 counted agglomerates in 18 samples, 199 were bound by Si interfaces (≈85.4%), 9 were bound by CaMgFe interfaces (≈3.9%), and the remaining 25 interfaces were of indeterminate enrichment. This observation indicates that the process leading to the formation of Si interfaces may occur more frequently than the process leading to the formation of CaMgFe interfaces (discussed further in Chapter 8). Furthermore, Si interfaces are observed at all attachment locations: exterior, surface, and interior, while CaMgFe interfaces are only observed for exterior and surface agglomerates. This observation is consistent with with the proposal by Weisz (2016) that the CaMgFe interface is the result of a late-stage deposition from the vapor term in the fireball as exterior and surface agglomerates arrived later in time than interior agglomerates [68]. Of the 225

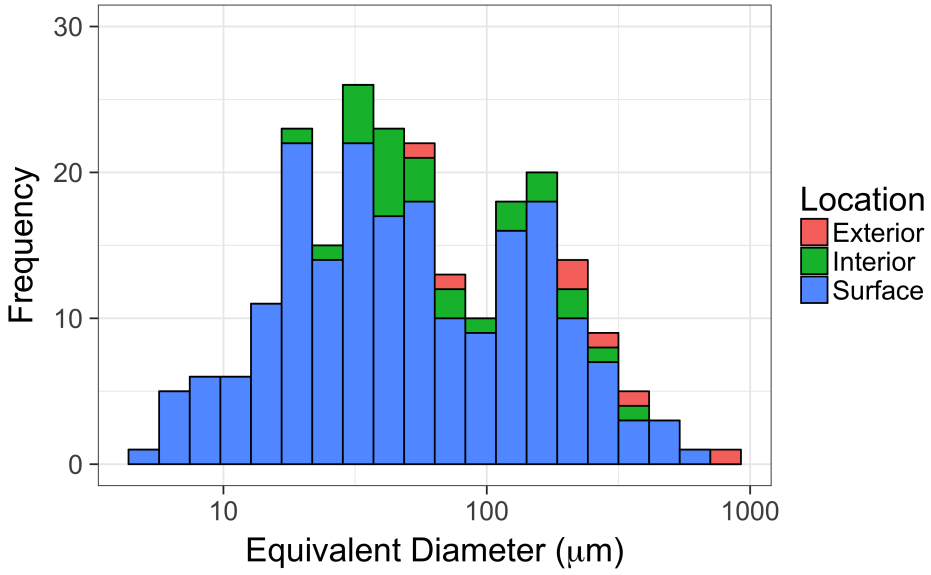

Figure 3.10: Histogram of agglomerate equivalent diameters in 18 samples, colored by their location of attachment (n = 233; number of bins = 20). The median agglomerate diameter is ∼48 μm. Data are tabulated in Appendix A.1.

counted interior and surface agglomerates, 197 are bounded by Si interfaces (≈87.5%), 6 are bounded by CaMgFe interfaces (≈2.7%), and the enrichment at the remaining 22 surface and interior interfaces were indeterminate. of the seven counted exterior agglomerates in the 18 samples, three exhibited CaMgFe interfaces, two exhibited Si interfaces, and the enrichment of the remaining two interfaces were indeterminate.

3.7 Down-selecting agglomerates

Once identified using compositional X-ray maps, agglomerates were down-selected, capturing the range of observed agglomerate features, including diameters, attachment locations, and types of compositional interfaces. Figures 3.11 and 3.12 show histograms of the sizes of down-selected agglomerates and their locations of attachment. This subset was additionally characterized by EDS and EDS and SIMS, respectively (Chapters 4 and 5), see Table 3.2.

To address if the major element composition or U isotope composition of small agglomerates is different than their hosts or larger agglomerates, the first down-selection criteria was agglomerate dimension. The equivalent diameter of agglomerates down-selected for study in this dissertation range from ∼15 μm to 1 mm. Twenty of the 58 agglomerates (35%) characterized by EDS (Chapter 4) and 18 of the 37 agglomerates characterized with SIMS (49%; Chapter 5) are less than 100 μm in diameter.

Next, because attachment location implies agglomerates collided with the host at dif-

ferent times and temperatures, agglomerates were down-selected to establish relationships in populations of exterior, surface, and interior agglomerates. To determine if the location of attachment for agglomerates is correlated with differences in formation processes or in the incorporation of anthropogenic U from the vapor phase, agglomerates attached to the exterior of fallout samples represent 17 of the 58 (≈29%) of the agglomerates characterized with EDS (9 of the 37, or 24% of the agglomerates characterized with SIMS). Agglomerates residing at the surface of the host glass represent 30 of the 58 (≈52%) of the agglomerates characterized with EDS and 20 of the 37 (54%) of the agglomerates characterized by SIMS. Finally, interior agglomerates represent 11 of the 58 (≈19%) of the agglomerates characterized with EDS and 9 of the 37 agglomerates (24%) of the agglomerates characterized with SIMS.

The compositional interface of an agglomerate is related to the vapor phase the agglomerate and host prior to agglomeration [68]. Studying agglomerates with different compositional interfaces provides evidence of how these different ambient environments affect the formation, volatilization, or incorporation of radionuclides into different agglomerates. Of the 58 total agglomerates downselected for further characterization with EDS, 37 exhibit Si compositional interfaces and 16 exhibit CaMgFe interfaces (5 interfaces had indeterminate enrichments). Of the 40 surface and interior agglomerates downselected for further characterization with EDS whose enrichments could be measured, 35 exhibited Si interfaces (87.5%) and the remaining 5 exhibited CaMgFe interfaces (12.5%).[2] In contrast, exterior agglomerates are predominantly bounded by CaMgFe interfaces. Of the 13 exterior agglomerates downselected for further characterization with EDS whose enrichments could be measured, 11 exhibited CaMgFe interfaces (≈84.5%) and 2 exhibited Si interfaces (≈15.5%).[3] Furthermore, in the 11 additional samples that had agglomerates downselected for further characterization, not including the 4 already studied by Weisz (2016), four samples preserved agglomerates with CaMgFe interfaces (FLD10, FLD14, FLD18, and U1B.2). However, as will be further explored in Chapter 8 and 9, Si interfaces may also appear adjacent to CaMgFe interfaces and appear more diffuse than CaMgFe interfaces in these instances, indicating an earlier formation time and two that distinct processes lead to the formation of Si and CaMgFe interfaces.

Once agglomerates were down-selected, they were characterized with EDS raster analyses to measure their chemical compositions, SIMS in the agglomerate and over their interface to characterize their U isotope composition and the behavior of ^{235}U at the interface (Chapter 9), and their interfaces characterized with high magnification, quantitative compositional X-ray mapping with EDS to determine the enrichment and depletion of major elements across the interfaces (Chapter 4).

[2]A total of 43 surface and interior agglomerates were downselected for further characterization using EDS. However, two of the compositional interfaces of those agglomerates had indeterminate enrichments.

[3]A total of 15 exterior agglomerates were downselected for for further characterization using EDS. However, two of the compositional interfaces of those agglomerates had indeterminate enrichments.

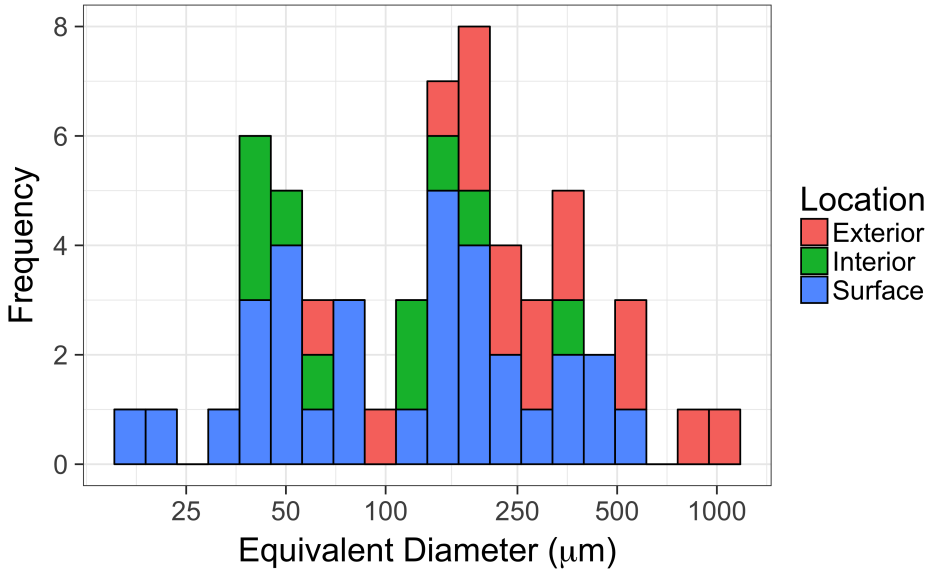

Figure 3.11: Histogram showing the size distribution of agglomerates down-selected for further characterization by EDS (n=53 in 15 samples; histogram has 20 bins). Note the log x-axis. Colors denote the location of the agglomerate as defined in the text and depicted in Figure 3.1.

Table 3.2: Table of agglomerates analyzed by EDS, sorted by sample. Also noted are the agglomerate attachment locations, their compositional interface type (as described in the text), and whether they were also analyzed by SIMS to measure their U isotopic composition ($^{235}U/^{238}U$ ratio).

Sample	Agglomerates	Diameter (equiv., μm)	Location	Interface Type	Characterized by SIMS
AA.B	B1	384	Exterior	CaMgFe	X
	B2	70	Surface	CaMgFe	X
	B3	590	Exterior	CaMgFe	
AE.C	C1	200	Exterior	CaMgFe	X
	C2	207	Exterior	CaMgFe	X
	C3	106	Exterior	CaMgFe	
	C4	264	Exterior	CaMgFe	
AG.D	D1	201	Exterior	CaMgFe	
	D2	283	Exterior	CaMgFe	X
AH.E	E1	178	Exterior	CaMgFe	X
	E2	341	Exterior	CaMgFe	
FLD10	FLD10.L	1089	Exterior	CaMgFe	X
FLD14	FLD14.1	157	Surface	Si	X
	FLD14.L	856	Exterior	CaMgFe	X
FLD17	FLD17.1	209	Exterior	Si	
	FLD17.2	355	Surface	Si	
	FLD17.int.1	111	Interior	Si	
	FLD17.int.2	62	Interior	Si	X
	FLD17.tail	143	Exterior	Indeterminate	
FLD18	FLD18.1	60	Exterior	CaMgFe	X
	FLD18.2	124	Interior	Si	X
	FLD18.3	166	Interior	Si	
	FLD18.4	336	Surface	CaMgFe	

FLD21	FLD21.1	401	Surface	Si	
	FLD21.L	206	Exterior	Indeterminate	
FLD23	FLD23.1.1	46	Surface	Si	X
	FLD23.1.2	47	Surface	Si	X
	FLD23.1.3	47	Surface	Si	X
	FLD23.2.1	21	Surface	Si	X
	FLD23.2.2	31	Surface	Si	X
	FLD23.3.1	40	Surface	Si	X
	FLD23.3.2	17	Surface	Si	X
	FLD23.4.1	42	Surface	Si	X
	FLD23.4.2	43	Surface	Si	X
	FLD23.5.1	60	Surface	Si	X
	FLD23.L	498	Exterior	Si	X
FLD4.3	FLD4.3.1	39	Interior	Si	X
	FLD4.3.2	41	Interior	Si	X
	FLD4.3.3	53	Interior	Si	X
	FLD4.3.4	70	Surface	Si	
	FLD4.3.5	41	Interior	Si	X
	FLD4.3.UA	46	Surface	Si	
FLD4.4	FLD4.4.1	244	Surface	Si	
	FLD4.4.2	163	Surface	Si	
U1B	U1B.2	84	Surface	CaMgFe	X
	U1B.L	195	Interior	Si	X
U3	U3.1	134	Surface	Si	X
	U3.2	191	Surface	Si	X
	U3.3	262	Surface	Si	X
	U3.4	125	Surface	Si	X
	U3.5	146	Surface	Si	X
U4	U4.1	553	Surface	Indeterminate	X
	U4.2	335	Interior	Si	X
	U4.3	465	Surface	Indeterminate	X
	U4.4	178	Surface	Si	
	U4.5	171	Surface	Si	
	U4.6	154	Surface	Si	
	U4.7	247	Surface	Indeterminate	
Total	**58**		**Exterior: 17** **Surface: 30** **Interior: 11**	**CaMgFe: 16** **Si: 37** **Indeterminate: 5**	**Exterior: 9** **Surface: 20** **Interior: 9** **CaMgFe: 11** **Si: 25** **Indeterminate: 2**

3.8 Conclusion

This chapter discusses how agglomerates are identified, where they are located in samples, their frequency, and the compositional interface. The chapter also explains the criteria used for down-selection and the rationale for down-selecting agglomerates to ensure smaller agglomerates, agglomerates at different locations, and agglomerates with different compositional interfaces were represented in the sample subset subsequently characterized with EDS and with both EDS and SIMS.

The next chapter details the use of EDS to generate X-ray compositional maps of entire samples, measure the major element composition of the host and agglomerates using individual raster analyses, and generate high resolution X-ray compositional maps of compositional

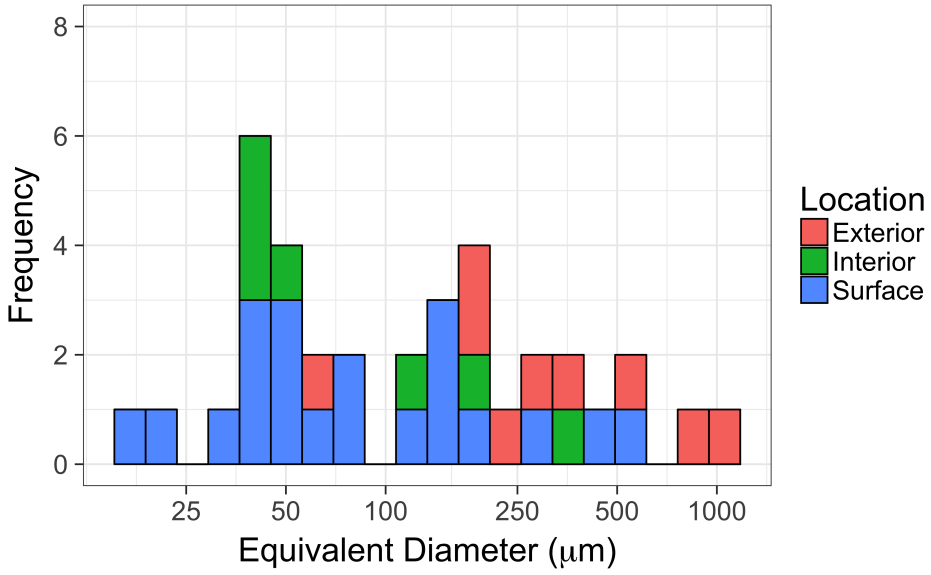

Figure 3.12: Histogram showing the size distribution of agglomerates down-selected for further characterization by SIMS (n=37 in 13 samples; histogram has 20 bins). Note the log x-axis. Colors denote the location of the agglomerate (Figure 3.1). The axes are the same as in Figure 3.11 to allow for comparison between the two plots.

interfaces.

Chapter 4

Major Element Compositions of Fallout

4.1 Chapter overview

This chapter describes how energy-dispersive X-ray spectroscopy (EDS) is used to characterize fallout populations of host objects, agglomerates, and unmelted soil. In this study, three types of EDS data are collected: (1) Rastered EDS analyses (≈10-15 μm in diameter) to characterize the major element composition of hosts and agglomerates, (2) qualitative EDS compositional X-ray maps to identify agglomerates, and (3) quantified EDS compositional X-ray maps taken at high magnification to characterize the major element behavior at compositional interfaces.

This chapter primarily discusses the results the EDS raster analyses, which are used to quantitatively measure the major element composition across a population of host objects and agglomerates using series of ∼10–15 μm diameter rasters. The major element compositions of host objects and agglomerates obtained from these analyses are compared to one another to illustrate the compositional similarity between the two populations. This comparison reveals that agglomerate compositions are a subset of host populations, indicating agglomerates and hosts are derived from the same carrier material. These two populations are then compared to EDS raster analyses of unmelted soil collected near ground zero, the precursor carrier material for forming glassy fallout. These data sets are used to show that with respect to major element composition, both host objects and agglomerates are consistent with being a mixture of minerals present in the soil. Finally, the compositions of host objects and agglomerates measured with EDS rasters are used to explore whether host objects and agglomerates experienced measurable loss of volatile alkali oxides as a function of their diameter, as would be expected when externally-heating a melt to high temperatures. (Smaller melts are expected lose relatively more of their alkali oxides due to their increased surface area/volume ratio.)

Qualitative compositional X-ray maps are used to characterize and describe composi-

tional relationships and textures in host objects and agglomerates.[1] These maps reveal that agglomerates tend to be more thoroughly mixed and glassy, containing fewer unmelted minerals than host objects. These maps also reveal that outlying compositions are not always unmelted mineral phases, but in two samples, U2 and FLD25, appear to have been fully melted. Autoradiographs of these samples also reveal that these outlying compositions incorporated relatively little activity compared to the rest of the sample. Compositional X-ray maps of a region in sample FLD10 are also used to discuss the fallout formation implications of a region in sample FLD10 that exhibits a continuous transition from unmelted rock near its center to a partially-melted region to a glassy region and its periphery, indicating external heating formed this sample of glassy fallout.

4.2 Variables and datasets used in this chapter

The major element composition data on host objects consists of approximately 3,500 EDS raster measurements taken in grid patterns across 37 of the 49 host objects. In the glassy fallout population studied here, there are eight elements measurable by EDS with reasonable uncertainties (<15% 1RSD): Si, Al, Na, K, Ca, Fe, Ti, and Mg. This study reports these measured elements as oxide weight percentages, assuming the elements are present as SiO_2, Al_2O_3, Na_2O, K_2O, CaO, FeO_T, TiO_2, and MgO, respectively.[2]

In measurements of host objects, these oxides are usually present at the following concentrations:

- >50 wt.% SiO_2 (observed range spans from 57 to 103 wt.%)
- >10 wt.% Al_2O_3 (observed range spans from 0 to 24 wt.%)
- >1 wt.% and <10 wt.%: Na_2O, K_2O, CaO, and FeO (observed ranges span from 0 to 8, 10, 10, and 16 wt.%, respectively)
- <1 wt.%: TiO_2 and MgO (observed ranges span from 0 to 6 and 7 wt.%, respectively)

Due to chemical heterogeneity, however, there is considerable variance about these values, particularly when analyzing minerals that may have remained unmelted or regions in fallout that were partially, but incompletely melted.

[1] While the method of X-ray compositional mapping is discussed in this chapter, *qualitative* X-ray compositional maps are primarily shown and discussed in Chapter 3 to identify and count agglomerates and *quantitative* X-ray maps are shown and discussed in Chapters 8 and 9 to characterize the composition at interfaces.

[2] This analysis assumes all Fe is present as FeO, hence the T subscript in FeO_T standing for "total." The actual Fe oxidation state was not independently determined (see [69] for discussion).

4.3 Energy-dispersive X-ray spectroscopy

EDS is a technique used to qualitatively or quantitatively determine the chemical composition of a sample. EDS relies on detecting X-rays produced between the primary electron beam and electrons in the sample. Two types of X-rays are produced through these interactions: continuum X-rays and characteristic X-rays. Continuum X-rays are primarily responsible for the background in X-ray energy spectra, and characteristic X-rays are the signals that can be processed to determine the sample's composition.

Continuum X-rays

Continuum X-rays are created from the continuous deceleration and scattering primary electrons experience as they travel through the sample. Each scattering event produces an X-ray with energy $\Delta E = h\nu$, where h is Planck's constant and ν is the frequency of the resulting X-ray. Because the primary electrons can lose any amount of energy up to their incoming kinetic energy in a scattering event, this creates a continuum of X-rays from low energy up to the energy of the primary beam. Most energy losses are small, producing a large background of X-rays with low energy. Continuum radiation constitutes the background in an EDS spectrum and must be fit and subtracted.

Characteristic X-rays

Characteristic X-rays are produced when inner shell electrons are ejected from their orbitals by primary beam electrons. The primary electron beam energy used in this study carries enough energy to eject inner shell electrons of the eight characterized elements. The SEM was operated to accelerate primary beam electrons to a kinetic energy 15 keV and the binding energies for the inner most shell electrons for the major elements of interest in glassy fallout range from 1.071 keV (for Na) to 7.112 keV (for Fe).

Ejecting an inner shell electron leaves the atom in an excited and ionized state. The ion quickly de-excites ($\sim$1 ps) through a set of available transitions from an electron in a higher orbital down to the inner orbital vacancy (Figure 4.1) [92]. The difference in binding energies is often emitted as a "characteristic X-ray" ($\Delta E_{\text{binding}} = h\nu$), as the energy difference between these orbitals is well-defined and element-dependent. While there are several transitions available (and some forbidden), the L to K transition (emitting a K_α X-ray) is the most intense for the major elements characterized in these fallout glasses (Si, Al, Na, K, Ca, Fe, Ti, and Mg) and was used to quantify the compositions in these glassy fallout samples.

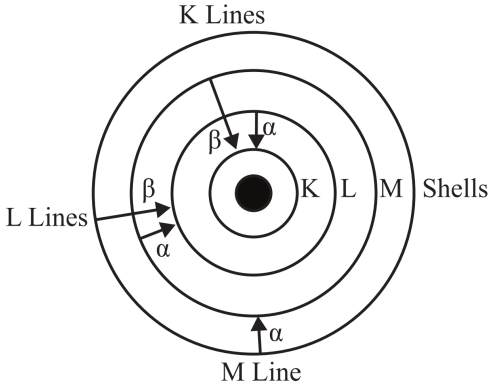

Figure 4.1: Electron transitions leading to common characteristic X-rays from the K, L, and M shells. Adapted from [93]. All major elements in this dissertation rely on quantifying the K_α transitions.

X-ray detection and processing

The EDS detector in this study uses a lithium-compensated (also referred to as "lithium-drifted") Si or "Si(Li)" semiconductor to detect X-rays emissions in the SEM.[3] EDS semiconductor detectors detect X-rays of all energies that impinge on the detector and disperses them by energy, creating an energy spectrum that contains the continuum X-ray background with characteristic X-ray peaks (Figure 4.2). This study used a Bruker Flash 6-60 EDS spectrometer with a 10 mm^2 Si(Li) detector mounted on an FEI Inspect-F SEM.

EDS detectors create mobile charge carriers (electron-hole pairs) in direct proportion to the energy of the absorbed X-ray. As the X-ray enters a detector, it will deposit most of its energy into an electron (now called the photoelectron), ejecting it from its orbital where it is free to scatter through the solid, depositing the energy absorbed from the X-ray. As the photoelectron scatters through the detector it creates electron-hole pairs until it dissipates all of its kinetic energy. In the case of Si(Li), for every 3.76 eV of energy the incoming X-ray carries, one electron on average will be promoted to the conduction band, creating one electron-hole pair. For X-rays with keV energies, hundreds to thousands of electron-hole pairs are typically produced for each incoming X-ray. However, this is a statistical process, producing a distribution around some mean number of electron-hole pairs produced for an X-ray of a given energy. This distribution is the energy resolution of the detector, which is typically 130 eV at FWHM of Mn's K_α X-ray energy (5.90 keV).[4]

[3]Li is used to compensate for the excess holes created by the low levels of impurities present in high-purity Si [93].While Li is a dopant, it does not alter the band gap between the valence and conduction bands like other dopants are intended to. The band gap remains 3.76 eV.

[4]The resolution decreases slowly with increasing energy; the resolution at the Mn K_α X-ray energy is cited because of convention [94].

An applied voltage causes electrons and holes to migrate to opposite ends of the crystal, creating an electronic signal. Because the number of electron-hole pairs created is proportional to the energy of the absorbed X-ray, the amplitude of this signal is also proportional to the energy of the absorbed X-ray. A pre-amplifier converts this charge to a voltage, which is then shaped and amplified by a linear amplifier, and then a multichannel analyzer sorts the pulses by voltage [94]. The software converts this histogram of counts versus detected voltage into a histogram of counts versus incoming X-ray energy, creating the energy spectrum that an operator uses to qualitatively or quantitatively measure a sample's composition.

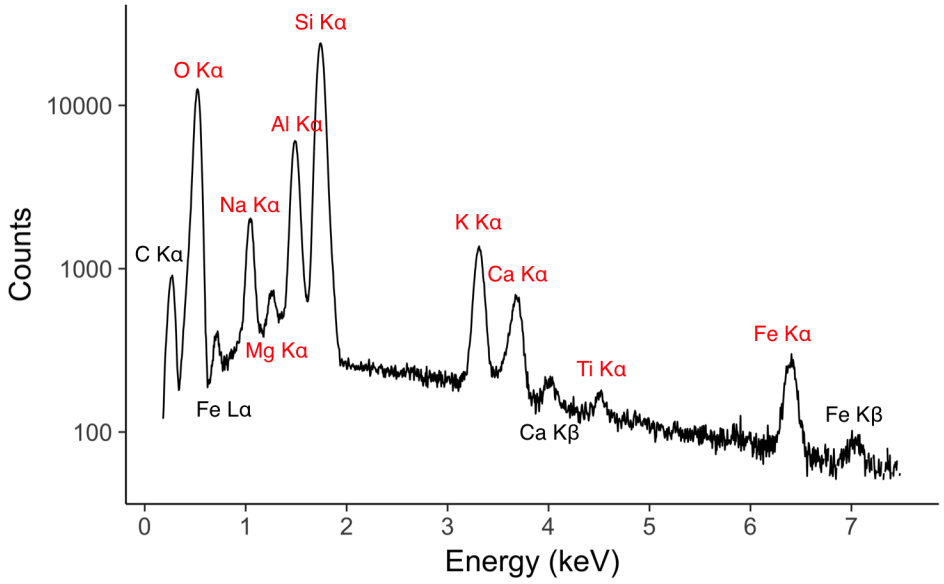

Figure 4.2: A typical EDS spectra from a glassy fallout sample (FLD10) in the range of 0–7.5 keV. Note the log scale on the y-axis. Characteristic X-rays of elements characterized in this study are noted in red. The K_α peaks are fit and quantified after the X-ray continuum has been fit and subtracted. This analysis was taken with the standard operating parameters described in the text. The widths of the peaks are due to the energy resolution of the spectrometer, which is relatively poor compared to the natural linewidth of characteristic X-ray emission (≈2 eV for Ca at FWHM) [92].

Quantifying an EDS spectrum

This study uses ESPIRIT 2 software (bundled with the Bruker EDS) to quantify EDS spectra using the Kα emissions for all measured elements: O, Si, Al, Na, K, Ca, Fe, Ti, and Mg. After collecting an EDS spectrum, the ESPIRIT 2 software uses an internal algorithm (known as a "ZAF correction"), which is a standardless quantification procedure, to calculate the elemental weight percent of each element of interest in the sample. First, the continuum X-ray background is modeled based on operating conditions and subtracted. Next, the

algorithm corrects for three matrix factors (Z, A, and F factors) that take into account the primary effects that alter X-ray yields between different elements.

The Z correction

The **Z** in ZAF refers to two corrections, one for the sample's stopping power and one for backscatter of primary beam electrons, both of which depend on the average atomic number (Z) of the analysis volume. The first correction is for the inelastic scattering primary beam electrons undergo with inner shell electrons as the travel into the sample, which decreases with increasing Z [92]. Stopping power is defined as the rate of energy loss ($-dE/dx$, which can be approximated using the Bethe-Bloch equation) divided by the sample's mass density, ρ:

$$S = -\frac{1}{\rho}\frac{dE}{dx}. \tag{4.1}$$

The backscatter correction corrects for primary beam electrons that backscatter out of the sample, primarily due to scattering events with nuclei. This effect becomes more pronounced with increasing average atomic number ($\propto \ln(\bar{Z})$) [92, 95]. For samples with higher Z, more electrons are backscattered out of the sample, and fewer X-rays are generated in the sample as a result. These two effects trend in opposite directions (stopping power decreases with Z and backscattering increases with Z), so the overall **Z** correction factor is usually small [87].

The A correction

The **A** refers to the correction for the self-absorption of X-rays as they exit the sample, attenuating the number of X-rays escaping the sample surface. Absorption is usually the largest correction and it depends strongly and nonlinearly on the X-ray energy and the sample's composition [93]. Because primary electrons eject inner shell electrons from some finite depth below the sample surface, the X-rays must travel some finite distance to escape the sample. As X-rays produced at some depth x, with some intensity I_0, travel towards the surface, they are absorbed by bound electrons, which are subsequently ejected, creating photoelectrons, with kinetic energies equal to the X-ray energy minus their binding energy. The attenuation follows Beer's Law:

$$\frac{I}{I_0} = \exp\left(-\frac{\mu}{\rho}(\rho x)\right) \tag{4.2}$$

where I is the X-ray intensity once the X-ray has escaped the sample, μ/ρ is the mass absorption coefficient, ρ is the density, and x is the distance traveled in the sample along a straight line from where the X-rays were Figure to the face of the detector window [92].

The F correction

Absorption causes atoms to emit secondary characteristic X-rays, or fluoresce, which is the **F** correction. As primary X-rays (both characteristic and continuum) leave the sample, they may be absorbed by inner shell electrons from other atoms in the sample. The inner shell electron may be ejected, and higher vacancy electrons will drop to fill the inner shell vacancy, releasing a characteristic X-ray [85]. In this case, these X-rays are called secondary X-rays and this processes is called secondary fluorescence.

The primary characteristic X-ray must have energy greater than the absorption edge of the photoelectron it creates. For example, the presence of Fe (with its Kα X-ray energy of 6.404 keV) can cause secondary fluorescence in all the other major elements present in these samples (after Fe, Ti has the highest K absorption edge at 4.966 keV). In the absence of a fluorescence correction, Fe would appear to be less abundant, and the other elements more abundant due to photoelectrons from other elements in the sample, which are created by absorbing Fe's Kα X-ray and then release characteristic X-rays of their own.

Sum totals

Sum totals are the sum of the ZAF-corrected and quantified concentrations of a single analysis for all characterized major element oxides. Ideally, sum totals should equal 100 wt.%, but rarely do. Deviations from 100% are meaningful and primarily reflect analytical uncertainties, but can also indicate charging effects, an element that is present in the sample but was not quantified, topographical effects that were ignored, excessive volatilization of alkalis, or an improper quantification scheme [92]. In this study, the only retained EDS analyses are those whose eight oxides sum to between 96% and 104%, where values greater 100% are likely due to assumed stoichiometries.

Carbon and oxygen

Carbon and oxygen are present in the samples – carbon as a $\sim$10 nm conductive coating and oxygen at approximately 45 wt.%. These elements are included in the software's matrix corrections. In this study, C was selected as the conductive coating in the ESPIRIT 2 software. This built-in option deconvolutes and fits the C K_α X-ray to incorporate it into the ZAF correction, but does not report it as part of the sample's composition. Despite being the most abundance element in these fallout samples, O's K_α line has a high uncertainty due to its low energy, making its measured abundance susceptible to slight variations in C coating thickness and its convolution with C's K_α and Fe's L_α lines. Despite its high uncertainty, the ZAF software reports the calculated wt.% for O, but this was not used for reporting chemical compositions.

EDS grid analyses

To characterize the compositions of host objects in glassy fallout, 100 EDS raster analyses were conducted in a grid pattern at a fixed magnification of 150x across host objects (herein called the "EDS host object grid analyses"; Figure 4.3). The grid pattern ensures the raster analyses and complete EDS dataset are unbiased, sampling compositions randomly across the host object. Using a fixed magnification and a constant number of rasters ensures that the number of analyses per host object is based on its cross-sectional area. At 150x magnification, 100 evenly-spaced square EDS rasters were manually drawn in a grid pattern across the field of view (with each raster having a dimension ∼10-15 μm across its diagonal). Rasters drawn over voids, fractures, or on epoxy were rejected. For the EDS host object grid analyses, EDS X-ray compositional maps and BSE images were later used to exclude EDS rasters taken in features resembling agglomerates and interfaces between agglomerates and host objects. For EDS raster analyses collected within agglomerates, these same compositional maps were used to confirm the identity of agglomerates and also to exclude raster analyses that overlapped the compositional interface or sampled the host object. Raster analyses were used instead of "point" or "spot" analyses ($\leq$1 μm beam diameter at the sample surface) because high primary beam currents and long analysis times can volatilize species such as Na and K (discussed below).

All EDS raster analyses were collected for a live time of 30 s, with EDS detector dead times kept between ≈10-20%.[5] The analyses were conducted with samples set 10 mm from exit aperture of the electron beam column in the SEM (called the "working distance"), 15 kV accelerating voltage, and "spot size" of 5. Spot size is a term used by the FEI Inspect SEM software as a proxy for primary beam current, and can be set by the user in steps of 0.5 between the values 3 and 6. A spot size of 5 corresponds to a primary e^- beam current of approximately 1 nA.

Accuracy and precision of EDS analyses

The goal of generating of the EDS host object grid analyses is to characterize the variations in the major element chemical composition of populations of agglomerates, host objects, and unmelted soil collected proximate to ground zero (discussed below). EDS analysis with a standardless quantification procedure is suitable to measure these compositional variations in a large sample suite. The chemical composition of most SIMS analyses locations were measured 3–4 times and averaged, with the standard deviation of that average presented as the 1σ uncertainty. Operating conditions were kept constant, and the majority of EDS raster analyses were conducted over the period of several months to minimize systematic uncertainties (for EDS analyses of hosts and agglomerates).

[5]The dead time is the percentage of time the detector spends processing current signals; during this time it does not process new incoming x-rays.

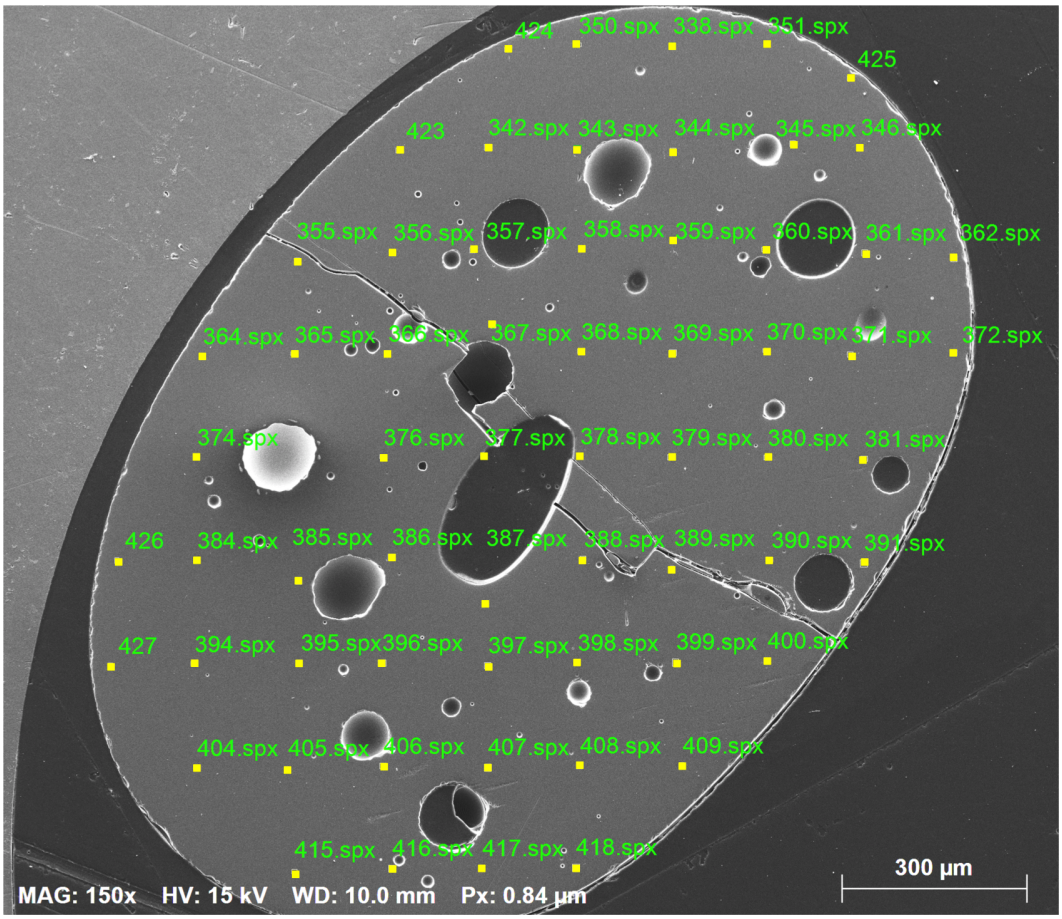

Figure 4.3: Secondary electron image of a grid of EDS rasters (yellow boxes with green labels as identifiers) collected on sample FLD25 at a magnification of 150x. Rasters were manually drawn and are approximately 10–15 μm across the diagonal.

Accuracy

To determine the systematic bias of the EDS's internal standardless ZAF correction, a reference standard was used to compare EDS measurements to the standard's literature values and to measurements of the standard using EPMA (WDS) from [68] (Figure 4.4). The analyzed reference material is Basalt Columbia River 1 (BCR-1, U.S. Geological Survey), which has a basaltic composition. The BCR-1 material was provided as a powder and fused into a glass at LLNL so it could be analyzed using techniques such as EDS, WDS, and SIMS. The major element composition of glassy fallout samples used in this study are more silicic than BCR-1, but BCR-1 provides a basis to compare the accuracy of standardized WDS and standardless EDS techniques. In addition, Ti and Mg are present above the percent level in BCR-1 ($\approx$1.3 and 2.1 wt.%, respectively), though present at $\sim$0.5 wt.% or below in these glassy fallout samples. A rhyolitic standard would be the best compositional comparison

with this suite of glasy fallout samples. However, this compositional comparison is most important for determining alkali mobility [96].

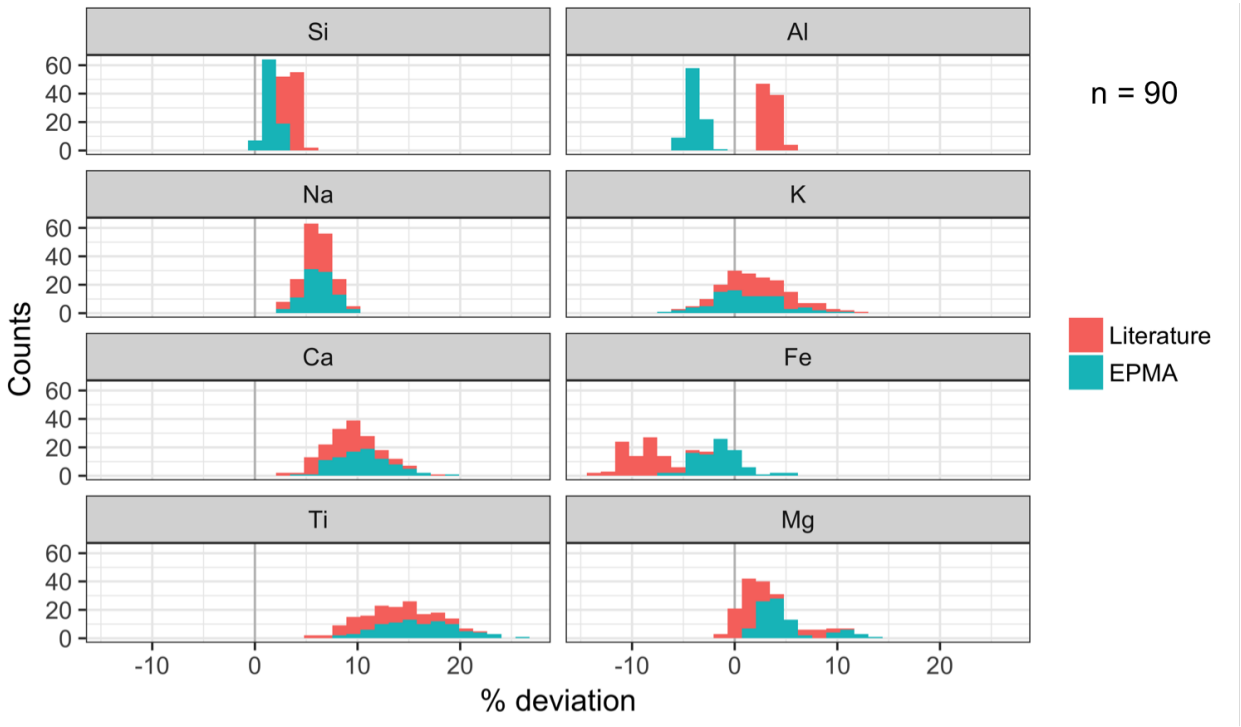

Figure 4.4: Histograms showing the EDS analyses deviations from the literature values [97] and the standardized EPMA measurements [68]. On BCR-1, 90 ∼10 μm raster EDS analyses were collected using the operating conditions described in the text (Table 4.3). Individual uncertainties are not shown to highlight the systematic bias of the ZAF quantification scheme. Note that the standardized EPMA analyses and BCR-1 literature values do not agree (within 1σ, see Table 4.1) for Al and Fe: the EPMA systematically measures a higher Al concentration and lower Fe concentration. Inaccuracies between the EDS and measured EPMA values or literature values are within 10%, except for Ca and Ti. One possibility for the deviation from the literature values is that BCR-1 was provided as a powder and then fused into glass at LLNL, which may have slightly modified the composition.

Precision

For the operating conditions used in this dissertation, EDS achieves ∼5% precision for most elements with abundances >1 wt.% in a single analysis (Table 4.2). Longer counting times can in some cases achieve better precision, but ∼5% is acceptable and shorter counting times prevent excessive alkali loss (discussed below) [68]. The resulting uncertainty is not limited by counting statistics, but instead by uncertainties in fitting the continuum background and deconvolving and fitting the characteristic X-ray peaks in the 1–2 keV range (Na, Mg, Al, and Si; Table 4.2). The analytical uncertainty is dominated by uncertainty in the ZAF

Table 4.1: Summary of historic measurements on BCR-1 (reproduced from [97]) compared with standardized EPMA measurements by Weisz (2016) [68]. Results from [68] assumed oxide stoichiometries, so no O or sum total is shown. The results that are outside 1σ are highlighted in bold.

Element	Literature	±	1σ	EPMA	±	1σ
Si	25.27	±	0.17	25.78	±	0.24
Al	**7.22**	±	**0.13**	**7.78**	±	**0.06**
Na	2.43	±	0.09	2.43	±	0.07
K	1.40	±	0.03	1.42	±	0.03
Ca	4.97	±	0.11	4.89	±	0.05
Fe	**9.38**	±	**0.25**	**8.68**	±	**0.14**
Ti	1.34	±	0.06	1.31	±	0.03
Mg	2.10	±	0.08	2.05	±	0.02
O	45.10	±	0.40	-		-
Sum	99.95	±	0.55	-		-

correction and fitting routines from Bruker's ESPIRIT 2 software package, as spot-to-spot precision (reproducibility) of EDS analyses is typically ∼1% (Table 4.3).

Table 4.2: Concentration, counts, and their associated uncertainties from a single EDS raster analysis (∼10 μm diameter raster, 30 s live time, ∼15% dead time) on fallout sample U1B. These concentrations are typical for glassy fallout from this test. Elements are ordered by their K_α X-ray energy.

Element	K_α (keV)	Weight %	±	1σ	1RSD (%)	Counts	±	1RSD (%)
O	0.53	48.03	±	5.32	11.07	154555	±	0.25
Na	1.04	1.52	±	0.12	8.01	12752	±	0.89
Mg	1.25	0.48	±	0.05	10.85	5455	±	1.35
Al	1.49	7.68	±	0.38	4.97	98914	±	0.32
Si	1.74	33.88	±	1.43	4.22	431200	±	0.15
K	3.13	2.75	±	0.11	4.05	25358	±	0.63
Ca	3.69	0.95	±	0.06	5.93	7202	±	1.18
Ti	4.51	0.27	±	0.04	13.48	1462	±	2.62
Fe	6.40	2.19	±	0.10	4.39	6879	±	1.21
Sum	-	97.74	±	7.60	7.78	-		-

Electron-beam induced alkali loss

Ideally, <1 μm EDS analyses would be used to characterize the chemical heterogeneity in glassy fallout while minimally overlapping regions of differing composition. However, such small "spot" analyses may mobilize and volatilize alkalis due to beam-induced heating of the analytical volume and sample charging [96]. Na and K volatilization in fallout from spot analyses has previously been demonstrated in EPMA analyses of glassy fallout [68].

Table 4.3: Mean, 1σ, and 1RSD for 90 EDS rasters (raster diameter ≈10 μm) on the BCR-1 standard. This table shows the spot-to-spot precision of EDS analyses.

Element	Mean	±	1σ	1RSD(%)
Si	26.18	±	0.15	0.55
Al	7.47	±	0.05	0.73
Na	2.58	±	0.04	1.39
K	1.44	±	0.05	3.29
Ca	5.41	±	0.13	2.46
Fe	8.55	±	0.20	2.37
Ti	1.52	±	0.05	3.21
Mg	2.15	±	0.06	2.73
O	44.71	±	0.10	0.23

These effects can largely be mitigated by using EDS rasters or diffuse primary beams, short counting times, low currents, and high accelerating potentials [96, 98].

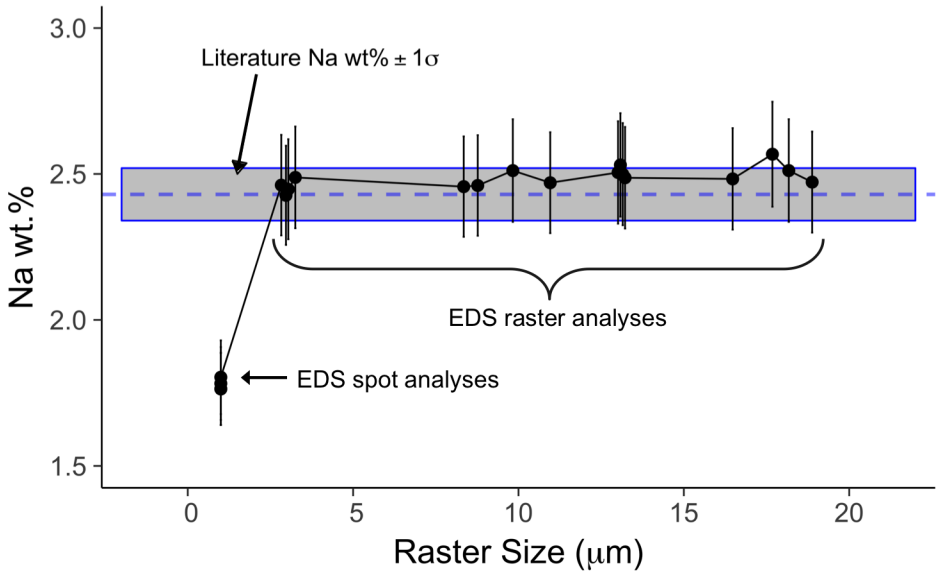

Figure 4.5: Variation of Na EDS measurements (as elemental wt.%) as a function of raster diameter on BCR-1. The first points are "spot" analyses (*i.e.*, not rasters) and are arbitrarily set to 1 μm, but are likely smaller. Rasters are hand-drawn and circular, which leads to the slight variation in raster diameters (measured later using ImageJ) [86]. The dashed line is the BCR-1 literature value for the Na composition in wt.% and the gray band is its 1σ uncertainty. Data are tabulated in Table E.2 in Appendix E.

To understand and minimize alkali volatilization from single EDS analyses, EDS rasters of different sizes were used to measure the composition of the BCR-1 standard. Figure 4.5 shows that raster diameters >5 μm do not volatilize Na in BCR-1. However, Na may be more

mobile in glassy fallout samples than in the BCR-1 standard. In order to determine whether Na volatilizes more easily from glassy fallout than the BCR-1 standard, three overlaid EDS raster analyzes were used to analyze, in immediate succession, the composition of BCR-1 and a representative glassy region of fallout from sample FLD10 (Figure 4.7). Figure 4.7 shows the Na and K composition relative to the composition of the first raster in BCR-1 and glassy fallout. In both BCR-1 and glassy fallout, K volatilization is observed to be negligible. In contrast, while Na volatilization is negligible in BCR-1, Na decreases with each successive EDS analysis in glassy fallout, indicating Na may be volatilizing during multiple successive analyses in glassy fallout and that Na may be more mobile in BCR-1 than in glassy fallout. As a result, to ensure Na was minimally volatilized from glassy fallout during EDS raster analyses, only EDS rasters with diameters $\geq$10 μm were used when analyzing glassy fallout with EDS. Furthermore, in order to capture the composition of a region previously analyzed with SIMS, the approach of overlaying multiple EDS rasters was frequently used to measure the composition of a SIMS analytical crater when the crater topography was wide and shallow to not affect the analysis (otherwise, EDS rasters were placed adjacent to and surrounding the analytical crater; Figure 4.6). To report the most accurate composition for Na in these cases, if the measured Na wt.% decreased over successive EDS raster analyses, the concentration from the first analysis was used and the uncertainty for Na was taken as the uncertainty from a typical, single analysis ($\approx$8%) instead of the standard deviation of the successive raster measurements.

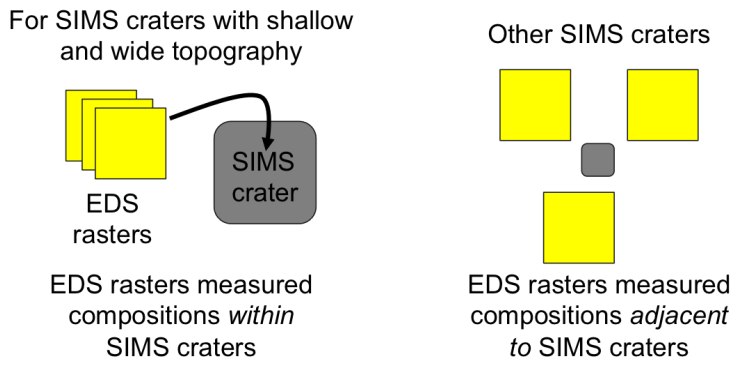

Figure 4.6: Schematic detailing how compositions of SIMS analytical regions were measured with EDS rasters. When the topography of the SIMS crater was shallow and wide, EDS rasters were placed directly in the analytical crater to measure its composition. Otherwise, EDS rasters were collected adjacent to the SIMS crater.

4.4 EDS compositional X-ray maps

EDS compositional X-ray maps were collected for two purposes. First, qualitative X-ray maps of entire samples were used to identify agglomerates and determine their size, location,

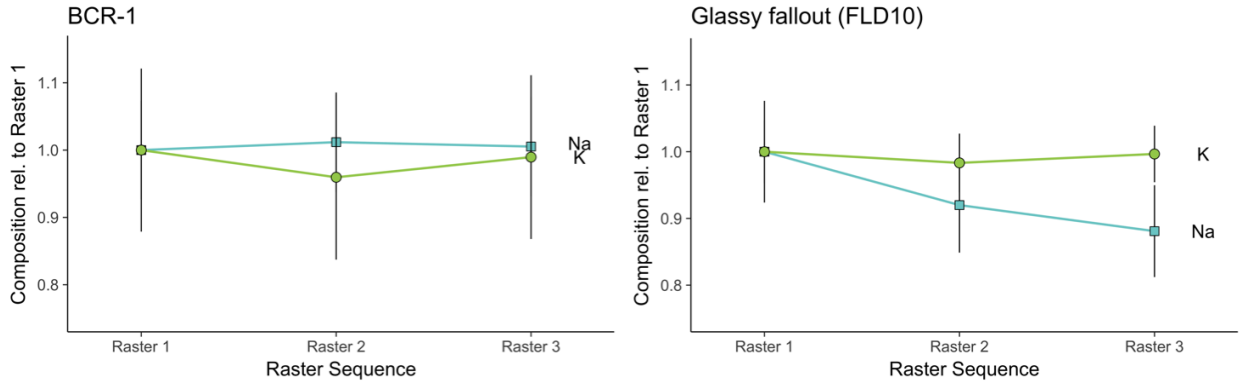

Figure 4.7: Relative same spot variation of Na and K from successive EDS rasters over the same region for BCR-1 (on left) and a representative example of glassy fallout from sample FLD10 (on right). Na and K compositions are normalized to the first measurement in the raster sequence ("Raster 1"). Uncertainties are 1σ. BCR-1 does not appear to volatilize Na under the operating conditions described in the text, while some analyses in fallout volatilized Na. Neither BCR-1 or fallout was observed to volatilize K in overlapping raster analyses. Data are tabulated in Table E.1 in Appendix E.

and frequency (discussed in Chapter 3). Second, high-magnification quantitative X-ray maps were collected over compositional interfaces between agglomerates and hosts to characterize the behavior of major elements at the interface (discussed in Chapter 8).

To collect EDS X-ray maps, a field of view is subdivided into pixels, over which the primary electron beam is rastered. An X-ray spectrum is collected in each pixel, independently fit, the background independently subtracted, and characteristic X-ray peaks independently integrated to determine the number of counts of each element in that pixel. These maps may also be quantified, but the Bruker's ESPRIT 2 software does not output an uncertainty in this case. Due to the large number of pixels in an image (often exceeding several million) and the short dwell time per pixel (typically set to 8 μs/pixel), one needs to collect maps for several days for large samples to obtain a high signal-to-noise ratio, which can be time prohibitive. There are several alternatives. First, descriptive (qualitative) X-ray maps, particularly for the most abundant elements, Si and Al, can be obtained on the order of hours. Second, when mapping at higher magnification and lower pixel resolution, sufficient counts per pixel, even for minor elements, can be achieved on the order of hours, particularly when averaging multiple adjacent pixels (*i.e.*, using pixel smoothing).

Whole sample mapping

Interfaces between host objects and agglomerates are usually, but not always, easily visible in BSE images (Figure 4.8) [68]. X-ray maps can be used to definitively locate agglomerates that are difficult to identify using BSE images alone because many interface compositions do not appreciably deviate in $\bar{Z}$ from the bulk average (Figure 4.8). X-ray maps used to identify and count agglomerated objects were typically collected for between 15–24 hours at currents

sufficient to increase the deadtime to ∼50% (spot size 5.5 or 6.0). The resolution of these maps depended on the sample, but were approximately 1800x1800 pixels at magnifications above 100x (minimum field of view is ≈2.4x2.4 mm). These operating conditions were sufficient to resolve agglomerates ∼5–10 μm in diameter. Images of larger samples were stitched together from multiple maps. Al maps were used to identify agglomerates because of the relatively high abundance of Al in these samples (∼13 wt.% Al_2O_3 in the glassy regions of fallout) and the consistent observed depletion across both CaMgFe and Si interfaces. Examples of whole sample Al compositional X-ray maps are shown in Figure 4.9.

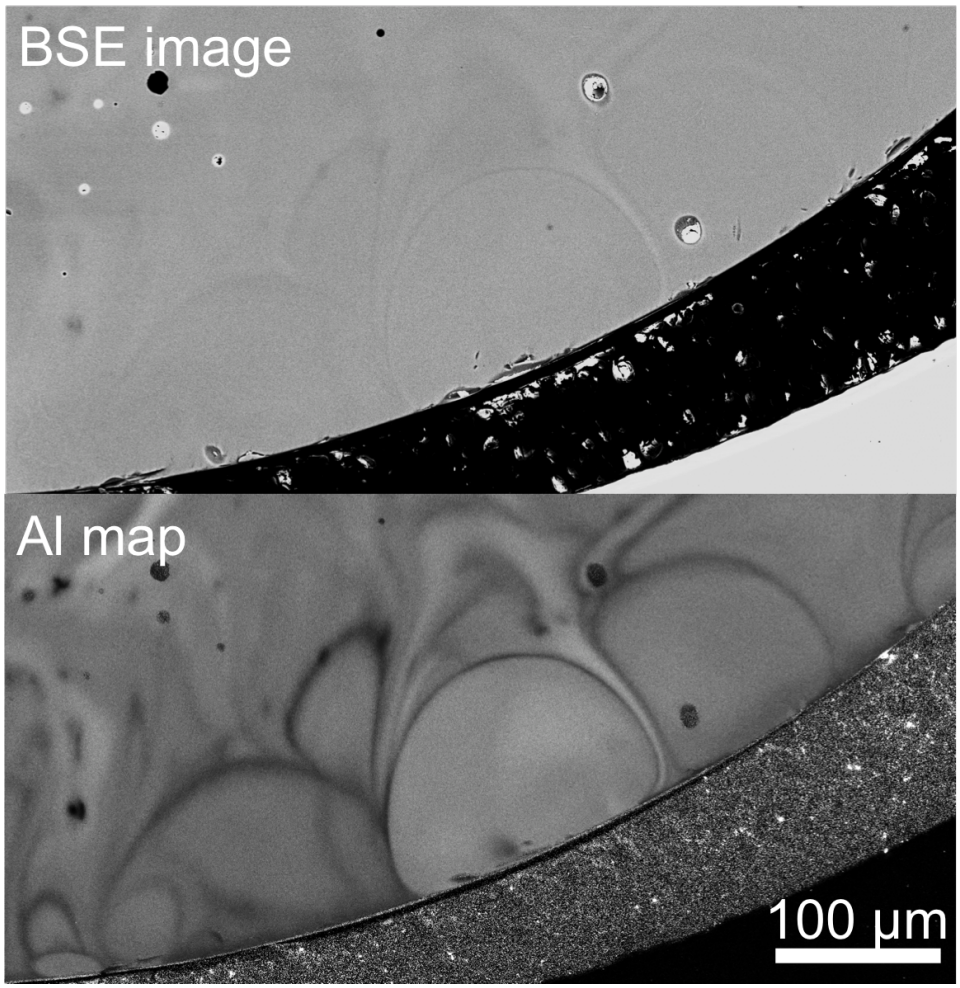

Figure 4.8: Comparison between a BSE image (top) and Al X-ray compositional map (bottom) of the same location at the periphery of sample U3. The compositional interfaces of surface agglomerates are more visible in the Al X-ray compositional map.

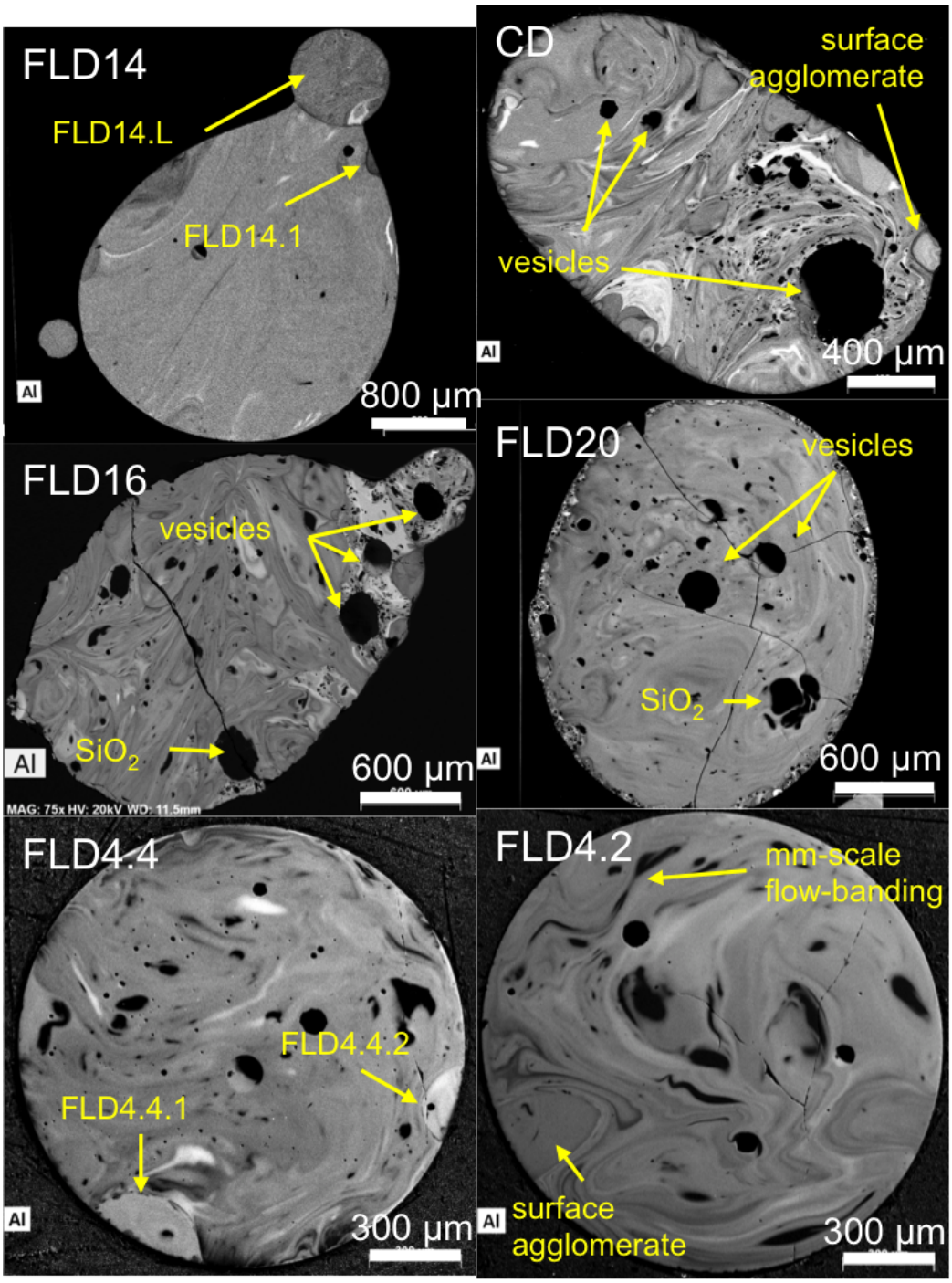

Figure 4.9: Examples of Al compositional X-ray maps of select samples. These types of maps are used to identify agglomerates and qualitatively characterize textures and morphology in cross-sections of fallout. Examples of features common in fallout cross-sections such as agglomerates, vesicles, flow-banding, and high SiO_2 regions (unmelted or partially-melted quartz) are noted. Agglomerates characterized in this study are also noted.

Interface mapping and line scans

Quantified, high-magnification compositional X-ray maps were collected to determine the composition of interfaces between agglomerates and hosts (discussed in Chapter 8). The magnification of these maps varied, but were sufficient to resolve ∼10–20 μm on either side of the interface.

Each quantified map of an interface was collected until pixels at the interface contained at least 1000 background-subtracted counts of Si and several hundred counts of Al (∼2–3 hours). Other elements such as Fe, Ca, and Al contained ∼30 counts per pixel. After the maps were quantified, ImageJ image analysis software was used to extract line profiles of pixel values in a direction perpendicular to the interface [86]. Line profiles were smoothed using 50 pixels or more to estimate and reduce the uncertainty of the line profiles. The smoothed scans were extracted at regions along the interface that showed the least amount of curvature to avoid artificially increasing the apparent width of the interface (Figure 8.3). The location of the profile was selected to transect regions that were approximately homogeneous on both the agglomerate and host side of the interface.

As previously noted, Bruker's ESPIRIT 2 software does not calculate uncertainties for quantified compositional X-ray maps. To estimate the uncertainty of each smoothed step in the line scan, a one pixel wide line scan whose length was equal to the number of pixels used for smoothing was drawn perpendicular to the line scan across the interface. To estimate the uncertainty of the line profile, the standard error of the mean (SEOM) of these samples was calculated (≥20 samples, depending on the number of smoothed pixels). The uncertainties presented in tables and figures of extracted traverses of compositional interfaces from quantified X-ray compositional maps are the 2 times the standard error the mean (2SEOM). These data are presented and discussed in Chapters 8 and 9.

4.5 The major element composition of host objects

Host object compositions were measured using 3,698 EDS raster analyses collected in grid patterns across 37 samples. Table 4.4 shows the mean composition of these analyses, Table 4.6 shows the mean composition of these analyses for each sample, and Figure 4.10 shows the distributions for each of the major element oxides from these measurements as kernel density estimates (KDEs).

The mean major element composition of host objects

In terms of exposed cross-sectional area, the host objects dominate the population compared to agglomerates (discussed in Chapter 3). Therefore, major element compositions of host objects are largely representative of the fallout population as a whole. The average composition of the host objects is rich in SiO_2, which is present at 73.8 ± 4.1 wt.% oxide (mean ± 1σ; Table 4.4). The next most abundant oxide is Al_2O_3, present at an average concentration of 13.6 ± 2.1 wt.%, followed by the alkali oxides with K_2O slightly enriched

on average compared to Na_2O (averages of 3.8 ± 0.7 and 3.3 ± 0.7 wt.%, respectively). On average, FeO and CaO are present at similar concentrations: 2.8 ± 0.8 and 2.1 ± 1.0 wt.%, respectively, and MgO and TiO_2 are present at under 1 wt.%, with average concentrations of 0.6 ± 0.3 and 0.3 ± 0.2 wt%, respectively.

TiO_2, MgO, and CaO have the largest RSDs, varying between 44.3 and 53.7%. The large RSD for TiO_2 and MgO can be explained, at least in part, by their large analytical uncertainties due to their low abundances. The analytical uncertainties on MgO and TiO_2 are approximately 15% 1σ relative (mean relative 1σ uncertainties are 17.7 and 12.8%, respectively). In contrast, the mean analytical uncertainty on CaO is 4.8% 1σ relative. The RSD of the average composition of CaO instead reflects Ca heterogeneity among the glassy, partially-melted, and unmelted phases of the analyzed fallout samples (best shown in Figure 4.10).

Table 4.4: Mean oxide values for major elements collected from 3,698 EDS raster measurements on 37 host fallout glasses.

Oxide	Mean (wt.%)	1σ (wt.%)	1RSD (%)
SiO_2	73.77	4.12	5.58
Al_2O_3	13.59	2.16	15.92
Na_2O	3.26	0.70	21.51
K_2O	3.80	0.70	18.49
CaO	2.12	0.99	46.93
FeO	2.77	0.76	27.61
TiO_2	0.32	0.17	53.74
MgO	0.60	0.26	44.32

Kernel density estimates of major element concentrations in host objects

Kernel density estimates (KDEs) show the distribution of each of the measured major element oxides across the 37 characterized hosts (Figure 4.10). KDEs are a smoothed approximation of a distribution using point data (essentially, a smoothed histogram). The method is non-parametric, making few assumptions about the underlying data except the shape of the kernel (Gaussian, rectangular, triangular, etc.) and the bandwidth (analogous to bin widths in histograms). Given the assumption of Gaussian uncertainties for analyses performed by EDS, a Gaussian kernel is used here. The bandwidths are determined independently for each element based on the variance in the overall (n = 3,698) EDS host dataset for that variable, following Ward and Jones' "oversmoothed bandwidth selector" [99]. These bandwidths are applied to all subsequent histograms and KDEs overlaid with host grid analyses KDEs shown in Figure 4.10. The bandwidths are 0.44 for SiO_2, 0.16 for Al_2O_3, 0.08 for Na_2O, 0.06 for K_2O, 0.09 for CaO, 0.05 for FeO, 0.01 for TiO_2, and 0.03 for MgO.

The Gaussian KDEs of the measured compositions reveal primarily unimodal distributions, except for CaO, which has peaks near 0, at 1.81 wt.%, and 3.31 wt.%. As previously observed by CaO's high RSD, the multiple CaO peaks visible using the KDE approach confirms the high degree of Ca heterogeneity in these fallout samples.

The tails of all the individual KDE distributions are long, suggesting the presence of outliers, likely unmelted or partially-melted mineral compositions. In the case of K_2O, CaO, FeO, TiO_2, and MgO the range of the x-axis was truncated, excluding a total of 54 analyses, to show the details of the distribution instead of the extent of the scaling towards anomalous measurements rich in these oxides. The ranges of K_2O, CaO, FeO, TiO_2, and MgO compositions extend to 10.1, 10.2, 16.1, 5.8 and 6.9 wt.%, respectively. The outliers were measured on samples FLD3.2, FLD9, FLD10, and FLD11, which appear (via BSE images and X-ray compositional maps) to contain large unmelted and partially-melted regions. However, in the case of K_2O, most of the outlying measurements were performed on sample FLD25, which contains a melted, felsic composition. The significance of these outlying compositions are discussed more below and in Chapter 6.

The relative uniformity of the distributions in Figure 4.10 suggests that relatively similar mixing between similar starting materials (mineral phases) occurred across all 37 samples, particularly with respect to SiO_2, Al_2O_3, Na_2O, K_2O, and FeO. The multimodal features in CaO suggest that there were multiple sources of CaO incorporated into the fallout glasses. In particular, the resolvable peaks at 1.81 and 3.31 wt.% CaO suggest at least two major sources of Ca contributed to the CaO observed in this fallout population.

Comparison of major element dissolution analyses with spatially-resolved data

Figure 4.10 also shows the mean $\pm$ 2σ values for dissolution measurements of glassy fallout from the same nuclear test from [100]. Using ICP-MS, 81 glassy fallout samples ranging in mass from 0.03 to 205 mg (compared to the range of 2.5 to 193 mg for the 23 of 49 samples that were massed in this study; Table 2.1) were dissolved and analyzed for major and trace elements by Dr. Josh Wimpenny of LLNL. Each measurement represents the average composition of an entire sample. Due to the ICP-MS analytical procedure, the Si concentration was not directly measured, but instead was was determined by difference of the other elements present at the percent level (including Mn, which is present at an average of 0.09 wt.% oxide). Therefore, the ICP-MS major element composition is constrained to sum to 100.

The mean values for major element oxides based on the spatial EDS measurements (this study) and those determined by bulk dissolution measurements (Wimpenny et al., *in draft*) agree within 1σ (Table 4.5). These data highlight the utility of spatial compositional analyses—on average, the EDS data reflect the bulk composition of fallout, yet measure a greatly expanded range of compositions that would otherwise be obscured. Finally, the strong agreement between host object EDS data and bulk dissolution data suggests that the

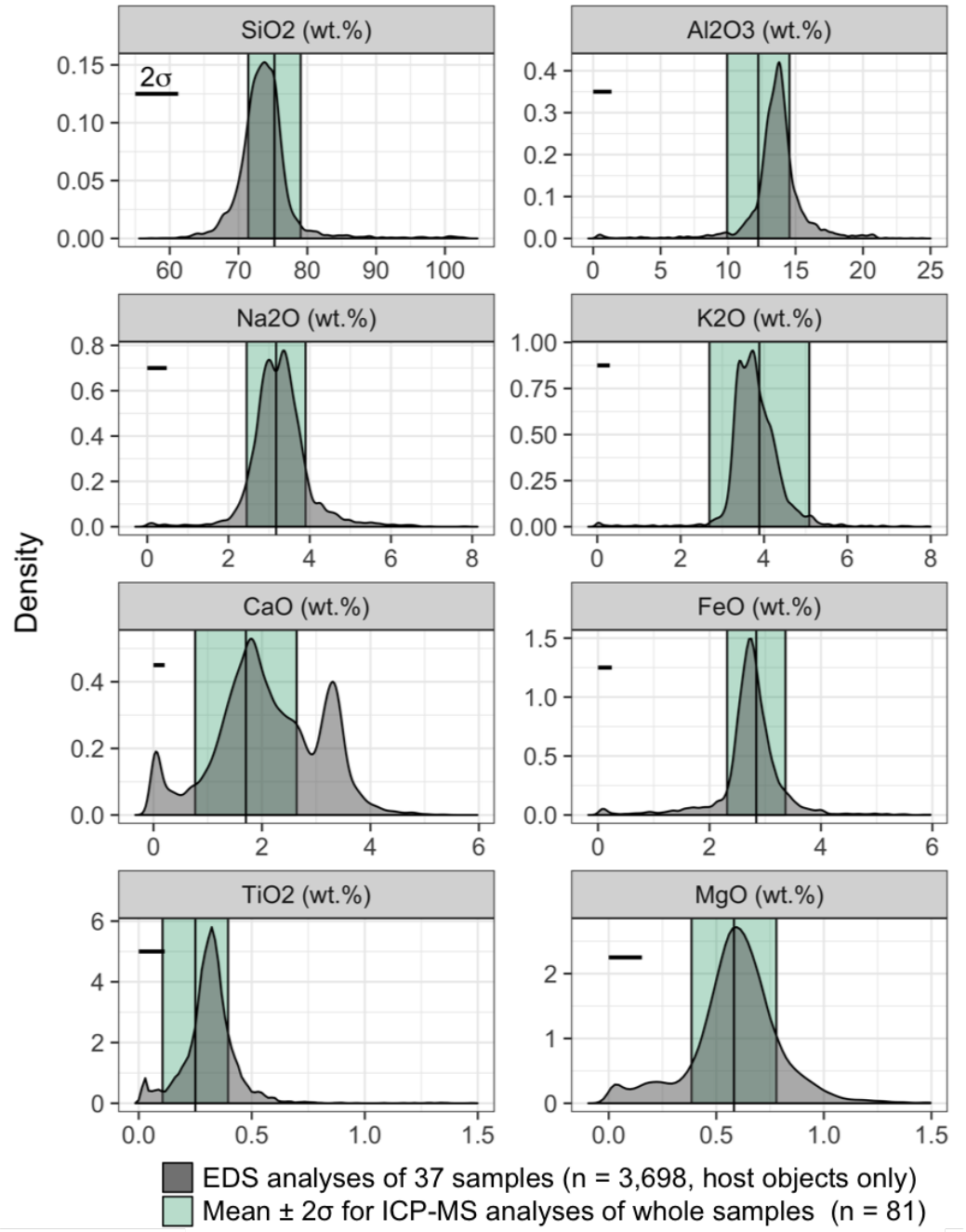

Figure 4.10: Kernel density estimates of the host compositions measured with EDS for this study (data tables in Appendix B). Fifty-four analyses are excluded from this figure to allow the peaks of the distributions to be easily viewed and compared to other major element oxides (see text for discussion). The green band denotes the mean ± 2σ of 81 ICP-MS analyses of wholly dissolved pieces of fallout from this test [100]. The bar in the top left of each plot shows the mean analytical 2σ uncertainty for a single representative EDS measurement for that major element oxide.

assumption of using spatial data as a proxy for bulk fallout data is appropriate, at least for the characterization of major element compositions.

The RSDs of the mean of the bulk dissolution data are typically lower than the EDS composite data by a factor of two or more, except in the case of K_2O (15.4% for the bulk data compared to 18.7% for the EDS data). However, in both datasets CaO still has one of the highest RSDs (27.6% for bulk data and 47.2% for EDS data), despite being present at the percent level. This is in comparison to Mg and Ti, whose maximum measured concentrations were 0.86 wt.% MgO and 0.43 wt.% TiO_2 in the bulk dissolution dataset, yet have comparable RSDs to CaO. These results reinforce the presence of a large degree of Ca heterogeneity from sample to sample and that there likely are multiple sources of Ca-rich minerals in the soil that contribute to the CaO heterogeneity ultimately measured in the glassy fallout. CaO must have been incorporated into different samples in differing amounts. This behavior is in contrast to other oxides present at the several percent level or greater, which appear to be relatively well-mixed amongst the sample suite, as exemplified by the quasi-unimodal behavior of their KDEs (Figure 4.10).

Table 4.5: Comparison between EDS measurements on host objects (this study) and bulk dissolution measurements of fallout measured using ICP-MS [100].

	Host object EDS Data (n = 3,698)			Bulk ICP-MS Data (n = 81)		
Oxide	Mean	±	1σ	Mean	±	1σ
SiO_2	73.77	±	4.07	75.22	±	1.90
Al_2O_3	13.59	±	2.16	12.24	±	1.16
Na_2O	3.26	±	0.70	3.17	±	0.36
K_2O	3.80	±	0.71	3.89	±	0.60
CaO	2.12	±	1.00	1.70	±	0.47
FeO	2.76	±	0.78	2.84	±	0.26
TiO_2	0.32	±	0.18	0.25	±	0.07
MgO	0.60	±	0.27	0.58	±	0.10

Major element compositions of individual hosts

The average major element compositions of individual samples (based on EDS rasters performed in a grid pattern across individual objects) shows that most sample compositions largely mirror the overall KDEs (Figure 4.11 and Table 4.6). However, there are several samples whose average compositions contain outliers of potential significance (noted in Figure 4.11).

The average CaO compositions obtained from individual samples span a wide range, from values as low as 0.86 wt.% CaO in FLD3.2, a sample observed to primarily contain unmelted or partially-melted regions, to values as high as 3.34 wt.% CaO in FLD14, a sample observed

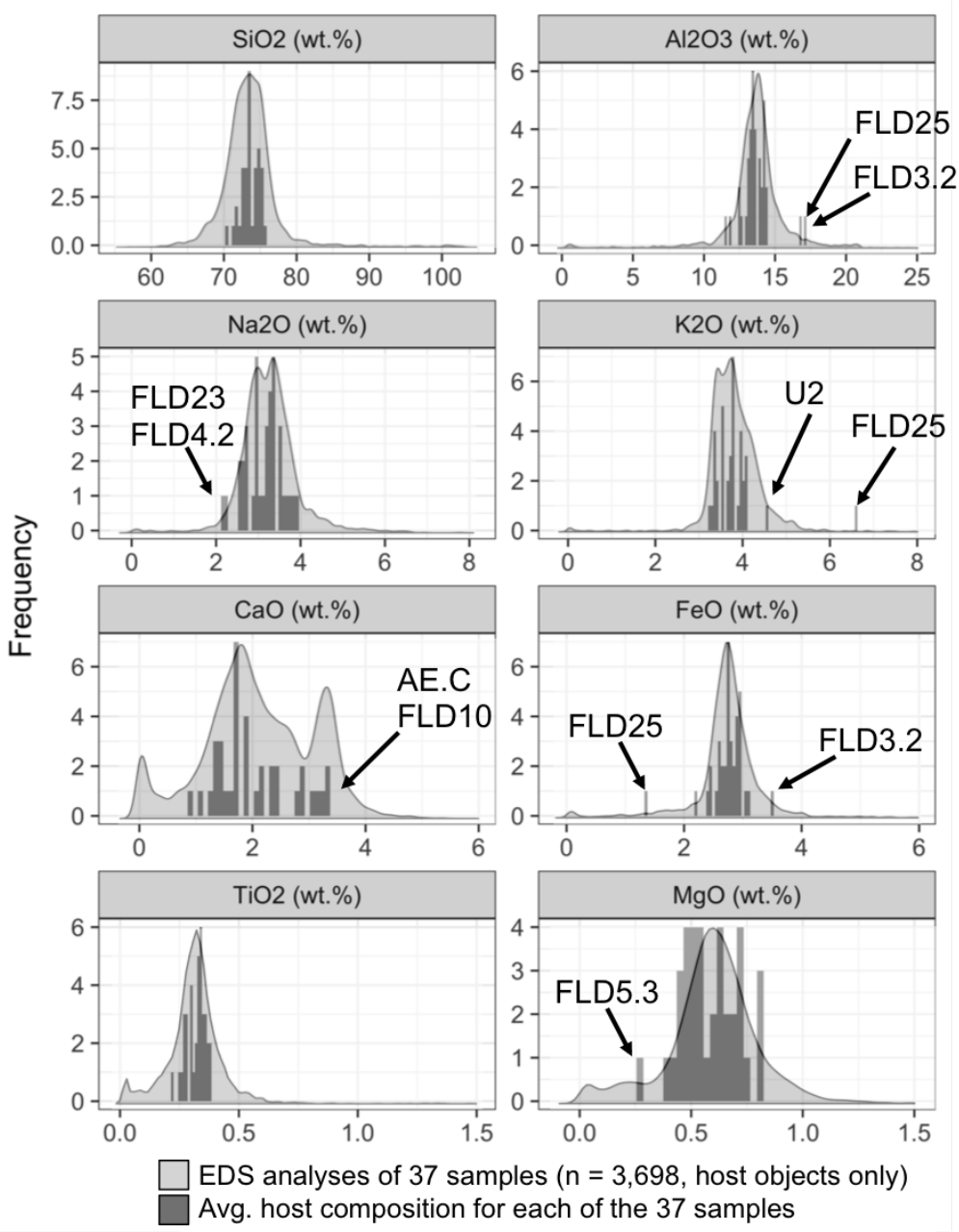

Figure 4.11: Histogram showing the average host object composition overlaid with the host KDE from Figure 4.10. The maximum of each KDE has been scaled to match the maximum of the histogram in each panel. The binwidth for each major element is the same as the bandwidth for the KDE (as noted in the text). The third peak in the CaO KDE is due to the large percentage of EDS grid analyses (≈19% of the total) that were performed on samples with average CaO concentrations >3 wt.%. While the majority of samples have similar average compositions, there are notable outliers in the FeO, K_2O, and Al_2O_3 panels. Average host compositions are tabulated in Table 4.6 and the EDS raster data used for the host KDEs are tabulated in Appendix B.

in its X-ray compositional map to be well-mixed and glassy (*i.e.*, composed of a mixture of compositions that melted, inhomogeneously mixed, and subsequently quenched). This wide variation in average CaO composition from sample to sample helps explain the width of the sample population's KDE. The third peak in the CaO KDE at 3.31 wt.% is likely due to a few samples with a high CaO content, again suggesting a heterogeneous distribution of Ca in the precursor soil, and subsequently, in the samples (Figure 4.11). There are five samples with mean CaO concentrations greater than 3% (samples FLD13, FLD14, FLD15, FLD20, and FLD21; Table 4.6). In total, there were 693 retained EDS analyses on these fives samples, representing nearly 19% of the total number of host EDS analyses. This suggests that even when considering average composition on a per samples basis, inter-sample variation (at least in oxides such as CaO for this sample population) should be considered.

The four host objects most enriched in CaO (FLD14, FLD13, FLD21, and FLD15; Table 4.6) all also appear compositionally well-mixed in compositional X-ray maps (Appendix A), which is confirmed by their relatively small CaO 1RSDs: 5.2%, 5.3%, 15.3%, and 9.0%, as compared to the sample average 1RSD for CaO of 32.2%. This suggests that samples that were more extensively heated or spent longer in the fireball had more of an opportunity to incorporate and homogenize any mineral or other sources of CaO into their volume.

Table 4.6: Mean compositions of host objects calculated from the grid-based EDS raster analyses sorted by equivalent diameter.

	Sample	n	Equiv. d (mm)	SiO_2	1σ	Al_2O_3	1σ	Na_2O	1σ	K_2O	1σ	CaO	1σ	FeO	1σ	TiO_2	1σ	MgO	1σ
	Mean	**3698**	–	**73.77**	**4.07**	**13.59**	**2.16**	**3.26**	**0.70**	**3.80**	**0.70**	**2.12**	**0.99**	**2.77**	**0.76**	**0.32**	**0.17**	**0.60**	**0.27**
1	FLD9	393	7.27	72.55	4.35	13.98	2.39	3.38	0.65	3.94	0.57	2.03	0.85	2.96	0.77	0.35	0.15	0.63	0.44
2	FLD13	264	4.67	75.23	1.18	13.87	0.43	2.95	0.13	3.36	0.10	3.31	0.18	2.64	0.13	0.27	0.06	0.58	0.04
3	FLD11	164	4.46	73.12	3.97	14.38	2.09	3.49	0.51	3.98	0.53	2.88	1.38	2.95	0.62	0.36	0.11	0.80	0.55
4	FLD10	343	4.40	74.59	6.79	12.48	3.27	3.81	1.22	3.97	0.96	1.34	1.20	2.80	1.79	0.30	0.47	0.38	0.28
5	FLD12	219	3.21	73.01	2.96	14.26	1.59	3.52	0.41	4.09	0.45	1.67	0.48	2.94	0.50	0.36	0.11	0.72	0.18
6	FLD14	89	2.89	75.14	0.85	14.21	0.38	2.91	0.13	3.35	0.11	3.34	0.17	2.77	0.12	0.25	0.05	0.61	0.04
7	AA.B	174	2.82	74.85	4.64	12.52	2.02	3.38	0.58	3.52	0.57	1.72	0.41	2.44	0.39	0.27	0.05	0.67	0.08
8	FLD15	144	2.45	73.40	1.21	12.91	0.39	3.34	0.12	3.75	0.11	3.15	0.28	2.74	0.12	0.30	0.03	0.55	0.05
9	AG.D	127	2.41	75.21	4.80	13.49	2.43	2.97	0.57	3.54	0.66	1.92	0.56	2.68	0.50	0.32	0.08	0.62	0.14
10	U3	72	2.37	73.40	1.98	13.28	0.71	2.99	0.27	3.77	0.19	2.75	0.61	2.92	0.30	0.33	0.05	0.71	0.10
11	FLD17	39	2.35	74.14	2.15	13.63	1.34	3.31	0.28	3.98	0.37	2.34	0.57	2.71	0.33	0.28	0.06	0.61	0.11
12	AH.E	55	2.30	75.18	1.67	13.68	0.90	3.61	0.34	3.75	0.18	1.22	0.40	3.03	0.18	0.36	0.07	0.76	0.17
13	FLD20	105	2.29	74.35	4.76	13.05	2.19	3.30	0.58	3.77	0.65	3.03	0.71	2.67	0.48	0.33	0.08	0.68	0.11
14	U4	74	2.23	71.56	1.47	14.39	0.98	2.96	0.26	3.55	0.21	2.91	0.82	2.87	0.15	0.34	0.05	0.63	0.05
15	AE.C	188	2.22	73.61	4.33	13.27	2.13	3.91	0.76	4.07	0.62	1.44	0.75	2.75	0.50	0.30	0.10	0.55	0.22
16	FLD16	75	2.15	73.58	3.31	14.06	1.76	3.03	0.50	4.00	0.35	1.62	0.43	2.96	0.45	0.38	0.11	0.64	0.15
17	FLD23	47	1.93	74.96	7.64	11.47	3.30	2.13	0.58	3.54	0.90	1.92	0.70	2.38	0.67	0.27	0.08	0.50	0.15
18	FLD18	90	1.82	73.79	3.33	13.44	1.52	3.13	0.50	3.80	0.49	2.40	0.60	2.77	0.32	0.33	0.06	0.71	0.17
19	CD	79	1.82	73.19	2.47	14.31	1.30	3.18	0.32	3.80	0.36	1.75	0.42	2.93	0.38	0.37	0.09	0.69	0.14
20	FLD21	91	1.78	74.85	2.21	13.53	0.99	2.98	0.21	3.51	0.23	3.25	0.50	2.59	0.20	0.28	0.07	0.72	0.08
21	CC	97	1.76	73.53	4.74	13.49	2.36	3.39	0.55	3.88	0.56	2.12	0.55	2.92	0.53	0.34	0.10	0.65	0.16
22	U1A	60	1.58	72.79	2.41	13.49	0.98	3.26	0.40	3.38	0.25	1.86	0.30	2.88	0.21	0.31	0.04	0.46	0.05
23	U2	67	1.54	73.45	2.17	13.15	0.92	3.33	0.43	4.57	0.39	1.42	0.76	2.19	0.78	0.28	0.10	0.48	0.23
24	FLD3.1	70	1.52	74.77	2.71	14.31	1.25	2.62	0.27	3.77	0.25	1.75	0.54	2.79	0.30	0.35	0.07	0.55	0.19
25	FLD3.3	62	1.51	75.59	1.48	13.91	0.65	2.56	0.19	3.67	0.18	1.92	0.39	2.75	0.15	0.33	0.04	0.47	0.07
26	FLD4.2	49	1.48	73.62	3.87	14.20	1.98	2.26	0.23	3.40	0.18	1.68	0.37	2.45	0.27	0.30	0.05	0.43	0.09
27	FLD4.3	55	1.47	71.72	2.41	14.07	1.55	3.22	0.47	4.01	0.20	1.69	0.61	3.11	0.27	0.38	0.08	0.82	0.22
28	FLD4.1	69	1.46	73.54	2.16	13.33	0.81	2.68	0.15	3.44	0.15	2.45	0.25	2.58	0.17	0.32	0.04	0.51	0.06
29	FLD4.4	61	1.42	74.49	3.71	13.48	2.12	2.53	0.29	3.31	0.31	2.17	0.46	2.92	0.30	0.35	0.07	0.80	0.21
30	FLD3.2	33	1.40	71.48	7.73	17.16	4.37	2.71	0.91	3.71	1.22	0.86	0.44	3.48	1.79	0.37	0.18	0.45	0.25
31	FLD25	47	1.39	70.46	3.17	16.82	3.34	3.67	0.52	6.61	1.99	2.38	1.62	1.36	1.01	0.22	0.08	0.44	0.21
32	U1B	60	1.34	72.66	3.92	13.65	1.92	3.55	0.53	3.36	0.35	1.39	0.27	2.84	0.29	0.34	0.07	0.55	0.07
33	FLD5.3	31	1.10	73.30	2.32	11.89	1.03	3.75	0.32	4.10	0.21	1.12	0.88	2.74	0.27	0.26	0.09	0.28	0.19
34	FLD5.2	36	1.10	72.67	3.69	13.08	1.82	3.17	0.40	3.76	0.34	1.43	0.38	2.61	0.47	0.34	0.10	0.48	0.14
35	FLD5.5	18	1.01	73.11	1.86	13.36	1.40	2.65	0.33	3.76	0.32	1.31	0.38	2.56	0.40	0.33	0.10	0.47	0.12
36	FLD5.1	27	0.99	74.24	6.43	12.58	2.98	2.69	0.56	3.26	0.69	1.49	0.43	2.75	0.63	0.34	0.09	0.51	0.13
37	FLD5.4	24	0.94	72.28	5.26	13.42	3.13	3.32	0.52	3.65	0.40	1.69	0.81	2.78	0.45	0.34	0.10	0.51	0.16

The outliers in the KDE plots of Al_2O_3, K_2O, and FeO belong to samples FLD25, FLD3.2, and U2. The outlying compositions in FLD3.2 were sampled in locations that contain large regions that appear, through visual inspection of its compositional maps, to be unmelted or partially-melted (and contain little to no radioactivity), so EDS measurements in these regions likely reflect unmelted minerals derived from soil (Figure 2.17 shows the autoradiograph for FLD3.2). Figure 4.12 outlines these regions using a Ca compositional map for U2, Al compositional map for FLD25, and BSE image for FLD3.2.[6] In contrast, the outlying compositions in U2 and FLD25 were measured in compositional regions that appear partially melted in EDS compositional maps (Figure 4.12) and contain radioactivity in their respective autoradiographs (Figures 2.19 and 2.16), albeit with less intensity relative to the rest of the sample. These observations indicate these compositional regions were heated thoroughly enough by the fireball to melt and partially incorporate some radionuclides from the vapor phase. These two observations suggest that these outlying compositional regions in U2 and FLD25 retain compositions more representative of an unmelted mineral compositions in soil and incorporated relatively little radionuclides into the melt compared to other regions in these samples. Such a situation could occur relatively late in the fireball formation process or at the periphery of the fireball, when and where the concentration of radionuclides in the vapor term is relatively low.

To quantitate the U isotope composition of the outlying major element composition region in U2, SIMS measurements were conducted in this region by Lewis et al. (2015) [60]. While all U isotope measurements in this region of U2 were enriched relative to natural ($0.02 < {}^{235}U/{}^{238}U < 1$), the U isotope ratios measured in this region are amongst the lowest enrichments measured in fallout from this event (U isotope compositions in fallout is discussed further in Chapter 5) [60, 67, 101].

4.6 The major element composition of agglomerates

The composition of the characterized agglomerates overlaps that of the host object population (and the bulk sample compositions measured via ICP-MS) within 1σ (Tables 4.7, 4.8, and Figure 4.13). Fifty-eight agglomerates in 15 samples were characterized by EDS raster analyses. Despite overall compositional similarity to host objects, agglomerate compositions span a more restricted range. This suggests that agglomerates contain few unmelted and partially-melted regions, consistent with textural observations (Chapter 3 and Appendix A),indicating agglomerates were thoroughly transformed in the fireball. Similarly, the histograms of the average compositions measured in agglomerates largely overlaps those of the host object KDEs (Figure 4.13). This demonstrates that the agglomerate compositions are not greatly different from the host objects, except that agglomerate compositions span a

[6]Samples FLD9 and FLD10 also contain large partially-melted and unmelted regions, but do not appear as outliers because the measurements in these host objects also include large areas of glassy regions. The resulting mean major element compositions of FLD9 and FLD10 collected by EDS is close to the collective host object mean.

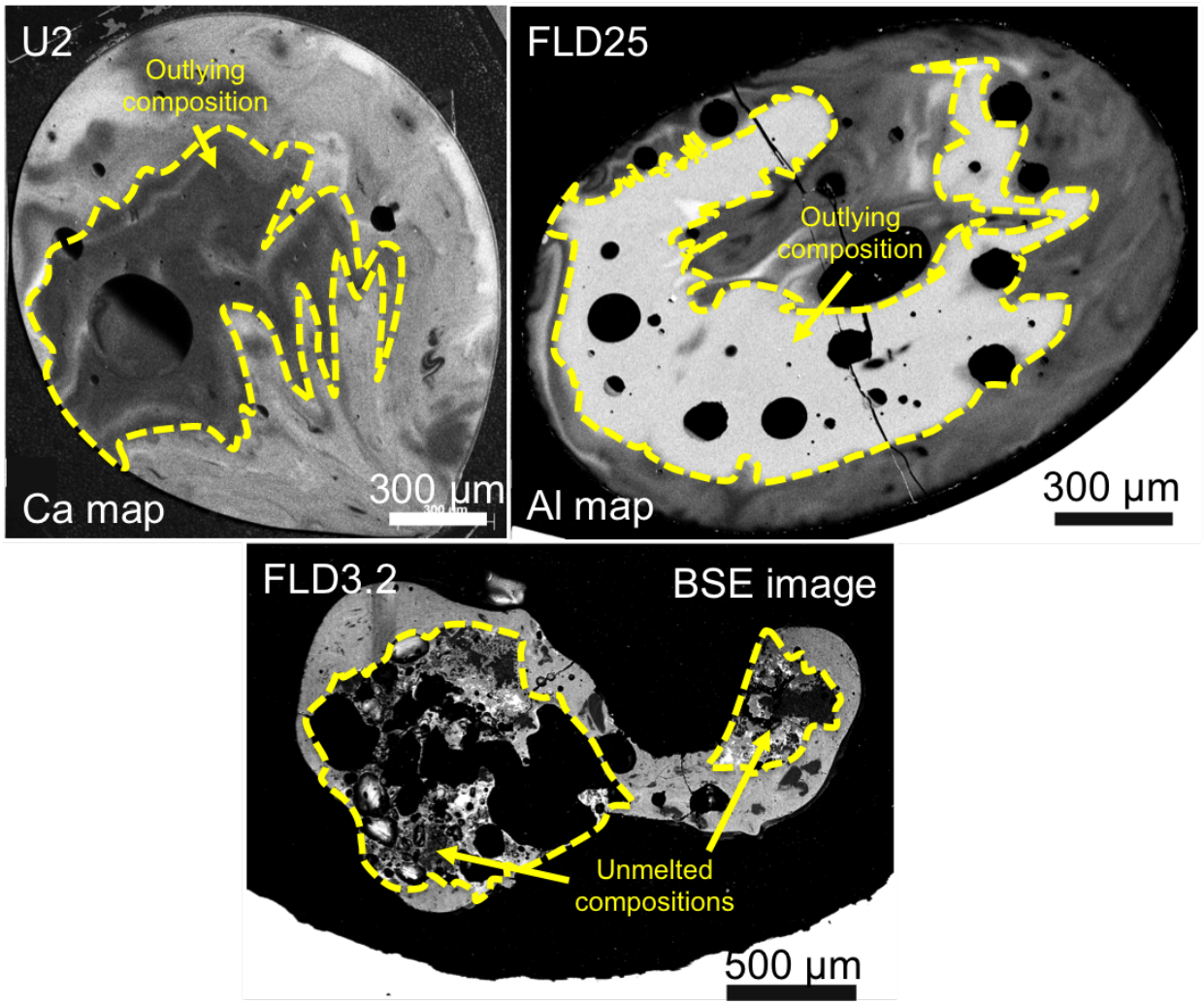

Figure 4.12: Ca map of sample U2, Al map of sample FLD25, and BSE image of sample FLD3.2 highlighting outlying compositional regions in each of these samples. The outlying compositional regions in U2 and FLD25 are glassy, while the outlying composition in FLD3.2 contains unmelted and partially-melted mineral textures and is highly vesiculated. The outlying compositions correspond to the low activity regions in the autoradiographs of U2 and FLD25 autoradiographs (Figures 2.19 and 2.16) and the region nearly devoid of activity in FLD3.2 (Figure 2.17).

narrower range. Notable exceptions are the Na_2O and K_2O content of the agglomerates, which, on average, have lower concentrations than those observed in the host objects (Table 4.7; the means are still well within 1σ of each other). This difference in alkali compositions are explored further below to determine if agglomerates experienced significant volatile loss.

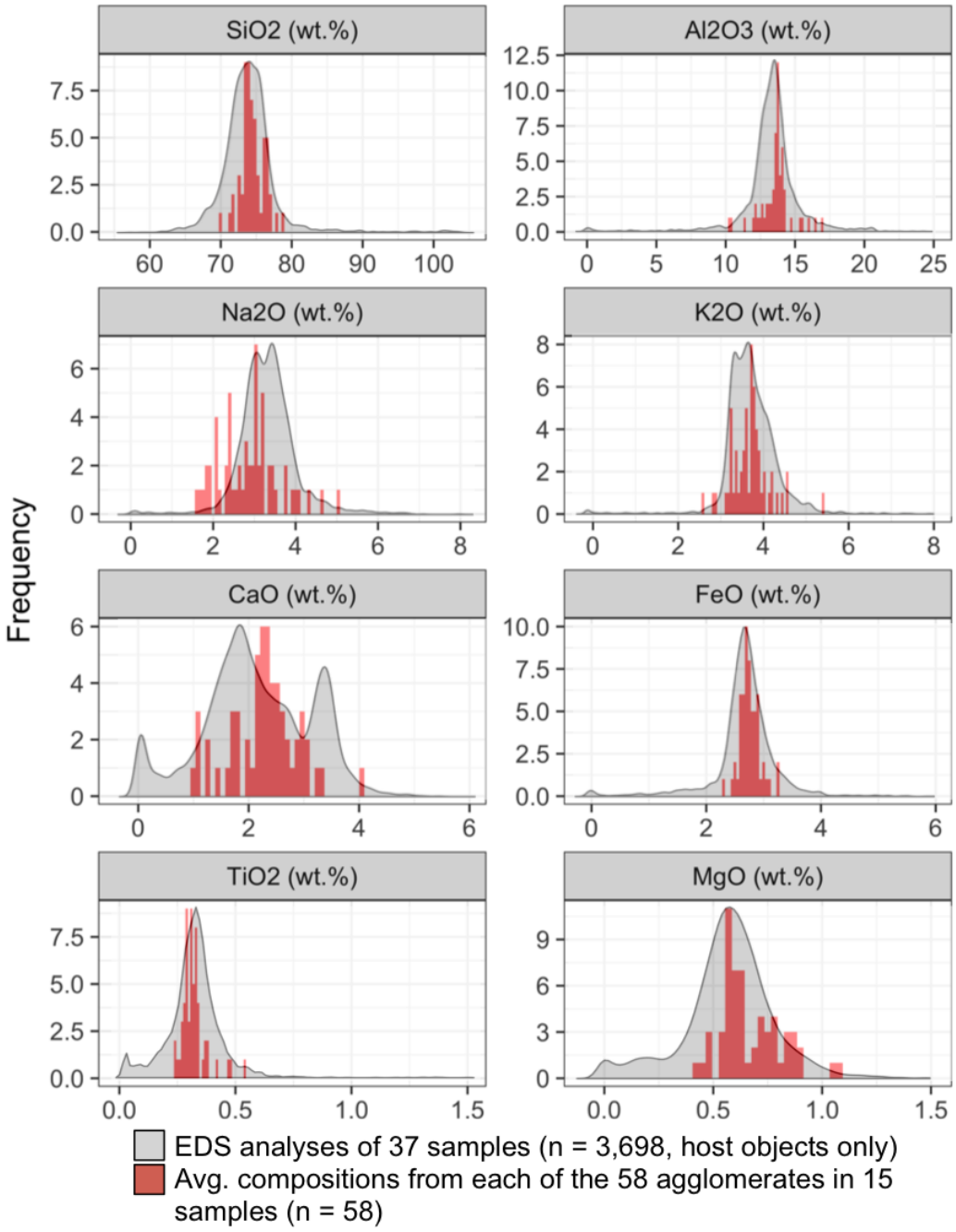

Figure 4.13: Smoothed histograms of the host compositions (shown in grey; data tabulated in Appendix B) with overlaid histograms of average compositions of individual agglomerates (shown in red; data tabulated in Table 4.8). Distributions of agglomerate compositions largely overlay host compositions. CaO appears more unimodal, likely because agglomerates are more well-mixed.

Table 4.7: The mean compositions of host object population ($n = 3,698$) and agglomerate population ($n = 679$) from EDS raster measurements.

	Host composition			Agglomerate composition		
Oxide	Mean	±	1σ	Mean	±	1σ
SiO_2	73.77	±	4.07	74.19	±	2.34
Al_2O_3	13.59	±	2.16	13.75	±	1.34
Na_2O	3.26	±	0.70	3.02	±	0.73
K_2O	3.80	±	0.71	3.59	±	0.45
CaO	2.12	±	1.00	2.40	±	0.63
FeO	2.76	±	0.78	2.74	±	0.27
TiO_2	0.32	±	0.18	0.31	±	0.07
MgO	0.60	±	0.27	0.68	±	0.14

Major element compositions of individual agglomerates

Several agglomerates have mean compositions that fallout outside of the general distribution (Figure 4.13 and Table 4.8). For example, agglomerate FLD21.L, a surface agglomerate in sample FLD21, has a mean CaO concentration nearly 70% higher than the mean CaO concentration from all EDS raster analyses within agglomerates (Tables 4.7 and 4.8). The other characterized agglomerate on sample FLD21, FLD21.1, is also enriched in CaO relative to the agglomerate mean of CaO (3.06 wt.% CaO, nearly 30% greater than the agglomerate mean). This deviation is less notable when compared to the mean CaO concentration of the host object FLD21 (3.25 ± 0.50 wt.%; Table 4.6). In this case, agglomerate FLD21.1 is depleted relative to host object FLD21 by ∼-6% and agglomerate FLD21.L enriched by 24% relative to host object FLD21. Comparing agglomerates to the hosts to which they are attached may provide a more accurate basis for understanding general differences (or similarities) in the compositions of the host object and agglomerate population.

Table 4.8: Mean compositions of agglomerates measured using n EDS raster analyses across the agglomerates sorted by equivalent diameter. The first row shows the mean of all EDS raster analyses within all agglomerates.

	Sample	Agglomerate	n	Equiv. d (μm)	SiO_2	1σ	Al_2O_3	1σ	Na_2O	1σ	K_2O	1σ	CaO	1σ	FeO	1σ	TiO_2	1σ	MgO	1σ
	Mean	**Mean**	**679**	–	**74.19**	**2.34**	**13.75**	**1.34**	**3.02**	**0.73**	**3.58**	**0.45**	**2.40**	**0.63**	**2.74**	**0.27**	**0.31**	**0.07**	**0.68**	**0.14**
1	FLD10	FLD10.L	30	1089	73.93	1.31	13.11	0.33	3.07	0.18	3.61	0.16	2.27	0.18	2.81	0.13	0.33	0.05	0.49	0.04
2	FLD14	FLD14.L	75	856	74.21	1.54	13.73	0.63	2.99	0.29	3.43	0.15	3.26	0.28	2.64	0.09	0.29	0.04	0.68	0.13
3	AA.B	B3	56	590	73.34	1.82	13.46	0.96	3.80	0.39	3.66	0.24	2.35	0.27	2.51	0.16	0.27	0.05	0.74	0.05
4	U4	U4.1	13	553	74.46	1.33	13.79	0.36	2.29	0.33	3.26	0.12	2.36	0.10	2.91	0.10	0.28	0.05	0.63	0.04
5	FLD23	FLD23.L	8	498	73.33	0.47	12.95	0.33	2.05	0.15	3.36	0.22	2.98	0.30	2.61	0.06	0.28	0.01	0.55	0.02
6	U4	U4.3	29	465	76.39	1.44	13.55	0.34	2.19	0.18	3.37	0.17	2.52	0.20	2.71	0.07	0.28	0.02	0.76	0.05
7	FLD21	FLD21.1	10	401	76.42	1.11	13.25	0.29	2.75	0.25	3.32	0.21	3.06	0.18	2.71	0.19	0.31	0.06	0.67	0.05
8	AA.B	B1	43	384	73.92	1.35	13.72	0.62	3.78	0.23	3.60	0.25	2.45	0.32	2.63	0.17	0.29	0.07	0.77	0.06
9	FLD17	FLD17.2	21	355	76.03	1.04	13.26	0.37	3.02	0.06	3.49	0.07	3.00	0.18	2.75	0.07	0.29	0.03	0.58	0.03
10	AH.E	E2	13	341	76.26	1.59	13.59	0.78	3.16	0.12	3.25	0.11	2.00	0.15	2.83	0.15	0.31	0.06	0.77	0.04
11	FLD18	FLD18.4	23	336	73.55	1.08	13.93	0.57	3.10	0.36	3.57	0.34	2.55	0.24	2.77	0.13	0.33	0.04	0.59	0.04
12	U4	U4.2	7	335	73.59	1.18	12.85	0.23	2.91	0.07	3.26	0.08	2.73	0.09	2.65	0.15	0.28	0.06	0.41	0.04
13	AG.D	D2	19	283	73.53	6.38	13.81	3.42	3.36	0.81	3.51	0.83	1.80	0.55	2.74	0.66	0.37	0.12	0.71	0.17
14	AE.C	C4	9	264	71.85	1.88	12.40	0.72	4.61	0.29	4.42	0.13	1.71	0.63	2.59	0.31	0.34	0.09	0.57	0.19
15	U3	U3.3	13	262	74.51	0.58	13.42	0.18	3.33	0.09	3.69	0.11	2.87	0.13	2.74	0.06	0.32	0.01	0.91	0.03
16	U4	U4.7	12	247	76.04	0.69	14.14	0.37	2.61	0.08	3.13	0.13	2.55	0.24	2.90	0.09	0.29	0.02	0.77	0.02
17	FLD4.4	FLD4.4.1	19	244	72.40	4.19	16.46	2.40	2.04	0.23	2.61	0.23	2.18	0.36	3.11	0.37	0.38	0.08	0.72	0.10
18	FLD17	FLD17.1	8	209	76.45	2.23	12.51	1.39	3.19	0.30	3.70	0.23	2.24	0.61	2.84	0.09	0.29	0.03	0.57	0.05
19	AE.C	C2	14	207	76.46	0.80	13.17	0.64	3.19	0.20	3.23	0.08	2.67	0.15	2.65	0.10	0.26	0.06	0.58	0.03
20	FLD21	FLD21.L	8	206	73.77	1.50	14.02	0.41	2.46	0.09	2.86	0.12	4.03	0.10	2.65	0.08	0.25	0.05	0.62	0.03
21	AG.D	D1	10	201	73.93	1.30	13.63	0.94	3.94	0.34	4.35	0.35	1.46	0.17	2.53	0.18	0.29	0.06	0.56	0.04
22	AE.C	C1	12	200	73.32	0.99	14.19	0.64	4.31	0.67	4.12	0.47	2.13	0.20	2.72	0.09	0.31	0.05	0.62	0.03
23	U1B	U1B.L	25	195	71.44	2.18	15.60	0.62	2.40	0.14	3.61	0.10	1.61	0.13	3.26	0.17	0.48	0.05	0.83	0.06
24	U3	U3.2	6	191	74.55	1.41	12.91	0.68	2.37	0.11	3.71	0.03	2.63	0.07	3.02	0.15	0.28	0.05	0.62	0.12
25	AH.E	E1	9	178	73.29	1.60	13.72	0.42	4.09	0.63	4.54	0.52	1.10	0.10	2.61	0.19	0.32	0.04	0.73	0.04
26	U4	U4.4	9	178	73.34	2.80	15.42	1.61	3.03	0.23	3.17	0.20	2.86	0.44	2.81	0.22	0.32	0.05	0.84	0.07
27	U4	U4.5	4	171	74.12	1.55	14.02	0.32	3.48	0.13	3.90	0.13	2.07	0.18	2.85	0.07	0.32	0.03	0.76	0.03
28	FLD18	FLD18.3	9	166	74.38	1.42	13.75	0.25	2.63	0.13	3.26	0.11	2.40	0.14	2.79	0.11	0.33	0.04	0.56	0.04
29	FLD4.4	FLD4.4.2	12	163	69.84	1.32	16.96	1.28	2.38	0.08	2.84	0.18	2.41	0.19	3.25	0.14	0.42	0.05	0.80	0.05
30	FLD14	FLD14.1	7	157	73.23	1.87	12.18	0.27	2.94	0.58	4.19	0.12	2.93	0.19	2.48	0.06	0.27	0.02	0.61	0.16
31	U4	U4.6	5	154	74.42	1.53	14.67	1.08	2.89	0.10	3.36	0.14	2.13	0.25	2.95	0.06	0.36	0.02	0.86	0.04
32	U3	U3.5	7	146	74.12	0.94	13.62	0.22	3.23	0.05	3.79	0.06	2.67	0.04	2.75	0.05	0.31	0.02	0.88	0.02
33	FLD17	FLD17.tail	6	143	74.67	0.90	12.73	0.39	3.48	0.11	3.90	0.06	2.54	0.35	2.87	0.13	0.29	0.02	0.61	0.05
34	U3	U3.1	7	134	73.29	1.90	13.83	0.70	2.40	0.17	3.25	0.09	3.31	0.22	2.91	0.11	0.31	0.03	0.64	0.10
35	U3	U3.4	6	125	75.18	0.96	13.51	0.56	3.19	0.18	3.80	0.07	2.63	0.13	2.88	0.09	0.33	0.03	0.86	0.02
36	FLD18	FLD18.2	28	124	74.85	1.38	13.98	0.48	2.29	0.68	3.85	0.17	1.71	0.36	2.62	0.24	0.33	0.03	0.70	0.15
37	FLD17	FLD17.int.1	6	111	77.00	1.16	12.72	0.61	3.01	0.08	3.70	0.03	1.95	0.09	2.70	0.08	0.29	0.02	0.56	0.03
38	AE.C	C3	4	106	73.51	1.35	11.29	0.59	5.00	1.05	5.42	0.07	1.72	0.12	2.29	0.06	0.24	0.02	0.47	0.03
39	U1B	U1B.2	9	84	73.02	1.29	12.19	1.59	3.97	0.91	4.58	0.34	1.06	0.29	2.78	0.60	0.31	0.03	0.46	0.05
40	AA.B	B2	4	70	72.63	1.30	13.61	0.54	3.56	0.73	4.19	0.06	2.38	0.14	2.43	0.06	0.24	0.06	0.77	0.10

41	FLD4.3	FLD4.3.4	4	70	74.87	0.60	13.81	0.73	3.02	0.19	3.85	0.04	1.28	0.03	3.02	0.19	0.47	0.03	1.09	0.03
42	FLD17	FLD17.int.2	4	62	75.32	0.59	13.76	0.13	2.77	0.06	4.00	0.05	3.04	0.09	2.72	0.07	0.31	0.03	0.84	0.03
43	FLD18	FLD18.1	5	60	73.75	0.81	13.79	0.82	2.86	0.30	3.72	0.24	2.80	0.17	2.83	0.06	0.31	0.02	0.71	0.17
44	FLD23	FLD23.5.1	4	60	73.85	0.47	13.68	0.24	2.81	0.11	3.79	0.07	2.39	0.16	2.58	0.09	0.30	0.03	0.56	0.06
45	FLD4.3	FLD4.3.3	3	53	78.74	0.48	10.31	0.38	1.65	0.17	3.60	0.07	1.01	0.08	2.76	0.10	0.29	0.04	0.42	0.03
46	FLD23	FLD23.1.2	3	47	75.78	0.45	13.97	0.24	1.96	0.08	3.78	0.08	2.29	0.15	2.72	0.06	0.33	0.04	0.58	0.03
47	FLD23	FLD23.1.3	3	47	76.47	2.49	14.06	0.27	2.06	0.24	3.74	0.13	2.17	0.29	2.73	0.14	0.34	0.03	0.61	0.04
48	FLD23	FLD23.1.1	3	46	75.39	0.87	14.04	0.14	1.95	0.17	3.71	0.04	2.58	0.09	2.64	0.07	0.34	0.02	0.58	0.02
49	FLD4.3	FLD4.3.UA	4	46	72.50	0.80	13.94	0.98	1.80	0.03	3.60	0.17	1.79	0.09	2.91	0.19	0.37	0.03	0.90	0.20
50	FLD23	FLD23.4.2	6	43	74.08	0.74	13.74	0.52	3.02	0.13	3.99	0.07	2.17	0.21	2.68	0.11	0.32	0.02	0.62	0.06
51	FLD23	FLD23.4.1	5	42	74.79	0.60	13.78	0.07	2.77	0.16	3.82	0.15	2.24	0.06	2.61	0.02	0.31	0.03	0.61	0.01
52	FLD4.3	FLD4.3.2	3	41	78.04	0.87	10.43	0.51	1.64	0.17	3.56	0.06	1.27	0.09	2.75	0.08	0.30	0.01	0.48	0.02
53	FLD4.3	FLD4.3.5	2	41	71.51	0.66	15.99	0.53	3.20	0.31	3.92	0.01	1.77	0.12	3.03	0.01	0.54	0.00	1.06	0.02
54	FLD23	FLD23.3.1	4	40	74.75	0.82	14.07	0.22	2.42	0.22	3.73	0.04	2.31	0.12	2.70	0.02	0.33	0.04	0.62	0.01
55	FLD4.3	FLD4.3.1	3	39	76.34	2.10	11.96	0.33	1.77	0.18	3.85	0.05	1.04	0.08	2.92	0.12	0.38	0.05	0.54	0.01
56	FLD23	FLD23.2.2	4	31	76.18	1.20	14.16	0.37	2.08	0.34	3.76	0.03	2.38	0.11	2.71	0.07	0.34	0.03	0.61	0.04
57	FLD23	FLD23.2.1	2	21	77.03	0.51	14.25	0.15	1.84	0.16	3.76	0.05	2.37	0.19	2.66	0.02	0.33	0.05	0.61	0.04
58	FLD23	FLD23.3.2	2	17	74.98	0.90	13.56	0.63	2.59	0.01	3.99	0.06	2.25	0.26	2.71	0.07	0.30	0.00	0.58	0.05

Deviations of agglomerate compositions from their host objects

Earlier work (Lewis et al. (2015)) suggested that fallout glasses may form in disparate parts of fireball, based on the observations that each object incorporated a different mixture of soil and bomb vapor [60]. A more appropriate basis for understanding formation relationships is to compare the major element composition of agglomerates directly to the hosts they are attached to, as at some point, it is evident that the two objects were in close proximity when still molten.

While individual agglomerates may show large deviations from the composition of the host to which they are attached, collectively, the median agglomerate composition deviation from the median of its host object composition is close to 0 (Figure 4.14 and Table 4.9). MgO has the greatest median deviation at +10.4%, followed by CaO at +6.1%. The median deviation of agglomerates suggests a slight overall enrichment of agglomerates in so-called "refractory" oxides (CaO, TiO_2, and Al_2O_3) and "moderately volatile" species (SiO_2, FeO, and MgO) relative to "volatile" species (Na_2O, and K_2O) [102]. The alkali oxides are the only major element oxides where agglomerates have median deviations from their host objects of less than zero. Na_2O and K_2O have median deviations of -3.61% and -1.14%, respectively. This is discussed further below when analyzing agglomerate and host compositions for volatile loss.

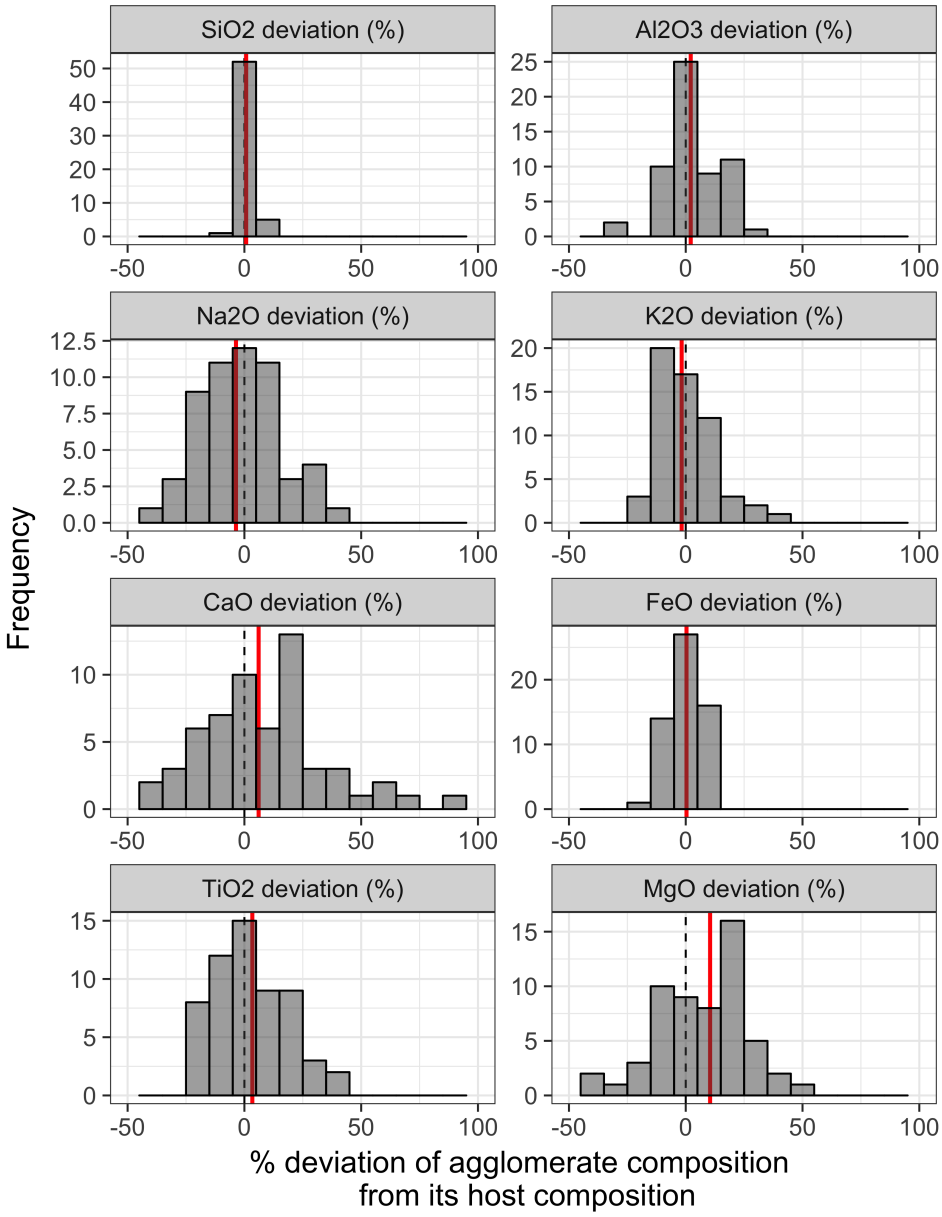

Figure 4.14: Histograms (bin width = 10%) showing the percent deviation of the average composition of each of the 58 agglomerates from their respective average host compositions. The vertical red line denotes the median deviation in each panel. The dashed vertical line denotes 0% deviation. While there are large deviations across the agglomerate population, the median values for each major element oxide are close to 0, with MgO having the greatest average deviation of +10.4% and CaO having the next greatest deviation at +6.1%. Medians are used instead of means to minimize the influence of outliers on the overall compositional deviation. Data are tabulated in Table 4.9.

Table 4.9: Percent deviation of average agglomerate compositions (Table 4.8) from the average compositions of their host objects for 15 samples (Table 4.6).

	Host	Agglomerate	SiO_2 dev.	Al_2O_3 dev.	Na_2O dev.	K_2O dev.	CaO dev.	FeO dev.	TiO_2 dev.	MgO dev.
1	–	**Median dev.**	**0.75**	**2.14**	**-3.61**	**-1.14**	**6.09**	**0.33**	**3.39**	**10.43**
2	AA.B	B1	-2.02	7.51	12.28	4.05	37.02	3.03	1.16	11.15
3		B2	-1.24	9.58	11.69	2.34	42.85	7.95	8.65	15.66
4		B3	-2.97	8.70	5.19	19.12	38.77	-0.26	-10.08	15.66
5	AE.C	C1	-2.40	-6.59	18.03	8.60	18.84	-5.75	11.92	3.75
6		C2	3.87	-0.79	-18.33	-20.64	85.56	-3.57	-14.42	5.57
7		C3	-0.14	-14.95	28.01	33.17	19.54	-16.67	-21.00	-14.45
8		C4	-0.40	6.90	10.35	1.23	48.03	-1.02	2.04	12.85
9	AG.D	D1	-1.70	1.00	32.79	22.97	-23.80	-5.48	-8.88	-9.59
10		D2	-2.23	2.34	13.24	-0.77	-6.05	2.36	16.26	14.62
11	AH.E	E1	1.44	-0.66	-12.57	-13.30	64.11	-6.61	-13.63	1.43
12		E2	-2.51	0.29	13.16	21.11	-9.74	-13.87	-10.84	-3.84
13	FLD10	FLD10.L	-0.89	5.06	-19.49	-9.05	69.69	0.43	9.84	30.63
14	FLD14	FLD14.1	-1.24	-3.36	2.75	2.37	-2.50	-4.63	16.25	11.79
15		FLD14.L	-2.54	-14.27	1.03	25.05	-12.37	-10.41	8.23	0.29
16	FLD17	FLD17.1	2.60	-3.17	3.77	-3.07	23.30	-1.99	-16.93	-11.57
17		FLD17.2	3.11	-8.23	-3.77	-7.09	-4.10	4.65	4.74	-6.66
18		FLD17.int.1	2.54	-2.73	-8.90	-12.36	28.44	1.33	4.74	-5.02
19		FLD17.int.2	3.85	-6.69	-9.20	-7.09	-16.52	-0.51	4.74	-8.30
20		FLD17.tail	0.71	-6.62	4.98	-2.06	8.74	5.75	4.74	-0.11
21	FLD18	FLD18.1	-0.33	3.65	-0.97	-5.93	6.38	-0.08	0.83	-17.17
22		FLD18.2	-0.06	2.61	-8.64	-1.98	16.81	2.08	-5.28	-0.33
23		FLD18.3	1.43	4.02	-26.85	1.44	-28.66	-5.50	0.83	-1.73
24		FLD18.4	0.80	2.31	-15.99	-14.10	0.13	0.64	0.83	-21.38
25	FLD21	FLD21.1	2.10	-2.09	-7.58	-5.50	-5.88	4.48	11.91	-6.87
26		FLD21.L	-1.44	3.60	-17.33	-18.59	23.96	2.17	-9.75	-13.82
27	FLD23	FLD23.1.1	-2.18	12.93	-3.91	-5.04	55.08	9.63	4.80	9.71
28		FLD23.1.2	-0.23	20.17	29.84	7.96	16.57	9.63	16.03	21.68
29		FLD23.1.3	-1.18	19.82	41.56	12.77	12.92	12.57	19.77	23.67
30		FLD23.2.1	-1.48	19.29	31.71	7.11	24.37	8.37	12.28	11.70
31		FLD23.2.2	1.09	21.82	-8.13	6.83	19.17	14.25	23.51	15.69
32		FLD23.3.1	2.01	22.61	-3.44	5.70	12.92	14.67	27.26	21.68
33		FLD23.3.2	2.76	24.27	-13.75	6.27	23.33	11.73	23.51	21.68
34		FLD23.4.1	1.62	23.48	-2.50	6.27	23.85	13.83	27.26	21.68
35		FLD23.4.2	-0.28	22.70	13.43	5.42	20.21	13.41	23.51	23.67
36		FLD23.5.1	0.02	18.25	21.40	12.77	17.09	13.83	12.28	15.69
37		FLD23.L	0.57	22.43	-8.60	4.85	34.26	10.89	27.26	15.69
38	FLD4.3	FLD4.3.1	1.09	-0.91	-44.07	-10.24	5.80	-6.39	-2.21	9.31
39		FLD4.3.2	4.40	-1.83	-6.16	-4.00	-24.35	-2.85	24.22	32.39
40		FLD4.3.3	-0.29	13.66	-0.57	-2.26	4.62	-2.53	42.73	28.75
41		FLD4.3.4	6.45	-14.98	-45.00	-4.00	-38.53	-6.07	0.44	-34.41
42		FLD4.3.5	8.82	-25.86	-49.04	-11.23	-24.94	-11.53	-20.71	-41.70

43		FLD4.3.UA	9.79	-26.71	-48.73	-10.24	-40.30	-11.21	-23.35	-48.99
44	FLD4.4	FLD4.4.1	-6.24	25.85	-6.10	-14.18	11.29	11.20	18.40	-0.30
45		FLD4.4.2	-2.80	22.14	-19.51	-21.13	0.67	6.41	7.13	-10.27
46	U1B	U1B.2	-1.67	14.29	-32.38	7.47	15.85	14.74	40.48	50.25
47		U1B.L	0.50	-10.69	11.86	36.35	-23.73	-2.16	-9.27	-16.73
48	U3	U3.1	2.42	1.75	6.55	0.88	-4.51	-1.31	-1.10	21.42
49		U3.2	-0.16	4.16	-19.84	-13.72	20.19	-0.29	-7.09	-9.64
50		U3.3	1.51	1.07	11.22	-2.04	4.21	-6.11	-4.09	28.48
51		U3.4	0.97	2.58	7.88	0.61	-3.05	-5.77	-7.09	24.24
52		U3.5	1.56	-2.77	-20.84	-1.51	-4.51	3.48	-16.08	-12.47
53	U4	U4.1	4.15	-11.87	2.39	0.35	-22.75	-1.91	-21.26	-16.38
54		U4.2	2.84	-10.72	-1.69	-8.16	-6.42	-7.69	-17.46	-35.66
55		U4.3	2.49	7.17	2.39	-10.64	-1.81	-2.26	-6.68	32.53
56		U4.4	3.58	-2.56	17.59	9.93	-28.93	-0.87	-6.68	19.91
57		U4.5	4.00	1.96	-2.34	-5.29	-26.87	2.61	4.98	35.69
58		U4.6	6.26	-1.72	-11.81	-11.77	-12.45	0.87	-15.43	21.49
59		U4.7	4.06	-4.16	-22.62	-8.11	-18.97	1.22	-18.35	-0.60

4.7 Comparing fallout to proximate soil and unmelted/partially-melted rock

The composition of fallout from this event has been shown to be representative of local soil, which is unsurprising since local soils can generally donate the majority of mass interacting with a fireball in near-surface events [57, 60, 67]. As shown in Table 1.1, the estimated mass of soil melted or vaporized in near surface tests ranges from ∼160–250 T of soil melted and vaporized per kT of device yield. To understand the formation of glassy fallout, an understanding of the composition of rocks and minerals in soil proximate to the event is important. This enables an understanding of which compositions can be explained by the simple melting and mixing of rocks and minerals in the soil and which compositions require additional, potentially anthropogenic components to explain their compositions.

Proximate soil collections and analyses

Several sediment samples were collected proximate to ground zero and away from the radioactive plume's direction of travel. Previously characterized aliquots of soil show that the sediment is consistent with being rhyolitic (igneous-derived sediment with $\gtrapprox$70 wt.% SiO_2), and primarily contains quartz, plagioclase feldspars, and alkali feldspars [57, 100].[7] Plagioclase feldspars are minerals that range in composition from albite ($NaAlSi_3O_8$) to anorthite ($CaAl_2Si_2O_8$). The alkali feldspars are minerals that range in composition from anorthite to orthoclase ($KAlSi_3O_8$), the potassium feldspar endmember. There are no natural feldspar minerals with compositions between orthoclase and anorthite.

For this study, sediment was also analyzed using EDS raster analyses and compositional X-ray maps to target and identify mineral compositions. Similar to the methods used glassy fallout, the unmelted sediment was mounted in epoxy and polished flat. SEM/EDS was then used to analyze the composition of several of the minerals in the sediment and characterize their morphology. Combined with compositional X-ray mapping, SEM/EDS analyses helped to identify mineral phases (Figure 4.15). As with other EDS analyses, only those analyses with sum totals between 96 and 104 were retained. In these sediments, much of the soil is porous, silty, and readily disintegrates when interrogated with a high energy electron beam. Because of this, out of 345 total EDS raster analyses of the soil, only 192 had sum totals between 96 and 104 and were retained. As a result, these soil analyses may not fully represent compositions that exist in the soils as carbonates, clays, or other sediments that easily volatilize or disintegrate under a focused electron beam.

[7] The aliquots of soil were analyzed using ICP-MS, which, due to the dissolution procedure cannot measure SiO_2 directly. SiO_2 concentrations was calculated by difference the ICP-MS analyses and confirmed with EDS.

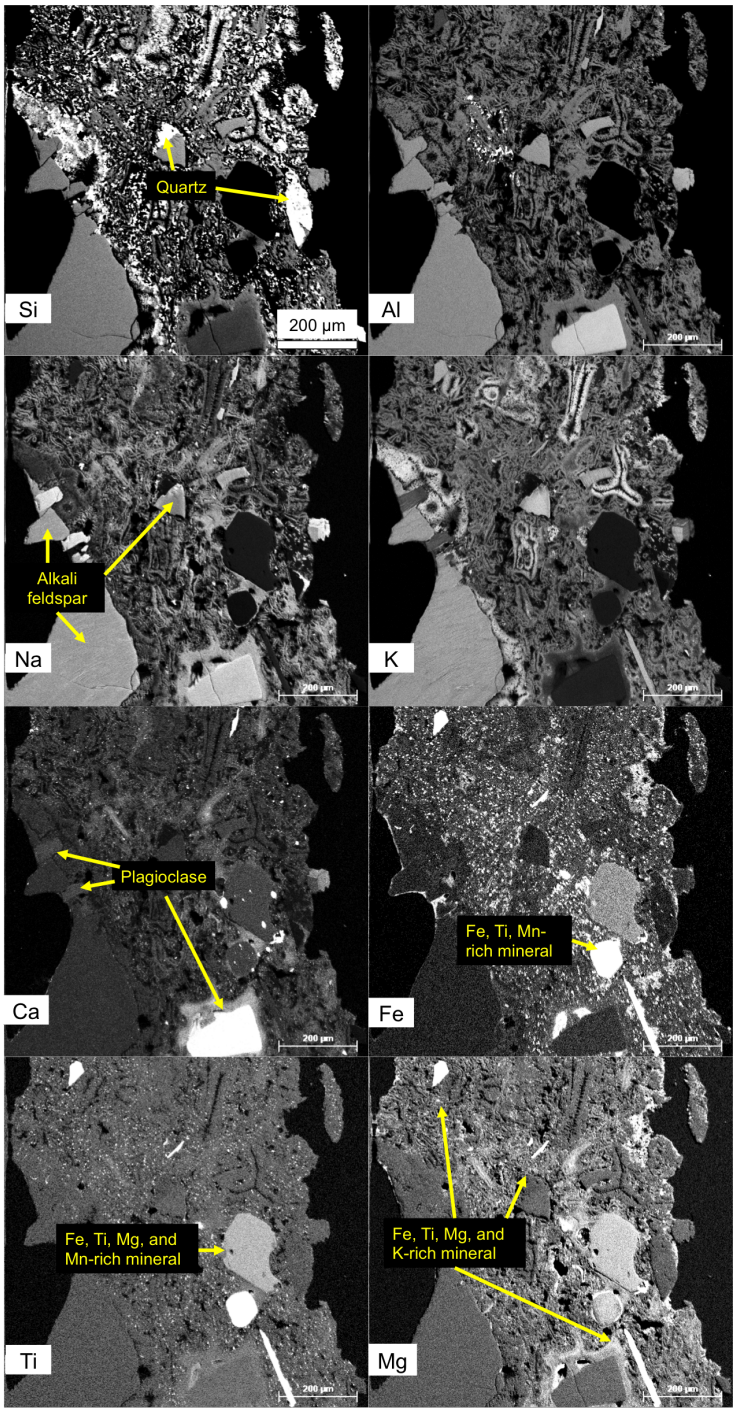

Figure 4.15: Compositional maps of a portion of sediment.The largest phases are tentatively identified based on composition. The porous, fine grained matrix contains many smaller minerals that are relatively enriched in Si, Al, Ca, and Fe.

Partially-melted/unmelted regions in fallout samples

Several samples such as FLD3.2, FLD9, FLD10, FLD11 contain large partially-melted or unmelted regions that appear to retain and preserve precursor soil (Figure 4.16). In one of these samples, FLD10, EDS raster analyses collected across the partially-melted and unmelted regions have been separated from those analyses in the glassy phases (using BSE and compositional maps as a guide) to highlight compositional similarities and differences. The glassy region appears primarily on the sample's surface and transitions to a partially-melted region, then to an unmelted region at the sample's interior. This sequence suggests the millimeter-scale rock was externally-heated. Autoradiography shows activity only in the glassy outer portions of the sample (Figure 2.13).

The glassy region, as seen in the Si compositional X-ray map (Figure 4.16), shows compositional flow-banding, diffuse compositional heterogeneities, and few vesicles. The partially-melted region also shows some flow-banding and deformation of some minerals, but in contrast to the glassy region, contains many SiO_2 regions with diffuse boundaries, consistent with partially-melted and/or relict quartz. While all the other mineral compositions appear to have been melted and begun to mix, the quartz grains in this intermediate region are incompletely melted, suggesting that this region was heated to at least the melting points of quartz, but did not sustain these temperatures for long enough to completely melt the quartz grains. The large number of vesicles, as noted in other studies (*e.g.*, [66]) suggest out-gassing of volatile species during the rapid heating and cooling. The glassy region in FLD10 does not show the same vesicularity as the partially-melted region. One explanation may be that the sample was heated to high enough temperatures to allow volatilized gases to escape. In contrast, the partially-melted region in FLD10 may have remained relatively cool, highly viscous, trapping gases as they volatilized. The unmelted region of FLD10 retains primarily mineralogic textures and vesicles. Both the glassy and partially-melted regions in FLD10 contain radioactivity (Figure 4.16). This suggests the bomb vapor was able to condense onto sample FLD10 and become incorporated in both of these regions. In contrast, the unmelted regions contain little to no activity.

Higher magnification compositional maps in FLD10 (Figure 4.17) show that the transition from unmelted to partially-melted to glassy regions in sample FLD10 is continuous.The unmelted region begins in the top right of each panel of Figure 4.17, transitions to partially-melted in the center of each panel, and finally glassy in the bottom left of each panel. In the top right, the Si compositional map shows regular, euhedral SiO_2-rich regions, likely quartz. The Al and Na concentrations are correlated in locations in this region, and retain euhedral boundaries as well, suggestive of alkali feldspars. In the partially-melted region, which occurs about halfway between the top right and bottom left corners, the Si-rich regions retain a mixture of angular and diffuse boundaries that are stretched in the direction of the compositionally heterogeneous flow-banding, transverse to the unmelted region. This region must have experienced temperatures at or exceeding 2000 K, the approximate melting point of quartz [46]. The bright flowbands in the partially-melted regions visible in the BSE image, Ca X-ray map, and partially in the Fe X-ray map appear to emanate from the diffuse Ca

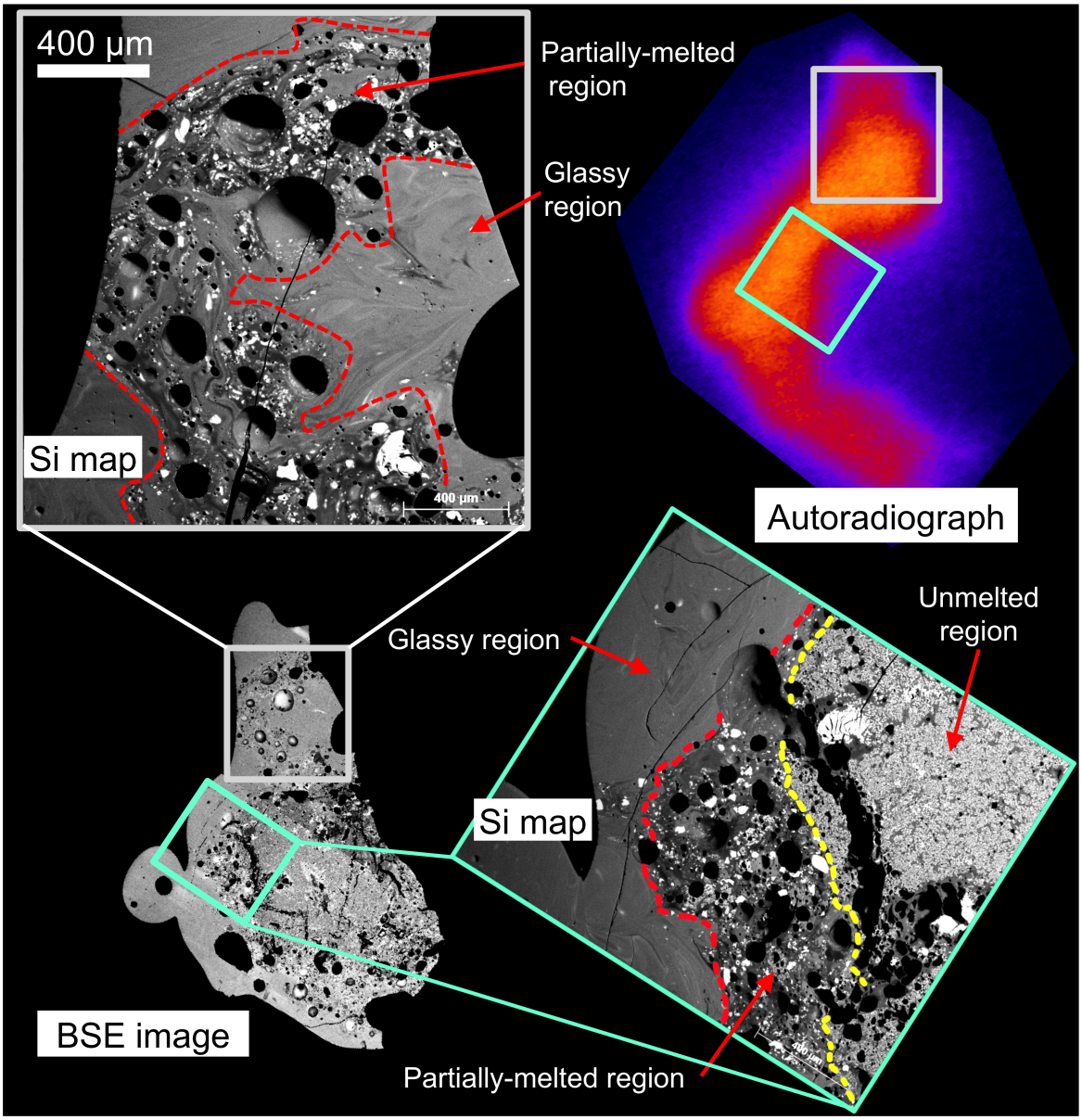

Figure 4.16: Si compositional maps showing regions in FLD10 that transition from unmelted to glassy. Inset Si X-ray map locations are shown by the green and white boxes in the BSE image, optical image, and autoradiograph. The scale bar corresponds to both inset Si maps. Both the glassy and partially-melted regions contain radioactivity, while the unmelted region contains no radioactivity.

and Fe regions, visible near the bottom right of the Ca X-ray map and in the center of the Fe X-ray map, respectively. The Ca and Fe-rich flow bands then flow into and become incorporated into the glassy region. Melting minerals to high temperatures (and low enough

viscosity) allows the compositions mix well, forming a glassy phase that reflects the average major element composition of the multi-mineralic precursor.

No compositional interfaces are observed in the Al and Si panels. This bolsters the argument that the Si and Al compositional interfaces used to identify agglomerates (particularly those fully incorporated into host objects) are not formed from compositional heterogeneities in the melt or convective patterns of minerals melting in place and then experiencing bulk flow. Instead, these compositional boundaries may result from some other process due to agglomeration. The origin of compositional boundaries between agglomerates and host objects will be further explored in Chapter 8.

Host and agglomerate compositions compared to soil measurements and partially-melted/unmelted fallout compositions

The composition of glassy fallout has previously been observed to primarily reflect a mixture of lithologies found in the surrounding soil [57, 60]. To better establish the relationship of the composition of glassy fallout with that of the surrounding soil, EDS raster measurements of soil grains and the partially-melted and unmelted regions of sample FLD10 are compared with host object and agglomerate compositions using different pairs of major element oxides (Figures 4.18, 4.20, and 4.19). Each of these plots shows two panels, with the left panel overlaying the host object compositions ($n = 3,698$), the agglomerate compositions ($n = 679$), the soil compositions ($n = 192$), and compositional measurements on FLD10 performed on the partially-melted/unmelted region ($n = 168$).[8] The right panel shows these same data points as transparent black circles, to highlight the density of measured compositions and shows clustering and overlap of compositions. The right panel also shows the relative location for quartz and feldspar endmembers (orthoclase, albite, and anorthite), as well as and outlying soil, agglomerate, and host compositions representative of mineral types as measured by EDS.

The compositional groups defined by these data include:

- Quartz-like, classified based on its high silica content: $\geq$90 wt.% SiO_2
- Mafic, classified based on its high CaO, high FeO, and high MgO content: CaO $\geq$ 8 wt.%, FeO $\geq$ 5 wt.%, and MgO $\geq$ 2 wt.%
- Felsic, classified based on its high Al_2O_3 and high alkali or CaO content (feldspar-like): $Al_2O_3 \geq 20$ wt.% and $Na_2O + K_2O \geq 10$ wt.% or CaO $\geq$ 5 wt.%

Al_2O_3 vs. SiO_2

Al_2O_3 and SiO_2 are the two most abundant oxides in these fallout samples. Plotting the Al_2O_3 and SiO_2 compositional relationships of the host objects, agglomerates, soil, and

[8] Data are tabulated in Appendices B and C.

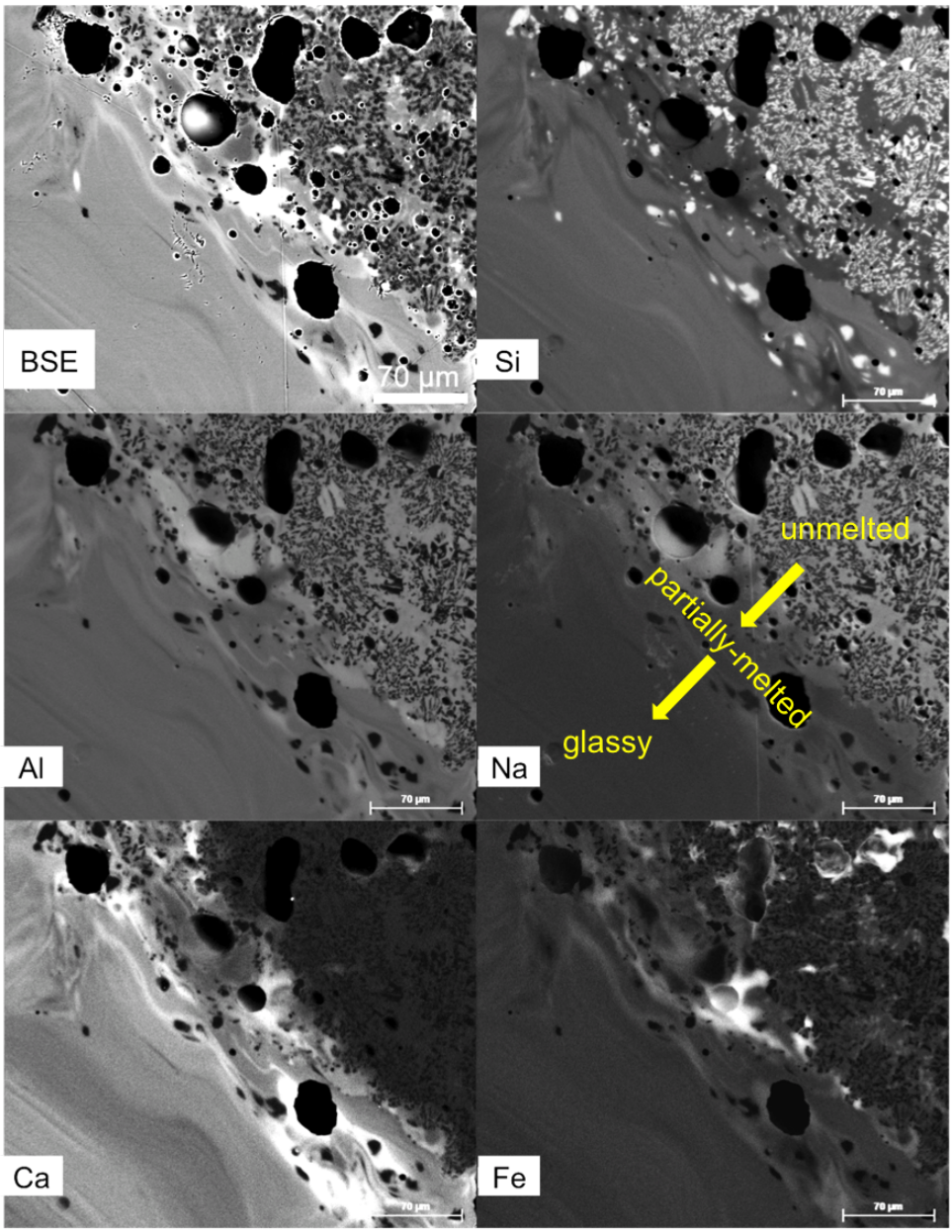

Figure 4.17: A BSE image and corresponding Si, Al, Na, Ca, and Fe compositional X-ray maps of a region on sample FLD10 showing an unmelted to glassy transition. In the unmelted region (top right corner of each panel), minerals in the Si compositional map retain sharp boundaries and are fairly evenly distributed. In the partially-melted region (center of each panel) the boundaries of SiO_2-rich objects become diffuse. Compositional flow-banding (visible in the Ca compositional X-ray map) indicates the viscous flow of partially-melted minerals. The glassy region (bottom left of each panel), is compositionally well-mixed. The flow-banding direction in the glassy and partially-melted regions run transverse to the unmelted boundary. Compositional interfaces, such as those used to identify agglomerates, are absent.

partially-melted/unmelted compositions in FLD10 shows that the majority of these compositions plot in a narrow band extending from quartz-like compositions along a line through orthoclase and albite endmembers and towards anorthite (Figure 4.18). The soil and partially-melted/unmelted compositions on FLD10 appear to overlap the host object and agglomerate measurements because feldspar endmembers plot along a single band from a high SiO_2, low Al_2O_3 composition to low SiO_2, high Al_2O_3 compositions. Measured compositions that plot towards low SiO_2 and Al_2O_3 values include the mafic component and a few other anomalous compositions that are enriched in FeO and TiO_2. Fewer than 20 analyses represent this mafic composition, a minor component of the composition expressed in fallout (comprising less than 0.5% of the total number of EDS measurements). The majority of fallout compositions are consistent with a mixing between felsic and quartz minerals, with a small number of anomalous compositions. However, the majority of measurements (right panel, Figure 4.18) show a tightly clustered composition, reflective of the general compositional homogeneity of this glassy fallout population.

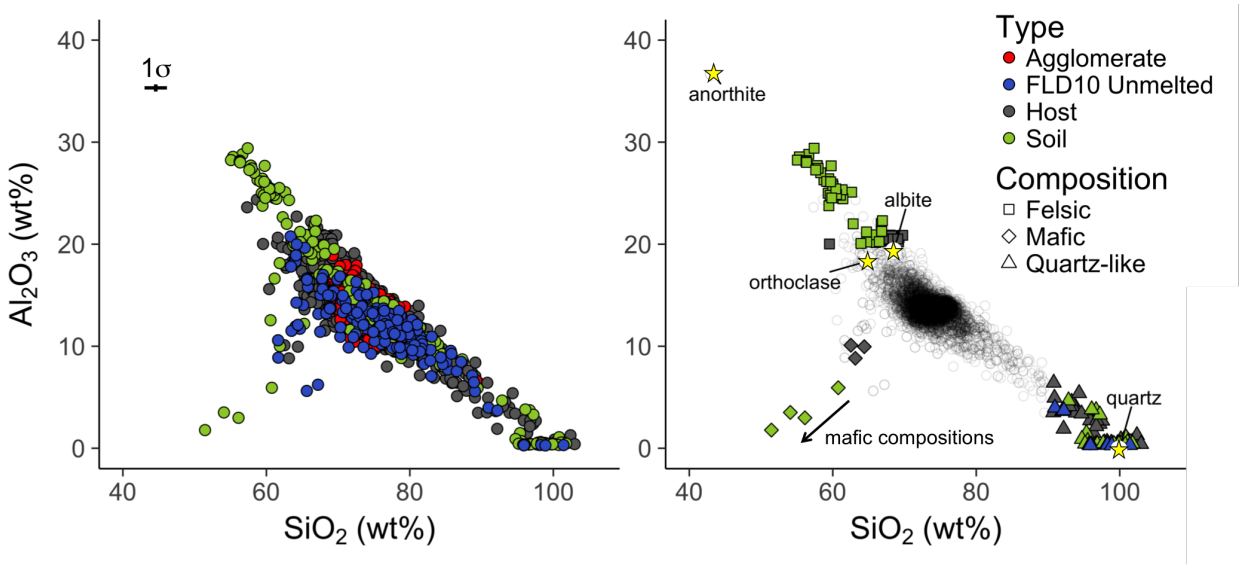

Figure 4.18: Bivariate plot of Al_2O_3 vs. SiO_2 showing EDS analyses of host objects, agglomerates, unmelted soil, and partially-melted/unmelted compositions from sample FLD10 (left panel) and a density plot of these same analyses with outlying compositions and feldspar and quartz endmembers marked (right panel). All of the agglomerate measurements and the majority of host, soil, and partially-melted/unmelted FLD10 measurements lie on a mixing line between quartz (100% SiO_2) and an Al-rich, Si-poor composition, likely feldspars. Soil and partially-melted/unmelted compositions in FLD10 appear to overlap the host and agglomerate compositions because the feldspar endmembers plot along a single band between anorthite and quartz. While the majority of compositions are densely clustered, reflective of a high degree of compositional homogeneity, the high density region is again stretched between the feldspar endmembers and quartz, suggesting mafic compositions contribute only a minor component of the precursor minerals that mixed to form the glassy host objects and agglomerates (right panel). Data are tabulated in Appendices B, C, and D.

CaO vs. Al_2O_3

Ca is one of the most variable major elements analyzed in this study (Figure 4.10). In a plot of CaO and Al_2O_3, the soil compositions define the greatest range, with all host and agglomerate compositions appearing as a subset (Figure 4.19). The unmelted/partially-melted measurements on FLD10 are confined to an even narrower range, being restricted to compositions with CaO <4 wt.%. This suggests that the unmelted soil preserved in FLD10 may only contain a subset of minerals found in the precursor lithology. Alternatively, because the partially-melted/unmelted compositions characterized in FLD10 were part of the EDS rasters taken in a grid patterns and were not targeted, EDS analyses collected from fine grained calcic minerals may overlap other compositions, obfuscating the endmember Ca component.

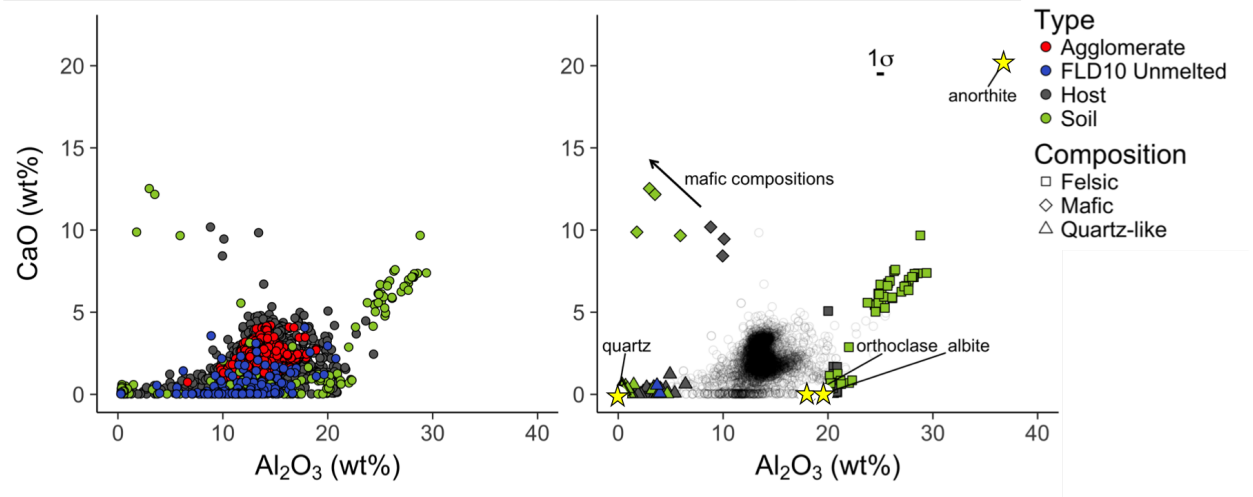

Figure 4.19: Bivariate plot of CaO vs. SiO_2 showing host analyses, agglomerate analyses, soil analyses, and the partially-melted/unmelted compositions from sample FLD10 (left panel) and a density plot of these same analyses with outlying compositions and feldspar and quartz endmembers marked (right panel). All high Ca compositions measured in the host objects are bounded by soil compositions as well, suggesting that host object and agglomerate CaO and Al_2O_3 compositions can be well explained as a mixture of minerals originating from the soil. Data are tabulated in Appendices B, C, and D.

Alkalis vs. Al_2O_3

Comparing the alkali oxide content relative to Al_2O_3 illustrates how the unmelted soil and partially-melted/unmelted region on sample FLD10 bound the host and agglomerate compositions (Figure 4.20). The unmelted/partially-melted compositions form the edges of a triangle whose vertices are defined by quartz, anorthite, and orthoclase. Host object and agglomerate compositions occupy regions inside the triangle. The unmelted/partially-melted FLD10 compositions plot primarily between quartz and orthoclase, following a line that

intercepts the quartz end member between the orthoclase and albite endmembers, but are generally depleted in Al_2O_3 relative to pure feldspar compositions. The soil compositions are bimodal, clustering towards quartz-like compositions, or following a trend that plots between anorthite (Ca-rich) and albite (Na-rich), orthoclase (K-rich) feldspars.

The majority of host compositions form a tight cluster at in the triangle's interior (Figure 4.20). The agglomerate compositions span a more limited range, appearing as a subset of the host compositions, close to the host object mean. Only a single EDS measurement in an agglomerate extends towards more quartz-like compositions. The felsic compositions mostly plot within a triangle formed by feldspar endmembers, while mafic compositions tend to plot towards the quartz-like compositions, being depleted in alkalis and alumina relative to the bulk.

The left panel of Figure 4.20 shows a different perspective of the soil measurements compared to the host and agglomerate measurements—the soil measurements and the compositional measurements on the partially-melted/unmelted regions of FLD10 sharply bound the host object and agglomerate compositions. This indicates that the major element compositions of the host objects have become enriched in Al due to the addition of felsic compositions in to the glassy melt, or through other processes.

4.8 Evidence for volatile loss

When soil is swept into the fireball and heated, volatile species such as alkalis may be lost from the soil melt if the heating is sustained for a long enough duration.[9] Given the modeled and experimental determination of quenching timescales on the order of seconds in fallout, appreciable loss of volatile major elements is not expected [10, 44]. If volatile loss occurs mainly from the surface of the melt, examination of host objects or agglomerates as a function of size may provide a method by which times and temperatures of heating may be estimated.

To volatilize species from a silicate melt, volatiles must first migrate through the melt to its surface and then evaporate from the melt's surface. In experimental studies of Na_2O, among other volatile species such as C, S, and F, the rate of volatilization from the surface of the melt (instead of diffusion through the melt) has been shown to be the rate-limiting reaction and is therefore proportional to the surface area of the melt (at a given concentration and partial pressure above the melt) [104, 105]. The mass loss due to volatilization follows the expected exponential Arrhenius relationship [105]:

$$\frac{\partial m_i}{\partial t} = -\mathrm{SA} \cdot C_i \cdot k_i(T) \tag{4.3}$$

where SA is the surface area, C_i is the molar concentration of species i in the melt, and $k_i(T)$ is the Arrhenius reaction rate: $k_{i0} \exp -E_i/RT$, where k_{i0} is the reaction rate

[9] Experimental work on chondrules, common features found in meteorites, suggests that temperatures of ∼1600 K need to be sustained for several minutes to evaporate an appreciable amount (∼1 wt.%) of alkalis from the chondrule melt [103].

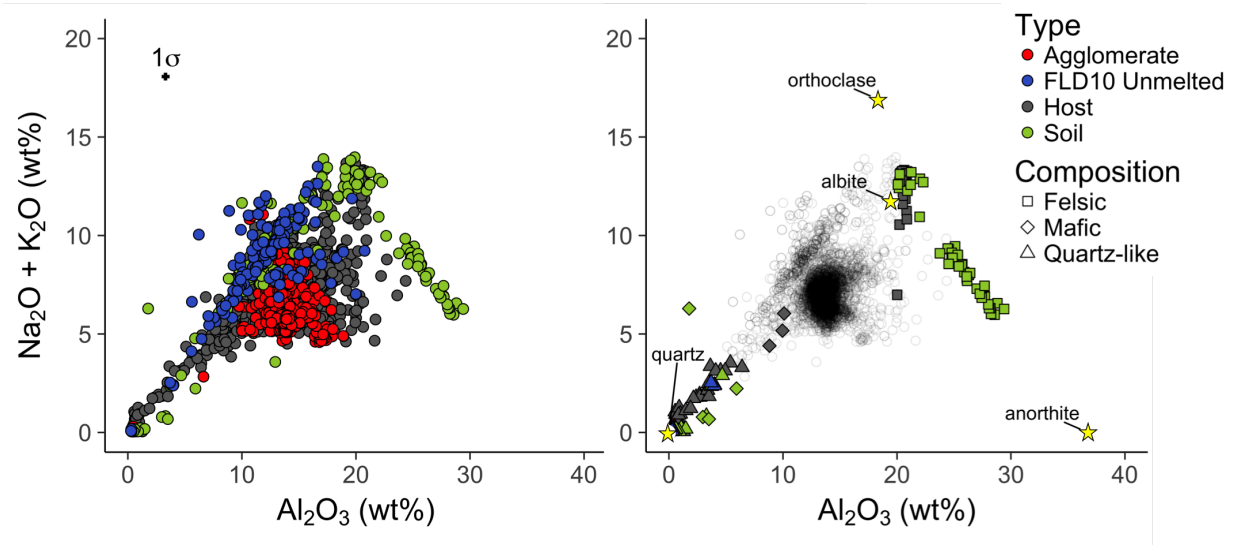

Figure 4.20: Bivariate plots of Na_2O + K_2 plotted vs. Al_2O_3 showing host analyses, agglomerate analyses, soil analyses, and the partially-melted/unmelted compositions from sample FLD10 (left panel) and a density plot of these same analyses with outlying compositions and feldspar and quartz endmembers marked (right panel). Orthoclase, anorthite, and quartz form the vertices of a triangle that bound almost all measured compositions. The soil analyses and partially-melted/unmelted compositions from FLD10 bound the agglomerate and host object analyses, which, due to mixing of mineral compositions, cluster within the interior of the triangle. While the soil analyses span Al_2O_3 concentrations from 0 wt.% to ∼30 wt.%, the partially-melted/unmelted compositions from FLD10 are restricted to Al_2O_3 concentrations less than ∼20 wt.%, consistent with the majority of the agglomerate and host object compositions, possibly because these EDS raster analyses were conducted in a grid-based pattern and the rasters may have overlapped multiple mineral compositions. Data are tabulated in Appendices B, C, and D.

constant, E_i is the activation energy of the reaction, and R and T are the gas constant and temperature, respectively. Instead of the absolute mass loss rate, the mass loss rate per unit volume (assuming a homogeneously distributed species) can be used to compare the relative mass loss for melts of different sizes:

$$\frac{\partial m_i/\mathrm{V}}{\partial t} = -\frac{\mathrm{SA}}{\mathrm{V}} \cdot C_i \cdot k_i(T) \tag{4.4}$$

The mass loss per unit volume of species i for a spherical melt is proportional to its surface area divided by its volume, or its inverse radius.[10] For multiple spherical melts with similar starting compositions, densities, and experiencing the same ambient environment for identical times, mass loss from volatilization between melts of two different sizes should be equal to the inverse ratio of their radiis. Plotting the average concentration of the alkali oxides versus $1/r$ (the inverse of an agglomerate or host object's equivalent radii) yields no

[10]Volume is assumed constant in Eqn. 4.4 because Na_2O and K_2O are present at a few weight percent and only minor evaporative loss is expected for a flash heating followed by rapid quenching [106].

trend suggesting volatile loss occurred (Figure 4.21). If the fireball is heterogeneous, it likely is too simplistic to assume these melts had identical beginning concentrations, identical ambient environments, or were heated to the same temperatures for the same amount of time.

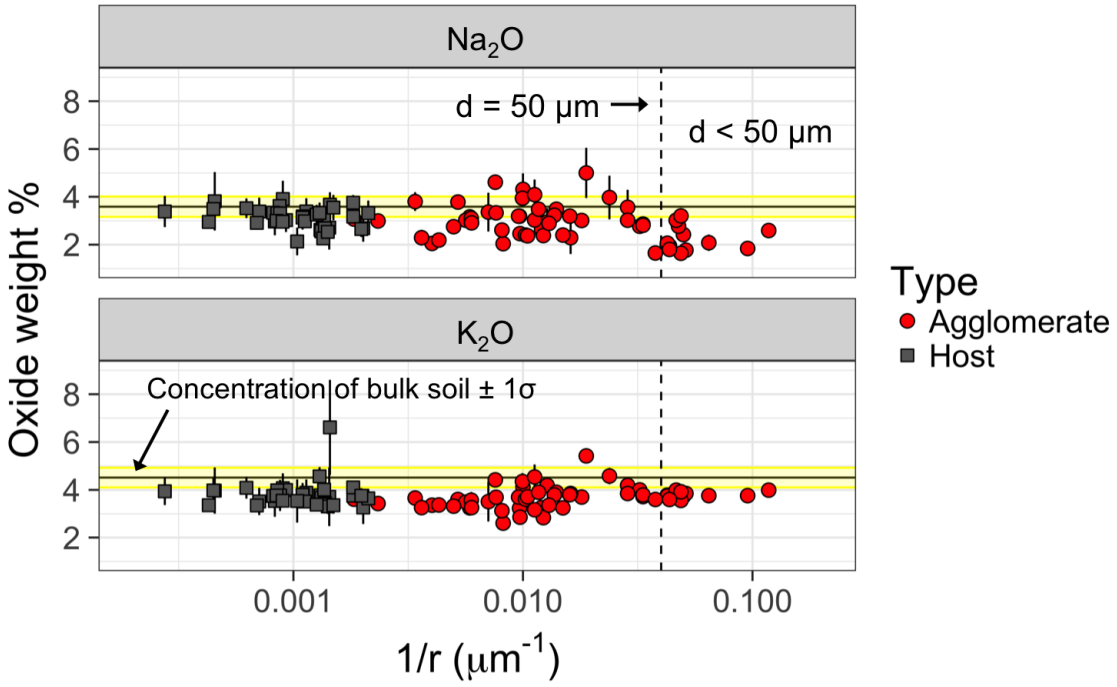

Figure 4.21: Plots of alkali concentrations (in oxide weight %) from the average composition of hosts and agglomerates (taken from Tables 4.6 and 4.8) as a function of the inverse equivalent radius of the object (calculated from its area exposed in cross-section). Uncertainties are 1σ of the mean alkali concentration for each object. The horizontal line and and yellow band correspond to the mean concentration of each of the alkali oxides in six ICP-MS dissolution analyses of bulk soil samples and 1σ about this mean, respectively [100].

The smallest agglomerates (d <50 μm) show a greater depletion in Na_2O, on average, relative to the rest of the agglomerates and the host objects (Figure 4.21 and Table 4.10). However, this behavior is not mirrored in K_2O concentration relationships. If agglomerates with $d < 50$ μm are excluded, the calculated mean Na_2O concentration increases from 2.88 wt.% to 3.06 wt.%, which more closely mirrors the average host and bulk fallout Na_2O concentrations of 3.13 and 3.17 wt.%, respectively. The agglomerates with diameters < 50 μm are from two samples: FLD23 and FLD4.3. There are nine agglomerates characterized in FLD23 with equivalent diameters less than 50 μm and they have an average Na_2O concentration of 2.29 $\pm$ 0.42 wt.%, which is greater than the average Na_2O content of the host sample FLD23 of 2.13 $\pm$ 0.58 (mean $\pm$ 1σ). The other four agglomerates with equivalent diameters less than 50 μm are incorporated into FLD4.3. Their average Na_2O concentration

Table 4.10: Mean and standard deviations of bulk soil analyses (ICP-MS; data from [100]), average compositions of entire hosts, agglomerates, and agglomerates greater and less than 50 μm in diameter (EDS).

	Na_2O (wt.%)		K_2O (wt.%)	
	Mean	1σ	Mean	1σ
Bulk soil (n=6)	3.59	0.43	4.52	0.41
Host and agglomerates (n=95)	2.97	0.65	3.74	0.49
Hosts (n=37)	3.13	0.43	3.80	0.55
Agglomerates (n=58)	2.88	0.74	3.70	0.45
Agglomerates >50 μm (n=45)	3.06	0.69	3.67	0.50
Agglomerates <50 μm (n=13)	2.24	0.51	3.79	0.13

is 2.10 ± 0.74 (mean ± 1σ), which is almost 30% less than the average Na_2O content of the host object FLD4.3 (3.22 ± 0.47 wt.%). Three of the four characterized agglomerates from FLD4.3 have a Na_2O concentration of 1.80 wt.% or below (1σs for these agglomerates are all less than 0.20 wt.% absolute; Table 4.8).

Ultimately, these data show no systematic volatile loss as a function of agglomerate or host object size. The agglomerates less than 50 μm in FLD23 actually have a *higher* average Na_2O content than the host FLD23, and one out of the four agglomerates less than 50 μm characterized in sample FLD4.3 has a comparable Na_2O concentration to the host. U content may help distinguish to what extent these objects interacted with the ambient environment (the fireball), and whether agglomerates depleted in alkalis are unique only in their Na_2O composition or if this relates to the degree with their incorporation of bomb vapor as well (discussed in Chapter 5).

4.9 Conclusion

EDS compositional analyses of host objects and agglomerates reveal several conclusions. First, from the EDS host analyses in 37 samples, fallout from this test is compositionally homogeneous (Figure 4.10). Most major element oxides resemble unimodal distributions with well-defined average compositions standard deviations less than 30% for all measured oxides except CaO, TiO_2, and MgO. However, fallout also contains unmelted and partially-melted compositions, which contribute to the tailing of the distributions shown in Figure 4.10. The transition from an unmelted to a partially-melted to a glassy composition is demonstrated in sample FLD10 (Figure 4.17), consistent with a rock heated from the exterior. Analysis of regions using ∼10–15 μm EDS rasters reveals compositions spanning a much wider range than those obtained through bulk dissolution analyses, which homogenize regions of compositional heterogeneity in the fallout glasses. The high CaO 1RSD and multi-modal nature of the KDE of CaO suggests CaO is highly heterogeneous and points towards multiple major sources of CaO being incorporated into fallout. While Weisz (2016) hypothesized there may be an anthropogenic source of CaO, such as concrete, comparing CaO compositions in fallout to

CaO compositions in unmelted soil shows that the unmelted soil compositions bound the glassy fallout compositions (Figure 4.19), indicating the CaO in glassy fallout from this test is consistent with a mixture of mineral compositions in the surrounding lithology.

The 58 agglomerates incorporated onto or into host objects in 15 samples characterized by EDS resemble the host compositions, but span a more restricted range for each major element oxide. These data indicate that as a separate population, agglomerates tend to be more well-mixed than hosts. This observation is supported by BSE images and compositional X-ray maps of agglomerates, which show they tend to exhibit few unmelted or partially-melted textures and were thoroughly melted by the blast (Figure 4.13). The median deviations in mean major element compositions between agglomerates and *their* host objects are small, with MgO having the greatest median deviation of +10.4%, followed by CaO at +6.1%. These deviations suggest that statistically, agglomerates do not grossly deviate from the hosts to which they are attached, indicating a local scale homogeneity of the carrier material in the fireball.

EDS analyses of unmelted sediment collected near ground zero show that compositions bound the host and agglomerate compositions. The host object and agglomerate major element compositions are consistent with the melting and mixing of minerals from the surrounding lithology. These fallout compositions primarily span the range from quartz-like to felsic with a small number of mafic compositions and other anomalous compositions identified (primarily high FeO/TiO_2 measurements).

Sample FLD10 retains an unmelted/rocky interior (Figures 4.16 and 4.17), which transitions to a partially-melted region, and finally to a glassy region towards the sample's periphery. The transition occurs over $\sim$100 μm. This transition of textures and compositions indicates exterior heating, which melted the surface of the rock, and subsequently heated the rock towards the center. The heating was sufficient to completely melt some minerals and partially-melt others, but the interior remained comparatively cool and unmelted. The transitions between these regions are continuous and show no compositional interfaces like those used to identify agglomerates (local Al_2O_3 depletions and either SiO_2 or CaO/MgO/FeO enrichments; Chapter 3), strengthening the hypothesis that compositional interfaces are a product of the agglomeration process rather than flow-banding, compositional heterogeneity, or simply minerals melting in place. In FLD10, partially-melted regions contain some radioactivity. While these regions were not as thoroughly heated as the fully melted regions (but still reached temperatures of at least the melting point of quartz, $\sim$2000 K), bomb vapor either diffusively or convectively mixed into these regions.

There no evidence for systematic volatile loss among hosts or agglomerates as a function of an object's surface area, as might be expected when externally heating a melt (Figure 4.21). This could reflect the limited heating duration (on the order of seconds) or be complicated by the thermal heterogeneities of the fireball or by variable residence times of the melts in the fireball. [10, 44].

As two separate populations, the major element compositions of hosts and agglomerates are remarkably similar to each other, indicating a generally similar precursor carrier melt. In particular, the surprising compositional similarity of agglomerates relative to *their* hosts

indicates a local scale major element homogeneity. However, What is not clear is whether the host objects and their associated agglomerates experienced a similar or different vapor environment in the fireball. To address this question, the next chapter focuses on U isotope measurements (as a proxy for the bomb vapor) in both populations to analyze differences and similarities in carrier melt-bomb vapor interactions between agglomerates and *their* host objects.

Chapter 5

Bomb Vapor Contributions to Fallout

5.1 Chapter overview

In Chapter 4, the major element compositions of host objects and agglomerates were compared, revealing that agglomerate compositions are a subset of host compositions, and the major element compositions of both host objects and agglomerates are consistent with the mixing of minerals present in the local lithology. In this chapter, differences in incorporation of bomb vapor into agglomerates and host objects is measured and discussed, using unfissioned U fuel (^{235}U) as a proxy. Using secondary ion mass spectrometry, the U isotopic composition (the ^{235}U/^{238}U composition) of host objects and agglomerates are quantified and compared. Possible scenarios that could lead to different U incorporation among agglomerates, depending on their location of attachment (exterior, surface, or interior) are also discussed.

To characterize the U content in agglomerates and hosts, present at concentrations of <100 ppm, an analytical technique more sensitive than EDS or EPMA, but with comparable spatial resolution, must be used. Secondary ion mass spectrometry was used to measure two U isotopes, ^{235}U and ^{238}U, at locations within the glassy regions of 14 glassy fallout samples. All 323 measured ^{235}U/^{238}U ratios are greater than natural (^{235}U/^{238}U $\approx$ 0.00725), showing that all glassy regions of fallout volumetrically incorporated some amount of enriched U. The magnitude of ratios between different regions, such as agglomerates and hosts, or regions of different compositions within single samples, highlights differential incorporation of unfissioned U from the device, and therefore, bomb vapor from the fireball. A systematic enrichment or depletion in the ^{235}U/^{238}U ratio between the agglomerates and host objects would suggest different fireball and formation conditions between the two, potentially in time or local fireball environment, which could elucidate the deviations between theory and experiment noted in Chapter 1.

In Chapter 4, no systematic difference was found in the major element composition between agglomerates and host objects. Agglomerate compositions appear to be a subset of host compositions, spanning a more restricted compositional range, and exhibiting few

partially-melted/unmelted regions. Similar to major element compositions in Chapter 4, the U isotope data of agglomerates and host objects to bound host object relationships with their associated agglomerates and generalize the interfaces of the two population with fireball vapor.

5.2 Secondary ion mass spectrometry

Secondary ion mass spectrometry (SIMS) is an analytical technique that can provide *in situ* isotopic and compositional information at a spatial resolution of 10 μm and below, with sub-ppm sensitivities for most elements. The technique is ideal for measuring ppm levels of residual fuel in these glassy fallout samples, where the scale of compositional heterogeneity and the dimensions of some of the agglomerates approaches $\sim$10 μm (Figure 3.7) [60].

SIMS is a quasi-destructive analytical technique. A primary ion beam, generated in an ion source and accelerated to $\approx$10 keV energies, sputters the surface of the sample. During sputtering, atoms from the sample are liberated from the sample surface. The majority of these atoms remain neutral, but a small percentage, typically 1–2%, depending on the element, are liberated as ions. These ions, called "secondary ions", are then extracted into the mass spectrometer for analysis. All three SIMS instruments used in this dissertation (discussed below) are double-focusing magnetic sector mass spectrometers, meaning the secondary ion beam is sorted by both energy and momentum before ions are detected and counted. Ions are detected using either current or pulse counting techniques, creating a mass spectrum (counts as a function of mass), 2D ion image (rastered beam, detected as a function of position), and/or a depth profile (raster or spot collected as a function of time) (Figure 5.1). The simplest SIMS instruments are made with a single detector, and can only detect a single mass at a time, so the magnetic field must be changed to direct ions of a different mass into the detector. More complex SIMS instruments use several detectors to count ions from different masses simultaneously while the magnetic field remains static.

Instruments

The fallout samples in this study were characterized over five years using three different SIMS instruments: an IMS-3f (at LLNL), IMS-1280 (at LANL), and NanoSIMS (at LLNL), all manufactured by CAMECA. Of the three, the IMS-3f is the simplest and most representative of the SIMS diagram in Figure 5.1. The IMS-1280 is an evolution of the IMS-3f that includes a larger geometry magnet for improved mass resolution and a multi-collector system that can analyze five masses simultaneously. Finally, the NanoSIMS, which was used to collect ion images, uses a novel plasma ion source and unique geometry to achieve nanometer-scale spatial resolution (if desired). Most samples were characterized using SIMS in a single analytical session using a single instrument. However, several samples were analyzed in multiple analytical sessions, using two or three instruments (Table 5.1). The operating conditions for each instrument are discussed below.

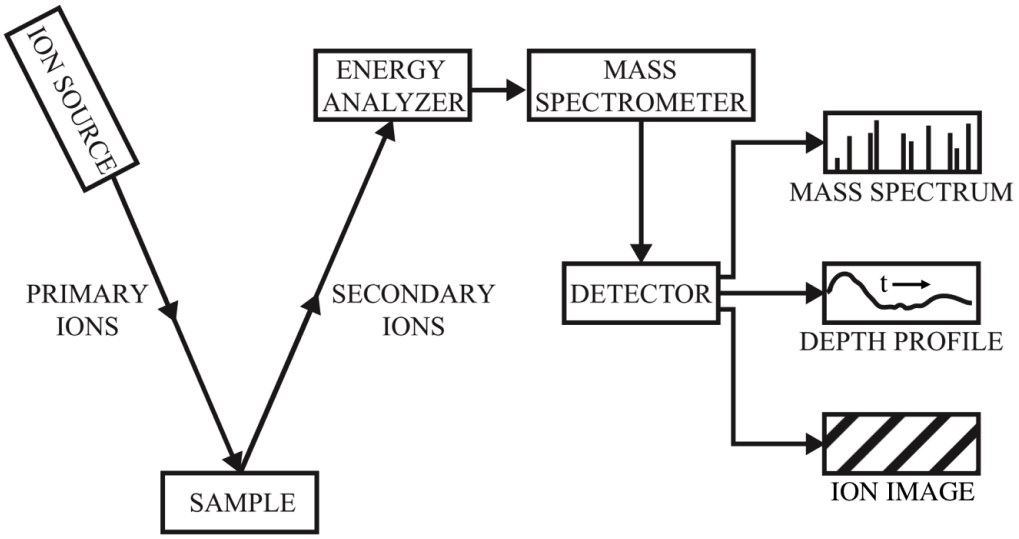

Figure 5.1: A schematic of a double-focusing SIMS instrument with a single detector. Two of the instruments in this study, the CAMECA NanoSIMS and the CAMECA IMS-1280, use multiple detectors that collect ions simultaneously. Adapted from [107].

SIMS analyses of samples

The primary beam

O^- ions were used as the primary beam for all instruments and analytical sessions in this study. While O_2^+ creates a higher secondary ion yield for U^+ and UO^+ ions (by a factor of $\sim$2), O^- is typically used when analyzing insulating samples to neutralize positive charge build-up in the analysis crater [108]. In addition, in the NanoSIMS, the primary ion beam must be opposite in polarity to the secondary ion beam because of its unique co-axial extraction system where the primary beam enters and the secondary beam is extracted through the same aperture, which sits just above the sample surface.

The ion source

The CAMECA IMS-3f and IMS-1280 use a duoplasmatron to generate O^- ions for the primary ion beam. The duoplasmatron has been the standard ion source since the 1960s for producing beams from gases, as it can efficiently produce ions from gases in either polarity. In addition, the user has their choice of using monomers, dimers, and other molecules (*e.g.*, CO_2^-) for the primary beam. In SIMS, duoplasmatrons are most frequently used to create

Table 5.1: SIMS analysis campaigns (instrument and year) sorted by host object. Designations in **bold** were analysis campaigns that specifically targeted comparing the U isotope ratio of agglomerates to the host objects they are attached or incorporated into.

Sample ID	No. Agglomerates Analyzed	SIMS Instrument (Analysis Year)
U1A	0	IMS-1280 (2012)
U1B	2	IMS-3f (2012), IMS-1280 (2012), **NanoSIMS (2016, 2017)**
U2	0	IMS-3f (2012), IMS-1280 (2012)
U3	2	IMS-3f (2012), IMS-1280 (2012)
U4	3	IMS-3f (2012), IMS-1280 (2012)
FLD10	1	**NanoSIMS (2017)**
FLD14	2	**NanoSIMS (2017)**
FLD15	0	IMS-1280 (2015)
FLD16	0	IMS-1280 (2015)
FLD17	1	**NanoSIMS (2017)**
FLD18	2	IMS-1280 (2015), **NanoSIMS (2016, 2017)**
FLD20	0	IMS-1280 (2015)
FLD23	11	**NanoSIMS (2016, 2017)**
FLD4.3	4	**NanoSIMS (2017)**
AA.B	3	**NanoSIMS (2015)** in [67]
AE.C	2	**NanoSIMS (2015)** in [67]
AG.D	2	**NanoSIMS (2015)** in [67]
AH.E	1	**NanoSIMS (2015)** in [67]

either positive or negative O ion beams, and reliably do so with high brightness (>10 A cm^{-2} sr^{-1}) and narrow energy spreads (∼10 eV) [109].

To form the plasma, the duoplasmatrons in the IMS-3f and IMS-1280 use a current applied through a high-purity O_2 gas to strike an arc between a Ni cathode and the ferrous Fe anode. The Ni cathode bombards the O_2 gas with electrons, ionizing it and forming a plasma. The plasma is constricted by an inhomogeneous magnetic field near the aperture located at the anode, where it is extracted and steered through a magnet to allow only the ions of interest to enter into the primary column. In contrast, the NanoSIMS uses an inductively-coupled plasma source to generate its O^- primary beam. The NanoSIMS ion source, the Hyperion II (manufactured by Oregon Physics), is capable of a ∼100x increase in beam brightness over the duoplasmatron and is capable of operating at much higher spatial resolutions (∼50 nm) with narrower energy spreads (≈3–4 eV) [110]. The primary beam column (which houses the ion optics of the primary beam) for all three instruments consists of a series of electrostatic lenses, deflectors, and octopole stigmators, which allow the user to adjust the shape, size, and intensity of the primary beam. On the IMS-3f and IMS-1280, which have similar primary columns, the beam can be varied between ≈1–200 μm in diameter, and the current between 0.1–1000 nA. For this study, on the IMS-3f, the beam diameter ranged from 10–30 μm and the beam current was set to approximately 5

nA. On the IMS-1280, samples were analyzed with a 25–40 μm beam rastered in a square at approximately 25 nA.

Sputtering

Sputtering is the controlled erosion of a solid surface from bombardment by an energetic ion beam and is the process that SIMS uses to generate ions from solid samples. It is a complex and incompletely understood process that can be described qualitatively, but no first-principles model adequately describes sputtering from complex surfaces such as heterogeneous, amorphous aluminosilicates, such as glassy fallout [111].

As energetic O^- ions bombard the surface, they transfer their energy to atoms in the sample through elastic and inelastic scattering. The atoms in the sample that are struck by primary beam ions are called "primary knock-on" atoms and they transfer their energy to atoms surrounding them [112]. Those atoms continue to transfer energy and momentum to other atoms, creating a "collision cascade" (Figure 5.2) [112]. If an atom receives sufficient kinetic energy in excess of its binding energy (≈10–30 eV) and momentum in a direction away from the sample, it may escape the sample surface.

Sputtered atoms are ejected from only the top few atomic layers of the sample and can be liberated as neutral atoms, ions, and as monomers or molecules [113]. As a result, it is necessary to "pre-sputter" the sample surface before collecting data to remove contamination layers and/or the conductive coating. The number of atoms of a species sputtered as ions per incident primary beam ion is called the secondary ion yield. For positive ions sputtered from the same matrix, the yield roughly decreases exponentially with the ionization potential of the element. For example, the positive secondary ion yield of Group I and II elements, with low ionization potentials, is greater than for Au, Th, or U (Figure 5.3). U^+ is not shown in Figure 5.3, but its *useful* secondary positive ion yield (that is, ions *detected* per incoming primary beam ion) when sputtered from silicate matrices is almost identical to Th^+ [114].[1]

The energy distribution of sputtered atoms that are liberated as ions peaks at kinetic energies between 5–10 eV and has an exponential tails that extends up to ∼100 eV [113]. However, molecules can be produced as well (M^+, MO^+, MO_2^+, MOH^+, etc., where M is a metal or metalloid that can form positive ions). In the case of geological samples, these molecular ions create complex mass spectra that have many interfering isobars. Fortunately, there are several methods to filter out isobaric interferences. When they cannot be filtered out, one can usually estimate and subtract their contribution (discussed below).

Finally, relative ion yields for isotopes of the same element are not identical. Lighter isotopes are preferentially sputtered relative to heavier isotopes. This mass-based fractionation is usually small (at the percent level). Because no first-principles understanding of the

[1]Useful secondary positive ion yield is different from positive ion yield in that it counts the number of ions *detected* not *produced*, so this depends on the instrument, operator, and tuning conditions. The useful secondary ion yield will always be lower than the secondary ion yield, due to transmission losses in the instrument and detection inefficiencies.

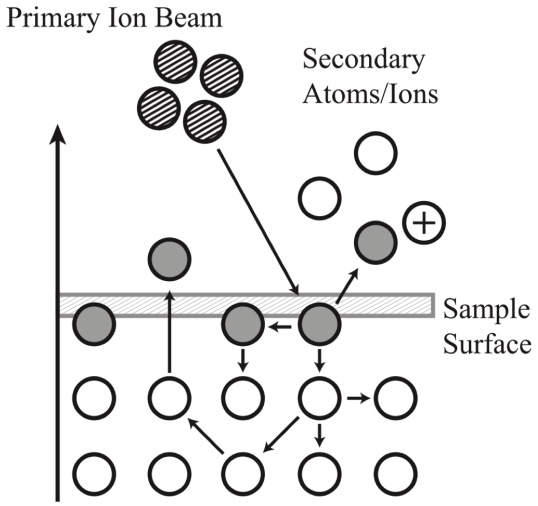

Figure 5.2: A schematic of the sputtering process and the a collision cascade.

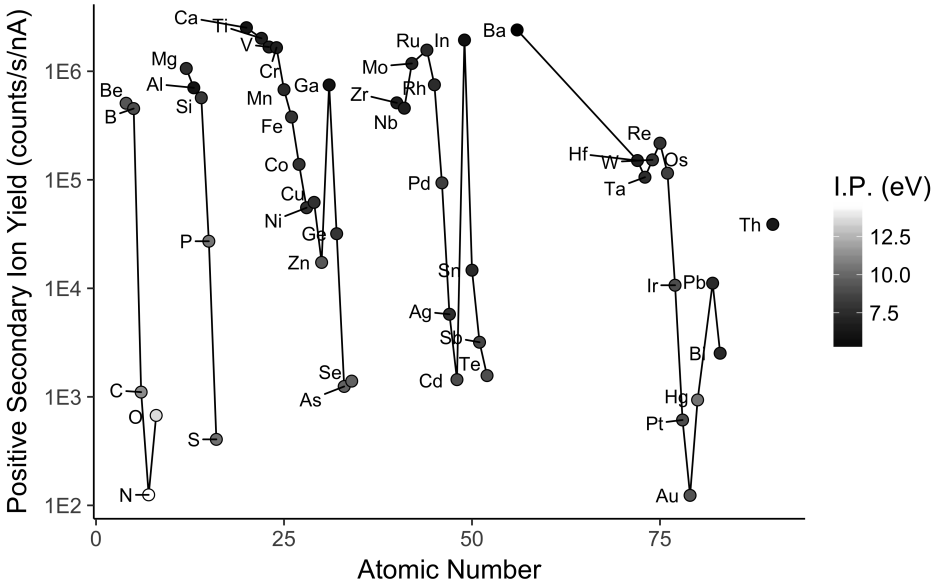

Figure 5.3: Plot of positive secondary ion yield vs. atomic number from bombardment with an O^- beam. Shading of the points correspond to their ionization potential in eV (I.P. in the legend). Lines connect elements from the same row in the periodic table. Adapted from [115].

sputtering process exists, this fractionation is corrected by measuring standards with similar matrices and compositions to the unknown (Figure 5.6).

The secondary beam and column

Once sputtered, secondary ions are accelerated into the secondary column through an aperture in an extraction electrode just above the sample surface.[2] The secondary column preserves the ion image of the sample surface as the secondary beam is transported through the mass spectrometer, allowing for real-time ion mapping and imaging of the sample surface (for the IMS-3f and IMS-1280). The NanoSIMS forms ion images through rastering the primary beam over a region.

After the extraction electrodes, the transfer optics focus the ion image of the sample surface onto the field aperture, which sits just behind the entrance slit. The field aperture and entrance slit are both physical apertures, but with different functions. The field aperture limits or expands the field of view the sample surface, which, allows the user to only sample, image, and count ions from the very center of a SIMS crater and not the crater edges. The entrance slit is used to remove secondary ions that are off-axis from the majority of the secondary beam, either due to deviations in position, energy, or momentum, and contribute to the finite width of ion peaks at the detector end of the spectrometer. By narrowing the entrance slit, these aberrant ions are removed, narrowing the width of ion peaks and improving the separation between ions of similar mass, allowing the spectrometer to resolve isobaric interferences.

Next, the secondary ion beam passes through the electrostatic analyzer, a pair of curved electrostatic plates of opposite voltage. The inner plate is opposite in voltage to the secondary ions, attracting them to the inner plate. The radius of curvature of ions through the analyzer is proportional to their kinetic energy,

$$F_E = zE = F_{\text{centrip}} = \frac{mv^2}{r_{\text{curvature}}} \longrightarrow r_{\text{curvature}} = \frac{mv^2}{zE}, \tag{5.1}$$

where F_E is the magnitude of force due to an electric field perpendicular to an ion's trajectory, F_{centrip} is the centripetal force an object experiences traveling on a circular path, z is the ion's net charge, E is the magnitude of the electric field, and $r_{\text{curvature}}$ is resulting the radius of curvature of an ion with charge z and kinetic energy $1/2mv^2$, passing through a field E perpendicular to its trajectory. Ions of lower kinetic energy are more easily deflected by the E-field than higher energy ions, leading to a spatial distribution of ions by energy. The secondary beam then passes through the spectrometer lens, which can be narrowed or translated to select high energy ions, low energy ions, or both. Next, the secondary beam enters the magnet, which disperses secondary ions by momentum:

$$F_B = zvB = F_{\text{centrip}} = \frac{mv^2}{r_{\text{curvature}}} \longrightarrow r_{\text{curvature}} = \frac{mv}{zB}, \tag{5.2}$$

[2]The following description of the secondary column primarily relates to the design of the IMS-3f for simplicity and clarity. In the IMS-1280 and NanoSIMS, additional deflection plates, quadrupoles, and lenses control higher order aberrations and alignment of the secondary beam in the magnet and detection system. Altering the voltages on these electrodes is an important aspect of tuning the secondary column, but only the primary components of the mass spectrometer are discussed here.

where where F_B is the magnitude of force due to a magnetic field perpendicular to an ion's trajectory, F_{centrip} is the centripetal force an object experiences traveling on a circular path, z is the ion's net charge, B is the magnitude of the electric field, and $r_{\text{curvature}}$ is resulting the radius of curvature of an ion with charge z and kinetic energy $1/2mv^2$, passing through a field B perpendicular to its velocity. Alternatively, the ion's kinetic energy can be expressed as KE= zV, and solving Equation 5.2 for $v = Bzr_{\text{curvature}}/m$, the resulting dispersion can be expressed in terms of an ion's mass-to-charge ratio m/z:

$$zV = \frac{mv^2}{2} \longrightarrow zV = \frac{mB^2z^2r_{\text{curvature}}^2}{2m^2} \longrightarrow \frac{m}{z} = \frac{B^2r_{\text{curvature}}^2}{2V}. \tag{5.3}$$

After ions are dispersed by the magnetic field, they pass through the exit slit, which is a physical aperture that can be narrowed to reduce the range of ions with $\Delta r_{\text{curvature}}$ incident on the detector. (This, in combination with the entrance slit, is one method double-focusing mass spectrometers can resolve isobaric interferences.) For multi-collector systems, the exit slits are physically mounted on each of the detectors and for mono-collector systems, the exit slit is positioned just after the magnet. Finally, a series of lenses and deflector plates guide the mass-filtered secondary ion beam, preserving the location from where they were first sputtered (again, allowing ion imaging and mapping), onto detectors where they are counted.

Ion detection

To form ratios between different isotopes, ions were counted using an electron multiplier (EM) or a Faraday cup (FC). The EM and FC determine count rates using pulse counting and current measurement, respectively. At low count rates ($<10^6$ cps), the EM is used due to a background $\sim$6 orders of magnitude below the FC's background ($\sim10^4$ cps). At high count rates ($>10^6$ cps), the Faraday cup is often used to avoid excessive dead time losses and damaging the EM's sensitive dynode surfaces. However, when using multiple detectors to detect ions, the relative efficiencies of the detectors must be known. Frequently, instead of switching to the FC for high count rate isotopes, many users simply reduce the primary beam current and, therefore, secondary beam current, to allow them to measure all isotopes on the EM.

The IMS-3f has a single electron multiplier and Faraday cup that uses electrostatic deflectors to switch between the two during an analysis. The multi-collector setup on the IMS-1280 has five electron multipliers with two Faraday cups, one on the low mass side and one on the high mass side. The NanoSIMS multi-collector system also has five electron multiplier detectors, with a single Faraday cup on the low mass side. The IMS-1280 has the advantage of being able to measure the major and minor isotopes of U using a single static magnetic field. In the NanoSIMS, the magnet insufficiently disperses $^{235}U^+$ and $^{238}U^+$ ions, preventing the electron multipliers from getting close enough to measure both ions using a single, static magnetic field, so two magnetic fields must be used.

EMs were used for all analytical sessions, except for some 2012 measurements on the IMS-3f, when the intensity of $^{30}Si^{+}$ was too high for the EM. When shifting between an EM and Faraday cup during the same analytical session, the relative detection efficiency of the EM (Faraday cup has an assumed efficiency of 1) must be measured. Relative detection efficiencies of EMs are usually >0.9.

Electron multiplier

The EM is the standard ion detector in SIMS. It has low background noise, typically <0.1 counts per second (cps), and as a result, is able to detect and count single ions. EMs enhance the signal from incoming ions using a series of dynodes (Figure 5.4). First, an ion transmitted through the instrument strikes the conversion dynode, made of a low work function material, which readily ejects secondary electrons. An applied potential accelerates these electrons to the next dynode, where they bombard the surface, creating more secondary electrons. Those electrons are accelerated to the next, and so on, creating an electron cascade. The EMs for all three SIMS instruments use 18 dynodes to achieve gains of up to 10^7 electrons are detected per incoming ion from the sample. These electrons are collected at the anode and read as a single pulse. The pulse is converted to a voltage, amplified by the pre-amplifier, and then passed to a discriminator, which filters out low energy noise before the pulse is counted.

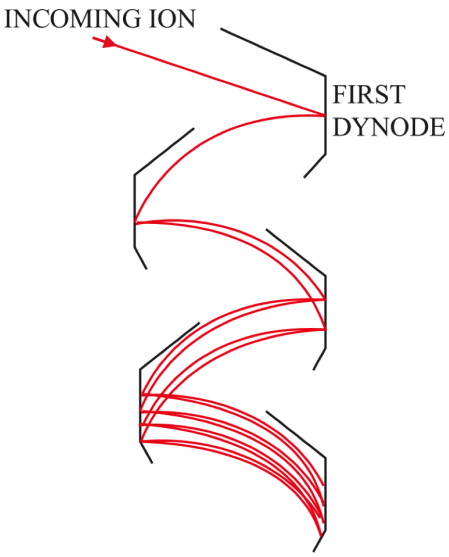

Figure 5.4: Schematic of an ion from the sample striking the conversion dynode of an EM, creating an electron cascade. Reproduced from [60].

From an ion striking the conversion dynode to being read by the counter, EM signal processing takes a non-negligible amount of time (≈30–50 ns). During this time, signals created

by other incoming ions are rejected. This deadtime (τ) must be properly characterized to correct for lost counts, In addition, the dead time changes as the EM ages, so it must be periodically re-characterized. The measured count rate differs from the true count rate by

$$C_{\text{true}} = \frac{C_{\text{meas}}}{1 - \tau C_{\text{meas}}}. \tag{5.4}$$

The deadtime correction is nearly negligible at count rates below $\sim 10^3$ cps ($C_{\text{true}}/C_{\text{meas}} = 1.00004$, assuming $\tau = 40$ ns), but important for count rates above $\sim 10^4$ cps. At even higher count rates ($\sim 10^6$ cps), small variations in the deadtime lead to large changes in the count rate, so the deadtime must be carefully characterized. High count rates can also damage the conversion dynode surface, so either the primary current must be reduced or the user must switch over to the Faraday cup detector, which is more robust and does not suffer from dead time losses.

Faraday cup

A Faraday cup counts ions by measuring ion current. It consists of a tilted metallic electrode located within a grounded, metallic cup. The electrode is tilted to prevent secondary electrons, created by the bombardment of the ion beam on the electrode from escaping the cup and are instead collected by the grounded cup walls. As the titled electrode collects the positive ions from the ion beam, electrons travel across a high resistance load resistor to neutralize the positive charge. Current across the resistor produces a voltage that is measured and the number of positive ions collected on the electrode is calculated. However, the high resistance of the load resistor causes a great deal of thermal noise, producing a background of spurious, random voltages across the resistor, creating a high background of $\sim 10^4$ cps.

Faraday cups are always used to measure primary beam currents, due to their potentially high intensity (up to several μA) and are sometimes used to measure secondary ion beam currents, when the intensity is too great for an electron multiplier ($>10^6$ cps). In this study, only the 2012 analytical session on the IMS-3f used the FC, and only infrequently, when the intensity of $^{30}Si^+$ was too great for the EM. In other circumstances, when secondary ion beam intensities approached 10^6 cps, the primary ion beam current was turned down so all ions could be measured on EMs.

Isobaric interferences and mass resolving power

The measured signal intensity from a mass spectrometer corresponds to ions of a small range of masses about the nominal mass (Δm about m), rather than one isotope of a single mass. This dispersion is caused by the finite width of the secondary ion energy distribution and the physical width of entrance slits, exit slits, and conversion dynode on the EM. Isobaric interferences (ions with the same nominal mass) can be separated in two ways: either by taking advantage of the different energy distributions between atomic and molecular ions and altering the energy bandpass of the spectrometer accordingly, or by increasing the "mass

resolving power". The ability of a mass spectrometer to separate ions of near identical mass is known as its mass resolving power and is calculated as $m/\Delta m$, where m is the nominal mass and Δm is the difference in mass defects between the interfering ion and ion of interest about m.[3] In this study, the mass resolving power is increased to separate isobaric interferences because both atomic and molecular ions were often analyzed in the same analytical session and increasing the mass resolving power generally reduces transmission less than energy filtering [116].

Mass resolving power is variable and set by the operator, but the higher the mass resolving power, the greater the ability to distinguish between ions of similar masses. The different SIMS instruments used in this study are capable of different mass resolving powers: the IMS-3f is capable of mass resolving powers greater than 5,000, while the IMS-1280 and NanoSIMS are capable of mass resolving powers exceeding 12,000. Not all interferences can or need to be resolved (Figure 5.5). Some unresolvable interferences have a negligible contribution, such as $^{234}UH^+$ interfering at $^{235}U^+$ in this study. First, ^{234}U is already at a low abundance in this fallout($^{234}U/^{238}U < 0.1$) [60]. Second, hydride formation is low with approximately 2.5 cps detected at mass 239 ($^{238}UH^+$) for every 10^4 cps detected at mass 238 (as measured on the U500 standard). If there is an unresolvable interference with a non-negligible contribution, one may monitor that interference using a different isotope of an element that comprises the interference. Assuming an isotopic composition, the contribution of the unresolvable interference can be estimated and the subtracted from the measured mass of interest.

Higher mass resolving power reduces transmission of secondary ions through the instrument because physical plates (*i.e.*, the entrance and exit slits) are used to block ions from (a) entering the mass spectrometer and (b) impinging on the detector. The IMS-3f and IMS-1280 have continuously variable entrance and exit slits, while the NanoSIMS has five discrete slit widths. Narrowing the entrance slit removes aberrant ions far from the center line of the mass spectrometer ("the optical axis"). Narrowing the exit slits physically reduces the peak width before the ions are detected to remove tails from isobaric interferences.

For the analytical sessions in this study, the instruments operated at a mass resolving power ∼3000–4000, sufficient to resolve most non-negligible isobaric interferences [60]. Non-negligible interferences in this study were primarily at low mass, such as silicon hydrides interfering on $^{30}Si^+$ and $^{27}Al_2{}^+$ interfering on $^{54}Fe^+$. At the masses of U and UO, non-hydride isobaric interferences were primarily from combinations of Pb isotopes and isotopes of major elements, such as $^{208}Pb^{27}Al^+$ interfering at mass 235 or $^{208}Pb^{30}Si^+$ interfering at mass 238. Pb was present at <1 cps when monitoring $^{208}Pb^+$ for possible sources of isobaric interferences on fallout in 2012. $^{238}U^1H^+$ and $^{238}U^{16}O^1H^+$ was monitored on the IMS-1280 and the IMS-3f during several analyses on the U500 standard to measure the contribution from $^{234}U^1H^+$ and $^{234}U^{16}O^1H^+$. $^{238}U^{16}O^1H^+$ contributed approximately 2.5 cps for every 10^4 cps of $^{238}U^{16}O^+$ ($^{238}U^1H/^{238}U \approx 0.00025$ from 50 measurements on U500). Given the abundance of $^{234}U^+$ in fallout (<1 at.%) relative to $^{235}U^+$ (usually >75 at.%), a hydride interference is a negligible correction for $^{235}U^+$ in this study. During the IMS-1280 studies,

[3] In this work, two ions are considered resolved when their overlap is <10% of their peak heights.

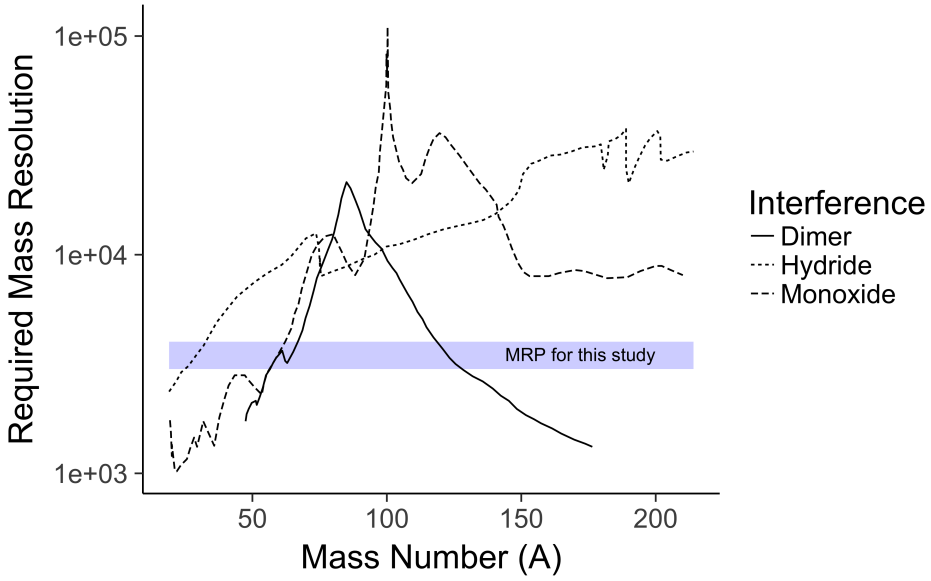

Figure 5.5: Mass resolving power required to resolve three common isobaric interferences: dimers, hydrides, and monoxides. The horizontal band denotes the approximate range of mass resolving powers used in this study. Plot adapted from [117].

the contribution of $^{235}U^{1}H^{+}$ to the 236 mass peak was removed by subtracting the calculated $^{235}U^{1}H^{+}$ contribution from monitoring $^{238}U^{1}H^{+}$ (mass 239):

$$^{236}U^{+}_{\text{cts}} = (\text{Cts at mass } 236) - \frac{^{238}U^{1}H^{+}_{\text{cts}}}{^{238}U^{+}_{\text{cts}}} \times {}^{235}U^{+}_{\text{cts}}. \tag{5.5}$$

This correction was small, with $^{235}U^{1}H^{+}$ contributing approximately 0.5 cps to $^{236}U^{+}$ (≈25–50 cps).

Standards

Many instrumental factors and physical processes affect how efficiently an ion is sputtered from a sample, transmitted through an instrument, detected, and counted. These factors not only vary between instruments and operators, but may vary from day-to-day on the same instrument.

Instead for accounting for these instrumental biases individually, SIMS relies on measurements of standard materials to correct for instrumental bias collectively. Effective and useful standards are completely characterized (*i.e.*, major and trace element concentrations and isotopic ratios are known), similar in major element composition to the unknown (referred to as being "matrix-matched"), and similar in isotopic composition to the trace elements of

interest (*i.e.*, a standard with non-natural U isotopic composition is better for SIMS studies of fallout than one with natural U isotopic composition).

In total, three U-doped, calcium aluminosilicate glasses were used as standards (Tables 5.2 and 5.3). The glasses were fabricated at LLNL and doped with U_3O_3 powders of known and certified U isotopic compositions. For the majority of SIMS analyses, a single glass standard doped with ≈350 ppm U of non-natural isotopic composition was used ("LLNL U500" in Table 5.2). Another set of SIMS analyses, performed at LANL in 2012, used a higher concentration U standard (≈3500 ppm U) made with the same base glass material and U dopant ("LANL U500" in Table 5.2). The U dopant in both standards is a U_3O_8 powdered Certified Reference Material (CRM) from New Brunswick Laboratory with a $^{235}U/^{238}U$ ratio of ≈1 (Table 5.2). However, early SIMS isotopic measurements suggested that the ratio in the final formulated glass deviated from the CRM certificate. MC-ICP-MS analyses of the glass revealed a slight deviation in the isotopic ratios from certificate values, likely from contamination from some other non-natural U source in the laboratory used to create the doped glass.

The third U-doped glass standard, CAS-53-500, was used during the 2017 NanoSIMS analytical session. The U dopant was New Brunswick Laboratories Nuclear Forensic Reference Material 2 (NFRM U-2), with a nominal $^{235}U/^{238}U$ ratio of ≈1.13. Similar to the U500 standards, MC-ICP-MS analyses revealed its U isotopic composition deviated from the certified ratios of the base U powder (see [101]). While the CAS-53-500 U isotopic composition is similar to that of the U500 glasses, its major element composition is different, being fused from a different eutectic (the CAS-3 eutectic) in the CaO-Al_2O_3-SiO_2 system (Tables 5.3).

Table 5.2: U concentrations and U isotopic ratios of the U-bearing glass standards as measured by MC-ICP-MS. Included are the certified U isotopic ratios from the NBL CRM certificate for U500 and NFRM U-2 for comparison and reference. To calculate the fractionation factors, U500 MC-ICP-MS measurements were performed by K. Treinen and R. Williams and CAS-53-500 MC-ICP-MS measurements performed by G. Eppich were used (documented in [101]).

Standard	U Conc. (μg/g)	±	2σ	$^{235}U/^{238}U$	±	2σ	$^{234}U/^{238}U$	±	2σ	$^{236}U/^{238}U$	±	2σ
LLNL U500 (meas.)	359.1	±	1.2	0.9618	±	0.0013	0.010044	±	0.000006	0.001479	±	0.000006
LANL U500 (meas.)	3490	±	12	0.9949	±	0.0014	0.010371	±	0.000006	0.001521	±	0.000005
NBL U500 Cert.	-	±	-	0.9997	±	0.0028	0.010422	±	0.000038	0.001519	±	0.000012
CAS-53-500 (meas.)	331.5	±	4.1	1.1253	±	0.0004	0.010622	±	0.000002	0.007773	±	0.000004
NFRM U-2 Cert.	-	±	-	1.1340	±	0.0020	0.008067	±	0.000028	0.005691	±	0.000013

Table 5.3: Nominal compositions of the base glasses used to make the U500 standards and CAS-53-500 standard.

Standard	Si wt.%	Al wt.%	Ca wt.%
U500 glass	15.0	19.6	22.2
CAS-53-500 glass	29.0	7.7	16.8

The fractionation factor

The deviation of standards measurements from their known values is used to collectively account for sputtering and instrumental fractionation effects. This ratio, called the fractionation factor, is then used to correct measurements made on the unknown:

$$\text{Sample ratio}_{\text{true}} = \frac{\text{Standard ratio}_{\text{true}}}{\text{Standard ratio}_{\text{measured}}} \times \text{Sample ratio}_{\text{measured}}. \tag{5.6}$$

For these analyses, the correction is small, at the percent or permil level, and is usually slightly less than 1, as sputtering preferentially sputters lighter isotopes relative to heavier ones (Figure 5.6). The fractionation factor can be greater than 1 for multi-collector analyses because of differences between EM age or where the secondary ion beam strikes each EM's conversion dynode surface. Finally, the uncertainty in the fractionation correction is typically small as well (at the permil level), and is added in quadrature with the uncertainty from the measured ratio.

SIMS instrument operating conditions

IMS-3f

The CAMECA IMS-3f is capable of per mil precision and produce count rates of ∼100 cps on $^{235}U^{16}O^{+}$ for tens of ppm U at a spot size ≈10–30 μm and primary beam currents of ≈5-10 nA O^{-}. Given these operating conditions, per mil precision were typically achieved in these samples with ∼1 hr analyses.

The CAMECA IMS-3f was used in 2012 to characterize the heterogeneity of U isotopes in U1B, U2, U3, and U4 by conducting approximately linear traverses across the samples and not attempting to target and characterize agglomerates [60]. However, when reexamining the analysis craters by SEM/EDS, it was determined that several agglomerates had been analyzed. The data from these agglomerates are included in this dataset, along with the host object U isotope dataset from the other SIMS analysis craters.

IMS-1280

The CAMECA IMS-1280 is a large geometry multi-collector SIMS instrument, with high transmission of secondary ions through the mass spectrometer. As a result, the instrument can achieve sub-per-mil precision in an analytical session of just a few minutes. Count rates on this instrument were approximately an order-of-magnitude larger, yielding ∼1000 cps on $^{235}U^{+}$ for most measurements at 25 nA primary beam currents.

Data from two analytical sessions using the IMS-1280 are included in this dissertation. First, M. Zimmer and W. Kinman of Los Alamos National Laboratory (LANL) analyzed samples U1A, U1B, U2, U3 and U4 for major and minor U isotopes ($^{234}U^{+}$, $^{235}U^{+}$, $^{236}U^{+}$, $^{238}U^{+}$, and $^{238}U^{1}H^{+}$ to correct for hydride formation) in 2012. They conducted traverses across the samples without regard to agglomerates, similar to the study of the U-series of

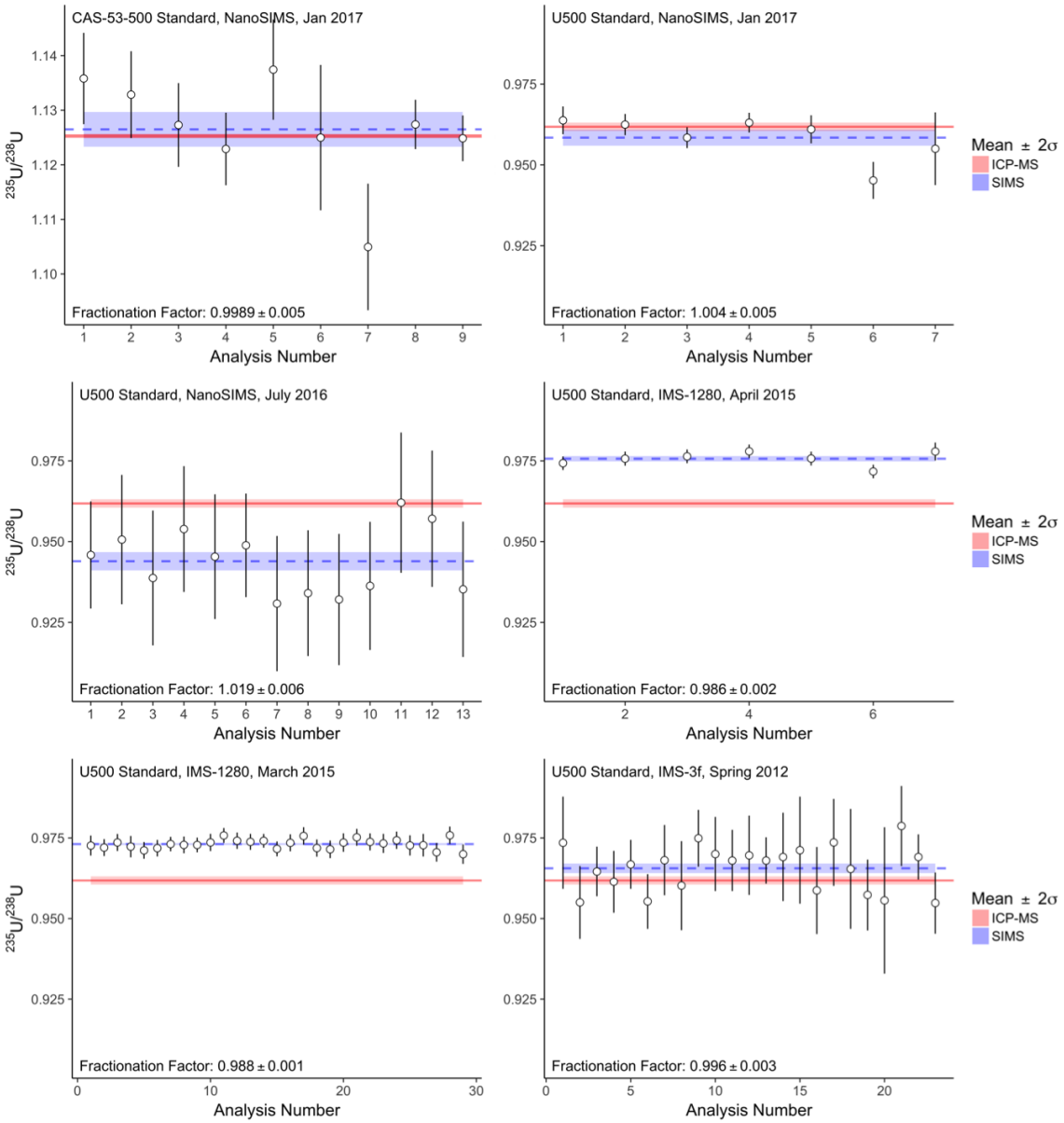

Figure 5.6: SIMS measurements of the $^{235}U/^{238}U$ ratio on CAS-53-500 (top left) and ≈350 ppm U500 standard (the remaining plots) from all SIMS sessions between 2012–2017 in reverse chronological order. LANL's analysis of the ≈3500 ppm U500 standard during the analytical campaign on their IMS-1280 in 2012 is detailed in [60]. For all plots, the blue dashed line and blue band are the mean and 2SEOM of the SIMS measurements, respectively. The red line and band are the mean and 2SEOM band of three ICP-MS measurements on each of the standard glasses. For the U500 plots, the y-axis is the same to ease comparison between results from the U500-doped glasses with two different concentrations. Data are tabulated in Appendix F.

samples on the IMS-3f in Lewis (2012) and was combined with these results for publication [60]. In 2015, LANL's IMS-1280 was used with assistance from T. Williamson and C. Bonamici to analyze samples FLD15, FLD16, FLD18, FLD20 in linear traverses, again not specifically targeting agglomerates. During this analytical session, the $^{234}U^{+}$, $^{235}U^{+}$, $^{238}U^{+}$, and $^{238}U^{1}H^{+}$ ions were measured. $^{236}U^{+}$ was also measured in select analyses.

NanoSIMS

The CAMECA NanoSIMS is a SIMS instrument primarily built for sub-micron scale imaging. Typical operating conditions for fallout glasses were primary beam currents of 0.1–0.5 nA and square rasters of 10-20 μm (the beam diameter is much smaller than this, typically $\approx$1 μm, but rastered over the 10-20 μm region). Under these operating conditions, percent precision can be obtained with $\sim$1 hr analyses [118]. While the primary ion beam current is an order-of-magnitude lower than the IMS-3f, the instrument's ability to transmit secondary ions through the secondary column without loss is higher, so count rates on $^{235}U^{16}O^{+}$ were $\approx$50–150 cps, similar to the IMS-3f.

The NanoSIMS was used (with assistance from J. Matzel and P. Weber) for two analytical sessions, one in July 2016 and January 2017. These measurements took advantage of the small spatial resolution of the NanoSIMS to target agglomerates in samples U1B, FLD10, FLD14, FLD17, FLD18, FLD23, and FLD4.3.

Determining chemical compositions of SIMS analysis regions

To combine U isotope and major element composition data, EDS rasters were collected from within and around SIMS analyses craters.

For the IMS-3f, the operating conditions created $\approx$10-30 μm diameter analysis craters, with depths on the order of several microns (Figure 5.7). To measure the composition using EDS, several rasters were manually drawn around the crater and averaged. However, due to the scale of compositional heterogeneity in glassy fallout, this can lead to sampling a composition with EDS that is not similar in composition to the region analyzed by SIMS. Data with this behavior were omitted from this study.

For the IMS-1280, operating conditions created analysis craters that tended to be wider and shallower than the IMS-3f, $\approx$30 μm squares, but shallow ($<$1 μm deep) and Gaussian-shaped (Figure 5.7). In contrast to IMS-3f analysis craters, EDS rasters were often able to sample the composition of the crater directly, depending on its depth and topography.

Finally, analysis craters from the NanoSIMS were shallow and square. This topography allowed for the use of manually-drawn EDS raster directly in the analyses crater to measure the major element composition within the crater in all cases (Figure 5.7).

While operating conditions between different analytical sessions varied, conditions within individual analytical sessions were approximately fixed (Table 5.4). For example, only approximate primary ion beam currents are known because the primary ion beam drifts with time (typically by less than a few percent). The mass resolving power is usually only mea-

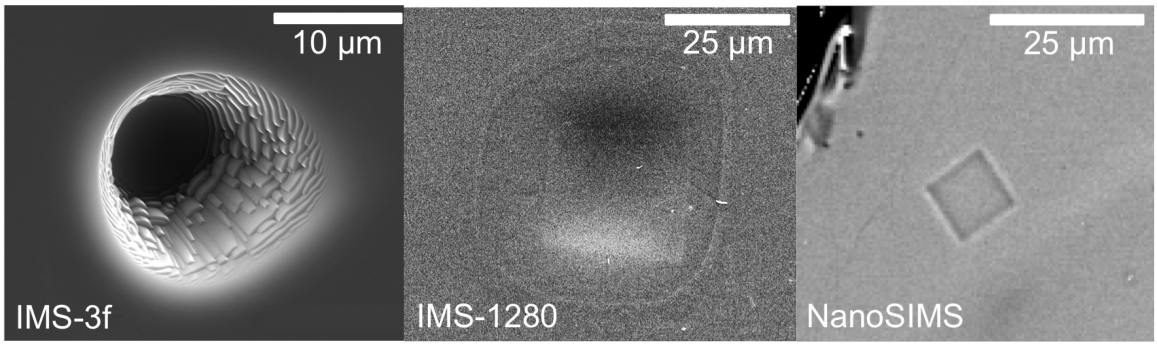

Figure 5.7: Electron images of craters created by the three different SIMS instruments used in this study: the IMS-3f (left; SE image), IMS-1280 (middle; SE image), and a 15 μm square raster from the NanoSIMS (right; BSE image).

sured while tuning, which is at the beginning of an analytical session. Although operating conditions vary from instrument to instrument, the SIMS measurements are comparable because they are linked through measurements of the standard glasses previously described. Standards measurements take place throughout the analytical session to account for variations in analytical conditions, if they occur. In one instance, during a 3 week analytical session at LANL that spanned from March 2015 to April 2015, the instrument was tuned at the beginning of the session and then re-tuned in early April, creating a slight variation in the measured fractionation factor (Figure 5.6). All fallout measurements made in March 2015 were corrected based on the March 2015 standards measurements and fallout measurements made in April 2015 were corrected based on the April 2015 standards measurements.

Table 5.4: Operating conditions for the analytical sessions in this study. "I (nA)" refers to the primary ion beam current and "$m\Delta m$" to the approximate mass resolving power the instrument operated at.

Instrument	Year	~I (nA)	~ $m/\Delta m$	Standard	Detectors and Ions	Crater Sizes (μm)	Pixels	Pre-sputter time (min.)	Analytical time (min.)	Cycles
IMS-3f	2012	5	3000	U500	Table 5.5	10–30	-	5	60	60–80
IMS-1280*	2012	25	4000	3500 ppm U500	Table 5.6	30–40	-	2	15	50–60
IMS-1280	2015	25	4000	U500	Table 5.6	30–40	-	2	15	50–60
NanoSIMS	2016	0.2	4000	U500	Table 5.7	15–20	64x64	10	120	100–200
NanoSIMS	2017	0.4	4000	U500/CAS-53-500	Table 5.7	15–20	64x64	10	60	70–100

Running a SIMS analysis

After the SIMS instrument is tuned, the operator decides the masses to measure (Table 5.5). Typically, a low mass and high mass are chosen as reference masses. For example, for the NanoSIMS runs in 2016 and 2017, $^{42}Ca^{+}$ was the reference mass at low masses (reference for $^{30}Si^{+}$ and $^{54}Fe^{+}$) and $^{235}UO^{+}$ was a reference at high mass for $^{235}U^{+}$, $^{238}U^{+}$, and $^{238}UO^{+}$. Measurements of reference masses were fit in the beginning of, and during, an analysis so the intermediate mass peaks could be re-centered if instrument drift has occurred. Generally,

a measurement of the secondary ion distribution of reference mass ions was performed and the instrument software applies a voltage offset to the sample stage to ensure the energy distributions of the reference ion masses did not shift. This accounts for instrumental drift during an analysis and other masses were assumed to drift with the reference mass. Magnetic field or energy distribution shifts applied to the reference masses were applied to all other masses.

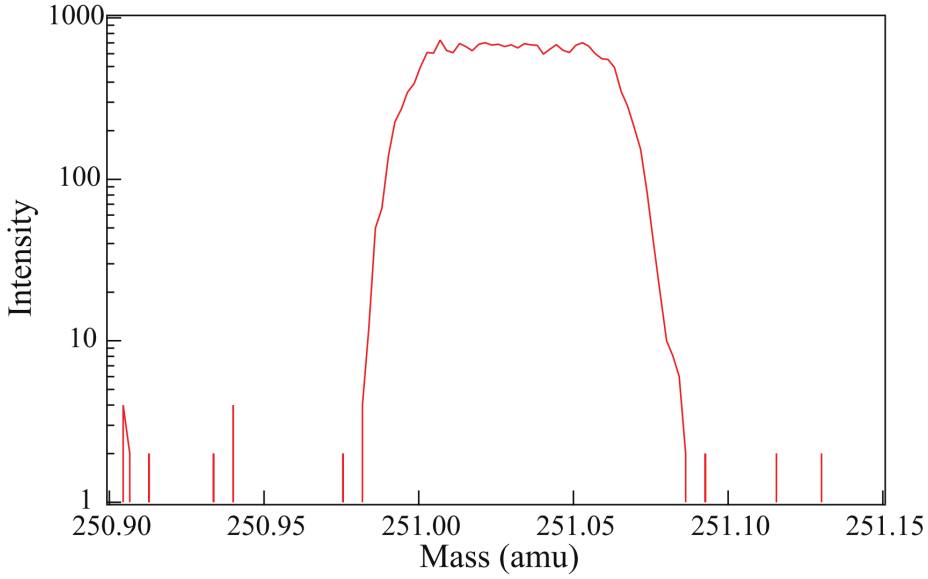

Figure 5.8: High resolution mass scan about mass 251 ($^{235}U^{16}O^{-}$) from a standard glass not used in this study. High resolution scans throughout an analysis use the slope and heights of either side of the peak to locate the approximate center of the peak, which the software considers the number of counts of particular ion. Due to slight drifts throughout the run, small variations in the noise on the peak top are averaged out. In this study, drift was much typically only a few percent of the full peak width.

SIMS instruments count ions in cycles. For a mono-collector instrument, ions at particular mass are counted for user-determined period of time (between 1-10 s/cycle depending on the ion's count rate). The magnetic field is then changed, the next mass in the mass table is counted, and so on. One cycle happens after all ions in the mass table have been counted once and the magnetic field returns to measure the first mass in the mass table (Table 5.5). For the multi-collector system on the IMS-1280, where only one magnetic field was used, the total run is split up into a user-defined number of cycles, typically 15-25 cycles under our operating conditions (Table 5.6). For the multi-collector system on the NanoSIMS, where two magnetic fields were used, one cycle was defined similarly to the mono-collector setup, but all masses at a particular magnetic field were counted for the same duration (Table 5.7).

Table 5.5: Mass table for IMS-3f SIMS measurements of fallout. This is a mono-collector system, so all ions were measured on the same EM, except when the intensity of $^{30}Si^+$ exceeded 10^6 cps, when measurements of $^{30}Si^+$ was moved to the FC. $^{30}Si^+$ was added in the latter half of the analysis campaign and was measured only samples U3 and U4. Before $^{30}Si^+$ was added, the mass table consisted of masses 248–254. Rest masses were used to allow the magnet to settle after large changes in magnetic field.

Nom. Mass	Ion	Detector
26.5	Rest Mass	EM
30	$^{30}Si^+$	EM/FC
247.5	Rest Mass	EM
251	$^{235}U^{16}O^+$	EM
254	$^{238}U^{16}O^+$	EM

Table 5.6: Mass table for the 2015 IMS-1280 analytical session on fallout. This is a multi-collector system. A static magnetic field was used and the EMs were arranged to collect the ions listed. The 2012 IMS-1280 analytical session is documented in [60] and used a mono-collector setup for samples U1A, U1B, U2, and U3 and a multi-collector setup for sample U4 (identical to the setup in this table). The mono-collector setup analyzed the same ions listed below, but on a single EM.

EM No.	Nominal Mass	Ion
EM1	234	$^{234}U^+$
EM2	235	$^{235}U^+$
EM3	236	$^{236}U^+$
EM4	238	$^{238}U^+$
EM5	239	$^{238}U^1H^+$

Isotopic ratios in SIMS

To form the reported isotope ratios, the ratio between analyzed ions is calculated for each cycle after applying several corrections (usually performed automatically by the instrument's software). Because sputtering continually removes atoms from the sample, the sputtered surface at time t_1 (when the instrument is counting, say, $^{235}U^+$) is different from the sputtered surface a few seconds later, at time t_2, when the instrument is counting, say, $^{238}U^+$. Another temporal effect is drift in the primary beam current, and therefore, secondary ion count rate, with time. When forming isotope ratios between ions collected on different magnetic fields, the counts are linearly time-interpolated to correct for these two effects. The time interpolation correction is usually small, ≈1–2%, and only applied when isotope ratios were formed between ions on different magnetic fields, such as in the case of a mono-collector analysis, or a multi-collector instrument using more than one field. Next, the counts were corrected for dead time losses. For U isotopes, where count rates are $\sim 10^2$ cps, this correction is negligible (but is automatically applied by the software). However, the dead time correction is important for isotopes of major elements, where count rates are $\sim 10^4$–10^5. Finally, the user can remove aberrant cycles. This is necessary when pre-sputtering times were insuffi-

Table 5.7: Mass table for both the 2016 and 2017 NanoSIMS analytical sessions. While this is a multi-collector system, two magnetic fields were used, one that included light elements and ions of ^{235}U, and the other that only included the ions of of ^{238}U. Note both the atomic and monoxide ions of ^{235}U and ^{238}U were analyzed. However, due to the higher secondary ion yield of the monoxide ions, and therefore, better precision, monoxide ratios were used in this study. Atomic ions of U were both measured on the same EM (EM4) and monoxide ions of U were both measured on the same EM (EM5).

	B-Field 1		**B-Field 2**	
EM No.	Nominal Mass	Ion	Nominal Mass	Ion
EM1	30	$^{30}Si^+$	-	-
EM2	42	$^{42}Ca^+$	-	-
EM3	54	$^{54}Fe^+$	-	-
EM4	235	$^{235}U^+$	238	$^{238}U^+$
EM5	251	$^{235}U^{16}O^+$	254	$^{238}U^{16}O^+$

cient to remove contamination layers on the sample, the primary beam current rapidly and unexpectedly fluctuates, or other transients occur in the instrument.

The final reported isotope ratio is the mean of the ratio of ions for each cycle, with its uncertainty presented as 2SEOM. This ratio and uncertainty were then corrected for mass fractionation, with the ratio's uncertainty and the fractionation factor's uncertainty summed in quadrature. Data are tabulated in Appendix F.

U/major element ratios in SIMS

U-major element ratios can be used to calculate the concentration of U or serve as a proxy for U concentration if the chosen major element is largely invariant in the sample. To calculate the ratio of U to major elements in fallout using SIMS, the (^{235}U+^{238}U)/^{30}Si or (^{235}U+^{238}U)/^{42}Ca ratio is measured on fallout and compared to the known (^{235}U+^{238}U)/^{30}Si or (^{235}U+^{238}U)/^{42}Ca ratio in the U-bearing silicate standards (Table 5.8). The total U is assumed to be $^{235}U^{16}O^+$ + $^{238}U^{16}O^+$ and that minor isotopes are negligible. Ca or Si is used in the denominator due to their presence in the standard glasses and in glassy fallout. (^{235}U+^{238}U)/^{30}Si is commonly used as a proxy for U concentration because the Si content typically varies ∼20% in the glassy regions of these fallout samples (Figure 4.10).

In addition to mass-based fractionation, the secondary ion yield of different elements must be considered when forming ratios between isotopes of different elements. The correction, which for elemental ratios is called the "relative sensitivity factor" (RSF), is defined as:

$$\mathrm{RSF} = \frac{\left[\frac{\mathrm{U}}{^{30}\mathrm{Si}}\right]_{\mathrm{known,std}}}{\left[\frac{\mathrm{U}}{^{30}\mathrm{Si}}\right]_{\mathrm{measured,std}}}. \tag{5.7}$$

Strictly, the RSF is the relative variation due to secondary ion yield, fractionation, transmission, and detection, between two elements. For simplicity it is used here between

Table 5.8: (^{235}U+^{238}U)/^{30}Si and (^{235}U+^{238}U)/^{42}Ca atomic ratios on U500 and CAS-53-500 and their measured values from three different analytical sessions (assuming nominal major element compositions and 5% uncertainties about those compositions). The EM used to measure ^{30}Si during the NanoSIMS (2016) analytical session had a failing pre-amplifier, leading to the anomalously high measured U/^{30}Si ratio. The RSF is obtained by dividing the known value by the measured value. Uncertainties are summed in quadrature.

Analytical Session	Standard	U/^{30}Si	±	2σ	U/^{42}Ca	±	2σ
-	U500	0.0092	±	0.0005	0.0425	±	0.0021
-	CAS-53-500	0.0044	±	0.0002	0.0517	±	0.0017
IMS-3f (2012)	U500	0.0293	±	0.0016	-	±	-
NanoSIMS (2016)	U500	0.2872	±	0.0008	0.0105	±	0.0003
NanoSIMS (2017)	U500	0.0532	±	0.0153	0.0085	±	0.0002
NanoSIMS (2017)	CAS-53-500	0.0064	±	0.0009	0.0093	±	0.0006

^{235}U, ^{238}U and ^{30}Si. The RSF correction accounts for difference in secondary ion yield between different elements. Unlike mass-based fractionation, which is typically a permil correction, the RSF measured in this study is ∼0.1 for (^{235}U+^{238}U)/^{30}Si and ∼5 for (^{235}U+^{238}U)/^{42}Ca. In addition, because different elements reach sputtering equilibrium at different rates, typically (^{235}U+^{238}U)/^{30}Si or (^{235}U+^{238}U)/^{42}Ca ratios take more cycles to reach a steady-state and have more scatter, leading to increased uncertainties compared to ratios of isotopes of the same element. Usually, the ^{235}U^{16}O/^{30}Si or ^{235}U^{16}O/^{42}Ca ratio increases from cycle to cycle before reaching sputtering equilibrium (Figure 5.9). In some analyses, the ^{235}U^{16}O/^{30}Si or ^{235}U^{16}O/^{42}Ca ratios were still increasing at the end of an analysis, although by <5% between cycles. This behavior results in an underestimation of the U concentration in these particular analyses.

To calculate U to major element ratios, the cycles were first subset and ^{235}U^{16}O/^{30}Si and ^{238}U^{16}O/^{30}Si ratios were summed, forming $\left[\mathrm{U}/^{30}\mathrm{Si}\right]_{\mathrm{measured,uncorrected}}$. Next, the corrected ratio is calculated by multiplying $\left[\mathrm{U}/^{30}\mathrm{Si}\right]_{\mathrm{measured,uncorrected}}$ by the relative sensitivity factor as measured on the standard with known U and Si concentrations:

$$\left[\frac{\mathrm{U}}{^{30}\mathrm{Si}}\right]_{\mathrm{measured,corrected}} = \frac{\left[\frac{\mathrm{U}}{^{30}\mathrm{Si}}\right]_{\mathrm{known,std}}}{\left[\frac{\mathrm{U}}{^{30}\mathrm{Si}}\right]_{\mathrm{measured,std}}} \times \left[\frac{\mathrm{U}}{^{30}\mathrm{Si}}\right]_{\mathrm{measured,uncorrected}}. \tag{5.8}$$

Uncertainties are summed in quadrature. ^{30}Si$^+$ and ^{42}Ca$^+$ were collected for all NanoSIMS measurements (2016 and 2017 analysis campaigns), so U/^{30}Si and U/^{42}Ca were calculated for measurements on samples U1B, FLD4.3, FLD10, FLD14, FLD17, FLD18, and FLD23 (Table 5.1).[4] ^{30}Si$^+$ was collected for a set of IMS-3f analyses (2012 analysis campaign), so the U/^{30}Si ratios were also calculated for several analyses on samples U2, U3, and U4 (Table 5.1). Data are tabulated in Appendix F.

[4]During the 2016 NanoSIMS campaign, EM1, which was used to count ^{30}Si$^+$, was malfunctioning. As a result, the U/^{30}Si data are omitted for these analyses and only the U/^{42}Ca ratios are reported.

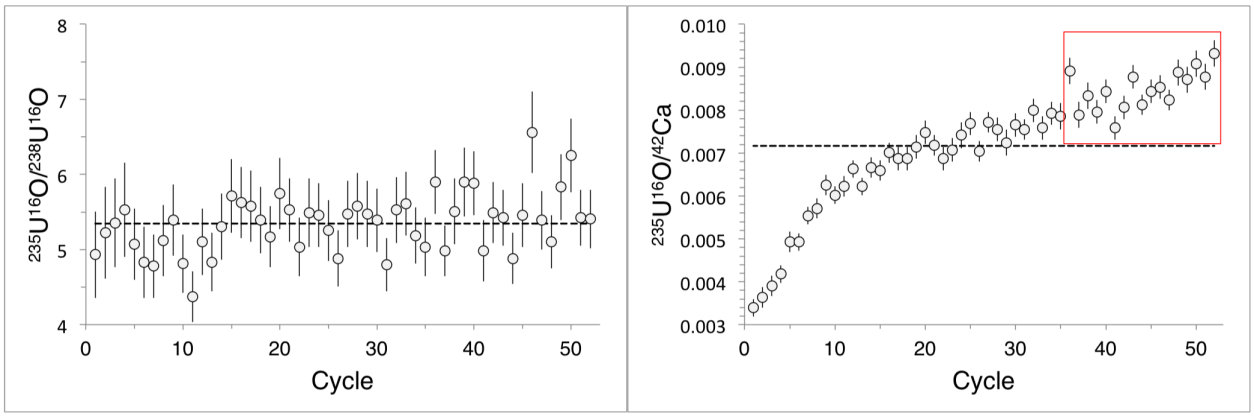

Figure 5.9: The $^{235}U^{16}O/^{238}U^{16}O$ ratio (left) and $^{235}U^{16}O/^{42}Ca$ ratio for each cycle from a NanoSIMS analysis on sample FLD23. The horizontal dashed lines are the mean of all cycles. Note the $^{235}U^{16}O/^{238}U^{16}O$ ratio deviates little from the mean between the first and last cycle, but the $^{235}U^{16}O/^{42}Ca$ ratio takes tens of cycles to approach sputtering equilibrium. In this analysis, all cycles were included when calculating the U isotope ratio. However, the $^{235}U^{16}O/^{42}Ca$ ratio is still increasing between cycles, even in the last few cycles. The red box indicates how the cycles were subset to calculate the $^{235}U^{16}O/^{42}Ca$ ratio for this run. Because the $^{235}U^{16}O/^{42}Ca$ ratio is still slightly increasing from cycle to cycle, this may lead to an underestimation of the concentration of U.

Analysis of NanoSIMS rasters in L'IMAGE

L'IMAGE image analysis software was used to calculate isotope ratios from NanoSIMS rasters [119]. Users can remove cycles, apply dead time corrections, calculate isotope ratios, and create and process ion and isotope ratio images. In this study, L'IMAGE was used in two ways: to calculate isotope ratios of entire rasters and to extract traverses across compositional interfaces. L'IMAGE shows an ion image in false color with the total number of counts per pixel, which is the sum of all retained cycles.

Calculation of isotope ratios from NanoSIMS rasters

Isotope ratios were calculated in select regions of interest (ROIs) (Figure 5.10). For analyses that did not occur at interfaces between agglomerated and host objects, the ROI was defined to be ≈5 pixels in from the edge of the image to avoid edge effects. Edge effects may occur when the primary ion beam sputters the sides of the crater, instead of sputtering material from the crater bottom, which can lead to unpredictable fractionation effects (Figure 5.11).

The intensities of $^{30}Si^+$ and $^{42}Ca^+$ do not spatially coincide in Figure 5.11. The ion images are from the U500 standard, which is assumed to be chemically homogeneous, and this mismatch is likely not due to chemical heterogeneity in the sample. Instead, these differences are interpreted as analytical artifacts due to elemental-dependent sputtering effects. When the isotope ratio the entire raster (excluding the edges) is averaged and calculated, these analytical artifacts are removed. The spatial variation of U/major element and major

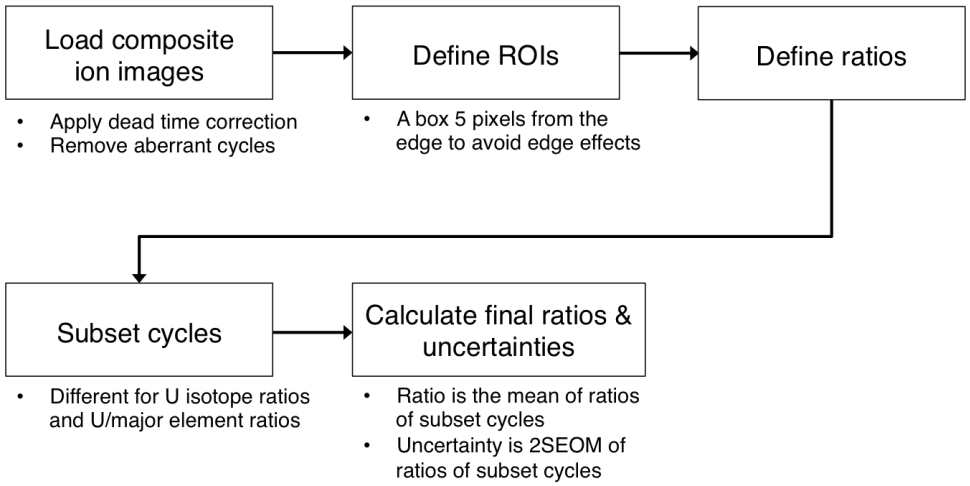

Figure 5.10: Flow diagram of processing steps in calculating isotope ratios from entire NanoSIMS rasters in L'IMAGE. Isotope ratios are tabulated in Appendix F.

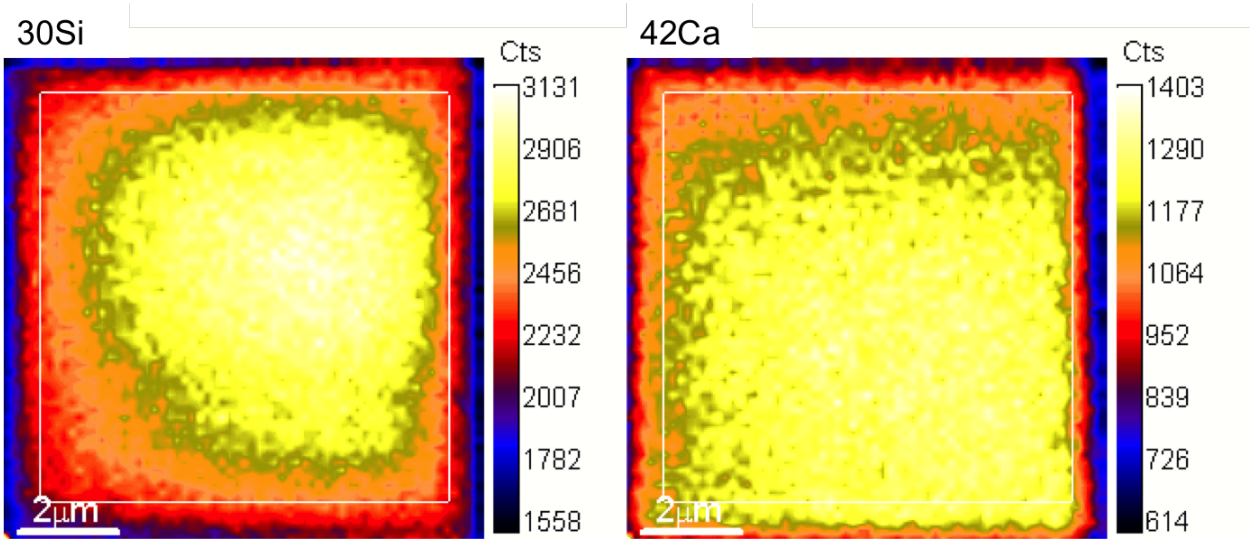

Figure 5.11: Example of NanoSIMS ion images ($^{30}Si^+$, left; $^{42}Ca^+$, right; scale bar is 2 μm) from sample FLD23, where pixel intensity represents the total number of counts in that pixel summed over all cycles. The white box is the user-defined ROI, drawn to exclude edge effects.

element/major element ratios is usually larger than the effects caused by these analytical artifacts, especially for compositional interfaces exhibiting enrichments in $^{235}U^+$, $^{42}Ca^+$, and $^{54}Fe^+$, such as those described in Weisz (2016) [67].

Cycles were sub-selected to capture steady-state conditions for the different isotope ratios. For U isotope ratios, the first 0–10 cycles were usually removed, which varied with the efficacy of the pre-sputtering (Figure 5.12). For U/major element isotope ratios, between first 50%

to 90% of cycles were removed. The cycle-to-cycle growth or decay of a U isotope/major element ratio is similar regardless of which U isotope is in the numerator ($^{235}U^{16}O^+$ or $^{238}U^{16}O^+$) so a subset of cycles were selected for both the $^{235}U^{16}O^+$/major element and $^{238}U^{16}O^+$/major element ratios using the $^{235}U^{16}O^+$/major element ratios (Figure 5.13). The cycle-to-cycle behavior of different $^{235}U^{16}O^+$/major element ratios is also similar, regardless of the major element isotope in the denominator, so a subset of cycles were selected based on the $^{235}U^{16}O^+/^{42}Ca^+$ cycle-to-cycle behavior and this subset was then applied to all U isotope/major element ratios (*e.g.*, $^{238}U^{16}O^+/^{54}Fe^+$, $^{235}U^{16}O^+/^{30}Si^+$, etc.; Figure 5.14).

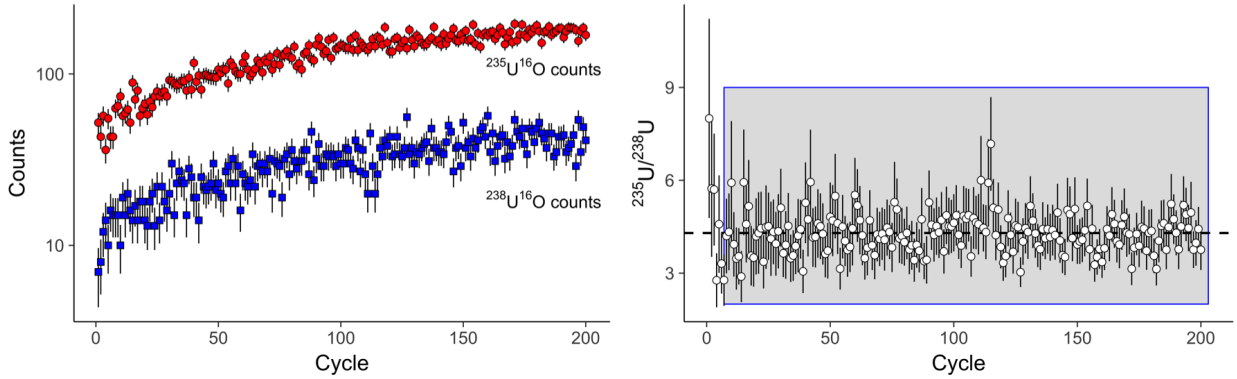

Figure 5.12: Plot of counts versus cycle for $^{235}U^{16}O^+$ and $^{238}U^{16}O^+$ (left; note the log scale) and the resulting $^{235}U/^{238}U$ ratio for each cycle (right) from a NanoSIMS analysis on sample FLD23. The grey box on the isotope ratio plot shows how the data were subset, removing the first 10 cycles. The dashed line is the average ratio of the subset cycles. While the number of counts increases for both ions from cycle to cycle, their growth is proportional: the resulting ratio (right panel) shows little drift when considered over many cycles, unlike like the plot of counts (left panel). Uncertainties in both plots are 1σ.

The reported isotope ratio is the mean of the isotope ratios from each subset cycle. The reported uncertainty is two standard errors of the mean (2SEOM) of the isotope ratios from cycle to cycle.

Line profiles across interfaces in L'IMAGE

U isotope behavior was quantified at compositional interfaces (following observations from Weisz [68]) using isotope ratio images calculated and output by L'IMAGE. The intensity in each pixel of an isotope ratio image corresponds to the ratio calculated within that pixel. These images were used to perform linescans across analyzed interfaces (Figure 5.15). Due to the low number of counts per pixel, linescans must be averaged or smoothed over several pixels to obtain isotope ratios with reasonable uncertainties. Line profiles were drawn perpendicular to interfaces and smoothed to improve precision while minimally affecting the measured width of the interface (10–50 pixel smoothing), similar to line profiles across interfaces in EDS described in Chapter 4 and discussed further in Chapters 8 and 9.

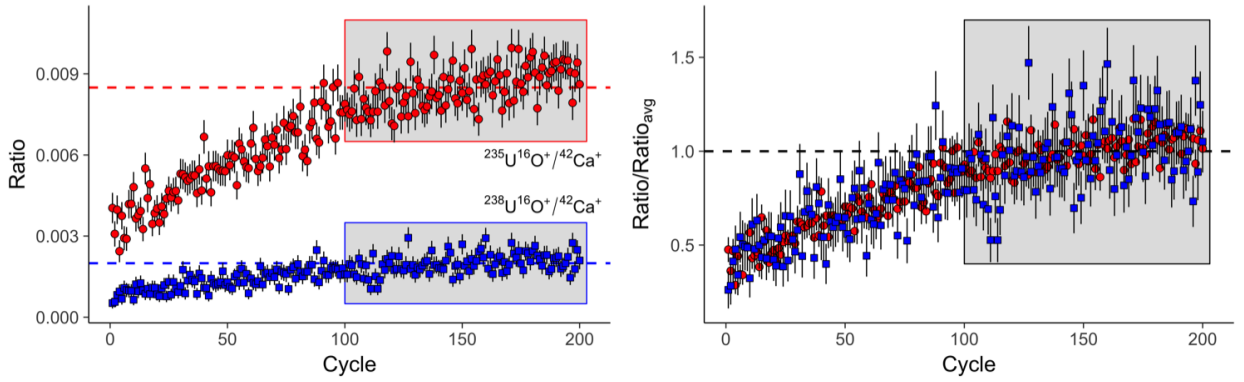

Figure 5.13: Plot of the $^{235}U^{16}O^+/^{42}Ca^+$ and $^{238}U^{16}O^+/^{42}Ca^+$ for each cycle (left panel) and the same ratios divided by their average from cycle 100–200 (right panel) from a NanoSIMS analysis on sample FLD23. The grey boxes in each plot shows how cycles were subset (removing the first 100 cycles). The dashed line on the left plot denotes the average ratio of the subset cycles. Cycles were subset to minimize the cycle-to-cycle drift of $^{235}U^{16}O^+/^{42}Ca^+$. This criterion was applied to the $^{238}U^{16}O^+/^{42}Ca^+$ ratio as well. While the ratio increases for both ions from cycle to cycle (left plot), their growth is proportional (right). Uncertainties in both plots are 1σ.

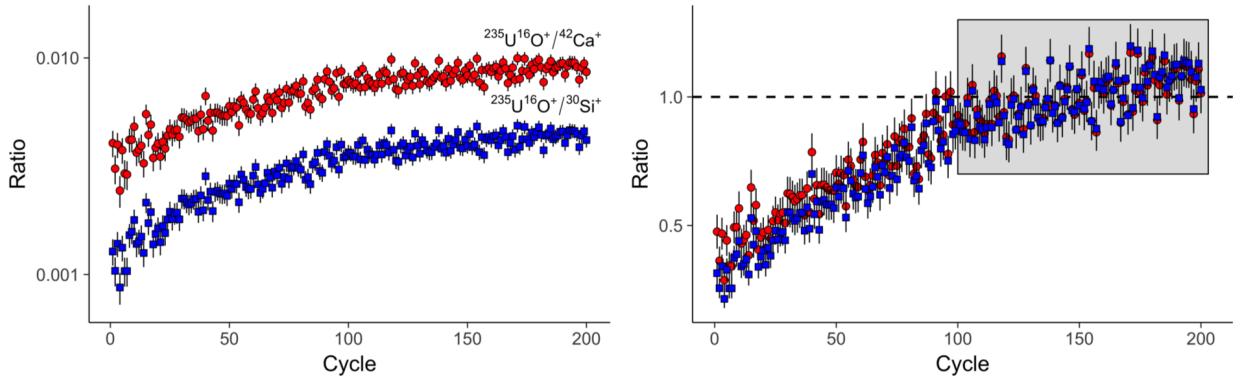

Figure 5.14: Plot of $^{235}U^{16}O^+/^{30}Si^+$ and $^{235}U^{16}O^+/^{42}Ca^+$ for each cycle (left plot) and the same ratios divided by their average from cycle 100–200 (right plot) from a NanoSIMS analysis on sample FLD23. Note the log scale on the left plot. The grey box on the right plot shows how this analysis was subset for U/major element ratios, removing the first 100 cycles. While cycles were subset based on the cycle-to-cycle drift of $^{235}U^{16}O^+/^{42}Ca^+$, the subset was also applied to the $^{235}U^{16}O^+/^{30}Si^+$ ratio as well. The values for all ratios increase from cycle-to-cycle (left plot) and increase at different rates initially (right plot, cycles<100) and their behavior from cycle 100–200 is similar (right plot). In individual cycles, the U/major element ratio is similar, implying that the ratio is largely controlled by fluctuations in the number of $^{235}U^{16}O^+$ counts in a particular cycle. Given that the $^{235}U^{16}O^+$ counts were typically much smaller than the number of counts in isotopes from the major elements, relatively small fluctuations in U counts may lead to non-negligible deviations in the overall ratio. Uncertainties in both plots are 1σ.

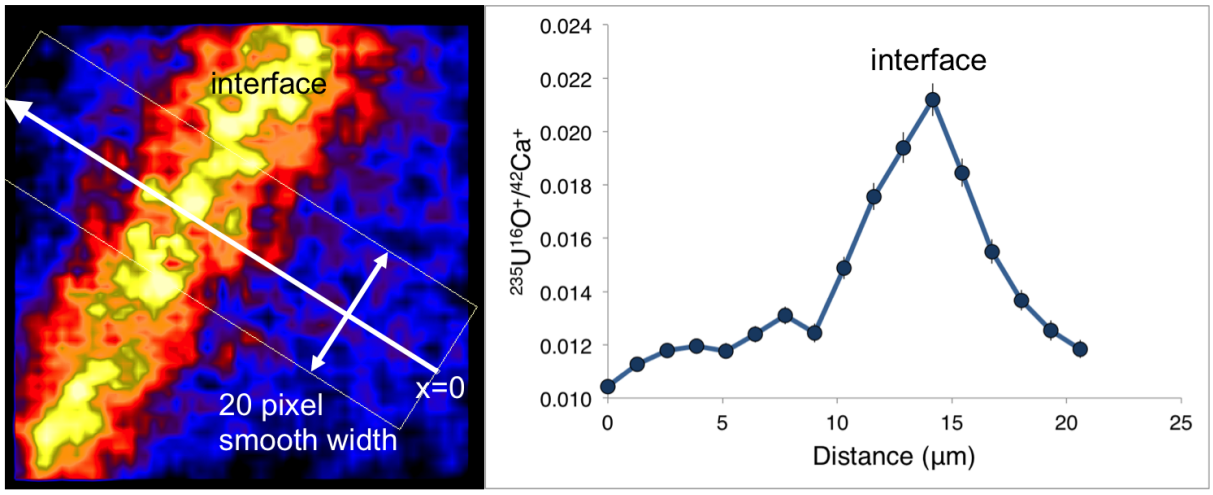

Figure 5.15: $^{235}U^{16}O^+/^{42}Ca^+$ image of the interface between interior agglomerate U1B.L and sample U1B (left panel) with the resulting extracted $^{235}U^{16}O/^{42}Ca$ line profile (right panel). Points in the line profile were sampled in 1 μm intervals. The profile was smoothed with a 20 pixel width and starts in the bottom right (at $x = 0$) of the image and moves across the image to the top left. The compositional interface separates U1B.L (interior agglomerate; right hand side of the raster) and U1B (the host object; left hand side of the raster). Data are tabulated in Appendix K.

Choosing SIMS locations

For the SIMS data collected on the IMS-3f and IMS-1280 instruments, SIMS analyses were performed in linear traverses across samples to characterize the U isotope heterogeneity of entire samples. For analyses on the NanoSIMS, agglomerates were targeted in the 2016 and 2017 analytical sessions, compositional interfaces were also targeted during the 2017 analytical session, and regions on the host glass near the agglomerates were targeted in the 2016 and 2017 analytical sessions.

Often only 1-2 NanoSIMS rasters (10–20 μm diameter rasters) fit within smaller agglomerates. If the agglomerate was large enough, NanoSIMS analyses were performed in a series of four or more NanoSIMS rasters in traverse starting in the agglomerate, crossing the compositional interface, and ending in the host (*e.g.*, the traverse from FLD14.L into FLD14 shown in Figure 5.16). However, only 1-2 U isotope measurements with agglomerates is likely sufficient as agglomerates tend to be more compositionally homogeneous than host glasses (Figure 5.16 and Table 3.2). In addition, prior studies indicate that compositional homogeneity in a single sample tends to be associated with U isotope homogeneity (further discussed below and shown in Figure 5.31) [60].

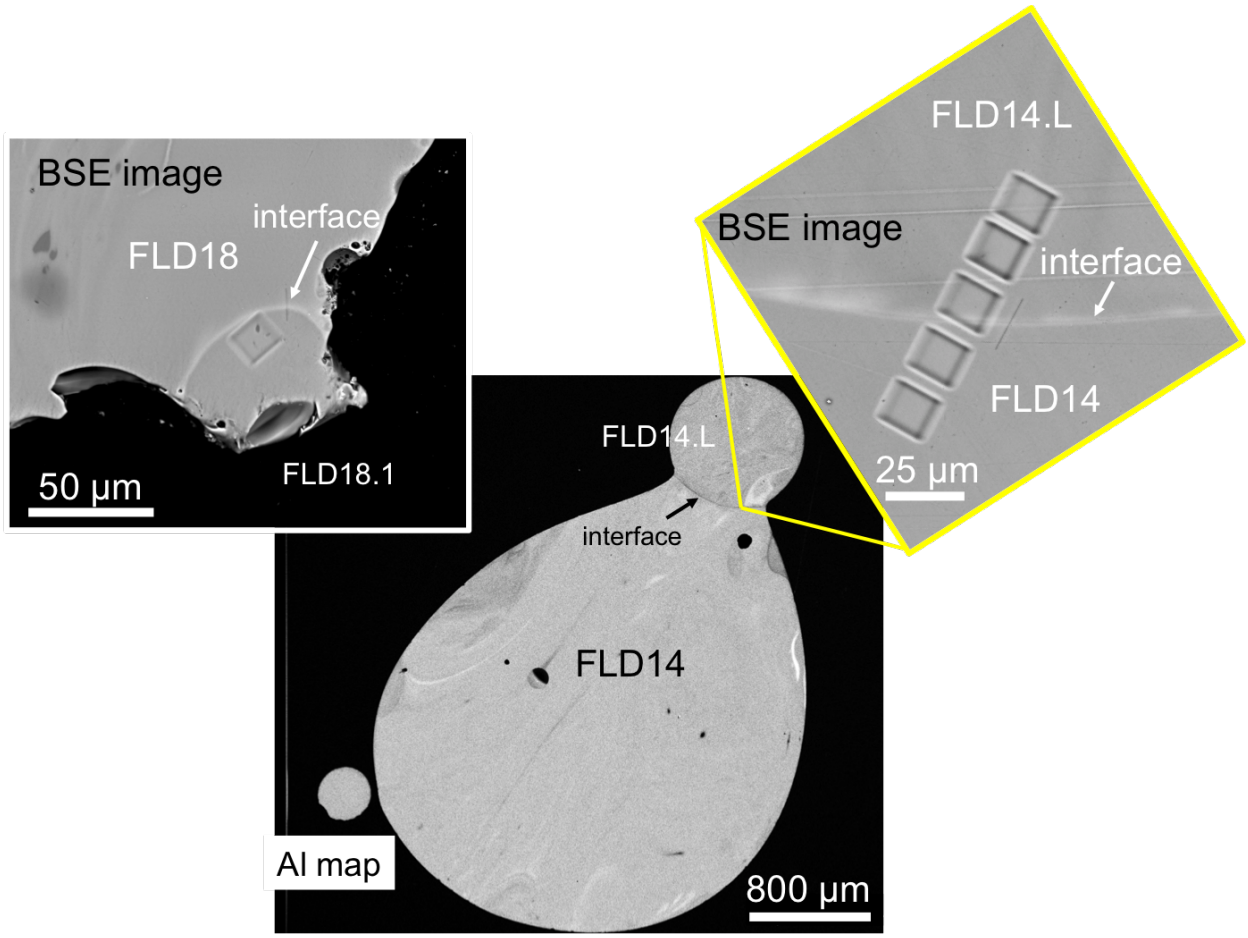

Figure 5.16: Backscatter electron images of NanoSIMS rasters from U isotope analyses of a large agglomerate (FLD14.L in sample FLD14, equivalent diameter of ≈850 μm; shown in top right BSE image) and small agglomerate (FLD18.1 in sample FLD18, equivalent diameter of ≈60 μm, shown in top left BSE image). Both are exterior agglomerates. The bottom image is an Al compositional map of sample FLD14.

5.3 SIMS Measurements

The $^{235}U/^{238}U$ isotope ratio

A histogram of all $^{235}U/^{238}U$ measurements (including hosts and agglomerates), 323 measurements in 14 samples, shows roughly unimodal distribution (Figure 5.17). The median $^{235}U/^{238}U$ ratio is 4.57 (25th and 75th percentiles are 3.30 and 5.94, respectively), roughly corresponding to a ^{235}U enrichment of 82% (neglecting the ^{234}U contribution, which is approximately 1% for oralloy [120]). The cumulative probability distribution in Figure 5.17 shows that 50% of the U isotope measurements fall between 3.30 and 5.94, corresponding to ^{235}U enrichments of approximately 76.7% and 85.6%. The lowest measured $^{235}U/^{238}U$ ratio is 0.02 ± 0.002 (2σ), approximately 2.8 times the natural $^{235}U/^{238}U$ ratio, and corre-

sponds to approximately a 2% enrichment in ^{235}U. The highest measured ^{235}U/^{238}U ratio is 11.84 ± 0.22 (2σ), corresponding to a ^{235}U enrichment of approximately 92%. These high and low values were observed in measurements of sample U1B and U2, respectively (further documented and discussed in [60]).

The wide observed range in uranium isotope ratios show that these materials are not only heterogeneously mixed with respect to major elements, but also with respect to anthropogenic material, as previously reported [57, 60]. The *major element* heterogeneity is consistent with the mixing of multiple molten minerals or measuring partially-melted/unmelted minerals in the host from several endmember compositions present in the soil. In contrast, the high *U isotope* heterogeneity reflects different regions in the fallout incorporating different amounts of anthropogenic U from the device. ^{235}U/^{238}U, ^{234}U/^{238}U, and ^{236}U/^{238}U measurements in fallout from this test have been shown to be consistent with two-component mixing between natural U and some enriched U endmember, whose ^{235}U/^{238}U ratio is at least 11.84 ± 0.22 [60]. Despite the wide range of measured ^{235}U/^{238}U ratios within and between samples, the unimodality and restricted range of the 25th and 75th percentiles (3.30 and 5.94; Figure 5.17) highlights that in most of analyzed regions, enriched U has mixed in to a similar extent.

^{235}U/^{238}U measurements in sample U2 and U3

There is a buildup of values below a ^{235}U/^{238}U ratio of ≈2 because the majority of ^{235}U/^{238}U ratios measured below 2 come from two samples: U2 and U3. Collectively, the SIMS analyses on samples U2 and U3 account for 36% of all the SIMS analyses conducted for this study (117 out of 323 SIMS analyses). To test for analytical bias, removing these measurements from the histogram in Figure 5.17 increases the median from 4.57 to 4.80 (a 5% increase) and increases the 25th and 75th percentiles to 3.93 and 6.34, respectively (a 19% and 7% increase, respectively; Figure 5.18).

Excluding the analyses on U2 and U3 do not appreciably change the statistics or the observations of the overall U isotope distribution. SIMS measurements on two samples account for a large percentage of the overall number of SIMS measurements and a majority of the low measured ^{235}U/^{238}U ratios (36 of the 39 ^{235}U/^{238}U ratios below 2 were measured in samples U2 and U3), but these measurements do not appear to greatly bias the overall dataset. Instead, U isotope measurements on samples U2 and U3 highlight that while the majority of measurements reflect a dominant anthropogenic U composition, there are regions in fallout where natural U from the soil strongly contributes to the overall U isotope ratio.

Following Lewis et al. 2015, assuming two-component isotopic mixing between a natural U and an endpoint enriched U end-member with a composition of oralloy [120]:

$$\frac{n_n}{n_f} = \frac{x_{235} - \frac{n_{235}}{n_{238}} x_{238}}{\frac{n_{235}}{n_{238}} y_{238} - y_{235}} \tag{5.9}$$

where $\frac{n_n}{n_f}$ represents the relative contribution of U atoms of natural isotopic composition

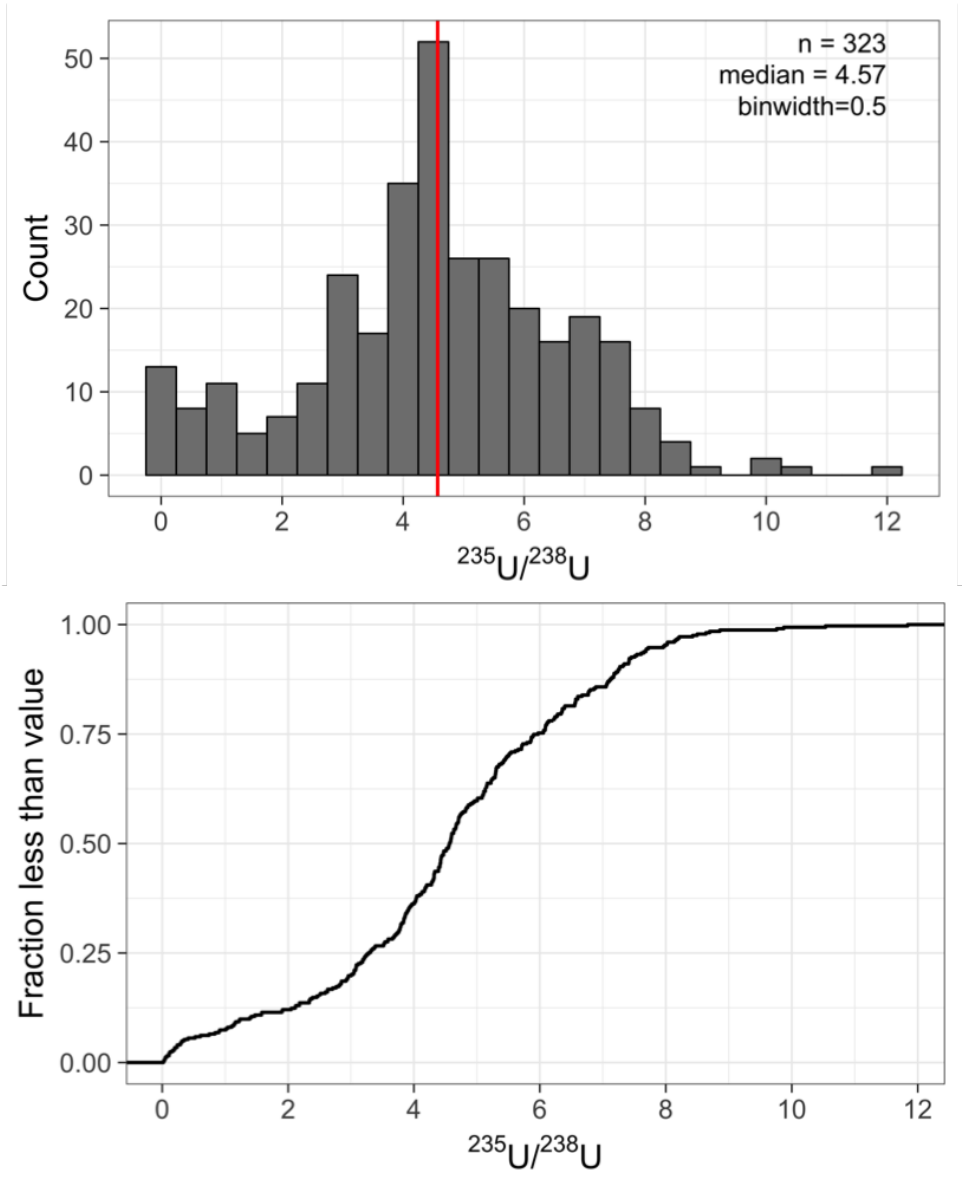

Figure 5.17: Histogram of all SIMS measurements of $^{235}U/^{238}U$ ratios in fallout from this test (top plot). The red vertical line denote the median of the measurements. The bin width is 0.50. The bottom plot shows a cumulative distribution function of these data. The inter-quartile range, encompassing the central 50% of all measurements (all measurements between the 25th and 75th percentile), lie between $^{235}U/^{238}U$ ratios of 3.30 and 5.94, corresponding to approximate ^{235}U enrichments of 77% to 86%. Data are tabulated in Appendix F.

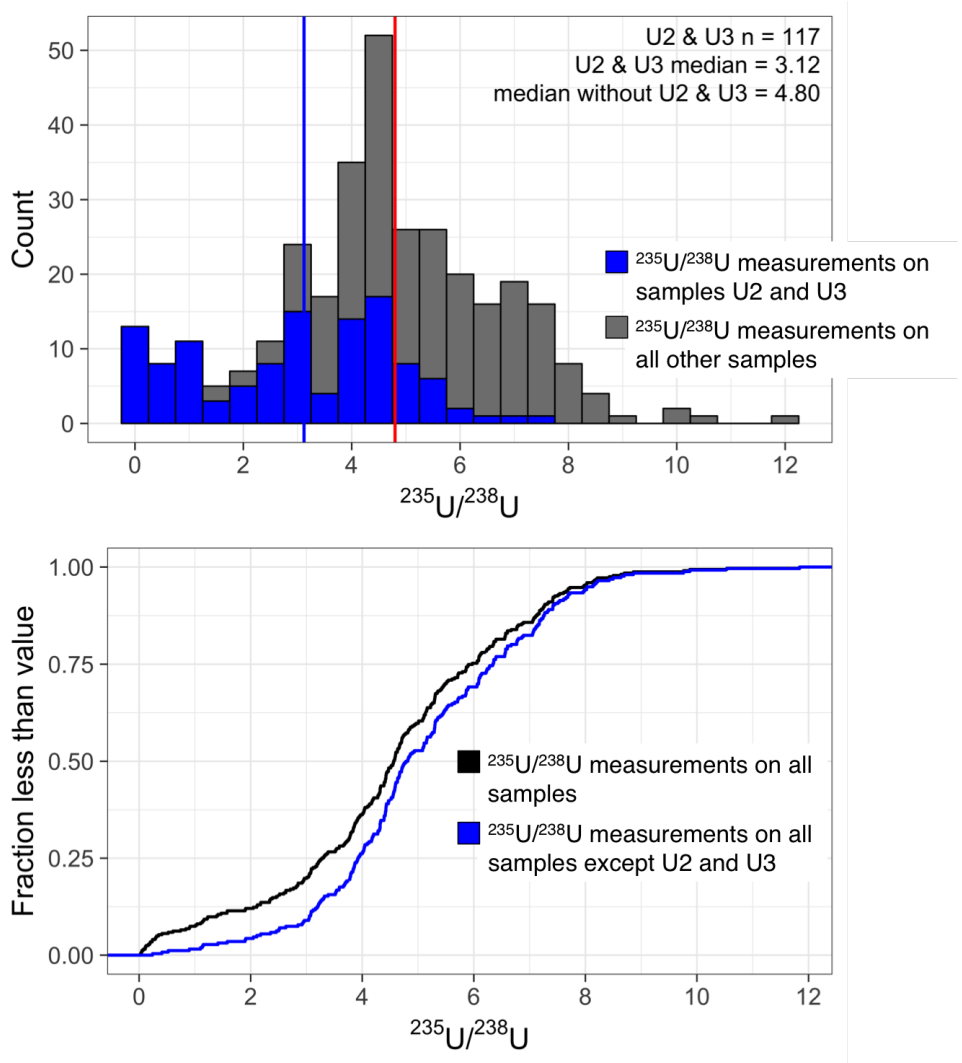

Figure 5.18: Histogram of all SIMS measurements with measurements on samples U2 and U3 separated into the blue histogram (top plot) and the cumulative distribution function showing all U isotope measurements (in black, as in Figure 5.17) compared with the cumulative distribution function of all U isotope measurements if SIMS measurements on samples U2 and U3 are excluded (bottom plot). Data are tabulated in Appendix F.

to enriched isotopic composition, and x_{235}, x_{238}, y_{235}, and y_{238} represent the abundances of ^{235}U and ^{238}U in natural U and abundances ^{235}U and ^{238}U in oralloy, respectively.[5]. Then the ratio where U atoms of natural and oralloy composition equally contribute is:

$$\frac{n_{235}}{n_{238}}y_{238} - y_{235} = x_{235} - \frac{n_{235}}{n_{238}}x_{238} \tag{5.10}$$

$$\frac{n_{235}}{n_{238}}(y_{238} + x_{238}) = x_{235} + y_{235} \tag{5.11}$$

$$\frac{n_{235}}{n_{238}} = \frac{x_{235} + y_{235}}{y_{238} + x_{238}} \tag{5.12}$$

$$\frac{n_{235}}{n_{238}} \approx 0.90. \tag{5.13}$$

There were 23 measurements where natural U is calculated as being the dominant contributor to the overall isotope ratio, all of which were in samples U2 or U3 (19 analyses in U2 and 4 analyses in U3). Assuming two component mixing between natural U and enriched U with the composition of oralloy, most regions in fallout are dominated by the anthropogenic contribution. However, 23 analyzed regions were dominated by the contribution of U of natural isotopic composition. If soil was the only contributor of natural U, these 23 regions incorporated U in a portion of the fireball without an appreciable amount enriched U in the ambient environment. This may be due to spatial heterogeneity in the fireball. Alternatively, these regions may not have been able to effectively incorporate enriched U, possibly because they were not thoroughly heated and/or remained too viscous. In the case of sample U2, the region in which the low ^{235}U/^{238}U ratios were measured appears thoroughly and completely melted, so low U isotope ratios may be due to forming in a fireball environment with little enriched U in the vapor term. The melted region is dominated by isotopically-natural U in U2 appears to have collided and partially-mixed with a region that is distinct in both major element composition and U isotope ratio (all the ^{235}U/^{238}U ratios in this region are >1, Figure 1.11). In contrast, in the case of U3, low ^{235}U/^{238}U ratios were measured near the center of the sample, around which there appear many partially-melted, compositionally heterogeneous regions (as demonstrated by the frequent, visible partially-melted quartz grains). The higher U isotope ratios in U3 were measured towards the sample's surface, which appears compositionally more well-mixed in major elements, and in and around the agglomerates that surround the periphery of the sample. All of the U isotope ratios measured in the agglomerates or that overlap the compositional interfaces between the agglomerates

[5]Standard radiochemical techniques were used to analyze the U isotopic composition of a piece of oxidized oralloy foil, yielding the following atomic abundances: x_{234}: 0.0102 ± 0.0002, x_{235}: 0.9317 ± 0.0138, x_{236}: 0.00443 ± 0.00006, and x_{238}: 0.0538 ± 0.0008 [120]. The calculated ^{235}U/^{238}U ratio is then 17.30 ± 0.27. Given the ≈1.5% uncertainties reported from this radiochemical analysis, it is reasonable to exclude other radionuclides measured in the oralloy, such as ^{233}U, ^{237}Np, and the isotopes of Pu, Am, and Th, as the most abundant of these species are present at concentrations more than three orders-of-magnitude below ^{236}U, the least abundant of the four U isotopes used in the calculation (3.6×10^{18} atoms/mL for ^{236}U compared to 1.3×10^{15} atoms/mL for ^{237}Np).

and host in sample U3 have a higher average U isotope composition than the host, due to the low $^{235}U/^{238}U$ values measured towards the sample's center. In the case of U3, it is more plausible that the interior regions of the sample were not as thoroughly heated as the exterior, preventing U from throughly mixing into the center of sample.

U isotope measurements by sample

In contrast to major element compositions, where samples (except for outliers such as FLD25) have similar compositions (Figure 4.11 and Table 4.6), grouping the U isotope measurements by sample shows that individual samples show large enrichments relative to other samples (Figure 5.20). Note that this compilation reflects *all* measurements in a sample, with no separation of agglomerate and host measurements.

Comparisons of U measurements by sample show that unlike the major element composition, different samples appear to incorporate vastly different amounts of enriched U, ranging from sample U2 with a mean $^{235}U/^{238}U$ ratio of 2.49 ± 1.93 ($n = 67$) to sample FLD4.3 with a mean $^{235}U/^{238}U$ ratio of 9.00 ± 1.27 ($n = 6$). Differences in mean $^{235}U/^{238}U$ content suggests that even while these samples were collected at similar locations from ground zero, the distribution of bomb vapor in fireball was highly heterogeneous, and heterogeneously incorporated into these samples (Figure 5.20 and Table 5.9). This is further bolstered by the bulk dissolution measurements that represent the average $^{235}U/^{238}U$ ratio of an entire sample, which spans a range from $^{235}U/^{238}U = 0.012 \pm 0.0003$ to 9.43 ± 0.04. Therefore, the average U isotopic compositions of entire samples are also highly heterogeneous, and the observed heterogeneity from the SIMS measurements is not simply an artifact of sampling micro-volumes of material with spatially-resolved techniques. Furthermore, the average U content of entire samples exhibits a more heterogeneous distribution than the major element composition of entire samples (Figure 5.20 and Table 5.9). With respect to major elements, the quadrature-summed standard deviation of the entire set of bulk dissolution data is approximately half that of the $^{235}U/^{238}U$ ratio, 0.85 (18.62% 1RSD) for major elements compared to 1.63 (30.22% 1RSD) for the $^{235}U/^{238}U$ ratio, respectively, indicating that from sample to sample, U is much more heterogeneous than the major element composition.[6] These observations show that the soil term incorporated into the fireball was fairly homogeneous (or was homogenized during incorporation) compared to the incorporation of condensing species from the cooling fireball plasma.

Minor isotopes

Minor isotopes of U (^{234}U and ^{236}U) were also measured during SIMS analyses performed with the IMS-1280 (Figure 5.21). This includes measurements on samples U1A, U1B, U2, U3,

[6]The quadrature-summed standard deviation for major elements is defined here as ME $1\sigma = \sqrt{1/8(\sigma^2_{SiO_2} + \sigma^2_{Al_2O_3} + \sigma^2_{Na_2O} + \sigma^2_{K_2O} + \sigma^2_{CaO} + \sigma^2_{FeO} + \sigma^2_{TiO_2} + \sigma^2_{MgO})}$.

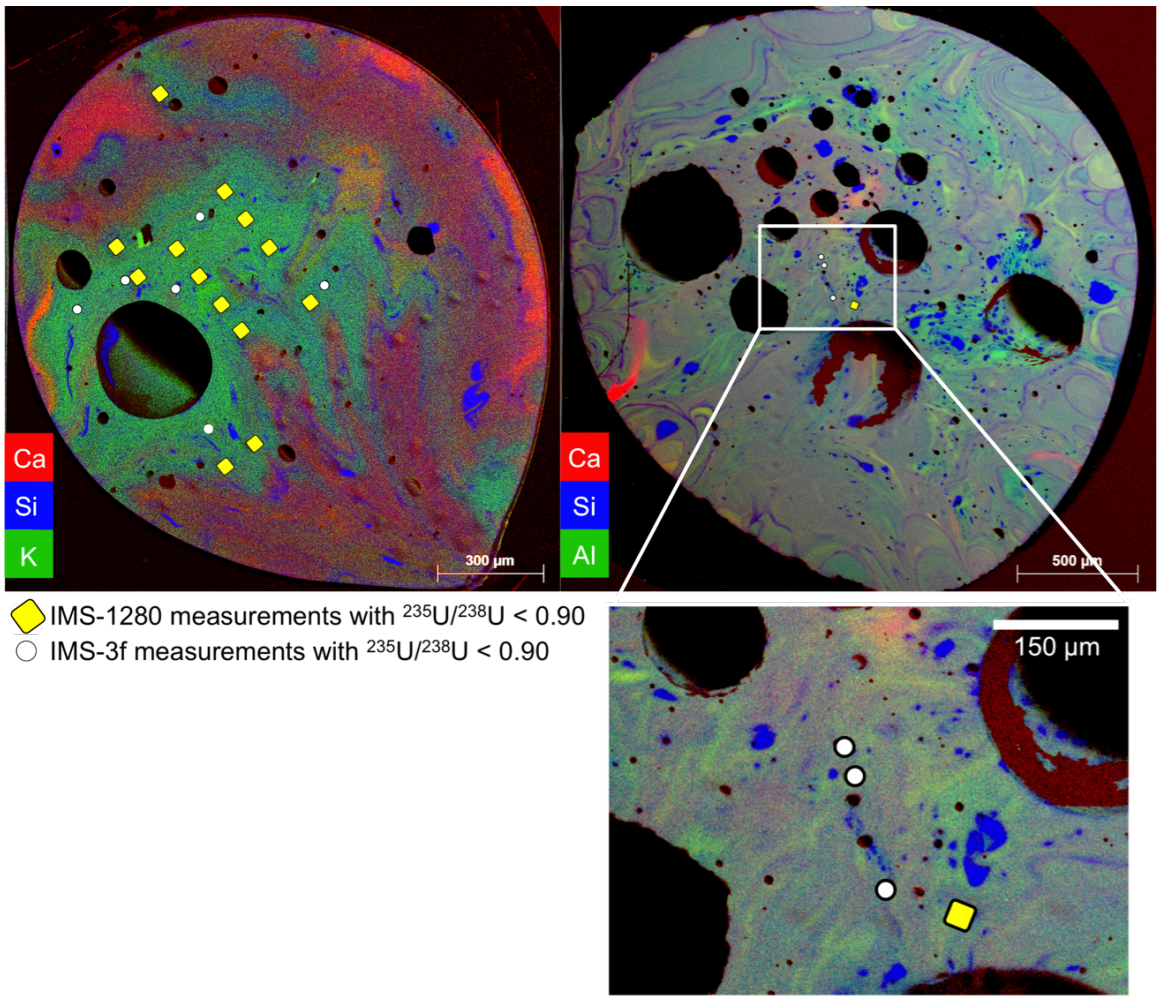

Figure 5.19: False color compositional maps of samples U2 (left) and U3 (right) where each of the RGB channels shows a different composition. For sample U2, red shows Ca, green shows K, and blue shows Si. These elements were selected to highlight the compositional differences between the two distinct regions. For sample U3, red shows Ca, green shows Al, and blue shows Si. These elements were selected to highlight the agglomerates present at the periphery of the sample, as well as partially-melted mineral compositions. The greener regions in U3 contain many partially-melted quartz grains, which appearing as blue shapes with regular boundaries in the composite image. The yellow squares and white circles correspond to IMS-1280 and IMS-3f measurements, respectively, where the $^{235}U/^{238}U$ ratio reflects a dominant natural U contribution, assuming a two component mixing between natural and enriched U end-members (see text). Data are tabulated in Appendix F.

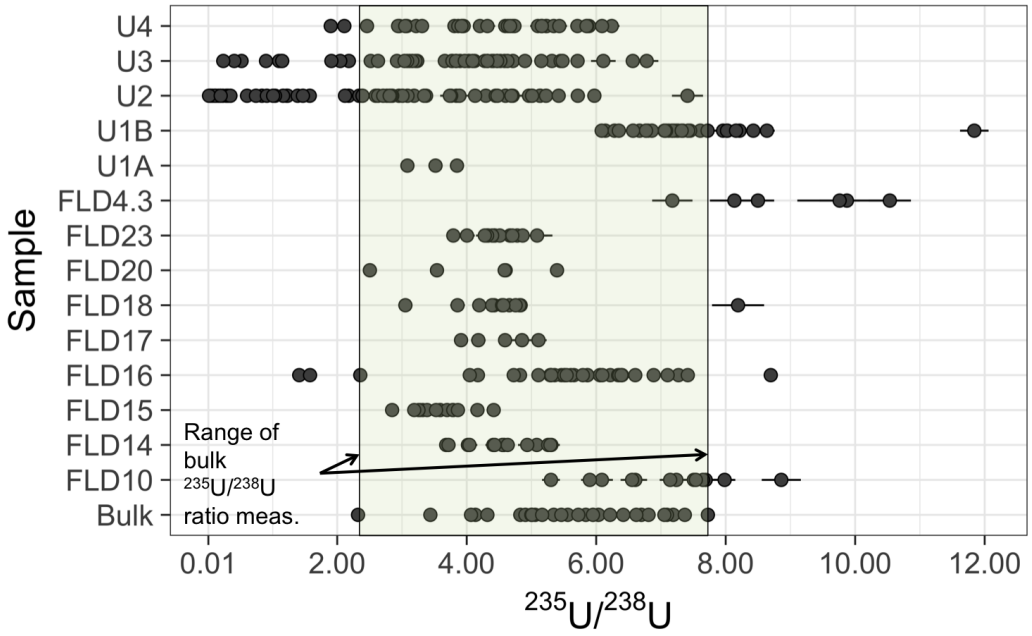

Figure 5.20: $^{235}U/^{238}U$ measurements in each sample (includes measurements of agglomerates, hosts, and over interfaces). Bulk refers to dissolution-based ICP-MS measurements of whole samples of glassy fallout from Eppich et al. (2014). The range of bulk U isotope measurements is also shown by the partially-transparent box. Summary statistics for this plot are given in Table 5.9. Data are tabulated in Appendix F.

U4, FLD15, FLD16, FLD18, and FLD20. The analytical conditions of these measurements are described above in Section 5.2.

A subset of these plots that only included U-series analyses were reported by Lewis et al. (2015) and demonstrated that three isotope plots of both $^{234}U/^{238}U$ vs. $^{235}U/^{238}U$ and $^{236}U/^{238}U$ vs. $^{235}U/^{238}U$ are highly linear, consistent with mixing between natural and enriched end-members (R^2 of 0.998 and 0.997, respectively). The plots in Figure 5.21 also include three measurements overlapping the interface between agglomerates and the host in sample U3, which plot on the same line as other host measurements and are indistinguishable from the all the other measurements shown. Therefore, the agglomerates (and the compositional interfaces, if enriched) are incorporating U from the same enriched U source, consistent with the host SIMS measurements.

From an analytical perspective, the minor isotope measurements highlight the robustness of the standard-based comparison for these SIMS measurements. The $^{234}U/^{238}U$ measurements in Figure 5.21 show measurements from nine samples, five of which were characterized using the IMS-1280 at LANL in 2013 and three of which were characterized using the same instrument in 2015. The consistency of the linear correlation across analytical sessions suggests that the standard corrections performed to account for instrumental bias are sufficient

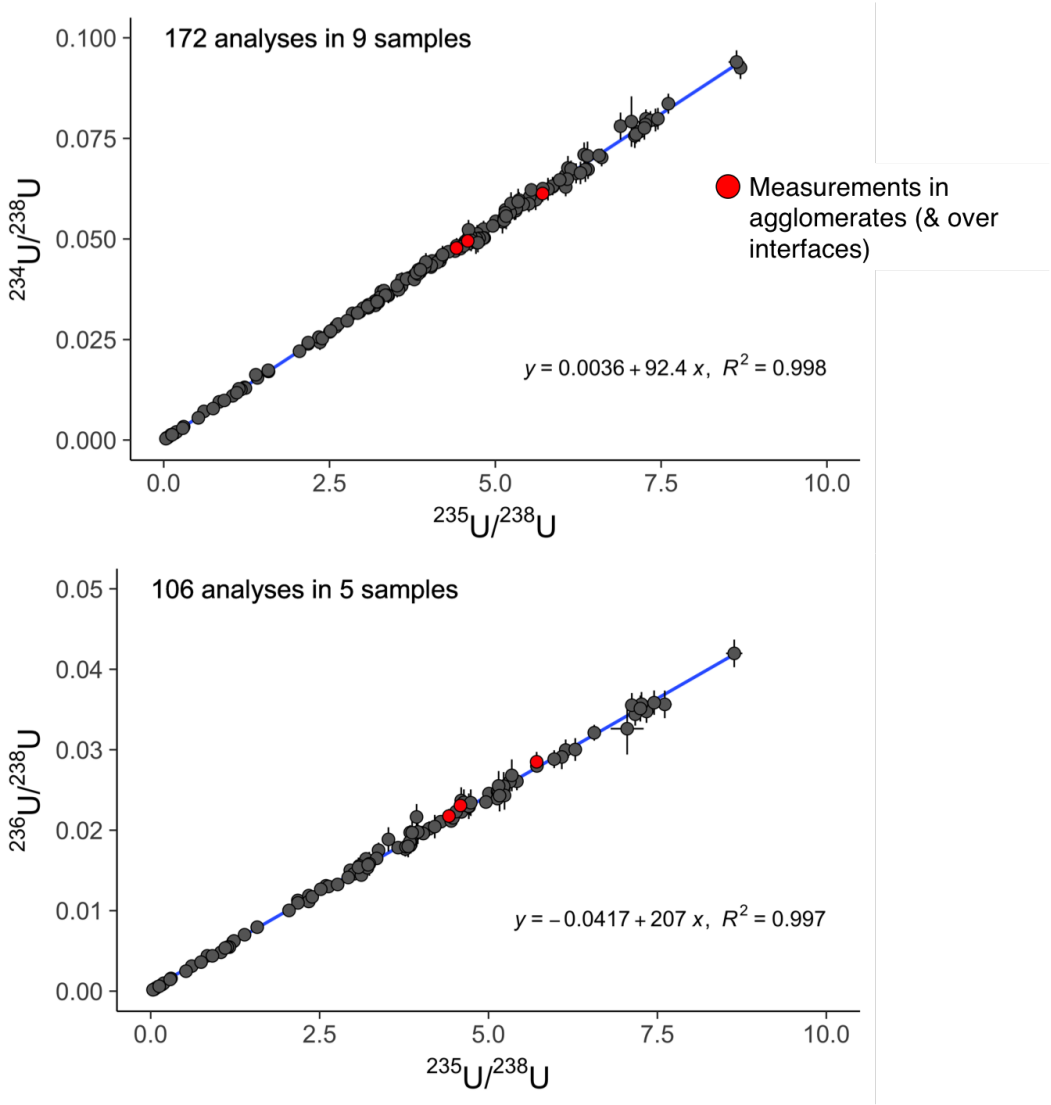

Figure 5.21: Three isotope plots of $^{234}U/^{238}U$ vs. $^{235}U/^{238}U$ (top panel) and $^{236}U/^{238}U$ vs. $^{235}U/^{238}U$ (bottom panel) from SIMS measurements in fallout. Red points correspond to the three measurements performed in agglomerates or over interfaces. There were 172 SIMS measurements of ^{234}U in nine samples, five of which were analyzed in 2013 and three of which were analyzed in 2015. There were 106 SIMS measurements of ^{236}U in five samples, all of which were analyzed in 2013. All three agglomerate/interface SIMS measurements follow the strongly linear trend of the host measurements, indicating agglomerates incorporated enriched and natural U end-members similarly to host objects. Data are tabulated in Appendix F.

Table 5.9: Mean $^{235}U/^{238}U$ measurements by SIMS grouped by sample (includes data collected in both host objects and their associated agglomerates). Bulk data refers to dissolution-based ICP-MS measurements of whole samples of glassy fallout reported by Eppich et al. (2014). Individual measurements are shown in Figure 5.20. Data are tabulated in Appendix F.

	Sample	n	Mean $^{235}U/^{238}U$	1σ
1	U4	35	4.40	1.18
2	U3	50	3.64	1.57
3	U2	67	2.49	1.93
4	U1B	35	7.36	1.01
5	U1A	3	3.48	0.38
6	FLD43	6	9.00	1.27
7	FLD23	18	4.46	0.31
8	FLD20	5	4.13	1.12
9	FLD18	12	4.69	1.21
10	FLD17	5	4.53	0.49
11	FLD16	36	5.54	1.46
12	FLD15	15	3.58	0.40
13	FLD14	14	4.57	0.56
14	FLD10	13	7.08	0.96
15	Bulk	28	5.62	1.27

to account for different instrumental conditions across analytical campaigns.

5.4 U isotope measurements in hosts and agglomerates

Unlike the major element compositions, where agglomerate compositions were a subset of host compositions, separating out SIMS measurements performed in agglomerates (including those that overlap interfaces between agglomerates and hosts) from those in hosts reveals two distinct distributions (Figure 5.22).[7] Host measurements span the widest range of U isotope values and exhibit the lowest overall enrichment, from $^{235}U/^{238}U = 0.02 \pm 0.002$ (the minimum of all measurements reported in this study) to 8.70 ± 0.09. In contrast, the minimum agglomerate measured $^{235}U/^{238}U$ ratio is almost 200 times greater than the minimum measured host $^{235}U/^{238}U$ ratio, and the maximum agglomerate $^{235}U/^{238}U$ ratio is

[7]Note that the sum of the host and agglomerate measurements is 283, less than the 323 total SIMS measurements (Figure 5.22). This is because some samples were polished and re-coated, which removed some of SIMS craters such that whether they were made in a host or agglomerate could not be verified, and so are excluded. The analyses most impacted by this are the LLNL measurements on U1B performed in 2012 and the LANL measurements of samples U4 performed in 2013, both of which are documented in Lewis et al. (2015) and include the maximum $^{235}U/^{238}U$ ratio measured in these samples, 11.84 ± 0.22.

1.2 times greater than the maximum measured host $^{235}U/^{238}U$ ratio (from 3.68 ± 0.09 to 10.54 ± 0.33).

As an ensemble, agglomerates exhibit a greater overall U isotope enrichment than the host objects. The median of the $^{235}U/^{238}U$ measurements for the agglomerates is approximately 22% higher than the median of the host objects (medians of 5.11 and 4.18, respectively; the differences between the means is greater with mean $^{235}U/^{238}U$ ratios of 5.77 and 4.04, respectively). The 25th and 75th percentiles of the $^{235}U/^{238}U$ measurements in the hosts and agglomerates span a range (75th percentile - 25th percentile) of 2.51 and 2.15, respectively, suggesting host objects incorporated enriched U more variably than characterized agglomerates. Fifty percent of the agglomerate and host $^{235}U/^{238}U$ ratios span from 4.41 (25th percentile) to 6.56 (75th percentile) and 2.83 (25th percentile) and 5.35 (75th percentile), respectively.

U isotope measurements by agglomerate and host

Figure 5.24 distinguishes $^{235}U/^{238}U$ ratio measurements performed in the host from those obtained in the agglomerate, and those that overlaps the compositional interface. The measurements that overlap interfaces were included with the agglomerate measurements when calculating the agglomerate U isotope composition. Interface measurements will be discussed further in Chapter 8. When these interfaces are enriched in Ca, Mg, and Fe (and subsequently ^{235}U), they increase the overall calculated composition of an agglomerate by <10%. However, when this type of compositional interface is absent, they may increase or decrease the calculated U isotope composition of the agglomerate depending on whether the host object is enriched in U relative to the agglomerate. Such enrichments and depletions are also limited to a maximum of a 10% (from a total of six such measurements).

For completeness, Figure 5.24 shows four additional samples not included in Figure 5.20, samples AH.E, AG.D, AE.C, and AA.B [67, 68]. Instead of processing raw data from the SIMS analyses, these data were extracted from the electronic annex provided by Weisz et al. (2016), which show the data from line scans of NanoSIMS rasters over compositional interfaces. To separate these NanoSIMS traverses into measurements obtained in the host or in an agglomerate, the $^{54}Fe/^{30}Si$ ratio as a function of distance was plotted (see the right panel of Figure 1.9) to determine the location of the interface. All the $^{235}U/^{238}U$ points from the baselines from both sides of the interface (the left side corresponding to the agglomerate and the right side corresponding to the host) were selected and averaged. The points in Figure 5.24 represent the mean and standard deviation of those baseline points for the agglomerates and hosts for samples AH.E, AG.D, AE.C, and AA.B. There is no host for sample AA.B because the analyzed interface was between two agglomerates attached to each other (B1 attached to B2) and one surface agglomerate (B3) residing at the surface of agglomerate B2. The large standard deviations reflect the poor counting statistics resulting from partially extracting data from a line scan across a NanoSIMS raster (instead of averaging the entire raster to obtain the $^{235}U/^{238}U$ ratio).

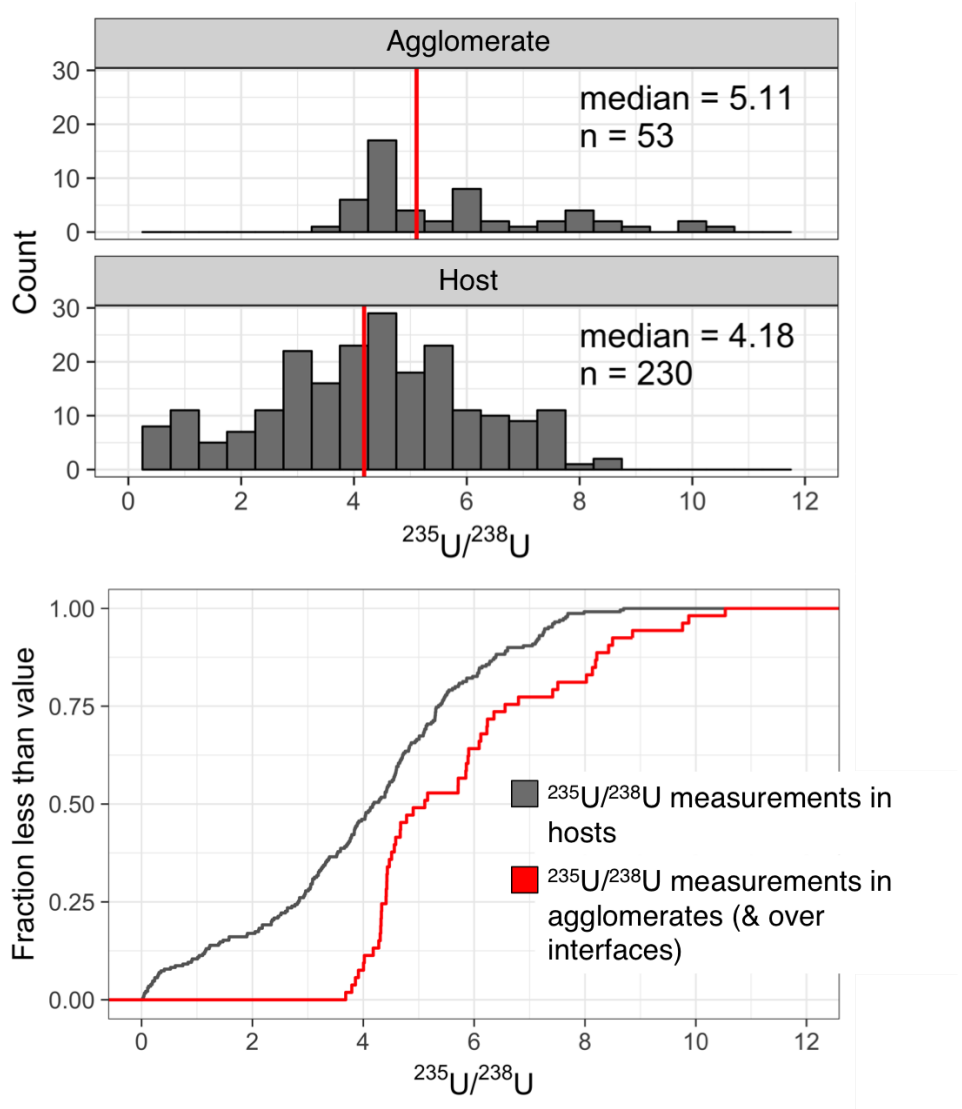

Figure 5.22: Histogram of $^{235}U/^{238}U$ measurements separated out into whether they were performed in an agglomerate (including overlapping compositional interfaces) or in the host objects (top plot). The bottom plot shows two cumulative distribution functions comparing the host and agglomerate $^{235}U/^{238}U$ distributions. There are no $^{235}U/^{238}U$ measurements in the agglomerates below ≈3.68, while approximately 39% of all the host measurements fall below this value. Data are tabulated in Appendix F.

Table 5.10: Mean host and agglomerate U isotope compositions, and the deviation of the mean agglomerate composition from the mean composition of its host. For n = 1, the 2σ uncertainty of the single measurement was used. Otherwise, the 1σ represents 1 standard deviation of the mean of the measurements in that object. Asterisks denote that the SIMS measurements that include SIMS measurements that also sampled the compositional interface and/or the host object in addition to the agglomerate. Data are tabulated in Appendix F.

	Host			**Agglomerate & Interfaces**				
Sample	n	$^{235}U/^{238}U$	1σ	Agglomerate	n	$^{235}U/^{238}U$	1σ	Dev. (%)
AE.C	1	5.73	0.68	C1	1	6.56	0.88	14.46
				C2	1	6.23	1.51	8.74
AG.D	1	6.27	1.25	D2	1	6.12	1.60	-2.43
AH.E	1	7.68	3.59	E1	1	7.42	1.17	-3.47
FLD10	10	6.98	0.84	FLD10.L	3*	7.42	1.48	6.36
FLD14	11	4.71	0.52	FLD14.1	1	4.41	0.10	-6.38
				FLD14.L	2*	3.85	0.24	-18.26
FLD17	2	4.72	0.19	FLD17.int.1	3*	4.40	0.63	-6.83
FLD18	10	4.42	0.52	FLD18.1	1*	3.86	0.11	-12.78
				FLD18.2	1	8.19	0.40	85.16
FLD23	4	4.76	0.29	FLD23.1.1	1	4.42	0.13	-7.10
				FLD23.1.2	1	4.43	0.01	-6.97
				FLD23.1.3	1	4.26	0.36	-10.60
				FLD23.2.1	1	4.31	0.13	-9.40
				FLD23.2.2	1	4.28	0.14	-10.14
				FLD23.3.1	1	4.31	0.12	-9.59
				FLD23.3.2	1	4.67	0.14	-2.02
				FLD23.4.1	1	4.67	0.15	-1.86
				FLD23.4.2	1	4.78	0.15	0.39
				FLD23.5.1	1	4.33	0.13	-9.16
				FLD23.L	2*	4.06	0.38	-14.70
FLD4.3	1	7.18	0.31	FLD4.3.1	1*	9.87	0.77	37.58
				FLD4.3.2	1	9.76	0.31	36.02
				FLD4.3.3	2*	9.52	1.44	32.63
				FLD4.3.5	1*	8.13	0.38	13.37
U1B	12	7.11	0.71	U1B.2	1	6.80	0.41	-4.45
				U1B.L	3*	8.22	0.20	15.53
U3	40	3.31	1.53	U3.1	1	4.90	0.11	48.12
				U3.2	1	4.47	0.11	35.12
				U3.3	1*	4.58	0.04	38.59
				U3.4	1*	5.71	0.07	72.67
				U3.5	1*	4.41	0.05	33.44
U4	11	3.44	1.19	U4.1	4	5.98	0.23	73.86
				U4.2	2	5.08	1.08	47.78
				U4.3	2	5.51	0.49	60.13

Two important trends are observed between agglomerates and hosts (Figure 5.27 and Table 5.10). First, agglomerates are not significantly different in U isotope composition from their associated host objects. Second, agglomerates attached in the same location (*i.e.*, exterior, surface, or interior) in the same host tend to exhibit similar isotopic ratios. These two observations mirror observations of the major element compositions of agglomerates compared with their hosts (Figure 4.14 and Table 4.9), strengthening the argument that host and agglomerate objects formed and collided in a localized environment. Similarly, agglomerates *within* the same sample tend to exhibit similar U isotope ratios. For example, agglomerates

FLD23.1.1 – FLD23.5.1 in sample FLD23 are a collection of ten surface agglomerates. The mean $^{235}U/^{238}U$ ratio of these agglomerates is 4.41 ± 0.21 (1σ; 1RSD <5%). Similarly, the four characterized agglomerates in FLD4.3 (FLD4.3.1, FLD4.3.2, FLD4.3.3, and FLD4.3.5) have a mean $^{235}U/^{238}U$ ratio of 9.32 ± 0.80 (1σ; 1RSD <10%). This suggests that agglomerates associated with a given host object likely formed under similar conditions and at similar times in the fireball.

Notable exceptions to this trend are found in the agglomerates that have different locations of attachment in the same sample (*e.g.,* a surface agglomerate compared to an interior agglomerate in the same sample). Examples of this are observed in samples FLD14 (FLD14.L and FLD14.1), U1B (U1B.L and U1B.2), FLD23 (the exterior-attached agglomerate FLD23.L and all the surface agglomerates), U4 (U4.1 and U4.3 are surface agglomerates, while U4.2 is an interior agglomerate) and FLD18 (FLD18.1 is attached at the exterior and FLD18.2 is an interior agglomerate). In these cases, the agglomerates attached in different locations in the host may have collided at different times and temperatures, and therefore, when the U isotope composition of the local fireball environment was different. In host object FLD14, FLD14.L is an exterior-attached agglomerate and is depleted relative to FLD14.1, which resides of the surface at FLD14 (FLD14.L and FLD14.1 have mean $^{235}U/^{238}U$ ratios of 3.85 ± 0.24 and 4.41 ± 0.10, respectively). Due to FLD14.1's location at the surface of FLD14, FLD14.1 likely collided with FLD14 earlier in time (when FLD14 was more molten), whereas FLD14.L must have attached at a time closer to the closure of FLD14. FLD18.2, an agglomerate that is completely incorporated into FLD18, is greatly enriched relative to FLD18.1, an exterior agglomerate. This morphological relationship suggests an earlier incorporation time for FLD18.2 than FLD18.1. U1B.L is also fully incorporated into the interior of its host, U1B. Similar to agglomerates FLD18 and FLD14, U1B.L is enriched relative to U1B.2, a surface agglomerate, which likely collided with U1B later in time, preventing it from being fully incorporated. All of the FLD23 surface agglomerates (FLD23.1.1–FLD23.5.1) share similar U isotope compositions, but are relatively enriched (but within one standard deviation of) the exterior agglomerate FLD23.L ($^{235}U/^{238}U = 4.06 \pm 0.38$).[8] Morphology and relative location (observed using compositional maps) show that FLD23.L must have collided and coalesced later with FLD23 than at least one of these agglomerates, FLD23.3.2, which is bound on one side by the the interface with FLD23.L and the host FLD23 (Figure 5.23). Finally, U4.2 ($^{235}U/^{238}U = 5.08 \pm 1.08$), an interior agglomerate is within one standard deviation of the U isotopic composition of surface agglomerates U4.1 and U4.3. In the case of U4, the fully incorporated agglomerate does not always appear more enriched than the less incorporated agglomerates.

Collectively, these four samples (excluding sample U4, where the interior agglomerate

[8]The reported U isotope composition of FLD23.L includes two SIMS measurements in FLD23.L, one within the agglomerate and one that overlapped the interface and significantly sampled the host FLD23 in addition to the agglomerate. Only including the measurement *within* FLD23.L, the measured $^{235}U/^{238}U$ ratio is 3.79 ± 0.08. The SIMS measurement over the interface between FLD23.L and FLD23 has a measured $^{235}U/^{238}U$ ratio of 4.33 ± 0.11. The mean and standard deviation of these two measurements is the reported $^{235}U/^{238}U$ ratio: 4.06 ± 0.38.

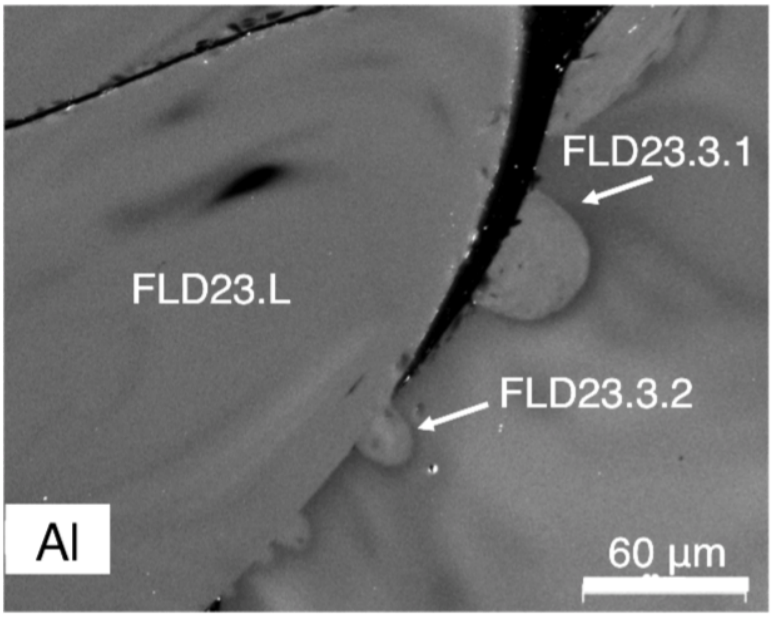

Figure 5.23: An Al compositional map showing agglomerates FLD23.L, FLD23.3.1, and FLD23.3.2 in sample FLD23. Agglomerate FLD23.3.2 is bound by the host and FLD23.L, so it must have collided with FLD23 prior to the agglomeration of FLD23.L.

does not show a ^{235}U enrichment relative to the surface agglomerates) suggest that agglomerates that collided and incorporated into their hosts earlier in time may have generally incorporated more U and more enriched U than agglomerates colliding and coalescing with the host object later in time. This could result from U condensing from the cloud earlier in time, while the vapor term in the fireball contained a greater density of enriched U. These earlier agglomerates served as condensing surfaces for the enriched U, after which latter agglomerates pass through a vapor environment less enriched in refractory device material. Bolstering this argument, the measured agglomerates in FLD4.3 are all interior agglomerates, are all enriched relative to their host, and contain the highest measured U isotope ratios in this study (Table 5.10).

Deviations in U isotope measurements between agglomerates and their hosts

As was observed with major element compositions, comparing the U isotope composition of agglomerates directly to their hosts (*e.g.*, the U isotope composition of agglomerate U1B.L to sample U1B) shows that statistically, agglomerates are not grossly different than hosts (Figure 5.25 and Table 5.10). The median deviation of an agglomerate's U isotopic composition relative to its host is +0.4% (Figure 5.25), well within the 2σ uncertainty of a single U isotope measurement. Collectively, the U isotopic composition of the agglomerates is no

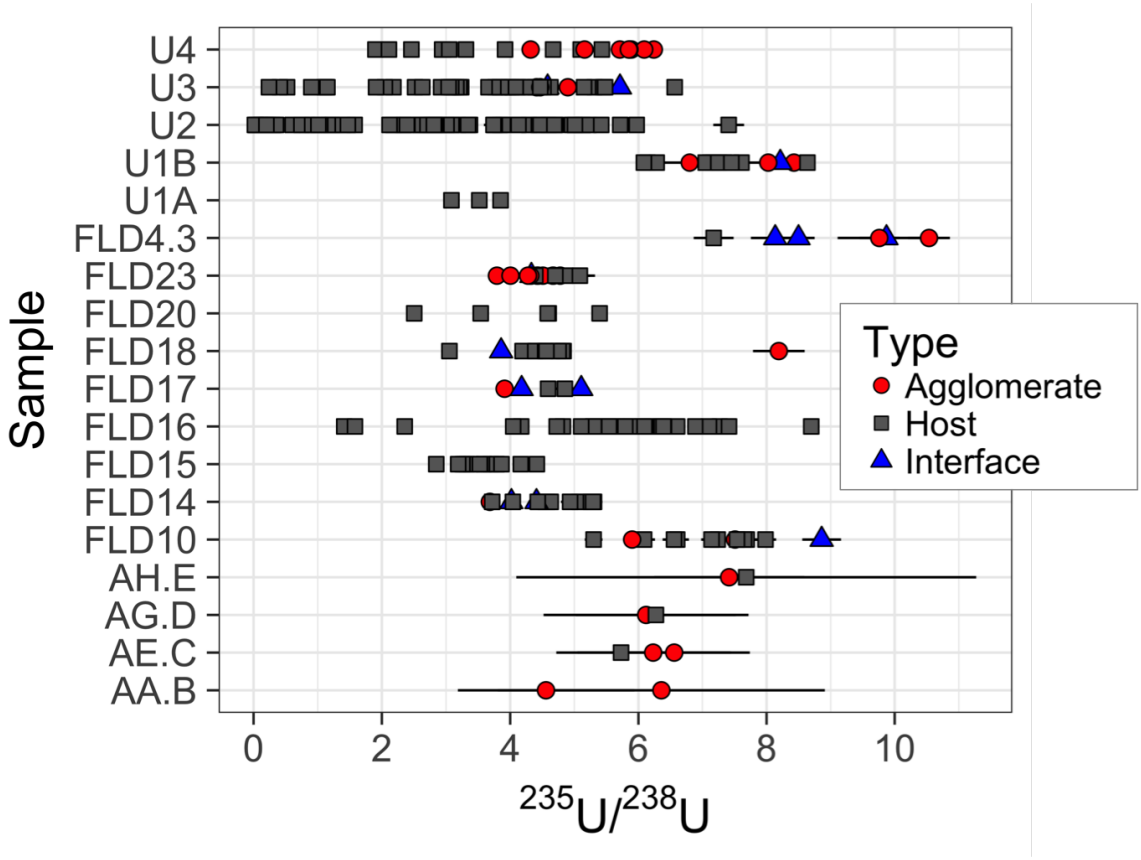

Figure 5.24: $^{235}U/^{238}U$ isotopic measurements separated by sample and location of measurement (n=302). Different markers refer to whether isotopic measurements were performed in the host, in an agglomerate, or overlapping a compositional interface between a host and agglomerate. Analyses over interfaces (blue triangles) are included when calculating agglomerate compositions. Data are tabulated in Appendix F.

different than the hosts they are attached to.

However, the distribution of deviations is not symmetric about 0. While the majority of deviations lie between -20% and +20% (27 of the 35 agglomerates, or 77%), deviations greater than 20% occur only as *positive* deviations, as demonstrated by the mean deviation being +15.0%, compared to the median deviation of +0.4%. The maximum deviation of an agglomerate from its host is observed in FLD18.2 from sample FLD18, which has an 85% higher measured $^{235}U/^{238}U$ ratio than the average of the host measurements in FLD18 (8.19 $\pm$ 0.40 and 4.42 $\pm$ 0.52, respectively). The most negative deviation is observed in the externally-attached agglomerate FLD14.L, where the $^{235}U/^{238}U$ isotopic composition is 18% lower (average of two measurements, one in the agglomerate and one over the interface) than the average U isotopic composition of host FLD14. As will be discussed in Chapter 8, the compositional interface of FLD14.L is *enriched* in $^{235}U/^{238}U$, which actually increases the average calculated composition of the agglomerate by approximately 5% (the $^{235}U/^{238}U$

ratio of FLD14.L is 3.85 ± 0.24 with the interface measurement included and 3.68 ± 0.09 with the interface measurement excluded).

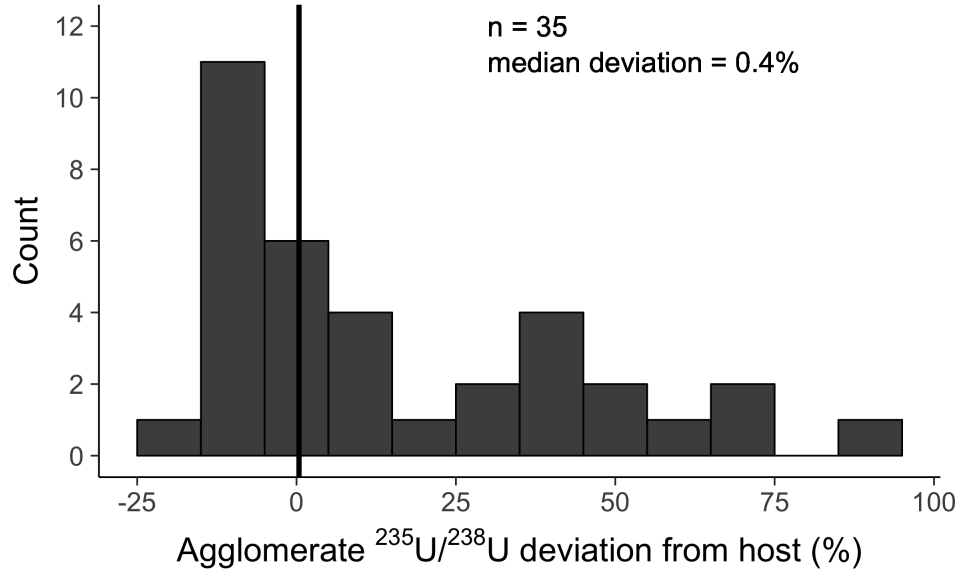

Figure 5.25: Histogram showing the deviations of the mean U isotope composition of each agglomerate from the mean U isotope composition of its host. Bins are 10% wide. The vertical line denotes the median deviation of 0.4%. Data are tabulated in Table 5.10.

Agglomerate U content and size

The samples in this study are glassy, millimeter-scale objects, and have major element compositions reflective of soil. Aircraft flying through the debris cloud after nuclear events have also collected small (micron scale), highly radioactive fallout particles on air filters [121]. These different size fractions of fallout may be formed by fundamentally different processes (*e.g.*, condensation of the ambient vapor into a soil melt versus direct vapor condensation of material). Fallout from surface bursts are modeled as reflecting the Heft distribution (Figure 1.2). In the Heft distribution, fallout objects are interpreted as a convolution of log-normal distributions as a function of diameter, where local fallout from ground collections generally being glassy and >10 μ, while air filter collections are not necessarily glassy and range from <1 μ to >100 μm. These populations are not only different because of their size, but also because of the partitioning of radionuclides among them. Volatile radionuclides are relatively enriched in smaller particles that reside longer in the fireball, and larger, glassy fallout particles are relatively enriched in refractory species [122]. It is the collision and agglomeration of these two populations that Freiling hypothesized [23] as possibly being responsible for the deviation between Miller's and Norman and Winchell's fractionation model and experimental data [50], which showed that actual, millimeter-scale fallout samples were more enriched

in volatile species more than either theory predicts (Figure 1.7). According the Heft distribution theory, agglomerates smaller than 100 μm could be derived from the cloud population *or* the local fallout population. In actuality, these populations refer to how these samples were collected (ground collects versus air filter collects) and *not* how they formed. That said, smaller particles may preserve evidence being formed of through a different physical process (such as the directly condensation vaporized material).

In this study, the smallest agglomerates ($\lessapprox$50 μm) exhibit two distinct behaviors with respect to U enrichment (Figure 5.26 and Table 5.11). These two groups come from two different samples, FLD4.3 and FLD23. The agglomerates from FLD23 are slightly depleted in their measured $^{235}U/^{238}U$ ratios relative to the host, with a mean depletion of -6.5%. Their $^{235}U/^{238}U$ ratios are reflective of the median of the entire set of 323 $^{235}U/^{238}U$ measurements (the mean of FLD23 agglomerates less than 50 μ in diameter is 4.45 $\pm$ 0.20 compared to the overall median of 323 U isotope measurements of 4.57). In contrast, the agglomerates from FLD4.3 show a large enrichment relative to their host, being enriched on average by +29%. Furthermore, the enriched population of small characterized agglomerates in FLD4.3 are all *internal* agglomerates, but the population of small characterized agglomerates in FLD23 are *surface* agglomerates. These two clusters suggest the possibility of two formation modes. The agglomerates in FLD4.3 likely formed from a vapor-dominated composition that incorporated into the host relatively early in the fallout formation process (while the host object was more molten). The agglomerates in FLD23 formed later in time, possibly from the breakup of a larger melt. This would explain why the U isotope composition of the FLD23 agglomerates are more reflective not only of the host FLD23, but also of the median of the collection of U isotope measurements. At sizes greater than 50 μm, the U isotope measurements of these groups disappear, and agglomerates become more reflective of the heterogeneities observed in bulk measurements (Figure 5.26).

5.5 U isotopes and major element composition

Major element composition of SIMS analysis locations compared to host grid analyses

After a SIMS analysis, EDS was used to measure the major element composition in (if the SIMS analysis crater was shallow enough) or adjacent to the SIMS crater to create a combined major element and U isotopic composition dataset (Figure 4.6; data discussed in Chapter 6 and are tabulated in Appendix G). Compared with the host KDEs presented in Chapter 4 (Figure 4.10), the compositions of the regions analyzed by SIMS lie primarily within the body of each of the major element KDEs. This reflects that SIMS analyses were primarily performed in glassy regions of fallout and not in the partially-melted/unmelted compositions that occupy the long tails of the KDEs (except for Na_2O, discussed below; Figure 5.27). There are two exceptions that have been excluded from Figure 5.27 to maintain the scaling used on previously shown KDE plots (Figures 4.10, 4.11, and 4.13) and ease comparison

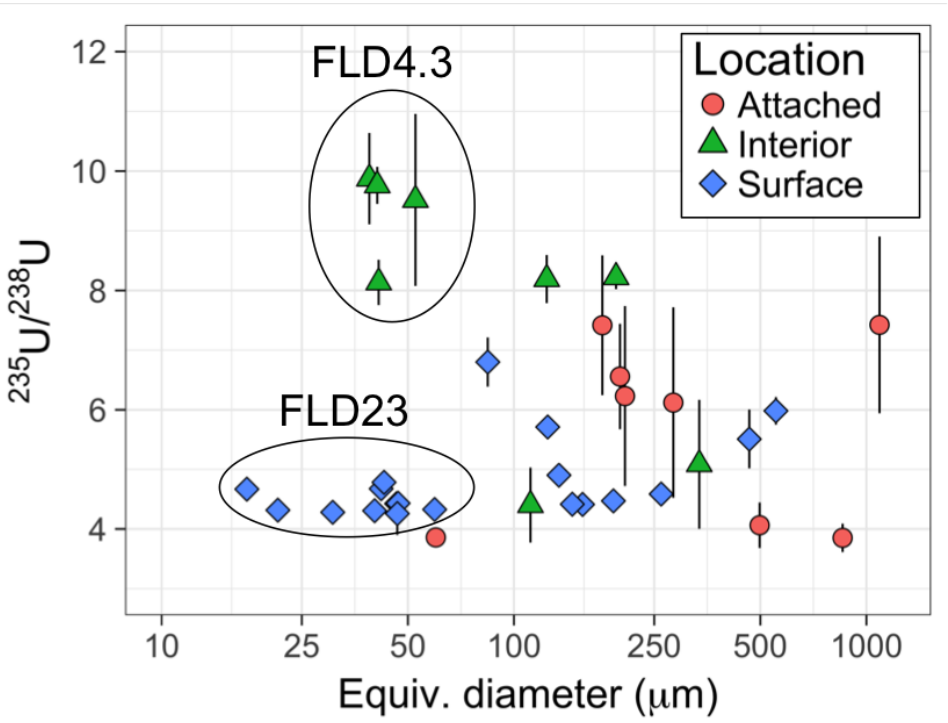

Figure 5.26: Plot of average $^{235}U/^{238}U$ ratio versus equivalent diameter for 35 different agglomerates characterized with SIMS. Shape and color refer to the location of the agglomerate (attached at the exterior, bounded by sample and the sample's surface, or fully incorporated into the sample; Figure 3.1). Data are tabulated in Table 5.11.

between them. These two SIMS analyses were conducted in high Ca regions in the hosts of samples U3 and FLD16 (Table 5.12).

There is a shift in the measured Na_2O compositions towards lower values for the compositions measured of the SIMS regions relative to the host KDE (Figure 5.27). This likely due to the volatilization of Na by the SIMS analysis and/or the topography of the crater. Measured major element compositions of three SIMS craters from sample U1A highlights this effect (Figure 5.29). Each point in Figure 5.29 represents the mean of three measurements either within or adjacent to SIMS crater (as noted in the legend) and the error bars are two times the standard deviation of these three measurements. All non-Na_2O compositions, except for a single K_2O composition (whose values differ by less than 5%), are within 2σ. In contrast, the Na_2O concentration, decreases by an average of 36% when EDS measurements are taken within the crater compared to when they are taken adjacent to the craters. As a result, while the Na_2O measurements of the SIMS analyses are reported in Appendix G, they are not used in any analysis of combining major element compositions and U isotope measurements.

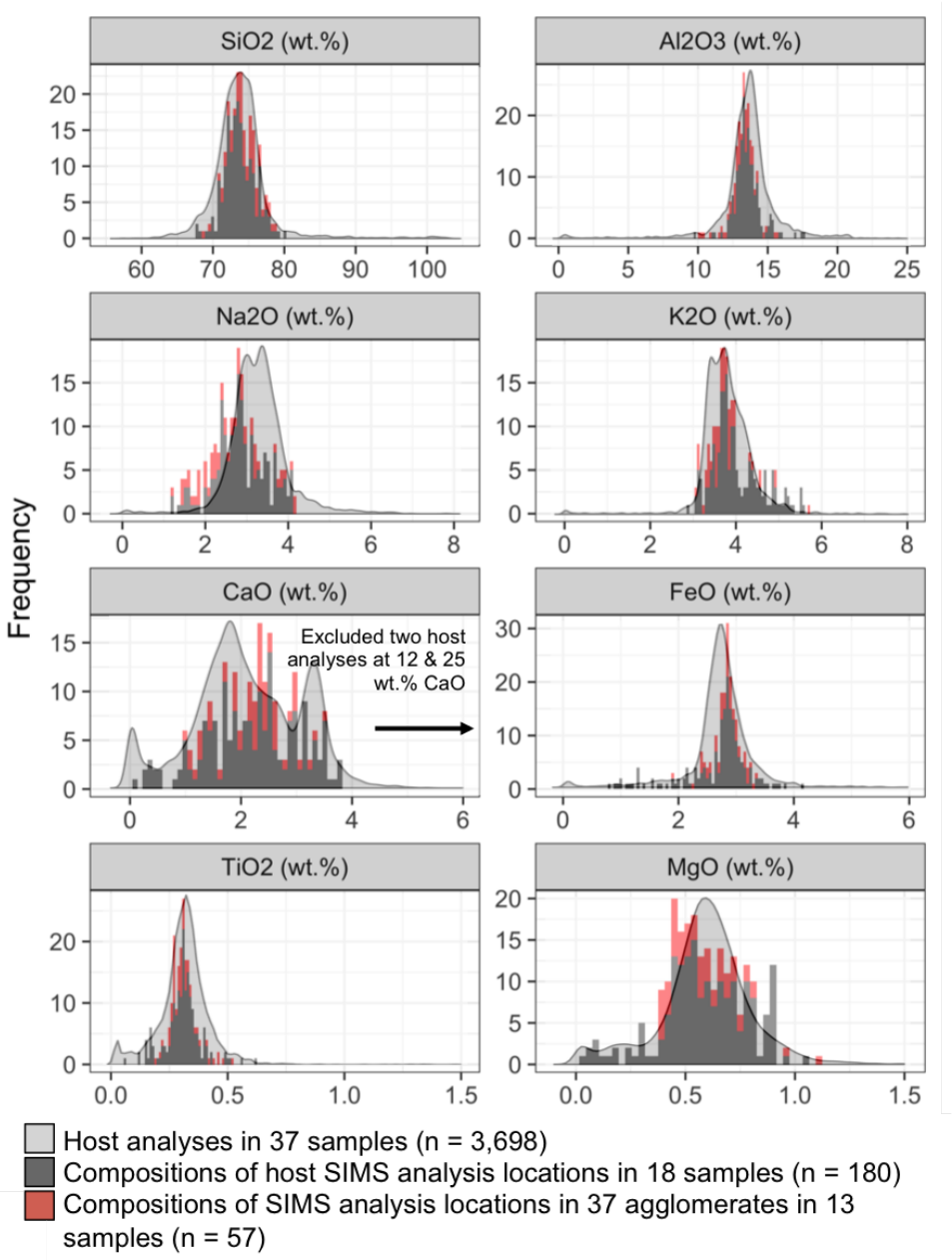

Figure 5.27: Major element compositions measured by EDS of within/adjacent to SIMS analysis craters (diagram shown in Figure 4.6) compared with the host KDEs (Figure 4.10). The deviation in the Na_2O measurements is likely due to the topography of the SIMS craters and/or Na volatilization during the SIMS analysis, and while reported in Appendix G, are not included in any analysis of the combined major element/U isotopic composition dataset in this dissertation. Data are tabulated in Appendix G.

Table 5.11: Mean U isotope composition of agglomerates characterized by SIMS sorted by equivalent diameter. U isotope data are tabulated in Appendix F.

Sample	Agglomerate	Equivalent diameter (μm)	$^{235}U/^{238}U$	1σ	Attachment location
FLD23	FLD23.3.2	17	4.67	0.14	Surface
FLD23	FLD23.2.1	21	4.31	0.13	Surface
FLD23	FLD23.2.2	31	4.28	0.14	Surface
FLD4.3	FLD4.3.1	39	9.87	0.77	Interior
FLD23	FLD23.3.1	40	4.31	0.12	Surface
FLD4.3	FLD4.3.2	41	9.76	0.31	Interior
FLD4.3	FLD4.3.5	41	8.13	0.38	Interior
FLD23	FLD23.4.1	42	4.67	0.15	Surface
FLD23	FLD23.4.2	43	4.78	0.15	Surface
FLD23	FLD23.1.1	46	4.42	0.13	Surface
FLD23	FLD23.1.3	47	4.26	0.36	Surface
FLD23	FLD23.1.2	47	4.43	0.01	Surface
FLD4.3	FLD4.3.3	53	9.52	1.44	Interior
FLD23	FLD23.5.1	60	4.33	0.13	Surface
FLD18	FLD18.1	60	3.86	0.11	Attached
U1B	U1B.2	84	6.80	0.41	Surface
FLD17	FLD17.int.1	111	4.40	0.63	Interior
FLD18	FLD18.2	124	8.19	0.40	Interior
U3	U3.4	125	5.71	0.07	Surface
U3	U3.1	134	4.90	0.11	Surface
U3	U3.5	146	4.41	0.05	Surface
FLD14	FLD14.1	157	4.41	0.10	Surface
AH.E	E1	178	7.42	1.17	Attached
U3	U3.2	191	4.47	0.11	Surface
U1B	U1B.L	195	8.22	0.20	Interior
AE.C	C1	200	6.56	0.88	Attached
AE.C	C2	207	6.23	1.51	Attached
U3	U3.3	262	4.58	0.04	Surface
AG.D	D2	283	6.12	1.60	Attached
U4	U4.2	335	5.08	1.08	Interior
U4	U4.3	465	5.51	0.49	Surface
FLD23	FLD23.L	498	4.06	0.38	Attached
U4	U4.1	553	5.98	0.23	Surface
FLD14	FLD14.L	856	3.85	0.24	Attached
FLD10	FLD10.L	1089	7.42	1.48	Attached

Table 5.12: Major element compositions excluded from Figure 5.27 due to anomalous CaO (see text). Major elements oxides are presented in weight percent.

Sample	SiO_2	1σ	Al_2O_3	1σ	Na_2O	1σ	K_2O	1σ	CaO	1σ	FeO	1σ	TiO_2	1σ	MgO	1σ
FLD16	62.41	2.64	13.47	0.68	3.08	0.23	2.84	0.11	12.08	0.48	3.77	0.19	0.38	0.11	1.05	0.15
U3	57.92	1.37	7.87	0.26	2.05	0.14	1.26	0.09	25.04	0.99	3.55	0.06	0.20	0.03	1.05	0.02

The correlation between U isotope heterogeneity and major element heterogeneity

Compositional homogeneity is strongly correlated with U isotopic homogeneity (Figure 5.31), such that samples that are well-mixed with respect to major elements tend to also be well-mixed with respect to U isotopes. The $^{235}U/^{238}U$ 1σ (absolute standard deviation) for all the host measurements in a single sample plotted against the standard deviation of

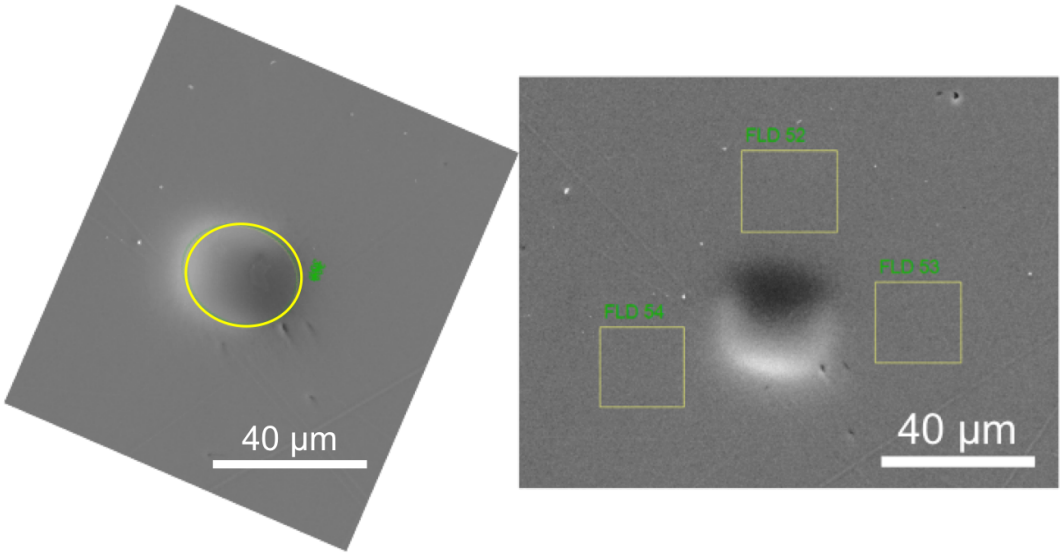

Figure 5.28: SE image showing how EDS rasters were collected to measure the composition *within* (left image) or *adjacent* to (right image) a SIMS analysis crater (data shown in Figure 5.29). The left panel shows three successive, overlaid rasters the right panel shows three EDS rasters *adjacent* to a SIMS analysis crater in the host of U1A from a IMS-1280 analysis. A combination of these approaches were used to characterize the composition of the regions analyzed with SIMS depending on the topography of the SIMS analytical crater (as shown in Figure 4.6). Although reported in Appendix G and not used for analysis of the combined major element/U isotopic dataset in this dissertation, if the analyzed region within the SIMS crater from successive, overlapping EDS raster analyses volatilized Na_2O from analysis to analysis, the first Na_2O composition was used as the measured value with the reported 1σ uncertainty taken to be the standard deviation of the Na_2O values of the three measurements.

the major element compositions (added in quadrature) of those SIMS analytical craters as measured by SIMS (excluding the Na_2O composition) highlights this observation.[9] The samples shown in Figure 5.31 were filtered to include only those with ten or more SIMS measurements in the hosts, to ensure the hosts were extensively characterized. Samples U2 and U4 (showcased in Figure 1.11 and discussed in [60]) were also excluded because their compositional heterogeneity is due to the incomplete mixing of two different melts with distinct major element and U isotope compositions that collided instead of the incomplete mixing of single melt. Therefore, Figure 5.31 shows U isotopic heterogeneity as a function of the total major element heterogeneity for well-characterized hosts that appear to have behaved as a single melt.

The most compositionally homogeneous samples shown in Figure 5.31 are FLD15, U1B, and FLD18. FLD15 and U1B exhibit flow-banding on the scale of the sample size, suggesting that physical mixing resulted in compositional homogenization (Figure 5.30). FLD18 also

[9]The standard deviations of the EDS measurements are the standard deviations from the means of entire agglomerate measurements added in quadrature: Major element $1\sigma = \sqrt{1/7(\sigma^2_{SiO_2} + \sigma^2_{Al_2O_3} + \sigma^2_{K_2O} + \sigma^2_{CaO} + \sigma^2_{FeO} + \sigma^2_{TiO_2} + \sigma^2_{MgO})}$.

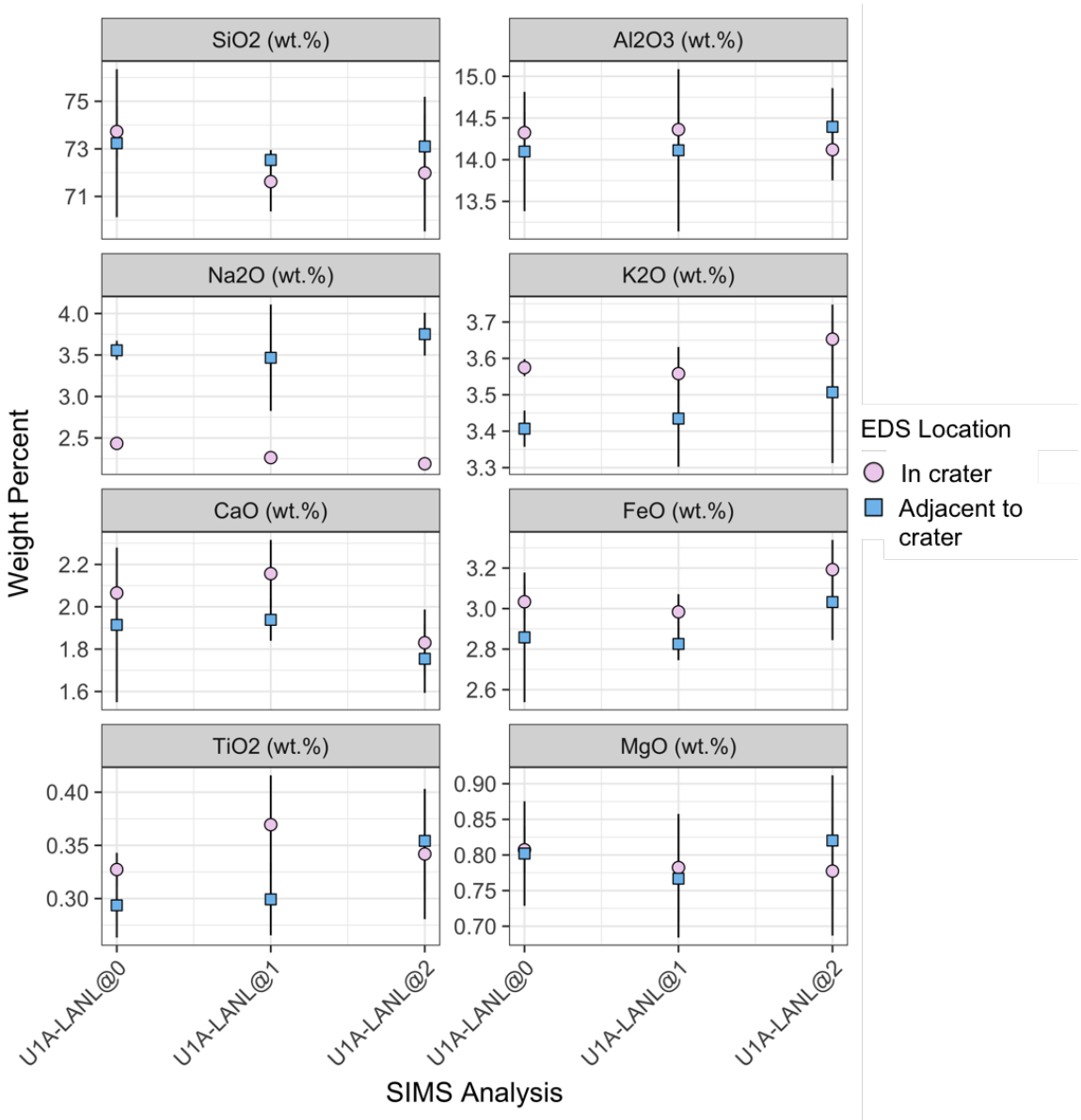

Figure 5.29: Major element compositions measured using EDS rasters within (circles) and adjacent to (squares) three IMS-1280 SIMS craters on sample U1A. Measurements within the SIMS crater were overlaid, successive analyses, while the measurements adjacent to the SIMS craters were conducted in different regions around the crater (as shown in Figure 5.28). Measurements represent the mean and 2 times the standard deviation of three measurements. Note the scale differences on the y-axes. All non-Na_2O analyses (except one K_2O analysis from SIMS analysis U1A-LANL@0, which is less than 5% different than the in and adjacent crater measurements) are within two standard deviations of each other. This suggests that EDS measurements within SIMS craters only affected the Na_2O measurements. While the measured Na_2O compositions from within/around SIMS analytical craters are tabulated in Appendix G, Na_2O is dropped from all analyses of the combined major element/U isotopic dataset in this dissertation.

contains these large scale, compositionally-homogeneous regions, but has smaller, more heterogeneous regions that appear partially-melted, and many of the high SiO_2 regions contain diffuse boundaries, suggestive of partially-melted quartz. In sample U3, the flow-banding is present at a smaller-scale, suggesting more localized mixing (Figures 5.30 and 5.19). Furthermore, U3 contains many high SiO_2 regions that appear to be partially-melted quartz, suggesting that this sample may not have been as thoroughly or extensively heated. These compositional textures may make sample-scale convective mixing prohibitive due to the high viscosity and/or of the lower heating temperature or duration.

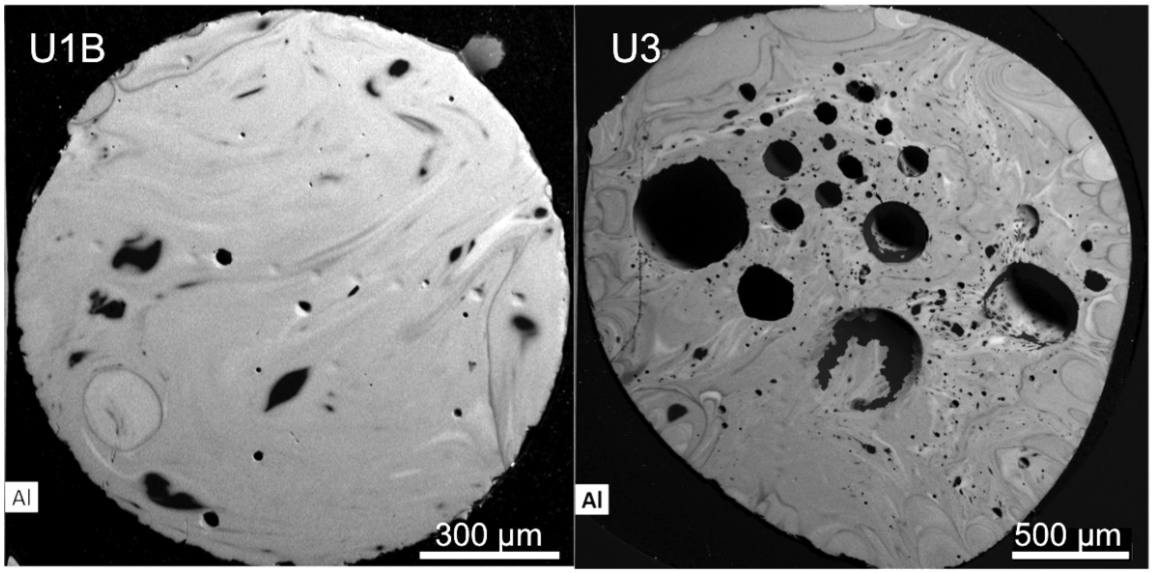

Figure 5.30: Al compositional maps of samples U1B (left panel) and U3 (right panel). Note the large-scale flow-banding in U1B and relatively even brightness of the Al map (excluding the black regions, which are high SiO_2 regions and the compositional interfaces) compared to sample U3. The large round black regions clustered towards the center of U3 are voids, which are much more abundant in U3 than U1B (which has two $\sim$50 μm voids visible near its center).

The observations in the most compositionally homogeneous and heterogeneous (and subsequently homogeneous and heterogeneous with respect to U isotopes) samples shows that physical mixing is the best explanation for thoroughly incorporating enriched U into these samples. At a given temperature, lower viscosity compositions may more effectively homogenize anthropogenic U that condenses from the vapor phase into the melt.

The correlation between major element homogeneity and U isotopic homogeneity justifies extrapolating from relatively few SIMS measurements within agglomerates. Using EDS-measured compositions of the entire agglomerate (*i.e.*, 10 μm rasters spaced approximately 10-15 μm apart across the entire exposed area of the agglomerate, instead using only compositions measured within SIMS craters), all agglomerates characterized with both EDS and SIMS have a major element standard deviation <1 (Figure 5.31). The fit obtained

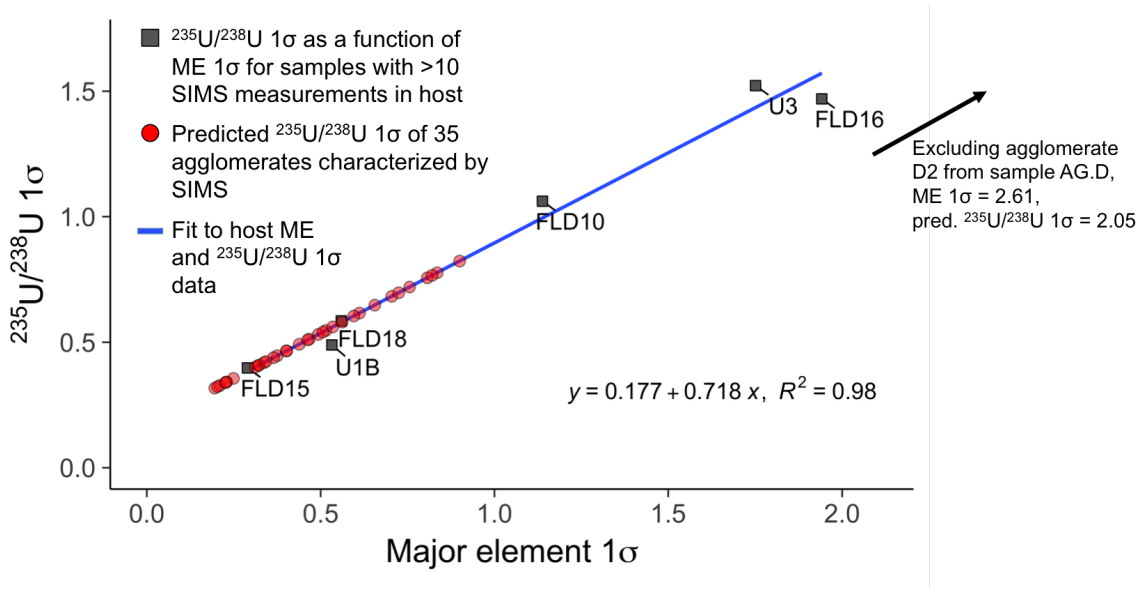

Figure 5.31: Plot of the standard deviation in U isotope ratio (^{235}U/^{238}U 1σ) of select host objects ($n > 10$) versus the standard deviation of EDS-measured major element compositions ("ME 1σ" in plot legend and text; excluding Na_2O) within/around SIMS craters in hosts with ten or more combined major element/U isotope analyses (*i.e.*, well characterized hosts). The blue line is a fit to the six host data points. The red points are the *predicted* ^{235}U/^{238}U 1σ for agglomerates using their calculated major element standard deviation. To calculate the major element standard deviations, the standard deviation of each of the individual major element oxides are summed in quadrature (excluding Na_2O; see text). Host objects that appear to have formed as the result of the collision and mixing of two distinct compositions (*i.e.*, samples U2 and U4) are excluded. This plot is generated using data tabulated in Appendix G

.

from the host SIMS measurements and the compositions of these craters is used to *predict* the ^{235}U/^{238}U standard deviation for agglomerates (shown as the red points in Figure 5.31). Except for agglomerate D2, all agglomerates have a predicted ^{235}U/^{238}U standard deviation of <1 as well. Excluded from Figure 5.31, agglomerate D2 is an exterior agglomerate of sample AG.D, with a major element 1σ = 2.61 and predicted ^{235}U/^{238}U 1σ = 2.05. The heterogeneity in this agglomerate is due to a single EDS measurement in a high SiO_2 region, likely partially-melted quartz, within the agglomerate. Excluding this single EDS measurements (*i.e.*, restricting composition measurements to the glassy regions instead of an incompletely melted mineral), reduces the major element standard deviation to 0.93 and *predicted* ^{235}U/^{238}U standard deviation to 0.85, within the range of all other agglomerates characterized by EDS and SIMS.

5.6 Conclusion

U isotope measurements in fallout reveal several previously unreported observations about fallout, hosts, agglomerates, and their formation processes. Fallout from this population is not only well-mixed with respect to major elements (Figure 4.10 and Chapter 4), but also in U isotope composition (Figure 5.17). The complete suite of $^{235}U/^{238}U$ measurements results in a quasi-unimodal distribution (n=323) with a median of 4.57, or approximately 82% enriched in ^{235}U (Figure 5.17). Three isotope plots of $^{234}U/^{238}U$ and $^{236}U/^{238}U$ vs. $^{235}U/^{238}U$ show strong linear correlations (R^2 = 0.998 and 0.997, respectively), continuing to support an interpretation of two component mixing with between natural and enriched end-members from this test (Figure 5.21) [60]. Assuming the enriched end-member has the composition of oralloy, the majority of $^{235}U/^{238}U$ measurements (300 of the 323) are dominated by contributions from this enriched source (presumably the device's fuel). Onlyl 23 measurements (measured in sample U2 and U3) reflect a dominant contribution from the natural end-member(s), which could be due to late melting and incorporation of carrier soil (sample U2) or partial melting of carrier soil, preventing efficient mixing and incorporation of condensed vapor from the ambient environment (sample U3) 5.19.

Comparisons of U isotope ratio measurements by sample shows that unlike the major element composition, different samples (including both hosts and agglomerates) appear to incorporate significantly different amounts of enriched U on average, ranging from sample U2 with $^{235}U/^{238}U = 2.49 \pm 1.93$ (n=67) to sample FLD4.3 with $^{235}U/^{238}U = 9.00 \pm 1.27$ (n=6) (Table 5.9). These differences in mean $^{235}U/^{238}U$ content shows the vapor environment in the fireball was highly heterogeneous. Even though samples were collected at similar distances from ground zero, the location of ground deposition has little relation to their degree of bomb vapor incorporation. The range in $^{235}U/^{238}U$ ratio measurements from bulk measurements of entire samples supports this conclusion (Figure 5.20 and Table 5.9).

U is more heterogeneously distributed from sample-to-sample than major elements. This suggests the soil term that was incorporated into the fireball was fairly homogeneous (or was homogenized during incorporation) compared to heterogeneities of vaporized species in the fireball, despite the soil term comprising the >99% of the composition of these samples. Within samples, U isotopic heterogeneity is strongly correlated with major element heterogeneity (Figure 5.31). Homogeneous samples preserve compositional flow-banding patterns on the scale of the sample size, suggesting these melts had time to homogenize not only their chemical compositions through physical mixing (convection), but that physical mixing also distributed and homogenized enriched U originally condensed onto the surface of the carrier soil melts.

Comparison between agglomerates and hosts

Unlike major element compositions, agglomerate $^{235}U/^{238}U$ ratio measurements do not appear as a subset of the measured host $^{235}U/^{238}U$ ratios (Figure 5.22). Instead, the agglomerate distribution is shifted towards higher enrichments in ^{235}U, with a minimum measured

$^{235}U/^{238}U$ ratio of 3.68 ± 0.09, while the minimum host measurement is near natural at $^{235}U/^{238}U$ equal to 0.02 ± 0.002. The maximum $^{235}U/^{238}U$ ratio measured a host object is 8.70 ± 0.09 (sample FLD16). In comparison, four agglomerate measurements in two samples (two of which overlap compositional interfaces) observed to have $^{235}U/^{238}U$ ratios greater than the host maximum. The histogram of measurements and comparison of cumulative distribution functions between hosts and agglomerates show that generally, agglomerates are enriched relative to hosts and have a higher median value as a collection. There were no measured $^{235}U/^{238}U$ ratios below 3.68, or a ^{235}U enrichment of approximately 78% (measured in FLD14.L the agglomerate attached to the exterior of FLD14) in agglomerates.

When comparing the U isotopic composition of an agglomerate and its host, the median deviation of the suite of U isotope ratio measurements ($n = 35$) is 0.4%, suggesting that statistically agglomerates and their hosts incorporate similar amounts of enriched U (Figure 5.25). However, the deviations are not symmetric about 0 (as highlighted by the *mean* deviation of +15.0%). The most negative deviation is 18% and the most positive deviation is +85%, indicating large differences in enrichment are due to agglomerates incorporating more enriched U than their hosts.

The combined evidence of isotopic and major element characterization of agglomerates and their hosts suggest that while hosts may experience a range of temperatures and melting within a single sample, agglomerates are primarily glassy and have been thoroughly transformed by the fireball. Statistically, agglomerate compositions and U content are no different than the hosts they are attached to, suggesting these agglomerations occurred in a small, localized region of the fireball. This would preclude the large heterogeneities shown to be present in sample-to-sample differences in measured U isotope ratios (Figures 5.20, 5.24 and Tables 5.9 and 5.10). Notable exceptions to this observation are samples U2 and U4, which exhibit two distinct compositions and U isotope distributions and, in the case of U2, formed from the collision of two comparably sized melts.

In four samples, U3, U4, FLD23, and FLD4.3, the agglomerates attached in the same location (*e.g.*, the surface agglomerates of FLD23) have similar isotope ratios and compositions to each other (Table 5.10). This suggests a common mode of formation, a common source of the agglomerates, and/or a collision at a similar time. These commonalities can be extrapolated to infer common a fireball temperature and local fireball vapor composition. These similarities will be explored in the next chapter, which uses multivariate analyses and approaches to explore the combined U isotopic and major element dataset.

Agglomerates attached in different locations in the same sample (*e.g.*, FLD14.L compared to FLD14.1, an exterior agglomerate in FLD14 compared to a surface agglomerate in FLD14), reveal that, in most cases, the agglomerate that collided with the host at earlier times and higher temperatures is *more* enriched than the agglomerate that collided with the same host later in time. This suggests that the local environment in the fireball earlier in time allowed more enriched U vapor to condense mix into the volume of these more fully incorporated agglomerates, and that this inventory and the degree of bomb vapor condensing decreased with time.

Agglomerates characterized in this study smaller than ∼50 μm are from two samples

(FLD23 and FLD4.3). The agglomerates <50 μm in FLD23 are slightly depleted in measured $^{235}U/^{238}U$ ratios relative to their host objects, with a mean depletion of -6.5% and are similar to the median of the full 323 collection of U isotope measurements. In contrast, agglomerates from FLD4.3 show a large enrichment relative to the host, enriched on average by +29%. While characterized agglomerates less than 50 μm come from only two samples, they exhibit two different relative enrichments to their host objects, and they are located in two different regions. The FLD23 agglomerates are all bound by the surface of the sample, while the agglomerates smaller than 50 μm in FLD4.3 have all been fully incorporated into sample FLD4.3. The enriched group (in FLD4.3), consists of interior agglomerates, all of which contain high U content, while the surface group (in FLD23), exhibits a U isotope ratio similar to the median $^{235}U/^{238}U$ ratio of the collection of U isotope measurements. This suggests two formation modes for the smallest agglomerates: those relatively enriched in an enriched vapor term incorporated this vapor relatively early in the fallout formation process, while the host object was more molten. In the second case, the small agglomerates may result from the prior breakup of a larger melt, explaining why its $^{235}U/^{238}U$ composition is more reflective not only of the host it is attached to, but also to the collection of U isotope measurements as a whole. At sizes greater than 50 μm, U isotope differences between these two groups disappear and the resulting U isotope compositions are more reflective of the heterogeneities of bulk measurements, suggesting they are now reflecting various (average) amounts of incorporation of vapor and molten soil.

The observation of collective U isotopic similarity between agglomerates and their associated host objects does not support the theory of Freiling et al. (1965) that agglomerates with grossly different radionuclide inventories were incorporated into host objects [5]. Furthermore, these agglomerates, if representative, are unable to appreciably alter the average radionuclide composition of the entire sample. While the characterized interior agglomerates in FLD4.3 are highly enriched in ^{235}U relative to their host FLD4.3, the sum total of their cross-sectional areas occupies an insignificant area within the exposed cross-section of the sample ($<<1\%$).

In Chapter 6, the multivariate relationships between major elements and U isotope compositions will be explored using Principal Components Analysis. This multivariate approach allows for the simultaneous visualization of all major element oxides in a single plot to determine if there are persistent correlations between pairs or groups of major element oxides and/or the U isotope composition. These correlations will be used to explore the possible end-member compositions contributing to the mixtures in the glassy phase and whether U isotope composition is correlated with major elements, as has been observed with Pu, Ca, Mg, and Fe in the case of the Trinity test [55, 58].

Chapter 6

Principal Components Analysis of Major Element and U Isotopic Compositions in Fallout

6.1 Chapter overview

In Chapters 4 and 5, each of the measured major elements and the $^{235}U/^{238}U$ ratios were treated separately to determine the relationship between agglomerates and hosts. In this and the next chapter, these variables are combined and analyzed simultaneously to establish the co-variance between major elements and the $^{235}U/^{238}U$ ratio.

In this chapter, principal components analysis (PCA) is conducted to visualize and analyze the major element relationships between the host objects, agglomerates, and unmelted soil compositions. In addition, PCA is used to determine the relationship between the major element composition and U isotope composition. In both cases, the principal components model is created using major element oxide data measured using EDS rasters in a grid pattern across the host objects ($n = 3,698$). The first model projects major element compositions (EDS data only) from agglomerates and unmelted soil through this model to visualize the sources of variance in the major element compositions. Result show the agglomerate compositional relationships relative to host objects, and that the dominant source of variance in the dataset are outlying compositions from measurements of unmelted mineral regions in the fallout.

To constrain the relationship between major element composition and U isotope composition, a combined dataset created from U isotope analyses by SIMS and major element analyses obtained from EDS rasters collected within/adjacent to the SIMS analytical craters is projected through the PCA model created using host object major element compositions (excluding Na_2O, as discussed in Chapter 5). This model is used to search for co-varying relationships between the unfissioned fuel and major elements in the glassy phases. Such variance has been previously observed at CaMgFe interfaces in fallout from this test and also

noted in studies of glassy fallout from the Pu-fueled Trinity test [55, 58, 66, 67].

Before generating the principal components model, the influence of analytical uncertainty in EDS major element data, outliers in the host object major element compositions, the handling of zeros in modeling compositional data with noisy variables (*e.g.*, TiO_2 and MgO, which are usually present at <1 wt.%) is also discussed.

6.2 Principal Components Analysis

While standard geochemical tools such as binary and ternary diagrams can relate the mixing between different chemical constituents in the soil, other multivariate visualization and statistical approaches enable a more comprehensive analysis of compositional relationships when major elements are derived from multiple sources (such as different minerals in the soil). The first and most fundamental approach in most multivariate analyses is principal components analysis (PCA). PCA is a widely-used technique for exploratory data analysis and dimension reduction in multivariate datasets. It solves several problems when dealing with a large number of variables. For example, only three variables can be easily visualized graphically at any one time, making visualization and interpretation unwieldy when dealing with a large number of variables. Furthermore, some variables may contain very little information or simply noise, and including them in the analysis may lead to spurious results. PCA solves these problems by generating principal components (PCs), which are linear combinations of the original variables and by definition, linearly independent from one another (*i.e.*, uncorrelated with one another). This transformation projects all of the original variables simultaneously in 2D space and removes correlations between variables. By removing the correlation between variables, PCs become ideal inputs for further multivariate analyses, including regression, classification, and discrimination methods [123, 124].

PCs are generated in such a way that the first PC explains the largest source of variance in the data set, the second explains the next largest source of variance (that is also orthogonal to the first PC), and so on. Higher order PCs capture the least variance and often are mostly capturing systematic noise and may be removed to reduce the overall number of dimensions in the dataset. Unlike the original variables, PCs are not necessarily physically meaningful, and accordingly, one must be careful with their interpretation [125].

PCs are usually viewed using a binary plot, called a *biplot*, which shows both the transformed dataset (the *scores*) and the weights of the original variables in 2D space (the *loadings*; Figure 6.1) [126–129]. The biplot uses any two of the PC components as the x and y-axes, the original variables (the major element oxides) are plotted as 2D vectors, with magnitudes in the x and y directions equal to their weights in those principal components. The angles between the vectors provide information about the correlation or anti-correlation between different original variables and reveal trends between the data and all variables simultaneously.

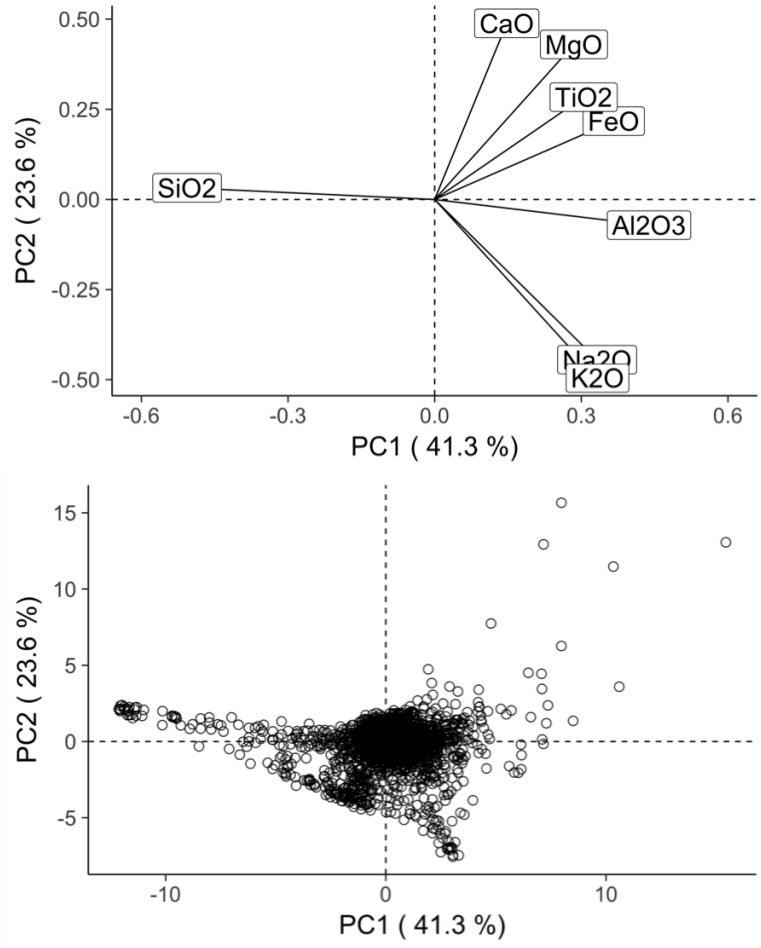

Figure 6.1: PC1 and PC2 loadings (top) and scores of the host major element oxide compositions measured using EDS (bottom). Conventionally, biplots combine the scores and loadings on the same plot. To ease viewing, they are split into two plots here.

Calculating principal components

One of the primary goals of PCA is reducing the number of original dimensions in a dataset, where the number of original dimensions in this study refers to the number of major element oxides and isotopic ratios included in a single analysis. PCA aims to reduce a dataset $\mathbf{X}$ of m_{obs} rows where each row is an observation or measurement (e.g., a single EDS analysis), and n_{var} columns, where each column is a variable (*i.e.*, SiO_2, Al_2O_3, Na_2O,...), to a new data matrix with fewer variables that better explain the observed variance in the data set. The new variables (called *latent* or *synthetic* variables) are the principal components (PCs). They are obtained through a rotation of the original variables into a new reference frame—one where PCs are oriented in the direction of greatest variance. There are the same number of PCs as there are original variables and they are mutually orthogonal, so the full set of PCs

form a linearly-independent set of basis vectors for the space spanned by the data. PCs are calculated such that the first PC (PC1) is oriented in the direction of the greatest variance, the next PC (PC2) is oriented the direction of next greatest variance orthogonal to PC1, PC3 is oriented in the direction of greatest variance that is orthogonal to both PC1 and PC2, and so on. The linear combination of the original variables, or weights, for a principal component are called the *loadings* of that PC. The coordinates of the original data in PC space are called the *scores*. The loadings show how the original variables are correlated or anti-correlated, revealing which variables contribute to the data's variance.

Transforming the original variables in the original data matrix $\mathbf{X}$ into principal components is subject to the constraints of maximizing the variance of PCs and minimizing the co-variance (redundancy) between PCs. Given two original variables A and B that form columns in $\mathbf{X}$ (*e.g.* SiO_2 and Al_2O_3), PCA simultaneously seeks to

$$\begin{aligned} \text{maximize: Var(A)} = \sigma_A^2 &= \frac{\sum_{i=1}^{m}(A_i - \bar{A})^2}{m} \\ \text{minimize: Cov(A,B)} = \sigma_{A,B}^2 &= \frac{\sum_{i=1}^{m}(A_i - \bar{A})(B_i - \bar{B})}{m}, \end{aligned} \tag{6.1}$$

where A_i denotes the value of A from a single measurement, $\bar{A}$ denotes the mean of all the measurements of A, and m denotes the total number of measurements. The requirements of Eqn. 6.1 are fulfilled by diagonalizing the covariance matrix, $\mathbf{C}$. The covariance matrix $\mathbf{C}$ is a square, symmetric matrix with variances along the diagonal and co-variances everywhere else and is calculated from the original data matrix $\mathbf{X}$ by $\mathbf{C} \equiv \frac{1}{n-1}\mathbf{X}'\mathbf{X}$. For example, for hypothetical variables A, B, and C, the covariance matrix is

$$\mathbf{C} = \begin{bmatrix} \sigma_A^2 & \sigma_{A,B}^2 & \sigma_{A,C}^2 \\ \sigma_{B,A}^2 & \sigma_B^2 & \sigma_{B,C}^2 \\ \sigma_{C,A}^2 & \sigma_{C,B}^2 & \sigma_C^2 \end{bmatrix} \tag{6.2}$$

Diagonalizing $\mathbf{C}$ fulfills the requirements of Equation 6.1, in that diagonalization of $\mathbf{C}$ simultaneously maximizes the variance and minimizes the covariance [130].

$\mathbf{C}$, being a symmetric matrix, is diagonalizable by a matrix of orthonormal eigenvectors:

$$\mathbf{C} = \frac{1}{m-1}\mathbf{Q}\mathbf{\Lambda}\mathbf{Q}' \tag{6.3}$$

where matrix $\mathbf{Q}$ contains the orthonormal eigenvectors and $\mathbf{\Lambda}$ is a diagonal matrix of the eigenvalues. Most algorithms do not calculate matrix $\mathbf{C}$ directly, but instead perform the diagonalization using the original matrix $\mathbf{X}$ and solving for the eigenvectors and eigenvalues of $\mathbf{C}$ using singular value decomposition (SVD), which decomposes the covariance matrix into three matrices,

$$\mathbf{X}_{m_{\text{obs}} \times n_{\text{var}}} = \mathbf{U}\mathbf{\Sigma}\mathbf{V}', \tag{6.4}$$

where $\mathbf{U}$ and $\mathbf{V}$ are orthogonal matrices ($\mathbf{VV'} = \mathbf{I}$) and $\mathbf{\Sigma}$ is a diagonal matrix of singular values. A requirement of PCA is that $\mathbf{C}$ is diagonalized, such that

$$\mathbf{X} = \mathbf{U\Sigma V'} \tag{6.5a}$$

$$\mathbf{C} = \frac{1}{m-1}\mathbf{X'X} = \frac{1}{m-1}(\mathbf{U\Sigma V'})'\mathbf{U\Sigma V'} \tag{6.5b}$$

$$\mathbf{C} = \frac{1}{m-1}\mathbf{V\Sigma U'U\Sigma V'} \tag{6.5c}$$

$$\mathbf{U} \text{ is orthogonal, so } \mathbf{C} = \frac{1}{m-1}\mathbf{V\Sigma^2 V'} \tag{6.5d}$$

Matrix $\mathbf{V}$ equals the matrix $\mathbf{Q}$ from Equation 6.3, which contains the orthonormal eigenvectors of $\mathbf{C}$ as its columns. Matrix $\mathbf{\Sigma^2}$ equals the matrix $\mathbf{\Lambda}$, which contains eigenvalues of $\mathbf{C}$ along its diagonal. Therefore, the singular values are actually $\sqrt{\lambda_i}$, where λ_i are the eigenvalues of $\mathbf{C}$. In the case of $\mathbf{C}$, $\lambda_i = \sigma_i^2$, the variances of the original variables of the data matrix $\mathbf{X}$ and the corresponding eigenvectors of $\mathbf{C}$ in the columns of $\mathbf{V}$ are the principal components of $\mathbf{X}$. To summarize, the eigenvalues and eigenvectors of the co-variance matrix $\mathbf{C}$ are the variances and PCs of the original data matrix $\mathbf{X}$.

In PCA, the eigenvalues along the diagonal of $\mathbf{\Sigma}$ are ordered in decreasing magnitude. Correspondingly, the eigenvectors in the columns of $\mathbf{V}$ are ordered by decreasing magnitude of the variance they explain. The rows of $\mathbf{V}$ then represent the original variables, with entries being the various weights for each PC. Finally, the rows of $\mathbf{U}$ contain the individual measurements transformed into PCA space—the *scores* [131].

While the covariance matrix $\mathbf{C}$ is used to introduce how to solve for PCs and eigenvalues, most PCA models in literature (and all models used in this study) pre-treat the data by subtracting some metric of the data's center (usually the mean or median) and scaling it to have a variance of one (or some other metric of the data's scatter). This variance-scaling creates a *correlation* matrix, instead of the unscaled covariance matrix. (The eigenvalues and eigenvectors of the correlation matrix are not equivalent to the covariance matrix.) Using the correlation matrix instead of the covariance matrix for PCA allows variables to be compared without the influence of different units (*e.g.*, when comparing weight percents to isotope ratios) or changes in absolute values. The resultant PCs instead reflect relative changes in the original variables.

Using PCA to model dataset variance

The primary goal of PCA is dimension reduction. By discarding PCs that contain little useful information, spurious variance due to analytical noise or bias can be removed from consideration. The more PCs retained, however, the better PCA replicates the original data matrix $\mathbf{X}$. If all of the PCs are retained, PCA replicates the data matrix $\mathbf{X}$ exactly. In a typical PCA model, only the first few PCs are retained for further analysis, as the latter PCs

subsequently describe decreasing amounts of variance and ideally contain noise or no useful information. Deviation between the model and the original data matrix $\mathbf{X}$ is captured in an error or residuals matrix $\mathbf{E}$ (Figure 6.2):

$$\mathbf{X}_{m_{\text{obs}} \times n_{\text{var}}} = \mathbf{U}_{m_{\text{obs}} \times p_{\text{ret}}} \mathbf{\Sigma}_{p_{\text{ret}} \times p_{\text{ret}}} \mathbf{V}'_{p_{\text{ret}} \times n_{\text{var}}} + \mathbf{E}_{m_{\text{obs}} \times n_{\text{var}}}, \tag{6.6}$$

where p_{ret} is the number of PCs retained in the model. The residuals matrix $\mathbf{E}$ is important in determining how well the PCA model fits the data and is used to find and describe data outliers (described further below).

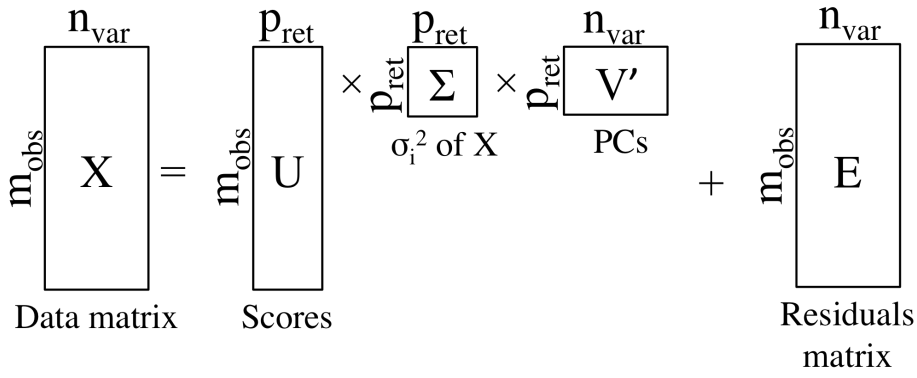

Figure 6.2: A pictorial representation of decomposing the data matrix with SVD and retaining a subset of principal components. Terms are as defined in the text.

When applied to inhomogeneous mixtures, such as the spatially resolved fallout glass compositions measured using EDS, the PCs may describe the end-member sources contributing to that mixture, such as quartz, feldspars, and mafic minerals [80]. PCs can also reveal multiple sources of the original variables (such as if CaO or FeO is derived from multiple end-member sources in the soil).

Determining the number of principal components to retain

There are several approaches to determine how many principal components to retain in a PCA model, all of which rely on the magnitude of variance explained by the principal components. These approaches generally rely on the *scree plot*, which is a plot of the eigenvalues (variances) as a function of principal component number, or, alternatively, a plot of cumulative proportion of the variance explained by each successive PC (Figure 6.3).

The first and simplest approach is *Kaiser's rule*, which argues that PCs with variances greater than 1 should be retained [125]. For the scree plot of the eigenvalues obtained from a PCA model of major element oxide compositions of host objects presented in Figure 6.3, only the first 3 PCs would be retained. This argument relies on the pre-treatment of data prior to PCA: because data are standardized to have of a variance of one and a mean of

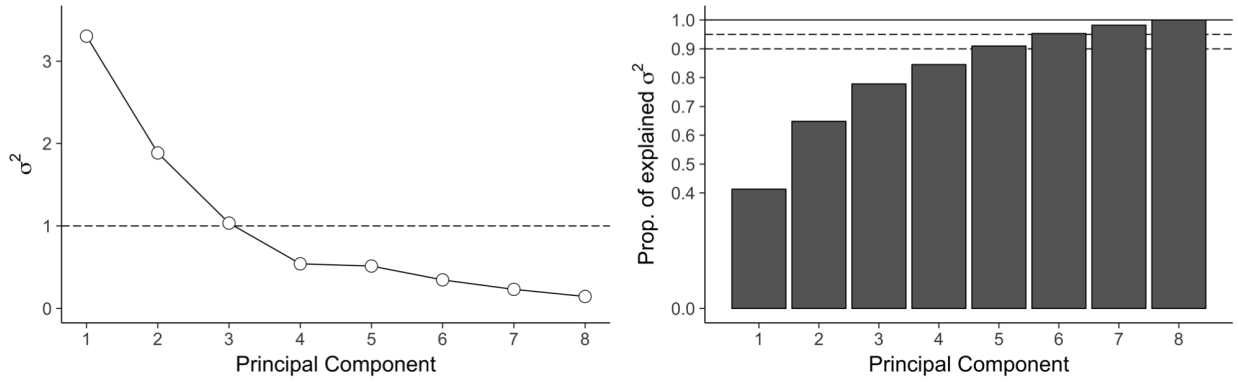

Figure 6.3: The magnitude of the variance (σ^2; also the magnitude of the eigenvalue) as a function of principal component number (left; called a scree plot) and cumulative variance explained as a function of principal component number (right) of the EDS grid data. There are eight PCs because eight original variables (oxides of Si, Al, Na, K, Ca, Fe, Ti, Mg) are included. The horizontal lines on the right plot show how many PCs must be retained to account for 90% and 95% of the total variance (retaining all 8 PCs replicates the data exactly and therefore explains all of the variance in dataset, defeating the purpose of using PCA for dimension reduction).

zero prior to PCA, if PCs have variances less than 1, then they explain less of the variance than the original variables did and should be discarded. This rule is often considered too conservative, however, and may result in discarding PCs that still explain important sources of variance [125]. The next and most employed test, and one test used in this study, was introduced by Cattell (1966) and is called the *scree test* [132]. It relies on using the scree plot to determine when the slope of the variance changes from steep to shallow, forming an elbow [132]. The elbow then is the number of PCs to retain. This "elbow" is visible at PC4 in the left plot of Figure 6.3 and supports retaining only the first 4 PCs. This a more subjective test, however, as in some scree plots, there may be multiple elbows or the shift in slope may be more subtle, such that determining on the number of retained PCs may ultimately be up for some degree of interpretation. This test, while somewhat subjective, has been successfully applied in many scenarios [125]. The last common test relies on retaining PCs that explain a set amount of variance of the original data set (*e.g.*, the right plot in Figure 6.3). Typically, the analytical uncertainty of the technique used to make the measurements, or arbitrarily a 90% or 95% cut off is applied. As can be seen in Figure 6.3, this approach results in the most number of PCs being retained (5 for a 90% cutoff and 6 for 95% cut off). It is not used here, however, because the uncertainty in the measurements is variable-dependent.

While the above tests are instructive and useful as a guide (suggesting retaining between 3 PCs for Kaiser's rule and 6 PCs for a 95% cut-off in the proportion of variance explained), noisy compositional data presents additional challenges. To better quantify how many PCs should be retained, for a robust model, a more rigorous noise-injection method is used here (as discussed below).

This method suggests that first 5 PCs primarily explain real variance in the dataset, and

therefore may be retained, and that PCs 6-8 primarily capture analytical noise in their PC directions and should be discarded.

Data pre-treatment

When performing multivariate analyses using variables with different variances and magnitudes, data are usually pre-treated to (a) give each variable equal weight in the analysis, (b) weight the variables using some *a priori* knowledge about each variable's importance to the analysis, and/or (c) transform the data to remove constraints such as closure. In this dissertation, each major element oxide variable is scaled and centered to give it equal weight in the PCA analysis.

Standard pre-treatment: scaling and centering

Standard (or "classical") pre-treatment of data prior to PCA refers to centering each variable by subtracting its mean, and then scaling each variable such that each variable has a variance equal to one:

$$x_{\text{std}} = \frac{x - \bar{x}}{\sigma_x}, \tag{6.7}$$

where x refers to each variable (SiO_2, Al_2O_3, etc.), σ_x is the variance in that variable, and $\bar{x}$ is the mean of that variable. For the dataset of major element oxide compositions of host objects, this is the mean composition of all the host measurements (Table 4.4), and x_{std} is the resulting pre-treated data used for PCA.

Standard pre-treatment is the simplest and most common data pre-treatment method. Data pre-treatment ensures that variables that have greater absolute values (such as SiO_2) are given equal treatment as minor variables (such as FeO, CaO, MgO, or TiO_2). In addition, scaling to unit variance ensures that measurement fluctuations are given equal weight and allows measurements of different units to be compared. When the data are non-Gaussian and contain many outlying compositions (as these compositional data are) other metrics have been proposed to pre-treating the data, such as subtracting by the median instead of the mean and using alternative scaling metrics [123, 131, 133]. These are known as "robust" pre-treatment methods and were formulated as an alternative to standard pre-treatment methods to resist the influence of outliers in generating the principal components. However, because fallout is consistent with being a mixture of mineral compositions present in the soil (which manifest as outliers) understanding and visualizing the correlations between soil mineral compositions is important to visualizing the compositional trends captured in the glassy phases of the fallout. Therefore, these compositional outliers *should* influence the PC space (as long as they are valid measurements). As a result, only standard pre-treatment (mean centering and scaling to unit variance, as shown in Equation 6.7) is used here.

Log-ratio transformations: opening compositional data

Compositional data are subject to the constraint of summing to 1, 100, or near these values. As a result, they do not represent absolute values, but relative values of a whole. Therefore, they do not populate n-dimensional positive real space, $\mathbb{R}^n$, where n is the number of variables (positive because compositional data are also subject to the constraint of non-negativity–all values must be positive). Instead they populate the $n-1$-dimensional simplex $\mathcal{S}^n$, which has dimension $n-1$ (if 7 of 8 variables are measured, the last one is known by difference, and is therefore not linearly independent) [134–136]. To transform from the $\mathcal{S}^n$ to $\mathbb{R}^n$, from a "closed" dataset to an "open" dataset, a set of log-ratio transformations have been proposed and are now widely used [136–139]. Transforming compositional data from closed to open is important to allow for the correct application of multivariate statistical techniques that rely on Euclidean distances between points (as will be done in Chapter 7).

The most used log-ratio transformation (also used here when conducting the similarity analyses in Chapter 7) is Aitchison's centered-log ratio (CLR) transformation [138], which transforms the compositional data from $\mathcal{S}^n$ to $\mathbb{R}^n$:

$$\mathrm{CLR}(x) = \left(\ln\left(\frac{x_1}{g(x)}\right), \ldots, \ln\left(\frac{x_n}{g(x)}\right)\right), \tag{6.8}$$

where $\mathrm{CLR}(x)$ is the transformed composition of a single measurement and $g(x)$ is the measurement's geometric mean [133, 135, 140].[1]

While some multivariate techniques require the data populate $\mathbb{R}^n$, PCA does not. Furthermore, whether log-ratio transformations are beneficial for compositional data prior to PCA is still debated. Recent comparisons between standard pre-treatment and log-ratio transformations in materials similar to fallout, such as major element data from alkaline glasses [141, 142], have shown that standard PCA can lead to more interpretable principal components and greater visual separation between sub-groups. This separation eases using further multivariate methods such as cluster analyses [143, 144]. For PCA in this study, standard pre-treatment is used because PCA is applied here as an exploratory and data visualization tool. However, when quantitatively measuring distances in multivariate space between agglomerates and hosts, most analyses rely on metrics that assume Euclidean distances. Thus, when performing similarity analyses between these objects using multidimensional scaling (Chapter 7), the data are first transformed to $\mathbb{R}^n$ using the centered log-ratio transformation then standardly pre-treated (Equation 6.7) to prevent low abundance and noisy variables from having outweighed importance in the multivariate analyses. This counters the increased influence of noise with the log-ratio transformation [140, 142, 145].

[1] The geometric mean is defined as $g(x) \equiv \sqrt[n]{x_1 x_2 \ldots x_n}$.

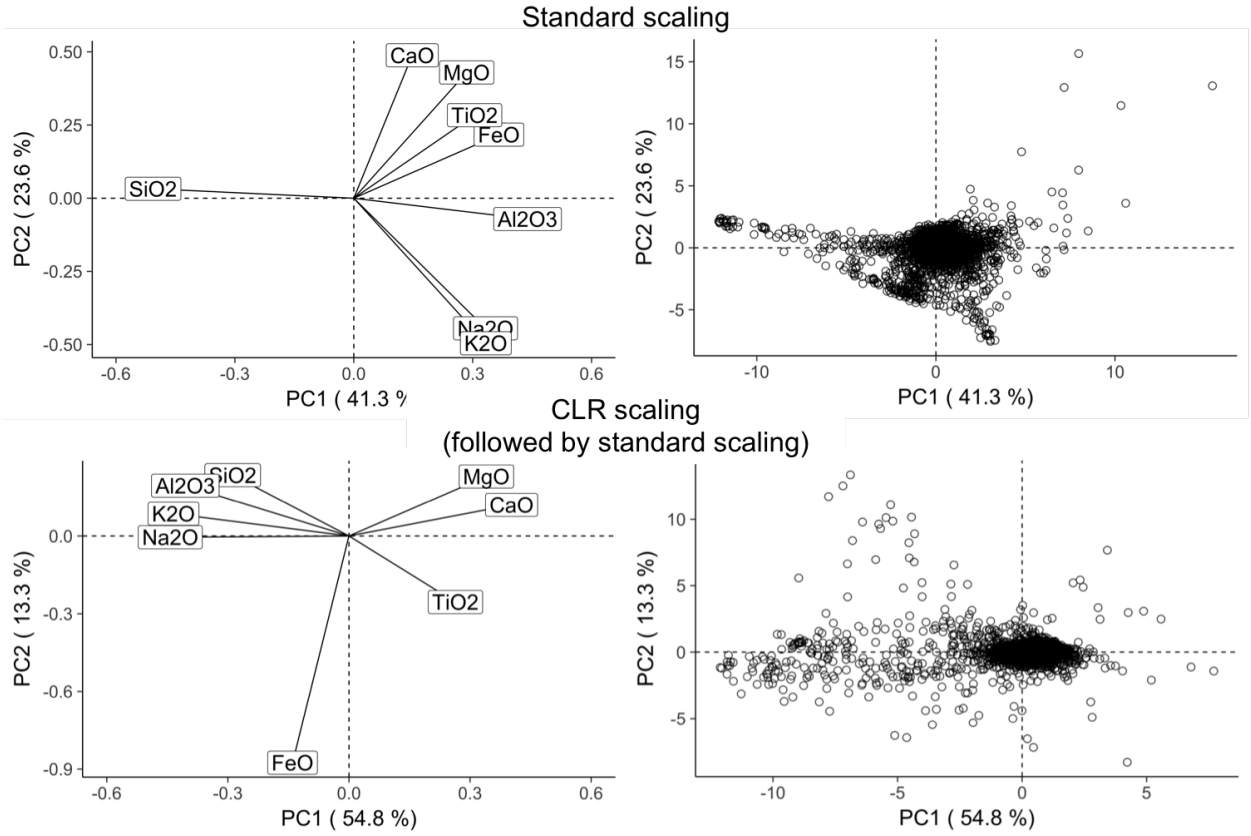

Figure 6.4: Plot showing the loadings and scores of PC1 vs. PC2 for host compositional data that were only standard scaled (top) and CLR scaled then standard scaled (bottom).

Dealing with zeros and detection limits

Many multivariate methods require matrix inversion. When there are zeros in the measurements, this can lead to singular matrices. Furthermore, analytical instruments have detection limits, yet may still report data below those detection limits, so care must be taken when analyzing those results. Usually, one either removes the measurements containing entries with zeros and replaces the values greater than zero but below the detection limit with some arbitrary value, typically one half the detection limit [146]. However, such an approach presents several potential problems. First, removing data with zeros may remove outliers important to understanding variance in the data. For this reason, many studies stick to standard scaling—it can handle zeros in data. Second, replacing entries below the detection limit but greater than zero with some fixed value may lead to spurious correlations and/or unintentionally add trends to data when none actually exist. When the number of measurements below the detection limits is small (less than 15%) the spurious correlation effect is also small [146]. In the case of the major element oxide compositional dataset of host objects,

which consists of 3,698 retained measurements, 290 of the measurements contained entries below the detection limits (approximately 7.8%), primarily in Ca (111 measurements), Ti (91 measurements), and Mg (68 measurements). Of those 290 measurements, 49 contained zeros, only in Ca (28 measurements) and Ti (24 measurements). Because the occurrence of measurements below the detection limit in the compositional data is below 15%, measured zeros and measurements below the detection limits were set to one half the detection limit of the EDS, 0.05 elemental wt.% (Figure 6.5). The detection limit of the EDS was determined to be 0.05 elemental wt.% because below this concentration, Bruker's ESPIRIT 2 EDS software stops reporting uncertainties for individual EDS raster measurements.

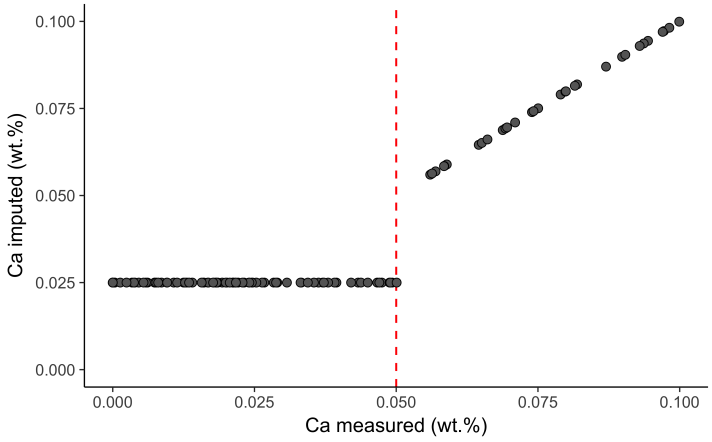

Figure 6.5: Imputed Ca values set to 0.025 wt.% (one half the approximate EDS detection limit) compared with the measured Ca values for major element compositions of host objects with Ca concentrations less than 0.1 wt.%. The vertical red line denotes the detection limit of 0.05 elemental wt.%.

6.3 Analytical uncertainty in PCA

Standard PCA assumes perfect data and does not take into account uncertainty in analytical measurements. Ignoring analytical uncertainty is often justified by assuming that the variance between measurements will be greater than the noise within a single measurement. However, some of the variables in this study, particularly MgO and TiO_2, have typical 1RSD uncertainties of ≈10–15% (their absolute uncertainty is ≈0.05 wt.%; see Chapter 4). Fe and Ca, important variables in this study because of previous findings of Ca being consistently associated with Pu from the Trinity test [55, 58, 66] and Fe being an anthropogenic component (from the tower), have 1RSDs of ≈5%.

To understand the effect of the analytical uncertainty on the resulting PCA model, a random noise-injection method is used here. This method generates *uncertainty perturbed matrices* (called "UP matrices" hereafter), produced from the original dataset and their associated analytical uncertainties. New PCA models are generated using these UP matrices

to determine how the UP matrices affect the generated multivariate models, following Duewer et al. (1976) [147]. This process is repeated many times (500-1000), to generate statistics reflecting the stability of each PC as a function of the analytical uncertainty in the data. By determining the correlation between the PCs generated from the UP matrices and the original data matrix, one can determine to what degree each PC is modeling true variance in the data or modeling analytical noise [147].

UP matrices are generated assuming Gaussian analytical uncertainties. The data matrix $\mathbf{X}$ contains the mean value and the 1σ uncertainty output by the ESPIRIT 2 EDS software and corresponds to 1 standard deviation about this mean. Then, a new composition is sampled from the normal distributions of each of different major elements ($\mathbf{x}_{ij}$ in $\mathbf{X}$) generated by their measured values and uncertainties to create a normal distribution defined by these parameters for each major element oxide. The distribution is then sampled for each measurement to generate the uncertainty-perturbed data matrix $\mathbf{X}^{\mathrm{UP}}$.

When taking a large number of EDS measurements in succession, however, the ESPIRIT 2 EDS software does not output analytical uncertainties. Instead, individual raster measurements are output with uncertainties. Given that the analytical conditions were kept approximately constant, the analytical uncertainties output by 53 measurements were fit to generate an uncertainty model (Figure 6.6). The composition of the subset of 53 measurements spans the range of compositions observed in the entire dataset—ranging from well-mixed compositions, representative of the average composition of glassy fallout from this test (Table 4.4) to end-member compositions of nearly-pure SiO_2, high FeO and Ti_2 compositions, mafic and felsic compositions (Figure 6.6).

Uncertainty for all major elements are well-fit by a function of the form $A/x + B$, with each element deviating only slightly in the best fit A and B parameters (Table 6.1 and Figure 6.6). This fit is empirical, as there is no physical reason the uncertainties should be so well fit by an equation of this form. As the software does not output uncertainties when concentrations are below 0.05 wt.%, this is used as the approximate detection limit for all elements in this study. Values below 0.05 wt.% were initially set to half the detection limit (0.025 wt.%). However, when injecting noise, entries may fall below the detection limits. As part of the UP matrix generation, entries in UP matrices that ended up below the detection limit are replaced with randomly generated concentrations between 0 and 0.05 elemental wt.%.

PCA of uncertainty perturbed (UP) matrices

One thousand UP matrices generated from the original data matrix $\mathbf{X}$ were used to determine the stability of the PC loadings. Comparing the mean variances from 1000 UP matrices to the original data matrix $\mathbf{X}$ shows that the shapes of the scree plots are similar and the elbow at PC4 is also reproduced (Figure 6.7). However, there is a deviation in the variance explained by PC1 and PCs 6–8 between the original data matrix and the mean of the 1000 UP matrices. The original data matrix explains more variance in the first PC, while the UP matrices explain more variance in the last three PCs. This suggests that the extra

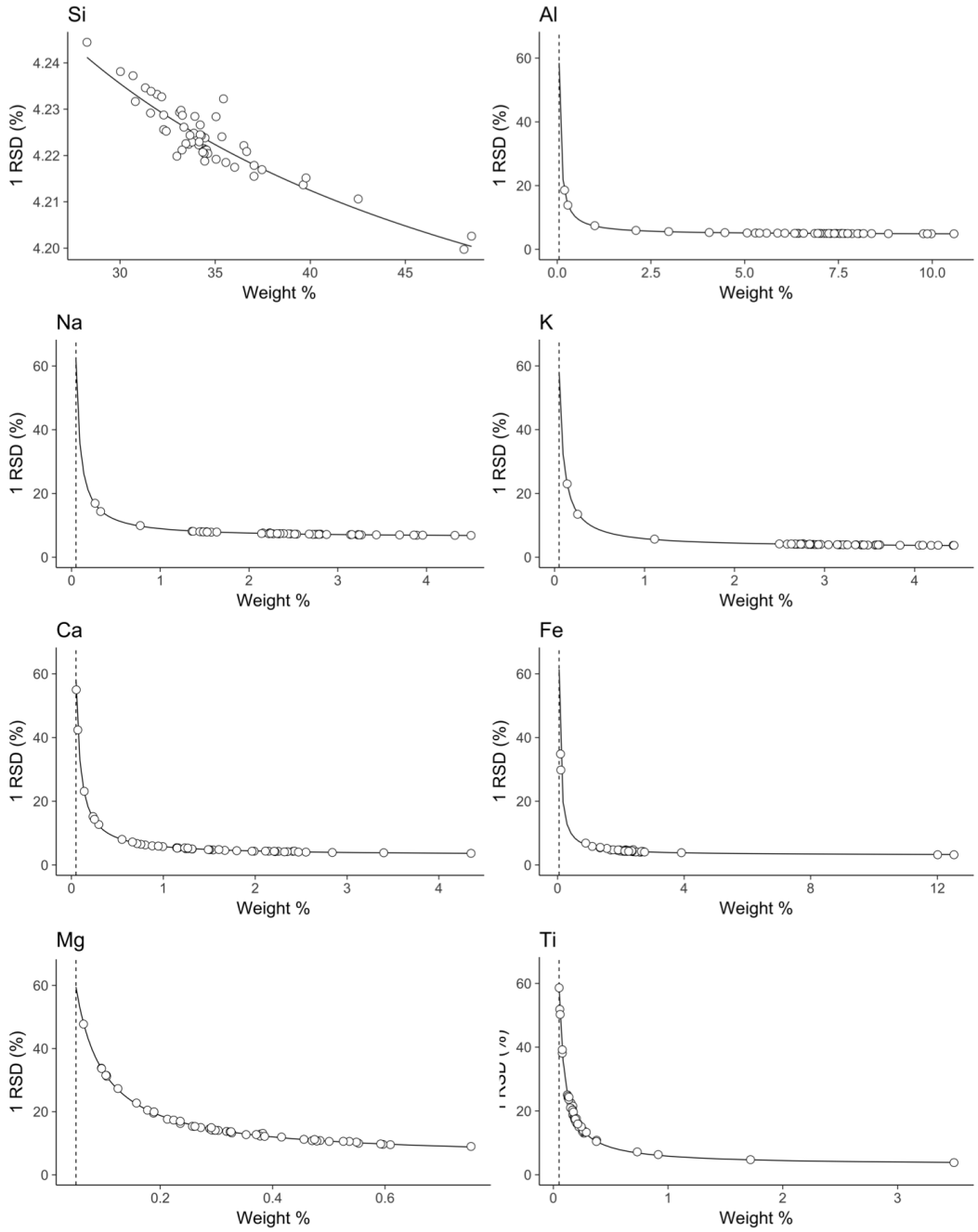

Figure 6.6: The 1RSD analytical uncertainty output by the ESPIRIT 2 EDS software as a function of the measured composition (in elemental wt.%). Plots show fits of $A/x + B$ (solid line; Table 6.1) from 53 EDS analyses (points) in various glassy fallout samples that span the range of compositions observed in fallout from this test. Vertical dashed lines intercept the x-axes at 0.05 wt.%, the approximate detection limit for the EDS under these conditions. These fits are used to calculate EDS uncertainties for all other EDS measurements in this study prior to converting the compositions to oxides, assuming the oxide stoichiometries of SiO_2, Al_2O_3, Na_2O, K_2O, CaO, FeO, TiO_2, and MgO. Data are tabulated in Appendix B.

Table 6.1: Non-linear least square fits of the equation $A/x + B$ to uncertainties from 53 EDS measurements. The 2σ refers to 95% confidence intervals of the fit. The fits primarily differ in their offsets, the B parameter of the fit. While Si has the largest standard error for the A parameter, the range of absolute uncertainties for Si measurements is small (ranging from about 4.20 wt.% for a composition consisting almost entirely of Si and O to about 4.24 wt.% for regions with relatively low abundances of Si).

Element	A	±	2σ	B	±	2σ
Si	2.77	±	0.17	4.14	±	0.01
Al	2.69	±	0.01	4.62	±	0.01
Na	2.77	±	0.02	6.18	±	0.02
K	2.75	±	0.01	3.06	±	0.01
Ca	2.76	±	0.01	3.01	±	0.02
Fe	2.92	±	0.02	3.08	±	0.04
Mg	2.77	±	0.01	3.05	±	0.06
Ti	2.71	±	0.02	5.22	±	0.16

variance explained in the first PC by the data matrix is artificial and due to some analytical bias. This bias is due to how EDS data are collected and the proximity of different counted characteristic X-rays for different elements. Elements with characteristic K_α X-rays close in energy, such as Na, Mg, Al, and Si co-vary during measurements. For example, if EDS slightly overestimates the Si concentration, it will also tend to slightly overestimate that Na, Mg, and Al concentrations. Consequently, this will result in an underestimation of the K, Ca, Fe, and Ti concentrations. Overall, this analytical artifact introduces artificial structure in the data, which is exposed and removed through the UP matrix approach.

Following Duewer et al., the correlation between the loadings of the UP matrices and the original data matrix can be used as another metric to estimate the number of PCs to retain [147]. This is calculated from the diagonal elements of the correlation matrix between the loadings of the data matrix and the UP matrix (Figure 6.8). Figure 6.8 shows the mean and standard deviations of the diagonals of 1000 correlation matrices created from the loadings of the data matrix and the loadings of 1000 generated UP matrices. PCs 1-3 appear unaffected by the injected noise. In contrast, PCs 4 and 5 appear to model some degree of noise, although still being strongly correlated with the original data matrix. Similarly, PC 6 is still largely correlated with the original data matrix, but its direction models more noise than PCs 4 and 5. Finally, PCs 7 and 8 predominantly describe analytical uncertainty, being only weakly correlated with the original data matrix. These results suggest that retaining up to PC 6 is reasonable. To avoid over-interpreting PCs that model a significant fraction of noise (PCs 6-8), the first 5 PCs are retained in this model, which describe approximately 90% of the total variance in the data set.

To visualize the correlation shown in Figure 6.8 and support these conclusions about how many PCs to retain, the loadings of the PCs generated using the original data matrix and a subset of three randomly chosen UP matrices are plotted (Figure 6.9). In Figure 6.9, the loadings of the PCs of the three UP matrices appear similar for the first four PCs.

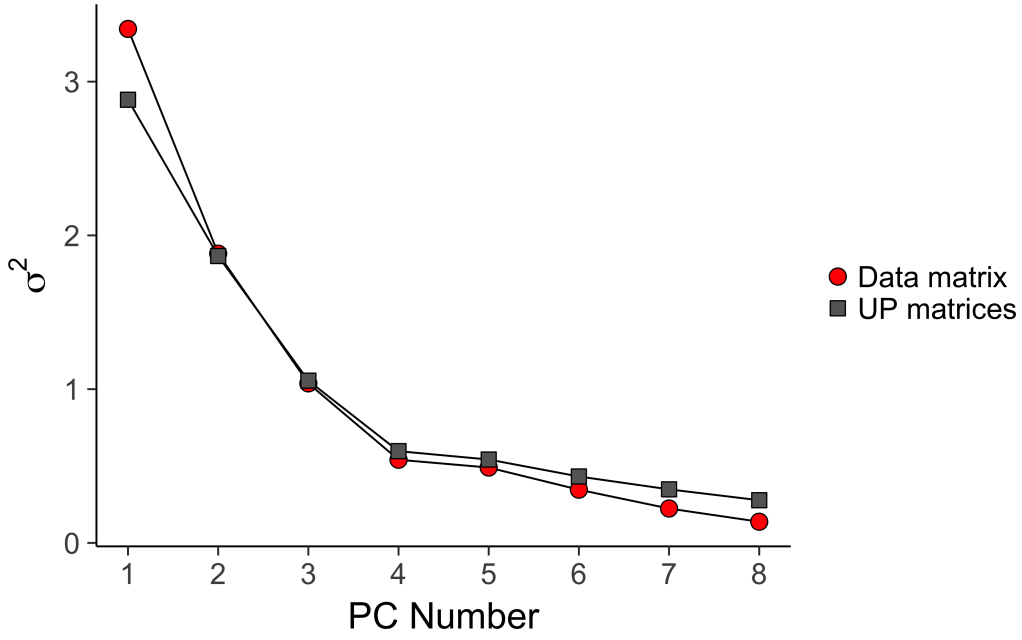

Figure 6.7: Scree plot of eigenvalues (variances) of the original compositional data of host objects **X** and the average variances from 1000 UP matrices generated using **X** and its modeled uncertainties. The standard deviations of the mean eigenvalues from the UP matrices are smaller than the points. The UP matrices reproduce a similar shape to the data matrix **X**, and would support retaining the same number of PCs at the elbow at PC4. The deviations between the UP matrices and the original data matrix **X** is due to bias introduced by the EDS method and software, resulting from similarities in the energy of the K_α X-rays of some elements.

In the fifth PC, the loadings are still similar, but there is variation between UP matrices, suggesting that PC5 is describing a small degree of noise in addition to real variance between major elements. PCs 6–8 appear to describe even more noise, creating PCs that show large deviations from the original data matrix as well as between UP matrices.

6.4 Outliers

The loadings of principal components in standard PCA are easily affected and skewed by outliers, both those from valid measurements with extreme values and those caused by artifacts that should be removed [148–152]. Because the major element composition of fallout glasses are consistent with being formed from inhomogeneous mixtures of rock-forming minerals, valid outliers should occur with some frequency, particularly in unmelted or partially-melted regions of samples.

Invalid measurements must be located and removed to ensure the PCA model is not unduly influenced by artifacts. For data analysis purposes, the EDS measurements were

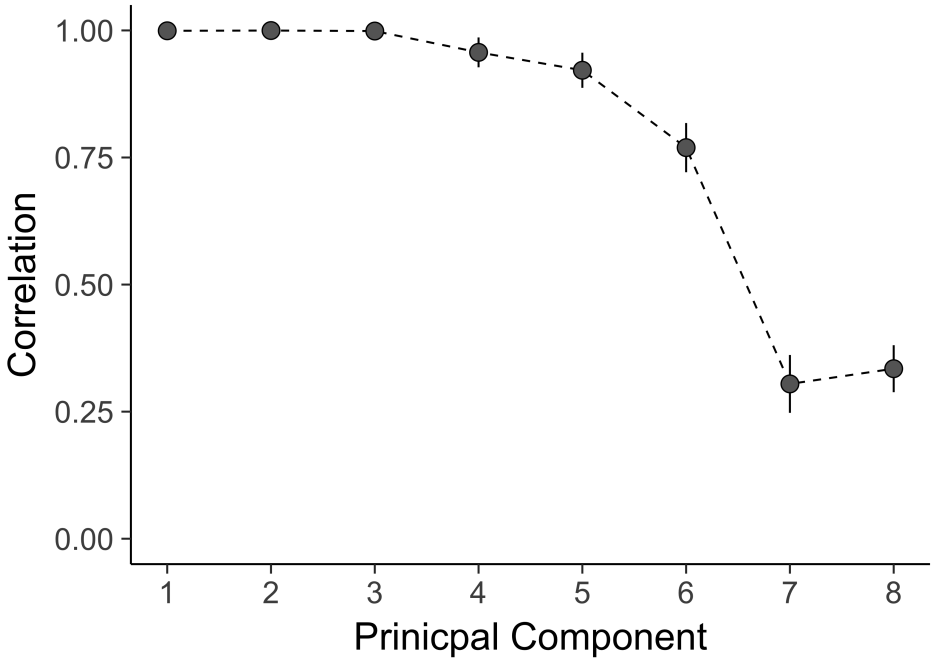

Figure 6.8: Correlations between principal components of the data matrix and 1000 UP matrices. Error bars represent one standard deviation. The first three principal components appear to be unaffected by noise. PCs 4 and 5 model a small noise component, with PC 6 modeling a greater degree of noise, but still containing variance related relationships between measurements. PCs 7 and 8 are dominated by noise.

previously restricted to between those with sum totals between 96 and 104%, removing the majority of invalid outliers. In the remaining dataset, however, is still possible that invalid compositional data may sum to between 96 and 104%.

Outliers are located using some metric to determine the center and spread of the data in multivariate space. The simplest and most common approach is to use the Mahalanobis distance to detector outliers [153], which is given by:

$$d_i = \sqrt{(\mathbf{x}_i - \mu)^T \mathbf{C}^{-1} (\mathbf{x}_i - \mu)}, \tag{6.9}$$

where $\mathbf{x}$ is a row vector containing the composition of the ith measurement, μ is a row vector containing the mean of each variable, and $\mathbf{C}$ is the covariance matrix. While the Mahalanobis distance is used routinely in other multivariate methods (such as classification, discriminant analysis, or assessing how well a PCA model performs) its use in outlier detection is limited when many outliers are present. When the data contain many outliers, the Mahalanobis distance often fails to outliers correctly (called "masking"), while other routinely used methods may label too many data points as outliers (called "swamping") [151]. Because valid outliers are expected to appear in these data due to the nature of fallout being heterogeneous mixtures, and should therefore be retained, an alternative outlier detection

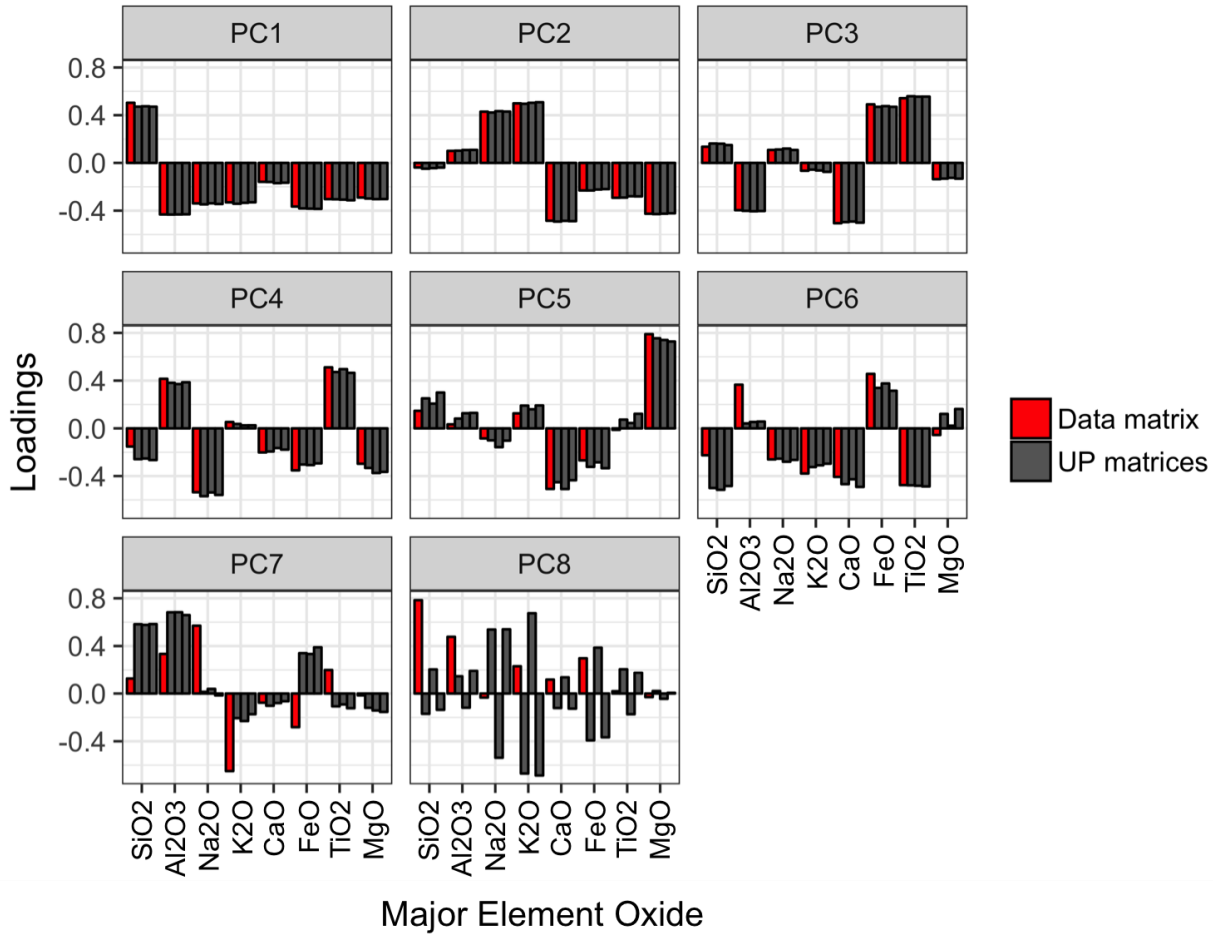

Figure 6.9: Histogram of loadings for PCs for the data matrix (red) and three random UP matrices (grey). Each histogram shows the loadings (y-axis) versus major element (x-axis) for a given principal component. Data are tabulated in Appendix H.

is used here. Originally proposed by Egan and Morgan (1998), their approach more accurately marks outliers than many other methods and is still reliable when a large percent of the data are outliers (between 20-45%) [151]. The approach is called "resampling by half-means" (RHM) and relies on calculating the distance from a point to the centroid of the distribution in multivariate space. First, RHM requires random sampling of 50% of the data set (without replacement). The mean and standard deviation of these data are calculated and then the entire data set are subtracted and scaled by these values, respectively. Then, the distance of each point to the centroid is calculated (called the "RHM distance"):

$$\mathbf{l} = \sqrt{\sum_{k=1}^{p} \left(\frac{\mathbf{X}_k - \mu_k^{RHM}}{\sigma_k^{RHM}} \right)^2}, \tag{6.10}$$

where $\mathbf{l}$ is a column vector containing the RHM distances, $\mathbf{X}_k$ is the column vector containing all measurements of the kth variable (*e.g.*, all the SiO_2 measurements), p the total number of variables (8 for the EDS dataset), and μ_k^{RHM} the mean of the 50% sampled data, and σ_k^{RHM} the standard deviation of the 50% sampled data. These distances are then plotted as a histogram. By convention, measurements beyond the 95th percentile are considered outliers and should be inspected. Each outlier in this thesis was compared to BSE and/or compositional maps to determine their potential validity to the overall dataset. Of the 5% of identified outliers (185 measurements), 79 (43%) are in high Si regions (>80 wt.% SiO_2), likely being EDS rasters on or overlapping relict quartz grains or partially-melted quartz. Of those 79, 43 (54%) are "quartz-like" compositions (*i.e.*, >90 wt.% SiO_2, as defined in Chapter 4).

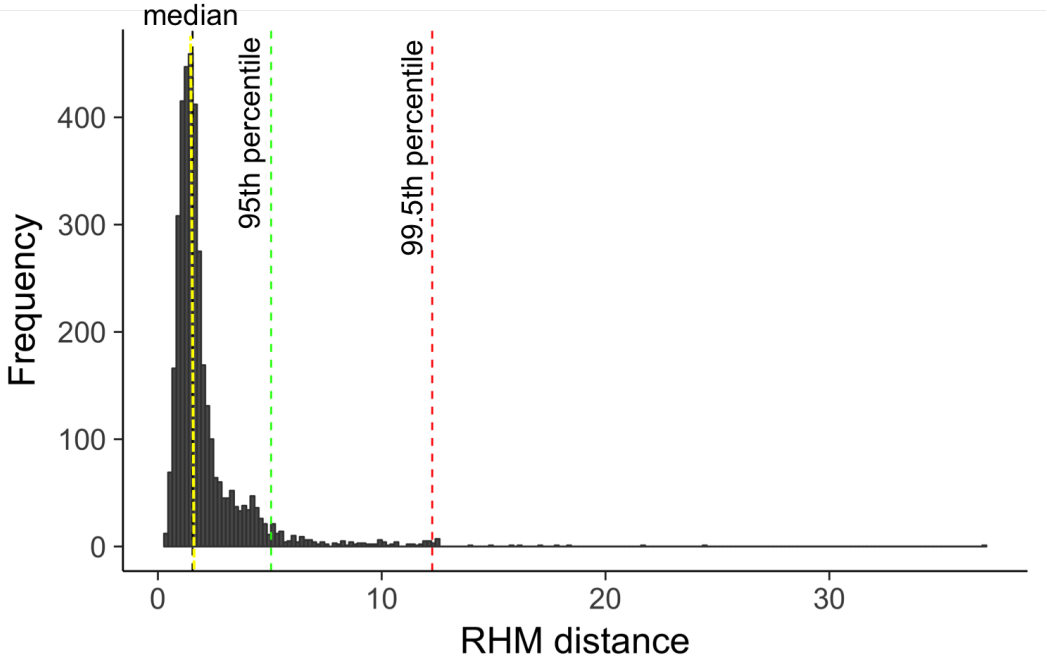

Figure 6.10: Histogram of RHM distances to the 50% sampled centroid, calculated from Equation 6.10. The histogram uses 200 bins. The 50th percentile (median), 95th percentile, and 99.5th percentile of RHM distances are marked with yellow, red, and green vertical dashed lines, respectively.

Of the remaining 106 outlying measurements, 78 are from samples FLD9, FLD10, FLD11 and FLD3.2. These samples were previously describe (Chapter 2) as having regions without radioactivity that appear vesicular and unmelted. Therefore, these measurements likely represent partially or unmelted minerals other than quartz in the soil near ground zero (Figure 4.16).

Of the remaining 28 outliers that are not high in silica or measured in samples FLD9, FLD10, FLD11, and FLD3.2, 22 were measured in sample FLD25. (Table 6.2 shows the aver-

age composition from these measurements.) These measurements were primarily conducted on the bright region visible the Al compositional map of FLD25. The mean composition of these measurements is felsic (see Chapter 4 and Figure 6.11). Since these measurements were all located in a single region and are of similar composition, the measurements are not invalid, but this composition in the host of FLD25 is likely an outlying composition compared to the other 37 host objects analyzed with EDS rasters. Also, interestingly, the optical image of FLD25 intact and unpolished shows that it is relatively colorless compared to the other fallout samples, which tend to be dark green in color (Figure 2.16). The remaining 6 outlying measurements were measured in samples FLD12, FLD16, FLD4.3, FLD5.4, and U3 (Table 6.3).

Table 6.2: Comparison of outlying compositions in FLD25 identified using Equation 6.10 with the mean and standard deviation of the host object major element oxide compositions.

Element oxide	FLD25 Mean (wt.%)	±	FLD25 1σ	EDS Host Mean (wt.%)	±	1σ
SiO_2	67.80	±	1.68	73.69	±	4.07
Al_2O_3	20.01	±	1.42	13.65	±	2.16
Na_2O	3.94	±	0.31	3.23	±	0.70
K_2O	8.44	±	1.05	3.81	±	0.71
CaO	0.87	±	0.92	2.17	±	1.00
FeO	0.37	±	0.45	2.78	±	0.78
TiO_2	0.18	±	0.06	0.32	±	0.18
MgO	0.24	±	0.11	0.59	±	0.27

Table 6.3: Remaining outlying compositions after excluding high Si regions and measurements on samples with large unmelted/partially melted regions. These compositions are felsic or trending towards felsic compositions, except for the composition measured in U3.

Sample	RHM Distance	SiO_2	Al_2O_3	Na_2O	K_2O	CaO	FeO	TiO_2	MgO	Sum
FLD12	5.57	69.00	19.47	4.96	5.90	0.84	1.33	0.15	0.26	101.91
FLD12	8.79	69.24	20.63	5.15	8.17	0.20	0.07	0.00	0.27	103.73
FLD16	6.84	66.01	20.91	4.57	5.20	1.10	0.70	0.96	0.12	99.56
FLD4.3	5.37	61.60	20.64	3.34	3.29	4.19	3.68	0.47	1.05	98.25
FLD5.4	6.93	57.32	23.62	3.72	3.24	4.47	3.81	0.57	0.76	97.51
U3	5.37	69.66	13.89	2.99	3.59	6.71	3.49	0.30	1.29	101.93

The 99.5% outliers (19 measurements) are found in 7 samples: AA.B, AG.D, FLD9, FLD10, FLD11, FLD3.2, and FLD5.1 (Table 6.4). All of the measurements in samples AA.B, AG.D, FLD3.2, and FLD5.1 are quartz-like, as are two of the measurements in FLD10. Their RHM distances are close to the 99.5 percentile cutoff of RHM distances equal to 12.25 (Figure 6.10). Two of the measurements (both in sample FLD11) are classified as mafic

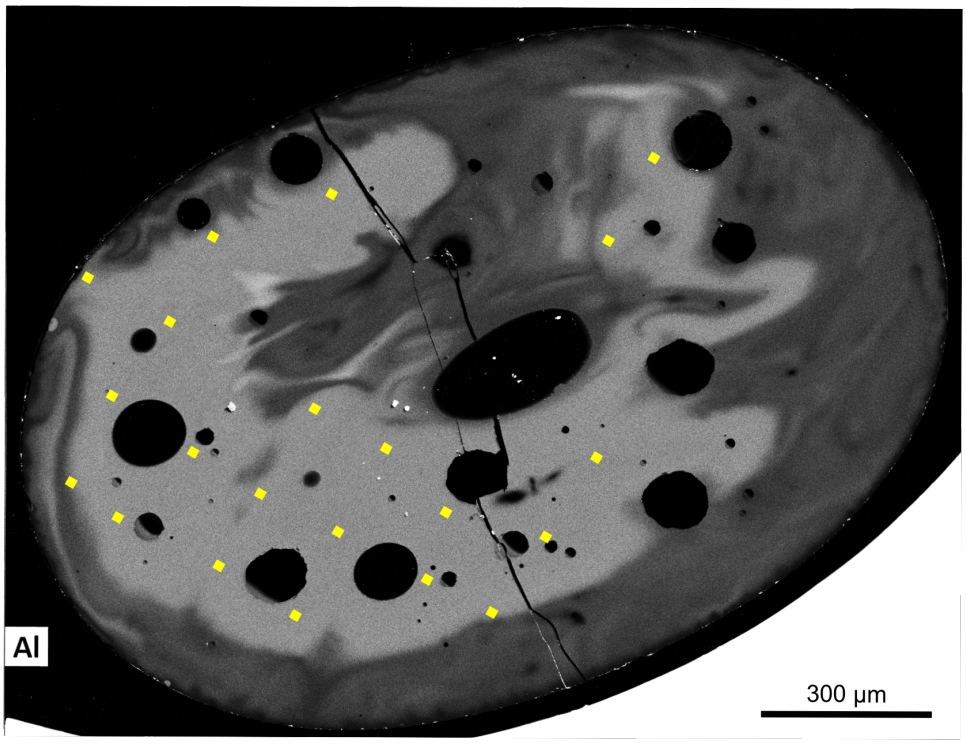

Figure 6.11: Al compositional map of sample FLD25. Yellow squares denote the locations of the outlying EDS measurements shown in Table 6.2. Tiny, bright white spots around the periphery of the sample are Al metal pieces from the sample holder that were removed during polishing, but lodged between the sample and the epoxy.

and none are classified as felsic (see Chapter 4). The remaining 99.5% outliers (and the two most outlying measurements) do not fall into the mineral-type compositional classifications defined in Chapter 4, but are primarily enriched in FeO, TiO_2, Na_2O, K_2O, and less frequently in MgO and CaO (highly enriched in one measurement each). These unclassified outliers suggest the presence of minor, but notable mineral components that may be able to explain co-variations of higher order principal components during the PC analysis.

Table 6.4: 99.5% outliers within the dataset of host object major element oxide compositions as determined and sorted by their RHM distances, classified according to the mineral-type definitions in Chapter 4.

Sample	RHM Distance	SiO_2	Al_2O_3	Na_2O	K_2O	CaO	FeO	TiO_2	MgO	Classification
FLD10	36.89	65.64	5.62	3.22	3.41	0.42	16.11	5.82	0.89	High Fe, Ti
FLD9	24.52	65.31	13.61	3.82	3.46	2.03	7.49	0.44	6.86	High Fe, Mg
FLD11	21.70	63.15	8.82	2.45	1.96	10.18	5.85	0.77	5.64	Mafic
FLD11	18.37	64.39	9.96	2.69	2.48	8.42	5.51	0.74	4.92	Mafic
FLD10	17.75	61.63	10.58	5.99	5.03	1.29	9.33	2.80	0.97	High Na, K, Fe
FLD10	17.17	67.25	13.16	3.52	4.62	3.11	2.57	3.23	0.61	High Na, K, Ca, Ti
FLD10	16.19	61.66	8.88	6.40	4.86	3.57	13.93	0.81	0.18	High Na, K, Fe
FLD10	15.78	68.35	13.23	5.20	5.33	0.33	5.04	2.87	0.31	High Na, K, Fe, Ti
FLD10	14.96	67.20	6.22	5.33	4.72	1.43	12.54	1.29	0.17	High Na, K, Fe, Ti
FLD10	13.93	64.19	14.27	5.75	5.57	0.43	3.44	2.52	0.44	High Na, K, Fe, Ti
FLD5.1	12.57	102.97	0.41	0.15	0.00	0.08	0.09	0.08	0.11	Quartz-like
AG.D	12.50	101.40	0.51	0.05	0.03	0.00	0.02	0.04	0.01	Quartz-like
FLD3.2	12.49	102.39	1.27	0.01	0.01	0.05	0.09	0.02	0.00	Quartz-like
FLD10	12.47	101.43	0.31	0.11	0.06	0.01	0.09	0.04	0.01	Quartz-like
FLD10	12.47	102.69	0.50	0.19	0.20	0.12	0.12	0.00	0.04	Quartz-like
AA.B	12.44	102.36	0.75	0.09	0.03	0.03	0.01	0.05	0.21	Quartz-like
FLD10	12.43	67.50	11.42	6.04	5.03	0.36	11.20	0.74	0.91	High Na, K, Fe
AG.D	12.31	100.27	0.50	0.03	0.04	0.00	0.08	0.00	0.10	Quartz-like
AG.D	12.28	100.21	0.56	0.10	0.01	0.02	0.03	0.06	0.04	Quartz-like

As expected, valid outliers are the largest source of variance in the dataset and therefore, control the loadings of the first several PCs (Figure 6.12 where measurements with RHM distances in the 95% percentile and above have been colored to show their influence on the PC space). While the correlations between different major element oxides will be discussed in the next section, the outliers, primarily composed of the end-member compositions of "quartz-like", "felsic", and "mafic" (as defined in Chapter 4), strongly influence the PC loadings. That the most mineral-like compositions are responsible for most of the variance in the dataset highlights that the origins of the glassy phase is consistent with originating from a mixture of mineral-like compositions.

6.5 PCA of the host compositional data

The previous sections used the major element oxide compositions of host objects ($n = 3,698$) to illustrate data pre-treatment, PC retention, assessing the amount of noise present in different PCs, and outlier detection and evaluation. This section explicitly discusses the results from the PCA analysis of the result dataset, including interpreting the PC loadings and scores, and possible interpretations of the PCs based on correlations between different major elements. This is followed by a comparison of the agglomerate EDS data with the model generated by the host object EDS data. The PC model generated by the host object EDS data is used to generate the PCA model because it was collected in an unbiased manner using grids of EDS rasters across the hosts. In contrast, EDS raster measurements of agglomerates were targeted and intended to capture the range of compositions in the agglomerate.

To form the PCA model, all eight major element oxides are retained for the PC analysis (retaining only those analyses with sums between 96 and 104 wt.%). Major element data below the detection limit were imputed to half the EDS detection limit. Next the data were pre-treated by subtracting the mean from each major element oxide and scaling each of these variables to have a variance equal to one. Following the PC analysis, the number of PCs retained was based on the correlation of PCs from the original data matrix with 1000 randomly-generated UP matrices, which showed that PCs 1-5 are greater than 90% correlated with the original data matrix, while PC 6, 7, and 8 are only ∼75%, ∼25%, and ∼26% correlated with the original data matrix, respectively (Figure 6.8). As a result, only PCs 1-5 are retained. Collectively they account for ∼91% of the total variance in the data set (Table 6.5). The loadings from this PC model are used to calculate the scores of the EDS measurements collected in the agglomerates and unmelted soil and project these data into the model.

As will be shown, the observations from these plots do not supplant the bivariate analyses shown in Chapter 4, but instead bolster them. The PCA analysis shows that the compositional measurements of the host objects are relatively homogeneous and that the variance in the compositional measurements of the hosts are again consistent with an origin of mixing between different minerals and compositions measured in the soil. The agglomerates remain a subset of the host compositions, as expected. The PCA analyses additionally highlights

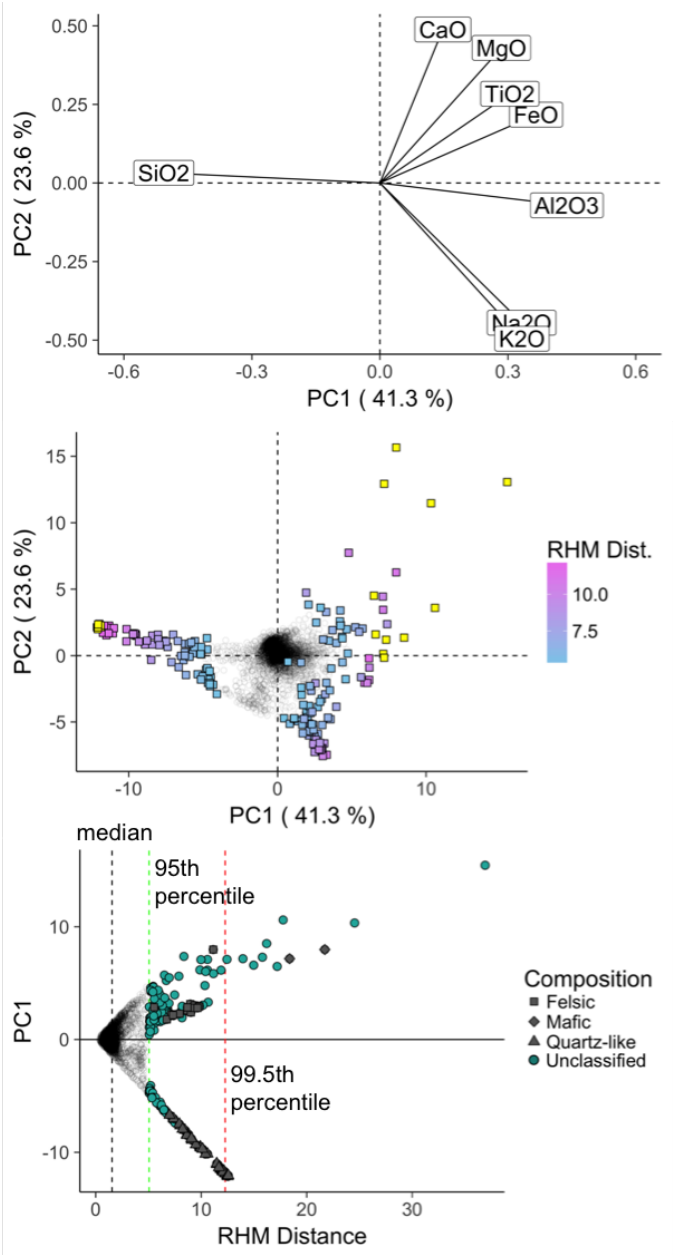

Figure 6.12: PC1 vs. PC2 for the dataset of major element oxide compositions of host objects. Outliers are highlighted as determined by the 95% percentile of the RHM distances. RHM distances in the 99.5% percentile are shown in yellow. The bottom plot shows PC1 plotted directly as a function of the RHM distances, highlighting the outliers' influence on PC1. The grey, green, and red vertical lines denote the 50th, 95th, and 99.5th percentiles, respectively. The slope of the edges of the cone-like shape becomes more gradual with each succeeding PC. Shapes correspond to end-member compositions, as defined in Chapter 4. Unclassified compositions, shown as blue circles, are discussed in the text, and primarily consist of high Fe compositions.

Table 6.5: Proportion of variance and cumulative proportion of variance explained by each PC of the PC analysis of the major element compositions of host objects. The dashed line denotes the PCs that were not retained for the PCA model.

PC	Var. Exp. (%)	Cumulative Var. Exp (%)
PC1	41.3	41.3
PC2	23.6	64.9
PC3	12.9	77.8
PC4	6.8	84.5
PC5	6.4	91.0
PC6	4.3	95.3
PC7	2.9	98.2
PC8	1.8	100.0

multiple source for some major elements (such as FeO and CaO) and reveals what compositions are the largest sources of variance in the data set. This enables an assessment of how different compositions in the soil contributed to the overall compositions of the glassy phases in the fallout.

PC1 and PC2

PC1 describes 41.3% of the overall variance in the data set of host compositional measurements (Figure 6.14 shows PC1 plotted against PC2). In PC1, SiO_2 has a negative loading, while all other major elements have positive loadings, with Al_2O_3 having the most positive loading. The variance PC1 is describing is due to the relatively large number of partially-melted and/or unmelted quartz minerals measured in the host, relative to the majority of the glassy phase. While the measured compositions plot densely near (0,0), there are a continuum of compositions that extend towards the quartz-like compositions (bottom panel of Figure 6.14). PC1 plotted against PC2 separates the end-member composition of "quartz-like" (as defined in Chapter 4) into quadrants II and III, while the remaining mafic and felsic end-members (including albite, anorthite, and orthoclase-like compositions) plot in quadrants I and IV.

PC2, which describes 23.6% of the overall variance in the data set, has little influence from SiO_2 and Al_2O_3, but separates Na_2O and K_2O from CaO, MgO, TiO_2, and FeO (top panel, Figure 6.14). This PC separates the alkali feldspar-like, plagioclase feldspar-like and mafic compositions into quadrants IV and I, respectively. The variance described by PC2 separates more alkali-rich compositions from compositions rich in CaO, FeO, TiO_2, and MgO. These latter compositions are largely mafic, but also include FeO, TiO_2-rich compositions.

SiO_2 has a large loading only in PC1. This shows that other than measurements in quartz and/or quartz-like compositions, SiO_2 varies relatively little and is not well associated with variations between other major elements in other PCs. Therefore, while 41.3% of the variance

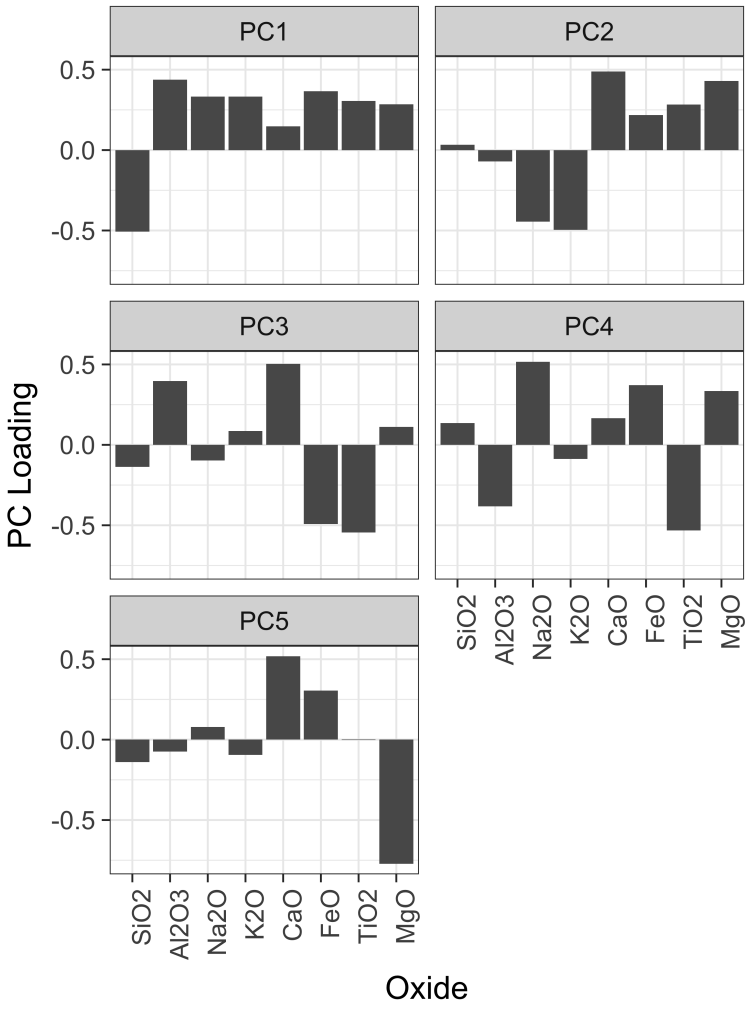

Figure 6.13: Loadings of the 5 retained principal components. Data are tabulated in Appendix H.

in the data is due to SiO_2, the remaining 49.7% of the variance is due to other, less abundant elements in the samples.

The first two PCs collectively describe 64.9% of the total variance in the EDS measurements (Table 6.5). The loadings of PC1 and PC2 are controlled by outlying measurements, as measured via their RHM distances (Figure 6.12). These outliers are only outliers in the sense that they are found primarily in samples with large unmelted or partially-melted regions, so likely represent partially-melted or unmelted minerals.

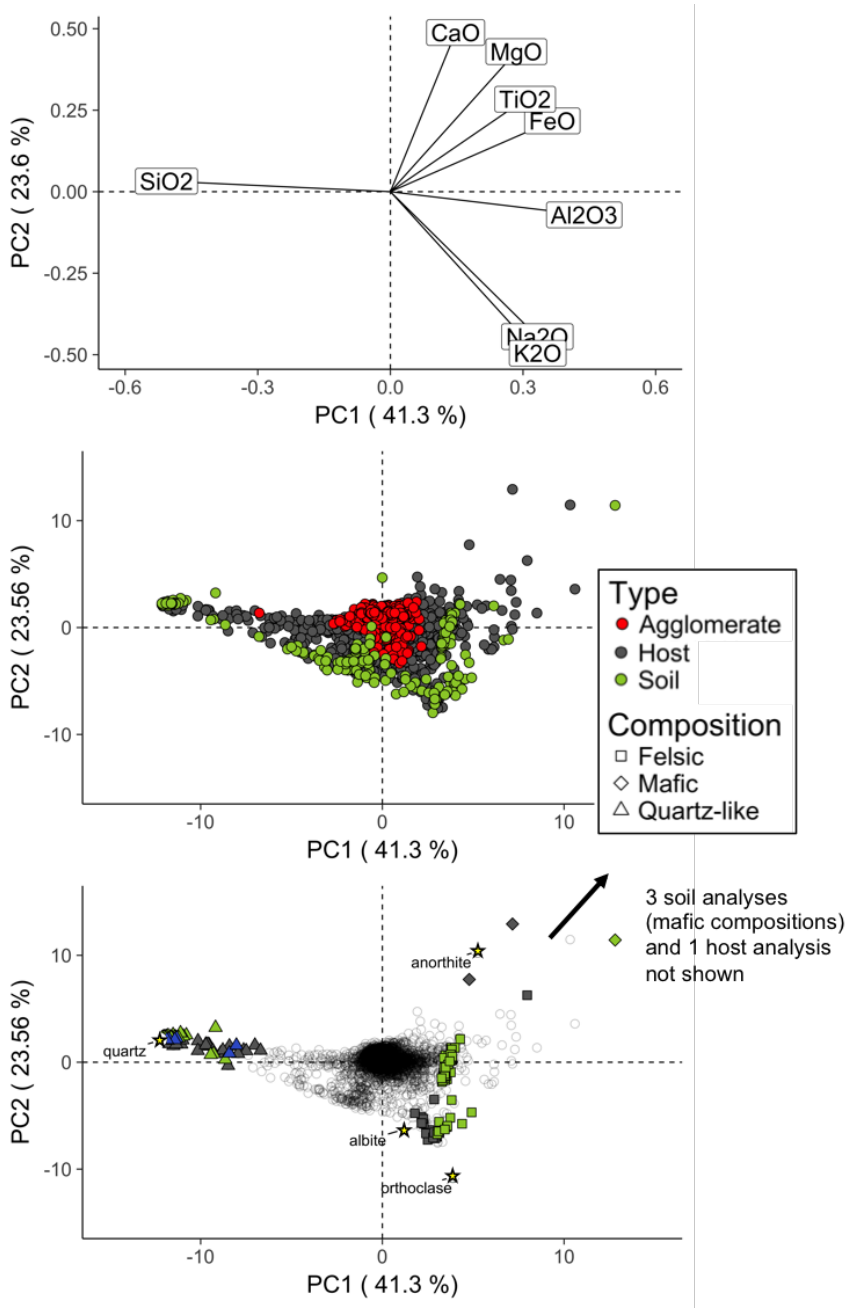

Figure 6.14: PC1 vs. PC2. The top plot shows the loadings of the PC model created using the EDS host grid data. The middle plot shows the EDS host grid data, the EDS agglomerate data, and EDS measurements of unmelted soil collected proximate to ground zero. The bottom plot renders the EDS host grid data partially transparent, showing a density plot of the host compositions. Outlying felsic, mafic, and quartz-like compositions, as defined in Chapter 4, are shown with different shapes and colored by whether they measured in hosts, agglomerates, or in unmelted soil. Quartz and feldspar endmember compositions are also plotted and marked.

PC3

PC3 captures 12.9% of the total variance. When plotted against PC2, PC3 highlights the variance due FeO, TiO_2-rich compositions (plotting in quadrants III and IV) and more plagioclase-like compositions (plotting in quadrants I and II), with little influence from K_2O, Na_2O, and SiO_2 (Figure 6.15). PC3 therefore separates the multiple sources of FeO, showing the association between FeO and TiO_2 as being separate from the association between FeO, CaO, and MgO derived from the mafic compositions (whose variance is captured by PC2). This FeO-TiO_2 association (highlighted by PC3) contributes less to the overall variance in the dataset than the variance due to mafic compositions (highlighted by PC2). Therefore, while the mafic compositions are a small overall contributor to the primary fallout composition (Figure 4.19), the FeO, TiO_2-rich minerals, observed in soil (noted in Figure 4.15 and compositions consistent with ilmenite are noted by [67]), have an even smaller overall contribution to the composition of the glassy phase in fallout.

PC4

PC4 (plotted versus PC2, Figure 6.16) separates the feldspathic compositions from more mafic compositions into each quadrant, with mafic, albite-like, orthoclase-like, and anorthite-like compositions falling into quadrants I, II, III, and IV, respectively. The association between Na_2O and CaO (from the continuum of compositions between albite and anorthite) is visible, as is the association between FeO, MgO, and CaO compositions. Quadrant IV distinguishes FeO, TiO_2-rich compositions all of which were measured in host objects, and specifically are part of the compositions measured in the unmelted/partially-melted region of FLD10 (see discussion in Chapter 4).

PC5

PC5 explains 6.4% of the overall variance. A plot of PC5 versus PC3 separates the FeO, CaO, and MgO (associated with mafic compositions) into FeO and CaO (positive loadings) and MgO (negative loading), with all other elements having little influence in PC5 (Figure 6.17). The FeO, TiO_2-rich compositions are separated into quadrant II, more CaO-rich compositions (plotting towards anorthite) into quadrant I, and the mafic compositions into quadrant I. The remaining felsic end-members and quartz plot near origin, along with fallout compositions that trend towards these end-members (bottom panel, Figure 6.17).

6.6 Combining U isotopic and major element compositions

A combined data set of U isotope ratios measured using SIMS and the major element compositions measured within/adjacent to the SIMS analysis craters ($n = 245$) was collected for

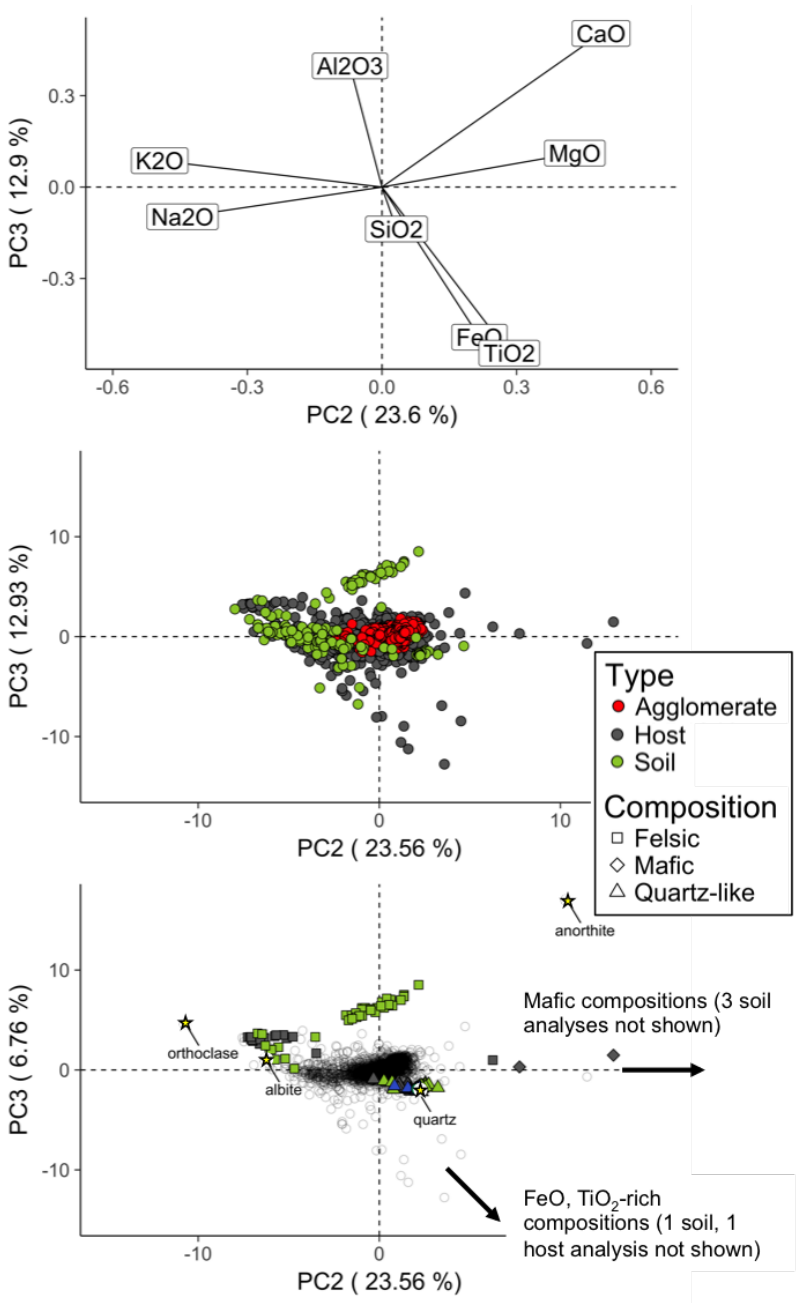

Figure 6.15: PC2 vs. PC3. The top plot shows the loadings of the PC model created using the EDS host grid data. The middle plot shows the EDS host grid data, the EDS agglomerate data, and EDS measurements of unmelted soil collected proximate to ground zero. The bottom plot renders the EDS host grid data partially transparent, showing a density plot of the host compositions. Outlying felsic, mafic, and quartz-like compositions, as defined in Chapter 4, are shown with different shapes and colored by whether they measured in hosts, agglomerates, or in unmelted soil. Quartz and feldspar endmember compositions are also plotted and marked.

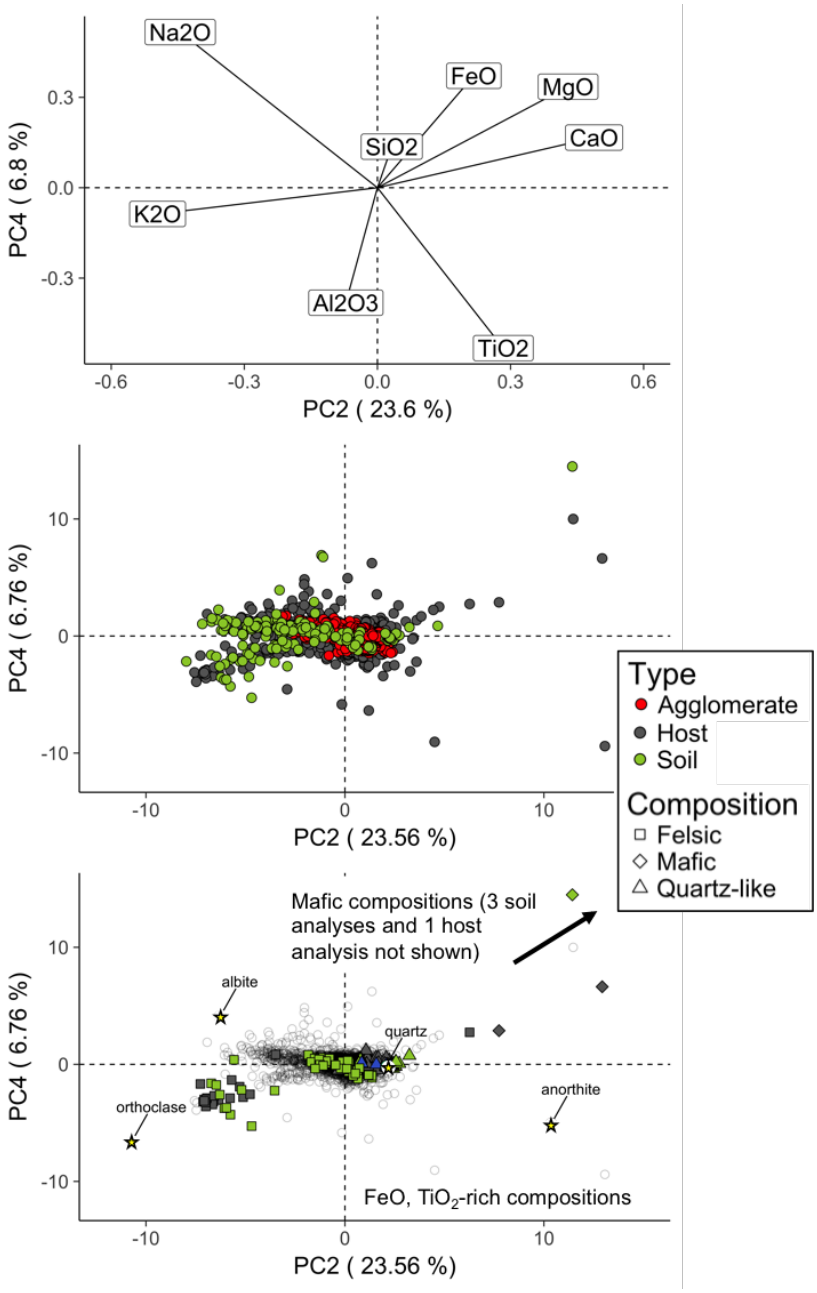

Figure 6.16: PC4 vs. PC2. The top plot shows the loadings of the PC model created using the EDS host grid data. The middle plot shows the EDS host grid data, the EDS agglomerate data, and EDS measurements of unmelted soil collected proximate to ground zero. The bottom plot renders the EDS host grid data partially transparent, showing a density plot of the host compositions. Outlying felsic, mafic, and quartz-like compositions, as defined in Chapter 4, are shown with different shapes and colored by whether they measured in hosts, agglomerates, or in unmelted soil. Quartz and feldspar endmember compositions are also plotted and marked.

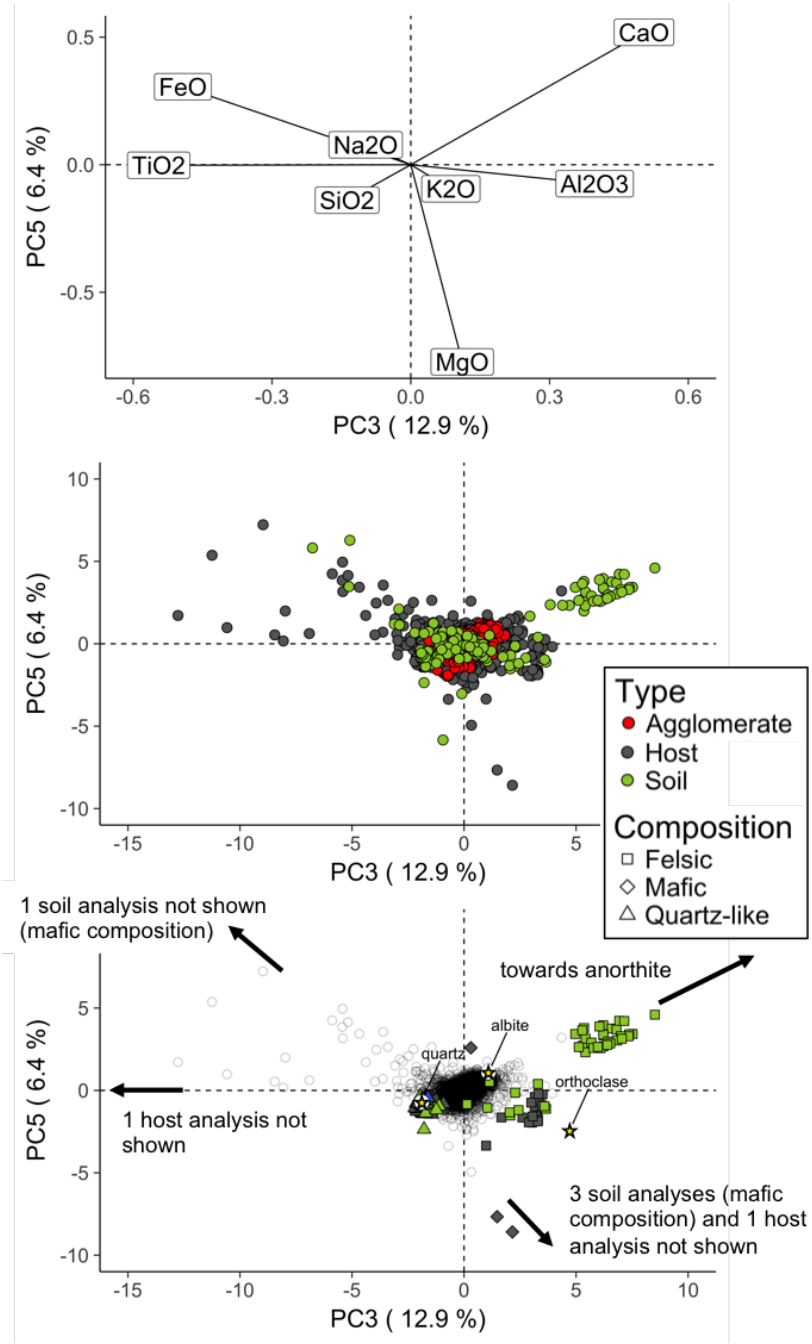

Figure 6.17: PC5 vs. PC3. The top plot shows the loadings of the PC model created using the EDS host grid data. The middle plot shows the EDS host grid data, the EDS agglomerate data, and EDS measurements of unmelted soil collected proximate to ground zero. The bottom plot renders the EDS host grid data partially transparent, showing a density plot of the host compositions. Outlying felsic, mafic, and quartz-like compositions, as defined in Chapter 4, are shown with different shapes and colored by whether they measured in hosts, agglomerates, or in unmelted soil. Quartz and feldspar endmember compositions are also plotted and marked.

several purposes. First, previous studies of Trinity show an association between unfissioned Pu fuel and Ca, Mg, and Fe [55, 58, 66, 80]. In historic fractionation models, Pu is considered to behave as a strongly refractory species, modeled as not fractionating from the benchmark refractory fission product, ^{95}Zr [5]. As noted in Chapter 1, U has historically modeled as behaving as a semi-volatile species in air bursts, but exhibits different fractionation behavior in surface bursts, depending on the detonation conditions and surrounding environment [47]. In high-yield coral bursts, U is observed to not fractionate from ^{95}Zr or ^{239}Pu, but in silicate surface bursts, U is observed to continue to behave with intermediate volatility (although behaving with a slightly more refractory nature than U in air bursts) [47]. The Weisz (2016) study of interfaces demonstrated a co-location of enriched U with CaO, MgO, and FeO at boundaries of hosts and exterior agglomerates (Table 3.1). A consistent association in the glassy phase between enriched U and CaO, FeO, and MgO could suggest that U in this event behaved chemically similar to how Pu behaved in Trinity. Understanding the behavior of U in this event will help inform and aid in predicting the chemical behavior of U in other tests. Associations between U and major element enrichments at compositional interfaces of agglomerates and U in the bulk of the glassy phase could support similar condensation conditions to those hypothesized to occur and created compositional interfaces [67], and may place constraints on the chemical speciation of U as it is incorporated into fallout melts. First order associations between U and major elements should be unexpected (unless there was a large anthropogenic source a major element also present in the soil, such as the steel tower in the case of Trinity). However, combined U isotopic and major element compositions projected into PCA space may also reveal higher order associations between the unfissioned fuel and major elements.

Comparison between major element compositions and the combined major element/U isotopic dataset

This chapter considers and conducts multivariate analyses of two separate data sets. First, the previously discussed and modeled major element data of agglomerates and hosts (discussed in above and in Chapter 4). A second dataset is also used, combining the U isotope analyses from SIMS and *targeted* EDS rasters from within/around the SIMS analyses craters to link the SIMS analysis locations with major element compositions (Figure 4.6). The combined major element/U isotope dataset excludes Na_2O, due to crater topography and possible Na volatilization by SIMS (discussed in Chapter 5). A schematic distinguishing these two datasets is shown in Figure 6.18.

Due to the time required for each SIMS analysis (>1 hr for a NanoSIMS analyses, excluding several days for tuning the instrument prior to an analysis and analyzing standards throughout the analytical campaign), fewer SIMS analyses were used to characterize agglomerates and hosts. Instead, these analyses were targeted and micro-volumes of material were sputtered to measure the U isotopic compositions of hosts and agglomerates. The correlation between U isotopic homogeneity and major element homogeneity from well-characterized

hosts using this combined major element/U isotope dataset (Figure 5.31) showed that while some agglomerates were characterized by only 1–2 SIMS analyses, the variance about these measured U isotopics is likely small (the predicted $^{235}U/^{238}U$ 1σ is <1 for all characterized agglomerates).

Further comparison between the two data sets is needed. Specifically, evaluating how well the few targeted analyses that comprise the combined major element composition/U isotope dataset represent entire objects (the major element-only dataset collected across entire agglomerates and host objects) is necessary to draw comparisons and conclusions between the two datasets. Note that these datasets *should not* be identical, as the EDS analyses characterizing the compositions across entire host objects included unmelted/partially-minerals in addition to glassy regions, whereas the SIMS analyses primarily targeted the glassy regions in agglomerates and host objects.

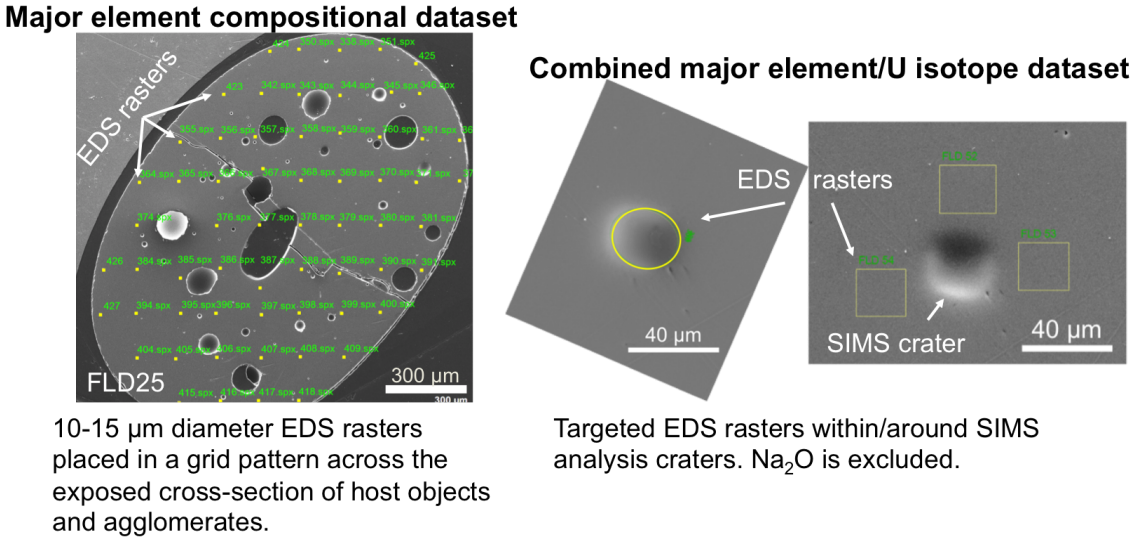

Figure 6.18: Examples of how the different EDS datasets discussed here were collected. In the figure on the left, the major element composition dataset, which was collected across host objects in grid patterns (data used to generate the PCA space) and collected in an approximate grid patterns across agglomerates to determine the composition of agglomerates (Table 4.8). In the second dataset (figure on right), to estimate the major element composition at the location of U isotope ratio measurements, 1–4 EDS rasters were collected within/around SIMS analysis craters. In this second dataset, Na_2O is excluded, as discussed in the text.

Figure 6.19 shows the deviation of the compositions from the combined EDS/SIMS dataset to the EDS grid-based major element dataset for agglomerates and host objects as a function of the number of EDS/SIMS analyses within the object. The mean composition is used to define an object's composition (both for the major element only and combined major element/U isotopic composition). The standard deviation about this mean is used to represent the variability in this composition for multiple measurements (shown as

error bars in Figure 6.19), and the analytical uncertainty is shown for single measurements. As would be expected, the combined major element/U isotope compositions deviating the most from the median major element composition of entire objects occur where only 1–2 SIMS analyses were used to characterize the object. Surprisingly, for all major elements, only five SIMS/EDS analyses are needed until the mean composition of the combined major element/U isotope dataset and major element dataset agree within uncertainty.

For two or more combined major element/U isotopic measurements in a single object, major elements with a relative deviation >15% from the compositions determined from the grid-based EDS analysis occur primarily in the MgO and TiO_2 compositions. While the *relative* deviation between datasets is >15% for the compositions of some objects in these major element oxides, because of their low abundance in fallout (usually <1 wt.%), the absolute deviation is small. Other major element oxides that exhibit deviations greater than 15% are primarily CaO compositions in the hosts FLD10 (CaO deviation: +93.6 ± 218.6%), FLD14 (CaO deviation: -20.0 ± 21.8%), U4 (CaO deviation: -15.6 ± 49.5%). In these cases, the *median absolute deviations* (instead of the standard deviation as used in Fig. 6.19) of the deviations in compositions between the grid-based EDS dataset and combined EDS/SIMS dataset overlap a 0% deviation, indicating these deviations are largely due to compositional heterogeneities within samples.

Bivariate plots of U versus major elements

Before including the $^{235}U/^{238}U$ ratio in the PCA model, it is illustrative to show the $^{235}U/^{238}U$ isotope ratio measurements as a function of major element concentrations in traditional bivariate plots (Figure 6.20). The bivariate plots in Figure 6.20 to reveal trends between the $^{235}U/^{238}U$ and major elements only for K_2O, CaO, FeO, and MgO at outlying compositions. Furthermore, perceived trends typically manifest only for single samples, not across the entire sample suite.

For example, the apparent correlation in the U bivariate plots (Figure 6.20) visible near the origins of the plots of $^{235}U/^{238}U$ as a function of CaO, FeO, MgO, and anti-correlation of $^{235}U/^{238}U$ as a function of K_2O at concentrations ≈4–6 wt.% were all measured in the host of sample U2. Sample U2 was previously noted to appear as the collision and partial mixing of two distinct melts, each of which had incorporated different amounts of enriched U prior to agglomeration (see Chapter 1) [60]. In compositional maps, this appears as a roughly bi-modal composition. Using a Ca compositional map (Figure 1.11), and noting locations of SIMS measurements made in these two regions, reveals a qualitative *co-location* between $^{235}U/^{238}U$ ratios <1 being measured in the Ca "depleted" region and $^{235}U/^{238}U$ >1 being measured in the Ca "enriched" region.[2] In this study, measured major element compositions from within and around the SIMS analysis craters directly (instead of averaging EPMA data

[2]The enriched region within U2 has a mean CaO concentration of 1.79 ± 0.20 wt.% (2σ) and the depleted region has a mean CaO concentration of 0.45 ± 0.24 wt.% (2σ) [60]. However, the depleted region is not only depleted relative to the enriched region, but also depleted relative to the average CaO concentration measured in the host EDS analyses (Table 4.4) of 2.12 ± 1.00 1σ.

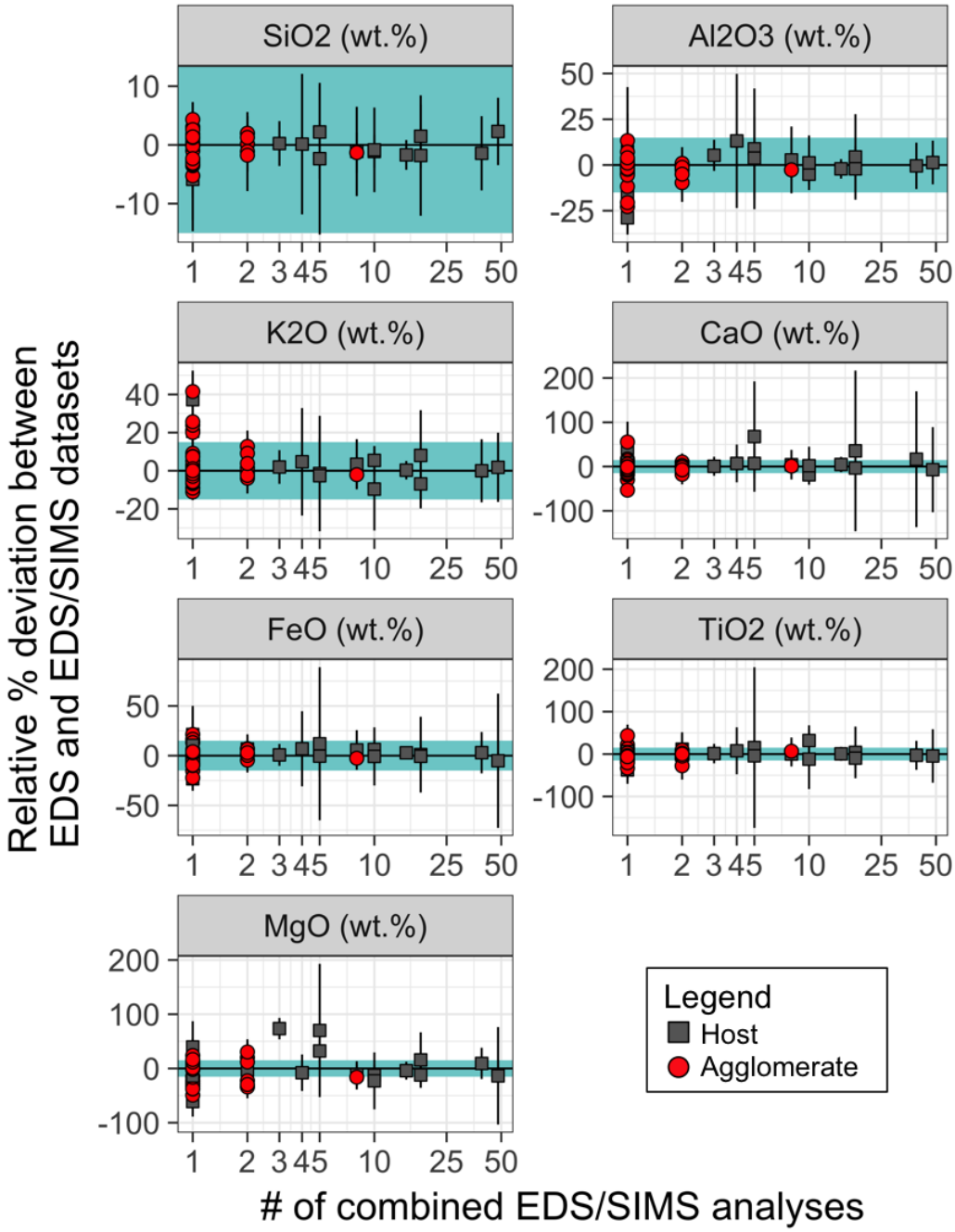

Figure 6.19: Percent deviation between the median major element composition of an object measured using grid-based patterns of EDS rasters across entire objects and the composition measured from the EDS rasters from within/around the SIMS craters as a function of the number of combined EDS/SIMS analyses within the object (Figure 6.18). Note the log x-axis. The blue band denotes ±15% relative deviation. The uncertainties are 1σ of the mean (for multiple measurements) or the 1σ analytical uncertainty for single measurements. Na_2O is excluded, as discussed in the text. Data are tabulated in Appendix G, Table 4.8, and Table 4.6.

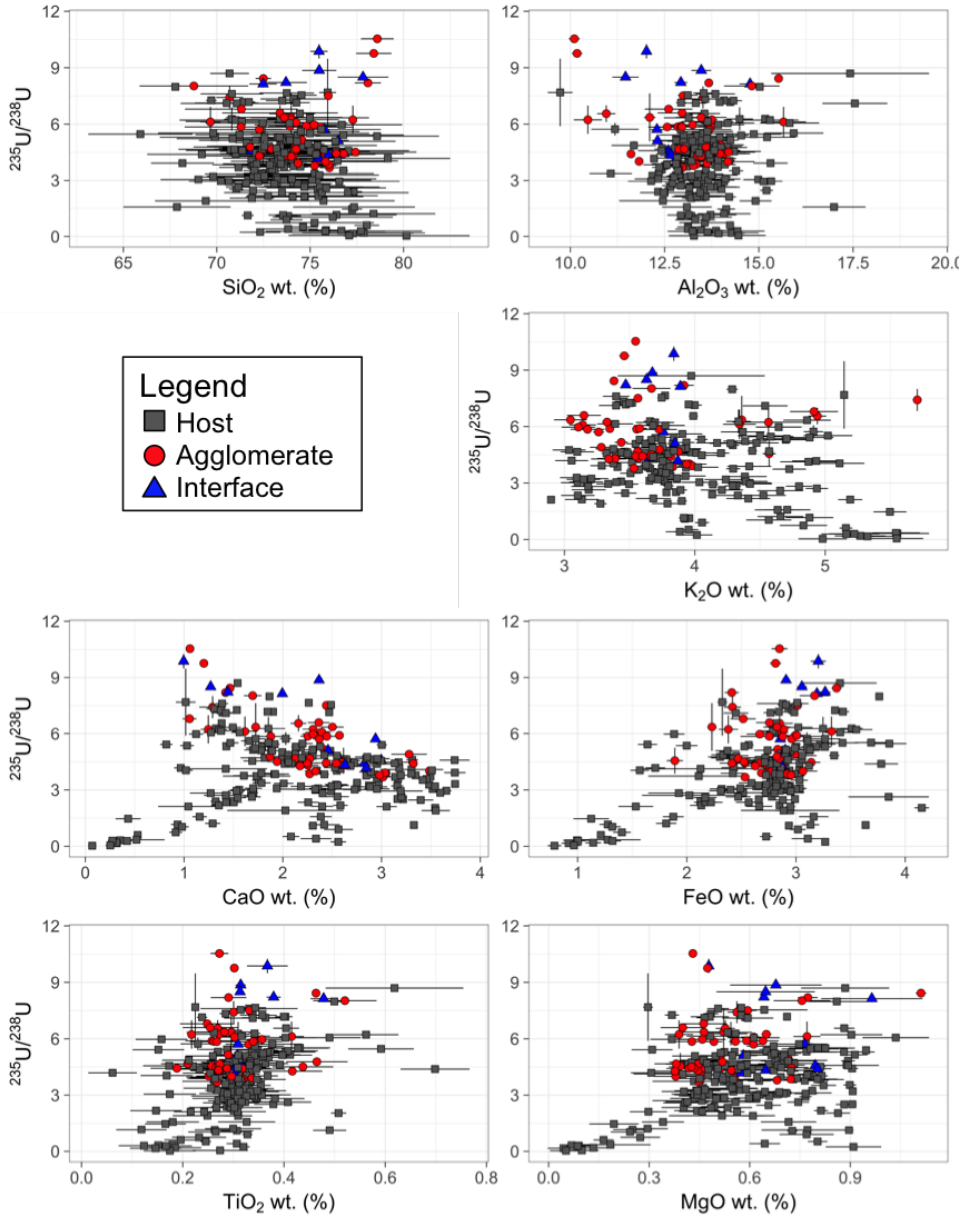

Figure 6.20: Bivariate plots showing SIMS measurements of $^{235}U/^{238}U$ ratios as a function of the major element composition measured using EDS rasters collected within/around the SIMS craters (Figure 6.18). Uncertainties are 1σ. Na_2O is excluded as discussed in the text. The shape and color of points correspond to whether the SIMS analysis was performed in a host, an agglomerate, or over an interface that significantly sampled both the host and agglomerate. To ease viewing of the plots, the plots exclude to two points with anomalous CaO compositions discussed in the text (Figure 6.23 and Table 5.12). Data are tabulated in Appendix G.

taken in a grid pattern, as was done in Lewis et al. (2015) to establish the co-location between U isotopic and major element composition) reveals not only a *co-location*, but a *correlation* between the U isotopic composition and CaO, FeO, MgO, and an anti-correlation with K_2O (Figure 6.21). However, due to this behavior being exhibited in a single sample that contains two melts of distinct major element and U isotopic compositions incompletely mixing prior to quenching, these correlations in $^{235}U/^{238}U$ as a function of CaO, FeO, MgO, and K_2O are likely not capturing some chemical behavior of U in the fireball. Instead, the trends visible in Figure 6.21 are most likely due to sampling regions with SIMS/EDS that have experienced different amounts of mixing between the two melts. That is, the finite sampling size of the SIMS craters and the EDS rasters sample different proportions of each of the melts, resulting in a correlation, but reflect analyses in regions where the melts have partially mixed prior to quenching.

Excluding these measurements removes any signification whole-population correlations between the $^{235}U/^{238}U$ ratio and CaO, FeO, and MgO at $^{235}U/^{238}U$ ratios < 2. A weak anti-correlation of the $^{235}U/^{238}U$ ratio with CaO concentration remains (Figure 6.22), consistent bulk dissolution ICP-MS data of whole glassy fallout samples from this test [57].

Excluded CaO outliers in U3 and FLD16

Two combined major element/U isotopic analyses performed in samples U3 and FLD16 are not shown in Figures 6.20-6.22 due to their anomalous CaO composition. These analyses are also not shown in some of the principal component analyses plots below (Table 6.6). The major element compositions of the regions where these SIMS analyses were performed do not fall under the definition of "mafic" as assigned in Chapter 4 (CaO $\geq$ 8 wt.%, FeO $\geq$ 5 wt.%, and MgO $\geq$ 2 wt.%). However, in addition to the notably high CaO concentration, FeO and MgO are also enriched relative to the average host composition (2.77 $\pm$ 0.76 wt.% for FeO and 0.60 $\pm$ 0.26 wt.% for MgO; Table 4.4).

Table 6.6: $^{235}U/^{238}U$ ratio and major element composition (as wt.% oxide) of single SIMS/EDS analyses in high CaO regions.

Sample	$^{235}U/^{238}U$	2σ	SiO_2	1σ	Al_2O_3	1σ	K_2O	1σ	CaO	1σ	FeO	1σ	TiO_2	1σ	MgO	1σ
FLD16	5.54	0.04	62.41	2.64	13.47	0.68	2.84	0.11	12.08	0.48	3.77	0.19	0.38	0.11	1.05	0.15
U3	5.45	0.11	57.92	1.37	7.87	0.26	1.26	0.09	25.04	0.99	3.55	0.06	0.20	0.03	1.05	0.02

6.7 Including U measurements in PCA

The combined major element/U isotopic composition dataset was projected through the PC model generated using the major element compositions of host objects to assess the potential association between enriched U and groups of major element oxides. Projecting the combined major element/U isotopic data set through the original PCA model ensures the PC space remains unbiased. This is important because in many cases, SIMS analyses were targeted

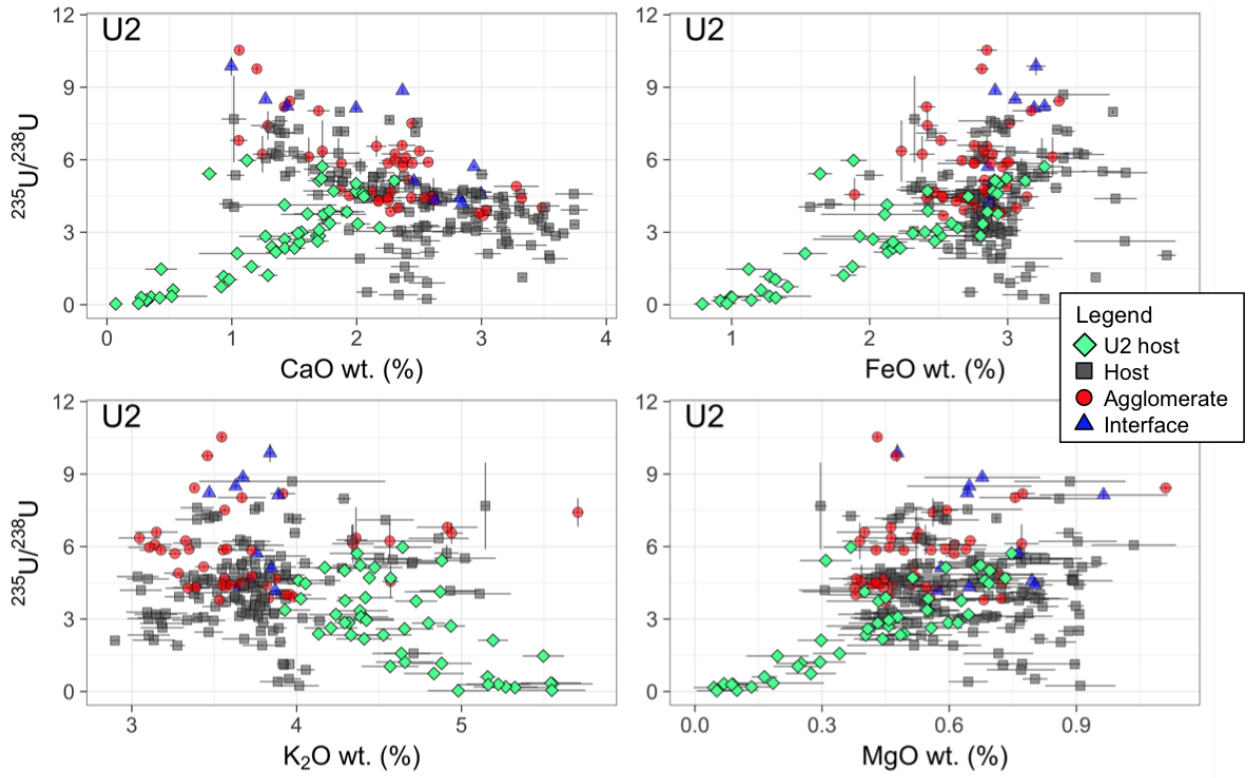

Figure 6.21: Bivariate plots showing $^{235}U/^{238}U$ ratio as a function of select major element oxides, those that exhibit a correlation with the $^{235}U/^{238}U$ ratio in sample U2 (n = 48, shown as green diamonds). Uncertainties are 1σ. To ease viewing of the plots, the plots exclude to two points with anomalous CaO compositions discussed in the text (Figure 6.23 and Table 5.12). Data are tabulated in Appendix G.

at particular agglomerates, interfaces between agglomerates and hosts, or particular regions within a host. Furthermore, there are fewer combined SIMS/EDS data (245 analyses in 18 samples) compared to the original grid-based host object compositional dataset (3,698 analyses in 37 samples), so fewer spurious compositions are required to influence the PC space.

The new PC model generated here is identical to that in Section 6.5, except that Na_2O is excluded (as discussed in Chapter 5). Excluding Na_2O does not appreciably alter the loadings of the PC analysis (compare Figures 6.24 and 6.13). This is likely because of the strong correlation between Na_2O and K_2O for the majority of measured compositions, rendering one of these variables unnecessary to fully account for the variance dataset, except at higher order PCs (*i.e.*, they are not linearly independent; Figure 6.25). The exception is for high values of K_2O and Na_2O, which are more "mineral-like" in their composition. In these instances, Na_2O and K_2O do become linearly independent, converging towards two different mixing end-members for the alkali feldspar compositions (albite and orthoclase, respectively). Because U is not used in generating the PC model, the EDS measurements

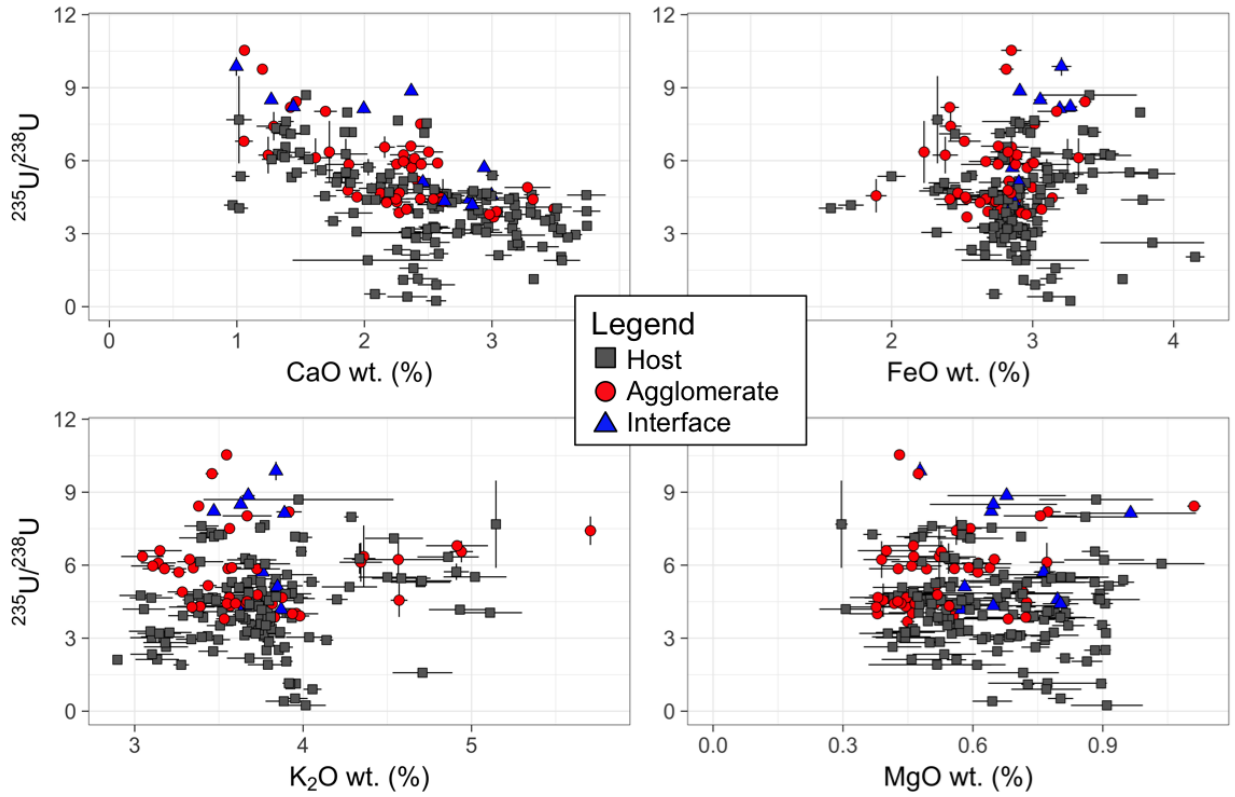

Figure 6.22: $^{235}U/^{238}U$ as a function of major element concentration (wt.% oxide) for CaO, FeO, K_2O, and MgO, with combined major element/U isotopic compositions measured in sample U2 removed. To ease viewing of the plots, the plots exclude to two points with anomalous CaO compositions discussed in the text (Figure 6.23 and Table 5.12). Data are tabulated in Appendix G.

from within and around the SIMS analytical craters are projected through the PC model and their points are colored according to their $^{235}U/^{238}U$ ratio.

Presentations for these PCA plots similar to the plots shown previously in Section 6.5. The top plot in Figures 6.26 and 6.27 show the loadings for the same pairs of PCs plotted in Section 6.5. The center plots in Figures 6.26 and 6.27 shows the full range spanned by the host object major element compositions (shown as partially-transparent "+" markers in all plots) used to generate the PC model with a box highlighting the inset shown in the bottom plot. These plots also show the two CaO compositions excluded in the insets shown in the bottom plots. The bottom plots in Figures 6.26 and 6.27 show individual combined major element/U isotopic ratio measurements are shown and shaded according to their U isotope ratio. The shape and outline color of these points correspond to whether the SIMS analysis was performed in an agglomerate (red circles), a host object (black squares), or over an interface where the host and agglomerate were both significantly sampled in the analysis (blue triangles).

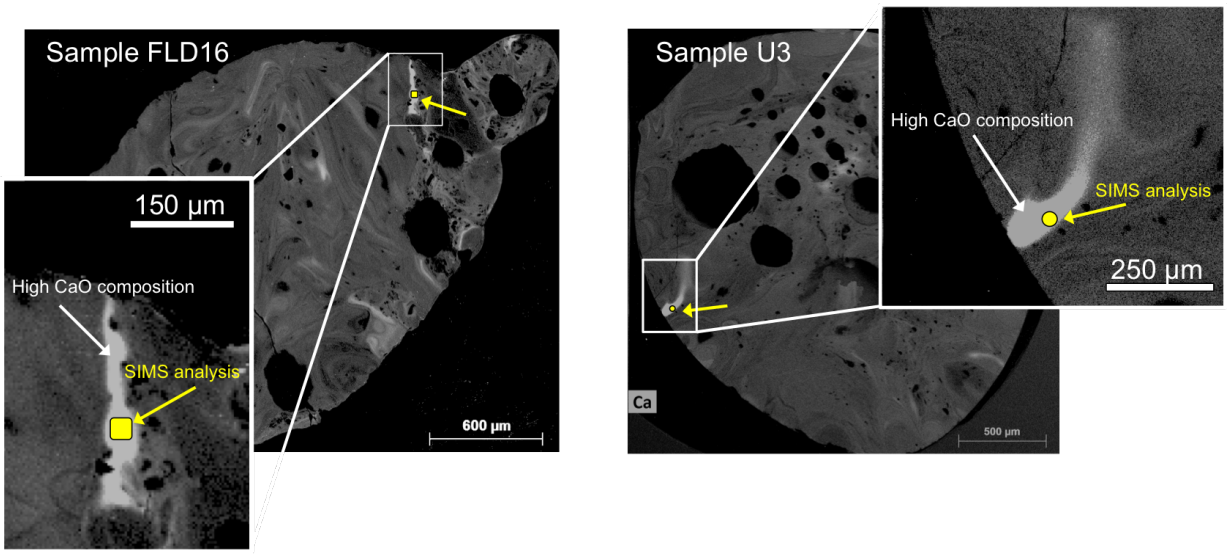

Figure 6.23: Ca compositional maps of U3 and FLD16 with insets showing the high Ca regions where the two SIMS analyses were performed. Data are tabulated in Appendix G.

Table 6.7: Comparison between variance explained by PCs for the PC model generated using the EDS host data excluding Na (used for SIMS and EDS combined measurements) and EDS host data including Na (Table 6.5). Five PCs are retained for both models, denoted by the horizontal line.

	Explained variance (%)		Cumulative exp. variance (%)	
PC	Exc. Na_2O	Inc. Na_2O	Exc. Na_2O	Inc. Na_2O
PC1	43.5	41.3	43.5	41.3
PC2	21.8	23.6	65.4	64.9
PC3	14.6	12.9	80.0	77.8
PC4	7.4	6.8	87.3	84.5
PC5	6.2	6.4	93.5	91.0
PC6	4.4	4.3	97.9	95.3
PC7	2.1	2.9	100.0	98.2
PC8	-	1.8	-	100.0

Given that the SIMS measurements were conducted in primarily glassy regions and the original PCA model was generated using data containing outlying compositions from partially-melted and unmelted regions of host objects, the major element compositions from within/around SIMS craters cluster near the origin (Figures 6.26-6.27). The two measurements made in regions with anomalous CaO compositions discussed above and shown in Figure 6.23 and Table 5.12 are excluded. This trend is replicated in all retained PCs, so they are shown and discussed collectively. While the majority of compositions cluster near the origin, the distribution of measurements in PCA space exhibits tailing, following the

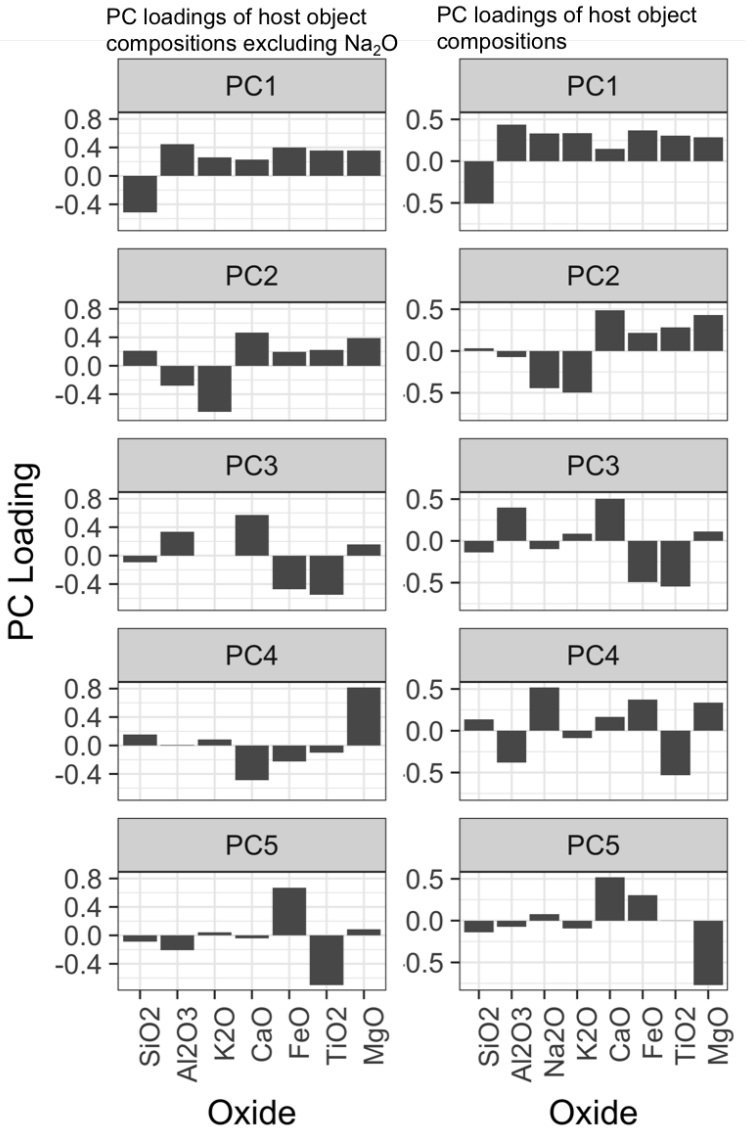

Figure 6.24: Loadings of the principal components for the PC analysis of the EDS host grid data when excluding Na_2O (left) compared to the PC loadings when all major element oxides are included. PC4 and PC5 have been interchanged between the two models, which is unsurprising, since they both describe similar amounts of variance in the original dataset (6.8 and 6.4%, respectively; Table 6.5). The inversion of PC4 on the left panel and PC5 on the right panel is insignificant because a PC4 and -1×PC4 are both orthogonal to all other PCs and are in directions that the describe the same amount of variance (known as "rotational ambiguity").

measurements of U2. Again, the perceived trend due to this tailing is most likely due to sampling regions that have experienced varying degrees of mixing between the melt compositions that comprise U2. This tailing is most pronounced in PCs that have strong loadings

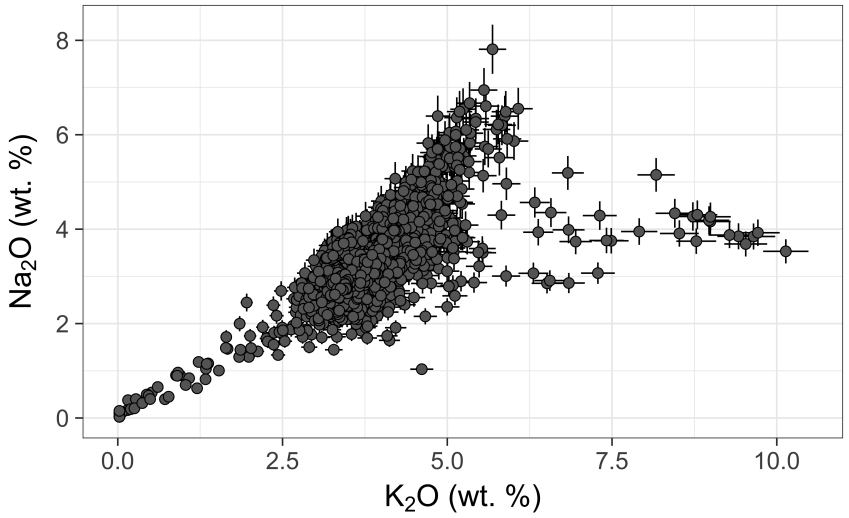

Figure 6.25: Na_2O vs. K_2O (as wt.%) for the host object compositions measured in a grid-based pattern with EDS. Note the strong correlation between the oxides for K_2O concentrations less than approximately 5.0 wt.%. Higher K_2O concentrations are representative of the solid solution ideal composition of alkali feldspars between albite and orthoclase, of which Na and K are linearly independent mixing end-members. Data are tabulated in Appendix B.

in K_2O, primarily PC2. Due to the a stronger separation of compositions in PC space, PC2 is used for three of the four PCA biplots shown in Figures 6.26-6.27.

In all PC plots, the most anomalous major element/U isotope measurements in U2 are not only outlying with respect to the combined major element/U isotope ratio dataset, but are outliers to the 3,698 grid-based EDS analyses of host objects as well. This further confirms that the region of outlying composition in sample U2 likely represents a soil composition that remained relatively unmixed with melts of other compositions, but did mix to a limited extent with the vapor term in the fireball since it is exhibits some (albeit a low) enrichment in ^{235}U. This cluster of ten points from sample U2 have a mean $^{235}U/^{238}U$ ratio of 0.38 ± 0.41 (1σ; compositions shown in Table 6.8). These ten points are also high in SiO_2 (mean of 77.37 ± 1.24 wt.% compared to 73.77 ± 4.12 wt.% for the mean of all host measurements) and K_2O (mean of 5.33 ± 0.20 wt.% compared to 3.80 ± 0.70 wt.% for the mean of all host measurements). Excluding these measurements in U2, the remaining compositions within/around the SIMS analytical craters follow the trends of the host object data measured in the grid-based pattern (shown as "+" markers in Figure 6.28), indicating that the majority of compositions sampled with SIMS are representative of the majority of compositions measured across 37 samples with 3,698 EDS rasters.

Compositions with intermediate $^{235}U/^{238}U$ values tend to plot with the majority of the EDS host compositions (Figure 6.29). This suggests that well-mixed, representative compositions do not tend to have outlying U isotopic compositions (either anomalously high or

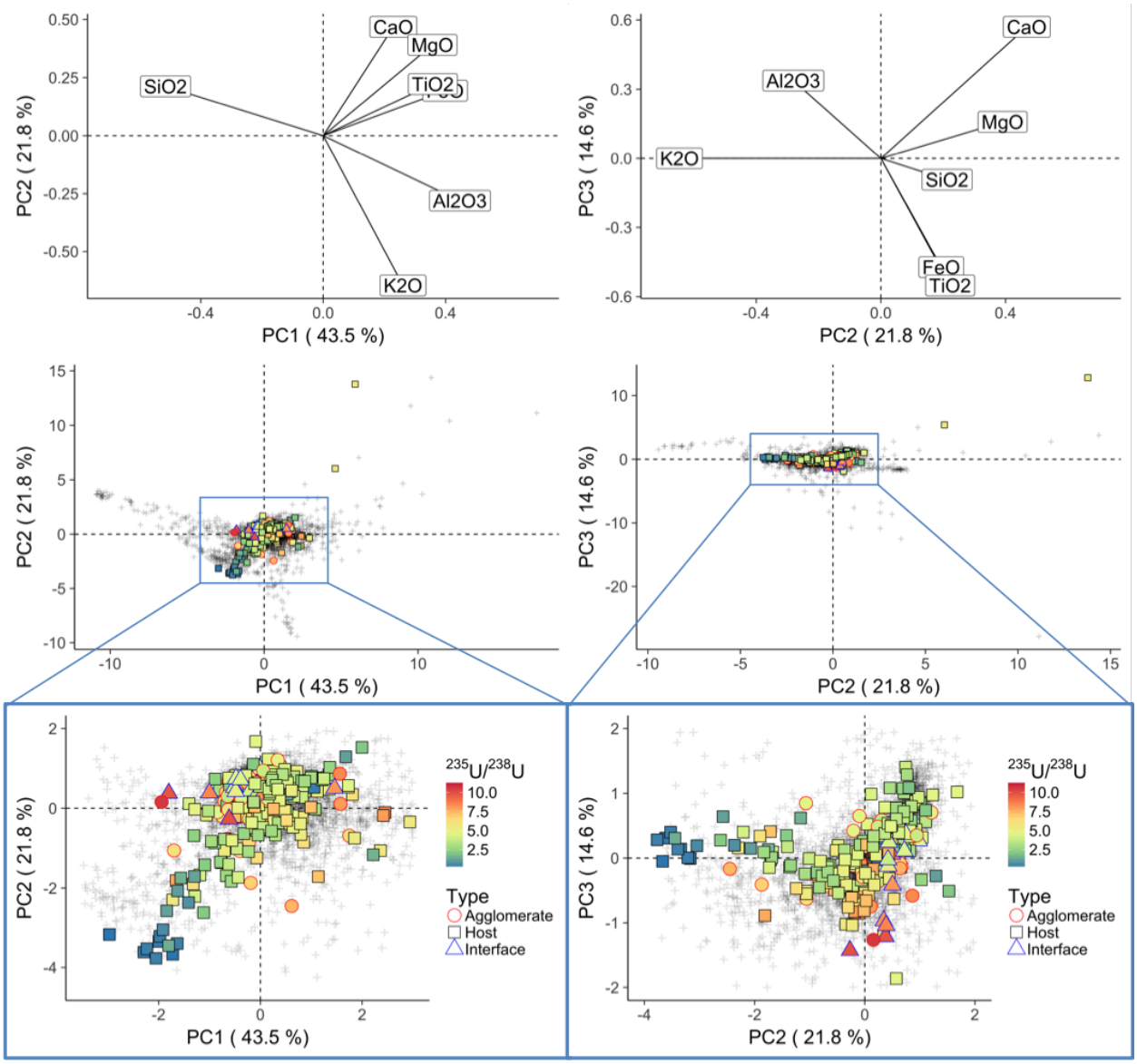

Figure 6.26: PC1 vs. PC2 (left plots) and PC2 vs. PC3 (right plots) where the combined major element composition/U isotope data have been projected through the original PCA model. The top panel shows the loadings. The center plots show the full range spanned by host compositions measured in a grid-based pattern using EDS (shown with partially-transparent + markers). The bottom plots show the scores of the major element compositions measured from within/around SIMS analytical craters ($n = 245$). The color of the points corresponds to the measured $^{235}U/^{238}U$ ratio and the shape and color of the outline corresponds to where the analysis was performed.

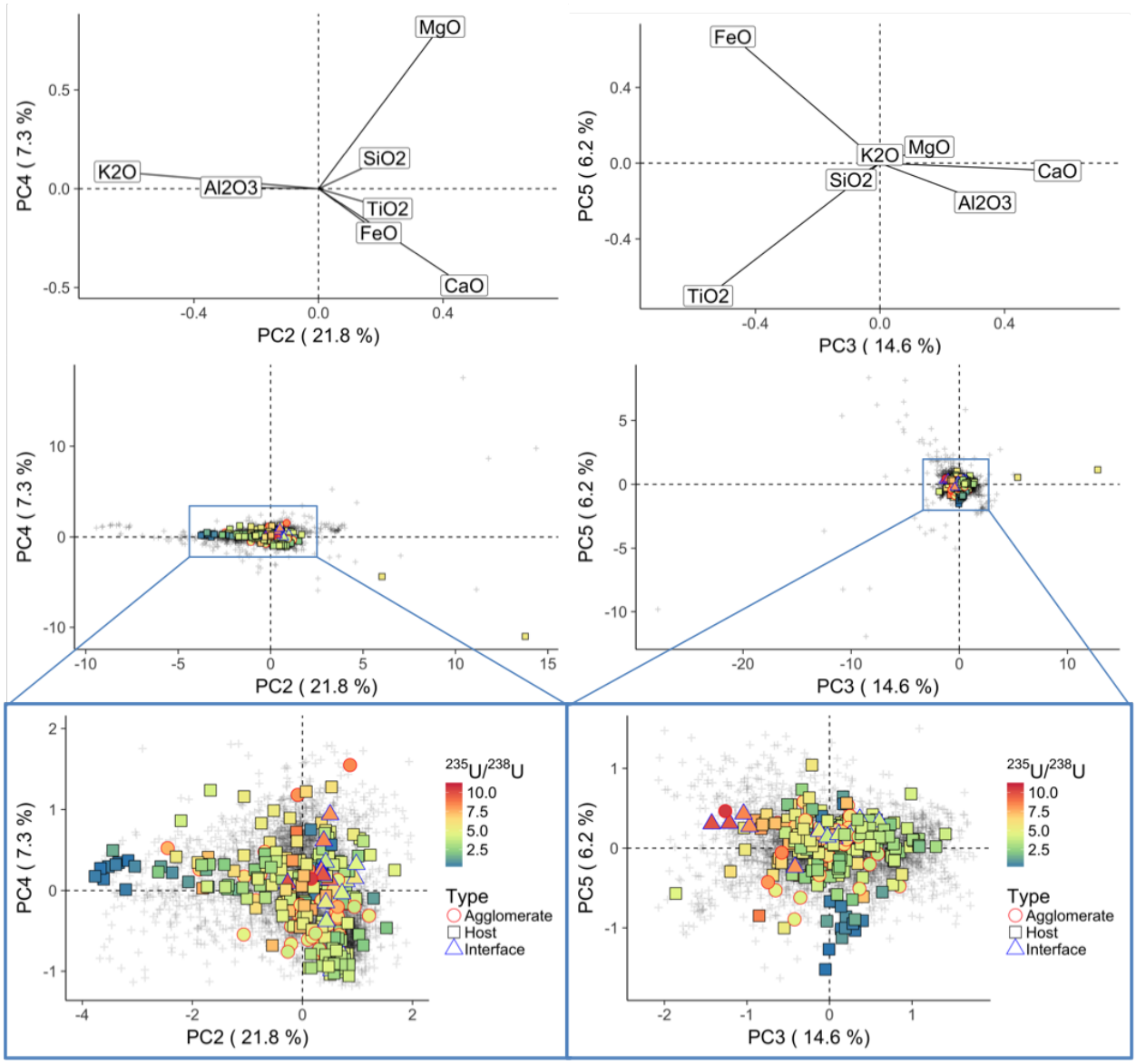

Figure 6.27: PC2 vs. PC4 (left plots) and PC3 vs. PC5 (right plots) where the combined major element composition/U isotope data have been projected through the original PCA model. The top panel shows the loadings. The center plots show the full range spanned by host compositions measured in a grid-based pattern using EDS (shown with partially-transparent + markers). The bottom plots show the scores of the major element compositions measured from within/around SIMS analytical craters ($n = 245$). The color of the points corresponds to the measured $^{235}U/^{238}U$ ratio and the shape and color of the outline corresponds to where the analysis was performed.

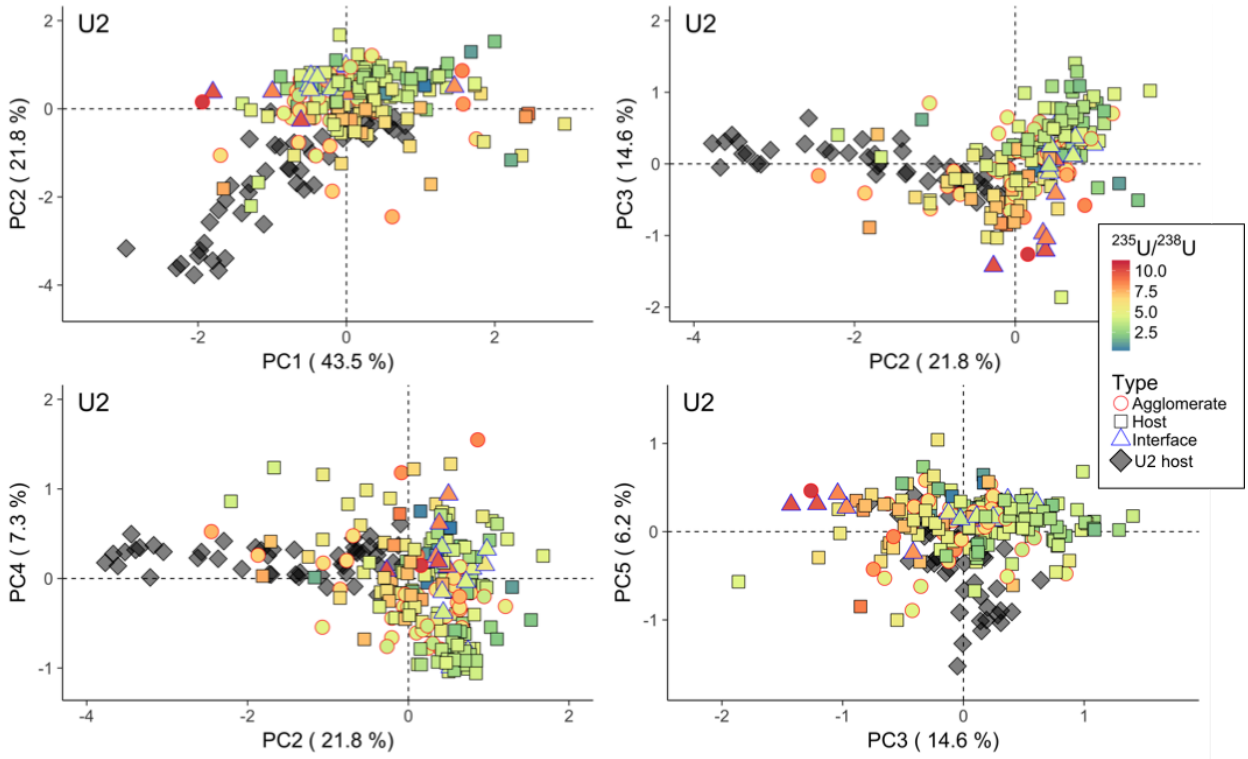

Figure 6.28: PC plots with U2 host measurements marked.

anomalously low $^{235}U/^{238}U$ ratios). Exceptions include the compositions with low $^{235}U/^{238}U$ ratios plotting near the origin in Figure 6.29. These points were measured near the center of sample U3, and discussed in Chapter 5 being located in a region that appears partially-melted. These regions did not efficiently incorporate enriched U, likely due to a high viscosity, preventing thorough bulk mixing and distribution of U into the center of U3. Similarly, the highest isotope ratios measured in this study, those in agglomerates FLD4.3.1-FLD4.3.3, do not follow the trend of the majority of compositions shown the plot of PC2 v.s PC3 (Figure 6.29). This suggests that objects with anomalous major element compositions may be more likely to preserve anomalous U isotope ratio compositions. In the case of U2, the outlying compositions in the PCA model are reflective of a relatively unmixed soil composition. In the case of FLD4.3, the outlying compositions are enriched in SiO_2, and have similar compositions to the Si interfaces that will be discussed in Chapter 8.

The only PC showing any correlation with the $^{235}U/^{238}U$ isotope composition is PC3, which exhibits a weak anti-correlation due to its negligible loading of K_2O and strong positive loading of CaO (Figure 6.30). PC3 separates the mafic and FeO, TiO_2-rich compositions, having CaO and MgO positively-loaded, with FeO and TiO_2 being negatively-loaded (likely correlated due to FeO, TiO_2-rich compositions in the precursor soil). In a plot of PC2 against PC3, the majority of compositions from the EDS host object analyses (the

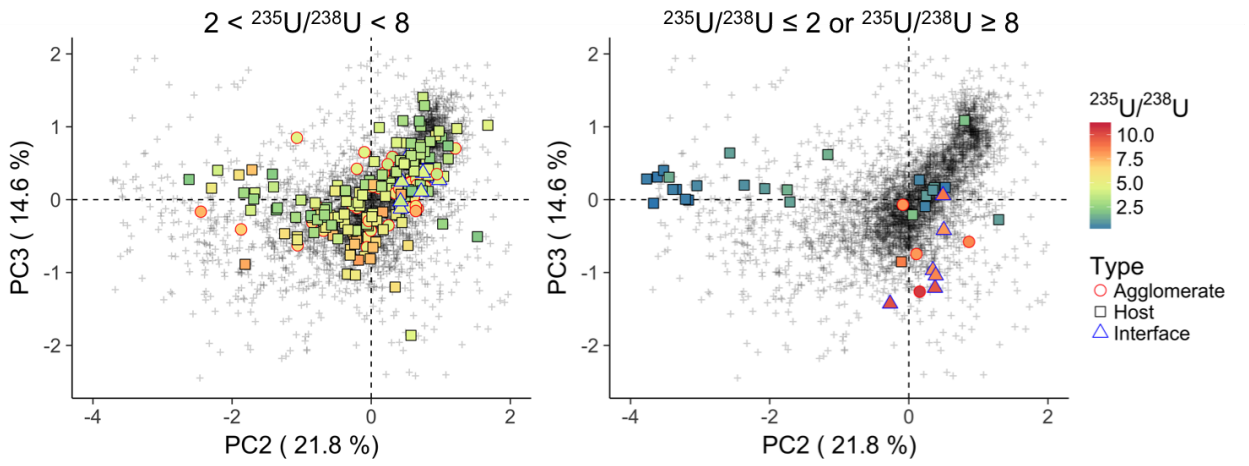

Figure 6.29: PC2 vs. PC3 showing compositions with intermediate $^{235}U/^{238}U$ isotope ratios ($2 < {}^{235}U/^{238}U > 8$; left panel) and outlying $^{235}U/^{238}U$ isotope ratios ($^{235}U/^{238}U < 2$ or $^{235}U/^{238}U > 8$; right panel).

partially-transparent "+" markers) and the compositions from within/around the SIMS analysis craters plot along a roughly one-to-one line intercepting the y-axis at the origin (Figure 6.30). The SIMS measurements conducted in the K_2O-rich, SiO_2-rich, and CaO-poor region in U2 plot near the x-axis in Quadrants II and III, meaning PC3 exerts little influence on these points, due to the negligible K_2O loading in PC3. This negligible K_2O loading coupled with strong loading of CaO yield a weak anti-correlation between PC3 and the $^{235}U/^{238}U$ ratio, remarkably similar to the bivariate plot of $^{235}U/^{238}U$ versus CaO, when the measurements in U2 are removed (compare Figures 6.30 and 6.22).

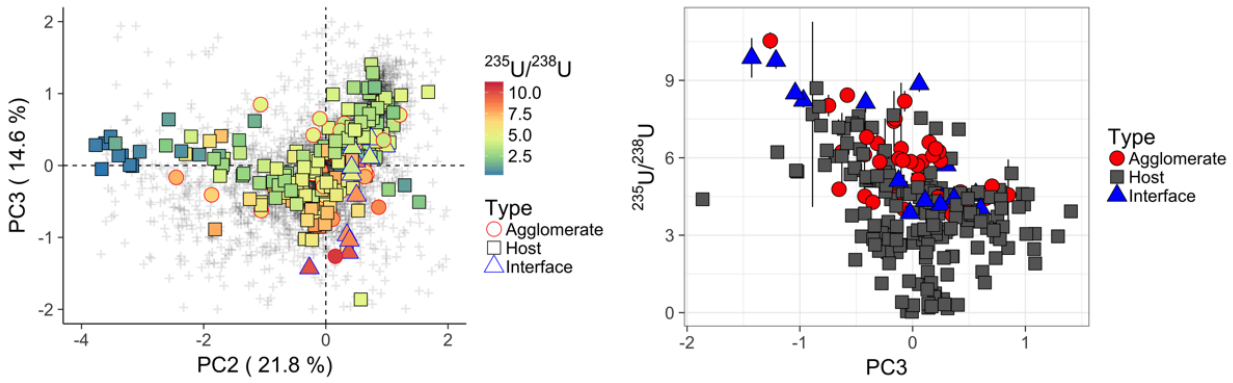

Figure 6.30: PC plots with U2 host measurements marked.

Table 6.8: Compositions of outlying measurements in sample U2 with their PC1 and PC2 coordinates arranged by their $^{235}U/^{238}U$ ratio.

PC1	PC2	$^{235}U/^{238}U$	2σ	SiO_2	1σ	Al_2O_3	1σ	K_2O	1σ	CaO	1σ	FeO	1σ	TiO_2	1σ	MgO	1σ
-2.97	-3.17	0.034	0.002	80.15	3.39	13.28	0.67	4.98	0.20	0.07	0.00	0.79	0.04	0.17	0.05	0.05	0.01
-1.72	-3.67	0.052	0.002	77.09	3.26	14.46	0.73	5.55	0.22	0.25	0.01	0.97	0.05	0.27	0.08	0.10	0.01
-2.29	-3.61	0.165	0.004	77.29	3.27	13.93	0.70	5.32	0.21	0.32	0.01	0.92	0.05	0.15	0.04	0.04	0.01
-2.00	-3.34	0.192	0.003	77.86	3.29	14.28	0.72	5.27	0.21	0.32	0.01	1.14	0.06	0.18	0.05	0.13	0.02
-1.98	-3.21	0.288	0.004	75.81	3.21	13.24	0.66	5.16	0.21	0.42	0.02	1.32	0.07	0.17	0.05	0.09	0.01
-2.23	-3.52	0.301	0.005	77.72	3.29	14.43	0.72	5.22	0.21	0.27	0.01	1.00	0.05	0.12	0.03	0.09	0.01
-2.05	-3.77	0.320	0.020	76.67	1.04	13.86	0.48	5.55	0.24	0.35	0.06	0.99	0.13	0.15	0.03	0.07	0.02
-1.63	-3.39	0.350	0.010	75.85	0.94	13.47	0.46	5.54	0.18	0.52	0.28	1.28	0.30	0.18	0.00	0.18	0.12
-1.92	-3.05	0.607	0.011	78.03	0.66	14.24	0.11	5.16	0.05	0.53	0.03	1.21	0.01	0.20	0.03	0.16	0.03
-1.80	-3.45	1.470	0.090	77.24	0.54	14.13	0.23	5.50	0.13	0.43	0.13	1.12	0.16	0.17	0.04	0.19	0.07

PCA projections by sample

Separating out measurements within individual samples, the influence that each sample contributes to apparent trend in PC space can be examined using PC2 and PC3, which creates the greatest separation in compositions in the combined major element/U isotopic dataset (Figures 6.31–6.32). While the collective distribution of compositional measurements spans a wide range in the PCA projection, measurements within individual samples tend to cluster closely. Counterexamples are measurements in samples U2, U1B, and FLD16, which exhibit a large range in their PC2 scores. The host measurements in U1B are tightly clustered, but combined major element/U isotopic measurements in the agglomerates U1B.2 and U1B.L deviate from the host compositions, contributing the range spanned by all measurements in U1B. Overall, however, host and agglomerate measurements of most samples tend occupy a relatively restricted region of PC space. This observation indicates hosts and agglomerates in the same sample tend to have similar compositions. To quantify how similar different objects are to each other (*e.g.*, hosts and agglomerates in the same sample) a different multivariate approach must be used, which will be shown and discussed in Chapter 7.

6.8 Conclusion

This chapter uses the multivariate approach of PCA and bivariate plots to visualize and analyze the two separate datasets collected in this dissertation: first the grid-based EDS analyses of host objects and agglomerates across entire objects and then the combined major element/U isotope dataset from measuring the major element compositions within/around SIMS analytical craters. The major element compositions of host objects ($n = 3,698$) was used to generate the PC space (Eqn. 6.7). To determine the number of PCs to retain, a noise-injection method using UP matrices was used. The first 5 PCs were largely stable to variations within analytical uncertainty, suggesting the first 5 PCs are primarily modeling true variance in the data instead of noise. These 5 PCs were shown to be controlled by unmelted/partially-melted compositions in the soil, bolstering the observation discussed in Chapter 4 that fallout from this event is dominantly formed from the melting and mixing of

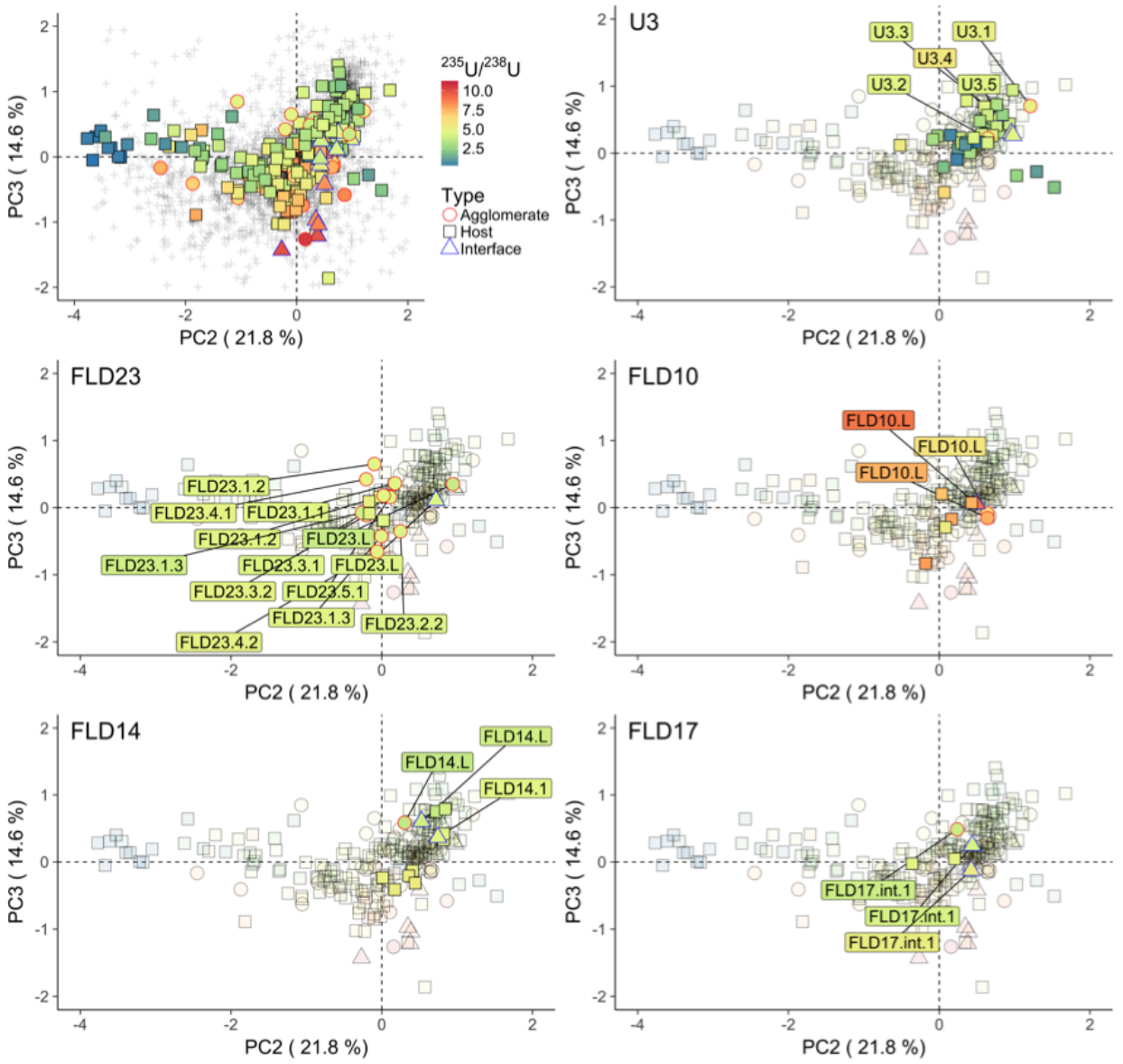

Figure 6.31: PC2 vs. PC3 of a PC space generated using the EDS host grid data, excluding Na_2O. Plots show the SIMS/EDS measurements performed in each sample with measurements in other samples shown as partially transparent, with measurements in agglomerates and over interfaces marked following the legend in the top left plot, which shows the full range spanned major element/U isotopic measurements in all samples. The color in the labels of these measurements also corresponds to their $^{235}U/^{238}U$ ratio following the legend (in case the marker is obscured by overlapping data). The loadings are shown in Figure 6.26.

minerals in the local lithology. Therefore, major element behavior in fallout is controlled by the environment immediately surrounding the nuclear event.

Bivariate plots of $^{235}U/^{238}U$ ratios as a function of each major element show no strong

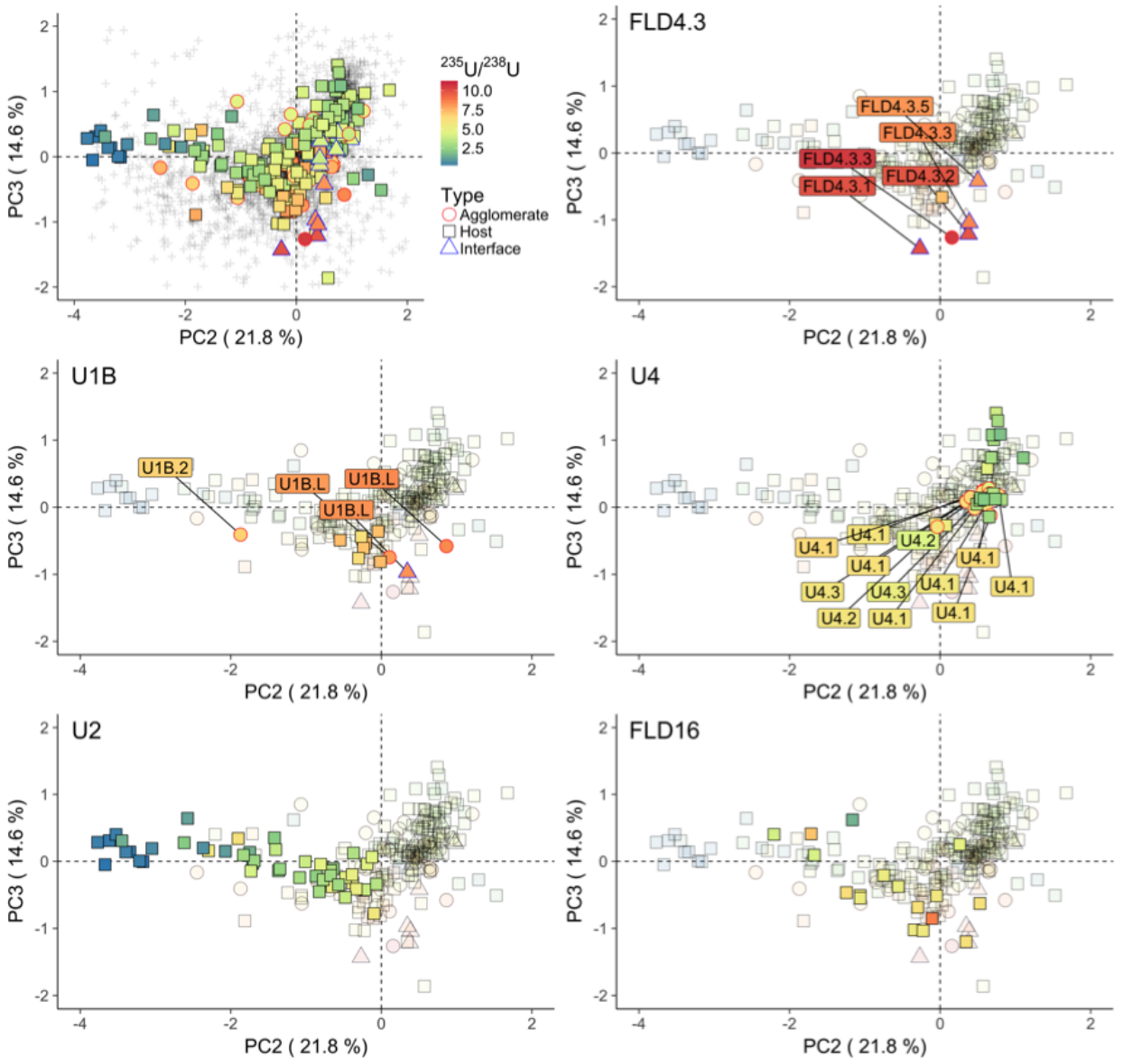

Figure 6.32: PC2 vs. PC3 of a PC space generated using the EDS host grid data, excluding Na_2O. Plots show the SIMS/EDS measurements performed in each sample with measurements in other samples shown as partially transparent, with measurements in agglomerates and over interfaces marked following the legend in the top left plot, which shows the full range spanned major element/U isotopic measurements in all samples. The color in the labels of these measurements also corresponds to their $^{235}U/^{238}U$ ratio following the legend (in case the marker is obscured by overlapping data). The loadings are shown in Figure 6.26.

trends with major element composition. This observation is in contrast to the documented associations between Pu and Ca, Mg, and Fe in fallout from the Trinity event, as well as the frequent association observed between U and Ca, Mg, and Fe at the compositional

interfaces of agglomerates in fallout from this event (discussed further in Chapters 8 and 9). One exception is the positive correlation between the $^{235}U/^{238}U$ ratio and CaO, MgO, FeO, which were measured in sample U2. However, as discussed, this anomaly is likely due to poor and incomplete physical mixing between two melts of distinct composition and the finite size of the SIMS analytical regions, instead of some chemical behavior (such as volatility). Excluding measurements in U2 reveals a weak anti-correlation between the remaining $^{235}U/^{238}U$ measurements and the CaO composition, consistent with data from bulk ICP-MS measurements of whole dissolved samples from this event (Figure 6.22) [57].

The combined major element/U isotope dataset ($n = 245$) was then projected through the original PC model. The majority of compositions from this dataset cluster near the origin, as they were primarily conducted in the glassy regions of fallout and contain few outlying compositions. The strongest trend between PCs and $^{235}U/^{238}U$ ratio is shown in the plots of PC2 versus PC3 (Figure 6.30), due to strong loadings of K_2O in PC2 (separating the compositions from sample U2) and a strong loading CaO and negligible loading of K_2O in PC3. When considering measurements by sample, examination of PC3 versus PC2 shows that measurements in agglomerates and their associated host objects tend to occupy similar, restricted regions in PC space (Figures 6.31 and 6.32). Compositional heterogeneity largely occurs *between* samples in this fallout population. The glassy regions of agglomerates and their host objects tend to be relatively similar to one another, with respect to both major elements and U isotope ratios. This observation further supports the conclusions of Chapters 4 and 5, indicating that the carrier melt and the vapor term of the fireball tend to exhibit homogeneity at the local scale. The major element and U isotopic compositional similarities between agglomerates and their associated hosts is visualized and quantified in Chapter 7.

Chapter 7

Compositional Similarity Analysis of Agglomerates and Host Objects

7.1 Chapter overview

In the next multivariate analysis, agglomerates and host objects are compared based on their compositional similarity. First, to visualize the compositional similarity of all analyzed host objects and agglomerates simultaneously, a technique known as Multidimensional Scaling (MDS) is used. MDS models and approximates the compositional similarities (the distance between objects in compositional space, also referred to as *dissimilarities*, because larger values indicate objects are farther apart, and therefore, more compositionally dissimilar) between all objects and projects these points onto a 2D map while maintaining, as closely as possible, the inter-object distances from the higher dimensional space. This technique creates a simple map that shows qualitatively the compositional similarity between all characterized agglomerates and host objects in a single representation.

Next, the compositional similarity between agglomerates and their associated host objects is quantitated (*i.e.*, not modeled, as in the case of MDS) by calculating the Euclidean distance from agglomerates to their associated host objects in full 7D compositional space. The more compositionally similar a pair of agglomerates and their host objects are (*i.e.*, the shorter the Euclidean distance between the two objects), the more likely they were formed from similar precursor melts. Greatly different compositions between a given set of agglomerates and their host objects suggests formation from distinct precursor melts prior to agglomeration or that or that agglomerates experienced a different fireball environment (*e.g.*, longer residence time, sourced from a different type of soil from a different part of the fireball, etc.) prior to colliding and coalescing with their associated host objects.

Both the MDS model and the Euclidean distance calculation are first performed for the major element dataset only to focus on the precursor/soil origins of these materials. Next, the combined major element/U isotopic dataset is explored to understand differences in how agglomerates and their host objects interacted with and incorporated the bomb vapor.

In Chapter 6, uncertainty perturbed matrices ("UP matrices") of the original data matrix were used to determine how sensitive different principal components were to the analytical uncertainty in the EDS measurements. In this chapter, UP matrices are used to calculate and show analytical uncertainties in the MDS projection and Euclidean distance calculations.

7.2 Multidimensional scaling

In Chapter 6, PCA was used to visualize and interpret relationships between *variables* (the major element oxides). This chapter visualizes and interprets relationships between *whole objects* (entire agglomerates and host objects). Two separate techniques are used here. First, to visualize the compositional relationships between all agglomerates and host objects simultaneously, a qualitative visualization technique known as Multidimensional Scaling (MDS) is used. Similar to PCA, the goal of MDS is dimension reduction. MDS reduces the number of dimensions of the original dataset by modeling the inter-object distances in full compositional space (7 dimensions in this study) and generating a lower dimensional projection of points (2 dimensions in this study) where each point corresponds to an object. This 2D mapping attempts to preserve the higher dimensional distances between objects in the lower dimensional mapping. These inter-object distances in 7D space are called *dissimilarities*, as objects more similar in composition are closer together (have smaller dissimilarities) and objects farther apart are more dissimilar (have larger dissimilarities). The dissimilarities of agglomerates and their host objects are represented by a single measure of their major element or combined major element/U isotopic composition. To reduce the influence of outlying compositions, the median composition is used here.

In this study, the multivariate compositional space is derived from the major element composition dataset collected by EDS or the combined major element/U isotopic dataset that includes U isotope ratios collected by SIMS and EDS rasters collected from within/around these SIMS analytical craters and excludes Na_2O (Figure 6.18). The dimensionality of the multivariate space is the same in both cases. In the analyses in this chapter, MgO is also excluded in both cases, as discussed below. What changes between the two datasets is the number of characterized objects (37 hosts and 58 agglomerates in the case of the EDS only dataset and 17 hosts, 31 agglomerates, and 10 interfaces in the case of the combined SIMS/EDS dataset) and the variance around the calculated compositions due to the overall number of measurements used to calculate the centroid of an object's composition.

Both PCA and MDS use square, symmetric matrices whose entries contain the relationship between either different variables (*e.g.*, SiO_2, Al_2O_3, etc., for PCA) or different objects (*e.g.*, host FLD10, agglomerate FLD4.3.3, etc., for MDS). However, in contrast to PCA, which uses a correlation matrix, a type of *similarity* matrix, where larger elements indicate stronger relationships between variables, MDS uses a *dissimilarity* matrix $\mathbf{D}$, where larger elements (d_{ij}) of $\mathbf{D}$ indicate that objects are less compositionally related. A commonly used measure of dissimilarity, and the measure of dissimilarity used here, is the Euclidean distance between objects [154, 155]. The Euclidean distance (d_{ij}) between two objects i and j is given

by

$$d_{ij} = \sqrt{(x_1^i - x_1^j)^2 + (x_2^i - x_2^j)^2 + \ldots + (x_n^i - x_n^j)^2}, \tag{7.1}$$

where the subscripts $1 \ldots n$ denote the different variables (*e.g.*, x_1 denotes the SiO_2 composition of an object, x_2 denotes the Al_2O_3 composition of an object, etc.).

For m objects, $m(m-1)/2$ distances must be computed to account for the distances between each pair of objects. Because the distance from any object to itself is 0 and $d_{ij} = d_{ji}$, $\mathbf{D}$ is an $m \times m$ triangular matrix with 0s for diagonal elements.

The elements of $\mathbf{D}$ are calculated using all n dimensions. MDS then models these dissimilarities in a lower dimensional space, such that:

$$\delta_{ij} \approx d_{ij}, \tag{7.2}$$

where δ_{ij}s are the modeled distances, which then comprise the elements of the modeled distance matrix $\mathbf{\Delta}$. Similar to PCA, if one retains all n dimensions, then $\mathbf{\Delta} \equiv \mathbf{D}$. Depending on the goodness of fit, two or three dimensions often satisfactorily represents the analytical dissimilarities (d_{ij}s) in full dimensional space between the objects [156]. Because MDS plots are used here to qualitatively explore and visualize similarities before the Euclidean distance between agglomerates and their host objects is quantitated (Sections 7.5 and 7.6), both datasets are projected and plotted in 2D.

The mapping between the analytical dissimilarities (d_{ij}s) and the representation of these dissimilarities in lower dimensional space with modeled distances (δ_{ij}s) requires some *a priori* knowledge or assumption of how d_{ij} is related to δ_{ij}. Some MDS models assume strong relationships, such as δ_{ij} being linearly related to d_{ij} [157]. That is, an increase in analytical dissimilarity between two objects results in a proportional increase in the modeled inter-point distance between those objects in the lower dimensional mapping. A more commonly used (albeit weaker criterion), and the one used in this study, is that of *monotonicity* between the higher dimensional and lower dimensional representations. Monotonicity means that the rank orders of the magnitudes δ_{ij} and d_{ij} are preserved [158, 159]. That is, if the analytical dissimilarities were placed in order of largest to smallest, the modeled distances would follow that same ordering. This type of MDS is known as *ordinal non-metric* MDS (referred to as nMDS herein). nMDS is used here because it provides a better representation in fewer dimensions than other forms of MDS [160].

Analytical dissimilarities rarely obey the monotonic constraint [158]. Instead, nMDS generates a monotonic fit to the analytical dissimilarities (d_{ij}s), which is used to map between the analytical dissimilarities in 7D space and the modeled distances in 2D space [161]. While the primary goal of nMDS is to find the optimum configuration of points in 2D with inter-point distances (δ_{ij}s) that best match the analytical dissimilarities (d_{ij}s), an intermediate step is that a monotonic function must be fit to the analytical dissimilarities (d_{ij}s) to satisfy the relationship between the higher and lower dimensional representations [161]. This monotonic fit contains approximated d_{ij}s referred to *disparities* ($\hat{d}_{ij}$s), which are then

used to approximate the analytical dissimilarities in the lower dimensional configuration of points in 2D. That is,

d_{ij}	$\longrightarrow$	$\hat{d_{ij}}$	$\longrightarrow$	δ_{ij}
analytical		monotonic		modeled
dissimilarities	$\longrightarrow$	disparities	$\longrightarrow$	distances

Goodness of fit of nMDS models

Similar to other methods of fitting models to analytical data, the goodness of fit in nMDS is measured by the normalized sum of the squared residuals, referred to as the *stress* (S) in MDS literature [157]. The goodness of fit of an nMDS model is how well the modeled distances in 2D (δ_{ij}s) match the disparities ($\hat{d_{ij}}$s) measured using the residuals between these values. That is,

$$S = \sqrt{\frac{\sum \left(\delta_{ij} - \hat{d_{ij}}\right)^2}{\sum \delta_{ij}^2}}. \tag{7.3}$$

Historically, MDS models with stresses between 0.1–0.2 are considered "fair", between 0.05–0.1 are considered "good", between 0.025–0.05 are excellent, and a stress <0.025 is considered "near-perfect" [158].[1]

The best fit configuration of points in lower dimensional space is found by minimizing the stress [161]. As a result, nMDS is an iteratively solved technique, unlike PCA [158, 159]. To find the minimum stress, the nMDS algorithm begins with a random configuration of points in the user-defined dimensionality of the lower dimensional projection (2D here; Fig. 7.1). The modeled inter-point distances (δ_{ij}s) in this lower dimensional mapping are calculated. A monotone regression, from which the disparities ($\hat{d_{ij}}$s) are extracted, is then conducted using the dataset of (d_{ij}, δ_{ij}) coordinate pairs. The stress (Eqn. 7.3) is then calculated between the disparities ($\hat{d_{ij}}$s) that comprise the regression and the modeled distances (d_{ij}s). The algorithm then iterates until the minimum stress is reached (typically fewer than 100 iterations). In this study, nMDS modeling is performed using the metaMDS function in the **vegan** package in the statistical programming language **R** [162], which follows the nMDS algorithm presented in [161].

The nMDS goodness of fit is visualized using a stress plot (Fig. 7.2) [157]. The stress plot shows the modeled distances in the 2D projection as a function of the 7D analytical dissimilarities for each pair of inter-object distances, which have coordinate pairs (d_{ij},δ_{ij}) and are shown as blue markers in Figure 7.2. The monotonic regression and disparities are

[1] A perfect fit indicates that there is a perfect monotonic relationship between the modeled distances (δ_{ij}s) and the disparities ($\hat{d_{ij}}$s).

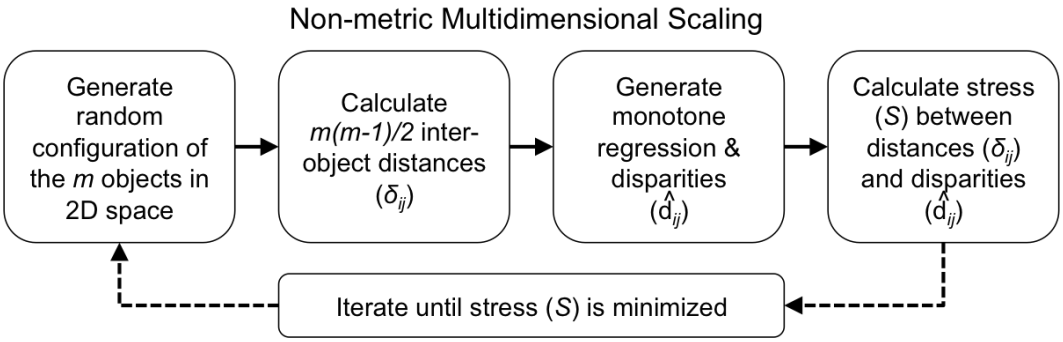

Figure 7.1: nMDS algorithm for finding the optimum lower dimensional configuration.

also plotted as a function of the dissimilarities (red line). The residuals used to calculate the stress (Eqn. 7.3) are the vertical distances between the (d_{ij},δ_{ij}) coordinate pairs (blue markers) and the (d_{ij},$\hat{d_{ij}}$) coordinate pairs (red line).

Calculating the dissimilarity matrix

Compositional data are represent parts of a whole and sum to approximately or exactly 100 wt.%, also known as a *closure constraint*. Due to closure, compositional data exist on the simplex $\mathcal{S}^n$ and not in real, Euclidean space $\mathbb{R}^n$. As a result, the data must be mapped to $\mathbb{R}^n$ prior to calculating the Euclidean distances between different objects, which is accomplished here using Aitchison's CLR transformation (as discussed in Chapter 6; Eqn. 6.8). These Euclidean distances between objects in 7D space represent the dissimilarities d_{ij} that are elements of the dissimilarity matrix $\mathbf{D}$. Following the CLR transformation, the data are pre-treated following the standard scaling method (Eqn. 6.7): the mean from each variable is subtracted and each variable is individually scaled to have a variance equal to 1, identical to the PCA data pretreatment used in Chapter 6.

The compositional centroid of an object

Agglomerates and host objects were characterized using one or more analyses (as described in Chapters 4–6). To calculate the distance between agglomerates and host objects a single distance must be used. In this case, some measure of the compositional centroid of the sample must be defined. To avoid the bias from outliers such as measurements in nearly-pure SiO_2 regions, the *median* compositions of agglomerates and host objects are used as the centroid and Euclidean distance is calculated between medians of different pairs of objects, which comprise the elements of the dissimilarity matrix used in the MDS model.

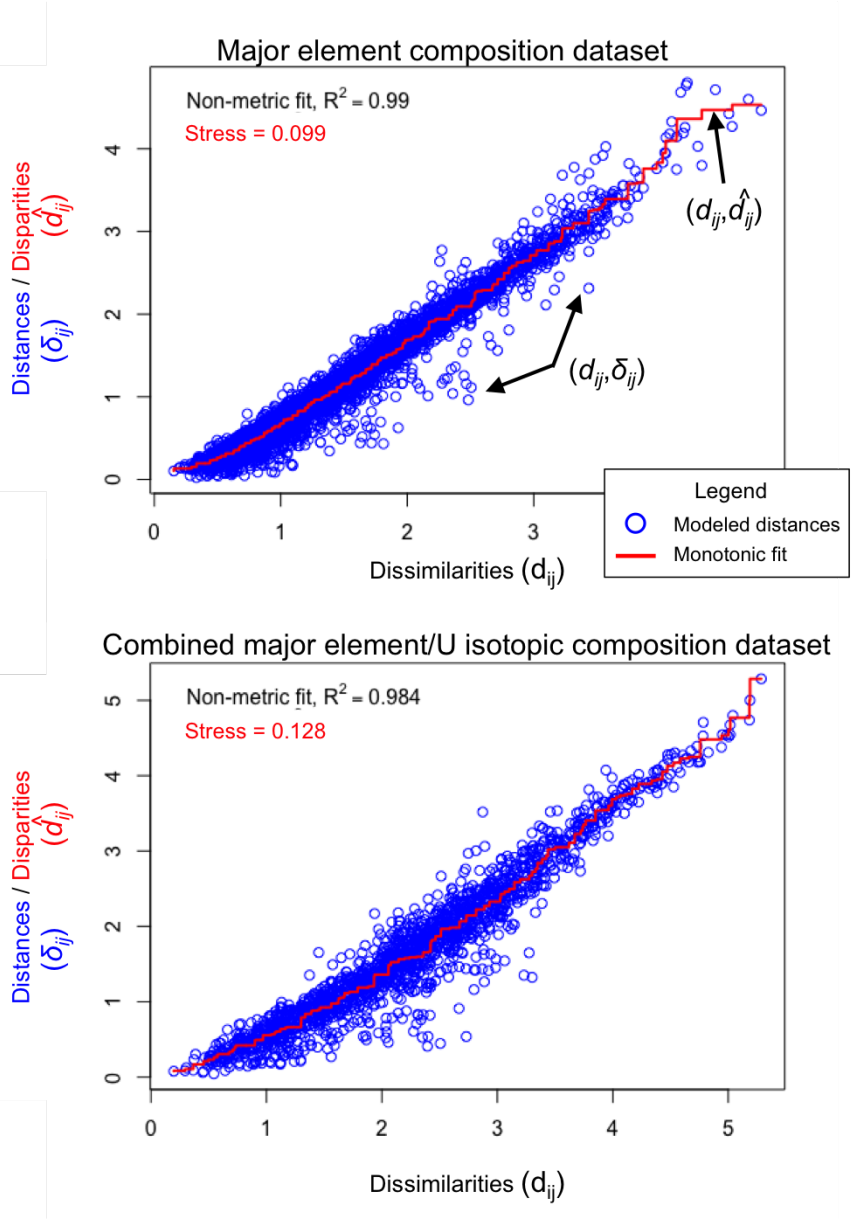

Figure 7.2: Stress plots of MDS models of the the major element compositional data set of hosts and agglomerates (top) and the combined major element/U isotopic dataset from EDS rasters taken within/around the SIMS craters (bottom). These plots show the modeled distances (δ_{ij}s) as a function of the analytical dissimilarities (d_{ij}s) (blue markers). The non-metric monotonic fit (which contains the disparities, $\hat{d_{ij}}$s) is also shown (red line) plotted as a function of the analytical dissimilarities (d_{ij}s). Modeled distances that have large vertical deviations from the monotonic fit contribute to large values of stress (Eqn. 7.3). The top plot is an example of a "good" fit with $S < 0.1$ and the bottom plot is an example of a "fair" fit with $0.1 < S < 0.2$.

Uncertainties in MDS

Like other multivariate techniques, MDS ignores analytical uncertainty and assumes that the distance between objects is much greater than the uncertainty in measuring that object's position in multivariate space. To model the effect of the analytical uncertainty on the final multivariate model in this dissertation, UP matrices are randomly generated to produce uncertainties in MDS space. The points in the following MDS plots correspond to the mean MDS coordinates for each object from the 500 UP matrix simulations and the uncertainties represent 2σ about these mean values (Fig. 7.3).

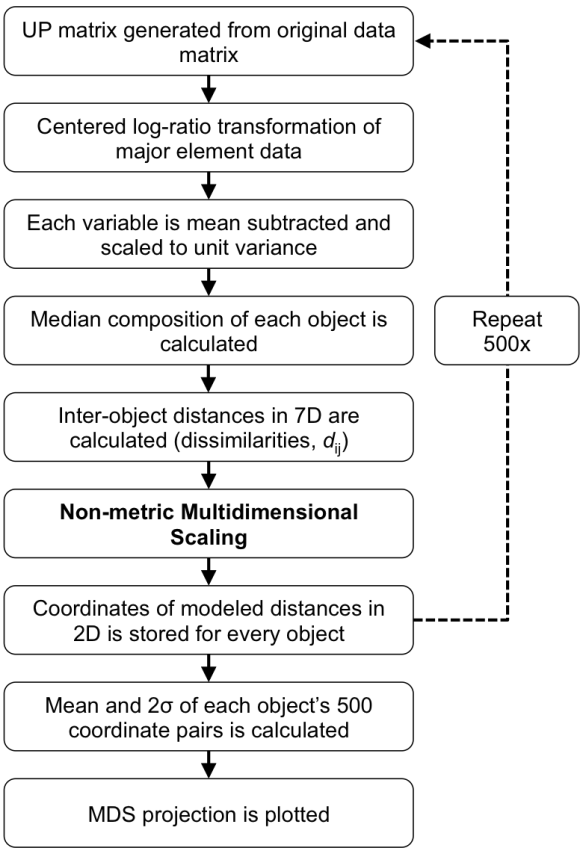

Figure 7.3: Flow chart for generating points and uncertainties in MDS plots. The nMDS step is shown in Figure 7.1.

First an UP matrix is generated using the original data matrix and its associated uncertainties. The data are CLR-transformed (Eqn. 6.8) to map the data to Euclidean $\mathbb{R}^n$ space, then standard scaled (Eqn. 6.7) so each variable carries equal weight in the model. The median composition of each object is then calculated from these data, which is used to calculate the Euclidean distance between objects in multivariate space (Eqn. 7.1.), forming the dissimilarity matrix D_{ij}. This dissimilarity matrix is used for the 2D nMDS modeling

(Fig. 7.1). After the MDS model converges, the MDS coordinates of each object is recorded and the process is repeated 500 times (limited by the computational power and memory of the computer system used). After 500 simulations, the mean of these coordinates for each object is used as the data point and the two times standard deviation of these coordinates is used as the 2σ uncertainty shown in the MDS plots.

Reading an MDS plot

Although points have coordinates in MDS space, these coordinates are arbitrary.[2] Unlike PCA, the axes in MDS are not meaningful and are not linear combinations of the original variables, so should not be interpreted as such. MDS plots are used to determine the relative similarity between objects only. The only meaning that can be assigned for two objects that plot in, say, quadrant I and one object that plots towards the bottom left of quadrant III is that the two objects in quadrant I are more similar than those objects are to the object plotting towards the bottom left in quadrant III. The plots are useful for searching for clustering, groupings of objects, outliers, and comparing the similarity of large number of objects in high dimensional space in a 2D or 3D plot.

7.3 MDS model of the major element only dataset

The median compositions of agglomerates and host objects were used to represent the compositions of objects in the MDS models. For the first MDS model, which uses the major element only dataset, the median major element compositions of agglomerate and host objects are calculated from the 3,698 EDS raster measurements taken in grid-based patterns across host objects (used to generate the PCA space in Chapter 6) and the 679 EDS measurements characterizing the agglomerates. These measurements characterized the major element compositions across a total of 95 objects: 37 host objects and 58 agglomerates.

The calculated stress from the converged solution of the non-metric MDS model is 0.099, considered a "good" fit [158]. While the fit is improved if more than 2 dimensions are used, a 2D MDS projection shows the approximate similarity between all objects clearly and simultaneously (Fig. 7.4; data tabulated in Appendix I). Figure 7.4 shows the modeled proximities of all agglomerates (red circles) and host objects (grey squares) with outliers marked. Examples of the compositional similarity or dissimilarity between agglomerates and their associated host objects are shown in Figure 7.5 for samples U1B, FLD4.3, FLD23, FLD14, FLD4.4, and AE.C.

Collectively, most of the host objects (grey squares) cluster close together near the origin, except for FLD25 (in quadrant III), FLD5.3 (in quadrant II), and FLD3.2 (in quadrant I). The reason for close proximity of most of the host objects is likely due to the relatively large number of EDS measurements performed per host, such that anomalous compositions tend to be averaged out. Using the median composition as an object's compositional centroid also

[2]While numbers are shown in the axes in MDS plots in this dissertation, that is not done customarily.

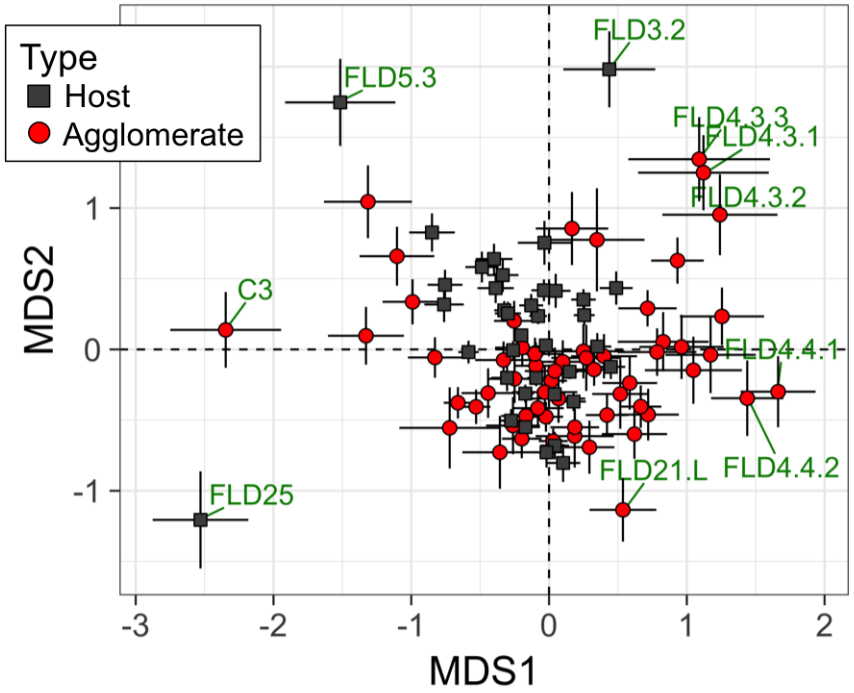

Figure 7.4: MDS modeled proximities of the median compositions of all agglomerates and host objects characterized with EDS in grid-based patterns (95 total objects). Points represent the mean of 500 non-metric MDS models generated using randomly-generated UP matrices and the uncertainties represent 2 standard deviations about that mean (Fig. 7.3). The proximity between objects highlights compositional similarity, while large distances between objects indicates those agglomerates or host objects are compositionally dissimilar. The majority of host objects tend to cluster towards the center, while agglomerates are more widely spread. Data are tabulated in Appendix I.

helps negate the influence of infrequent outlying compositions measured in host objects. In the case of FLD25, FLD3.2, and FLD5.3, much of the host objects contain outlying compositions, leading them to plot far from other host objects and agglomerates. The compositions of FLD25 and FLD3.2 have been previously discussed in Chapter 6: FLD25 contains a large region of primarily felsic composition and FLD3.2 appears largely unmelted/partially-melted from backscatter electron images. FLD5.3 is depleted in CaO, Al_2O_3, and MgO relative to the average bulk composition, and also exhibits a heterogeneous activity distribution (Table 4.6 and Figure 2.18).

In contrast to host objects, agglomerates tend to be less clustered near the origin. While agglomerates were previously noted as tending to be well-mixed due to their smaller size, fewer EDS measurements can be performed in each agglomerate, so a small number of outlying measurements may lead to an outlying composition. The spread of the agglomerates and tighter spread of the hosts in this MDS model are bolstered by the histograms in Figs. 4.11 and 4.13, which show the mean compositions of each object overlaid with the KDEs

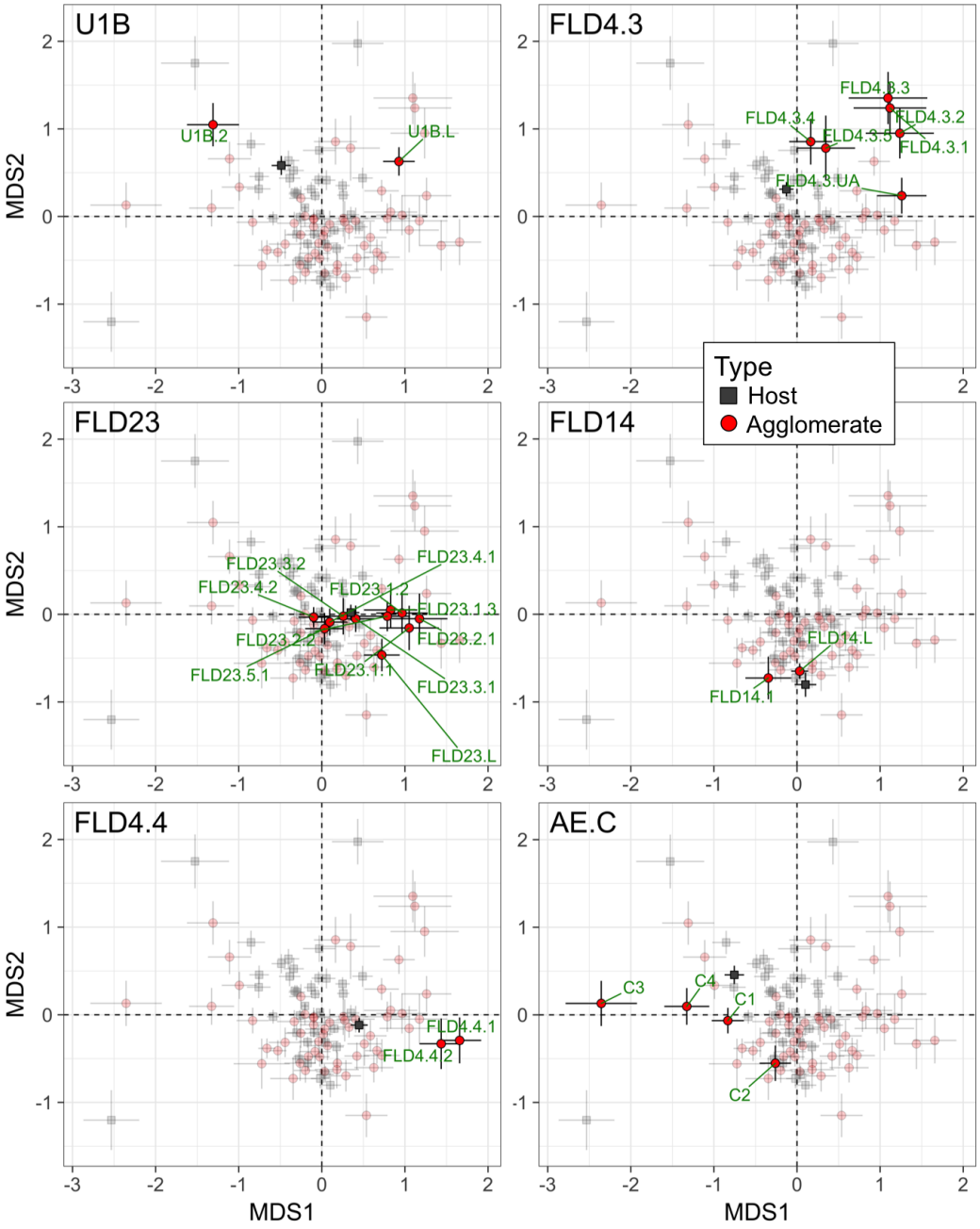

Figure 7.5: Examples of the relative compositional similarity between agglomerates and their host objects for the major element only dataset. The panels show the agglomerates and host objects of U1B, FLD4.3, FLD23, FLD14, FLD4.4, and AE.C while rendering all other characterized objects as partially transparent. These examples showcase several different compositional similarities between agglomerates and their host objects, as discussed in the text. Data are tabulated in Appendix I.

from the host object grid-based EDS measurements. These figures reveal a larger spread in mean agglomerate compositions relative to mean host object compositions.

There appears to be no segregation between the population of agglomerates and host objects, confirming that agglomerates and host objects do not preserve distinct compositional trends. Agglomerates and host objects *within the same sample* often have close proximities, however. Two examples of agglomerates compositionally similar to their host objects are FLD14, FLD23 (Figure 7.5), but while not shown, also include the agglomerates and host objects of U4, U3, FLD21, AA.B, AG.D, and FLD17 (Appendix I).

There are noteworthy exceptions: the agglomerates FLD4.3.1, FLD4.3.2, and FLD4.3.3, and FLD4.3.UA, plot far from FLD4.3, their host object (Figure 7.5). FLD4.3.1, FLD4.3.2, and FLD.4.3.3 are the agglomerates with the highest measured U isotope ratio in this study. In addition, the agglomerates U1B.2 and U1B.L plot far not only from their relatively compositionally homogeneous host object U1B (Figure 7.5 and Table 4.6), but plot even further from each other, suggesting a great degree of compositional dissimilarity between these agglomerates (unsurprisingly, U1B.L is an interior agglomerate while U1B.2 is a surface agglomerate).

While host objects are often similar to their associated agglomerates, agglomerates within the same sample are also often similar to *each other*. For example, the agglomerates in samples FLD14, FLD23, FLD4.4 and FLD4.3 (Figure 7.5), and while not shown, also include the agglomerates of FLD18, U3, U4, FLD21, AA.B, FLD17, and AG.D (11 of the 15 samples with both hosts and agglomerates characterized with EDS) have agglomerates that show one or more groupings in the MDS projection (Appendix I). This suggests that same-sample agglomerates tend to have similar compositions as well and therefore, may also be derived from similar precursor melts. In several instances (such as FLD4.4.1 and FLD4.4.2 in FLD4.4), agglomerates are compositionally similar to each other, but distinct in composition to the host object, which could be due to the breakup and agglomeration of parcels of melt distinct in composition to their respective host objects (and while not shown in Figure 7.5, other examples include the agglomerates of AA.B; Appendix I).

Samples with multiple clusters of compositionally similar agglomerates, such as sample FLD4.3 (FLD4.3.1, FLD4.3.2, and FLD4.3.3 form one group, FLD4.3.4, FLD4.3.5 form another, and FLD4.3.UA is distinct from both groups) suggest a formation history through agglomeration of multiple parcels of melt with distinct composition. This is bolstered by the observation that agglomerates FLD4.3.1, FLD4.3.2, and FLD4.3.3 are also spatially proximate to each other within sample FLD4.3, being within 80 μm of each other[3] and all are interior agglomerates. While FLD4.3.UA is within 100 μm of these agglomerates, FLD4.3.UA is a surface agglomerate, suggesting it collided at a later time. Similarly, the agglomerates FLD23.1.1, FLD23.1.2, FLD23.1.3 are all located spatially close to each other (within 150 μm of each other); FLD23.2.1, and FLD23.2.2 are within 50 μm of each other; agglomerates FLD23.4.1, FLD23.4.2, FLD23.5.1 are within approximately 300 μm of each

[3]These spatial distance were determined by measuring the distances between approximate centers of the furthest agglomerates.

other; and FLD23.3.1 and FLD23.3.2 are 85 μm apart. This consistent observation further shows that compositionally-similar agglomerates are often preserved at spatially proximate locations. However, in the case of agglomerates FLD4.4.1 and FLD4.4.2, two surface agglomerates that have similar compositions, are located on near-opposite sides of their host object, being spaced approximately 1 mm apart. Finally, having both spatial proximity and similar location of attachment (attached, surface, interior) does not necessarily imply compositional similarity, as exemplified by agglomerates C1 and C2 in sample AE.C (both attached agglomerates), spaced approximately 280 μm apart.

7.4 MDS model of combined major element/U isotopic dataset

To determine how the differing bomb vapor interactions between agglomerates and host objects affects their compositional similarity, U isotopic measurements are included in the second MDS model (Fig. 7.6). This model uses the same combined major element/U isotopic dataset as the PCA analysis in Section 6.7; tabulated in Appendix G) to calculate the median compositions of agglomerates and host objects, calculate the distances between these objects in compositional space, then model those distances with MD . In contrast to the PCA analysis, where the major element compositions of host objects taken in grid-based patterns were used to generate the PCA model and the combined major element/U isotopic dataset was projected through the PCA model, this MDS model directly uses the combined major element/U isotopic dataset to generate the MDS model.

The MDS model from the combined major element/U isotopic dataset uses the SiO_2, Al_2O_3, K_2O, CaO, FeO, and TiO_2 compositions from targeted EDS rasters within/around SIMS craters combined with the $^{235}U/^{238}U$ ratio from these SIMS analyses to project the 7-dimensional distances of 58 total objects into 2-dimensional space. These 58 objects include 17 host objects, 31 agglomerates in 13 samples, and 10 measurements of agglomerates over interfaces (in 6 samples) that also significantly sampled the host (defined here as >25% of the total crater or raster area overlapping the host).

For this model, SIMS rasters over the interface that significantly sampled the host were considered as separate compositions (shown as blue triangles), to avoid biasing the dataset. These ten measurements include five measurements for which there are at least one other SIMS/EDS measurements within the agglomerate itself (U1B.L, FLD10.L, FLD17.int.1, FLD23.L, and FLD4.3.3) and five measurements where these interfacial measurements are the only measurements characterizing the agglomerate (U3.3, U3.4, U3.5, FLD4.3.1, and FLD4.3.5). Of the five interfacial measurements where there are other SIMS/EDS measurements to characterize the agglomerate, four (U1B.L, FLD17.int.1, FLD23.L, and FLD4.3.3) are from agglomerates with Si interfaces. These interfacial compositions over Si interfaces plot between the agglomerate and the host in terms of proximity (Figure 7.7). Having the interfacial composition plot between the host object and the agglomerate for the four Si

interfaces suggests the Si interface itself does not greatly alter the overall composition of the measurement, as plotting between the agglomerate and host object is expected because both are sampled during the analysis.In contrast, the interfacial composition of the only agglomerate exhibiting a CaMgFe interface, FLD10.L, does not plot between FLD10.L and FLD10 in Figure 7.6. These interfaces are further discussed in Chapter 8 and 9.

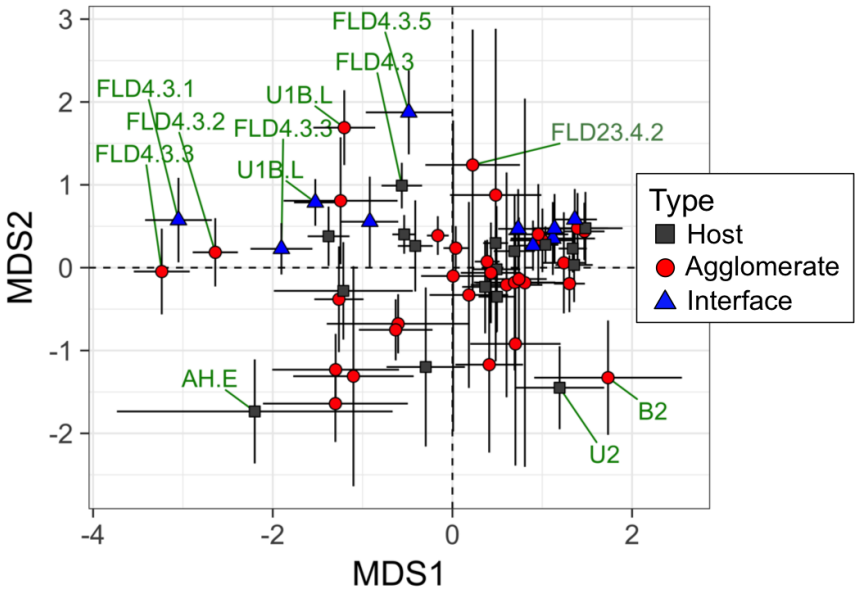

Figure 7.6: MDS plot of all agglomerates and host objects characterized with the combined major element/U isotopic dataset. Interfaces measurements are SIMS rasters that overlapped the host with more than 25% of the total crater or raster area occupied by the host. Points represent the mean of 500 non-metric MDS models generated using randomly-generated UP matrices and the uncertainties represent 2 standard deviations about that mean. The proximity between objects indicates major element/U isotopic compositional similarity, while large distances between objects shows that those objects are compositionally dissimilar. There are larger uncertainties in this MDS projection due to the fewer analyses used to characterize each object compared to the major element only dataset (Fig. 7.4). Outliers in the MDS projection are marked and data are tabulated in Appendix I.

Objects that clustered closely in the MDS plots using EDS raster data also tend to cluster closely in the combined EDS/SIMS MDS plots, despite using two different data sets. (Compare the clustering of agglomerates and host objects between the two MDS projections of U1B, FLD4.3, FLD23, and FLD14 in Figures 7.5 and 7.7). While they are two separate data sets, as shown in Chapter 6, the mean major element compositions of objects, as calculated from the two distinct datasets, do not deviate appreciably from one another when there are more than 1–2 combined major element/U isotopic measurements are used to calculate the composition of an object. However, what combined major element/U isotopic MDS model shows, in contrast to the major element MDS model discussed in Section 7.3, is that the differing extent that agglomerates and their host objects interacted with the bomb

vapor does not greatly alter the clustering when using only major element compositions to generate the MDS model. That is, agglomerates and hosts that exhibit similar major element compositions do not tend to exhibit grossly different U isotopic compositions.

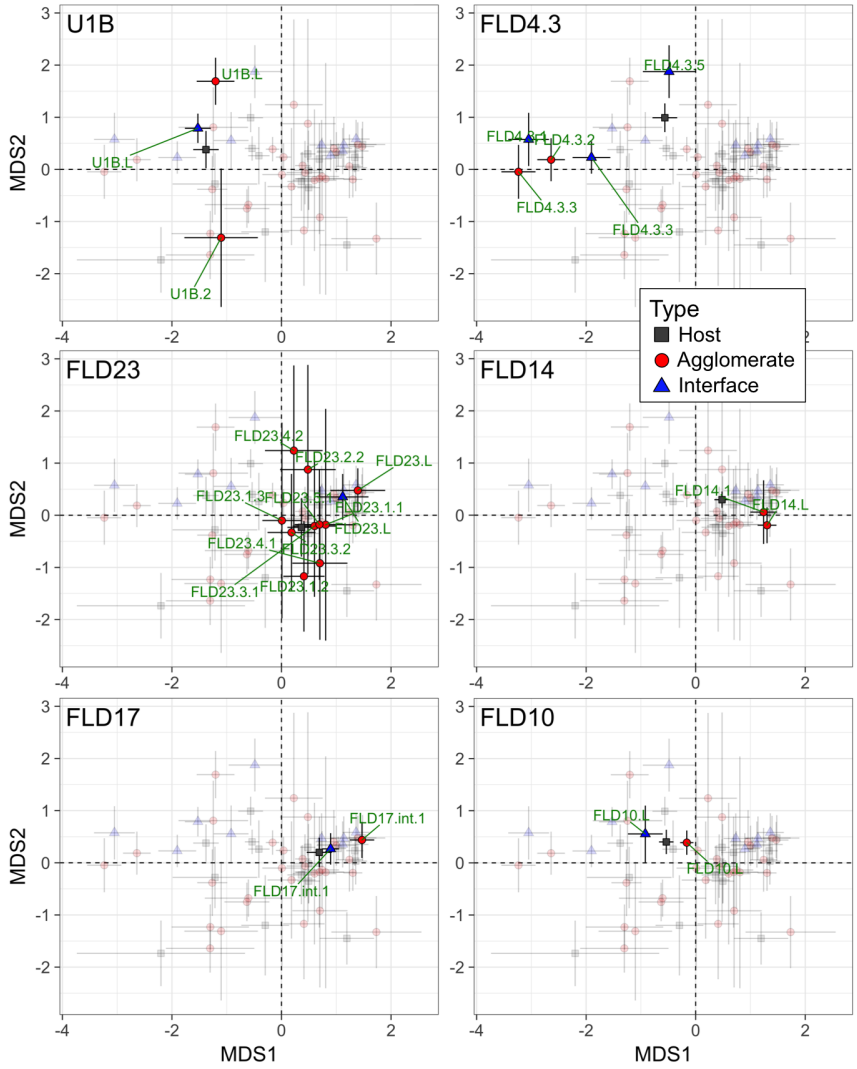

Figure 7.7: MDS plot of all agglomerates and host objects characterized with the combined major element/U isotopic dataset. Interfaces measurements are SIMS rasters that overlapped the host with more than 25% of the total crater or raster area occupied by the host. Points represent the mean of 500 non-metric MDS models generated using randomly-generated UP matrices and the uncertainties represent 2 standard deviations about that mean. The proximity of points highlights compositional similarity, while large distances between points shows that those points are compositionally dissimilar. The majority of host objects tend to cluster towards the center, while agglomerates have a wider spread. Data are tabulated in Appendix I.

7.5 Compositional similarity by sample

MDS models the Euclidean distances between agglomerates and hosts and projects them in 2D space to simultaneously visualize the similarity of all *all* characterized objects. When considering agglomerates and host objects in the same sample, only a single metric needs to be considered: the Euclidean distance from agglomerates to *their* associated host object (*e.g.*, the Euclidean distance between interior agglomerate U1B.L and host U1B; Figure 7.8). Collectively, these plots show that with respect to the data set of EDS rasters where entire objects were characterized, agglomerates tend to be compositionally similar to the associated host objects.

Figure 7.8 shows the compositional similarity of agglomerates relative to each of their hosts in three ways. First, in the top panel, the Euclidean distance (Eqn. 7.1) is plotted for each agglomerate relative to its host, with all other objects being shown as partially-transparent. The middle panel shows the distance of agglomerates to their hosts as a percentile of its distance all other objects characterized in this dissertation relative to that same host (including all other host objects and other agglomerates). For example, if an agglomerate is plotted at the 25th percentile relative to its host, 75% of all other characterized objects, both agglomerates and hosts, are more compositionally dissimilar to that particular host than the agglomerate. Finally, the last panel shows a cumulative distribution function (CDF) of the distance percentile of all agglomerates relative to their host objects. The agglomerates in the top two panels of Figure 7.8 are colored and shaped by their location of attachment and their uncertainties as 2σ about the mean from 500 UP matrix simulations, as described above. As a proxy for uncertainty in the CDF plot in the bottom panel of Figure 7.8, 500 UP matrices were generated and their CDFs drawn (shown in pale grey). The median of those 500 UP matrix simulations calculating the distance percentile from agglomerates to their respective hosts is shown in the bold red line.

The median CDF in Figure 7.8 shows that over 50% of all agglomerates are within the 25th distance percentile relative to their hosts (median percentile is 55% of all agglomerates, with the simulations ranging from 38% to 58%) and over 75% of all agglomerates are within the 50th distance percentile relative to their hosts (median percentile is 81% of all agglomerates, with the simulations ranging from 66% to 84%).

Collectively, the major element composition of agglomerates tend to be more similar in composition to their hosts than other hosts or agglomerates in other samples. This compositional similarity indicates that agglomerates and their host objects generally tend to be formed from similar precursor melts. This result is surprising given first the diversity of unmelted soil present in the lithology and second the turbulent mixing and rapid expansion that occurs within the fireball, which may incorporate, loft, and heat many thousands of tons of soil for each kT of yield (Table 1.1).

If agglomerates and their host objects are formed from similar parcels of precursor melts, lofted and melted soil likely did not travel far between formation and agglomeration before quenching. That is, melts are locally homogeneous. In addition, as an ensemble, the scale of compositional similarity suggests that melts do not travel far within the fireball before

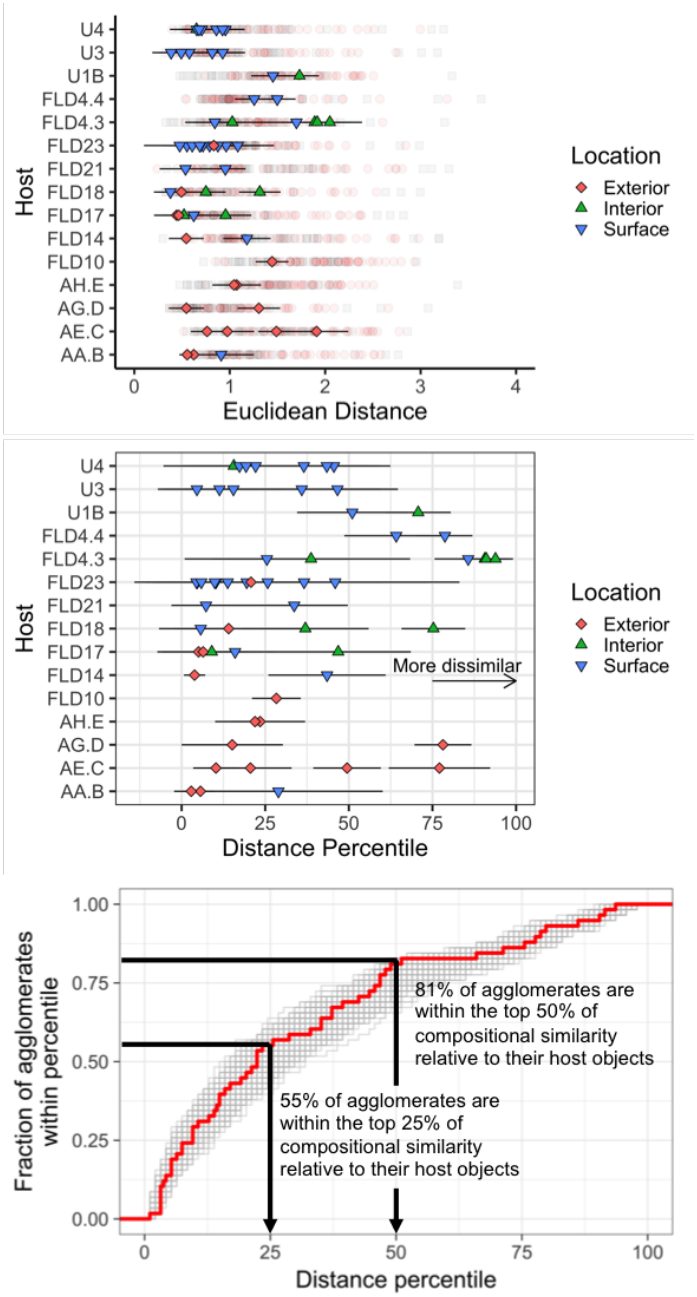

Figure 7.8: The similarity of agglomerates to their respective hosts for the EDS raster dataset characterizing entire objects. The top panel shows the Euclidean distance of agglomerates (colored and shaped by their attachment location) to their respective hosts, with all other objects shown as partially transparent. The middle panel shows these distances as a percentile, showing how similar agglomerates are relative to all other characterized objects. Uncertainties are 2σ for the top and middle panels. The bottom panel shows the cumulative distribution function of 500 randomly generated UP matrix configurations of the distance percentiles in grey with the median CDF highlighted in red. Data are tabulated in Appendix I.

colliding and agglomerating prior to quenching. Rapid cooling timescales (fallout formation occurs on timescales of order seconds [44, 67]) prevents complete incorporation and mixing of agglomerates and their host objects, preserving their distinct mixing patterns and textures and the compositional interface separating them, so they appear as distinct objects within the same sample while exhibiting similar major element compositions.

There are notable exceptions to the general trend of compositional similarity between agglomerates and their host objects. The agglomerates most dissimilar in composition to their host objects are the interior agglomerates FLD4.3.1, FLD4.3.2, and FLD4.3.3 incorporated into host FLD4.3. Notably these are also the agglomerates measured to be most enriched in U isotopes in this study and will be explored and discussed further in Chapter 9.

Finally, attached agglomerates appear to be more similar to their respective hosts than either surface or interior agglomerates (Fig. 7.8). Thirteen of the seventeen attached agglomerates characterized by EDS (≈76%) are within the 25th distance percentile, compared to of the 15 of the 31 surface agglomerates (≈44%) and 2 of the 10 interior agglomerates (20%). However, roughly the same percent of interior and surface agglomerates are within the 50th distance percentile: 15 of the 17 attached agglomerates (≈88%), 27 of the 31 (≈87%) on the surface agglomerates, but only 5 of the 10 (50%) interior agglomerates fall within the 50th distance percentile of their host. This suggests that interior agglomerates (melts that collided and accreted with their host melt at earlier times and higher temperatures), despite being fully incorporated into the host object and interacting with the host melt longer than other co-located surface or attached agglomerates, are to be formed from a more dissimilar parcel of melt relative to their associated host object.

7.6 Compositional and U isotopic similarity by sample

Next, to determine how including the bomb vapor interaction affects the similarity between agglomerates and their hosts, the combined major element/U isotopic dataset is used to compare the similarity between agglomerates and their respective hosts. Figure 7.9 shows the same three panel scheme explained in the section above except using the combined major element/U isotopic dataset. The top panel shows the Euclidean distance of agglomerates relative to their hosts (29 agglomerates in 12 hosts, whose color and shapes correspond to their location of attachment).[4] The middle panel shows these distances as percentiles, which shows each agglomerate's similarity to its associated host object relative to all other objects characterized with the combined SIMS/EDS approach. Finally, the bottom panel shows the cumulative distribution function of distance percentiles (from the middle panel) from the median of 500 UP matrix simulations.

[4]Excluding analyses over interfaces where the host was significantly sampled by the SIMS raster to avoid biasing the dataset.

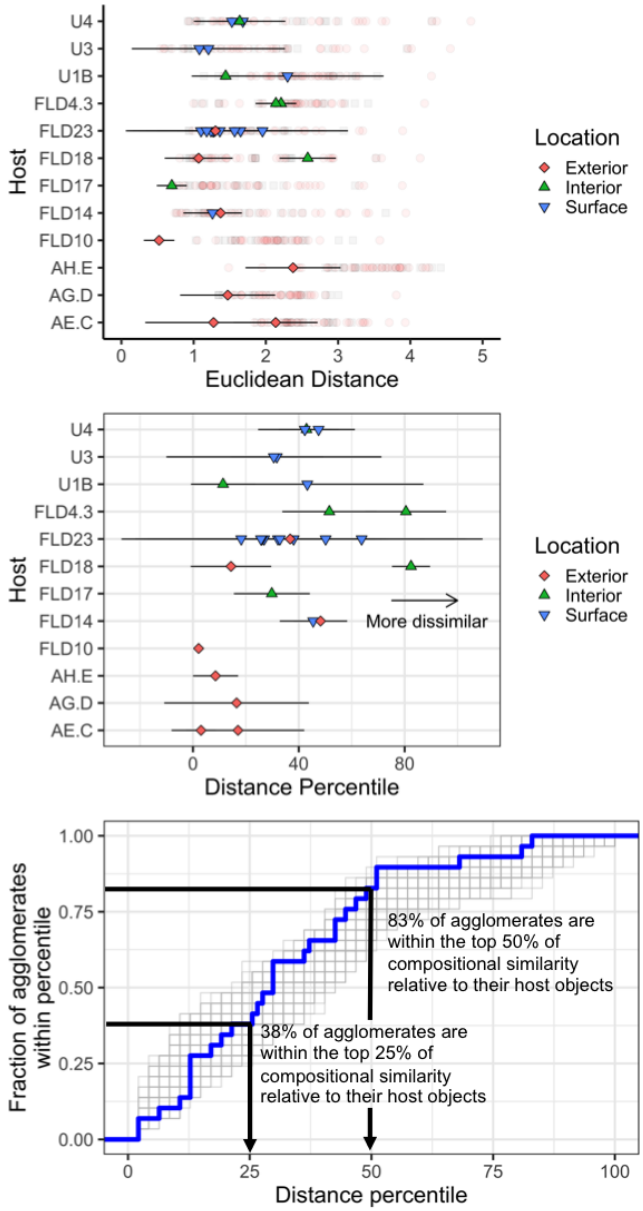

Figure 7.9: The similarity of agglomerates to their respective hosts for the combined major element/U isotopic dataset. The top panel shows the Euclidean distance of 29 agglomerates (colored and shaped by their attachment location) to their respective hosts, with all other objects shown as partially transparent. These plots exclude 5 agglomerates where the only SIMS analysis of the agglomerate also significantly sampled the host in addition to the interface and the agglomerate: FLD4.3.1, FLD4.3.5, U3.3, U3.4, and U3.5. The middle panel shows these distances as a percentile, showing how similar agglomerates are relative to all other characterized objects. Uncertainties are 2σ for the top and middle panels. The bottom panel shows the cumulative distribution function of 500 randomly generated UP matrix configurations of the distance percentiles in grey with the median CDF highlighted in blue. Data are tabulated in Appendix I.

The combined major element/U isotopic dataset has more uncertainty than the grid-based EDS dataset (shown in Figure 7.8) because of the fewer number of measurements per object. However, these data show a similar trend to the grid-based EDS: as a collection, agglomerates are more similar to their host objects than to other agglomerates or host objects in other samples. The CDF shows that from the 500 UP matrix simulations, the median percent of agglomerates that are within the 25th distance percentile are 38% (ranging from 24% to 58%), 83% are within the 50th distance percentile (ranging from 62% to 90%), and 93% of the agglomerates fall within the 75th distance percentile to their respective hosts (ranging from 79% to 100%). Overall, these results show not only compositional similarity between agglomerates and their respective hosts, but U isotopic similarity as well.

Similar to the grid-based EDS dataset, *exterior* agglomerates are most similar to their host objects, compared to both surface and interior agglomerates. The Euclidean distances of the combined major element/U isotopic compositions of 6 of the 8 attached agglomerates (75%) are within the 25th distance percentile of their hosts, while 0 of the 15 surface agglomerates, and 1 of the 6 interior agglomerates (≈17%) fall within the 25th percentile of their hosts. All eight attached agglomerates (100%) are within the 50th percentile in terms of similarity to their hosts, while 13 of the 15 surface agglomerates (≈87%) and 2 of the 5 interior agglomerates (40%) fall within the 50th percentile of their hosts. Again, the most dissimilar agglomerates are interior agglomerates, with FLD18.2 and FLD4.3.3 being more dissimilar to their hosts than more than 75% of the characterized objects (81st ± 5 and 81st ± 7 distance percentiles, respectively).

The compositional and U isotopic similarity between agglomerates and their host objects suggests that not only do they tend to be formed from similar precursor melts, but that agglomerates and host objects interacted similarly with the bomb vapor in the fireball. This observation suggests that agglomeration occurs in a localized environment in the fireball, as inter-sample U isotopic heterogeneity is extensive (see Chapter 5), even for samples this population, which were all collected at similar distance from ground zero.

7.7 Conclusion

Multidimensional scaling provides a means to visualize and compare the similarity between all the compositions of agglomerates and host objects characterized in this study simultaneously. In this chapter, an MDS model was first created using the grid-based EDS dataset alone (Figures 7.4). This first MDS model included SiO_2, Al_2O_3, Na_2O, K_2O, CaO, FeO, and TiO_2 as variables in calculating different objects' similarity based on their median composition for 95 total objects: 58 agglomerates in 15 samples and 37 host objects. This model using only major element compositions shows that host objects tend to be fairly tightly clustered, implying a high degree of similarity in their median compositions (with three exceptions in hosts FLD25, FLD3.2, and FLD5.3). The agglomerates, despite being well-mixed and compositionally quasi-homogeneous, exhibit a greater degree of scatter because they are more likely to contain anomalous compositions. Observations from the MDS plots alone

show that agglomerates and host objects in the same sample tend to cluster close together, whether it be host objects and agglomerates (*e.g.*, the host FLD23 and its associated agglomerates; Figure 7.5), or agglomerates clustering near other agglomerates located in or attached to the same host (*e.g.*, the agglomerates of FLD4.4; Figure 7.5).

This host-agglomerate similarity is also apparent in the second MDS model, created using the dataset of SIMS measurements of U isotopic ratios combined with EDS rasters from within/around those SIMS analysis craters (Figures 7.6). This MDS model shows how the addition of a bomb vapor component affects the compositional similarity between agglomerates and their host objects. The EDS/U MDS model included $^{235}U/^{238}U$, SiO_2, Al_2O_3, K_2O, CaO, FeO, and TiO_2 as variables in calculating different objects' similarity based on their median composition for 60 total objects: 33 agglomerates in 13 samples, 10 interface measurements that also significantly sampled the host object in 6 samples, and 17 host objects. This MDS model showed a greater degree of uncertainty because of fewer measurements per object, but agglomerates and their host objects that clustered closely in the major element only MDS model also tended cluster closely in the major element/U isotopic MDS model. This consistency between both MDS models indicate that agglomerates and their host objects that are compositionally similar also tend to have similar U isotopic compositions as well. Furthermore, all interface measurements over "Si" interfaces plotted between the agglomerate and the host, suggesting a shared similarity between the two objects. However, the interface measurement over FLD10.L, which is a "CaMgFe" interface did not, likely due to the existence of a deposition enriched in species such as Fe, Ca, Mg, and $^{235}U/^{238}U$ at the interface (discussed in Chapters 8 and 9).

Instead of relying on a qualitative 2-dimensional representation of 7-dimensional space to determine the compositional similarities between objects, the Euclidean distance for agglomerates relative to their hosts was calculated for both the major element and combined major element/U isotopic datasets (Figs. 7.8 and 7.9, respectively). These data quantify the observations from the MDS plots: agglomerates tend to be more similar to their hosts than other objects when both considering the EDS raster only dataset and the EDS/SIMS combined dataset. For the EDS raster dataset (Fig. 7.8), which includes more objects, the median CDF from the 500 UP matrix simulations shows that 55% of all agglomerates are compositionally more similar to their respective hosts than 75% of all other characterized objects (that is, they fall within the 25th distance percentile) and a median of 81% of agglomerates are compositionally more similar to their respective hosts than 50% of all other characterized objects. Similarly, when using the EDS/SIMS dataset, which adds U and excludes Na_2O, (Fig. 7.9), a median of 47% agglomerates fall within the 25th distance percentile of their respective hosts and a median of 83% agglomerates fall within the 50th distance percentile of their respective agglomerates.

The compositional similarity between agglomerates and their host objects suggests that agglomerates, as a collection, tend to likely have formed from similar precursor melts as their host objects. This suggests agglomerates were not formed some other material (such as a finer size fraction of soil), nor did agglomerates experience a grossly different environment in the fireball (such as excessive volatilization compared to their hosts).

The U isotopic and compositionally similarity between agglomerates and their hosts suggests that, as a collection, agglomerates and host objects also experienced similar ambient environments in the fireball prior to agglomeration. In addition to being formed from melts of similar compositions, agglomerates and their host objects tend to incorporate similar amounts of U from vapor phase in the fireball.

Finally, both datasets indicate that exterior agglomerates tend to be most similar to their host objects (≈76% and 75% of the exterior agglomerates falling within the 25th distance percentile in terms of similarity to their hosts for the EDS raster and EDS/SIMS datasets, respectively), followed by surface agglomerates, and then interior agglomerates. Exterior agglomerates are also observed to most frequently exhibit CaMgFe compositional interfaces between themselves and their host objects. This location of attachment (both the agglomerate and the host must have been relatively cool and near closure) and the proposal of these interfaces being a vapor deposition layer imply a late stage collision and accretion [68]. It is possible longer residence times in the fireball homogenize exterior agglomerates more than surface or interior agglomerates.

Both the major element and U isotopic compositions of agglomerates and host objects have been explored in Chapters 4-7. However, the compositional interfaces of agglomerates, while studied in recent works, have yet to be analyzed here [67, 68, 84]. In particular, the Si interface, which is observed bounding agglomerates in all attachment locations and appears with much greater frequency than CaMgFe interfaces (Chapter 3) requires study as it has not been previously noted in the fallout literature and may add insight into the fireball environment at the time of agglomeration.

Chapter 8 studies the major element behavior across the CaMgFe interfaces studied here, comparing the results to previous findings, then characterizes the major element behavior across Si interfaces. In Chapter 9, the U isotopic behavior across both CaMgFe and Si interfaces are also studied to understand how the two compare and possible scenarios that could lead to the formation of Si interfaces.

Chapter 8

Interface Major Element Compositions

8.1 Chapter overview

This study characterizes the major element and U isotopic composition of exterior, surface, and interior agglomerates. However, compositional interfaces may preserve the ambient vapor environment just prior to agglomeration, informing oxidation conditions and how the surfaces of melts interacted with the fireball prior to quenching. Two types of compositional interfaces between agglomerates and host objects are observed. The first interface type ("CaMgFe interfaces") tends to be enriched in CaO, FeO, and MgO and depleted in Al_2O_3. The second interface type ("Si interfaces") are enriched in SiO_2 and depleted in Al_2O_3 and all other major element oxides. While the behavior of major elements and the possible source of CaMgFe interfaces has been discussed in depth previously [67], the occurrence and source of Si interfaces has not been previously noted in the literature, despite being observed in this study to occur with a much higher frequency than CaMgFe interfaces (see Chapter 3) [67, 68, 84].

To characterize the behavior of major elements across compositional interfaces, quantified EDS compositional maps are used to extract smoothed line traverses perpendicular to the interface. From these maps, the major element composition of interfaces is determined and compared with EDS raster data of hosts, agglomerates, and unmelted soil first using bivariate plots and then by projecting the interface compositions into the PCA model generated in Chapter 6 from the grid-based EDS raster measurements of host objects ($n = 3,698$).

Previously unreported Si interfaces surround agglomerates at all attachment locations, while CaMgFe interfaces are observed only arround exterior and surface agglomerates. Si interface are also observed to surround host objects, a behavior unobserved in CaMgFe interfaces. The formation of Si interfaces is likely a condensation process, which occurs earlier than the formation of CaMgFe interfaces. The formation of Si interfaces is hypothesized to occur in dusty regions of the fireball, where the partial pressure of SiO_{gas} is high enough to

preferentially condense Si from the vapor phase onto the surface of melts.

8.2 Recent findings of CaMgFe interfaces

Weisz (2016), Weisz et al. (2017), and Weisz et al. (2018) studied the major element composition and U isotopic composition of interfaces between host objects and exterior agglomerates and two surface agglomerates in five samples [67, 68, 84]. Data from eight agglomerates across four samples are used in this dissertation: AA.B (agglomerates B1, B2, and B3), AE.C (agglomerates C1 and C2), AG.D (agglomerates D1 and D2), and AH.E (agglomerate E1).[1] In the nomenclature used in this dissertation, agglomerate B1 is an exterior agglomerate attached to agglomerate B3, which is an exterior agglomerate attached to the host of AA.B. Agglomerate B2 is a surface agglomerate of agglomerate B3, between B1 and B3. Agglomerates C1 and C2 are both exterior agglomerates attached to AE.C, agglomerates D1 and D2 are both exterior agglomerates attached to AG.D, and agglomerate E1 is an exterior agglomerate attached to sample AH.E, while agglomerate E2 is a surface agglomerate of sample AH.E. Figure 8.1 shows two of these studied CaMgFe interfaces in sample AG.D. Weisz conducted EPMA traverses across these interfaces to measure major element composition (SiO_2, Al_2O_3, Na_2O, K_2O, CaO, FeO, TiO_2, MgO, and MnO) of the interface using 1 μm diameter analyses spaced 1 μm apart across entire agglomerates and across interfaces. The behavior of U isotopes at CaMgFe interfaces was measured by sampling the interfaces using NanoSIMS rasters. Analyzed isotopes via NanoSIMS include: ^{235}U, ^{238}U, ^{30}Si, ^{44}Ca, and either ^{54}Fe or ^{56}Fe, and were used to produce NanoSIMS image of ^{235}U/^{238}U, ^{235}U/^{30}Si (used as a proxy for U concentration since the Si content was found to vary <10% across CaMgFe interfaces), ^{44}Ca/^{30}Si, and ^{54,56}Fe/^{30}Si (the latter two ratios serve as proxies for the Ca and Fe concentrations across the interface, respectively).

The compositional interfaces studied by Weisz (2016) were observed to be enriched in Ca, Fe, Mg, and ^{235}U and depleted in Al relative to the region immediately adjacent in either the agglomerate or host object. Table 8.1 tabulates the enrichments or depletions of characterized major element oxides and isotope ratios across the studied interfaces. Figure 8.2 shows the enrichment of four major element oxides across four interfaces as measured by Weisz using EPMA [68]. Weisz speculated that the source of these interface enrichments is a late-stage deposition of species in the vapor phase. This layer becomes trapped between two rapidly cooling, viscous, molten or partially-molten silicate objects, so has a limited amount of time to diffuse into both the agglomerate and host object before the melt quenches.

Using volatility arguments alone, the co-enrichment of Ca, Mg, and Fe and depletions of Al and Ti cannot be explained given the oxide forms assumed in this dissertation. Al_2O_3 has a similar boiling point to CaO (observed to be enriched in some interfaces) and is often co-located with CaO in a major mineral phase present in the soil—plagioclase. Weisz (2016) explains that the unknown speciation and variable oxygen fugacity within the fireball can

[1] This dissertation does not use data from agglomerate C3 in sample AE.C or agglomerate E2 in sample AH.E because NanoSIMS analyses were not conducted across their compositional interfaces.

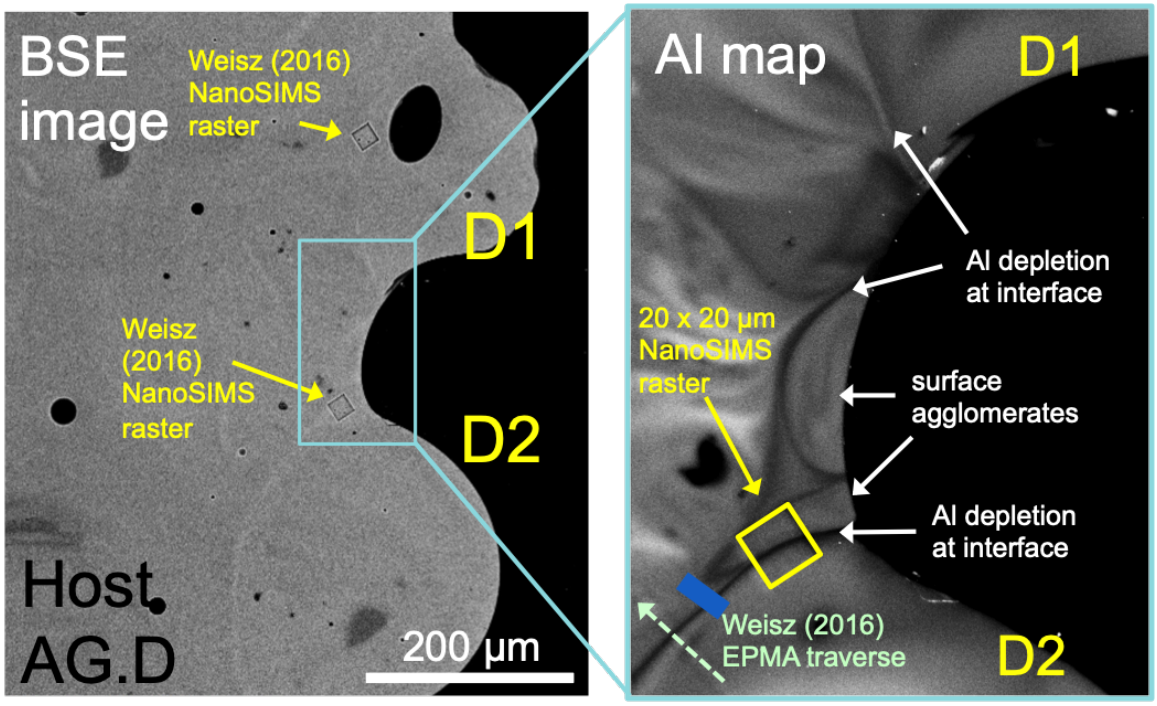

Figure 8.1: BSE image of CaMgFe interfaces previously characterized by Weisz (2016) for exterior agglomerates D1 and D2 (in sample AG.D). Inset Al compositional X-ray map highlights the respective enrichment and depletion of Al at the compositional interface. The Al compositional X-ray map on the far right shows two uncharacterized surface agglomerates between agglomerates D1 and D2.

significantly affect the condensation temperatures. While many fireball models assume a highly oxygenated fireball, several recent studies provide evidence for a highly-variable and partially-reducing fireball environment [44, 69].

To confirm the observations of Weisz (2016) and Weisz et al. (2017) regarding the location of CaMgFe interfaces and the major element behavior across these boundaries, three additional CaMgFe interfaces in three samples are characterized in this study. Two of these CaMgFe interfaces were subsequently sampled with NanoSIMS analyses to compare the behavior of enriched U across these boundaries with the findings of [67, 68]. All CaMgFe interfaces in this study (three new CaMgFe interfaces in three samples in addition to the eleven CaMgFe interfaces in five samples characterized by Weisz (2016)) bound either exterior or surface agglomerates, bolstering the argument that the source of this interface is a *late-stage* process.

8.3 Si interfaces

Si interfaces were first noted in this study when using qualitative compositional maps of whole samples to identify the size, frequency, and location of agglomerates (Figure 3.10).

Table 8.1: Summary of initial findings on CaMgFe interfaces, as first reported by Weisz (2016) and Weisz et al. (2017) showing the relative enrichment or depletion of major element oxides, the $^{235}U/^{30}Si$ ratio and $^{235}U/^{238}U$ ratio at 9 interfaces (11 total interface scans: two scans were conducted across agglomerates C1 and C3) in five samples. This summary was determined using the supplemental data tables from [67], which was analyzed independently for this study. Interface compositions are considered enriched if a point within 1 μm of the interface peak identified by Weisz et al. (2017) is greater than the mean of concentrations or ratios between 1 and 3 μm on both sides of the interface.

Element	Interface behavior
SiO_2	Enriched in 5 of 11 interfaces
Al_2O_3	**Depleted** in 10 of 11 interfaces
Na_2O	Enriched in 3 of 11 interfaces
K_2O	**Depleted** in 7 of 11 interfaces
CaO	Enriched in 11 of 11 interfaces
FeO	Enriched in 11 of 11 interfaces
TiO_2	**Depleted** in 6 of 11 interfaces
MgO	Enriched in 9 of 11 interfaces
$^{235}U/^{30}Si$	Enriched in 5 of 9 interfaces
$^{235}U/^{238}U$	Enriched in 6 of 9 interfaces

While CaMgFe interfaces are only observed to bound surface and exterior agglomerates, the discovery of Si interfaces revealed the preservation of interior agglomerates in these fallout samples, indicating some Si interfaces formed comparatively earlier to CaMgFe interfaces for agglomerates attached to the same host. While Si interfaces are observed to predominantly bound surface and interior agglomerates, they do infrequently bound exterior agglomerates as well, as discussed below. Furthermore, Si interfaces are observed to occur with greater frequency than CaMgFe agglomerates. Of the 233 agglomerates in 18 samples identified in Chapter 3, 200 are bounded by Si interfaces (∼86%). Given the frequency of Si interfaces, it is important to characterize major and trace element compositions across these boundaries to hypothesize under what conditions they might form and determine how they differ from CaMgFe interfaces.

8.4 EDS mapping of interfaces

To characterize compositional interfaces, this dissertation uses quantified EDS maps collected at resolutions of <0.3 μm/pixel. The magnification of these maps varied, but sampled at least ∼10 μm on either side of the interface. Each interface was mapped until pixels at the interface contained at least 1000 counts of Si and several hundred counts of Al, which took between 3–8 hours. Elements such as Fe, Ca, and Al contained ∼30–50 counts per pixel. Maps were then quantified using the internal ZAF quantification scheme of Bruker's ESPIRIT 2 software and then transformed to oxides, using the assumed stoichiometry discussed earlier in this dissertation (Section 4.2). In contrast to EDS raster analyses, compositions of quantified

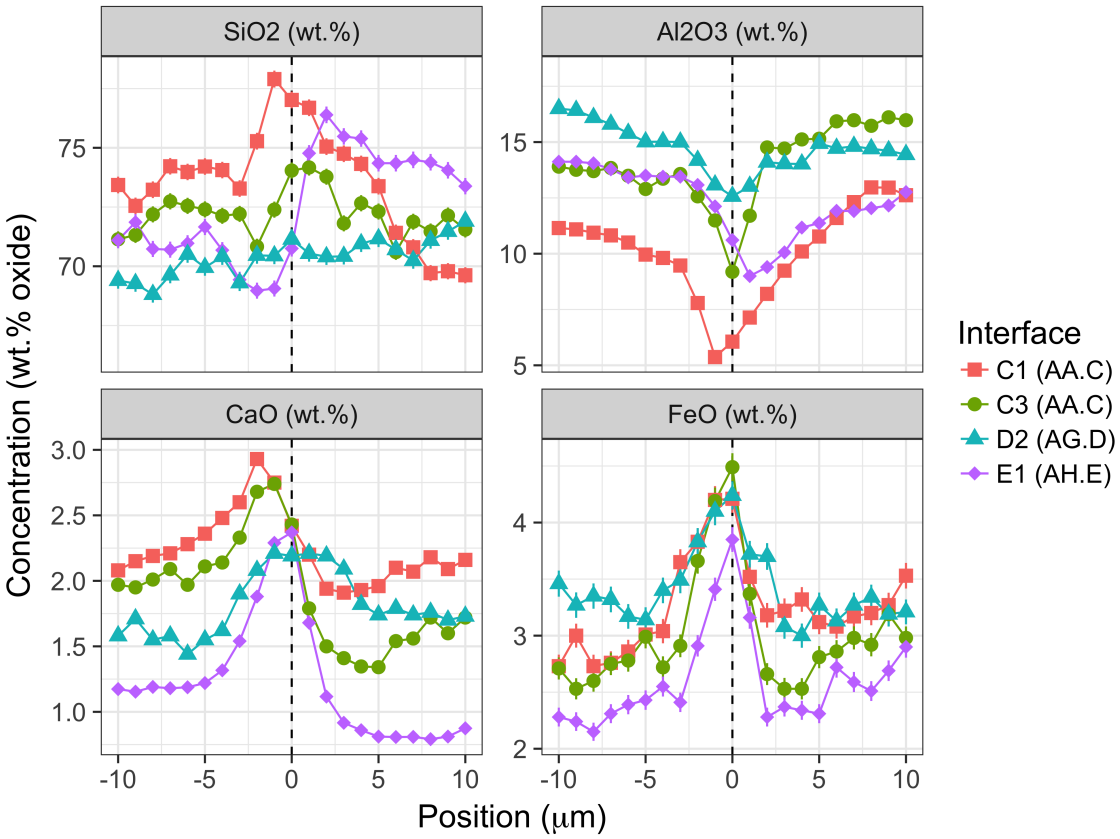

Figure 8.2: EPMA traverses across 4 CaMgFe interfaces (a subset of the 11 studied by Weisz (2016) and Weisz et al. (2017)) showing the major element behavior of SiO_2, Al_2O_3, CaO, and FeO across the interfaces. Plots are generated for this study using data from [67] and are centered at $x = 0$ μm based on their FeO maxima. Traverses were conducted using a 1 μm primary electron beam and analyses were spaced 1 μm apart. Traverses move from the agglomerate side on the left of each plot, across the interface at $x = 0$ μm, into the host object on the right. Uncertainties are 1σ and are smaller than the points in all panels except the FeO panel. The maxima in three of the four Si peaks relative to both the agglomerate and host object side are slightly offset relative to the FeO peak (C1's SiO_2 peak is offset by 1 μm towards the agglomerate, while C3 and E1 are offset towards the host object). While SiO_2 appears to be generally enriched near the interface, the relative change in SiO_2 composition is small, less than 10% compared to the agglomerate composition for all interfaces characterized in [67, 68]. This argument is used in [67, 68] to justify using the $^{235}U/^{30}Si$ ratio as a proxy for the U concentration across the interface. In contrast, the CaO and FeO interface compositions are enriched at CaMgFe interfaces, generally 50% or more relative to the agglomerate composition ($x < 0$ μm).

line scans were normalized to 100.

ImageJ image analysis software was used to extract linear profiles across the interfaces [86]. Line profiles were smoothed (*i.e.*, averaged) using widths of 50 pixels or more to reduce uncertainty. These smoothed scans were extracted along the region of the interface that exhibited the least amount of curvature to avoid artificially increasing the apparent width

of the interface and drawn roughly perpendicular to interface boundaries (Figure 8.3).

To determine the uncertainty of each smoothed step in the line scan, a one pixel wide line profile was drawn perpendicular to the line scan, with a length equal to the number of pixels used for smoothing (between 50–250 pixels long). Each pixel represents a sample of the composition along the interface traverse. The presented uncertainty is 2 times the standard error the mean (2SEOM) of these pixels ($\geq$50 pixels, depending on the number of pixels smoothed for that particular interface).

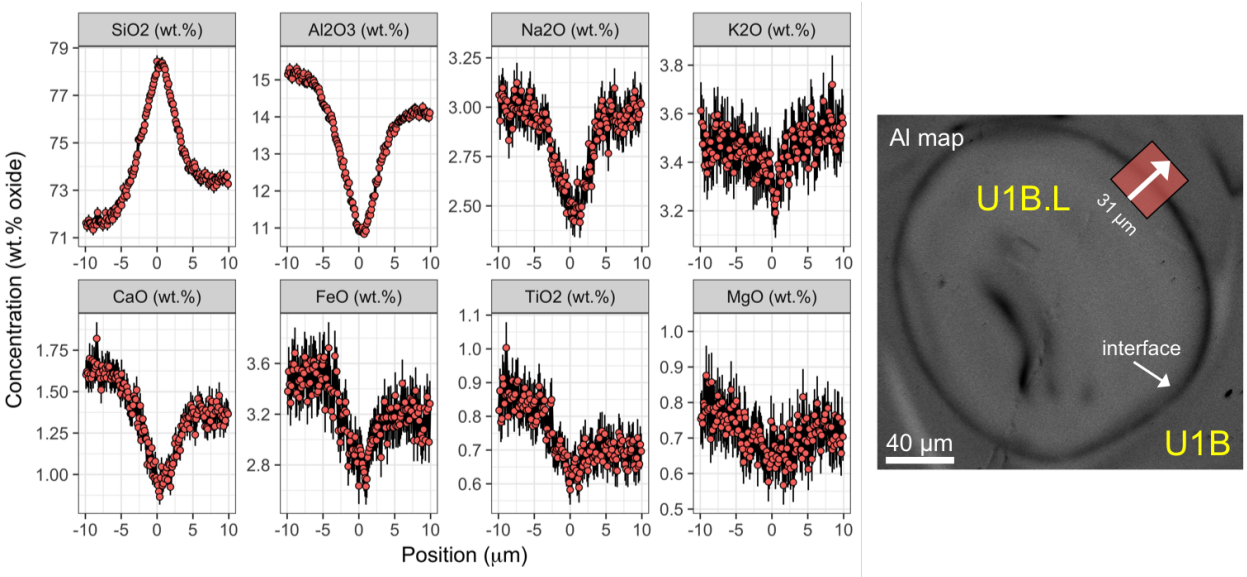

Figure 8.3: Al compositional map (on right) and extracted linear traverse across the interface between agglomerate U1B.L and host object U1B (on left). The interface traverse is extracted from an EDS compositional map (≈125 nm/pixel resolution) and smoothed using a line width of 250 pixels (≈31 μm). The y-axis for the plots are the compositions (as wt.% oxide) for each of the major elements analyzed using EDS. U1B.L's interface is an Si interface, so the interface traverse is centered at the SiO_2 maxima. The traverse begins in the agglomerate, passes over the interface near $x = 0$ μm and ends in the host. In this case, the centering is slightly off-center due to the noise in the SiO_2 peak with the maximum SiO_2 concentration being shifted slightly toward the agglomerate (<1 μm). Uncertainties are 2SEOM calculated assuming $n = 250$ (250 pixels were used for smoothing) and using the standard deviation from 250 pixels taken from a line drawn perpendicular to the interface traverse. For this Si (and most other Si interfaces), Si is the **only** analyzed major element enriched at the interface, while all other analyzed elements show a depletion or no measurable change across the interface.

If the interface was additionally characterized with NanoSIMS, the location of the EDS maps were deliberately collected near the location of the NanoSIMS raster. However, in some cases, excessive mapping of these regions pre-SIMS analysis (to plan for the NanoSIMS analysis) and post-SIMS analysis lead to Na_2O volatilization. In these instances, another section of the interface was mapped instead.

To compare EPMA traverses (such as those reported in [67, 68]) with EDS map traverses (this study) in both composition, width, and major element behavior across the interface,

several additional examples of traverses from EDS maps were collected near EPMA traverses (from Weisz (2016)). EDS map traverses taken near EPMA traverses show generally good agreement with the EPMA data. Figures 8.4 and 8.5 illustrate two such traverses in agglomerates C1 (from sample AA.C) and D2 (from sample AG.D), respectively for each of the major elements measured with EDS.[2] These two traverses extend to 10 μm on either side of the interface and were both centered using the FeO maxima.

For EDS map-based (map resolution of $\sim$0.14 μm/pixel and the traverse was smoothed using an $\sim$14 μm wide line) and EPMA-based traverses across the CaMgFe interface of agglomerate C1 (Fig. 8.4), SiO_2, Al_2O_3, CaO, FeO, and MgO show comparable compositions on the agglomerate side, at the interface, and on the host side. The EDS compositions of TiO_2 is systematically higher than the EPMA compositions, a trend not replicated in the traverse across Figure 8.5. While both traverses show similar compositional trends for Na_2O and K_2O (with Na_2O slowly increasing across the entirety of the traverse and K_2O increasing until the interface, rapidly decreasing across the interface and then slowly increasing again) the measured compositions are systematically different. The EDS-measured Na_2O composition is approximately 100% greater than the EPMA-measured composition across the entirety of the traverse ($\approx$2 wt.% for EPMA and $\approx$4 wt.% for EDS), with the K_2O composition measured by EDS being approximately 10% greater than the EPMA-measured composition across the entirety of the traverse. This trend is mimicked on the agglomerate side of the traverse across the interface of D2 (Figure 8.5). This suggests that Na_2O, and to a lesser extent, K_2O volatilized during the EPMA spot analyses, and that the EDS mapping technique used in this dissertation may minimize these effects. Finally, and most importantly, the enrichments and depletions observed in the EPMA traverses are replicated with the EDS map traverses across the interface of agglomerate C1.

In contrast, the agreement between the EDS map-based (map resolution of $\approx$0.25 μm/pixel and and the traverse was smoothed using an $\approx$31 μm wide line) and EPMA-based traverses across the interface of agglomerate D2 is not as strong, despite the traverses being taken $\sim$20 μm from each other (Fig. 8.5). The enrichments in CaO and FeO and depletion Al_2O_3 are replicated in the EDS map (again, both interfaces are centered based on their FeO maxima). However, the EDS map also shows a $\approx$5% enrichment in SiO_2 just prior to the interface. FeO and TiO_2 show the best agreement between these two approaches. While SiO_2 and Al_2O_3 strongly agreed across the C1 interface (Fig. 8.4), the compositions slightly disagree in the D2 traverse (by approximately 5 % and 10–15% relative for SiO_2 and Al_2O_3, respectively). The disagreement is small and may result from the compositional heterogeneity in the agglomerate, such as that visible in the Al compositional map (top right panel of Fig. 8.5).

These comparisons confirm relatively good agreement in compositions and enrichment trends of different major elements across CaMgFe interfaces studied previously. The quantified EDS maps suffer from increased uncertainty compared to the EPMA traverses even when smoothing by averaging a large number of pixels perpendicular to the interface. How-

[2]Weisz (2016) and Weisz et al. (2017) also measured MnO using EPMA.

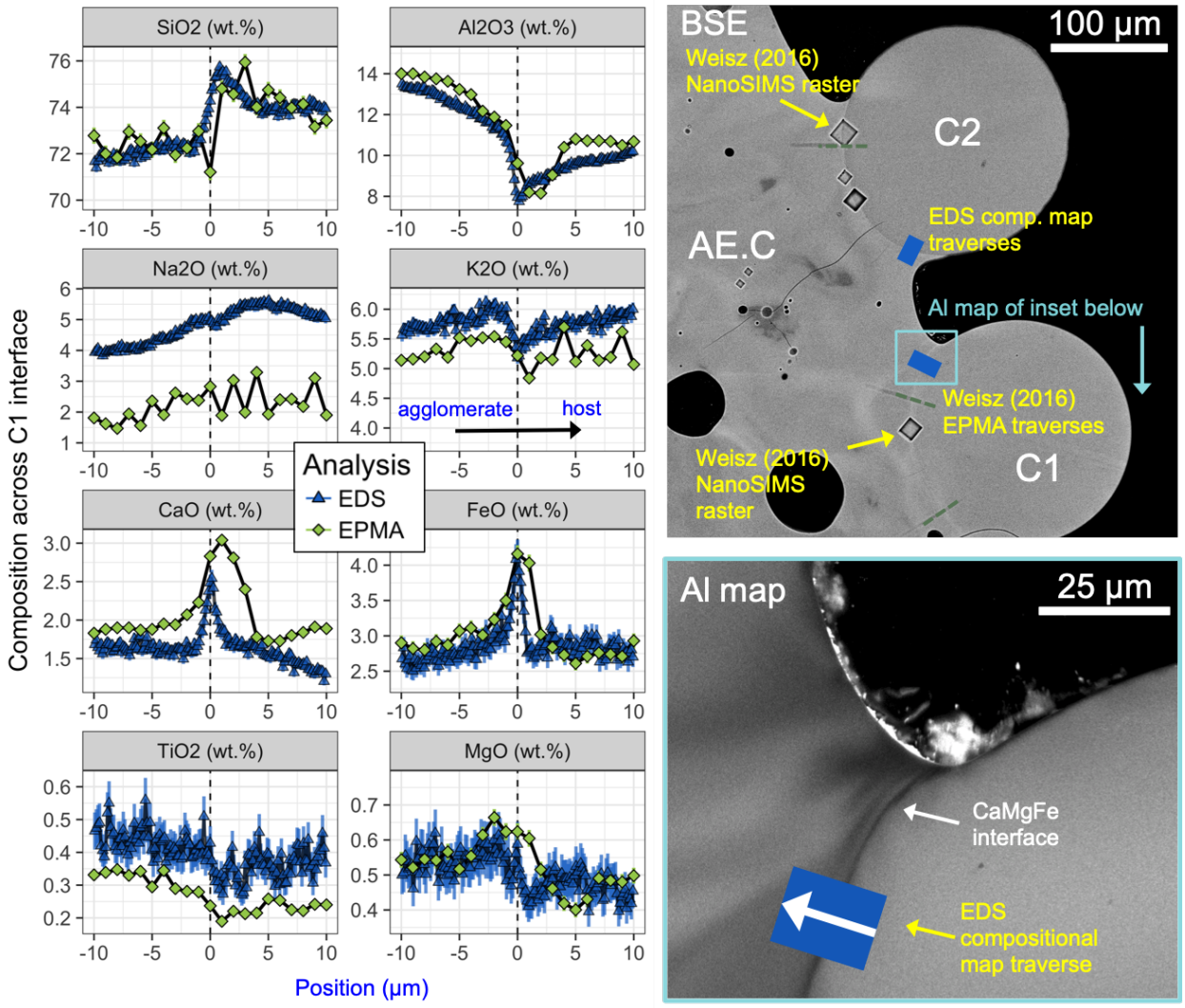

Figure 8.4: Comparison between EPMA (data taken from [67]) and EDS map-based traverses across the CaMgFe interface C1 in sample AA.C for each of the elements characterized using EDS in this study (left panel). The top right image shows a BSE image of sample AA.C with exterior agglomerates C1 and C2. The magnified inset in the bottom right shows an Al compositional map indicating the approximate location and width (13.6 μm/100 pixel smoothing width) of the traverse conducted using quantified EDS compositional maps. The point spacing of the EPMA traverse was 1 μm and the point spacing of the EDS traverse is 0.14 μm (the resolution of this map). Trends for most of the element oxides are replicated in the EDS map-based traverse as observed in the EPMA traverse. However, the EDS-derived Na_2O and K_2O traverses are systematically higher, possibly due to volatilization using the EPMA technique. The deviation between the EPMA and EDS TiO_2 traverses is possibly due to the different quantification schemes used for EPMA and EDS. Uncertainties are 1σ for the EPMA data and 2σ for the EDS map data.

ever, the EDS maps provide higher spatial resolution ($\leq$0.3 μm), and are therefore able to resolve enrichment trends not observed with EPMA (*e.g.*, the enrichment in Si just prior to

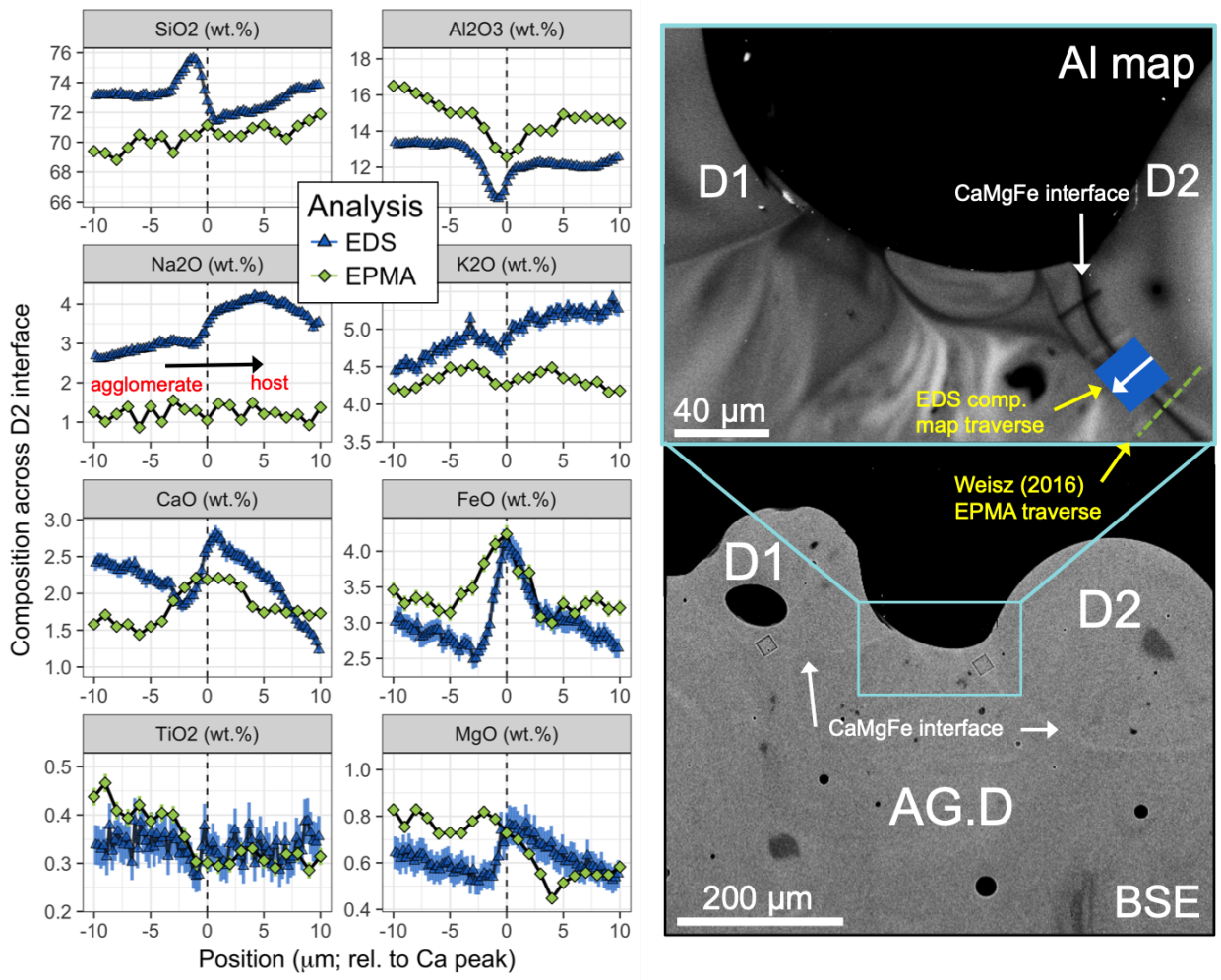

Figure 8.5: Comparison between EPMA and EDS compositional map scans across the CaMgFe interface D2 in sample AG.D (left panel). The bottom right panel shows a BSE image of sample AG.D and agglomerates D1 and D2, with the inset above (top right panel) showing an Al compositional map indicating where Weisz (2016) conducted the EPMA traverse, as well as the approximate location and width (30.7 μm/125 pixel smoothing width) of the traverse conducted using quantified EDS compositional maps (this study). The point spacing of the EPMA traverse is 1 μm and the point spacing of the EDS traverse is 0.25 μm, which is the pixel size for this map. However, there is likely some smearing effect due to the finite size of the electron beam, so the resolution of the EDS traverse is likely greater. The systematic disagreement between SiO_2 and Al_2O_3 between the two techniques may be due to compositional heterogeneity since the traverses were taken in different locations. Uncertainties are 1σ for the EPMA data and 2σ for the EDS map data.

the CaMgFe interface of agglomerate D2, Fig. 8.5), and do not appear to volatilize Na_2O or K_2O.

CaMgFe interfaces analyzed in this study

New CaMgFe interfaces analyzed for this study by both EDS and NanoSIMS are all exterior agglomerates: FLD10.L, FLD14.L, and FLD18.1. These CaMgFe interfaces show major element enrichments and depletions consistent with the previous observations of Weisz (2016) and Weisz et al. (2017) (Figure 8.6; ^{235}U enrichments are discussed in Chapter 9). The three interfaces are all observed to be enriched in FeO, CaO, and MgO (enrichments for all characterized major elements are shown in Appendix J). In addition, all three interfaces are depleted in Al across the interface and two of the three show minor, but resolvable, offset enrichments in SiO_2. These SiO_2 enrichments are offset within 2 μm of the FeO interface, and enriched ≈3–5 wt.% relative to the agglomerate or host composition.

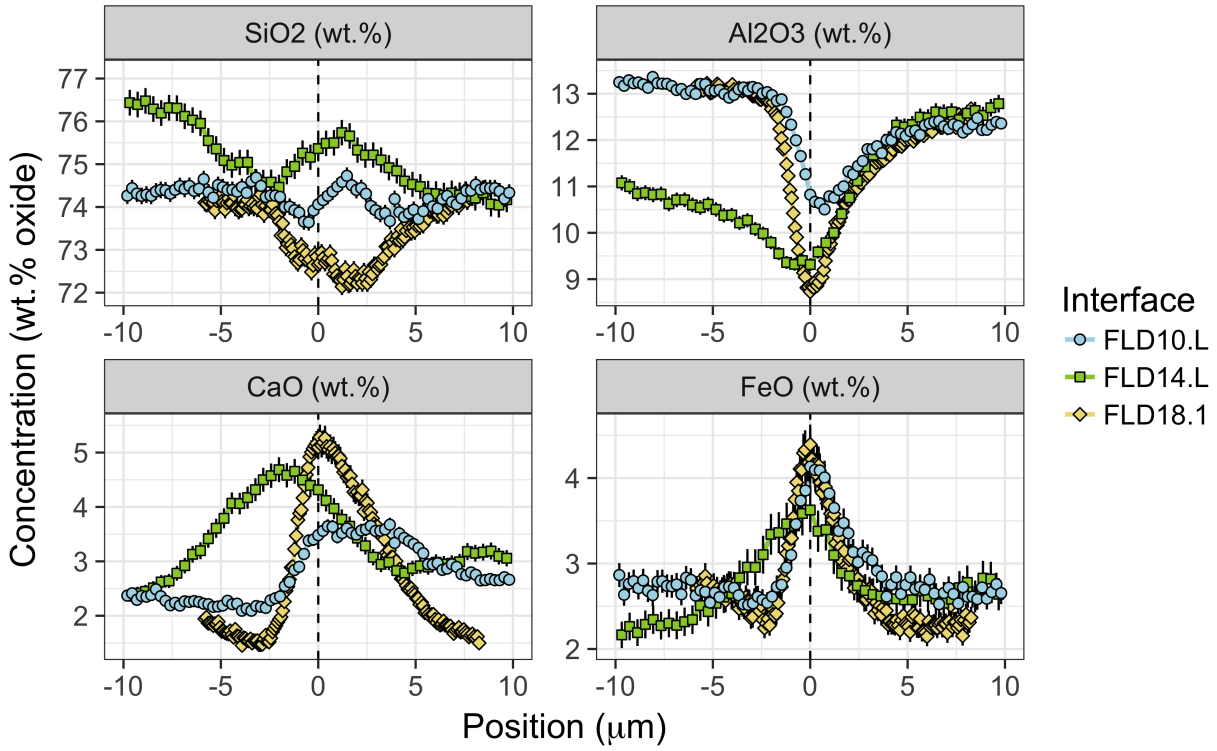

Figure 8.6: Traverses extracted from quantitative EDS compositional maps collected across the CaMgFe interfaces of FLD18.1, FLD14.L, and FLD10.L. All three are exterior agglomerates. The peaks are centered at $x = 0$ μm based on their FeO maxima. Similar to the interfaces studied by Weisz (2016), these interfaces uniformly exhibit enrichments in CaO, FeO, and MgO (not shown) and depletions in Al_2O_3. Two of the three interfaces (FLD10.L and FLD14.L) also exhibit enrichments in SiO_2 offset towards the host by ≈2 μm. Uncertainties are 2σ. Data are tabulated in Appendix J.

8.5 Si interfaces analyzed in this study

In contrast to CaMgFe interfaces, which show persistent enrichment of several major elements at the compositional interface of most (but not all) exterior agglomerates and some surface agglomerates, Si interfaces appear only enriched in SiO_2 and are observed to bound all three types of agglomerates: exterior, surface, and interior agglomerates. Figure 8.7 shows six examples of traverses extracted from quantified EDS maps across Si interfaces: FLD23.L is an exterior agglomerate, FLD14.1 is a surface agglomerate, and the remaining four agglomerates are interior agglomerates. In contrast to traverses of CaMgFe interfaces, these plots of Si interfaces are centered at $x = 0$ μm based on their maximum SiO_2 concentration.

Examples of EDS traverses along with compositional maps highlighting the width and location of these traverses are shown in Figures 8.8 and 8.9. The examples shown include both CaMgFe and Si interfaces, with CaMgFe interfaces being centered at the location of their FeO maxima and Si interfaces being centered at the location of their SiO_2 maxima. Figures 8.8 and 8.9 show the same four element oxides as Figures 8.6 and 8.7 along with Al maps showing the traverse across the interface. The color of the traverse shown in the Al map corresponds to the same color of the interface in the plot. The interface points are highlighted in the EDS traverse plots in Figures 8.6 and 8.7, with yellow points distinguishing which oxide was used for centering the peak (SiO_2 or FeO) and the white points about $x = 0$ μm showing the concentrations of the three other oxides for those peak points. Peak points are defined to be all points within 2σ of either the SiO_2 or FeO maximum (depending on the type of interface). These interface peak points used to characterize and discuss interface compositions and to project interface compositions into PCA space.

The first question about Si interfaces is one of their local, spatial occurrence. For example, do they occur surrounding agglomerates, the host objects, or both. CaMgFe interfaces present on on exterior and surface agglomerates have been observed to surround entire agglomerates, but have not been observed to surround the entire host. In contrast, Si maps show that both hosts and agglomerates can exhibit Si enrichment at their surfaces (Fig. 8.10).

Figure 8.10 shows three pairs of Si maps from samples FLD23, FLD14, and FLD4.3. The grayscale panel is an Si map with the red showing the thresholding used to produce the adjacent thresholded black and white panels. The red in the grayscale map and the black and white thresholded Si map highlight the Si enrichments at the surface of both host objects and agglomerates. FLD23 contains several small surface agglomerates (FLD23.3.1, FLD23.3.2, and several uncharacterized surface agglomerates) in addition to one large exterior agglomerate (FLD23.L). All characterized agglomerates in FLD23 appear to exhibit asymmetric Si interfaces that are narrow on the agglomerate side and more diffuse the side of the host object. Figure 8.9 shows interface traverses from nine agglomerates from FLD23. Si maps of agglomerates from this sample show Si enrichment not just at the interface between the surface agglomerate and FLD23, but also on FLD23's periphery away from agglomerates, suggesting that in FLD23 the Si interface is due to an Si enrichment on the host (see top right panels showing FLD23.L, FLD23.3.2, and FLD23.3.1 in Fig. 8.10). In the Si map

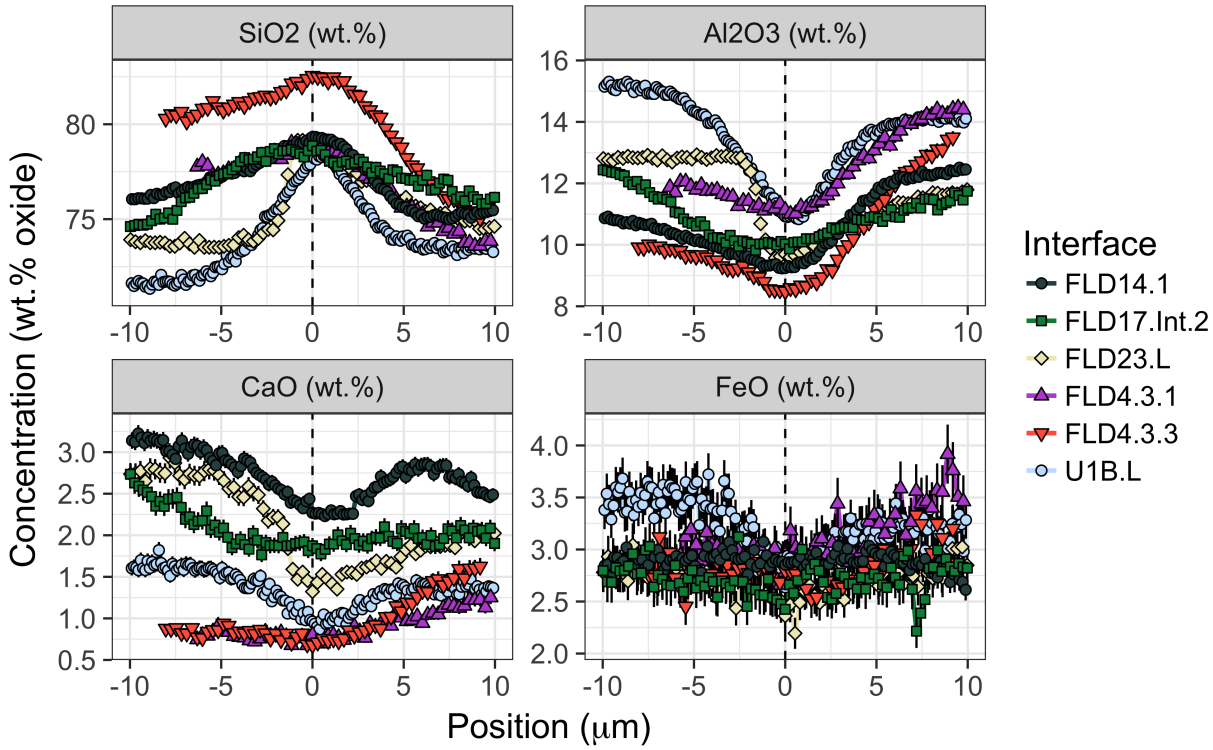

Figure 8.7: Example interface traverses extracted from quantitated EDS compositional maps across six Si interfaces. Peaks are centered at $x = 0$ μm based on their local maximum SiO_2 concentration. Traverses being in the agglomerate for $x < 0$ μm, pass the interface near $x = 0$ μm, and traverse into the host for $x > 0$ μm. FLD14.1 is a surface agglomerate, FLD23.L is an exterior agglomerate, and the remaining four are interior agglomerates. The SiO_2 enrichment at the interface can be as little as 5% relative compared to the agglomerate composition (*e.g.*, FLD4.3.3) and rarely exceeds 10%, consistent with this and previous findings of CaMgFe interfaces. The remaining characterized major element oxides are tabulated in Appendix J. All major element oxides not shown here, except, in several cases K_2O or FeO, are either depleted or show no measurable change in composition across the interface (discussed further below; see Figure 8.19).

of the magnified region shown in Figure 8.10, it can be seen that host object FLD23 also exhibits an Si enrichment at its surface when there is no surface agglomerate and is bounded by the epoxy. Similarly, host object FLD4.3 exhibits an Si enrichment at its periphery, as demonstrated by the interface between FLD4.3.UA and edge of FLD4.3 where there are no visible surface agglomerates. However, an Si map from taken on the other side of FLD4.3 does not show the same Si enrichment at the periphery of the host object. Finally, the panel containing host object FLD14 and agglomerates FLD14.1 and FLD14.L, shows that both the host and an agglomerate (FLD14.1) exhibit Si enrichment at their surfaces.

For internal agglomerates to preserve Si interfaces, either the agglomerate melt accumulated the enrichment at its periphery prior to agglomeration or the host melt accumulated an Si enrichment on its surface, which coated the agglomerate as it mixed into the host object.

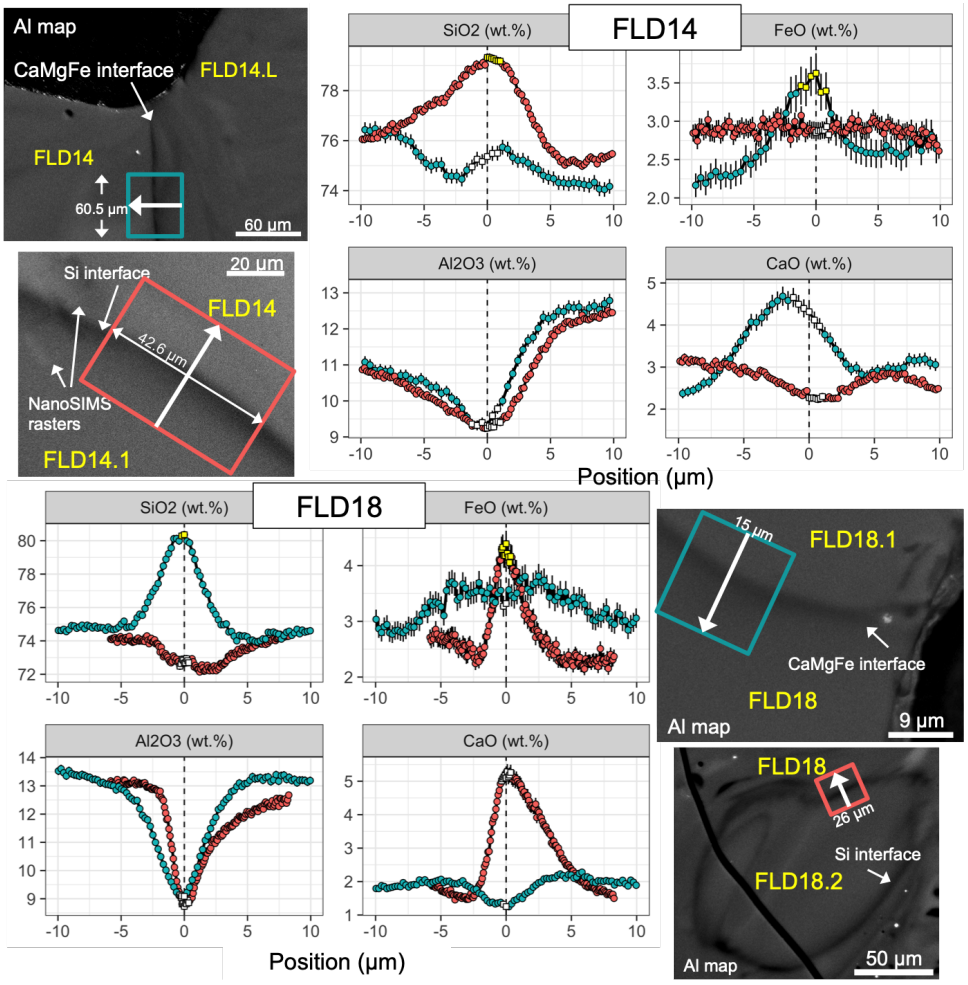

Figure 8.8: Traverses across compositional interfaces characterized by quantitative EDS compositional maps. Al compositional maps show the location and smoothing width of the interface traverses for SiO_2, FeO, Al_2O_3, and CaO. Si interfaces are centered based on their SiO_2 maxima and CaMgFe interfaces are centered based on their FeO maxima. The colors of the traverses in the compositional maps correspond to the colors of the traverses in the plots. Interface points are highlighted in the traverses, with yellow markers indicating which major element oxide (SiO_2 or FeO) was used to define the interface peak points for these interfaces, and white markers in the other panels highlighting those compositions for the other oxides. The top panel shows the two agglomerates characterized in FLD14: FLD14.L (and exterior agglomerate; CaMgFe interface) and FLD14.1 (a surface agglomerate; Si interface). The bottom panel shows FLD18.1 (an exterior agglomerate; CaMgFe interface) and FLD18.2 (an interior agglomerate; Si interface) in sample FLD18. Uncertainties are 2σ. Data are tabulated in Appendix J.

Some combination of both of these scenarios is also possible.

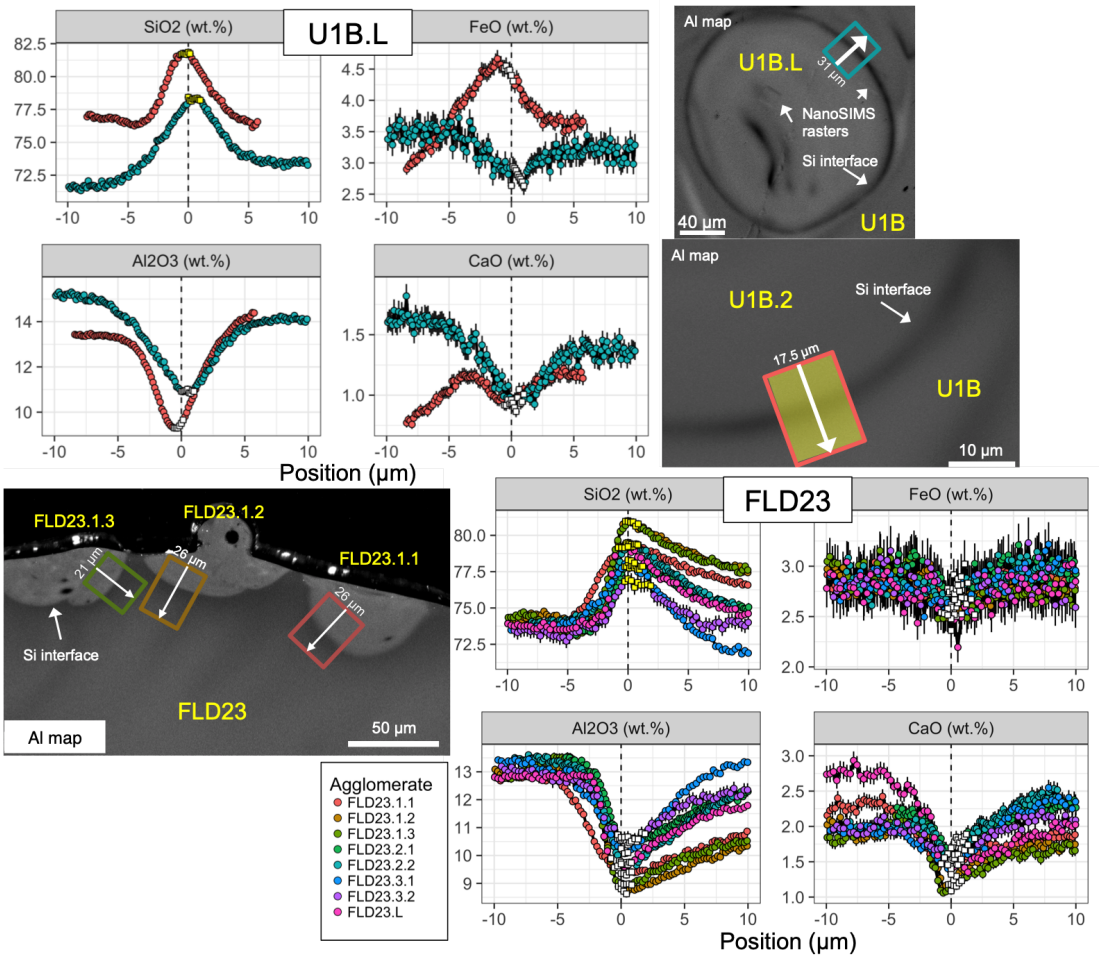

Figure 8.9: Traverses across compositional interfaces characterized by quantitative EDS compositional maps. Al compositional maps show the location and smoothing width of the interface traverses for SiO_2, FeO, Al_2O_3, and CaO. All agglomerates in this figure have Si interfaces and are centered based on their SiO_2 maxima. The colors of the traverses in the compositional maps correspond to the colors of the traverses in the plots. Interface points are highlighted in the traverses, with yellow markers indicating which major element oxide (SiO_2 or FeO) was used to define the interface peak points for these interfaces, and white markers in the other panels highlighting those compositions for the other oxides. The top row shows the two agglomerates characterized in U1B: U1B.L (an interior agglomerate) and FLD14.1 (a surface agglomerate). The bottom row shows eight interfaces from agglomerates in FLD23. Only the Al map highlighting the traverses of FLD23.1.1, FLD23.1.2, and FLD231.3 are shown here. All eight agglomerates plotted for FLD23 are surface agglomerates, except for FLD23.L, which is an exterior agglomerate. Uncertainties are 2σ. Data are tabulated in Appendix J.

8.6 Possible origins of Si interfaces

These Si enrichments surrounding agglomerates and/or hosts can plausibly arise through two scenarios: a process that preferentially allows Si to condense onto the surface of hosts

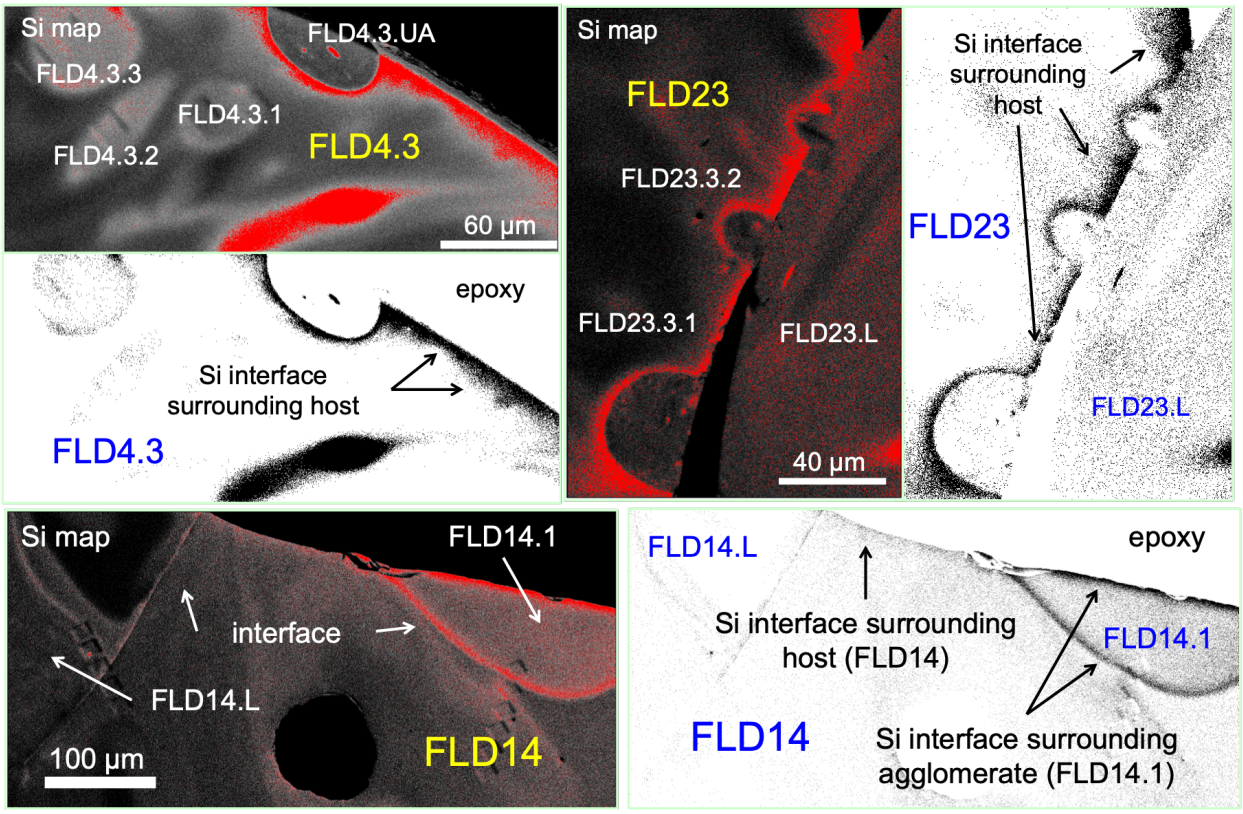

Figure 8.10: Si maps of magnified regions in the samples FLD23 (top right), FLD4.3 (top left), and FLD14 (bottom) highlighting Si interfaces surrounding hosts and their agglomerates. The grayscale Si map shows the thresholded region in red used to produce the black and white thresholded Si map, showing the location of Si interfaces overlaying the Si compositional maps. For FLD23, the Si interface appears created by an Si-enriched region surrounding the host. The interface for FLD4.3.UA in samples FLD4.3 is also likely due to an Si-enriched region surrounding the host. Finally, the agglomerate FLD14.1 in sample FLD14 exhibits an Si-enriched region surrounding the the agglomerate, while the host FLD14 exhibits a slight enrichment surrounding the host.

and/or agglomerates or a process that preferentially volatilizes all major elements at the surface of some agglomerates and hosts, leaving SiO_2 relatively enriched.

There are two plausible explanations for surfaces enrichments of one or several elemental species: condensation of those enriched species from a vapor phase or volatilization from the melt of other species that have a significant contribution to the overall composition.

In evaporative loss experiments in obsidian, which has a comparable major element composition to the average fallout composition (but is less silicic), Si behaves as a moderately volatile species, being more refractory than the alkalis, yet more volatile than Ca, Al, and Ti (and behaving with similar volatility to Fe and Mg) [102].[3] Gerasimov et al. (2005)

[3]Only general trends of major element volatility are given here (*i.e.,* alkalis behaving as volatiles, Si, Fe, and Mg behaving with intermediate volatility, and Ca, Ti, and Mg behaving as refractories) because the

notes that the compositions of glasses that were heated and quenched show a large variability in final chemical composition, largely reflective of differences in temperature history, which reflects varying degrees of mass loss. Given the observations of the last several chapters showing relative localized homogeneity with respect to U isotopes (agglomerates and their host objects tend to be more similar in U isotope composition than to other hosts or to other agglomerates), but significant heterogeneity when considering the collection of U isotopic measurements, the partial pressures of soil-derived species in the vapor phase are likely similarly heterogeneous and rapidly evolving as the fireball expands and cools. As a result, CaO, Al_2O_3, and TiO_2 are relatively *enriched* in the heated and quenched obsidian relative to the starting material because these species have proportionally volatilized the least. Thermodynamic calculations are consistent with these general volatility trends [102]. Given the experimental observations and theoretical calculations, if evaporative loss were the source of enrichment at the surface of host objects or agglomerates, Al_2O_3, CaO, and TiO_2 enrichment at the surface would be expected. Instead, however, SiO_2, an oxide with intermediate volatility, is enriched, so evaporative loss is discarded as a plausible source of these Si compositional interfaces and surface enrichments in host objects and agglomerates. Direct Si condensation from the vapor phase is the other plausible source of Si compositional interfaces.

Chondrules are a potential analogue to glassy fallout because chondrules are also thought to form through the flash heating and rapid cooling of rocky material. Chondrules are silicates found in primitive meteorites called chondrites, and commonly exhibit silica-enriched "rims" or "peripheries" (the nomenclature used in the cosomochemistry literature) [103, 163–166]. Chondrules may exhibit these silica-rich rims (part of a class of chondrules called type I chondrules) are thought to have formed in a similar manner to glassy fallout: flash heating of rocky material (in the early solar nebula) to ∼2000 K, which subsequently cooled at a rate on the order of 10–1000 K/h [167].[4] Studies have considered both evaporative loss and gas-melt condensation as the origin of the Si-enrichment in type I chondrules [103, 163, 168, 169]. However, recent experiments show that condensing $SiO_{(gas)}$ from the vapor phase can lead to a preferential enrichment of SiO_2 at the surface of silicate melts [103, 170]. $SiO_{(gas)}$ will preferentially condense from the vapor phase if the partial pressure of Si in the vapor phase is sufficiently high. This hypothesis has led to the speculation that chondrules with silica-enriched rims formed in a particularly dusty region of the solar nebula, which had a high concentration of fine grained silica that vaporized, increasing the partial pressure of $SiO_{(gas)}$ (the dominant Si species in the vapor phase at temperatures ≈2000 K), resulting in a preferential condensation of SiO from the vapor phase onto molten chondrules, which then cooled and crystallized.

Silica is the dominant major element oxide in soil from this test [57]. In addition, compositional X-ray maps of the soil mount show many fine-grained silica-rich regions (Fig. 4.15).

ambient environment in the fireball is still an open question [44, 69].

[4]This cooling timescale is rapid for cosmological timescales, but not compared to cooling timescales of a nuclear fireball. As a result, silica-enriched rims in chondrules are often crystalline.

As a result, it is possible regions of the fireball vaporized a large concentrations of fine quartz and silicious matrices (which may more easily vaporize than other soils due to their high surface area-to-volume ratio and ease with which they are lofted into the fireball). Given the relatively high boiling point of SiO_2, these regions with relatively high $SiO_{(gas)}$ partial pressures likely occurred at early times in the fireball. These regions could result in early time, localized Si deposition on the surfaces of melts passing through them.

8.7 Layered Si and CaMgFe interfaces

CaMgFe interfaces have only been observed at the interfaces of exterior and surface agglomerates in this and Weisz's study, while Si interfaces are observed at the interfaces of exterior, surface, and interior agglomerates. Therefore, it is likely the Si deposition occurs earlier than the CaMgFe deposition. In some cases, however, agglomerates exhibit compositional interfaces with multiple layers, including both Si and CaMgFe interfaces. If objects experience fireball environments with conditions leading to the formation of both types of enriched surface layers, the Si enrichment should occur first, followed by the CaMgFe layer. This temporal ordering of interfaces leads to a spatial ordering of interfaces around individual objects and limits the number of hypothesized permutations of multiply-layered interfaces that are observed between agglomerates and their host objects (*e.g.*, FLD10.L and FLD14.L).

Because both agglomerates and hosts are likely to experience similar fireball environments (given the U isotopic observations of agglomerates and hosts discussed in Chapters 5 and 7), but may also experience different fireball environments, some permutations of the ordering of compositional interfaces are possible (Figure 8.11). Figure 8.11 shows depositions that may result in double-layered interfaces, but given that both the host and agglomerate may preserve Si enrichments followed by a CaMgFe enrichment, interfaces with four layers may be possible. After agglomeration the two distinct CaMgFe interfaces in contact in between an Si interface on the agglomerate side and an Si interface on the host object side may diffuse together, leading to only three resolvable interfaces after the combined melt quenches.

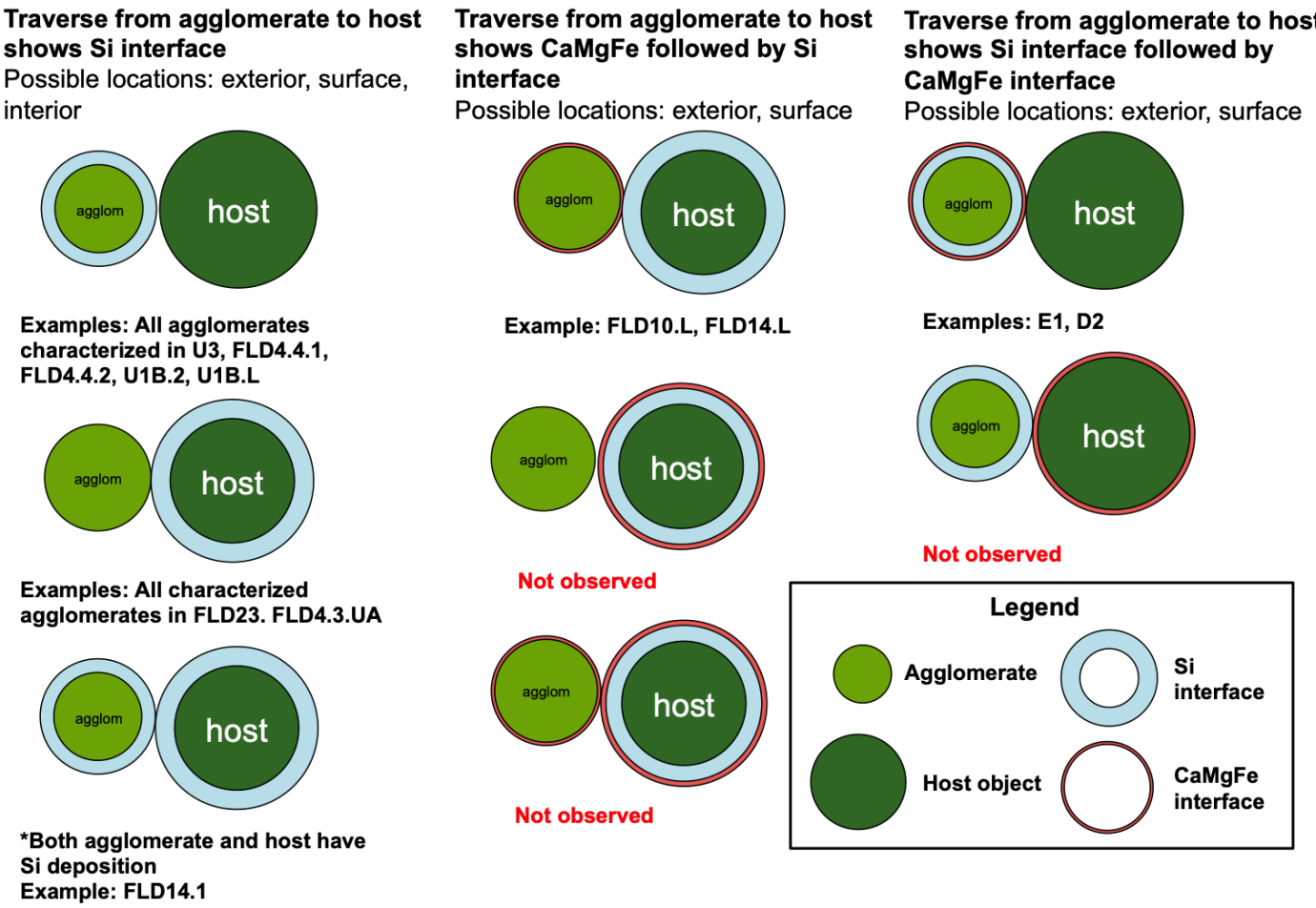

Figure 8.11: Scenarios that could lead to different interface and enrichment layers. Given observations of the relative width of the Si interfaces compared to the CaMgFe interfaces, an object coated first with a CaMgFe deposition layer followed by an Si deposition layer is not hypothesized to not occur. However, an agglomerate may be coated with Si and the host with a CaMgFe, leading to a preservation of an Si interface overlaid by a CaMgFe interface. However, this scenario was not observed in this study.

One clear example of a multiply-layered interface is the compositional interface between agglomerate FLD10.L and host FLD10 (Fig. 8.12). Figure 8.12 shows four compositional maps (Si, Fe, Al, and Ca) from the interface FLD10.L (shown on the right of each compositional map). There is a small surface agglomerate near the center of each map that shows a compositional interface enriched in Si shared between this agglomerate and the host (visible in the first and third panels) and a CaMgFe interface shared between this agglomerate and FLD10.L (visible in the second and fourth panels). This exemplifies the host's surface (FLD10) being relatively enriched in Si, while the agglomerate's surface (FLD10.L) is relatively enriched in CaMgFe. The differing behavior of the compositional interface of each side of the surface agglomerate suggests the Si enrichment first coated FLD10, the uncharacterized intermediate agglomerate then impacted FLD10, and finally, FLD10.L impacted FLD10. The more diffuse width of the Si interface relative to the CaMgFe interface suggests that the Si deposition occurred earlier, while the host object was more molten.

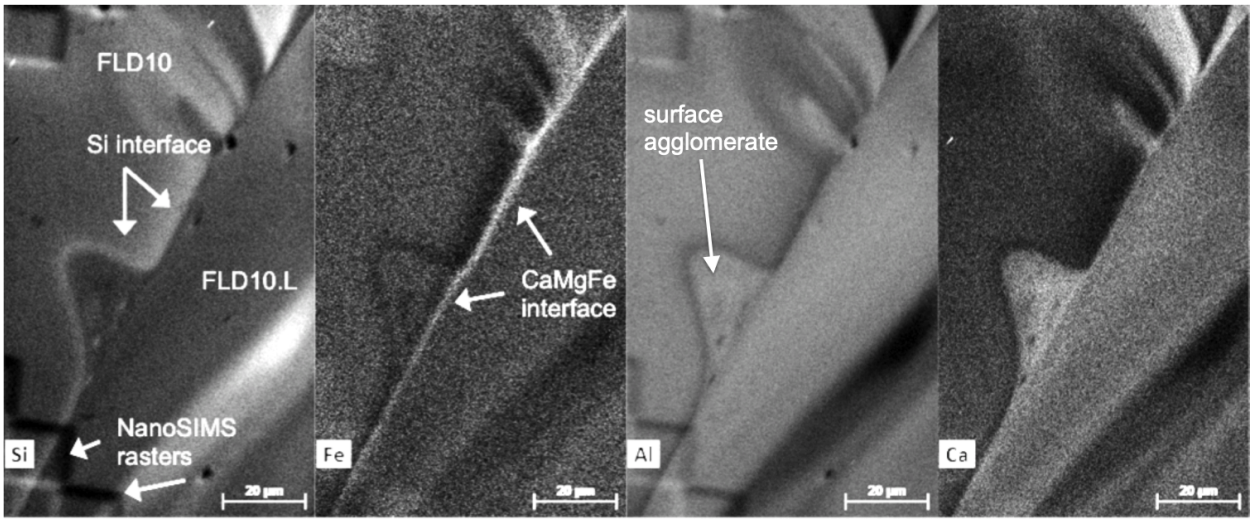

Figure 8.12: EDS compositional maps of the interface between FLD10.L and FLD10 showing two interfaces a CaMgFe interface at the boundary of agglomerate FLD10.L, followed by an Si interface between the CaMgFe interface and the host FLD10. A surface agglomerate near the center of the map preserves only a CaMgFe interface between itself and FLD10.L and an Si interface between itself and the host object FLD10. The Si interface appears more diffuse than the CaMgFe interface.

Further evidence for interfaces containing multiple layers include several traverses across CaMgFe interfaces with slightly offset enrichments that could be Si interfaces. These examples include agglomerate E1 in sample AH.E, agglomerate D2 in sample AG.D, and agglomerate FLD14.L in sample FLD14 (all exterior agglomerates; Figs. 8.2 and 8.6).

8.8 Interface compositions

The mean Si interface compositions (99 interface peak points from 16 interfaces in 5 samples) and CaMgFe interface compositions (46 interface peak points from 9 interfaces in 7 samples) extracted from quantified EDS compositional maps are within 1σ of the mean of the EDS raster measurements in the 37 hosts discussed in Chapter 4 (Table 8.2). However, the 1σ of the host EDS measurements is large because it includes EDS measurements of unmelted, partially-melted, and unmelted compositions. The mean Al_2O_3 values of both interface compositions (10.04 ± 1.28 wt.% Al_2O_3 for Si interfaces and 10.35 ± 1.57 wt.% Al_2O_3 for CaMgFe interfaces) are systematically depleted relative to the mean host object composition (13.59 ± 2.16 wt.%). This is consistent with the observations of persistent Al depletion at compositional interfaces between agglomerates and host objects. Similarly, the SiO_2 composition of Si interfaces is systematically enriched relative to the mean of both CaMgFe interface peak points and mean host object composition (79.10 ± 2.27 wt.% SiO_2 compared to 73.89 ± 1.53 wt.% SiO_2 and 73.77 ± 4.12 wt.% SiO_2, respectively). However, while the CaO and FeO means observed at CaMgFe interface peaks are enriched relative to the mean of the Si interface peak compositions and the mean host object composition, they are still within within 1σ of both (CaMgFe interface CaO mean = 3.17 ± 1.31 wt.% and FeO mean = 3.75 ± 0.59 wt.% compared to the Si interface CaO mean = 1.34 ± 0.46 wt.% and FeO mean = 2.85 ± 0.44 wt.% and the host object CaO mean = 2.12 ± 0.99 wt.% and FeO mean = 2.77 ± 0.76 wt.%). The mean MgO compositions at Si and CaMgFe interface peaks are both within 10% (relative) of the mean host object composition (0.60 ± 0.26 for the host object MgO mean composition compared to 0.54 ± 0.09 wt.% and 0.62 ± 0.14 for the Si and CaMgFe interface peak points, respectively). The large variances in MgO compositions can be attributed to the high analytical uncertainty of MgO in these analyses due to the low abundance of MgO in these samples. The relative uncertainty from a single representative MgO measurement is ≈15–20%. Given the enrichment for CaO and FeO from CaMgFe means compared to the host grid means is ≈50% relative, the average MgO concentration for CaMgFe interfaces is expected to also be enriched. However, it is likely that the relative enrichment of MgO across CaMgFe interfaces is smaller than the CaO and FeO enrichment, and may be unresolved within uncertainty, given the low abundance of MgO, or that the enrichment of MgO across CaMgFe interfaces is not as persistent as the CaO and FeO enrichments. Weisz (2016) observed that MgO was only enriched in 9 of 11 CaMgFe interfaces, while CaO and FeO were enriched in 11 of 11 interfaces analyzed with EPMA (Table 8.1). The EDS traverses across the interfaces of agglomerates C1 and D2 (blue triangles shown in Figs. 8.4 and 8.5, respectively) both show MgO enrichments at their CaMgFe interfaces, while only C1 shows an MgO enrichment when considering the EPMA data alone (green diamonds in Fig. 8.4).

Plotting the interface peak compositions in bivariate plots and differentiating between host object, agglomerate, and soil EDS raster analyses (similar to those shown in Figures 4.18 and 4.19) demonstrates that most interface peak compositions lie within the range of the compositions observed in the host objects. Additionally, outlying interface compositions are

Table 8.2: Comparison of the mean Si interface composition (16 interfaces in 5 samples), CaMgFe interface composition (9 interfaces in 7 samples), and the mean host object composition from grid-based EDS analyses (37 hosts).

	Si interfaces (n=99)		CaMgFe interfaces (n=46)		Host compositions (n=3,698)	
Oxide	Mean (wt.%)	1σ (wt.%)	Mean (wt.%)	1σ (wt.%)	Mean (wt.%)	1σ (wt.%)
SiO_2	79.10	2.27	73.89	1.53	73.77	4.12
Al_2O_3	10.04	1.28	10.35	1.57	13.59	2.16
Na_2O	2.12	0.71	3.23	0.73	3.26	0.70
K_2O	3.77	0.30	4.49	0.62	3.80	0.70
CaO	1.34	0.46	3.17	1.31	2.12	0.99
FeO	2.85	0.44	3.75	0.59	2.77	0.76
TiO_2	0.44	0.10	0.40	0.05	0.32	0.17
MgO	0.54	0.09	0.62	0.14	0.60	0.26

still well bounded (as are the host and agglomerate compositions) by EDS raster measurements of unmelted soil collected proximate to ground zero (Figure 8.13). The Al_2O_3 vs. SiO_2 plot in Figure 8.13 (top panel) is dominated by the mixing between feldspars (which trend towards high alumina concentrations in the top left of the plot), quartz (which trend towards high silica concentrations in the bottom right of the plot), and infrequently sampled mafic compositions (which trend towards low values of both alumina and silica, towards the plot's origin). Overlaying the compositions of the Si interfaces (upside down cyan triangles) and CaMgFe interfaces (golden triangles), the Al_2O_3 vs. SiO_2 plot (top left panel) in Figure 8.13 highlights the alumina depletion of the both the Si and CaMgFe interface compositions relative to the host object and agglomerate average values. All of the Si interface compositions follow a trend similar to that observed in the host object and agglomerate data, decreasing in Al_2O_3 proportionally as the SiO_2 composition increases. However, the CaMgFe interface points show relatively restricted range in SiO_2 compositions, falling between approximately 71 wt.% and 76 wt.% SiO_2, despite covering a similar range in Al_2O_3 compositions as observed at Si interfaces (which span from ≈75 wt.% to 86 wt.% SiO_2). Instead, CaMgFe interfaces follow a trend similar to the mafic compositions measured in the soil, exhibiting enrichments in CaO, MgO, and FeO concentrations that tend to be commensurate with depletions in their Al_2O_3 concentration.

The bottom panel of Figure 8.13 plots the concentration of CaO vs. Al_2O_3. This plot shows the enrichment at CaMgFe interfaces relative to the compositions for Si interfaces, host objects, and agglomerates. Many of the CaMgFe interface compositions overlap agglomerate or host compositions, while other CaMgFe compositions trend towards higher CaO concentrations at lower Al_2O_3 concentrations (similar to the mafic compositions; towards the top left of the plot). The CaMgFe interface compositions exhibiting this trend remain bounded by several outlying mafic compositions measured in host objects and unmelted soil, as in

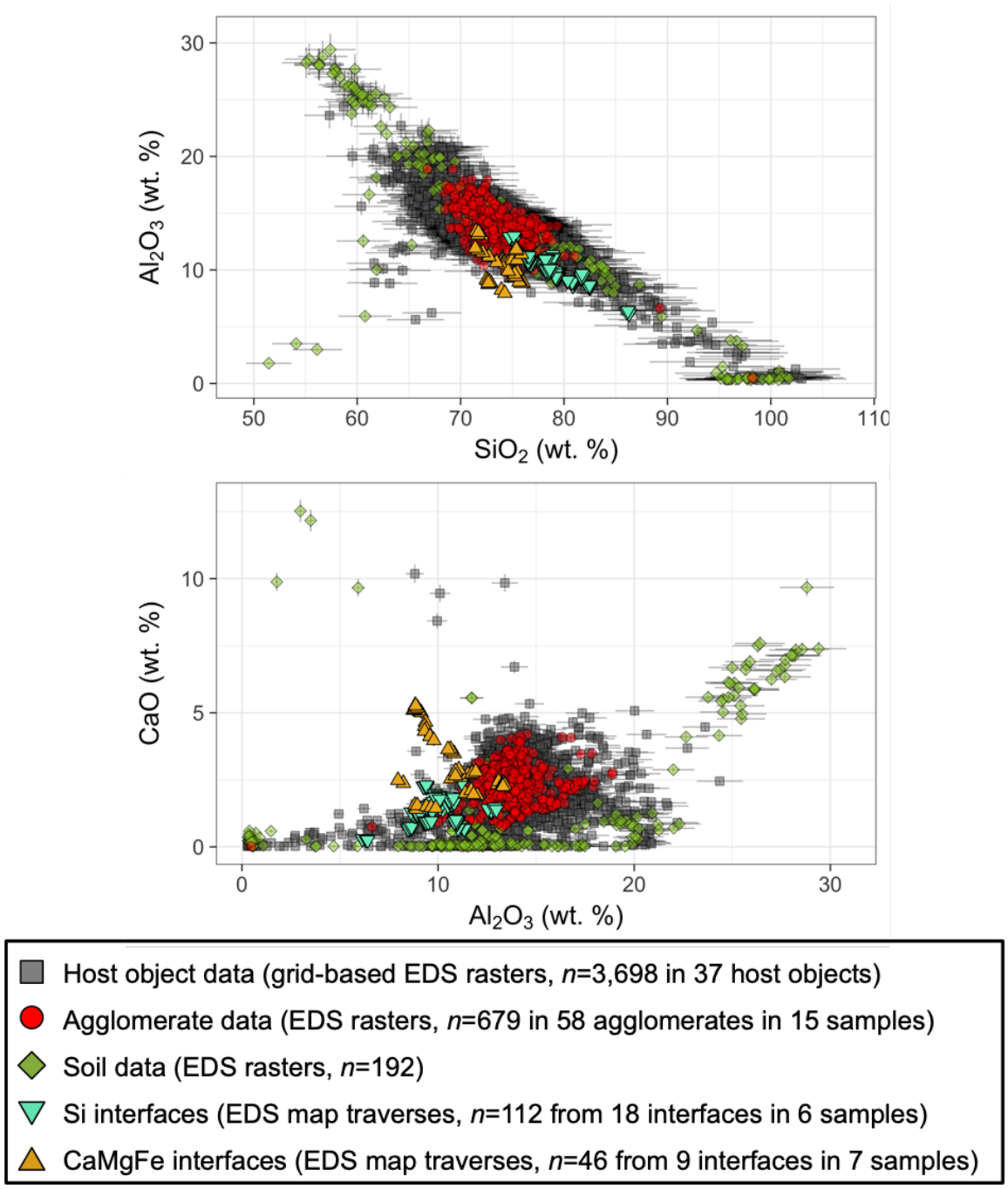

Figure 8.13: Bivariate plots showing compositions of host objects, agglomerates, and unmelted soil overlaid with Si and CaMgFe interface compositions. Uncertainties are 1σ and are smaller than the points for the interface compositions. Data are tabulated in Appendices B (for host object compositions), C (for agglomerate compositions), D (for unmelted soil compositions), and J (for Si and CaMgFe interface compositions).

Chapter 4. In contrast, the Si interface compositions again show a weak correlation consistent with the host object and agglomerate compositions (and fall well within the range spanned by most host objects and agglomerate values). Where as the Al_2O_3 concentration increases, the CaO concentration roughly increases as well, albeit with a large degree of scatter. This trend is mostly created by the Si interface values with the lowest Al_2O_3 and CaO concentrations, which correspond to the the highest SiO_2 concentrations in Al_2O_3 vs. SiO_2 panel. The interface with this outlying composition is that bounding agglomerate FLD4.3.UA (a surface agglomerate) and host FLD4.3, visible in the thresholded Si maps in Figure 8.10.

Interface compositions in PCA space

While general similarities in composition are evident in bivariate plots, to determine whether the compositions of Si and CaMgFe interfaces are consistent with the values measured in hosts or agglomerates, the interface compositions are plotted in PCA space. The interface data are projected in PCA space using the same PCA model generated by the host object EDS raster data discussed in Chapter 6, whose loadings and scores for PC1 v. PC2 are shown in Figure 6.1. The same PC1 v. PC2 biplot is used to project the Si and CaMgFe interface compositions. PC1 v. PC2 separates the Si and CaMgFe interface measurements, as values high in CaO, MgO, and FeO plot towards quadrant I and compositions high in SiO_2 plot towards quadrants II and III. Both sets of interface compositions will tend towards smaller values of PC1, as they both exhibit Al_2O_3 depletions at their interfaces.

Figures 8.14–8.16 shows several examples of both Si and CaMgFe interfaces in PCA space. Plotting both the Si and CaMgFe interfaces shows two trends. First, interface compositions (shown as triangles) tend to be distinct from their host compositions (EDS data collected from that particular host are shown as grey squares) and their agglomerate compositions (EDS data collected from that particular agglomerate are shown as filled in circles). Si interface compositions tend to plot towards quadrants II and III, in the direction of higher Si enrichment. CaMgFe interfaces tend to plot in quadrant I, in the direction greater CaO, MgO, and FeO enrichment.

The interface compositions in Figures 8.14–8.16 indicate that the interface compositions, for at least some interfaces, tend not to be represented in the compositional space of the interface's associated agglomerate or host object, suggesting variation in the interface composition cannot be simply due to compositional heterogeneity in the sample. Furthermore, in two cases, (the interface of FLD18.2 and the interface of FLD14.1) the interface compositions plot outside the collection of *all* measured host object compositions. In these interfaces, a composition not significantly represented in the 37 host objects is present. Collectively, these observations support the hypothesis of both the CaMgFe and Si interfaces not being sourced from chemical heterogeneity in the host melt, but rather as a result of fireball influenced processes, such as elemental-fractionated condensation.

Plotting all interface compositions in PCA space reveals additional observations from individual hosts and agglomerates (Figure 8.17). PC1 v. PC2 highlights that Si interface

points remain tightly clustered as they trend towards negative values of PC1, following more silicic compositions. As a result, Si interfaces trend span a much wider range in PC1 than CaMgFe interfaces. In contrast, CaMgFe interface points primarily group in quadrants I and IV, spanning a much wider range in PC2 than Si interfaces, likely due to the inconsistent enrichment of major elements across these interfaces (whereas Si interfaces tend to only be enriched in Si and depleted in all other major elements). However, plotting PC3 v. PC2 clusters both Si and CaMgFe interfaces closer together, distinguishing trends in the interface compositions from trends in the host object compositions. This clustering of both interface compositions is due to the observed depletion in Al_2O_3 across both types of interfaces.

Relative depletions across interfaces

To further investigate the hypothesis of an Si condensation process for Si interface formation (instead of an evaporative process that leads to the loss of all other major elements), the relative depletions of Al_2O_3, Na_2O, K_2O, CaO, and FeO were calculated across Si interfaces. TiO_2 and MgO were excluded due to their high analytical uncertainties. If the process leading to the Si enrichment at the periphery of hosts and agglomerates was predominantly evaporative, Na_2O and K_2O should preserve the highest relative depletions across Si interfaces (being most volatile species), followed by FeO (being moderately volatile), and finally CaO and Al_2O_3.

The *relative* depletion of these species across Si interfaces is calculated relative to the mean agglomerate composition (from the same quantified EDS map data), and calculated from the average of the agglomerate points prior to the interface (Fig. 8.18). Figure 8.18 shows a traverse across the Si interface of FLD23.L. The grey box outlined in red on the top panel shows the points used to calculate the mean agglomerate composition. The next panel shows the interface compositions determined using the points within 2σ of the SiO_2 maxima (as described above).

Interface compositions relative to mean agglomerate compositions were calculated for 16 Si interfaces in 8 samples: FLD23.1.1, FLD23.1.2, FLD23.2.1, FLD23.2.2, FLD23.3.1, FLD23.3.2, FLD23.L, FLD17.int.2, FLD18.2, FLD14.1, the Si interface of FLD10.L (this agglomerate has a CaMgFe interface as well), FLD4.3.1, FLD4.3.3, FLD4.3.UA, U1B.L, and U3.1 (Fig. 8.19). As the relative depletion of all oxides other than SiO_2 should depend on the relative enrichment of SiO_2 (due to the nature of compositional data), the data are plotted in Figure 8.19 as a function of the relative enrichment of SiO_2 (also relative to the mean agglomerate composition).

In contrast to the expected trend for an evaporative process, where the most volatile species should be the most depleted at the periphery of these samples, the refractory oxides of CaO and Al_2O_3 tend to be the *most* depleted. The CaO and Al_2O_3 compositions show the expected trend of larger SiO_2 enrichments leading to larger CaO and Al_2O_3 depletions. Observed depletions range from a ≈-5% relative depletion for Al_2O_3 when the SiO_2 enrichment was only ≈1.5% across the interface of agglomerate FLD4.3.1 to a ≈-79% depletion in CaO for an SiO_2 enrichment of ≈15% across the interface of agglomerate FLD4.3.UA.

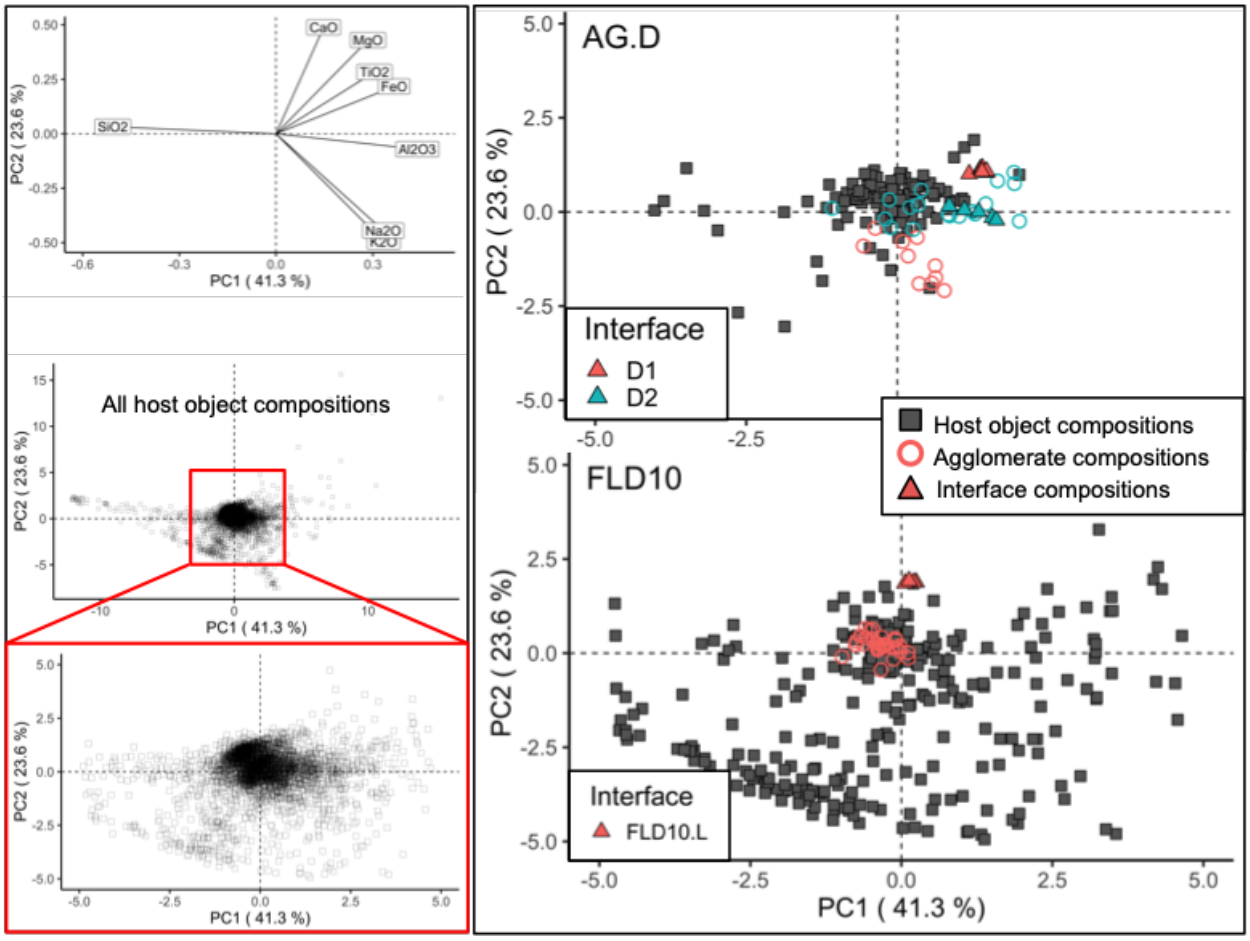

Figure 8.14: CaMgFe interface compositions projected into PCA space for interfaces across FLD10.L, D1, and D2 (all exterior agglomerates). The top left panel shows the loadings of PC1 v. PC2 and the grid-based host object analyses used to generate the PCA space. The center left panel shows the full range spanned by the host objects in PCA space. The red box is the magnified view shown in the plot in the bottom left (which shows the host object compositions in the magnified view) and the sample specific plots in the right panel. In the magnified PCA plots, which show interfaces characterized in sample FLD23 (top) and sample FLD4.3 (bottom), interface compositions are shown as filled triangles. The composition of the host object is shown as grey filled squares. The agglomerate composition is shown as unfilled circles. CaMgFe interface compositions are distinct from EDS analyses in either the host object or agglomerate plotted, but they do not exceed the range spanned the collective set of EDS host analyses and plot towards the majority of measured compositions. Data are tabulated in Appendix J using the PCA model shown in Appendix H.

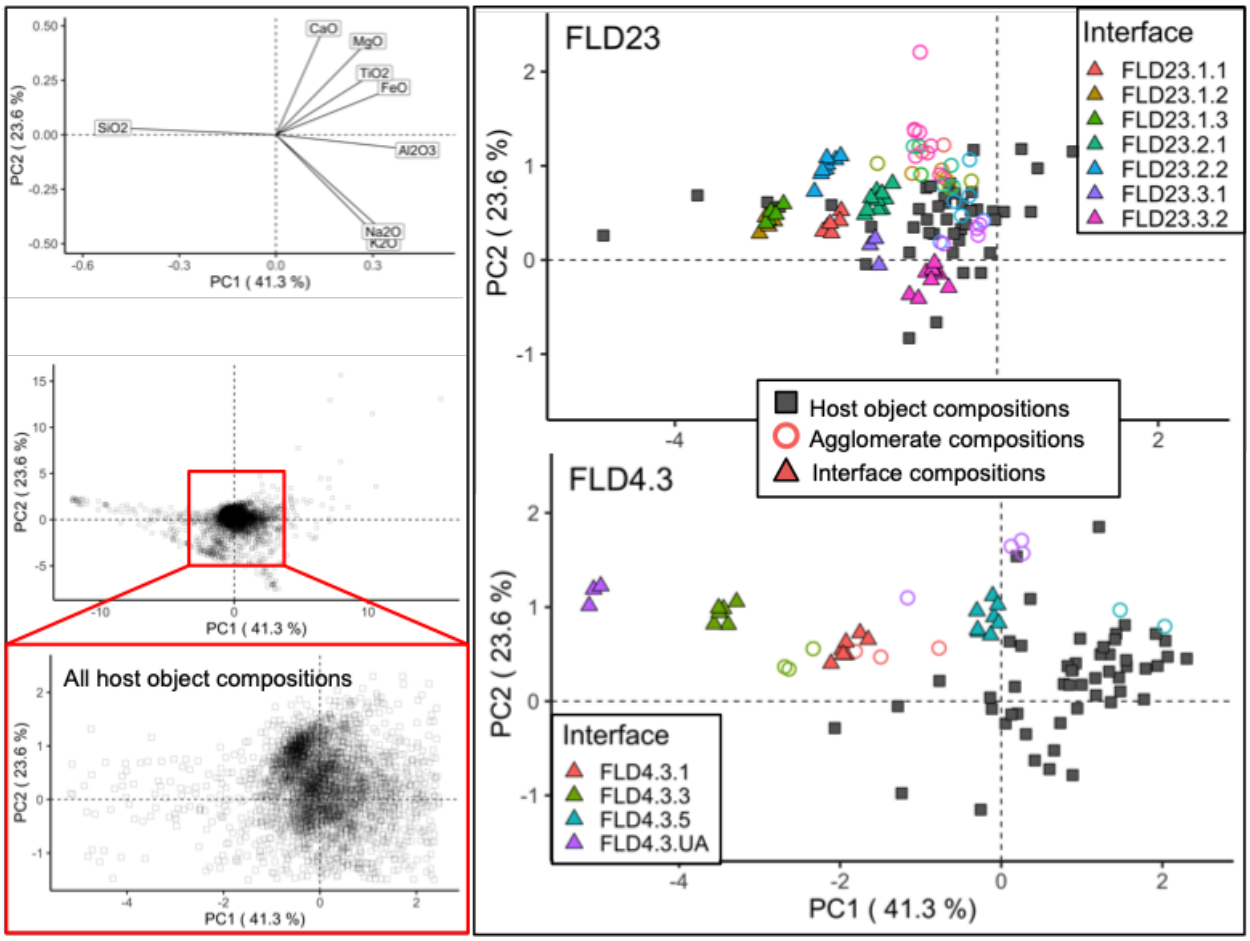

Figure 8.15: Si interface compositions projected into PCA space for 12 interfaces in samples FLD23 and FLD4.3. The top left panel shows the loadings of PC1 v. PC2 and the grid-based host object analyses used to generate the PCA space. The center left panel shows the full range spanned by the host objects in PCA space. The red box is the magnified view shown in the plot in the bottom left (which shows the host object compositions in the magnified view) and the sample specific plots in the right panel. In the magnified PCA plots, which show interfaces characterized in sample FLD23 (top) and sample FLD4.3 (bottom), interface compositions are shown as filled triangles. The composition of the host object is shown as grey filled squares. The agglomerate composition is shown as unfilled circles. Interface compositions tend to be distinct from both their associated agglomerate and host object (a counter-example is interface and agglomerate compositions of FLD4.3.1). Si interface peak compositions trend towards more negative values of PC1 (higher SiO_2 compositions), but do not exceed the range spanned by the EDS host compositions. Data are tabulated in Appendix J using the PCA model shown in Appendix H.

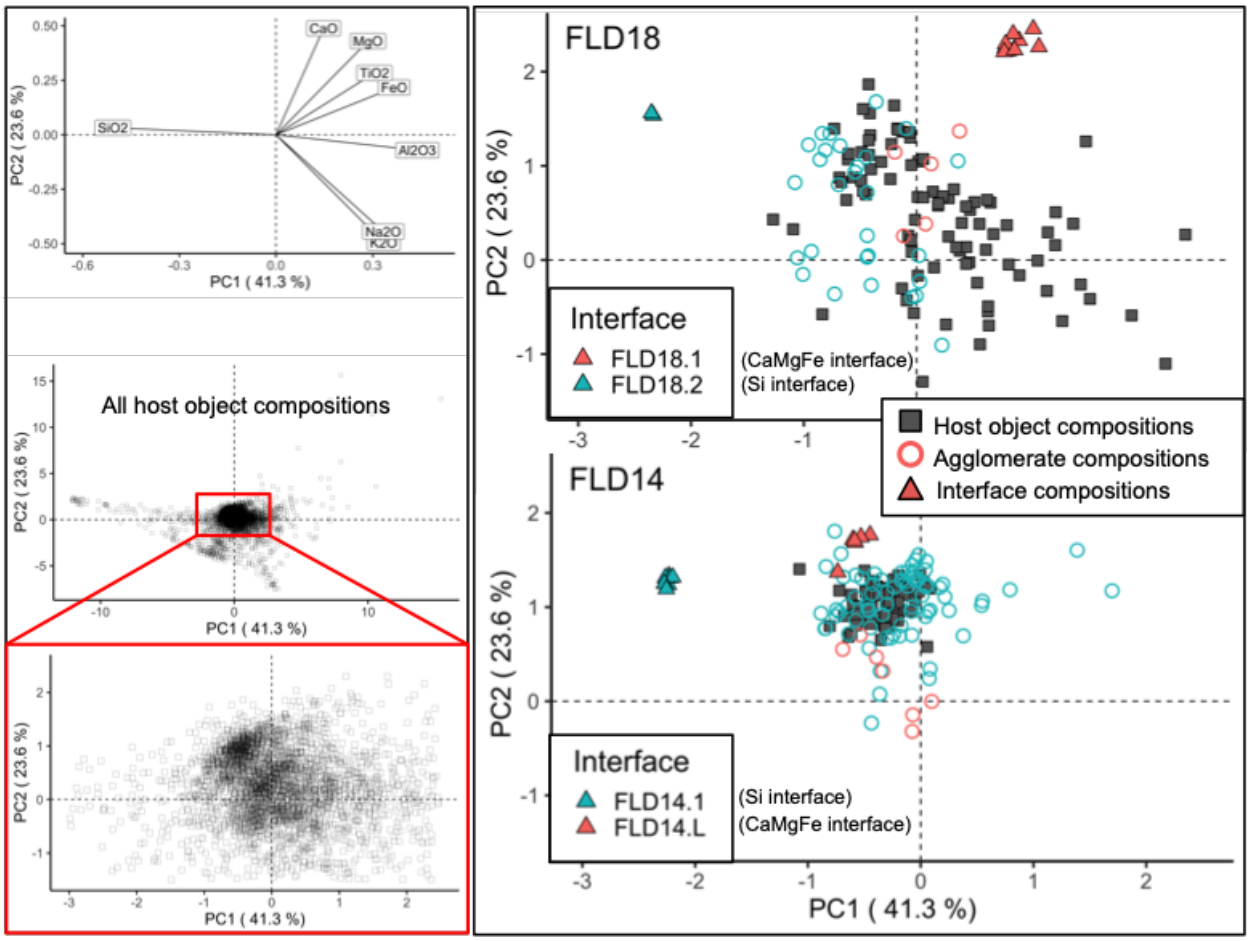

Figure 8.16: Interface compositions projected into PCA space 2 Si and 2 CaMgFe interfaces in samples FLD18 and FLD14. The top left panel shows the loadings of PC1 v. PC2 and the grid-based host object analyses used to generate the PCA space. The center left panel shows the full range spanned by the host objects in PCA space. The red box is the magnified view shown in the plot in the bottom left (which shows the host object compositions in the magnified view) and the sample specific plots in the right panel. In the magnified PCA plots, which show interfaces characterized in sample FLD18 (top) and sample FLD14 (bottom), interface compositions are shown as filled triangles. The composition of the host object is shown as grey filled squares. The agglomerate composition is shown as unfilled circles. Interface compositions tend to be distinct from both their associated agglomerate and host object. Si interface peak compositions trend towards more negative values of PC1 (higher SiO_2 compositions) and CaMgFe interface compositions tend towards quadrant I but do not exceed the range spanned by the EDS host compositions. Data are tabulated in Appendix J using the PCA model shown in Appendix H.

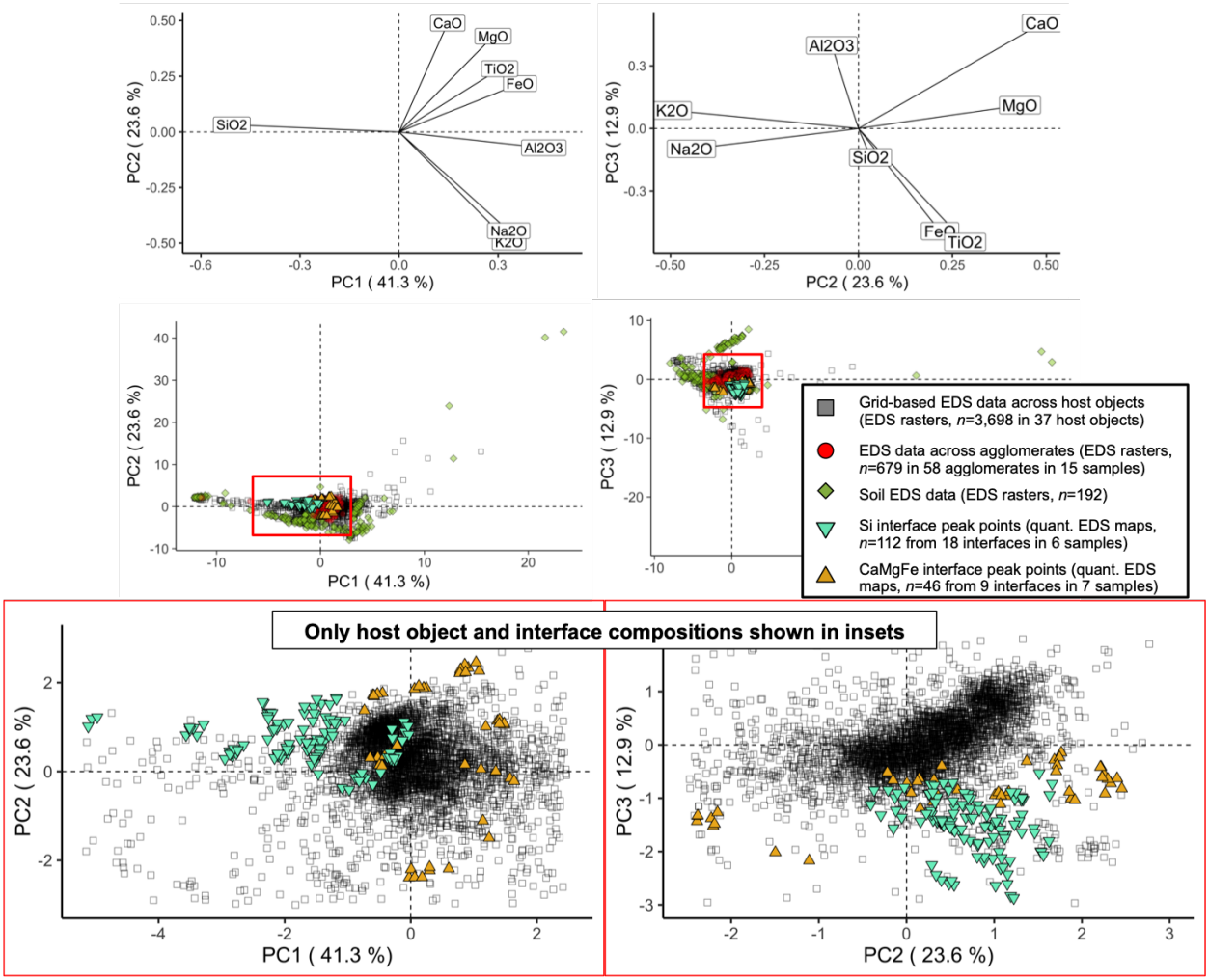

Figure 8.17: Compositions in PCA space for 18 Si interfaces in 6 samples ($n = 112$) and 9 CaMgFe interfaces in 7 samples ($n = 46$) collected using linear traverses extracted from quantified EDS maps. The top plots show the loadings of PC1 v. PC2 (left) and PC2 v. PC3 (right). The center plots shown the full range spanned by the major element compositions of host objects and unmelted soil. Si interface compositions are shown as upside down green triangles and CaMgFe compositions are shown as orange triangles. The host, agglomerate, and soil major element compositions are rendered partially transparent. The bottom plots shows the inset marked in the middle plots, but excludes the agglomerate and unmelted soil compositions for clarity. Data are tabulated in Appendices B (for host object compositions), C (for agglomerate compositions), D (for unmelted soil compositions), J (for Si and CaMgFe interface compositions), and H for the PCA model used to project the compositions into PCA space.

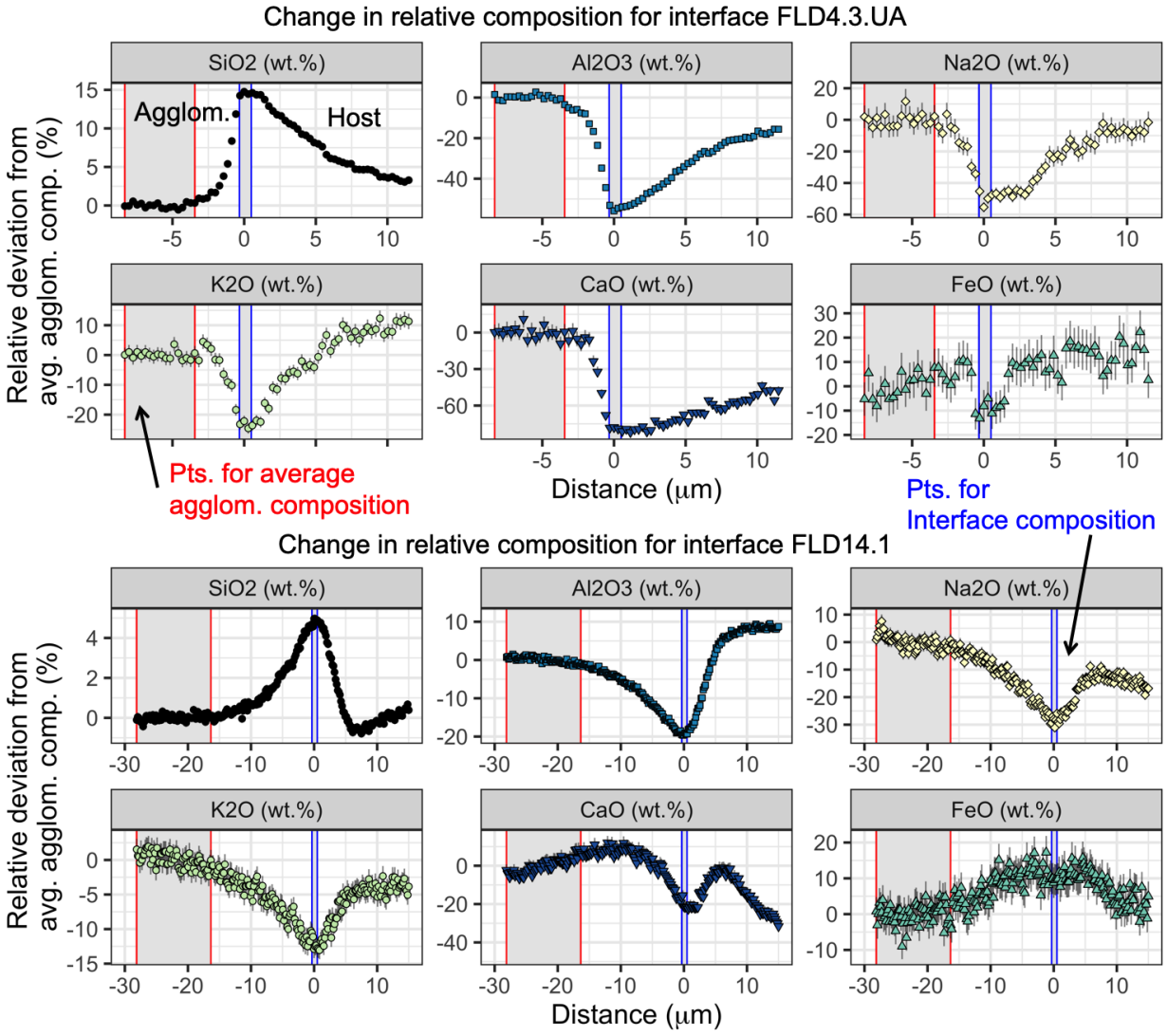

Figure 8.18: Example showing the change in major element composition across the interfaces of FLD4.3.UA (top panel) and FLD14.1 (bottom panel) relative to the average agglomerate composition. The traverses are centered at $x = 0$ μm based on their SiO_2 maxima. The agglomerate composition is sampled for values of $x < 0$ μm, and the host is sampled for values of $x > 0$ μm. The points used to determine the average agglomerate composition are shown in the red box. The blue box at the interface shows the interface peak points, used to determine the interface composition, selected based on the points within 2σ of the SiO_2 maxima for Si interfaces (and FeO maxima for CaMgFe interfaces). Data are tabulated in Appendix J.

K_2O and FeO tend to be the least relatively depleted at the interface relative to the agglomerate composition. This suggests that not only is SiO_2 is condensing at the periphery of fallout melts in the fireball, but small amounts of other relatively volatile vaporized species from the soil are co-condensing. This hypothesis is bolstered by the observation of four

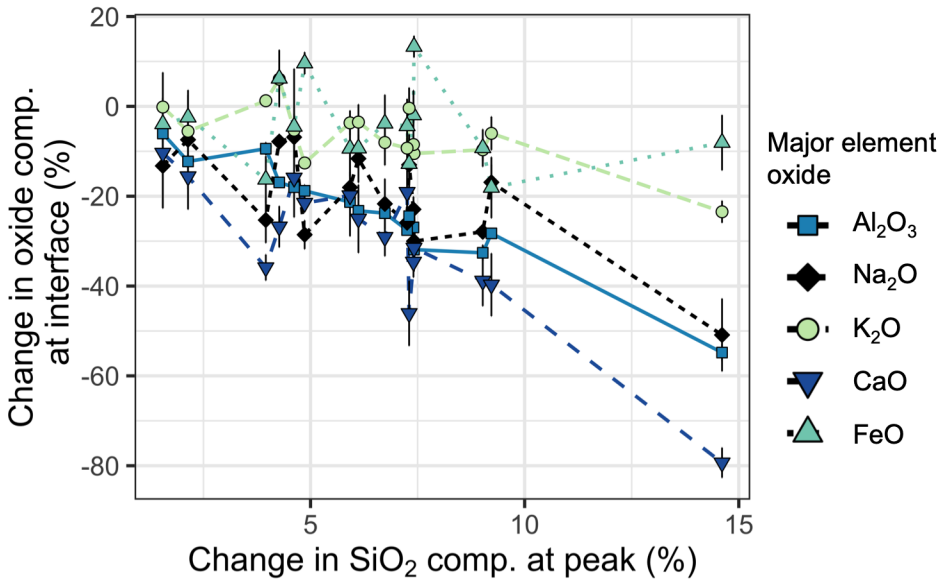

Figure 8.19: The relative change in major element oxides at 16 Si interfaces in 8 samples as a function of the relative enrichment of SiO_2 at the peak of that interface. The interfaces are listed in the text. Relative enrichments and depletions are calculated relative to the average agglomerate composition (≈40 points for each interface were sampled and averaged to determine the "agglomerate" composition). The plots shows 14 Si interfaces. The greatest relative depletions at interfaces tend to be from CaO, Al_2O_3, and Na_2O (possibly due to volatility). The smallest relative depletions (and sometimes enrichments) at the interfaces tend to be observed in FeO and K_2O. An evaporative process would lead the refractory oxides enriched. Instead, the Si interfaces likely reflect a condensation process where Si preferentially is deposited on the surface of agglomerates and hosts. The intermediate behavior of Na_2O could suggest that condensation and evaporation happened concurrently, leading to the preferential loss of Na_2O and higher relative depletions of Na_2O at the interfaces.

interfaces that show a K_2O and/or FeO *enrichment* at their interface relative to the mean agglomerate composition. Two interfaces are only enriched in FeO (FLD14.1 and FLD18.2, the two interface compositions that plotted *outside* the observed range of all EDS host grid analyses in PC1 v. PC2), one interface (FLD10.L) is slightly enriched in K_2O, and one interface (U3.1) is enriched in both FeO and K_2O by the same relative amount (the points overlap; Fig. 8.19).

Na_2O belies the inverted trend observed for K_2O, FeO, Al_2O_3, and CaO. Na_2O exhibits an intermediate behavior, tending to plot between K_2O, FeO and Al_2O_3 and CaO, instead of being the least depleted of the five major element oxides as the trend from the other species may suggest. This may be due to evaporation occurring at the surface of the fallout melts, enabling some Na_2O volatilization from the surface of the melts. Na_2O should volatilize before other species if the given local partial pressure of the other soil-derived species in the vapor phase does not affect the expected volatility order.

8.9 Implications for fallout formation

The presence of SiO_2 enrichments at the surfaces of agglomerates and hosts their observed frequency suggests and supports the hypothesis of a complex and rapidly-evolving vapor environment in the fireball. This is additionally supported by the existence of layered Si and CaMgFe interfaces. The occurrence of Si interfaces suggests that the fireball contains regions with high concentrations of vaporized silica. The Si interfaces are most likely due to high partial pressures of $SiO_{(gas)}$, which cause Si to condense from the vapor phases onto both agglomerates and hosts, rather than being an evaporative process that would leave Si enriched at the surface or peripheries of silicate melts. The hypothesis of high partial pressures of Si in the vapor above the precursor melts show that soil-dominated vapors can condense onto silicate melts. This vapor component most likely originates as finer soils that are easily lofted into the early fireball and vaporized.

For detonations in untested environments, this behavior suggests that high concentrations of fine material in the environment may vaporize more easily and result in those environmental compositions being enriched at interfaces of agglomerates and hosts in quenched fallout. This can be explored by analyzing fallout from tests where the local lithology is well known and characterized.

The diffuse character of Si interfaces surrounding host objects (Figures 8.10 and 8.12) coupled with the existence of Si interfaces on interior agglomerates suggest this Si-rich condensation occurred earlier than the deposition CaMgFe interfaces, which tend to have narrower widths and have only been observed on surface and exterior agglomerates. Enriched U incorporated into the bulk of agglomerates and host objects must occur prior to the formation of Si interfaces because enriched U appears mixed throughout the volume of these samples, while the Si remains enriched at sample peripheries and compositional interfaces. The U behavior at these interfaces is discussed in the next chapter.

8.10 Conclusion

This chapter explored the two types of compositional interfaces observed in fallout from this test: CaMgFe and previously unreported Si interfaces. CaMgFe interfaces have previously been characterized and the data presented here are consistent with prior observations. Both types of interfaces are likely due to condensation processes, with the Si condensation occurring earlier than the CaMgFe condensation. This leads to hypothesized permutations of how single and multiply-layered interfaces may be observed (many of which were observed and noted in this chapter; Figure 8.11). The interface compositions tend to be distinct from the associated agglomerate and host object, but are mostly bounded by the collection of host analyses discussed earlier in this dissertation. This suggests that the compositional heterogeneity in the soil is, in most cases, greater than compositional variations resulting from the condensing of the Si or CaMgFe species from the vapor phase. While formation of both interfaces is likely a result of condensation, the CaMgFe interface is known to co-condense

with an enriched U component from the vapor environment. How enriched U behaves at Si interfaces is discussed further in the next chapter.

Chapter 9

U Behavior at Compositional Interfaces

9.1 Chapter overview

EDS can measure elemental concentrations as low as 0.1–0.25 wt.% [93]. In glassy fallout studied in this dissertation, the only elements with abundances $\gtrapprox$0.1 wt.% are those appreciably concentrated in the emplacement environment (see Chapter 4). To determine the behavior of unfissioned U, which is present at ppm concentrations, SIMS analyses are necessary (see Chapter 5). In this chapter, the high-resolution imaging capability of the NanoSIMS is used to determine the behavior of ^{235}U at both CaMgFe and Si compositional interfaces between agglomerates and host objects. U has previously been observed to be relatively enriched at CaMgFe interfaces along with CaO, MgO, and FeO [67, 68]. The NanoSIMS analyses in these dissertation are used to corroborate the previous findings of [68] and [67] at CaMgFe interfaces and determine if U is co-located with Si at Si interfaces to establish a more thorough formation hypothesis for Si interfaces.

9.2 Previous findings of ^{235}U behavior at CaMgFe compositional interfaces

^{235}U behavior at CaMgFe interfaces has already been investigated at length in Weisz (2016), Weisz et al. (2017), and Weisz et al. (2018) [67, 68, 84]. These studies collected NanoSIMS isotope ratio images at nine interfaces in five samples (A1, B1, B2, B3, C1, C2, D1, D2, and E1 in samples A, AA.B, AE.C, AG.D, and AH.E). Figures 9.1 and 9.2 show the three primary isotope ratios (^{235}U/^{238}U, ^{235}U/^{30}Si, and ^{235}U/^{42}Ca) collected at these nine interfaces.[1] Images of NanoSIMS rasters from Weisz (2016) for agglomerates in AE.C (C1 and C2) and

[1]Weisz (2016) measured ^{44}Ca, but was converted to ^{42}Ca (assuming natural isotopic composition of Ca) to allow comparison to the ^{42}Ca NanoSIMS data collected in this study.

AG.D (D1 and D2) are shown in this dissertation (Figures 8.4 and 8.5, respectively). Table 9.1 summarizes the enrichment behavior of all nine interfaces.

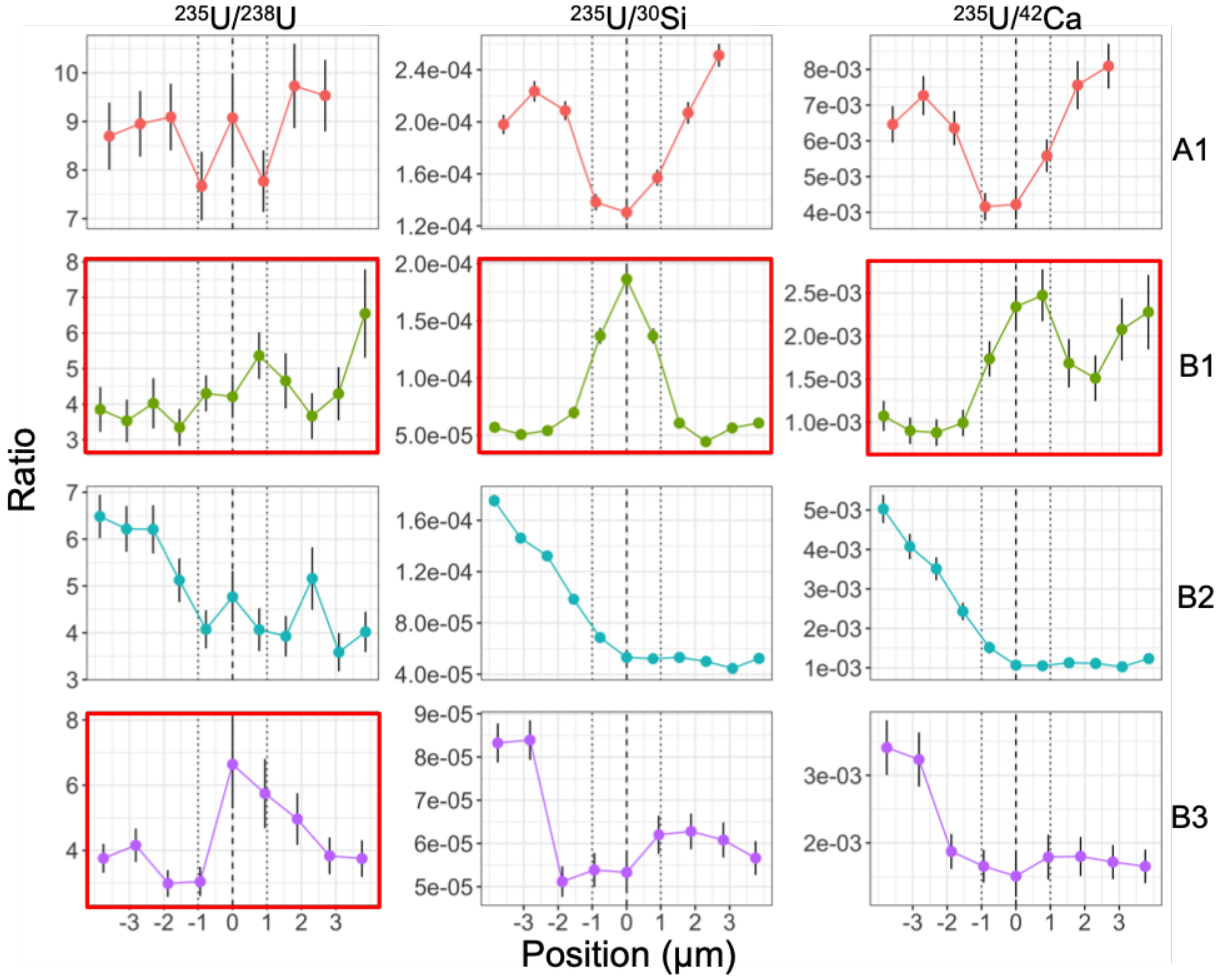

Figure 9.1: Extracted traverses from NanoSIMS rasters across four of the nine interfaces studied with NanoSIMS by [67] (A1 in sample A and B1, B2, and B3 in sample AA.B). Three ratios are shown: $^{235}U/^{238}U$, $^{235}U/^{30}Si$, and $^{235}U/^{42}Ca$. Interfaces were centered at $x = 0$ based on the designation of the interface location in [67]. The dotted lines show ± 1 μm about $x = 0$ μm, bounding the interface peak. Uncertainties are 2σ. Plots highlighted in red show an enrichment at the interface, as defined in the text and Table 9.1. These data were extracted from the supplementary tables provided in [67].

The Weisz data (Figures 9.1 and 9.2 and tabulated in Tables 9.1 and 8.1) indicate that an increase in Ca, Mg, and Fe concentrations occurs more frequently than an enrichment in the $^{235}U/^{238}U$ ratio or the U concentration (as given by the $^{235}U/^{30}Si$ ratio) at the CaMgFe interfaces. Additional observations of other CaMgFe interfaces for this study (the interfaces of FLD10.L, FLD14.L, and FLD18.1) confirm this behavior. In 14 CaMgFe interfaces (this includes the 11 CaMgFe interfaces from Weisz (2016) and the 3 CaMgFe interfaces studied

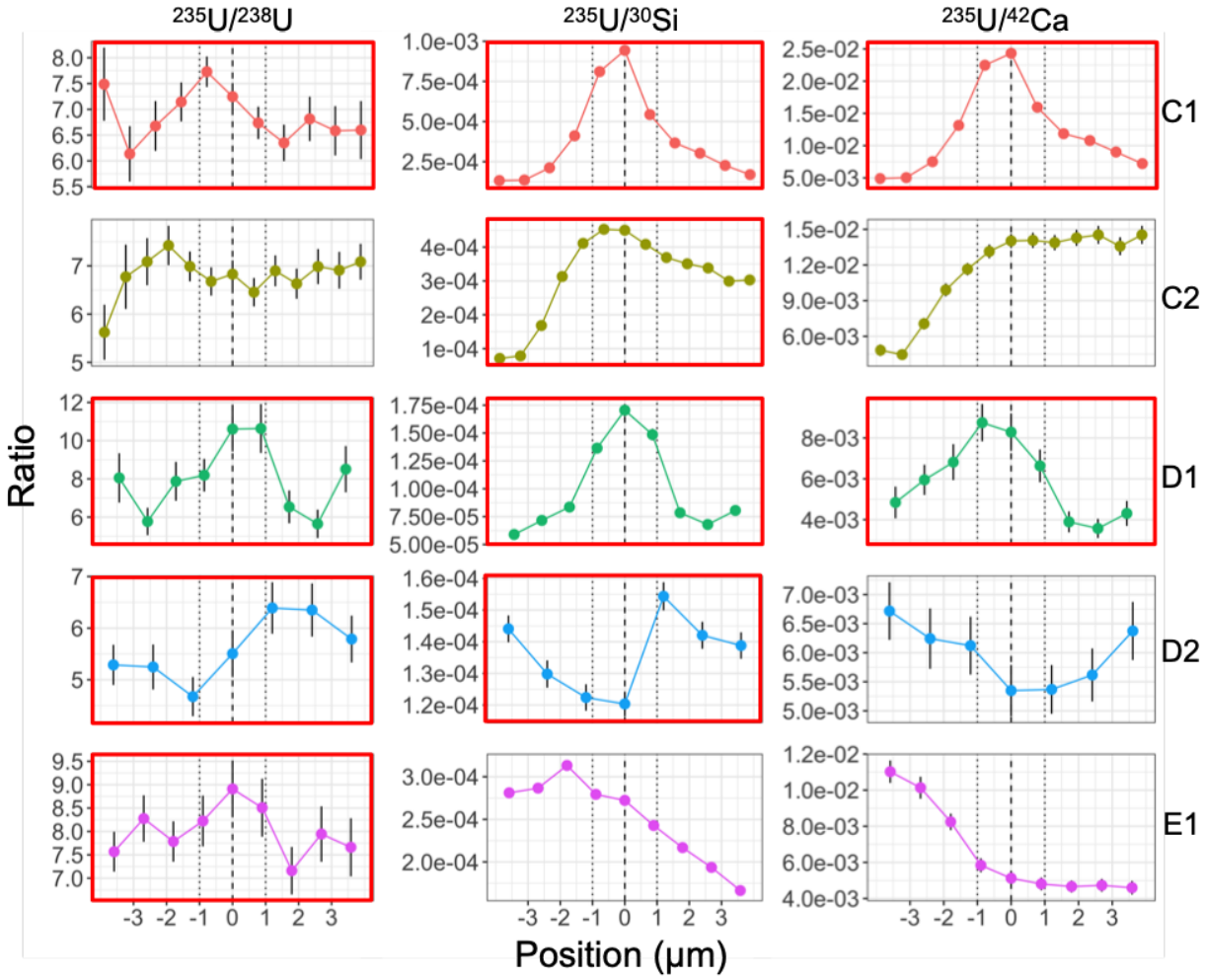

Figure 9.2: Extracted traverses from NanoSIMS rasters five of nine interfaces studied with NanoSIMS by [67] (C1 and C2 in sample AE.C, D1 and D2 in sample AG.D, and E1 in sample AH.E). Three ratios are shown: $^{235}U/^{238}U$, $^{235}U/^{30}Si$, and $^{235}U/^{42}Ca$. Interfaces were centered at $x = 0$ based on the designation of the interface location in [67]. The dotted lines show ± 1 μm about $x = 0$ μm, bounding the interface peak. Uncertainties are 2σ. Plots highlighted in red show an enrichment at the interface, as defined in the text and Table 9.1. These data were extracted from the supplementary tables provided in [67].

here), CaO is enriched at 14 of 14 interfaces, MgO is enriched at 12 of 14 (∼86%) of interfaces, and FeO is enriched at 14 of 14 interfaces.

Weisz (2016) observed that ^{235}U is enriched at 6 of 9 interfaces (∼67%) and the U concentration increases at 5 of 9 interfaces (∼56%). Furthermore, the interfaces enriched in $^{235}U/^{42}Ca$ are a subset of those interfaces enriched in both $^{235}U/^{238}U$ and $^{235}U/^{30}Si$. In these cases, the increase in U concentration at the interface is greater than the increase the CaO concentration at the interface (CaO commonly increases by a factor of 1.5 or more relative to the agglomerate composition; see Figures 8.4, 8.5, and 8.6). In contrast, the

Table 9.1: Observed relative enrichments extracted from NanoSIMS isotope ratio images at the interface of 9 agglomerates (Weisz (2016)) for $^{235}U/^{238}U$, $^{235}U/^{30}Si$, $^{235}U/^{42}Ca$, $^{42}Ca/^{30}Si$, and $^{235}U/^{238}U$ ratios. Interface compositions are considered enriched if a point within 1 μm of the interface (as identified by Weisz (2016)) is greater than the mean of the ratios between 1 and 3 μm on both the agglomerate and host object side of the interface.

Isotope Ratio	Relative enrichment behavior at interface
$^{235}U/^{238}U$	Enriched at **6**/9 interfaces (B1, B3, C1, D1, D2, E1)
$^{235}U/^{30}Si$	Enriched at **5**/9 interfaces (B1, C1, C2, D1, D2)
$^{235}U/^{42}Ca$	Enriched at **3**/9 interfaces (B1, C1, D1)
$^{42}Ca/^{30}Si$	Enriched at **9**/9 interfaces

SiO_2 enrichment is typically <10% at interfaces, and typically offset relative to the CaO and FeO enrichment (see Figures 8.4, 8.5, and 8.6 for representative examples). This behavior is consistent with deposition occurring over time in an evolving vapor, as discussed in Chapter 8. To confirm the observations of CaMgFe interfaces from Weisz (2016), all of which are exterior agglomerates (except for B2 which is a surface agglomerate of B3), NanoSIMS was used to characterize the behavior of U across two additional CaMgFe interfaces. These collective observations of CaMgFe interfaces are then compared to the behavior of U across Si interfaces.

9.3 New observations of U behavior at CaMgFe compositional interfaces

Two additional CaMgFe compositional interfaces were sampled with NanoSIMS in this study, both of which are exterior agglomerates: FLD14.L and FLD10.L (which exhibits a double-layered compositional interface). As described in Chapter 5 (and shown in Figure 5.15), L'IMAGE NanoSIMS image processing software was used to draw linear traverses approximately perpendicular to interfaces using as wide a smoothing as possible to minimize uncertainty, typically ≈10–25 pixels wide (or 2.3–5.8 μm wide), with square NanoSIMS rasters consisting of 64 pixels × 64 pixels and being 15 μm × 15 μm). The approach used to extract traverses is comparable to the procedure outlined in Weisz (2016), except that study generally used larger rasters at higher resolution (20 μm × 20 μm mapped at 256 pixels × 256 pixels) and maintained a constant smoothing width of the linear traverse (15 pixels or ∼1 μm) [67]. How EDS maps were collected and how the linear traverses were extracted are discussed in Section 8.4.

The interface of FLD14.L exhibits a relative enrichment in both ^{235}U and an increase in the U concentration at the interface (Figure 9.3). Three panels are shown in Figure 9.3.

Panel A shows a BSE image of FLD14.L with insets showing the location of the NanoSIMS raster analysis and where the quantified EDS map was taken. In the case of FLD14.L, the NanoSIMS analysis and EDS traverse were collected on opposite sides of FLD14.L, approximately 500 μm apart. This was to avoid the region near the NanoSIMS analysis where Na_2O had been volatilized due to long periods of collecting EDS compositional maps to plan where NanoSIMS analyses would take place. Panel B shows the NanoSIMS isotope ratio images of the $^{235}U/^{238}U$, $^{235}U/^{30}Si$, and $^{235}U/^{42}Ca$ ratios as false color maps for the NanoSIMS analysis that sampled the interface of FLD14.L. FLD14.L occupies most of this image, with the interface appearing as a band in the bottom right corner of each map. These and subsequent isotope ratio images shown in this chapter and Appendix K have not been corrected for mass-dependent fractionation between U isotopes (a $\sim$1% correction) or the relative secondary ion yield between different elements (corrections shown and discussed in Chapter 5), so the color scales shown in Panel B can only be used to infer relative changes between regions within a single isotope ratio image. Panel C shows the extracted traverses from the NanoSIMS isotope ratio maps and the quantified EDS map. These linear traverses *have* been corrected for fractionation and the differing secondary ion yields between different elements. The location of the extracted NanoSIMS traverse is shown with the blue arrow in Panel B.

In all traverses shown in this chapter, the plots are centered so the agglomerate plots at values of $x < 0$ μm, the interface is centered at $x = 0$ μm, and the host plots at values of $x > 0$ μm. For FLD14.L, the interface is centered in the NanoSIMS traverses by the $(^{235}U + ^{238}U)/^{30}Si$ ("$U/^{30}Si$") maximum. The EDS traverses are transformed to oxides and centered centered at $x = 0$ μm based on the FeO maximum, due to the observed consistent enrichment of FeO (along with CaO and MgO) at CaMgFe interfaces (Table 8.1) [67]. Because the NanoSIMS and EDS traverses are collected in different locations, and in this particular case, on opposite sides of the agglomerate, they may only approximate U isotopic and major element trends between one another. For example, in the last two panels of the EDS and NanoSIMS traverses of across the interface of FLD14.L, the $(^{235}U + ^{238}U)/^{42}Ca$ ("$U/^{42}Ca$") and $^{235}U/^{54}Fe$ plots have peaks at $x = 0$ μm, while the CaO plot is slightly offset towards the agglomerate side relative to the FeO peak.[2] Nonetheless, similar to interface D1 (Figure 9.2), the interface of FLD14.L exhibits enrichment in $^{235}U/^{238}U$, $U/^{30}Si$, and $U/^{42}Ca$ ratios, consistent with previous observations of CaMgFe interfaces (Table 9.1).

In contrast, the CaMgFe interface of the double-layered interface of FLD10.L exhibits an increase in the U concentration only and is relatively *depleted* in ^{235}U at the interface (Figs. 9.4 and 9.5). The EDS maps overlaid with NanoSIMS rasters are shown in Figure 9.4 with isotope ratio images and the extracted traverses are shown in Figure 9.5. Figure 9.4 shows FLD10.L on the left, followed by a CaMgFe interface, followed by the Si interface, ending with FLD10 on the right. The top set of compositional maps shows an expanded view of the interface, including an uncharacterized surface agglomerate where the CaMgFe interface

[2]The $^{235}U/^{54}Fe$ plot is uncorrected for fractionation and differing secondary ion yields between different elements because the U-doped glass bearing standards contained no added Fe.

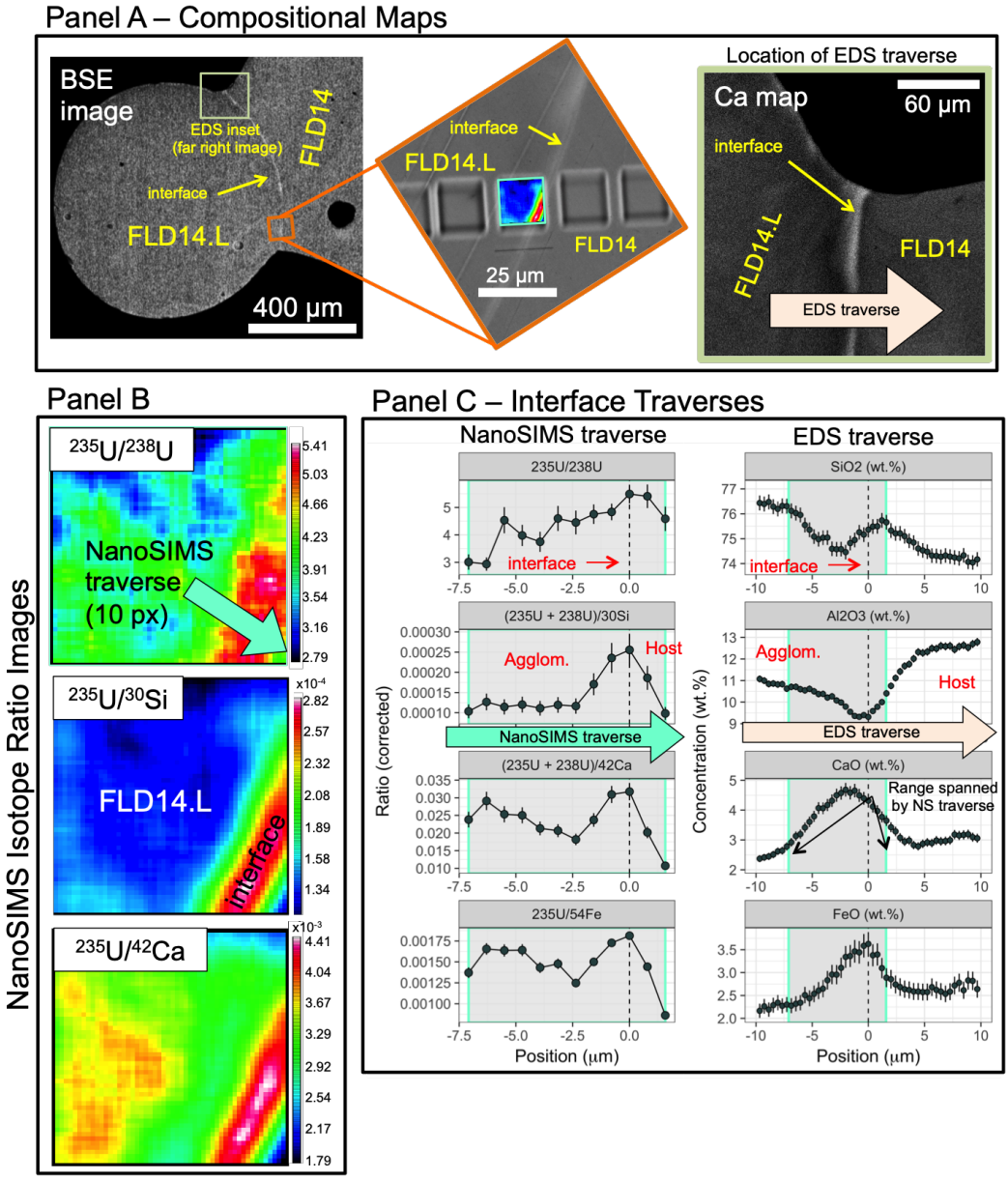

Figure 9.3: The behavior of U isotopes and major elements across interface FLD14.L (an exterior agglomerate with a CaMgFe interface). The insets in Panel A show the location of both the NanoSIMS analysis and the quantified EDS maps from which both interface traverses were extracted. Panel B shows the NanoSIMS isotope ratio images as false color maps for the analysis over the interface. Panel C shows the extracted interface traverses from both the NanoSIMS analysis and EDS maps. For the NanoSIMS traverse, the interface is centered at $x = 0$ μm based on the $(^{235}\mathrm{U}+^{238}\mathrm{U})/^{30}\mathrm{Si}$ peak. For the EDS traverse, the interface is centered at $x = 0$ μm based on the FeO maximum. The range of the extracted NanoSIMS traverse is projected onto the EDS traverse plots as a gray box. Uncertainties are 2σ. Data are tabulated in Appendix J and K.

passes behind the agglomerate and the Si interface passes in front of the agglomerate. The second row of images show the inset denoted by the orange box in the Si map on the top row overlaid with different isotope ratio images. The left side of the isotope ratio images corresponds to the CaMgFe interface and the blue band visible in the $^{235}U/^{30}Si$ and $^{235}U/^{42}Ca$ isotope ratio images (indicating a lower ratio) corresponds with the Si interface in the EDS compositional maps. The remainder of the isotope ratio image to the right of the blue band is the host FLD10. The extracted traverses for FLD10.L are centered based at $x = 0$ μm using the Si interface, corresponding to the $U/^{42}Ca$ minimum for the NanoSIMS traverse and the SiO_2 maximum for the EDS traverse. The CaMgFe interface (shown in the plots as a vertical dashed red line) is centered using the $U/^{42}Ca$ local maximum for the NanoSIMS traverse and the FeO maximum for the EDS traverse.

The depletion in the $^{235}U/^{238}U$ ratio at the CaMgFe interface likely occurs because agglomerate FLD10.L was not sampled in this NanoSIMS analysis. This particular NanoSIMS raster sampled only the CaMgFe interface (discussed in Chapter 8 as coating agglomerate FLD10.L), followed by the Si interface (discussed in Chapter 8 as coating host object FLD10) and the host FLD10. The observed depletion in the $^{235}U/^{238}U$ ratio may be due simply to differences in the U isotopic ratio between the CaMgFe interface and the host object. While FLD10.L was not sampled in the analysis shown in Figure 9.5, there were two additional NanoSIMS analyses were collected in FLD10.L. These analyses are spaced approximately 15 μm and 30 μm from the analysis shown in Figure 9.5 (visible in the top center Si compositional map of Figure 9.4), resulting in measured U isotope ratios (averaging the entire raster, as described in Chapter 5) of 7.51 $\pm$ 0.21 and 5.90 $\pm$ 0.14 (2σ), respectively. The $^{235}U/^{238}U$ ratio of the analysis 15 μm away is within 1σ uncertainty of the $^{235}U/^{238}U$ ratio at the CaMgFe interface (7.78 $\pm$ 0.39), suggesting no substantive enrichment. The analysis collected 30 μm away from the CaMgFe interface in FLD10.L falls outside this uncertainty.

9.4 U behavior at Si interfaces

Chapter 8 established that the only major element oxide enriched at Si interfaces is SiO_2. Given the hypothesis that this interface is the result of a condensation process, establishing the behavior of U at interfaces will help establish whether U tended to co-condense with Si from the vapor phase, as would be predicted if Si interfaces result from material condensing from the ambient environment in the fireball. Three examples of NanoSIMS raster images over Si interfaces are provided (Figures 9.6-9.9). In contrast to CaMgFe interfaces, no persistent enrichment in the $^{235}U/^{238}U$ ratio occurs across these three interfaces. Variations in isotope ratios are likely due to a combined decrease in the total U concentration and variation in either SiO_2 (which increases by <10%) or CaO (which decreases) concentration at the Si interface. Variations in the the $^{235}U/^{238}U$ ratio are best explained as variable enrichments between the agglomerate and the host.

The most well-defined Si interface sampled with NanoSIMS in this study is U1B.L. It is best visualized using the $^{235}U/^{42}Ca$ isotope ratio image (bottom map in Panel B, Fig.

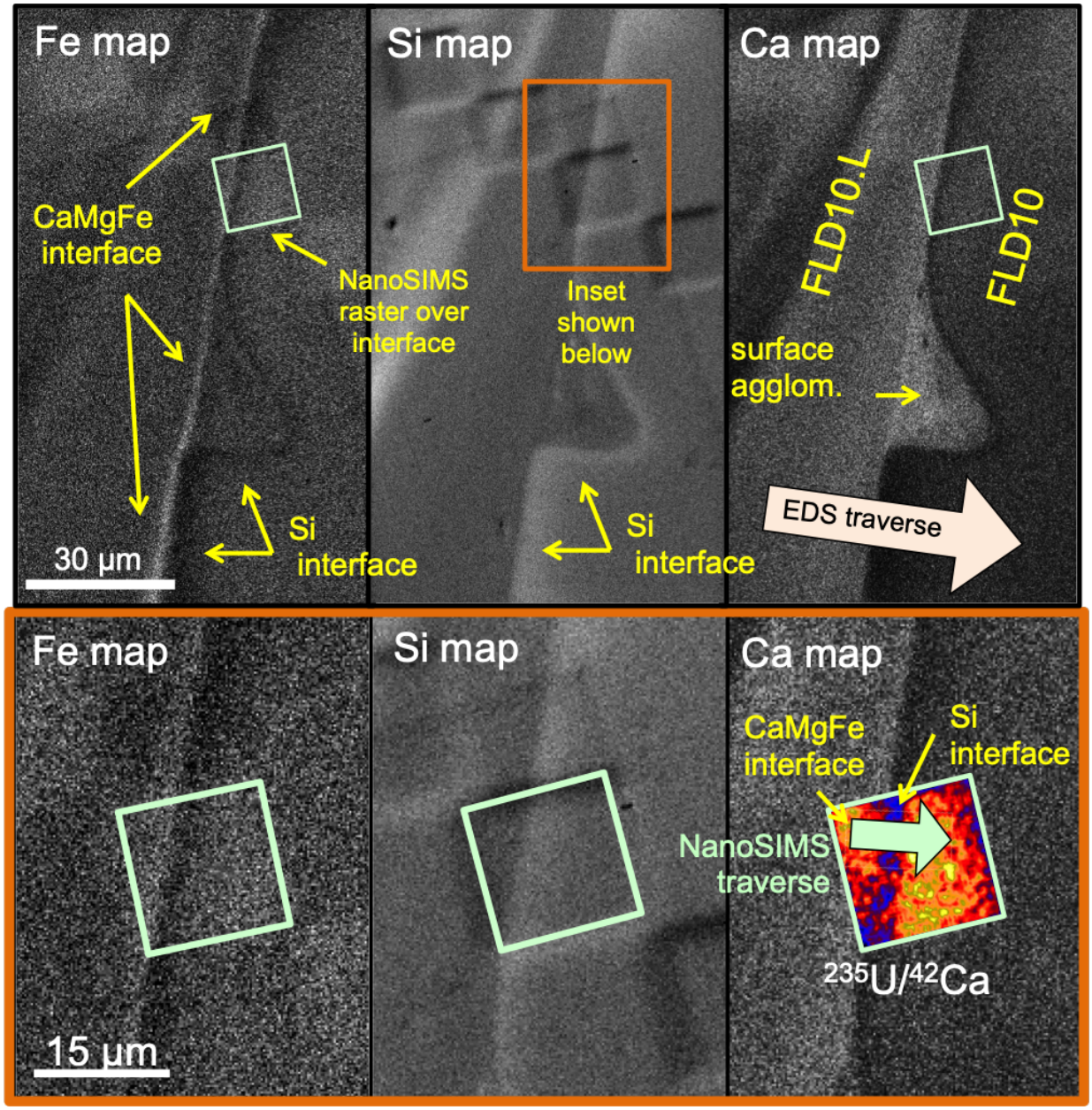

Figure 9.4: Compositional maps showing the double-layered interface between exterior agglomerate FLD10.L (left side of compositional maps) and FLD10 (right side of compositional maps). Moving from from FLD10.L to FLD10, the first interface is a CaMgFe interface, followed by an Si interface. The surface agglomerate exhibits a CaMgFe interface between itself and FLD10.L and an Si interface between itself and FLD10. This suggests the CaMgFe interface is consistent with a late stage deposition coating on the agglomerate, while the Si interface may have previously deposited on the host object, as hypothesized in Chapter 8. The bottom panels show the location of the NanoSIMS analyses over the interface with the $^{235}U/^{42}Ca$ isotope ratio image overlaid in the Ca panel. The extracted traverses are shown in Figure 9.5 and were conducted <100 μm from each other.

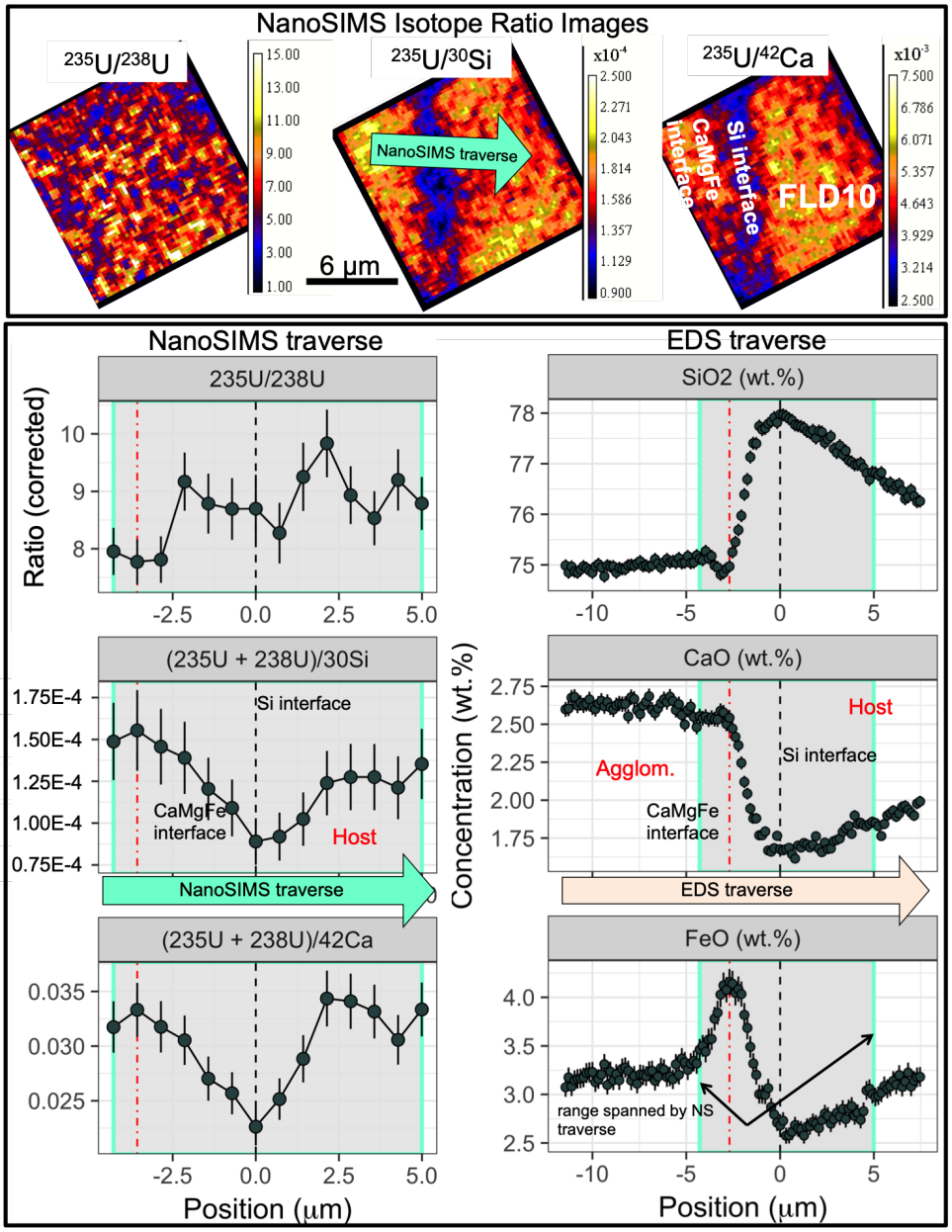

Figure 9.5: The U isotopic and major element behavior across the double-layered interface of FLD10.L (an exterior agglomerate). The top panel shows the NanoSIMS isotope ratio images. The bottom panel shows the extracted interface traverses from both the NanoSIMS analyses and EDS maps (location shown in 9.4). For the NanoSIMS traverse, the Si interface is centered at $x = 0$ μm based on the U/^{42}Ca minimum and the CaMgFe interface is identified based on the local U/^{42}Ca maximum. For the EDS traverse, the Si interface is centered at $x = 0$ μm based on its SiO_2 maximum and the CaMgFe interface is identified from the FeO maximum. The range of the extracted NanoSIMS traverse is projected onto the EDS traverse plots as a gray box. Uncertainties are 2σ. Data are tabulated in Appendix J and K.

9.6). Figure 9.6 is organized into Panels A, B, and C, similar to Figure 9.3 for FLD14.L, where Panel A shows the EDS compositional maps, Panel B shows the NanoSIMS isotope ratio images, and Panel C shows the extracted interface traverses for both datasets. The extracted NanoSIMS traverse for the interface of U1B.L was centered at $x = 0$ μm using the U/^{42}Ca maximum. The EDS traverse was centered at $x = 0$ μm using SiO_2 maximum. The traverses extracted from the isotope ratio images in L'IMAGE used a 20 pixel (6.4 μm) wide smoothing width (the NanoSIMS raster is 20 μm x 20 μm and contains 64 x 64 pixels). The EDS traverse used a 31 μm smoothing width and was taken approximately 50 μm from the NanoSIMS raster analysis.

The Si interface of U1B.L is not detectably enriched in ^{235}U/^{238}U at the interface's centroid, in contrast to the CaMgFe interface of FLD14.L (Fig. 9.3). Averaging the first five points in the agglomerate U1B.L (from $x \approx$-12 to -7.5 μm), yields a ^{235}U/^{238}U of 8.41 $\pm$ 1.61 (2σ), while the interface peak has a ^{235}U/^{238}U ratio of 8.13 $\pm$ 0.53, no change relative to the agglomerate.

Similar to previous findings of CaMgFe interfaces, SiO_2 enrichments across Si interfaces are also limited to <10% relative to the agglomerate composition (discussed further in Chapter 8). This limited increase in the SiO_2 concentration allows the U/^{30}Si ratio to serve as a proxy for the U concentration at Si interfaces, just as they do at CaMgFe interfaces. The U/^{30}Si ratio at the Si interface of U1B.L is depleted relative to the agglomerate. This depletion is such that the U/^{30}Si ratio of the host object and interface are consistent, while both their SiO_2 concentrations and ^{235}U/^{238}U ratios differ. Averaging the same 5 points in the agglomerate as done in the paragraph above, the average U/^{30}Si ratio in the agglomerate is $(1.87 \pm 0.24) \times 10^{-4}$ (2σ), compared to $(1.20 \pm 0.35) \times 10^{-4}$ (2σ) at the interface centroid, a 36% depletion (-38 $\pm$ 21% (2σ)). The increase in the SiO_2 concentration at the interface is insufficient to fully account for the depletion in the U/^{30}Si ratio, as [SiO_2] increases by $\sim$9% at the interface relative to the agglomerate composition ([SiO_2] = 71.7 $\pm$ 0.3 wt.% in U1B.L and 78.3 $\pm$ 0.2 wt.% (2σ) at the interface peak, an increase of 9.2 $\pm$ 0.5%). As a result, there must be a 30 $\pm$ 7% decrease in the U concentration at the interface to account for the U/^{30}Si depletion. This observed depletion in the U/^{30}Si ratio at Si interfaces is also visible in the Si interface of FLD10.L, where interface is depleted relative to both the agglomerate and the host object (Figure 9.5).

However, performing the same calculation using U/^{42}Ca does not result in the same decrease in U concentration at the Si interface. The U/^{42}Ca ratio at the interface exhibits a 89 $\pm$ 14% enrichment relative to the agglomerate, increasing from 0.067 $\pm$ 0.003 (2σ) in the agglomerate (averaging the same first five points) to 0.127 $\pm$ 0.008 (2σ) at the interface centroid. Based on the EDS interface traverse (bottom of Panel C; Figure 9.6), the average CaO concentration in the agglomerate is 1.57 $\pm$ 0.14 wt.% (2σ) and decreases to 0.95 $\pm$ 0.06 wt.% at the interface, a -40 $\pm$ 8 % depletion relative to the agglomerate composition. As a result, the required change in U concentration is an enrichment of +14 $\pm$ 18 %, which encompasses no change in U concentration within uncertainty. This discrepancy between the calculated change in U concentration at the interface between the U/^{30}Si and U/^{42}Ca ratios may be due the fact that the EDS and NanoSIMS traverses were conducted in different

locations.

In contrast to the interface between the interior agglomerate U1B.L and host U1B, the Si interface between the *exterior* agglomerate FLD23.L and host object FLD23, while also depleted in the U/^{30}Si ratio relative to the agglomerate composition, does *not* exhibit an enrichment in the U/^{42}Ca ratio at the interface (Figs. 9.7 and 9.8). The Al map on the right of Figure 9.8 shows FLD23.L on the left, FLD23 on the right, and the Si interface extending from the top right corner down across the image as a dark diffuse band. Between FLD23.L and FLD23 are several surface agglomerates, including FLD23.3.2 (characterized with SIMS) and two others (uncharacterized). The red arrow shows the direction and approximate smoothing width of the extracted EDS traverse. The insets (orange box, on left) are overlaid with false color NanoSIMS isotope ratio images, revealing that an uncharacterized surface agglomerate was sampled by the NanoSIMS analysis (bottom right of the false color NanoSIMS isotope ratio images in Figure 9.7). The small blue arrow in the ^{235}U/^{42}Ca NanoSIMS isotope ratio image (Ca map inset) shows the direction and approximate smoothing width (25 pixels or 5.9 μm) extracted from the 15 μm x 15 μm, 64 pixel x 64 pixel NanoSIMS raster. The uncharacterized surface agglomerate was avoided when extracting the NanoSIMS traverse.

Similar to U1B.L, the interface between FLD23.L and FLD23 exhibits no detectable enrichment in the ^{235}U/^{238}U ratio (Fig. 9.8). Instead, the ^{235}U/^{238}U ratio monotonically increases across the interface, beginning with a mean of 3.77 $\pm$ 0.30 in the agglomerate (averaging the first five points in the agglomerate) to 5.87 $\pm$ 0.15 in the host object (averaging the last four points in the host), an increase of (56 $\pm$ 13)% from FLD23.L to FLD23.

Also, similar to U1B.L, the interface exhibits a depletion in the U/^{30}Si ratio at the interface, which cannot be fully accounted for by the increase in the SiO_2 concentration at the interface. The U/^{30}Si ratio in the agglomerate is (1.52 $\pm$ 0.27) $\times$ 10^{-4} (averaging the first five points in the agglomerate) and is (0.71 $\pm$ 0.21) $\times$ 10^{-4} at the interface centroid, a $\sim$54% decrease (-53 $\pm$ 16% (2σ)). The SiO_2 concentration across the interface increases by $\sim$7% ([SiO_2] = 73.8 $\pm$ 0.5 wt.% in the agglomerate and 79.2 $\pm$ 0.1 at the interface). The U concentration at the interface must decrease by $\sim$50% at the interface to account for the observed depletion in the U/^{30}Si ratio (-50 $\pm$ 17% (2σ)).

The change in U concentration required to explain the variation in the U/^{42}Ca ratio at the interface is consistent with that of the U/^{30}Si ratio. The U/^{42}Ca ratio in the agglomerate is (2.26 $\pm$ 0.13) $\times$ 10^{-2} and is (1.71 $\pm$ 0.11) $\times$ 10^{-2} at the interface, a (-24 $\pm$ 11.5)% decrease. The CaO concentration decreases from 2.68 $\pm$ 0.26 wt.% in the agglomerate to 1.45 $\pm$ 0.19 wt.% at the interface, a (-46 $\pm$ 9)% reduction. The U concentration at the interface must decrease by 41 $\pm$ 9% to account for the observed U/^{42}Ca depletion, consistent with the required decrease for the U/^{30}Si ratio.

In contrast to the Si interfaces of FLD10.L, U1B.L, or FLD23.L, the NanoSIMS isotope ratio images for agglomerate FLD4.3.3 does not exhibit a marked maximum or minimum for any of the measured isotope ratios (Figure 9.9). These Si interfaces are apparent as a slight increase in brightness in the Si compositional map at the periphery of FLD4.3.3 (Panel A, Fig. 9.9) and the slight enrichment in SiO_2 (Panel C, Fig. 9.9), steadily increasing from

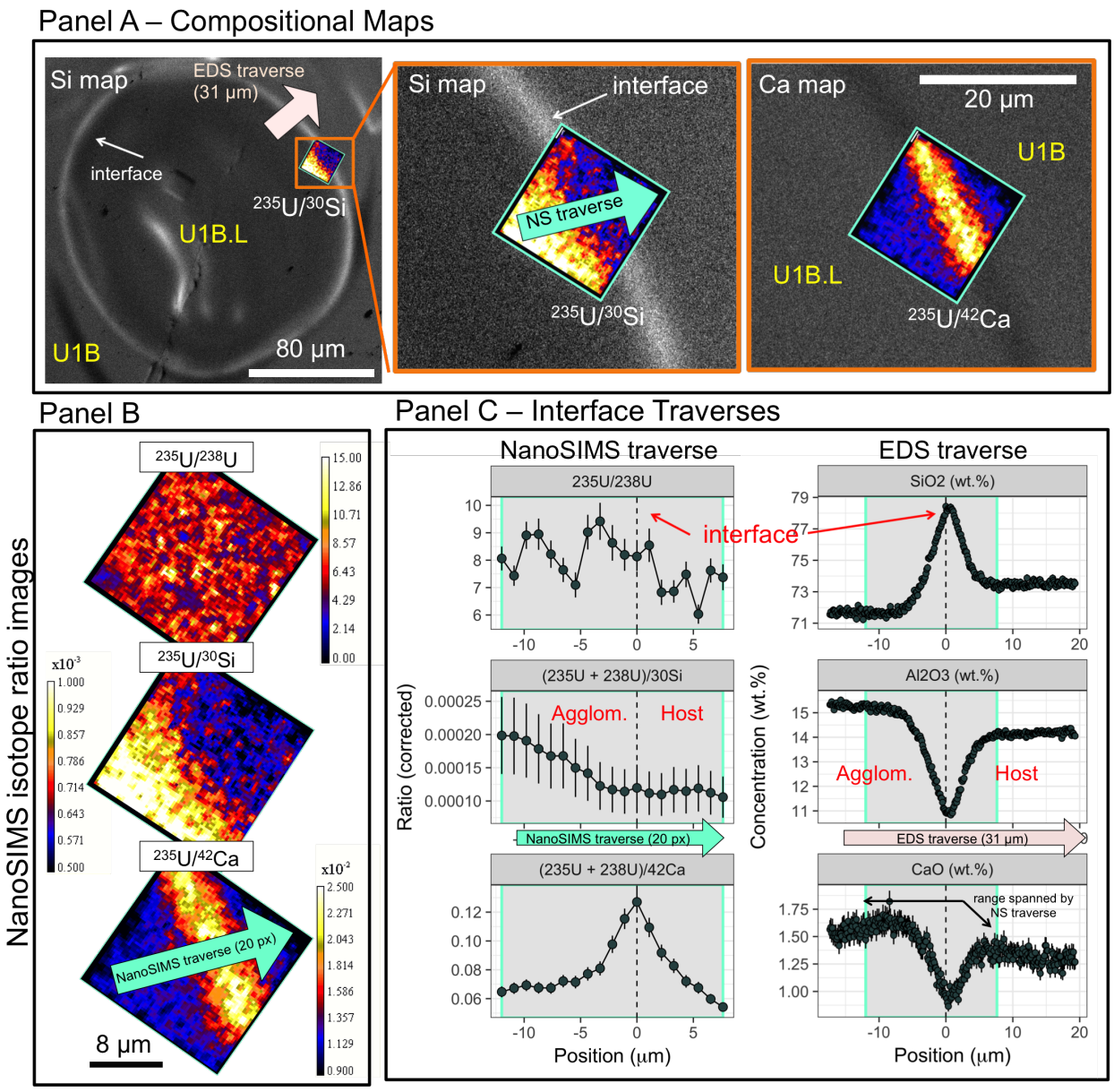

Figure 9.6: The U isotopic and major element behavior across Si interface U1B.L (an interior agglomerate). Panel A shows the location of both the NanoSIMS analysis and the quantified EDS map from which both interface traverses were extracted. Panel B shows the raw NanoSIMS isotope ratio images. Panel C shows the extracted interface traverses from both the NanoSIMS (corrected for fractionation) and EDS analyses. For the NanoSIMS traverse, the interface is centered at $x = 0$ μm based on the U/^{42}Ca maximum. For the EDS traverse, the interface is centered at $x = 0$ μm based on its SiO_2 maximum. The range of the extracted NanoSIMS traverse is projected onto the EDS traverse plots as a gray box. Uncertainties are 2σ. Data are tabulated in Appendix J and K.

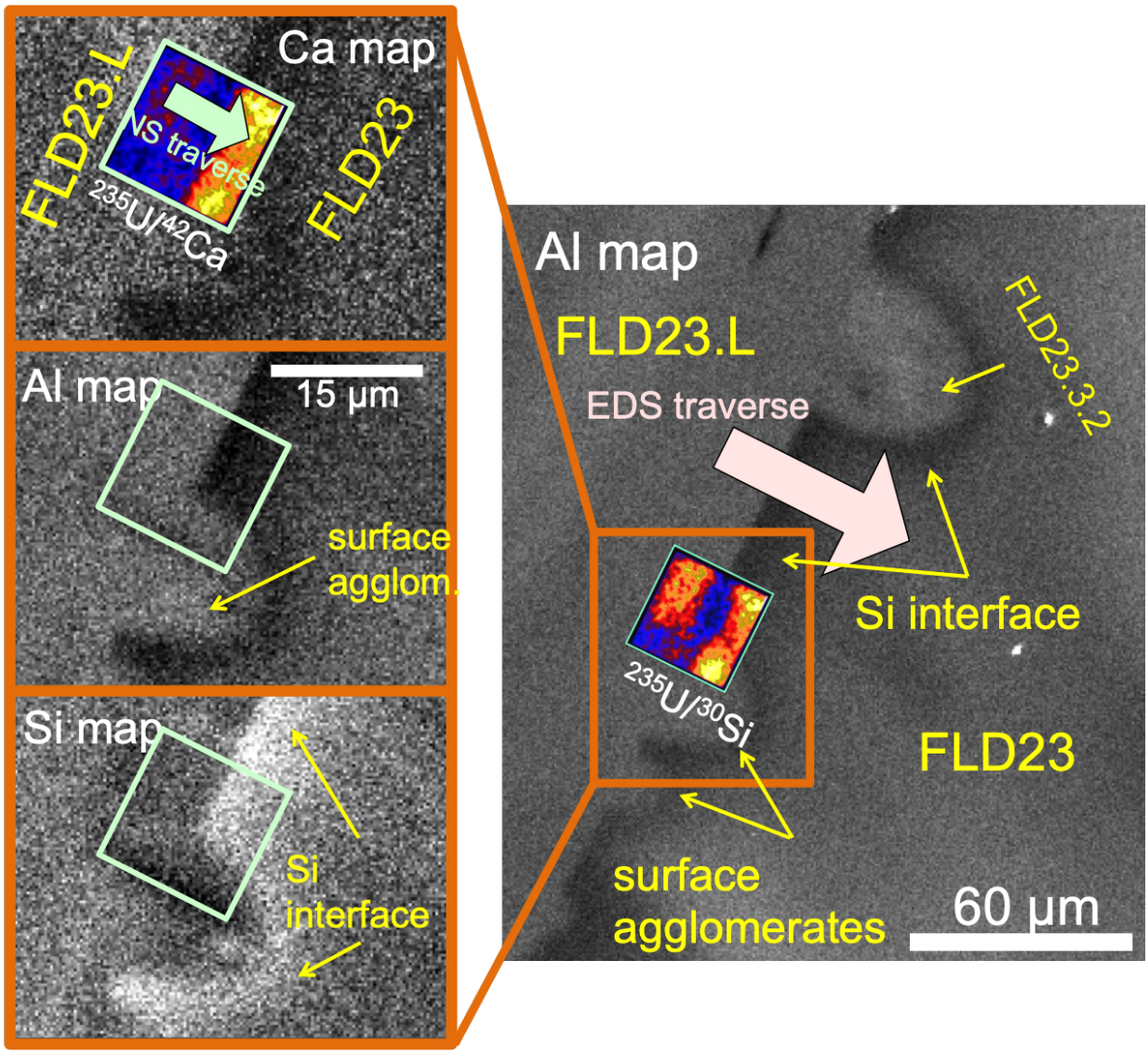

Figure 9.7: EDS Compositional maps showing the Si interface between exterior agglomerate FLD23.L (left side of compositional maps) and FLD23 (right side of compositional maps). The location of the linear traverse extracted from the quantified EDS map is shown as a red arrow. Surface agglomerates between FLD23.L and FLD23 are also visible. The inset (left set of compositional maps) shows the location of the NanoSIMS analysis and the direction and width of traverse extracted from the NanoSIMS raster analysis. The extracted traverses are shown in Figure 9.8 and were conducted <50 μm from each other over Si the interface.

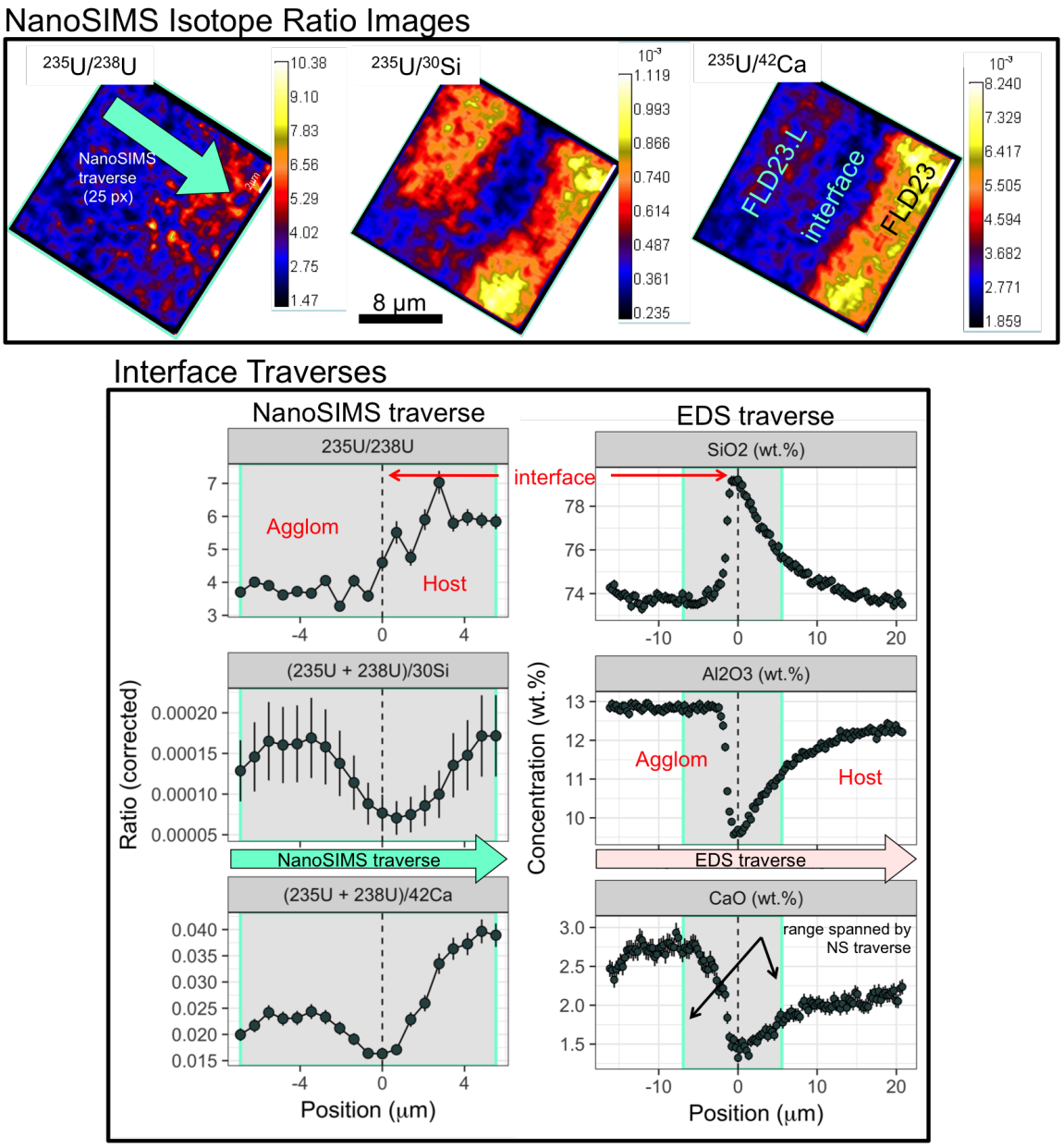

Figure 9.8: The U isotopic and major element behavior across the Si interface of FLD23.L (an exterior agglomerate). The top panel shows the NanoSIMS isotope ratio images as false color maps. The bottom panel shows the extracted interface traverses from both the NanoSIMS (corrected for fractionation) and EDS analyses (traverse locations shown in Figure 9.7). For the NanoSIMS traverse, the Si interface is centered at $x = 0$ μm based on the $(^{235}U+^{238}U)/^{42}Ca$ minimum and for the EDS traverse, the Si interface is centered at $x = 0$ μm based on its SiO_2 maximum. The range of the extracted NanoSIMS traverse is projected onto the EDS traverse plots as a gray box. Uncertainties are 2σ. Data are tabulated in Appendix J and K.

80.8 ± 0.7 wt.% (2σ) (averaged from the first sampled 5 μm within the agglomerate) to 82.4 ± 0.1 wt.%, a 2.0 ± 0.9 % enrichment relative to the agglomerate composition. Here, the $^{235}U/^{238}U$ shows a roughly decreasing trend moving from the agglomerate towards the host, with a possible local maximum at the interface. However, the $^{235}U/^{238}U$ ratio varies within both the agglomerate and the host, both containing points that have $^{235}U/^{238}U$ ratios greater than the $^{235}U/^{238}U$ ratio at the interface. In contrast, the $U/^{30}Si$ shows no variability within uncertainty.

The most marked variation between FLD4.3.3 and its host object is visible in the $U/^{42}Ca$ traverse, which shows an approximately constant trend for the first 6 μm followed by a steadily decreasing trend into the host object. As a result, $x = 0$ μm was set at the point just before the $U/^{42}Ca$ ratio begins its decreasing trend, which roughly aligns with the curved orange and red region visible in the $^{235}U/^{42}Ca$ false color image. The CaO concentration follows a similar trend to the $U/^{42}Ca$ plot, showing a roughly constant concentration in the agglomerate (0.85 ± 0.09 wt.% CaO for the first 5 μm), and in contrast to the NanoSIMS traverse shows a slight change outside 2σ uncertainty at the interface to 0.72 ± 0.03 (a -15 ± 9 % relative depletion at the interface), and steadily increasing into the host thereafter. While the trend suggests that the CaO concentration may still be increasing, averaging the last ≈2.5 μm collected in the host object yields a CaO concentration of 1.55 ± 0.15 wt.% CaO, an 83% ± 25% enrichment (2σ) relative to the agglomerate. The agglomerate exhibits a $U/^{42}Ca$ isotope ratio of 0.113 ± 0.01 (2σ) for the first ≈5 μm in the agglomerate (the first six points in the traverse) and the host object has a $U/^{42}Ca$ has a ratio of 0.064 ± 0.007 (2σ) for the final ≈3 μm in the host object (the last four points), a relative depletion of -44 ± 9 %. Despite a generally decreasing trend in the $^{235}U/^{238}U$ ratio traversing from the agglomerate to the host, within 2σ uncertainty the $^{235}U/^{238}U$ shows no change when averaging the same points in the agglomerate and the host ($^{235}U/^{238}U = 9.4 \pm 1.6$ in the agglomerate compared to 7.3 ± 2.7 in the host object). Excluding the high outlier in the host object (the first point included in the average at $x \approx 5$ μm) yields a mean $^{235}U/^{238}U$ ratio in the host of 6.6 ± 0.9, just outside 2σ uncertainties, which represents a -30 ± 13% depletion of the host relative to the agglomerate.

9.5 Implications for Si interface formation

The lack of enrichment in the $^{235}U/^{238}U$ ratio and depletion in the $(^{235}U+^{238}U)/^{30}Si$ ratio (U concentration) at most Si interfaces suggests Si did not co-condense with U from the vapor phase, unlike the observed frequent co-location of $^{235}U/^{238}U$ and $(^{235}U+^{238}U)/^{30}Si$ enrichment at CaMgFe interfaces (7/11 and 6/11 interfaces). As discussed in Chapter 8, the ubiquitous presence of Si interfaces surrounding exterior, surface, and interior agglomerates suggests this formation event occurred earlier than CaMgFe interfaces, which, by contrast, have only been observed at the interfaces between exterior and surface agglomerates and their host objects. The ordering of the double-layered interface at FLD10.L further supports this argument (Figure 9.4). The Si interface formation events occurring earlier than

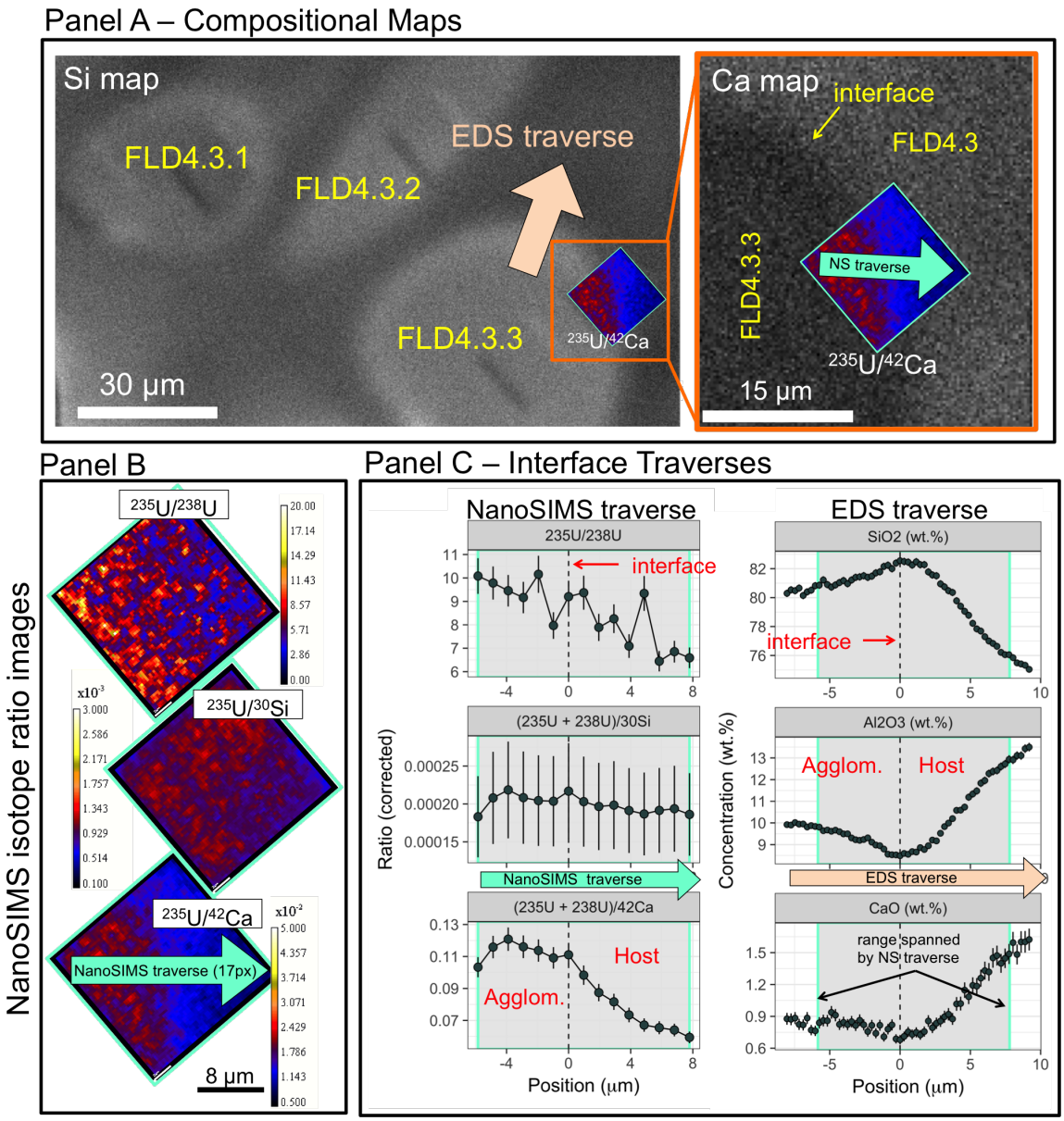

Figure 9.9: The U isotopic and major element behavior across the Si interface of FLD4.3.3 (an interior agglomerate). Panel A shows EDS compositional maps of agglomerates FLD4.3.1, FLD4.3.2, and FLD4.3.3. Arrows denote the location of the extracted traverses. Panel B shows the NanoSIMS isotope ratio images over the interface. Panel C shows the extracted interface traverses from both the NanoSIMS (corrected for fractionation) and EDS analyses (converted to oxides). For the NanoSIMS traverse, the interface is centered at $x = 0$ μm as described in the text. For the EDS traverse, the interface is centered at $x = 0$ μm based on its SiO_2 maximum. The range of the extracted NanoSIMS traverse is projected onto the EDS traverse plots as a gray box. Uncertainties are 2σ. Data are tabulated in Appendix J and K.

CaMgFe interfaces formed is also bolstered by the relative diffuseness of these interfaces, best visualized in the double-layered interface of FLD10.L (Fig. 9.5). Furthermore, the relative depletion of the U/^{30}Si ratio at three of the four Si interfaces (including the Si interface of FLD10.L) and no observed enrichment in the ^{235}U/^{238}U ratio at any of the Si interfaces suggests that the formation occurred in the absence of significant condensing enriched U from the vapor phase of the fireball.

The presence of multiple types of interfaces points to temporal and spatial heterogeneity of the ambient vapor environment, suggesting enriched U is first volumetrically incorporated into both host and agglomerate melts at early times. If these melts pass through an ambient environment dominated by vaporized Si derived from the soil, possibly from fine SiO_2 dominated minerals that are easily lofted and vaporized due to their small size and large surface area-to-volume ratio (similar to one hypothesized mechanism of formation of silica-rich rims in chondrules, as discussed in Chapter 8), an early deposition of the an Si interface occurs. This may be followed by a late stage condensation of CaO, MgO, FeO and enriched ^{235}U when the melts are near their quenching temperatures.

Despite the lack of observed ^{235}U/^{238}U enrichment at Si interfaces, there are three observed examples of both ^{235}U and Si enrichment. These appear not at interfaces, but in three interior agglomerates of FLD4.3. These interior agglomerates are enriched in ^{235}U (Figure 5.24) with an analysis over the interface of FLD4.3.1 having a ^{235}U/^{238}U ratio of 9.87 ± 0.77, an analysis within agglomerate FLD4.3.2 having a ^{235}U/^{238}U ratio of 9.76 ± 0.31, and an analysis within FLD4.3.3 having a ^{235}U/^{238}U ratio of 10.54 ± 0.33 (2σ). Notably, these three interior agglomerates have the highest U isotopic compositions of objects characterized in this study.

The Si contents of FLD4.3.1–FLD4.3.3 is also enriched relative to the average composition of host objects and agglomerates. These interior agglomerates have respective SiO_2 concentrations (in wt.%) of 76.3 ± 2.1, 78.0 ± 0.9, and 78.7 ± 0.5 (1σ), compared to the average of the host EDS data of 73.77 ± 4.07 (Tables 4.4 and 4.8). These SiO_2 concentrations are not outside 1σ of the host EDS average because of the large number of high SiO_2 regions (likely resulting from frequent measurements of unmelted, partially-melted, and completely melted but incompletely mixed quartz) in many of the samples, but are comparable to the SiO_2 concentrations to the peaks of many of the Si interfaces discussed in Chapter 8. If more agglomerates similarly enriched in ^{235}U and SiO_2 are found and characterized in other samples from this event, it would support the hypothesis that some vapor phase material was preserved in some samples at locations other than compositional interfaces, and that the ambient conditions when these agglomerates formed and impacted the host object allowed both Si and U to condense simultaneously.

9.6 Conclusion

The isotope ratio images that sampled CaMgFe interfaces in this study are consistent with previous findings of the behavior of U isotope ratios at these interfaces. The ^{235}U/^{238}U ratio

(in the case of FLD14.L) and/or the $^{235}U/^{30}Si$ (in the case of both FLD14.L and FLD10.L) ratios tend to be enriched across CaMgFe interfaces, supporting a co-condensation of enriched U with the major element species enriched at these interfaces. In contrast, Si interfaces, first reported here, show no detectable enrichment in the $^{235}U/^{238}U$ ratio. Variations in the $(^{235}U + ^{238}U)/^{30}Si$ and $(^{235}U + ^{238}U)/^{42}Ca$ ratios are best explained by a decrease in the U concentration at the interface combined with major element variations across the interface. This suggests a vapor environment dominated by Si at early times, despite prior incorporation of U into the bulk of the melt, and enhanced U deposition at later times resulting in the formation of CaMgFe interfaces. Three examples of interior agglomerates (within a single sample, FLD4.3) whose *bulk* compositions are both enriched in Si and highly enriched in ^{235}U relative to average may be evidence of distinct, condensation dominated formation mechanisms. Similar features found in other samples from this event may point to largely vapor-derived materials preserved in localized early agglomerates *within* host objects, when the ambient fireball environment was suitable for both an Si-rich and U-rich vapor to co-condense and form agglomerates <25 μm in diameter.

Chapter 10

Conclusion

Fallout formation models are empirical, relying on decades old data from a limited number of testing environments. These data show that radionuclides fractionate, and the overall size distribution of fallout particles is sensitive not only to the height of burst, but also to the surrounding lithology. Future concerns are that nuclear explosions may occur in city centers, where the structural materials incorporated into the fireball are significantly different than historic testing environments. This demonstrates a need to more thoroughly understand and predict how fallout may form in untested environments to better inform military, local, and public response in such an event. Predication and real time modeling is particularly challenging in the case of the near-surface burst, where due to the complex coupling between the fireball, the air, and the ground, fallout formation is most poorly understood.

To better understand fallout formation, the role of agglomeration and condensation in altering fallout formation predictions must be studied. Historically, the effect of agglomeration on altering the size distribution and radionuclide content of fallout in near-surface bursts has been ignored, despite a cited pressing need to understand its effect on fallout formation, to possibly account for major discrepancies between observations and models. Some explanation for this discrepancy may result from a lack of understanding of agglomeration's role in fallout formation. As shown in the Heft distribution of fallout (Figure 1.2), fallout particles of small sizes ($\sim$10 μm) may be formed through entirely different formation mechanisms (*e.g.*, primary condensation) and have entirely different radionuclide inventories than larger fallout particles. Through turbulent collisions in the fireball, these smaller fallout melts may agglomerate onto and become incorporated into larger melts, altering the overall radionuclide content of a fallout sample when analyzed in aggregate. This hypothesis, that agglomeration incorporates objects with significantly different radionuclide contents into larger hosts, may explain, in part, the deviation between thermodynamic models of radionuclide fractionation and the observed fractionation as a function of particles size (Figure 1.7).

To determine if this hypothesis is plausible, this dissertation studied the role agglomerates play in forming larger glassy fallout and the possible origins of these agglomerates by characterizing the major element and U isotopic compositions of host objects and agglomerates. First, agglomerates were compared as a separate population to the host object population.

Then, agglomerates were directly compared to their associated host objects. This study, using a larger dataset than any recent study on fallout, allows for conclusions to be drawn about the relationships between agglomerates and host objects, and in particular, how different agglomerates are to *their* hosts, as well as whether there is evidence that agglomerate have distinctive formation formation origins or experienced a significantly different fireball environment prior to collision and coalescence.

10.1 Initial sample characterization

This study characterized agglomerates and hosts starting from an initial sample suite of 49 glassy fallout samples. While previous studies of fallout from this test have focused on mm-scale fallout, the samples studied here were selected from a range of sizes, from approximately 250 μm up to nearly 1 cm in dimension. Starting with optical microscopy, whole unpolished samples were imaged (Figures 2.3–2.6), many of which contain frequent visible agglomeration on their exteriors (Figure 2.7). Backscatter electron micrographs of samples in cross-section reveal heterogeneous compositional textures such as flow-banding and regularly-shaped compositional regions, suggesting incomplete mixing and unmelted or partially-melted minerals, respectively. Furthermore, BSE images reveal compositional agglomerate textures. CaMgFe interfaces are also readily identified in BSE images. However, Si interfaces can also be identified in BSE images, with slightly more difficulty (*e.g.,* Figure 4.8). Autoradiography of all 49 samples (Figure 2.10) shows that samples can exhibit a wide range of activity distributions, from homogeneous to extremely heterogeneous. Many of the heterogeneous activity distributions can be attributed to vesiculation (*e.g.*, AH.E, FLD1, FLD23, FLD17) or individual minerals or entire regions within samples that were partially-melted or may have remained unmelted (*e.g.*, AG.D, FLD3.2, FLD7, FLD10). However, the heterogeneous activity distributions in many samples (*e.g.*, AE.C, FLD12, U2, U4, FLD4.2, FLD4.3, FLD4.4, FLD16, FLD25) appear due to compositional heterogeneity in the sample, suggesting that these different compositional regions also incorporated differing amounts of radionuclides from the ambient environment and along with major elements, were incompletely mixed into the melt prior to the melt quenching. Due to the resolution of autoradiography (particularly in fallout dominated by β emission) and the size of agglomerates characterized in this study, only several exterior agglomerates were identified as contained visibly differing amounts of radioactivity than their hosts—agglomerates B1 and B3 in sample AA.B and agglomerates C1 and C2 in AE.C.

The 49 samples were downselected (Figure 2.1) for further characterization, ensuring the down-selected populations were representative of the initial sample suite by including samples covering the observed range of dimensions, chemical heterogeneity, total activity and distribution of activity. Samples analyzed previously with SIMS were also included. The downselected samples were analyzed for their major element composition using EDS raster analyses (37 samples), to identify agglomerates using EDS compositional mapping (counted in 18 samples; Figure 3.9), and characterize a downselection of agglomerates using EDS

raster analyses (53 agglomerates in 15 samples) to compare the major element composition of agglomerates and hosts.

10.2 Identifying and counting agglomerates

Si and Al X-ray compositional maps reveal a higher frequency of agglomerates within samples than visibly attached to the exterior of unpolished samples (Fig. 3.9). However, agglomerates still occupy of a relatively small, but not insignificant, area of any given sample's total cross-sectional area, indicating that the host object is volumetrically dominant. Agglomerates are observed to occupy between 0 and approximately 20% of the exposed cross-sectional area of samples. Therefore, in samples where agglomerates contribute significantly to the total area, agglomerates could alter the average radionuclide inventory of an entire sample if their radionuclide concentrations were significantly different from that of their host object. Size distributions of agglomerates in host objects exhibit three primary trends: samples with few to no visible agglomerates (*e.g.*, U2, FLD20, FLD28), samples with few agglomerates that occupy a large portion of the visible cross-section (*e.g.*, U4, FLD5.4, and FLD14), and samples containing many smaller agglomerates (*e.g.*, FLD23, CC, and U3). This suggests that agglomeration generally occurs while the host object is still relatively molten, allowing the agglomerate impact to deform the host, as opposed to close to closure and nearly solidified. The variation in attachment location shows that fallout experiences varying degrees of agglomeration. While this study cannot discern agglomerates that arrived very early in time and were fully incorporated and mixed into the host, the total proportion of the sample is dominated (>80% or greater) by the host. In cross-section, surface agglomerates are observed to be by far the most frequently type of agglomerate, while the collection counted exterior, surface, and interior agglomerates show a roughly log-normal distribution with a mean equivalent diameter of 141 μm, with equivalent diameters of identified agglomerates ranging from 5–855 μm.

Compositional maps also revealed a new type of compositional interface, the Si interface. Like CaMgFe interfaces, Si interfaces tend to consistently be depleted in Al, however, unlike CaMgFe interfaces, they only tend to be enriched in Si (typically <10% enriched). Si interfaces are observed with greater frequency than CaMgFe interfaces and are observed at all agglomerate locations: exterior, surface, and interior. In contrast, CaMgFe interfaces have only been observed at the interface of exterior and surface agglomerates and their hosts, consistent with being a late-stage deposition process.

10.3 Major element compositions of hosts & agglomerates

Next, hosts and agglomerates were characterized for their major element compositions using EDS. EDS analyses of fallout, both hosts and agglomerates, reveal several conclusions. First,

from the EDS host analyses in 37 samples, fallout from this test is highly homogeneous (Fig. 4.10). However, fallout also contains unmelted and partially-melted compositions, which contribute to the tailing of the distributions shown in Figure 4.10. These host analyses resemble bulk dissolution analyses, agreeing within 1σ. However, the EDS analyses span a much wider range, confirming the internal of the heterogeneity of the fallout glasses and poor mixing of the precursor soil melts.

The 58 agglomerates in 15 samples characterized by EDS resemble the host compositions, but span a more restricted range, indicating agglomerates tend to be thoroughly melted and more well-mixed than hosts 4.13. When calculating the deviation between an agglomerate's composition from its associated host, the deviations tend to be small, with MgO having the greatest median deviation of +10.4%, followed by CaO at +6.1%. These deviations show that statistically, agglomerates do not grossly deviate in major element composition from the hosts to which they are attached, suggesting hosts and their agglomerates were derived from silicate melts of similar compositions or that there is a localized homogenization of the carrier material prior to agglomeration.

Targeted EDS analyses of the unmelted soil show that soil compositions bound the host and agglomerate compositions, indicating that the host and agglomerate compositions are consistent with a mixture of molten minerals in the surrounding lithology. These compositions primarily span the range from quartz-like to felsic with a small number of mafic compositions and other anomalous compositions (primarily high FeO and TiO_2 compositions). These observations are consistent with previous studies and bolster the argument that these compositions were molten and not vaporized during their interaction with the fireball.

Finally, there is no evidence for systematic volatile loss of major elements among hosts or agglomerates (through analyzing their Na_2O and K_2O compositions), as may be expected when externally heating a melt to high temperatures (Fig. 4.21).

10.4 U isotopic composition of agglomerates and hosts

Whole sample U isotopic observations

Fallout from this test is not only well-mixed with respect to major elements, but U isotopes as well (Figs. 4.10 and 5.17). $^{235}U/^{238}U$ measurements show a quasi-unimodal distribution (n=323) with a median of 4.57, or approximately 82% enriched in ^{235}U (Fig. 5.17). When considering the entire suite of U isotope measurements, the 25th to 75th percentile of U enrichments span from 77% to 86% enriched in ^{235}U. However, the inter-sample U isotopic heterogeneity is greater, indicating the vapor term in the fireball is similarly heterogeneous. Three isotope plots of $^{234}U/^{238}U$ and $^{236}U/^{238}U$ vs. $^{235}U/^{238}U$ show strong linear correlations ($R^2 = 0.998$ and 0.997, respectively), consistent with the mixing between natural and enriched end-members (Fig. 5.21). Assuming the enriched end-member has the composition

of oralloy and come from the device, the majority of $^{235}U/^{238}U$ measurements (300 of the 323) are dominated by contributions from the device, while 23 measurements, measured on sample U2 and U3, reflect a dominant contribution from sources with natural U isotopic composition, which could be due to late melting and incorporation of a melt (sample U2) or only partial melting of a melt, preventing efficient mixing and incorporation of condensed vapor from the ambient environment, which appears in other enriched in other parts of the sample (sample U3; Figure 5.19).

Comparisons of U measurements by sample show that, unlike the major element composition, different samples (including both hosts and agglomerates) appear to incorporate very different amounts of enriched U, ranging from sample U2 with $^{235}U/^{238}U = 2.49 \pm 1.93$ (n=67) to sample FLD4.3 with $^{235}U/^{238}U = 9.00 \pm 1.27$ (n=6). These differences in mean $^{235}U/^{238}U$ content suggests that even though these samples were collected from similar distances from ground zero, the ambient environment in fireball is highly heterogeneous, leading to melts incorporating greatly different amounts of enriched U. The range in $^{235}U/^{238}U$ ratio measurements from bulk measurements of entire samples agree with this result (Fig. 5.20 and Table 5.9). With respect to major elements for the bulk dissolution measurements, the quadrature-summed standard deviation is approximately half that of the $^{235}U/^{238}U$ ratio, 0.85 (18.62% 1RSD) for major elements compared to 1.63 (30.22% 1RSD) for the $^{235}U/^{238}U$ ratio, respectively, revealing that from sample to sample, U is more heterogeneously distributed from sample-to-sample than major elements. This suggests the soil term incorporated into the fireball was fairly homogeneous (or was homogenized during incorporation) compared to heterogeneities of vaporized species in the fireball.

Finally, U isotopic heterogeneity is strongly correlated with major element heterogeneity (Fig. 5.31). Homogeneous samples have flow-banding patterns on the scale of the sample size, suggesting these melts had time to mostly homogenize not only their chemical compositions through bulk mixing (convection), but that bulk mixing may have also distributed and homogenize the anthropogenic U that condensed onto the surface of these melts. Following a fit from $^{235}U/^{238}U$ 1σs of hosts and the compositions from within/adjacent to the SIMS analytical craters, the predicted $^{235}U/^{238}U$ 1σ for all agglomerates characterized by SIMS is $^{235}U/^{238}U$ 1σ <1.0.

Comparison of U isotopic compositions between agglomerates and hosts

Unlike major element composition observations, agglomerate $^{235}U/^{238}U$ ratios do not appear as a subset of the measured host $^{235}U/^{238}U$ ratios (Fig. 5.22). Instead, the agglomerate distribution is shifted towards higher enrichments in ^{235}U, with a minimum measured $^{235}U/^{238}U$ ratio of 3.68 ± 0.09, while the minimum host measurement is near natural at $^{235}U/^{238}U$ equal to 0.02 ± 0.002. The maximum $^{235}U/^{238}U$ ratio measured in the host is 8.70 ± 0.09 measured on sample FLD16. In comparison, there are four agglomerate measurements in two samples (two of which overlap compositional interfaces) with $^{235}U/^{238}U$ ratios greater than the host

maximum. The histogram of measurements and comparison of cumulative distribution functions between hosts and agglomerates show that generally, agglomerates are enriched relative to hosts, have a higher median value as a population, and have no measured $^{235}U/^{238}U$ ratios below 3.68, or a ^{235}U enrichment of approximately 78% (measured in FLD14.L the agglomerate attached to the exterior of FLD14). (The next two lowest U isotope measurements were also measured in agglomerates attached to the exterior of hosts: 3.79 ± 0.08 in agglomerate FLD23.L and 3.86 ± 0.11 in agglomerate FLD18.1, attached to samples FLD23 and FLD18, respectively).

When comparing an agglomerate's U isotopic composition to that of its associated host, the median suggests there is no difference between them when considering the collection of measurements (median deviation is 0.4%; Fig. 5.25). However, the deviations are not symmetric about 0 (as demonstrated by the mean deviation of +15.0%). The most negative deviation is 18% (in FLD14.L, an exterior-attached agglomerate where a a SIMS measurement that overlaps a ^{235}U-enriched compositional interface was included when calculating its U isotopic composition), but the most positive deviation is +85% (in FLD18.2, an interior agglomerate in sample FLD18, where there are 10 measurements of the U isotopic composition in the host). Both isotopic and major element characterization of agglomerates and their hosts suggest that while hosts may experience a range of temperatures and melting within a single sample, agglomerates are well-mixed and have been thoroughly transformed by the fireball. Statistically, their compositions and U content are no different than the hosts they are attached to, suggesting these objects primarily formed in small, localized region of the fireball, mostly avoiding the large heterogeneities shown to be present with the large sample-to-sample differences in measured U isotope ratios (Figs. 5.20, 5.24 and Tables 5.9 and 5.10). Notable exceptions to this observation are samples U2 and U4, which exhibit two distinct major element compositions and U isotope distributions from the agglomeration multiple melts with distinct major element and U isotope compositions.

In four samples, U3, U4, FLD23, and FLD4.3, the agglomerates attached in the same location (*e.g.*, the surface agglomerates of FLD23) have similar isotope ratios and compositions to each other (Table 5.10). This supports a common mode of formation, a common source of the agglomerates, and/or a collision at a similar time, and as a result, fireball temperature and ambient fireball composition. Agglomerates attached in different locations in the same sample (*e.g.,* FLD14.L compared to FLD14.1, an exterior agglomerate in FLD14 compared to a surface agglomerate in FLD14), shows that, in most cases, the agglomerate that collided with the host at likely earlier times and higher temperatures is *more* enriched in ^{235}U than the agglomerate that collided with the host later. This suggests that the ambient environment in the fireball earlier in time allowed more U to condense onto the surface and mix into the volume of the more fully incorporated and earlier arriving agglomerates.

Finally, agglomerates characterized in this study smaller than ≈50 μm occur in two samples, samples FLD23 and FLD4.3. The agglomerates from FLD23 are slightly depleted in their measured $^{235}U/^{238}U$ ratios relative to the host, with a mean depletion of -6.5% and are similar to the median of the full 323 collection of U isotope measurements. In contrast, the agglomerates from FLD4.3 show a relatively large enrichment to the host,

being enriched on average by +29% (the single $^{235}U/^{238}U$ isotope measurement in the host FLD4.3 is 7.18 ± 0.31 and the mean and standard deviation of the FLD4.3 agglomerates less than 50 μm in diameter is 9.32 ± 0.80). Agglomerates less than 50 μm exhibit two different relative enrichments to their host object and they are located in two different regions: the FLD23 agglomerates are surface agglomerates, while the agglomerates smaller than 50 μm in FLD4.3 are interior agglomerates. This may indicate two formation modes exist for the smallest characterized agglomerates: one relatively enriched in an anthropogenic vapor term that was incorporated into samples relatively early in the fallout formation process (while the sample was more molten and able to fully incorporate agglomerates) and one possibly from the breakup of a larger object, explaining why its $^{235}U/^{238}U$ composition is more reflective not only of the host it is attached to, but statistics of the U isotope measurements as a whole. At sizes greater than 50 μm, the variations in the U isotope compositions between these two groups disappear. At larger sizes, U isotope compositions are more reflective of the heterogeneities of bulk measurements, suggesting the variation is dominantly reflecting variable incorporation of vapor and molten soil.

10.5 Principal Components Analysis

The multivariate approach of PCA (and some bivariate methods) was used to visualize and analyze the two separate datasets collected in this dissertation: first the EDS raster analyses ($n = 3,698$ for the host dataset) across entire objects in a grid-based pattern and then the combined dataset of U isotopic data from SIMS combined with the compositions from within/around these analytical craters measured with EDS rasters ($n = 245$).

The EDS raster analyses taken in a grid-based pattern across host objects was used to generate the PC space. To determine the number of PCs to retain, a noise-injection method using UP matrices was used, which showed that when injecting random noise in the data proportional to the analytical uncertainty in individual measurements and different major elements, the first 5 PCs were largely stable to this perturbation, suggesting the first 5 PCs are primarily modeling true variance in the data instead of analytical noise. These first 5 PCs were shown to be controlled by outliers, which are primarily quartz-like, mafic, felsic, or Fe, Ti-rich compositions. That is, the PC space is controlled by, and the greatest sources of variance are due to, unmelted/partially-melted compositions in the soil.

Bivariate plots of the $^{235}U/^{238}U$ versus each of the major elements showed no strong trends with composition. This observation presents a contrast to the documented association between Pu and Ca, Mg, and Fe in Trinity and the association between U concentration (using $^{235}U/^{30}Si$ as a proxy) at CaMgFe compositional interfaces [55, 61, 66–68]. The exception was the positive correlation between the $^{235}U/^{238}U$ ratio and CaO, MgO, FeO, which were measured in sample U2. However, this exception is likely due to physical mixing of roughly two melts of distinct composition and sampling regions that experienced different amounts of mixing between the two melts, rather than chemical behavior, such as volatility leading to the co-condensation of U, CaO, FeO, and MgO from the vapor phase. Exclud-

ing these measurements results in a weak anti-correlation between the $^{235}U/^{238}U$ ratio and CaO, consistent with bulk ICP-MS measurements of whole dissolved samples from the same U-fueled event (Fig. 6.22) [57]. Apparent trends or co-locations in other samples, such as U4 or FLD4.3, can be explained through agglomeration and that these agglomerated melts had a distinct U and major element composition.

Projecting the major element compositions from within/around the SIMS analysis craters into the PC model shows the majority of compositions cluster near the origin, as they were primarily conducted in the glassy regions of fallout and contain few outlying compositions. The strongest trend between composition and $^{235}U/^{238}U$ ratio is shown in the plots of PC2 versus PC3 (Fig. 6.28), due to a strong loading of K_2O in PC2 (separating the compositions from sample U2) and the separation of CaO into the first quadrant (allowing the compositions from SIMS measurements in the agglomerates of FLD4.3 to plot in quadrants III and IV), with $^{235}U/^{238}U$ of intermediate compositions overlaying the majority of EDS host measurements near the origin (Fig. 6.29). A direct plot of the $^{235}U/^{238}U$ ratio as a function of PC3 shows a weak anti-correlation (strongly affected by the low $^{235}U/^{238}U$ ratios and 0 PC3 scores for several measurements in the apparently partially-melted center of host U3), which is strongly influenced by the CaO concentration. Sample by sample, plots of PC3 vs. PC2 show that most samples (agglomerates and their associated host objects) occupy a restricted region of space, pointing to the relative compositional homogeneity within most samples and the relative similarity of agglomerates to their respective hosts.

10.6 Interpreting compositional similarity between host objects & agglomerates

Multidimensional scaling provides a means to directly visualize and compare the similarity between all the agglomerates and hosts characterized in this study simultaneously. MDS models were created for the two datasets: the EDS raster only dataset (Figures 7.4 and 7.5) and the combined U isotope/EDS raster from around the SIMS craters dataset (Figures 7.6 and 7.7). The EDS raster model calculated different objects' similarity based on their median major element composition for 95 total objects: 58 agglomerates in 15 samples and 37 hosts. The EDS-only model shows that host objects are fairly tightly clustered, implying a high degree of similarity (with three exceptions in hosts FLD25, FLD3.2, and FLD5.3), while the agglomerates, despite being well-mixed and quasi-homogeneous compositionally, exhibit a greater degree of scatter because they are more likely to contain anomalous compositions due to fewer measurements within the agglomerate. Observations from the MDS plots show that objects in the same sample tend to cluster close together, whether it be hosts and agglomerates (*e.g.*, FLD23 in Figure 7.5), or agglomerates clustering near other agglomerates from the same sample (*e.g.*, FLD4.4 in Figure 7.5). The major element/U isotopic MDS model calculated different objects' similarity based on their median combined U isotopic/major element composition for 60 total objects: 33 agglomerates in 13 samples,

10 interface measurements that significantly sampled the agglomerate and the host in 6 samples, and 17 host objects. This MDS model showed a greater degree of uncertainty because of fewer measurements per object, but objects that were similar in the EDS-only MDS model also tended to be similar in the major element/U isotopic combined MDS model. Furthermore, all interface measurements over "Si interfaces" plotted between the agglomerate and the host, suggesting a shared similarity between the two objects. However, the interface measurement over FLD10.L, which is a double-layered interface did not, likely due to the CaMgFe deposition layer.

Next, the exact Euclidean distance for agglomerates relative to their hosts was calculated for major element and combined major element/U isotopic datasets (Figures 7.8 and 7.9, respectively). Plots as a function of the distance percentile (how many objects are more similar at a given distance from the host object) and the cumulative distribution function (CDF) of these distance percentiles show what fraction of agglomerates fall within a given degree of similarity to their host objects. The data from these plots bolster the observations from the MDS plots: agglomerates tend to be more similar to their hosts than other objects when both considering the EDS raster only dataset and the EDS/SIMS combined dataset. For the EDS-only dataset (Figure 7.8), which includes more objects, the median CDF from the 500 UP matrix simulations shows that 55% of all agglomerates are compositionally more similar to their respective hosts than 75% of all other characterized objects (that is, they fall within the 25th distance percentile) and a median of 81% of agglomerates are compositionally more similar to their respective hosts than 50% of all other characterized objects. Similarly, when using the EDS/SIMS dataset (Figure 7.9), a median of 47% agglomerates fall within the 25th distance percentile of their respective hosts and a median of 83% agglomerates fall within the 50th distance percentile of their respective agglomerates. The compositional similarity between agglomerates and their hosts suggests that agglomerates, as a collection, tend to likely formed from similar parcels of melt to their hosts. This observation implies that agglomerates were not formed some other material (such as a finer size fraction of soil) or experienced a grossly different environment in the fireball (such as excessive volatilization compared to their host objects).

The U isotopic and major element compositional similarity between agglomerates and their hosts indicates that, as a collection, agglomerates and hosts experienced similar ambient environments in the fireball, and in addition to their being formed from melts of similar compositions and interacted similarly with the bomb vapor term in the fireball. These observations bolster the hypothesis of Glesston (1966) that the mean free paths of melt parcels in the fireball tend to be small [10]. Furthermore, as a collection, agglomerates and host objects likely incorporated anthropogenic material through similar physical processes and the population of agglomerates do not show evidence formation through some different mechanism (*e.g.*, primary condensation of material from the vapor phase) compared to the host (condensation of material in the vapor phase onto, and subsequently mixing into, the silicate melt). Three possible exceptions in interior agglomerates FLD4.3.1, FLD4.3.2, and FLD4.3.3 are discussed below. Finally, both datasets suggest that attached agglomerates tend to be most similar (≈76% and 75% of the attached agglomerates falling within the 25th

distance percentile in terms of similarity to their hosts for the EDS raster and EDS/SIMS datasets, respectively), followed by surface agglomerates, and then interior agglomerates.

10.7 Compositional interfaces

Major element compositions of interfaces

Two types of compositional interfaces were observed (Si and CaMgFe interfaces) and analyzed. CaMgFe interfaces have previously been well-characterized and the data presented here are consistent with observations presented in [67, 68]. However, it was shown that using quantified EDS mapping to characterize interfaces may result in less Na volatilization and gives higher spatial resolution than EPMA, although EPMA is a standardized technique. Both types of interfaces are likely due to condensation processes, with the Si condensation occurring earlier than the CaMgFe condensation. This leads to hypothesized permutations of how single and multiply-layered interfaces may be observed (many of which were observed and noted in this chapter; Fig. 8.11). The interface compositions extracted from EDS maps tend to be distinct from the agglomerate and host, but are mostly bounded by the collection of host grid EDS raster analyses discussed earlier in this dissertation. This suggests that the compositional heterogeneity in the partially-melted and unmelted regions in fallout is greater than any alteration of the composition of melt surfaces due to he preferential condensation of Si or Ca/Mg/Fe species from the vapor phase. While both are likely condensation effects, the CaMgFe interface has been observed to be frequently co-located with enriched U and increases in U concentration, likely due to co-condensation of the soil-derived and bomb vapor-derived species from the vapor term [67, 68].

U behavior at interfaces

NanoSIMS ion images sampling CaMgFe interfaces in this study are consistent with previous findings of the behavior of U isotope ratios at these interfaces [67, 68]. The $^{235}U/^{238}U$ ratio and/or the $^{235}U/^{30}Si$ ratios tend to be enriched across CaMgFe interfaces, suggesting a co-condensation of enriched U with the major element species enriched at these interfaces. In contrast, Si interfaces do not show an enrichment in $^{235}U/^{238}U$. Changes in the $^{235}U/^{238}U$ ratio can be attributed to variable U isotopic enrichment between the agglomerate and host object. Furthermore, the U concentration tends to *decrease* at Si interfaces. Other variations in the $(^{235}U + ^{238}U)/^{30}Si$ and $(^{235}U + ^{238}U)/^{42}Ca$ ratios can be attributed to major element variations across the interfaces. This suggests these condensations occurred in a vapor environment dominated by Si, allowing an Si-dominated vapor to condense, but not appreciable amounts of enriched U from the vapor term, despite U being incorporated into the bulk of the melt at early times and also likely condensing later with Ca, Mg, and Fe to form CaMgFe interfaces. However, there are three examples of interior agglomerates (FLD4.3.1, FLD4.3.2, and FLD4.3.3) whose bulk (*not* their interfaces) are both enriched

in SiO_2 and ^{235}U relative to average. If similar features are found in other samples from this test, this may point to largely vapor-derived materials preserved within samples not at interfaces and a fireball environment suitable for both an Si-rich and U-rich vapor to co-condense. However, these agglomerates occur too infrequently to appreciably alter the overall radionuclide composition of FLD4.3, counter to the hypothesis of Freiling et al. (1965) [5].

10.8 Future Work

While this study elaborates on the origin and role of agglomerates in the formation of fallout from this U-fueled event and provides the most modern comprehensive spatially-resolved study of glassy fallout to date, it has its limitations and the observations made pose a variety of new questions.

Fallout formation varies considerably from event to event, dependent not only on the yield, height of burst, and other detonation conditions, but on the surrounding environment as well. This study, while seeking to characterize a population of host objects and agglomerates, is limited to a single (U-fueled) event where the surrounding geology was consistent with being rhyolitic and fairly homogeneous. How does the frequency and behavior of agglomerates change in other events that take place in other geologies? Studying agglomeration in aerodynamic glassy fallout from the Trinity event may present an interesting contrast due to its different and more heterogeneous surrounding lithology. The geology of the Trinity site is primarily arkosic sand, which tends not to be a silicic as the soil surrounding this event, and is constituted primarily of quartz, a large proportion of feldspars, and carbonates [30, 35, 58].

The interior agglomerates of FLD4.3.1, FLD4.3.2, and FLD4.3.3 are major element compositional and U isotopic outliers in this study. They indicate that $\sim$20 μm size agglomerates, with compositions possibly primarily derived from the vapor term of the fireball, may be preserved in glassy fallout. While these agglomerates are all found within a single sample FLD4.3, a search should be conducted specifically to locate agglomerates of this type in other samples. Agglomerates FLD4.3.1–FLD4.3.3 may compare to other fallout populations, such as those collected on filters by aircraft passing through the debris cloud at early times.

While ^{235}U was used as a proxy for the amount of bomb vapor incorporation into agglomerates and host objects, its volatility behavior is variable depending on the detonation conditions, ranging from semi-volatile in air bursts to strongly refractory in MT-scale detonations over coral [5, 47]. However, as observed in Lewis et al. (2015), ^{235}U enrichment is co-located with autoradiograph intensity in samples U2 and U4. The autoradiographs are dominated by β emissions, as discussed in Chapter 2, which are likely derived from fission and activation products, indicating a possible correlation between actinide and fission/activation product incorporation in agglomerates and host objects. The incorporation of other radionuclides (*e.g.*, ^{89}Sr as a volatile-behaving archetype and ^{95}Zr as a refractory-behaving archetype) relative to ^{235}U remains relatively unconstrained (*i.e.*, studied in a restricted set

of detonation environments and conditions) [47, 121]. Investigating this co-location further may help elucidate U volatility behavior in this event and serve as a basis to predict its behavior in other events.

This study of interfaces here and in [67, 68] in aerodynamic glassy fallout can be directly applied to studies of ground glass. Hermes and Strickfaden (2005) have proposed that melts from the fireball rain down on the surrounding soil and are still molten when they fall to the surface, adhering to ground glass [31]. The confirmation of preserved compositional interfaces in this fallout morphology could confirm their hypothesis. In addition, the major and trace element behavior at these interfaces would provide insight into the fireball environment as these melts were ejected from the fireball.

This is the first study to document the presence of Si compositional interfaces in fallout. While Si-rich interfaces have been studied in chondrules and chondrule analogues, the origin of Si interfaces and conditions that allow them to form in fallout requires further study. Furthermore, while Si interfaces may form due to the particular lithology surrounding this event, it is unclear how are the compositional interfaces may differ between nuclear events that take place in different geologies. Interfaces offer the opportunity to study condensation and oxidation conditions that occur in the fireball at the time when the interfaces form. While the enrichment of ^{235}U is observed to be invariable at Si interfaces, but there may be other radionuclides whose composition could be studied across these interfaces that would further elucidate the fireball environment and relative to when these Si interfaces formed.

This study reveals that agglomerates are unlikely to be responsible for the deviations between historical models and observations, as previously hypothesized. However, the major element and U isotopic compositional similarity between agglomerates and their associated host objects indicates formation from common precursor melts and similar interaction with the bomb vapor. These similarities suggest that agglomeration tends to occur over small spatial scales in the fireball. Over these small scales, the carrier melts and bomb vapor term is locally quasi-homogeneous. Finally, the observation and analysis of Si interfaces reveals that another condensation process, in addition to the late-stage deposition of CaMgFe interfaces, is preserved within glassy fallout. These Si interfaces form earlier in time than CaMgFe interfaces and are likely sourced from regions of the fireball with high concentrations of vaporized environmental material. Collectively, the study of agglomerates yields useful information about formation processes within the fireball, such as the frequency of agglomeration, scales of both carrier material and bomb vapor homogeneity, and ambient vapor compositions and conditions at different times of fallout formation and agglomeration.

Bibliography

1. Spencer, L., Chilton, A. & C.M., E. *Structure Shielding Against Fallout Gamma Rays from Nuclear Detonations* (U.S. Department of Commerce, Washington, D.C., 1980).
2. Glasstone, S. & Dolan, P. *The Effects of Nuclear Weapons* (U.S. Department of Defense, 1964).
3. Norman, J. H. & Winchell, P. *Cloud Chemistry of Fallout Formation* in *Fallout Phenomena Symposium, Proceedings Part I* (ed Mikhail, S.) (1966).
4. Crocker, G., O'Connor, J. & Freiling, E. *Physical and Radiochemical Properties of Fallout Particles* tech. rep. AD0623485 (U.S. Naval Radiological Defense Laboratory, 1965).
5. Freiling, E. C., Crocker, G. R. & Adams, C. E. *Nuclear Debris Formation* in *Radioactive Fallout from Nuclear Weapons Tests: Proceedings of the Second Conference* (ed Klement, A. W.) (U.S. Atomic Energy Commission, 1965), 1–44.
6. (ed Mikhail, S.) *Fallout Phenomena Symposium* AD0488164. Office of Civil Defense, Defense Atomic Support Agency (Monterey, CA, 1966).
7. (ed Klement, A. W.) *Radioactive Fallout from Nuclear Tests: Proceedings of a Conference* (Atomic Energy Commission, 1961).
8. Willis, J. *The History of Fallout Prediction* MA thesis (1979).
9. Stone, R. Test blasts simulate a nuclear attack on a U.S. port. *Science* (2017).
10. Izrael, I. *Radioactive Fallout After Nuclear Explosions and Accidents* (Elsevier Science, 2002).
11. *The Effects on the Atmosphere of a Major Nuclear Exchange* (National Academies Press, 1985).
12. Moresco, P. *First principles modeling of the formation of nuclear debris* tech. rep. October (AWE, 2012).
13. Crocker, G., O'Connor, J. & Freiling, E. Physical and radiochemical properties of fallout particles. *Health Physics* **12,** 1099 (1966).
14. Nathans, M. W., Thews, R., Holland, W. D. & Benson, P. A. Particle size distribution in clouds from nuclear airbursts. *Journal of Geophysical Research* **75,** 7559–7572 (1970).

15. Benson, P., Gleit, C. E. & Leventhal, L. *Radiochemical Fractionation Characteristics of Single Particles from High-Yield Air Bursts* in *Radioactive Fallout from Nuclear Weapons tests: Proceedings of the Second Conference* (ed Klement, A. W.) (U.S. Atomic Energy Commission, 1965), 98–107.

16. *Operation Ivy, Project 5.4b: Fallout and Cloud-particle Studies* tech. rep. AD0363630 (Chemical and Radiological Laboratories, Army Chemical Center, 1953).

17. Martin, C. *Fallout Fractionation in Silicate Soils* PhD thesis (Air Force Institute of Technology, 1983).

18. Freiling, E. C. & Kay, M. A. Radionuclide Fractionation in Air-Burst Debris. *Nature* **209,** 236–238 (1966).

19. Russell, I. *Operation Sun Beam, Shot Johnie Boy, Project Officers Report–Project 2.13: Radioisotope Fractionation and Particle Size Characteristics of a Low-Yield Surface Nuclear Detonation* tech. rep. (Air Force Weapons Laboratory, 1965).

20. Miller, C. *A Theory of Formation of Fallout From Land-Surface Nuclear Detonations and Decay of the Fission Products* tech. rep. AD0241240 (U.S. Naval Radiological Defense Laboratory, 1960).

21. Freiling, E. C. *Fractionation in Surface Bursts* in *Radioactive Fallout from Nuclear Tests: Proceedings of a Conference* (ed Klement, A. W.) (U.S. Atomic Energy Commission, 1962), 25–46.

22. Wallace, J. & Hobbs, P. in *Atmospheric Science: An Introductory Survey* 2nd edition, 209–270 (Academic Press, 2006).

23. Freiling, E. C. *Fractionation III. Estimation of Degree of Fractionation and Radionuclide Partition for Nuclear Debris* tech. rep. USNRDL-TR-680 (Naval Radiological Defense Laboratory, 1963).

24. Freiling, E. *Particle Formation and Fractionation in Air Bursts* in *Radioactive Fallout from Nuclear Tests: Proceedings of a Conference held in Germantown, Maryland* (Germantown, Maryland, 1961), 47–59.

25. Stewart, K. The condensation of a vapour to an assembly of droplets or particles. *Trans. Faraday Soc.* **52,** 161–173 (1956).

26. Friedlander, S. *Theory of Self-Preserving Size Distributions in a Coagulating Dispersion* in *Radioactive Fallout from Nuclear Weapons Tests: Proceedings of the Second Conference* (ed Klement, A. W.) (U.S. Atomic Energy Commission, 1965), 253–259.

27. Heft, R. E. in *Radionuclides in the Environment* (ed Freiling, E. C.) 254–281 (American Chemical Society, 1970).

28. Parekh, P. P. *et al.* Radioactivity in Trinitite six decades later. *Journal of Environmental Radioactivity* **85,** 103–120 (2006).

29. Adams, C., Farlow, N. & Schell, W. The compositions, structures and origins of radioactive fallout particles. *Geochemica et Cosmochimica Acts* **18,** 42–56 (1960).

30. Eby, N, Hermes, R, Charnley, N & Smoliga, J. Trinitite – the atomic rock. *Geology Today* **26,** 180–185 (2010).

31. Hermes, R. E. & Strickfaden, W. B. A new look at trinitite. *Nucl. Weapons J.* 2–7 (2005).

32. Tompkins, R. C., Russell, I. J. & Nathans, M. W. in (ed Freiling, E. C.) 381–400 (American Chemical Society, 1970).

33. Mackin, J., Zigman, P., Love, D., Macdonald, D. & Sam, D. Radiochemical analysis of individual fallout particles. *Journal of Inorganic Nuclear Chemistry* **15,** 20–36 (1960).

34. Williamson Jr., W. *Investigation and correlation of some physical parameters of fallout material* tech. rep. AD0144368 (U.S. Naval Radiological Defense Laboratory, 1957).

35. Eby, G. *et al.* Trinitite redux: mineralogy and petrology. *American Mineralogist* **100,** 427–441 (2015).

36. Freiling, E. & Kay, M. *Radionuclide fractionation in air-burst debris* tech. rep. USNRDL-TR-933 (U.S. Naval Radiological Defense Laboratory, 1965).

37. Hicks, H. G. Calculation of the concentration of any radionuclide deposited on the ground by offsite fallout from a nuclear detonation. *Health Physics* **42,** 585–600 (1982).

38. Heft, R. E. & Steele, W. A. *Procedures for the Systematic Separation and Analysis of Radioactive Particles from Nuclear Detonations* tech. rep. ADA382858 (Lawrence Radiation Laboratory, Livermore, CA, 1968).

39. Peters, W. & Paffrath, D. Investigation on correlations between fractionation effects and particle size distributions in fission product samples. *J Geophys Research* **75,** 2991–2998 (1970).

40. Chan, H. K. *Activity-Size Relationship of Fallout Particles from Two Shots, Operation Redwing* tech. rep. AD0233607 (U.S. Naval Radiological Defense Laboratory, 1959).

41. Cook, C. S., Mather, R. L., Johnson, R. F. & Tomnovec, F. M. Fractionation of Nuclear Weapon Debris. *Nature* **187,** 1100–1101 (1960).

42. *Worldwide Effects of Atomic Weapons – Project Sunshine* (U.S. Atomic Energy Commission, 1953).

43. Norman, J. H. & Winchell, P. *Cloud Chemistry of Fallout Formation: Final Report* tech. rep. ADA995398 (General Atomic, 1967).

44. Cassata, W. *et al.* When the dust settles: stable xenon isotope constraints on the formation of nuclear fallout. *Journal of environmental radioactivity* **137,** 88–95 (2014).

45. Trabalka, J. R. & Kocher, D. C. *Bounding Analysis of Effects of Fractionation of Radionuclides in Fallout on Estimation of Doses to Atomic Veterans* tech. rep. AD1045478 (Senes Oak Ridge, Inc., 2007).

46. Rankin, D. W. *CRC handbook of chemistry and physics, edited by David R. Lide* (Taylor & Francis, 2009).

47. Crocker, G., Kawahara, F. & Freiling, E. *Radiochemical Data Correlations on Debris from Silicate Bursts* in *Radioactive Fallout from Nuclear Weapons Tests: Proceedings of the Second Conference* (ed Klement, A. W.) (U.S. Atomic Energy Commission, 1965), 72–81.

48. Miller, C. *Biological and Radiological Effects of Fallout from Nuclear Explosions* tech. rep. AD0476572 (Stanford Research Institute, 1964).

49. Korts, R. F. & Norman, J. H. *A Calculational Model for Condensed State Diffusion Controlled Fission Product Absorption During Fallout Formation* tech. rep. D0651755 (General Atomic, 1967).

50. Norman, J., Winchell, P., Dixon, J., Roos, B. & Korts, R. in *Radionuclides in the Environment* (ed Freiling, E.) 13–34 (American Chemical Society, Washington, D.C., 1970).

51. Atkatz, D. & Bragg, C. Determining the yield of the Trinity nuclear device via gammaray spectroscopy. *American Journal of Physics* **63,** 411–413 (1995).

52. Schlauf, D. *et al.* Trinitite redux: Comment on Determining the yield of the Trinity nuclear device via gamma-ray spectroscopy, by David Atkatz and Christopher Bragg [Am. J. Phys. 63 (5), 411413 (1995)]. *American Journal of Physics* **65,** 1110–1112 (1997).

53. Bellucci, J. J. *et al.* Distribution and behavior of some radionuclides associated with the Trinity nuclear test. *Journal of Radioanalytical and Nuclear Chemistry* **295,** 2049–2057 (2013).

54. Bellucci, J. J. & Simonetti, A. Nuclear forensics: searching for nuclear device debris in trinitite-hosted inclusions. *Journal of Radioanalytical and Nuclear Chemistry* **293,** 313–319 (2012).

55. Plutonium segregation in glassy aerodynamic fallout from a nuclear weapon test. *Dalton Transactions* **46,** 1770–1778 (2017).

56. Bellucci, J. J., Snape, J. F., Whitehouse, M. W. & Nemchin, A. A. Direct Pb isotopic analysis of a nuclear fallout debris particle from the Trinity nuclear test. *Analytical Chemistry* (2016).

57. Eppich, G. R., Knight, K. B., Jacomb-Hood, T. W., Spriggs, G. D. & Hutcheon, I. D. Constraints on fallout melt glass formation from a near-surface nuclear test. *Journal of Radioanalytical and Nuclear Chemistry* **302,** 593–609 (2014).

58. Fahey, A., Zeissler, C., Newbury, D., Davis, J. & Lindstrom, R. Postdetonation Nuclear Debris for Attribution. *Proceedings of the National Academy* **107,** 20207–20212 (2010).

59. Belloni, F., Himbert, J., Marzocchi, O. & Romanello, V. Investigating incorporation and distribution of radionuclides in trinitite. *Journal of Environmental Radioactivity* **102,** 852–862 (2011).

60. Lewis, L. *et al.* Spatially-resolved analyses of aerodynamic fallout from a uranium-fueled nuclear test. *Journal of Environmental Radioactivity* **148,** 183–195 (2015).

61. Wallace, C. *et al.* A multi-method approach for determination of radionuclide distribution in trinitite. *Journal of Radioanalytical and Nuclear Chemistry* **298,** 993–1003 (2013).

62. Bellucci, J. J., Simonetti, A., Wallace, C., Koeman, E. C. & Burns, P. C. Lead isotopic composition of trinitite melt glass: Evidence for the presence of Canadian industrial lead in the first atomic weapon test. *Analytical Chemistry* **85,** 7588–7593 (2013).

63. Bellucci, J. J., Simonetti, A., Koeman, E. C., Wallace, C. & Burns, P. C. A detailed geochemical investigation of post-nuclear detonation trinitite glass at high spatial resolution: delineating anthropogenic vs. natural components. *Chemical Geology* **365,** 69–86 (2014).

64. Sharp, N. *et al.* Rapid analysis of trinitite with nuclear forensic applications for post-detonation material analyses. *Journal of Radioanalytical and Nuclear Chemistry* **302,** 57–67 (2014).

65. Donohue, P. H., Simonetti, A., Koeman, E. C., Mana, S. & Burns, P. C. Nuclear forensic applications involving high spatial resolution analysis of Trinitite cross-sections. *Journal of Radioanalytical and Nuclear Chemistry* **306,** 457–467 (2015).

66. Bonamici, C. E. *et al.* A geochemical approach to constraining the formation of glassy fallout debris from nuclear tests. *Contributions to Mineralogy and Petrology* **172,** 2 (2017).

67. Weisz, D. G. *et al.* Deposition of vaporized species onto glassy fallout from a near-surface nuclear test. *Geochimica et Cosmochimica Acta* (2017).

68. Weisz, D. G. *Mass Transport of Condensed Species in Aerodynamic Fallout Glass from a Near-Surface Nuclear Test* PhD thesis (University of California, Berkeley, 2016).

69. Pacold, J. *et al.* Chemical speciation of U, Fe, and Pu in melt glass from nuclear weapons testing. *Journal of Applied Physics* **119,** 195102 (2016).

70. Bainbridge, K. *Trinity* tech. rep. (Los Alamos Scientific Lab., NM (USA), 1976).

71. Malik, J. *The Yields of the Hiroshima and Nagasaki Nuclear Explosions* tech. rep. (Los Alamos National Laboratory, Los Alamos, NM, 1985).

72. Adams, C. & O'Connor, J. *The Nature of Individual Radioactive Particles VI. Fallout Particles from a Tower Shot, Operation Redwing* tech. rep. USNRDL-TR-208 (U.S. Naval Radiological Defense Laboratory, 1957).

73. Adams, C. E., Quan, J. T. & Balkwell, W. R. in *Radionuclides in the Environment* (ed Freiling, E.) 35–62 (American Chemical Society, Washington, D.C., 1970).

74. Glass, B., Senftle, F., Muenow, D., Aggrey, K. & Thorpe, A. *Atomic Bomb Glass Beads: Tektite and Microtektite Analogs* in *Second International Conference on Natural Glasses* (Prague, 1987), 361–369.

75. Giuli, G., Pratesi, G., Eeckhout, S. G., Koeberl, C. & Paris, E. Iron reduction in silicate glass produced during the 1945 nuclear test at the Trinity site (Alamogordo, New Mexico, USA). *Geological Society of America Special Papers* **465,** 653–660 (2010).

76. Bunch, T. E. *et al.* Very high-temperature impact melt products as evidence for cosmic airbursts and impacts 12,900 years ago. *Proceedings of the National Academy of Sciences* **109,** E1903–E1912 (2012).

77. Sheffer, A. & Dyar, M. *57Fe Mossbauer Spectroscopy of Fulgurites: Implications for Chemical Reduction* in *Lunar and Planetary Science XXXV* (2004), 57–58.

78. Sheffer, A. A. *Chemical Reduction of Silicates by Meteorite Impacts and Lightning Strikes* PhD thesis (University of Arizona, 2007).

79. Storebo, P. Formation of radioactivity size distributions in nuclear bomb debris. *Journal of Aerosol Science* **5,** 557–577 (1974).

80. Fitzgerald, M, Knight, K., Matzel, J. & Czerwinksi, K. Interpreting mixing relationships in energetic melts to estimate vapor contribution and composition. *In Draft* (2018).

81. Dustin, M. K., Koeman, E. C., Simonetti, A., Torrano, Z. & Burns, P. C. Comparative Investigation between In Situ Laser Ablation Versus Bulk Sample (Solution Mode) Inductively Coupled Plasma Mass Spectrometry (ICP-MS) Analysis of Trinitite Post-Detonation Materials. *Applied Spectroscopy,* 0003702816662597 (2016).

82. Zhang, Y. Diffusion in Minerals and Melts: Theoretical Background. *Reviews in Mineralogy and Geochemistry* **72,** 5–59 (2010).

83. Johnson, B. C. & Melosh, H. J. Formation of spherules in impact produced vapor plumes. *Icarus* **217,** 416–430 (2012).

84. Weisz, D. G. *et al.* Diffusive mass transport in agglomerated glassy fallout from a near-surface nuclear test. *Geochimica et Cosmochimica Acta* **223,** 377–388 (2018).

85. Newbury, D. E. & Ritchie, N. W. M. Performing elemental microanalysis with high accuracy and high precision by scanning electron microscopy/silicon drift detector energy-dispersive X-ray spectrometry (SEM/SDD-EDS). *Journal of Materials Science* **50,** 493–518 (2015).

86. Schneider, C. A., Rasband, W. S. & Eliceiri, K. W. NIH Image to ImageJ: 25 years of image analysis. *Nature methods* **9,** 671 (2012).

87. Goldstein, J. *Scanning electron microscopy and X-ray microanalysis* (Springer, 2003).

88. Parsons-Davis, T. *et al.* Application of modern autoradiography to nuclear forensic analysis. *Forensic Science International* **286,** 223–232 (2018).

89. Prasad, M. S. & Khedekar, V. Impact microcrater morphology on Australasian microtektites. *Meteoritics & Planetary Science* **38,** 1351–1371 (2003).

90. Kyte, F., Omura, C. & Gersonde, R. Accretionary Growth of Impact Spherules. *Meteoritics and Planetary Science Supplement* **73,** 5376 (2010).

91. Glass, B., Senftle, F., Muenow, D., Aggrey, K. & Thorpe, A. *Atomic bomb glass beads: Tektite and microtektite analogs* in *Proceedings of the Second International Conference on Natural Glasses* (1987), 361–369.

92. Goldstein, J. *et al. Scanning Electron Microscopy and X-Ray Microanalysis* 3rd Edition (Springer, 2007).

93. Garratt-Reed, A. & Bell, D. *Energy-dispersive X-ray analysis in the electron microscope* (Garland Science, 2003).

94. Fitzgerald, R., Keil, K. & Heinrich, K. F. J. Solid-State Energy-Dispersion Spectrometer for Electron-Microprobe X-ray Analysis. *Science* **159,** 528–530 (1968).

95. Lloyd, G. Atomic number and crystallographic contrast images with the SEM: a review of backscattered electron techniques. *Mineralogical Magazine* **51,** 3–19 (1987).

96. Spray, J. G. & Rae, D. A. Quantitative Electron-Microprobe Analysis of Alkali Silicate Glasses: A Review and User Guide. *The Canadian Mineralogist* **33,** 323–332 (1995).

97. Gladney, E. S., Jones, E. A., Nickell, E. J. & Roelandts, I. 1988 Compilation of Elemental Concentration Data for USGS Basalt BCR-1. *Geostandards Newsletter* **14,** 209–359 (1990).

98. Morgan, G. B. V. & London, D. Optimizing the electron microprobe analysis of hydrous alkali aluminosilicate glasses. *American Mineralogist* **81,** 1176–1185 (1996).

99. Wand, M. & Jones, M. *Kernel Smoothing* First Edition (Chapman & Hall, London, 1995).

100. Wimpenny, J. B. *et al.* Characterizing major and trace element compositions in fallout melt glass from a near-surface nuclear test. *In Draft* (2018).

101. Eppich, G. *et al. Characterization of low concentration uranium glass working materials* tech. rep. LLNL-TR-645481 (Lawrence Livermore National Laboratory).

102. Gerasimov, M. V., Yakovlev, O. I., Dikov, Y. P. & Wlotzka, F. in *Large Meteorite Impacts III* (eds Kenkman, T., Horz, F. & Deutsch, A.) 1st, 351–366 (The Geological Society of America, Boulder, CO, 2005).

103. Hewins, R., Connolly, H., Lofgren Jr, G. & Libourel, G. *Experimental constraints on chondrule formation* in *Chondrites and the protoplanetary disk* **341** (2005), 286.

104. Tsuchiyama, A., Nagahara, H. & Kushiro, I. Volatilization of sodium from silicate melt spheres and its application to the formation of chondrules. *Geochimica et Cosmochimica Acta* **45,** 1357–1367 (1981).

105. Hashimoto, A. Evaporation metamorphism in the early solar nebulaEvaporation experiments on the melt FeO-MgO-SiO_2-CaO-Al_2O_3 and chemical fractionations of primitive materials. *Geochemical Journal* **17,** 111–145 (1983).

106. Georges, P, Libourel, G & Deloule, E. *Potassium condensation experiments and their bearing on chondrule formation* in *Lunar and Planetary Science Conference* **30** (1999).

107. Wilson, R., Stevie, F. & Magee, C. *Secondary Ion Mass Spectrometry: A Practical Handbook for Depth Profiling and Bulk Impurity Analysis* (Wiley & Sons, 1989).

108. Andersen, C., Roden, H. & Robinson, C. Negative Ion Bombardment of Insulators to Alleviate Surface Charge-Up. *Journal of Applied Physics* **40,** 3419 (1969).

109. Cherepin, V. *Secondary ion mass spectroscopy of solid surfaces* (VSP Books, 1987).

110. Smith, N., Tesch, P., Martin, N. & Kinion, D. A high brightness source for nano-probe secondary ion mass spectrometry. *Applied Surface Science* **255,** 1606–1609 (2008).

111. Werner, H. Quantitative secondary ion mass spectrometry: A review. *Surface and Interface Analysis* **2,** 56–74 (1980).

112. Slodzian, G. Some problems encountered in secondary ion emission applied to elementary analysis. *Surface Science* **48,** 161–186 (1975).

113. Williams, P. The sputtering process and sputtered ion emission. *Surface Science* **90,** 588–634 (1979).

114. Hervig, R. *et al.* Useful ion yields for Cameca IMS 3f and 6f SIMS: Limits on quantitative analysis. *Chemical geology* **227,** 83–99 (2006).

115. Storms, H., Brown, K. & Stein, J. Evaluation of a cesium positive ion source for secondary ion mass spectrometry. *Analytical Chemistry* **49,** 2023–2030 (1977).

116. De Groot, P. *Handbook of stable isotope analytical techniques* (Elsevier Science, 2004).

117. Shimizu, N. & Hart, S. Applications of the Ion Microprobe to Geochemistry and Cosmochemistry. *Annual Review of Earth and Planetary Science* **10,** 483–526 (1982).

118. Hoppe, P., Cohen, S. & Meibom, A. NanoSIMS: Technical Aspects and Applications in Cosmochemistry and Biological Geochemistry. *Geostandards and Geoanalytical Research* **37,** 111–154 (2013).

119. Nittler, L. R. *Interactive processing of SIMS images* (2011).

120. Moody, K. *Dissolved Oralloy Standards and the Origin of HEU* tech. rep. UCRL-ID-117611 (Lawrence Livermore National Laboratory, Livermore, CA).

121. Nathans, M. W. in *Radionuclides in the Environment* (ed Freiling, E.) 352–359 (American Chemical Society, Washington, D.C., 1970).

122. Freiling, E. *Experimental Determination of Input for the Prediction of Fallout Effects* in *Fallout Phenomena Symposium, Proceedings Part I* (ed Mikhail, S.) (1966).

123. Varmuza, K. & Filzmoser, P. *Introduction to multivariate statistical analysis in chemometrics* (CRC press, 2016).

124. Esbensen, K. & Geladi, P. in *Comprehensive Chemometrics* 211–226 (Elsevier, 2009).

125. Jolliffe, I. T. *Principal Component Analysis, Second Edition* **3,** 487 (2002).

126. Mellinger, M. Multivariate Data Analysis: Its Methods. *Chemometrics and Intelligent Laboratory Systems* **2,** 29–36 (1987).

127. Wold, S., Esbensen, K. I. M. & Geladi, P. Principal Component Analysis. *Chemometrics and Intelligent Laboratory Systems* **2,** 37–52 (1987).

128. Birks, H. Multivariate Analysis in Geology and Geochemistry : an Introduction. *Chemometrics and Intelligent Laboratory Systems* **2,** 15–28 (1987).

129. Braak, C. J. F. Principal Components Biplots and Alpha and Beta Diversity. *Ecology* **64,** 454–462 (1983).

130. Shlens, J. A tutorial on principal component analysis. *arXiv preprint arXiv:1404.1100* (2014).

131. Boogaart, K. G.V. D. & Tolosana-Delgado, R. *Analyzing Compositional Data with R* First (Springer, 2013).

132. Cattell, R. B. The scree test for the number of factors. *Multivariate behavioral research* **1,** 245–276 (1966).

133. Filzmoser, P., Hron, K. & Reimann, C. Principal component analysis for compositional data with outliers. *Environmetrics* **20,** 621–632 (2009).

134. Aitchison, J. Principal component analysis of compositional data. *Biometrika* **70,** 57–65 (1983).

135. Aitchison, J & Egozcue, J. J. Compositional Data Analysis : Where Are We and Where Should We Be Heading? *Mathematical Geology* **37,** 829–850 (2005).

136. *Compositional Data Analysis: Theory and Applications* First (eds Pawlowsky-Glahn, V. & Buccianti, A.) (John Wiley & Sons Ltd, West Sussex, United Kingdom, 2011).

137. Aitchison, J. The Statistical Analysis of Compositional Data. *Journal of the Royal Statistical Society: Series B (Statistical Methodology)* **44,** 139–177 (1982).

138. Aitchison, J. *The statistical analysis of compositional data* (Chapman and Hall London, 1986).

139. Whitten, E. H. T. Open and Closed Compositional Data in Petrology. *Mathematical Geology* **27,** 789–806 (1995).

140. Vermeesch, P. Multi-sample comparison of detrital age distributions. *Chemical Geology* **341,** 140–146 (2013).

141. Beardah, C. C., Baxter, M. J., Cool, H. E. M. & Jackson, C. M. *Compositional data analysis of archaeological glass: problems and possible solutions* in *Proceedings of the Compositional Data Analysis Workshop, CODAWORK* (2003), 279–300.

142. Baxter, M. J., Beardah, C. C., Cool, H. E. M. & Jackson, C. M. Compositional data analysis of some alkaline glasses. *Mathematical Geology* **37,** 183–196 (2005).

143. Iwamori, H *et al.* Classification of geochemical data based on multivariate statistical analyses: Complementary roles of cluster, principal component, and independent component analyses. *Geochemistry, Geophysics, Geosystems* **18,** 994–1012 (2017).

144. Tangri, D. & Wright, R. V. S. Multivariate analysis of compositional data: applied comparisons favour standard principal components analysis over Aitchison's log-linear contrast method. *Archaeometry* **35,** 103–115 (1993).

145. Templ, M., Filzmoser, P. & Reimann, C. Applied Geochemistry Cluster analysis applied to regional geochemical data: problems and possibilities. *Applied Geochemistry* **23,** 2198–2213 (2008).

146. Helsel, D. R. Fabricating data: How substituting values for nondetects can ruin results, and what can be done about it. *Chemosphere* **65,** 2434–2439 (2006).

147. Duewer, D. L., Kowalski, B. & Fasching, J. Improving the Reliability of Factor Analysis of Chemical Data by Utilizing the Measured Analytical Uncertainty. *Analytical Chemistry* **48,** 2002–2010 (1976).

148. Daszykowski, M, Kaczmarek, K, Heyden, Y. V. & Walczak, B. Robust statistics in data analysis A review of basic concepts. *Chemometrics and Intelligent Laboratory Systems* **85,** 203–219 (2007).

149. Filzmoser, P., Garrett, R. G. & Reimann, C. Multivariate outlier detection in exploration geochemistry. *Computers and Geosciences* **31,** 579–587 (2005).

150. De Maesschalck, R., Jouan-Rimbaud, D. & Massart, D. L. The Mahalanobis distance. *Chemometrics and Intelligent Laboratory Systems* **50,** 1–18 (2000).

151. Egan, W. J. & Morgan, S. L. Outlier Detection in Multivariate Analytical Chemical Data. *Analytical Chemistry* **70,** 2372–2379 (1998).

152. Cao, D.-S., Liang, Y.-Z., Xu, Q.-S., Li, H.-D. & Chen, X. A new strategy of outlier detection for QSAR/QSPR. *Journal of computational chemistry* **31,** 592–602 (2010).

153. Hodge, V. & Austin, J. A survey of outlier detection methodologies. *Artificial intelligence review* **22,** 85–126 (2004).

154. Everitt, B. S. & Dunn, G. *Applied Multivariate Data Analysis* 2nd (John Wiley & Sons Ltd, London).

155. Faith, D. P., Minchin, P. R. & Belbin, L. Compositional dissimilarity as a robust measure of ecological distance. *Vegetatio* **69,** 57–68 (1987).

156. Jaworska, N. & Chupetlovska-Anastasova, A. A Review of Multidimensional Scaling (MDS) and its Utility in Various Psychological Domains. *Tutorials in Quantitative Methods for Psychology* **5,** 1–10 (2009).

157. Borg, I. & Groenen, P. J. *Modern Multidimensional Scaling* 2nd edition (Springer, 2005).

158. Kruskal, J. B. Multidimensional scaling by optimizing goodness of fit to a nonmetric hypothesis. *Psychometrika* **29,** 1–27 (1964).

159. Shepard, R. N. The analysis of proximities: multidimensional scaling with an unknown distance function. I. *Psychometrika* **27,** 125–140 (1962).

160. Wickelmaier, F. An introduction to MDS. *Sound Quality Research Unit, Aalborg University, Denmark* **46** (2003).

161. Kruskal, J. B. Nonmetric multidimensional scaling: a numerical method. *Psychometrika* **29,** 115–129 (1964).

162. Oksanen, J. *et al. vegan: Community Ecology Package* R package version 2.4-4 (2017).

163. Krot, A. N., Libourel, G., Goodrich, C. a., Petaev, M. I. & Rais, A. Silica-rich igneous rims around magnesian chondrules in CR carbonaceous chondrites : Evidence for condensation origin from fractionated nebular gas. *Meteoritics & Planetary Science* **39,** 1931–1955 (2004).

164. Scott, E. R. & Krot, A. N. Chondrites and Their Components. *Treatise on Geochemistry: Second Edition* **1,** 65–137 (2013).

165. Alexander, C. M. O. Trace element contents of chondrule rims and interchondrule matrix in ordinary chondrites. *Geochimica et Cosmochimica Acta* **59,** 3247–3266 (1995).

166. Alexander, C. M. O. *Formation of Chondrules by Recycling and Volatile Loss* in *Proceedings of the 26th Lunar and Planetary Science Conference* (Alexander1994, 1994), 15–16.

167. Humayun, M. Chondrule cooling rates inferred from diffusive profiles in metal lumps from the Acfer 097 CR2 chondrite. *Meteoritics & Planetary Science* **47,** 1191–1208 (2012).

168. Libourel, G., Krot, A. N. & Tissandier, L. Role of gas-melt interaction during chondrule formation. *Earth and Planetary Science Letters* **251,** 232–240 (2006).

169. Hezel, D. C., Palme, H., Brenker, F. E. & Nasdala, L. Evidence for fractional condensation and reprocessing at high temperatures in CH chondrites. *Meteoritics & Planetary Science* **38,** 1199–1215 (2003).

170. Tissandier, L., Libourel, G. & Robert, F. Gas-melt interactions and their bearing on chondrule formation. *Meteoritics & Planetary Science* **37,** 1377–1389 (2002).

Appendix A

Agglomerates

Table A.1: Size, location, and frequency of agglomerates in 18 samples counted using Al and Si compositional maps. "Name" refers to agglomerates that were further characterized with EDS and/or SIMS. Interface types were confirmed with Si and Ca compositional maps. If, however, Ca enrichments were indeterminate, the interface type is labeled as indeterminate as a Si enrichment may be present at both Si interfaces and near CaMgFe interfaces. "% of Samp. Area" refers to the area occupied by the agglomerate relative to the *sample* (not just the host), expressed as a percentage. These data are used to generate Figures 3.8, 3.9, and 3.10.

Sample	Sample Area (μm^2)	Agglomerate Count	Name	Agglomerate Area (μm^2)	% of Samp. Area	Interface Type	Attachment Location
CC	2.43E+06	1	-	2.008E+04	8.28E-01	Si	Surface
CC	2.43E+06	2	-	7.334E+02	3.02E-02	Si	Surface
CC	2.43E+06	3	-	1.290E+03	5.32E-02	Si	Interior
CC	2.43E+06	4	-	4.329E+02	1.78E-02	Si	Surface
CC	2.43E+06	5	-	2.691E+03	1.11E-01	Si	Surface
CC	2.43E+06	6	-	3.056E+02	1.26E-02	Si	Interior
CC	2.43E+06	7	-	3.994E+04	1.65E+00	Si	Surface
CC	2.43E+06	8	-	6.553E+02	2.70E-02	Si	Interior
CC	2.43E+06	9	-	8.274E+03	3.41E-01	Si	Interior
CC	2.43E+06	10	-	6.519E+02	2.69E-02	Si	Surface
CC	2.43E+06	11	-	1.290E+02	5.32E-03	Si	Surface
CC	2.43E+06	12	-	3.378E+02	1.39E-02	Si	Surface
CC	2.43E+06	13	-	4.804E+02	1.98E-02	Si	Surface
CC	2.43E+06	14	-	7.402E+02	3.05E-02	Si	Surface
CC	2.43E+06	15	-	6.892E+02	2.84E-02	Si	Surface
CC	2.43E+06	16	-	1.766E+02	7.28E-03	Si	Surface
CC	2.43E+06	17	-	7.639E+02	3.15E-02	Si	Surface
CC	2.43E+06	18	-	3.565E+01	1.47E-03	Si	Surface
CC	2.43E+06	19	-	6.112E+01	2.52E-03	Si	Surface
CC	2.43E+06	20	-	3.056E+01	1.26E-03	Si	Surface
CC	2.43E+06	21	-	1.783E+03	7.35E-02	Si	Surface
CC	2.43E+06	22	-	4.675E+03	1.93E-01	Si	Surface
CC	2.43E+06	23	-	3.056E+01	1.26E-03	Si	Surface
CC	2.43E+06	24	-	5.297E+02	2.18E-02	Si	Surface
CC	2.43E+06	25	-	1.686E+03	6.95E-02	Si	Surface
CC	2.43E+06	26	-	4.036E+04	1.66E+00	Si	Surface
CC	2.43E+06	27	-	7.653E+03	3.16E-01	Si	Surface
CC	2.43E+06	28	-	9.988E+04	4.12E+00	Si	Surface
CC	2.43E+06	29	-	5.432E+02	2.24E-02	Si	Surface
CC	2.43E+06	30	-	1.830E+03	7.54E-02	Si	Surface
CC	2.43E+06	31	-	1.169E+04	4.82E-01	Si	Surface

CC	2.43E+06	32	-	3.429E+02	1.41E-02	Si	Surface
CC	2.43E+06	33	-	1.698E+02	7.00E-03	Si	Surface
CC	2.43E+06	34	-	2.292E+02	9.45E-03	Si	Surface
CC	2.43E+06	35	-	2.648E+02	1.09E-02	Si	Surface
CD	2.60E+06	1	-	1.951E+04	7.49E-01	CaMgFe	Surface
CD	2.60E+06	2	-	7.413E+03	2.85E-01	Si	Surface
CD	2.60E+06	3	-	4.450E+03	1.71E-01	Si	Surface
CD	2.60E+06	4	-	8.221E+03	3.16E-01	Si	Surface
CD	2.60E+06	5	-	8.619E+03	3.31E-01	Si	Surface
CD	2.60E+06	6	-	1.239E+03	4.76E-02	Si	Interior
CD	2.60E+06	7	-	6.825E+03	2.62E-01	Si	Surface
CD	2.60E+06	8	-	4.149E+03	1.59E-01	Si	Surface
CD	2.60E+06	9	-	7.612E+02	2.92E-02	Si	Interior
CD	2.60E+06	10	-	2.764E+03	1.06E-01	Si	Surface
CD	2.60E+06	11	-	1.176E+02	4.52E-03	Si	Surface
CD	2.60E+06	12	-	2.436E+02	9.35E-03	Si	Surface
CD	2.60E+06	13	-	4.567E+02	1.75E-02	Si	Surface
CD	2.60E+06	14	-	2.325E+02	8.93E-03	Si	Surface
CD	2.60E+06	15	-	1.064E+03	4.09E-02	Si	Surface
CD	2.60E+06	16	-	2.584E+04	9.92E-01	Si	Surface
CD	2.60E+06	17	-	6.844E+03	2.63E-01	Si	Surface
FLD14	6.54E+06	1	-	3.287E+04	5.02E-01	Si	Surface
FLD14	6.54E+06	2	FLD14.1	1.925E+04	2.94E-01	Si	Surface
FLD14	6.54E+06	3	FLD14.L	5.750E+05	8.79E+00	CaMgFe	Exterior
FLD14	6.54E+06	4	-	8.670E+04	1.32E+00	n.d.	Exterior
FLD17	4.34E+06	1	FLD17.Tail	2.770E+04	6.38E-01	CaMgFe	Exterior
FLD17	4.34E+06	2	FLD17.1	4.828E+04	1.11E+00	Si	Exterior
FLD17	4.34E+06	3	-	9.120E+02	2.10E-02	Si	Surface
FLD17	4.34E+06	4	-	6.974E+03	1.61E-01	Si	Surface
FLD17	4.34E+06	5	-	3.131E+03	7.21E-02	Si	Interior
FLD17	4.34E+06	6	FLD17.int.2	4.080E+03	9.39E-02	Si	Interior
FLD17	4.34E+06	7	FLD17.int.1	1.452E+04	3.34E-01	Si	Interior
FLD17	4.34E+06	8	FLD17.2	1.452E+05	3.34E+00	Si	Surface
FLD18	2.61E+06	1	FLD18.1	2.826E+03	1.08E-01	CaMgFe	Exterior
FLD18	2.61E+06	2	-	2.193E+02	8.39E-03	n.d.	Surface
FLD18	2.61E+06	3	-	3.180E+02	1.22E-02	n.d.	Surface
FLD18	2.61E+06	4	-	2.040E+04	7.80E-01	Si	Surface
FLD18	2.61E+06	5	-	2.500E+02	9.56E-03	n.d.	Surface
FLD18	2.61E+06	6	-	7.412E+02	2.84E-02	CaMgFe	Surface
FLD18	2.61E+06	7	-	2.401E+02	9.19E-03	n.d.	Surface
FLD18	2.61E+06	8	-	5.515E+02	2.11E-02	n.d.	Surface
FLD18	2.61E+06	9	-	1.272E+02	4.87E-03	n.d.	Surface
FLD18	2.61E+06	10	-	4.824E+01	1.85E-03	n.d.	Surface
FLD18	2.61E+06	11	-	9.210E+01	3.52E-03	n.d.	Surface
FLD18	2.61E+06	12	-	2.193E+01	8.39E-04	n.d.	Surface
FLD18	2.61E+06	13	-	3.289E+01	1.26E-03	n.d.	Surface
FLD18	2.61E+06	14	-	3.191E+02	1.22E-02	n.d.	Surface
FLD18	2.61E+06	15	-	2.664E+02	1.02E-02	n.d.	Surface
FLD18	2.61E+06	16	-	6.359E+01	2.43E-03	n.d.	Surface
FLD18	2.61E+06	17	-	1.053E+02	4.03E-03	n.d.	Surface
FLD18	2.61E+06	18	FLD18.3	2.152E+04	8.24E-01	Si	Interior
FLD18	2.61E+06	19	FLD18.4	8.890E+04	3.40E+00	CaMgFe	Surface
FLD18	2.61E+06	20	FLD18.2	1.205E+04	4.61E-01	Si	Interior
FLD20	4.11E+06	1	-	7.269E+03	1.77E-01	CaMgFe	Surface
FLD20	4.11E+06	2	-	2.909E+03	7.08E-02	Si	Interior
FLD20	4.11E+06	3	-	2.508E+03	6.11E-02	Si	Surface
FLD21	2.50E+06	1	FLD21.1	1.263E+05	5.06E+00	Si	Surface
FLD21	2.50E+06	2	FLD21.L	3.333E+04	1.33E+00	Si	Exterior
FLD23	2.91E+06	1	-	4.655E+03	1.60E-01	Si	Surface

FLD23	2.91E+06	2	-	1.155E+03	3.96E-02	Si	Surface
FLD23	2.91E+06	3	-	7.213E+02	2.48E-02	Si	Surface
FLD23	2.91E+06	4	FLD23.1.1	1.662E+03	5.70E-02	Si	Surface
FLD23	2.91E+06	5	FLD23.1.2	1.735E+03	5.95E-02	Si	Surface
FLD23	2.91E+06	6	FLD23.1.3	1.735E+03	5.95E-02	Si	Surface
FLD23	2.91E+06	7	FLD23.2.1	3.464E+02	1.19E-02	Si	Surface
FLD23	2.91E+06	8	FLD23.2.2	7.547E+02	2.59E-02	Si	Surface
FLD23	2.91E+06	9	-	1.838E+03	6.31E-02	Si	Surface
FLD23	2.91E+06	10	-	2.381E+02	8.17E-03	Si	Surface
FLD23	2.91E+06	11	-	8.069E+02	2.77E-02	Si	Surface
FLD23	2.91E+06	12	-	6.219E+02	2.13E-02	Si	Surface
FLD23	2.91E+06	13	-	2.155E+03	7.40E-02	Si	Surface
FLD23	2.91E+06	14	FLD23.3.1	1.300E+03	4.46E-02	Si	Surface
FLD23	2.91E+06	15	FLD23.3.2	2.270E+02	7.79E-03	Si	Surface
FLD23	2.91E+06	16	-	1.508E+02	5.17E-03	Si	Surface
FLD23	2.91E+06	17	FLD23.4.2	1.385E+03	4.75E-02	Si	Surface
FLD23	2.91E+06	18	FLD23.4.1	1.452E+03	4.98E-02	Si	Surface
FLD23	2.91E+06	19	FLD23.5.1	2.827E+03	9.70E-02	Si	Surface
FLD23	2.91E+06	20	-	3.324E+02	1.14E-02	Si	Surface
FLD23	2.91E+06	21	-	5.157E+02	1.77E-02	Si	Surface
FLD23	2.91E+06	22	-	7.658E+02	2.63E-02	Si	Surface
FLD23	2.91E+06	23	-	1.491E+02	5.11E-03	Si	Surface
FLD23	2.91E+06	24	-	1.628E+02	5.58E-03	Si	Surface
FLD23	2.91E+06	25	-	4.866E+02	1.67E-02	Si	Surface
FLD23	2.91E+06	26	FLD23.L	1.948E+05	6.68E+00	Si	Surface
FLD25	1.51E+06	1	-	3.553E+02	2.35E-02	Si	Surface
FLD25	1.51E+06	2	-	7.583E+01	5.02E-03	Si	Surface
FLD25	1.51E+06	3	-	9.288E+01	6.15E-03	Si	Surface
FLD25	1.51E+06	4	-	2.232E+02	1.48E-02	Si	Surface
FLD25	1.51E+06	5	-	4.857E+01	3.22E-03	Si	Surface
FLD25	1.51E+06	6	-	4.090E+01	2.71E-03	Si	Surface
FLD25	1.51E+06	7	-	2.658E+02	1.76E-02	Si	Surface
FLD25	1.51E+06	8	-	4.243E+02	2.81E-02	Si	Surface
FLD25	1.51E+06	9	-	7.822E+02	5.18E-02	Si	Surface
FLD28	1.80E+06	1	-	2.250E+02	1.25E-02	Si	Surface
FLD28	1.80E+06	2	-	1.920E+02	1.06E-02	Si	Surface
FLD4.2	1.73E+06	1	-	6.091E+04	3.52E+00	Si	Surface
FLD4.2	1.73E+06	2	-	4.560E+04	2.64E+00	Si	Surface
FLD4.2	1.73E+06	3	-	1.090E+04	6.31E-01	Si	Surface
FLD4.3	1.70E+06	1	FLD4.3.UA	1.670E+03	9.84E-02	Si	Surface
FLD4.3	1.70E+06	2	FLD4.3.1	1.186E+03	6.99E-02	Si	Interior
FLD4.3	1.70E+06	3	FLD4.3.2	1.315E+03	7.75E-02	Si	Interior
FLD4.3	1.70E+06	4	FLD4.3.3	2.166E+03	1.28E-01	Si	Interior
FLD4.3	1.70E+06	5	-	1.473E+03	8.68E-02	Si	Surface
FLD4.3	1.70E+06	6	FLD4.3.4	3.892E+03	2.29E-01	Si	Surface
FLD4.3	1.70E+06	7	-	1.127E+03	6.64E-02	Si	Surface
FLD4.3	1.70E+06	8	-	3.725E+03	2.19E-01	Si	Surface
FLD4.3	1.70E+06	9	-	7.352E+02	4.33E-02	Si	Surface
FLD4.3	1.70E+06	10	-	2.812E+02	1.66E-02	Si	Surface
FLD4.3	1.70E+06	11	-	4.737E+02	2.79E-02	Si	Surface
FLD4.3	1.70E+06	12	FLD4.3.5	1.340E+03	7.89E-02	Si	Interior
FLD4.3	1.70E+06	13	-	1.628E+03	9.59E-02	Si	Interior
FLD4.3	1.70E+06	14	-	9.942E+02	5.86E-02	Si	Surface
FLD4.3	1.70E+06	15	-	1.611E+03	9.49E-02	Si	Surface
FLD4.3	1.70E+06	16	-	1.480E+03	8.72E-02	Si	Surface
FLD4.4	1.58E+06	1	FLD4.4.1	4.690E+04	2.97E+00	Si	Surface
FLD4.4	1.58E+06	2	FLD4.4.2	2.076E+04	1.32E+00	Si	Surface
FLD4.4	1.58E+06	3	-	3.857E+02	2.45E-02	Si	Surface
FLD4.4	1.58E+06	4	-	3.029E+02	1.92E-02	Si	Surface

FLD5.4	7.00E+05	1	-	9.415E+03	1.35E+00	Si	Surface
FLD5.4	7.00E+05	2	-	3.141E+04	4.49E+00	Si	Surface
FLD5.4	7.00E+05	3	-	1.872E+03	2.67E-01	Si	Surface
FLD5.4	7.00E+05	4	-	2.112E+03	3.02E-01	Si	Surface
FLD5.4	7.00E+05	5	-	3.226E+04	4.61E+00	Si	Surface
FLD5.4	7.00E+05	6	-	9.823E+02	1.40E-01	Si	Surface
FLD5.4	7.00E+05	7	-	1.392E+04	1.99E+00	Si	Surface
FLD5.4	7.00E+05	8	-	1.230E+04	1.76E+00	Si	Surface
FLD5.4	7.00E+05	9	-	1.099E+04	1.57E+00	Si	Surface
FLD5.4	7.00E+05	10	-	2.667E+03	3.81E-01	Si	Surface
FLD5.4	7.00E+05	11	-	4.454E+03	6.36E-01	n.d.	Exterior
U1B	1.41E+06	1	U1B.2	5.570E+03	3.95E-01	CaMgFe	Surface
U1B	1.41E+06	2	-	1.098E+03	7.80E-02	CaMgFe	Surface
U1B	1.41E+06	3	-	8.385E+02	5.95E-02	Si	Surface
U1B	1.41E+06	4	-	5.000E+02	3.55E-02	n.d.	Surface
U1B	1.41E+06	5	U1B.L	2.981E+04	2.12E+00	Si	Interior
U2	1.86E+06	1	-	0.000E+00	0.00E+00	n.d.	N/A
U3	4.41E+06	1	U3.2	3.008E+04	6.83E-01	Si	Surface
U3	4.41E+06	2	-	2.719E+04	6.17E-01	Si	Interior
U3	4.41E+06	3	-	1.287E+04	2.92E-01	Si	Surface
U3	4.41E+06	4	-	2.418E+03	5.49E-02	Si	Surface
U3	4.41E+06	5	-	5.310E+04	1.21E+00	Si	Surface
U3	4.41E+06	6	-	1.918E+04	4.35E-01	Si	Surface
U3	4.41E+06	7	-	7.857E+02	1.78E-02	Si	Surface
U3	4.41E+06	8	-	4.492E+03	1.02E-01	Si	Surface
U3	4.41E+06	9	-	2.550E+04	5.79E-01	Si	Surface
U3	4.41E+06	10	U3.5	1.636E+04	3.71E-01	Si	Surface
U3	4.41E+06	11	-	4.069E+03	9.23E-02	Si	Surface
U3	4.41E+06	12	-	1.035E+04	2.35E-01	Si	Surface
U3	4.41E+06	13	-	9.286E+02	2.11E-02	Si	Interior
U3	4.41E+06	14	-	4.510E+02	1.02E-02	Si	Surface
U3	4.41E+06	15	-	1.705E+04	3.87E-01	Si	Surface
U3	4.41E+06	16	-	4.337E+03	9.84E-02	Si	Interior
U3	4.41E+06	17	-	1.777E+04	4.03E-01	Si	Surface
U3	4.41E+06	18	U3.1	1.399E+04	3.18E-01	Si	Surface
U3	4.41E+06	19	-	2.227E+03	5.05E-02	Si	Surface
U3	4.41E+06	20	-	2.332E+04	5.29E-01	Si	Surface
U3	4.41E+06	21	-	2.382E+03	5.40E-02	Si	Surface
U3	4.41E+06	22	-	1.426E+04	3.24E-01	Si	Surface
U3	4.41E+06	23	-	8.510E+02	1.93E-02	Si	Surface
U3	4.41E+06	24	-	4.939E+02	1.12E-02	Si	Interior
U3	4.41E+06	25	-	2.876E+03	6.53E-02	Si	Surface
U3	4.41E+06	26	U3.3	5.304E+04	1.20E+00	Si	Surface
U3	4.41E+06	27	-	1.041E+02	2.36E-03	Si	Surface
U3	4.41E+06	28	-	7.143E+01	1.62E-03	Si	Surface
U3	4.41E+06	29	-	7.347E+01	1.67E-03	Si	Surface
U3	4.41E+06	30	-	1.490E+02	3.38E-03	Si	Surface
U3	4.41E+06	31	-	3.586E+03	8.14E-02	Si	Surface
U3	4.41E+06	32	-	9.531E+02	2.16E-02	Si	Surface
U3	4.41E+06	33	-	2.886E+04	6.55E-01	Si	Surface
U3	4.41E+06	34	-	1.103E+04	2.50E-01	Si	Surface
U3	4.41E+06	35	-	2.068E+04	4.69E-01	Si	Interior
U3	4.41E+06	36	U3.4	1.186E+04	2.69E-01	Si	Surface
U3	4.41E+06	37	-	6.531E+02	1.48E-02	Si	Surface
U3	4.41E+06	38	-	1.633E+02	3.71E-03	Si	Surface
U3	4.41E+06	39	-	1.367E+02	3.10E-03	Si	Surface
U3	4.41E+06	40	-	1.730E+04	3.93E-01	Si	Surface
U3	4.41E+06	41	-	2.808E+03	6.37E-02	Si	Surface
U3	4.41E+06	42	-	9.592E+02	2.18E-02	Si	Interior

U3	4.41E+06	43	-	4.538E+04	1.03E+00	Si	Surface
U3	4.41E+06	44	-	2.612E+03	5.93E-02	Si	Surface
U3	4.41E+06	45	-	1.044E+04	2.37E-01	Si	Surface
U3	4.41E+06	46	-	4.538E+04	1.03E+00	Si	Surface
U3	4.41E+06	47	-	2.612E+03	5.93E-02	Si	Surface
U3	4.41E+06	48	-	1.044E+04	2.37E-01	Si	Surface
U3	4.41E+06	49	-	4.702E+03	1.07E-01	Si	Surface
U3	4.41E+06	50	-	2.592E+03	5.88E-02	Si	Surface
U3	4.41E+06	51	-	2.808E+03	6.37E-02	Si	Surface
U3	4.41E+06	52	-	8.918E+02	2.02E-02	Si	Surface
U3	4.41E+06	53	-	1.616E+04	3.67E-01	Si	Surface
U3	4.41E+06	54	-	2.017E+04	4.58E-01	Si	Surface
U3	4.41E+06	55	-	1.141E+04	2.59E-01	Si	Surface
U3	4.41E+06	56	-	2.465E+03	5.59E-02	Si	Surface
U4	3.90E+06	1	-	6.822E+04	1.75E+00	n.d.	Surface
U4	3.90E+06	2	U4.1	2.406E+05	6.16E+00	n.d.	Surface
U4	3.90E+06	3	-	1.319E+04	3.38E-01	n.d.	Surface
U4	3.90E+06	4	U4.3	1.699E+05	4.35E+00	n.d.	Surface
U4	3.90E+06	5	U4.4	2.494E+04	6.39E-01	Si	Surface
U4	3.90E+06	6	U4.2	8.839E+04	2.26E+00	Si	Interior
U4	3.90E+06	7	-	5.130E+04	1.31E+00	n.d.	Interior
U4	3.90E+06	8	U4.6	1.851E+04	4.74E-01	Si	Surface
U4	3.90E+06	9	U4.5	2.284E+04	5.85E-01	Si	Surface
U4	3.90E+06	10	U4.7	4.776E+04	1.22E+00	n.d.	Surface
U4	3.90E+06	11	-	5.614E+04	1.44E+00	n.d.	Surface

Appendix B

EDS Host Analyses

Table B.1: Compositions in hosts of 37 samples measured by EDS. Analytical procedure is detailed in Chapter 4. Uncertainties are calculated as detailed in Chapter 6. These data are also used to generate the PCA model in Chapter 6.

Sample	SiO_2	1σ	Al_2O_3	1σ	Na_2O	1σ	K_2O	1σ	CaO	1σ	FeO	1σ	TiO_2	1σ	MgO	1σ
AA.B	74.40	3.14	12.63	0.64	3.45	0.25	3.39	0.14	1.44	0.08	2.32	0.11	0.27	0.05	0.74	0.08
AA.B	72.81	3.08	13.16	0.66	3.77	0.27	3.68	0.15	1.55	0.09	2.55	0.12	0.30	0.06	0.77	0.09
AA.B	73.74	3.11	12.94	0.65	3.63	0.26	3.67	0.15	1.88	0.10	2.51	0.12	0.27	0.05	0.74	0.08
AA.B	72.07	3.05	12.46	0.63	3.30	0.24	3.71	0.15	1.87	0.09	2.44	0.11	0.28	0.06	0.68	0.08
AA.B	73.69	3.11	12.69	0.64	3.39	0.25	3.84	0.15	1.46	0.08	2.42	0.11	0.22	0.05	0.65	0.08
AA.B	76.47	3.23	13.45	0.67	3.58	0.26	3.63	0.14	1.48	0.08	2.58	0.12	0.26	0.05	0.78	0.09
AA.B	73.98	3.12	12.53	0.63	3.46	0.25	3.70	0.15	1.71	0.09	2.51	0.12	0.30	0.06	0.62	0.08
AA.B	97.19	4.09	2.38	0.16	0.90	0.09	0.88	0.06	0.16	0.04	0.60	0.06	0.06	0.05	0.35	0.06
AA.B	73.72	3.11	12.49	0.63	3.71	0.27	3.79	0.15	1.57	0.09	2.46	0.11	0.26	0.05	0.62	0.08
AA.B	71.92	3.04	13.48	0.67	3.42	0.25	3.79	0.15	1.56	0.09	2.51	0.11	0.22	0.05	0.71	0.08
AA.B	96.83	4.07	3.02	0.19	0.91	0.09	0.95	0.06	0.23	0.05	0.57	0.06	0.05	0.05	0.34	0.06
AA.B	95.88	4.03	2.72	0.18	0.96	0.10	0.91	0.06	0.03	0.04	0.47	0.05	0.10	0.05	0.30	0.06
AA.B	73.33	3.10	11.96	0.60	3.33	0.24	3.76	0.15	1.50	0.08	2.26	0.11	0.28	0.05	0.63	0.08
AA.B	93.87	3.95	4.01	0.24	1.19	0.11	1.23	0.07	0.34	0.05	0.79	0.06	0.10	0.05	0.42	0.07
AA.B	72.92	3.08	13.20	0.66	3.69	0.27	3.82	0.15	1.65	0.09	2.58	0.12	0.31	0.06	0.72	0.08
AA.B	74.81	3.16	13.32	0.67	3.76	0.27	3.70	0.15	1.75	0.09	2.47	0.11	0.29	0.06	0.80	0.09
AA.B	74.98	3.17	12.99	0.65	3.63	0.26	3.76	0.15	1.72	0.09	2.43	0.11	0.29	0.06	0.65	0.08
AA.B	102.36	4.30	0.75	0.09	0.09	0.04	0.03	0.03	0.03	0.04	0.03	0.04	0.03	0.05	0.21	0.06
AA.B	100.92	4.24	1.00	0.10	0.38	0.06	0.16	0.04	0.07	0.04	0.25	0.05	0.03	0.05	0.23	0.06
AA.B	71.13	3.01	12.79	0.64	3.37	0.25	3.78	0.15	1.80	0.09	2.62	0.12	0.30	0.06	0.72	0.08
AA.B	75.94	3.21	13.22	0.66	3.45	0.25	3.49	0.14	1.89	0.10	2.49	0.11	0.25	0.05	0.71	0.08
AA.B	74.80	3.16	12.82	0.64	3.31	0.24	3.68	0.15	1.90	0.10	2.62	0.12	0.17	0.05	0.73	0.08
AA.B	74.96	3.17	12.71	0.64	3.37	0.25	3.68	0.15	1.81	0.09	2.48	0.11	0.29	0.06	0.69	0.08
AA.B	71.65	3.03	12.43	0.63	3.32	0.24	3.73	0.15	1.64	0.09	2.52	0.12	0.34	0.06	0.66	0.08
AA.B	73.06	3.09	12.43	0.63	3.31	0.24	3.78	0.15	1.72	0.09	2.52	0.12	0.29	0.06	0.67	0.08
AA.B	75.31	3.18	12.91	0.65	3.50	0.25	3.64	0.14	1.88	0.10	2.58	0.12	0.31	0.06	0.69	0.08
AA.B	73.15	3.09	12.47	0.63	3.49	0.25	3.73	0.15	1.59	0.09	2.50	0.11	0.29	0.06	0.64	0.08
AA.B	72.69	3.07	12.52	0.63	2.97	0.22	3.70	0.15	1.92	0.10	2.47	0.11	0.27	0.05	0.67	0.08
AA.B	73.33	3.10	12.24	0.62	3.10	0.23	3.73	0.15	1.94	0.10	2.55	0.12	0.24	0.05	0.65	0.08
AA.B	75.06	3.17	13.06	0.65	3.11	0.23	3.70	0.15	2.15	0.10	2.60	0.12	0.34	0.06	0.67	0.08
AA.B	73.78	3.12	13.08	0.66	2.74	0.21	3.26	0.13	1.93	0.10	2.48	0.11	0.29	0.06	0.65	0.08
AA.B	75.05	3.17	13.64	0.68	2.87	0.21	3.24	0.13	1.92	0.10	2.56	0.12	0.26	0.05	0.74	0.08
AA.B	78.12	3.30	12.98	0.65	2.89	0.22	3.20	0.13	1.65	0.09	2.46	0.11	0.22	0.05	0.68	0.08
AA.B	74.03	3.13	12.64	0.64	2.85	0.21	3.42	0.14	1.77	0.09	2.55	0.12	0.26	0.05	0.72	0.08
AA.B	72.66	3.07	12.78	0.64	3.02	0.22	3.64	0.14	1.90	0.10	2.71	0.12	0.32	0.06	0.69	0.08
AA.B	71.55	3.02	12.40	0.62	3.23	0.24	3.64	0.14	1.73	0.09	2.55	0.12	0.27	0.05	0.65	0.08
AA.B	80.87	3.41	11.08	0.56	2.70	0.20	3.18	0.13	1.51	0.08	2.11	0.10	0.20	0.05	0.58	0.08

AA.B	71.56	3.02	13.28	0.67	3.45	0.25	3.76	0.15	1.82	0.09	2.53	0.12	0.30	0.06	0.71	0.08
AA.B	73.12	3.09	12.07	0.61	2.90	0.22	3.57	0.14	1.73	0.09	2.35	0.11	0.26	0.05	0.68	0.08
AA.B	73.01	3.08	12.92	0.65	2.88	0.22	3.45	0.14	1.90	0.10	2.35	0.11	0.29	0.06	0.66	0.08
AA.B	73.06	3.09	13.59	0.68	2.98	0.22	3.51	0.14	2.03	0.10	2.58	0.12	0.30	0.06	0.73	0.08
AA.B	74.98	3.17	12.80	0.64	2.81	0.21	3.36	0.14	1.88	0.10	2.56	0.12	0.32	0.06	0.72	0.08
AA.B	74.75	3.16	13.09	0.66	2.77	0.21	3.28	0.13	1.94	0.10	2.46	0.11	0.25	0.05	0.67	0.08
AA.B	73.16	3.09	13.40	0.67	2.73	0.21	3.28	0.13	2.21	0.11	2.61	0.12	0.27	0.05	0.76	0.08
AA.B	73.89	3.12	13.87	0.69	2.94	0.22	3.24	0.13	2.21	0.11	2.55	0.12	0.28	0.06	0.76	0.08
AA.B	76.88	3.24	12.62	0.63	2.99	0.22	3.83	0.15	2.45	0.11	2.47	0.11	0.29	0.06	0.63	0.08
AA.B	74.74	3.16	13.12	0.66	3.25	0.24	3.66	0.15	2.54	0.11	2.48	0.11	0.29	0.06	0.63	0.08
AA.B	74.51	3.15	13.60	0.68	3.23	0.24	3.67	0.15	2.60	0.12	2.50	0.11	0.32	0.06	0.68	0.08
AA.B	76.54	3.23	11.99	0.61	3.05	0.23	3.46	0.14	2.05	0.10	2.25	0.11	0.26	0.05	0.72	0.08
AA.B	75.14	3.17	12.16	0.61	3.18	0.23	3.63	0.14	2.28	0.11	2.49	0.11	0.27	0.05	0.69	0.08
AA.B	72.80	3.08	13.17	0.66	2.97	0.22	3.49	0.14	1.86	0.09	2.50	0.11	0.30	0.06	0.69	0.08
AA.B	75.59	3.19	13.56	0.68	3.41	0.25	3.67	0.15	2.48	0.11	2.47	0.11	0.29	0.06	0.72	0.08
AA.B	76.17	3.22	14.35	0.71	3.44	0.25	3.59	0.14	2.67	0.12	2.46	0.11	0.29	0.06	0.79	0.09
AA.B	72.99	3.08	13.49	0.68	3.46	0.25	3.71	0.15	1.40	0.08	2.53	0.12	0.32	0.06	0.64	0.08
AA.B	74.93	3.16	12.88	0.65	3.68	0.27	3.52	0.14	1.74	0.09	2.52	0.12	0.23	0.05	0.70	0.08
AA.B	72.29	3.05	12.33	0.62	3.56	0.26	3.70	0.15	2.18	0.10	2.48	0.11	0.28	0.06	0.67	0.08
AA.B	74.66	3.15	12.80	0.64	3.86	0.28	3.50	0.14	2.14	0.10	2.48	0.11	0.27	0.05	0.68	0.08
AA.B	75.15	3.17	12.84	0.64	4.00	0.28	3.50	0.14	2.02	0.10	2.43	0.11	0.26	0.05	0.68	0.08
AA.B	72.15	3.05	12.30	0.62	3.81	0.27	3.68	0.15	2.10	0.10	2.40	0.11	0.24	0.05	0.64	0.08
AA.B	72.23	3.05	13.74	0.69	3.44	0.25	3.58	0.14	1.69	0.09	2.62	0.12	0.29	0.06	0.70	0.08
AA.B	71.46	3.02	12.63	0.64	3.71	0.27	3.79	0.15	1.41	0.08	2.66	0.12	0.27	0.05	0.65	0.08
AA.B	74.64	3.15	12.94	0.65	3.68	0.27	3.57	0.14	1.55	0.09	2.46	0.11	0.29	0.06	0.70	0.08
AA.B	74.73	3.16	13.18	0.66	3.23	0.24	3.10	0.13	1.53	0.08	2.48	0.11	0.28	0.06	0.69	0.08
AA.B	73.12	3.09	12.46	0.63	3.55	0.26	3.60	0.14	1.86	0.09	2.55	0.12	0.34	0.06	0.64	0.08
AA.B	75.14	3.17	12.91	0.65	3.83	0.27	3.47	0.14	1.48	0.08	2.59	0.12	0.19	0.05	0.63	0.08
AA.B	72.43	3.06	13.21	0.66	3.46	0.25	3.65	0.14	1.50	0.08	2.59	0.12	0.21	0.05	0.64	0.08
AA.B	72.69	3.07	12.96	0.65	3.53	0.26	3.62	0.14	1.46	0.08	2.61	0.12	0.25	0.05	0.65	0.08
AA.B	70.82	2.99	13.17	0.66	3.55	0.26	3.66	0.15	1.48	0.08	2.52	0.12	0.32	0.06	0.66	0.08
AA.B	73.23	3.09	12.83	0.64	3.67	0.26	3.68	0.15	1.51	0.08	2.47	0.11	0.29	0.06	0.65	0.08
AA.B	75.30	3.18	12.89	0.65	3.66	0.26	3.46	0.14	1.77	0.09	2.42	0.11	0.24	0.05	0.69	0.08
AA.B	71.51	3.02	12.45	0.63	3.35	0.24	3.51	0.14	1.84	0.09	2.52	0.12	0.29	0.06	0.65	0.08
AA.B	71.73	3.03	13.26	0.66	3.42	0.25	3.60	0.14	1.60	0.09	2.50	0.11	0.25	0.05	0.64	0.08
AA.B	73.60	3.11	13.06	0.66	3.62	0.26	3.72	0.15	1.47	0.08	2.40	0.11	0.26	0.05	0.64	0.08
AA.B	73.03	3.09	12.95	0.65	3.60	0.26	3.61	0.14	1.44	0.08	2.52	0.12	0.14	0.05	0.63	0.08
AA.B	73.39	3.10	12.84	0.64	3.53	0.26	3.64	0.14	1.45	0.08	2.48	0.11	0.27	0.05	0.66	0.08
AA.B	71.36	3.02	12.88	0.65	3.52	0.26	3.69	0.15	1.44	0.08	2.48	0.11	0.22	0.05	0.68	0.08
AA.B	75.92	3.21	13.28	0.67	3.66	0.26	3.37	0.14	1.45	0.08	2.43	0.11	0.26	0.05	0.64	0.08
AA.B	81.49	3.44	9.14	0.47	2.66	0.20	2.84	0.12	1.18	0.07	1.93	0.10	0.20	0.05	0.58	0.08
AA.B	74.56	3.15	13.44	0.67	3.66	0.26	3.57	0.14	1.80	0.09	2.72	0.12	0.31	0.06	0.75	0.08
AA.B	74.06	3.13	12.36	0.62	3.48	0.25	3.71	0.15	1.41	0.08	2.50	0.11	0.26	0.05	0.63	0.08
AA.B	72.14	3.05	12.77	0.64	3.47	0.25	3.64	0.14	1.54	0.08	2.43	0.11	0.24	0.05	0.69	0.08
AA.B	73.68	3.11	12.90	0.65	3.70	0.27	3.75	0.15	1.54	0.09	2.47	0.11	0.28	0.05	0.64	0.08
AA.B	73.11	3.09	12.32	0.62	3.69	0.27	3.84	0.15	1.55	0.09	2.38	0.11	0.32	0.06	0.64	0.08
AA.B	73.74	3.11	12.57	0.63	3.84	0.28	3.79	0.15	1.61	0.09	2.43	0.11	0.26	0.05	0.55	0.07
AA.B	73.35	3.10	12.50	0.63	3.80	0.27	3.71	0.15	1.65	0.09	2.52	0.12	0.27	0.05	0.61	0.08
AA.B	74.58	3.15	13.82	0.69	3.11	0.23	3.28	0.13	2.12	0.10	2.64	0.12	0.32	0.06	0.75	0.08
AA.B	74.21	3.13	12.88	0.65	3.35	0.24	3.57	0.14	2.13	0.10	2.53	0.12	0.27	0.05	0.69	0.08
AA.B	73.34	3.10	12.69	0.64	3.34	0.24	3.58	0.14	1.97	0.10	2.47	0.11	0.23	0.05	0.68	0.08
AA.B	75.40	3.18	12.70	0.64	3.71	0.27	3.69	0.15	1.86	0.09	2.37	0.11	0.26	0.05	0.69	0.08
AA.B	73.22	3.09	12.62	0.63	3.58	0.26	3.63	0.14	1.90	0.10	2.48	0.11	0.29	0.06	0.70	0.08
AA.B	73.03	3.09	12.55	0.63	3.61	0.26	3.76	0.15	2.05	0.10	2.52	0.12	0.28	0.06	0.69	0.08
AA.B	72.38	3.06	12.62	0.63	3.49	0.25	3.68	0.15	2.14	0.10	2.47	0.11	0.23	0.05	0.65	0.08
AA.B	73.56	3.11	12.72	0.64	3.55	0.26	3.61	0.14	1.93	0.10	2.58	0.12	0.28	0.06	0.67	0.08
AA.B	72.53	3.06	12.67	0.64	3.40	0.25	3.79	0.15	1.99	0.10	2.73	0.12	0.37	0.06	0.71	0.08
AA.B	74.79	3.16	12.68	0.64	3.67	0.26	3.84	0.15	1.50	0.08	2.53	0.12	0.27	0.05	0.62	0.08
AA.B	73.56	3.11	13.01	0.65	3.77	0.27	3.84	0.15	1.87	0.09	2.53	0.12	0.35	0.06	0.75	0.08
AA.B	74.47	3.14	13.13	0.66	3.68	0.27	3.66	0.15	1.76	0.09	2.54	0.12	0.26	0.05	0.72	0.08
AA.B	74.22	3.13	12.89	0.65	3.60	0.26	3.54	0.14	1.66	0.09	2.52	0.12	0.28	0.06	0.70	0.08
AA.B	73.86	3.12	13.05	0.65	3.68	0.26	3.72	0.15	1.81	0.09	2.61	0.12	0.36	0.06	0.69	0.08

AA.B	73.13	3.09	12.46	0.63	3.53	0.26	3.74	0.15	1.67	0.09	2.51	0.12	0.28	0.05	0.63	0.08
AA.B	75.56	3.19	12.84	0.64	3.68	0.27	3.55	0.14	1.31	0.08	2.39	0.11	0.21	0.05	0.61	0.08
AA.B	74.50	3.15	13.42	0.67	3.72	0.27	3.53	0.14	1.38	0.08	2.56	0.12	0.29	0.06	0.65	0.08
AA.B	75.64	3.19	13.13	0.66	3.38	0.25	3.37	0.14	2.09	0.10	2.57	0.12	0.26	0.05	0.67	0.08
AA.B	73.98	3.12	13.84	0.69	3.44	0.25	3.43	0.14	2.55	0.12	2.71	0.12	0.30	0.06	0.72	0.08
AA.B	73.71	3.11	13.30	0.67	3.49	0.25	3.66	0.15	2.47	0.11	2.60	0.12	0.37	0.06	0.76	0.08
AA.B	72.85	3.08	12.76	0.64	3.61	0.26	3.81	0.15	1.78	0.09	2.64	0.12	0.30	0.06	0.67	0.08
AA.B	74.19	3.13	12.66	0.64	3.55	0.26	3.83	0.15	1.81	0.09	2.59	0.12	0.25	0.05	0.70	0.08
AA.B	74.19	3.13	12.96	0.65	3.59	0.26	3.73	0.15	1.60	0.09	2.59	0.12	0.32	0.06	0.65	0.08
AA.B	74.09	3.13	13.79	0.69	3.74	0.27	3.80	0.15	2.09	0.10	2.68	0.12	0.32	0.06	0.78	0.09
AA.B	74.15	3.13	12.83	0.64	3.49	0.25	3.76	0.15	2.10	0.10	2.50	0.11	0.29	0.06	0.64	0.08
AA.B	73.26	3.09	13.54	0.68	3.64	0.26	3.74	0.15	1.27	0.08	2.45	0.11	0.22	0.05	0.63	0.08
AA.B	73.77	3.12	13.18	0.66	3.46	0.25	3.66	0.15	1.55	0.09	2.59	0.12	0.22	0.05	0.69	0.08
AA.B	73.45	3.10	13.19	0.66	3.52	0.26	3.73	0.15	1.83	0.09	2.56	0.12	0.31	0.06	0.68	0.08
AA.B	74.74	3.16	13.29	0.67	2.92	0.22	3.28	0.13	1.91	0.10	2.59	0.12	0.33	0.06	0.76	0.08
AA.B	75.56	3.19	12.91	0.65	3.21	0.24	3.42	0.14	1.94	0.10	2.61	0.12	0.29	0.06	0.63	0.08
AA.B	76.62	3.23	13.00	0.65	3.33	0.24	3.41	0.14	1.89	0.10	2.52	0.12	0.25	0.05	0.69	0.08
AA.B	74.27	3.14	12.71	0.64	3.79	0.27	3.66	0.15	1.45	0.08	2.54	0.12	0.30	0.06	0.69	0.08
AA.B	73.96	3.12	12.67	0.64	3.73	0.27	3.57	0.14	1.47	0.08	2.52	0.12	0.25	0.05	0.69	0.08
AA.B	73.58	3.11	12.73	0.64	3.69	0.27	3.59	0.14	1.91	0.10	2.56	0.12	0.28	0.05	0.71	0.08
AA.B	72.53	3.06	12.79	0.64	3.56	0.26	3.65	0.15	1.66	0.09	2.56	0.12	0.29	0.06	0.69	0.08
AA.B	73.14	3.09	12.47	0.63	3.64	0.26	3.70	0.15	1.30	0.08	2.56	0.12	0.27	0.05	0.65	0.08
AA.B	73.66	3.11	12.94	0.65	3.63	0.26	3.64	0.14	1.30	0.08	2.35	0.11	0.26	0.05	0.64	0.08
AA.B	74.34	3.14	12.76	0.64	3.61	0.26	3.60	0.14	1.35	0.08	2.59	0.12	0.28	0.06	0.68	0.08
AA.B	72.89	3.08	13.35	0.67	3.65	0.26	3.60	0.14	1.41	0.08	2.57	0.12	0.25	0.05	0.62	0.08
AA.B	75.54	3.19	13.00	0.65	3.53	0.26	3.38	0.14	1.91	0.10	2.46	0.11	0.26	0.05	0.64	0.08
AA.B	75.78	3.20	12.94	0.65	3.52	0.26	3.52	0.14	1.82	0.09	2.52	0.12	0.28	0.05	0.68	0.08
AA.B	75.14	3.17	12.84	0.64	3.44	0.25	3.59	0.14	1.65	0.09	2.61	0.12	0.23	0.05	0.70	0.08
AA.B	74.40	3.14	12.93	0.65	3.57	0.26	3.65	0.15	1.56	0.09	2.51	0.12	0.31	0.06	0.66	0.08
AA.B	71.44	3.02	13.10	0.66	3.67	0.26	3.78	0.15	1.71	0.09	2.75	0.12	0.27	0.05	0.70	0.08
AA.B	73.53	3.11	12.58	0.63	3.71	0.27	3.65	0.15	1.66	0.09	2.50	0.11	0.22	0.05	0.69	0.08
AA.B	76.11	3.21	12.87	0.65	3.91	0.28	3.68	0.15	1.64	0.09	2.54	0.12	0.23	0.05	0.70	0.08
AA.B	72.12	3.05	12.10	0.61	3.65	0.26	3.72	0.15	1.66	0.09	2.46	0.11	0.24	0.05	0.65	0.08
AA.B	75.09	3.17	12.63	0.64	3.90	0.28	3.56	0.14	1.81	0.09	2.45	0.11	0.24	0.05	0.63	0.08
AA.B	75.35	3.18	12.88	0.65	3.52	0.26	3.54	0.14	1.73	0.09	2.32	0.11	0.27	0.05	0.68	0.08
AA.B	75.09	3.17	12.89	0.65	3.47	0.25	3.58	0.14	1.67	0.09	2.55	0.12	0.17	0.05	0.69	0.08
AA.B	74.16	3.13	12.88	0.65	3.53	0.26	3.65	0.14	1.70	0.09	2.45	0.11	0.29	0.06	0.66	0.08
AA.B	74.98	3.17	12.87	0.65	3.63	0.26	3.65	0.15	1.62	0.09	2.43	0.11	0.31	0.06	0.67	0.08
AA.B	74.25	3.14	12.81	0.64	3.49	0.25	3.52	0.14	1.70	0.09	2.39	0.11	0.33	0.06	0.66	0.08
AA.B	73.35	3.10	12.60	0.63	3.54	0.26	3.67	0.15	1.75	0.09	2.44	0.11	0.24	0.05	0.64	0.08
AA.B	73.56	3.11	12.65	0.64	3.52	0.26	3.56	0.14	1.80	0.09	2.64	0.12	0.33	0.06	0.65	0.08
AA.B	73.93	3.12	12.94	0.65	3.77	0.27	3.45	0.14	1.68	0.09	2.60	0.12	0.29	0.06	0.72	0.08
AA.B	76.82	3.24	13.25	0.66	3.85	0.28	3.72	0.15	1.61	0.09	2.51	0.12	0.26	0.05	0.69	0.08
AA.B	75.02	3.17	12.78	0.64	3.73	0.27	3.74	0.15	1.58	0.09	2.59	0.12	0.32	0.06	0.69	0.08
AA.B	75.52	3.19	12.63	0.64	3.81	0.27	3.82	0.15	1.51	0.08	2.53	0.12	0.32	0.06	0.63	0.08
AA.B	74.63	3.15	12.67	0.64	3.82	0.27	3.94	0.15	1.69	0.09	2.43	0.11	0.23	0.05	0.68	0.08
AA.B	73.82	3.12	12.40	0.62	3.80	0.27	3.92	0.15	1.66	0.09	2.44	0.11	0.22	0.05	0.61	0.08
AA.B	75.02	3.17	12.41	0.62	3.65	0.26	3.67	0.15	1.59	0.09	2.40	0.11	0.31	0.06	0.64	0.08
AA.B	71.85	3.04	15.27	0.76	3.48	0.25	3.46	0.14	1.92	0.10	2.71	0.12	0.32	0.06	0.76	0.08
AA.B	71.78	3.03	13.56	0.68	3.16	0.23	3.30	0.13	1.61	0.09	2.59	0.12	0.34	0.06	0.66	0.08
AA.B	72.50	3.06	13.55	0.68	3.26	0.24	3.37	0.14	1.73	0.09	2.55	0.12	0.33	0.06	0.70	0.08
AA.B	75.12	3.17	12.67	0.64	3.64	0.26	3.76	0.15	1.72	0.09	2.53	0.12	0.28	0.06	0.64	0.08
AA.B	72.50	3.06	12.17	0.61	3.40	0.25	3.75	0.15	1.55	0.09	2.38	0.11	0.22	0.05	0.59	0.08
AA.B	74.93	3.16	12.96	0.65	3.64	0.26	3.69	0.15	1.52	0.08	2.47	0.11	0.25	0.05	0.65	0.08
AA.B	75.78	3.20	12.99	0.65	3.86	0.28	3.74	0.15	1.63	0.09	2.56	0.12	0.27	0.05	0.64	0.08
AA.B	73.41	3.10	12.70	0.64	3.75	0.27	3.85	0.15	1.58	0.09	2.58	0.12	0.28	0.06	0.67	0.08
AA.B	73.68	3.11	12.39	0.62	3.68	0.27	3.75	0.15	1.59	0.09	2.54	0.12	0.28	0.06	0.63	0.08
AA.B	73.59	3.11	12.50	0.63	3.72	0.27	3.72	0.15	1.68	0.09	2.45	0.11	0.24	0.05	0.67	0.08
AA.B	74.74	3.16	13.14	0.66	3.82	0.27	3.62	0.14	1.51	0.08	2.55	0.12	0.24	0.05	0.69	0.08
AA.B	74.91	3.16	13.01	0.65	3.48	0.25	3.64	0.14	2.25	0.11	2.45	0.11	0.24	0.05	0.70	0.08
AA.B	74.95	3.16	13.09	0.66	3.52	0.26	3.71	0.15	2.30	0.11	2.50	0.11	0.29	0.06	0.73	0.08
AA.B	72.78	3.07	12.80	0.64	3.36	0.25	3.77	0.15	2.30	0.11	2.55	0.12	0.27	0.05	0.67	0.08

AA.B	75.00	3.17	12.71	0.64	3.69	0.27	3.73	0.15	1.67	0.09	2.44	0.11	0.25	0.05	0.70	0.08
AA.B	72.83	3.08	12.80	0.64	3.66	0.26	3.85	0.15	1.72	0.09	2.54	0.12	0.33	0.06	0.72	0.08
AA.B	72.74	3.07	12.36	0.62	3.54	0.26	3.78	0.15	1.60	0.09	2.54	0.12	0.25	0.05	0.60	0.08
AA.B	73.67	3.11	12.59	0.63	3.71	0.27	3.66	0.15	1.69	0.09	2.52	0.12	0.24	0.05	0.70	0.08
AA.B	74.47	3.14	13.04	0.65	3.77	0.27	3.72	0.15	1.73	0.09	2.54	0.12	0.27	0.05	0.67	0.08
AA.B	74.32	3.14	12.95	0.65	3.54	0.26	3.61	0.14	1.46	0.08	2.46	0.11	0.28	0.06	0.68	0.08
AA.B	73.16	3.09	14.05	0.70	3.68	0.27	3.78	0.15	1.31	0.08	2.68	0.12	0.35	0.06	0.71	0.08
AA.B	74.86	3.16	13.06	0.66	3.53	0.26	3.70	0.15	1.88	0.10	2.55	0.12	0.26	0.05	0.69	0.08
AA.B	74.42	3.14	13.73	0.69	2.95	0.22	3.18	0.13	2.20	0.10	2.42	0.11	0.29	0.06	0.68	0.08
AA.B	74.73	3.16	13.12	0.66	3.37	0.25	3.56	0.14	2.33	0.11	2.46	0.11	0.25	0.05	0.75	0.08
AA.B	74.08	3.13	13.05	0.65	3.43	0.25	3.60	0.14	2.32	0.11	2.33	0.11	0.26	0.05	0.80	0.09
AA.B	73.86	3.12	12.98	0.65	3.52	0.26	3.68	0.15	2.32	0.11	2.47	0.11	0.24	0.05	0.72	0.08
AA.B	76.21	3.22	12.91	0.65	3.77	0.27	3.63	0.14	1.71	0.09	2.38	0.11	0.27	0.05	0.67	0.08
AE.C	72.24	3.05	14.65	0.73	3.52	0.26	3.68	0.15	1.69	0.09	3.12	0.13	0.40	0.06	0.75	0.08
AE.C	71.92	3.04	13.61	0.68	4.51	0.32	4.59	0.17	1.86	0.09	2.30	0.11	0.28	0.05	0.46	0.07
AE.C	71.53	3.02	13.45	0.67	5.59	0.38	5.12	0.19	1.65	0.09	3.21	0.14	0.24	0.05	0.75	0.08
AE.C	76.51	3.23	13.16	0.66	4.56	0.32	4.41	0.17	1.28	0.08	2.36	0.11	0.31	0.06	0.44	0.07
AE.C	73.70	3.11	14.28	0.71	4.60	0.32	4.00	0.16	1.26	0.08	2.62	0.12	0.25	0.05	0.63	0.08
AE.C	70.26	2.97	15.05	0.75	4.57	0.32	4.32	0.17	1.25	0.08	3.28	0.14	0.31	0.06	0.49	0.07
AE.C	73.49	3.10	12.37	0.62	3.89	0.28	4.45	0.17	1.21	0.08	2.70	0.12	0.33	0.06	0.70	0.08
AE.C	71.64	3.03	14.45	0.72	5.00	0.35	4.86	0.18	1.18	0.07	2.69	0.12	0.35	0.06	0.71	0.08
AE.C	70.52	2.98	14.08	0.70	4.95	0.34	4.70	0.18	1.32	0.08	2.48	0.11	0.44	0.06	0.67	0.08
AE.C	71.09	3.01	15.58	0.77	4.68	0.33	4.33	0.17	1.49	0.08	2.46	0.11	0.36	0.06	0.71	0.08
AE.C	69.53	2.94	14.70	0.73	4.69	0.33	4.73	0.18	1.15	0.07	2.83	0.13	0.43	0.06	0.67	0.08
AE.C	69.49	2.94	13.87	0.69	5.42	0.37	5.18	0.19	1.15	0.07	2.43	0.11	0.39	0.06	0.63	0.08
AE.C	71.14	3.01	13.22	0.66	5.32	0.37	5.00	0.19	0.96	0.07	2.88	0.13	0.30	0.06	0.57	0.08
AE.C	74.55	3.15	13.00	0.65	4.99	0.35	4.37	0.17	0.77	0.06	2.54	0.12	0.27	0.05	0.44	0.07
AE.C	72.88	3.08	13.21	0.66	5.23	0.36	4.47	0.17	0.66	0.06	2.91	0.13	0.32	0.06	0.49	0.07
AE.C	76.69	3.24	11.58	0.59	4.38	0.31	4.38	0.17	0.03	0.04	2.74	0.12	0.19	0.05	0.23	0.06
AE.C	75.05	3.17	12.39	0.62	5.46	0.38	4.98	0.19	0.63	0.06	2.52	0.12	0.26	0.05	0.36	0.06
AE.C	75.37	3.18	11.78	0.60	5.12	0.35	4.67	0.18	0.13	0.04	2.78	0.12	0.18	0.05	0.11	0.05
AE.C	76.45	3.23	10.54	0.54	4.09	0.29	4.29	0.16	0.03	0.04	2.87	0.13	0.20	0.05	0.16	0.05
AE.C	77.94	3.29	11.72	0.59	4.15	0.29	4.54	0.17	0.06	0.04	2.06	0.10	0.09	0.05	0.03	0.05
AE.C	79.02	3.33	11.78	0.60	4.40	0.31	4.68	0.18	0.22	0.05	1.76	0.09	0.09	0.05	0.05	0.05
AE.C	72.35	3.06	11.29	0.57	4.87	0.34	5.08	0.19	0.27	0.05	2.59	0.12	0.16	0.05	0.23	0.06
AE.C	71.76	3.03	13.45	0.67	4.10	0.29	4.18	0.16	0.99	0.07	3.07	0.13	0.32	0.06	0.60	0.08
AE.C	69.77	2.95	12.00	0.61	5.02	0.35	5.15	0.19	0.48	0.05	3.17	0.14	0.33	0.06	0.36	0.06
AE.C	74.81	3.16	13.94	0.70	3.81	0.27	3.98	0.16	1.76	0.09	2.51	0.11	0.33	0.06	0.61	0.08
AE.C	76.28	3.22	13.91	0.69	3.35	0.25	3.54	0.14	1.52	0.08	2.69	0.12	0.31	0.06	0.64	0.08
AE.C	72.36	3.06	13.89	0.69	3.30	0.24	3.60	0.14	1.84	0.09	3.01	0.13	0.32	0.06	0.70	0.08
AE.C	71.27	3.01	16.63	0.82	2.86	0.21	2.87	0.12	3.45	0.14	2.76	0.12	0.33	0.06	0.57	0.07
AE.C	73.00	3.08	13.33	0.67	3.31	0.24	3.78	0.15	1.40	0.08	2.89	0.13	0.35	0.06	0.68	0.08
AE.C	72.11	3.05	14.08	0.70	3.15	0.23	3.39	0.14	2.20	0.10	2.84	0.13	0.33	0.06	0.66	0.08
AE.C	74.31	3.14	14.43	0.72	3.00	0.22	3.08	0.13	2.55	0.12	2.76	0.12	0.27	0.05	0.60	0.08
AE.C	71.98	3.04	15.98	0.79	2.86	0.21	2.93	0.12	3.20	0.13	2.78	0.12	0.35	0.06	0.60	0.08
AE.C	72.18	3.05	13.02	0.65	3.01	0.22	3.48	0.14	1.84	0.09	2.84	0.13	0.30	0.06	0.65	0.08
AE.C	72.44	3.06	16.47	0.81	2.76	0.21	2.84	0.12	3.40	0.14	2.75	0.12	0.30	0.06	0.61	0.08
AE.C	71.71	3.03	14.27	0.71	3.12	0.23	3.58	0.14	1.54	0.08	3.10	0.13	0.46	0.06	0.76	0.09
AE.C	71.75	3.03	13.24	0.66	3.56	0.26	4.01	0.16	1.24	0.08	2.85	0.13	0.33	0.06	0.56	0.07
AE.C	73.95	3.12	13.97	0.70	3.39	0.25	3.57	0.14	1.87	0.09	2.88	0.13	0.34	0.06	0.70	0.08
AE.C	75.12	3.17	13.80	0.69	3.25	0.24	3.56	0.14	1.53	0.08	2.81	0.12	0.36	0.06	0.64	0.08
AE.C	72.55	3.07	15.71	0.78	3.35	0.24	3.57	0.14	1.80	0.09	3.15	0.13	0.41	0.06	0.89	0.09
AE.C	73.37	3.10	13.39	0.67	3.02	0.22	3.61	0.14	1.92	0.10	2.98	0.13	0.28	0.05	0.60	0.08
AE.C	72.99	3.08	15.18	0.75	2.55	0.20	2.81	0.12	2.84	0.12	2.32	0.11	0.28	0.06	0.47	0.07
AE.C	74.61	3.15	13.38	0.67	2.71	0.21	3.09	0.13	1.77	0.09	2.75	0.12	0.36	0.06	0.71	0.08
AE.C	71.67	3.03	14.28	0.71	3.22	0.24	3.66	0.15	1.71	0.09	2.87	0.13	0.44	0.06	0.80	0.09
AE.C	72.95	3.08	14.11	0.70	3.53	0.26	3.87	0.15	1.73	0.09	3.00	0.13	0.36	0.06	0.66	0.08
AE.C	74.21	3.13	14.34	0.71	3.52	0.26	3.66	0.15	1.53	0.08	3.00	0.13	0.36	0.06	0.67	0.08
AE.C	71.23	3.01	14.54	0.72	3.18	0.23	3.55	0.14	1.76	0.09	2.89	0.13	0.42	0.06	0.82	0.09
AE.C	72.85	3.08	14.16	0.71	3.36	0.25	3.63	0.14	1.78	0.09	3.02	0.13	0.38	0.06	0.69	0.08
AE.C	73.86	3.12	14.53	0.72	3.41	0.25	3.66	0.15	1.83	0.09	2.92	0.13	0.34	0.06	0.76	0.08
AE.C	72.90	3.08	13.96	0.70	3.16	0.23	3.57	0.14	1.93	0.10	2.88	0.13	0.39	0.06	0.72	0.08

AE.C	70.58	2.98	13.94	0.70	3.61	0.26	3.89	0.15	1.28	0.08	3.26	0.14	0.46	0.06	0.61	0.08
AE.C	69.91	2.96	13.28	0.67	4.66	0.33	4.43	0.17	1.39	0.08	3.15	0.13	0.41	0.06	0.74	0.08
AE.C	74.30	3.14	12.08	0.61	4.13	0.29	4.42	0.17	0.32	0.05	2.34	0.11	0.14	0.05	0.08	0.05
AE.C	80.82	3.41	10.04	0.52	3.06	0.23	3.61	0.14	0.97	0.07	2.62	0.12	0.23	0.05	0.54	0.07
AE.C	73.20	3.09	14.61	0.73	3.61	0.26	3.78	0.15	1.33	0.08	3.16	0.14	0.32	0.06	0.67	0.08
AE.C	76.82	3.24	13.62	0.68	3.17	0.23	3.49	0.14	1.79	0.09	2.84	0.13	0.36	0.06	0.69	0.08
AE.C	72.63	3.07	13.61	0.68	3.17	0.23	3.54	0.14	1.84	0.09	2.73	0.12	0.42	0.06	0.60	0.08
AE.C	69.31	2.93	14.96	0.74	3.91	0.28	4.05	0.16	1.82	0.09	3.87	0.16	0.55	0.06	0.76	0.08
AE.C	71.98	3.04	14.51	0.72	3.90	0.28	4.15	0.16	1.83	0.09	3.04	0.13	0.30	0.06	0.77	0.09
AE.C	66.95	2.83	16.12	0.80	4.10	0.29	3.98	0.16	2.96	0.13	3.25	0.14	0.31	0.06	0.79	0.09
AE.C	71.91	3.04	13.58	0.68	4.46	0.31	4.30	0.17	1.61	0.09	2.85	0.13	0.31	0.06	0.70	0.08
AE.C	71.62	3.03	13.43	0.67	4.18	0.30	4.34	0.17	1.63	0.09	3.22	0.14	0.42	0.06	0.81	0.09
AE.C	72.75	3.07	13.05	0.65	3.89	0.28	4.10	0.16	2.33	0.11	3.63	0.15	0.41	0.06	0.77	0.09
AE.C	77.02	3.25	12.77	0.64	3.50	0.25	3.98	0.16	1.36	0.08	2.80	0.12	0.32	0.06	0.66	0.08
AE.C	72.38	3.06	13.27	0.66	3.67	0.26	3.97	0.15	1.71	0.09	3.18	0.14	0.35	0.06	0.79	0.09
AE.C	75.02	3.17	13.10	0.66	3.81	0.27	4.15	0.16	1.32	0.08	2.80	0.12	0.24	0.05	0.64	0.08
AE.C	73.72	3.11	13.63	0.68	3.47	0.25	3.70	0.15	1.50	0.08	2.70	0.12	0.42	0.06	0.63	0.08
AE.C	68.68	2.91	15.51	0.77	4.45	0.31	4.33	0.17	2.89	0.13	2.73	0.12	0.41	0.06	0.68	0.08
AE.C	78.22	3.30	10.84	0.55	3.27	0.24	3.83	0.15	0.96	0.07	2.30	0.11	0.13	0.05	0.45	0.07
AE.C	70.43	2.98	13.02	0.65	5.55	0.38	4.97	0.19	3.01	0.13	3.14	0.13	0.26	0.05	0.66	0.08
AE.C	75.52	3.19	13.15	0.66	3.97	0.28	4.61	0.17	0.90	0.07	2.15	0.10	0.14	0.05	0.28	0.06
AE.C	63.53	2.69	18.05	0.89	4.15	0.29	4.08	0.16	2.31	0.11	3.57	0.15	0.54	0.06	1.03	0.10
AE.C	71.20	3.01	15.66	0.78	3.87	0.28	3.92	0.15	2.24	0.11	3.18	0.14	0.34	0.06	0.70	0.08
AE.C	73.76	3.12	12.61	0.63	3.84	0.28	4.16	0.16	1.48	0.08	3.29	0.14	0.40	0.06	0.69	0.08
AE.C	70.92	3.00	14.13	0.70	3.98	0.28	4.21	0.16	1.76	0.09	3.42	0.14	0.48	0.06	0.91	0.09
AE.C	70.79	2.99	14.21	0.71	4.13	0.29	4.16	0.16	1.71	0.09	3.64	0.15	0.38	0.06	0.89	0.09
AE.C	76.59	3.23	9.70	0.50	3.78	0.27	4.20	0.16	1.07	0.07	2.26	0.11	0.28	0.05	0.60	0.08
AE.C	74.98	3.17	12.91	0.65	4.57	0.32	4.48	0.17	1.73	0.09	2.28	0.11	0.27	0.05	0.50	0.07
AE.C	89.48	3.77	6.49	0.35	2.24	0.18	2.70	0.12	0.84	0.06	1.62	0.09	0.11	0.05	0.40	0.07
AE.C	75.65	3.19	14.49	0.72	3.62	0.26	3.82	0.15	1.59	0.09	2.73	0.12	0.29	0.06	0.71	0.08
AE.C	75.09	3.17	12.38	0.62	3.60	0.26	3.97	0.15	1.30	0.08	2.52	0.12	0.34	0.06	0.62	0.08
AE.C	77.22	3.26	9.95	0.51	3.19	0.23	3.64	0.14	0.94	0.07	3.30	0.14	0.30	0.06	0.58	0.08
AE.C	72.17	3.05	13.52	0.68	4.59	0.32	4.61	0.17	1.39	0.08	3.00	0.13	0.38	0.06	0.68	0.08
AE.C	78.30	3.30	11.10	0.56	4.41	0.31	4.09	0.16	0.03	0.04	2.91	0.13	0.14	0.05	0.03	0.05
AE.C	74.90	3.16	11.92	0.60	3.25	0.24	3.52	0.14	1.71	0.09	2.35	0.11	0.24	0.05	0.45	0.07
AE.C	73.50	3.10	14.03	0.70	3.38	0.25	3.64	0.14	2.36	0.11	2.67	0.12	0.25	0.05	0.58	0.08
AE.C	74.10	3.13	13.78	0.69	4.27	0.30	4.20	0.16	1.84	0.09	2.27	0.11	0.32	0.06	0.51	0.07
AE.C	70.72	2.99	15.32	0.76	4.27	0.30	4.24	0.16	1.44	0.08	3.14	0.13	0.29	0.06	0.71	0.08
AE.C	69.34	2.93	15.53	0.77	4.24	0.30	4.35	0.17	1.87	0.10	2.87	0.13	0.36	0.06	0.64	0.08
AE.C	71.81	3.03	13.86	0.69	4.17	0.30	4.36	0.17	1.17	0.07	3.06	0.13	0.32	0.06	0.49	0.07
AE.C	77.90	3.29	10.12	0.52	3.48	0.25	4.08	0.16	0.19	0.04	2.14	0.10	0.19	0.05	0.07	0.05
AE.C	75.69	3.20	13.21	0.66	4.26	0.30	4.49	0.17	0.12	0.04	2.16	0.10	0.10	0.05	0.03	0.05
AE.C	74.67	3.15	13.77	0.69	3.87	0.28	3.79	0.15	2.08	0.10	2.35	0.11	0.29	0.06	0.50	0.07
AE.C	73.63	3.11	13.87	0.69	3.93	0.28	3.95	0.15	1.94	0.10	2.30	0.11	0.30	0.06	0.52	0.07
AE.C	72.17	3.05	14.65	0.73	4.47	0.31	3.95	0.15	1.59	0.09	2.92	0.13	0.36	0.06	0.79	0.09
AE.C	75.73	3.20	11.22	0.57	4.09	0.29	4.40	0.17	0.03	0.04	2.26	0.11	0.11	0.05	0.15	0.05
AE.C	77.97	3.29	12.10	0.61	4.45	0.31	4.43	0.17	0.03	0.04	2.23	0.11	0.03	0.05	0.05	0.05
AE.C	79.05	3.33	11.74	0.59	4.45	0.31	4.27	0.16	0.03	0.04	2.21	0.11	0.15	0.05	0.03	0.05
AE.C	75.21	3.18	12.69	0.64	4.01	0.29	4.23	0.16	0.88	0.06	2.59	0.12	0.20	0.05	0.42	0.07
AE.C	79.03	3.33	11.57	0.59	4.32	0.30	4.36	0.17	0.03	0.04	2.50	0.11	0.20	0.05	0.03	0.05
AE.C	76.75	3.24	11.33	0.57	3.76	0.27	4.22	0.16	0.26	0.05	2.78	0.12	0.16	0.05	0.18	0.05
AE.C	78.95	3.33	11.64	0.59	4.28	0.30	4.36	0.17	0.03	0.04	2.28	0.11	0.06	0.05	0.03	0.05
AE.C	77.81	3.28	11.22	0.57	4.18	0.30	4.15	0.16	0.28	0.05	2.64	0.12	0.09	0.05	0.07	0.05
AE.C	75.24	3.18	12.57	0.63	4.86	0.34	4.62	0.17	1.70	0.09	2.15	0.10	0.24	0.05	0.45	0.07
AE.C	74.99	3.17	13.25	0.66	3.98	0.28	4.14	0.16	1.96	0.10	2.45	0.11	0.27	0.05	0.46	0.07
AE.C	70.65	2.99	16.71	0.82	4.54	0.32	4.37	0.17	1.33	0.08	2.64	0.12	0.39	0.06	0.69	0.08
AE.C	69.56	2.94	16.62	0.82	4.18	0.30	3.88	0.15	1.76	0.09	2.79	0.12	0.43	0.06	0.63	0.08
AE.C	84.00	3.54	8.73	0.45	2.79	0.21	3.35	0.14	0.50	0.05	1.73	0.09	0.12	0.05	0.27	0.06
AE.C	74.27	3.14	13.74	0.69	4.00	0.28	4.22	0.16	1.76	0.09	2.60	0.12	0.38	0.06	0.46	0.07
AE.C	73.45	3.10	12.99	0.65	3.97	0.28	4.29	0.16	1.80	0.09	2.65	0.12	0.26	0.05	0.48	0.07
AE.C	72.99	3.08	12.94	0.65	3.90	0.28	4.27	0.16	1.93	0.10	2.63	0.12	0.32	0.06	0.55	0.07
AE.C	80.51	3.40	10.76	0.55	3.24	0.24	3.98	0.16	0.20	0.04	2.22	0.11	0.15	0.05	0.03	0.05

AE.C	76.17	3.22	12.59	0.63	3.79	0.27	4.27	0.16	0.76	0.06	2.46	0.11	0.20	0.05	0.35	0.06
AE.C	69.61	2.94	14.45	0.72	5.25	0.36	4.75	0.18	1.53	0.08	3.17	0.14	0.39	0.06	0.92	0.09
AE.C	72.35	3.06	13.79	0.69	3.89	0.28	4.40	0.17	1.48	0.08	2.72	0.12	0.23	0.05	0.72	0.08
AE.C	70.22	2.97	14.73	0.73	3.71	0.27	3.93	0.15	2.18	0.10	3.79	0.15	0.43	0.06	0.73	0.08
AE.C	75.59	3.19	13.11	0.66	3.43	0.25	3.78	0.15	1.58	0.09	2.74	0.12	0.34	0.06	0.55	0.07
AE.C	72.51	3.06	11.89	0.60	3.77	0.27	4.23	0.16	1.19	0.07	3.83	0.16	0.32	0.06	0.37	0.06
AE.C	86.23	3.63	7.95	0.42	2.72	0.21	3.12	0.13	0.30	0.05	1.69	0.09	0.15	0.05	0.17	0.05
AE.C	68.28	2.89	14.73	0.73	4.29	0.30	4.82	0.18	1.25	0.08	2.88	0.13	0.34	0.06	0.64	0.08
AE.C	70.47	2.98	13.05	0.65	4.43	0.31	4.49	0.17	2.32	0.11	3.43	0.14	0.29	0.06	0.86	0.09
AE.C	71.52	3.02	13.07	0.66	4.59	0.32	4.66	0.18	2.02	0.10	2.89	0.13	0.16	0.05	0.49	0.07
AE.C	68.60	2.90	13.03	0.65	4.75	0.33	4.60	0.17	1.85	0.09	3.19	0.14	0.41	0.06	0.96	0.10
AE.C	72.24	3.05	15.32	0.76	3.37	0.25	3.46	0.14	2.87	0.13	2.91	0.13	0.38	0.06	0.70	0.08
AE.C	73.77	3.12	15.10	0.75	3.73	0.27	3.77	0.15	1.77	0.09	2.70	0.12	0.37	0.06	0.51	0.07
AE.C	74.09	3.13	13.68	0.68	3.76	0.27	4.30	0.17	1.14	0.07	2.62	0.12	0.27	0.05	0.49	0.07
AE.C	73.10	3.09	13.58	0.68	4.36	0.31	4.57	0.17	1.49	0.08	2.77	0.12	0.26	0.05	0.46	0.07
AE.C	74.90	3.16	11.20	0.57	3.68	0.26	4.38	0.17	1.02	0.07	2.84	0.13	0.30	0.06	0.29	0.06
AE.C	73.19	3.09	12.50	0.63	4.19	0.30	4.56	0.17	1.26	0.08	3.42	0.14	0.24	0.05	0.38	0.07
AE.C	72.97	3.08	12.77	0.64	4.81	0.34	4.91	0.18	1.20	0.07	2.19	0.11	0.27	0.05	0.33	0.06
AE.C	73.78	3.12	14.66	0.73	3.50	0.25	3.81	0.15	2.20	0.10	2.47	0.11	0.30	0.06	0.47	0.07
AE.C	72.83	3.08	14.02	0.70	3.86	0.28	4.30	0.16	1.03	0.07	2.66	0.12	0.33	0.06	0.64	0.08
AE.C	70.25	2.97	12.57	0.63	3.82	0.27	4.30	0.17	1.33	0.08	3.47	0.14	0.40	0.06	1.12	0.10
AE.C	73.87	3.12	12.78	0.64	4.08	0.29	4.26	0.16	1.59	0.09	2.97	0.13	0.34	0.06	0.58	0.08
AE.C	68.25	2.89	12.06	0.61	4.26	0.30	4.58	0.17	1.06	0.07	5.23	0.20	0.44	0.06	0.46	0.07
AE.C	68.43	2.89	13.64	0.68	4.98	0.35	4.91	0.18	1.16	0.07	2.70	0.12	0.33	0.06	0.51	0.07
AE.C	71.45	3.02	14.32	0.71	4.21	0.30	4.66	0.18	1.23	0.08	2.72	0.12	0.29	0.06	0.68	0.08
AE.C	75.19	3.17	13.02	0.65	4.20	0.30	4.47	0.17	1.36	0.08	2.64	0.12	0.30	0.06	0.47	0.07
AE.C	72.01	3.04	12.99	0.65	3.86	0.28	4.23	0.16	1.72	0.09	2.77	0.12	0.36	0.06	0.58	0.08
AE.C	72.13	3.05	13.97	0.70	4.34	0.31	4.47	0.17	0.82	0.06	2.77	0.12	0.34	0.06	0.55	0.07
AE.C	76.06	3.21	12.17	0.61	4.55	0.32	4.64	0.18	0.45	0.05	2.10	0.10	0.11	0.05	0.34	0.06
AE.C	71.05	3.00	17.12	0.84	4.70	0.33	4.46	0.17	2.06	0.10	2.51	0.12	0.29	0.06	0.52	0.07
AE.C	68.72	2.91	14.69	0.73	4.11	0.29	4.37	0.17	2.10	0.10	2.68	0.12	0.28	0.06	0.64	0.08
AE.C	67.91	2.87	16.01	0.79	4.26	0.30	4.25	0.16	2.03	0.10	3.60	0.15	0.57	0.06	0.95	0.09
AE.C	69.11	2.92	14.22	0.71	4.64	0.32	4.62	0.17	1.58	0.09	3.49	0.15	0.52	0.06	0.88	0.09
AE.C	73.73	3.11	11.84	0.60	4.66	0.33	5.03	0.19	1.52	0.08	2.48	0.11	0.21	0.05	0.44	0.07
AE.C	85.02	3.58	6.83	0.37	3.16	0.23	3.71	0.15	0.64	0.06	1.57	0.09	0.03	0.05	0.29	0.06
AE.C	69.92	2.96	15.40	0.76	3.41	0.25	3.85	0.15	2.38	0.11	2.69	0.12	0.40	0.06	0.65	0.08
AE.C	73.07	3.09	14.84	0.74	4.30	0.30	4.09	0.16	1.44	0.08	2.63	0.12	0.39	0.06	0.72	0.08
AE.C	71.61	3.03	14.58	0.73	4.31	0.30	4.22	0.16	1.50	0.08	3.03	0.13	0.38	0.06	0.83	0.09
AE.C	74.69	3.15	14.72	0.73	3.88	0.28	3.89	0.15	2.00	0.10	3.08	0.13	0.38	0.06	0.72	0.08
AE.C	77.88	3.29	11.78	0.60	4.10	0.29	4.35	0.17	0.03	0.04	2.19	0.11	0.18	0.05	0.23	0.06
AE.C	75.73	3.20	10.89	0.55	3.82	0.27	4.17	0.16	0.24	0.05	2.52	0.12	0.18	0.05	0.33	0.06
AE.C	73.40	3.10	11.81	0.60	4.26	0.30	4.52	0.17	0.03	0.04	2.70	0.12	0.18	0.05	0.08	0.05
AE.C	73.31	3.10	11.15	0.57	5.57	0.38	4.84	0.18	1.11	0.07	2.70	0.12	0.26	0.05	0.45	0.07
AE.C	70.20	2.97	13.56	0.68	5.01	0.35	4.87	0.18	1.14	0.07	2.97	0.13	0.31	0.06	0.50	0.07
AE.C	70.90	3.00	14.94	0.74	4.67	0.33	4.35	0.17	1.44	0.08	2.91	0.13	0.48	0.06	0.65	0.08
AE.C	74.68	3.15	13.08	0.66	4.56	0.32	4.72	0.18	1.82	0.09	2.34	0.11	0.32	0.06	0.49	0.07
AE.C	73.04	3.09	14.46	0.72	4.20	0.30	4.25	0.16	1.57	0.09	2.56	0.12	0.39	0.06	0.57	0.07
AE.C	70.59	2.98	14.41	0.72	4.90	0.34	4.93	0.18	1.51	0.08	3.18	0.14	0.36	0.06	0.57	0.07
AE.C	68.90	2.91	14.62	0.73	3.88	0.28	4.27	0.16	2.54	0.12	3.08	0.13	0.31	0.06	0.73	0.08
AE.C	76.09	3.21	10.15	0.52	3.68	0.27	4.13	0.16	0.47	0.05	2.55	0.12	0.16	0.05	0.27	0.06
AE.C	71.20	3.01	13.57	0.68	4.19	0.30	4.38	0.17	1.44	0.08	2.96	0.13	0.29	0.06	0.69	0.08
AE.C	74.36	3.14	14.30	0.71	4.69	0.33	4.90	0.18	1.26	0.08	2.22	0.11	0.16	0.05	0.37	0.06
AE.C	68.59	2.90	14.81	0.74	5.33	0.37	5.11	0.19	1.55	0.09	2.97	0.13	0.35	0.06	0.64	0.08
AE.C	68.21	2.89	14.56	0.72	4.58	0.32	4.80	0.18	1.37	0.08	3.15	0.13	0.42	0.06	0.73	0.08
AE.C	63.48	2.69	18.21	0.89	4.63	0.32	4.13	0.16	4.12	0.16	3.08	0.13	0.38	0.06	0.78	0.09
AE.C	72.37	3.06	13.99	0.70	3.18	0.23	3.24	0.13	2.75	0.12	2.73	0.12	0.32	0.06	0.55	0.07
AE.C	69.83	2.95	14.37	0.72	4.03	0.29	4.14	0.16	1.37	0.08	3.00	0.13	0.40	0.06	0.68	0.08
AE.C	71.98	3.04	14.07	0.70	3.68	0.27	4.03	0.16	1.52	0.08	2.80	0.12	0.36	0.06	0.62	0.08
AE.C	87.91	3.70	5.64	0.31	1.74	0.15	2.01	0.09	0.51	0.05	1.51	0.08	0.18	0.05	0.39	0.07
AE.C	71.87	3.04	13.57	0.68	3.05	0.23	3.38	0.14	1.77	0.09	2.72	0.12	0.28	0.05	0.56	0.07
AE.C	100.72	4.23	0.55	0.08	0.54	0.07	0.52	0.05	0.03	0.04	0.07	0.04	0.03	0.05	0.07	0.05
AE.C	71.69	3.03	15.30	0.76	3.34	0.24	3.30	0.13	2.28	0.11	2.81	0.12	0.44	0.06	0.71	0.08

AE.C	93.29	3.92	4.53	0.26	1.47	0.13	1.67	0.08	0.39	0.05	1.39	0.08	0.12	0.05	0.36	0.06
AE.C	71.88	3.04	13.91	0.69	3.00	0.22	3.46	0.14	1.78	0.09	2.84	0.13	0.37	0.06	0.59	0.08
AE.C	71.86	3.04	13.70	0.68	3.67	0.26	4.41	0.17	1.05	0.07	2.35	0.11	0.44	0.06	0.57	0.07
AE.C	72.57	3.07	14.35	0.71	3.17	0.23	3.33	0.14	2.49	0.11	2.70	0.12	0.29	0.06	0.54	0.07
AE.C	72.28	3.05	13.01	0.65	3.36	0.25	3.85	0.15	1.40	0.08	2.75	0.12	0.32	0.06	0.63	0.08
AE.C	77.52	3.27	11.37	0.58	2.76	0.21	3.42	0.14	1.12	0.07	2.26	0.11	0.27	0.05	0.41	0.07
AE.C	69.95	2.96	15.38	0.76	3.99	0.28	4.48	0.17	1.24	0.08	2.53	0.12	0.32	0.06	0.63	0.08
AE.C	73.73	3.11	13.45	0.67	3.07	0.23	3.58	0.14	1.71	0.09	2.90	0.13	0.33	0.06	0.60	0.08
AE.C	72.14	3.05	14.61	0.73	3.28	0.24	3.64	0.14	1.83	0.09	3.12	0.13	0.38	0.06	0.79	0.09
AE.C	73.98	3.12	13.78	0.69	3.05	0.23	3.38	0.14	2.37	0.11	2.61	0.12	0.34	0.06	0.60	0.08
AE.C	74.31	3.14	13.14	0.66	3.22	0.24	3.60	0.14	1.32	0.08	2.48	0.11	0.33	0.06	0.56	0.07
AE.C	74.94	3.16	13.64	0.68	3.20	0.24	3.67	0.15	1.68	0.09	2.91	0.13	0.35	0.06	0.65	0.08
AE.C	73.19	3.09	13.44	0.67	2.81	0.21	3.47	0.14	2.32	0.11	2.88	0.13	0.33	0.06	0.58	0.08
AE.C	71.75	3.03	13.78	0.69	3.19	0.24	3.74	0.15	1.44	0.08	3.10	0.13	0.31	0.06	0.68	0.08
AE.C	74.90	3.16	13.80	0.69	2.90	0.22	3.18	0.13	2.51	0.11	2.87	0.13	0.33	0.06	0.58	0.08
AG.D	74.34	3.14	12.79	0.64	3.37	0.25	3.90	0.15	1.93	0.10	2.78	0.12	0.33	0.06	0.66	0.08
AG.D	75.41	3.18	13.88	0.69	2.83	0.21	3.74	0.15	1.71	0.09	2.11	0.10	0.26	0.05	0.49	0.07
AG.D	73.94	3.12	14.63	0.73	2.85	0.21	3.35	0.14	2.20	0.10	2.73	0.12	0.32	0.06	0.72	0.08
AG.D	74.12	3.13	14.27	0.71	2.64	0.20	3.25	0.13	2.04	0.10	2.58	0.12	0.34	0.06	0.63	0.08
AG.D	73.12	3.09	14.23	0.71	2.52	0.19	3.03	0.13	2.05	0.10	2.85	0.13	0.34	0.06	0.65	0.08
AG.D	71.92	3.04	15.73	0.78	3.33	0.24	3.71	0.15	2.02	0.10	3.02	0.13	0.39	0.06	0.77	0.09
AG.D	70.63	2.99	14.29	0.71	2.86	0.21	3.41	0.14	2.36	0.11	2.83	0.13	0.40	0.06	0.67	0.08
AG.D	73.59	3.11	13.91	0.69	3.20	0.24	3.71	0.15	1.76	0.09	2.66	0.12	0.35	0.06	0.62	0.08
AG.D	73.81	3.12	14.74	0.73	3.42	0.25	3.57	0.14	1.81	0.09	2.41	0.11	0.33	0.06	0.61	0.08
AG.D	77.37	3.27	12.32	0.62	4.10	0.29	4.73	0.18	1.35	0.08	2.42	0.11	0.34	0.06	0.60	0.08
AG.D	76.88	3.24	13.12	0.66	2.82	0.21	3.74	0.15	1.17	0.07	2.12	0.10	0.30	0.06	0.86	0.09
AG.D	73.13	3.09	14.06	0.70	3.03	0.23	3.60	0.14	2.11	0.10	2.73	0.12	0.36	0.06	0.65	0.08
AG.D	73.70	3.11	14.11	0.70	2.82	0.21	3.19	0.13	2.49	0.11	2.71	0.12	0.31	0.06	0.64	0.08
AG.D	74.29	3.14	12.59	0.63	3.33	0.24	4.00	0.16	2.78	0.12	2.74	0.12	0.24	0.05	0.59	0.08
AG.D	72.62	3.07	13.74	0.69	3.23	0.24	3.64	0.14	2.83	0.12	2.91	0.13	0.29	0.06	0.74	0.08
AG.D	72.36	3.06	14.99	0.74	3.23	0.24	3.68	0.15	2.38	0.11	2.67	0.12	0.40	0.06	0.68	0.08
AG.D	73.32	3.10	13.19	0.66	3.36	0.25	3.95	0.15	1.60	0.09	2.81	0.12	0.15	0.05	0.42	0.07
AG.D	74.32	3.14	14.34	0.71	3.34	0.24	3.75	0.15	1.71	0.09	2.35	0.11	0.34	0.06	0.54	0.07
AG.D	71.48	3.02	13.43	0.67	3.43	0.25	3.85	0.15	2.00	0.10	2.90	0.13	0.32	0.06	0.71	0.08
AG.D	74.35	3.14	14.20	0.71	3.28	0.24	4.17	0.16	1.43	0.08	2.93	0.13	0.33	0.06	0.74	0.08
AG.D	75.86	3.20	13.31	0.67	2.73	0.21	3.56	0.14	1.82	0.09	2.66	0.12	0.32	0.06	0.59	0.08
AG.D	77.14	3.26	12.49	0.63	2.66	0.20	3.37	0.14	1.70	0.09	2.53	0.12	0.25	0.05	0.54	0.07
AG.D	75.19	3.17	13.72	0.69	2.97	0.22	3.58	0.14	2.25	0.11	2.85	0.13	0.33	0.06	0.65	0.08
AG.D	74.18	3.13	12.42	0.63	3.10	0.23	3.80	0.15	2.48	0.11	2.86	0.13	0.30	0.06	0.61	0.08
AG.D	76.06	3.21	13.84	0.69	3.28	0.24	3.81	0.15	1.98	0.10	2.69	0.12	0.34	0.06	0.65	0.08
AG.D	73.07	3.09	12.91	0.65	3.43	0.25	4.16	0.16	1.74	0.09	2.82	0.12	0.31	0.06	0.61	0.08
AG.D	72.96	3.08	13.69	0.68	3.28	0.24	3.69	0.15	2.05	0.10	2.85	0.13	0.32	0.06	0.67	0.08
AG.D	71.68	3.03	14.04	0.70	3.27	0.24	3.60	0.14	2.26	0.11	2.65	0.12	0.37	0.06	0.64	0.08
AG.D	74.27	3.14	14.64	0.73	2.96	0.22	3.34	0.14	1.94	0.10	2.65	0.12	0.42	0.06	0.62	0.08
AG.D	100.21	4.21	0.56	0.08	0.10	0.04	0.03	0.03	0.03	0.04	0.03	0.04	0.06	0.05	0.03	0.05
AG.D	101.40	4.26	0.51	0.07	0.03	0.04	0.03	0.03	0.03	0.04	0.03	0.04	0.03	0.05	0.03	0.05
AG.D	100.27	4.21	0.50	0.07	0.03	0.04	0.03	0.03	0.03	0.04	0.08	0.04	0.03	0.05	0.10	0.05
AG.D	74.71	3.15	11.99	0.61	3.06	0.23	3.63	0.14	2.45	0.11	2.55	0.12	0.26	0.05	0.59	0.08
AG.D	72.37	3.06	13.22	0.66	3.09	0.23	3.74	0.15	1.89	0.10	2.95	0.13	0.28	0.06	0.61	0.08
AG.D	75.24	3.18	13.32	0.67	2.75	0.21	3.38	0.14	2.08	0.10	2.58	0.12	0.30	0.06	0.58	0.08
AG.D	72.26	3.05	13.11	0.66	2.98	0.22	3.70	0.15	2.41	0.11	3.09	0.13	0.32	0.06	0.69	0.08
AG.D	73.90	3.12	14.93	0.74	2.97	0.22	3.48	0.14	1.95	0.10	2.89	0.13	0.42	0.06	0.69	0.08
AG.D	72.68	3.07	13.70	0.68	3.27	0.24	4.23	0.16	2.09	0.10	3.02	0.13	0.43	0.06	0.83	0.09
AG.D	73.16	3.09	14.92	0.74	3.42	0.25	4.09	0.16	2.01	0.10	2.89	0.13	0.44	0.06	0.88	0.09
AG.D	75.59	3.19	13.15	0.66	3.30	0.24	4.09	0.16	1.52	0.08	2.74	0.12	0.40	0.06	0.75	0.08
AG.D	74.63	3.15	13.88	0.69	3.49	0.25	3.91	0.15	1.97	0.10	2.83	0.12	0.35	0.06	0.66	0.08
AG.D	76.01	3.21	13.53	0.68	3.55	0.26	4.01	0.16	1.87	0.09	2.85	0.13	0.36	0.06	0.63	0.08
AG.D	76.11	3.21	14.11	0.70	3.37	0.25	3.75	0.15	2.06	0.10	2.78	0.12	0.33	0.06	0.69	0.08
AG.D	76.69	3.24	13.88	0.69	3.05	0.23	3.61	0.14	1.97	0.10	3.16	0.14	0.33	0.06	0.65	0.08
AG.D	74.12	3.13	13.72	0.69	2.94	0.22	3.50	0.14	2.36	0.11	2.80	0.12	0.31	0.06	0.66	0.08
AG.D	73.67	3.11	14.48	0.72	2.97	0.22	3.68	0.15	2.29	0.11	3.04	0.13	0.35	0.06	0.72	0.08
AG.D	74.62	3.15	13.28	0.67	2.88	0.22	3.56	0.14	1.90	0.10	2.73	0.12	0.29	0.06	0.58	0.08

AG.D	74.90	3.16	13.42	0.67	4.32	0.30	4.86	0.18	1.28	0.08	2.71	0.12	0.31	0.06	0.49	0.07
AG.D	73.22	3.09	15.06	0.75	2.96	0.22	3.56	0.14	1.50	0.08	3.35	0.14	0.37	0.06	0.76	0.08
AG.D	76.88	3.24	12.90	0.65	2.82	0.21	3.46	0.14	1.98	0.10	2.72	0.12	0.30	0.06	0.55	0.07
AG.D	74.21	3.13	13.74	0.69	3.02	0.22	3.65	0.15	2.10	0.10	2.85	0.13	0.33	0.06	0.69	0.08
AG.D	74.88	3.16	14.45	0.72	3.25	0.24	3.77	0.15	2.04	0.10	2.72	0.12	0.42	0.06	0.67	0.08
AG.D	76.88	3.24	13.96	0.70	2.80	0.21	3.50	0.14	2.07	0.10	2.80	0.12	0.27	0.05	0.63	0.08
AG.D	75.36	3.18	13.93	0.70	3.16	0.23	3.51	0.14	2.08	0.10	2.70	0.12	0.34	0.06	0.57	0.08
AG.D	75.45	3.19	14.17	0.71	2.94	0.22	3.44	0.14	2.25	0.11	2.81	0.12	0.28	0.05	0.67	0.08
AG.D	73.13	3.09	13.86	0.69	3.11	0.23	3.66	0.15	2.03	0.10	2.94	0.13	0.34	0.06	0.66	0.08
AG.D	73.22	3.09	14.49	0.72	3.68	0.27	4.06	0.16	2.57	0.12	2.56	0.12	0.44	0.06	0.71	0.08
AG.D	82.65	3.48	10.76	0.55	2.68	0.20	3.56	0.14	1.07	0.07	2.15	0.10	0.13	0.05	0.48	0.07
AG.D	77.09	3.25	13.47	0.67	3.72	0.27	4.45	0.17	1.31	0.08	2.49	0.11	0.17	0.05	0.78	0.09
AG.D	74.15	3.13	13.91	0.69	2.96	0.22	3.71	0.15	2.09	0.10	2.82	0.12	0.30	0.06	0.68	0.08
AG.D	75.81	3.20	13.75	0.69	2.94	0.22	3.59	0.14	2.19	0.10	2.90	0.13	0.35	0.06	0.65	0.08
AG.D	74.75	3.16	13.86	0.69	2.92	0.22	3.63	0.14	2.36	0.11	2.90	0.13	0.35	0.06	0.67	0.08
AG.D	72.02	3.04	14.39	0.72	3.03	0.23	3.71	0.15	2.01	0.10	3.03	0.13	0.42	0.06	0.70	0.08
AG.D	74.06	3.13	14.24	0.71	2.59	0.20	3.16	0.13	2.18	0.10	2.84	0.13	0.34	0.06	0.61	0.08
AG.D	73.12	3.09	14.82	0.74	2.96	0.22	3.55	0.14	1.97	0.10	3.17	0.14	0.38	0.06	0.79	0.09
AG.D	71.92	3.04	13.99	0.70	2.91	0.22	3.68	0.15	2.10	0.10	2.97	0.13	0.30	0.06	0.65	0.08
AG.D	77.18	3.26	13.57	0.68	2.73	0.21	3.36	0.14	1.92	0.10	3.01	0.13	0.32	0.06	0.65	0.08
AG.D	74.13	3.13	14.15	0.71	3.50	0.25	3.97	0.15	2.62	0.12	2.95	0.13	0.39	0.06	0.85	0.09
AG.D	79.85	3.37	11.85	0.60	2.86	0.21	3.49	0.14	1.61	0.09	2.49	0.11	0.24	0.05	0.53	0.07
AG.D	76.71	3.24	11.51	0.58	3.22	0.24	3.80	0.15	1.58	0.09	3.08	0.13	0.26	0.05	0.60	0.08
AG.D	76.92	3.25	13.51	0.68	3.50	0.25	3.67	0.15	1.77	0.09	2.62	0.12	0.30	0.06	0.60	0.08
AG.D	73.34	3.10	13.57	0.68	3.21	0.24	3.63	0.14	1.86	0.09	2.80	0.12	0.30	0.06	0.50	0.07
AG.D	73.59	3.11	14.25	0.71	3.43	0.25	3.58	0.14	2.05	0.10	3.06	0.13	0.29	0.06	0.65	0.08
AG.D	73.53	3.11	12.29	0.62	3.34	0.24	3.78	0.15	1.86	0.09	2.91	0.13	0.29	0.06	0.56	0.07
AG.D	71.99	3.04	13.69	0.68	2.90	0.22	3.43	0.14	2.00	0.10	2.89	0.13	0.54	0.06	0.69	0.08
AG.D	74.21	3.13	13.97	0.70	3.09	0.23	3.69	0.15	1.93	0.10	2.68	0.12	0.29	0.06	0.65	0.08
AG.D	75.69	3.20	13.49	0.67	3.03	0.23	3.49	0.14	1.97	0.10	2.63	0.12	0.37	0.06	0.60	0.08
AG.D	74.91	3.16	14.69	0.73	2.59	0.20	3.00	0.13	2.00	0.10	2.88	0.13	0.31	0.06	0.65	0.08
AG.D	82.67	3.48	8.71	0.45	2.29	0.18	2.93	0.12	0.71	0.06	1.66	0.09	0.24	0.05	0.42	0.07
AG.D	76.72	3.24	13.68	0.68	3.88	0.28	3.88	0.15	1.51	0.08	3.14	0.13	0.31	0.06	0.57	0.07
AG.D	72.58	3.07	15.58	0.77	2.72	0.21	3.07	0.13	2.29	0.11	2.66	0.12	0.36	0.06	0.67	0.08
AG.D	78.16	3.30	12.24	0.62	3.23	0.24	4.33	0.17	0.99	0.07	2.05	0.10	0.24	0.05	0.50	0.07
AG.D	73.10	3.09	13.77	0.69	2.83	0.21	3.56	0.14	2.33	0.11	2.96	0.13	0.32	0.06	0.79	0.09
AG.D	73.40	3.10	14.19	0.71	2.87	0.21	3.35	0.14	2.03	0.10	2.82	0.12	0.35	0.06	0.70	0.08
AG.D	68.49	2.90	17.65	0.87	2.69	0.20	2.85	0.12	3.14	0.13	2.64	0.12	0.34	0.06	0.65	0.08
AG.D	75.37	3.18	13.35	0.67	2.55	0.20	3.02	0.13	1.68	0.09	2.52	0.12	0.35	0.06	0.56	0.07
AG.D	83.36	3.51	9.80	0.50	2.76	0.21	3.16	0.13	1.21	0.07	2.14	0.10	0.23	0.05	0.50	0.07
AG.D	68.67	2.90	18.44	0.90	2.74	0.21	2.75	0.12	3.69	0.15	2.57	0.12	0.36	0.06	0.63	0.08
AG.D	74.03	3.13	14.66	0.73	2.72	0.21	3.32	0.14	1.93	0.10	2.75	0.12	0.31	0.06	0.67	0.08
AG.D	67.41	2.85	18.12	0.89	2.52	0.19	2.67	0.12	3.30	0.14	2.83	0.13	0.44	0.06	0.62	0.08
AG.D	74.16	3.13	13.69	0.68	2.56	0.20	3.41	0.14	1.85	0.09	2.79	0.12	0.33	0.06	0.64	0.08
AG.D	72.40	3.06	15.50	0.77	2.68	0.20	3.00	0.13	2.17	0.10	2.80	0.12	0.38	0.06	0.62	0.08
AG.D	73.74	3.11	14.07	0.70	3.22	0.24	3.54	0.14	2.30	0.11	3.04	0.13	0.34	0.06	0.65	0.08
AG.D	81.60	3.44	10.74	0.55	1.92	0.16	2.49	0.11	1.49	0.08	1.78	0.09	0.31	0.06	0.49	0.07
AG.D	74.19	3.13	13.65	0.68	2.71	0.21	3.29	0.13	1.81	0.09	2.93	0.13	0.32	0.06	0.66	0.08
AG.D	74.58	3.15	14.59	0.73	3.06	0.23	3.71	0.15	1.85	0.09	2.67	0.12	0.34	0.06	0.62	0.08
AG.D	72.97	3.08	15.70	0.78	2.69	0.20	3.37	0.14	2.28	0.11	2.35	0.11	0.37	0.06	0.60	0.08
AG.D	74.07	3.13	13.86	0.69	3.01	0.22	3.67	0.15	2.11	0.10	2.85	0.13	0.34	0.06	0.68	0.08
AG.D	74.65	3.15	13.02	0.65	2.84	0.21	3.50	0.14	1.97	0.10	2.71	0.12	0.31	0.06	0.57	0.07
AG.D	69.03	2.92	16.97	0.84	3.07	0.23	3.68	0.15	1.92	0.10	3.12	0.13	0.54	0.06	0.94	0.09
AG.D	71.21	3.01	15.43	0.76	3.28	0.24	3.77	0.15	2.35	0.11	2.69	0.12	0.39	0.06	0.66	0.08
AG.D	72.78	3.08	14.13	0.70	3.04	0.23	3.85	0.15	2.08	0.10	2.79	0.12	0.36	0.06	0.66	0.08
AG.D	76.40	3.22	14.43	0.72	2.83	0.21	3.38	0.14	1.75	0.09	2.60	0.12	0.34	0.06	0.63	0.08
AG.D	75.16	3.17	13.61	0.68	3.00	0.22	3.62	0.14	1.96	0.10	2.71	0.12	0.35	0.06	0.66	0.08
AG.D	77.14	3.26	12.47	0.63	2.80	0.21	3.61	0.14	1.65	0.09	2.73	0.12	0.26	0.05	0.57	0.07
AG.D	71.25	3.01	14.27	0.71	3.00	0.22	3.85	0.15	2.49	0.11	2.88	0.13	0.36	0.06	0.75	0.08
AG.D	72.65	3.07	13.54	0.68	3.06	0.23	3.68	0.15	2.04	0.10	2.94	0.13	0.34	0.06	0.79	0.09
AG.D	73.15	3.09	15.61	0.77	2.61	0.20	3.20	0.13	2.04	0.10	2.88	0.13	0.36	0.06	0.62	0.08
AG.D	75.45	3.19	14.36	0.72	2.97	0.22	3.59	0.14	2.32	0.11	2.71	0.12	0.35	0.06	0.62	0.08

AG.D	71.00	3.00	13.94	0.70	2.65	0.20	3.58	0.14	2.15	0.10	3.10	0.13	0.30	0.06	0.70	0.08
AG.D	75.10	3.17	13.99	0.70	2.80	0.21	3.38	0.14	1.90	0.10	2.64	0.12	0.33	0.06	0.61	0.08
AG.D	73.78	3.12	13.78	0.69	2.86	0.21	3.43	0.14	2.37	0.11	2.96	0.13	0.33	0.06	0.67	0.08
AG.D	85.42	3.60	9.13	0.47	2.16	0.17	3.26	0.13	0.94	0.07	2.01	0.10	0.24	0.05	0.54	0.07
AG.D	73.21	3.09	14.70	0.73	3.13	0.23	3.72	0.15	2.12	0.10	3.09	0.13	0.40	0.06	0.69	0.08
AG.D	75.15	3.17	13.88	0.69	3.31	0.24	3.89	0.15	1.99	0.10	2.88	0.13	0.36	0.06	0.65	0.08
AG.D	80.32	3.39	11.87	0.60	3.20	0.24	4.30	0.17	0.26	0.05	2.06	0.10	0.06	0.05	0.03	0.05
AG.D	77.37	3.26	13.87	0.69	2.87	0.21	3.46	0.14	1.81	0.09	2.61	0.12	0.32	0.06	0.58	0.08
AG.D	74.44	3.14	14.48	0.72	2.94	0.22	3.46	0.14	1.89	0.10	2.77	0.12	0.36	0.06	0.60	0.08
AG.D	75.02	3.17	13.84	0.69	2.67	0.20	3.46	0.14	2.11	0.10	2.66	0.12	0.29	0.06	0.61	0.08
AG.D	74.36	3.14	14.55	0.72	3.05	0.23	3.77	0.15	1.88	0.10	2.51	0.12	0.35	0.06	0.60	0.08
AG.D	73.40	3.10	13.58	0.68	3.12	0.23	3.99	0.16	2.03	0.10	2.89	0.13	0.28	0.05	0.66	0.08
AG.D	74.28	3.14	14.80	0.74	3.40	0.25	3.92	0.15	1.58	0.09	3.43	0.14	0.38	0.06	0.60	0.08
AG.D	79.07	3.34	12.60	0.63	3.73	0.27	4.54	0.17	0.34	0.05	2.18	0.11	0.03	0.05	0.12	0.05
AG.D	78.49	3.31	12.89	0.65	3.48	0.25	4.30	0.16	0.67	0.06	2.44	0.11	0.19	0.05	0.36	0.06
AG.D	75.66	3.19	13.83	0.69	3.13	0.23	3.65	0.15	2.49	0.11	2.83	0.12	0.34	0.06	0.70	0.08
AG.D	73.09	3.09	14.49	0.72	2.95	0.22	3.58	0.14	2.32	0.11	2.99	0.13	0.35	0.06	0.68	0.08
AG.D	73.58	3.11	13.62	0.68	3.09	0.23	3.72	0.15	2.08	0.10	2.96	0.13	0.29	0.06	0.69	0.08
AH.E	73.39	3.10	13.79	0.69	3.63	0.26	3.68	0.15	1.26	0.08	3.10	0.13	0.39	0.06	0.84	0.09
AH.E	74.63	3.15	15.11	0.75	3.38	0.25	3.48	0.14	1.91	0.10	3.05	0.13	0.43	0.06	0.82	0.09
AH.E	76.43	3.23	12.77	0.64	3.44	0.25	3.59	0.14	1.13	0.07	3.13	0.13	0.44	0.06	0.82	0.09
AH.E	73.18	3.09	14.52	0.72	3.62	0.26	3.71	0.15	1.37	0.08	3.02	0.13	0.43	0.06	0.85	0.09
AH.E	74.47	3.14	13.63	0.68	3.85	0.28	3.78	0.15	0.99	0.07	3.19	0.14	0.37	0.06	0.73	0.08
AH.E	76.84	3.24	13.47	0.67	3.51	0.25	3.60	0.14	1.07	0.07	2.91	0.13	0.37	0.06	0.84	0.09
AH.E	73.76	3.12	13.54	0.68	3.43	0.25	3.75	0.15	1.19	0.07	3.16	0.14	0.38	0.06	0.86	0.09
AH.E	73.07	3.09	13.83	0.69	3.66	0.26	3.81	0.15	1.06	0.07	3.16	0.14	0.33	0.06	0.83	0.09
AH.E	73.94	3.12	13.86	0.69	3.92	0.28	3.79	0.15	1.07	0.07	3.23	0.14	0.38	0.06	0.78	0.09
AH.E	74.03	3.13	14.64	0.73	3.46	0.25	3.70	0.15	1.38	0.08	3.19	0.14	0.44	0.06	0.94	0.09
AH.E	73.96	3.12	14.71	0.73	3.49	0.25	3.67	0.15	1.35	0.08	3.14	0.13	0.41	0.06	0.92	0.09
AH.E	72.48	3.06	13.84	0.69	3.58	0.26	3.79	0.15	1.27	0.08	2.94	0.13	0.42	0.06	0.78	0.09
AH.E	74.77	3.16	13.05	0.65	3.77	0.27	3.74	0.15	0.92	0.07	3.00	0.13	0.33	0.06	0.61	0.08
AH.E	73.37	3.10	14.00	0.70	3.54	0.26	3.64	0.14	1.32	0.08	3.08	0.13	0.43	0.06	0.90	0.09
AH.E	73.87	3.12	13.36	0.67	3.34	0.24	3.66	0.15	1.48	0.08	3.03	0.13	0.40	0.06	0.83	0.09
AH.E	75.63	3.19	14.36	0.72	3.54	0.26	3.78	0.15	1.34	0.08	2.75	0.12	0.33	0.06	0.78	0.09
AH.E	74.33	3.14	13.70	0.68	3.56	0.26	3.68	0.15	1.57	0.09	2.94	0.13	0.39	0.06	0.83	0.09
AH.E	77.90	3.29	11.56	0.59	3.94	0.28	3.88	0.15	0.73	0.06	2.86	0.13	0.30	0.06	0.40	0.07
AH.E	73.11	3.09	14.21	0.71	4.28	0.30	3.89	0.15	0.77	0.06	3.71	0.15	0.47	0.06	0.82	0.09
AH.E	74.76	3.16	12.42	0.63	3.80	0.27	4.01	0.16	0.63	0.06	3.09	0.13	0.24	0.05	0.46	0.07
AH.E	75.80	3.20	14.18	0.71	3.50	0.25	3.49	0.14	1.66	0.09	3.18	0.14	0.36	0.06	0.87	0.09
AH.E	75.69	3.20	14.19	0.71	3.82	0.27	3.63	0.14	1.77	0.09	2.80	0.12	0.34	0.06	0.57	0.07
AH.E	78.03	3.29	12.16	0.61	3.92	0.28	3.78	0.15	1.00	0.07	2.77	0.12	0.24	0.05	0.50	0.07
AH.E	77.24	3.26	13.72	0.69	3.53	0.26	3.81	0.15	1.24	0.08	2.95	0.13	0.32	0.06	0.71	0.08
AH.E	72.23	3.05	12.92	0.65	3.51	0.25	3.81	0.15	1.00	0.07	2.92	0.13	0.32	0.06	0.73	0.08
AH.E	77.22	3.26	12.81	0.64	3.61	0.26	3.99	0.16	0.77	0.06	3.38	0.14	0.32	0.06	0.56	0.07
AH.E	74.24	3.14	12.88	0.65	2.40	0.19	4.35	0.17	1.42	0.08	2.90	0.13	0.30	0.06	0.76	0.08
AH.E	73.13	3.09	14.08	0.70	3.41	0.25	3.52	0.14	1.64	0.09	3.29	0.14	0.43	0.06	1.00	0.10
AH.E	77.81	3.28	12.39	0.62	3.96	0.28	3.94	0.15	0.60	0.06	2.99	0.13	0.26	0.05	0.52	0.07
AH.E	73.52	3.11	15.16	0.75	3.91	0.28	3.87	0.15	1.16	0.07	3.05	0.13	0.42	0.06	0.94	0.09
AH.E	76.26	3.22	13.00	0.65	3.94	0.28	3.87	0.15	0.74	0.06	3.10	0.13	0.29	0.06	0.60	0.08
AH.E	72.70	3.07	13.96	0.70	3.53	0.26	3.75	0.15	1.22	0.08	3.20	0.14	0.39	0.06	0.89	0.09
AH.E	78.43	3.31	11.28	0.57	4.28	0.30	4.02	0.16	0.21	0.04	3.06	0.13	0.21	0.05	0.21	0.06
AH.E	74.77	3.16	13.19	0.66	3.97	0.28	3.81	0.15	0.81	0.06	2.98	0.13	0.29	0.06	0.72	0.08
AH.E	74.28	3.14	14.28	0.71	3.34	0.24	3.59	0.14	1.43	0.08	3.33	0.14	0.46	0.06	0.97	0.10
AH.E	76.11	3.21	13.77	0.69	3.21	0.24	3.67	0.15	1.57	0.09	2.98	0.13	0.38	0.06	0.93	0.09
AH.E	76.98	3.25	14.04	0.70	3.30	0.24	3.49	0.14	1.91	0.10	2.74	0.12	0.26	0.05	0.80	0.09
AH.E	77.81	3.28	13.10	0.66	3.36	0.25	3.53	0.14	1.41	0.08	2.80	0.12	0.35	0.06	0.87	0.09
AH.E	75.69	3.20	14.34	0.71	3.42	0.25	3.89	0.15	1.28	0.08	2.79	0.12	0.37	0.06	0.81	0.09
AH.E	74.27	3.14	13.23	0.66	3.24	0.24	3.58	0.14	1.23	0.08	3.15	0.13	0.47	0.06	0.88	0.09
AH.E	75.80	3.20	14.57	0.73	3.77	0.27	3.79	0.15	1.25	0.08	2.99	0.13	0.41	0.06	0.80	0.09
AH.E	74.17	3.13	13.82	0.69	3.31	0.24	3.69	0.15	1.54	0.08	3.00	0.13	0.37	0.06	0.78	0.09
AH.E	75.59	3.19	15.13	0.75	3.12	0.23	3.31	0.13	2.01	0.10	2.83	0.13	0.35	0.06	0.84	0.09
AH.E	75.75	3.20	14.98	0.74	3.45	0.25	3.59	0.14	1.57	0.09	2.99	0.13	0.45	0.06	1.03	0.10

AH.E	74.90	3.16	13.63	0.68	3.60	0.26	3.84	0.15	0.99	0.07	3.01	0.13	0.36	0.06	0.83	0.09
AH.E	77.25	3.26	13.26	0.66	4.13	0.29	3.78	0.15	0.71	0.06	2.96	0.13	0.26	0.05	0.56	0.07
AH.E	75.07	3.17	13.01	0.65	4.07	0.29	4.03	0.16	0.74	0.06	3.02	0.13	0.28	0.05	0.56	0.07
AH.E	73.65	3.11	13.79	0.69	3.35	0.24	3.77	0.15	1.47	0.08	3.02	0.13	0.24	0.05	0.77	0.09
AH.E	74.74	3.16	14.54	0.72	3.40	0.25	3.97	0.15	1.14	0.07	2.65	0.12	0.39	0.06	0.86	0.09
AH.E	76.56	3.23	14.00	0.70	3.60	0.26	3.54	0.14	1.79	0.09	2.93	0.13	0.33	0.06	0.78	0.09
AH.E	76.29	3.22	13.81	0.69	3.40	0.25	3.64	0.14	1.74	0.09	3.00	0.13	0.39	0.06	0.79	0.09
AH.E	74.77	3.16	15.00	0.74	3.46	0.25	3.66	0.15	1.34	0.08	3.01	0.13	0.50	0.06	0.87	0.09
AH.E	74.17	3.13	14.32	0.71	3.94	0.28	3.79	0.15	1.15	0.07	3.12	0.13	0.31	0.06	0.81	0.09
AH.E	76.82	3.24	14.02	0.70	3.90	0.28	3.74	0.15	1.49	0.08	2.87	0.13	0.36	0.06	0.70	0.08
AH.E	79.02	3.33	11.44	0.58	4.43	0.31	4.00	0.16	0.21	0.04	3.21	0.14	0.28	0.05	0.27	0.06
CC	72.78	3.08	13.76	0.69	3.35	0.24	3.76	0.15	2.33	0.11	2.69	0.12	0.30	0.06	0.56	0.07
CC	74.48	3.15	13.18	0.66	3.46	0.25	3.65	0.15	2.62	0.12	2.78	0.12	0.29	0.06	0.66	0.08
CC	70.45	2.98	13.72	0.69	3.29	0.24	3.61	0.14	2.35	0.11	2.95	0.13	0.42	0.06	0.68	0.08
CC	71.69	3.03	12.80	0.64	3.60	0.26	3.80	0.15	2.66	0.12	2.83	0.13	0.30	0.06	0.59	0.08
CC	70.44	2.98	14.43	0.72	3.95	0.28	4.18	0.16	2.58	0.12	2.70	0.12	0.36	0.06	0.63	0.08
CC	73.84	3.12	13.24	0.66	3.41	0.25	3.77	0.15	2.72	0.12	2.71	0.12	0.26	0.05	0.60	0.08
CC	74.35	3.14	13.02	0.65	3.20	0.24	3.63	0.14	2.12	0.10	2.71	0.12	0.28	0.05	0.47	0.07
CC	73.88	3.12	13.27	0.66	3.24	0.24	3.60	0.14	2.38	0.11	2.72	0.12	0.27	0.05	0.54	0.07
CC	75.44	3.19	13.15	0.66	3.16	0.23	3.59	0.14	1.97	0.10	2.54	0.12	0.32	0.06	0.51	0.07
CC	72.86	3.08	12.94	0.65	3.80	0.27	4.03	0.16	2.40	0.11	2.79	0.12	0.34	0.06	0.62	0.08
CC	75.22	3.18	13.38	0.67	3.29	0.24	3.79	0.15	2.94	0.13	2.78	0.12	0.27	0.05	0.66	0.08
CC	74.54	3.15	13.85	0.69	3.59	0.26	3.86	0.15	2.54	0.12	2.81	0.12	0.31	0.06	0.62	0.08
CC	101.73	4.27	0.61	0.08	0.50	0.07	0.44	0.05	0.15	0.04	0.09	0.04	0.09	0.05	0.03	0.05
CC	70.38	2.98	12.98	0.65	3.51	0.25	4.18	0.16	2.07	0.10	2.78	0.12	0.37	0.06	0.55	0.07
CC	74.00	3.13	13.07	0.66	3.35	0.24	3.79	0.15	2.27	0.11	2.86	0.13	0.30	0.06	0.59	0.08
CC	69.32	2.93	14.52	0.72	4.05	0.29	4.08	0.16	2.65	0.12	3.43	0.14	0.53	0.06	0.75	0.08
CC	74.95	3.16	12.24	0.62	3.74	0.27	3.90	0.15	2.07	0.10	2.99	0.13	0.27	0.05	0.58	0.08
CC	73.64	3.11	13.12	0.66	3.88	0.28	4.23	0.16	1.25	0.08	2.39	0.11	0.14	0.05	0.45	0.07
CC	75.12	3.17	9.68	0.50	3.91	0.28	4.01	0.16	1.72	0.09	2.83	0.13	0.22	0.05	0.52	0.07
CC	75.15	3.17	14.18	0.71	3.42	0.25	3.69	0.15	2.81	0.12	2.64	0.12	0.33	0.06	0.56	0.07
CC	71.01	3.00	13.55	0.68	3.44	0.25	4.17	0.16	1.49	0.08	2.95	0.13	0.34	0.06	0.62	0.08
CC	70.37	2.98	14.18	0.71	3.54	0.26	3.99	0.16	2.99	0.13	3.05	0.13	0.38	0.06	0.73	0.08
CC	73.72	3.11	13.99	0.70	3.37	0.25	3.81	0.15	2.54	0.12	2.90	0.13	0.34	0.06	0.68	0.08
CC	73.52	3.11	12.44	0.63	3.32	0.24	4.05	0.16	1.76	0.09	3.57	0.15	0.63	0.07	0.70	0.08
CC	71.29	3.01	13.80	0.69	3.46	0.25	4.02	0.16	2.44	0.11	3.75	0.15	0.52	0.06	0.82	0.09
CC	71.92	3.04	13.30	0.67	3.61	0.26	4.14	0.16	1.78	0.09	3.42	0.14	0.38	0.06	0.73	0.08
CC	72.04	3.04	13.65	0.68	3.63	0.26	3.81	0.15	2.04	0.10	2.82	0.12	0.29	0.06	0.52	0.07
CC	72.22	3.05	13.47	0.67	3.94	0.28	4.17	0.16	1.93	0.10	3.01	0.13	0.29	0.06	0.66	0.08
CC	74.15	3.13	11.62	0.59	3.95	0.28	4.10	0.16	2.11	0.10	2.51	0.12	0.26	0.05	0.49	0.07
CC	75.15	3.17	12.46	0.63	3.36	0.25	3.86	0.15	2.67	0.12	2.96	0.13	0.27	0.05	0.53	0.07
CC	74.38	3.14	11.25	0.57	2.91	0.22	3.74	0.15	2.29	0.11	2.72	0.12	0.26	0.05	0.49	0.07
CC	73.50	3.10	15.09	0.75	3.63	0.26	3.91	0.15	1.74	0.09	3.13	0.13	0.37	0.06	0.75	0.08
CC	71.56	3.02	14.57	0.72	3.72	0.27	4.18	0.16	1.60	0.09	3.34	0.14	0.34	0.06	0.72	0.08
CC	72.51	3.06	12.96	0.65	3.53	0.26	4.12	0.16	2.33	0.11	3.01	0.13	0.28	0.06	0.61	0.08
CC	68.89	2.91	15.65	0.78	3.30	0.24	4.07	0.16	2.28	0.11	3.40	0.14	0.56	0.06	0.83	0.09
CC	100.56	4.23	0.60	0.08	0.40	0.06	0.27	0.04	0.03	0.04	0.15	0.04	0.03	0.05	0.03	0.05
CC	70.77	2.99	13.90	0.69	4.11	0.29	4.22	0.16	1.89	0.10	2.75	0.12	0.25	0.05	0.52	0.07
CC	74.93	3.16	12.02	0.61	3.23	0.24	4.09	0.16	2.41	0.11	3.02	0.13	0.29	0.06	0.59	0.08
CC	74.35	3.14	13.50	0.68	3.58	0.26	3.92	0.15	3.33	0.14	2.91	0.13	0.39	0.06	0.64	0.08
CC	75.66	3.19	13.16	0.66	2.90	0.22	3.37	0.14	2.74	0.12	2.72	0.12	0.24	0.05	0.51	0.07
CC	74.56	3.15	14.22	0.71	3.21	0.24	3.62	0.14	2.89	0.13	2.82	0.12	0.30	0.06	0.59	0.08
CC	72.82	3.08	14.38	0.72	3.54	0.26	3.86	0.15	2.30	0.11	3.14	0.13	0.41	0.06	0.78	0.09
CC	70.65	2.99	16.30	0.81	3.80	0.27	4.15	0.16	1.75	0.09	3.16	0.14	0.38	0.06	0.95	0.09
CC	78.54	3.31	12.20	0.62	3.26	0.24	4.19	0.16	0.63	0.06	2.56	0.12	0.13	0.05	0.29	0.06
CC	70.61	2.98	16.11	0.80	3.68	0.27	4.26	0.16	2.49	0.11	3.29	0.14	0.44	0.06	0.90	0.09
CC	70.16	2.97	15.58	0.77	3.60	0.26	4.14	0.16	2.52	0.11	3.16	0.14	0.35	0.06	0.77	0.09
CC	73.88	3.12	13.83	0.69	3.33	0.24	3.86	0.15	2.16	0.10	2.52	0.12	0.28	0.06	0.53	0.07
CC	67.61	2.86	18.64	0.91	4.37	0.31	4.14	0.16	2.52	0.11	2.89	0.13	0.35	0.06	0.83	0.09
CC	69.82	2.95	14.88	0.74	4.29	0.30	4.33	0.17	1.93	0.10	3.04	0.13	0.34	0.06	0.78	0.09
CC	76.88	3.24	12.54	0.63	3.74	0.27	4.26	0.16	2.39	0.11	2.54	0.12	0.27	0.05	0.53	0.07
CC	75.21	3.18	14.13	0.70	3.70	0.27	4.03	0.16	2.56	0.12	2.66	0.12	0.31	0.06	0.52	0.07

CC	72.07	3.05	14.33	0.71	3.37	0.25	3.96	0.15	1.61	0.09	3.14	0.13	0.43	0.06	0.71	0.08
CC	73.14	3.09	13.77	0.69	3.40	0.25	4.06	0.16	1.78	0.09	3.20	0.14	0.30	0.06	0.70	0.08
CC	70.07	2.96	16.04	0.79	3.64	0.26	4.27	0.16	2.06	0.10	3.37	0.14	0.56	0.06	0.95	0.09
CC	71.12	3.01	14.40	0.72	3.57	0.26	4.19	0.16	1.93	0.10	3.27	0.14	0.45	0.06	0.85	0.09
CC	71.29	3.01	13.58	0.68	3.38	0.25	4.06	0.16	2.07	0.10	3.06	0.13	0.39	0.06	0.71	0.08
CC	73.27	3.10	14.53	0.72	3.23	0.24	3.70	0.15	2.50	0.11	3.04	0.13	0.34	0.06	0.69	0.08
CC	72.31	3.06	14.24	0.71	3.24	0.24	3.74	0.15	2.72	0.12	2.97	0.13	0.36	0.06	0.63	0.08
CC	73.58	3.11	13.99	0.70	3.56	0.26	3.85	0.15	2.40	0.11	2.76	0.12	0.26	0.05	0.57	0.07
CC	72.26	3.05	14.49	0.72	3.39	0.25	3.52	0.14	2.49	0.11	2.56	0.12	0.26	0.05	0.60	0.08
CC	74.85	3.16	14.00	0.70	3.59	0.26	3.86	0.15	2.67	0.12	2.74	0.12	0.18	0.05	0.57	0.07
CC	75.73	3.20	13.25	0.66	3.27	0.24	3.78	0.15	2.38	0.11	2.78	0.12	0.33	0.06	0.62	0.08
CC	73.41	3.10	13.53	0.68	3.34	0.24	3.90	0.15	2.00	0.10	3.02	0.13	0.41	0.06	0.71	0.08
CC	72.99	3.08	13.25	0.66	3.38	0.25	3.96	0.15	2.92	0.13	3.04	0.13	0.22	0.05	0.68	0.08
CC	72.42	3.06	14.04	0.70	2.66	0.20	4.06	0.16	2.40	0.11	3.11	0.13	0.32	0.06	0.78	0.09
CC	70.91	3.00	14.74	0.73	2.55	0.20	4.16	0.16	2.04	0.10	3.56	0.15	0.41	0.06	0.82	0.09
CC	69.78	2.95	15.11	0.75	3.68	0.26	4.28	0.16	1.87	0.09	3.65	0.15	0.41	0.06	0.79	0.09
CC	74.67	3.15	13.76	0.69	3.16	0.23	3.79	0.15	2.54	0.12	2.55	0.12	0.27	0.05	0.49	0.07
CC	71.91	3.04	14.55	0.72	3.42	0.25	3.79	0.15	2.42	0.11	2.93	0.13	0.39	0.06	0.68	0.08
CC	74.58	3.15	12.69	0.64	3.67	0.26	4.06	0.16	1.35	0.08	2.81	0.12	0.25	0.05	0.58	0.08
CC	72.56	3.07	12.44	0.63	3.28	0.24	3.85	0.15	1.33	0.08	2.97	0.13	0.26	0.05	0.60	0.08
CC	72.04	3.04	14.91	0.74	3.40	0.25	3.88	0.15	1.78	0.09	3.23	0.14	0.47	0.06	0.83	0.09
CC	73.37	3.10	12.37	0.62	3.10	0.23	4.02	0.16	1.95	0.10	3.20	0.14	0.34	0.06	0.66	0.08
CC	72.37	3.06	11.61	0.59	2.96	0.22	4.14	0.16	1.89	0.10	2.73	0.12	0.27	0.05	0.54	0.07
CC	71.95	3.04	15.12	0.75	3.54	0.26	4.22	0.16	2.24	0.11	3.27	0.14	0.31	0.06	0.80	0.09
CC	72.22	3.05	14.75	0.73	2.54	0.19	4.01	0.16	2.14	0.10	3.11	0.13	0.41	0.06	0.77	0.09
CC	71.30	3.01	15.75	0.78	2.69	0.20	4.27	0.16	1.61	0.09	3.75	0.15	0.44	0.06	0.64	0.08
CC	68.67	2.90	16.47	0.81	3.86	0.28	4.06	0.16	2.82	0.12	3.60	0.15	0.59	0.06	1.09	0.10
CC	75.10	3.17	13.58	0.68	3.31	0.24	3.82	0.15	2.57	0.12	2.64	0.12	0.28	0.05	0.64	0.08
CC	80.50	3.39	9.72	0.50	2.89	0.22	3.34	0.14	1.70	0.09	2.18	0.10	0.25	0.05	0.50	0.07
CC	73.08	3.09	13.97	0.70	3.76	0.27	3.92	0.15	2.10	0.10	2.74	0.12	0.32	0.06	0.64	0.08
CC	72.64	3.07	13.99	0.70	3.50	0.25	4.13	0.16	2.25	0.11	2.89	0.13	0.44	0.06	0.65	0.08
CC	84.08	3.54	9.68	0.50	2.56	0.20	3.42	0.14	0.93	0.07	1.80	0.09	0.27	0.05	0.41	0.07
CC	70.07	2.96	13.81	0.69	3.31	0.24	4.14	0.16	1.93	0.10	3.59	0.15	0.51	0.06	0.77	0.09
CC	72.42	3.06	15.78	0.78	3.73	0.27	4.05	0.16	1.77	0.09	3.51	0.15	0.46	0.06	0.87	0.09
CC	73.94	3.12	12.89	0.65	3.08	0.23	3.83	0.15	2.00	0.10	2.77	0.12	0.33	0.06	0.57	0.07
CC	72.06	3.05	15.41	0.76	3.60	0.26	3.83	0.15	2.39	0.11	3.26	0.14	0.45	0.06	0.87	0.09
CC	77.63	3.28	11.09	0.56	3.06	0.23	3.83	0.15	1.13	0.07	2.77	0.12	0.32	0.06	0.50	0.07
CC	73.42	3.10	12.88	0.65	3.31	0.24	4.07	0.16	1.80	0.09	2.80	0.12	0.36	0.06	0.59	0.08
CC	65.91	2.79	16.68	0.82	3.87	0.28	4.03	0.16	2.08	0.10	3.54	0.15	0.62	0.07	0.98	0.10
CC	73.15	3.09	13.96	0.70	3.75	0.27	4.35	0.17	2.42	0.11	3.04	0.13	0.38	0.06	0.69	0.08
CC	70.44	2.98	16.34	0.81	3.81	0.27	4.06	0.16	1.92	0.10	3.44	0.14	0.40	0.06	0.93	0.09
CC	70.34	2.97	12.97	0.65	3.18	0.23	4.03	0.16	1.74	0.09	3.09	0.13	0.39	0.06	0.73	0.08
CC	72.55	3.07	13.39	0.67	3.35	0.24	3.95	0.15	1.57	0.09	3.74	0.15	0.43	0.06	0.73	0.08
CC	74.75	3.16	13.76	0.69	3.32	0.24	3.86	0.15	1.78	0.09	2.93	0.13	0.34	0.06	0.66	0.08
CC	73.97	3.12	13.93	0.70	3.46	0.25	3.76	0.15	2.26	0.11	2.96	0.13	0.34	0.06	0.66	0.08
CC	73.82	3.12	13.84	0.69	3.70	0.27	4.02	0.16	2.08	0.10	2.97	0.13	0.42	0.06	0.69	0.08
CD	72.75	3.07	15.20	0.75	2.90	0.22	3.45	0.14	1.63	0.09	2.64	0.12	0.36	0.06	0.64	0.08
CD	72.18	3.05	15.56	0.77	2.80	0.21	3.22	0.13	2.00	0.10	2.99	0.13	0.34	0.06	0.72	0.08
CD	75.92	3.20	13.27	0.66	3.15	0.23	3.80	0.15	1.51	0.08	2.72	0.12	0.24	0.05	0.66	0.08
CD	73.10	3.09	14.06	0.70	3.28	0.24	3.83	0.15	1.41	0.08	3.12	0.13	0.40	0.06	0.81	0.09
CD	69.45	2.94	16.30	0.80	3.28	0.24	3.53	0.14	2.68	0.12	3.15	0.13	0.37	0.06	0.74	0.08
CD	71.65	3.03	13.65	0.68	3.12	0.23	4.27	0.16	2.07	0.10	3.06	0.13	0.40	0.06	0.63	0.08
CD	72.80	3.08	12.92	0.65	3.06	0.23	3.95	0.15	1.61	0.09	2.52	0.12	0.34	0.06	0.59	0.08
CD	73.40	3.10	15.05	0.75	3.46	0.25	3.91	0.15	1.53	0.08	3.31	0.14	0.37	0.06	0.82	0.09
CD	70.55	2.98	17.47	0.86	2.84	0.21	3.09	0.13	2.33	0.11	2.85	0.13	0.35	0.06	0.71	0.08
CD	67.62	2.86	17.57	0.86	2.34	0.18	2.71	0.12	2.88	0.13	3.19	0.14	0.37	0.06	0.74	0.08
CD	73.75	3.12	14.21	0.71	3.07	0.23	3.48	0.14	1.78	0.09	3.12	0.13	0.39	0.06	0.68	0.08
CD	84.26	3.55	11.51	0.58	3.12	0.23	4.10	0.16	0.22	0.05	0.47	0.05	0.07	0.05	0.03	0.05
CD	71.34	3.02	14.37	0.72	3.41	0.25	4.07	0.16	2.07	0.10	3.20	0.14	0.48	0.06	0.72	0.08
CD	70.71	2.99	14.29	0.71	3.36	0.25	3.89	0.15	1.83	0.09	3.09	0.13	0.41	0.06	0.78	0.09
CD	73.89	3.12	14.29	0.71	2.85	0.21	3.39	0.14	2.00	0.10	3.00	0.13	0.37	0.06	0.69	0.08
CD	75.02	3.17	14.12	0.70	2.61	0.20	3.13	0.13	2.00	0.10	3.00	0.13	0.31	0.06	0.67	0.08

CD	74.72	3.16	11.60	0.59	2.64	0.20	3.54	0.14	1.19	0.07	2.68	0.12	0.30	0.06	0.56	0.07
CD	73.81	3.12	13.05	0.65	3.21	0.24	3.80	0.15	1.94	0.10	2.82	0.12	0.31	0.06	0.67	0.08
CD	74.12	3.13	14.52	0.72	3.40	0.25	4.14	0.16	1.29	0.08	2.65	0.12	0.24	0.05	0.58	0.08
CD	72.44	3.06	14.29	0.71	3.17	0.23	3.99	0.16	1.54	0.08	3.05	0.13	0.48	0.06	0.82	0.09
CD	76.78	3.24	11.63	0.59	2.72	0.21	3.70	0.15	1.25	0.08	2.51	0.12	0.21	0.05	0.49	0.07
CD	71.89	3.04	15.03	0.75	3.52	0.26	4.22	0.16	2.12	0.10	2.87	0.13	0.20	0.05	0.70	0.08
CD	74.95	3.16	13.54	0.68	2.88	0.22	3.68	0.15	1.56	0.09	2.92	0.13	0.28	0.05	0.53	0.07
CD	72.34	3.06	13.05	0.65	3.08	0.23	3.92	0.15	1.17	0.07	2.74	0.12	0.35	0.06	0.64	0.08
CD	72.80	3.08	13.61	0.68	2.97	0.22	3.69	0.15	1.41	0.08	2.98	0.13	0.37	0.06	0.68	0.08
CD	74.23	3.13	13.83	0.69	3.00	0.22	3.47	0.14	1.36	0.08	3.00	0.13	0.34	0.06	0.74	0.08
CD	69.93	2.96	16.62	0.82	3.80	0.27	4.59	0.17	1.76	0.09	2.69	0.12	0.30	0.06	0.55	0.07
CD	69.00	2.92	15.89	0.79	3.59	0.26	4.29	0.16	1.84	0.09	3.45	0.14	0.45	0.06	0.80	0.09
CD	75.26	3.18	13.28	0.67	3.40	0.25	4.43	0.17	1.84	0.09	2.84	0.13	0.35	0.06	0.70	0.08
CD	71.33	3.01	13.80	0.69	3.03	0.23	4.02	0.16	1.71	0.09	3.42	0.14	0.60	0.07	0.62	0.08
CD	71.24	3.01	15.41	0.76	3.10	0.23	3.99	0.16	2.00	0.10	2.68	0.12	0.44	0.06	0.61	0.08
CD	71.32	3.01	14.18	0.71	3.56	0.26	4.18	0.16	1.27	0.08	3.55	0.15	0.34	0.06	0.55	0.07
CD	76.26	3.22	13.69	0.68	3.15	0.23	3.88	0.15	1.34	0.08	2.89	0.13	0.33	0.06	0.70	0.08
CD	73.21	3.09	14.35	0.71	3.28	0.24	3.87	0.15	1.72	0.09	3.46	0.14	0.37	0.06	0.84	0.09
CD	74.94	3.16	14.13	0.70	2.81	0.21	3.26	0.13	1.98	0.10	2.91	0.13	0.32	0.06	0.70	0.08
CD	75.01	3.17	15.12	0.75	3.35	0.24	3.89	0.15	1.56	0.09	3.20	0.14	0.42	0.06	0.83	0.09
CD	76.31	3.22	14.20	0.71	2.93	0.22	3.61	0.14	1.38	0.08	2.88	0.13	0.35	0.06	0.65	0.08
CD	76.63	3.23	11.46	0.58	3.14	0.23	4.11	0.16	0.57	0.06	2.68	0.12	0.20	0.05	0.31	0.06
CD	74.03	3.13	13.78	0.69	2.76	0.21	3.48	0.14	1.81	0.09	2.76	0.12	0.36	0.06	0.63	0.08
CD	74.59	3.15	14.38	0.72	2.97	0.22	3.52	0.14	1.88	0.10	3.05	0.13	0.44	0.06	0.76	0.08
CD	73.66	3.11	14.31	0.71	2.84	0.21	3.50	0.14	1.69	0.09	3.13	0.13	0.44	0.06	0.66	0.08
CD	72.58	3.07	14.15	0.71	3.28	0.24	4.02	0.16	1.82	0.09	3.28	0.14	0.44	0.06	0.93	0.09
CD	74.73	3.16	14.61	0.73	3.22	0.24	3.63	0.14	2.00	0.10	2.96	0.13	0.34	0.06	0.71	0.08
CD	76.17	3.22	13.07	0.66	2.81	0.21	3.42	0.14	1.65	0.09	3.08	0.13	0.31	0.06	0.71	0.08
CD	74.41	3.14	12.99	0.65	3.16	0.23	3.76	0.15	1.54	0.08	2.79	0.12	0.31	0.06	0.61	0.08
CD	72.33	3.06	14.02	0.70	3.30	0.24	3.84	0.15	1.56	0.09	3.03	0.13	0.41	0.06	0.76	0.09
CD	76.12	3.21	11.69	0.59	3.22	0.24	3.77	0.15	1.66	0.09	2.63	0.12	0.24	0.05	0.50	0.07
CD	72.27	3.05	14.40	0.72	3.64	0.26	4.15	0.16	2.41	0.11	2.90	0.13	0.52	0.06	0.80	0.09
CD	70.62	2.99	15.52	0.77	2.40	0.19	2.98	0.12	2.20	0.10	2.93	0.13	0.40	0.06	0.57	0.08
CD	73.47	3.10	12.87	0.65	2.65	0.20	3.46	0.14	1.83	0.09	2.81	0.12	0.41	0.06	0.68	0.08
CD	71.77	3.03	15.75	0.78	3.56	0.26	3.83	0.15	1.85	0.09	2.92	0.13	0.30	0.06	0.91	0.09
CD	75.00	3.17	14.10	0.70	3.16	0.23	4.01	0.16	1.46	0.08	2.64	0.12	0.38	0.06	0.67	0.08
CD	72.90	3.08	14.32	0.71	3.33	0.24	4.13	0.16	2.00	0.10	2.97	0.13	0.29	0.06	0.77	0.09
CD	72.89	3.08	13.24	0.66	3.56	0.26	4.32	0.17	1.47	0.08	2.55	0.12	0.34	0.06	0.51	0.07
CD	72.44	3.06	15.11	0.75	3.44	0.25	3.94	0.15	1.70	0.09	3.16	0.14	0.32	0.06	0.82	0.09
CD	73.55	3.11	14.58	0.73	3.41	0.25	3.94	0.15	1.40	0.08	3.18	0.14	0.33	0.06	0.80	0.09
CD	68.38	2.89	14.77	0.73	3.93	0.28	4.41	0.17	2.87	0.13	3.44	0.14	0.68	0.07	1.08	0.10
CD	71.57	3.02	14.71	0.73	3.44	0.25	4.05	0.16	1.42	0.08	3.00	0.13	0.35	0.06	0.77	0.09
CD	76.21	3.22	13.87	0.69	3.26	0.24	3.89	0.15	1.35	0.08	2.67	0.12	0.35	0.06	0.67	0.08
CD	76.88	3.24	12.25	0.62	3.67	0.26	4.28	0.16	2.18	0.10	3.31	0.14	0.37	0.06	0.78	0.09
CD	76.11	3.21	14.39	0.72	3.11	0.23	3.64	0.14	1.61	0.09	2.62	0.12	0.33	0.06	0.66	0.08
CD	73.29	3.10	13.32	0.67	3.91	0.28	4.40	0.17	1.49	0.08	2.51	0.12	0.28	0.05	0.59	0.08
CD	71.61	3.03	14.00	0.70	3.86	0.28	4.28	0.16	1.99	0.10	2.84	0.13	0.37	0.06	0.68	0.08
CD	75.13	3.17	12.32	0.62	2.90	0.22	3.58	0.14	1.42	0.08	2.73	0.12	0.45	0.06	0.71	0.08
CD	73.46	3.10	15.45	0.77	3.45	0.25	3.83	0.15	2.25	0.11	3.37	0.14	0.42	0.06	0.89	0.09
CD	73.01	3.08	15.29	0.76	3.47	0.25	4.00	0.16	1.87	0.09	3.43	0.14	0.38	0.06	0.81	0.09
CD	73.63	3.11	14.44	0.72	3.32	0.24	4.02	0.16	1.68	0.09	3.04	0.13	0.40	0.06	0.88	0.09
CD	73.76	3.12	14.79	0.74	2.99	0.22	3.68	0.15	1.65	0.09	3.11	0.13	0.60	0.07	0.84	0.09
CD	72.69	3.07	16.21	0.80	3.02	0.22	3.39	0.14	1.93	0.10	2.85	0.13	0.41	0.06	0.68	0.08
CD	73.61	3.11	15.21	0.75	3.53	0.26	4.13	0.16	1.91	0.10	3.01	0.13	0.35	0.06	0.71	0.08
CD	72.57	3.07	14.36	0.72	3.26	0.24	3.91	0.15	2.25	0.11	3.08	0.13	0.29	0.06	0.79	0.09
CD	72.59	3.07	13.88	0.69	3.12	0.23	3.74	0.15	1.85	0.09	2.85	0.13	0.41	0.06	0.64	0.08
CD	74.42	3.14	14.45	0.72	3.06	0.23	3.53	0.14	2.00	0.10	2.72	0.12	0.34	0.06	0.65	0.08
CD	72.93	3.08	14.66	0.73	2.89	0.22	3.38	0.14	2.08	0.10	2.85	0.13	0.36	0.06	0.67	0.08
CD	71.18	3.01	14.19	0.71	3.17	0.23	3.71	0.15	2.06	0.10	2.75	0.12	0.33	0.06	0.62	0.08
CD	70.75	2.99	14.91	0.74	3.27	0.24	3.95	0.15	1.56	0.09	3.46	0.14	0.39	0.06	0.75	0.08
CD	67.65	2.86	17.56	0.86	3.26	0.24	3.37	0.14	2.14	0.10	3.09	0.13	0.56	0.06	0.77	0.09
CD	68.45	2.90	16.33	0.81	3.16	0.23	3.55	0.14	1.94	0.10	3.02	0.13	0.48	0.06	0.75	0.08

CD	72.00	3.04	16.12	0.80	3.37	0.25	4.08	0.16	1.77	0.09	2.86	0.13	0.34	0.06	0.60	0.08
FLD10	69.57	2.94	13.52	0.68	3.58	0.26	4.17	0.16	1.78	0.09	3.06	0.13	0.50	0.06	1.22	0.11
FLD10	80.72	3.40	9.35	0.48	2.34	0.18	3.07	0.13	1.36	0.08	2.23	0.11	0.18	0.05	0.42	0.07
FLD10	88.74	3.74	7.33	0.39	1.81	0.15	2.51	0.11	0.24	0.05	1.27	0.08	0.09	0.05	0.13	0.05
FLD10	69.80	2.95	13.09	0.66	3.21	0.24	3.87	0.15	2.66	0.12	2.70	0.12	0.32	0.06	0.53	0.07
FLD10	72.72	3.07	11.76	0.60	3.22	0.24	3.94	0.15	1.87	0.09	2.28	0.11	0.33	0.06	0.54	0.07
FLD10	73.00	3.08	12.98	0.65	2.93	0.22	3.32	0.14	2.87	0.13	2.43	0.11	0.30	0.06	0.39	0.07
FLD10	73.36	3.10	13.51	0.68	3.19	0.23	3.51	0.14	1.65	0.09	2.64	0.12	0.30	0.06	0.47	0.07
FLD10	73.32	3.10	13.01	0.65	3.39	0.25	3.82	0.15	1.69	0.09	2.75	0.12	0.36	0.06	0.43	0.07
FLD10	67.22	2.84	16.88	0.83	4.45	0.31	4.28	0.16	2.31	0.11	2.06	0.10	0.14	0.05	0.37	0.06
FLD10	69.44	2.94	14.71	0.73	3.88	0.28	4.34	0.17	1.76	0.09	2.87	0.13	0.32	0.06	0.66	0.08
FLD10	71.37	3.02	12.52	0.63	3.00	0.22	3.47	0.14	2.84	0.12	2.62	0.12	0.26	0.05	0.44	0.07
FLD10	71.15	3.01	12.57	0.63	3.14	0.23	3.58	0.14	2.70	0.12	2.74	0.12	0.34	0.06	0.43	0.07
FLD10	73.54	3.11	13.30	0.67	3.09	0.23	3.37	0.14	2.18	0.10	2.55	0.12	0.34	0.06	0.54	0.07
FLD10	72.07	3.05	13.06	0.66	3.23	0.24	3.51	0.14	2.41	0.11	2.71	0.12	0.29	0.06	0.49	0.07
FLD10	73.56	3.11	12.23	0.62	3.47	0.25	3.74	0.15	2.14	0.10	2.60	0.12	0.22	0.05	0.52	0.07
FLD10	70.24	2.97	14.62	0.73	3.91	0.28	3.67	0.15	1.25	0.08	2.35	0.11	0.47	0.06	0.55	0.07
FLD10	73.12	3.09	12.84	0.64	3.17	0.23	3.56	0.14	2.08	0.10	2.84	0.13	0.30	0.06	0.48	0.07
FLD10	73.32	3.10	13.11	0.66	3.13	0.23	3.69	0.15	2.23	0.11	2.83	0.13	0.32	0.06	0.56	0.07
FLD10	71.94	3.04	12.53	0.63	3.23	0.24	3.57	0.14	2.78	0.12	2.48	0.11	0.28	0.05	0.45	0.07
FLD10	71.32	3.01	12.65	0.64	3.17	0.23	3.48	0.14	3.00	0.13	2.64	0.12	0.18	0.05	0.51	0.07
FLD10	71.85	3.04	12.79	0.64	3.13	0.23	3.64	0.14	2.70	0.12	2.63	0.12	0.27	0.05	0.44	0.07
FLD10	71.96	3.04	12.79	0.64	3.42	0.25	4.60	0.17	0.98	0.07	4.83	0.19	0.31	0.06	0.47	0.07
FLD10	70.88	3.00	13.68	0.68	3.02	0.22	3.27	0.13	3.09	0.13	2.52	0.12	0.29	0.06	0.39	0.07
FLD10	73.14	3.09	12.93	0.65	3.22	0.24	3.55	0.14	2.19	0.10	2.62	0.12	0.28	0.06	0.53	0.07
FLD10	70.19	2.97	13.24	0.66	3.12	0.23	3.80	0.15	1.99	0.10	2.88	0.13	0.35	0.06	0.51	0.07
FLD10	73.73	3.11	12.50	0.63	3.10	0.23	3.41	0.14	2.57	0.12	2.65	0.12	0.31	0.06	0.46	0.07
FLD10	73.56	3.11	13.03	0.65	3.02	0.22	3.29	0.13	2.68	0.12	2.46	0.11	0.36	0.06	0.50	0.07
FLD10	71.57	3.02	12.69	0.64	3.05	0.23	3.49	0.14	2.67	0.12	2.61	0.12	0.32	0.06	0.42	0.07
FLD10	90.97	3.83	3.97	0.23	1.04	0.10	1.34	0.07	0.07	0.04	1.14	0.07	0.03	0.05	0.11	0.05
FLD10	72.18	3.05	12.23	0.62	3.07	0.23	3.51	0.14	2.98	0.13	2.52	0.12	0.19	0.05	0.52	0.07
FLD10	75.57	3.19	13.22	0.66	3.33	0.24	3.66	0.15	1.76	0.09	2.76	0.12	0.29	0.06	0.34	0.06
FLD10	72.28	3.05	13.25	0.66	3.01	0.22	3.73	0.15	2.45	0.11	2.82	0.12	0.32	0.06	0.55	0.07
FLD10	71.78	3.03	15.62	0.77	3.48	0.25	4.17	0.16	1.77	0.09	2.55	0.12	0.25	0.05	0.62	0.08
FLD10	72.39	3.06	15.63	0.77	2.50	0.19	2.72	0.12	3.14	0.13	2.97	0.13	0.30	0.06	0.47	0.07
FLD10	71.50	3.02	13.73	0.69	3.10	0.23	3.56	0.14	2.41	0.11	2.66	0.12	0.34	0.06	0.53	0.07
FLD10	75.87	3.20	12.81	0.64	3.02	0.22	4.69	0.18	0.74	0.06	0.99	0.07	0.12	0.05	0.09	0.05
FLD10	92.21	3.88	3.70	0.22	1.16	0.11	1.37	0.08	0.55	0.05	0.97	0.07	0.20	0.05	0.32	0.06
FLD10	71.92	3.04	14.00	0.70	3.22	0.24	3.84	0.15	2.50	0.11	2.36	0.11	0.27	0.05	0.44	0.07
FLD10	76.45	3.23	12.11	0.61	3.23	0.24	3.55	0.14	1.47	0.08	2.52	0.12	0.14	0.05	0.24	0.06
FLD10	72.93	3.08	13.30	0.67	3.00	0.22	3.79	0.15	2.47	0.11	2.65	0.12	0.30	0.06	0.48	0.07
FLD10	71.54	3.02	14.47	0.72	2.76	0.21	3.33	0.14	2.71	0.12	2.71	0.12	0.31	0.06	0.53	0.07
FLD10	75.95	3.21	13.05	0.65	2.79	0.21	3.35	0.14	1.95	0.10	2.92	0.13	0.29	0.06	0.51	0.07
FLD10	72.60	3.07	14.54	0.72	2.58	0.20	2.75	0.12	3.54	0.15	2.74	0.12	0.39	0.06	0.49	0.07
FLD10	65.15	2.76	14.04	0.70	3.84	0.28	4.43	0.17	1.79	0.09	8.45	0.30	1.47	0.09	1.19	0.11
FLD10	67.25	2.85	13.16	0.66	3.52	0.26	4.62	0.17	3.11	0.13	2.57	0.12	3.23	0.15	0.61	0.08
FLD10	71.11	3.01	14.11	0.70	3.43	0.25	3.97	0.15	2.60	0.12	2.89	0.13	0.42	0.06	0.62	0.08
FLD10	71.63	3.03	14.32	0.71	2.55	0.20	3.06	0.13	1.95	0.10	3.02	0.13	0.35	0.06	0.46	0.07
FLD10	72.56	3.07	12.31	0.62	2.78	0.21	3.47	0.14	3.06	0.13	2.75	0.12	0.33	0.06	0.46	0.07
FLD10	72.98	3.08	13.22	0.66	2.25	0.18	2.90	0.12	3.01	0.13	2.76	0.12	0.26	0.05	0.50	0.07
FLD10	73.47	3.10	14.25	0.71	2.62	0.20	2.88	0.12	3.55	0.15	2.72	0.12	0.31	0.06	0.46	0.07
FLD10	63.37	2.69	20.76	1.01	4.69	0.33	4.54	0.17	2.18	0.10	3.04	0.13	0.45	0.06	0.97	0.10
FLD10	64.06	2.71	18.31	0.90	4.21	0.30	4.64	0.18	2.57	0.12	3.97	0.16	0.51	0.06	1.21	0.11
FLD10	74.78	3.16	12.47	0.63	2.80	0.21	3.34	0.14	2.50	0.11	2.71	0.12	0.33	0.06	0.39	0.07
FLD10	72.97	3.08	15.04	0.75	3.08	0.23	3.41	0.14	2.67	0.12	2.87	0.13	0.32	0.06	0.44	0.07
FLD10	73.10	3.09	12.58	0.63	3.11	0.23	3.72	0.15	3.33	0.14	2.90	0.13	0.30	0.06	0.52	0.07
FLD10	78.29	3.30	11.91	0.60	2.89	0.22	4.05	0.16	1.17	0.07	1.01	0.07	0.10	0.05	0.15	0.05
FLD10	72.01	3.04	14.49	0.72	3.75	0.27	4.76	0.18	1.76	0.09	2.68	0.12	0.35	0.06	0.52	0.07
FLD10	72.99	3.08	13.13	0.66	2.80	0.21	3.55	0.14	2.80	0.12	2.78	0.12	0.38	0.06	0.37	0.06
FLD10	72.69	3.07	12.40	0.62	3.52	0.26	4.31	0.17	1.15	0.07	3.36	0.14	0.90	0.07	0.59	0.08
FLD10	64.14	2.72	18.91	0.93	4.46	0.31	4.71	0.18	1.10	0.07	2.76	0.12	0.61	0.07	1.15	0.11
FLD10	69.90	2.96	16.54	0.82	3.95	0.28	4.85	0.18	1.51	0.08	1.86	0.10	0.19	0.05	0.03	0.05

FLD10	72.68	3.07	13.22	0.66	3.15	0.23	3.71	0.15	2.60	0.12	2.46	0.11	0.32	0.06	0.50	0.07
FLD10	74.20	3.13	12.18	0.61	3.40	0.25	3.91	0.15	2.43	0.11	2.56	0.12	0.29	0.06	0.39	0.07
FLD10	71.09	3.00	13.95	0.70	3.63	0.26	3.77	0.15	3.11	0.13	2.96	0.13	0.41	0.06	0.61	0.08
FLD10	73.19	3.09	13.14	0.66	3.42	0.25	3.78	0.15	2.37	0.11	2.78	0.12	0.34	0.06	0.49	0.07
FLD10	81.44	3.43	10.94	0.56	4.19	0.30	3.92	0.15	0.03	0.04	1.62	0.09	0.03	0.05	0.22	0.06
FLD10	81.61	3.44	10.50	0.54	3.64	0.26	3.56	0.14	0.03	0.04	1.37	0.08	0.03	0.05	0.16	0.05
FLD10	72.13	3.05	13.16	0.66	3.64	0.26	4.31	0.17	1.44	0.08	4.07	0.16	0.44	0.06	0.21	0.06
FLD10	80.47	3.39	9.16	0.47	2.35	0.18	3.47	0.14	0.49	0.05	2.34	0.11	0.30	0.06	0.46	0.07
FLD10	75.30	3.18	12.72	0.64	3.41	0.25	3.74	0.15	2.20	0.10	2.66	0.12	0.30	0.06	0.45	0.07
FLD10	73.38	3.10	12.37	0.62	3.46	0.25	4.06	0.16	2.26	0.11	2.71	0.12	0.29	0.06	0.46	0.07
FLD10	72.56	3.07	13.02	0.65	3.33	0.24	3.98	0.16	2.16	0.10	2.72	0.12	0.32	0.06	0.55	0.07
FLD10	73.73	3.11	13.25	0.66	3.57	0.26	3.93	0.15	2.27	0.11	2.56	0.12	0.34	0.06	0.60	0.08
FLD10	78.05	3.29	12.63	0.64	4.77	0.33	4.54	0.17	0.03	0.04	1.80	0.09	0.10	0.05	0.16	0.05
FLD10	71.70	3.03	13.59	0.68	5.55	0.38	5.25	0.19	0.31	0.05	3.87	0.16	0.13	0.05	0.10	0.05
FLD10	79.13	3.34	12.29	0.62	4.72	0.33	4.28	0.16	0.12	0.04	2.06	0.10	0.10	0.05	0.03	0.05
FLD10	67.53	2.86	15.03	0.75	4.39	0.31	4.64	0.18	1.24	0.08	3.26	0.14	0.21	0.05	0.35	0.06
FLD10	75.08	3.17	12.93	0.65	3.41	0.25	4.58	0.17	0.72	0.06	0.96	0.07	0.15	0.05	0.49	0.07
FLD10	71.97	3.04	12.26	0.62	3.46	0.25	4.26	0.16	2.10	0.10	3.09	0.13	0.28	0.05	0.40	0.07
FLD10	74.72	3.16	13.31	0.67	3.54	0.26	3.73	0.15	2.38	0.11	2.72	0.12	0.33	0.06	0.49	0.07
FLD10	71.85	3.04	12.55	0.63	3.28	0.24	3.86	0.15	2.37	0.11	2.67	0.12	0.25	0.05	0.45	0.07
FLD10	80.54	3.40	12.46	0.63	4.58	0.32	4.40	0.17	0.03	0.04	1.59	0.09	0.03	0.05	0.23	0.06
FLD10	74.60	3.15	9.26	0.48	4.30	0.30	4.18	0.16	1.15	0.07	5.40	0.20	0.19	0.05	0.20	0.06
FLD10	75.36	3.18	13.71	0.69	5.52	0.38	4.81	0.18	0.03	0.04	2.56	0.12	0.14	0.05	0.13	0.05
FLD10	76.91	3.25	12.92	0.65	4.68	0.33	4.83	0.18	0.03	0.04	2.01	0.10	0.06	0.05	0.03	0.05
FLD10	63.43	2.69	17.81	0.87	3.71	0.27	3.87	0.15	4.07	0.16	3.70	0.15	0.42	0.06	1.48	0.12
FLD10	73.20	3.09	12.94	0.65	3.71	0.27	4.23	0.16	2.54	0.12	3.55	0.15	0.36	0.06	0.52	0.07
FLD10	73.21	3.09	12.96	0.65	3.09	0.23	3.57	0.14	2.61	0.12	2.77	0.12	0.34	0.06	0.44	0.07
FLD10	72.19	3.05	13.09	0.66	3.21	0.24	3.58	0.14	3.99	0.16	2.95	0.13	0.40	0.06	0.65	0.08
FLD10	71.61	3.03	13.04	0.65	3.16	0.23	3.72	0.15	2.95	0.13	2.49	0.11	0.36	0.06	0.53	0.07
FLD10	78.10	3.30	11.10	0.56	4.35	0.31	4.35	0.17	0.03	0.04	2.81	0.12	0.08	0.05	0.17	0.05
FLD10	80.46	3.39	11.84	0.60	4.25	0.30	4.28	0.16	0.03	0.04	1.66	0.09	0.03	0.05	0.20	0.06
FLD10	68.35	2.89	13.23	0.66	5.20	0.36	5.33	0.20	0.33	0.05	5.04	0.19	2.87	0.14	0.31	0.06
FLD10	70.66	2.99	13.33	0.67	3.11	0.23	4.39	0.17	2.08	0.10	4.73	0.18	0.31	0.06	1.13	0.10
FLD10	75.82	3.20	13.41	0.67	3.08	0.23	3.42	0.14	2.73	0.12	2.89	0.13	0.39	0.06	0.50	0.07
FLD10	75.18	3.17	13.07	0.66	3.20	0.24	3.79	0.15	2.46	0.11	2.88	0.13	0.30	0.06	0.47	0.07
FLD10	72.06	3.05	13.21	0.66	3.17	0.23	3.44	0.14	3.49	0.14	2.71	0.12	0.31	0.06	0.63	0.08
FLD10	72.60	3.07	15.43	0.76	5.83	0.40	5.34	0.20	0.07	0.04	2.87	0.13	0.06	0.05	0.21	0.06
FLD10	65.37	2.77	19.65	0.96	5.87	0.40	6.01	0.22	1.20	0.07	0.35	0.05	0.03	0.05	0.03	0.05
FLD10	77.42	3.27	11.39	0.58	4.21	0.30	4.50	0.17	0.71	0.06	4.29	0.17	0.23	0.05	0.14	0.05
FLD10	69.39	2.93	15.38	0.76	4.09	0.29	4.06	0.16	1.67	0.09	3.41	0.14	0.46	0.06	0.89	0.09
FLD10	74.56	3.15	12.90	0.65	2.93	0.22	3.56	0.14	2.90	0.13	2.56	0.12	0.27	0.05	0.42	0.07
FLD10	73.42	3.10	12.24	0.62	2.73	0.21	3.44	0.14	3.14	0.13	2.39	0.11	0.33	0.06	0.51	0.07
FLD10	73.90	3.12	12.78	0.64	3.20	0.24	3.72	0.15	2.88	0.13	2.73	0.12	0.28	0.05	0.48	0.07
FLD10	76.01	3.21	10.22	0.52	2.90	0.22	5.21	0.19	0.27	0.05	3.71	0.15	0.15	0.05	0.09	0.05
FLD10	67.90	2.87	15.78	0.78	4.34	0.31	4.81	0.18	1.58	0.09	3.97	0.16	0.67	0.07	0.78	0.09
FLD10	76.90	3.25	14.33	0.71	3.11	0.23	3.75	0.15	2.07	0.10	2.69	0.12	0.31	0.06	0.50	0.07
FLD10	73.18	3.09	13.95	0.70	3.41	0.25	3.63	0.14	2.08	0.10	2.77	0.12	0.44	0.06	0.54	0.07
FLD10	72.11	3.05	12.80	0.64	3.13	0.23	3.51	0.14	3.14	0.13	2.62	0.12	0.34	0.06	0.44	0.07
FLD10	75.41	3.18	13.18	0.66	2.92	0.22	3.18	0.13	3.41	0.14	2.43	0.11	0.34	0.06	0.52	0.07
FLD10	71.25	3.01	12.55	0.63	3.00	0.22	3.56	0.14	2.62	0.12	2.69	0.12	0.35	0.06	0.44	0.07
FLD10	67.90	2.87	16.99	0.84	3.96	0.28	4.57	0.17	1.59	0.09	3.43	0.14	0.53	0.06	1.04	0.10
FLD10	73.27	3.10	15.19	0.75	3.45	0.25	4.73	0.18	0.98	0.07	1.81	0.09	0.18	0.05	0.38	0.06
FLD10	75.49	3.19	12.48	0.63	3.12	0.23	3.77	0.15	2.67	0.12	2.45	0.11	0.19	0.05	0.50	0.07
FLD10	74.30	3.14	12.98	0.65	3.04	0.23	3.70	0.15	2.59	0.12	2.52	0.12	0.32	0.06	0.48	0.07
FLD10	73.05	3.09	13.61	0.68	3.52	0.26	3.71	0.15	2.53	0.11	3.16	0.14	0.41	0.06	0.48	0.07
FLD10	73.33	3.10	13.57	0.68	3.20	0.24	3.43	0.14	2.54	0.12	2.77	0.12	0.27	0.05	0.47	0.07
FLD10	78.54	3.31	12.60	0.63	3.26	0.24	3.51	0.14	1.70	0.09	2.56	0.12	0.22	0.05	0.34	0.06
FLD10	73.60	3.11	13.70	0.68	3.03	0.22	3.38	0.14	3.06	0.13	3.37	0.14	0.27	0.05	0.48	0.07
FLD10	70.26	2.97	16.85	0.83	4.23	0.30	4.81	0.18	1.31	0.08	2.95	0.13	0.41	0.06	0.74	0.08
FLD10	73.79	3.12	14.54	0.72	3.24	0.24	4.73	0.18	1.11	0.07	2.24	0.11	0.27	0.05	0.59	0.08
FLD10	68.86	2.91	15.84	0.78	3.78	0.27	4.31	0.17	2.25	0.11	2.94	0.13	1.22	0.08	0.79	0.09
FLD10	75.12	3.17	12.69	0.64	3.09	0.23	3.70	0.15	1.88	0.10	2.69	0.12	0.28	0.06	0.31	0.06

FLD10	85.88	3.62	6.39	0.35	1.68	0.14	2.26	0.10	0.99	0.07	1.84	0.09	0.15	0.05	0.27	0.06
FLD10	74.92	3.16	13.27	0.66	3.18	0.23	3.57	0.14	1.98	0.10	2.83	0.13	0.35	0.06	0.42	0.07
FLD10	77.66	3.28	14.62	0.73	2.50	0.19	2.86	0.12	2.74	0.12	2.70	0.12	0.33	0.06	0.48	0.07
FLD10	74.77	3.16	14.01	0.70	3.25	0.24	3.63	0.14	2.68	0.12	2.63	0.12	0.31	0.06	0.50	0.07
FLD10	85.30	3.59	7.71	0.41	2.86	0.21	2.78	0.12	0.03	0.04	1.02	0.07	0.05	0.05	0.16	0.05
FLD10	67.77	2.87	16.44	0.81	5.47	0.38	5.20	0.19	1.32	0.08	3.56	0.15	0.19	0.05	0.22	0.06
FLD10	75.09	3.17	10.51	0.54	3.54	0.26	4.52	0.17	0.08	0.04	2.39	0.11	0.08	0.05	0.03	0.05
FLD10	64.23	2.72	19.99	0.98	3.61	0.26	3.42	0.14	2.95	0.13	3.49	0.15	0.63	0.07	1.25	0.11
FLD10	93.89	3.95	3.48	0.21	1.14	0.11	1.35	0.07	0.26	0.05	0.83	0.06	0.05	0.05	0.09	0.05
FLD10	74.30	3.14	12.55	0.63	3.34	0.24	3.41	0.14	2.80	0.12	2.68	0.12	0.33	0.06	0.51	0.07
FLD10	86.54	3.64	7.55	0.40	2.87	0.22	2.95	0.12	0.11	0.04	1.73	0.09	0.30	0.06	0.12	0.05
FLD10	70.63	2.99	14.46	0.72	3.48	0.25	4.49	0.17	1.11	0.07	2.47	0.11	0.27	0.05	0.68	0.08
FLD10	77.51	3.27	12.01	0.61	4.28	0.30	4.84	0.18	0.09	0.04	2.68	0.12	0.07	0.05	0.22	0.06
FLD10	68.02	2.88	14.63	0.73	3.93	0.28	4.53	0.17	1.12	0.07	3.64	0.15	0.47	0.06	0.71	0.08
FLD10	70.28	2.97	14.07	0.70	3.60	0.26	4.53	0.17	1.13	0.07	4.58	0.18	0.28	0.05	0.77	0.09
FLD10	99.01	4.16	0.43	0.07	0.17	0.05	0.15	0.04	0.03	0.04	0.13	0.04	0.03	0.05	0.03	0.05
FLD10	75.06	3.17	12.34	0.62	3.49	0.25	4.19	0.16	1.44	0.08	2.39	0.11	0.23	0.05	0.37	0.06
FLD10	72.38	3.06	13.05	0.65	3.47	0.25	3.71	0.15	2.33	0.11	2.87	0.13	0.34	0.06	0.44	0.07
FLD10	73.71	3.11	14.76	0.73	5.40	0.37	5.09	0.19	0.44	0.05	2.10	0.10	0.03	0.05	0.09	0.05
FLD10	79.10	3.34	10.94	0.56	4.08	0.29	3.97	0.15	0.03	0.04	1.62	0.09	0.11	0.05	0.03	0.05
FLD10	80.34	3.39	10.01	0.51	2.56	0.20	3.32	0.13	1.48	0.08	2.28	0.11	0.17	0.05	0.55	0.07
FLD10	67.03	2.84	18.45	0.90	4.26	0.30	4.11	0.16	1.73	0.09	2.79	0.12	0.33	0.06	0.91	0.09
FLD10	80.28	3.39	9.35	0.48	2.41	0.19	2.84	0.12	0.78	0.06	2.49	0.11	0.28	0.05	0.43	0.07
FLD10	66.57	2.82	16.53	0.82	4.56	0.32	4.78	0.18	1.79	0.09	3.37	0.14	0.52	0.06	0.65	0.08
FLD10	70.03	2.96	12.96	0.65	3.76	0.27	4.44	0.17	2.40	0.11	3.55	0.15	1.34	0.09	0.55	0.07
FLD10	68.61	2.90	14.21	0.71	3.94	0.28	4.07	0.16	3.22	0.14	5.40	0.20	0.72	0.07	0.73	0.08
FLD10	74.15	3.13	13.40	0.67	3.44	0.25	3.73	0.15	1.98	0.10	2.59	0.12	0.30	0.06	0.43	0.07
FLD10	64.68	2.74	11.72	0.59	6.36	0.43	5.14	0.19	2.32	0.11	8.81	0.31	0.70	0.07	0.33	0.06
FLD10	81.72	3.45	10.20	0.52	3.80	0.27	3.74	0.15	0.03	0.04	1.45	0.08	0.08	0.05	0.03	0.05
FLD10	71.50	3.02	14.41	0.72	3.39	0.25	4.29	0.16	1.28	0.08	2.41	0.11	0.29	0.06	0.55	0.07
FLD10	67.87	2.87	16.57	0.82	4.64	0.32	4.51	0.17	0.92	0.07	3.89	0.16	0.03	0.05	0.40	0.07
FLD10	67.45	2.85	17.51	0.86	4.29	0.30	4.17	0.16	2.66	0.12	3.81	0.16	0.38	0.06	0.88	0.09
FLD10	66.05	2.80	16.27	0.80	3.94	0.28	4.07	0.16	2.65	0.12	4.98	0.19	0.60	0.07	1.28	0.11
FLD10	67.73	2.87	15.40	0.76	3.66	0.26	4.37	0.17	1.69	0.09	5.13	0.20	0.47	0.06	0.85	0.09
FLD10	72.11	3.05	13.42	0.67	3.69	0.27	3.92	0.15	2.97	0.13	2.73	0.12	0.34	0.06	0.56	0.07
FLD10	72.95	3.08	12.64	0.64	3.35	0.24	3.80	0.15	2.62	0.12	2.91	0.13	0.36	0.06	0.44	0.07
FLD10	67.20	2.84	6.22	0.34	5.33	0.37	4.72	0.18	1.43	0.08	12.54	0.43	1.29	0.09	0.17	0.05
FLD10	80.54	3.40	11.83	0.60	4.51	0.32	4.08	0.16	0.03	0.04	1.67	0.09	0.03	0.05	0.22	0.06
FLD10	80.26	3.38	12.58	0.63	4.69	0.33	4.35	0.17	0.03	0.04	1.86	0.09	0.05	0.05	0.17	0.05
FLD10	67.31	2.85	16.67	0.82	4.07	0.29	4.25	0.16	2.04	0.10	3.06	0.13	0.74	0.07	0.90	0.09
FLD10	76.06	3.21	14.49	0.72	4.15	0.29	4.20	0.16	0.89	0.07	2.16	0.10	0.20	0.05	0.38	0.07
FLD10	75.39	3.18	12.74	0.64	3.12	0.23	4.63	0.18	0.61	0.06	1.36	0.08	0.22	0.05	0.26	0.06
FLD10	63.98	2.71	19.78	0.97	3.76	0.27	3.88	0.15	2.68	0.12	3.35	0.14	1.17	0.08	1.17	0.11
FLD10	68.09	2.88	16.56	0.82	3.47	0.25	4.12	0.16	3.24	0.14	3.18	0.14	0.44	0.06	1.04	0.10
FLD10	69.52	2.94	13.11	0.66	3.67	0.26	4.43	0.17	2.49	0.11	2.57	0.12	0.16	0.05	0.41	0.07
FLD10	73.95	3.12	13.53	0.68	3.60	0.26	3.82	0.15	2.83	0.12	3.69	0.15	0.30	0.06	0.52	0.07
FLD10	78.51	3.31	11.77	0.60	4.45	0.31	4.36	0.17	0.03	0.04	1.79	0.09	0.09	0.05	0.03	0.05
FLD10	78.41	3.31	11.51	0.58	5.07	0.35	4.21	0.16	0.43	0.05	3.98	0.16	0.09	0.05	0.18	0.05
FLD10	61.49	2.61	20.07	0.98	4.42	0.31	4.18	0.16	3.51	0.14	2.24	0.11	0.31	0.06	0.36	0.06
FLD10	70.20	2.97	16.14	0.80	4.64	0.32	5.01	0.19	1.13	0.07	3.28	0.14	0.38	0.06	0.47	0.07
FLD10	85.06	3.58	9.05	0.47	2.00	0.16	1.85	0.09	1.30	0.08	1.92	0.10	0.20	0.05	0.44	0.07
FLD10	70.80	2.99	14.86	0.74	3.80	0.27	4.43	0.17	1.53	0.08	2.73	0.12	0.42	0.06	0.71	0.08
FLD10	65.54	2.78	17.71	0.87	3.64	0.26	4.24	0.16	3.50	0.14	3.36	0.14	0.46	0.06	1.08	0.10
FLD10	68.40	2.89	15.56	0.77	3.69	0.27	3.98	0.16	3.13	0.13	3.49	0.15	0.48	0.06	0.79	0.09
FLD10	85.69	3.61	9.55	0.49	3.66	0.26	3.18	0.13	0.03	0.04	1.37	0.08	0.05	0.05	0.14	0.05
FLD10	67.76	2.87	16.63	0.82	6.55	0.44	6.08	0.22	0.03	0.04	2.77	0.12	0.03	0.05	0.17	0.05
FLD10	71.47	3.02	9.88	0.51	4.28	0.30	4.21	0.16	2.18	0.10	6.73	0.25	0.36	0.06	0.03	0.05
FLD10	71.72	3.03	14.33	0.71	3.80	0.27	3.48	0.14	3.05	0.13	5.04	0.19	0.59	0.06	0.78	0.09
FLD10	73.40	3.10	13.53	0.68	3.21	0.24	4.33	0.17	0.93	0.07	2.88	0.13	0.30	0.06	0.44	0.07
FLD10	63.77	2.70	19.18	0.94	4.54	0.32	5.23	0.19	0.97	0.07	4.53	0.18	0.35	0.06	0.79	0.09
FLD10	69.18	2.93	17.18	0.85	4.57	0.32	6.33	0.23	0.67	0.06	2.44	0.11	0.07	0.05	0.25	0.06
FLD10	70.10	2.96	14.18	0.71	3.60	0.26	4.19	0.16	2.98	0.13	2.37	0.11	0.21	0.05	0.49	0.07

FLD10	71.93	3.04	14.39	0.72	3.46	0.25	3.82	0.15	1.78	0.09	2.89	0.13	0.32	0.06	0.67	0.08
FLD10	83.06	3.50	10.94	0.56	3.99	0.28	3.97	0.15	0.03	0.04	1.48	0.08	0.03	0.05	0.17	0.05
FLD10	81.03	3.42	11.58	0.59	4.38	0.31	4.25	0.16	0.03	0.04	1.71	0.09	0.03	0.05	0.03	0.05
FLD10	82.89	3.49	9.65	0.50	3.70	0.27	3.64	0.14	0.03	0.04	1.45	0.08	0.03	0.05	0.17	0.05
FLD10	69.02	2.92	14.94	0.74	3.61	0.26	4.22	0.16	1.73	0.09	3.81	0.16	0.50	0.06	0.97	0.10
FLD10	83.04	3.50	9.45	0.49	2.75	0.21	3.55	0.14	0.75	0.06	2.18	0.10	0.09	0.05	0.23	0.06
FLD10	88.70	3.73	7.12	0.38	2.77	0.21	2.68	0.12	0.03	0.04	1.05	0.07	0.03	0.05	0.05	0.05
FLD10	78.83	3.33	12.69	0.64	4.94	0.34	4.66	0.18	0.03	0.04	1.90	0.10	0.03	0.05	0.03	0.05
FLD10	77.21	3.26	12.98	0.65	5.06	0.35	4.73	0.18	0.03	0.04	1.88	0.10	0.03	0.05	0.03	0.05
FLD10	58.68	2.49	24.36	1.18	3.78	0.27	3.91	0.15	2.45	0.11	4.94	0.19	0.76	0.07	1.66	0.13
FLD10	67.11	2.84	16.70	0.82	5.13	0.36	5.54	0.20	0.71	0.06	2.18	0.11	0.07	0.05	0.23	0.06
FLD10	98.82	4.15	0.53	0.08	0.12	0.05	0.06	0.04	0.03	0.04	0.07	0.04	0.03	0.05	0.03	0.05
FLD10	72.59	3.07	13.73	0.69	3.06	0.23	3.23	0.13	3.55	0.15	2.34	0.11	0.27	0.05	0.43	0.07
FLD10	71.60	3.03	12.39	0.62	2.92	0.22	3.53	0.14	2.77	0.12	2.75	0.12	0.37	0.06	0.71	0.08
FLD10	74.62	3.15	13.45	0.67	3.34	0.24	3.64	0.14	2.64	0.12	2.80	0.12	0.31	0.06	0.59	0.08
FLD10	76.82	3.24	12.48	0.63	4.81	0.34	4.50	0.17	0.03	0.04	1.69	0.09	0.06	0.05	0.03	0.05
FLD10	73.40	3.10	13.99	0.70	5.48	0.38	4.83	0.18	0.03	0.04	2.09	0.10	0.08	0.05	0.05	0.05
FLD10	85.09	3.58	8.45	0.44	3.17	0.23	3.17	0.13	0.20	0.04	2.01	0.10	0.10	0.05	0.16	0.05
FLD10	79.93	3.37	9.92	0.51	3.81	0.27	3.66	0.15	0.09	0.04	1.70	0.09	0.03	0.05	0.03	0.05
FLD10	64.08	2.71	11.94	0.60	6.54	0.44	5.24	0.19	1.53	0.08	9.32	0.33	0.60	0.07	0.13	0.05
FLD10	84.58	3.56	8.24	0.43	3.24	0.24	3.15	0.13	0.08	0.04	1.31	0.08	0.05	0.05	0.19	0.05
FLD10	61.63	2.61	10.58	0.54	5.99	0.41	5.03	0.19	1.29	0.08	9.33	0.33	2.80	0.13	0.97	0.10
FLD10	65.64	2.78	5.62	0.31	3.22	0.24	3.41	0.14	0.42	0.05	16.11	0.54	5.82	0.23	0.89	0.09
FLD10	98.30	4.13	0.33	0.07	0.03	0.04	0.03	0.03	0.03	0.04	0.13	0.04	0.03	0.05	0.03	0.05
FLD10	74.01	3.13	11.73	0.59	5.82	0.40	4.71	0.18	0.72	0.06	6.48	0.24	0.32	0.06	0.09	0.05
FLD10	77.34	3.26	13.13	0.66	5.22	0.36	4.66	0.18	0.03	0.04	1.82	0.09	0.03	0.05	0.23	0.06
FLD10	81.59	3.44	9.77	0.50	3.69	0.27	3.67	0.15	0.03	0.04	1.59	0.09	0.08	0.05	0.08	0.05
FLD10	75.64	3.19	12.85	0.65	4.79	0.33	4.77	0.18	0.03	0.04	1.87	0.10	0.03	0.05	0.15	0.05
FLD10	72.45	3.06	11.19	0.57	4.91	0.34	4.65	0.18	0.03	0.04	4.14	0.17	0.13	0.05	0.09	0.05
FLD10	67.50	2.86	11.42	0.58	6.04	0.41	5.03	0.19	0.36	0.05	11.20	0.38	0.74	0.07	0.91	0.09
FLD10	80.04	3.38	10.95	0.56	4.30	0.30	4.08	0.16	0.03	0.04	1.53	0.08	0.03	0.05	0.03	0.05
FLD10	76.08	3.21	11.46	0.58	4.74	0.33	4.46	0.17	0.10	0.04	2.45	0.11	0.08	0.05	0.16	0.05
FLD10	78.42	3.31	11.47	0.58	4.63	0.32	4.33	0.17	0.03	0.04	1.73	0.09	0.03	0.05	0.17	0.05
FLD10	71.04	3.00	14.39	0.72	6.07	0.41	5.13	0.19	0.10	0.04	3.43	0.14	0.23	0.05	0.26	0.06
FLD10	77.19	3.26	12.38	0.62	4.93	0.34	4.61	0.17	0.03	0.04	2.23	0.11	0.03	0.05	0.10	0.05
FLD10	78.71	3.32	12.99	0.65	5.21	0.36	4.56	0.17	0.03	0.04	2.15	0.10	0.06	0.05	0.28	0.06
FLD10	73.19	3.09	13.13	0.66	5.33	0.37	4.93	0.18	0.35	0.05	3.02	0.13	0.13	0.05	0.17	0.05
FLD10	73.55	3.11	9.91	0.51	5.54	0.38	4.75	0.18	0.62	0.06	7.80	0.28	0.41	0.06	0.03	0.05
FLD10	73.56	3.11	12.23	0.62	5.62	0.39	4.77	0.18	0.80	0.06	4.81	0.19	0.34	0.06	0.10	0.05
FLD10	78.29	3.30	12.63	0.64	4.77	0.33	4.42	0.17	0.06	0.04	1.88	0.10	0.17	0.05	0.26	0.06
FLD10	63.51	2.69	11.51	0.58	6.49	0.44	5.19	0.19	1.80	0.09	9.91	0.34	0.35	0.06	0.03	0.05
FLD10	77.22	3.26	12.69	0.64	5.00	0.35	4.54	0.17	0.41	0.05	2.50	0.11	0.03	0.05	0.15	0.05
FLD10	80.66	3.40	10.10	0.52	4.16	0.30	3.98	0.16	0.19	0.04	2.42	0.11	0.35	0.06	0.16	0.05
FLD10	77.79	3.28	11.17	0.57	4.43	0.31	4.42	0.17	0.03	0.04	2.80	0.12	0.64	0.07	0.03	0.05
FLD10	81.40	3.43	9.47	0.49	3.57	0.26	3.71	0.15	0.14	0.04	1.76	0.09	0.06	0.05	0.07	0.05
FLD10	74.97	3.17	13.37	0.67	5.50	0.38	5.04	0.19	0.03	0.04	3.11	0.13	0.28	0.05	0.21	0.06
FLD10	64.19	2.72	14.27	0.71	5.75	0.39	5.57	0.20	0.43	0.05	3.44	0.14	2.52	0.13	0.44	0.07
FLD10	87.15	3.67	8.47	0.44	2.96	0.22	3.06	0.13	0.03	0.04	1.48	0.08	0.06	0.05	0.15	0.05
FLD10	89.08	3.75	5.58	0.31	1.92	0.16	2.20	0.10	0.03	0.04	1.04	0.07	0.03	0.05	0.08	0.05
FLD10	74.94	3.16	15.25	0.76	5.74	0.39	5.04	0.19	0.03	0.04	2.00	0.10	0.05	0.05	0.26	0.06
FLD10	76.33	3.22	13.71	0.68	5.16	0.36	4.83	0.18	0.08	0.04	1.97	0.10	0.03	0.05	0.05	0.05
FLD10	79.83	3.37	11.52	0.58	4.27	0.30	4.39	0.17	0.03	0.04	1.65	0.09	0.03	0.05	0.16	0.05
FLD10	71.13	3.01	13.72	0.69	6.00	0.41	5.13	0.19	0.76	0.06	4.38	0.17	0.12	0.05	0.25	0.06
FLD10	70.30	2.97	10.93	0.56	5.20	0.36	4.82	0.18	1.11	0.07	6.12	0.23	0.31	0.06	0.07	0.05
FLD10	64.40	2.73	12.10	0.61	6.67	0.45	5.34	0.20	1.77	0.09	9.22	0.32	0.45	0.06	0.18	0.05
FLD10	78.37	3.31	11.97	0.60	4.59	0.32	4.48	0.17	0.03	0.04	1.93	0.10	0.05	0.05	0.19	0.05
FLD10	77.96	3.29	11.35	0.58	4.46	0.31	4.32	0.17	0.03	0.04	2.39	0.11	0.03	0.05	0.16	0.05
FLD10	72.95	3.08	15.00	0.74	6.03	0.41	5.35	0.20	0.25	0.05	3.18	0.14	0.10	0.05	0.05	0.05
FLD10	78.54	3.31	11.77	0.60	4.49	0.32	4.28	0.16	0.03	0.04	1.52	0.08	0.03	0.05	0.15	0.05
FLD10	78.55	3.31	11.91	0.60	4.48	0.31	4.25	0.16	0.10	0.04	1.77	0.09	0.03	0.05	0.14	0.05
FLD10	76.46	3.23	12.65	0.64	4.64	0.32	4.66	0.18	0.28	0.05	2.64	0.12	0.10	0.05	0.18	0.05
FLD10	79.63	3.36	9.70	0.50	3.73	0.27	3.85	0.15	0.09	0.04	1.51	0.08	0.05	0.05	0.03	0.05

FLD10	74.35	3.14	13.40	0.67	5.01	0.35	4.82	0.18	0.06	0.04	2.16	0.10	0.07	0.05	0.14	0.05
FLD10	77.72	3.28	11.84	0.60	4.69	0.33	4.48	0.17	0.03	0.04	2.48	0.11	0.03	0.05	0.10	0.05
FLD10	77.91	3.29	11.73	0.59	4.63	0.32	4.43	0.17	0.03	0.04	2.12	0.10	0.03	0.05	0.03	0.05
FLD10	81.01	3.42	12.12	0.61	4.50	0.32	4.20	0.16	0.03	0.04	1.65	0.09	0.03	0.05	0.20	0.06
FLD10	77.98	3.29	11.43	0.58	4.37	0.31	4.26	0.16	0.03	0.04	1.53	0.08	0.03	0.05	0.03	0.05
FLD10	72.54	3.06	16.30	0.80	6.34	0.43	5.43	0.20	0.29	0.05	2.56	0.12	0.03	0.05	0.25	0.06
FLD10	65.79	2.79	15.81	0.78	6.95	0.47	5.56	0.20	0.67	0.06	3.39	0.14	0.08	0.05	0.50	0.07
FLD10	76.43	3.23	13.47	0.67	5.03	0.35	4.75	0.18	0.03	0.04	2.03	0.10	0.03	0.05	0.09	0.05
FLD10	95.87	4.03	0.29	0.06	0.10	0.04	0.03	0.03	0.06	0.04	0.08	0.04	0.03	0.05	0.13	0.05
FLD10	79.86	3.37	11.19	0.57	4.27	0.30	4.05	0.16	0.03	0.04	1.83	0.09	0.07	0.05	0.03	0.05
FLD10	78.24	3.30	11.71	0.59	4.51	0.32	4.47	0.17	0.03	0.04	1.70	0.09	0.03	0.05	0.03	0.05
FLD10	79.65	3.36	11.91	0.60	4.93	0.34	4.45	0.17	0.03	0.04	2.11	0.10	0.10	0.05	0.03	0.05
FLD10	61.66	2.61	8.88	0.46	6.40	0.43	4.86	0.18	3.57	0.15	13.93	0.47	0.81	0.07	0.18	0.05
FLD10	67.84	2.87	15.60	0.77	6.61	0.45	5.59	0.20	0.70	0.06	4.41	0.17	0.15	0.05	0.18	0.05
FLD10	78.69	3.32	11.01	0.56	4.59	0.32	4.30	0.17	0.07	0.04	2.40	0.11	0.15	0.05	0.21	0.06
FLD10	95.91	4.03	0.29	0.06	0.12	0.05	0.03	0.03	0.11	0.04	0.07	0.04	0.03	0.05	0.03	0.05
FLD10	73.29	3.10	13.91	0.69	5.68	0.39	4.87	0.18	0.27	0.05	2.99	0.13	0.08	0.05	0.44	0.07
FLD10	77.57	3.27	9.83	0.51	4.73	0.33	4.14	0.16	0.82	0.06	4.95	0.19	0.28	0.05	0.19	0.05
FLD10	78.22	3.30	9.89	0.51	4.05	0.29	3.86	0.15	0.03	0.04	1.93	0.10	0.13	0.05	0.13	0.05
FLD10	73.99	3.12	15.05	0.75	6.10	0.42	5.29	0.20	0.03	0.04	2.08	0.10	0.06	0.05	0.23	0.06
FLD10	101.43	4.26	0.31	0.07	0.11	0.04	0.06	0.04	0.03	0.04	0.09	0.04	0.03	0.05	0.03	0.05
FLD10	65.64	2.78	16.64	0.82	7.81	0.52	5.69	0.21	0.07	0.04	2.14	0.10	0.03	0.05	0.05	0.05
FLD10	78.49	3.31	13.47	0.67	5.22	0.36	4.65	0.18	0.03	0.04	1.86	0.10	0.05	0.05	0.24	0.06
FLD10	98.89	4.16	0.28	0.06	0.05	0.04	0.03	0.03	0.03	0.04	0.03	0.04	0.03	0.05	0.03	0.05
FLD10	76.54	3.23	12.17	0.61	4.82	0.34	4.35	0.17	0.06	0.04	1.95	0.10	0.03	0.05	0.21	0.06
FLD10	65.28	2.76	15.14	0.75	5.89	0.40	4.97	0.19	0.93	0.07	3.88	0.16	0.12	0.05	0.18	0.05
FLD10	64.99	2.75	16.05	0.79	6.39	0.43	5.87	0.21	0.09	0.04	2.80	0.12	0.08	0.05	0.03	0.05
FLD10	88.94	3.74	6.46	0.35	2.39	0.19	2.36	0.11	0.03	0.04	0.86	0.06	0.03	0.05	0.15	0.05
FLD10	76.99	3.25	12.02	0.61	4.72	0.33	4.29	0.16	0.03	0.04	1.75	0.09	0.14	0.05	0.08	0.05
FLD10	65.68	2.78	16.51	0.81	6.27	0.43	5.43	0.20	0.53	0.05	2.11	0.10	0.12	0.05	0.16	0.05
FLD10	83.01	3.50	7.06	0.38	3.07	0.23	2.84	0.12	0.03	0.04	1.74	0.09	0.11	0.05	0.23	0.06
FLD10	84.30	3.55	8.91	0.46	3.54	0.26	3.14	0.13	0.03	0.04	1.25	0.08	0.06	0.05	0.03	0.05
FLD10	78.81	3.32	9.24	0.48	3.46	0.25	3.74	0.15	0.03	0.04	1.28	0.08	0.03	0.05	0.12	0.05
FLD10	67.49	2.86	17.18	0.85	6.49	0.44	5.89	0.21	0.03	0.04	2.19	0.11	0.08	0.05	0.12	0.05
FLD10	76.54	3.23	10.45	0.53	4.09	0.29	3.95	0.15	0.03	0.04	1.46	0.08	0.07	0.05	0.03	0.05
FLD10	68.60	2.90	15.00	0.74	5.68	0.39	5.18	0.19	0.33	0.05	3.07	0.13	0.74	0.07	0.24	0.06
FLD10	70.66	2.99	14.96	0.74	5.70	0.39	5.20	0.19	0.10	0.04	2.31	0.11	0.06	0.05	0.22	0.06
FLD10	73.01	3.08	12.87	0.65	5.00	0.35	4.56	0.17	0.03	0.04	2.09	0.10	0.10	0.05	0.05	0.05
FLD10	78.59	3.32	9.89	0.51	3.98	0.28	3.78	0.15	0.03	0.04	1.89	0.10	0.03	0.05	0.20	0.06
FLD10	71.56	3.02	12.34	0.62	3.02	0.22	3.35	0.14	2.60	0.12	2.77	0.12	0.28	0.05	0.48	0.07
FLD10	78.82	3.33	10.01	0.51	2.77	0.21	3.37	0.14	0.54	0.05	2.25	0.11	0.73	0.07	0.19	0.05
FLD10	76.58	3.23	11.25	0.57	4.13	0.29	4.07	0.16	0.03	0.04	1.63	0.09	0.07	0.05	0.03	0.05
FLD10	68.98	2.92	13.80	0.69	5.52	0.38	5.16	0.19	0.03	0.04	3.10	0.13	0.06	0.05	0.03	0.05
FLD10	81.98	3.46	8.26	0.43	2.94	0.22	3.27	0.13	0.03	0.04	1.25	0.08	0.03	0.05	0.03	0.05
FLD10	77.65	3.28	11.39	0.58	4.34	0.31	4.07	0.16	0.07	0.04	1.82	0.09	0.03	0.05	0.25	0.06
FLD10	74.82	3.16	13.23	0.66	4.99	0.35	4.60	0.17	0.03	0.04	1.84	0.09	0.03	0.05	0.22	0.06
FLD10	72.12	3.05	10.88	0.55	4.88	0.34	4.36	0.17	0.06	0.04	3.87	0.16	0.20	0.05	0.61	0.08
FLD10	72.22	3.05	13.49	0.67	3.48	0.25	4.29	0.16	0.92	0.07	2.64	0.12	0.22	0.05	0.42	0.07
FLD10	102.69	4.31	0.50	0.07	0.19	0.05	0.20	0.04	0.12	0.04	0.12	0.04	0.03	0.05	0.03	0.05
FLD10	73.44	3.10	12.53	0.63	3.86	0.28	4.23	0.16	1.62	0.09	2.56	0.12	0.20	0.05	0.42	0.07
FLD10	75.89	3.20	11.99	0.61	4.52	0.32	4.48	0.17	0.03	0.04	1.56	0.09	0.03	0.05	0.03	0.05
FLD10	85.81	3.61	9.26	0.48	3.43	0.25	3.23	0.13	0.03	0.04	1.17	0.07	0.03	0.05	0.21	0.06
FLD10	82.86	3.49	8.58	0.45	3.31	0.24	3.12	0.13	0.03	0.04	1.36	0.08	0.03	0.05	0.03	0.05
FLD10	74.90	3.16	11.40	0.58	5.05	0.35	4.45	0.17	0.03	0.04	3.92	0.16	0.15	0.05	0.18	0.05
FLD10	74.79	3.16	11.40	0.58	3.00	0.22	3.87	0.15	1.92	0.10	2.53	0.12	0.25	0.05	0.42	0.07
FLD10	67.66	2.86	14.63	0.73	3.76	0.27	4.03	0.16	1.77	0.09	3.41	0.14	0.48	0.06	0.87	0.09
FLD10	85.64	3.61	6.84	0.37	1.88	0.15	2.75	0.12	0.46	0.05	2.44	0.11	0.35	0.06	0.22	0.06
FLD10	72.27	3.05	12.27	0.62	3.33	0.24	4.01	0.16	1.64	0.09	3.47	0.14	0.34	0.06	0.52	0.07
FLD10	72.64	3.07	13.29	0.67	5.38	0.37	4.88	0.18	0.03	0.04	3.17	0.14	0.03	0.05	0.19	0.05
FLD10	73.53	3.11	12.08	0.61	4.74	0.33	4.41	0.17	0.03	0.04	3.27	0.14	0.03	0.05	0.26	0.06
FLD10	78.25	3.30	12.56	0.63	4.68	0.33	4.51	0.17	0.06	0.04	1.65	0.09	0.03	0.05	0.21	0.06
FLD10	68.97	2.92	13.08	0.66	3.38	0.25	3.86	0.15	2.77	0.12	3.01	0.13	0.36	0.06	0.60	0.08

FLD10	70.12	2.96	12.43	0.63	3.47	0.25	4.13	0.16	2.78	0.12	2.45	0.11	0.22	0.05	0.69	0.08
FLD10	89.07	3.75	4.97	0.28	1.29	0.12	1.99	0.09	0.71	0.06	0.93	0.07	0.07	0.05	0.20	0.06
FLD10	77.87	3.29	11.22	0.57	4.01	0.29	4.14	0.16	0.03	0.04	1.39	0.08	0.07	0.05	0.18	0.05
FLD10	70.33	2.97	11.86	0.60	4.91	0.34	4.75	0.18	0.03	0.04	4.23	0.17	0.49	0.06	0.43	0.07
FLD10	80.34	3.39	9.60	0.50	3.46	0.25	3.72	0.15	0.03	0.04	1.30	0.08	0.03	0.05	0.13	0.05
FLD10	67.99	2.88	14.20	0.71	3.96	0.28	4.20	0.16	1.85	0.09	3.18	0.14	0.15	0.05	0.48	0.07
FLD10	86.52	3.64	6.42	0.35	1.62	0.14	2.28	0.10	0.46	0.05	1.26	0.08	0.16	0.05	0.17	0.05
FLD10	71.35	3.02	11.93	0.60	3.51	0.25	4.24	0.16	2.76	0.12	2.12	0.10	0.19	0.05	0.63	0.08
FLD10	78.74	3.32	9.15	0.47	2.71	0.21	3.19	0.13	1.38	0.08	1.91	0.10	0.19	0.05	0.55	0.07
FLD10	74.77	3.16	11.23	0.57	3.48	0.25	4.44	0.17	0.70	0.06	3.13	0.13	1.08	0.08	0.20	0.06
FLD10	68.86	2.91	13.69	0.68	4.87	0.34	4.77	0.18	0.60	0.06	2.76	0.12	0.43	0.06	0.15	0.05
FLD10	73.39	3.10	12.78	0.64	3.25	0.24	3.37	0.14	2.32	0.11	2.83	0.12	0.33	0.06	0.44	0.07
FLD10	72.26	3.05	13.10	0.66	3.30	0.24	3.36	0.14	2.40	0.11	2.69	0.12	0.35	0.06	0.44	0.07
FLD10	73.75	3.12	11.80	0.60	3.08	0.23	3.31	0.13	2.34	0.11	2.53	0.12	0.25	0.05	0.37	0.06
FLD10	69.66	2.95	13.63	0.68	3.93	0.28	4.19	0.16	2.00	0.10	2.43	0.11	0.14	0.05	0.56	0.07
FLD10	81.08	3.42	9.18	0.48	2.23	0.18	3.18	0.13	0.72	0.06	2.21	0.11	0.42	0.06	0.68	0.08
FLD10	71.19	3.01	12.42	0.63	3.12	0.23	3.30	0.13	4.76	0.18	2.47	0.11	0.41	0.06	0.61	0.08
FLD10	73.70	3.11	13.08	0.66	3.22	0.24	3.61	0.14	2.08	0.10	2.53	0.12	0.30	0.06	0.47	0.07
FLD10	72.71	3.07	12.73	0.64	3.57	0.26	3.87	0.15	2.54	0.12	2.45	0.11	0.23	0.05	0.53	0.07
FLD10	75.14	3.17	13.83	0.69	3.88	0.28	4.65	0.18	0.34	0.05	1.53	0.08	0.21	0.05	0.21	0.06
FLD10	72.15	3.05	12.23	0.62	3.17	0.23	3.90	0.15	1.70	0.09	2.52	0.12	0.28	0.05	0.39	0.07
FLD10	73.93	3.12	11.91	0.60	3.05	0.23	3.88	0.15	1.82	0.09	1.53	0.08	0.09	0.05	0.35	0.06
FLD10	68.09	2.88	13.61	0.68	3.58	0.26	3.80	0.15	4.80	0.18	2.08	0.10	0.16	0.05	0.49	0.07
FLD10	72.57	3.07	13.08	0.66	3.36	0.25	3.73	0.15	2.20	0.10	2.71	0.12	0.37	0.06	0.57	0.07
FLD10	81.54	3.44	8.94	0.46	2.47	0.19	3.40	0.14	0.35	0.05	1.57	0.09	0.03	0.05	0.03	0.05
FLD10	72.10	3.05	13.01	0.65	3.13	0.23	3.56	0.14	2.54	0.12	2.85	0.13	0.37	0.06	0.60	0.08
FLD10	62.77	2.66	17.69	0.87	4.30	0.30	4.29	0.16	3.13	0.13	3.28	0.14	0.34	0.06	0.34	0.06
FLD10	78.28	3.30	12.06	0.61	2.78	0.21	4.09	0.16	0.48	0.05	1.13	0.07	0.39	0.06	0.40	0.07
FLD10	71.07	3.00	13.23	0.66	3.39	0.25	3.86	0.15	1.85	0.09	2.78	0.12	0.33	0.06	0.54	0.07
FLD10	66.24	2.80	16.40	0.81	3.86	0.28	4.03	0.16	3.30	0.14	2.01	0.10	0.13	0.05	0.25	0.06
FLD10	66.57	2.82	14.42	0.72	3.13	0.23	3.70	0.15	4.86	0.18	2.75	0.12	1.33	0.09	0.71	0.08
FLD10	73.50	3.10	13.52	0.68	3.22	0.24	3.60	0.14	1.85	0.09	2.68	0.12	0.29	0.06	0.50	0.07
FLD10	70.26	2.97	13.17	0.66	3.39	0.25	3.66	0.15	2.65	0.12	2.65	0.12	0.32	0.06	0.51	0.07
FLD10	77.43	3.27	11.01	0.56	3.07	0.23	3.74	0.15	1.35	0.08	2.14	0.10	0.21	0.05	0.37	0.06
FLD11	69.86	2.95	17.25	0.85	3.27	0.24	3.84	0.15	2.65	0.12	3.44	0.14	0.57	0.06	1.19	0.11
FLD11	73.17	3.09	13.24	0.66	3.05	0.23	3.73	0.15	3.81	0.15	2.75	0.12	0.41	0.06	0.72	0.08
FLD11	72.37	3.06	13.23	0.66	3.13	0.23	3.59	0.14	2.76	0.12	2.58	0.12	0.30	0.06	0.60	0.08
FLD11	74.23	3.14	13.31	0.67	3.24	0.24	3.90	0.15	3.51	0.14	2.62	0.12	0.30	0.06	0.70	0.08
FLD11	70.56	2.98	16.11	0.80	4.05	0.29	4.73	0.18	2.66	0.12	1.89	0.10	0.15	0.05	0.44	0.07
FLD11	75.17	3.17	13.77	0.69	3.23	0.24	3.93	0.15	3.49	0.14	2.42	0.11	0.25	0.05	0.57	0.07
FLD11	75.05	3.17	13.69	0.68	3.26	0.24	3.76	0.15	3.42	0.14	2.80	0.12	0.29	0.06	0.74	0.08
FLD11	71.96	3.04	15.75	0.78	2.91	0.22	3.21	0.13	4.37	0.17	2.73	0.12	0.29	0.06	0.63	0.08
FLD11	73.87	3.12	13.15	0.66	2.78	0.21	3.27	0.13	3.89	0.16	2.58	0.12	0.25	0.05	0.57	0.07
FLD11	72.87	3.08	16.59	0.82	4.00	0.29	4.52	0.17	1.60	0.09	2.71	0.12	0.49	0.06	0.72	0.08
FLD11	67.89	2.87	17.35	0.85	2.98	0.22	3.17	0.13	4.99	0.19	2.74	0.12	0.43	0.06	0.66	0.08
FLD11	68.58	2.90	15.41	0.76	3.31	0.24	3.82	0.15	3.03	0.13	3.57	0.15	0.50	0.06	0.97	0.10
FLD11	74.56	3.15	13.89	0.69	3.28	0.24	3.81	0.15	3.35	0.14	2.65	0.12	0.36	0.06	0.69	0.08
FLD11	70.63	2.99	15.63	0.77	3.80	0.27	4.39	0.17	2.35	0.11	3.50	0.15	0.52	0.06	1.06	0.10
FLD11	68.16	2.88	17.40	0.86	3.74	0.27	4.13	0.16	1.81	0.09	3.35	0.14	0.55	0.06	0.88	0.09
FLD11	74.37	3.14	16.37	0.81	3.95	0.28	4.63	0.18	1.01	0.07	2.59	0.12	0.38	0.06	0.67	0.08
FLD11	70.90	3.00	15.63	0.77	3.63	0.26	4.20	0.16	2.43	0.11	3.64	0.15	0.43	0.06	0.77	0.09
FLD11	71.25	3.01	14.56	0.72	3.61	0.26	4.30	0.16	2.15	0.10	3.12	0.13	0.33	0.06	0.80	0.09
FLD11	72.26	3.05	13.87	0.69	3.46	0.25	3.99	0.16	3.12	0.13	2.89	0.13	0.41	0.06	0.78	0.09
FLD11	75.30	3.18	13.58	0.68	3.48	0.25	4.24	0.16	2.28	0.11	2.43	0.11	0.35	0.06	0.60	0.08
FLD11	72.60	3.07	14.24	0.71	3.66	0.26	4.03	0.16	3.35	0.14	2.86	0.13	0.37	0.06	0.83	0.09
FLD11	68.28	2.89	13.41	0.67	3.43	0.25	3.10	0.13	9.84	0.34	3.11	0.13	0.18	0.05	1.04	0.10
FLD11	72.48	3.06	15.71	0.78	3.44	0.25	4.13	0.16	1.72	0.09	2.94	0.13	0.47	0.06	0.85	0.09
FLD11	69.72	2.95	17.07	0.84	4.34	0.31	4.73	0.18	1.81	0.09	3.09	0.13	0.33	0.06	0.56	0.07
FLD11	67.89	2.87	17.20	0.85	3.85	0.28	4.28	0.16	1.99	0.10	3.58	0.15	0.48	0.06	1.00	0.10
FLD11	68.06	2.88	19.18	0.94	4.02	0.29	3.89	0.15	3.08	0.13	3.18	0.14	0.49	0.06	1.05	0.10
FLD11	69.96	2.96	17.74	0.87	3.63	0.26	3.60	0.14	4.15	0.16	2.70	0.12	0.31	0.06	0.68	0.08
FLD11	68.85	2.91	15.59	0.77	3.76	0.27	4.32	0.17	2.16	0.10	3.19	0.14	0.37	0.06	0.90	0.09

FLD11	72.74	3.07	15.29	0.76	3.64	0.26	4.05	0.16	2.88	0.13	3.12	0.13	0.36	0.06	0.75	0.08
FLD11	71.42	3.02	15.62	0.77	3.34	0.24	3.79	0.15	3.04	0.13	2.95	0.13	0.42	0.06	0.77	0.09
FLD11	74.76	3.16	13.63	0.68	3.07	0.23	3.93	0.15	2.50	0.11	3.14	0.13	0.32	0.06	0.71	0.08
FLD11	69.30	2.93	16.56	0.82	3.74	0.27	4.55	0.17	2.49	0.11	3.09	0.13	0.51	0.06	0.90	0.09
FLD11	69.39	2.93	17.34	0.85	3.87	0.28	4.39	0.17	1.85	0.09	3.44	0.14	0.47	0.06	0.94	0.09
FLD11	71.30	3.01	14.29	0.71	3.79	0.27	3.91	0.15	3.82	0.15	3.41	0.14	0.30	0.06	0.93	0.09
FLD11	94.33	3.97	5.39	0.30	1.41	0.12	2.12	0.10	0.07	0.04	0.20	0.04	0.05	0.05	0.03	0.05
FLD11	72.02	3.04	16.74	0.83	3.72	0.27	4.45	0.17	1.33	0.08	3.14	0.13	0.35	0.06	0.74	0.08
FLD11	67.59	2.86	14.32	0.71	3.60	0.26	4.01	0.16	4.28	0.17	4.05	0.16	0.41	0.06	1.10	0.10
FLD11	67.18	2.84	17.19	0.85	3.96	0.28	4.28	0.16	4.44	0.17	3.36	0.14	0.42	0.06	1.02	0.10
FLD11	72.87	3.08	13.75	0.69	3.56	0.26	4.06	0.16	2.32	0.11	3.50	0.15	0.28	0.06	1.07	0.10
FLD11	75.38	3.18	12.38	0.62	3.36	0.25	4.67	0.18	1.38	0.08	3.45	0.14	0.36	0.06	0.59	0.08
FLD11	72.15	3.05	16.19	0.80	3.72	0.27	4.27	0.16	2.80	0.12	3.29	0.14	0.38	0.06	0.99	0.10
FLD11	73.86	3.12	14.99	0.74	2.92	0.22	3.30	0.13	4.11	0.16	2.64	0.12	0.34	0.06	0.65	0.08
FLD11	71.21	3.01	15.93	0.79	3.70	0.27	4.62	0.17	2.31	0.11	2.79	0.12	0.52	0.06	0.69	0.08
FLD11	70.16	2.97	15.06	0.75	3.53	0.26	4.36	0.17	3.75	0.15	2.80	0.12	0.33	0.06	0.71	0.08
FLD11	70.89	3.00	17.16	0.84	4.00	0.29	4.19	0.16	4.43	0.17	1.94	0.10	0.26	0.05	0.63	0.08
FLD11	72.19	3.05	15.12	0.75	3.42	0.25	3.98	0.16	3.19	0.13	2.95	0.13	0.39	0.06	0.83	0.09
FLD11	66.90	2.83	19.56	0.96	3.50	0.25	5.54	0.20	1.67	0.09	3.73	0.15	0.59	0.06	1.39	0.12
FLD11	77.24	3.26	11.89	0.60	3.36	0.25	4.17	0.16	3.10	0.13	2.28	0.11	0.13	0.05	0.57	0.08
FLD11	71.55	3.02	14.29	0.71	3.43	0.25	3.81	0.15	2.89	0.13	3.03	0.13	0.37	0.06	0.82	0.09
FLD11	72.85	3.08	14.35	0.71	2.98	0.22	3.46	0.14	3.15	0.13	2.53	0.12	0.36	0.06	0.65	0.08
FLD11	97.55	4.10	2.69	0.18	0.84	0.09	1.08	0.07	0.33	0.05	0.92	0.07	0.03	0.05	0.27	0.06
FLD11	71.77	3.03	15.13	0.75	3.01	0.22	3.63	0.14	3.27	0.14	2.90	0.13	0.30	0.06	0.60	0.08
FLD11	75.32	3.18	13.37	0.67	2.95	0.22	3.60	0.14	3.29	0.14	2.58	0.12	0.21	0.05	0.52	0.07
FLD11	74.08	3.13	14.09	0.70	3.40	0.25	4.13	0.16	1.44	0.08	3.40	0.14	0.53	0.06	0.93	0.09
FLD11	74.19	3.13	14.81	0.74	3.69	0.27	4.14	0.16	1.16	0.07	3.27	0.14	0.32	0.06	0.53	0.07
FLD11	73.34	3.10	12.73	0.64	3.42	0.25	4.15	0.16	3.54	0.15	2.92	0.13	0.34	0.06	0.73	0.08
FLD11	69.56	2.94	16.88	0.83	2.86	0.21	2.79	0.12	4.65	0.18	2.84	0.13	0.38	0.06	0.66	0.08
FLD11	72.36	3.06	14.58	0.73	3.90	0.28	4.26	0.16	2.75	0.12	2.84	0.13	0.28	0.06	0.69	0.08
FLD11	74.78	3.16	14.15	0.71	3.68	0.27	3.90	0.15	2.66	0.12	3.11	0.13	0.47	0.06	0.84	0.09
FLD11	81.95	3.45	11.72	0.59	3.88	0.28	4.51	0.17	0.03	0.04	1.70	0.09	0.08	0.05	0.03	0.05
FLD11	68.22	2.89	16.31	0.81	5.35	0.37	5.14	0.19	0.39	0.05	4.01	0.16	0.28	0.05	0.28	0.06
FLD11	74.44	3.14	13.29	0.67	3.47	0.25	3.85	0.15	2.05	0.10	3.03	0.13	0.38	0.06	0.70	0.08
FLD11	72.99	3.08	14.49	0.72	3.63	0.26	3.80	0.15	2.80	0.12	2.77	0.12	0.34	0.06	0.64	0.08
FLD11	71.27	3.01	14.39	0.72	3.48	0.25	3.89	0.15	2.51	0.11	3.12	0.13	0.39	0.06	1.00	0.10
FLD11	70.97	3.00	16.05	0.79	3.05	0.23	3.23	0.13	4.09	0.16	2.68	0.12	0.35	0.06	0.60	0.08
FLD11	73.07	3.09	14.84	0.74	3.51	0.25	4.10	0.16	2.83	0.12	3.01	0.13	0.47	0.06	0.81	0.09
FLD11	72.37	3.06	15.90	0.79	3.70	0.27	3.93	0.15	2.01	0.10	3.08	0.13	0.52	0.06	0.81	0.09
FLD11	71.75	3.03	14.43	0.72	3.72	0.27	4.31	0.17	1.33	0.08	3.16	0.14	0.36	0.06	0.78	0.09
FLD11	71.78	3.03	13.75	0.69	3.57	0.26	3.78	0.15	3.38	0.14	3.66	0.15	0.38	0.06	0.67	0.08
FLD11	71.69	3.03	17.13	0.84	4.08	0.29	4.19	0.16	2.58	0.12	2.94	0.13	0.40	0.06	0.79	0.09
FLD11	75.06	3.17	14.09	0.70	3.32	0.24	4.35	0.17	1.42	0.08	3.04	0.13	0.41	0.06	0.59	0.08
FLD11	72.19	3.05	14.76	0.73	3.70	0.27	4.02	0.16	3.30	0.14	3.26	0.14	0.34	0.06	0.93	0.09
FLD11	70.99	3.00	15.26	0.76	3.01	0.22	3.25	0.13	4.01	0.16	2.70	0.12	0.35	0.06	0.62	0.08
FLD11	71.94	3.04	15.22	0.76	3.11	0.23	3.20	0.13	4.04	0.16	2.34	0.11	0.31	0.06	0.59	0.08
FLD11	75.15	3.17	14.07	0.70	2.96	0.22	3.48	0.14	3.89	0.16	2.64	0.12	0.27	0.05	0.60	0.08
FLD11	74.85	3.16	14.06	0.70	3.37	0.25	3.88	0.15	2.94	0.13	2.54	0.12	0.32	0.06	0.63	0.08
FLD11	70.49	2.98	16.16	0.80	4.38	0.31	4.20	0.16	3.40	0.14	3.30	0.14	0.28	0.06	0.82	0.09
FLD11	76.29	3.22	13.24	0.66	3.72	0.27	4.50	0.17	1.92	0.10	2.80	0.12	0.28	0.05	0.51	0.07
FLD11	74.31	3.14	13.65	0.68	3.57	0.26	3.89	0.15	3.03	0.13	2.61	0.12	0.34	0.06	0.63	0.08
FLD11	72.58	3.07	13.61	0.68	3.93	0.28	4.01	0.16	3.72	0.15	2.79	0.12	0.40	0.06	0.72	0.08
FLD11	69.39	2.93	16.71	0.82	4.39	0.31	4.02	0.16	2.76	0.12	2.62	0.12	0.38	0.06	0.84	0.09
FLD11	74.92	3.16	12.53	0.63	3.69	0.27	3.50	0.14	4.21	0.17	2.73	0.12	0.32	0.06	0.78	0.09
FLD11	89.12	3.75	7.05	0.38	1.87	0.15	2.87	0.12	0.59	0.06	1.22	0.08	0.13	0.05	0.31	0.06
FLD11	67.72	2.87	16.49	0.81	3.94	0.28	4.04	0.16	3.27	0.14	3.39	0.14	0.52	0.06	1.00	0.10
FLD11	74.32	3.14	14.88	0.74	4.26	0.30	4.02	0.16	1.81	0.09	2.54	0.12	0.30	0.06	0.75	0.08
FLD11	73.77	3.12	15.11	0.75	3.22	0.24	3.41	0.14	3.95	0.16	2.60	0.12	0.32	0.06	0.70	0.08
FLD11	71.99	3.04	14.54	0.72	3.76	0.27	4.13	0.16	3.74	0.15	3.13	0.13	0.42	0.06	0.97	0.10
FLD11	73.83	3.12	15.03	0.75	3.98	0.28	4.65	0.18	2.09	0.10	2.40	0.11	0.32	0.06	0.63	0.08
FLD11	70.83	2.99	16.46	0.81	4.02	0.29	4.34	0.17	2.37	0.11	2.81	0.12	0.37	0.06	0.87	0.09
FLD11	70.32	2.97	13.65	0.68	3.68	0.27	3.97	0.15	2.80	0.12	4.66	0.18	0.50	0.06	1.63	0.13

FLD11	72.58	3.07	12.57	0.63	3.62	0.26	3.79	0.15	3.92	0.16	3.30	0.14	0.35	0.06	1.15	0.11
FLD11	71.89	3.04	12.54	0.63	3.64	0.26	3.98	0.16	3.65	0.15	3.20	0.14	0.44	0.06	1.24	0.11
FLD11	73.49	3.10	15.58	0.77	3.21	0.24	3.57	0.14	4.17	0.16	2.81	0.12	0.39	0.06	0.64	0.08
FLD11	75.52	3.19	13.10	0.66	3.43	0.25	3.99	0.16	3.35	0.14	2.87	0.13	0.31	0.06	0.72	0.08
FLD11	75.49	3.19	13.22	0.66	3.76	0.27	4.43	0.17	2.50	0.11	2.84	0.13	0.32	0.06	0.71	0.08
FLD11	75.20	3.17	13.37	0.67	3.64	0.26	4.17	0.16	3.28	0.14	2.93	0.13	0.36	0.06	0.71	0.08
FLD11	74.85	3.16	12.85	0.65	3.48	0.25	4.16	0.16	3.34	0.14	2.69	0.12	0.33	0.06	0.67	0.08
FLD11	75.79	3.20	13.27	0.66	3.30	0.24	3.95	0.15	3.24	0.14	2.77	0.12	0.37	0.06	0.73	0.08
FLD11	69.17	2.93	20.22	0.99	5.70	0.39	4.85	0.18	0.61	0.06	2.16	0.10	0.07	0.05	0.83	0.09
FLD11	74.18	3.13	14.05	0.70	3.56	0.26	4.10	0.16	2.21	0.11	2.86	0.13	0.31	0.06	0.73	0.08
FLD11	74.83	3.16	13.79	0.69	3.37	0.25	3.85	0.15	2.88	0.13	2.95	0.13	0.33	0.06	0.68	0.08
FLD11	76.35	3.22	14.36	0.72	3.09	0.23	4.02	0.16	1.03	0.07	2.72	0.12	0.24	0.05	0.50	0.07
FLD11	72.52	3.06	15.85	0.78	3.67	0.26	4.05	0.16	2.04	0.10	3.00	0.13	0.40	0.06	0.89	0.09
FLD11	68.56	2.90	17.03	0.84	4.12	0.29	4.08	0.16	1.37	0.08	3.64	0.15	0.64	0.07	0.90	0.09
FLD11	73.79	3.12	11.92	0.60	3.32	0.24	3.67	0.15	4.02	0.16	4.44	0.17	0.27	0.05	1.36	0.12
FLD11	83.01	3.50	9.39	0.49	2.40	0.19	3.07	0.13	2.42	0.11	1.76	0.09	0.16	0.05	0.50	0.07
FLD11	74.91	3.16	13.95	0.70	3.52	0.26	4.21	0.16	1.89	0.10	2.90	0.13	0.32	0.06	0.66	0.08
FLD11	77.75	3.28	12.06	0.61	3.06	0.23	3.89	0.15	1.24	0.08	2.72	0.12	0.36	0.06	0.64	0.08
FLD11	77.19	3.26	13.20	0.66	3.47	0.25	4.44	0.17	1.43	0.08	2.00	0.10	0.21	0.05	0.48	0.07
FLD11	71.48	3.02	14.53	0.72	3.43	0.25	4.38	0.17	1.19	0.07	3.08	0.13	0.41	0.06	0.71	0.08
FLD11	74.37	3.14	13.56	0.68	3.09	0.23	3.65	0.15	4.31	0.17	3.00	0.13	0.31	0.06	0.82	0.09
FLD11	73.55	3.11	14.82	0.74	2.76	0.21	3.25	0.13	3.98	0.16	2.62	0.12	0.30	0.06	0.59	0.08
FLD11	71.03	3.00	14.69	0.73	3.24	0.24	3.65	0.15	4.18	0.16	2.58	0.12	0.34	0.06	0.66	0.08
FLD11	73.19	3.09	12.74	0.64	3.28	0.24	3.72	0.15	3.72	0.15	3.13	0.13	0.29	0.06	0.87	0.09
FLD11	73.40	3.10	15.16	0.75	3.75	0.27	4.45	0.17	1.42	0.08	2.92	0.13	0.31	0.06	0.56	0.07
FLD11	70.07	2.96	14.50	0.72	3.36	0.25	3.85	0.15	3.41	0.14	4.03	0.16	0.48	0.06	0.79	0.09
FLD11	71.75	3.03	14.99	0.74	3.71	0.27	4.49	0.17	1.59	0.09	3.65	0.15	0.58	0.06	0.81	0.09
FLD11	72.48	3.06	15.12	0.75	3.76	0.27	4.39	0.17	1.61	0.09	3.06	0.13	0.40	0.06	0.70	0.08
FLD11	75.22	3.18	14.13	0.70	3.47	0.25	3.81	0.15	3.32	0.14	2.65	0.12	0.37	0.06	0.65	0.08
FLD11	74.16	3.13	14.39	0.72	3.54	0.26	4.19	0.16	2.60	0.12	3.07	0.13	0.50	0.06	0.79	0.09
FLD11	72.27	3.05	14.86	0.74	3.61	0.26	3.96	0.15	3.82	0.15	2.63	0.12	0.48	0.06	0.66	0.08
FLD11	75.38	3.18	14.03	0.70	3.29	0.24	3.79	0.15	3.09	0.13	2.88	0.13	0.41	0.06	0.81	0.09
FLD11	73.09	3.09	14.63	0.73	3.50	0.25	4.13	0.16	2.85	0.12	2.57	0.12	0.29	0.06	0.72	0.08
FLD11	73.84	3.12	13.75	0.69	3.73	0.27	4.26	0.16	3.57	0.15	2.52	0.12	0.31	0.06	0.70	0.08
FLD11	72.96	3.08	13.85	0.69	3.51	0.25	4.37	0.17	1.21	0.07	2.88	0.13	0.29	0.06	0.64	0.08
FLD11	69.77	2.95	15.67	0.78	4.17	0.30	4.58	0.17	2.12	0.10	2.85	0.13	0.17	0.05	0.47	0.07
FLD11	75.12	3.17	14.24	0.71	3.09	0.23	3.68	0.15	3.54	0.15	2.76	0.12	0.30	0.06	0.71	0.08
FLD11	74.46	3.14	15.46	0.77	3.07	0.23	4.30	0.17	1.16	0.07	2.37	0.11	0.41	0.06	0.60	0.08
FLD11	73.02	3.08	13.50	0.68	3.38	0.25	4.46	0.17	2.02	0.10	3.89	0.16	0.37	0.06	0.68	0.08
FLD11	72.68	3.07	13.59	0.68	3.62	0.26	4.09	0.16	3.32	0.14	2.87	0.13	0.31	0.06	0.75	0.08
FLD11	72.41	3.06	14.19	0.71	3.52	0.26	3.94	0.15	3.28	0.14	3.67	0.15	0.43	0.06	1.29	0.11
FLD11	75.30	3.18	14.08	0.70	3.61	0.26	3.99	0.16	2.90	0.13	2.92	0.13	0.32	0.06	0.77	0.09
FLD11	79.36	3.35	11.63	0.59	2.87	0.22	3.56	0.14	2.33	0.11	2.45	0.11	0.27	0.05	0.53	0.07
FLD11	73.05	3.09	13.40	0.67	3.29	0.24	3.92	0.15	2.97	0.13	3.08	0.13	0.39	0.06	0.75	0.08
FLD11	73.99	3.13	14.24	0.71	3.61	0.26	4.07	0.16	3.73	0.15	2.50	0.11	0.28	0.05	0.66	0.08
FLD11	73.65	3.11	13.12	0.66	3.79	0.27	4.10	0.16	2.56	0.12	3.47	0.14	0.39	0.06	0.89	0.09
FLD11	74.72	3.16	14.15	0.71	3.38	0.25	4.11	0.16	3.57	0.15	2.36	0.11	0.32	0.06	0.61	0.08
FLD11	71.58	3.02	14.67	0.73	3.41	0.25	3.51	0.14	5.33	0.20	3.54	0.15	0.43	0.06	1.22	0.11
FLD11	69.97	2.96	13.82	0.69	3.43	0.25	4.18	0.16	3.65	0.15	3.18	0.14	0.39	0.06	0.79	0.09
FLD11	71.63	3.03	15.70	0.78	3.49	0.25	3.70	0.15	4.14	0.16	3.06	0.13	0.33	0.06	0.75	0.08
FLD11	74.40	3.14	14.90	0.74	3.53	0.26	4.34	0.17	1.43	0.08	2.82	0.12	0.56	0.06	0.76	0.09
FLD11	72.89	3.08	13.57	0.68	3.58	0.26	3.98	0.16	3.05	0.13	3.36	0.14	0.36	0.06	0.79	0.09
FLD11	73.10	3.09	14.30	0.71	3.16	0.23	3.74	0.15	3.63	0.15	2.80	0.12	0.32	0.06	0.63	0.08
FLD11	73.52	3.11	13.82	0.69	3.44	0.25	4.05	0.16	3.37	0.14	2.39	0.11	0.24	0.05	0.59	0.08
FLD11	73.58	3.11	14.42	0.72	3.70	0.27	4.12	0.16	3.78	0.15	2.59	0.12	0.30	0.06	0.64	0.08
FLD11	73.77	3.12	13.07	0.66	3.60	0.26	4.11	0.16	4.12	0.16	2.80	0.12	0.17	0.05	0.77	0.09
FLD11	75.03	3.17	13.34	0.67	3.62	0.26	3.99	0.16	3.26	0.14	2.97	0.13	0.38	0.06	0.82	0.09
FLD11	73.91	3.12	13.80	0.69	3.59	0.26	4.14	0.16	2.52	0.11	3.06	0.13	0.35	0.06	0.79	0.09
FLD11	71.45	3.02	15.02	0.75	3.56	0.26	4.26	0.16	2.22	0.11	3.23	0.14	0.40	0.06	0.74	0.08
FLD11	71.38	3.02	15.10	0.75	3.65	0.26	4.11	0.16	3.39	0.14	3.16	0.14	0.47	0.06	1.29	0.11
FLD11	73.41	3.10	14.47	0.72	3.46	0.25	4.04	0.16	2.23	0.11	3.54	0.15	0.39	0.06	1.16	0.11
FLD11	73.64	3.11	14.18	0.71	3.47	0.25	4.17	0.16	1.82	0.09	3.37	0.14	0.53	0.06	0.88	0.09

FLD11	72.40	3.06	14.86	0.74	3.66	0.26	4.26	0.16	1.80	0.09	2.92	0.13	0.42	0.06	0.76	0.08
FLD11	72.62	3.07	15.85	0.78	3.52	0.26	4.45	0.17	1.83	0.09	3.48	0.15	0.59	0.06	0.79	0.09
FLD11	80.21	3.38	11.80	0.60	3.05	0.23	4.31	0.17	1.02	0.07	2.53	0.12	0.32	0.06	0.39	0.07
FLD11	64.39	2.73	9.96	0.51	2.69	0.20	2.48	0.11	8.42	0.29	5.51	0.21	0.74	0.07	4.92	0.30
FLD11	63.15	2.68	8.82	0.46	2.45	0.19	1.96	0.09	10.18	0.35	5.85	0.22	0.77	0.07	5.64	0.34
FLD11	73.83	3.12	14.79	0.74	3.90	0.28	4.51	0.17	1.85	0.09	2.85	0.13	0.26	0.05	0.52	0.07
FLD11	74.44	3.14	13.67	0.68	3.29	0.24	3.77	0.15	3.62	0.15	2.91	0.13	0.36	0.06	0.78	0.09
FLD11	72.10	3.05	16.55	0.82	3.96	0.28	4.37	0.17	3.11	0.13	2.55	0.12	0.36	0.06	0.64	0.08
FLD11	74.39	3.14	14.10	0.70	3.55	0.26	4.00	0.16	3.07	0.13	3.00	0.13	0.33	0.06	0.66	0.08
FLD11	76.04	3.21	13.80	0.69	3.85	0.28	4.46	0.17	1.50	0.08	2.94	0.13	0.31	0.06	0.49	0.07
FLD11	75.83	3.20	13.19	0.66	3.31	0.24	3.87	0.15	2.67	0.12	2.76	0.12	0.30	0.06	0.53	0.07
FLD11	74.51	3.15	13.81	0.69	3.90	0.28	4.32	0.17	1.73	0.09	3.30	0.14	0.30	0.06	0.67	0.08
FLD12	72.84	3.08	16.15	0.80	3.88	0.28	4.10	0.16	2.04	0.10	2.73	0.12	0.34	0.06	0.78	0.09
FLD12	70.56	2.98	15.55	0.77	3.84	0.28	4.12	0.16	2.42	0.11	3.38	0.14	0.46	0.06	0.99	0.10
FLD12	84.60	3.56	9.64	0.50	2.59	0.20	3.40	0.14	0.84	0.06	1.99	0.10	0.11	0.05	0.51	0.07
FLD12	73.20	3.09	14.55	0.72	3.59	0.26	4.60	0.17	1.49	0.08	2.49	0.11	0.28	0.05	0.66	0.08
FLD12	76.58	3.23	13.20	0.66	3.41	0.25	3.99	0.16	1.46	0.08	2.56	0.12	0.42	0.06	0.70	0.08
FLD12	75.57	3.19	15.25	0.76	3.05	0.23	3.36	0.14	1.84	0.09	2.69	0.12	0.38	0.06	0.70	0.08
FLD12	73.23	3.09	14.75	0.73	3.76	0.27	4.20	0.16	2.75	0.12	2.51	0.12	0.42	0.06	0.79	0.09
FLD12	69.00	2.92	19.47	0.95	4.96	0.34	5.90	0.21	0.84	0.06	1.33	0.08	0.15	0.05	0.26	0.06
FLD12	69.49	2.94	15.96	0.79	3.59	0.26	4.04	0.16	1.56	0.09	3.08	0.13	0.54	0.06	0.88	0.09
FLD12	76.20	3.22	13.25	0.66	3.37	0.25	4.07	0.16	1.62	0.09	2.63	0.12	0.19	0.05	0.62	0.08
FLD12	71.96	3.04	14.59	0.73	3.62	0.26	4.18	0.16	1.86	0.09	3.35	0.14	0.44	0.06	0.97	0.10
FLD12	85.74	3.61	8.37	0.44	2.17	0.17	3.07	0.13	0.76	0.06	2.14	0.10	0.19	0.05	0.46	0.07
FLD12	73.47	3.10	14.36	0.72	3.41	0.25	4.48	0.17	1.42	0.08	2.92	0.13	0.27	0.05	0.61	0.08
FLD12	69.84	2.95	14.81	0.74	3.61	0.26	4.05	0.16	2.01	0.10	3.36	0.14	0.55	0.06	1.27	0.11
FLD12	71.12	3.01	15.67	0.78	3.77	0.27	4.17	0.16	1.97	0.10	2.64	0.12	0.51	0.06	0.79	0.09
FLD12	76.75	3.24	11.13	0.57	2.93	0.22	4.03	0.16	0.86	0.06	2.36	0.11	0.19	0.05	0.40	0.07
FLD12	68.85	2.91	14.84	0.74	3.92	0.28	4.75	0.18	1.63	0.09	3.38	0.14	0.44	0.06	0.75	0.08
FLD12	70.80	2.99	14.10	0.70	3.51	0.25	4.11	0.16	1.63	0.09	2.87	0.13	0.34	0.06	0.66	0.08
FLD12	69.10	2.92	14.58	0.73	3.57	0.26	4.00	0.16	1.74	0.09	3.21	0.14	0.49	0.06	0.84	0.09
FLD12	75.81	3.20	13.45	0.67	3.20	0.24	3.78	0.15	1.82	0.09	2.95	0.13	0.35	0.06	0.71	0.08
FLD12	75.83	3.20	13.14	0.66	2.54	0.20	3.22	0.13	1.78	0.09	2.65	0.12	0.33	0.06	0.60	0.08
FLD12	72.96	3.08	16.21	0.80	3.82	0.27	4.64	0.18	1.44	0.08	2.60	0.12	0.28	0.06	0.65	0.08
FLD12	74.97	3.17	15.96	0.79	3.69	0.27	4.49	0.17	1.18	0.07	2.29	0.11	0.33	0.06	0.90	0.09
FLD12	69.60	2.94	16.22	0.80	4.02	0.29	4.30	0.17	2.42	0.11	2.62	0.12	0.27	0.05	1.02	0.10
FLD12	74.39	3.14	13.28	0.67	3.26	0.24	4.03	0.16	1.49	0.08	2.89	0.13	0.33	0.06	0.77	0.09
FLD12	71.93	3.04	14.41	0.72	3.61	0.26	4.14	0.16	1.65	0.09	3.37	0.14	0.58	0.06	0.79	0.09
FLD12	72.51	3.06	15.11	0.75	3.71	0.27	4.14	0.16	1.07	0.07	2.88	0.13	0.37	0.06	0.61	0.08
FLD12	87.73	3.69	7.33	0.39	2.18	0.17	2.78	0.12	0.49	0.05	1.98	0.10	0.14	0.05	0.40	0.07
FLD12	75.21	3.18	14.72	0.73	2.75	0.21	3.14	0.13	2.12	0.10	2.98	0.13	0.41	0.06	0.61	0.08
FLD12	73.98	3.12	14.05	0.70	3.32	0.24	3.98	0.16	1.57	0.09	2.74	0.12	0.38	0.06	0.71	0.08
FLD12	71.36	3.02	15.31	0.76	3.66	0.26	4.21	0.16	1.49	0.08	3.13	0.13	0.44	0.06	0.80	0.09
FLD12	75.98	3.21	13.13	0.66	3.14	0.23	3.97	0.15	1.50	0.08	3.20	0.14	0.21	0.05	0.67	0.08
FLD12	73.75	3.11	13.58	0.68	3.20	0.24	4.03	0.16	1.74	0.09	3.00	0.13	0.40	0.06	0.74	0.08
FLD12	72.48	3.06	13.77	0.69	3.14	0.23	3.90	0.15	1.97	0.10	2.86	0.13	0.29	0.06	0.65	0.08
FLD12	71.80	3.03	14.79	0.73	3.61	0.26	3.99	0.16	1.65	0.09	3.32	0.14	0.38	0.06	0.80	0.09
FLD12	70.78	2.99	14.17	0.71	3.79	0.27	3.99	0.16	1.73	0.09	4.22	0.17	0.66	0.07	0.90	0.09
FLD12	74.32	3.14	12.08	0.61	3.11	0.23	3.61	0.14	2.48	0.11	2.77	0.12	0.67	0.07	1.05	0.10
FLD12	69.08	2.92	15.92	0.79	3.85	0.28	4.33	0.17	1.88	0.10	3.22	0.14	0.46	0.06	0.87	0.09
FLD12	70.68	2.99	17.27	0.85	4.00	0.29	4.23	0.16	2.18	0.10	3.34	0.14	0.40	0.06	0.93	0.09
FLD12	71.66	3.03	16.16	0.80	3.81	0.27	4.14	0.16	2.14	0.10	2.35	0.11	0.25	0.05	1.05	0.10
FLD12	72.05	3.04	15.53	0.77	3.61	0.26	4.08	0.16	2.44	0.11	3.44	0.14	0.35	0.06	1.56	0.13
FLD12	76.20	3.22	14.22	0.71	3.39	0.25	3.79	0.15	1.79	0.09	3.02	0.13	0.33	0.06	0.76	0.08
FLD12	70.87	3.00	14.62	0.73	3.56	0.26	4.37	0.17	0.87	0.06	2.94	0.13	0.31	0.06	0.56	0.07
FLD12	66.95	2.83	17.74	0.87	4.05	0.29	4.21	0.16	2.11	0.10	3.41	0.14	0.42	0.06	0.62	0.08
FLD12	72.77	3.07	13.03	0.65	3.57	0.26	4.18	0.16	1.48	0.08	3.18	0.14	0.20	0.05	0.60	0.08
FLD12	70.83	2.99	13.52	0.68	3.22	0.24	4.20	0.16	1.09	0.07	3.26	0.14	0.40	0.06	0.55	0.07
FLD12	68.77	2.91	16.27	0.80	3.93	0.28	4.17	0.16	1.71	0.09	3.32	0.14	0.36	0.06	1.01	0.10
FLD12	75.63	3.19	14.82	0.74	2.74	0.21	3.39	0.14	2.63	0.12	2.61	0.12	0.30	0.06	0.59	0.08
FLD12	76.41	3.23	13.93	0.70	2.68	0.20	3.23	0.13	2.02	0.10	2.82	0.12	0.18	0.05	0.69	0.08
FLD12	74.20	3.13	13.96	0.70	3.33	0.24	4.13	0.16	1.73	0.09	3.32	0.14	0.38	0.06	0.84	0.09

FLD12	70.26	2.97	15.74	0.78	3.64	0.26	4.36	0.17	1.79	0.09	3.22	0.14	0.46	0.06	0.92	0.09
FLD12	74.62	3.15	14.03	0.70	3.17	0.23	3.71	0.15	1.41	0.08	2.62	0.12	0.35	0.06	0.56	0.07
FLD12	72.47	3.06	13.63	0.68	3.36	0.25	4.06	0.16	1.54	0.08	2.99	0.13	0.47	0.06	0.69	0.08
FLD12	75.58	3.19	14.58	0.73	2.69	0.20	3.17	0.13	1.84	0.09	2.88	0.13	0.37	0.06	0.65	0.08
FLD12	69.89	2.96	14.58	0.73	3.81	0.27	4.19	0.16	1.99	0.10	4.87	0.19	0.60	0.07	0.76	0.09
FLD12	68.50	2.90	15.75	0.78	3.74	0.27	4.18	0.16	1.91	0.10	3.90	0.16	0.41	0.06	0.96	0.10
FLD12	71.57	3.02	12.75	0.64	3.30	0.24	4.16	0.16	1.18	0.07	3.02	0.13	0.58	0.06	0.73	0.08
FLD12	70.92	3.00	17.08	0.84	3.76	0.27	4.13	0.16	2.22	0.11	3.81	0.16	0.54	0.06	1.10	0.10
FLD12	72.58	3.07	13.72	0.69	3.52	0.26	4.41	0.17	1.44	0.08	3.21	0.14	0.34	0.06	0.69	0.08
FLD12	70.35	2.97	16.49	0.81	4.01	0.29	4.40	0.17	2.15	0.10	3.45	0.14	0.37	0.06	0.80	0.09
FLD12	73.92	3.12	14.21	0.71	2.62	0.20	3.30	0.13	1.89	0.10	2.59	0.12	0.39	0.06	0.61	0.08
FLD12	74.20	3.13	14.72	0.73	3.02	0.22	3.45	0.14	2.00	0.10	2.68	0.12	0.18	0.05	0.63	0.08
FLD12	68.47	2.90	15.07	0.75	3.75	0.27	3.96	0.15	2.09	0.10	4.37	0.17	0.71	0.07	0.92	0.09
FLD12	68.05	2.88	17.05	0.84	4.05	0.29	4.18	0.16	2.14	0.10	3.46	0.14	0.53	0.06	0.96	0.10
FLD12	72.15	3.05	14.00	0.70	3.75	0.27	4.58	0.17	1.03	0.07	2.88	0.13	0.31	0.06	0.66	0.08
FLD12	72.07	3.05	15.31	0.76	3.75	0.27	4.38	0.17	1.68	0.09	2.74	0.12	0.37	0.06	0.67	0.08
FLD12	71.09	3.01	16.60	0.82	4.00	0.29	4.23	0.16	1.93	0.10	3.43	0.14	0.49	0.06	0.94	0.09
FLD12	71.93	3.04	13.97	0.70	3.44	0.25	4.30	0.16	1.21	0.08	3.45	0.14	0.42	0.06	0.67	0.08
FLD12	69.23	2.93	14.17	0.71	3.50	0.25	4.09	0.16	1.96	0.10	3.59	0.15	0.46	0.06	0.88	0.09
FLD12	71.15	3.01	14.67	0.73	3.52	0.26	4.24	0.16	1.87	0.09	3.01	0.13	0.41	0.06	0.83	0.09
FLD12	70.37	2.97	15.22	0.76	3.56	0.26	4.14	0.16	1.63	0.09	2.97	0.13	0.45	0.06	0.85	0.09
FLD12	68.66	2.90	15.17	0.75	3.56	0.26	3.83	0.15	2.15	0.10	4.71	0.18	0.49	0.06	0.96	0.10
FLD12	73.93	3.12	13.83	0.69	3.64	0.26	4.14	0.16	1.62	0.09	2.83	0.13	0.40	0.06	0.74	0.08
FLD12	69.16	2.92	17.26	0.85	3.83	0.27	4.23	0.16	2.66	0.12	2.44	0.11	0.47	0.06	0.63	0.08
FLD12	70.91	3.00	15.51	0.77	3.68	0.27	4.11	0.16	1.45	0.08	3.15	0.13	0.33	0.06	0.83	0.09
FLD12	74.43	3.14	14.02	0.70	3.27	0.24	4.10	0.16	1.69	0.09	2.67	0.12	0.51	0.06	0.78	0.09
FLD12	72.42	3.06	14.88	0.74	3.57	0.26	3.96	0.15	2.10	0.10	2.75	0.12	0.32	0.06	0.87	0.09
FLD12	72.72	3.07	13.87	0.69	3.59	0.26	4.36	0.17	1.68	0.09	2.97	0.13	0.29	0.06	0.54	0.07
FLD12	69.44	2.94	15.28	0.76	3.90	0.28	4.53	0.17	1.46	0.08	3.31	0.14	0.37	0.06	0.90	0.09
FLD12	72.05	3.04	13.68	0.68	3.75	0.27	4.15	0.16	1.67	0.09	3.02	0.13	0.32	0.06	0.75	0.08
FLD12	69.24	2.93	20.63	1.01	5.15	0.36	8.17	0.28	0.20	0.04	0.07	0.04	0.03	0.05	0.27	0.06
FLD12	75.64	3.19	13.64	0.68	3.16	0.23	4.87	0.18	1.53	0.08	2.73	0.12	0.27	0.05	0.62	0.08
FLD12	71.77	3.03	13.18	0.66	3.03	0.23	4.54	0.17	1.39	0.08	2.52	0.12	0.34	0.06	0.61	0.08
FLD12	72.44	3.06	13.81	0.69	3.33	0.24	4.05	0.16	1.73	0.09	3.04	0.13	0.42	0.06	0.77	0.09
FLD12	71.06	3.00	14.64	0.73	3.55	0.26	4.54	0.17	1.08	0.07	2.85	0.13	0.45	0.06	0.75	0.08
FLD12	79.06	3.33	13.29	0.67	2.98	0.22	3.58	0.14	0.82	0.06	2.25	0.11	0.27	0.05	0.64	0.08
FLD12	71.65	3.03	16.24	0.80	3.59	0.26	4.03	0.16	1.45	0.08	3.03	0.13	0.38	0.06	0.91	0.09
FLD12	69.94	2.96	14.21	0.71	3.95	0.28	4.42	0.17	0.87	0.06	2.73	0.12	0.32	0.06	0.70	0.08
FLD12	73.47	3.10	11.71	0.59	3.57	0.26	4.34	0.17	0.74	0.06	2.74	0.12	0.20	0.05	0.12	0.05
FLD12	71.72	3.03	13.34	0.67	4.25	0.30	4.37	0.17	1.14	0.07	3.37	0.14	0.39	0.06	0.51	0.07
FLD12	73.53	3.11	14.69	0.73	3.59	0.26	3.91	0.15	1.83	0.09	3.07	0.13	0.46	0.06	0.78	0.09
FLD12	73.77	3.12	12.49	0.63	3.90	0.28	4.13	0.16	1.72	0.09	2.83	0.13	0.32	0.06	0.72	0.08
FLD12	70.82	2.99	15.66	0.78	3.97	0.28	4.41	0.17	1.13	0.07	3.35	0.14	0.38	0.06	0.64	0.08
FLD12	73.71	3.11	13.50	0.68	3.36	0.25	3.95	0.15	1.78	0.09	2.78	0.12	0.35	0.06	0.69	0.08
FLD12	74.82	3.16	13.07	0.66	3.80	0.27	4.29	0.16	1.61	0.09	2.67	0.12	0.34	0.06	0.71	0.08
FLD12	74.28	3.14	13.83	0.69	3.46	0.25	4.05	0.16	1.69	0.09	2.74	0.12	0.32	0.06	0.74	0.08
FLD12	71.88	3.04	14.96	0.74	3.62	0.26	3.86	0.15	1.75	0.09	2.98	0.13	0.41	0.06	0.84	0.09
FLD12	73.17	3.09	14.39	0.72	3.74	0.27	4.11	0.16	1.86	0.09	2.72	0.12	0.34	0.06	0.68	0.08
FLD12	73.19	3.09	12.81	0.64	3.32	0.24	4.22	0.16	1.29	0.08	2.86	0.13	0.38	0.06	0.73	0.08
FLD12	73.01	3.08	13.67	0.68	3.59	0.26	4.13	0.16	1.55	0.09	2.85	0.13	0.32	0.06	0.75	0.08
FLD12	70.96	3.00	14.87	0.74	3.75	0.27	4.26	0.16	1.59	0.09	3.26	0.14	0.40	0.06	0.84	0.09
FLD12	72.24	3.05	15.32	0.76	3.92	0.28	4.11	0.16	1.97	0.10	3.03	0.13	0.38	0.06	0.81	0.09
FLD12	74.65	3.15	14.16	0.71	3.68	0.27	3.94	0.15	1.63	0.09	2.84	0.13	0.43	0.06	0.67	0.08
FLD12	73.33	3.10	14.89	0.74	3.05	0.23	3.60	0.14	2.14	0.10	2.59	0.12	0.41	0.06	0.60	0.08
FLD12	70.55	2.98	15.89	0.79	3.88	0.28	4.13	0.16	1.91	0.10	3.17	0.14	0.39	0.06	0.87	0.09
FLD12	74.63	3.15	14.66	0.73	3.64	0.26	3.88	0.15	1.67	0.09	3.05	0.13	0.39	0.06	0.94	0.09
FLD12	70.69	2.99	14.50	0.72	3.46	0.25	4.13	0.16	2.19	0.10	3.08	0.13	0.46	0.06	0.88	0.09
FLD12	71.39	3.02	13.52	0.68	3.31	0.24	3.90	0.15	1.86	0.09	2.84	0.13	0.33	0.06	0.71	0.08
FLD12	72.71	3.07	13.98	0.70	3.53	0.26	4.15	0.16	1.68	0.09	2.75	0.12	0.36	0.06	0.74	0.08
FLD12	70.50	2.98	13.29	0.67	3.37	0.25	4.10	0.16	1.74	0.09	2.77	0.12	0.38	0.06	0.63	0.08
FLD12	69.90	2.96	14.33	0.71	3.51	0.25	4.16	0.16	1.54	0.08	3.56	0.15	0.38	0.06	0.83	0.09
FLD12	78.22	3.30	11.86	0.60	2.96	0.22	3.84	0.15	0.86	0.06	2.23	0.11	0.30	0.06	0.46	0.07

FLD12	68.65	2.90	14.95	0.74	3.51	0.25	4.35	0.17	1.26	0.08	3.25	0.14	0.55	0.06	0.65	0.08
FLD12	74.64	3.15	13.10	0.66	3.40	0.25	4.23	0.16	1.26	0.08	2.76	0.12	0.20	0.05	0.75	0.08
FLD12	72.74	3.07	14.51	0.72	2.83	0.21	3.21	0.13	1.98	0.10	2.86	0.13	0.33	0.06	0.74	0.08
FLD12	73.09	3.09	13.78	0.69	3.47	0.25	3.94	0.15	1.78	0.09	2.67	0.12	0.38	0.06	0.70	0.08
FLD12	74.31	3.14	13.94	0.70	3.44	0.25	3.86	0.15	1.81	0.09	2.83	0.13	0.44	0.06	0.77	0.09
FLD12	75.93	3.21	13.81	0.69	2.83	0.21	3.35	0.14	2.69	0.12	2.63	0.12	0.35	0.06	0.62	0.08
FLD12	72.19	3.05	14.49	0.72	3.39	0.25	3.86	0.15	1.88	0.10	3.16	0.14	0.35	0.06	0.74	0.08
FLD12	75.04	3.17	13.78	0.69	3.09	0.23	3.40	0.14	2.61	0.12	2.98	0.13	0.30	0.06	0.61	0.08
FLD12	69.57	2.94	13.58	0.68	4.13	0.29	4.09	0.16	3.44	0.14	2.78	0.12	0.31	0.06	0.68	0.08
FLD12	71.80	3.03	14.49	0.72	3.39	0.25	4.02	0.16	1.82	0.09	2.93	0.13	0.35	0.06	0.72	0.08
FLD12	73.47	3.10	13.33	0.67	3.59	0.26	4.13	0.16	2.29	0.11	3.81	0.16	0.46	0.06	1.17	0.11
FLD12	73.97	3.12	12.86	0.65	3.60	0.26	4.00	0.16	1.68	0.09	2.78	0.12	0.27	0.05	0.69	0.08
FLD12	76.29	3.22	12.74	0.64	2.98	0.22	3.59	0.14	1.72	0.09	2.83	0.12	0.22	0.05	0.65	0.08
FLD12	72.23	3.05	15.09	0.75	3.25	0.24	3.91	0.15	1.27	0.08	3.08	0.13	0.44	0.06	0.88	0.09
FLD12	72.28	3.05	13.06	0.65	2.87	0.21	3.29	0.13	2.47	0.11	2.65	0.12	0.30	0.06	0.58	0.08
FLD12	73.64	3.11	13.90	0.69	3.54	0.26	4.07	0.16	1.83	0.09	3.14	0.13	0.41	0.06	0.78	0.09
FLD12	74.65	3.15	13.46	0.67	3.20	0.24	3.94	0.15	1.75	0.09	2.80	0.12	0.48	0.06	0.77	0.09
FLD12	77.07	3.25	13.98	0.70	2.67	0.20	3.13	0.13	2.77	0.12	2.57	0.12	0.24	0.05	0.65	0.08
FLD12	71.60	3.03	13.98	0.70	3.33	0.24	3.83	0.15	1.89	0.10	3.08	0.13	0.38	0.06	0.71	0.08
FLD12	76.19	3.22	14.01	0.70	2.95	0.22	3.44	0.14	2.29	0.11	2.61	0.12	0.31	0.06	0.59	0.08
FLD12	73.30	3.10	14.49	0.72	3.52	0.26	4.13	0.16	1.79	0.09	2.70	0.12	0.31	0.06	0.60	0.08
FLD12	73.86	3.12	14.44	0.72	3.37	0.25	3.97	0.15	1.81	0.09	2.86	0.13	0.33	0.06	0.70	0.08
FLD12	73.42	3.10	12.05	0.61	3.80	0.27	4.45	0.17	1.29	0.08	2.81	0.12	0.22	0.05	0.58	0.08
FLD12	70.82	2.99	18.85	0.92	4.48	0.31	4.74	0.18	1.66	0.09	2.02	0.10	0.19	0.05	0.65	0.08
FLD12	75.20	3.18	15.08	0.75	3.09	0.23	3.55	0.14	1.94	0.10	2.71	0.12	0.34	0.06	0.63	0.08
FLD12	72.77	3.07	14.00	0.70	2.72	0.21	3.24	0.13	1.87	0.09	2.79	0.12	0.31	0.06	0.63	0.08
FLD12	71.26	3.01	14.91	0.74	3.62	0.26	4.12	0.16	1.18	0.07	3.01	0.13	0.40	0.06	0.83	0.09
FLD12	75.12	3.17	14.20	0.71	3.52	0.26	4.14	0.16	1.53	0.08	2.81	0.12	0.34	0.06	0.64	0.08
FLD12	71.47	3.02	12.71	0.64	3.52	0.26	4.08	0.16	1.80	0.09	3.29	0.14	0.31	0.06	0.76	0.09
FLD12	74.55	3.15	13.70	0.68	3.35	0.25	3.83	0.15	2.35	0.11	2.70	0.12	0.33	0.06	0.65	0.08
FLD12	71.95	3.04	14.39	0.72	3.40	0.25	3.88	0.15	1.90	0.10	2.96	0.13	0.39	0.06	0.78	0.09
FLD12	75.92	3.20	14.02	0.70	3.29	0.24	3.68	0.15	2.58	0.12	2.80	0.12	0.22	0.05	0.66	0.08
FLD12	72.73	3.07	13.68	0.68	3.42	0.25	3.91	0.15	2.78	0.12	2.78	0.12	0.31	0.06	0.66	0.08
FLD12	74.45	3.14	14.02	0.70	3.29	0.24	3.87	0.15	1.72	0.09	2.76	0.12	0.26	0.05	0.71	0.08
FLD12	73.00	3.08	13.49	0.67	4.00	0.28	4.32	0.17	0.95	0.07	3.21	0.14	0.21	0.05	0.56	0.07
FLD12	73.18	3.09	13.31	0.67	3.46	0.25	4.04	0.16	1.80	0.09	2.90	0.13	0.32	0.06	0.65	0.08
FLD12	73.77	3.12	13.30	0.67	3.93	0.28	4.33	0.17	1.54	0.08	2.81	0.12	0.36	0.06	0.67	0.08
FLD12	70.83	2.99	14.11	0.70	3.69	0.27	3.93	0.15	2.03	0.10	3.27	0.14	0.48	0.06	0.75	0.08
FLD12	77.60	3.27	13.21	0.66	2.27	0.18	3.60	0.14	0.61	0.06	1.54	0.09	0.05	0.05	0.49	0.07
FLD12	73.20	3.09	13.88	0.69	3.69	0.27	4.00	0.16	2.41	0.11	3.22	0.14	0.34	0.06	0.81	0.09
FLD12	75.69	3.20	12.79	0.64	3.28	0.24	4.24	0.16	1.07	0.07	2.55	0.12	0.28	0.06	0.52	0.07
FLD12	73.54	3.11	14.80	0.74	3.29	0.24	4.21	0.16	1.24	0.08	2.56	0.12	0.33	0.06	0.66	0.08
FLD12	71.79	3.03	14.21	0.71	4.24	0.30	4.43	0.17	1.50	0.08	3.29	0.14	0.46	0.06	0.66	0.08
FLD12	76.34	3.22	11.57	0.59	3.28	0.24	3.90	0.15	1.73	0.09	3.00	0.13	0.33	0.06	0.71	0.08
FLD12	65.07	2.76	16.12	0.80	4.46	0.31	4.56	0.17	1.67	0.09	3.79	0.15	0.44	0.06	0.81	0.09
FLD12	70.85	2.99	15.02	0.75	3.58	0.26	4.03	0.16	1.99	0.10	3.27	0.14	0.45	0.06	0.85	0.09
FLD12	72.05	3.04	14.19	0.71	4.33	0.31	4.49	0.17	1.02	0.07	3.23	0.14	0.32	0.06	0.55	0.07
FLD12	74.15	3.13	14.18	0.71	3.33	0.24	4.00	0.16	1.70	0.09	2.85	0.13	0.33	0.06	0.71	0.08
FLD12	74.15	3.13	13.87	0.69	3.72	0.27	4.19	0.16	0.94	0.07	2.88	0.13	0.19	0.05	0.40	0.07
FLD12	75.42	3.18	14.16	0.71	3.63	0.26	3.98	0.16	2.07	0.10	3.10	0.13	0.32	0.06	1.10	0.10
FLD12	75.31	3.18	11.64	0.59	3.61	0.26	3.97	0.15	1.51	0.08	3.18	0.14	0.35	0.06	0.69	0.08
FLD12	72.91	3.08	14.75	0.73	3.71	0.27	4.24	0.16	1.94	0.10	3.17	0.14	0.40	0.06	0.80	0.09
FLD12	71.70	3.03	13.87	0.69	3.50	0.25	4.30	0.17	1.90	0.10	2.94	0.13	0.43	0.06	0.74	0.08
FLD12	73.52	3.11	13.84	0.69	3.36	0.25	3.75	0.15	1.87	0.09	2.63	0.12	0.28	0.05	0.61	0.08
FLD12	73.30	3.10	14.18	0.71	3.43	0.25	4.15	0.16	1.64	0.09	3.07	0.13	0.36	0.06	0.95	0.10
FLD12	85.83	3.62	8.52	0.45	2.35	0.18	3.30	0.13	0.53	0.05	2.35	0.11	0.19	0.05	0.50	0.07
FLD12	72.62	3.07	14.01	0.70	3.46	0.25	4.20	0.16	1.27	0.08	2.71	0.12	0.43	0.06	0.84	0.09
FLD12	74.60	3.15	13.75	0.69	3.54	0.26	4.15	0.16	1.61	0.09	3.08	0.13	0.42	0.06	0.71	0.08
FLD12	69.64	2.94	15.05	0.75	3.65	0.26	4.21	0.16	1.24	0.08	3.31	0.14	0.40	0.06	0.71	0.08
FLD12	73.72	3.11	14.73	0.73	3.81	0.27	4.11	0.16	1.76	0.09	3.17	0.14	0.30	0.06	0.74	0.08
FLD12	71.42	3.02	13.67	0.68	3.85	0.28	4.45	0.17	0.94	0.07	3.45	0.14	0.35	0.06	0.43	0.07
FLD12	71.99	3.04	14.70	0.73	3.55	0.26	4.04	0.16	1.89	0.10	3.28	0.14	0.29	0.06	0.86	0.09

FLD12	72.44	3.06	13.85	0.69	3.64	0.26	4.27	0.16	1.21	0.07	3.18	0.14	0.44	0.06	0.70	0.08
FLD12	78.80	3.32	12.49	0.63	3.25	0.24	3.88	0.15	1.31	0.08	2.82	0.12	0.35	0.06	0.64	0.08
FLD12	74.22	3.13	15.03	0.75	3.71	0.27	4.60	0.17	0.96	0.07	1.51	0.08	0.26	0.05	0.45	0.07
FLD12	75.71	3.20	13.50	0.68	3.40	0.25	4.03	0.16	1.39	0.08	2.76	0.12	0.26	0.05	0.71	0.08
FLD12	73.56	3.11	13.94	0.70	3.69	0.27	4.33	0.17	1.63	0.09	2.87	0.13	0.34	0.06	0.68	0.08
FLD12	75.74	3.20	13.13	0.66	3.85	0.28	4.18	0.16	1.64	0.09	3.46	0.14	0.34	0.06	0.54	0.07
FLD12	73.97	3.12	13.57	0.68	3.52	0.26	4.11	0.16	1.80	0.09	2.62	0.12	0.40	0.06	0.68	0.08
FLD12	72.49	3.06	14.13	0.70	3.72	0.27	4.28	0.16	1.92	0.10	3.30	0.14	0.46	0.06	0.85	0.09
FLD12	71.31	3.01	14.29	0.71	3.65	0.26	4.14	0.16	1.37	0.08	3.43	0.14	0.55	0.06	0.93	0.09
FLD12	76.39	3.22	14.05	0.70	3.57	0.26	4.07	0.16	1.41	0.08	2.77	0.12	0.15	0.05	0.66	0.08
FLD12	73.26	3.09	13.53	0.68	3.68	0.27	4.29	0.16	1.05	0.07	3.33	0.14	0.35	0.06	0.45	0.07
FLD12	74.31	3.14	13.05	0.65	3.39	0.25	4.15	0.16	1.55	0.09	2.83	0.13	0.38	0.06	0.68	0.08
FLD12	71.14	3.01	13.18	0.66	3.63	0.26	4.37	0.17	1.05	0.07	3.26	0.14	0.37	0.06	0.52	0.07
FLD12	72.29	3.05	12.86	0.65	3.45	0.25	4.04	0.16	1.65	0.09	2.79	0.12	0.33	0.06	0.80	0.09
FLD12	78.48	3.31	11.32	0.57	3.16	0.23	3.94	0.15	0.36	0.05	1.88	0.10	0.05	0.05	0.24	0.06
FLD12	74.39	3.14	14.44	0.72	3.65	0.26	4.12	0.16	1.58	0.09	3.05	0.13	0.32	0.06	0.66	0.08
FLD12	76.05	3.21	12.74	0.64	3.40	0.25	4.16	0.16	0.63	0.06	2.58	0.12	0.15	0.05	0.34	0.06
FLD12	73.31	3.10	14.22	0.71	3.49	0.25	3.99	0.16	1.90	0.10	3.10	0.13	0.35	0.06	0.70	0.08
FLD12	69.92	2.96	16.09	0.80	4.01	0.29	4.19	0.16	1.43	0.08	3.58	0.15	0.45	0.06	0.68	0.08
FLD12	75.61	3.19	13.90	0.69	3.39	0.25	3.84	0.15	1.52	0.08	2.61	0.12	0.28	0.05	0.70	0.08
FLD12	72.16	3.05	15.34	0.76	3.70	0.27	4.26	0.16	1.33	0.08	2.22	0.11	0.31	0.06	0.59	0.08
FLD12	75.22	3.18	13.89	0.69	3.81	0.27	4.24	0.16	1.80	0.09	2.88	0.13	0.28	0.06	0.65	0.08
FLD12	75.66	3.19	11.67	0.59	3.31	0.24	4.13	0.16	0.67	0.06	2.61	0.12	0.03	0.05	0.31	0.06
FLD12	74.18	3.13	13.67	0.68	3.32	0.24	3.98	0.16	1.88	0.10	2.84	0.13	0.37	0.06	0.71	0.08
FLD12	69.90	2.96	14.76	0.73	3.69	0.27	4.16	0.16	1.56	0.09	3.26	0.14	0.26	0.05	0.79	0.09
FLD12	74.63	3.15	14.18	0.71	3.48	0.25	4.15	0.16	1.78	0.09	2.72	0.12	0.33	0.06	0.64	0.08
FLD12	73.72	3.11	14.10	0.70	3.76	0.27	4.33	0.17	1.88	0.10	2.62	0.12	0.31	0.06	0.68	0.08
FLD12	69.51	2.94	19.17	0.94	4.18	0.30	4.39	0.17	1.73	0.09	2.00	0.10	0.21	0.05	0.62	0.08
FLD12	74.71	3.15	12.52	0.63	3.43	0.25	4.14	0.16	1.51	0.08	2.77	0.12	0.33	0.06	0.61	0.08
FLD12	70.76	2.99	16.14	0.80	3.92	0.28	4.25	0.16	1.64	0.09	3.05	0.13	0.37	0.06	0.68	0.08
FLD12	68.86	2.91	17.66	0.87	3.89	0.28	4.14	0.16	2.24	0.11	3.22	0.14	0.34	0.06	1.00	0.10
FLD12	77.50	3.27	10.80	0.55	3.65	0.26	4.29	0.16	2.27	0.11	2.72	0.12	0.18	0.05	0.62	0.08
FLD12	73.75	3.12	14.26	0.71	3.83	0.27	4.40	0.17	1.52	0.08	3.02	0.13	0.54	0.06	0.76	0.08
FLD12	73.06	3.09	16.45	0.81	3.96	0.28	4.01	0.16	2.01	0.10	2.97	0.13	0.34	0.06	0.91	0.09
FLD12	73.45	3.10	15.15	0.75	3.66	0.26	4.09	0.16	1.31	0.08	2.37	0.11	0.43	0.06	0.73	0.08
FLD12	76.02	3.21	13.43	0.67	3.60	0.26	4.42	0.17	2.09	0.10	2.73	0.12	0.36	0.06	0.77	0.09
FLD12	73.33	3.10	14.79	0.74	3.62	0.26	3.94	0.15	2.15	0.10	2.98	0.13	0.44	0.06	0.87	0.09
FLD12	70.22	2.97	15.26	0.76	3.50	0.25	4.02	0.16	1.58	0.09	3.75	0.15	0.58	0.06	0.99	0.10
FLD12	68.35	2.89	13.95	0.70	3.52	0.26	4.40	0.17	1.76	0.09	3.54	0.15	0.53	0.06	0.76	0.09
FLD12	71.82	3.04	15.43	0.76	3.49	0.25	3.92	0.15	1.67	0.09	4.02	0.16	0.54	0.06	0.95	0.10
FLD12	71.62	3.03	14.61	0.73	3.74	0.27	4.17	0.16	2.11	0.10	3.99	0.16	0.55	0.06	1.33	0.11
FLD12	74.30	3.14	13.00	0.65	3.26	0.24	4.03	0.16	1.34	0.08	3.13	0.13	0.31	0.06	0.92	0.09
FLD12	68.79	2.91	16.54	0.82	4.06	0.29	4.37	0.17	1.85	0.09	3.24	0.14	0.43	0.06	0.72	0.08
FLD12	68.87	2.91	16.18	0.80	3.94	0.28	4.44	0.17	1.89	0.10	3.28	0.14	0.38	0.06	0.78	0.09
FLD12	71.21	3.01	14.51	0.72	3.95	0.28	4.32	0.17	1.46	0.08	2.69	0.12	0.34	0.06	0.58	0.08
FLD13	75.67	3.19	14.40	0.72	2.96	0.22	3.28	0.13	3.47	0.14	2.83	0.13	0.26	0.05	0.65	0.08
FLD13	74.21	3.13	14.25	0.71	3.14	0.23	3.52	0.14	4.30	0.17	2.92	0.13	0.29	0.06	0.73	0.08
FLD13	74.22	3.13	13.93	0.70	3.06	0.23	3.44	0.14	3.46	0.14	2.61	0.12	0.27	0.05	0.64	0.08
FLD13	73.37	3.10	13.63	0.68	2.98	0.22	3.41	0.14	3.06	0.13	2.65	0.12	0.19	0.05	0.59	0.08
FLD13	73.90	3.12	13.76	0.69	3.00	0.22	3.35	0.14	3.40	0.14	2.65	0.12	0.30	0.06	0.59	0.08
FLD13	72.74	3.07	13.26	0.66	2.77	0.21	3.48	0.14	3.37	0.14	2.78	0.12	0.24	0.05	0.54	0.07
FLD13	75.03	3.17	13.52	0.68	3.06	0.23	3.49	0.14	3.61	0.15	2.61	0.12	0.26	0.05	0.67	0.08
FLD13	72.40	3.06	13.60	0.68	2.95	0.22	3.31	0.13	3.55	0.15	2.57	0.12	0.27	0.05	0.55	0.07
FLD13	75.00	3.17	14.13	0.70	2.99	0.22	3.28	0.13	3.27	0.14	2.61	0.12	0.24	0.05	0.56	0.07
FLD13	75.65	3.19	13.51	0.68	3.11	0.23	3.38	0.14	3.43	0.14	2.66	0.12	0.25	0.05	0.56	0.07
FLD13	74.67	3.15	13.45	0.67	3.03	0.22	3.33	0.14	3.25	0.14	2.72	0.12	0.30	0.06	0.56	0.07
FLD13	76.17	3.22	13.82	0.69	3.18	0.23	3.31	0.13	3.19	0.13	2.68	0.12	0.24	0.05	0.58	0.08
FLD13	74.28	3.14	14.59	0.73	2.95	0.22	3.30	0.13	3.29	0.14	2.68	0.12	0.40	0.06	0.63	0.08
FLD13	76.21	3.22	14.14	0.71	3.12	0.23	3.29	0.13	3.31	0.14	2.64	0.12	0.23	0.05	0.58	0.08
FLD13	72.92	3.08	13.37	0.67	2.85	0.21	3.31	0.13	3.33	0.14	2.75	0.12	0.24	0.05	0.55	0.07
FLD13	76.52	3.23	13.87	0.69	3.09	0.23	3.27	0.13	3.14	0.13	2.64	0.12	0.23	0.05	0.58	0.08
FLD13	75.17	3.17	13.77	0.69	2.84	0.21	3.33	0.14	3.24	0.14	2.62	0.12	0.21	0.05	0.59	0.08

FLD13	75.67	3.19	14.44	0.72	3.00	0.22	3.44	0.14	3.40	0.14	2.58	0.12	0.31	0.06	0.60	0.08
FLD13	76.24	3.22	14.09	0.70	3.02	0.22	3.30	0.13	3.39	0.14	2.75	0.12	0.35	0.06	0.53	0.07
FLD13	74.87	3.16	13.70	0.68	2.99	0.22	3.50	0.14	3.51	0.14	2.73	0.12	0.27	0.05	0.60	0.08
FLD13	73.77	3.12	14.37	0.72	2.79	0.21	3.07	0.13	3.09	0.13	2.33	0.11	0.33	0.06	0.56	0.07
FLD13	76.57	3.23	14.03	0.70	3.17	0.23	3.43	0.14	3.16	0.13	2.57	0.12	0.32	0.06	0.60	0.08
FLD13	74.89	3.16	13.77	0.69	2.97	0.22	3.35	0.14	3.30	0.14	2.60	0.12	0.30	0.06	0.56	0.07
FLD13	75.44	3.19	13.91	0.69	3.04	0.23	3.23	0.13	3.18	0.13	2.70	0.12	0.22	0.05	0.55	0.07
FLD13	76.50	3.23	14.22	0.71	3.19	0.24	3.25	0.13	3.13	0.13	2.51	0.12	0.29	0.06	0.60	0.08
FLD13	76.04	3.21	14.11	0.70	3.15	0.23	3.26	0.13	3.22	0.14	2.57	0.12	0.28	0.05	0.63	0.08
FLD13	74.69	3.15	13.66	0.68	2.94	0.22	3.43	0.14	3.46	0.14	2.76	0.12	0.19	0.05	0.57	0.08
FLD13	76.53	3.23	14.36	0.72	2.85	0.21	3.12	0.13	3.17	0.13	2.75	0.12	0.19	0.05	0.63	0.08
FLD13	76.23	3.22	13.89	0.69	2.94	0.22	3.53	0.14	2.92	0.13	2.56	0.12	0.35	0.06	0.64	0.08
FLD13	71.40	3.02	17.02	0.84	2.92	0.22	2.98	0.12	3.60	0.15	3.22	0.14	0.40	0.06	0.76	0.09
FLD13	76.13	3.21	14.44	0.72	2.90	0.22	3.15	0.13	3.16	0.13	2.64	0.12	0.27	0.05	0.55	0.07
FLD13	75.21	3.18	14.92	0.74	3.21	0.24	3.37	0.14	3.54	0.15	2.67	0.12	0.30	0.06	0.63	0.08
FLD13	72.16	3.05	12.96	0.65	2.94	0.22	3.34	0.14	3.63	0.15	2.69	0.12	0.21	0.05	0.53	0.07
FLD13	74.14	3.13	13.66	0.68	3.04	0.23	3.37	0.14	3.40	0.14	2.45	0.11	0.24	0.05	0.58	0.08
FLD13	76.27	3.22	13.74	0.69	2.95	0.22	3.39	0.14	3.17	0.13	2.55	0.12	0.21	0.05	0.56	0.07
FLD13	75.25	3.18	13.56	0.68	2.80	0.21	3.39	0.14	3.28	0.14	2.61	0.12	0.31	0.06	0.58	0.08
FLD13	76.86	3.24	13.98	0.70	2.90	0.22	3.33	0.14	3.37	0.14	2.42	0.11	0.23	0.05	0.61	0.08
FLD13	73.93	3.12	13.86	0.69	2.69	0.20	3.28	0.13	2.30	0.11	2.89	0.13	0.41	0.06	0.58	0.08
FLD13	75.42	3.18	13.88	0.69	2.95	0.22	3.34	0.14	3.16	0.13	2.78	0.12	0.36	0.06	0.66	0.08
FLD13	75.01	3.17	13.85	0.69	3.00	0.22	3.29	0.13	3.28	0.14	2.47	0.11	0.30	0.06	0.60	0.08
FLD13	75.72	3.20	13.40	0.67	3.07	0.23	3.44	0.14	3.25	0.14	2.52	0.12	0.23	0.05	0.54	0.07
FLD13	75.62	3.19	13.09	0.66	3.06	0.23	3.36	0.14	3.30	0.14	2.37	0.11	0.29	0.06	0.61	0.08
FLD13	75.26	3.18	13.85	0.69	2.86	0.21	3.45	0.14	3.25	0.14	2.82	0.12	0.29	0.06	0.57	0.07
FLD13	73.42	3.10	13.78	0.69	2.87	0.22	3.31	0.13	3.18	0.13	2.82	0.12	0.38	0.06	0.52	0.07
FLD13	76.39	3.22	13.56	0.68	2.94	0.22	3.34	0.14	3.22	0.14	2.78	0.12	0.27	0.05	0.66	0.08
FLD13	72.42	3.06	12.85	0.65	2.79	0.21	3.43	0.14	3.45	0.14	2.69	0.12	0.24	0.05	0.54	0.07
FLD13	75.85	3.20	13.63	0.68	3.07	0.23	3.48	0.14	3.29	0.14	2.78	0.12	0.20	0.05	0.64	0.08
FLD13	75.76	3.20	13.72	0.69	3.04	0.23	3.36	0.14	3.32	0.14	2.57	0.12	0.27	0.05	0.60	0.08
FLD13	76.45	3.23	13.61	0.68	3.09	0.23	3.38	0.14	3.38	0.14	2.66	0.12	0.14	0.05	0.59	0.08
FLD13	75.77	3.20	13.43	0.67	3.20	0.24	3.30	0.13	3.27	0.14	2.57	0.12	0.22	0.05	0.55	0.07
FLD13	74.98	3.17	13.36	0.67	3.17	0.23	3.29	0.13	3.40	0.14	2.61	0.12	0.16	0.05	0.60	0.08
FLD13	76.51	3.23	13.82	0.69	3.05	0.23	3.32	0.13	2.93	0.13	2.79	0.12	0.29	0.06	0.59	0.08
FLD13	76.48	3.23	14.09	0.70	2.95	0.22	3.48	0.14	3.26	0.14	2.80	0.12	0.22	0.05	0.67	0.08
FLD13	76.33	3.22	13.96	0.70	3.04	0.23	3.31	0.13	3.11	0.13	2.67	0.12	0.20	0.05	0.60	0.08
FLD13	75.77	3.20	14.17	0.71	3.09	0.23	3.41	0.14	3.43	0.14	2.66	0.12	0.22	0.05	0.65	0.08
FLD13	76.17	3.22	14.11	0.70	3.10	0.23	3.24	0.13	3.23	0.14	2.62	0.12	0.28	0.05	0.59	0.08
FLD13	75.37	3.18	14.05	0.70	3.08	0.23	3.33	0.14	3.27	0.14	2.51	0.12	0.16	0.05	0.57	0.07
FLD13	74.19	3.13	13.51	0.68	3.10	0.23	3.43	0.14	3.23	0.14	2.56	0.12	0.31	0.06	0.56	0.07
FLD13	75.82	3.20	13.73	0.69	2.76	0.21	3.35	0.14	3.35	0.14	2.53	0.12	0.28	0.05	0.55	0.07
FLD13	75.47	3.19	14.05	0.70	3.02	0.22	3.32	0.14	3.34	0.14	2.50	0.11	0.19	0.05	0.56	0.07
FLD13	75.06	3.17	13.75	0.69	2.94	0.22	3.34	0.14	3.17	0.13	2.83	0.13	0.25	0.05	0.60	0.08
FLD13	74.12	3.13	13.32	0.67	2.89	0.22	3.36	0.14	3.17	0.13	2.74	0.12	0.30	0.06	0.54	0.07
FLD13	75.01	3.17	13.44	0.67	2.96	0.22	3.41	0.14	3.18	0.13	2.87	0.13	0.22	0.05	0.50	0.07
FLD13	75.90	3.20	14.00	0.70	3.24	0.24	3.42	0.14	3.33	0.14	2.54	0.12	0.25	0.05	0.58	0.08
FLD13	74.26	3.14	14.18	0.71	2.97	0.22	3.27	0.13	3.34	0.14	2.75	0.12	0.28	0.05	0.63	0.08
FLD13	75.57	3.19	13.22	0.66	2.81	0.21	3.33	0.14	3.15	0.13	2.60	0.12	0.20	0.05	0.53	0.07
FLD13	74.65	3.15	13.27	0.67	2.95	0.22	3.40	0.14	3.20	0.13	2.58	0.12	0.23	0.05	0.54	0.07
FLD13	75.74	3.20	14.53	0.72	2.95	0.22	3.41	0.14	3.50	0.14	2.76	0.12	0.21	0.05	0.58	0.08
FLD13	75.15	3.17	14.03	0.70	3.03	0.23	3.19	0.13	3.12	0.13	2.77	0.12	0.28	0.06	0.58	0.08
FLD13	76.69	3.24	13.76	0.69	3.14	0.23	3.50	0.14	3.14	0.13	2.56	0.12	0.31	0.06	0.67	0.08
FLD13	75.40	3.18	13.50	0.68	3.15	0.23	3.67	0.15	3.09	0.13	2.62	0.12	0.28	0.06	0.58	0.08
FLD13	73.30	3.10	13.73	0.69	2.95	0.22	3.22	0.13	3.38	0.14	2.56	0.12	0.28	0.05	0.54	0.07
FLD13	75.85	3.20	14.12	0.70	2.81	0.21	3.41	0.14	3.53	0.14	2.60	0.12	0.28	0.05	0.61	0.08
FLD13	69.85	2.95	13.42	0.67	2.71	0.21	3.34	0.14	3.48	0.14	2.74	0.12	0.28	0.06	0.52	0.07
FLD13	73.56	3.11	13.73	0.69	2.98	0.22	3.51	0.14	3.37	0.14	3.14	0.13	0.20	0.05	0.67	0.08
FLD13	74.18	3.13	13.82	0.69	2.93	0.22	3.26	0.13	3.30	0.14	2.44	0.11	0.32	0.06	0.56	0.07
FLD13	75.77	3.20	13.61	0.68	3.06	0.23	3.51	0.14	3.26	0.14	2.61	0.12	0.32	0.06	0.53	0.07
FLD13	76.10	3.21	13.83	0.69	3.34	0.24	3.50	0.14	3.03	0.13	2.55	0.12	0.36	0.06	0.59	0.08
FLD13	74.74	3.16	13.59	0.68	3.09	0.23	3.37	0.14	3.21	0.14	2.62	0.12	0.25	0.05	0.56	0.07

FLD13	74.89	3.16	13.83	0.69	3.18	0.23	3.43	0.14	3.10	0.13	2.82	0.12	0.38	0.06	0.60	0.08
FLD13	76.50	3.23	14.10	0.70	2.97	0.22	3.24	0.13	3.24	0.14	2.59	0.12	0.21	0.05	0.58	0.08
FLD13	73.63	3.11	13.60	0.68	3.06	0.23	3.36	0.14	3.31	0.14	2.66	0.12	0.29	0.06	0.56	0.07
FLD13	74.53	3.15	14.34	0.71	3.02	0.22	3.23	0.13	3.26	0.14	2.64	0.12	0.18	0.05	0.69	0.08
FLD13	75.97	3.21	13.99	0.70	2.96	0.22	3.40	0.14	3.34	0.14	2.67	0.12	0.31	0.06	0.59	0.08
FLD13	75.51	3.19	13.81	0.69	2.93	0.22	3.45	0.14	3.26	0.14	2.63	0.12	0.33	0.06	0.55	0.07
FLD13	75.05	3.17	14.33	0.71	3.05	0.23	3.29	0.13	3.39	0.14	2.73	0.12	0.24	0.05	0.57	0.07
FLD13	76.60	3.23	13.85	0.69	2.92	0.22	3.27	0.13	3.24	0.14	2.63	0.12	0.19	0.05	0.53	0.07
FLD13	76.23	3.22	13.92	0.69	3.00	0.22	3.49	0.14	3.26	0.14	2.63	0.12	0.30	0.06	0.64	0.08
FLD13	76.29	3.22	14.29	0.71	3.13	0.23	3.37	0.14	3.16	0.13	2.72	0.12	0.22	0.05	0.52	0.07
FLD13	75.74	3.20	13.23	0.66	3.16	0.23	3.52	0.14	3.22	0.14	2.48	0.11	0.38	0.06	0.58	0.08
FLD13	75.43	3.18	13.95	0.70	3.16	0.23	3.38	0.14	3.21	0.14	2.81	0.12	0.29	0.06	0.59	0.08
FLD13	76.72	3.24	14.00	0.70	2.99	0.22	3.37	0.14	3.27	0.14	2.59	0.12	0.26	0.05	0.61	0.08
FLD13	75.41	3.18	13.65	0.68	3.00	0.22	3.35	0.14	3.24	0.14	2.54	0.12	0.24	0.05	0.60	0.08
FLD13	75.87	3.20	13.79	0.69	2.99	0.22	3.41	0.14	3.36	0.14	2.62	0.12	0.33	0.06	0.49	0.07
FLD13	75.79	3.20	13.98	0.70	3.20	0.24	3.46	0.14	3.20	0.14	2.83	0.12	0.19	0.05	0.60	0.08
FLD13	73.31	3.10	13.46	0.67	2.82	0.21	3.39	0.14	3.36	0.14	2.69	0.12	0.37	0.06	0.54	0.07
FLD13	74.12	3.13	13.54	0.68	3.11	0.23	3.45	0.14	3.17	0.13	2.46	0.11	0.35	0.06	0.57	0.08
FLD13	76.45	3.23	13.98	0.70	2.86	0.21	3.31	0.13	3.26	0.14	2.56	0.12	0.22	0.05	0.53	0.07
FLD13	73.88	3.12	13.77	0.69	3.00	0.22	3.30	0.13	3.39	0.14	2.66	0.12	0.18	0.05	0.53	0.07
FLD13	75.37	3.18	13.79	0.69	3.21	0.24	3.38	0.14	3.15	0.13	2.70	0.12	0.27	0.05	0.52	0.07
FLD13	75.35	3.18	14.14	0.71	2.98	0.22	3.28	0.13	3.24	0.14	2.65	0.12	0.30	0.06	0.60	0.08
FLD13	74.25	3.14	13.34	0.67	3.09	0.23	3.41	0.14	3.19	0.13	2.34	0.11	0.29	0.06	0.59	0.08
FLD13	75.45	3.19	13.90	0.69	3.18	0.23	3.35	0.14	3.11	0.13	2.80	0.12	0.32	0.06	0.60	0.08
FLD13	75.97	3.21	14.02	0.70	2.94	0.22	3.30	0.13	3.23	0.14	2.67	0.12	0.22	0.05	0.59	0.08
FLD13	74.72	3.16	14.12	0.70	3.05	0.23	3.32	0.13	3.27	0.14	2.66	0.12	0.28	0.05	0.60	0.08
FLD13	75.24	3.18	13.55	0.68	3.15	0.23	3.49	0.14	3.09	0.13	2.66	0.12	0.30	0.06	0.57	0.07
FLD13	75.28	3.18	13.82	0.69	3.09	0.23	3.27	0.13	3.18	0.13	2.73	0.12	0.29	0.06	0.57	0.08
FLD13	74.13	3.13	13.87	0.69	2.72	0.21	3.20	0.13	3.49	0.14	2.60	0.12	0.36	0.06	0.57	0.08
FLD13	76.04	3.21	13.90	0.69	3.01	0.22	3.52	0.14	3.28	0.14	2.65	0.12	0.24	0.05	0.56	0.07
FLD13	76.31	3.22	13.11	0.66	3.04	0.23	3.25	0.13	3.20	0.14	2.69	0.12	0.17	0.05	0.57	0.07
FLD13	75.93	3.21	13.76	0.69	2.96	0.22	3.25	0.13	3.16	0.13	2.44	0.11	0.24	0.05	0.54	0.07
FLD13	75.69	3.20	13.84	0.69	3.09	0.23	3.32	0.14	3.38	0.14	2.54	0.12	0.28	0.05	0.59	0.08
FLD13	76.31	3.22	13.85	0.69	3.27	0.24	3.46	0.14	3.16	0.13	2.47	0.11	0.31	0.06	0.54	0.07
FLD13	74.93	3.16	13.60	0.68	2.98	0.22	3.25	0.13	3.31	0.14	2.78	0.12	0.35	0.06	0.63	0.08
FLD13	75.40	3.18	13.97	0.70	3.03	0.22	3.28	0.13	3.31	0.14	2.59	0.12	0.23	0.05	0.58	0.08
FLD13	75.36	3.18	14.09	0.70	2.96	0.22	3.39	0.14	3.38	0.14	2.58	0.12	0.27	0.05	0.63	0.08
FLD13	76.57	3.23	14.03	0.70	3.05	0.23	3.40	0.14	3.23	0.14	2.71	0.12	0.32	0.06	0.59	0.08
FLD13	77.23	3.26	13.75	0.69	2.97	0.22	3.51	0.14	3.19	0.13	2.46	0.11	0.25	0.05	0.57	0.08
FLD13	76.68	3.24	13.74	0.69	2.75	0.21	3.36	0.14	3.22	0.14	2.51	0.11	0.17	0.05	0.61	0.08
FLD13	76.70	3.24	13.83	0.69	2.96	0.22	3.30	0.13	3.16	0.13	2.66	0.12	0.21	0.05	0.52	0.07
FLD13	77.17	3.26	13.38	0.67	2.91	0.22	3.35	0.14	3.35	0.14	2.58	0.12	0.27	0.05	0.45	0.07
FLD13	75.92	3.20	14.25	0.71	2.91	0.22	3.51	0.14	3.43	0.14	2.84	0.13	0.29	0.06	0.60	0.08
FLD13	74.94	3.16	13.58	0.68	2.85	0.21	3.28	0.13	3.29	0.14	2.67	0.12	0.30	0.06	0.52	0.07
FLD13	69.79	2.95	17.17	0.85	3.04	0.23	3.25	0.13	4.16	0.16	2.99	0.13	0.39	0.06	0.65	0.08
FLD13	75.66	3.19	13.79	0.69	2.94	0.22	3.36	0.14	3.36	0.14	2.57	0.12	0.29	0.06	0.56	0.07
FLD13	76.55	3.23	13.60	0.68	3.06	0.23	3.24	0.13	3.23	0.14	2.70	0.12	0.20	0.05	0.51	0.07
FLD13	76.43	3.23	14.41	0.72	2.95	0.22	3.26	0.13	3.33	0.14	2.54	0.12	0.38	0.06	0.62	0.08
FLD13	75.38	3.18	13.33	0.67	3.11	0.23	3.44	0.14	3.24	0.14	2.68	0.12	0.25	0.05	0.61	0.08
FLD13	75.34	3.18	13.85	0.69	2.78	0.21	3.36	0.14	3.30	0.14	2.66	0.12	0.21	0.05	0.56	0.07
FLD13	77.16	3.26	13.79	0.69	2.87	0.22	3.45	0.14	3.32	0.14	2.48	0.11	0.19	0.05	0.55	0.07
FLD13	75.45	3.19	13.68	0.68	3.02	0.22	3.28	0.13	3.07	0.13	2.59	0.12	0.28	0.06	0.54	0.07
FLD13	75.10	3.17	13.83	0.69	2.85	0.21	3.39	0.14	3.43	0.14	2.54	0.12	0.25	0.05	0.58	0.08
FLD13	75.64	3.19	13.99	0.70	2.88	0.22	3.20	0.13	3.25	0.14	2.63	0.12	0.27	0.05	0.57	0.07
FLD13	72.20	3.05	13.43	0.67	2.84	0.21	3.41	0.14	3.40	0.14	2.74	0.12	0.26	0.05	0.59	0.08
FLD13	75.82	3.20	13.90	0.69	2.97	0.22	3.29	0.13	3.23	0.14	2.64	0.12	0.12	0.05	0.55	0.07
FLD13	75.55	3.19	14.34	0.71	2.95	0.22	3.30	0.13	3.31	0.14	2.70	0.12	0.33	0.06	0.67	0.08
FLD13	74.50	3.15	13.60	0.68	2.81	0.21	3.30	0.13	3.38	0.14	2.52	0.12	0.31	0.06	0.55	0.07
FLD13	76.32	3.22	13.76	0.69	3.01	0.22	3.34	0.14	3.25	0.14	2.73	0.12	0.14	0.05	0.59	0.08
FLD13	74.41	3.14	13.53	0.68	2.89	0.22	3.40	0.14	3.16	0.13	2.58	0.12	0.32	0.06	0.53	0.07
FLD13	75.49	3.19	13.97	0.70	2.91	0.22	3.30	0.13	3.31	0.14	2.50	0.11	0.20	0.05	0.63	0.08
FLD13	73.13	3.09	13.64	0.68	2.86	0.21	3.57	0.14	3.41	0.14	2.58	0.12	0.30	0.06	0.57	0.08

FLD13	75.25	3.18	13.76	0.69	3.02	0.22	3.34	0.14	3.20	0.14	2.61	0.12	0.21	0.05	0.58	0.08
FLD13	75.16	3.17	14.17	0.71	2.93	0.22	3.27	0.13	3.43	0.14	2.60	0.12	0.21	0.05	0.62	0.08
FLD13	71.83	3.04	13.83	0.69	2.62	0.20	3.15	0.13	3.50	0.14	2.63	0.12	0.23	0.05	0.58	0.08
FLD13	74.32	3.14	13.73	0.69	2.80	0.21	3.34	0.14	3.17	0.13	2.69	0.12	0.22	0.05	0.54	0.07
FLD13	75.53	3.19	14.36	0.71	2.98	0.22	3.26	0.13	3.26	0.14	2.65	0.12	0.31	0.06	0.61	0.08
FLD13	73.92	3.12	13.32	0.67	2.91	0.22	3.44	0.14	3.37	0.14	2.55	0.12	0.33	0.06	0.57	0.07
FLD13	76.09	3.21	14.14	0.70	2.82	0.21	3.20	0.13	3.53	0.14	2.58	0.12	0.35	0.06	0.52	0.07
FLD13	76.66	3.24	14.19	0.71	2.88	0.22	3.27	0.13	3.42	0.14	2.58	0.12	0.39	0.06	0.60	0.08
FLD13	74.64	3.15	13.84	0.69	2.75	0.21	3.30	0.13	3.30	0.14	2.68	0.12	0.26	0.05	0.57	0.07
FLD13	76.52	3.23	14.25	0.71	3.07	0.23	3.29	0.13	3.01	0.13	2.61	0.12	0.38	0.06	0.60	0.08
FLD13	74.61	3.15	13.44	0.67	2.69	0.20	3.16	0.13	3.15	0.13	2.73	0.12	0.29	0.06	0.57	0.07
FLD13	76.77	3.24	13.30	0.67	3.10	0.23	3.49	0.14	3.12	0.13	2.49	0.11	0.17	0.05	0.54	0.07
FLD13	76.14	3.21	13.61	0.68	2.99	0.22	3.46	0.14	3.41	0.14	2.65	0.12	0.22	0.05	0.57	0.08
FLD13	74.28	3.14	13.78	0.69	2.83	0.21	3.47	0.14	3.37	0.14	2.77	0.12	0.33	0.06	0.57	0.07
FLD13	76.43	3.23	13.80	0.69	3.07	0.23	3.42	0.14	3.04	0.13	2.58	0.12	0.20	0.05	0.58	0.08
FLD13	74.48	3.15	13.87	0.69	2.79	0.21	3.41	0.14	3.22	0.14	2.75	0.12	0.36	0.06	0.58	0.08
FLD13	75.48	3.19	14.02	0.70	2.91	0.22	3.37	0.14	3.19	0.13	2.77	0.12	0.23	0.05	0.57	0.07
FLD13	75.79	3.20	13.81	0.69	2.93	0.22	3.24	0.13	3.19	0.13	2.76	0.12	0.36	0.06	0.58	0.08
FLD13	75.66	3.19	13.92	0.70	2.95	0.22	3.33	0.14	3.20	0.13	2.64	0.12	0.24	0.05	0.55	0.07
FLD13	75.97	3.21	14.08	0.70	3.01	0.22	3.40	0.14	3.21	0.14	2.65	0.12	0.33	0.06	0.65	0.08
FLD13	73.68	3.11	13.71	0.69	2.84	0.21	3.25	0.13	3.33	0.14	2.61	0.12	0.25	0.05	0.63	0.08
FLD13	75.85	3.20	14.01	0.70	3.00	0.22	3.29	0.13	3.23	0.14	2.70	0.12	0.27	0.05	0.62	0.08
FLD13	76.38	3.22	14.04	0.70	2.93	0.22	3.31	0.13	3.22	0.14	2.64	0.12	0.31	0.06	0.63	0.08
FLD13	73.22	3.09	13.68	0.68	2.76	0.21	3.31	0.13	3.48	0.14	2.50	0.11	0.32	0.06	0.56	0.07
FLD13	75.08	3.17	13.71	0.69	3.03	0.23	3.20	0.13	3.16	0.13	2.61	0.12	0.31	0.06	0.56	0.07
FLD13	75.57	3.19	13.92	0.69	2.93	0.22	3.35	0.14	3.33	0.14	2.57	0.12	0.26	0.05	0.60	0.08
FLD13	75.65	3.19	13.97	0.70	2.92	0.22	3.35	0.14	3.35	0.14	2.51	0.11	0.30	0.06	0.57	0.08
FLD13	75.85	3.20	14.15	0.71	2.90	0.22	3.27	0.13	3.40	0.14	2.60	0.12	0.34	0.06	0.63	0.08
FLD13	77.19	3.26	13.33	0.67	3.14	0.23	3.30	0.13	3.28	0.14	2.72	0.12	0.34	0.06	0.62	0.08
FLD13	75.29	3.18	13.51	0.68	2.93	0.22	3.29	0.13	3.27	0.14	2.87	0.13	0.25	0.05	0.53	0.07
FLD13	75.99	3.21	13.84	0.69	2.92	0.22	3.40	0.14	3.19	0.13	2.26	0.11	0.20	0.05	0.59	0.08
FLD13	75.18	3.17	13.37	0.67	2.94	0.22	3.39	0.14	3.26	0.14	2.47	0.11	0.38	0.06	0.52	0.07
FLD13	75.61	3.19	13.66	0.68	2.80	0.21	3.23	0.13	3.30	0.14	2.62	0.12	0.24	0.05	0.53	0.07
FLD13	75.30	3.18	13.80	0.69	2.94	0.22	3.68	0.15	3.34	0.14	2.62	0.12	0.23	0.05	0.55	0.07
FLD13	76.59	3.23	13.88	0.69	2.99	0.22	3.43	0.14	3.22	0.14	2.58	0.12	0.20	0.05	0.57	0.08
FLD13	77.04	3.25	13.62	0.68	3.15	0.23	3.54	0.14	3.26	0.14	2.57	0.12	0.26	0.05	0.55	0.07
FLD13	74.54	3.15	13.69	0.68	2.74	0.21	3.33	0.14	3.24	0.14	2.80	0.12	0.20	0.05	0.49	0.07
FLD13	74.64	3.15	13.61	0.68	2.95	0.22	3.52	0.14	3.16	0.13	2.62	0.12	0.20	0.05	0.53	0.07
FLD13	76.17	3.22	13.74	0.69	2.81	0.21	3.41	0.14	3.37	0.14	2.72	0.12	0.18	0.05	0.52	0.07
FLD13	76.40	3.22	13.61	0.68	2.89	0.22	3.44	0.14	3.36	0.14	2.56	0.12	0.32	0.06	0.53	0.07
FLD13	73.74	3.11	13.57	0.68	2.91	0.22	3.59	0.14	3.06	0.13	2.76	0.12	0.15	0.05	0.62	0.08
FLD13	74.66	3.15	13.77	0.69	3.05	0.23	3.57	0.14	3.17	0.13	2.72	0.12	0.25	0.05	0.61	0.08
FLD13	75.14	3.17	13.98	0.70	2.85	0.21	3.35	0.14	3.56	0.15	2.71	0.12	0.26	0.05	0.59	0.08
FLD13	75.85	3.20	13.86	0.69	2.95	0.22	3.49	0.14	3.48	0.14	2.56	0.12	0.34	0.06	0.60	0.08
FLD13	73.00	3.08	13.34	0.67	2.71	0.21	3.44	0.14	3.35	0.14	2.45	0.11	0.23	0.05	0.54	0.07
FLD13	74.85	3.16	13.62	0.68	2.86	0.21	3.42	0.14	3.42	0.14	2.67	0.12	0.23	0.05	0.57	0.07
FLD13	75.13	3.17	13.88	0.69	3.14	0.23	3.48	0.14	3.21	0.14	2.67	0.12	0.30	0.06	0.63	0.08
FLD13	75.56	3.19	13.78	0.69	2.96	0.22	3.39	0.14	3.31	0.14	2.42	0.11	0.36	0.06	0.62	0.08
FLD13	76.35	3.22	13.95	0.70	3.18	0.23	3.43	0.14	3.11	0.13	2.57	0.12	0.30	0.06	0.64	0.08
FLD13	72.60	3.07	14.05	0.70	2.92	0.22	3.36	0.14	3.65	0.15	2.63	0.12	0.25	0.05	0.62	0.08
FLD13	74.46	3.14	14.07	0.70	2.82	0.21	3.20	0.13	3.24	0.14	2.73	0.12	0.17	0.05	0.61	0.08
FLD13	75.16	3.17	13.41	0.67	3.13	0.23	3.46	0.14	3.35	0.14	2.64	0.12	0.36	0.06	0.50	0.07
FLD13	72.97	3.08	13.38	0.67	2.80	0.21	3.34	0.14	3.33	0.14	2.64	0.12	0.32	0.06	0.55	0.07
FLD13	75.45	3.19	13.93	0.70	2.87	0.22	3.29	0.13	3.09	0.13	2.78	0.12	0.34	0.06	0.57	0.07
FLD13	75.46	3.19	14.15	0.71	2.87	0.22	3.34	0.14	3.30	0.14	2.54	0.12	0.23	0.05	0.54	0.07
FLD13	75.69	3.20	13.97	0.70	2.86	0.21	3.33	0.14	3.22	0.14	2.66	0.12	0.32	0.06	0.59	0.08
FLD13	73.72	3.11	13.52	0.68	2.84	0.21	3.42	0.14	3.30	0.14	2.52	0.12	0.27	0.05	0.59	0.08
FLD13	75.52	3.19	13.94	0.70	2.83	0.21	3.43	0.14	3.39	0.14	2.76	0.12	0.29	0.06	0.53	0.07
FLD13	74.05	3.13	13.61	0.68	2.83	0.21	3.42	0.14	3.38	0.14	2.75	0.12	0.28	0.05	0.54	0.07
FLD13	74.87	3.16	13.79	0.69	2.86	0.21	3.35	0.14	3.49	0.14	2.57	0.12	0.29	0.06	0.55	0.07
FLD13	76.21	3.22	13.84	0.69	2.91	0.22	3.39	0.14	3.20	0.14	2.64	0.12	0.17	0.05	0.59	0.08
FLD13	74.16	3.13	13.68	0.68	2.78	0.21	3.29	0.13	3.37	0.14	2.50	0.11	0.28	0.05	0.52	0.07

FLD13	74.79	3.16	13.82	0.69	2.86	0.21	3.51	0.14	3.45	0.14	2.75	0.12	0.33	0.06	0.61	0.08
FLD13	76.25	3.22	14.12	0.70	2.81	0.21	3.47	0.14	3.52	0.14	2.65	0.12	0.16	0.05	0.61	0.08
FLD13	75.50	3.19	14.02	0.70	2.84	0.21	3.37	0.14	3.44	0.14	2.38	0.11	0.26	0.05	0.58	0.08
FLD13	75.99	3.21	13.77	0.69	2.85	0.21	3.38	0.14	3.38	0.14	2.52	0.12	0.30	0.06	0.51	0.07
FLD13	74.15	3.13	13.49	0.67	2.83	0.21	3.40	0.14	3.55	0.15	2.49	0.11	0.33	0.06	0.55	0.07
FLD13	74.41	3.14	14.32	0.71	2.78	0.21	3.24	0.13	3.45	0.14	2.80	0.12	0.30	0.06	0.62	0.08
FLD13	75.95	3.21	13.87	0.69	3.09	0.23	3.43	0.14	3.24	0.14	2.78	0.12	0.20	0.05	0.60	0.08
FLD13	73.80	3.12	13.52	0.68	2.86	0.21	3.31	0.13	3.41	0.14	2.60	0.12	0.19	0.05	0.55	0.07
FLD13	73.95	3.12	14.75	0.73	2.80	0.21	3.26	0.13	3.73	0.15	2.71	0.12	0.29	0.06	0.58	0.08
FLD13	74.61	3.15	14.00	0.70	2.76	0.21	3.24	0.13	3.40	0.14	2.51	0.12	0.32	0.06	0.56	0.07
FLD13	74.51	3.15	13.74	0.69	3.00	0.22	3.55	0.14	3.30	0.14	2.61	0.12	0.38	0.06	0.55	0.07
FLD13	75.16	3.17	14.02	0.70	2.91	0.22	3.24	0.13	3.37	0.14	2.61	0.12	0.20	0.05	0.55	0.07
FLD13	76.53	3.23	13.83	0.69	3.01	0.22	3.33	0.14	3.27	0.14	2.50	0.11	0.16	0.05	0.55	0.07
FLD13	76.39	3.22	14.43	0.72	3.02	0.22	3.29	0.13	3.39	0.14	2.34	0.11	0.18	0.05	0.57	0.08
FLD13	74.60	3.15	13.53	0.68	2.79	0.21	3.46	0.14	3.16	0.13	2.86	0.13	0.18	0.05	0.55	0.07
FLD13	75.17	3.17	14.02	0.70	2.86	0.21	3.39	0.14	3.37	0.14	2.71	0.12	0.24	0.05	0.57	0.07
FLD13	74.63	3.15	13.70	0.68	2.93	0.22	3.33	0.14	3.30	0.14	2.72	0.12	0.24	0.05	0.56	0.07
FLD13	75.06	3.17	13.83	0.69	2.85	0.21	3.39	0.14	3.17	0.13	2.70	0.12	0.21	0.05	0.54	0.07
FLD13	75.55	3.19	13.86	0.69	2.87	0.21	3.32	0.13	3.14	0.13	2.62	0.12	0.24	0.05	0.51	0.07
FLD13	76.05	3.21	13.56	0.68	2.72	0.21	3.29	0.13	3.31	0.14	2.68	0.12	0.18	0.05	0.53	0.07
FLD13	76.12	3.21	14.23	0.71	2.96	0.22	3.36	0.14	3.24	0.14	2.69	0.12	0.23	0.05	0.57	0.07
FLD13	76.45	3.23	14.19	0.71	2.87	0.22	3.37	0.14	3.15	0.13	2.58	0.12	0.38	0.06	0.60	0.08
FLD13	71.90	3.04	13.68	0.68	2.73	0.21	3.40	0.14	3.34	0.14	2.63	0.12	0.22	0.05	0.50	0.07
FLD13	75.05	3.17	14.12	0.70	2.82	0.21	3.27	0.13	3.33	0.14	2.79	0.12	0.27	0.05	0.58	0.08
FLD13	76.06	3.21	13.99	0.70	2.79	0.21	3.31	0.13	3.44	0.14	2.90	0.13	0.22	0.05	0.62	0.08
FLD13	76.69	3.24	13.52	0.68	2.91	0.22	3.43	0.14	3.40	0.14	2.76	0.12	0.20	0.05	0.59	0.08
FLD13	75.42	3.18	14.01	0.70	2.91	0.22	3.39	0.14	3.34	0.14	2.41	0.11	0.27	0.05	0.57	0.07
FLD13	75.41	3.18	13.99	0.70	2.85	0.21	3.38	0.14	3.48	0.14	2.99	0.13	0.37	0.06	0.57	0.07
FLD13	74.88	3.16	14.00	0.70	2.91	0.22	3.33	0.14	3.43	0.14	2.48	0.11	0.24	0.05	0.55	0.07
FLD13	73.43	3.10	13.85	0.69	2.92	0.22	3.19	0.13	3.42	0.14	2.64	0.12	0.29	0.06	0.54	0.07
FLD13	74.75	3.16	14.15	0.71	2.81	0.21	3.53	0.14	3.77	0.15	2.47	0.11	0.22	0.05	0.62	0.08
FLD13	74.07	3.13	15.20	0.75	2.93	0.22	3.33	0.14	3.64	0.15	2.76	0.12	0.24	0.05	0.56	0.07
FLD13	74.97	3.17	13.47	0.67	2.78	0.21	3.29	0.13	3.17	0.13	2.73	0.12	0.28	0.05	0.58	0.08
FLD13	75.85	3.20	13.82	0.69	2.70	0.20	3.30	0.13	3.45	0.14	2.53	0.12	0.30	0.06	0.61	0.08
FLD13	74.92	3.16	14.20	0.71	2.73	0.21	3.33	0.14	3.79	0.15	2.59	0.12	0.28	0.06	0.64	0.08
FLD13	76.75	3.24	13.82	0.69	2.86	0.21	3.49	0.14	3.40	0.14	2.56	0.12	0.30	0.06	0.61	0.08
FLD13	76.95	3.25	14.19	0.71	2.98	0.22	3.25	0.13	3.30	0.14	2.43	0.11	0.30	0.06	0.52	0.07
FLD13	75.46	3.19	13.74	0.69	2.91	0.22	3.39	0.14	3.47	0.14	2.59	0.12	0.24	0.05	0.61	0.08
FLD13	75.54	3.19	13.73	0.69	2.88	0.22	3.38	0.14	3.44	0.14	2.55	0.12	0.23	0.05	0.56	0.07
FLD13	75.26	3.18	14.04	0.70	2.89	0.22	3.38	0.14	3.83	0.15	2.39	0.11	0.31	0.06	0.58	0.08
FLD13	75.71	3.20	14.28	0.71	3.00	0.22	3.33	0.14	3.51	0.14	2.71	0.12	0.30	0.06	0.68	0.08
FLD13	76.48	3.23	14.11	0.70	2.91	0.22	3.34	0.14	3.46	0.14	2.71	0.12	0.34	0.06	0.59	0.08
FLD13	74.47	3.14	13.53	0.68	3.02	0.22	3.52	0.14	3.22	0.14	2.75	0.12	0.31	0.06	0.57	0.07
FLD13	75.13	3.17	14.04	0.70	2.88	0.22	3.51	0.14	3.06	0.13	2.64	0.12	0.29	0.06	0.60	0.08
FLD13	75.79	3.20	14.21	0.71	2.84	0.21	3.35	0.14	3.33	0.14	2.61	0.12	0.33	0.06	0.60	0.08
FLD13	75.47	3.19	13.57	0.68	2.84	0.21	3.38	0.14	3.33	0.14	2.59	0.12	0.21	0.05	0.57	0.07
FLD13	75.08	3.17	14.38	0.72	2.93	0.22	3.37	0.14	3.45	0.14	2.67	0.12	0.25	0.05	0.56	0.07
FLD13	74.48	3.15	13.64	0.68	3.03	0.22	3.37	0.14	3.36	0.14	2.75	0.12	0.23	0.05	0.58	0.08
FLD13	75.82	3.20	13.91	0.69	2.85	0.21	3.43	0.14	3.25	0.14	2.63	0.12	0.28	0.05	0.63	0.08
FLD13	76.42	3.23	13.93	0.70	2.98	0.22	3.37	0.14	3.28	0.14	2.60	0.12	0.31	0.06	0.57	0.07
FLD13	76.31	3.22	14.05	0.70	2.73	0.21	3.30	0.13	3.42	0.14	2.63	0.12	0.33	0.06	0.58	0.08
FLD13	75.87	3.20	13.92	0.69	2.89	0.22	3.57	0.14	3.26	0.14	2.72	0.12	0.18	0.05	0.60	0.08
FLD13	75.46	3.19	13.98	0.70	2.89	0.22	3.18	0.13	3.19	0.13	2.75	0.12	0.36	0.06	0.50	0.07
FLD13	75.72	3.20	14.30	0.71	2.85	0.21	3.48	0.14	3.88	0.16	2.58	0.12	0.37	0.06	0.62	0.08
FLD13	75.90	3.20	14.06	0.70	2.84	0.21	3.38	0.14	3.36	0.14	2.60	0.12	0.19	0.05	0.60	0.08
FLD13	76.30	3.22	13.94	0.70	2.89	0.22	3.36	0.14	3.30	0.14	2.94	0.13	0.30	0.06	0.57	0.07
FLD13	75.96	3.21	14.52	0.72	3.01	0.22	3.33	0.14	3.46	0.14	2.71	0.12	0.34	0.06	0.62	0.08
FLD13	75.41	3.18	13.83	0.69	2.88	0.22	3.38	0.14	3.47	0.14	2.66	0.12	0.20	0.05	0.60	0.08
FLD13	75.71	3.20	14.36	0.72	2.85	0.21	3.39	0.14	3.40	0.14	2.67	0.12	0.29	0.06	0.60	0.08
FLD13	74.95	3.16	13.90	0.69	3.27	0.24	3.27	0.13	3.28	0.14	2.56	0.12	0.27	0.05	0.60	0.08
FLD13	75.77	3.20	13.70	0.68	2.98	0.22	3.24	0.13	3.16	0.13	2.72	0.12	0.28	0.05	0.59	0.08
FLD14	75.46	3.19	14.54	0.72	3.06	0.23	3.31	0.13	3.47	0.14	2.86	0.13	0.22	0.05	0.58	0.08

FLD14	74.77	3.16	14.13	0.70	2.90	0.22	3.26	0.13	3.22	0.14	2.65	0.12	0.20	0.05	0.64	0.08
FLD14	74.80	3.16	14.47	0.72	2.94	0.22	3.31	0.13	3.09	0.13	2.67	0.12	0.23	0.05	0.59	0.08
FLD14	74.18	3.13	14.20	0.71	3.09	0.23	3.24	0.13	3.18	0.13	2.81	0.12	0.23	0.05	0.64	0.08
FLD14	75.81	3.20	14.33	0.71	3.01	0.22	3.33	0.14	3.40	0.14	3.08	0.13	0.28	0.06	0.63	0.08
FLD14	74.58	3.15	14.11	0.70	2.94	0.22	3.22	0.13	3.37	0.14	2.77	0.12	0.32	0.06	0.65	0.08
FLD14	75.45	3.19	14.41	0.72	2.72	0.21	3.38	0.14	3.39	0.14	2.71	0.12	0.24	0.05	0.64	0.08
FLD14	74.97	3.17	14.06	0.70	2.91	0.22	3.31	0.13	3.37	0.14	2.78	0.12	0.26	0.05	0.63	0.08
FLD14	74.31	3.14	14.33	0.71	2.69	0.20	3.22	0.13	3.49	0.14	2.80	0.12	0.22	0.05	0.59	0.08
FLD14	76.21	3.22	14.31	0.71	2.83	0.21	3.24	0.13	3.26	0.14	2.62	0.12	0.24	0.05	0.64	0.08
FLD14	76.00	3.21	14.23	0.71	2.94	0.22	3.36	0.14	3.33	0.14	2.61	0.12	0.33	0.06	0.62	0.08
FLD14	73.82	3.12	13.96	0.70	2.82	0.21	3.37	0.14	3.52	0.14	2.84	0.13	0.24	0.05	0.63	0.08
FLD14	76.63	3.23	14.10	0.70	3.04	0.23	3.27	0.13	3.17	0.13	2.68	0.12	0.27	0.05	0.58	0.08
FLD14	74.17	3.13	13.89	0.69	2.85	0.21	3.30	0.13	3.49	0.14	2.68	0.12	0.30	0.06	0.57	0.07
FLD14	74.73	3.16	13.92	0.69	2.81	0.21	3.19	0.13	3.26	0.14	2.51	0.12	0.35	0.06	0.62	0.08
FLD14	75.87	3.20	13.27	0.66	2.83	0.21	3.74	0.15	3.35	0.14	2.81	0.12	0.22	0.05	0.63	0.08
FLD14	76.43	3.23	14.34	0.71	2.76	0.21	3.19	0.13	3.38	0.14	2.86	0.13	0.28	0.06	0.64	0.08
FLD14	74.29	3.14	13.96	0.70	2.90	0.22	3.42	0.14	3.32	0.14	2.75	0.12	0.26	0.05	0.59	0.08
FLD14	75.48	3.19	14.37	0.72	2.93	0.22	3.39	0.14	3.36	0.14	2.84	0.13	0.24	0.05	0.72	0.08
FLD14	75.62	3.19	14.18	0.71	3.09	0.23	3.45	0.14	3.28	0.14	2.76	0.12	0.37	0.06	0.64	0.08
FLD14	74.47	3.14	14.14	0.71	2.91	0.22	3.34	0.14	3.39	0.14	2.66	0.12	0.18	0.05	0.60	0.08
FLD14	75.68	3.19	14.41	0.72	2.83	0.21	3.29	0.13	3.41	0.14	2.77	0.12	0.15	0.05	0.62	0.08
FLD14	74.85	3.16	14.00	0.70	3.05	0.23	3.44	0.14	3.28	0.14	2.79	0.12	0.31	0.06	0.60	0.08
FLD14	74.11	3.13	12.29	0.62	3.16	0.23	3.56	0.14	3.30	0.14	2.86	0.13	0.30	0.06	0.57	0.07
FLD14	74.52	3.15	14.16	0.71	2.63	0.20	3.33	0.14	3.44	0.14	2.86	0.13	0.21	0.05	0.57	0.07
FLD14	76.99	3.25	14.48	0.72	2.54	0.19	2.99	0.12	3.35	0.14	2.47	0.11	0.21	0.05	0.62	0.08
FLD14	74.43	3.14	14.33	0.71	2.90	0.22	3.33	0.14	3.50	0.14	2.78	0.12	0.37	0.06	0.62	0.08
FLD14	75.46	3.19	14.27	0.71	2.84	0.21	3.38	0.14	3.38	0.14	2.67	0.12	0.20	0.05	0.58	0.08
FLD14	74.28	3.14	14.15	0.71	2.89	0.22	3.32	0.14	3.44	0.14	2.93	0.13	0.28	0.05	0.58	0.08
FLD14	75.82	3.20	14.25	0.71	3.03	0.23	3.33	0.14	3.13	0.13	2.62	0.12	0.16	0.05	0.60	0.08
FLD14	75.97	3.21	14.47	0.72	2.99	0.22	3.22	0.13	3.39	0.14	2.82	0.12	0.21	0.05	0.57	0.07
FLD14	73.92	3.12	14.29	0.71	2.94	0.22	3.36	0.14	3.58	0.15	2.79	0.12	0.32	0.06	0.62	0.08
FLD14	76.63	3.23	12.98	0.65	3.25	0.24	3.43	0.14	3.19	0.13	2.88	0.13	0.30	0.06	0.59	0.08
FLD14	75.04	3.17	14.29	0.71	3.00	0.22	3.28	0.13	3.38	0.14	2.64	0.12	0.20	0.05	0.60	0.08
FLD14	76.04	3.21	14.06	0.70	3.00	0.22	3.41	0.14	3.16	0.13	2.72	0.12	0.17	0.05	0.61	0.08
FLD14	74.00	3.13	14.06	0.70	2.71	0.21	3.28	0.13	3.35	0.14	2.74	0.12	0.22	0.05	0.65	0.08
FLD14	75.67	3.19	14.51	0.72	3.06	0.23	3.36	0.14	3.25	0.14	2.74	0.12	0.20	0.05	0.66	0.08
FLD14	74.47	3.14	14.82	0.74	2.77	0.21	3.17	0.13	3.41	0.14	2.88	0.13	0.27	0.05	0.50	0.07
FLD14	76.32	3.22	14.35	0.71	2.87	0.22	3.29	0.13	3.31	0.14	2.88	0.13	0.20	0.05	0.68	0.08
FLD14	74.11	3.13	14.06	0.70	2.75	0.21	3.27	0.13	3.24	0.14	2.80	0.12	0.29	0.06	0.60	0.08
FLD14	73.93	3.12	14.28	0.71	2.71	0.21	3.41	0.14	3.49	0.14	2.87	0.13	0.26	0.05	0.56	0.07
FLD14	76.01	3.21	14.60	0.73	2.97	0.22	3.29	0.13	3.29	0.14	2.75	0.12	0.24	0.05	0.72	0.08
FLD14	75.06	3.17	14.33	0.71	3.02	0.22	3.38	0.14	3.31	0.14	2.95	0.13	0.29	0.06	0.68	0.08
FLD14	75.92	3.20	14.68	0.73	2.95	0.22	3.25	0.13	3.43	0.14	2.76	0.12	0.19	0.05	0.62	0.08
FLD14	75.29	3.18	14.19	0.71	2.87	0.22	3.33	0.14	3.43	0.14	2.90	0.13	0.20	0.05	0.58	0.08
FLD14	75.42	3.18	14.30	0.71	3.01	0.22	3.43	0.14	3.36	0.14	2.95	0.13	0.21	0.05	0.56	0.07
FLD14	75.56	3.19	14.45	0.72	2.90	0.22	3.38	0.14	3.36	0.14	2.75	0.12	0.28	0.06	0.61	0.08
FLD14	75.72	3.20	14.39	0.72	2.86	0.21	3.32	0.14	3.43	0.14	3.00	0.13	0.27	0.05	0.63	0.08
FLD14	75.28	3.18	14.26	0.71	3.13	0.23	3.41	0.14	3.36	0.14	2.64	0.12	0.27	0.05	0.64	0.08
FLD14	74.74	3.16	14.22	0.71	3.04	0.23	3.46	0.14	3.28	0.14	2.71	0.12	0.25	0.05	0.63	0.08
FLD14	76.28	3.22	14.31	0.71	2.91	0.22	3.34	0.14	3.44	0.14	2.68	0.12	0.18	0.05	0.64	0.08
FLD14	74.11	3.13	14.16	0.71	2.72	0.21	3.37	0.14	3.57	0.15	2.63	0.12	0.17	0.05	0.57	0.07
FLD14	75.51	3.19	14.26	0.71	2.90	0.22	3.29	0.13	3.47	0.14	2.68	0.12	0.31	0.06	0.52	0.07
FLD14	75.85	3.20	14.37	0.72	3.04	0.23	3.30	0.13	3.38	0.14	2.88	0.13	0.28	0.05	0.60	0.08
FLD14	75.92	3.20	14.53	0.72	3.04	0.23	3.37	0.14	3.46	0.14	2.74	0.12	0.21	0.05	0.59	0.08
FLD14	76.68	3.24	13.48	0.67	3.01	0.22	3.38	0.14	3.14	0.13	2.56	0.12	0.21	0.05	0.63	0.08
FLD14	74.40	3.14	13.90	0.69	2.93	0.22	3.46	0.14	3.26	0.14	2.75	0.12	0.26	0.05	0.55	0.07
FLD14	75.53	3.19	14.34	0.71	2.97	0.22	3.33	0.14	3.42	0.14	2.75	0.12	0.28	0.05	0.63	0.08
FLD14	74.54	3.15	14.44	0.72	2.84	0.21	3.18	0.13	3.26	0.14	2.73	0.12	0.20	0.05	0.65	0.08
FLD14	75.86	3.20	14.39	0.72	2.88	0.22	3.43	0.14	3.32	0.14	2.87	0.13	0.30	0.06	0.58	0.08
FLD14	75.70	3.20	13.85	0.69	2.89	0.22	3.42	0.14	3.31	0.14	2.73	0.12	0.33	0.06	0.63	0.08
FLD14	73.59	3.11	13.67	0.68	2.89	0.22	3.53	0.14	3.18	0.13	2.67	0.12	0.25	0.05	0.60	0.08
FLD14	74.57	3.15	14.44	0.72	2.89	0.22	3.26	0.13	3.56	0.15	2.67	0.12	0.23	0.05	0.69	0.08

FLD14	74.90	3.16	13.87	0.69	2.97	0.22	3.35	0.14	3.37	0.14	2.58	0.12	0.26	0.05	0.57	0.07
FLD14	75.45	3.19	14.17	0.71	2.85	0.21	3.30	0.13	3.22	0.14	2.57	0.12	0.17	0.05	0.63	0.08
FLD14	75.32	3.18	14.28	0.71	2.99	0.22	3.35	0.14	3.31	0.14	2.93	0.13	0.26	0.05	0.62	0.08
FLD14	75.75	3.20	14.62	0.73	3.04	0.23	3.30	0.13	3.29	0.14	2.85	0.13	0.30	0.06	0.65	0.08
FLD14	76.31	3.22	14.29	0.71	3.11	0.23	3.29	0.13	3.27	0.14	2.54	0.12	0.26	0.05	0.57	0.07
FLD14	74.58	3.15	14.32	0.71	3.01	0.22	3.49	0.14	3.41	0.14	2.93	0.13	0.22	0.05	0.64	0.08
FLD14	74.70	3.15	13.64	0.68	3.01	0.22	3.57	0.14	3.19	0.13	2.81	0.12	0.24	0.05	0.54	0.07
FLD14	74.73	3.16	14.40	0.72	3.00	0.22	3.32	0.13	3.46	0.14	2.77	0.12	0.15	0.05	0.56	0.07
FLD14	74.82	3.16	14.16	0.71	3.03	0.23	3.41	0.14	3.39	0.14	2.85	0.13	0.25	0.05	0.55	0.07
FLD14	75.29	3.18	14.15	0.71	2.95	0.22	3.38	0.14	3.26	0.14	2.81	0.12	0.25	0.05	0.65	0.08
FLD14	73.79	3.12	13.86	0.69	2.82	0.21	3.46	0.14	3.24	0.14	2.73	0.12	0.25	0.05	0.57	0.07
FLD14	73.52	3.11	13.86	0.69	2.86	0.21	3.56	0.14	3.41	0.14	2.78	0.12	0.17	0.05	0.57	0.08
FLD14	74.40	3.14	14.81	0.74	2.75	0.21	3.14	0.13	3.38	0.14	2.82	0.12	0.24	0.05	0.51	0.07
FLD14	74.63	3.15	14.51	0.72	3.14	0.23	3.32	0.13	3.47	0.14	2.82	0.12	0.31	0.06	0.68	0.08
FLD14	75.69	3.20	14.10	0.70	2.93	0.22	3.37	0.14	3.28	0.14	2.73	0.12	0.26	0.05	0.61	0.08
FLD14	73.75	3.12	13.87	0.69	2.78	0.21	3.48	0.14	3.45	0.14	2.87	0.13	0.29	0.06	0.53	0.07
FLD14	76.18	3.22	14.43	0.72	2.90	0.22	3.43	0.14	3.32	0.14	2.67	0.12	0.23	0.05	0.64	0.08
FLD14	75.51	3.19	14.22	0.71	2.92	0.22	3.47	0.14	3.52	0.14	2.80	0.12	0.28	0.05	0.58	0.08
FLD14	74.37	3.14	14.06	0.70	2.77	0.21	3.33	0.14	3.56	0.15	2.80	0.12	0.26	0.05	0.56	0.07
FLD14	73.95	3.12	15.20	0.75	2.74	0.21	3.14	0.13	3.50	0.14	2.76	0.12	0.21	0.05	0.54	0.07
FLD14	74.98	3.17	14.31	0.71	2.72	0.21	3.40	0.14	3.41	0.14	2.86	0.13	0.23	0.05	0.59	0.08
FLD14	73.64	3.11	14.72	0.73	2.81	0.21	3.37	0.14	3.44	0.14	3.09	0.13	0.25	0.05	0.62	0.08
FLD14	75.30	3.18	14.29	0.71	2.94	0.22	3.66	0.15	2.08	0.10	2.93	0.13	0.43	0.06	0.64	0.08
FLD14	76.65	3.24	14.03	0.70	2.77	0.21	3.32	0.13	3.42	0.14	2.62	0.12	0.23	0.05	0.63	0.08
FLD14	75.38	3.18	14.38	0.72	2.76	0.21	3.41	0.14	3.49	0.14	2.84	0.13	0.30	0.06	0.65	0.08
FLD14	76.01	3.21	14.53	0.72	2.88	0.22	3.38	0.14	3.39	0.14	2.59	0.12	0.18	0.05	0.63	0.08
FLD15	73.02	3.08	12.98	0.65	3.39	0.25	3.79	0.15	3.57	0.15	2.74	0.12	0.30	0.06	0.63	0.08
FLD15	72.64	3.07	12.67	0.64	3.42	0.25	3.92	0.15	2.60	0.12	2.74	0.12	0.29	0.06	0.39	0.07
FLD15	72.11	3.05	12.92	0.65	3.20	0.24	3.69	0.15	3.09	0.13	2.95	0.13	0.33	0.06	0.57	0.07
FLD15	72.27	3.05	13.18	0.66	3.42	0.25	3.86	0.15	2.78	0.12	2.82	0.12	0.32	0.06	0.58	0.08
FLD15	71.36	3.02	12.42	0.63	3.30	0.24	3.78	0.15	3.00	0.13	2.71	0.12	0.28	0.05	0.54	0.07
FLD15	71.54	3.02	12.75	0.64	3.19	0.23	3.78	0.15	3.76	0.15	2.71	0.12	0.31	0.06	0.62	0.08
FLD15	75.36	3.18	12.90	0.65	3.56	0.26	3.62	0.14	2.86	0.12	2.67	0.12	0.29	0.06	0.55	0.07
FLD15	72.89	3.08	13.00	0.65	3.46	0.25	3.80	0.15	3.52	0.14	2.68	0.12	0.33	0.06	0.55	0.07
FLD15	72.58	3.07	12.58	0.63	3.33	0.24	4.00	0.16	2.75	0.12	2.48	0.11	0.29	0.06	0.43	0.07
FLD15	72.53	3.06	12.73	0.64	3.35	0.24	3.77	0.15	3.19	0.13	2.72	0.12	0.28	0.05	0.53	0.07
FLD15	72.61	3.07	13.01	0.65	3.43	0.25	3.84	0.15	2.83	0.12	2.76	0.12	0.31	0.06	0.57	0.07
FLD15	71.28	3.01	12.65	0.64	3.29	0.24	3.76	0.15	3.21	0.14	2.84	0.13	0.33	0.06	0.53	0.07
FLD15	71.58	3.03	12.77	0.64	3.27	0.24	3.84	0.15	3.61	0.15	2.80	0.12	0.30	0.06	0.57	0.07
FLD15	72.24	3.05	12.50	0.63	3.26	0.24	3.72	0.15	2.89	0.13	2.63	0.12	0.26	0.05	0.46	0.07
FLD15	72.96	3.08	13.00	0.65	3.36	0.25	3.67	0.15	3.32	0.14	2.76	0.12	0.29	0.06	0.59	0.08
FLD15	73.04	3.09	12.92	0.65	3.32	0.24	3.77	0.15	3.17	0.13	2.65	0.12	0.30	0.06	0.55	0.07
FLD15	75.33	3.18	13.65	0.68	3.53	0.26	3.66	0.15	3.05	0.13	2.69	0.12	0.30	0.06	0.60	0.08
FLD15	74.04	3.13	13.27	0.66	3.35	0.24	3.70	0.15	3.46	0.14	2.77	0.12	0.28	0.06	0.59	0.08
FLD15	72.55	3.07	13.01	0.65	3.31	0.24	3.91	0.15	2.69	0.12	2.71	0.12	0.26	0.05	0.54	0.07
FLD15	73.03	3.09	12.90	0.65	3.31	0.24	3.72	0.15	3.40	0.14	2.66	0.12	0.33	0.06	0.59	0.08
FLD15	72.70	3.07	11.54	0.58	3.10	0.23	3.67	0.15	2.98	0.13	2.66	0.12	0.26	0.05	0.58	0.08
FLD15	72.48	3.06	12.91	0.65	3.39	0.25	3.74	0.15	3.27	0.14	2.50	0.11	0.37	0.06	0.53	0.07
FLD15	71.34	3.02	12.77	0.64	3.27	0.24	3.79	0.15	3.02	0.13	2.62	0.12	0.28	0.06	0.50	0.07
FLD15	72.41	3.06	12.88	0.65	3.43	0.25	3.68	0.15	3.29	0.14	2.60	0.12	0.29	0.06	0.55	0.07
FLD15	73.90	3.12	12.80	0.64	3.34	0.24	3.76	0.15	3.10	0.13	2.62	0.12	0.25	0.05	0.54	0.07
FLD15	71.71	3.03	12.76	0.64	3.34	0.24	3.72	0.15	3.37	0.14	2.75	0.12	0.36	0.06	0.61	0.08
FLD15	72.44	3.06	12.97	0.65	3.32	0.24	3.76	0.15	3.33	0.14	2.64	0.12	0.27	0.05	0.60	0.08
FLD15	71.59	3.03	12.82	0.64	3.14	0.23	3.55	0.14	3.22	0.14	2.83	0.12	0.31	0.06	0.57	0.08
FLD15	71.83	3.04	12.31	0.62	3.33	0.24	3.90	0.15	2.70	0.12	2.58	0.12	0.27	0.05	0.38	0.07
FLD15	73.09	3.09	12.88	0.65	3.40	0.25	3.76	0.15	3.33	0.14	2.69	0.12	0.31	0.06	0.58	0.08
FLD15	74.93	3.16	13.16	0.66	3.48	0.25	3.77	0.15	3.20	0.14	2.74	0.12	0.31	0.06	0.59	0.08
FLD15	73.13	3.09	13.37	0.67	3.26	0.24	3.72	0.15	2.88	0.13	2.93	0.13	0.41	0.06	0.64	0.08
FLD15	74.27	3.14	12.84	0.65	3.33	0.24	3.68	0.15	2.95	0.13	2.63	0.12	0.31	0.06	0.52	0.07
FLD15	71.71	3.03	12.81	0.64	3.28	0.24	3.79	0.15	3.79	0.15	2.81	0.12	0.41	0.06	0.65	0.08
FLD15	73.44	3.10	13.02	0.65	3.38	0.25	3.74	0.15	3.49	0.14	2.75	0.12	0.28	0.05	0.59	0.08
FLD15	72.33	3.06	12.74	0.64	3.28	0.24	3.80	0.15	3.66	0.15	2.63	0.12	0.33	0.06	0.61	0.08

FLD15	71.34	3.02	12.96	0.65	3.30	0.24	3.83	0.15	2.90	0.13	2.96	0.13	0.35	0.06	0.62	0.08
FLD15	73.12	3.09	13.18	0.66	3.43	0.25	3.88	0.15	2.95	0.13	2.83	0.12	0.32	0.06	0.57	0.07
FLD15	73.41	3.10	12.63	0.64	3.34	0.24	3.70	0.15	3.35	0.14	2.60	0.12	0.32	0.06	0.53	0.07
FLD15	73.44	3.10	12.87	0.65	3.10	0.23	3.68	0.15	2.59	0.12	2.83	0.13	0.35	0.06	0.56	0.07
FLD15	72.75	3.07	12.58	0.63	3.32	0.24	3.64	0.14	3.17	0.13	2.58	0.12	0.34	0.06	0.55	0.07
FLD15	73.03	3.09	12.79	0.64	3.36	0.25	3.88	0.15	2.85	0.12	2.70	0.12	0.32	0.06	0.49	0.07
FLD15	76.50	3.23	11.81	0.60	3.22	0.24	3.55	0.14	2.69	0.12	2.48	0.11	0.28	0.05	0.50	0.07
FLD15	73.60	3.11	13.11	0.66	3.45	0.25	3.75	0.15	3.55	0.15	2.78	0.12	0.29	0.06	0.62	0.08
FLD15	73.26	3.09	12.91	0.65	3.34	0.24	3.70	0.15	2.94	0.13	2.70	0.12	0.25	0.05	0.55	0.07
FLD15	72.20	3.05	12.87	0.65	3.35	0.24	3.73	0.15	3.36	0.14	2.78	0.12	0.28	0.06	0.55	0.07
FLD15	74.13	3.13	12.73	0.64	3.38	0.25	3.70	0.15	3.21	0.14	2.76	0.12	0.26	0.05	0.50	0.07
FLD15	73.60	3.11	12.52	0.63	3.47	0.25	3.81	0.15	2.75	0.12	2.71	0.12	0.28	0.05	0.48	0.07
FLD15	73.13	3.09	12.86	0.65	3.35	0.24	3.72	0.15	3.13	0.13	2.75	0.12	0.28	0.06	0.57	0.08
FLD15	73.03	3.09	13.32	0.67	3.12	0.23	3.62	0.14	3.07	0.13	2.82	0.12	0.33	0.06	0.55	0.07
FLD15	72.68	3.07	12.89	0.65	3.42	0.25	3.80	0.15	3.18	0.13	2.66	0.12	0.25	0.05	0.53	0.07
FLD15	71.78	3.03	12.51	0.63	3.24	0.24	3.78	0.15	3.44	0.14	2.80	0.12	0.32	0.06	0.63	0.08
FLD15	75.56	3.19	13.20	0.66	3.48	0.25	3.62	0.14	3.26	0.14	2.72	0.12	0.30	0.06	0.58	0.08
FLD15	71.62	3.03	12.38	0.62	3.04	0.23	3.76	0.15	3.76	0.15	2.84	0.13	0.33	0.06	0.50	0.07
FLD15	73.62	3.11	13.04	0.65	3.39	0.25	3.71	0.15	3.13	0.13	2.85	0.13	0.33	0.06	0.54	0.07
FLD15	74.31	3.14	12.30	0.62	3.19	0.24	3.72	0.15	3.08	0.13	2.55	0.12	0.28	0.06	0.53	0.07
FLD15	71.36	3.02	12.64	0.64	3.28	0.24	3.89	0.15	3.06	0.13	2.79	0.12	0.26	0.05	0.57	0.07
FLD15	74.08	3.13	13.69	0.68	3.41	0.25	3.61	0.14	2.99	0.13	2.86	0.13	0.36	0.06	0.52	0.07
FLD15	74.29	3.14	13.10	0.66	3.47	0.25	3.91	0.15	2.38	0.11	2.84	0.13	0.33	0.06	0.65	0.08
FLD15	74.50	3.15	13.39	0.67	3.39	0.25	3.72	0.15	2.99	0.13	2.58	0.12	0.29	0.06	0.51	0.07
FLD15	74.26	3.14	13.22	0.66	3.54	0.26	3.77	0.15	2.60	0.12	2.79	0.12	0.32	0.06	0.58	0.08
FLD15	74.28	3.14	13.34	0.67	3.43	0.25	3.56	0.14	2.88	0.13	2.90	0.13	0.30	0.06	0.50	0.07
FLD15	74.58	3.15	13.04	0.65	3.43	0.25	3.69	0.15	3.08	0.13	2.82	0.12	0.28	0.06	0.60	0.08
FLD15	72.78	3.07	12.87	0.65	3.39	0.25	3.78	0.15	3.05	0.13	2.69	0.12	0.30	0.06	0.54	0.07
FLD15	74.75	3.16	13.11	0.66	3.46	0.25	3.66	0.15	2.64	0.12	2.62	0.12	0.25	0.05	0.48	0.07
FLD15	73.04	3.09	12.66	0.64	3.38	0.25	3.78	0.15	3.13	0.13	2.62	0.12	0.28	0.05	0.50	0.07
FLD15	74.91	3.16	13.20	0.66	3.48	0.25	3.70	0.15	3.31	0.14	2.75	0.12	0.29	0.06	0.62	0.08
FLD15	72.34	3.06	12.82	0.64	3.44	0.25	3.81	0.15	3.37	0.14	2.77	0.12	0.29	0.06	0.60	0.08
FLD15	74.00	3.13	13.02	0.65	3.16	0.23	3.52	0.14	3.25	0.14	3.00	0.13	0.31	0.06	0.58	0.08
FLD15	73.35	3.10	13.62	0.68	3.34	0.24	3.72	0.15	3.13	0.13	2.73	0.12	0.30	0.06	0.53	0.07
FLD15	73.54	3.11	13.03	0.65	3.43	0.25	3.79	0.15	3.32	0.14	2.69	0.12	0.33	0.06	0.59	0.08
FLD15	71.61	3.03	12.58	0.63	2.90	0.22	3.78	0.15	3.55	0.15	2.73	0.12	0.34	0.06	0.45	0.07
FLD15	73.85	3.12	12.98	0.65	3.35	0.24	3.76	0.15	3.16	0.13	2.78	0.12	0.26	0.05	0.56	0.07
FLD15	73.84	3.12	13.03	0.65	3.30	0.24	3.75	0.15	3.52	0.14	2.68	0.12	0.33	0.06	0.53	0.07
FLD15	74.15	3.13	12.87	0.65	3.31	0.24	3.65	0.15	3.15	0.13	2.67	0.12	0.30	0.06	0.53	0.07
FLD15	71.40	3.02	12.40	0.62	3.23	0.24	3.74	0.15	3.19	0.13	2.71	0.12	0.27	0.05	0.46	0.07
FLD15	73.69	3.11	12.89	0.65	3.41	0.25	3.82	0.15	3.36	0.14	2.77	0.12	0.36	0.06	0.57	0.07
FLD15	72.82	3.08	12.76	0.64	3.25	0.24	3.79	0.15	3.39	0.14	2.70	0.12	0.36	0.06	0.58	0.08
FLD15	72.25	3.05	13.67	0.68	3.58	0.26	3.90	0.15	2.64	0.12	2.58	0.12	0.23	0.05	0.57	0.07
FLD15	73.24	3.09	13.19	0.66	3.43	0.25	3.84	0.15	2.79	0.12	2.85	0.13	0.29	0.06	0.58	0.08
FLD15	72.24	3.05	12.76	0.64	3.31	0.24	3.77	0.15	3.02	0.13	2.62	0.12	0.36	0.06	0.59	0.08
FLD15	74.72	3.16	12.37	0.62	3.31	0.24	3.78	0.15	3.10	0.13	2.67	0.12	0.27	0.05	0.53	0.07
FLD15	74.09	3.13	13.08	0.66	3.43	0.25	3.70	0.15	3.05	0.13	2.68	0.12	0.27	0.05	0.56	0.07
FLD15	73.95	3.12	13.22	0.66	3.44	0.25	3.80	0.15	3.15	0.13	2.69	0.12	0.34	0.06	0.55	0.07
FLD15	74.22	3.13	12.62	0.63	3.45	0.25	3.74	0.15	3.11	0.13	2.80	0.12	0.26	0.05	0.53	0.07
FLD15	72.91	3.08	13.05	0.65	3.47	0.25	3.85	0.15	3.34	0.14	2.77	0.12	0.28	0.05	0.59	0.08
FLD15	74.06	3.13	12.84	0.64	3.56	0.26	3.78	0.15	3.14	0.13	2.79	0.12	0.33	0.06	0.58	0.08
FLD15	72.44	3.06	12.81	0.64	3.51	0.25	3.80	0.15	3.16	0.13	2.72	0.12	0.31	0.06	0.55	0.07
FLD15	74.14	3.13	12.98	0.65	3.33	0.24	3.62	0.14	3.30	0.14	2.85	0.13	0.26	0.05	0.62	0.08
FLD15	74.77	3.16	13.23	0.66	3.31	0.24	3.73	0.15	3.00	0.13	2.84	0.13	0.38	0.06	0.54	0.07
FLD15	74.26	3.14	12.89	0.65	3.39	0.25	3.80	0.15	3.01	0.13	2.70	0.12	0.29	0.06	0.51	0.07
FLD15	73.20	3.09	12.63	0.64	3.13	0.23	3.88	0.15	2.80	0.12	2.76	0.12	0.26	0.05	0.37	0.06
FLD15	75.64	3.19	12.64	0.64	3.29	0.24	3.58	0.14	3.03	0.13	2.61	0.12	0.27	0.05	0.54	0.07
FLD15	73.35	3.10	12.96	0.65	3.37	0.25	3.75	0.15	3.35	0.14	2.78	0.12	0.30	0.06	0.55	0.07
FLD15	71.85	3.04	12.66	0.64	3.35	0.24	3.95	0.15	3.16	0.13	2.71	0.12	0.27	0.05	0.51	0.07
FLD15	73.61	3.11	12.82	0.64	3.28	0.24	3.85	0.15	3.23	0.14	2.67	0.12	0.30	0.06	0.51	0.07
FLD15	73.53	3.11	13.03	0.65	3.46	0.25	3.74	0.15	3.07	0.13	2.74	0.12	0.32	0.06	0.52	0.07
FLD15	71.51	3.02	13.24	0.66	3.35	0.25	3.88	0.15	3.40	0.14	2.74	0.12	0.32	0.06	0.57	0.08

FLD15	73.48	3.10	13.62	0.68	3.44	0.25	3.74	0.15	3.18	0.13	2.89	0.13	0.38	0.06	0.58	0.08
FLD15	75.89	3.20	12.64	0.64	3.44	0.25	3.83	0.15	2.73	0.12	2.56	0.12	0.28	0.05	0.47	0.07
FLD15	73.87	3.12	13.16	0.66	3.38	0.25	3.73	0.15	2.72	0.12	2.75	0.12	0.31	0.06	0.58	0.08
FLD15	74.50	3.15	13.16	0.66	3.38	0.25	3.74	0.15	3.51	0.14	2.74	0.12	0.31	0.06	0.60	0.08
FLD15	74.76	3.16	12.95	0.65	3.48	0.25	3.78	0.15	3.32	0.14	2.67	0.12	0.30	0.06	0.55	0.07
FLD15	73.03	3.09	12.89	0.65	3.35	0.24	3.81	0.15	3.43	0.14	2.68	0.12	0.38	0.06	0.58	0.08
FLD15	72.47	3.06	12.86	0.65	3.31	0.24	3.80	0.15	3.61	0.15	2.76	0.12	0.36	0.06	0.59	0.08
FLD15	73.52	3.11	13.14	0.66	3.21	0.24	3.78	0.15	3.10	0.13	2.94	0.13	0.31	0.06	0.60	0.08
FLD15	71.16	3.01	12.55	0.63	3.32	0.24	3.89	0.15	3.41	0.14	2.76	0.12	0.33	0.06	0.49	0.07
FLD15	73.96	3.12	12.59	0.63	3.30	0.24	3.79	0.15	2.34	0.11	2.74	0.12	0.23	0.05	0.44	0.07
FLD15	73.97	3.12	13.22	0.66	3.39	0.25	3.67	0.15	3.44	0.14	2.85	0.13	0.29	0.06	0.57	0.08
FLD15	73.97	3.12	13.09	0.66	3.27	0.24	3.64	0.14	3.39	0.14	2.65	0.12	0.30	0.06	0.51	0.07
FLD15	74.57	3.15	12.96	0.65	3.38	0.25	3.86	0.15	2.97	0.13	2.68	0.12	0.28	0.06	0.52	0.07
FLD15	74.87	3.16	12.47	0.63	3.46	0.25	3.84	0.15	2.90	0.13	2.99	0.13	0.27	0.05	0.53	0.07
FLD15	74.20	3.13	12.43	0.63	3.43	0.25	3.75	0.15	2.68	0.12	2.69	0.12	0.30	0.06	0.45	0.07
FLD15	73.82	3.12	13.14	0.66	3.39	0.25	3.87	0.15	3.82	0.15	2.67	0.12	0.38	0.06	0.66	0.08
FLD15	74.76	3.16	13.17	0.66	3.40	0.25	3.67	0.15	3.25	0.14	2.64	0.12	0.28	0.06	0.59	0.08
FLD15	73.44	3.10	12.92	0.65	3.32	0.24	3.77	0.15	3.55	0.15	2.75	0.12	0.31	0.06	0.56	0.07
FLD15	71.90	3.04	13.40	0.67	3.38	0.25	3.93	0.15	2.98	0.13	2.83	0.12	0.36	0.06	0.59	0.08
FLD15	73.70	3.11	13.03	0.65	3.37	0.25	3.72	0.15	3.14	0.13	2.84	0.13	0.29	0.06	0.59	0.08
FLD15	73.29	3.10	12.91	0.65	3.21	0.24	3.83	0.15	3.25	0.14	2.66	0.12	0.29	0.06	0.58	0.08
FLD15	72.49	3.06	12.71	0.64	3.33	0.24	3.77	0.15	3.36	0.14	2.74	0.12	0.29	0.06	0.54	0.07
FLD15	75.00	3.17	13.25	0.66	3.36	0.25	3.66	0.15	3.05	0.13	2.55	0.12	0.32	0.06	0.52	0.07
FLD15	75.63	3.19	13.17	0.66	3.17	0.23	3.56	0.14	3.15	0.13	2.96	0.13	0.28	0.06	0.69	0.08
FLD15	74.63	3.15	13.67	0.68	2.94	0.22	3.18	0.13	3.44	0.14	2.66	0.12	0.30	0.06	0.57	0.08
FLD15	77.79	3.28	10.84	0.55	2.88	0.22	3.43	0.14	2.92	0.13	2.36	0.11	0.30	0.06	0.51	0.07
FLD15	74.15	3.13	12.90	0.65	3.58	0.26	3.86	0.15	2.73	0.12	3.01	0.13	0.31	0.06	0.50	0.07
FLD15	72.80	3.08	12.68	0.64	3.32	0.24	3.79	0.15	3.24	0.14	2.81	0.12	0.28	0.06	0.54	0.07
FLD15	72.58	3.07	12.30	0.62	3.22	0.24	3.81	0.15	3.27	0.14	2.72	0.12	0.26	0.05	0.50	0.07
FLD15	71.32	3.01	13.35	0.67	3.35	0.24	3.75	0.15	3.36	0.14	2.93	0.13	0.34	0.06	0.52	0.07
FLD15	73.85	3.12	12.96	0.65	3.30	0.24	3.78	0.15	3.36	0.14	2.77	0.12	0.33	0.06	0.57	0.07
FLD15	72.56	3.07	12.74	0.64	3.38	0.25	3.79	0.15	3.24	0.14	2.81	0.12	0.30	0.06	0.57	0.07
FLD15	73.70	3.11	12.61	0.63	3.28	0.24	3.77	0.15	3.46	0.14	2.73	0.12	0.25	0.05	0.56	0.07
FLD15	73.98	3.12	13.33	0.67	2.96	0.22	3.21	0.13	3.07	0.13	2.77	0.12	0.33	0.06	0.55	0.07
FLD15	73.35	3.10	13.16	0.66	3.14	0.23	3.60	0.14	3.07	0.13	2.84	0.13	0.31	0.06	0.54	0.07
FLD15	76.09	3.21	13.30	0.67	3.44	0.25	3.58	0.14	3.16	0.13	2.80	0.12	0.28	0.06	0.59	0.08
FLD15	74.18	3.13	13.40	0.67	3.48	0.25	3.83	0.15	2.96	0.13	2.89	0.13	0.32	0.06	0.57	0.07
FLD15	72.85	3.08	12.95	0.65	3.32	0.24	3.71	0.15	3.78	0.15	2.98	0.13	0.32	0.06	0.59	0.08
FLD15	72.83	3.08	12.51	0.63	3.39	0.25	3.90	0.15	3.19	0.13	2.74	0.12	0.26	0.05	0.54	0.07
FLD15	72.83	3.08	12.74	0.64	3.27	0.24	3.74	0.15	3.33	0.14	2.87	0.13	0.26	0.05	0.58	0.08
FLD15	74.46	3.14	12.92	0.65	3.41	0.25	3.77	0.15	2.93	0.13	2.76	0.12	0.32	0.06	0.50	0.07
FLD15	75.60	3.19	13.64	0.68	3.23	0.24	3.71	0.15	2.95	0.13	2.46	0.11	0.29	0.06	0.52	0.07
FLD15	75.08	3.17	13.85	0.69	3.21	0.24	3.68	0.15	3.15	0.13	2.62	0.12	0.32	0.06	0.53	0.07
FLD15	73.03	3.09	13.02	0.65	3.11	0.23	3.67	0.15	3.08	0.13	3.15	0.13	0.36	0.06	0.61	0.08
FLD15	73.68	3.11	12.72	0.64	3.38	0.25	3.85	0.15	3.10	0.13	2.62	0.12	0.27	0.05	0.56	0.07
FLD15	74.02	3.13	13.48	0.67	3.39	0.25	3.63	0.14	3.05	0.13	2.72	0.12	0.29	0.06	0.59	0.08
FLD16	75.49	3.19	12.44	0.63	2.95	0.22	3.81	0.15	1.89	0.10	3.14	0.13	0.42	0.06	0.59	0.08
FLD16	81.71	3.44	10.43	0.53	2.56	0.20	3.67	0.15	0.92	0.07	2.78	0.12	0.28	0.06	0.57	0.08
FLD16	71.96	3.04	13.81	0.69	2.78	0.21	3.87	0.15	1.84	0.09	2.90	0.13	0.35	0.06	0.65	0.08
FLD16	72.34	3.06	13.07	0.66	2.74	0.21	3.79	0.15	1.74	0.09	3.01	0.13	0.34	0.06	0.59	0.08
FLD16	73.70	3.11	13.12	0.66	2.96	0.22	3.85	0.15	1.80	0.09	3.07	0.13	0.37	0.06	0.60	0.08
FLD16	70.76	2.99	15.77	0.78	3.28	0.24	4.09	0.16	1.47	0.08	3.37	0.14	0.45	0.06	0.76	0.08
FLD16	74.25	3.14	13.97	0.70	2.10	0.17	3.59	0.14	2.88	0.13	2.96	0.13	0.27	0.05	0.52	0.07
FLD16	82.47	3.48	10.79	0.55	2.47	0.19	3.90	0.15	0.86	0.06	2.36	0.11	0.34	0.06	0.53	0.07
FLD16	67.02	2.84	15.68	0.78	3.75	0.27	4.20	0.16	2.50	0.11	3.97	0.16	0.43	0.06	0.91	0.09
FLD16	73.23	3.09	13.85	0.69	2.93	0.22	3.67	0.15	2.32	0.11	2.98	0.13	0.35	0.06	0.60	0.08
FLD16	75.60	3.19	12.53	0.63	2.92	0.22	3.84	0.15	1.36	0.08	2.58	0.12	0.27	0.05	0.47	0.07
FLD16	71.41	3.02	16.18	0.80	2.57	0.20	3.57	0.14	1.50	0.08	3.06	0.13	0.47	0.06	0.66	0.08
FLD16	75.55	3.19	13.33	0.67	2.63	0.20	3.63	0.14	0.98	0.07	2.68	0.12	0.29	0.06	0.34	0.06
FLD16	68.58	2.90	14.82	0.74	3.22	0.24	4.14	0.16	1.43	0.08	3.67	0.15	0.43	0.06	0.67	0.08
FLD16	70.07	2.96	15.07	0.75	3.40	0.25	4.01	0.16	1.74	0.09	3.39	0.14	0.44	0.06	0.76	0.09
FLD16	75.54	3.19	12.88	0.65	3.08	0.23	4.05	0.16	1.62	0.09	2.82	0.12	0.34	0.06	0.52	0.07

FLD16	73.91	3.12	14.11	0.70	3.46	0.25	4.01	0.16	2.04	0.10	2.99	0.13	0.40	0.06	0.73	0.08
FLD16	75.45	3.19	13.71	0.68	3.15	0.23	3.87	0.15	1.80	0.09	2.70	0.12	0.33	0.06	0.61	0.08
FLD16	72.48	3.06	14.50	0.72	2.53	0.19	3.60	0.14	1.34	0.08	3.17	0.14	0.51	0.06	0.70	0.08
FLD16	73.27	3.10	14.93	0.74	2.64	0.20	3.66	0.15	1.28	0.08	3.09	0.13	0.38	0.06	0.64	0.08
FLD16	73.43	3.10	14.60	0.73	2.80	0.21	3.60	0.14	2.59	0.12	2.82	0.12	0.38	0.06	0.65	0.08
FLD16	76.38	3.22	13.78	0.69	2.87	0.22	3.93	0.15	1.46	0.08	2.87	0.13	0.27	0.05	0.62	0.08
FLD16	73.88	3.12	14.04	0.70	3.12	0.23	4.12	0.16	1.45	0.08	2.93	0.13	0.33	0.06	0.58	0.08
FLD16	71.98	3.04	15.28	0.76	2.20	0.17	3.65	0.15	1.27	0.08	3.35	0.14	0.45	0.06	0.92	0.09
FLD16	76.26	3.22	12.29	0.62	2.78	0.21	3.71	0.15	1.26	0.08	2.98	0.13	0.33	0.06	0.59	0.08
FLD16	74.50	3.15	13.88	0.69	3.37	0.25	4.36	0.17	1.39	0.08	3.08	0.13	0.43	0.06	0.88	0.09
FLD16	79.60	3.36	10.55	0.54	3.03	0.23	4.12	0.16	1.30	0.08	2.39	0.11	0.24	0.05	0.45	0.07
FLD16	69.80	2.95	16.26	0.80	3.34	0.24	4.11	0.16	1.77	0.09	3.12	0.13	0.42	0.06	0.72	0.08
FLD16	73.27	3.10	13.01	0.65	2.88	0.22	3.97	0.15	1.46	0.08	3.43	0.14	0.42	0.06	0.66	0.08
FLD16	68.01	2.88	15.19	0.75	3.51	0.25	4.15	0.16	1.92	0.10	3.95	0.16	0.40	0.06	0.72	0.08
FLD16	71.05	3.00	17.16	0.84	3.53	0.26	3.88	0.15	1.76	0.09	3.36	0.14	0.54	0.06	0.83	0.09
FLD16	74.11	3.13	14.07	0.70	2.76	0.21	3.77	0.15	2.52	0.11	2.82	0.12	0.34	0.06	0.69	0.08
FLD16	73.17	3.09	13.91	0.69	2.73	0.21	3.69	0.15	1.58	0.09	2.82	0.12	0.36	0.06	0.69	0.08
FLD16	76.87	3.24	12.82	0.64	2.98	0.22	3.94	0.15	1.84	0.09	2.77	0.12	0.32	0.06	0.57	0.07
FLD16	71.97	3.04	14.34	0.71	3.36	0.25	4.48	0.17	1.62	0.09	3.20	0.14	0.43	0.06	0.77	0.09
FLD16	70.16	2.97	14.91	0.74	3.18	0.23	4.18	0.16	1.64	0.09	3.38	0.14	0.44	0.06	0.87	0.09
FLD16	77.34	3.26	12.81	0.64	2.83	0.21	3.73	0.15	1.10	0.07	2.67	0.12	0.31	0.06	0.56	0.07
FLD16	75.42	3.18	13.44	0.67	3.22	0.24	4.04	0.16	2.18	0.10	2.74	0.12	0.30	0.06	0.54	0.07
FLD16	78.98	3.33	11.91	0.60	2.51	0.19	3.69	0.15	0.93	0.07	2.28	0.11	0.23	0.05	0.53	0.07
FLD16	72.83	3.08	14.98	0.74	2.80	0.21	3.86	0.15	1.63	0.09	3.20	0.14	0.50	0.06	0.93	0.09
FLD16	74.54	3.15	13.22	0.66	3.26	0.24	4.34	0.17	1.42	0.08	2.94	0.13	0.35	0.06	0.50	0.07
FLD16	75.99	3.21	13.46	0.67	2.15	0.17	4.67	0.18	1.06	0.07	1.92	0.10	0.30	0.06	0.57	0.07
FLD16	79.47	3.35	11.73	0.59	2.46	0.19	3.83	0.15	1.96	0.10	2.12	0.10	0.26	0.05	0.40	0.07
FLD16	65.15	2.76	18.14	0.89	3.61	0.26	4.16	0.16	1.78	0.09	3.54	0.15	0.67	0.07	1.03	0.10
FLD16	77.13	3.26	13.02	0.65	3.25	0.24	3.96	0.15	1.72	0.09	3.08	0.13	0.31	0.06	0.59	0.08
FLD16	67.87	2.87	18.75	0.92	4.68	0.33	4.62	0.17	1.48	0.08	3.01	0.13	0.32	0.06	1.14	0.10
FLD16	70.02	2.96	15.25	0.76	3.09	0.23	3.97	0.15	1.98	0.10	3.18	0.14	0.44	0.06	0.74	0.08
FLD16	70.12	2.96	14.26	0.71	2.55	0.20	4.49	0.17	1.64	0.09	2.84	0.13	0.31	0.06	0.72	0.08
FLD16	66.01	2.79	20.91	1.02	4.57	0.32	5.20	0.19	1.10	0.07	0.70	0.06	0.96	0.08	0.12	0.05
FLD16	77.31	3.26	12.61	0.63	3.31	0.24	4.04	0.16	1.33	0.08	2.75	0.12	0.43	0.06	0.54	0.07
FLD16	73.63	3.11	13.53	0.68	3.37	0.25	4.18	0.16	1.85	0.09	2.54	0.12	0.34	0.06	0.45	0.07
FLD16	72.26	3.05	11.40	0.58	4.06	0.29	4.90	0.18	1.62	0.09	3.01	0.13	0.25	0.05	0.55	0.07
FLD16	67.45	2.85	14.96	0.74	4.12	0.29	4.95	0.18	1.18	0.07	3.13	0.13	0.56	0.06	0.63	0.08
FLD16	70.87	3.00	15.64	0.77	3.16	0.23	4.24	0.16	1.96	0.10	3.19	0.14	0.39	0.06	0.73	0.08
FLD16	75.25	3.18	13.54	0.68	2.34	0.18	3.19	0.13	1.82	0.09	3.31	0.14	0.32	0.06	0.54	0.07
FLD16	74.35	3.14	13.55	0.68	2.99	0.22	4.12	0.16	1.17	0.07	3.17	0.14	0.45	0.06	0.64	0.08
FLD16	71.25	3.01	14.28	0.71	3.27	0.24	4.01	0.16	1.80	0.09	3.45	0.14	0.52	0.06	0.75	0.08
FLD16	71.71	3.03	13.66	0.68	2.92	0.22	4.16	0.16	2.44	0.11	3.05	0.13	0.48	0.06	0.76	0.08
FLD16	74.76	3.16	13.82	0.69	2.94	0.22	3.74	0.15	1.81	0.09	3.14	0.13	0.39	0.06	0.55	0.07
FLD16	75.31	3.18	13.61	0.68	2.77	0.21	3.69	0.15	1.68	0.09	2.76	0.12	0.35	0.06	0.55	0.07
FLD16	73.44	3.10	16.05	0.79	3.39	0.25	4.19	0.16	1.44	0.08	2.78	0.12	0.33	0.06	0.64	0.08
FLD16	70.64	2.99	15.66	0.78	2.81	0.21	3.71	0.15	1.51	0.08	3.54	0.15	0.48	0.06	0.82	0.09
FLD16	76.58	3.23	12.93	0.65	2.84	0.21	3.90	0.15	1.30	0.08	2.72	0.12	0.23	0.05	0.52	0.07
FLD16	75.04	3.17	12.75	0.64	1.85	0.15	3.69	0.15	0.97	0.07	2.82	0.12	0.26	0.05	0.56	0.07
FLD16	77.82	3.28	10.79	0.55	3.02	0.22	4.05	0.16	1.28	0.08	2.97	0.13	0.30	0.06	0.50	0.07
FLD16	73.37	3.10	15.04	0.75	2.98	0.22	3.87	0.15	1.62	0.09	3.08	0.13	0.38	0.06	0.70	0.08
FLD16	72.81	3.08	15.39	0.76	3.05	0.23	3.94	0.15	1.81	0.09	3.43	0.14	0.41	0.06	0.73	0.08
FLD16	73.17	3.09	12.78	0.64	3.32	0.24	4.63	0.18	1.59	0.09	3.05	0.13	0.42	0.06	0.64	0.08
FLD16	72.88	3.08	14.74	0.73	3.15	0.23	3.98	0.16	1.59	0.09	3.15	0.13	0.37	0.06	0.67	0.08
FLD16	76.15	3.21	12.96	0.65	3.13	0.23	4.08	0.16	1.06	0.07	3.48	0.15	0.24	0.05	0.54	0.07
FLD16	73.07	3.09	16.09	0.80	2.78	0.21	3.64	0.14	0.93	0.07	2.73	0.12	0.38	0.06	0.55	0.07
FLD16	75.39	3.18	13.61	0.68	2.88	0.22	3.71	0.15	1.24	0.08	2.64	0.12	0.27	0.05	0.41	0.07
FLD16	75.37	3.18	13.43	0.67	2.55	0.20	3.64	0.14	2.47	0.11	2.59	0.12	0.19	0.05	0.57	0.07
FLD16	74.57	3.15	13.75	0.69	2.62	0.20	3.96	0.15	1.99	0.10	2.80	0.12	0.30	0.06	0.58	0.08
FLD16	73.70	3.11	15.05	0.75	3.81	0.27	4.42	0.17	1.79	0.09	2.79	0.12	0.42	0.06	0.64	0.08
FLD17	73.81	3.12	13.04	0.65	3.24	0.24	3.89	0.15	3.02	0.13	2.77	0.12	0.27	0.05	0.63	0.08
FLD17	75.56	3.19	13.77	0.69	3.05	0.23	3.50	0.14	2.76	0.12	2.77	0.12	0.26	0.05	0.62	0.08
FLD17	72.20	3.05	13.34	0.67	3.35	0.24	3.91	0.15	2.43	0.11	2.79	0.12	0.28	0.05	0.62	0.08

FLD17	73.44	3.10	13.04	0.65	3.25	0.24	3.82	0.15	2.08	0.10	2.85	0.13	0.28	0.06	0.65	0.08
FLD17	72.79	3.08	13.06	0.66	2.98	0.22	3.68	0.15	2.39	0.11	2.82	0.12	0.27	0.05	0.72	0.08
FLD17	72.95	3.08	13.00	0.65	3.57	0.26	3.94	0.15	2.90	0.13	2.55	0.12	0.23	0.05	0.56	0.07
FLD17	74.15	3.13	12.67	0.64	3.51	0.25	3.90	0.15	2.25	0.11	2.74	0.12	0.24	0.05	0.62	0.08
FLD17	76.07	3.21	13.49	0.68	3.46	0.25	4.08	0.16	2.45	0.11	2.88	0.13	0.29	0.06	0.62	0.08
FLD17	75.16	3.17	12.49	0.63	3.06	0.23	3.59	0.14	2.75	0.12	2.69	0.12	0.32	0.06	0.55	0.07
FLD17	77.21	3.26	13.45	0.67	3.13	0.23	3.63	0.14	2.75	0.12	2.78	0.12	0.28	0.05	0.66	0.08
FLD17	72.64	3.07	13.38	0.67	3.27	0.24	4.08	0.16	2.33	0.11	3.05	0.13	0.33	0.06	0.70	0.08
FLD17	70.91	3.00	14.38	0.72	3.52	0.26	3.83	0.15	2.24	0.11	3.06	0.13	0.36	0.06	0.78	0.09
FLD17	76.76	3.24	12.89	0.65	3.18	0.23	3.69	0.15	2.63	0.12	2.71	0.12	0.17	0.05	0.52	0.07
FLD17	74.30	3.14	14.16	0.71	3.39	0.25	4.02	0.16	2.33	0.11	3.10	0.13	0.32	0.06	0.74	0.08
FLD17	75.04	3.17	13.81	0.69	3.45	0.25	4.00	0.16	2.43	0.11	2.80	0.12	0.34	0.06	0.72	0.08
FLD17	73.53	3.11	13.17	0.66	3.31	0.24	4.00	0.16	2.07	0.10	3.22	0.14	0.36	0.06	0.79	0.09
FLD17	72.51	3.06	13.55	0.68	3.41	0.25	3.94	0.15	2.51	0.11	2.78	0.12	0.32	0.06	0.64	0.08
FLD17	73.28	3.10	12.92	0.65	3.60	0.26	3.94	0.15	2.98	0.13	2.67	0.12	0.24	0.05	0.58	0.08
FLD17	75.52	3.19	13.48	0.67	3.23	0.24	3.88	0.15	2.33	0.11	2.81	0.12	0.32	0.06	0.66	0.08
FLD17	76.61	3.23	13.23	0.66	3.24	0.24	3.98	0.16	2.29	0.11	2.85	0.13	0.31	0.06	0.73	0.08
FLD17	73.25	3.09	17.04	0.84	3.79	0.27	5.11	0.19	1.72	0.09	2.19	0.11	0.25	0.05	0.53	0.07
FLD17	69.52	2.94	15.92	0.79	3.86	0.28	5.08	0.19	1.80	0.09	1.86	0.09	0.18	0.05	0.36	0.06
FLD17	75.68	3.19	13.51	0.68	3.16	0.23	3.83	0.15	2.45	0.11	2.93	0.13	0.29	0.06	0.74	0.08
FLD17	75.02	3.17	13.81	0.69	3.15	0.23	4.14	0.16	2.95	0.13	2.70	0.12	0.27	0.05	0.57	0.08
FLD17	73.81	3.12	12.35	0.62	3.24	0.24	3.84	0.15	2.49	0.11	2.62	0.12	0.26	0.05	0.60	0.08
FLD17	75.25	3.18	14.67	0.73	3.10	0.23	3.60	0.14	3.29	0.14	2.75	0.12	0.34	0.06	0.65	0.08
FLD17	74.87	3.16	13.89	0.69	3.09	0.23	3.69	0.15	3.04	0.13	3.06	0.13	0.32	0.06	0.73	0.08
FLD17	76.08	3.21	12.12	0.61	3.03	0.22	4.07	0.16	0.63	0.06	2.20	0.11	0.10	0.05	0.36	0.06
FLD17	74.32	3.14	14.01	0.70	3.19	0.23	3.99	0.16	1.64	0.09	2.63	0.12	0.33	0.06	0.54	0.07
FLD17	73.02	3.08	13.81	0.69	3.31	0.24	4.05	0.16	2.02	0.10	2.91	0.13	0.32	0.06	0.67	0.08
FLD17	69.09	2.92	18.85	0.92	4.24	0.30	5.04	0.19	1.39	0.08	1.41	0.08	0.13	0.05	0.31	0.06
FLD17	73.79	3.12	12.11	0.61	3.49	0.25	4.37	0.17	1.22	0.08	2.59	0.12	0.26	0.05	0.36	0.06
FLD17	71.99	3.04	13.36	0.67	3.57	0.26	4.23	0.16	1.93	0.10	2.57	0.12	0.27	0.05	0.55	0.07
FLD17	70.74	2.99	14.23	0.71	3.59	0.26	4.08	0.16	2.19	0.10	2.69	0.12	0.26	0.05	0.63	0.08
FLD17	74.19	3.13	12.71	0.64	3.42	0.25	4.02	0.16	2.92	0.13	2.83	0.13	0.24	0.05	0.65	0.08
FLD17	78.43	3.31	13.10	0.66	2.86	0.21	3.77	0.15	1.80	0.09	2.56	0.12	0.32	0.06	0.62	0.08
FLD17	76.22	3.22	12.30	0.62	2.90	0.22	3.79	0.15	2.39	0.11	2.84	0.13	0.27	0.05	0.57	0.07
FLD17	73.11	3.09	15.57	0.77	2.97	0.22	3.48	0.14	3.40	0.14	3.07	0.13	0.36	0.06	0.65	0.08
FLD17	78.80	3.32	11.95	0.60	3.14	0.23	3.85	0.15	1.92	0.10	2.74	0.12	0.25	0.05	0.65	0.08
FLD18	72.62	3.07	12.66	0.64	3.76	0.27	4.47	0.17	1.98	0.10	2.36	0.11	0.31	0.06	0.40	0.07
FLD18	72.74	3.07	13.58	0.68	3.43	0.25	3.95	0.15	2.17	0.10	2.95	0.13	0.35	0.06	0.64	0.08
FLD18	71.93	3.04	13.01	0.65	3.51	0.25	4.19	0.16	1.80	0.09	2.71	0.12	0.30	0.06	0.56	0.07
FLD18	71.31	3.01	13.26	0.66	3.64	0.26	4.07	0.16	2.13	0.10	2.84	0.13	0.33	0.06	0.80	0.09
FLD18	73.99	3.12	13.20	0.66	3.20	0.24	3.82	0.15	2.61	0.12	2.72	0.12	0.33	0.06	0.58	0.08
FLD18	72.99	3.08	13.78	0.69	3.74	0.27	4.25	0.16	2.18	0.10	2.78	0.12	0.34	0.06	0.61	0.08
FLD18	72.15	3.05	12.93	0.65	3.10	0.23	3.87	0.15	3.07	0.13	2.84	0.13	0.35	0.06	0.63	0.08
FLD18	75.05	3.17	13.73	0.69	2.81	0.21	3.42	0.14	2.48	0.11	2.88	0.13	0.35	0.06	0.89	0.09
FLD18	73.77	3.12	13.23	0.66	3.28	0.24	3.99	0.16	2.09	0.10	2.82	0.12	0.31	0.06	0.58	0.08
FLD18	73.13	3.09	13.03	0.65	2.66	0.20	3.52	0.14	2.47	0.11	2.75	0.12	0.34	0.06	0.53	0.07
FLD18	74.50	3.15	13.67	0.68	3.23	0.24	3.79	0.15	2.55	0.12	2.80	0.12	0.30	0.06	0.82	0.09
FLD18	73.02	3.08	13.11	0.66	3.15	0.23	3.86	0.15	2.72	0.12	2.77	0.12	0.28	0.06	0.56	0.07
FLD18	72.47	3.06	13.01	0.65	2.61	0.20	3.47	0.14	3.15	0.13	2.70	0.12	0.34	0.06	0.46	0.07
FLD18	71.89	3.04	12.66	0.64	3.80	0.27	4.23	0.16	2.29	0.11	2.83	0.13	0.40	0.06	0.54	0.07
FLD18	71.63	3.03	13.24	0.66	3.53	0.26	3.92	0.15	2.62	0.12	2.76	0.12	0.33	0.06	0.56	0.07
FLD18	72.69	3.07	12.80	0.64	3.37	0.25	4.00	0.16	2.01	0.10	2.63	0.12	0.27	0.05	0.55	0.07
FLD18	75.41	3.18	12.58	0.63	2.78	0.21	3.58	0.14	2.85	0.12	2.63	0.12	0.22	0.05	0.38	0.06
FLD18	76.29	3.22	13.47	0.67	2.79	0.21	3.58	0.14	3.19	0.13	2.59	0.12	0.29	0.06	0.75	0.08
FLD18	73.75	3.12	13.34	0.67	3.10	0.23	3.74	0.15	2.64	0.12	2.84	0.13	0.31	0.06	0.79	0.09
FLD18	75.67	3.19	13.50	0.68	2.79	0.21	3.47	0.14	2.83	0.12	2.72	0.12	0.29	0.06	0.77	0.09
FLD18	71.14	3.01	15.79	0.78	3.85	0.28	4.20	0.16	2.11	0.10	2.42	0.11	0.32	0.06	0.95	0.10
FLD18	73.33	3.10	13.49	0.67	3.72	0.27	4.36	0.17	1.07	0.07	2.67	0.12	0.36	0.06	0.76	0.08
FLD18	72.26	3.05	14.63	0.73	3.72	0.27	4.07	0.16	2.43	0.11	3.03	0.13	0.36	0.06	0.97	0.10
FLD18	68.55	2.90	14.96	0.74	3.81	0.27	4.30	0.17	2.05	0.10	3.26	0.14	0.48	0.06	1.02	0.10
FLD18	73.46	3.10	12.33	0.62	3.58	0.26	4.03	0.16	1.93	0.10	2.77	0.12	0.36	0.06	0.87	0.09
FLD18	73.07	3.09	14.19	0.71	3.58	0.26	4.32	0.17	2.16	0.10	2.86	0.13	0.33	0.06	0.82	0.09

FLD18	73.32	3.10	12.86	0.65	2.47	0.19	3.39	0.14	2.59	0.12	2.83	0.12	0.32	0.06	0.48	0.07
FLD18	74.69	3.15	13.85	0.69	2.79	0.21	3.60	0.14	2.44	0.11	2.96	0.13	0.32	0.06	0.83	0.09
FLD18	100.65	4.23	0.90	0.09	0.66	0.08	0.61	0.05	0.03	0.04	0.29	0.05	0.03	0.05	0.20	0.06
FLD18	75.83	3.20	13.77	0.69	2.65	0.20	3.36	0.14	3.33	0.14	2.67	0.12	0.29	0.06	0.80	0.09
FLD18	75.67	3.19	13.99	0.70	2.71	0.20	3.29	0.13	2.79	0.12	2.73	0.12	0.28	0.06	0.81	0.09
FLD18	69.19	2.93	14.85	0.74	3.89	0.28	4.63	0.18	2.04	0.10	3.05	0.13	0.31	0.06	0.87	0.09
FLD18	70.29	2.97	14.24	0.71	3.85	0.28	4.26	0.16	1.29	0.08	2.83	0.12	0.34	0.06	0.87	0.09
FLD18	71.51	3.02	14.35	0.71	3.57	0.26	4.19	0.16	2.22	0.11	2.66	0.12	0.44	0.06	0.87	0.09
FLD18	73.80	3.12	13.55	0.68	3.41	0.25	4.03	0.16	2.07	0.10	2.72	0.12	0.35	0.06	0.83	0.09
FLD18	73.34	3.10	13.56	0.68	3.73	0.27	4.09	0.16	1.97	0.10	2.65	0.12	0.28	0.06	0.86	0.09
FLD18	77.75	3.28	12.33	0.62	2.84	0.21	3.43	0.14	2.14	0.10	2.67	0.12	0.31	0.06	0.51	0.07
FLD18	75.88	3.20	13.59	0.68	2.65	0.20	3.49	0.14	2.72	0.12	2.59	0.12	0.34	0.06	0.82	0.09
FLD18	73.14	3.09	13.10	0.66	2.50	0.19	3.43	0.14	2.39	0.11	2.95	0.13	0.34	0.06	0.75	0.08
FLD18	73.40	3.10	13.24	0.66	2.58	0.20	3.37	0.14	2.78	0.12	2.93	0.13	0.29	0.06	0.48	0.07
FLD18	72.09	3.05	13.56	0.68	2.63	0.20	3.47	0.14	2.94	0.13	2.83	0.12	0.31	0.06	0.49	0.07
FLD18	72.22	3.05	14.37	0.72	3.59	0.26	4.09	0.16	2.33	0.11	2.90	0.13	0.37	0.06	0.91	0.09
FLD18	71.55	3.02	13.55	0.68	3.17	0.23	3.91	0.15	2.32	0.11	3.53	0.15	0.61	0.07	0.90	0.09
FLD18	74.09	3.13	13.33	0.67	2.94	0.22	3.60	0.14	2.77	0.12	2.74	0.12	0.31	0.06	0.81	0.09
FLD18	73.01	3.08	13.67	0.68	3.44	0.25	4.01	0.16	2.16	0.10	3.00	0.13	0.37	0.06	0.88	0.09
FLD18	72.26	3.05	13.53	0.68	3.37	0.25	3.99	0.16	2.15	0.10	2.87	0.13	0.35	0.06	0.84	0.09
FLD18	71.63	3.03	13.65	0.68	3.55	0.26	3.95	0.15	2.08	0.10	3.16	0.14	0.45	0.06	0.90	0.09
FLD18	74.58	3.15	14.44	0.72	3.19	0.24	3.78	0.15	1.90	0.10	2.93	0.13	0.37	0.06	0.88	0.09
FLD18	76.48	3.23	13.70	0.68	2.63	0.20	3.44	0.14	2.45	0.11	2.70	0.12	0.30	0.06	0.77	0.09
FLD18	75.56	3.19	13.74	0.69	2.69	0.20	3.55	0.14	2.53	0.11	2.77	0.12	0.34	0.06	0.75	0.08
FLD18	75.67	3.19	13.36	0.67	2.55	0.20	3.42	0.14	2.36	0.11	2.82	0.12	0.28	0.06	0.79	0.09
FLD18	75.72	3.20	13.32	0.67	2.38	0.18	3.26	0.13	2.50	0.11	2.89	0.13	0.30	0.06	0.74	0.08
FLD18	74.56	3.15	13.79	0.69	2.69	0.20	3.42	0.14	2.90	0.13	2.90	0.13	0.33	0.06	0.77	0.09
FLD18	73.47	3.10	12.71	0.64	3.08	0.23	3.91	0.15	3.13	0.13	2.75	0.12	0.28	0.05	0.71	0.08
FLD18	73.93	3.12	13.26	0.66	3.15	0.23	3.85	0.15	2.50	0.11	2.78	0.12	0.33	0.06	0.85	0.09
FLD18	73.23	3.09	13.60	0.68	3.28	0.24	3.99	0.16	2.63	0.12	2.77	0.12	0.27	0.05	0.82	0.09
FLD18	72.23	3.05	13.77	0.69	3.49	0.25	4.29	0.16	1.71	0.09	2.98	0.13	0.38	0.06	0.92	0.09
FLD18	72.76	3.07	13.66	0.68	3.17	0.23	3.80	0.15	3.05	0.13	2.59	0.12	0.31	0.06	0.79	0.09
FLD18	74.56	3.15	14.53	0.72	3.38	0.25	4.08	0.16	1.90	0.10	2.77	0.12	0.37	0.06	0.86	0.09
FLD18	74.99	3.17	13.56	0.68	3.31	0.24	3.96	0.15	1.89	0.10	2.76	0.12	0.33	0.06	0.55	0.07
FLD18	76.07	3.21	14.15	0.71	2.81	0.21	3.28	0.13	3.41	0.14	2.78	0.12	0.32	0.06	0.81	0.09
FLD18	74.38	3.14	13.44	0.67	2.61	0.20	3.20	0.13	3.39	0.14	2.68	0.12	0.29	0.06	0.72	0.08
FLD18	72.90	3.08	13.67	0.68	2.93	0.22	3.52	0.14	3.19	0.13	2.71	0.12	0.30	0.06	0.71	0.08
FLD18	72.00	3.04	13.66	0.68	3.10	0.23	4.04	0.16	2.37	0.11	2.81	0.12	0.35	0.06	0.77	0.09
FLD18	75.31	3.18	12.60	0.63	2.70	0.20	3.67	0.15	2.66	0.12	2.64	0.12	0.27	0.05	0.71	0.08
FLD18	73.62	3.11	13.52	0.68	3.34	0.24	4.01	0.16	2.57	0.12	2.88	0.13	0.37	0.06	0.89	0.09
FLD18	72.80	3.08	13.27	0.66	3.25	0.24	3.91	0.15	2.58	0.12	2.82	0.12	0.37	0.06	0.82	0.09
FLD18	71.38	3.02	14.37	0.72	3.59	0.26	4.28	0.16	1.57	0.09	2.90	0.13	0.35	0.06	0.87	0.09
FLD18	70.45	2.98	16.71	0.82	4.26	0.30	4.64	0.18	1.59	0.09	2.86	0.13	0.34	0.06	0.88	0.09
FLD18	76.25	3.22	12.63	0.64	3.34	0.24	4.10	0.16	1.06	0.07	2.17	0.10	0.16	0.05	0.36	0.06
FLD18	70.72	2.99	12.62	0.63	3.55	0.26	4.29	0.16	1.77	0.09	3.28	0.14	0.33	0.06	0.49	0.07
FLD18	74.43	3.14	13.98	0.70	2.77	0.21	3.43	0.14	3.13	0.13	2.78	0.12	0.32	0.06	0.77	0.09
FLD18	73.47	3.10	13.66	0.68	2.79	0.21	3.40	0.14	3.06	0.13	2.75	0.12	0.26	0.05	0.47	0.07
FLD18	72.00	3.04	13.37	0.67	3.20	0.24	3.99	0.16	2.50	0.11	2.74	0.12	0.29	0.06	0.52	0.07
FLD18	72.80	3.08	13.19	0.66	3.26	0.24	4.00	0.16	2.80	0.12	2.78	0.12	0.35	0.06	0.59	0.08
FLD18	72.58	3.07	13.32	0.67	3.28	0.24	3.96	0.15	2.46	0.11	2.93	0.13	0.35	0.06	0.60	0.08
FLD18	73.34	3.10	13.25	0.66	3.20	0.24	3.92	0.15	2.01	0.10	3.09	0.13	0.40	0.06	0.91	0.09
FLD18	73.25	3.09	14.52	0.72	3.98	0.28	4.55	0.17	1.59	0.09	2.89	0.13	0.41	0.06	1.01	0.10
FLD18	75.24	3.18	13.91	0.69	2.64	0.20	3.38	0.14	2.10	0.10	2.83	0.12	0.33	0.06	0.54	0.07
FLD18	74.84	3.16	11.81	0.60	3.03	0.22	3.99	0.16	1.28	0.08	2.74	0.12	0.29	0.06	0.48	0.07
FLD18	76.07	3.21	14.57	0.73	2.77	0.21	3.41	0.14	3.21	0.14	2.74	0.12	0.31	0.06	0.79	0.09
FLD18	75.27	3.18	14.25	0.71	2.77	0.21	3.40	0.14	3.21	0.14	2.72	0.12	0.31	0.06	0.78	0.09
FLD18	72.20	3.05	13.24	0.66	3.16	0.23	3.58	0.14	2.87	0.12	2.82	0.12	0.32	0.06	0.48	0.07
FLD18	72.90	3.08	13.46	0.67	3.15	0.23	3.99	0.16	2.69	0.12	2.77	0.12	0.33	0.06	0.80	0.09
FLD18	72.44	3.06	12.74	0.64	3.06	0.23	3.84	0.15	2.77	0.12	2.89	0.13	0.39	0.06	0.60	0.08
FLD18	73.04	3.09	13.02	0.65	3.29	0.24	4.15	0.16	1.84	0.09	2.75	0.12	0.30	0.06	0.50	0.07
FLD18	74.25	3.14	14.83	0.74	2.26	0.18	3.08	0.13	3.88	0.16	2.74	0.12	0.34	0.06	0.51	0.07
FLD18	75.06	3.17	14.02	0.70	2.79	0.21	3.41	0.14	3.06	0.13	2.70	0.12	0.31	0.06	0.50	0.07

FLD18	75.19	3.17	13.49	0.67	3.19	0.24	3.96	0.15	1.91	0.10	2.68	0.12	0.34	0.06	0.74	0.08
FLD18	75.35	3.18	13.80	0.69	3.18	0.23	3.76	0.15	2.61	0.12	2.73	0.12	0.31	0.06	0.81	0.09
FLD20	78.47	3.31	11.02	0.56	3.37	0.25	4.03	0.16	2.67	0.12	2.44	0.11	0.25	0.05	0.62	0.08
FLD20	71.99	3.04	13.06	0.66	3.16	0.23	3.58	0.14	4.71	0.18	3.10	0.13	0.29	0.06	0.77	0.09
FLD20	72.65	3.07	13.49	0.68	3.16	0.23	3.55	0.14	3.85	0.15	2.73	0.12	0.36	0.06	0.81	0.09
FLD20	72.33	3.06	13.44	0.67	3.30	0.24	3.89	0.15	2.50	0.11	2.71	0.12	0.24	0.05	0.71	0.08
FLD20	72.26	3.05	14.10	0.70	3.69	0.27	3.85	0.15	2.60	0.12	2.84	0.13	0.39	0.06	0.76	0.08
FLD20	71.98	3.04	14.44	0.72	3.63	0.26	4.24	0.16	2.53	0.11	2.29	0.11	0.38	0.06	0.69	0.08
FLD20	77.87	3.29	12.45	0.63	3.30	0.24	4.05	0.16	1.57	0.09	1.44	0.08	0.09	0.05	0.29	0.06
FLD20	73.01	3.08	13.04	0.65	3.28	0.24	3.72	0.15	3.05	0.13	2.73	0.12	0.33	0.06	0.68	0.08
FLD20	70.68	2.99	13.89	0.69	3.31	0.24	3.68	0.15	3.10	0.13	2.82	0.12	0.36	0.06	0.74	0.08
FLD20	70.41	2.98	13.71	0.69	3.80	0.27	3.89	0.15	3.16	0.13	3.04	0.13	0.44	0.06	0.80	0.09
FLD20	74.25	3.14	13.14	0.66	3.52	0.26	3.84	0.15	3.33	0.14	3.15	0.14	0.36	0.06	0.71	0.08
FLD20	74.28	3.14	13.10	0.66	3.29	0.24	3.75	0.15	3.29	0.14	2.72	0.12	0.30	0.06	0.64	0.08
FLD20	73.40	3.10	13.34	0.67	3.31	0.24	3.82	0.15	3.43	0.14	2.51	0.12	0.40	0.06	0.72	0.08
FLD20	72.38	3.06	13.10	0.66	3.47	0.25	4.21	0.16	2.70	0.12	2.58	0.12	0.32	0.06	0.69	0.08
FLD20	72.69	3.07	13.33	0.67	3.37	0.25	3.59	0.14	4.77	0.18	2.98	0.13	0.34	0.06	0.86	0.09
FLD20	77.77	3.28	13.48	0.67	3.60	0.26	3.97	0.15	2.44	0.11	1.70	0.09	0.19	0.05	0.55	0.07
FLD20	72.36	3.06	14.45	0.72	3.69	0.27	3.80	0.15	3.56	0.15	2.63	0.12	0.35	0.06	0.68	0.08
FLD20	71.12	3.01	14.35	0.71	3.23	0.24	3.70	0.15	3.25	0.14	2.66	0.12	0.36	0.06	0.76	0.08
FLD20	70.75	2.99	14.13	0.70	3.25	0.24	3.68	0.15	3.15	0.13	2.80	0.12	0.40	0.06	0.74	0.08
FLD20	71.32	3.01	13.60	0.68	3.28	0.24	3.70	0.15	2.77	0.12	2.60	0.12	0.39	0.06	0.72	0.08
FLD20	75.47	3.19	12.99	0.65	3.31	0.24	3.82	0.15	2.88	0.13	2.57	0.12	0.28	0.06	0.57	0.07
FLD20	74.62	3.15	13.13	0.66	3.26	0.24	3.65	0.14	3.60	0.15	2.70	0.12	0.33	0.06	0.75	0.08
FLD20	74.40	3.14	13.22	0.66	3.33	0.24	3.74	0.15	4.45	0.17	2.83	0.12	0.29	0.06	0.74	0.08
FLD20	74.90	3.16	13.17	0.66	3.22	0.24	3.58	0.14	3.51	0.14	2.80	0.12	0.40	0.06	0.76	0.08
FLD20	74.35	3.14	13.86	0.69	3.26	0.24	3.61	0.14	2.88	0.13	2.68	0.12	0.35	0.06	0.68	0.08
FLD20	72.39	3.06	13.37	0.67	3.32	0.24	3.75	0.15	2.76	0.12	2.59	0.12	0.37	0.06	0.67	0.08
FLD20	73.18	3.09	13.31	0.67	3.20	0.24	3.63	0.14	3.26	0.14	2.65	0.12	0.35	0.06	0.69	0.08
FLD20	72.93	3.08	13.90	0.69	3.26	0.24	3.61	0.14	3.05	0.13	2.82	0.12	0.32	0.06	0.78	0.09
FLD20	71.66	3.03	14.05	0.70	3.38	0.25	3.84	0.15	3.41	0.14	2.60	0.12	0.38	0.06	0.73	0.08
FLD20	74.77	3.16	14.05	0.70	3.46	0.25	3.80	0.15	3.19	0.13	2.90	0.13	0.28	0.06	0.71	0.08
FLD20	72.10	3.05	14.18	0.71	3.21	0.24	3.59	0.14	3.58	0.15	2.84	0.13	0.44	0.06	0.69	0.08
FLD20	72.72	3.07	13.13	0.66	3.01	0.22	3.70	0.15	2.58	0.12	3.11	0.13	0.39	0.06	0.67	0.08
FLD20	75.36	3.18	14.00	0.70	3.29	0.24	3.62	0.14	3.37	0.14	2.75	0.12	0.25	0.05	0.67	0.08
FLD20	74.85	3.16	13.78	0.69	3.30	0.24	3.67	0.15	2.55	0.12	2.66	0.12	0.28	0.06	0.61	0.08
FLD20	72.43	3.06	13.37	0.67	3.11	0.23	3.67	0.15	3.18	0.13	2.79	0.12	0.35	0.06	0.72	0.08
FLD20	73.30	3.10	14.07	0.70	3.55	0.26	3.55	0.14	3.43	0.14	3.01	0.13	0.42	0.06	0.71	0.08
FLD20	72.46	3.06	13.22	0.66	3.15	0.23	3.73	0.15	2.98	0.13	2.79	0.12	0.36	0.06	0.68	0.08
FLD20	73.82	3.12	13.41	0.67	3.21	0.24	3.69	0.15	3.00	0.13	2.69	0.12	0.31	0.06	0.78	0.09
FLD20	73.43	3.10	13.46	0.67	3.32	0.24	3.60	0.14	3.27	0.14	2.81	0.12	0.39	0.06	0.78	0.09
FLD20	74.10	3.13	14.40	0.72	3.54	0.26	3.95	0.15	3.28	0.14	2.83	0.13	0.40	0.06	0.69	0.08
FLD20	74.71	3.15	13.80	0.69	3.29	0.24	3.77	0.15	3.22	0.14	2.76	0.12	0.35	0.06	0.71	0.08
FLD20	72.57	3.07	12.84	0.64	3.00	0.22	3.75	0.15	3.14	0.13	2.55	0.12	0.33	0.06	0.59	0.08
FLD20	71.90	3.04	13.37	0.67	3.08	0.23	3.53	0.14	3.69	0.15	3.28	0.14	0.36	0.06	0.79	0.09
FLD20	74.85	3.16	12.97	0.65	3.06	0.23	3.54	0.14	3.49	0.14	2.73	0.12	0.36	0.06	0.70	0.08
FLD20	74.72	3.16	13.08	0.66	3.11	0.23	3.58	0.14	3.41	0.14	2.66	0.12	0.35	0.06	0.71	0.08
FLD20	74.03	3.13	14.11	0.70	3.25	0.24	3.68	0.15	3.48	0.14	2.71	0.12	0.34	0.06	0.74	0.08
FLD20	101.71	4.27	0.54	0.08	0.21	0.05	0.25	0.04	0.06	0.04	0.12	0.04	0.08	0.05	0.18	0.05
FLD20	96.80	4.07	2.71	0.18	0.89	0.09	0.90	0.06	0.42	0.05	0.76	0.06	0.03	0.05	0.28	0.06
FLD20	72.95	3.08	14.01	0.70	3.39	0.25	3.76	0.15	3.42	0.14	2.93	0.13	0.37	0.06	0.81	0.09
FLD20	72.68	3.07	12.10	0.61	3.61	0.26	4.44	0.17	3.60	0.15	3.64	0.15	0.47	0.06	0.76	0.09
FLD20	74.10	3.13	13.70	0.68	3.26	0.24	3.78	0.15	3.33	0.14	2.61	0.12	0.30	0.06	0.62	0.08
FLD20	74.71	3.15	13.57	0.68	3.18	0.23	3.57	0.14	3.35	0.14	2.81	0.12	0.29	0.06	0.71	0.08
FLD20	75.12	3.17	13.04	0.65	3.04	0.23	3.77	0.15	3.21	0.14	2.53	0.12	0.23	0.05	0.61	0.08
FLD20	75.01	3.17	13.14	0.66	3.10	0.23	3.62	0.14	3.67	0.15	2.87	0.13	0.27	0.05	0.69	0.08
FLD20	74.27	3.14	13.06	0.66	3.13	0.23	3.75	0.15	3.44	0.14	2.58	0.12	0.36	0.06	0.63	0.08
FLD20	72.77	3.07	13.74	0.69	3.18	0.23	3.69	0.15	3.40	0.14	2.94	0.13	0.32	0.06	0.76	0.09
FLD20	100.73	4.23	1.01	0.10	0.47	0.07	0.47	0.05	0.13	0.04	0.67	0.06	0.03	0.05	0.22	0.06
FLD20	73.74	3.11	11.09	0.56	4.28	0.30	4.97	0.19	2.27	0.11	2.63	0.12	0.20	0.05	0.66	0.08
FLD20	75.38	3.18	13.38	0.67	3.12	0.23	3.70	0.15	3.33	0.14	2.89	0.13	0.39	0.06	0.70	0.08
FLD20	73.68	3.11	13.61	0.68	3.01	0.22	3.77	0.15	3.22	0.14	2.71	0.12	0.30	0.06	0.71	0.08

FLD20	72.97	3.08	12.83	0.64	2.97	0.22	3.70	0.15	2.69	0.12	2.73	0.12	0.42	0.06	0.67	0.08
FLD20	74.21	3.13	13.94	0.70	3.30	0.24	3.74	0.15	2.83	0.12	2.76	0.12	0.37	0.06	0.69	0.08
FLD20	72.34	3.06	13.64	0.68	3.08	0.23	3.63	0.14	3.31	0.14	2.83	0.13	0.28	0.06	0.71	0.08
FLD20	72.87	3.08	13.80	0.69	3.26	0.24	3.67	0.15	3.11	0.13	2.97	0.13	0.36	0.06	0.76	0.08
FLD20	72.84	3.08	14.01	0.70	3.45	0.25	3.91	0.15	2.85	0.12	2.56	0.12	0.37	0.06	0.70	0.08
FLD20	74.36	3.14	14.22	0.71	3.23	0.24	3.87	0.15	3.59	0.15	2.73	0.12	0.32	0.06	0.71	0.08
FLD20	75.05	3.17	14.03	0.70	3.08	0.23	3.63	0.14	3.21	0.14	2.78	0.12	0.35	0.06	0.70	0.08
FLD20	73.71	3.11	13.84	0.69	2.94	0.22	3.66	0.15	3.28	0.14	2.71	0.12	0.39	0.06	0.74	0.08
FLD20	75.22	3.18	14.09	0.70	3.23	0.24	3.75	0.15	3.43	0.14	2.88	0.13	0.40	0.06	0.73	0.08
FLD20	72.96	3.08	14.00	0.70	3.21	0.24	3.82	0.15	3.42	0.14	2.78	0.12	0.37	0.06	0.78	0.09
FLD20	73.91	3.12	13.61	0.68	3.23	0.24	4.30	0.16	2.82	0.12	2.66	0.12	0.29	0.06	0.72	0.08
FLD20	73.86	3.12	13.99	0.70	3.57	0.26	4.46	0.17	3.19	0.13	2.70	0.12	0.36	0.06	0.66	0.08
FLD20	72.96	3.08	13.23	0.66	3.38	0.25	4.23	0.16	3.18	0.13	2.78	0.12	0.32	0.06	0.59	0.08
FLD20	75.80	3.20	11.80	0.60	4.30	0.30	4.87	0.18	2.51	0.11	2.38	0.11	0.26	0.05	0.68	0.08
FLD20	74.02	3.13	10.69	0.55	4.13	0.29	4.80	0.18	2.36	0.11	2.76	0.12	0.27	0.05	0.59	0.08
FLD20	72.68	3.07	13.84	0.69	3.57	0.26	3.78	0.15	3.11	0.13	3.03	0.13	0.37	0.06	0.79	0.09
FLD20	73.84	3.12	13.47	0.67	3.38	0.25	3.71	0.15	2.94	0.13	2.86	0.13	0.34	0.06	0.66	0.08
FLD20	74.00	3.13	13.23	0.66	3.45	0.25	3.78	0.15	2.25	0.11	2.51	0.12	0.33	0.06	0.56	0.07
FLD20	75.15	3.17	13.05	0.65	3.08	0.23	3.63	0.14	3.07	0.13	2.81	0.12	0.31	0.06	0.63	0.08
FLD20	75.03	3.17	13.23	0.66	3.73	0.27	4.18	0.16	3.58	0.15	3.01	0.13	0.32	0.06	0.71	0.08
FLD20	79.62	3.36	9.05	0.47	3.54	0.26	4.26	0.16	2.70	0.12	2.62	0.12	0.10	0.05	0.47	0.07
FLD20	74.26	3.14	13.42	0.67	3.51	0.25	3.95	0.15	3.32	0.14	2.46	0.11	0.31	0.06	0.57	0.07
FLD20	69.55	2.94	11.93	0.60	4.85	0.34	5.22	0.19	4.12	0.16	2.44	0.11	0.23	0.05	0.88	0.09
FLD20	75.25	3.18	12.72	0.64	3.83	0.27	4.31	0.17	2.76	0.12	2.52	0.12	0.29	0.06	0.62	0.08
FLD20	72.88	3.08	13.71	0.69	3.75	0.27	4.26	0.16	3.07	0.13	2.75	0.12	0.39	0.06	0.73	0.08
FLD20	74.17	3.13	13.96	0.70	3.46	0.25	3.67	0.15	3.05	0.13	2.70	0.12	0.32	0.06	0.74	0.08
FLD20	71.72	3.03	13.80	0.69	3.95	0.28	4.34	0.17	2.77	0.12	2.63	0.12	0.36	0.06	0.69	0.08
FLD20	75.12	3.17	12.84	0.65	3.49	0.25	4.02	0.16	2.11	0.10	2.65	0.12	0.24	0.05	0.52	0.07
FLD20	72.43	3.06	13.83	0.69	3.33	0.24	3.85	0.15	3.46	0.14	2.93	0.13	0.38	0.06	0.78	0.09
FLD20	71.29	3.01	14.41	0.72	3.34	0.24	3.78	0.15	2.99	0.13	3.05	0.13	0.36	0.06	0.78	0.09
FLD20	72.07	3.05	14.45	0.72	3.26	0.24	3.74	0.15	3.32	0.14	2.75	0.12	0.43	0.06	0.76	0.09
FLD20	72.47	3.06	13.81	0.69	3.24	0.24	3.75	0.15	2.92	0.13	2.93	0.13	0.40	0.06	0.75	0.08
FLD20	73.80	3.12	14.18	0.71	3.49	0.25	3.74	0.15	2.70	0.12	3.00	0.13	0.36	0.06	0.73	0.08
FLD20	68.15	2.88	11.53	0.58	4.94	0.34	5.06	0.19	2.84	0.12	3.95	0.16	0.32	0.06	0.56	0.07
FLD20	75.47	3.19	13.61	0.68	3.40	0.25	3.59	0.14	3.85	0.15	2.86	0.13	0.29	0.06	0.76	0.08
FLD20	73.52	3.11	13.23	0.66	3.22	0.24	3.81	0.15	3.02	0.13	2.56	0.12	0.37	0.06	0.66	0.08
FLD20	71.87	3.04	13.39	0.67	3.15	0.23	3.75	0.15	3.08	0.13	2.59	0.12	0.39	0.06	0.67	0.08
FLD20	74.31	3.14	14.20	0.71	3.52	0.26	3.76	0.15	3.44	0.14	2.88	0.13	0.36	0.06	0.80	0.09
FLD20	81.03	3.42	11.09	0.56	2.94	0.22	3.38	0.14	2.32	0.11	2.06	0.10	0.16	0.05	0.59	0.08
FLD20	71.32	3.01	14.90	0.74	3.54	0.26	3.85	0.15	2.30	0.11	2.98	0.13	0.44	0.06	0.80	0.09
FLD20	73.10	3.09	13.48	0.67	3.23	0.24	3.73	0.15	2.70	0.12	3.00	0.13	0.36	0.06	0.67	0.08
FLD20	73.78	3.12	13.63	0.68	3.40	0.25	4.08	0.16	2.76	0.12	2.62	0.12	0.35	0.06	0.74	0.08
FLD20	73.49	3.10	13.43	0.67	3.37	0.25	3.71	0.15	3.44	0.14	3.01	0.13	0.29	0.06	0.70	0.08
FLD20	74.46	3.14	12.61	0.63	3.33	0.24	4.27	0.16	1.65	0.09	1.79	0.09	0.30	0.06	0.51	0.07
FLD20	71.94	3.04	14.60	0.73	3.69	0.27	4.23	0.16	2.62	0.12	2.49	0.11	0.36	0.06	0.76	0.08
FLD21	76.25	3.22	13.88	0.69	3.13	0.23	3.67	0.15	3.32	0.14	2.49	0.11	0.22	0.05	0.75	0.08
FLD21	74.19	3.13	13.49	0.68	3.01	0.22	3.48	0.14	3.55	0.15	2.72	0.12	0.36	0.06	0.73	0.08
FLD21	75.27	3.18	13.77	0.69	3.04	0.23	3.37	0.14	3.73	0.15	2.66	0.12	0.20	0.05	0.73	0.08
FLD21	73.34	3.10	13.62	0.68	3.09	0.23	3.53	0.14	3.57	0.15	2.63	0.12	0.35	0.06	0.74	0.08
FLD21	74.97	3.17	13.72	0.69	3.16	0.23	3.41	0.14	3.43	0.14	2.62	0.12	0.25	0.05	0.73	0.08
FLD21	75.64	3.19	13.97	0.70	3.10	0.23	3.43	0.14	3.77	0.15	2.68	0.12	0.33	0.06	0.77	0.09
FLD21	73.62	3.11	12.85	0.65	2.89	0.22	3.43	0.14	3.42	0.14	2.58	0.12	0.27	0.05	0.63	0.08
FLD21	76.47	3.23	14.10	0.70	2.69	0.20	2.86	0.12	3.92	0.16	2.66	0.12	0.19	0.05	0.63	0.08
FLD21	73.59	3.11	13.23	0.66	3.03	0.23	3.47	0.14	3.88	0.16	2.71	0.12	0.20	0.05	0.74	0.08
FLD21	77.13	3.25	12.97	0.65	2.94	0.22	3.54	0.14	2.63	0.12	2.54	0.12	0.26	0.05	0.67	0.08
FLD21	76.76	3.24	14.05	0.70	3.15	0.23	3.51	0.14	2.42	0.11	2.78	0.12	0.20	0.05	0.68	0.08
FLD21	74.67	3.15	14.01	0.70	2.81	0.21	3.32	0.13	3.45	0.14	2.45	0.11	0.21	0.05	0.67	0.08
FLD21	74.83	3.16	13.55	0.68	3.08	0.23	3.48	0.14	3.33	0.14	2.61	0.12	0.37	0.06	0.63	0.08
FLD21	73.74	3.11	13.52	0.68	2.83	0.21	3.53	0.14	3.40	0.14	2.78	0.12	0.27	0.05	0.72	0.08
FLD21	74.03	3.13	13.73	0.69	2.96	0.22	3.48	0.14	3.75	0.15	2.57	0.12	0.25	0.05	0.81	0.09
FLD21	73.98	3.12	13.79	0.69	3.07	0.23	3.56	0.14	3.58	0.15	2.51	0.12	0.26	0.05	0.74	0.08
FLD21	73.84	3.12	13.89	0.69	2.98	0.22	3.54	0.14	3.49	0.14	2.70	0.12	0.23	0.05	0.73	0.08

FLD21	73.78	3.12	13.81	0.69	3.05	0.23	3.51	0.14	3.71	0.15	2.55	0.12	0.31	0.06	0.76	0.09
FLD21	76.99	3.25	13.46	0.67	2.93	0.22	3.36	0.14	3.54	0.15	2.50	0.11	0.28	0.05	0.72	0.08
FLD21	73.00	3.08	13.20	0.66	2.93	0.22	3.54	0.14	3.54	0.15	2.67	0.12	0.26	0.05	0.71	0.08
FLD21	74.38	3.14	13.26	0.66	2.96	0.22	3.46	0.14	3.34	0.14	2.75	0.12	0.50	0.06	0.69	0.08
FLD21	74.87	3.16	13.85	0.69	3.16	0.23	3.58	0.14	3.26	0.14	2.52	0.12	0.31	0.06	0.72	0.08
FLD21	75.88	3.20	13.72	0.69	3.09	0.23	3.60	0.14	3.35	0.14	2.34	0.11	0.25	0.05	0.79	0.09
FLD21	75.38	3.18	13.90	0.69	3.14	0.23	3.54	0.14	2.75	0.12	2.43	0.11	0.31	0.06	0.76	0.09
FLD21	73.16	3.09	13.42	0.67	3.02	0.22	3.54	0.14	2.78	0.12	2.52	0.12	0.26	0.05	0.77	0.09
FLD21	74.33	3.14	13.81	0.69	3.06	0.23	3.60	0.14	3.25	0.14	2.46	0.11	0.15	0.05	0.73	0.08
FLD21	70.91	3.00	12.85	0.65	2.87	0.22	3.45	0.14	3.35	0.14	2.65	0.12	0.29	0.06	0.76	0.08
FLD21	74.71	3.15	13.83	0.69	2.90	0.22	3.55	0.14	3.52	0.14	2.51	0.12	0.36	0.06	0.75	0.08
FLD21	74.97	3.17	13.50	0.68	2.88	0.22	3.60	0.14	3.80	0.15	2.46	0.11	0.16	0.05	0.70	0.08
FLD21	74.83	3.16	13.60	0.68	2.94	0.22	3.57	0.14	3.41	0.14	2.67	0.12	0.27	0.05	0.71	0.08
FLD21	75.79	3.20	13.57	0.68	2.97	0.22	3.55	0.14	3.07	0.13	2.71	0.12	0.22	0.05	0.66	0.08
FLD21	75.98	3.21	13.65	0.68	3.08	0.23	3.59	0.14	3.24	0.14	2.81	0.12	0.33	0.06	0.78	0.09
FLD21	73.74	3.11	13.51	0.68	3.08	0.23	3.35	0.14	3.29	0.14	3.03	0.13	0.65	0.07	0.72	0.08
FLD21	71.89	3.04	15.27	0.76	3.29	0.24	3.58	0.14	3.13	0.13	2.98	0.13	0.34	0.06	0.97	0.10
FLD21	74.80	3.16	13.63	0.68	3.01	0.22	3.33	0.14	3.29	0.14	2.65	0.12	0.26	0.05	0.67	0.08
FLD21	75.51	3.19	13.60	0.68	2.88	0.22	3.74	0.15	2.29	0.11	2.49	0.11	0.24	0.05	0.77	0.09
FLD21	76.01	3.21	13.60	0.68	2.95	0.22	3.58	0.14	3.22	0.14	2.70	0.12	0.19	0.05	0.75	0.08
FLD21	75.32	3.18	13.80	0.69	2.96	0.22	3.67	0.15	2.87	0.12	2.54	0.12	0.36	0.06	0.69	0.08
FLD21	73.76	3.12	13.61	0.68	3.08	0.23	3.43	0.14	3.18	0.13	2.81	0.12	0.31	0.06	0.72	0.08
FLD21	75.94	3.21	13.96	0.70	3.09	0.23	3.49	0.14	3.64	0.15	2.72	0.12	0.26	0.05	0.85	0.09
FLD21	73.36	3.10	13.49	0.68	2.97	0.22	3.52	0.14	3.46	0.14	2.60	0.12	0.35	0.06	0.72	0.08
FLD21	73.99	3.13	13.44	0.67	3.00	0.22	3.41	0.14	3.50	0.14	2.33	0.11	0.29	0.06	0.74	0.08
FLD21	75.35	3.18	13.71	0.69	2.92	0.22	3.81	0.15	2.33	0.11	2.48	0.11	0.33	0.06	0.70	0.08
FLD21	71.52	3.02	12.80	0.64	2.77	0.21	3.77	0.15	2.67	0.12	2.50	0.11	0.33	0.06	0.74	0.08
FLD21	73.37	3.10	13.82	0.69	2.98	0.22	3.39	0.14	3.93	0.16	2.89	0.13	0.29	0.06	0.75	0.08
FLD21	74.02	3.13	13.77	0.69	3.05	0.23	3.59	0.14	3.03	0.13	2.65	0.12	0.30	0.06	0.74	0.08
FLD21	74.23	3.13	13.58	0.68	2.89	0.22	3.53	0.14	3.79	0.15	2.54	0.12	0.23	0.05	0.77	0.09
FLD21	73.76	3.12	13.60	0.68	3.01	0.22	3.53	0.14	3.45	0.14	2.85	0.13	0.27	0.05	0.76	0.08
FLD21	75.84	3.20	13.05	0.65	2.96	0.22	3.67	0.15	2.78	0.12	2.46	0.11	0.24	0.05	0.75	0.08
FLD21	74.32	3.14	13.66	0.68	3.04	0.23	3.41	0.14	3.41	0.14	2.86	0.13	0.37	0.06	0.75	0.08
FLD21	72.04	3.04	13.29	0.67	2.92	0.22	3.37	0.14	3.56	0.15	2.62	0.12	0.25	0.05	0.73	0.08
FLD21	76.24	3.22	13.99	0.70	2.78	0.21	3.44	0.14	3.31	0.14	2.52	0.12	0.25	0.05	0.74	0.08
FLD21	76.58	3.23	13.56	0.68	2.85	0.21	3.39	0.14	3.30	0.14	2.55	0.12	0.29	0.06	0.72	0.08
FLD21	72.97	3.08	13.60	0.68	2.97	0.22	3.50	0.14	4.04	0.16	2.71	0.12	0.31	0.06	0.74	0.08
FLD21	76.69	3.24	13.82	0.69	3.13	0.23	3.71	0.15	2.76	0.12	2.68	0.12	0.27	0.05	0.63	0.08
FLD21	75.07	3.17	14.03	0.70	2.97	0.22	3.62	0.14	2.74	0.12	2.66	0.12	0.27	0.05	0.83	0.09
FLD21	72.95	3.08	14.19	0.71	3.05	0.23	3.83	0.15	2.98	0.13	2.94	0.13	0.38	0.06	0.85	0.09
FLD21	75.72	3.20	13.26	0.66	2.95	0.22	3.61	0.14	2.68	0.12	2.49	0.11	0.23	0.05	0.70	0.08
FLD21	75.03	3.17	13.59	0.68	3.00	0.22	3.49	0.14	3.65	0.15	2.66	0.12	0.35	0.06	0.75	0.08
FLD21	72.06	3.05	13.38	0.67	2.97	0.22	3.38	0.14	3.26	0.14	2.79	0.12	0.26	0.05	0.72	0.08
FLD21	75.44	3.18	12.87	0.65	2.80	0.21	3.74	0.15	2.52	0.11	2.54	0.12	0.27	0.05	0.61	0.08
FLD21	74.91	3.16	13.72	0.69	3.11	0.23	3.47	0.14	3.43	0.14	2.51	0.12	0.26	0.05	0.83	0.09
FLD21	75.19	3.17	13.64	0.68	3.03	0.22	3.71	0.15	3.09	0.13	2.67	0.12	0.40	0.06	0.73	0.08
FLD21	90.90	3.83	4.94	0.28	1.29	0.12	1.84	0.09	1.23	0.08	1.37	0.08	0.22	0.05	0.31	0.06
FLD21	74.88	3.16	13.98	0.70	2.94	0.22	3.53	0.14	3.74	0.15	2.46	0.11	0.28	0.05	0.71	0.08
FLD21	75.09	3.17	14.00	0.70	3.00	0.22	3.59	0.14	3.73	0.15	2.68	0.12	0.24	0.05	0.76	0.08
FLD21	73.30	3.10	13.31	0.67	2.90	0.22	3.52	0.14	3.46	0.14	2.64	0.12	0.22	0.05	0.68	0.08
FLD21	74.10	3.13	13.62	0.68	2.99	0.22	3.63	0.14	3.01	0.13	2.54	0.12	0.30	0.06	0.69	0.08
FLD21	74.80	3.16	13.51	0.68	3.04	0.23	3.48	0.14	2.98	0.13	2.73	0.12	0.17	0.05	0.65	0.08
FLD21	76.82	3.24	12.86	0.65	3.01	0.22	3.47	0.14	3.01	0.13	2.56	0.12	0.28	0.05	0.64	0.08
FLD21	75.40	3.18	13.76	0.69	2.97	0.22	3.58	0.14	3.28	0.14	2.72	0.12	0.28	0.05	0.72	0.08
FLD21	75.79	3.20	13.82	0.69	3.09	0.23	3.51	0.14	3.23	0.14	2.47	0.11	0.25	0.05	0.77	0.09
FLD21	74.86	3.16	13.55	0.68	3.05	0.23	3.45	0.14	3.46	0.14	2.60	0.12	0.17	0.05	0.75	0.08
FLD21	75.73	3.20	13.96	0.70	3.04	0.23	3.72	0.15	3.62	0.15	2.80	0.12	0.28	0.05	0.78	0.09
FLD21	74.20	3.13	13.85	0.69	3.01	0.22	3.46	0.14	4.09	0.16	2.70	0.12	0.21	0.05	0.77	0.09
FLD21	77.61	3.27	13.33	0.67	3.06	0.23	3.71	0.15	2.66	0.12	2.30	0.11	0.21	0.05	0.64	0.08
FLD21	75.85	3.20	13.74	0.69	2.94	0.22	3.67	0.15	2.90	0.13	2.61	0.12	0.33	0.06	0.79	0.09
FLD21	75.50	3.19	14.05	0.70	3.12	0.23	3.42	0.14	2.63	0.12	2.53	0.12	0.26	0.05	0.68	0.08
FLD21	74.56	3.15	13.75	0.69	3.11	0.23	3.52	0.14	2.39	0.11	2.50	0.11	0.22	0.05	0.64	0.08

FLD21	72.11	3.05	13.62	0.68	2.78	0.21	3.80	0.15	3.68	0.15	2.48	0.11	0.30	0.06	0.71	0.08
FLD21	73.45	3.10	14.71	0.73	2.98	0.22	3.93	0.15	3.73	0.15	2.41	0.11	0.23	0.05	0.73	0.08
FLD21	73.35	3.10	13.40	0.67	2.94	0.22	3.52	0.14	3.93	0.16	2.71	0.12	0.32	0.06	0.75	0.08
FLD21	74.07	3.13	13.51	0.68	2.96	0.22	3.52	0.14	3.84	0.15	2.63	0.12	0.22	0.05	0.74	0.08
FLD21	73.91	3.12	13.51	0.68	3.00	0.22	3.60	0.14	3.61	0.15	2.60	0.12	0.40	0.06	0.71	0.08
FLD21	75.17	3.17	13.48	0.67	3.11	0.23	3.50	0.14	3.30	0.14	2.60	0.12	0.31	0.06	0.72	0.08
FLD21	78.45	3.31	12.30	0.62	3.12	0.23	3.70	0.15	1.77	0.09	2.20	0.11	0.23	0.05	0.44	0.07
FLD21	72.86	3.08	13.58	0.68	3.09	0.23	3.67	0.15	2.55	0.12	2.45	0.11	0.27	0.05	0.63	0.08
FLD21	73.94	3.12	14.00	0.70	3.00	0.22	3.36	0.14	3.23	0.14	2.43	0.11	0.20	0.05	0.69	0.08
FLD21	74.65	3.15	13.77	0.69	2.79	0.21	3.57	0.14	3.74	0.15	2.71	0.12	0.32	0.06	0.78	0.09
FLD21	77.64	3.28	13.44	0.67	3.05	0.23	3.41	0.14	2.65	0.12	2.57	0.12	0.21	0.05	0.70	0.08
FLD21	73.28	3.10	13.75	0.69	2.99	0.22	3.31	0.13	3.27	0.14	2.40	0.11	0.21	0.05	0.66	0.08
FLD23	79.31	3.35	8.82	0.46	1.45	0.13	3.28	0.13	1.60	0.09	1.94	0.10	0.14	0.05	0.45	0.07
FLD23	70.78	2.99	13.21	0.66	2.47	0.19	3.87	0.15	2.31	0.11	2.78	0.12	0.29	0.06	0.61	0.08
FLD23	72.59	3.07	13.10	0.66	2.63	0.20	4.18	0.16	1.63	0.09	2.21	0.11	0.23	0.05	0.43	0.07
FLD23	71.81	3.03	12.93	0.65	2.49	0.19	3.83	0.15	1.91	0.10	2.58	0.12	0.29	0.06	0.48	0.07
FLD23	72.04	3.04	12.57	0.63	2.63	0.20	3.77	0.15	2.24	0.11	2.68	0.12	0.30	0.06	0.52	0.07
FLD23	72.70	3.07	11.80	0.60	2.40	0.19	3.88	0.15	1.92	0.10	2.68	0.12	0.29	0.06	0.54	0.07
FLD23	71.04	3.00	13.18	0.66	2.49	0.19	4.17	0.16	1.85	0.09	2.59	0.12	0.29	0.06	0.51	0.07
FLD23	71.24	3.01	13.29	0.67	2.29	0.18	3.95	0.15	2.40	0.11	2.61	0.12	0.27	0.05	0.60	0.08
FLD23	69.45	2.94	13.34	0.67	2.61	0.20	4.11	0.16	2.82	0.12	2.81	0.12	0.31	0.06	0.60	0.08
FLD23	69.39	2.93	13.30	0.67	2.40	0.19	4.07	0.16	3.10	0.13	2.82	0.12	0.37	0.06	0.64	0.08
FLD23	70.64	2.99	12.97	0.65	2.47	0.19	4.05	0.16	2.32	0.11	2.79	0.12	0.30	0.06	0.67	0.08
FLD23	68.51	2.90	14.13	0.70	2.40	0.19	3.93	0.15	2.84	0.12	3.19	0.14	0.37	0.06	0.71	0.08
FLD23	77.85	3.28	9.46	0.49	1.78	0.15	3.55	0.14	1.31	0.08	2.31	0.11	0.22	0.05	0.57	0.07
FLD23	72.21	3.05	12.78	0.64	2.35	0.18	3.80	0.15	2.18	0.10	2.71	0.12	0.32	0.06	0.59	0.08
FLD23	71.85	3.04	12.95	0.65	2.18	0.17	3.68	0.15	2.45	0.11	2.55	0.12	0.30	0.06	0.57	0.08
FLD23	74.35	3.14	12.38	0.62	1.91	0.16	3.77	0.15	1.46	0.08	2.51	0.12	0.24	0.05	0.32	0.06
FLD23	78.49	3.31	9.98	0.51	1.72	0.14	3.32	0.14	1.32	0.08	2.37	0.11	0.26	0.05	0.44	0.07
FLD23	72.58	3.07	12.83	0.64	1.99	0.16	3.62	0.14	2.10	0.10	2.61	0.12	0.30	0.06	0.53	0.07
FLD23	73.25	3.09	12.86	0.65	2.17	0.17	3.94	0.15	2.35	0.11	2.24	0.11	0.30	0.06	0.52	0.07
FLD23	71.81	3.03	12.91	0.65	2.45	0.19	3.87	0.15	2.00	0.10	2.51	0.12	0.33	0.06	0.51	0.07
FLD23	72.61	3.07	13.34	0.67	2.35	0.18	4.12	0.16	1.25	0.08	2.52	0.12	0.34	0.06	0.57	0.08
FLD23	72.41	3.06	13.06	0.65	2.07	0.17	3.85	0.15	2.18	0.10	2.64	0.12	0.35	0.06	0.56	0.07
FLD23	71.50	3.02	13.54	0.68	2.15	0.17	3.75	0.15	2.26	0.11	2.76	0.12	0.31	0.06	0.56	0.07
FLD23	71.98	3.04	12.92	0.65	2.07	0.17	3.76	0.15	2.68	0.12	2.81	0.12	0.39	0.06	0.57	0.08
FLD23	70.48	2.98	13.66	0.68	2.35	0.18	3.85	0.15	1.96	0.10	2.89	0.13	0.27	0.05	0.62	0.08
FLD23	101.21	4.25	0.71	0.08	0.32	0.06	0.37	0.04	0.03	0.04	0.10	0.04	0.03	0.05	0.03	0.05
FLD23	100.15	4.21	0.85	0.09	0.40	0.06	0.49	0.05	0.13	0.04	0.34	0.05	0.03	0.05	0.03	0.05
FLD23	94.67	3.98	3.39	0.21	0.82	0.09	1.33	0.07	0.44	0.05	0.57	0.06	0.03	0.05	0.11	0.05
FLD23	72.78	3.07	13.29	0.67	2.30	0.18	3.64	0.14	2.27	0.11	2.64	0.12	0.28	0.05	0.54	0.07
FLD23	71.52	3.02	12.93	0.65	2.76	0.21	3.98	0.16	1.95	0.10	2.63	0.12	0.34	0.06	0.58	0.08
FLD23	74.52	3.15	11.31	0.57	2.65	0.20	3.68	0.15	2.43	0.11	2.58	0.12	0.36	0.06	0.64	0.08
FLD23	71.50	3.02	13.04	0.65	2.55	0.20	3.74	0.15	2.46	0.11	2.60	0.12	0.29	0.06	0.57	0.07
FLD23	72.65	3.07	12.45	0.63	2.27	0.18	3.77	0.15	1.82	0.09	2.37	0.11	0.24	0.05	0.46	0.07
FLD23	73.90	3.12	11.56	0.59	1.94	0.16	3.79	0.15	1.92	0.10	2.40	0.11	0.23	0.05	0.46	0.07
FLD23	72.89	3.08	11.85	0.60	2.30	0.18	3.66	0.15	2.09	0.10	2.64	0.12	0.28	0.05	0.53	0.07
FLD23	72.34	3.06	12.29	0.62	2.38	0.18	3.78	0.15	2.09	0.10	2.48	0.11	0.27	0.05	0.50	0.07
FLD23	72.28	3.05	12.73	0.64	2.41	0.19	3.89	0.15	2.08	0.10	2.67	0.12	0.29	0.06	0.52	0.07
FLD23	72.08	3.05	12.75	0.64	2.27	0.18	3.69	0.15	2.31	0.11	2.55	0.12	0.29	0.06	0.56	0.07
FLD23	73.25	3.09	12.19	0.61	2.46	0.19	3.67	0.15	2.21	0.11	2.33	0.11	0.28	0.05	0.50	0.07
FLD23	72.44	3.06	12.21	0.62	2.37	0.18	3.76	0.15	2.36	0.11	2.51	0.12	0.30	0.06	0.55	0.07
FLD23	71.32	3.01	13.46	0.67	2.25	0.18	3.83	0.15	2.02	0.10	2.62	0.12	0.28	0.06	0.55	0.07
FLD23	83.68	3.53	7.99	0.42	1.77	0.15	2.94	0.12	1.24	0.08	1.27	0.08	0.17	0.05	0.32	0.06
FLD23	70.24	2.97	13.04	0.65	2.27	0.18	3.87	0.15	2.96	0.13	3.35	0.14	0.32	0.06	0.61	0.08
FLD23	96.37	4.05	1.49	0.12	0.40	0.06	0.72	0.06	0.15	0.04	0.75	0.06	0.09	0.05	0.19	0.05
FLD23	76.27	3.22	10.36	0.53	2.09	0.17	3.64	0.14	1.91	0.10	2.18	0.10	0.23	0.05	0.60	0.08
FLD23	72.76	3.07	11.95	0.60	2.35	0.18	3.94	0.15	1.94	0.10	2.69	0.12	0.32	0.06	0.61	0.08
FLD23	73.54	3.11	11.84	0.60	2.69	0.20	4.11	0.16	1.08	0.07	2.51	0.11	0.23	0.05	0.41	0.07
FLD25	72.16	3.05	14.03	0.70	3.64	0.26	4.50	0.17	4.07	0.16	2.30	0.11	0.34	0.06	0.62	0.08
FLD25	73.65	3.11	12.62	0.63	4.49	0.32	4.70	0.18	4.27	0.17	2.34	0.11	0.32	0.06	0.69	0.08
FLD25	70.42	2.98	14.80	0.74	3.84	0.28	4.41	0.17	4.56	0.18	2.39	0.11	0.39	0.06	0.68	0.08

FLD25	74.17	3.13	12.64	0.64	3.38	0.25	4.26	0.16	3.31	0.14	2.30	0.11	0.28	0.06	0.44	0.07
FLD25	71.14	3.01	14.20	0.71	3.73	0.27	4.90	0.18	4.51	0.17	2.30	0.11	0.20	0.05	0.69	0.08
FLD25	67.67	2.86	20.59	1.00	4.16	0.30	8.99	0.31	0.07	0.04	0.09	0.04	0.16	0.05	0.26	0.06
FLD25	67.97	2.88	20.76	1.01	3.91	0.28	8.52	0.29	0.48	0.05	0.14	0.04	0.16	0.05	0.27	0.06
FLD25	67.14	2.84	20.59	1.00	4.27	0.30	8.73	0.30	0.21	0.04	0.22	0.04	0.29	0.06	0.28	0.06
FLD25	67.68	2.86	17.67	0.87	3.94	0.28	6.38	0.23	3.22	0.14	1.62	0.09	0.35	0.06	0.48	0.07
FLD25	71.57	3.02	13.85	0.69	3.88	0.28	4.90	0.18	4.59	0.18	2.38	0.11	0.27	0.05	0.76	0.08
FLD25	70.37	2.98	14.55	0.72	4.06	0.29	4.87	0.18	4.41	0.17	2.37	0.11	0.32	0.06	0.70	0.08
FLD25	72.78	3.07	14.95	0.74	3.90	0.28	3.95	0.15	4.36	0.17	2.28	0.11	0.20	0.05	0.67	0.08
FLD25	69.05	2.92	20.85	1.02	3.75	0.27	7.49	0.26	1.42	0.08	0.64	0.06	0.17	0.05	0.14	0.05
FLD25	65.19	2.76	19.93	0.97	3.84	0.28	9.65	0.33	0.06	0.04	0.03	0.04	0.14	0.05	0.22	0.06
FLD25	63.76	2.70	19.15	0.94	3.53	0.26	10.14	0.34	0.03	0.04	0.03	0.04	0.26	0.05	0.18	0.05
FLD25	68.55	2.90	20.76	1.01	3.75	0.27	8.78	0.30	0.60	0.06	0.20	0.04	0.18	0.05	0.07	0.05
FLD25	67.45	2.85	20.30	0.99	4.19	0.30	8.97	0.31	0.20	0.04	0.10	0.04	0.17	0.05	0.29	0.06
FLD25	67.99	2.88	20.89	1.02	4.26	0.30	8.99	0.31	0.12	0.04	0.08	0.04	0.19	0.05	0.32	0.06
FLD25	75.05	3.17	12.66	0.64	4.34	0.31	4.98	0.19	3.92	0.16	1.95	0.10	0.19	0.05	0.66	0.08
FLD25	72.17	3.05	15.81	0.78	3.01	0.22	5.89	0.21	3.32	0.14	1.95	0.10	0.33	0.06	0.60	0.08
FLD25	65.77	2.78	19.95	0.97	3.92	0.28	9.71	0.33	0.10	0.04	0.14	0.04	0.12	0.05	0.21	0.06
FLD25	67.92	2.87	20.40	0.99	3.69	0.27	9.53	0.33	0.08	0.04	0.10	0.04	0.24	0.05	0.27	0.06
FLD25	67.04	2.84	20.46	1.00	3.85	0.28	9.42	0.32	0.24	0.05	0.07	0.04	0.14	0.05	0.27	0.06
FLD25	68.29	2.89	20.75	1.01	3.95	0.28	7.91	0.28	1.21	0.08	0.27	0.05	0.16	0.05	0.14	0.05
FLD25	67.85	2.87	20.86	1.02	4.30	0.30	8.79	0.30	0.65	0.06	0.16	0.04	0.22	0.05	0.03	0.05
FLD25	66.77	2.83	19.31	0.94	4.35	0.31	6.57	0.23	1.99	0.10	0.75	0.06	0.16	0.05	0.25	0.06
FLD25	72.77	3.07	14.88	0.74	3.11	0.23	4.33	0.17	3.71	0.15	2.37	0.11	0.24	0.05	0.77	0.09
FLD25	68.20	2.88	20.82	1.01	3.88	0.28	9.28	0.32	0.16	0.04	0.11	0.04	0.13	0.05	0.28	0.06
FLD25	71.01	3.00	13.71	0.69	2.86	0.21	6.84	0.24	2.36	0.11	1.93	0.10	0.32	0.06	0.46	0.07
FLD25	68.40	2.89	20.51	1.00	4.29	0.30	7.31	0.26	1.69	0.09	0.68	0.06	0.07	0.05	0.18	0.05
FLD25	73.38	3.10	13.68	0.68	2.81	0.21	5.08	0.19	3.15	0.13	2.35	0.11	0.28	0.05	0.62	0.08
FLD25	71.28	3.01	14.11	0.70	2.85	0.21	6.51	0.23	3.44	0.14	2.28	0.11	0.09	0.05	0.73	0.08
FLD25	73.82	3.12	13.93	0.70	2.91	0.22	6.56	0.23	3.15	0.13	1.63	0.09	0.28	0.05	0.52	0.07
FLD25	76.11	3.21	12.67	0.64	3.35	0.25	4.75	0.18	3.57	0.15	2.40	0.11	0.17	0.05	0.57	0.07
FLD25	67.03	2.84	20.50	1.00	4.34	0.31	8.45	0.29	0.37	0.05	0.18	0.04	0.17	0.05	0.30	0.06
FLD25	74.70	3.15	12.46	0.63	4.11	0.29	5.14	0.19	3.76	0.15	1.95	0.10	0.27	0.05	0.64	0.08
FLD25	72.43	3.06	14.39	0.72	2.80	0.21	3.80	0.15	4.22	0.17	2.56	0.12	0.33	0.06	0.61	0.08
FLD25	70.42	2.98	16.35	0.81	3.07	0.23	6.31	0.23	2.58	0.12	1.55	0.09	0.16	0.05	0.44	0.07
FLD25	72.14	3.05	14.73	0.73	3.07	0.23	7.29	0.26	2.72	0.12	1.85	0.09	0.31	0.06	0.56	0.07
FLD25	67.87	2.87	19.82	0.97	3.76	0.27	7.42	0.26	2.68	0.12	0.69	0.06	0.09	0.05	0.32	0.06
FLD25	69.72	2.95	17.50	0.86	3.74	0.27	6.95	0.25	2.33	0.11	1.24	0.08	0.17	0.05	0.32	0.06
FLD25	74.65	3.15	14.24	0.71	2.85	0.21	4.76	0.18	3.63	0.15	2.30	0.11	0.22	0.05	0.62	0.08
FLD25	72.06	3.05	14.25	0.71	2.79	0.21	5.02	0.19	3.45	0.14	2.74	0.12	0.28	0.06	0.62	0.08
FLD25	69.75	2.95	20.87	1.02	3.99	0.28	6.84	0.24	1.68	0.09	0.46	0.05	0.16	0.05	0.13	0.05
FLD25	73.96	3.12	14.17	0.71	3.79	0.27	4.08	0.16	3.94	0.16	2.58	0.12	0.28	0.05	0.64	0.08
FLD25	74.71	3.15	12.94	0.65	2.79	0.21	3.85	0.15	3.86	0.15	2.33	0.11	0.08	0.05	0.63	0.08
FLD25	77.58	3.27	10.48	0.54	3.39	0.25	4.26	0.16	3.34	0.14	2.35	0.11	0.26	0.05	0.56	0.07
FLD9	74.57	3.15	13.05	0.65	3.50	0.25	3.76	0.15	2.09	0.10	2.66	0.12	0.32	0.06	0.55	0.07
FLD9	74.28	3.14	13.32	0.67	3.34	0.24	3.66	0.15	2.59	0.12	2.70	0.12	0.31	0.06	0.55	0.07
FLD9	71.91	3.04	14.58	0.73	3.21	0.24	3.36	0.14	2.76	0.12	2.73	0.12	0.35	0.06	0.57	0.08
FLD9	76.02	3.21	13.30	0.67	3.37	0.25	3.59	0.14	2.23	0.11	2.66	0.12	0.33	0.06	0.53	0.07
FLD9	74.09	3.13	14.53	0.72	3.22	0.24	3.17	0.13	2.61	0.12	2.66	0.12	0.30	0.06	0.56	0.07
FLD9	71.18	3.01	13.23	0.66	3.46	0.25	4.20	0.16	1.71	0.09	2.70	0.12	0.30	0.06	0.63	0.08
FLD9	74.99	3.17	14.43	0.72	3.35	0.25	3.38	0.14	2.18	0.10	2.67	0.12	0.24	0.05	0.56	0.07
FLD9	71.22	3.01	14.19	0.71	3.17	0.23	3.61	0.14	2.60	0.12	2.59	0.12	0.38	0.06	0.52	0.07
FLD9	71.95	3.04	14.08	0.70	3.33	0.24	3.72	0.15	2.00	0.10	3.04	0.13	0.37	0.06	0.71	0.08
FLD9	73.18	3.09	14.28	0.71	3.63	0.26	3.82	0.15	2.10	0.10	2.70	0.12	0.28	0.05	0.69	0.08
FLD9	85.96	3.62	8.28	0.43	2.56	0.20	2.90	0.12	0.90	0.07	1.58	0.09	0.14	0.05	0.35	0.06
FLD9	71.59	3.03	14.47	0.72	3.74	0.27	4.03	0.16	2.15	0.10	2.70	0.12	0.33	0.06	0.58	0.08
FLD9	84.50	3.56	9.75	0.50	3.48	0.25	3.55	0.14	0.03	0.04	1.16	0.07	0.03	0.05	0.22	0.06
FLD9	73.28	3.10	13.86	0.69	3.53	0.26	3.99	0.16	1.72	0.09	2.85	0.13	0.37	0.06	0.62	0.08
FLD9	79.07	3.34	12.63	0.64	3.65	0.26	4.23	0.16	0.41	0.05	2.46	0.11	0.17	0.05	0.15	0.05
FLD9	72.40	3.06	15.13	0.75	3.81	0.27	3.91	0.15	2.16	0.10	3.00	0.13	0.45	0.06	0.70	0.08
FLD9	79.74	3.36	11.90	0.60	3.55	0.26	3.80	0.15	1.33	0.08	2.36	0.11	0.24	0.05	0.32	0.06
FLD9	74.82	3.16	13.71	0.68	3.35	0.24	3.63	0.14	1.88	0.10	2.98	0.13	0.32	0.06	0.52	0.07

FLD9	75.27	3.18	13.67	0.68	3.36	0.25	3.57	0.14	1.82	0.09	2.51	0.12	0.26	0.05	0.42	0.07
FLD9	75.07	3.17	14.01	0.70	3.62	0.26	4.08	0.16	1.67	0.09	2.72	0.12	0.32	0.06	0.59	0.08
FLD9	72.81	3.08	13.54	0.68	3.37	0.25	3.73	0.15	2.54	0.12	2.79	0.12	0.30	0.06	0.56	0.07
FLD9	69.15	2.92	16.65	0.82	4.12	0.29	4.26	0.16	2.14	0.10	2.84	0.13	0.27	0.05	0.58	0.08
FLD9	65.20	2.76	17.02	0.84	3.79	0.27	4.09	0.16	1.99	0.10	3.58	0.15	0.56	0.06	1.37	0.12
FLD9	74.11	3.13	13.99	0.70	3.16	0.23	3.63	0.14	1.89	0.10	2.81	0.12	0.30	0.06	0.54	0.07
FLD9	73.11	3.09	13.79	0.69	3.58	0.26	3.86	0.15	2.26	0.11	2.81	0.12	0.33	0.06	0.61	0.08
FLD9	77.43	3.27	12.01	0.61	3.37	0.25	3.73	0.15	1.46	0.08	2.46	0.11	0.32	0.06	0.52	0.07
FLD9	87.41	3.68	8.51	0.44	3.12	0.23	3.19	0.13	0.03	0.04	0.92	0.07	0.03	0.05	0.26	0.06
FLD9	69.47	2.94	15.26	0.76	3.51	0.25	4.02	0.16	1.40	0.08	2.99	0.13	0.48	0.06	0.74	0.08
FLD9	74.94	3.16	13.37	0.67	3.21	0.24	3.59	0.14	2.76	0.12	2.87	0.13	0.25	0.05	0.56	0.07
FLD9	71.81	3.03	13.52	0.68	3.41	0.25	4.05	0.16	1.59	0.09	2.74	0.12	0.35	0.06	0.46	0.07
FLD9	74.46	3.14	13.31	0.67	3.35	0.24	3.85	0.15	1.80	0.09	2.71	0.12	0.31	0.06	0.52	0.07
FLD9	72.36	3.06	14.51	0.72	3.46	0.25	3.77	0.15	1.84	0.09	2.93	0.13	0.34	0.06	0.46	0.07
FLD9	76.18	3.22	13.57	0.68	3.43	0.25	3.62	0.14	2.59	0.12	2.58	0.12	0.27	0.05	0.51	0.07
FLD9	69.52	2.94	14.31	0.71	3.44	0.25	3.99	0.16	1.73	0.09	3.99	0.16	0.60	0.07	0.83	0.09
FLD9	73.33	3.10	15.14	0.75	3.73	0.27	3.91	0.15	1.78	0.09	3.04	0.13	0.43	0.06	0.54	0.07
FLD9	75.07	3.17	12.60	0.63	3.00	0.22	3.36	0.14	2.59	0.12	2.63	0.12	0.29	0.06	0.56	0.07
FLD9	72.02	3.04	14.70	0.73	3.55	0.26	3.78	0.15	2.89	0.13	3.16	0.14	0.40	0.06	1.19	0.11
FLD9	75.25	3.18	13.53	0.68	3.34	0.24	3.66	0.15	1.99	0.10	2.66	0.12	0.35	0.06	0.56	0.07
FLD9	64.63	2.74	17.97	0.88	3.96	0.28	4.04	0.16	1.93	0.10	3.41	0.14	0.58	0.06	1.65	0.13
FLD9	73.90	3.12	13.32	0.67	3.57	0.26	4.32	0.17	1.46	0.08	2.55	0.12	0.23	0.05	0.45	0.07
FLD9	73.50	3.10	12.46	0.63	3.59	0.26	4.24	0.16	0.86	0.06	2.26	0.11	0.14	0.05	0.40	0.07
FLD9	67.96	2.88	18.20	0.89	3.79	0.27	3.92	0.15	1.45	0.08	3.15	0.13	0.45	0.06	1.11	0.10
FLD9	70.75	2.99	14.13	0.70	3.23	0.24	3.87	0.15	1.56	0.09	2.91	0.13	0.41	0.06	0.64	0.08
FLD9	74.96	3.17	13.05	0.65	2.90	0.22	3.40	0.14	2.72	0.12	2.67	0.12	0.29	0.06	0.52	0.07
FLD9	76.13	3.21	13.30	0.67	3.44	0.25	3.90	0.15	2.08	0.10	2.75	0.12	0.14	0.05	0.64	0.08
FLD9	76.09	3.21	15.39	0.76	3.97	0.28	4.32	0.17	0.79	0.06	2.69	0.12	0.23	0.05	0.40	0.07
FLD9	75.78	3.20	13.14	0.66	3.30	0.24	3.59	0.14	2.43	0.11	2.53	0.12	0.25	0.05	0.43	0.07
FLD9	75.40	3.18	13.56	0.68	3.50	0.25	3.86	0.15	1.72	0.09	2.73	0.12	0.34	0.06	0.57	0.07
FLD9	76.52	3.23	13.29	0.67	3.40	0.25	4.07	0.16	0.91	0.07	3.09	0.13	0.19	0.05	0.39	0.07
FLD9	68.14	2.88	16.32	0.81	3.66	0.26	4.04	0.16	1.72	0.09	3.31	0.14	0.41	0.06	0.87	0.09
FLD9	74.58	3.15	13.46	0.67	3.27	0.24	3.57	0.14	2.89	0.13	2.65	0.12	0.32	0.06	0.63	0.08
FLD9	68.31	2.89	16.93	0.83	3.97	0.28	4.37	0.17	1.76	0.09	3.16	0.14	0.23	0.05	0.59	0.08
FLD9	74.04	3.13	13.40	0.67	3.32	0.24	3.71	0.15	2.67	0.12	2.68	0.12	0.30	0.06	0.55	0.07
FLD9	73.14	3.09	14.70	0.73	3.25	0.24	3.79	0.15	1.37	0.08	2.70	0.12	0.48	0.06	0.79	0.09
FLD9	76.52	3.23	13.40	0.67	3.09	0.23	3.48	0.14	2.63	0.12	2.63	0.12	0.26	0.05	0.55	0.07
FLD9	84.78	3.57	7.66	0.41	2.21	0.17	3.01	0.13	0.93	0.07	1.73	0.09	0.09	0.05	0.29	0.06
FLD9	75.11	3.17	15.00	0.74	3.83	0.27	4.24	0.16	0.73	0.06	2.73	0.12	0.32	0.06	0.45	0.07
FLD9	76.73	3.24	13.37	0.67	3.53	0.26	3.74	0.15	1.92	0.10	2.89	0.13	0.37	0.06	0.52	0.07
FLD9	74.60	3.15	12.86	0.65	3.03	0.22	3.84	0.15	1.56	0.09	3.15	0.13	0.32	0.06	0.50	0.07
FLD9	74.97	3.17	12.66	0.64	3.13	0.23	3.64	0.14	1.70	0.09	3.41	0.14	0.56	0.06	0.59	0.08
FLD9	67.81	2.87	16.69	0.82	3.62	0.26	4.10	0.16	1.69	0.09	3.28	0.14	0.52	0.06	0.93	0.09
FLD9	73.56	3.11	12.82	0.64	3.29	0.24	3.84	0.15	2.47	0.11	2.60	0.12	0.28	0.06	0.53	0.07
FLD9	71.15	3.01	14.53	0.72	3.84	0.27	4.15	0.16	2.05	0.10	3.02	0.13	0.32	0.06	0.64	0.08
FLD9	72.49	3.06	15.56	0.77	3.67	0.26	4.21	0.16	2.05	0.10	3.16	0.14	0.34	0.06	0.68	0.08
FLD9	76.74	3.24	12.02	0.61	4.42	0.31	4.34	0.17	0.03	0.04	1.32	0.08	0.03	0.05	0.03	0.05
FLD9	69.07	2.92	20.51	1.00	5.19	0.36	6.83	0.24	1.25	0.08	0.13	0.04	0.06	0.05	0.30	0.06
FLD9	74.36	3.14	13.93	0.70	3.56	0.26	4.08	0.16	1.33	0.08	2.86	0.13	0.23	0.05	0.41	0.07
FLD9	73.16	3.09	13.34	0.67	3.23	0.24	4.02	0.16	1.54	0.08	2.81	0.12	0.32	0.06	0.42	0.07
FLD9	76.92	3.25	13.40	0.67	3.43	0.25	3.69	0.15	2.02	0.10	2.58	0.12	0.28	0.05	0.53	0.07
FLD9	73.51	3.11	14.60	0.73	3.21	0.24	3.49	0.14	2.36	0.11	2.86	0.13	0.30	0.06	0.49	0.07
FLD9	74.77	3.16	14.57	0.72	3.66	0.26	4.08	0.16	1.79	0.09	2.92	0.13	0.31	0.06	0.64	0.08
FLD9	74.28	3.14	13.15	0.66	3.18	0.23	3.60	0.14	1.84	0.09	3.52	0.15	0.30	0.06	0.54	0.07
FLD9	74.78	3.16	13.59	0.68	3.38	0.25	3.75	0.15	1.83	0.09	2.93	0.13	0.32	0.06	0.52	0.07
FLD9	69.32	2.93	16.16	0.80	3.72	0.27	4.32	0.17	2.49	0.11	3.20	0.14	0.36	0.06	1.10	0.10
FLD9	73.20	3.09	14.65	0.73	3.33	0.24	3.46	0.14	3.29	0.14	2.96	0.13	0.32	0.06	0.76	0.08
FLD9	73.09	3.09	13.42	0.67	3.46	0.25	4.15	0.16	1.21	0.07	3.01	0.13	0.50	0.06	0.60	0.08
FLD9	69.41	2.94	18.43	0.90	6.11	0.42	5.75	0.21	0.03	0.04	1.75	0.09	0.03	0.05	0.28	0.06
FLD9	66.01	2.79	17.28	0.85	5.91	0.40	5.91	0.21	0.10	0.04	1.98	0.10	0.05	0.05	0.24	0.06
FLD9	72.22	3.05	14.77	0.73	5.43	0.37	5.33	0.20	0.03	0.04	2.97	0.13	0.06	0.05	0.23	0.06
FLD9	77.91	3.29	13.00	0.65	2.48	0.19	3.37	0.14	1.49	0.08	2.10	0.10	0.21	0.05	0.49	0.07

FLD9	74.79	3.16	12.85	0.65	3.32	0.24	3.89	0.15	2.30	0.11	2.87	0.13	0.38	0.06	0.51	0.07
FLD9	71.82	3.04	15.96	0.79	3.46	0.25	4.03	0.16	1.62	0.09	3.03	0.13	0.39	0.06	0.79	0.09
FLD9	70.60	2.98	14.23	0.71	3.13	0.23	3.80	0.15	1.65	0.09	3.61	0.15	0.44	0.06	0.76	0.09
FLD9	72.63	3.07	15.07	0.75	3.70	0.27	3.95	0.15	1.98	0.10	2.83	0.13	0.37	0.06	0.58	0.08
FLD9	67.53	2.86	16.45	0.81	3.72	0.27	4.08	0.16	1.93	0.10	4.04	0.16	0.54	0.06	0.94	0.09
FLD9	75.33	3.18	14.07	0.70	3.48	0.25	4.00	0.16	1.49	0.08	2.49	0.11	0.28	0.06	0.42	0.07
FLD9	70.57	2.98	16.41	0.81	3.45	0.25	3.85	0.15	1.81	0.09	2.95	0.13	0.48	0.06	0.96	0.10
FLD9	75.97	3.21	13.61	0.68	3.26	0.24	3.75	0.15	1.83	0.09	2.57	0.12	0.32	0.06	0.46	0.07
FLD9	68.06	2.88	17.31	0.85	3.92	0.28	4.41	0.17	1.74	0.09	2.83	0.13	0.43	0.06	0.72	0.08
FLD9	75.00	3.17	13.56	0.68	2.92	0.22	3.31	0.13	2.81	0.12	2.53	0.12	0.30	0.06	0.51	0.07
FLD9	74.32	3.14	12.85	0.65	3.38	0.25	4.11	0.16	1.16	0.07	2.92	0.13	0.30	0.06	0.48	0.07
FLD9	62.20	2.64	19.73	0.96	4.02	0.29	3.95	0.15	3.54	0.15	3.80	0.16	0.53	0.06	0.85	0.09
FLD9	77.22	3.26	13.25	0.66	3.19	0.23	3.99	0.16	1.21	0.08	2.49	0.11	0.18	0.05	0.51	0.07
FLD9	75.98	3.21	13.30	0.67	3.59	0.26	3.92	0.15	2.03	0.10	2.48	0.11	0.26	0.05	0.54	0.07
FLD9	69.03	2.92	14.45	0.72	3.58	0.26	4.11	0.16	2.03	0.10	3.56	0.15	0.35	0.06	0.56	0.07
FLD9	76.11	3.21	12.84	0.64	3.41	0.25	3.87	0.15	1.77	0.09	2.83	0.13	0.32	0.06	0.58	0.08
FLD9	73.25	3.09	12.54	0.63	3.22	0.24	3.94	0.15	1.67	0.09	2.39	0.11	0.33	0.06	0.53	0.07
FLD9	73.82	3.12	13.84	0.69	3.27	0.24	4.03	0.16	1.89	0.10	2.84	0.13	0.26	0.05	0.48	0.07
FLD9	69.32	2.93	14.46	0.72	3.87	0.28	4.98	0.19	1.03	0.07	2.57	0.12	0.19	0.05	0.31	0.06
FLD9	72.28	3.05	14.19	0.71	3.65	0.26	3.90	0.15	1.91	0.10	2.74	0.12	0.33	0.06	0.64	0.08
FLD9	71.43	3.02	13.99	0.70	3.68	0.27	4.17	0.16	1.74	0.09	3.25	0.14	0.28	0.06	0.92	0.09
FLD9	70.97	3.00	16.21	0.80	3.52	0.26	4.29	0.16	1.73	0.09	3.29	0.14	0.46	0.06	0.86	0.09
FLD9	70.94	3.00	17.33	0.85	6.20	0.42	5.83	0.21	0.03	0.04	1.64	0.09	0.03	0.05	0.24	0.06
FLD9	76.66	3.24	13.22	0.66	3.16	0.23	3.80	0.15	2.36	0.11	2.55	0.12	0.38	0.06	0.50	0.07
FLD9	75.24	3.18	12.60	0.63	3.34	0.24	3.91	0.15	2.23	0.11	2.80	0.12	0.30	0.06	0.42	0.07
FLD9	74.08	3.13	13.68	0.68	3.45	0.25	3.82	0.15	2.24	0.11	2.91	0.13	0.36	0.06	0.57	0.07
FLD9	71.64	3.03	13.60	0.68	3.70	0.27	4.26	0.16	1.57	0.09	3.54	0.15	0.44	0.06	0.54	0.07
FLD9	74.77	3.16	13.78	0.69	3.54	0.26	4.11	0.16	1.77	0.09	3.01	0.13	0.34	0.06	0.69	0.08
FLD9	70.10	2.96	13.89	0.69	3.67	0.26	4.24	0.16	1.76	0.09	2.91	0.13	0.33	0.06	0.60	0.08
FLD9	72.01	3.04	13.30	0.67	3.69	0.27	4.41	0.17	1.33	0.08	3.05	0.13	0.29	0.06	0.45	0.07
FLD9	68.97	2.92	14.76	0.73	3.96	0.28	4.32	0.17	1.99	0.10	4.02	0.16	0.54	0.06	0.68	0.08
FLD9	76.42	3.23	13.54	0.68	2.94	0.22	3.42	0.14	2.26	0.11	2.39	0.11	0.23	0.05	0.45	0.07
FLD9	68.98	2.92	17.48	0.86	4.00	0.29	4.35	0.17	1.55	0.09	3.20	0.14	0.40	0.06	0.87	0.09
FLD9	70.68	2.99	17.92	0.88	3.69	0.27	4.00	0.16	1.92	0.10	2.97	0.13	0.33	0.06	1.03	0.10
FLD9	96.73	4.07	2.15	0.15	0.70	0.08	1.03	0.06	0.03	0.04	0.60	0.06	0.03	0.05	0.03	0.05
FLD9	76.54	3.23	13.85	0.69	3.51	0.25	4.20	0.16	1.69	0.09	2.08	0.10	0.13	0.05	0.63	0.08
FLD9	67.61	2.86	19.71	0.96	3.39	0.25	3.53	0.14	2.27	0.11	3.22	0.14	0.55	0.06	1.19	0.11
FLD9	67.88	2.87	17.52	0.86	6.22	0.42	5.77	0.21	0.10	0.04	3.41	0.14	0.03	0.05	0.29	0.06
FLD9	74.93	3.16	14.06	0.70	3.54	0.26	4.07	0.16	1.60	0.09	2.64	0.12	0.33	0.06	0.58	0.08
FLD9	74.41	3.14	14.53	0.72	3.34	0.24	3.63	0.14	2.00	0.10	2.54	0.12	0.30	0.06	0.42	0.07
FLD9	66.31	2.81	18.13	0.89	4.49	0.32	4.48	0.17	1.38	0.08	3.72	0.15	0.60	0.07	0.53	0.07
FLD9	65.54	2.77	18.57	0.91	2.91	0.22	3.41	0.14	2.82	0.12	4.02	0.16	0.66	0.07	1.74	0.14
FLD9	64.18	2.72	18.22	0.89	4.27	0.30	4.64	0.18	1.77	0.09	3.30	0.14	0.51	0.06	1.18	0.11
FLD9	75.30	3.18	10.73	0.55	3.65	0.26	4.50	0.17	0.12	0.04	2.67	0.12	0.03	0.05	0.03	0.05
FLD9	70.31	2.97	16.21	0.80	3.44	0.25	4.25	0.16	1.60	0.09	3.12	0.13	0.33	0.06	0.70	0.08
FLD9	88.28	3.72	6.93	0.37	1.56	0.13	2.36	0.11	0.60	0.06	1.59	0.09	0.36	0.06	0.39	0.07
FLD9	67.13	2.84	17.29	0.85	3.52	0.26	3.95	0.15	2.46	0.11	3.35	0.14	0.57	0.06	1.29	0.11
FLD9	70.29	2.97	17.01	0.84	3.39	0.25	3.98	0.16	1.74	0.09	2.90	0.13	0.43	0.06	0.97	0.10
FLD9	66.50	2.81	16.99	0.84	3.61	0.26	3.83	0.15	2.80	0.12	4.07	0.16	0.60	0.06	1.72	0.14
FLD9	65.93	2.79	20.31	0.99	3.25	0.24	3.69	0.15	2.19	0.10	3.20	0.14	0.56	0.06	1.13	0.10
FLD9	82.42	3.47	11.66	0.59	2.54	0.19	3.35	0.14	0.88	0.07	2.07	0.10	0.09	0.05	0.55	0.07
FLD9	71.26	3.01	15.60	0.77	3.83	0.27	4.25	0.16	1.92	0.10	3.06	0.13	0.47	0.06	0.74	0.08
FLD9	75.00	3.17	13.46	0.67	3.48	0.25	3.82	0.15	2.17	0.10	2.74	0.12	0.30	0.06	0.54	0.07
FLD9	77.50	3.27	13.45	0.67	4.19	0.30	4.60	0.17	0.29	0.05	2.41	0.11	0.09	0.05	0.26	0.06
FLD9	70.95	3.00	16.67	0.82	4.31	0.30	4.29	0.16	1.90	0.10	3.01	0.13	0.48	0.06	0.84	0.09
FLD9	67.68	2.86	15.56	0.77	3.76	0.27	4.40	0.17	1.58	0.09	3.58	0.15	0.36	0.06	0.63	0.08
FLD9	72.60	3.07	16.26	0.80	3.15	0.23	3.57	0.14	1.50	0.08	2.99	0.13	0.40	0.06	0.69	0.08
FLD9	68.42	2.89	15.33	0.76	3.68	0.27	4.44	0.17	1.27	0.08	3.34	0.14	0.36	0.06	0.88	0.09
FLD9	74.01	3.13	14.45	0.72	3.44	0.25	3.82	0.15	1.64	0.09	2.69	0.12	0.32	0.06	0.52	0.07
FLD9	72.99	3.08	13.27	0.66	3.07	0.23	3.68	0.15	2.14	0.10	3.55	0.15	0.43	0.06	0.57	0.07
FLD9	75.78	3.20	15.37	0.76	3.29	0.24	3.74	0.15	1.30	0.08	2.78	0.12	0.42	0.06	0.82	0.09
FLD9	67.91	2.87	17.48	0.86	4.60	0.32	4.73	0.18	1.42	0.08	2.85	0.13	0.32	0.06	0.76	0.09

FLD9	77.35	3.26	13.68	0.68	3.97	0.28	4.26	0.16	0.76	0.06	2.27	0.11	0.14	0.05	0.20	0.06
FLD9	69.81	2.95	17.32	0.85	4.47	0.31	4.71	0.18	1.28	0.08	3.69	0.15	0.33	0.06	0.68	0.08
FLD9	67.76	2.87	17.49	0.86	4.74	0.33	4.80	0.18	1.61	0.09	3.90	0.16	0.45	0.06	0.65	0.08
FLD9	71.16	3.01	13.85	0.69	3.27	0.24	4.05	0.16	1.19	0.07	4.03	0.16	0.42	0.06	0.71	0.08
FLD9	66.86	2.83	18.14	0.89	4.19	0.30	4.71	0.18	2.00	0.10	3.42	0.14	0.42	0.06	0.83	0.09
FLD9	67.62	2.86	17.27	0.85	4.70	0.33	5.15	0.19	1.06	0.07	3.12	0.13	0.51	0.06	0.44	0.07
FLD9	81.13	3.42	11.00	0.56	3.21	0.24	4.09	0.16	0.82	0.06	2.69	0.12	0.08	0.05	0.33	0.06
FLD9	75.00	3.17	15.33	0.76	3.52	0.26	4.15	0.16	1.30	0.08	2.41	0.11	0.31	0.06	0.63	0.08
FLD9	74.08	3.13	16.63	0.82	3.35	0.25	4.03	0.16	1.95	0.10	2.50	0.11	0.36	0.06	0.71	0.08
FLD9	72.43	3.06	15.45	0.77	3.08	0.23	3.95	0.15	1.96	0.10	3.19	0.14	0.42	0.06	1.05	0.10
FLD9	72.58	3.07	16.51	0.81	3.22	0.24	3.98	0.16	1.71	0.09	2.90	0.13	0.51	0.06	0.84	0.09
FLD9	75.41	3.18	12.61	0.63	3.26	0.24	4.27	0.16	1.37	0.08	5.19	0.20	0.41	0.06	0.63	0.08
FLD9	67.94	2.87	14.58	0.73	4.53	0.32	4.85	0.18	1.76	0.09	4.50	0.18	0.12	0.05	0.25	0.06
FLD9	68.89	2.91	17.16	0.84	4.84	0.34	4.85	0.18	1.26	0.08	3.72	0.15	0.15	0.05	0.43	0.07
FLD9	83.72	3.53	9.19	0.48	2.75	0.21	2.80	0.12	1.55	0.09	2.29	0.11	0.24	0.05	0.60	0.08
FLD9	71.60	3.03	16.49	0.81	3.61	0.26	4.36	0.17	1.83	0.09	3.01	0.13	0.42	0.06	1.05	0.10
FLD9	70.72	2.99	17.93	0.88	3.47	0.25	4.42	0.17	1.54	0.08	2.77	0.12	0.36	0.06	0.81	0.09
FLD9	70.54	2.98	14.30	0.71	3.35	0.24	4.20	0.16	1.94	0.10	3.99	0.16	0.78	0.07	0.77	0.09
FLD9	67.38	2.85	14.61	0.73	5.74	0.39	5.13	0.19	2.15	0.10	5.54	0.21	0.23	0.05	0.18	0.05
FLD9	71.32	3.01	15.93	0.79	4.33	0.31	4.69	0.18	2.42	0.11	2.59	0.12	0.26	0.05	0.64	0.08
FLD9	65.56	2.78	18.14	0.89	3.59	0.26	4.26	0.16	2.62	0.12	4.34	0.17	0.55	0.06	1.61	0.13
FLD9	76.13	3.21	14.43	0.72	3.39	0.25	5.00	0.19	0.74	0.06	1.72	0.09	0.15	0.05	0.33	0.06
FLD9	65.71	2.78	14.92	0.74	5.70	0.39	5.62	0.21	0.24	0.05	6.58	0.24	0.09	0.05	0.16	0.05
FLD9	70.23	2.97	13.89	0.69	5.26	0.36	5.19	0.19	1.92	0.10	6.37	0.23	0.24	0.05	0.25	0.06
FLD9	75.49	3.19	13.53	0.68	2.85	0.21	4.62	0.17	1.50	0.08	3.92	0.16	0.19	0.05	0.88	0.09
FLD9	63.08	2.67	19.54	0.95	3.78	0.27	4.24	0.16	2.22	0.11	4.60	0.18	0.71	0.07	1.67	0.13
FLD9	72.18	3.05	15.62	0.77	3.87	0.28	4.51	0.17	1.76	0.09	3.10	0.13	0.25	0.05	0.92	0.09
FLD9	64.06	2.71	19.53	0.95	4.01	0.29	4.01	0.16	3.16	0.13	4.99	0.19	0.65	0.07	2.84	0.19
FLD9	68.54	2.90	17.78	0.87	4.70	0.33	5.01	0.19	1.59	0.09	3.67	0.15	0.42	0.06	0.56	0.07
FLD9	75.01	3.17	12.85	0.65	3.03	0.23	3.49	0.14	2.30	0.11	3.65	0.15	0.48	0.06	1.26	0.11
FLD9	75.50	3.19	15.23	0.76	3.11	0.23	4.07	0.16	0.79	0.06	2.21	0.11	0.30	0.06	0.64	0.08
FLD9	73.52	3.11	14.76	0.73	3.96	0.28	4.31	0.17	1.53	0.08	3.13	0.13	0.32	0.06	0.75	0.08
FLD9	75.71	3.20	13.17	0.66	3.35	0.25	3.63	0.14	3.50	0.14	3.02	0.13	0.26	0.05	0.90	0.09
FLD9	72.82	3.08	14.54	0.72	3.36	0.25	4.07	0.16	1.53	0.08	2.94	0.13	0.39	0.06	0.67	0.08
FLD9	74.68	3.15	12.79	0.64	3.26	0.24	3.63	0.14	3.42	0.14	2.53	0.12	0.25	0.05	0.74	0.08
FLD9	75.65	3.19	13.58	0.68	3.49	0.25	3.91	0.15	2.68	0.12	2.48	0.11	0.59	0.06	0.62	0.08
FLD9	70.78	2.99	14.74	0.73	3.86	0.28	4.17	0.16	2.10	0.10	3.77	0.15	0.52	0.06	0.65	0.08
FLD9	69.67	2.95	14.94	0.74	3.74	0.27	4.22	0.16	3.11	0.13	4.23	0.17	0.53	0.06	0.90	0.09
FLD9	71.27	3.01	13.04	0.65	3.33	0.24	3.56	0.14	3.97	0.16	4.68	0.18	0.67	0.07	1.48	0.12
FLD9	71.74	3.03	15.91	0.79	4.56	0.32	4.68	0.18	1.30	0.08	3.33	0.14	0.36	0.06	0.54	0.07
FLD9	68.76	2.91	15.15	0.75	4.60	0.32	4.73	0.18	2.19	0.10	2.89	0.13	0.23	0.05	0.43	0.07
FLD9	75.04	3.17	13.05	0.65	3.47	0.25	3.87	0.15	3.05	0.13	2.47	0.11	0.28	0.06	0.67	0.08
FLD9	74.72	3.16	13.32	0.67	3.30	0.24	3.65	0.15	3.62	0.15	2.71	0.12	0.34	0.06	0.74	0.08
FLD9	72.46	3.06	13.65	0.68	3.47	0.25	4.03	0.16	2.66	0.12	2.89	0.13	0.37	0.06	0.62	0.08
FLD9	74.50	3.15	13.16	0.66	3.29	0.24	3.79	0.15	3.70	0.15	2.70	0.12	0.33	0.06	0.73	0.08
FLD9	71.98	3.04	14.42	0.72	3.84	0.28	4.35	0.17	2.64	0.12	2.85	0.13	0.28	0.06	0.61	0.08
FLD9	69.89	2.96	16.31	0.81	4.24	0.30	4.44	0.17	2.41	0.11	3.25	0.14	1.27	0.09	0.77	0.09
FLD9	75.61	3.19	13.38	0.67	3.56	0.26	4.04	0.16	2.78	0.12	2.37	0.11	0.35	0.06	0.55	0.07
FLD9	74.81	3.16	12.70	0.64	3.30	0.24	3.82	0.15	3.14	0.13	2.54	0.12	0.29	0.06	0.68	0.08
FLD9	72.82	3.08	14.16	0.71	3.84	0.28	4.41	0.17	1.98	0.10	2.39	0.11	0.40	0.06	0.64	0.08
FLD9	72.18	3.05	12.86	0.65	3.75	0.27	4.42	0.17	2.16	0.10	3.97	0.16	0.33	0.06	0.68	0.08
FLD9	67.85	2.87	17.83	0.88	5.52	0.38	5.79	0.21	0.43	0.05	2.81	0.12	0.07	0.05	0.03	0.05
FLD9	66.44	2.81	15.37	0.76	4.04	0.29	4.45	0.17	2.07	0.10	5.49	0.21	0.55	0.06	0.61	0.08
FLD9	66.70	2.82	15.24	0.76	4.25	0.30	4.84	0.18	1.73	0.09	4.48	0.18	0.43	0.06	0.54	0.07
FLD9	71.62	3.03	13.77	0.69	3.61	0.26	4.35	0.17	2.21	0.11	2.56	0.12	0.27	0.05	0.50	0.07
FLD9	70.18	2.97	15.87	0.78	4.26	0.30	4.64	0.18	2.13	0.10	2.76	0.12	0.28	0.05	0.52	0.07
FLD9	78.56	3.31	12.85	0.65	3.33	0.24	4.33	0.17	0.87	0.06	2.13	0.10	0.32	0.06	0.29	0.06
FLD9	69.28	2.93	17.72	0.87	3.78	0.27	4.39	0.17	1.86	0.09	3.07	0.13	0.52	0.06	0.98	0.10
FLD9	70.82	2.99	18.39	0.90	3.62	0.26	4.14	0.16	1.79	0.09	3.20	0.14	0.54	0.06	1.02	0.10
FLD9	68.21	2.89	16.45	0.81	3.44	0.25	3.95	0.15	2.17	0.10	5.19	0.20	0.58	0.06	1.07	0.10
FLD9	67.84	2.87	16.99	0.84	3.80	0.27	4.25	0.16	2.11	0.10	5.17	0.20	0.87	0.07	0.91	0.09
FLD9	73.47	3.10	14.52	0.72	3.76	0.27	4.53	0.17	1.72	0.09	2.86	0.13	0.33	0.06	0.85	0.09

FLD9	65.31	2.77	13.61	0.68	3.82	0.27	3.46	0.14	2.03	0.10	7.49	0.27	0.44	0.06	6.86	0.41
FLD9	71.34	3.02	16.67	0.82	3.28	0.24	4.13	0.16	1.63	0.09	3.74	0.15	0.48	0.06	0.82	0.09
FLD9	69.18	2.93	17.90	0.88	3.42	0.25	4.17	0.16	2.12	0.10	3.46	0.14	0.39	0.06	1.23	0.11
FLD9	72.49	3.06	15.42	0.76	3.17	0.23	4.13	0.16	1.51	0.08	3.28	0.14	0.52	0.06	0.78	0.09
FLD9	71.82	3.04	15.47	0.77	3.76	0.27	4.76	0.18	1.07	0.07	2.36	0.11	0.33	0.06	0.45	0.07
FLD9	64.23	2.72	22.71	1.10	4.49	0.32	4.29	0.16	3.68	0.15	2.04	0.10	0.19	0.05	0.71	0.08
FLD9	77.23	3.26	12.76	0.64	2.32	0.18	3.49	0.14	2.15	0.10	1.17	0.07	0.17	0.05	0.73	0.08
FLD9	89.13	3.75	8.39	0.44	1.63	0.14	2.53	0.11	0.81	0.06	0.32	0.05	0.03	0.05	0.34	0.06
FLD9	70.07	2.96	16.89	0.83	3.85	0.28	4.22	0.16	1.56	0.09	4.09	0.16	0.53	0.06	1.12	0.10
FLD9	66.32	2.81	17.70	0.87	3.75	0.27	4.61	0.17	1.51	0.08	4.92	0.19	0.59	0.06	0.72	0.08
FLD9	70.62	2.99	15.85	0.78	3.57	0.26	4.26	0.16	1.62	0.09	2.96	0.13	0.36	0.06	0.79	0.09
FLD9	75.66	3.19	13.38	0.67	3.27	0.24	4.19	0.16	1.25	0.08	4.47	0.18	0.37	0.06	0.80	0.09
FLD9	69.48	2.94	19.03	0.93	3.54	0.26	4.52	0.17	1.37	0.08	3.36	0.14	0.42	0.06	1.36	0.12
FLD9	59.54	2.53	20.02	0.98	3.52	0.26	3.46	0.14	5.07	0.19	6.11	0.23	0.60	0.06	2.85	0.19
FLD9	67.73	2.87	15.25	0.76	4.17	0.30	4.89	0.18	1.06	0.07	4.67	0.18	0.54	0.06	0.65	0.08
FLD9	71.94	3.04	15.21	0.75	3.74	0.27	4.49	0.17	1.47	0.08	2.91	0.13	0.36	0.06	0.83	0.09
FLD9	78.70	3.32	11.62	0.59	2.83	0.21	3.92	0.15	0.78	0.06	2.35	0.11	0.19	0.05	0.38	0.06
FLD9	69.41	2.94	17.84	0.88	3.37	0.25	4.39	0.17	2.17	0.10	3.18	0.14	0.48	0.06	1.04	0.10
FLD9	68.75	2.91	19.26	0.94	3.73	0.27	3.99	0.16	2.22	0.11	3.79	0.15	0.48	0.06	1.46	0.12
FLD9	69.67	2.95	16.37	0.81	4.53	0.32	4.74	0.18	1.31	0.08	3.84	0.16	0.52	0.06	0.81	0.09
FLD9	73.05	3.09	15.04	0.75	3.78	0.27	4.66	0.18	0.97	0.07	3.02	0.13	0.37	0.06	0.55	0.07
FLD9	73.78	3.12	13.35	0.67	3.09	0.23	3.73	0.15	2.01	0.10	2.73	0.12	0.29	0.06	0.50	0.07
FLD9	67.73	2.87	14.81	0.74	3.08	0.23	4.32	0.17	1.65	0.09	3.13	0.13	0.52	0.06	0.83	0.09
FLD9	81.40	3.43	7.14	0.38	1.85	0.15	2.87	0.12	0.69	0.06	2.91	0.13	0.18	0.05	0.35	0.06
FLD9	68.11	2.88	14.93	0.74	3.75	0.27	4.47	0.17	1.17	0.07	3.55	0.15	0.55	0.06	0.61	0.08
FLD9	70.99	3.00	12.61	0.63	2.83	0.21	3.49	0.14	2.78	0.12	2.80	0.12	0.42	0.06	0.48	0.07
FLD9	66.68	2.82	16.08	0.79	3.54	0.26	4.15	0.16	1.92	0.10	3.31	0.14	0.40	0.06	0.66	0.08
FLD9	76.55	3.23	10.31	0.53	2.78	0.21	3.86	0.15	1.83	0.09	3.07	0.13	0.28	0.06	0.45	0.07
FLD9	70.04	2.96	14.82	0.74	3.33	0.24	4.30	0.17	1.42	0.08	2.89	0.13	0.38	0.06	0.63	0.08
FLD9	70.27	2.97	14.58	0.73	3.03	0.22	4.07	0.16	1.42	0.08	2.61	0.12	0.20	0.05	0.48	0.07
FLD9	74.19	3.13	11.74	0.59	2.79	0.21	3.81	0.15	1.96	0.10	2.63	0.12	0.36	0.06	0.43	0.07
FLD9	92.18	3.88	1.90	0.14	0.45	0.07	0.77	0.06	0.03	0.04	0.48	0.05	0.11	0.05	0.09	0.05
FLD9	67.14	2.84	16.86	0.83	3.43	0.25	4.11	0.16	1.93	0.10	4.08	0.16	0.53	0.06	0.79	0.09
FLD9	71.07	3.00	12.81	0.64	3.35	0.24	4.80	0.18	0.76	0.06	4.13	0.17	0.36	0.06	0.22	0.06
FLD9	70.83	2.99	12.46	0.63	3.25	0.24	4.00	0.16	2.34	0.11	2.87	0.13	0.33	0.06	0.45	0.07
FLD9	71.43	3.02	12.95	0.65	2.57	0.20	3.23	0.13	2.73	0.12	2.73	0.12	0.34	0.06	0.39	0.07
FLD9	66.79	2.83	15.38	0.76	3.82	0.27	4.38	0.17	1.71	0.09	3.50	0.15	0.58	0.06	0.87	0.09
FLD9	66.62	2.82	15.62	0.77	3.20	0.24	4.04	0.16	1.85	0.09	3.17	0.14	1.36	0.09	0.88	0.09
FLD9	71.41	3.02	13.94	0.70	3.29	0.24	3.95	0.15	2.09	0.10	2.47	0.11	0.29	0.06	0.52	0.07
FLD9	71.44	3.02	12.06	0.61	3.04	0.23	3.87	0.15	2.20	0.10	2.89	0.13	0.35	0.06	0.52	0.07
FLD9	72.01	3.04	11.35	0.58	3.04	0.23	3.73	0.15	2.87	0.13	2.83	0.12	0.28	0.06	0.43	0.07
FLD9	70.85	3.00	13.13	0.66	2.80	0.21	3.42	0.14	2.72	0.12	2.62	0.12	0.31	0.06	0.44	0.07
FLD9	72.06	3.05	12.04	0.61	3.08	0.23	3.87	0.15	1.75	0.09	2.78	0.12	0.35	0.06	0.47	0.07
FLD9	79.24	3.34	10.11	0.52	3.07	0.23	4.20	0.16	0.07	0.04	2.02	0.10	0.09	0.05	0.16	0.05
FLD9	72.68	3.07	11.76	0.60	2.95	0.22	4.09	0.16	1.75	0.09	2.66	0.12	0.29	0.06	0.44	0.07
FLD9	67.71	2.87	15.50	0.77	4.02	0.29	4.37	0.17	1.40	0.08	3.29	0.14	0.43	0.06	0.52	0.07
FLD9	73.94	3.12	11.76	0.59	3.50	0.25	4.49	0.17	0.03	0.04	2.46	0.11	0.03	0.05	0.03	0.05
FLD9	69.45	2.94	14.77	0.73	2.98	0.22	3.77	0.15	1.37	0.08	3.31	0.14	0.48	0.06	0.60	0.08
FLD9	70.22	2.97	12.75	0.64	3.16	0.23	3.76	0.15	2.60	0.12	2.99	0.13	0.35	0.06	0.73	0.08
FLD9	69.20	2.93	14.40	0.72	3.28	0.24	3.99	0.16	2.05	0.10	2.65	0.12	0.35	0.06	0.51	0.07
FLD9	67.42	2.85	15.29	0.76	3.28	0.24	4.16	0.16	2.15	0.10	2.69	0.12	0.48	0.06	0.57	0.07
FLD9	71.60	3.03	12.85	0.65	2.88	0.22	3.68	0.15	2.23	0.11	2.90	0.13	0.33	0.06	0.45	0.07
FLD9	70.77	2.99	13.27	0.66	3.25	0.24	3.82	0.15	2.24	0.11	3.07	0.13	0.34	0.06	0.51	0.07
FLD9	67.62	2.86	16.09	0.80	4.16	0.29	4.58	0.17	1.65	0.09	2.89	0.13	0.49	0.06	0.47	0.07
FLD9	64.62	2.74	15.92	0.79	3.35	0.24	4.02	0.16	3.15	0.13	3.76	0.15	0.53	0.06	1.00	0.10
FLD9	70.94	3.00	12.85	0.65	3.00	0.22	3.65	0.15	2.43	0.11	2.64	0.12	0.35	0.06	0.47	0.07
FLD9	71.75	3.03	12.75	0.64	2.98	0.22	3.90	0.15	1.97	0.10	2.84	0.13	0.34	0.06	0.46	0.07
FLD9	71.19	3.01	12.29	0.62	2.98	0.22	3.82	0.15	2.08	0.10	2.83	0.13	0.35	0.06	0.47	0.07
FLD9	69.00	2.92	14.28	0.71	3.80	0.27	4.49	0.17	1.07	0.07	3.27	0.14	0.39	0.06	0.61	0.08
FLD9	71.06	3.00	12.77	0.64	3.17	0.23	3.92	0.15	2.73	0.12	2.84	0.13	0.32	0.06	0.45	0.07
FLD9	69.80	2.95	15.68	0.78	3.45	0.25	3.91	0.15	2.70	0.12	3.71	0.15	0.33	0.06	0.42	0.07
FLD9	73.20	3.09	13.31	0.67	2.55	0.20	3.23	0.13	2.68	0.12	2.87	0.13	0.32	0.06	0.47	0.07

FLD9	89.51	3.77	3.47	0.21	1.00	0.10	1.53	0.08	0.53	0.05	0.90	0.07	0.13	0.05	0.21	0.06
FLD9	71.83	3.04	13.09	0.66	3.11	0.23	3.93	0.15	2.21	0.11	2.86	0.13	0.43	0.06	0.48	0.07
FLD9	70.73	2.99	13.15	0.66	2.63	0.20	3.26	0.13	3.06	0.13	2.79	0.12	0.33	0.06	0.49	0.07
FLD9	73.37	3.10	12.62	0.63	3.01	0.22	3.53	0.14	2.76	0.12	2.79	0.12	0.34	0.06	0.41	0.07
FLD9	69.67	2.95	14.20	0.71	3.30	0.24	4.00	0.16	2.11	0.10	2.75	0.12	0.39	0.06	0.57	0.08
FLD9	71.46	3.02	13.89	0.69	2.61	0.20	3.02	0.13	3.09	0.13	2.92	0.13	0.32	0.06	0.43	0.07
FLD9	70.57	2.98	12.21	0.62	3.11	0.23	3.98	0.16	2.57	0.12	2.91	0.13	0.35	0.06	0.47	0.07
FLD9	70.57	2.98	13.36	0.67	2.77	0.21	3.44	0.14	2.36	0.11	2.93	0.13	0.48	0.06	0.53	0.07
FLD9	70.14	2.97	13.32	0.67	2.86	0.21	3.57	0.14	2.44	0.11	3.05	0.13	0.31	0.06	0.50	0.07
FLD9	70.90	3.00	13.22	0.66	3.39	0.25	3.84	0.15	2.26	0.11	2.97	0.13	0.39	0.06	0.59	0.08
FLD9	70.17	2.97	13.40	0.67	2.72	0.21	3.45	0.14	2.72	0.12	2.99	0.13	0.31	0.06	0.48	0.07
FLD9	71.99	3.04	13.01	0.65	3.11	0.23	3.70	0.15	2.55	0.12	2.72	0.12	0.34	0.06	0.45	0.07
FLD9	69.91	2.96	13.38	0.67	3.15	0.23	3.54	0.14	3.40	0.14	2.94	0.13	0.40	0.06	0.53	0.07
FLD9	73.71	3.11	11.37	0.58	3.00	0.22	3.96	0.15	0.96	0.07	3.13	0.13	0.24	0.05	0.26	0.06
FLD9	67.44	2.85	14.86	0.74	3.55	0.26	4.15	0.16	1.77	0.09	3.80	0.15	0.51	0.06	0.62	0.08
FLD9	69.78	2.95	13.35	0.67	3.21	0.24	3.88	0.15	2.38	0.11	2.82	0.12	0.38	0.06	0.49	0.07
FLD9	63.92	2.71	18.39	0.90	3.75	0.27	4.16	0.16	3.78	0.15	2.73	0.12	0.17	0.05	0.74	0.08
FLD9	71.16	3.01	12.45	0.63	2.99	0.22	3.70	0.15	2.72	0.12	2.83	0.12	0.28	0.05	0.47	0.07
FLD9	67.36	2.85	15.83	0.78	3.07	0.23	3.72	0.15	1.73	0.09	3.19	0.14	0.54	0.06	0.83	0.09
FLD9	75.20	3.18	10.79	0.55	2.62	0.20	3.76	0.15	1.61	0.09	2.46	0.11	0.45	0.06	0.38	0.06
FLD9	68.42	2.89	14.56	0.72	3.24	0.24	3.92	0.15	2.11	0.10	3.03	0.13	0.40	0.06	0.61	0.08
FLD9	70.67	2.99	13.09	0.66	2.92	0.22	3.88	0.15	2.33	0.11	2.73	0.12	0.35	0.06	0.79	0.09
FLD9	73.60	3.11	11.43	0.58	2.91	0.22	3.69	0.15	2.33	0.11	2.56	0.12	0.41	0.06	0.49	0.07
FLD9	70.33	2.97	12.49	0.63	3.08	0.23	3.85	0.15	3.06	0.13	2.70	0.12	0.33	0.06	0.52	0.07
FLD9	72.65	3.07	12.64	0.64	3.06	0.23	3.60	0.14	2.25	0.11	2.85	0.13	0.34	0.06	0.50	0.07
FLD9	71.16	3.01	11.82	0.60	2.93	0.22	3.70	0.15	2.86	0.12	2.90	0.13	0.30	0.06	0.49	0.07
FLD9	71.26	3.01	12.48	0.63	3.47	0.25	4.24	0.16	2.31	0.11	2.90	0.13	0.40	0.06	0.61	0.08
FLD9	69.35	2.93	12.41	0.62	3.45	0.25	4.16	0.16	2.21	0.11	3.58	0.15	0.53	0.06	0.62	0.08
FLD9	62.52	2.65	10.10	0.52	3.03	0.23	3.01	0.13	9.45	0.32	5.98	0.22	0.78	0.07	1.66	0.13
FLD9	66.68	2.82	14.83	0.74	3.72	0.27	4.40	0.17	2.43	0.11	3.17	0.14	0.48	0.06	0.81	0.09
FLD9	71.66	3.03	12.48	0.63	3.30	0.24	4.42	0.17	1.79	0.09	2.83	0.13	0.27	0.05	0.33	0.06
FLD9	72.13	3.05	12.66	0.64	3.36	0.25	4.03	0.16	1.94	0.10	2.81	0.12	0.35	0.06	0.55	0.07
FLD9	69.06	2.92	13.00	0.65	3.40	0.25	3.97	0.15	2.50	0.11	3.08	0.13	0.45	0.06	0.64	0.08
FLD9	70.98	3.00	11.80	0.60	3.15	0.23	3.90	0.15	2.70	0.12	3.37	0.14	0.44	0.06	0.72	0.08
FLD9	70.17	2.97	12.81	0.64	3.15	0.23	3.83	0.15	2.49	0.11	3.17	0.14	0.35	0.06	0.55	0.07
FLD9	73.99	3.12	11.03	0.56	2.94	0.22	3.86	0.15	1.85	0.09	2.50	0.11	0.20	0.05	0.43	0.07
FLD9	76.80	3.24	8.01	0.42	2.60	0.20	4.14	0.16	0.47	0.05	3.98	0.16	0.05	0.05	0.14	0.05
FLD9	71.35	3.02	12.68	0.64	3.08	0.23	3.64	0.14	2.54	0.11	2.78	0.12	0.33	0.06	0.45	0.07
FLD9	71.51	3.02	12.35	0.62	3.36	0.25	4.04	0.16	2.41	0.11	2.70	0.12	0.33	0.06	0.44	0.07
FLD9	70.63	2.99	12.90	0.65	2.85	0.21	3.54	0.14	2.72	0.12	2.65	0.12	0.30	0.06	0.42	0.07
FLD9	70.83	2.99	13.05	0.65	2.88	0.22	3.77	0.15	2.33	0.11	2.86	0.13	0.30	0.06	0.48	0.07
FLD9	70.43	2.98	13.62	0.68	2.85	0.21	3.34	0.14	2.98	0.13	2.58	0.12	0.35	0.06	0.43	0.07
FLD9	71.44	3.02	12.30	0.62	2.87	0.21	3.72	0.15	2.79	0.12	2.60	0.12	0.29	0.06	0.46	0.07
FLD9	71.60	3.03	12.30	0.62	3.14	0.23	3.80	0.15	2.10	0.10	2.60	0.12	0.27	0.05	0.39	0.07
FLD9	71.10	3.01	12.35	0.62	3.12	0.23	3.91	0.15	2.01	0.10	2.76	0.12	0.33	0.06	0.45	0.07
FLD9	72.64	3.07	11.80	0.60	2.85	0.21	3.64	0.14	2.52	0.11	2.76	0.12	0.23	0.05	0.46	0.07
FLD9	68.65	2.90	14.79	0.73	3.75	0.27	4.23	0.16	1.69	0.09	2.47	0.11	0.17	0.05	0.56	0.07
FLD9	71.25	3.01	14.17	0.71	2.76	0.21	3.18	0.13	3.25	0.14	2.87	0.13	0.35	0.06	0.47	0.07
FLD9	70.99	3.00	11.99	0.61	3.18	0.23	4.02	0.16	1.97	0.10	3.20	0.14	0.34	0.06	0.45	0.07
FLD9	72.00	3.04	13.09	0.66	2.46	0.19	3.23	0.13	2.16	0.10	2.82	0.12	0.30	0.06	0.47	0.07
FLD9	71.26	3.01	12.80	0.64	2.93	0.22	3.57	0.14	2.70	0.12	2.91	0.13	0.30	0.06	0.47	0.07
FLD9	69.80	2.95	14.20	0.71	2.56	0.20	3.07	0.13	3.22	0.14	2.79	0.12	0.38	0.06	0.45	0.07
FLD9	69.09	2.92	14.58	0.73	2.61	0.20	3.03	0.13	3.33	0.14	2.74	0.12	0.41	0.06	0.42	0.07
FLD9	72.79	3.08	11.67	0.59	2.91	0.22	3.52	0.14	2.72	0.12	3.08	0.13	0.20	0.05	0.48	0.07
FLD9	70.42	2.98	12.93	0.65	3.11	0.23	3.93	0.15	2.23	0.11	2.95	0.13	0.38	0.06	0.52	0.07
FLD9	72.19	3.05	11.39	0.58	3.14	0.23	3.66	0.15	2.15	0.10	2.71	0.12	0.31	0.06	0.46	0.07
FLD9	78.26	3.30	9.44	0.49	2.53	0.19	3.40	0.14	1.63	0.09	2.34	0.11	0.16	0.05	0.29	0.06
FLD9	74.52	3.15	13.71	0.69	2.15	0.17	2.87	0.12	2.41	0.11	2.67	0.12	0.29	0.06	0.48	0.07
FLD9	77.04	3.25	13.37	0.67	2.84	0.21	3.31	0.13	2.55	0.12	2.66	0.12	0.27	0.05	0.54	0.07
FLD9	78.90	3.33	12.87	0.65	2.85	0.21	3.38	0.14	2.43	0.11	2.62	0.12	0.24	0.05	0.52	0.07
FLD9	78.73	3.32	11.58	0.59	2.55	0.20	3.39	0.14	2.23	0.11	2.69	0.12	0.20	0.05	0.48	0.07
FLD9	76.70	3.24	13.90	0.69	3.04	0.23	3.50	0.14	2.50	0.11	2.73	0.12	0.32	0.06	0.52	0.07

FLD9	75.30	3.18	13.58	0.68	3.35	0.25	4.26	0.16	1.95	0.10	2.67	0.12	0.29	0.06	0.68	0.08
FLD9	74.03	3.13	12.73	0.64	3.28	0.24	4.06	0.16	1.91	0.10	3.35	0.14	0.43	0.06	0.72	0.08
FLD9	72.01	3.04	13.62	0.68	3.47	0.25	3.96	0.15	3.35	0.14	3.94	0.16	0.51	0.06	1.19	0.11
FLD9	71.28	3.01	12.42	0.63	2.83	0.21	3.35	0.14	2.98	0.13	2.67	0.12	0.31	0.06	0.41	0.07
FLD9	70.34	2.97	13.02	0.65	3.31	0.24	3.97	0.15	2.11	0.10	2.85	0.13	0.24	0.05	0.52	0.07
FLD9	71.14	3.01	12.74	0.64	3.13	0.23	3.65	0.15	2.71	0.12	2.59	0.12	0.30	0.06	0.41	0.07
FLD9	83.38	3.51	6.89	0.37	1.80	0.15	2.37	0.11	0.99	0.07	1.85	0.09	0.13	0.05	0.33	0.06
FLD9	67.08	2.84	14.23	0.71	3.35	0.25	4.01	0.16	2.88	0.13	3.57	0.15	0.40	0.06	0.66	0.08
FLD9	69.69	2.95	13.12	0.66	3.51	0.25	4.42	0.17	1.96	0.10	3.10	0.13	0.35	0.06	0.51	0.07
FLD9	67.38	2.85	15.75	0.78	3.61	0.26	4.17	0.16	2.02	0.10	3.09	0.13	0.47	0.06	0.64	0.08
FLD9	72.93	3.08	12.65	0.64	3.16	0.23	3.96	0.15	1.72	0.09	2.85	0.13	0.41	0.06	0.50	0.07
FLD9	69.69	2.95	13.14	0.66	3.32	0.24	3.89	0.15	2.43	0.11	3.01	0.13	0.32	0.06	0.53	0.07
FLD9	70.66	2.99	12.69	0.64	3.16	0.23	3.72	0.15	2.39	0.11	2.69	0.12	0.35	0.06	0.40	0.07
FLD9	70.36	2.97	13.26	0.66	3.33	0.24	3.79	0.15	2.64	0.12	3.02	0.13	0.35	0.06	0.51	0.07
FLD9	70.18	2.97	13.45	0.67	3.41	0.25	4.16	0.16	1.73	0.09	2.74	0.12	0.42	0.06	0.55	0.07
FLD9	70.53	2.98	12.33	0.62	3.25	0.24	3.77	0.15	2.54	0.12	2.95	0.13	0.27	0.05	0.56	0.07
FLD9	71.75	3.03	11.36	0.58	3.08	0.23	3.77	0.15	2.60	0.12	2.88	0.13	0.35	0.06	0.50	0.07
FLD9	72.07	3.05	12.33	0.62	3.16	0.23	3.90	0.15	2.28	0.11	2.92	0.13	0.28	0.05	0.63	0.08
FLD9	71.74	3.03	12.23	0.62	3.13	0.23	3.72	0.15	2.59	0.12	3.01	0.13	0.27	0.05	0.59	0.08
FLD9	77.77	3.28	9.58	0.49	2.64	0.20	3.53	0.14	1.56	0.09	2.27	0.11	0.20	0.05	0.38	0.06
FLD9	69.95	2.96	12.75	0.64	3.35	0.25	4.36	0.17	2.29	0.11	2.88	0.13	0.35	0.06	0.57	0.07
FLD9	70.93	3.00	12.47	0.63	3.37	0.25	4.26	0.16	1.56	0.09	3.16	0.14	0.41	0.06	0.50	0.07
FLD9	69.14	2.92	13.21	0.66	3.50	0.25	4.19	0.16	2.11	0.10	3.10	0.13	0.41	0.06	0.54	0.07
FLD9	71.87	3.04	15.07	0.75	3.54	0.26	4.15	0.16	2.53	0.11	3.06	0.13	0.47	0.06	0.76	0.08
FLD9	74.36	3.14	13.65	0.68	3.55	0.26	4.01	0.16	2.55	0.12	2.68	0.12	0.35	0.06	0.66	0.08
FLD9	73.95	3.12	12.26	0.62	3.38	0.25	4.13	0.16	2.39	0.11	2.80	0.12	0.55	0.06	0.63	0.08
FLD9	72.82	3.08	14.56	0.72	2.94	0.22	3.27	0.13	3.02	0.13	2.63	0.12	0.32	0.06	0.49	0.07
FLD9	76.29	3.22	13.90	0.69	3.00	0.22	3.38	0.14	2.81	0.12	2.75	0.12	0.32	0.06	0.59	0.08
FLD9	74.89	3.16	13.49	0.67	3.04	0.23	3.47	0.14	2.69	0.12	2.67	0.12	0.33	0.06	0.54	0.07
FLD9	75.43	3.18	13.29	0.67	3.30	0.24	3.67	0.15	2.70	0.12	2.75	0.12	0.30	0.06	0.59	0.08
FLD9	74.13	3.13	13.38	0.67	3.21	0.24	3.45	0.14	2.84	0.12	2.61	0.12	0.31	0.06	0.53	0.07
FLD9	78.69	3.32	11.95	0.60	3.26	0.24	3.81	0.15	2.16	0.10	2.21	0.11	0.31	0.06	0.49	0.07
FLD9	77.15	3.26	12.62	0.63	3.43	0.25	4.05	0.16	2.05	0.10	2.66	0.12	0.27	0.05	0.55	0.07
FLD9	74.70	3.15	13.99	0.70	3.11	0.23	3.57	0.14	2.96	0.13	2.75	0.12	0.36	0.06	0.54	0.07
FLD9	73.47	3.10	13.01	0.65	3.12	0.23	3.73	0.15	3.34	0.14	2.65	0.12	0.35	0.06	0.54	0.07
FLD9	75.57	3.19	13.47	0.67	3.07	0.23	3.59	0.14	2.75	0.12	2.64	0.12	0.28	0.06	0.51	0.07
FLD9	75.26	3.18	13.48	0.67	2.75	0.21	3.35	0.14	3.01	0.13	2.71	0.12	0.32	0.06	0.58	0.08
FLD9	73.97	3.12	13.33	0.67	2.97	0.22	3.42	0.14	3.15	0.13	2.57	0.12	0.32	0.06	0.54	0.07
FLD9	74.37	3.14	13.95	0.70	3.44	0.25	4.17	0.16	1.97	0.10	2.91	0.13	0.36	0.06	0.68	0.08
FLD9	75.47	3.19	12.63	0.64	3.31	0.24	4.06	0.16	2.14	0.10	2.59	0.12	0.27	0.05	0.59	0.08
FLD9	73.90	3.12	14.22	0.71	3.68	0.27	4.20	0.16	2.49	0.11	2.94	0.13	0.43	0.06	0.59	0.08
FLD9	74.35	3.14	13.23	0.66	3.35	0.24	3.87	0.15	2.39	0.11	2.55	0.12	0.24	0.05	0.57	0.07
FLD9	74.05	3.13	14.14	0.71	2.57	0.20	3.26	0.13	2.94	0.13	2.72	0.12	0.39	0.06	0.54	0.07
FLD9	76.99	3.25	13.82	0.69	2.47	0.19	3.07	0.13	2.95	0.13	2.88	0.13	0.29	0.06	0.57	0.07
FLD9	74.96	3.16	13.64	0.68	2.76	0.21	3.32	0.13	3.03	0.13	2.65	0.12	0.38	0.06	0.47	0.07
FLD9	72.92	3.08	14.94	0.74	3.52	0.26	3.99	0.16	2.79	0.12	2.92	0.13	0.42	0.06	0.79	0.09
FLD9	76.36	3.22	13.87	0.69	3.44	0.25	4.02	0.16	2.14	0.10	2.80	0.12	0.32	0.06	0.61	0.08
FLD9	74.56	3.15	13.60	0.68	3.47	0.25	3.96	0.15	3.15	0.13	2.51	0.12	0.34	0.06	0.56	0.07
FLD9	76.60	3.23	12.31	0.62	2.97	0.22	3.64	0.14	2.55	0.12	2.47	0.11	0.26	0.05	0.53	0.07
FLD9	79.09	3.34	12.64	0.64	2.20	0.17	2.93	0.12	2.04	0.10	2.69	0.12	0.26	0.05	0.46	0.07
FLD9	74.87	3.16	14.01	0.70	2.30	0.18	3.05	0.13	2.33	0.11	2.77	0.12	0.38	0.06	0.50	0.07
FLD9	76.28	3.22	13.55	0.68	3.03	0.22	3.89	0.15	2.11	0.10	2.77	0.12	0.38	0.06	0.57	0.08
FLD9	72.08	3.05	15.77	0.78	3.57	0.26	4.10	0.16	2.45	0.11	2.48	0.11	0.28	0.05	0.51	0.07
FLD9	74.50	3.15	13.82	0.69	3.03	0.22	3.72	0.15	2.65	0.12	2.65	0.12	0.30	0.06	0.53	0.07
FLD9	75.29	3.18	13.42	0.67	2.74	0.21	3.33	0.14	2.54	0.12	2.74	0.12	0.31	0.06	0.47	0.07
FLD9	75.18	3.17	13.78	0.69	3.21	0.24	4.06	0.16	1.96	0.10	2.74	0.12	0.37	0.06	0.62	0.08
FLD9	73.22	3.09	12.86	0.65	2.97	0.22	3.72	0.15	3.11	0.13	2.68	0.12	0.33	0.06	0.53	0.07
FLD9	75.95	3.21	14.29	0.71	3.09	0.23	3.84	0.15	2.11	0.10	2.85	0.13	0.35	0.06	0.59	0.08
FLD9	75.66	3.19	13.67	0.68	3.16	0.23	3.75	0.15	2.48	0.11	2.87	0.13	0.30	0.06	0.65	0.08
FLD9	75.31	3.18	13.32	0.67	3.09	0.23	3.71	0.15	2.69	0.12	2.71	0.12	0.30	0.06	0.61	0.08
FLD9	75.16	3.17	13.96	0.70	3.04	0.23	3.78	0.15	2.52	0.11	2.85	0.13	0.40	0.06	0.61	0.08
FLD9	75.72	3.20	13.33	0.67	2.81	0.21	3.55	0.14	2.99	0.13	2.73	0.12	0.33	0.06	0.58	0.08

FLD9	77.75	3.28	13.16	0.66	2.89	0.22	3.43	0.14	2.83	0.12	2.91	0.13	0.27	0.05	0.65	0.08
FLD9	77.18	3.26	13.53	0.68	2.86	0.21	3.50	0.14	2.84	0.12	2.71	0.12	0.30	0.06	0.49	0.07
FLD9	75.37	3.18	13.23	0.66	2.98	0.22	3.55	0.14	2.53	0.11	2.81	0.12	0.26	0.05	0.50	0.07
FLD3.1	75.00	3.17	13.79	0.69	2.60	0.20	3.70	0.15	1.43	0.08	2.76	0.12	0.31	0.06	0.47	0.07
FLD3.1	77.88	3.29	14.23	0.71	2.74	0.21	3.59	0.14	1.42	0.08	2.72	0.12	0.34	0.06	0.50	0.07
FLD3.1	76.13	3.21	13.85	0.69	2.59	0.20	3.68	0.15	1.03	0.07	2.94	0.13	0.45	0.06	0.41	0.07
FLD3.1	71.50	3.02	14.88	0.74	3.62	0.26	4.69	0.18	1.51	0.08	2.56	0.12	0.27	0.05	0.59	0.08
FLD3.1	73.79	3.12	14.22	0.71	3.07	0.23	3.87	0.15	2.08	0.10	2.84	0.13	0.39	0.06	0.66	0.08
FLD3.1	73.24	3.09	15.48	0.77	3.07	0.23	4.02	0.16	1.73	0.09	2.71	0.12	0.44	0.06	0.62	0.08
FLD3.1	75.59	3.19	11.95	0.60	2.64	0.20	4.27	0.16	0.99	0.07	2.93	0.13	0.23	0.05	0.26	0.06
FLD3.1	74.24	3.14	13.67	0.68	2.77	0.21	3.88	0.15	1.95	0.10	2.86	0.13	0.34	0.06	0.56	0.07
FLD3.1	72.59	3.07	14.79	0.74	3.20	0.24	4.07	0.16	2.33	0.11	2.78	0.12	0.37	0.06	0.83	0.09
FLD3.1	74.51	3.15	14.45	0.72	2.82	0.21	3.68	0.15	1.64	0.09	3.26	0.14	0.42	0.06	0.61	0.08
FLD3.1	76.53	3.23	13.33	0.67	2.64	0.20	4.01	0.16	1.17	0.07	2.69	0.12	0.26	0.05	0.33	0.06
FLD3.1	74.62	3.15	13.93	0.70	2.73	0.21	3.83	0.15	1.87	0.09	2.84	0.13	0.36	0.06	0.58	0.08
FLD3.1	72.67	3.07	13.69	0.68	2.90	0.22	3.93	0.15	1.89	0.10	3.13	0.13	0.38	0.06	0.58	0.08
FLD3.1	73.69	3.11	14.16	0.71	2.80	0.21	3.80	0.15	1.49	0.08	3.62	0.15	0.47	0.06	1.73	0.14
FLD3.1	79.84	3.37	11.55	0.58	2.47	0.19	3.82	0.15	1.11	0.07	2.01	0.10	0.31	0.06	0.33	0.06
FLD3.1	70.95	3.00	14.20	0.71	2.84	0.21	4.17	0.16	1.97	0.10	3.75	0.15	0.44	0.06	0.47	0.07
FLD3.1	73.25	3.09	15.10	0.75	2.38	0.18	3.46	0.14	1.60	0.09	2.75	0.12	0.51	0.06	0.91	0.09
FLD3.1	76.01	3.21	14.54	0.72	2.72	0.21	3.93	0.15	1.07	0.07	2.75	0.12	0.31	0.06	0.46	0.07
FLD3.1	77.55	3.27	13.71	0.69	2.69	0.20	3.91	0.15	1.23	0.08	2.76	0.12	0.28	0.05	0.41	0.07
FLD3.1	75.53	3.19	14.18	0.71	2.62	0.20	3.83	0.15	1.75	0.09	2.44	0.11	0.35	0.06	0.46	0.07
FLD3.1	72.23	3.05	13.90	0.69	2.99	0.22	4.00	0.16	2.50	0.11	2.85	0.13	0.32	0.06	0.62	0.08
FLD3.1	77.65	3.28	12.57	0.63	2.54	0.19	3.95	0.15	1.91	0.10	2.68	0.12	0.27	0.05	0.50	0.07
FLD3.1	77.08	3.25	14.43	0.72	2.48	0.19	3.68	0.15	1.52	0.08	2.67	0.12	0.37	0.06	0.76	0.08
FLD3.1	77.46	3.27	13.10	0.66	2.56	0.20	3.83	0.15	1.43	0.08	2.46	0.11	0.26	0.05	0.36	0.06
FLD3.1	76.93	3.25	13.41	0.67	2.57	0.20	3.84	0.15	1.22	0.08	2.97	0.13	0.32	0.06	0.48	0.07
FLD3.1	77.56	3.27	13.92	0.69	2.36	0.18	3.73	0.15	1.60	0.09	2.81	0.12	0.34	0.06	0.48	0.07
FLD3.1	77.30	3.26	13.35	0.67	2.33	0.18	3.69	0.15	1.70	0.09	2.80	0.12	0.35	0.06	0.57	0.07
FLD3.1	77.21	3.26	14.11	0.70	2.30	0.18	3.39	0.14	1.77	0.09	2.60	0.12	0.29	0.06	0.43	0.07
FLD3.1	73.96	3.12	15.01	0.75	2.64	0.20	3.65	0.15	2.12	0.10	2.86	0.13	0.40	0.06	0.62	0.08
FLD3.1	73.87	3.12	14.56	0.72	2.59	0.20	3.72	0.15	2.22	0.11	3.01	0.13	0.42	0.06	0.69	0.08
FLD3.1	63.50	2.69	20.35	0.99	2.98	0.22	3.55	0.14	2.73	0.12	2.97	0.13	0.40	0.06	0.59	0.08
FLD3.1	71.38	3.02	15.45	0.77	2.60	0.20	3.54	0.14	1.94	0.10	3.02	0.13	0.45	0.06	0.61	0.08
FLD3.1	71.11	3.01	15.78	0.78	3.13	0.23	3.85	0.15	1.68	0.09	2.77	0.12	0.36	0.06	0.55	0.07
FLD3.1	74.66	3.15	14.12	0.70	2.69	0.20	3.96	0.15	1.67	0.09	2.75	0.12	0.30	0.06	0.34	0.06
FLD3.1	75.34	3.18	14.27	0.71	2.44	0.19	3.79	0.15	1.97	0.10	3.05	0.13	0.40	0.06	0.54	0.07
FLD3.1	76.47	3.23	14.28	0.71	2.38	0.19	3.70	0.15	1.66	0.09	2.72	0.12	0.35	0.06	0.57	0.07
FLD3.1	76.97	3.25	13.80	0.69	2.57	0.20	3.56	0.14	1.34	0.08	2.85	0.13	0.33	0.06	0.66	0.08
FLD3.1	73.40	3.10	14.86	0.74	2.68	0.20	3.91	0.15	2.05	0.10	2.83	0.13	0.44	0.06	0.61	0.08
FLD3.1	79.46	3.35	12.15	0.61	2.30	0.18	3.64	0.14	1.58	0.09	2.44	0.11	0.23	0.05	0.46	0.07
FLD3.1	73.53	3.11	14.16	0.71	2.55	0.20	3.61	0.14	2.26	0.11	2.90	0.13	0.39	0.06	0.60	0.08
FLD3.1	75.63	3.19	13.97	0.70	2.75	0.21	3.64	0.14	1.83	0.09	2.42	0.11	0.28	0.06	0.55	0.07
FLD3.1	74.91	3.16	14.39	0.72	2.46	0.19	3.98	0.16	1.32	0.08	2.88	0.13	0.37	0.06	0.60	0.08
FLD3.1	81.49	3.44	11.85	0.60	2.14	0.17	3.36	0.14	0.91	0.07	1.87	0.10	0.24	0.05	0.30	0.06
FLD3.1	75.74	3.20	14.03	0.70	2.63	0.20	3.91	0.15	1.24	0.08	2.79	0.12	0.32	0.06	0.56	0.07
FLD3.1	72.38	3.06	15.19	0.75	2.79	0.21	4.04	0.16	1.77	0.09	2.84	0.13	0.30	0.06	0.62	0.08
FLD3.1	75.19	3.17	14.74	0.73	2.19	0.17	3.30	0.13	1.89	0.10	2.82	0.12	0.35	0.06	0.59	0.08
FLD3.1	75.51	3.19	14.09	0.70	2.26	0.18	3.42	0.14	1.74	0.09	2.70	0.12	0.30	0.06	0.53	0.07
FLD3.1	72.20	3.05	14.41	0.72	2.72	0.21	3.96	0.15	2.20	0.10	3.06	0.13	0.37	0.06	0.55	0.07
FLD3.1	74.75	3.16	14.71	0.73	2.55	0.20	3.87	0.15	2.02	0.10	2.71	0.12	0.36	0.06	0.50	0.07
FLD3.1	72.23	3.05	15.13	0.75	2.62	0.20	3.92	0.15	1.98	0.10	3.31	0.14	0.45	0.06	0.69	0.08
FLD3.1	75.94	3.21	14.80	0.74	2.36	0.18	3.36	0.14	2.07	0.10	2.77	0.12	0.29	0.06	0.52	0.07
FLD3.1	76.48	3.23	14.57	0.73	2.39	0.19	3.65	0.15	1.46	0.08	2.95	0.13	0.32	0.06	0.58	0.08
FLD3.1	75.26	3.18	12.66	0.64	2.57	0.20	3.92	0.15	1.63	0.09	2.14	0.10	0.27	0.05	0.37	0.06
FLD3.1	72.28	3.05	15.35	0.76	2.45	0.19	3.68	0.15	1.65	0.09	3.19	0.14	0.44	0.06	0.61	0.08
FLD3.1	74.15	3.13	15.05	0.75	2.52	0.19	3.83	0.15	1.72	0.09	2.87	0.13	0.37	0.06	0.54	0.07
FLD3.1	78.12	3.30	13.06	0.66	2.49	0.19	3.42	0.14	2.68	0.12	2.55	0.12	0.29	0.06	0.49	0.07
FLD3.1	73.75	3.12	14.19	0.71	2.60	0.20	3.43	0.14	2.31	0.11	2.71	0.12	0.28	0.06	0.52	0.07
FLD3.1	80.32	3.39	13.44	0.67	2.02	0.16	3.33	0.14	0.95	0.07	2.70	0.12	0.35	0.06	0.38	0.07
FLD3.1	68.93	2.92	18.12	0.89	2.48	0.19	3.46	0.14	4.03	0.16	2.55	0.12	0.36	0.06	0.49	0.07

FLD3.1	75.45	3.19	13.36	0.67	2.34	0.18	3.47	0.14	2.64	0.12	2.51	0.12	0.24	0.05	0.40	0.07
FLD3.1	73.84	3.12	13.63	0.68	2.82	0.21	3.98	0.16	2.76	0.12	2.42	0.11	0.28	0.06	0.47	0.07
FLD3.1	76.77	3.24	13.72	0.69	2.16	0.17	3.39	0.14	1.84	0.09	2.92	0.13	0.42	0.06	0.60	0.08
FLD3.1	72.78	3.07	15.15	0.75	2.84	0.21	4.01	0.16	2.27	0.11	3.05	0.13	0.41	0.06	0.63	0.08
FLD3.1	73.72	3.11	15.41	0.76	2.45	0.19	3.66	0.15	1.66	0.09	3.14	0.13	0.46	0.06	0.63	0.08
FLD3.1	73.00	3.08	14.58	0.73	2.45	0.19	3.66	0.15	1.01	0.07	3.09	0.13	0.42	0.06	0.43	0.07
FLD3.1	74.40	3.14	15.38	0.76	3.17	0.23	4.12	0.16	2.18	0.10	2.39	0.11	0.35	0.06	0.56	0.07
FLD3.1	75.28	3.18	14.28	0.71	2.36	0.18	3.91	0.15	0.80	0.06	2.75	0.12	0.36	0.06	0.48	0.07
FLD3.1	74.70	3.15	15.08	0.75	2.56	0.20	3.91	0.15	1.11	0.07	2.80	0.12	0.34	0.06	0.47	0.07
FLD3.1	73.30	3.10	14.61	0.73	2.71	0.21	4.05	0.16	1.08	0.07	2.83	0.12	0.29	0.06	0.42	0.07
FLD3.1	72.90	3.08	15.19	0.75	2.77	0.21	3.68	0.15	1.36	0.08	2.69	0.12	0.49	0.06	0.65	0.08
FLD3.2	71.27	3.01	17.59	0.86	2.43	0.19	3.18	0.13	1.06	0.07	3.32	0.14	0.42	0.06	0.49	0.07
FLD3.2	62.65	2.66	17.95	0.88	3.35	0.24	4.76	0.18	0.88	0.06	6.08	0.23	0.51	0.06	0.48	0.07
FLD3.2	66.24	2.80	22.20	1.08	3.51	0.25	4.43	0.17	0.90	0.07	2.96	0.13	0.34	0.06	0.85	0.09
FLD3.2	68.75	2.91	20.01	0.98	2.53	0.19	3.28	0.13	1.34	0.08	3.11	0.13	0.44	0.06	0.88	0.09
FLD3.2	67.04	2.84	20.18	0.98	4.12	0.29	5.08	0.19	0.59	0.06	3.20	0.14	0.21	0.05	0.30	0.06
FLD3.2	71.67	3.03	16.59	0.82	2.70	0.20	3.38	0.14	0.87	0.06	2.99	0.13	0.37	0.06	0.45	0.07
FLD3.2	64.95	2.75	17.37	0.85	4.30	0.30	5.82	0.21	0.34	0.05	6.80	0.25	0.89	0.07	0.25	0.06
FLD3.2	72.45	3.06	16.22	0.80	2.88	0.22	3.92	0.15	0.67	0.06	3.27	0.14	0.24	0.05	0.25	0.06
FLD3.2	70.74	2.99	17.92	0.88	2.80	0.21	3.74	0.15	0.95	0.07	3.31	0.14	0.40	0.06	0.48	0.07
FLD3.2	73.25	3.09	16.82	0.83	2.28	0.18	3.23	0.13	1.00	0.07	2.99	0.13	0.38	0.06	0.45	0.07
FLD3.2	66.68	2.82	19.31	0.94	2.61	0.20	3.61	0.14	1.15	0.07	3.45	0.14	0.46	0.06	0.51	0.07
FLD3.2	71.55	3.02	16.13	0.80	2.72	0.21	3.81	0.15	0.93	0.07	3.12	0.13	0.39	0.06	0.44	0.07
FLD3.2	72.49	3.06	18.52	0.91	2.54	0.19	3.48	0.14	0.97	0.07	3.20	0.14	0.36	0.06	0.48	0.07
FLD3.2	72.25	3.05	19.12	0.94	1.96	0.16	2.66	0.11	1.33	0.08	3.23	0.14	0.48	0.06	0.64	0.08
FLD3.2	90.74	3.82	3.51	0.21	0.63	0.08	1.20	0.07	0.03	0.04	1.17	0.07	0.03	0.05	0.06	0.05
FLD3.2	69.13	2.92	19.87	0.97	2.75	0.21	3.36	0.14	1.19	0.07	3.39	0.14	0.45	0.06	0.82	0.09
FLD3.2	69.19	2.93	20.04	0.98	2.80	0.21	3.39	0.14	1.19	0.07	3.50	0.15	0.45	0.06	0.57	0.07
FLD3.2	67.49	2.86	19.61	0.96	2.26	0.18	2.94	0.12	1.34	0.08	3.46	0.14	0.46	0.06	0.66	0.08
FLD3.2	81.21	3.42	13.97	0.70	1.87	0.15	2.63	0.11	0.79	0.06	2.60	0.12	0.34	0.06	0.37	0.06
FLD3.2	75.07	3.17	15.53	0.77	4.09	0.29	5.28	0.19	0.13	0.04	3.16	0.14	0.09	0.05	0.06	0.05
FLD3.2	76.04	3.21	14.02	0.70	4.39	0.31	4.97	0.19	0.38	0.05	1.58	0.09	0.03	0.05	0.19	0.06
FLD3.2	69.17	2.93	18.61	0.91	2.46	0.19	3.46	0.14	1.09	0.07	3.50	0.15	0.44	0.06	0.45	0.07
FLD3.2	69.63	2.94	18.66	0.91	2.79	0.21	3.45	0.14	1.10	0.07	3.46	0.14	0.39	0.06	0.48	0.07
FLD3.2	66.63	2.82	21.71	1.06	2.57	0.20	3.17	0.13	1.52	0.08	3.74	0.15	0.52	0.06	0.64	0.08
FLD3.2	69.20	2.93	18.64	0.91	2.36	0.18	3.14	0.13	1.18	0.07	3.88	0.16	0.49	0.06	0.53	0.07
FLD3.2	70.36	2.97	19.17	0.94	2.97	0.22	4.23	0.16	0.92	0.07	3.35	0.14	0.45	0.06	0.36	0.06
FLD3.2	60.39	2.56	15.60	0.77	3.21	0.24	5.48	0.20	0.76	0.06	11.15	0.38	0.17	0.05	0.38	0.06
FLD3.2	102.39	4.30	1.27	0.11	0.03	0.04	0.03	0.03	0.03	0.04	0.09	0.04	0.03	0.05	0.03	0.05
FLD3.2	71.44	3.02	16.43	0.81	2.48	0.19	4.29	0.16	0.62	0.06	3.20	0.14	0.39	0.06	0.31	0.06
FLD3.2	67.18	2.84	20.63	1.01	2.05	0.16	3.31	0.13	1.38	0.08	3.83	0.16	0.54	0.06	0.63	0.08
FLD3.2	75.87	3.20	15.01	0.75	3.59	0.26	5.53	0.20	0.05	0.04	1.69	0.09	0.08	0.05	0.03	0.05
FLD3.2	67.08	2.84	21.64	1.05	1.91	0.16	2.75	0.12	1.64	0.09	3.51	0.15	0.60	0.07	1.07	0.10
FLD3.2	68.54	2.90	16.53	0.82	3.51	0.25	5.47	0.20	0.20	0.04	3.49	0.15	0.31	0.06	0.08	0.05
FLD3.3	74.86	3.16	13.70	0.68	2.53	0.19	3.68	0.15	1.92	0.10	2.67	0.12	0.36	0.06	0.51	0.07
FLD3.3	76.16	3.21	13.54	0.68	2.49	0.19	3.56	0.14	2.19	0.10	2.54	0.12	0.29	0.06	0.41	0.07
FLD3.3	75.06	3.17	14.00	0.70	2.56	0.20	3.73	0.15	1.80	0.09	2.80	0.12	0.34	0.06	0.46	0.07
FLD3.3	73.76	3.12	14.27	0.71	2.62	0.20	3.56	0.14	2.58	0.12	2.70	0.12	0.31	0.06	0.46	0.07
FLD3.3	73.84	3.12	13.75	0.69	2.72	0.21	3.57	0.14	2.60	0.12	2.78	0.12	0.33	0.06	0.50	0.07
FLD3.3	76.82	3.24	13.25	0.66	2.59	0.20	3.80	0.15	1.26	0.08	2.72	0.12	0.27	0.05	0.41	0.07
FLD3.3	75.98	3.21	13.40	0.67	2.45	0.19	3.80	0.15	1.32	0.08	2.77	0.12	0.33	0.06	0.40	0.07
FLD3.3	72.92	3.08	14.63	0.73	2.61	0.20	3.97	0.15	1.69	0.09	3.09	0.13	0.37	0.06	0.55	0.07
FLD3.3	74.88	3.16	13.54	0.68	2.46	0.19	3.66	0.15	1.68	0.09	2.65	0.12	0.31	0.06	0.45	0.07
FLD3.3	75.68	3.19	13.05	0.65	2.46	0.19	3.71	0.15	1.81	0.09	2.67	0.12	0.32	0.06	0.41	0.07
FLD3.3	77.27	3.26	14.39	0.72	2.51	0.19	3.66	0.15	1.94	0.10	2.81	0.12	0.37	0.06	0.48	0.07
FLD3.3	75.43	3.18	13.86	0.69	2.62	0.20	3.69	0.15	2.18	0.10	2.71	0.12	0.33	0.06	0.47	0.07
FLD3.3	76.17	3.22	13.74	0.69	2.58	0.20	3.91	0.15	1.22	0.08	2.82	0.12	0.32	0.06	0.40	0.07
FLD3.3	73.15	3.09	15.11	0.75	2.91	0.22	3.91	0.15	1.53	0.08	3.03	0.13	0.46	0.06	0.64	0.08
FLD3.3	74.37	3.14	14.49	0.72	2.55	0.20	3.76	0.15	1.85	0.09	2.78	0.12	0.38	0.06	0.57	0.07
FLD3.3	72.91	3.08	13.33	0.67	2.37	0.18	3.73	0.15	2.23	0.11	2.68	0.12	0.30	0.06	0.47	0.07
FLD3.3	76.02	3.21	13.85	0.69	2.69	0.20	3.56	0.14	2.33	0.11	2.71	0.12	0.32	0.06	0.50	0.07
FLD3.3	75.17	3.17	14.47	0.72	2.52	0.19	3.77	0.15	1.99	0.10	2.99	0.13	0.35	0.06	0.49	0.07

FLD3.3	75.42	3.18	14.39	0.72	2.59	0.20	3.73	0.15	1.86	0.09	2.75	0.12	0.34	0.06	0.52	0.07
FLD3.3	75.19	3.17	14.11	0.70	2.55	0.20	3.89	0.15	1.68	0.09	2.95	0.13	0.34	0.06	0.52	0.07
FLD3.3	77.80	3.28	13.70	0.68	2.60	0.20	3.70	0.15	1.76	0.09	2.75	0.12	0.30	0.06	0.50	0.07
FLD3.3	75.19	3.17	13.75	0.69	2.72	0.21	3.90	0.15	1.25	0.08	2.68	0.12	0.32	0.06	0.36	0.06
FLD3.3	75.68	3.19	14.03	0.70	2.74	0.21	3.72	0.15	1.80	0.09	2.66	0.12	0.35	0.06	0.52	0.07
FLD3.3	73.74	3.11	15.30	0.76	2.69	0.20	3.60	0.14	2.20	0.10	3.03	0.13	0.36	0.06	0.58	0.08
FLD3.3	75.01	3.17	13.34	0.67	2.47	0.19	3.60	0.14	2.36	0.11	2.61	0.12	0.30	0.06	0.46	0.07
FLD3.3	78.20	3.30	13.39	0.67	2.63	0.20	3.57	0.14	2.07	0.10	2.65	0.12	0.33	0.06	0.41	0.07
FLD3.3	77.55	3.27	13.61	0.68	2.56	0.20	3.79	0.15	1.36	0.08	2.65	0.12	0.35	0.06	0.38	0.06
FLD3.3	75.97	3.21	14.22	0.71	2.58	0.20	3.59	0.14	2.19	0.10	2.68	0.12	0.38	0.06	0.56	0.07
FLD3.3	74.82	3.16	14.54	0.72	2.68	0.20	3.82	0.15	1.76	0.09	2.87	0.13	0.37	0.06	0.55	0.07
FLD3.3	75.34	3.18	14.66	0.73	2.65	0.20	3.80	0.15	1.63	0.09	2.91	0.13	0.35	0.06	0.58	0.08
FLD3.3	74.84	3.16	14.61	0.73	2.92	0.22	3.83	0.15	1.26	0.08	2.82	0.12	0.36	0.06	0.58	0.08
FLD3.3	77.22	3.26	13.42	0.67	2.81	0.21	3.86	0.15	1.18	0.07	2.69	0.12	0.26	0.05	0.30	0.06
FLD3.3	73.63	3.11	14.05	0.70	2.65	0.20	3.72	0.15	2.06	0.10	2.74	0.12	0.35	0.06	0.48	0.07
FLD3.3	75.26	3.18	14.18	0.71	2.74	0.21	3.83	0.15	1.58	0.09	2.82	0.12	0.36	0.06	0.52	0.07
FLD3.3	75.68	3.19	14.30	0.71	2.44	0.19	3.62	0.14	2.19	0.10	2.75	0.12	0.33	0.06	0.45	0.07
FLD3.3	75.79	3.20	14.26	0.71	2.67	0.20	3.72	0.15	1.96	0.10	2.94	0.13	0.37	0.06	0.52	0.07
FLD3.3	74.56	3.15	13.72	0.69	2.65	0.20	3.78	0.15	1.98	0.10	2.68	0.12	0.35	0.06	0.44	0.07
FLD3.3	74.91	3.16	13.80	0.69	2.62	0.20	3.76	0.15	1.78	0.09	2.77	0.12	0.29	0.06	0.48	0.07
FLD3.3	75.06	3.17	13.81	0.69	2.75	0.21	3.83	0.15	1.70	0.09	2.81	0.12	0.31	0.06	0.40	0.07
FLD3.3	74.83	3.16	14.08	0.70	2.57	0.20	3.65	0.14	2.36	0.11	2.74	0.12	0.31	0.06	0.47	0.07
FLD3.3	76.54	3.23	13.47	0.67	2.57	0.20	3.79	0.15	1.62	0.09	2.81	0.12	0.31	0.06	0.44	0.07
FLD3.3	75.13	3.17	14.15	0.71	2.66	0.20	3.59	0.14	2.27	0.11	2.70	0.12	0.29	0.06	0.49	0.07
FLD3.3	73.05	3.09	14.16	0.71	2.68	0.20	3.70	0.15	2.21	0.11	2.83	0.12	0.35	0.06	0.45	0.07
FLD3.3	75.61	3.19	13.78	0.69	2.56	0.20	3.69	0.15	1.81	0.09	2.66	0.12	0.36	0.06	0.47	0.07
FLD3.3	75.29	3.18	14.71	0.73	2.89	0.22	3.69	0.15	2.10	0.10	2.71	0.12	0.35	0.06	0.50	0.07
FLD3.3	77.97	3.29	13.46	0.67	2.52	0.19	3.78	0.15	1.47	0.08	2.80	0.12	0.30	0.06	0.50	0.07
FLD3.3	81.25	3.43	11.09	0.56	2.10	0.17	3.59	0.14	1.12	0.07	2.05	0.10	0.26	0.05	0.29	0.06
FLD3.3	75.45	3.19	14.45	0.72	2.75	0.21	3.71	0.15	2.29	0.11	2.86	0.13	0.38	0.06	0.51	0.07
FLD3.3	77.12	3.25	13.94	0.70	2.76	0.21	3.68	0.15	1.80	0.09	2.79	0.12	0.32	0.06	0.49	0.07
FLD3.3	75.02	3.17	12.88	0.65	2.39	0.19	3.73	0.15	1.84	0.09	2.78	0.12	0.28	0.06	0.43	0.07
FLD3.3	76.91	3.25	13.77	0.69	2.74	0.21	3.82	0.15	1.52	0.08	2.69	0.12	0.35	0.06	0.44	0.07
FLD3.3	75.07	3.17	13.29	0.67	2.34	0.18	3.58	0.14	1.99	0.10	2.76	0.12	0.35	0.06	0.44	0.07
FLD3.3	73.42	3.10	14.55	0.72	2.05	0.16	3.11	0.13	2.17	0.10	2.74	0.12	0.35	0.06	0.53	0.07
FLD3.3	75.10	3.17	15.23	0.76	2.39	0.19	3.32	0.13	1.62	0.09	2.69	0.12	0.32	0.06	0.54	0.07
FLD3.3	78.50	3.31	13.06	0.65	2.40	0.19	3.52	0.14	2.08	0.10	2.46	0.11	0.30	0.06	0.40	0.07
FLD3.3	76.31	3.22	13.67	0.68	2.45	0.19	3.54	0.14	2.44	0.11	2.62	0.12	0.35	0.06	0.42	0.07
FLD3.3	75.64	3.19	13.63	0.68	2.38	0.18	3.58	0.14	2.39	0.11	2.62	0.12	0.32	0.06	0.45	0.07
FLD3.3	77.01	3.25	13.93	0.70	2.53	0.19	3.63	0.14	2.16	0.10	2.83	0.12	0.27	0.05	0.46	0.07
FLD3.3	75.42	3.18	14.99	0.74	2.06	0.17	2.99	0.12	2.31	0.11	2.81	0.12	0.33	0.06	0.54	0.07
FLD3.3	75.02	3.17	13.40	0.67	2.51	0.19	3.54	0.14	2.82	0.12	2.63	0.12	0.30	0.06	0.42	0.07
FLD3.3	76.45	3.23	13.62	0.68	2.31	0.18	3.36	0.14	2.48	0.11	2.85	0.13	0.27	0.05	0.42	0.07
FLD3.3	76.92	3.25	13.77	0.69	2.01	0.16	3.12	0.13	2.39	0.11	2.74	0.12	0.29	0.06	0.42	0.07
FLD4.1	72.53	3.06	13.31	0.67	2.62	0.20	3.49	0.14	2.41	0.11	2.66	0.12	0.36	0.06	0.56	0.07
FLD4.1	75.31	3.18	13.11	0.66	2.96	0.22	3.51	0.14	2.81	0.12	2.31	0.11	0.26	0.05	0.41	0.07
FLD4.1	73.63	3.11	13.06	0.66	2.66	0.20	3.18	0.13	3.16	0.13	2.31	0.11	0.25	0.05	0.40	0.07
FLD4.1	74.37	3.14	13.40	0.67	2.57	0.20	3.03	0.13	3.13	0.13	2.50	0.11	0.25	0.05	0.39	0.07
FLD4.1	71.75	3.03	13.47	0.67	2.82	0.21	3.60	0.14	2.57	0.12	2.44	0.11	0.36	0.06	0.53	0.07
FLD4.1	71.45	3.02	13.42	0.67	2.83	0.21	3.53	0.14	2.50	0.11	2.60	0.12	0.32	0.06	0.49	0.07
FLD4.1	73.06	3.09	13.65	0.68	2.98	0.22	3.44	0.14	2.47	0.11	2.63	0.12	0.35	0.06	0.57	0.07
FLD4.1	71.26	3.01	13.40	0.67	2.87	0.22	3.44	0.14	2.55	0.12	2.73	0.12	0.33	0.06	0.56	0.07
FLD4.1	70.45	2.98	13.49	0.67	2.87	0.22	3.49	0.14	2.49	0.11	2.80	0.12	0.38	0.06	0.53	0.07
FLD4.1	72.54	3.06	13.87	0.69	2.83	0.21	3.54	0.14	2.25	0.11	2.89	0.13	0.37	0.06	0.58	0.08
FLD4.1	73.96	3.12	13.36	0.67	2.73	0.21	3.49	0.14	2.14	0.10	2.51	0.12	0.31	0.06	0.57	0.07
FLD4.1	72.07	3.05	13.35	0.67	2.75	0.21	3.43	0.14	2.56	0.12	2.62	0.12	0.34	0.06	0.53	0.07
FLD4.1	72.74	3.07	13.30	0.67	2.67	0.20	3.48	0.14	2.60	0.12	2.53	0.12	0.33	0.06	0.56	0.07
FLD4.1	72.27	3.05	13.20	0.66	2.80	0.21	3.38	0.14	2.48	0.11	2.66	0.12	0.32	0.06	0.53	0.07
FLD4.1	71.00	3.00	13.22	0.66	2.87	0.22	3.55	0.14	2.43	0.11	2.74	0.12	0.50	0.06	0.53	0.07
FLD4.1	73.16	3.09	13.24	0.66	2.66	0.20	3.40	0.14	2.58	0.12	2.59	0.12	0.33	0.06	0.49	0.07
FLD4.1	73.77	3.12	13.39	0.67	2.73	0.21	3.49	0.14	2.24	0.11	2.47	0.11	0.26	0.05	0.42	0.07
FLD4.1	74.05	3.13	12.88	0.65	2.65	0.20	3.44	0.14	2.32	0.11	2.54	0.12	0.36	0.06	0.46	0.07

FLD4.1	73.46	3.10	13.75	0.69	2.72	0.21	3.52	0.14	2.29	0.11	2.61	0.12	0.35	0.06	0.55	0.07
FLD4.1	72.71	3.07	14.31	0.71	2.75	0.21	3.41	0.14	2.42	0.11	2.57	0.12	0.35	0.06	0.57	0.07
FLD4.1	74.12	3.13	13.05	0.65	2.81	0.21	3.52	0.14	2.58	0.12	2.53	0.12	0.29	0.06	0.48	0.07
FLD4.1	72.24	3.05	13.18	0.66	2.71	0.20	3.44	0.14	2.37	0.11	2.67	0.12	0.29	0.06	0.54	0.07
FLD4.1	73.12	3.09	12.99	0.65	2.75	0.21	3.38	0.14	2.46	0.11	2.65	0.12	0.35	0.06	0.50	0.07
FLD4.1	74.25	3.14	14.21	0.71	2.75	0.21	3.41	0.14	2.30	0.11	2.76	0.12	0.36	0.06	0.61	0.08
FLD4.1	73.57	3.11	12.87	0.65	2.65	0.20	3.53	0.14	2.30	0.11	2.55	0.12	0.31	0.06	0.47	0.07
FLD4.1	73.47	3.10	13.20	0.66	2.60	0.20	3.40	0.14	2.55	0.12	2.59	0.12	0.32	0.06	0.48	0.07
FLD4.1	72.53	3.06	13.33	0.67	2.56	0.20	3.44	0.14	2.33	0.11	2.57	0.12	0.32	0.06	0.52	0.07
FLD4.1	73.84	3.12	13.23	0.66	2.76	0.21	3.60	0.14	2.30	0.11	2.64	0.12	0.30	0.06	0.48	0.07
FLD4.1	73.65	3.11	14.25	0.71	2.86	0.21	3.39	0.14	2.39	0.11	2.60	0.12	0.35	0.06	0.55	0.07
FLD4.1	72.19	3.05	13.22	0.66	2.66	0.20	3.45	0.14	2.59	0.12	2.66	0.12	0.34	0.06	0.53	0.07
FLD4.1	72.30	3.05	12.73	0.64	2.71	0.21	3.46	0.14	2.52	0.11	2.51	0.12	0.26	0.05	0.50	0.07
FLD4.1	72.60	3.07	13.42	0.67	2.65	0.20	3.50	0.14	2.52	0.11	2.68	0.12	0.30	0.06	0.50	0.07
FLD4.1	73.44	3.10	13.39	0.67	2.59	0.20	3.49	0.14	2.28	0.11	2.66	0.12	0.34	0.06	0.54	0.07
FLD4.1	74.54	3.15	13.75	0.69	2.74	0.21	3.60	0.14	2.17	0.10	2.44	0.11	0.22	0.05	0.38	0.06
FLD4.1	73.44	3.10	13.50	0.68	2.66	0.20	3.51	0.14	2.12	0.10	2.72	0.12	0.32	0.06	0.51	0.07
FLD4.1	72.98	3.08	13.26	0.66	2.61	0.20	3.43	0.14	2.43	0.11	2.63	0.12	0.33	0.06	0.45	0.07
FLD4.1	72.33	3.06	13.18	0.66	2.57	0.20	3.43	0.14	2.44	0.11	2.60	0.12	0.32	0.06	0.51	0.07
FLD4.1	71.03	3.00	14.37	0.72	2.74	0.21	3.57	0.14	2.45	0.11	2.70	0.12	0.37	0.06	0.60	0.08
FLD4.1	71.71	3.03	13.62	0.68	2.74	0.21	3.50	0.14	2.53	0.11	2.71	0.12	0.33	0.06	0.56	0.07
FLD4.1	73.74	3.11	13.47	0.67	2.78	0.21	3.47	0.14	2.35	0.11	2.41	0.11	0.33	0.06	0.52	0.07
FLD4.1	71.87	3.04	13.33	0.67	2.86	0.21	3.51	0.14	2.40	0.11	2.53	0.12	0.36	0.06	0.52	0.07
FLD4.1	73.47	3.10	13.61	0.68	2.66	0.20	3.49	0.14	2.45	0.11	2.67	0.12	0.31	0.06	0.50	0.07
FLD4.1	74.72	3.16	13.76	0.69	2.56	0.20	3.47	0.14	2.36	0.11	2.65	0.12	0.31	0.06	0.49	0.07
FLD4.1	73.50	3.10	13.29	0.67	2.62	0.20	3.44	0.14	2.39	0.11	2.65	0.12	0.32	0.06	0.49	0.07
FLD4.1	74.12	3.13	12.91	0.65	2.49	0.19	3.39	0.14	2.50	0.11	2.54	0.12	0.32	0.06	0.49	0.07
FLD4.1	75.41	3.18	13.28	0.67	2.65	0.20	3.31	0.13	2.39	0.11	2.58	0.12	0.32	0.06	0.51	0.07
FLD4.1	72.79	3.08	13.59	0.68	2.72	0.21	3.57	0.14	2.40	0.11	2.48	0.11	0.31	0.06	0.55	0.07
FLD4.1	73.62	3.11	13.66	0.68	2.77	0.21	3.55	0.14	2.41	0.11	2.64	0.12	0.29	0.06	0.57	0.07
FLD4.1	71.98	3.04	13.69	0.68	2.73	0.21	3.61	0.14	2.31	0.11	2.73	0.12	0.33	0.06	0.54	0.07
FLD4.1	73.17	3.09	13.09	0.66	2.62	0.20	3.43	0.14	2.60	0.12	2.47	0.11	0.28	0.05	0.46	0.07
FLD4.1	73.51	3.11	12.99	0.65	2.68	0.20	3.41	0.14	2.51	0.11	2.56	0.12	0.34	0.06	0.54	0.07
FLD4.1	73.31	3.10	13.43	0.67	2.44	0.19	3.46	0.14	2.52	0.11	2.66	0.12	0.34	0.06	0.49	0.07
FLD4.1	72.88	3.08	14.10	0.70	2.77	0.21	3.58	0.14	2.63	0.12	2.55	0.12	0.34	0.06	0.60	0.08
FLD4.1	75.50	3.19	13.48	0.67	2.60	0.20	3.34	0.14	2.95	0.13	2.51	0.12	0.31	0.06	0.54	0.07
FLD4.1	73.88	3.12	13.70	0.68	2.68	0.20	3.42	0.14	2.66	0.12	2.57	0.12	0.35	0.06	0.51	0.07
FLD4.1	75.56	3.19	12.45	0.63	2.41	0.19	3.32	0.13	1.82	0.09	2.41	0.11	0.31	0.06	0.49	0.07
FLD4.1	75.35	3.18	13.29	0.67	2.72	0.21	3.54	0.14	2.37	0.11	2.52	0.12	0.27	0.05	0.51	0.07
FLD4.1	74.48	3.15	12.71	0.64	2.70	0.20	3.42	0.14	2.42	0.11	2.45	0.11	0.25	0.05	0.45	0.07
FLD4.1	74.64	3.15	13.69	0.68	2.48	0.19	3.50	0.14	2.54	0.12	2.68	0.12	0.37	0.06	0.54	0.07
FLD4.1	73.67	3.11	14.26	0.71	2.78	0.21	3.51	0.14	2.53	0.11	2.72	0.12	0.33	0.06	0.55	0.07
FLD4.1	74.07	3.13	13.56	0.68	2.64	0.20	3.51	0.14	2.44	0.11	2.74	0.12	0.32	0.06	0.55	0.07
FLD4.1	76.24	3.22	12.35	0.62	2.66	0.20	3.41	0.14	2.63	0.12	2.49	0.11	0.23	0.05	0.49	0.07
FLD4.1	74.16	3.13	13.32	0.67	2.61	0.20	3.31	0.13	2.15	0.10	2.36	0.11	0.31	0.06	0.52	0.07
FLD4.1	88.13	3.71	7.59	0.40	1.82	0.15	2.45	0.11	1.22	0.08	1.57	0.09	0.18	0.05	0.28	0.06
FLD4.1	74.98	3.17	13.23	0.66	2.70	0.20	3.45	0.14	2.52	0.11	2.60	0.12	0.33	0.06	0.56	0.07
FLD4.1	71.18	3.01	13.69	0.68	2.64	0.20	3.46	0.14	2.58	0.12	2.64	0.12	0.36	0.06	0.59	0.08
FLD4.1	72.50	3.06	13.52	0.68	2.51	0.19	3.51	0.14	2.71	0.12	2.66	0.12	0.34	0.06	0.55	0.07
FLD4.1	74.49	3.15	14.06	0.70	2.62	0.20	3.46	0.14	2.56	0.12	2.56	0.12	0.31	0.06	0.56	0.07
FLD4.1	74.22	3.13	13.59	0.68	2.68	0.20	3.44	0.14	2.48	0.11	2.53	0.12	0.29	0.06	0.50	0.07
FLD4.2	72.63	3.07	14.06	0.70	2.11	0.17	3.41	0.14	1.97	0.10	2.61	0.12	0.32	0.06	0.44	0.07
FLD4.2	71.93	3.04	14.21	0.71	2.44	0.19	3.52	0.14	1.82	0.09	2.66	0.12	0.34	0.06	0.52	0.07
FLD4.2	72.65	3.07	12.72	0.64	2.24	0.18	3.47	0.14	1.73	0.09	2.49	0.11	0.33	0.06	0.42	0.07
FLD4.2	69.64	2.94	15.39	0.76	2.52	0.19	3.47	0.14	1.93	0.10	2.66	0.12	0.31	0.06	0.45	0.07
FLD4.2	71.42	3.02	15.23	0.76	2.51	0.19	3.33	0.14	1.87	0.09	2.49	0.11	0.29	0.06	0.47	0.07
FLD4.2	70.98	3.00	14.67	0.73	2.15	0.17	3.25	0.13	1.97	0.10	2.94	0.13	0.40	0.06	0.69	0.08
FLD4.2	73.87	3.12	13.46	0.67	2.26	0.18	3.36	0.14	1.61	0.09	2.59	0.12	0.30	0.06	0.46	0.07
FLD4.2	70.48	2.98	14.75	0.73	2.36	0.18	3.49	0.14	1.75	0.09	2.50	0.11	0.32	0.06	0.40	0.07
FLD4.2	73.90	3.12	13.17	0.66	2.14	0.17	3.42	0.14	1.35	0.08	2.17	0.10	0.24	0.05	0.39	0.07
FLD4.2	80.87	3.41	11.02	0.56	1.98	0.16	3.06	0.13	1.15	0.07	1.86	0.10	0.22	0.05	0.30	0.06
FLD4.2	70.59	2.98	15.45	0.77	2.48	0.19	3.51	0.14	1.85	0.09	2.45	0.11	0.31	0.06	0.45	0.07

FLD4.2	71.05	3.00	15.61	0.77	2.49	0.19	3.43	0.14	1.93	0.10	2.58	0.12	0.31	0.06	0.48	0.07
FLD4.2	73.88	3.12	13.31	0.67	2.23	0.18	3.45	0.14	1.66	0.09	2.56	0.12	0.28	0.05	0.45	0.07
FLD4.2	81.71	3.44	9.42	0.49	1.72	0.14	2.80	0.12	1.03	0.07	1.95	0.10	0.21	0.05	0.29	0.06
FLD4.2	68.14	2.88	17.17	0.85	2.54	0.19	3.58	0.14	2.11	0.10	2.55	0.12	0.32	0.06	0.44	0.07
FLD4.2	71.53	3.02	15.84	0.78	2.57	0.20	3.67	0.15	1.71	0.09	2.52	0.12	0.31	0.06	0.46	0.07
FLD4.2	69.63	2.94	15.31	0.76	2.40	0.19	3.42	0.14	2.16	0.10	2.61	0.12	0.36	0.06	0.48	0.07
FLD4.2	79.94	3.37	12.91	0.65	2.09	0.17	3.48	0.14	1.10	0.07	2.11	0.10	0.22	0.05	0.37	0.06
FLD4.2	69.93	2.96	15.38	0.76	2.40	0.19	3.44	0.14	1.88	0.10	2.60	0.12	0.36	0.06	0.46	0.07
FLD4.2	81.49	3.44	9.01	0.47	1.71	0.14	3.10	0.13	0.69	0.06	1.75	0.09	0.18	0.05	0.19	0.05
FLD4.2	71.80	3.03	15.47	0.77	2.49	0.19	3.54	0.14	1.82	0.09	2.54	0.12	0.29	0.06	0.42	0.07
FLD4.2	84.28	3.55	8.05	0.42	1.50	0.13	2.91	0.12	0.86	0.06	1.58	0.09	0.15	0.05	0.18	0.05
FLD4.2	71.00	3.00	14.53	0.72	2.49	0.19	3.72	0.15	1.31	0.08	2.42	0.11	0.28	0.05	0.33	0.06
FLD4.2	81.20	3.42	12.87	0.65	2.18	0.17	3.36	0.14	1.22	0.08	2.12	0.10	0.21	0.05	0.35	0.06
FLD4.2	71.31	3.01	14.65	0.73	2.25	0.18	3.62	0.14	1.54	0.08	2.52	0.12	0.34	0.06	0.39	0.07
FLD4.2	73.33	3.10	15.71	0.78	2.31	0.18	3.36	0.14	1.73	0.09	2.46	0.11	0.32	0.06	0.44	0.07
FLD4.2	75.31	3.18	13.36	0.67	2.26	0.18	3.50	0.14	1.32	0.08	2.44	0.11	0.31	0.06	0.40	0.07
FLD4.2	80.46	3.39	11.39	0.58	2.07	0.17	3.05	0.13	1.05	0.07	1.82	0.09	0.20	0.05	0.24	0.06
FLD4.2	70.38	2.98	15.84	0.78	2.39	0.19	3.34	0.14	2.12	0.10	2.70	0.12	0.35	0.06	0.51	0.07
FLD4.2	77.80	3.28	12.22	0.62	2.06	0.17	3.35	0.14	1.84	0.09	2.46	0.11	0.25	0.05	0.34	0.06
FLD4.2	74.10	3.13	14.65	0.73	2.28	0.18	3.46	0.14	1.69	0.09	2.64	0.12	0.34	0.06	0.47	0.07
FLD4.2	70.97	3.00	15.76	0.78	2.39	0.19	3.53	0.14	2.00	0.10	2.61	0.12	0.33	0.06	0.48	0.07
FLD4.2	71.40	3.02	15.81	0.78	2.47	0.19	3.46	0.14	1.71	0.09	2.42	0.11	0.28	0.06	0.39	0.07
FLD4.2	73.99	3.13	14.55	0.72	2.47	0.19	3.65	0.15	1.23	0.08	2.38	0.11	0.26	0.05	0.59	0.08
FLD4.2	70.01	2.96	17.09	0.84	2.51	0.19	3.37	0.14	2.11	0.10	2.59	0.12	0.31	0.06	0.51	0.07
FLD4.2	74.14	3.13	13.90	0.69	2.13	0.17	3.37	0.14	2.03	0.10	2.61	0.12	0.29	0.06	0.48	0.07
FLD4.2	75.17	3.17	13.59	0.68	2.16	0.17	3.32	0.13	1.80	0.09	2.48	0.11	0.31	0.06	0.53	0.07
FLD4.2	70.58	2.98	16.09	0.80	2.36	0.18	3.39	0.14	2.08	0.10	2.82	0.12	0.32	0.06	0.51	0.07
FLD4.2	71.08	3.00	15.63	0.77	2.36	0.18	3.44	0.14	1.83	0.09	2.66	0.12	0.27	0.05	0.41	0.07
FLD4.2	75.02	3.17	13.66	0.68	2.09	0.17	3.40	0.14	1.54	0.08	2.37	0.11	0.27	0.05	0.38	0.06
FLD4.2	77.71	3.28	11.89	0.60	1.87	0.15	3.26	0.13	1.33	0.08	2.46	0.11	0.28	0.06	0.38	0.07
FLD4.2	75.90	3.20	13.87	0.69	2.23	0.18	3.59	0.14	1.44	0.08	2.37	0.11	0.30	0.06	0.41	0.07
FLD4.2	73.80	3.12	14.39	0.72	2.25	0.18	3.59	0.14	1.53	0.08	2.34	0.11	0.29	0.06	0.40	0.07
FLD4.2	70.02	2.96	15.88	0.79	2.36	0.18	3.50	0.14	1.85	0.09	2.56	0.12	0.31	0.06	0.39	0.07
FLD4.2	70.00	2.96	16.30	0.81	2.38	0.18	3.49	0.14	2.09	0.10	2.74	0.12	0.34	0.06	0.49	0.07
FLD4.2	70.75	2.99	16.49	0.81	2.38	0.19	3.27	0.13	2.26	0.11	2.51	0.12	0.32	0.06	0.46	0.07
FLD4.2	75.33	3.18	14.27	0.71	2.14	0.17	3.36	0.14	1.59	0.09	2.64	0.12	0.37	0.06	0.50	0.07
FLD4.2	73.19	3.09	13.90	0.69	2.20	0.17	3.34	0.14	1.87	0.09	2.64	0.12	0.32	0.06	0.43	0.07
FLD4.2	71.24	3.01	16.13	0.80	2.43	0.19	3.23	0.13	2.15	0.10	2.61	0.12	0.29	0.06	0.46	0.07
FLD4.3	70.14	2.97	12.94	0.65	3.32	0.24	4.30	0.17	1.75	0.09	3.00	0.13	0.37	0.06	0.53	0.07
FLD4.3	71.63	3.03	13.14	0.66	3.45	0.25	4.24	0.16	1.45	0.08	2.92	0.13	0.29	0.06	0.92	0.09
FLD4.3	68.82	2.91	13.92	0.69	3.74	0.27	4.41	0.17	1.92	0.10	3.38	0.14	0.43	0.06	1.19	0.11
FLD4.3	74.38	3.14	12.64	0.64	2.85	0.21	3.58	0.14	2.66	0.12	3.07	0.13	0.40	0.06	0.96	0.10
FLD4.3	71.46	3.02	14.15	0.71	3.66	0.26	4.12	0.16	2.05	0.10	3.28	0.14	0.43	0.06	0.95	0.09
FLD4.3	61.60	2.61	20.64	1.01	3.34	0.24	3.29	0.13	4.19	0.16	3.68	0.15	0.47	0.06	1.05	0.10
FLD4.3	70.24	2.97	14.07	0.70	3.30	0.24	4.00	0.16	1.82	0.09	3.21	0.14	0.40	0.06	0.96	0.10
FLD4.3	71.78	3.03	14.14	0.70	3.39	0.25	4.06	0.16	1.96	0.10	3.10	0.13	0.35	0.06	0.84	0.09
FLD4.3	71.37	3.02	13.88	0.69	3.80	0.27	4.00	0.16	0.92	0.07	3.24	0.14	0.34	0.06	0.69	0.08
FLD4.3	72.68	3.07	12.60	0.63	1.64	0.14	4.12	0.16	1.10	0.07	3.16	0.14	0.35	0.06	0.43	0.07
FLD4.3	72.73	3.07	14.48	0.72	3.36	0.25	3.90	0.15	1.67	0.09	2.95	0.13	0.34	0.06	0.89	0.09
FLD4.3	71.88	3.04	14.05	0.70	3.23	0.24	4.13	0.16	2.09	0.10	2.86	0.13	0.34	0.06	0.92	0.09
FLD4.3	71.69	3.03	13.45	0.67	3.31	0.24	3.89	0.15	1.16	0.07	2.79	0.12	0.33	0.06	0.71	0.08
FLD4.3	73.02	3.08	12.58	0.63	3.35	0.24	3.82	0.15	1.31	0.08	3.29	0.14	0.25	0.05	0.70	0.08
FLD4.3	65.72	2.78	18.60	0.91	4.24	0.30	4.24	0.16	3.41	0.14	2.94	0.13	0.32	0.06	1.14	0.10
FLD4.3	70.65	2.99	14.71	0.73	1.74	0.15	4.09	0.16	1.89	0.10	3.43	0.14	0.60	0.07	0.97	0.10
FLD4.3	72.87	3.08	14.34	0.71	3.18	0.23	4.05	0.16	1.90	0.10	3.19	0.14	0.39	0.06	0.86	0.09
FLD4.3	72.64	3.07	13.78	0.69	3.05	0.23	4.02	0.16	1.78	0.09	2.91	0.13	0.29	0.06	0.64	0.08
FLD4.3	71.00	3.00	14.81	0.74	3.26	0.24	3.92	0.15	2.02	0.10	3.02	0.13	0.43	0.06	0.86	0.09
FLD4.3	68.65	2.90	16.26	0.80	3.38	0.25	4.01	0.16	2.51	0.11	3.00	0.13	0.41	0.06	0.96	0.10
FLD4.3	71.68	3.03	15.02	0.75	3.41	0.25	3.98	0.16	1.41	0.08	3.34	0.14	0.49	0.06	0.87	0.09
FLD4.3	70.17	2.97	13.93	0.70	3.55	0.26	4.11	0.16	1.74	0.09	3.50	0.15	0.32	0.06	0.84	0.09
FLD4.3	72.46	3.06	13.93	0.70	3.26	0.24	3.94	0.15	1.65	0.09	3.07	0.13	0.37	0.06	0.94	0.09
FLD4.3	71.89	3.04	14.61	0.73	3.68	0.27	4.19	0.16	1.58	0.09	2.90	0.13	0.42	0.06	1.06	0.10

FLD4.3	77.05	3.25	11.50	0.58	2.74	0.21	3.69	0.15	1.11	0.07	2.89	0.13	0.32	0.06	0.53	0.07
FLD4.3	72.24	3.05	13.57	0.68	2.84	0.21	3.58	0.14	2.11	0.10	3.00	0.13	0.32	0.06	0.69	0.08
FLD4.3	73.74	3.11	12.76	0.64	3.04	0.23	3.95	0.15	1.53	0.08	2.96	0.13	0.34	0.06	0.63	0.08
FLD4.3	72.28	3.05	14.53	0.72	3.32	0.24	3.99	0.16	1.88	0.10	2.99	0.13	0.31	0.06	0.88	0.09
FLD4.3	72.14	3.05	15.05	0.75	3.48	0.25	3.90	0.15	1.47	0.08	3.29	0.14	0.38	0.06	1.01	0.10
FLD4.3	78.97	3.33	10.15	0.52	2.90	0.22	3.60	0.14	0.59	0.06	2.16	0.10	0.30	0.06	0.69	0.08
FLD4.3	71.79	3.03	14.29	0.71	3.14	0.23	3.92	0.15	1.40	0.08	3.01	0.13	0.39	0.06	0.93	0.09
FLD4.3	70.29	2.97	14.75	0.73	3.79	0.27	4.18	0.16	2.26	0.11	3.17	0.14	0.42	0.06	1.02	0.10
FLD4.3	72.56	3.07	13.28	0.67	3.02	0.22	3.97	0.16	1.80	0.09	2.69	0.12	0.32	0.06	0.78	0.09
FLD4.3	70.74	2.99	14.96	0.74	3.62	0.26	4.31	0.17	1.74	0.09	3.17	0.14	0.44	0.06	0.94	0.09
FLD4.3	72.14	3.05	15.07	0.75	3.28	0.24	3.94	0.15	1.97	0.10	3.38	0.14	0.48	0.06	0.98	0.10
FLD4.3	71.99	3.04	14.58	0.73	3.31	0.24	3.98	0.16	1.95	0.10	3.31	0.14	0.48	0.06	0.96	0.10
FLD4.3	72.51	3.06	13.40	0.67	3.45	0.25	4.05	0.16	0.91	0.07	3.14	0.13	0.32	0.06	0.69	0.08
FLD4.3	69.75	2.95	13.99	0.70	3.08	0.23	3.94	0.15	1.53	0.08	3.55	0.15	0.43	0.06	0.94	0.09
FLD4.3	72.59	3.07	13.65	0.68	3.06	0.23	3.85	0.15	1.08	0.07	2.81	0.12	0.32	0.06	0.77	0.09
FLD4.3	71.02	3.00	14.15	0.71	3.34	0.24	4.11	0.16	1.83	0.09	2.94	0.13	0.41	0.06	0.90	0.09
FLD4.3	73.38	3.10	12.68	0.64	3.04	0.23	3.84	0.15	1.81	0.09	3.01	0.13	0.37	0.06	0.53	0.07
FLD4.3	69.20	2.93	15.22	0.75	3.34	0.24	4.04	0.16	1.43	0.08	3.50	0.15	0.58	0.06	0.89	0.09
FLD4.3	73.98	3.12	11.03	0.56	2.82	0.21	3.90	0.15	0.78	0.06	3.28	0.14	0.23	0.05	0.21	0.06
FLD4.3	75.47	3.19	12.40	0.62	3.55	0.26	4.20	0.16	0.38	0.05	2.82	0.12	0.15	0.05	0.12	0.05
FLD4.3	70.60	2.98	15.03	0.75	3.32	0.24	4.01	0.16	1.63	0.09	3.69	0.15	0.49	0.06	1.01	0.10
FLD4.3	70.38	2.98	14.52	0.72	3.28	0.24	4.15	0.16	1.74	0.09	2.82	0.12	0.42	0.06	0.83	0.09
FLD4.3	70.35	2.97	13.63	0.68	3.06	0.23	3.90	0.15	1.92	0.10	3.18	0.14	0.36	0.06	0.93	0.09
FLD4.3	71.68	3.03	14.55	0.72	3.31	0.24	4.14	0.16	1.56	0.09	2.88	0.13	0.35	0.06	0.86	0.09
FLD4.3	71.69	3.03	13.31	0.67	3.47	0.25	4.18	0.16	1.16	0.07	3.04	0.13	0.43	0.06	0.53	0.07
FLD4.3	72.33	3.06	12.85	0.65	3.27	0.24	4.03	0.16	0.86	0.06	3.06	0.13	0.27	0.05	0.35	0.06
FLD4.3	72.33	3.06	14.24	0.71	2.24	0.18	4.10	0.16	1.55	0.09	2.92	0.13	0.34	0.06	0.83	0.09
FLD4.3	72.50	3.06	14.06	0.70	1.91	0.16	4.22	0.16	1.70	0.09	2.95	0.13	0.41	0.06	0.93	0.09
FLD4.3	71.92	3.04	13.96	0.70	3.45	0.25	4.25	0.16	1.94	0.10	3.58	0.15	0.44	0.06	0.94	0.09
FLD4.3	72.11	3.05	15.44	0.76	3.73	0.27	4.13	0.16	2.06	0.10	3.38	0.14	0.35	0.06	1.05	0.10
FLD4.3	73.58	3.11	14.45	0.72	3.33	0.24	4.08	0.16	1.45	0.08	3.18	0.14	0.49	0.06	1.08	0.10
FLD4.4	71.22	3.01	15.97	0.79	2.38	0.18	2.98	0.12	2.32	0.11	2.86	0.13	0.48	0.06	0.84	0.09
FLD4.4	71.37	3.02	15.90	0.79	2.31	0.18	2.82	0.12	2.08	0.10	2.89	0.13	0.38	0.06	0.86	0.09
FLD4.4	74.91	3.16	12.57	0.63	2.38	0.18	3.13	0.13	1.93	0.10	2.85	0.13	0.33	0.06	0.83	0.09
FLD4.4	74.28	3.14	13.86	0.69	2.51	0.19	3.34	0.14	1.89	0.10	2.78	0.12	0.31	0.06	0.87	0.09
FLD4.4	76.01	3.21	12.30	0.62	2.48	0.19	3.37	0.14	2.63	0.12	2.81	0.12	0.32	0.06	0.99	0.10
FLD4.4	72.21	3.05	14.10	0.70	2.62	0.20	3.51	0.14	2.44	0.11	2.90	0.13	0.41	0.06	0.96	0.10
FLD4.4	73.62	3.11	13.70	0.68	2.51	0.19	3.33	0.14	2.14	0.10	2.98	0.13	0.32	0.06	0.92	0.09
FLD4.4	75.07	3.17	12.41	0.62	2.37	0.18	3.32	0.14	1.71	0.09	2.98	0.13	0.35	0.06	0.82	0.09
FLD4.4	74.29	3.14	13.41	0.67	2.43	0.19	3.16	0.13	1.97	0.10	2.98	0.13	0.35	0.06	0.80	0.09
FLD4.4	72.94	3.08	14.19	0.71	2.46	0.19	3.28	0.13	2.21	0.11	3.20	0.14	0.39	0.06	1.03	0.10
FLD4.4	73.46	3.10	14.82	0.74	2.57	0.20	3.32	0.13	2.16	0.10	3.30	0.14	0.43	0.06	1.00	0.10
FLD4.4	75.42	3.18	14.69	0.73	2.78	0.21	3.46	0.14	2.16	0.10	2.88	0.13	0.33	0.06	0.91	0.09
FLD4.4	76.35	3.22	12.07	0.61	2.46	0.19	3.38	0.14	2.15	0.10	2.61	0.12	0.37	0.06	0.93	0.09
FLD4.4	72.22	3.05	14.36	0.72	2.60	0.20	3.31	0.13	2.31	0.11	3.27	0.14	0.43	0.06	0.98	0.10
FLD4.4	72.94	3.08	13.88	0.69	2.58	0.20	3.37	0.14	2.16	0.10	3.03	0.13	0.39	0.06	0.94	0.09
FLD4.4	72.19	3.05	14.01	0.70	2.58	0.20	3.44	0.14	2.17	0.10	3.02	0.13	0.41	0.06	0.91	0.09
FLD4.4	80.51	3.40	9.56	0.49	2.11	0.17	3.05	0.13	1.53	0.08	2.47	0.11	0.26	0.05	0.46	0.07
FLD4.4	73.82	3.12	13.73	0.69	2.68	0.20	3.44	0.14	2.20	0.10	2.90	0.13	0.35	0.06	0.95	0.09
FLD4.4	70.26	2.97	16.87	0.83	2.52	0.19	3.27	0.13	2.59	0.12	3.27	0.14	0.41	0.06	0.93	0.09
FLD4.4	68.04	2.88	16.85	0.83	3.21	0.24	3.56	0.14	2.27	0.11	3.08	0.13	0.39	0.06	0.59	0.08
FLD4.4	72.97	3.08	12.68	0.64	2.70	0.20	3.61	0.14	2.20	0.10	3.13	0.13	0.31	0.06	0.98	0.10
FLD4.4	74.58	3.15	13.89	0.69	2.75	0.21	3.57	0.14	2.71	0.12	2.87	0.13	0.48	0.06	1.10	0.10
FLD4.4	73.46	3.10	13.27	0.66	2.65	0.20	3.49	0.14	2.55	0.12	2.86	0.13	0.40	0.06	0.98	0.10
FLD4.4	74.05	3.13	13.66	0.68	2.70	0.20	3.47	0.14	2.21	0.11	2.92	0.13	0.40	0.06	1.01	0.10
FLD4.4	75.12	3.17	11.08	0.56	2.20	0.17	3.22	0.13	1.89	0.10	2.47	0.11	0.25	0.05	0.57	0.08
FLD4.4	75.42	3.18	13.92	0.69	2.66	0.20	3.27	0.13	2.31	0.11	2.85	0.13	0.39	0.06	0.97	0.10
FLD4.4	77.26	3.26	11.82	0.60	2.35	0.18	3.18	0.13	1.87	0.09	2.69	0.12	0.27	0.05	0.71	0.08
FLD4.4	84.76	3.57	8.03	0.42	1.86	0.15	2.76	0.12	1.10	0.07	2.37	0.11	0.21	0.05	0.34	0.06
FLD4.4	67.93	2.87	19.94	0.97	2.62	0.20	2.97	0.12	3.26	0.14	3.31	0.14	0.41	0.06	0.94	0.09
FLD4.4	76.40	3.22	13.09	0.66	2.74	0.21	3.53	0.14	1.57	0.09	2.32	0.11	0.26	0.05	0.38	0.06
FLD4.4	71.56	3.02	15.90	0.79	3.05	0.23	3.63	0.14	2.98	0.13	3.08	0.13	0.34	0.06	1.03	0.10

FLD4.4	73.97	3.12	14.22	0.71	2.80	0.21	3.58	0.14	2.37	0.11	2.90	0.13	0.34	0.06	0.93	0.09
FLD4.4	74.14	3.13	13.36	0.67	2.61	0.20	3.43	0.14	2.09	0.10	3.14	0.13	0.40	0.06	0.95	0.09
FLD4.4	73.93	3.12	13.88	0.69	2.54	0.19	3.25	0.13	2.19	0.10	2.92	0.13	0.35	0.06	0.85	0.09
FLD4.4	72.46	3.06	12.98	0.65	2.59	0.20	3.34	0.14	1.81	0.09	2.90	0.13	0.26	0.05	0.49	0.07
FLD4.4	76.00	3.21	14.33	0.71	2.47	0.19	3.29	0.13	2.23	0.11	2.92	0.13	0.37	0.06	0.87	0.09
FLD4.4	73.96	3.12	13.21	0.66	2.43	0.19	3.30	0.13	2.10	0.10	2.93	0.13	0.35	0.06	0.54	0.07
FLD4.4	73.55	3.11	13.15	0.66	2.71	0.21	3.49	0.14	3.32	0.14	2.99	0.13	0.35	0.06	1.05	0.10
FLD4.4	69.35	2.93	13.54	0.68	2.98	0.22	3.61	0.14	1.93	0.10	3.22	0.14	0.40	0.06	0.96	0.10
FLD4.4	74.61	3.15	14.60	0.73	2.92	0.22	3.56	0.14	2.26	0.11	2.98	0.13	0.36	0.06	0.97	0.10
FLD4.4	72.44	3.06	13.75	0.69	2.67	0.20	3.47	0.14	2.16	0.10	3.14	0.13	0.42	0.06	0.98	0.10
FLD4.4	75.13	3.17	14.03	0.70	2.69	0.20	3.42	0.14	2.23	0.11	2.98	0.13	0.34	0.06	0.87	0.09
FLD4.4	86.01	3.62	6.44	0.35	1.48	0.13	2.02	0.10	0.68	0.06	2.09	0.10	0.09	0.05	0.27	0.06
FLD4.4	76.43	3.23	14.20	0.71	2.44	0.19	3.16	0.13	2.13	0.10	2.92	0.13	0.37	0.06	0.87	0.09
FLD4.4	74.72	3.16	13.99	0.70	2.55	0.20	3.26	0.13	2.39	0.11	2.95	0.13	0.34	0.06	0.65	0.08
FLD4.4	73.17	3.09	12.92	0.65	2.39	0.19	3.43	0.14	2.66	0.12	3.09	0.13	0.32	0.06	0.68	0.08
FLD4.4	73.33	3.10	13.55	0.68	2.66	0.20	3.51	0.14	2.75	0.12	3.03	0.13	0.36	0.06	0.67	0.08
FLD4.4	74.07	3.13	14.34	0.71	2.80	0.21	3.57	0.14	2.37	0.11	3.27	0.14	0.43	0.06	1.01	0.10
FLD4.4	74.65	3.15	12.08	0.61	2.48	0.19	3.57	0.14	1.87	0.09	2.73	0.12	0.29	0.06	0.61	0.08
FLD4.4	72.46	3.06	14.21	0.71	2.75	0.21	3.61	0.14	2.12	0.10	3.25	0.14	0.43	0.06	1.00	0.10
FLD4.4	70.98	3.00	14.99	0.74	2.69	0.20	3.34	0.14	2.15	0.10	3.07	0.13	0.41	0.06	0.60	0.08
FLD4.4	79.33	3.35	12.03	0.61	2.30	0.18	3.20	0.13	1.86	0.09	2.69	0.12	0.31	0.06	0.48	0.07
FLD4.4	74.67	3.15	13.59	0.68	2.59	0.20	3.44	0.14	2.48	0.11	3.10	0.13	0.33	0.06	0.69	0.08
FLD4.4	72.94	3.08	14.56	0.72	2.55	0.20	3.36	0.14	2.42	0.11	3.11	0.13	0.44	0.06	0.66	0.08
FLD4.4	75.20	3.18	14.47	0.72	2.60	0.20	3.34	0.14	2.45	0.11	3.26	0.14	0.38	0.06	1.02	0.10
FLD4.4	76.43	3.23	11.01	0.56	2.25	0.18	3.33	0.14	1.86	0.09	2.76	0.12	0.33	0.06	0.55	0.07
FLD4.4	90.80	3.82	6.41	0.35	1.44	0.13	1.86	0.09	0.62	0.06	1.59	0.09	0.16	0.05	0.31	0.06
FLD4.4	75.99	3.21	14.30	0.71	2.80	0.21	3.34	0.14	2.16	0.10	2.91	0.13	0.35	0.06	0.99	0.10
FLD4.4	73.18	3.09	14.35	0.71	2.54	0.19	3.37	0.14	2.23	0.11	3.15	0.13	0.46	0.06	0.64	0.08
FLD4.4	74.10	3.13	14.02	0.70	2.55	0.20	3.36	0.14	2.37	0.11	3.06	0.13	0.36	0.06	0.63	0.08
FLD4.4	70.97	3.00	13.04	0.65	2.52	0.19	3.50	0.14	2.23	0.11	3.31	0.14	0.39	0.06	0.62	0.08
FLD5.1	78.79	3.32	12.42	0.63	2.79	0.21	3.43	0.14	0.92	0.07	2.64	0.12	0.29	0.06	0.30	0.06
FLD5.1	72.04	3.04	12.62	0.63	2.97	0.22	3.63	0.14	1.63	0.09	2.79	0.12	0.30	0.06	0.51	0.07
FLD5.1	70.39	2.98	13.35	0.67	3.19	0.23	3.77	0.15	1.62	0.09	3.19	0.14	0.42	0.06	0.50	0.07
FLD5.1	73.40	3.10	11.47	0.58	2.85	0.21	3.43	0.14	1.56	0.09	2.84	0.13	0.37	0.06	0.49	0.07
FLD5.1	72.80	3.08	14.02	0.70	2.93	0.22	3.39	0.14	1.56	0.09	2.98	0.13	0.36	0.06	0.53	0.07
FLD5.1	71.24	3.01	14.01	0.70	2.76	0.21	3.25	0.13	1.61	0.09	2.95	0.13	0.34	0.06	0.55	0.07
FLD5.1	71.62	3.03	14.80	0.74	2.88	0.22	3.38	0.14	1.66	0.09	3.06	0.13	0.33	0.06	0.72	0.08
FLD5.1	77.11	3.25	11.27	0.57	2.55	0.20	3.16	0.13	1.21	0.08	2.53	0.12	0.32	0.06	0.42	0.07
FLD5.1	73.84	3.12	13.49	0.67	2.84	0.21	3.15	0.13	1.60	0.09	2.75	0.12	0.38	0.06	0.49	0.07
FLD5.1	102.97	4.33	0.41	0.07	0.15	0.05	0.03	0.03	0.08	0.04	0.09	0.04	0.08	0.05	0.11	0.05
FLD5.1	74.28	3.14	11.28	0.57	2.49	0.19	3.16	0.13	1.32	0.08	2.78	0.12	0.21	0.05	0.66	0.08
FLD5.1	75.31	3.18	11.21	0.57	2.57	0.20	3.24	0.13	1.33	0.08	2.83	0.13	0.34	0.06	0.46	0.07
FLD5.1	77.06	3.25	11.20	0.57	2.48	0.19	3.12	0.13	1.15	0.07	2.68	0.12	0.31	0.06	0.56	0.07
FLD5.1	66.79	2.83	16.64	0.82	3.08	0.23	3.34	0.14	2.25	0.11	3.01	0.13	0.38	0.06	0.64	0.08
FLD5.1	79.82	3.37	8.46	0.44	2.02	0.16	2.71	0.12	0.97	0.07	1.72	0.09	0.17	0.05	0.34	0.06
FLD5.1	70.93	3.00	13.35	0.67	2.88	0.22	3.44	0.14	1.41	0.08	3.06	0.13	0.41	0.06	0.56	0.07
FLD5.1	70.18	2.97	14.23	0.71	2.88	0.22	3.46	0.14	1.79	0.09	3.03	0.13	0.42	0.06	0.54	0.07
FLD5.1	72.29	3.05	14.28	0.71	2.99	0.22	3.37	0.14	1.60	0.09	2.93	0.13	0.33	0.06	0.51	0.07
FLD5.1	73.52	3.11	12.96	0.65	2.55	0.20	3.20	0.13	1.43	0.08	2.78	0.12	0.42	0.06	0.54	0.07
FLD5.1	72.37	3.06	14.15	0.71	2.88	0.22	3.48	0.14	1.65	0.09	2.97	0.13	0.39	0.06	0.58	0.08
FLD5.1	73.19	3.09	13.06	0.66	2.80	0.21	3.60	0.14	1.77	0.09	2.81	0.12	0.31	0.06	0.51	0.07
FLD5.1	73.95	3.12	12.12	0.61	2.64	0.20	3.47	0.14	1.61	0.09	2.88	0.13	0.33	0.06	0.52	0.07
FLD5.1	73.90	3.12	12.17	0.61	2.76	0.21	3.55	0.14	1.60	0.09	2.75	0.12	0.29	0.06	0.43	0.07
FLD5.1	67.74	2.87	16.50	0.81	3.12	0.23	3.65	0.15	2.31	0.11	3.36	0.14	0.41	0.06	0.73	0.08
FLD5.1	71.83	3.04	14.57	0.73	2.80	0.21	3.53	0.14	2.04	0.10	2.89	0.13	0.33	0.06	0.55	0.07
FLD5.1	73.97	3.12	13.83	0.69	3.13	0.23	3.90	0.15	1.16	0.07	2.32	0.11	0.36	0.06	0.40	0.07
FLD5.1	73.04	3.09	11.81	0.60	2.62	0.20	3.31	0.13	1.40	0.08	3.67	0.15	0.53	0.06	0.57	0.07
FLD5.2	72.62	3.07	12.14	0.61	3.52	0.26	3.72	0.15	2.65	0.12	3.43	0.14	0.35	0.06	0.67	0.08
FLD5.2	73.93	3.12	12.55	0.63	3.07	0.23	3.56	0.14	1.33	0.08	2.72	0.12	0.34	0.06	0.40	0.07
FLD5.2	70.71	2.99	15.11	0.75	3.55	0.26	3.73	0.15	1.51	0.08	3.00	0.13	0.37	0.06	0.64	0.08
FLD5.2	70.02	2.96	13.98	0.70	3.49	0.25	3.85	0.15	1.47	0.08	2.69	0.12	0.39	0.06	0.54	0.07
FLD5.2	74.86	3.16	12.30	0.62	2.82	0.21	3.25	0.13	1.96	0.10	2.65	0.12	0.28	0.05	0.46	0.07

FLD5.2	73.94	3.12	13.00	0.65	3.12	0.23	3.60	0.14	1.45	0.08	2.69	0.12	0.29	0.06	0.36	0.06
FLD5.2	76.42	3.23	11.50	0.58	2.78	0.21	3.80	0.15	0.85	0.06	1.55	0.09	0.16	0.05	0.29	0.06
FLD5.2	69.73	2.95	14.26	0.71	3.38	0.25	4.03	0.16	1.36	0.08	2.45	0.11	0.35	0.06	0.49	0.07
FLD5.2	68.84	2.91	14.84	0.74	3.40	0.25	3.69	0.15	1.60	0.09	3.46	0.14	0.54	0.06	0.84	0.09
FLD5.2	71.73	3.03	13.41	0.67	3.07	0.23	3.82	0.15	1.38	0.08	2.81	0.12	0.43	0.06	0.52	0.07
FLD5.2	73.79	3.12	13.76	0.69	3.13	0.23	3.62	0.14	1.41	0.08	2.68	0.12	0.37	0.06	0.55	0.07
FLD5.2	70.49	2.98	13.71	0.69	3.17	0.23	3.80	0.15	1.42	0.08	2.76	0.12	0.43	0.06	0.50	0.07
FLD5.2	71.84	3.04	13.34	0.67	3.22	0.24	3.93	0.15	1.40	0.08	2.59	0.12	0.35	0.06	0.46	0.07
FLD5.2	71.84	3.04	13.17	0.66	3.36	0.25	3.73	0.15	1.05	0.07	2.53	0.12	0.35	0.06	0.41	0.07
FLD5.2	72.38	3.06	13.74	0.69	3.29	0.24	3.58	0.14	1.24	0.08	2.96	0.13	0.40	0.06	0.43	0.07
FLD5.2	71.35	3.02	13.08	0.66	3.10	0.23	3.83	0.15	1.43	0.08	2.49	0.11	0.32	0.06	0.49	0.07
FLD5.2	69.54	2.94	13.92	0.69	3.20	0.24	3.82	0.15	1.62	0.09	2.93	0.13	0.44	0.06	0.60	0.08
FLD5.2	72.13	3.05	13.47	0.67	3.28	0.24	3.84	0.15	1.60	0.09	2.59	0.12	0.46	0.06	0.43	0.07
FLD5.2	72.44	3.06	12.94	0.65	3.08	0.23	3.78	0.15	1.61	0.09	2.58	0.12	0.32	0.06	0.36	0.06
FLD5.2	87.44	3.68	6.08	0.33	1.33	0.12	2.43	0.11	0.83	0.06	2.17	0.10	0.22	0.05	0.24	0.06
FLD5.2	73.13	3.09	14.34	0.71	3.17	0.23	3.58	0.14	1.45	0.08	2.95	0.13	0.40	0.06	0.66	0.08
FLD5.2	67.80	2.87	15.24	0.76	3.36	0.25	3.75	0.15	1.93	0.10	3.04	0.13	0.46	0.06	0.62	0.08
FLD5.2	73.59	3.11	12.43	0.63	3.05	0.23	3.72	0.15	1.23	0.08	2.20	0.11	0.18	0.05	0.38	0.06
FLD5.2	70.72	2.99	14.73	0.73	3.23	0.24	3.81	0.15	1.67	0.09	2.82	0.12	0.36	0.06	0.61	0.08
FLD5.2	71.91	3.04	14.56	0.72	3.29	0.24	4.16	0.16	1.07	0.07	1.68	0.09	0.18	0.05	0.25	0.06
FLD5.2	69.62	2.94	14.78	0.73	3.16	0.23	3.60	0.14	1.66	0.09	3.14	0.13	0.40	0.06	0.66	0.08
FLD5.2	69.58	2.94	15.20	0.75	3.53	0.26	3.71	0.15	1.70	0.09	3.06	0.13	0.50	0.06	0.73	0.08
FLD5.2	70.59	2.98	13.92	0.69	3.06	0.23	3.79	0.15	1.58	0.09	2.85	0.13	0.38	0.06	0.58	0.08
FLD5.2	69.99	2.96	14.08	0.70	3.43	0.25	3.86	0.15	1.47	0.08	2.49	0.11	0.40	0.06	0.47	0.07
FLD5.2	73.88	3.12	11.41	0.58	3.50	0.25	4.15	0.16	1.93	0.10	2.52	0.12	0.22	0.05	0.38	0.07
FLD5.2	72.08	3.05	13.56	0.68	3.55	0.26	4.48	0.17	1.13	0.07	1.95	0.10	0.22	0.05	0.37	0.06
FLD5.2	75.90	3.20	11.08	0.56	3.04	0.23	3.83	0.15	1.53	0.08	2.36	0.11	0.24	0.05	0.36	0.06
FLD5.2	74.82	3.16	11.71	0.59	3.00	0.22	3.69	0.15	0.97	0.07	2.48	0.11	0.39	0.06	0.52	0.07
FLD5.2	72.57	3.07	12.14	0.61	3.42	0.25	4.50	0.17	1.18	0.07	2.82	0.12	0.43	0.06	0.44	0.07
FLD5.2	71.20	3.01	12.70	0.64	3.63	0.26	3.93	0.15	1.42	0.08	2.74	0.12	0.38	0.06	0.40	0.07
FLD5.2	82.80	3.49	8.62	0.45	2.43	0.19	3.22	0.13	0.45	0.05	1.22	0.08	0.14	0.05	0.24	0.06
FLD5.3	74.81	3.16	11.34	0.58	3.88	0.28	4.28	0.16	0.27	0.05	2.77	0.12	0.20	0.05	0.11	0.05
FLD5.3	72.15	3.05	13.33	0.67	3.59	0.26	3.94	0.15	2.13	0.10	2.80	0.12	0.33	0.06	0.53	0.07
FLD5.3	73.08	3.09	12.71	0.64	4.20	0.30	4.33	0.17	0.08	0.04	3.15	0.14	0.19	0.05	0.25	0.06
FLD5.3	75.37	3.18	11.57	0.59	3.82	0.27	4.33	0.17	0.39	0.05	2.65	0.12	0.14	0.05	0.16	0.05
FLD5.3	75.07	3.17	11.34	0.58	3.72	0.27	4.25	0.16	0.30	0.05	2.81	0.12	0.15	0.05	0.05	0.05
FLD5.3	74.34	3.14	10.69	0.55	3.87	0.28	4.25	0.16	0.74	0.06	2.61	0.12	0.19	0.05	0.11	0.05
FLD5.3	70.28	2.97	13.25	0.66	4.16	0.30	4.04	0.16	1.82	0.09	2.97	0.13	0.34	0.06	0.44	0.07
FLD5.3	71.39	3.02	12.93	0.65	4.12	0.29	4.13	0.16	1.53	0.08	2.58	0.12	0.35	0.06	0.38	0.07
FLD5.3	71.83	3.04	11.88	0.60	3.93	0.28	4.17	0.16	0.98	0.07	3.01	0.13	0.32	0.06	0.24	0.06
FLD5.3	74.39	3.14	10.81	0.55	3.68	0.27	4.23	0.16	0.21	0.04	2.49	0.11	0.12	0.05	0.16	0.05
FLD5.3	74.34	3.14	11.38	0.58	3.92	0.28	4.26	0.16	0.09	0.04	2.87	0.13	0.22	0.05	0.09	0.05
FLD5.3	73.99	3.13	10.84	0.55	3.86	0.28	4.24	0.16	0.09	0.04	2.80	0.12	0.19	0.05	0.22	0.06
FLD5.3	77.17	3.26	9.71	0.50	3.29	0.24	3.67	0.15	1.12	0.07	2.72	0.12	0.15	0.05	0.24	0.06
FLD5.3	72.49	3.06	12.51	0.63	3.68	0.27	4.20	0.16	2.12	0.10	2.84	0.13	0.39	0.06	0.53	0.07
FLD5.3	70.83	2.99	14.22	0.71	3.46	0.25	4.06	0.16	1.01	0.07	2.39	0.11	0.39	0.06	0.52	0.07
FLD5.3	74.29	3.14	10.77	0.55	3.55	0.26	4.12	0.16	0.76	0.06	2.83	0.13	0.18	0.05	0.20	0.06
FLD5.3	69.82	2.95	12.49	0.63	3.64	0.26	4.01	0.16	2.89	0.13	2.53	0.12	0.35	0.06	0.47	0.07
FLD5.3	74.34	3.14	11.23	0.57	3.89	0.28	4.28	0.16	0.42	0.05	2.62	0.12	0.14	0.05	0.10	0.05
FLD5.3	71.34	3.02	12.17	0.61	3.48	0.25	4.02	0.16	2.06	0.10	2.86	0.13	0.36	0.06	0.48	0.07
FLD5.3	74.04	3.13	11.17	0.57	3.76	0.27	4.37	0.17	0.39	0.05	2.82	0.12	0.21	0.05	0.07	0.05
FLD5.3	77.38	3.27	11.42	0.58	3.56	0.26	3.63	0.14	1.23	0.08	1.69	0.09	0.12	0.05	0.17	0.05
FLD5.3	76.56	3.23	11.49	0.58	4.04	0.29	4.18	0.16	0.76	0.06	2.95	0.13	0.25	0.05	0.14	0.05
FLD5.3	72.75	3.07	12.26	0.62	3.82	0.27	4.20	0.16	0.98	0.07	2.62	0.12	0.32	0.06	0.30	0.06
FLD5.3	75.85	3.20	11.21	0.57	3.51	0.25	4.13	0.16	0.38	0.05	2.70	0.12	0.20	0.05	0.08	0.05
FLD5.3	72.70	3.07	11.40	0.58	3.40	0.25	3.87	0.15	1.87	0.09	2.68	0.12	0.36	0.06	0.36	0.06
FLD5.3	66.19	2.80	14.31	0.71	4.81	0.34	4.34	0.17	3.69	0.15	3.32	0.14	0.44	0.06	0.88	0.09
FLD5.3	73.63	3.11	12.30	0.62	3.96	0.28	4.26	0.16	0.72	0.06	2.71	0.12	0.30	0.06	0.17	0.05
FLD5.3	74.45	3.14	11.22	0.57	3.43	0.25	3.95	0.15	0.67	0.06	2.63	0.12	0.14	0.05	0.16	0.05
FLD5.3	71.86	3.04	12.10	0.61	3.24	0.24	3.68	0.15	2.14	0.10	2.71	0.12	0.30	0.06	0.47	0.07
FLD5.3	73.91	3.12	12.42	0.63	3.65	0.26	3.96	0.15	1.23	0.08	2.97	0.13	0.32	0.06	0.37	0.06
FLD5.3	71.78	3.03	12.17	0.61	3.37	0.25	3.79	0.15	1.59	0.09	2.80	0.12	0.27	0.05	0.33	0.06

FLD5.4	71.46	3.02	13.48	0.67	3.02	0.22	3.43	0.14	1.76	0.09	2.86	0.13	0.34	0.06	0.62	0.08
FLD5.4	81.74	3.45	8.34	0.44	2.56	0.20	3.09	0.13	0.88	0.07	1.98	0.10	0.18	0.05	0.29	0.06
FLD5.4	72.02	3.04	13.83	0.69	3.54	0.26	3.89	0.15	1.44	0.08	2.75	0.12	0.29	0.06	0.35	0.06
FLD5.4	74.25	3.14	12.88	0.65	3.22	0.24	3.60	0.14	1.37	0.08	2.51	0.12	0.31	0.06	0.36	0.06
FLD5.4	70.06	2.96	14.06	0.70	4.22	0.30	4.18	0.16	1.53	0.08	3.09	0.13	0.31	0.06	0.60	0.08
FLD5.4	72.25	3.05	12.80	0.64	3.52	0.26	3.64	0.14	1.53	0.08	2.74	0.12	0.28	0.05	0.46	0.07
FLD5.4	69.38	2.93	14.94	0.74	3.97	0.28	4.22	0.16	1.29	0.08	3.05	0.13	0.43	0.06	0.56	0.07
FLD5.4	73.67	3.11	11.86	0.60	3.18	0.23	3.79	0.15	1.20	0.07	2.68	0.12	0.32	0.06	0.35	0.06
FLD5.4	57.32	2.43	23.62	1.14	3.72	0.27	3.24	0.13	4.47	0.17	3.81	0.16	0.57	0.06	0.76	0.08
FLD5.4	75.07	3.17	12.87	0.65	3.24	0.24	3.53	0.14	1.54	0.08	2.79	0.12	0.27	0.05	0.42	0.07
FLD5.4	72.53	3.06	12.98	0.65	3.05	0.23	3.46	0.14	1.52	0.08	2.83	0.13	0.29	0.06	0.38	0.06
FLD5.4	75.52	3.19	11.90	0.60	2.99	0.22	3.45	0.14	1.25	0.08	2.47	0.11	0.16	0.05	0.39	0.07
FLD5.4	69.27	2.93	13.93	0.70	3.62	0.26	3.67	0.15	2.28	0.11	3.30	0.14	0.47	0.06	0.64	0.08
FLD5.4	70.82	2.99	15.10	0.75	3.28	0.24	3.46	0.14	1.56	0.09	3.33	0.14	0.44	0.06	0.72	0.08
FLD5.4	73.67	3.11	12.61	0.63	3.05	0.23	3.48	0.14	1.41	0.08	2.62	0.12	0.33	0.06	0.40	0.07
FLD5.4	68.88	2.91	14.53	0.72	3.88	0.28	4.13	0.16	1.47	0.08	2.67	0.12	0.48	0.06	0.62	0.08
FLD5.4	73.30	3.10	12.15	0.61	2.97	0.22	3.57	0.14	1.35	0.08	2.61	0.12	0.34	0.06	0.37	0.06
FLD5.4	68.89	2.91	14.40	0.72	3.74	0.27	4.09	0.16	2.91	0.13	3.07	0.13	0.39	0.06	0.66	0.08
FLD5.4	65.96	2.79	16.38	0.81	4.00	0.29	4.19	0.16	3.07	0.13	2.79	0.12	0.42	0.06	0.78	0.09
FLD5.4	73.83	3.12	13.31	0.67	3.71	0.27	4.08	0.16	1.36	0.08	2.49	0.11	0.32	0.06	0.51	0.07
FLD5.4	86.57	3.65	5.11	0.29	1.86	0.15	2.50	0.11	0.46	0.05	1.53	0.08	0.11	0.05	0.19	0.05
FLD5.4	73.54	3.11	13.24	0.66	2.97	0.22	3.46	0.14	1.48	0.08	2.87	0.13	0.30	0.06	0.58	0.08
FLD5.4	72.23	3.05	13.30	0.67	2.84	0.21	3.58	0.14	1.54	0.09	2.69	0.12	0.44	0.06	0.48	0.07
FLD5.4	72.47	3.06	14.42	0.72	3.46	0.25	3.77	0.15	1.87	0.09	3.15	0.13	0.36	0.06	0.63	0.08
FLD5.5	72.64	3.07	13.64	0.68	2.88	0.22	3.80	0.15	1.31	0.08	2.68	0.12	0.30	0.06	0.36	0.06
FLD5.5	71.87	3.04	13.55	0.68	2.70	0.20	3.90	0.15	1.15	0.07	2.59	0.12	0.33	0.06	0.49	0.07
FLD5.5	71.31	3.01	13.56	0.68	2.28	0.18	3.36	0.14	1.78	0.09	2.82	0.12	0.36	0.06	0.59	0.08
FLD5.5	70.79	2.99	15.34	0.76	2.88	0.22	3.75	0.15	1.46	0.08	2.83	0.12	0.53	0.06	0.65	0.08
FLD5.5	77.16	3.26	13.93	0.70	2.86	0.21	3.95	0.15	0.74	0.06	1.21	0.07	0.12	0.05	0.17	0.05
FLD5.5	75.20	3.18	13.63	0.68	2.82	0.21	3.98	0.16	1.03	0.07	2.15	0.10	0.18	0.05	0.41	0.07
FLD5.5	75.63	3.19	10.89	0.55	2.30	0.18	3.70	0.15	1.10	0.07	2.60	0.12	0.28	0.05	0.51	0.07
FLD5.5	71.58	3.03	14.85	0.74	2.69	0.20	3.93	0.15	0.91	0.07	2.18	0.10	0.29	0.06	0.49	0.07
FLD5.5	74.02	3.13	11.85	0.60	2.19	0.17	3.66	0.15	1.05	0.07	2.61	0.12	0.33	0.06	0.54	0.07
FLD5.5	74.06	3.13	12.45	0.63	2.35	0.18	3.63	0.14	1.18	0.07	2.78	0.12	0.29	0.06	0.42	0.07
FLD5.5	72.57	3.07	12.88	0.65	2.88	0.22	4.00	0.16	1.32	0.08	2.84	0.13	0.29	0.06	0.53	0.07
FLD5.5	74.57	3.15	10.64	0.54	3.45	0.25	4.52	0.17	1.52	0.08	2.54	0.12	0.31	0.06	0.39	0.07
FLD5.5	69.68	2.95	15.17	0.75	2.60	0.20	3.31	0.13	1.99	0.10	2.72	0.12	0.43	0.06	0.45	0.07
FLD5.5	73.52	3.11	13.03	0.65	2.42	0.19	3.58	0.14	1.47	0.08	2.60	0.12	0.35	0.06	0.39	0.07
FLD5.5	71.79	3.03	15.53	0.77	2.71	0.21	3.40	0.14	1.99	0.10	2.84	0.13	0.46	0.06	0.64	0.08
FLD5.5	73.13	3.09	13.39	0.67	3.05	0.23	3.97	0.15	1.75	0.09	2.75	0.12	0.33	0.06	0.41	0.07
FLD5.5	72.52	3.06	13.89	0.69	2.22	0.17	3.20	0.13	1.19	0.07	2.92	0.13	0.44	0.06	0.63	0.08
FLD5.5	73.88	3.12	12.22	0.62	2.47	0.19	3.94	0.15	0.71	0.06	2.40	0.11	0.29	0.06	0.32	0.06
U1A	70.78	2.99	13.47	0.67	3.58	0.26	3.44	0.14	1.76	0.09	2.57	0.12	0.25	0.05	0.36	0.06
U1A	72.05	3.04	13.97	0.70	3.70	0.27	3.25	0.13	1.78	0.09	2.99	0.13	0.35	0.06	0.50	0.07
U1A	71.15	3.01	14.23	0.71	3.67	0.26	3.53	0.14	2.10	0.10	2.99	0.13	0.30	0.06	0.45	0.07
U1A	71.78	3.03	13.65	0.68	3.52	0.26	3.41	0.14	1.76	0.09	2.93	0.13	0.28	0.06	0.42	0.07
U1A	73.11	3.09	11.86	0.60	3.57	0.26	3.59	0.14	1.41	0.08	2.75	0.12	0.28	0.05	0.36	0.06
U1A	70.45	2.98	14.03	0.70	3.56	0.26	3.32	0.13	1.92	0.10	2.84	0.13	0.31	0.06	0.42	0.07
U1A	72.07	3.05	13.65	0.68	3.60	0.26	3.39	0.14	1.82	0.09	3.02	0.13	0.30	0.06	0.47	0.07
U1A	72.08	3.05	13.48	0.67	3.42	0.25	3.20	0.13	1.89	0.10	2.87	0.13	0.27	0.05	0.50	0.07
U1A	71.56	3.02	13.29	0.67	3.58	0.26	3.50	0.14	1.87	0.10	2.88	0.13	0.31	0.06	0.48	0.07
U1A	73.08	3.09	14.43	0.72	2.98	0.22	2.97	0.12	2.32	0.11	2.93	0.13	0.37	0.06	0.48	0.07
U1A	71.62	3.03	13.31	0.67	3.61	0.26	3.48	0.14	1.76	0.09	2.87	0.13	0.31	0.06	0.45	0.07
U1A	72.81	3.08	12.60	0.63	3.84	0.28	3.65	0.14	1.54	0.08	3.03	0.13	0.32	0.06	0.52	0.07
U1A	73.35	3.10	12.73	0.64	3.68	0.27	3.54	0.14	1.55	0.09	2.95	0.13	0.26	0.05	0.46	0.07
U1A	73.99	3.12	12.42	0.63	3.21	0.24	3.01	0.13	1.57	0.09	2.53	0.12	0.25	0.05	0.36	0.06
U1A	69.57	2.94	13.95	0.70	3.19	0.23	3.51	0.14	2.18	0.10	3.01	0.13	0.35	0.06	0.49	0.07
U1A	77.42	3.27	12.73	0.64	2.74	0.21	2.90	0.12	1.73	0.09	2.73	0.12	0.31	0.06	0.42	0.07
U1A	78.11	3.30	11.85	0.60	3.10	0.23	3.05	0.13	1.39	0.08	2.52	0.12	0.26	0.05	0.34	0.06
U1A	69.47	2.94	14.53	0.72	3.28	0.24	3.48	0.14	2.70	0.12	3.35	0.14	0.34	0.06	0.63	0.08
U1A	71.50	3.02	13.62	0.68	3.46	0.25	3.39	0.14	1.80	0.09	3.00	0.13	0.32	0.06	0.44	0.07
U1A	71.56	3.02	12.86	0.65	3.53	0.26	3.60	0.14	1.58	0.09	3.08	0.13	0.33	0.06	0.47	0.07

U1A	70.57	2.98	13.77	0.69	3.39	0.25	3.42	0.14	1.84	0.09	2.92	0.13	0.30	0.06	0.43	0.07
U1A	73.70	3.11	14.26	0.71	2.89	0.22	3.11	0.13	2.09	0.10	2.74	0.12	0.31	0.06	0.49	0.07
U1A	71.27	3.01	13.44	0.67	3.66	0.26	3.67	0.15	1.83	0.09	3.03	0.13	0.38	0.06	0.50	0.07
U1A	72.24	3.05	13.56	0.68	3.66	0.26	3.61	0.14	1.87	0.09	2.85	0.13	0.34	0.06	0.51	0.07
U1A	70.83	2.99	14.24	0.71	3.64	0.26	3.60	0.14	1.97	0.10	2.87	0.13	0.31	0.06	0.45	0.07
U1A	71.97	3.04	13.93	0.70	3.48	0.25	3.58	0.14	1.79	0.09	2.97	0.13	0.31	0.06	0.49	0.07
U1A	72.34	3.06	14.08	0.70	3.39	0.25	3.55	0.14	1.80	0.09	2.93	0.13	0.31	0.06	0.47	0.07
U1A	71.36	3.02	13.22	0.66	3.01	0.22	3.46	0.14	1.74	0.09	2.85	0.13	0.28	0.06	0.43	0.07
U1A	71.98	3.04	14.43	0.72	2.78	0.21	3.52	0.14	2.25	0.11	2.95	0.13	0.32	0.06	0.52	0.07
U1A	74.02	3.13	13.92	0.69	2.90	0.22	3.08	0.13	2.38	0.11	2.97	0.13	0.29	0.06	0.50	0.07
U1A	73.36	3.10	14.87	0.74	3.34	0.24	2.98	0.12	1.97	0.10	2.95	0.13	0.34	0.06	0.49	0.07
U1A	72.18	3.05	14.14	0.71	3.53	0.26	3.45	0.14	1.91	0.10	2.97	0.13	0.36	0.06	0.47	0.07
U1A	73.39	3.10	14.53	0.72	3.56	0.26	3.34	0.14	1.92	0.10	2.85	0.13	0.33	0.06	0.46	0.07
U1A	71.74	3.03	13.65	0.68	2.93	0.22	3.42	0.14	1.85	0.09	2.92	0.13	0.31	0.06	0.48	0.07
U1A	73.35	3.10	13.63	0.68	3.70	0.27	3.57	0.14	1.81	0.09	2.75	0.12	0.27	0.05	0.47	0.07
U1A	72.12	3.05	13.77	0.69	3.52	0.26	3.48	0.14	1.93	0.10	2.95	0.13	0.35	0.06	0.45	0.07
U1A	68.91	2.91	13.95	0.70	3.35	0.24	3.52	0.14	2.27	0.11	3.31	0.14	0.39	0.06	0.55	0.07
U1A	74.81	3.16	13.07	0.66	3.41	0.25	3.48	0.14	1.68	0.09	2.72	0.12	0.28	0.05	0.39	0.07
U1A	73.89	3.12	13.21	0.66	3.37	0.25	3.67	0.15	1.73	0.09	3.03	0.13	0.36	0.06	0.53	0.07
U1A	73.09	3.09	13.85	0.69	2.26	0.18	3.12	0.13	2.35	0.11	2.84	0.13	0.29	0.06	0.50	0.07
U1A	72.02	3.04	13.11	0.66	3.38	0.25	3.56	0.14	1.95	0.10	3.00	0.13	0.33	0.06	0.48	0.07
U1A	74.82	3.16	13.68	0.68	3.50	0.25	3.53	0.14	1.70	0.09	3.06	0.13	0.32	0.06	0.50	0.07
U1A	71.78	3.03	14.21	0.71	3.26	0.24	3.56	0.14	1.78	0.09	3.01	0.13	0.33	0.06	0.45	0.07
U1A	73.07	3.09	13.64	0.68	3.01	0.22	3.40	0.14	1.96	0.10	2.78	0.12	0.27	0.05	0.48	0.07
U1A	71.31	3.01	13.23	0.66	3.00	0.22	3.58	0.14	1.54	0.09	2.81	0.12	0.33	0.06	0.39	0.07
U1A	78.47	3.31	11.57	0.59	2.52	0.19	3.16	0.13	1.18	0.07	2.25	0.11	0.22	0.05	0.34	0.06
U1A	71.18	3.01	13.60	0.68	2.86	0.21	3.60	0.14	1.77	0.09	2.96	0.13	0.31	0.06	0.46	0.07
U1A	75.49	3.19	13.43	0.67	2.92	0.22	3.42	0.14	1.73	0.09	3.02	0.13	0.35	0.06	0.48	0.07
U1A	74.13	3.13	13.82	0.69	2.67	0.20	3.39	0.14	1.96	0.10	3.04	0.13	0.33	0.06	0.50	0.07
U1A	73.81	3.12	14.57	0.72	2.57	0.20	3.30	0.13	1.84	0.09	2.97	0.13	0.31	0.06	0.46	0.07
U1A	71.05	3.00	13.84	0.69	3.40	0.25	3.60	0.14	1.82	0.09	3.12	0.13	0.35	0.06	0.46	0.07
U1A	70.65	2.99	13.32	0.67	3.49	0.25	3.60	0.14	1.85	0.09	2.90	0.13	0.33	0.06	0.41	0.07
U1A	71.43	3.02	14.09	0.70	3.33	0.24	3.69	0.15	2.24	0.11	2.85	0.13	0.32	0.06	0.48	0.07
U1A	71.46	3.02	13.83	0.69	2.45	0.19	3.10	0.13	2.28	0.11	3.03	0.13	0.33	0.06	0.47	0.07
U1A	70.63	2.99	13.84	0.69	3.70	0.27	3.61	0.14	1.86	0.09	2.92	0.13	0.38	0.06	0.42	0.07
U1A	81.95	3.45	8.61	0.45	2.17	0.17	2.41	0.11	0.97	0.07	2.19	0.11	0.24	0.05	0.37	0.06
U1A	80.08	3.38	11.42	0.58	2.34	0.18	2.90	0.12	1.32	0.08	2.33	0.11	0.20	0.05	0.34	0.06
U1A	72.65	3.07	14.65	0.73	3.45	0.25	3.37	0.14	2.31	0.11	2.83	0.13	0.30	0.06	0.49	0.07
U1A	72.35	3.06	12.52	0.63	3.36	0.25	3.25	0.13	1.80	0.09	2.74	0.12	0.29	0.06	0.48	0.07
U1A	74.22	3.13	14.23	0.71	3.39	0.25	3.16	0.13	2.15	0.10	2.95	0.13	0.33	0.06	0.49	0.07
U1B	91.98	3.87	3.64	0.22	1.72	0.14	1.65	0.08	0.47	0.05	1.63	0.09	0.06	0.05	0.38	0.06
U1B	72.40	3.06	12.67	0.64	3.72	0.27	3.38	0.14	2.23	0.11	2.87	0.13	0.32	0.06	0.57	0.07
U1B	71.74	3.03	13.55	0.68	3.94	0.28	3.53	0.14	1.77	0.09	2.75	0.12	0.28	0.06	0.55	0.07
U1B	71.26	3.01	13.63	0.68	4.28	0.30	3.76	0.15	1.53	0.08	2.65	0.12	0.32	0.06	0.57	0.07
U1B	69.55	2.94	13.77	0.69	4.26	0.30	3.95	0.15	1.60	0.09	2.79	0.12	0.40	0.06	0.59	0.08
U1B	76.57	3.23	12.29	0.62	3.66	0.26	3.35	0.14	1.33	0.08	2.64	0.12	0.28	0.06	0.59	0.08
U1B	72.58	3.07	13.70	0.68	3.80	0.27	3.41	0.14	1.23	0.08	2.93	0.13	0.36	0.06	0.58	0.08
U1B	69.96	2.96	14.06	0.70	3.73	0.27	3.45	0.14	1.37	0.08	2.93	0.13	0.35	0.06	0.56	0.07
U1B	70.96	3.00	14.05	0.70	3.88	0.28	3.47	0.14	1.31	0.08	2.97	0.13	0.31	0.06	0.48	0.07
U1B	70.97	3.00	13.73	0.69	3.97	0.28	3.47	0.14	1.21	0.07	3.03	0.13	0.28	0.05	0.51	0.07
U1B	72.30	3.05	14.48	0.72	3.73	0.27	3.35	0.14	1.31	0.08	2.96	0.13	0.36	0.06	0.60	0.08
U1B	71.75	3.03	14.09	0.70	3.73	0.27	3.42	0.14	1.34	0.08	2.87	0.13	0.37	0.06	0.61	0.08
U1B	72.86	3.08	14.03	0.70	3.63	0.26	3.31	0.13	1.41	0.08	2.92	0.13	0.40	0.06	0.60	0.08
U1B	71.15	3.01	13.82	0.69	3.86	0.28	3.55	0.14	1.32	0.08	3.03	0.13	0.33	0.06	0.58	0.08
U1B	71.31	3.01	13.77	0.69	4.06	0.29	3.62	0.14	1.14	0.07	3.01	0.13	0.41	0.06	0.46	0.07
U1B	72.17	3.05	14.00	0.70	3.74	0.27	3.25	0.13	1.39	0.08	2.84	0.13	0.36	0.06	0.54	0.07
U1B	69.86	2.95	13.76	0.69	3.86	0.28	3.63	0.14	1.49	0.08	2.82	0.12	0.34	0.06	0.57	0.08
U1B	71.78	3.03	14.17	0.71	3.67	0.26	3.48	0.14	1.36	0.08	3.14	0.13	0.35	0.06	0.57	0.07
U1B	73.38	3.10	14.06	0.70	3.75	0.27	3.37	0.14	1.36	0.08	2.91	0.13	0.38	0.06	0.56	0.07
U1B	72.85	3.08	14.33	0.71	3.78	0.27	3.33	0.14	1.36	0.08	3.07	0.13	0.36	0.06	0.55	0.07
U1B	71.58	3.03	14.38	0.72	3.94	0.28	3.34	0.14	1.44	0.08	2.94	0.13	0.33	0.06	0.56	0.07
U1B	71.43	3.02	13.75	0.69	4.02	0.29	3.56	0.14	1.31	0.08	2.97	0.13	0.35	0.06	0.55	0.07

U1B	71.86	3.04	14.14	0.71	3.61	0.26	3.32	0.14	1.41	0.08	2.99	0.13	0.32	0.06	0.59	0.08
U1B	76.16	3.22	12.07	0.61	3.48	0.25	3.35	0.14	1.30	0.08	2.47	0.11	0.32	0.06	0.55	0.07
U1B	71.91	3.04	14.19	0.71	3.89	0.28	3.54	0.14	1.11	0.07	2.74	0.12	0.35	0.06	0.62	0.08
U1B	72.05	3.04	14.66	0.73	3.41	0.25	3.21	0.13	1.49	0.08	2.92	0.13	0.29	0.06	0.50	0.07
U1B	73.09	3.09	14.10	0.70	3.75	0.27	3.41	0.14	1.39	0.08	2.96	0.13	0.38	0.06	0.57	0.07
U1B	72.55	3.07	13.69	0.68	3.82	0.27	3.50	0.14	1.29	0.08	2.81	0.12	0.35	0.06	0.45	0.07
U1B	72.25	3.05	13.50	0.68	3.64	0.26	3.42	0.14	1.30	0.08	2.90	0.13	0.33	0.06	0.50	0.07
U1B	72.17	3.05	14.53	0.72	3.70	0.27	3.36	0.14	1.41	0.08	2.76	0.12	0.36	0.06	0.58	0.08
U1B	69.46	2.94	14.52	0.72	3.56	0.26	3.43	0.14	1.59	0.09	2.86	0.13	0.44	0.06	0.59	0.08
U1B	72.35	3.06	14.30	0.71	3.60	0.26	3.27	0.13	1.56	0.09	2.74	0.12	0.30	0.06	0.60	0.08
U1B	72.58	3.07	14.19	0.71	3.77	0.27	3.44	0.14	1.46	0.08	2.83	0.13	0.38	0.06	0.57	0.07
U1B	92.97	3.91	4.11	0.24	1.48	0.13	1.64	0.08	0.27	0.05	1.31	0.08	0.09	0.05	0.22	0.06
U1B	70.61	2.98	15.32	0.76	3.61	0.26	3.46	0.14	1.56	0.09	3.07	0.13	0.49	0.06	0.72	0.08
U1B	71.64	3.03	13.80	0.69	3.80	0.27	3.51	0.14	1.09	0.07	2.88	0.13	0.32	0.06	0.42	0.07
U1B	70.17	2.97	13.91	0.69	3.47	0.25	3.34	0.14	1.47	0.08	2.99	0.13	0.33	0.06	0.57	0.07
U1B	71.94	3.04	14.34	0.71	3.40	0.25	3.30	0.13	1.50	0.08	2.96	0.13	0.40	0.06	0.57	0.07
U1B	71.87	3.04	14.92	0.74	3.38	0.25	3.16	0.13	1.56	0.09	2.69	0.12	0.40	0.06	0.54	0.07
U1B	71.70	3.03	14.33	0.71	3.40	0.25	3.20	0.13	1.53	0.08	3.06	0.13	0.42	0.06	0.69	0.08
U1B	70.94	3.00	14.03	0.70	3.60	0.26	3.45	0.14	1.43	0.08	2.86	0.13	0.38	0.06	0.56	0.07
U1B	70.68	2.99	14.04	0.70	3.58	0.26	3.38	0.14	1.39	0.08	2.91	0.13	0.38	0.06	0.59	0.08
U1B	73.59	3.11	12.37	0.62	3.45	0.25	3.37	0.14	1.10	0.07	2.56	0.12	0.33	0.06	0.55	0.07
U1B	72.03	3.04	13.89	0.69	2.15	0.17	3.57	0.14	1.23	0.08	2.91	0.13	0.33	0.06	0.53	0.07
U1B	72.96	3.08	14.18	0.71	3.61	0.26	3.36	0.14	1.36	0.08	2.86	0.13	0.26	0.05	0.53	0.07
U1B	73.56	3.11	14.17	0.71	3.39	0.25	3.27	0.13	1.52	0.08	2.90	0.13	0.32	0.06	0.58	0.08
U1B	71.04	3.00	14.01	0.70	3.45	0.25	3.33	0.14	1.59	0.09	2.99	0.13	0.35	0.06	0.55	0.07
U1B	71.73	3.03	13.39	0.67	3.49	0.25	3.33	0.14	1.35	0.08	2.87	0.13	0.29	0.06	0.53	0.07
U1B	69.92	2.96	15.03	0.75	3.46	0.25	3.23	0.13	1.74	0.09	2.97	0.13	0.33	0.06	0.59	0.08
U1B	72.59	3.07	13.93	0.70	3.66	0.26	3.52	0.14	1.81	0.09	2.84	0.13	0.33	0.06	0.61	0.08
U1B	72.32	3.06	14.17	0.71	1.69	0.14	3.79	0.15	1.35	0.08	3.00	0.13	0.39	0.06	0.54	0.07
U1B	72.12	3.05	14.70	0.73	3.48	0.25	3.44	0.14	1.85	0.09	3.16	0.14	0.40	0.06	0.73	0.08
U1B	72.76	3.07	13.85	0.69	3.65	0.26	3.45	0.14	1.34	0.08	2.80	0.12	0.30	0.06	0.48	0.07
U1B	71.80	3.03	14.15	0.71	3.55	0.26	3.34	0.14	1.36	0.08	2.98	0.13	0.38	0.06	0.54	0.07
U1B	73.01	3.08	14.31	0.71	3.39	0.25	3.17	0.13	1.52	0.08	2.87	0.13	0.39	0.06	0.58	0.08
U1B	71.51	3.02	13.84	0.69	3.44	0.25	3.27	0.13	1.42	0.08	2.88	0.13	0.38	0.06	0.54	0.07
U1B	73.38	3.10	14.19	0.71	3.65	0.26	3.33	0.14	1.50	0.08	2.81	0.12	0.34	0.06	0.59	0.08
U1B	71.72	3.03	14.15	0.71	3.72	0.27	3.55	0.14	1.34	0.08	3.03	0.13	0.33	0.06	0.51	0.07
U1B	71.56	3.02	13.93	0.70	3.37	0.25	3.50	0.14	1.33	0.08	2.94	0.13	0.33	0.06	0.50	0.07
U1B	72.48	3.06	14.26	0.71	3.70	0.27	3.43	0.14	1.32	0.08	2.71	0.12	0.38	0.06	0.54	0.07
U2	71.93	3.04	12.69	0.64	3.54	0.26	4.33	0.17	2.38	0.11	2.72	0.12	0.31	0.06	0.58	0.08
U2	74.51	3.15	13.13	0.66	3.46	0.25	4.03	0.16	2.95	0.13	2.89	0.13	0.31	0.06	0.78	0.09
U2	71.12	3.01	12.57	0.63	2.96	0.22	4.32	0.17	2.41	0.11	2.52	0.12	0.29	0.06	0.57	0.08
U2	75.51	3.19	13.35	0.67	3.54	0.26	4.62	0.17	0.91	0.07	1.44	0.08	0.15	0.05	0.33	0.06
U2	70.75	2.99	13.61	0.68	3.61	0.26	4.40	0.17	2.04	0.10	2.80	0.12	0.38	0.06	0.63	0.08
U2	75.03	3.17	12.51	0.63	3.77	0.27	4.95	0.18	0.65	0.06	1.73	0.09	0.20	0.05	0.36	0.06
U2	76.97	3.25	10.43	0.53	2.98	0.22	4.02	0.16	2.01	0.10	2.74	0.12	0.28	0.05	0.64	0.08
U2	73.29	3.10	12.53	0.63	3.11	0.23	4.35	0.17	1.43	0.08	2.43	0.11	0.25	0.05	0.53	0.07
U2	72.72	3.07	12.24	0.62	3.04	0.23	4.42	0.17	1.56	0.09	2.14	0.10	0.25	0.05	0.41	0.07
U2	78.80	3.32	13.01	0.65	3.47	0.25	4.72	0.18	0.37	0.05	0.80	0.06	0.12	0.05	0.03	0.05
U2	72.86	3.08	13.42	0.67	3.41	0.25	4.18	0.16	1.71	0.09	2.55	0.12	0.34	0.06	0.56	0.07
U2	71.97	3.04	13.78	0.69	3.54	0.26	4.39	0.17	1.76	0.09	2.55	0.12	0.35	0.06	0.67	0.08
U2	79.12	3.34	12.39	0.62	2.59	0.20	5.12	0.19	0.16	0.04	0.92	0.07	0.11	0.05	0.19	0.05
U2	75.82	3.20	14.08	0.70	3.52	0.26	5.10	0.19	0.36	0.05	0.95	0.07	0.10	0.05	0.23	0.06
U2	74.53	3.15	13.50	0.68	3.46	0.25	4.80	0.18	0.64	0.06	1.36	0.08	0.15	0.05	0.24	0.06
U2	74.11	3.13	13.27	0.66	3.18	0.23	4.49	0.17	1.42	0.08	1.88	0.10	0.17	0.05	0.41	0.07
U2	72.98	3.08	13.42	0.67	3.32	0.24	4.25	0.16	1.91	0.10	2.74	0.12	0.33	0.06	0.71	0.08
U2	69.38	2.93	14.36	0.72	3.97	0.28	4.19	0.16	3.79	0.15	2.92	0.13	0.30	0.06	0.88	0.09
U2	75.48	3.19	9.90	0.51	3.27	0.24	4.36	0.17	1.99	0.10	2.91	0.13	0.16	0.05	0.60	0.08
U2	73.55	3.11	13.50	0.68	2.87	0.22	5.41	0.20	0.95	0.07	1.38	0.08	0.16	0.05	0.27	0.06
U2	75.14	3.17	14.22	0.71	3.73	0.27	5.30	0.20	0.21	0.04	0.84	0.06	0.19	0.05	0.07	0.05
U2	74.23	3.14	14.13	0.70	3.83	0.27	5.21	0.19	0.59	0.06	1.36	0.08	0.27	0.05	0.24	0.06
U2	74.17	3.13	13.39	0.67	3.38	0.25	5.10	0.19	0.27	0.05	0.85	0.06	0.10	0.05	0.10	0.05
U2	76.24	3.22	11.45	0.58	3.22	0.24	4.65	0.18	1.19	0.07	2.11	0.10	0.29	0.06	0.48	0.07

U2	72.96	3.08	13.57	0.68	3.51	0.25	4.17	0.16	2.17	0.10	2.87	0.13	0.27	0.05	0.72	0.08
U2	77.40	3.27	12.16	0.61	3.80	0.27	5.10	0.19	0.97	0.07	1.49	0.08	0.19	0.05	0.26	0.06
U2	76.57	3.23	13.80	0.69	3.70	0.27	5.11	0.19	0.06	0.04	0.86	0.06	0.15	0.05	0.03	0.05
U2	73.52	3.11	12.20	0.62	2.35	0.18	5.00	0.19	0.57	0.06	1.95	0.10	0.27	0.05	0.30	0.06
U2	71.81	3.03	12.05	0.61	3.37	0.25	4.84	0.18	1.19	0.07	2.14	0.10	0.30	0.06	0.55	0.07
U2	71.41	3.02	13.37	0.67	3.27	0.24	4.18	0.16	1.89	0.10	2.74	0.12	0.36	0.06	0.70	0.08
U2	71.24	3.01	13.50	0.68	3.39	0.25	4.34	0.17	2.06	0.10	2.72	0.12	0.31	0.06	0.64	0.08
U2	75.54	3.19	13.93	0.70	3.87	0.28	5.15	0.19	0.60	0.06	1.35	0.08	0.26	0.05	0.25	0.06
U2	74.10	3.13	13.73	0.69	3.74	0.27	5.12	0.19	0.39	0.05	1.37	0.08	0.14	0.05	0.32	0.06
U2	75.56	3.19	14.19	0.71	3.82	0.27	5.23	0.19	0.11	0.04	0.93	0.07	0.15	0.05	0.11	0.05
U2	73.35	3.10	13.07	0.66	3.34	0.24	4.60	0.17	1.56	0.09	2.24	0.11	0.36	0.06	0.47	0.07
U2	74.80	3.16	13.04	0.65	3.11	0.23	5.00	0.19	0.25	0.05	0.91	0.07	0.16	0.05	0.03	0.05
U2	76.45	3.23	14.05	0.70	3.71	0.27	4.98	0.19	0.62	0.06	1.09	0.07	0.23	0.05	0.19	0.06
U2	70.78	2.99	13.87	0.69	3.74	0.27	4.87	0.18	1.67	0.09	2.78	0.12	0.36	0.06	0.64	0.08
U2	70.61	2.98	13.05	0.65	3.22	0.24	4.19	0.16	1.95	0.10	2.83	0.12	0.37	0.06	0.62	0.08
U2	73.66	3.11	11.52	0.58	3.18	0.23	4.31	0.17	2.08	0.10	2.85	0.13	0.33	0.06	0.64	0.08
U2	75.77	3.20	13.93	0.70	3.80	0.27	4.90	0.18	0.30	0.05	1.10	0.07	0.16	0.05	0.11	0.05
U2	74.45	3.14	13.49	0.67	3.17	0.23	4.27	0.16	1.62	0.09	2.17	0.10	0.27	0.05	0.45	0.07
U2	71.72	3.03	12.82	0.64	3.53	0.26	4.44	0.17	1.50	0.08	2.44	0.11	0.32	0.06	0.52	0.07
U2	72.03	3.04	13.43	0.67	2.90	0.22	4.28	0.16	1.82	0.09	2.25	0.11	0.34	0.06	0.64	0.08
U2	72.48	3.06	13.78	0.69	3.51	0.25	4.59	0.17	1.46	0.08	2.63	0.12	0.30	0.06	0.57	0.07
U2	70.20	2.97	13.67	0.68	3.72	0.27	4.51	0.17	2.64	0.12	2.91	0.13	0.35	0.06	0.74	0.08
U2	72.55	3.07	12.53	0.63	2.97	0.22	4.12	0.16	1.79	0.09	3.06	0.13	0.60	0.07	0.65	0.08
U2	74.69	3.15	10.92	0.56	2.87	0.22	4.11	0.16	1.67	0.09	2.65	0.12	0.29	0.06	0.58	0.08
U2	70.16	2.97	14.56	0.72	3.53	0.26	4.19	0.16	2.23	0.11	3.04	0.13	0.35	0.06	0.88	0.09
U2	73.59	3.11	13.37	0.67	3.27	0.24	4.51	0.17	1.14	0.07	1.71	0.09	0.23	0.05	0.38	0.06
U2	73.34	3.10	13.61	0.68	2.98	0.22	4.16	0.16	1.75	0.09	2.47	0.11	0.32	0.06	0.62	0.08
U2	71.68	3.03	13.00	0.65	3.18	0.23	4.25	0.16	1.68	0.09	2.69	0.12	0.39	0.06	0.64	0.08
U2	74.89	3.16	12.00	0.61	3.26	0.24	4.12	0.16	2.10	0.10	2.95	0.13	0.33	0.06	0.64	0.08
U2	72.70	3.07	13.54	0.68	3.23	0.24	4.14	0.16	1.63	0.09	2.94	0.13	0.36	0.06	0.63	0.08
U2	69.62	2.94	13.61	0.68	3.14	0.23	4.27	0.16	1.83	0.09	3.11	0.13	0.40	0.06	0.72	0.08
U2	71.40	3.02	13.40	0.67	2.93	0.22	4.30	0.17	1.77	0.09	2.74	0.12	0.38	0.06	0.64	0.08
U2	73.32	3.10	13.96	0.70	3.34	0.24	4.53	0.17	1.53	0.08	2.13	0.10	0.32	0.06	0.47	0.07
U2	70.33	2.97	13.79	0.69	3.31	0.24	4.29	0.16	2.17	0.10	2.89	0.13	0.43	0.06	0.63	0.08
U2	72.62	3.07	12.78	0.64	3.45	0.25	4.48	0.17	1.88	0.10	2.97	0.13	0.40	0.06	0.64	0.08
U2	71.73	3.03	12.77	0.64	3.06	0.23	4.23	0.16	1.67	0.09	3.05	0.13	0.31	0.06	0.66	0.08
U2	75.50	3.19	13.55	0.68	3.60	0.26	5.08	0.19	0.28	0.05	0.96	0.07	0.13	0.05	0.10	0.05
U2	72.67	3.07	13.08	0.66	3.52	0.26	4.77	0.18	1.42	0.08	1.82	0.09	0.27	0.05	0.37	0.06
U2	71.16	3.01	14.15	0.71	1.03	0.10	4.61	0.17	1.47	0.08	3.33	0.14	0.37	0.06	0.71	0.08
U2	72.28	3.05	12.95	0.65	3.27	0.24	4.28	0.16	1.74	0.09	3.00	0.13	0.37	0.06	0.76	0.08
U2	74.32	3.14	12.54	0.63	3.24	0.24	4.17	0.16	1.34	0.08	2.98	0.13	0.32	0.06	0.66	0.08
U2	70.41	2.98	13.34	0.67	3.08	0.23	4.24	0.16	1.65	0.09	3.23	0.14	0.37	0.06	0.70	0.08
U2	75.62	3.19	14.73	0.73	3.98	0.28	5.11	0.19	1.14	0.07	1.09	0.07	0.13	0.05	0.24	0.06
U3	72.53	3.06	13.99	0.70	3.36	0.25	3.78	0.15	3.30	0.14	2.74	0.12	0.30	0.06	0.70	0.08
U3	74.74	3.16	11.95	0.60	2.90	0.22	3.50	0.14	3.07	0.13	2.72	0.12	0.30	0.06	0.66	0.08
U3	74.82	3.16	11.85	0.60	3.05	0.23	3.74	0.15	2.84	0.12	2.79	0.12	0.26	0.05	0.74	0.08
U3	75.75	3.20	13.10	0.66	3.10	0.23	3.75	0.15	2.39	0.11	2.37	0.11	0.29	0.06	0.63	0.08
U3	70.09	2.96	15.02	0.75	3.47	0.25	4.05	0.16	1.65	0.09	3.30	0.14	0.35	0.06	0.71	0.08
U3	71.91	3.04	13.11	0.66	3.20	0.24	3.90	0.15	2.57	0.12	3.34	0.14	0.33	0.06	0.71	0.08
U3	72.65	3.07	13.35	0.67	3.25	0.24	3.62	0.14	2.19	0.10	2.63	0.12	0.30	0.06	0.60	0.08
U3	71.64	3.03	13.13	0.66	3.06	0.23	3.66	0.15	2.31	0.11	2.72	0.12	0.38	0.06	0.69	0.08
U3	72.64	3.07	13.50	0.68	3.10	0.23	3.81	0.15	2.72	0.12	2.94	0.13	0.36	0.06	0.74	0.08
U3	72.86	3.08	13.70	0.68	2.84	0.21	3.55	0.14	2.96	0.13	2.70	0.12	0.33	0.06	0.74	0.08
U3	73.35	3.10	13.86	0.69	3.27	0.24	3.84	0.15	2.93	0.13	3.04	0.13	0.28	0.06	0.84	0.09
U3	71.63	3.03	12.80	0.64	3.31	0.24	4.07	0.16	2.97	0.13	4.02	0.16	0.47	0.06	0.79	0.09
U3	71.91	3.04	12.83	0.64	3.22	0.24	3.86	0.15	2.88	0.13	3.54	0.15	0.37	0.06	0.69	0.08
U3	77.19	3.26	11.64	0.59	2.88	0.22	3.42	0.14	2.26	0.11	2.74	0.12	0.30	0.06	0.61	0.08
U3	72.46	3.06	12.62	0.63	3.40	0.25	3.83	0.15	2.58	0.12	2.77	0.12	0.34	0.06	0.66	0.08
U3	73.23	3.09	12.63	0.64	3.18	0.23	4.01	0.16	2.67	0.12	2.65	0.12	0.38	0.06	0.63	0.08
U3	76.75	3.24	13.13	0.66	2.87	0.21	3.63	0.14	2.76	0.12	2.84	0.13	0.32	0.06	0.70	0.08
U3	69.78	2.95	14.07	0.70	3.04	0.23	4.02	0.16	2.76	0.12	3.03	0.13	0.39	0.06	0.75	0.08
U3	71.60	3.03	13.14	0.66	3.26	0.24	3.97	0.15	3.24	0.14	3.03	0.13	0.32	0.06	0.74	0.08

U3	72.80	3.08	12.76	0.64	3.06	0.23	4.02	0.16	3.35	0.14	3.49	0.15	0.40	0.06	0.77	0.09
U3	69.64	2.95	14.38	0.72	3.78	0.27	4.02	0.16	2.56	0.12	3.40	0.14	0.38	0.06	0.70	0.08
U3	72.83	3.08	12.89	0.65	3.23	0.24	3.64	0.14	2.57	0.12	2.89	0.13	0.35	0.06	0.71	0.08
U3	77.19	3.26	12.36	0.62	2.80	0.21	3.64	0.14	2.66	0.12	2.66	0.12	0.30	0.06	0.58	0.08
U3	75.24	3.18	13.40	0.67	2.89	0.22	3.72	0.15	2.82	0.12	2.79	0.12	0.30	0.06	0.67	0.08
U3	75.27	3.18	13.77	0.69	2.97	0.22	3.74	0.15	2.72	0.12	2.84	0.13	0.33	0.06	0.71	0.08
U3	74.10	3.13	13.54	0.68	2.52	0.19	3.63	0.14	2.53	0.11	2.82	0.12	0.35	0.06	0.62	0.08
U3	72.48	3.06	13.64	0.68	2.81	0.21	3.98	0.16	2.88	0.13	3.06	0.13	0.35	0.06	0.83	0.09
U3	69.66	2.95	13.89	0.69	2.99	0.22	3.59	0.14	6.71	0.24	3.49	0.15	0.30	0.06	1.29	0.11
U3	72.14	3.05	13.75	0.69	3.57	0.26	3.97	0.15	2.58	0.12	2.89	0.13	0.37	0.06	0.72	0.08
U3	72.39	3.06	14.11	0.70	3.75	0.27	3.72	0.15	3.24	0.14	2.67	0.12	0.36	0.06	0.67	0.08
U3	74.22	3.13	13.28	0.67	2.76	0.21	3.53	0.14	2.76	0.12	3.04	0.13	0.35	0.06	0.73	0.08
U3	75.31	3.18	13.57	0.68	2.92	0.22	3.51	0.14	2.68	0.12	2.80	0.12	0.32	0.06	0.65	0.08
U3	69.18	2.93	13.44	0.67	2.78	0.21	4.14	0.16	2.19	0.10	3.24	0.14	0.35	0.06	0.69	0.08
U3	73.00	3.08	13.37	0.67	2.99	0.22	3.89	0.15	2.82	0.12	3.08	0.13	0.30	0.06	0.83	0.09
U3	74.73	3.16	12.32	0.62	2.56	0.20	3.66	0.15	2.67	0.12	2.65	0.12	0.32	0.06	0.65	0.08
U3	72.08	3.05	14.29	0.71	3.38	0.25	3.99	0.16	1.68	0.09	3.18	0.14	0.33	0.06	0.69	0.08
U3	74.78	3.16	11.64	0.59	3.25	0.24	3.65	0.15	2.63	0.12	2.86	0.13	0.22	0.05	0.70	0.08
U3	75.65	3.19	13.94	0.70	2.81	0.21	3.48	0.14	2.82	0.12	2.63	0.12	0.31	0.06	0.59	0.08
U3	75.04	3.17	13.78	0.69	2.78	0.21	3.60	0.14	2.44	0.11	2.80	0.12	0.28	0.06	0.65	0.08
U3	75.11	3.17	13.42	0.67	2.55	0.20	3.65	0.15	2.44	0.11	2.95	0.13	0.29	0.06	0.68	0.08
U3	72.57	3.07	13.69	0.68	2.88	0.22	3.98	0.16	2.58	0.12	2.75	0.12	0.36	0.06	0.74	0.08
U3	72.60	3.07	13.04	0.65	2.52	0.19	3.78	0.15	2.61	0.12	2.80	0.12	0.30	0.06	0.65	0.08
U3	74.95	3.16	13.38	0.67	2.77	0.21	3.51	0.14	2.79	0.12	2.73	0.12	0.30	0.06	0.66	0.08
U3	71.34	3.02	13.75	0.69	3.06	0.23	3.95	0.15	2.55	0.12	3.20	0.14	0.37	0.06	0.81	0.09
U3	72.87	3.08	13.92	0.70	3.00	0.22	3.60	0.14	3.08	0.13	3.64	0.15	0.48	0.06	0.80	0.09
U3	76.15	3.21	12.77	0.64	2.73	0.21	3.72	0.15	2.81	0.12	2.81	0.12	0.17	0.05	0.69	0.08
U3	73.11	3.09	14.22	0.71	3.00	0.22	3.76	0.15	3.77	0.15	3.16	0.14	0.38	0.06	0.91	0.09
U3	73.37	3.10	13.63	0.68	2.78	0.21	3.90	0.15	2.91	0.13	3.01	0.13	0.29	0.06	0.77	0.09
U3	75.02	3.17	12.83	0.64	2.64	0.20	3.66	0.15	2.78	0.12	3.06	0.13	0.30	0.06	0.84	0.09
U3	70.17	2.97	14.22	0.71	2.93	0.22	3.99	0.16	2.77	0.12	3.20	0.14	0.41	0.06	0.85	0.09
U3	71.33	3.01	13.43	0.67	3.05	0.23	4.11	0.16	2.27	0.11	3.25	0.14	0.39	0.06	0.72	0.08
U3	73.77	3.12	13.26	0.66	2.82	0.21	3.75	0.15	2.69	0.12	2.70	0.12	0.31	0.06	0.62	0.08
U3	73.11	3.09	14.13	0.70	2.72	0.21	3.33	0.14	3.68	0.15	2.66	0.12	0.34	0.06	0.65	0.08
U3	75.08	3.17	13.53	0.68	3.20	0.24	3.97	0.15	2.50	0.11	2.96	0.13	0.38	0.06	0.79	0.09
U3	72.66	3.07	13.64	0.68	3.06	0.23	3.94	0.15	2.69	0.12	2.93	0.13	0.41	0.06	0.67	0.08
U3	77.66	3.28	11.76	0.59	2.67	0.20	3.47	0.14	2.67	0.12	2.81	0.12	0.33	0.06	0.65	0.08
U3	72.35	3.06	13.69	0.68	3.29	0.24	3.86	0.15	3.18	0.13	3.01	0.13	0.35	0.06	0.69	0.08
U3	73.12	3.09	13.25	0.66	3.00	0.22	3.76	0.15	2.40	0.11	2.67	0.12	0.36	0.06	0.69	0.08
U3	75.01	3.17	12.37	0.62	2.83	0.21	3.68	0.15	2.70	0.12	2.86	0.13	0.32	0.06	0.69	0.08
U3	72.57	3.07	12.97	0.65	2.94	0.22	3.77	0.15	2.34	0.11	2.77	0.12	0.31	0.06	0.63	0.08
U3	72.59	3.07	12.74	0.64	3.19	0.24	3.65	0.15	2.23	0.11	2.61	0.12	0.30	0.06	0.56	0.07
U3	72.44	3.06	13.01	0.65	3.15	0.23	3.65	0.14	2.49	0.11	2.79	0.12	0.28	0.05	0.70	0.08
U3	71.73	3.03	14.26	0.71	3.09	0.23	3.89	0.15	2.70	0.12	3.11	0.13	0.41	0.06	0.79	0.09
U3	76.61	3.23	12.08	0.61	2.68	0.20	3.58	0.14	2.58	0.12	2.49	0.11	0.27	0.05	0.51	0.07
U3	75.47	3.19	13.62	0.68	2.86	0.21	3.56	0.14	2.87	0.12	2.91	0.13	0.36	0.06	0.69	0.08
U3	77.67	3.28	12.40	0.62	2.80	0.21	3.56	0.14	2.53	0.11	2.69	0.12	0.34	0.06	0.68	0.08
U3	70.78	2.99	14.42	0.72	2.97	0.22	3.82	0.15	3.77	0.15	3.04	0.13	0.39	0.06	0.89	0.09
U3	73.93	3.12	12.98	0.65	2.59	0.20	3.99	0.16	2.23	0.11	2.56	0.12	0.33	0.06	0.59	0.08
U3	72.34	3.06	12.95	0.65	2.79	0.21	3.67	0.15	2.96	0.13	2.79	0.12	0.30	0.06	0.63	0.08
U3	74.77	3.16	13.01	0.65	2.88	0.22	3.79	0.15	2.16	0.10	2.38	0.11	0.25	0.05	0.64	0.08
U3	74.80	3.16	12.83	0.64	2.87	0.22	4.05	0.16	2.63	0.12	3.08	0.13	0.40	0.06	0.70	0.08
U3	72.81	3.08	13.24	0.66	2.88	0.22	3.74	0.15	2.56	0.12	2.56	0.12	0.30	0.06	0.64	0.08
U4	70.57	2.98	13.34	0.67	3.15	0.23	3.82	0.15	1.86	0.09	2.90	0.13	0.32	0.06	0.68	0.08
U4	74.09	3.13	12.97	0.65	2.68	0.20	3.18	0.13	2.59	0.12	2.68	0.12	0.27	0.05	0.53	0.07
U4	70.58	2.98	13.48	0.67	3.19	0.23	3.64	0.14	2.05	0.10	2.95	0.13	0.38	0.06	0.66	0.08
U4	71.80	3.03	13.55	0.68	3.32	0.24	3.70	0.15	1.95	0.10	2.78	0.12	0.32	0.06	0.58	0.08
U4	74.93	3.16	13.39	0.67	3.17	0.23	3.81	0.15	1.76	0.09	2.71	0.12	0.28	0.06	0.58	0.08
U4	72.37	3.06	13.89	0.69	3.29	0.24	3.90	0.15	2.03	0.10	3.03	0.13	0.34	0.06	0.70	0.08
U4	71.32	3.01	14.02	0.70	2.85	0.21	3.51	0.14	2.86	0.12	2.85	0.13	0.33	0.06	0.65	0.08
U4	74.59	3.15	12.83	0.64	2.85	0.21	3.52	0.14	2.51	0.11	2.64	0.12	0.23	0.05	0.54	0.07
U4	72.84	3.08	13.40	0.67	3.22	0.24	3.80	0.15	1.70	0.09	2.96	0.13	0.35	0.06	0.70	0.08

U4	71.12	3.01	14.12	0.70	3.46	0.25	3.68	0.15	2.03	0.10	3.00	0.13	0.45	0.06	0.75	0.08
U4	72.55	3.07	14.61	0.73	3.36	0.25	3.72	0.15	2.17	0.10	3.15	0.13	0.38	0.06	0.72	0.08
U4	72.86	3.08	13.50	0.68	2.75	0.21	3.39	0.14	2.82	0.12	2.86	0.13	0.34	0.06	0.59	0.08
U4	70.15	2.97	15.01	0.75	2.84	0.21	3.46	0.14	3.59	0.15	2.81	0.12	0.34	0.06	0.64	0.08
U4	72.21	3.05	14.29	0.71	3.40	0.25	3.82	0.15	1.81	0.09	3.06	0.13	0.33	0.06	0.70	0.08
U4	70.34	2.97	13.81	0.69	3.26	0.24	3.86	0.15	2.04	0.10	3.04	0.13	0.41	0.06	0.65	0.08
U4	71.90	3.04	13.89	0.69	3.24	0.24	3.63	0.14	2.08	0.10	3.12	0.13	0.36	0.06	0.70	0.08
U4	71.27	3.01	12.81	0.64	3.08	0.23	3.80	0.15	1.86	0.09	2.83	0.12	0.28	0.05	0.63	0.08
U4	75.30	3.18	13.34	0.67	2.57	0.20	3.24	0.13	2.57	0.12	2.54	0.12	0.34	0.06	0.59	0.08
U4	70.37	2.98	14.88	0.74	2.77	0.21	3.48	0.14	3.51	0.14	2.75	0.12	0.34	0.06	0.63	0.08
U4	70.77	2.99	14.98	0.74	3.05	0.23	3.56	0.14	3.20	0.14	2.87	0.13	0.37	0.06	0.65	0.08
U4	70.40	2.98	13.63	0.68	3.19	0.24	3.81	0.15	1.94	0.10	3.18	0.14	0.38	0.06	0.69	0.08
U4	72.06	3.04	13.78	0.69	2.73	0.21	3.36	0.14	3.13	0.13	2.86	0.13	0.37	0.06	0.63	0.08
U4	68.47	2.90	15.40	0.76	2.55	0.20	3.36	0.14	4.03	0.16	2.96	0.13	0.39	0.06	0.62	0.08
U4	71.07	3.00	14.92	0.74	2.86	0.21	3.41	0.14	3.56	0.15	2.79	0.12	0.33	0.06	0.63	0.08
U4	69.80	2.95	14.37	0.72	2.64	0.20	3.49	0.14	3.56	0.15	2.68	0.12	0.38	0.06	0.58	0.08
U4	71.66	3.03	15.04	0.75	2.91	0.22	3.49	0.14	3.49	0.14	2.78	0.12	0.32	0.06	0.61	0.08
U4	72.90	3.08	13.76	0.69	3.01	0.22	3.76	0.15	2.05	0.10	2.83	0.13	0.41	0.06	0.58	0.08
U4	71.93	3.04	13.97	0.70	3.34	0.24	3.89	0.15	1.90	0.10	3.12	0.13	0.39	0.06	0.71	0.08
U4	70.80	2.99	15.32	0.76	3.31	0.24	3.63	0.14	3.41	0.14	2.82	0.12	0.34	0.06	0.63	0.08
U4	69.83	2.95	16.33	0.81	2.83	0.21	3.24	0.13	4.01	0.16	2.96	0.13	0.40	0.06	0.68	0.08
U4	70.76	2.99	15.26	0.76	2.73	0.21	3.40	0.14	3.63	0.15	2.84	0.13	0.27	0.05	0.65	0.08
U4	71.83	3.04	14.90	0.74	2.80	0.21	3.41	0.14	3.54	0.15	2.79	0.12	0.36	0.06	0.65	0.08
U4	71.05	3.00	15.89	0.79	2.85	0.21	3.41	0.14	3.92	0.16	2.89	0.13	0.32	0.06	0.68	0.08
U4	70.65	2.99	15.21	0.75	3.13	0.23	3.55	0.14	3.50	0.14	2.98	0.13	0.31	0.06	0.64	0.08
U4	72.62	3.07	13.87	0.69	3.31	0.24	3.77	0.15	2.02	0.10	2.92	0.13	0.37	0.06	0.60	0.08
U4	71.83	3.04	13.26	0.66	3.08	0.23	3.91	0.15	1.85	0.09	2.88	0.13	0.28	0.05	0.56	0.07
U4	71.47	3.02	14.01	0.70	3.25	0.24	3.75	0.15	1.92	0.10	2.99	0.13	0.29	0.06	0.64	0.08
U4	71.48	3.02	15.00	0.74	2.74	0.21	3.43	0.14	3.64	0.15	2.78	0.12	0.37	0.06	0.60	0.08
U4	70.70	2.99	15.58	0.77	2.78	0.21	3.42	0.14	3.91	0.16	2.68	0.12	0.40	0.06	0.66	0.08
U4	70.71	2.99	16.02	0.79	2.88	0.22	3.40	0.14	3.97	0.16	2.91	0.13	0.35	0.06	0.71	0.08
U4	71.25	3.01	15.08	0.75	2.87	0.21	3.36	0.14	3.47	0.14	2.79	0.12	0.36	0.06	0.64	0.08
U4	73.14	3.09	12.94	0.65	3.02	0.22	3.69	0.15	2.14	0.10	2.94	0.13	0.32	0.06	0.64	0.08
U4	71.51	3.02	13.48	0.67	3.22	0.24	3.86	0.15	1.99	0.10	2.93	0.13	0.37	0.06	0.61	0.08
U4	66.62	2.82	17.73	0.87	2.18	0.17	3.18	0.13	4.81	0.18	3.29	0.14	0.40	0.06	0.74	0.08
U4	71.18	3.01	15.55	0.77	2.84	0.21	3.39	0.14	3.82	0.15	2.94	0.13	0.27	0.05	0.66	0.08
U4	74.47	3.15	13.97	0.70	2.74	0.21	3.40	0.14	3.35	0.14	2.73	0.12	0.21	0.05	0.60	0.08
U4	70.18	2.97	15.11	0.75	2.78	0.21	3.45	0.14	3.75	0.15	2.88	0.13	0.35	0.06	0.63	0.08
U4	72.12	3.05	14.50	0.72	3.01	0.22	3.41	0.14	3.13	0.13	3.03	0.13	0.38	0.06	0.70	0.08
U4	73.37	3.10	13.08	0.66	2.60	0.20	3.23	0.13	2.58	0.12	2.69	0.12	0.29	0.06	0.55	0.07
U4	72.71	3.07	15.05	0.75	3.04	0.23	3.45	0.14	3.70	0.15	2.80	0.12	0.35	0.06	0.70	0.08
U4	69.88	2.95	15.38	0.76	2.73	0.21	3.47	0.14	3.84	0.15	2.80	0.12	0.35	0.06	0.61	0.08
U4	72.82	3.08	15.59	0.77	2.93	0.22	3.49	0.14	3.52	0.14	2.82	0.12	0.33	0.06	0.61	0.08
U4	71.46	3.02	15.40	0.76	2.86	0.21	3.29	0.13	3.61	0.15	2.84	0.13	0.33	0.06	0.60	0.08
U4	70.67	2.99	14.14	0.71	3.26	0.24	3.92	0.15	1.87	0.09	3.20	0.14	0.44	0.06	0.61	0.08
U4	71.27	3.01	13.49	0.67	3.35	0.24	3.75	0.15	2.06	0.10	2.94	0.13	0.36	0.06	0.66	0.08
U4	70.55	2.98	13.14	0.66	3.06	0.23	3.89	0.15	1.91	0.10	3.00	0.13	0.41	0.06	0.66	0.08
U4	72.04	3.04	14.85	0.74	2.89	0.22	3.46	0.14	3.53	0.14	2.77	0.12	0.33	0.06	0.59	0.08
U4	71.42	3.02	13.56	0.68	3.14	0.23	3.76	0.15	1.86	0.09	2.96	0.13	0.38	0.06	0.66	0.08
U4	74.58	3.15	13.50	0.68	2.86	0.21	3.27	0.13	2.89	0.13	2.74	0.12	0.35	0.06	0.60	0.08
U4	70.88	3.00	14.11	0.70	3.30	0.24	3.79	0.15	1.94	0.10	3.09	0.13	0.33	0.06	0.68	0.08
U4	70.45	2.98	13.17	0.66	3.02	0.22	3.69	0.15	2.17	0.10	2.93	0.13	0.34	0.06	0.59	0.08
U4	71.44	3.02	14.78	0.73	2.86	0.21	3.44	0.14	3.53	0.15	2.71	0.12	0.22	0.05	0.66	0.08
U4	71.81	3.03	15.02	0.75	2.87	0.21	3.41	0.14	3.52	0.14	2.72	0.12	0.34	0.06	0.63	0.08
U4	70.00	2.96	15.08	0.75	2.76	0.21	3.40	0.14	3.61	0.15	2.95	0.13	0.32	0.06	0.58	0.08
U4	71.68	3.03	15.27	0.76	2.83	0.21	3.45	0.14	3.68	0.15	2.83	0.13	0.29	0.06	0.57	0.08
U4	72.24	3.05	13.88	0.69	3.46	0.25	3.86	0.15	1.84	0.09	3.00	0.13	0.33	0.06	0.70	0.08
U4	70.92	3.00	13.00	0.65	2.86	0.21	3.68	0.15	2.69	0.12	2.70	0.12	0.37	0.06	0.54	0.07
U4	72.44	3.06	13.88	0.69	2.74	0.21	3.47	0.14	3.37	0.14	2.39	0.11	0.36	0.06	0.58	0.08
U4	69.91	2.96	15.52	0.77	2.73	0.21	3.33	0.14	3.86	0.15	2.92	0.13	0.43	0.06	0.65	0.08
U4	72.63	3.07	15.34	0.76	2.95	0.22	3.31	0.13	3.69	0.15	2.91	0.13	0.35	0.06	0.64	0.08
U4	70.58	2.98	15.02	0.75	2.74	0.21	3.46	0.14	3.72	0.15	2.87	0.13	0.33	0.06	0.60	0.08

U4	70.05	2.96	14.78	0.73	2.71	0.21	3.41	0.14	3.65	0.15	2.77	0.12	0.35	0.06	0.60	0.08
U4	70.71	2.99	15.20	0.75	2.74	0.21	3.38	0.14	3.79	0.15	2.85	0.13	0.32	0.06	0.67	0.08
U4	74.32	3.14	13.52	0.68	2.61	0.20	3.29	0.13	2.66	0.12	2.90	0.13	0.34	0.06	0.53	0.07

Appendix C

EDS Agglomerate Analyses

This Appendix contains the EDS raster data collected across agglomerates and BSE images and/or compositional maps identifying the 58 agglomerates characterized for their major element compositions with EDS.

Table C.1: Compositions of 58 agglomerates in 15 samples measured by EDS. Analytical procedure is detailed in Chapter 4. Uncertainties are calculated as detailed in Chapter 6.

Sample	Agglom-erate	SiO_2	1σ	Al_2O_3	1σ	Na_2O	1σ	K_2O	1σ	CaO	1σ	FeO	1σ	TiO_2	1σ	MgO	1σ
AA.B	B1	75.78	3.20	12.63	0.64	3.66	0.26	3.29	0.13	2.59	0.12	2.47	0.11	0.25	0.05	0.73	0.08
AA.B	B1	75.15	3.17	12.78	0.64	3.76	0.27	3.43	0.14	2.52	0.11	2.43	0.11	0.23	0.05	0.76	0.08
AA.B	B1	70.13	2.96	13.34	0.67	3.88	0.28	3.76	0.15	2.22	0.11	2.74	0.12	0.33	0.06	0.87	0.09
AA.B	B1	75.87	3.20	13.75	0.69	3.88	0.28	3.42	0.14	2.30	0.11	2.72	0.12	0.22	0.05	0.80	0.09
AA.B	B1	74.58	3.15	12.41	0.63	3.60	0.26	3.47	0.14	2.26	0.11	2.53	0.12	0.23	0.05	0.71	0.08
AA.B	B1	75.01	3.17	14.13	0.70	3.63	0.26	3.36	0.14	2.93	0.13	2.49	0.11	0.28	0.06	0.79	0.09
AA.B	B1	76.40	3.22	13.30	0.67	3.63	0.26	3.25	0.13	2.78	0.12	2.32	0.11	0.29	0.06	0.74	0.08
AA.B	B1	74.66	3.15	13.83	0.69	3.77	0.27	3.52	0.14	2.61	0.12	2.55	0.12	0.31	0.06	0.79	0.09
AA.B	B1	74.26	3.14	13.19	0.66	3.59	0.26	3.38	0.14	2.64	0.12	2.63	0.12	0.32	0.06	0.68	0.08
AA.B	B1	75.57	3.19	12.37	0.62	3.66	0.26	3.46	0.14	2.67	0.12	2.64	0.12	0.30	0.06	0.72	0.08
AA.B	B1	73.86	3.12	13.79	0.69	3.90	0.28	3.88	0.15	2.75	0.12	2.97	0.13	0.25	0.05	0.81	0.09
AA.B	B1	75.32	3.18	14.47	0.72	3.63	0.26	3.27	0.13	2.85	0.12	2.63	0.12	0.14	0.05	0.83	0.09
AA.B	B1	74.66	3.15	13.43	0.67	3.83	0.27	3.56	0.14	2.32	0.11	2.66	0.12	0.33	0.06	0.77	0.09
AA.B	B1	74.53	3.15	13.78	0.69	3.43	0.25	3.27	0.13	2.87	0.13	2.64	0.12	0.29	0.06	0.68	0.08
AA.B	B1	72.78	3.08	14.17	0.71	3.82	0.27	3.49	0.14	2.65	0.12	2.57	0.12	0.34	0.06	0.79	0.09
AA.B	B1	73.30	3.10	13.71	0.69	3.72	0.27	3.64	0.14	2.49	0.11	2.41	0.11	0.34	0.06	0.77	0.09
AA.B	B1	73.44	3.10	14.15	0.71	3.48	0.25	3.27	0.13	3.08	0.13	2.53	0.12	0.30	0.06	0.75	0.08
AA.B	B1	74.18	3.13	13.69	0.68	3.67	0.26	3.42	0.14	2.71	0.12	2.54	0.12	0.36	0.06	0.76	0.08
AA.B	B1	73.46	3.10	13.42	0.67	3.60	0.26	3.46	0.14	2.54	0.11	2.59	0.12	0.37	0.06	0.82	0.09
AA.B	B1	74.91	3.16	14.08	0.70	3.69	0.27	3.50	0.14	2.54	0.12	2.55	0.12	0.23	0.05	0.80	0.09
AA.B	B1	73.50	3.10	14.38	0.72	4.03	0.29	3.86	0.15	2.02	0.10	3.07	0.13	0.39	0.06	0.88	0.09
AA.B	B1	73.72	3.11	14.35	0.71	4.18	0.30	3.93	0.15	1.92	0.10	2.96	0.13	0.22	0.05	0.74	0.08
AA.B	B1	74.00	3.13	14.01	0.70	3.60	0.26	3.43	0.14	2.88	0.13	2.58	0.12	0.30	0.06	0.66	0.08
AA.B	B1	72.71	3.07	13.97	0.70	3.61	0.26	3.36	0.14	2.85	0.12	2.63	0.12	0.22	0.05	0.70	0.08
AA.B	B1	72.23	3.05	14.24	0.71	3.70	0.27	3.56	0.14	2.75	0.12	2.98	0.13	0.25	0.05	0.81	0.09
AA.B	B1	71.42	3.02	13.62	0.68	3.52	0.26	3.49	0.14	2.42	0.11	2.53	0.12	0.41	0.06	0.79	0.09
AA.B	B1	73.89	3.12	14.06	0.70	3.71	0.27	3.50	0.14	2.41	0.11	2.56	0.12	0.24	0.05	0.75	0.08
AA.B	B1	72.27	3.05	14.36	0.72	3.98	0.28	3.86	0.15	2.13	0.10	2.87	0.13	0.41	0.06	0.86	0.09
AA.B	B1	71.88	3.04	14.17	0.71	4.07	0.29	3.73	0.15	2.29	0.11	2.77	0.12	0.36	0.06	0.76	0.08
AA.B	B1	75.07	3.17	14.63	0.73	3.76	0.27	3.34	0.14	2.93	0.13	2.57	0.12	0.24	0.05	0.74	0.08
AA.B	B1	74.88	3.16	13.93	0.70	3.80	0.27	3.57	0.14	2.44	0.11	2.66	0.12	0.29	0.06	0.79	0.09
AA.B	B1	75.19	3.17	13.40	0.67	3.76	0.27	3.74	0.15	2.18	0.10	2.41	0.11	0.13	0.05	0.78	0.09
AA.B	B1	72.24	3.05	14.27	0.71	4.08	0.29	4.04	0.16	1.64	0.09	2.98	0.13	0.37	0.06	0.82	0.09
AA.B	B1	73.54	3.11	14.29	0.71	3.96	0.28	3.93	0.15	2.27	0.11	2.75	0.12	0.33	0.06	0.81	0.09
AA.B	B1	74.07	3.13	13.90	0.69	4.21	0.30	4.03	0.16	1.96	0.10	2.64	0.12	0.30	0.06	0.70	0.08
AA.B	B1	73.23	3.09	12.83	0.64	3.48	0.25	3.49	0.14	2.55	0.12	2.46	0.11	0.17	0.05	0.69	0.08
AA.B	B1	71.49	3.02	13.63	0.68	3.74	0.27	3.70	0.15	2.34	0.11	2.61	0.12	0.38	0.06	0.83	0.09
AA.B	B1	74.82	3.16	14.04	0.70	3.92	0.28	3.65	0.15	2.16	0.10	2.57	0.12	0.23	0.05	0.87	0.09
AA.B	B1	72.48	3.06	14.35	0.71	4.22	0.30	4.20	0.16	2.06	0.10	2.82	0.12	0.29	0.06	0.87	0.09
AA.B	B1	74.14	3.13	14.43	0.72	4.35	0.31	4.06	0.16	2.31	0.11	2.62	0.12	0.31	0.06	0.77	0.09
AA.B	B1	75.40	3.18	12.85	0.65	3.98	0.28	3.81	0.15	1.98	0.10	2.55	0.12	0.29	0.06	0.64	0.08

AA.B	B1	73.70	3.11	13.53	0.68	3.77	0.27	3.61	0.14	2.51	0.11	2.53	0.12	0.37	0.06	0.66	0.08
AA.B	B1	74.69	3.15	12.18	0.61	3.18	0.23	3.81	0.15	2.18	0.10	2.41	0.11	0.31	0.06	0.70	0.08
AA.B	B2	73.43	3.10	13.39	0.67	4.64	0.32	4.25	0.16	2.24	0.11	2.42	0.11	0.31	0.06	0.91	0.09
AA.B	B2	70.76	2.99	13.23	0.66	3.31	0.24	4.14	0.16	2.36	0.11	2.37	0.11	0.19	0.05	0.68	0.08
AA.B	B2	73.62	3.11	13.40	0.67	3.22	0.24	4.23	0.16	2.58	0.12	2.51	0.12	0.21	0.05	0.75	0.08
AA.B	B2	72.71	3.07	14.41	0.72	3.05	0.23	4.13	0.16	2.36	0.11	2.41	0.11	0.28	0.05	0.76	0.08
AA.B	B3	74.50	3.15	13.00	0.65	3.04	0.23	3.91	0.15	2.59	0.12	2.46	0.11	0.21	0.05	0.76	0.08
AA.B	B3	73.84	3.12	13.74	0.69	3.98	0.28	3.74	0.15	2.30	0.11	2.42	0.11	0.27	0.05	0.73	0.08
AA.B	B3	72.25	3.05	13.90	0.69	4.16	0.29	3.80	0.15	2.24	0.11	2.70	0.12	0.30	0.06	0.82	0.09
AA.B	B3	73.39	3.10	13.70	0.68	4.46	0.31	3.95	0.15	2.29	0.11	2.71	0.12	0.28	0.06	0.85	0.09
AA.B	B3	70.45	2.98	12.22	0.62	4.48	0.31	4.02	0.16	2.35	0.11	2.72	0.12	0.25	0.05	0.82	0.09
AA.B	B3	74.38	3.14	13.94	0.70	3.96	0.28	3.51	0.14	2.55	0.12	2.52	0.12	0.29	0.06	0.74	0.08
AA.B	B3	75.70	3.20	14.45	0.72	3.83	0.27	3.23	0.13	2.46	0.11	2.55	0.12	0.32	0.06	0.74	0.08
AA.B	B3	69.30	2.93	13.72	0.69	3.92	0.28	3.85	0.15	2.81	0.12	2.67	0.12	0.33	0.06	0.75	0.08
AA.B	B3	74.10	3.13	13.89	0.69	3.98	0.28	3.57	0.14	2.44	0.11	2.70	0.12	0.35	0.06	0.90	0.09
AA.B	B3	73.70	3.11	14.29	0.71	3.60	0.26	3.31	0.13	2.70	0.12	2.62	0.12	0.27	0.05	0.80	0.09
AA.B	B3	73.08	3.09	13.66	0.68	3.92	0.28	3.62	0.14	2.52	0.11	2.51	0.12	0.31	0.06	0.67	0.08
AA.B	B3	69.73	2.95	13.73	0.69	4.08	0.29	4.01	0.16	2.93	0.13	2.59	0.12	0.24	0.05	0.69	0.08
AA.B	B3	72.37	3.06	13.21	0.66	4.13	0.29	3.89	0.15	2.25	0.11	2.47	0.11	0.27	0.05	0.69	0.08
AA.B	B3	73.01	3.08	13.33	0.67	4.24	0.30	4.04	0.16	2.27	0.11	2.49	0.11	0.29	0.06	0.76	0.08
AA.B	B3	71.27	3.01	13.58	0.68	4.19	0.30	4.07	0.16	2.42	0.11	2.38	0.11	0.29	0.06	0.70	0.08
AA.B	B3	71.35	3.02	15.04	0.75	4.45	0.31	4.28	0.16	2.01	0.10	1.95	0.10	0.16	0.05	0.72	0.08
AA.B	B3	74.72	3.16	12.99	0.65	2.69	0.20	3.95	0.15	2.50	0.11	2.46	0.11	0.18	0.05	0.72	0.08
AA.B	B3	72.26	3.05	14.10	0.70	2.44	0.19	3.53	0.14	2.53	0.11	2.68	0.12	0.21	0.05	0.71	0.08
AA.B	B3	73.91	3.12	13.60	0.68	3.09	0.23	3.56	0.14	2.49	0.11	2.52	0.12	0.29	0.06	0.77	0.09
AA.B	B3	73.94	3.12	13.76	0.69	3.55	0.26	3.39	0.14	2.56	0.12	2.52	0.12	0.32	0.06	0.81	0.09
AA.B	B3	75.44	3.19	13.72	0.69	3.60	0.26	3.36	0.14	2.47	0.11	2.46	0.11	0.26	0.05	0.75	0.08
AA.B	B3	72.27	3.05	14.41	0.72	3.67	0.26	3.36	0.14	2.67	0.12	2.68	0.12	0.26	0.05	0.73	0.08
AA.B	B3	75.18	3.17	13.96	0.70	3.57	0.26	3.40	0.14	2.42	0.11	2.45	0.11	0.33	0.06	0.75	0.08
AA.B	B3	72.39	3.06	15.15	0.75	3.78	0.27	3.32	0.14	2.74	0.12	2.69	0.12	0.27	0.05	0.74	0.08
AA.B	B3	72.16	3.05	14.40	0.72	3.84	0.28	3.52	0.14	2.66	0.12	2.54	0.12	0.19	0.05	0.68	0.08
AA.B	B3	73.45	3.10	13.87	0.69	3.97	0.28	3.62	0.14	2.36	0.11	2.67	0.12	0.31	0.06	0.83	0.09
AA.B	B3	78.33	3.30	10.16	0.52	3.17	0.23	3.21	0.13	1.48	0.08	2.09	0.10	0.27	0.05	0.63	0.08
AA.B	B3	74.91	3.16	12.42	0.63	3.83	0.27	3.75	0.15	2.12	0.10	2.65	0.12	0.32	0.06	0.67	0.08
AA.B	B3	71.96	3.04	14.42	0.72	3.47	0.25	3.29	0.13	2.64	0.12	2.55	0.12	0.28	0.05	0.75	0.08
AA.B	B3	73.27	3.10	13.77	0.69	3.72	0.27	3.60	0.14	2.51	0.11	2.50	0.11	0.26	0.05	0.74	0.08
AA.B	B3	74.31	3.14	12.62	0.63	3.80	0.27	3.72	0.15	2.07	0.10	2.48	0.11	0.15	0.05	0.71	0.08
AA.B	B3	70.89	3.00	13.53	0.68	3.85	0.28	3.64	0.14	2.11	0.10	2.40	0.11	0.29	0.06	0.74	0.08
AA.B	B3	72.42	3.06	14.46	0.72	3.84	0.28	3.56	0.14	2.51	0.11	2.55	0.12	0.29	0.06	0.72	0.08
AA.B	B3	73.81	3.12	13.36	0.67	3.78	0.27	3.59	0.14	2.42	0.11	2.54	0.12	0.26	0.05	0.71	0.08
AA.B	B3	73.29	3.10	13.33	0.67	4.06	0.29	3.90	0.15	2.18	0.10	2.52	0.12	0.33	0.06	0.74	0.08
AA.B	B3	76.40	3.22	11.47	0.58	3.57	0.26	3.47	0.14	2.21	0.11	2.37	0.11	0.23	0.05	0.65	0.08
AA.B	B3	76.23	3.22	12.11	0.61	3.65	0.26	3.49	0.14	2.22	0.11	2.41	0.11	0.29	0.06	0.65	0.08
AA.B	B3	72.69	3.07	13.33	0.67	3.86	0.28	3.76	0.15	2.22	0.11	2.55	0.12	0.36	0.06	0.74	0.08
AA.B	B3	71.92	3.04	13.65	0.68	3.89	0.28	3.73	0.15	1.94	0.10	2.47	0.11	0.26	0.05	0.74	0.08
AA.B	B3	75.14	3.17	12.53	0.63	3.66	0.26	3.54	0.14	2.31	0.11	2.47	0.11	0.33	0.06	0.75	0.08

AA.B	B3	74.26	3.14	12.06	0.61	3.69	0.27	3.65	0.15	2.31	0.11	2.42	0.11	0.27	0.05	0.65	0.08
AA.B	B3	78.81	3.32	10.83	0.55	3.12	0.23	3.21	0.13	1.78	0.09	2.08	0.10	0.25	0.05	0.75	0.08
AA.B	B3	71.90	3.04	14.41	0.72	3.93	0.28	3.74	0.15	2.32	0.11	2.69	0.12	0.27	0.05	0.73	0.08
AA.B	B3	72.50	3.06	13.45	0.67	3.95	0.28	3.75	0.15	1.92	0.10	2.65	0.12	0.27	0.05	0.67	0.08
AA.B	B3	73.37	3.10	12.85	0.65	3.81	0.27	3.61	0.14	2.16	0.10	2.75	0.12	0.31	0.06	0.67	0.08
AA.B	B3	72.39	3.06	13.51	0.68	3.84	0.27	3.54	0.14	2.34	0.11	2.58	0.12	0.26	0.05	0.70	0.08
AA.B	B3	73.61	3.11	13.16	0.66	3.84	0.28	3.66	0.15	2.28	0.11	2.50	0.11	0.36	0.06	0.73	0.08
AA.B	B3	74.47	3.14	12.32	0.62	3.75	0.27	3.54	0.14	2.15	0.10	2.43	0.11	0.26	0.05	0.77	0.09
AA.B	B3	72.36	3.06	13.57	0.68	3.93	0.28	3.73	0.15	2.39	0.11	2.68	0.12	0.27	0.05	0.77	0.09
AA.B	B3	70.76	2.99	14.99	0.74	3.98	0.28	3.66	0.15	2.78	0.12	2.56	0.12	0.29	0.06	0.75	0.08
AA.B	B3	73.33	3.10	13.78	0.69	3.66	0.26	3.48	0.14	2.48	0.11	2.44	0.11	0.19	0.05	0.75	0.08
AA.B	B3	72.69	3.07	13.46	0.67	3.99	0.28	3.88	0.15	2.50	0.11	2.53	0.12	0.28	0.06	0.83	0.09
AA.B	B3	75.08	3.17	12.92	0.65	3.98	0.28	3.76	0.15	1.74	0.09	2.39	0.11	0.20	0.05	0.68	0.08
AA.B	B3	73.17	3.09	13.62	0.68	4.16	0.29	3.87	0.15	2.15	0.10	2.36	0.11	0.31	0.06	0.71	0.08
AA.B	B3	72.34	3.06	14.72	0.73	4.08	0.29	4.03	0.16	2.36	0.11	2.48	0.11	0.26	0.05	0.75	0.08
AA.B	B3	72.17	3.05	13.37	0.67	4.12	0.29	3.96	0.15	2.47	0.11	2.38	0.11	0.30	0.06	0.70	0.08
AE.C	C2	76.53	3.23	12.14	0.61	3.08	0.23	3.11	0.13	2.51	0.11	2.49	0.11	0.23	0.05	0.60	0.08
AE.C	C2	74.90	3.16	12.26	0.62	3.23	0.24	3.09	0.13	2.48	0.11	2.49	0.11	0.21	0.05	0.57	0.08
AE.C	C2	76.62	3.23	14.01	0.70	3.34	0.24	3.16	0.13	2.81	0.12	2.77	0.12	0.25	0.05	0.63	0.08
AE.C	C2	75.85	3.20	13.64	0.68	3.34	0.24	3.25	0.13	2.60	0.12	2.78	0.12	0.35	0.06	0.61	0.08
AE.C	C2	76.67	3.24	12.40	0.62	3.32	0.24	3.13	0.13	2.39	0.11	2.56	0.12	0.26	0.05	0.63	0.08
AE.C	C2	76.35	3.22	13.26	0.66	3.29	0.24	3.29	0.13	2.60	0.12	2.67	0.12	0.20	0.05	0.55	0.07
AE.C	C2	75.46	3.19	13.03	0.65	3.41	0.25	3.30	0.13	2.51	0.11	2.80	0.12	0.26	0.05	0.56	0.07
AE.C	C2	76.42	3.23	12.65	0.64	2.68	0.20	3.29	0.13	2.79	0.12	2.65	0.12	0.19	0.05	0.53	0.07
AE.C	C1	71.96	3.04	13.59	0.68	5.26	0.36	4.74	0.18	1.85	0.09	2.62	0.12	0.28	0.06	0.62	0.08
AE.C	C1	74.26	3.14	14.38	0.72	2.87	0.22	3.90	0.15	2.22	0.11	2.67	0.12	0.29	0.06	0.62	0.08
AE.C	C1	74.25	3.14	13.75	0.69	4.76	0.33	4.40	0.17	1.95	0.10	2.76	0.12	0.23	0.05	0.57	0.08
AE.C	C1	73.97	3.12	14.26	0.71	4.45	0.31	3.77	0.15	2.12	0.10	2.82	0.12	0.22	0.05	0.63	0.08
AE.C	C1	73.15	3.09	13.15	0.66	5.37	0.37	4.99	0.19	2.04	0.10	2.63	0.12	0.31	0.06	0.58	0.08
AE.C	C1	72.92	3.08	13.69	0.68	4.64	0.32	4.53	0.17	1.93	0.10	2.68	0.12	0.33	0.06	0.58	0.08
AE.C	C1	72.55	3.07	13.80	0.69	4.26	0.30	4.20	0.16	1.98	0.10	2.71	0.12	0.34	0.06	0.63	0.08
AE.C	C1	74.29	3.14	14.48	0.72	3.84	0.28	3.63	0.14	2.42	0.11	2.69	0.12	0.28	0.06	0.59	0.08
AE.C	C1	74.33	3.14	14.55	0.72	4.02	0.29	3.61	0.14	2.24	0.11	2.72	0.12	0.36	0.06	0.65	0.08
AE.C	C1	72.73	3.07	15.16	0.75	4.01	0.29	3.70	0.15	2.53	0.11	2.67	0.12	0.33	0.06	0.66	0.08
AE.C	C1	73.94	3.12	14.10	0.70	3.90	0.28	3.71	0.15	2.13	0.10	2.94	0.13	0.33	0.06	0.60	0.08
AE.C	C1	71.50	3.02	15.34	0.76	4.39	0.31	4.20	0.16	2.16	0.10	2.77	0.12	0.39	0.06	0.65	0.08
AE.C	C2	76.86	3.24	13.79	0.69	3.40	0.25	3.30	0.13	2.73	0.12	2.72	0.12	0.36	0.06	0.59	0.08
AE.C	C2	76.29	3.22	13.21	0.66	3.12	0.23	3.27	0.13	2.80	0.12	2.57	0.12	0.32	0.06	0.56	0.07
AE.C	C2	77.14	3.26	13.84	0.69	3.28	0.24	3.29	0.13	2.72	0.12	2.65	0.12	0.35	0.06	0.62	0.08
AE.C	C2	76.16	3.21	13.87	0.69	3.15	0.23	3.30	0.13	2.90	0.13	2.68	0.12	0.21	0.05	0.56	0.07
AE.C	C2	78.30	3.30	12.80	0.64	3.03	0.22	3.18	0.13	2.67	0.12	2.60	0.12	0.22	0.05	0.53	0.07
AE.C	C2	76.92	3.25	13.49	0.68	3.04	0.23	3.22	0.13	2.82	0.12	2.61	0.12	0.24	0.05	0.56	0.07
AG.D	D1	72.69	3.07	14.50	0.72	4.24	0.30	4.84	0.18	1.36	0.08	2.51	0.12	0.19	0.05	0.57	0.07
AG.D	D1	72.63	3.07	13.94	0.70	3.92	0.28	4.86	0.18	1.30	0.08	2.50	0.11	0.26	0.05	0.51	0.07
AG.D	D1	73.05	3.09	14.10	0.70	3.95	0.28	4.67	0.18	1.14	0.07	2.17	0.10	0.31	0.06	0.49	0.07
AG.D	D1	73.85	3.12	15.50	0.77	4.13	0.29	4.49	0.17	1.43	0.08	2.35	0.11	0.24	0.05	0.55	0.07

AG.D	D1	72.77	3.07	13.04	0.65	4.40	0.31	4.34	0.17	1.60	0.09	2.74	0.12	0.27	0.05	0.60	0.08
AG.D	D1	76.51	3.23	12.65	0.64	3.81	0.27	3.96	0.15	1.49	0.08	2.40	0.11	0.26	0.05	0.61	0.08
AG.D	D1	75.50	3.19	14.00	0.70	3.93	0.28	4.03	0.16	1.70	0.09	2.74	0.12	0.37	0.06	0.61	0.08
AG.D	D1	73.49	3.10	12.87	0.65	3.79	0.27	4.01	0.16	1.55	0.09	2.65	0.12	0.33	0.06	0.57	0.07
AG.D	D1	74.71	3.15	12.57	0.63	3.14	0.23	4.09	0.16	1.44	0.08	2.63	0.12	0.37	0.06	0.56	0.07
AG.D	D1	74.13	3.13	13.12	0.66	4.07	0.29	4.18	0.16	1.60	0.09	2.59	0.12	0.31	0.06	0.54	0.07
AG.D	D2	74.27	3.14	14.02	0.70	3.62	0.26	3.87	0.15	1.38	0.08	2.79	0.12	0.35	0.06	0.67	0.08
AG.D	D2	70.68	2.99	14.22	0.71	3.61	0.26	3.69	0.15	1.74	0.09	2.91	0.13	0.38	0.06	0.69	0.08
AG.D	D2	73.35	3.10	12.95	0.65	3.55	0.26	3.56	0.14	1.84	0.09	2.56	0.12	0.32	0.06	0.59	0.08
AG.D	D2	70.78	2.99	15.14	0.75	3.60	0.26	3.79	0.15	1.59	0.09	2.99	0.13	0.41	0.06	0.81	0.09
AG.D	D2	70.07	2.96	16.45	0.81	3.62	0.26	3.48	0.14	1.96	0.10	3.26	0.14	0.53	0.06	0.88	0.09
AG.D	D2	73.98	3.12	13.65	0.68	3.40	0.25	3.36	0.14	2.04	0.10	2.59	0.12	0.32	0.06	0.71	0.08
AG.D	D2	71.95	3.04	14.61	0.73	3.89	0.28	3.73	0.15	2.35	0.11	2.79	0.12	0.34	0.06	0.67	0.08
AG.D	D2	69.69	2.95	14.76	0.73	3.51	0.25	3.81	0.15	1.42	0.08	3.11	0.13	0.45	0.06	0.72	0.08
AG.D	D2	73.25	3.09	14.47	0.72	3.31	0.24	3.49	0.14	2.56	0.12	2.95	0.13	0.36	0.06	0.65	0.08
AG.D	D2	98.20	4.13	0.48	0.07	0.12	0.04	0.19	0.04	0.03	0.04	0.17	0.04	0.03	0.05	0.13	0.05
AG.D	D2	69.60	2.94	14.97	0.74	3.80	0.27	3.78	0.15	2.52	0.11	2.80	0.12	0.43	0.06	0.74	0.08
AG.D	D2	72.07	3.05	15.32	0.76	3.56	0.26	3.79	0.15	1.39	0.08	2.90	0.13	0.43	0.06	0.76	0.08
AG.D	D2	69.45	2.94	16.35	0.81	3.44	0.25	3.43	0.14	2.19	0.10	3.26	0.14	0.50	0.06	0.93	0.09
AG.D	D2	74.95	3.16	13.46	0.67	3.72	0.27	3.73	0.15	2.00	0.10	2.76	0.12	0.40	0.06	0.80	0.09
AG.D	D2	75.04	3.17	13.94	0.70	3.16	0.23	4.16	0.16	1.75	0.09	2.61	0.12	0.29	0.06	0.62	0.08
AG.D	D2	76.60	3.23	12.14	0.61	3.13	0.23	3.50	0.14	1.94	0.10	2.66	0.12	0.24	0.05	0.58	0.08
AG.D	D2	70.70	2.99	15.78	0.78	3.46	0.25	3.58	0.14	2.00	0.10	3.09	0.13	0.54	0.06	0.89	0.09
AG.D	D2	68.75	2.91	15.77	0.78	3.93	0.28	4.08	0.16	1.77	0.09	2.98	0.13	0.44	0.06	0.84	0.09
AG.D	D2	73.59	3.11	14.00	0.70	3.40	0.25	3.59	0.14	1.65	0.09	2.87	0.13	0.30	0.06	0.78	0.09
AH.E	E1	76.57	3.23	13.09	0.66	4.08	0.29	4.02	0.16	0.97	0.07	2.53	0.12	0.25	0.05	0.66	0.08
AH.E	E1	73.64	3.11	14.00	0.70	4.22	0.30	4.12	0.16	1.21	0.07	2.79	0.12	0.36	0.06	0.80	0.09
AH.E	E1	74.23	3.13	13.73	0.69	4.33	0.31	4.51	0.17	1.09	0.07	2.62	0.12	0.35	0.06	0.70	0.08
AH.E	E1	73.56	3.11	14.15	0.71	4.06	0.29	4.49	0.17	1.14	0.07	2.67	0.12	0.37	0.06	0.74	0.08
AH.E	E1	72.97	3.08	13.97	0.70	3.92	0.28	3.88	0.15	1.19	0.07	2.88	0.13	0.34	0.06	0.74	0.08
AH.E	E1	73.50	3.10	14.23	0.71	2.83	0.21	4.47	0.17	1.10	0.07	2.81	0.12	0.27	0.05	0.76	0.09
AH.E	E1	71.16	3.01	13.08	0.66	3.62	0.26	5.50	0.20	1.25	0.08	2.41	0.11	0.35	0.06	0.73	0.08
AH.E	E1	72.51	3.06	13.60	0.68	4.75	0.33	4.96	0.19	0.95	0.07	2.33	0.11	0.29	0.06	0.69	0.08
AH.E	E1	71.47	3.02	13.68	0.68	4.97	0.34	4.92	0.18	1.02	0.07	2.48	0.11	0.27	0.05	0.71	0.08
AH.E	E2	75.53	3.19	14.00	0.70	3.19	0.24	3.26	0.13	2.11	0.10	2.68	0.12	0.31	0.06	0.79	0.09
AH.E	E2	76.23	3.22	14.06	0.70	3.27	0.24	3.35	0.14	2.10	0.10	2.78	0.12	0.43	0.06	0.80	0.09
AH.E	E2	75.36	3.18	13.28	0.67	3.21	0.24	3.22	0.13	1.93	0.10	2.81	0.12	0.28	0.06	0.78	0.09
AH.E	E2	76.48	3.23	13.56	0.68	3.17	0.23	3.36	0.14	2.12	0.10	2.86	0.13	0.36	0.06	0.76	0.09
AH.E	E2	76.05	3.21	13.55	0.68	3.10	0.23	3.30	0.13	2.02	0.10	2.98	0.13	0.32	0.06	0.80	0.09
AH.E	E2	75.11	3.17	13.91	0.69	3.11	0.23	3.30	0.13	2.09	0.10	2.87	0.13	0.30	0.06	0.77	0.09
AH.E	E2	75.16	3.17	13.62	0.68	3.22	0.24	3.20	0.13	1.98	0.10	2.92	0.13	0.33	0.06	0.76	0.08
AH.E	E2	75.36	3.18	14.41	0.72	2.97	0.22	3.24	0.13	2.12	0.10	2.78	0.12	0.36	0.06	0.84	0.09
AH.E	E2	81.00	3.42	11.21	0.57	2.90	0.22	2.92	0.12	1.59	0.09	2.46	0.11	0.16	0.05	0.71	0.08
AH.E	E2	75.30	3.18	13.99	0.70	3.20	0.24	3.26	0.13	2.13	0.10	2.87	0.13	0.29	0.06	0.72	0.08
AH.E	E2	75.61	3.19	13.38	0.67	3.32	0.24	3.31	0.13	1.96	0.10	2.81	0.12	0.33	0.06	0.73	0.08
AH.E	E2	76.87	3.24	13.96	0.70	3.30	0.24	3.32	0.14	1.89	0.10	2.82	0.12	0.32	0.06	0.80	0.09

AH.E	E2	77.35	3.26	13.78	0.69	3.06	0.23	3.20	0.13	1.97	0.10	3.13	0.13	0.28	0.06	0.79	0.09
FLD10	FLD10.L	71.82	3.04	13.82	0.69	2.96	0.22	3.48	0.14	2.53	0.11	2.91	0.13	0.19	0.05	0.48	0.07
FLD10	FLD10.L	75.18	3.17	13.63	0.68	3.29	0.24	3.52	0.14	2.20	0.10	2.92	0.13	0.28	0.05	0.56	0.07
FLD10	FLD10.L	73.76	3.12	12.61	0.63	2.99	0.22	3.40	0.14	2.07	0.10	2.51	0.12	0.31	0.06	0.50	0.07
FLD10	FLD10.L	75.68	3.19	12.81	0.64	3.10	0.23	3.52	0.14	2.17	0.10	2.93	0.13	0.32	0.06	0.49	0.07
FLD10	FLD10.L	73.10	3.09	13.05	0.65	3.30	0.24	3.75	0.15	2.05	0.10	2.79	0.12	0.33	0.06	0.48	0.07
FLD10	FLD10.L	73.10	3.09	13.13	0.66	3.20	0.24	3.84	0.15	2.04	0.10	2.99	0.13	0.39	0.06	0.51	0.07
FLD10	FLD10.L	74.06	3.13	12.90	0.65	3.42	0.25	3.83	0.15	1.96	0.10	2.67	0.12	0.30	0.06	0.47	0.07
FLD10	FLD10.L	72.72	3.07	12.96	0.65	3.33	0.24	3.92	0.15	2.13	0.10	2.75	0.12	0.39	0.06	0.51	0.07
FLD10	FLD10.L	74.73	3.16	13.28	0.67	2.90	0.22	3.43	0.14	2.45	0.11	2.85	0.13	0.33	0.06	0.54	0.07
FLD10	FLD10.L	74.79	3.16	12.93	0.65	3.04	0.23	3.53	0.14	2.32	0.11	2.81	0.12	0.37	0.06	0.48	0.07
FLD10	FLD10.L	74.20	3.13	12.67	0.64	3.10	0.23	3.69	0.15	2.15	0.10	2.86	0.13	0.39	0.06	0.44	0.07
FLD10	FLD10.L	72.13	3.05	12.70	0.64	3.10	0.23	3.78	0.15	2.35	0.11	2.90	0.13	0.33	0.06	0.52	0.07
FLD10	FLD10.L	75.08	3.17	13.47	0.67	3.23	0.24	3.56	0.14	2.36	0.11	2.83	0.13	0.35	0.06	0.49	0.07
FLD10	FLD10.L	73.26	3.09	13.18	0.66	3.13	0.23	3.68	0.15	2.22	0.11	2.83	0.12	0.34	0.06	0.51	0.07
FLD10	FLD10.L	74.47	3.14	13.42	0.67	3.28	0.24	3.63	0.14	2.07	0.10	2.92	0.13	0.37	0.06	0.55	0.07
FLD10	FLD10.L	74.00	3.13	13.27	0.66	3.13	0.23	3.54	0.14	2.45	0.11	2.78	0.12	0.33	0.06	0.45	0.07
FLD10	FLD10.L	72.73	3.07	13.20	0.66	3.23	0.24	3.72	0.15	2.26	0.11	2.88	0.13	0.33	0.06	0.51	0.07
FLD10	FLD10.L	76.52	3.23	12.66	0.64	3.11	0.23	3.66	0.15	2.01	0.10	2.52	0.12	0.26	0.05	0.52	0.07
FLD10	FLD10.L	75.79	3.20	13.48	0.67	2.97	0.22	3.41	0.14	2.37	0.11	2.86	0.13	0.28	0.06	0.44	0.07
FLD10	FLD10.L	71.92	3.04	13.09	0.66	2.83	0.21	3.53	0.14	2.48	0.11	2.81	0.12	0.27	0.05	0.50	0.07
FLD10	FLD10.L	74.62	3.15	13.70	0.68	2.82	0.21	3.33	0.14	2.60	0.12	2.67	0.12	0.34	0.06	0.47	0.07
FLD10	FLD10.L	73.73	3.11	13.13	0.66	2.88	0.22	3.34	0.14	2.44	0.11	2.65	0.12	0.31	0.06	0.45	0.07
FLD10	FLD10.L	74.46	3.14	12.96	0.65	3.06	0.23	3.66	0.15	2.15	0.10	2.83	0.13	0.37	0.06	0.45	0.07
FLD10	FLD10.L	75.73	3.20	13.59	0.68	3.18	0.23	3.67	0.15	2.08	0.10	3.01	0.13	0.40	0.06	0.59	0.08
FLD10	FLD10.L	71.97	3.04	12.67	0.64	2.87	0.21	3.55	0.14	2.34	0.11	2.88	0.13	0.29	0.06	0.43	0.07
FLD10	FLD10.L	72.92	3.08	12.82	0.64	2.75	0.21	3.45	0.14	2.55	0.12	2.80	0.12	0.31	0.06	0.47	0.07
FLD10	FLD10.L	74.82	3.16	13.06	0.66	3.00	0.22	3.80	0.15	2.16	0.10	2.97	0.13	0.35	0.06	0.53	0.07
FLD10	FLD10.L	75.47	3.19	13.29	0.67	3.18	0.23	3.74	0.15	2.41	0.11	2.73	0.12	0.36	0.06	0.45	0.07
FLD10	FLD10.L	72.31	3.06	12.90	0.65	2.90	0.22	3.72	0.15	2.40	0.11	2.92	0.13	0.33	0.06	0.53	0.07
FLD10	FLD10.L	72.90	3.08	12.95	0.65	2.79	0.21	3.50	0.14	2.45	0.11	2.67	0.12	0.28	0.06	0.47	0.07
FLD14	FLD14.L	74.58	3.15	13.35	0.67	3.62	0.26	3.79	0.15	3.07	0.13	2.47	0.11	0.26	0.05	0.76	0.08
FLD14	FLD14.L	72.65	3.07	13.47	0.67	3.14	0.23	3.47	0.14	3.14	0.13	2.59	0.12	0.28	0.06	0.75	0.08
FLD14	FLD14.L	74.68	3.15	14.18	0.71	3.16	0.23	3.37	0.14	3.31	0.14	2.59	0.12	0.30	0.06	0.81	0.09
FLD14	FLD14.L	72.90	3.08	13.17	0.66	3.14	0.23	3.60	0.14	3.16	0.13	2.51	0.12	0.32	0.06	0.74	0.08
FLD14	FLD14.L	74.83	3.16	13.83	0.69	3.04	0.23	3.32	0.13	2.77	0.12	2.63	0.12	0.24	0.05	0.78	0.09
FLD14	FLD14.L	71.97	3.04	13.00	0.65	2.97	0.22	3.58	0.14	2.69	0.12	2.48	0.11	0.31	0.06	0.47	0.07
FLD14	FLD14.L	75.93	3.21	13.24	0.66	3.97	0.28	3.75	0.15	3.22	0.14	2.59	0.12	0.22	0.05	0.78	0.09
FLD14	FLD14.L	73.03	3.09	13.27	0.66	2.93	0.22	3.49	0.14	3.13	0.13	2.56	0.12	0.29	0.06	0.44	0.07
FLD14	FLD14.L	74.06	3.13	13.53	0.68	2.97	0.22	3.34	0.14	3.22	0.14	2.73	0.12	0.29	0.06	0.77	0.09
FLD14	FLD14.L	74.36	3.14	14.25	0.71	3.03	0.23	3.31	0.13	3.27	0.14	2.58	0.12	0.29	0.06	0.81	0.09
FLD14	FLD14.L	73.55	3.11	14.26	0.71	3.09	0.23	3.53	0.14	2.71	0.12	2.71	0.12	0.27	0.05	0.90	0.09
FLD14	FLD14.L	72.50	3.06	13.24	0.66	3.07	0.23	3.42	0.14	3.28	0.14	2.53	0.12	0.28	0.06	0.50	0.07
FLD14	FLD14.L	73.93	3.12	13.47	0.67	3.16	0.23	3.51	0.14	3.28	0.14	2.53	0.12	0.28	0.05	0.74	0.08
FLD14	FLD14.L	73.85	3.12	13.65	0.68	2.99	0.22	3.37	0.14	3.42	0.14	2.62	0.12	0.30	0.06	0.77	0.09
FLD14	FLD14.L	74.90	3.16	13.94	0.70	2.99	0.22	3.46	0.14	3.32	0.14	2.61	0.12	0.33	0.06	0.78	0.09

FLD14	FLD14.L	73.89	3.12	13.58	0.68	2.93	0.22	3.29	0.13	3.24	0.14	2.64	0.12	0.33	0.06	0.76	0.08
FLD14	FLD14.L	73.71	3.11	13.41	0.67	3.08	0.23	3.55	0.14	3.22	0.14	2.76	0.12	0.32	0.06	0.83	0.09
FLD14	FLD14.L	70.84	2.99	12.89	0.65	2.95	0.22	3.57	0.14	3.30	0.14	2.61	0.12	0.31	0.06	0.48	0.07
FLD14	FLD14.L	73.10	3.09	13.45	0.67	3.07	0.23	3.54	0.14	3.54	0.15	2.76	0.12	0.31	0.06	0.75	0.08
FLD14	FLD14.L	74.15	3.13	13.85	0.69	2.94	0.22	3.35	0.14	3.43	0.14	2.67	0.12	0.33	0.06	0.74	0.08
FLD14	FLD14.L	72.27	3.05	13.58	0.68	2.83	0.21	3.32	0.14	3.65	0.15	2.71	0.12	0.32	0.06	0.69	0.08
FLD14	FLD14.L	76.24	3.22	13.55	0.68	2.90	0.22	3.32	0.13	3.30	0.14	2.63	0.12	0.27	0.05	0.75	0.08
FLD14	FLD14.L	74.83	3.16	13.60	0.68	2.94	0.22	3.34	0.14	2.93	0.13	2.61	0.12	0.29	0.06	0.78	0.09
FLD14	FLD14.L	73.58	3.11	14.11	0.70	3.19	0.23	3.64	0.14	2.66	0.12	2.75	0.12	0.39	0.06	0.91	0.09
FLD14	FLD14.L	75.31	3.18	13.81	0.69	3.16	0.23	3.54	0.14	3.16	0.13	2.59	0.12	0.28	0.06	0.81	0.09
FLD14	FLD14.L	72.31	3.06	14.52	0.72	3.27	0.24	3.50	0.14	2.99	0.13	2.75	0.12	0.40	0.06	0.88	0.09
FLD14	FLD14.L	74.11	3.13	13.12	0.66	2.89	0.22	3.52	0.14	3.07	0.13	2.59	0.12	0.30	0.06	0.72	0.08
FLD14	FLD14.L	73.10	3.09	13.47	0.67	2.83	0.21	3.28	0.13	3.59	0.15	2.64	0.12	0.29	0.06	0.43	0.07
FLD14	FLD14.L	73.81	3.12	13.54	0.68	2.91	0.22	3.31	0.13	3.57	0.15	2.72	0.12	0.27	0.05	0.45	0.07
FLD14	FLD14.L	74.72	3.16	13.76	0.69	2.88	0.22	3.30	0.13	3.37	0.14	2.56	0.12	0.28	0.06	0.72	0.08
FLD14	FLD14.L	74.98	3.17	13.57	0.68	3.00	0.22	3.44	0.14	3.24	0.14	2.74	0.12	0.33	0.06	0.79	0.09
FLD14	FLD14.L	70.99	3.00	12.99	0.65	2.85	0.21	3.50	0.14	3.43	0.14	2.66	0.12	0.30	0.06	0.44	0.07
FLD14	FLD14.L	75.51	3.19	13.76	0.69	2.93	0.22	3.28	0.13	3.21	0.14	2.60	0.12	0.26	0.05	0.76	0.08
FLD14	FLD14.L	73.13	3.09	13.72	0.69	3.14	0.23	3.50	0.14	3.31	0.14	2.69	0.12	0.32	0.06	0.76	0.08
FLD14	FLD14.L	72.61	3.07	13.42	0.67	2.08	0.17	3.43	0.14	3.38	0.14	2.65	0.12	0.31	0.06	0.44	0.07
FLD14	FLD14.L	74.72	3.16	14.19	0.71	2.95	0.22	3.31	0.13	3.74	0.15	2.71	0.12	0.30	0.06	0.77	0.09
FLD14	FLD14.L	75.01	3.17	14.16	0.71	2.94	0.22	3.40	0.14	3.72	0.15	2.61	0.12	0.31	0.06	0.75	0.08
FLD14	FLD14.L	74.38	3.14	14.00	0.70	2.95	0.22	3.29	0.13	3.64	0.15	2.76	0.12	0.29	0.06	0.75	0.08
FLD14	FLD14.L	73.92	3.12	13.51	0.68	2.95	0.22	3.37	0.14	3.41	0.14	2.77	0.12	0.29	0.06	0.76	0.09
FLD14	FLD14.L	75.19	3.17	14.34	0.71	3.03	0.22	3.35	0.14	3.33	0.14	2.70	0.12	0.32	0.06	0.82	0.09
FLD14	FLD14.L	74.83	3.16	13.42	0.67	2.95	0.22	3.40	0.14	3.39	0.14	2.69	0.12	0.33	0.06	0.75	0.08
FLD14	FLD14.L	75.36	3.18	13.79	0.69	3.08	0.23	3.32	0.13	3.25	0.14	2.67	0.12	0.28	0.06	0.77	0.09
FLD14	FLD14.L	76.67	3.24	14.20	0.71	2.12	0.17	3.31	0.13	3.14	0.13	2.66	0.12	0.29	0.06	0.79	0.09
FLD14	FLD14.L	73.48	3.10	13.44	0.67	2.00	0.16	3.39	0.14	3.46	0.14	2.65	0.12	0.31	0.06	0.43	0.07
FLD14	FLD14.L	75.59	3.19	13.80	0.69	2.90	0.22	3.27	0.13	3.36	0.14	2.66	0.12	0.26	0.05	0.75	0.08
FLD14	FLD14.L	75.05	3.17	13.91	0.69	3.00	0.22	3.34	0.14	3.31	0.14	2.70	0.12	0.28	0.06	0.77	0.09
FLD14	FLD14.L	76.16	3.21	13.18	0.66	2.96	0.22	3.51	0.14	3.13	0.13	2.55	0.12	0.32	0.06	0.77	0.09
FLD14	FLD14.L	73.38	3.10	13.70	0.68	3.01	0.22	3.49	0.14	3.57	0.15	2.63	0.12	0.29	0.06	0.74	0.08
FLD14	FLD14.L	73.83	3.12	13.76	0.69	3.01	0.22	3.54	0.14	3.40	0.14	2.67	0.12	0.30	0.06	0.48	0.07
FLD14	FLD14.L	74.41	3.14	13.30	0.67	2.14	0.17	3.45	0.14	3.21	0.14	2.71	0.12	0.25	0.05	0.71	0.08
FLD14	FLD14.L	73.34	3.10	13.56	0.68	3.01	0.22	3.48	0.14	3.36	0.14	2.78	0.12	0.27	0.05	0.72	0.08
FLD14	FLD14.L	74.78	3.16	13.84	0.69	3.05	0.23	3.43	0.14	3.48	0.14	2.63	0.12	0.29	0.06	0.74	0.08
FLD14	FLD14.L	70.58	2.98	16.33	0.81	3.12	0.23	3.54	0.14	4.10	0.16	2.73	0.12	0.37	0.06	0.84	0.09
FLD14	FLD14.L	74.87	3.16	13.52	0.68	3.02	0.22	3.45	0.14	3.54	0.15	2.63	0.12	0.29	0.06	0.76	0.08
FLD14	FLD14.L	72.93	3.08	13.89	0.69	3.39	0.25	3.67	0.15	3.22	0.14	2.66	0.12	0.29	0.06	0.74	0.08
FLD14	FLD14.L	72.31	3.06	14.60	0.73	3.35	0.24	3.45	0.14	3.57	0.15	2.73	0.12	0.26	0.05	0.78	0.09
FLD14	FLD14.L	75.44	3.19	13.20	0.66	3.33	0.24	3.54	0.14	2.88	0.13	2.54	0.12	0.29	0.06	0.75	0.08
FLD14	FLD14.L	73.91	3.12	12.62	0.63	3.33	0.24	3.86	0.15	2.70	0.12	2.29	0.11	0.26	0.05	0.64	0.08
FLD14	FLD14.L	73.64	3.11	13.72	0.69	3.06	0.23	3.48	0.14	2.75	0.12	2.68	0.12	0.34	0.06	0.78	0.09
FLD14	FLD14.L	68.46	2.90	16.78	0.83	3.18	0.23	3.78	0.15	4.07	0.16	2.57	0.12	0.36	0.06	0.76	0.09
FLD14	FLD14.L	72.71	3.07	12.84	0.64	2.65	0.20	3.68	0.15	3.31	0.14	2.61	0.12	0.31	0.06	0.45	0.07

FLD14	FLD14.1	74.52	3.15	11.77	0.60	3.82	0.27	4.06	0.16	2.64	0.12	2.48	0.11	0.27	0.05	0.74	0.08
FLD14	FLD14.1	76.31	3.22	12.47	0.63	2.88	0.22	4.00	0.16	3.04	0.13	2.54	0.12	0.25	0.05	0.77	0.09
FLD14	FLD14.1	74.39	3.14	12.44	0.63	2.76	0.21	4.20	0.16	2.91	0.13	2.44	0.11	0.25	0.05	0.72	0.08
FLD14	FLD14.1	71.58	3.03	11.97	0.60	2.06	0.16	4.19	0.16	3.10	0.13	2.55	0.12	0.28	0.06	0.39	0.07
FLD14	FLD14.1	71.79	3.03	12.06	0.61	3.22	0.24	4.32	0.17	2.76	0.12	2.47	0.11	0.30	0.06	0.46	0.07
FLD14	FLD14.1	71.44	3.02	12.14	0.61	2.51	0.19	4.29	0.16	3.18	0.13	2.48	0.11	0.28	0.05	0.46	0.07
FLD14	FLD14.1	72.59	3.07	12.39	0.62	3.32	0.24	4.29	0.16	2.89	0.13	2.38	0.11	0.26	0.05	0.71	0.08
FLD14	FLD14.L	74.24	3.14	14.59	0.73	3.20	0.24	3.34	0.14	3.25	0.14	2.58	0.12	0.23	0.05	0.59	0.08
FLD14	FLD14.L	76.17	3.22	13.85	0.69	3.06	0.23	3.26	0.13	3.05	0.13	2.67	0.12	0.30	0.06	0.56	0.07
FLD14	FLD14.L	76.14	3.21	13.23	0.66	2.99	0.22	3.27	0.13	2.86	0.12	2.56	0.12	0.26	0.05	0.59	0.08
FLD14	FLD14.L	76.32	3.22	14.06	0.70	2.86	0.21	3.29	0.13	3.19	0.13	2.68	0.12	0.28	0.06	0.62	0.08
FLD14	FLD14.L	76.06	3.21	13.89	0.69	2.92	0.22	3.16	0.13	3.45	0.14	2.58	0.12	0.21	0.05	0.50	0.07
FLD14	FLD14.L	76.68	3.24	13.43	0.67	3.01	0.22	3.35	0.14	3.08	0.13	2.55	0.12	0.23	0.05	0.60	0.08
FLD14	FLD14.L	76.15	3.21	14.13	0.70	2.98	0.22	3.26	0.13	3.09	0.13	2.79	0.12	0.32	0.06	0.54	0.07
FLD14	FLD14.L	76.10	3.21	13.88	0.69	2.83	0.21	3.16	0.13	3.46	0.14	2.79	0.12	0.31	0.06	0.57	0.07
FLD14	FLD14.L	75.20	3.18	13.30	0.67	2.89	0.22	3.19	0.13	2.99	0.13	2.49	0.11	0.32	0.06	0.56	0.07
FLD14	FLD14.L	74.50	3.15	12.96	0.65	3.54	0.26	3.83	0.15	2.85	0.12	2.47	0.11	0.17	0.05	0.54	0.07
FLD14	FLD14.L	75.92	3.20	13.86	0.69	2.95	0.22	3.39	0.14	3.05	0.13	2.72	0.12	0.24	0.05	0.53	0.07
FLD14	FLD14.L	75.53	3.19	14.11	0.70	2.90	0.22	3.24	0.13	3.36	0.14	2.59	0.12	0.20	0.05	0.61	0.08
FLD14	FLD14.L	75.28	3.18	13.71	0.69	2.84	0.21	3.27	0.13	3.44	0.14	2.87	0.13	0.18	0.05	0.50	0.07
FLD14	FLD14.L	75.94	3.21	13.43	0.67	2.92	0.22	3.29	0.13	3.12	0.13	2.66	0.12	0.27	0.05	0.55	0.07
FLD17	FLD17.int.2	74.73	3.16	13.81	0.69	2.79	0.21	4.07	0.16	3.16	0.13	2.78	0.12	0.31	0.06	0.84	0.09
FLD17	FLD17.int.2	75.15	3.17	13.58	0.68	2.79	0.21	3.96	0.15	3.06	0.13	2.65	0.12	0.33	0.06	0.85	0.09
FLD17	FLD17.int.2	75.29	3.18	13.88	0.69	2.69	0.20	4.01	0.16	2.98	0.13	2.77	0.12	0.27	0.05	0.80	0.09
FLD17	FLD17.int.2	76.13	3.21	13.79	0.69	2.81	0.21	3.96	0.15	2.98	0.13	2.66	0.12	0.34	0.06	0.86	0.09
FLD17	FLD17.1	74.85	3.16	12.92	0.65	3.07	0.23	3.55	0.14	2.88	0.13	2.76	0.12	0.28	0.06	0.61	0.08
FLD17	FLD17.1	73.67	3.11	13.72	0.69	3.77	0.27	4.11	0.16	1.51	0.08	2.92	0.13	0.29	0.06	0.52	0.07
FLD17	FLD17.1	76.56	3.23	13.30	0.67	3.08	0.23	3.49	0.14	2.84	0.12	2.86	0.13	0.27	0.05	0.56	0.07
FLD17	FLD17.1	80.09	3.38	11.23	0.57	2.93	0.22	3.54	0.14	2.17	0.10	2.67	0.12	0.24	0.05	0.54	0.07
FLD17	FLD17.1	75.57	3.19	12.23	0.62	3.37	0.25	4.01	0.16	1.51	0.08	2.93	0.13	0.33	0.06	0.54	0.07
FLD17	FLD17.1	76.38	3.22	13.28	0.67	3.14	0.23	3.59	0.14	2.66	0.12	2.81	0.12	0.30	0.06	0.59	0.08
FLD17	FLD17.1	75.05	3.17	13.64	0.68	3.31	0.24	3.74	0.15	2.68	0.12	2.88	0.13	0.32	0.06	0.67	0.08
FLD17	FLD17.1	79.40	3.35	9.76	0.50	2.82	0.21	3.57	0.14	1.63	0.09	2.86	0.13	0.26	0.05	0.52	0.07
FLD17	FLD17.tail	73.32	3.10	12.89	0.65	3.44	0.25	3.94	0.15	2.02	0.10	2.84	0.13	0.27	0.05	0.55	0.07
FLD17	FLD17.tail	74.70	3.15	13.42	0.67	3.56	0.26	3.93	0.15	2.73	0.12	2.83	0.12	0.27	0.05	0.67	0.08
FLD17	FLD17.tail	74.59	3.15	12.66	0.64	3.44	0.25	3.91	0.15	2.35	0.11	2.89	0.13	0.30	0.06	0.62	0.08
FLD17	FLD17.tail	74.69	3.15	12.64	0.64	3.51	0.25	3.89	0.15	2.36	0.11	2.76	0.12	0.27	0.05	0.55	0.07
FLD17	FLD17.tail	76.14	3.21	12.37	0.62	3.30	0.24	3.79	0.15	2.90	0.13	2.78	0.12	0.28	0.06	0.63	0.08
FLD17	FLD17.tail	74.54	3.15	12.42	0.63	3.62	0.26	3.96	0.15	2.87	0.13	3.11	0.13	0.33	0.06	0.65	0.08
FLD17	FLD17.int.1	77.92	3.29	12.64	0.64	2.99	0.22	3.77	0.15	1.79	0.09	2.64	0.12	0.26	0.05	0.55	0.07
FLD17	FLD17.int.1	75.72	3.20	13.08	0.66	2.99	0.22	3.67	0.15	1.88	0.10	2.78	0.12	0.28	0.05	0.56	0.07
FLD17	FLD17.int.1	76.79	3.24	13.21	0.66	3.06	0.23	3.69	0.15	1.98	0.10	2.75	0.12	0.30	0.06	0.60	0.08
FLD17	FLD17.int.1	77.58	3.27	11.54	0.58	2.85	0.21	3.70	0.15	2.00	0.10	2.59	0.12	0.28	0.06	0.51	0.07
FLD17	FLD17.int.1	75.60	3.19	13.02	0.65	3.06	0.23	3.70	0.15	2.03	0.10	2.77	0.12	0.32	0.06	0.56	0.07
FLD17	FLD17.int.1	78.39	3.31	12.82	0.64	3.08	0.23	3.68	0.15	2.02	0.10	2.71	0.12	0.31	0.06	0.59	0.08
FLD17	FLD17.2	74.03	3.13	13.06	0.66	2.95	0.22	3.65	0.15	3.25	0.14	2.83	0.12	0.25	0.05	0.60	0.08

FLD17	FLD17.2	77.01	3.25	12.97	0.65	2.99	0.22	3.48	0.14	3.06	0.13	2.72	0.12	0.27	0.05	0.55	0.07
FLD17	FLD17.2	76.45	3.23	13.19	0.66	3.11	0.23	3.54	0.14	3.01	0.13	2.77	0.12	0.32	0.06	0.58	0.08
FLD17	FLD17.2	76.35	3.22	13.65	0.68	2.96	0.22	3.53	0.14	3.13	0.13	2.76	0.12	0.32	0.06	0.61	0.08
FLD17	FLD17.2	76.26	3.22	13.67	0.68	3.01	0.22	3.41	0.14	3.24	0.14	2.87	0.13	0.25	0.05	0.64	0.08
FLD17	FLD17.2	76.47	3.23	13.20	0.66	2.93	0.22	3.36	0.14	2.92	0.13	2.80	0.12	0.29	0.06	0.59	0.08
FLD17	FLD17.2	73.60	3.11	12.94	0.65	2.95	0.22	3.56	0.14	2.96	0.13	2.71	0.12	0.32	0.06	0.55	0.07
FLD17	FLD17.2	77.23	3.26	12.47	0.63	3.13	0.23	3.54	0.14	2.78	0.12	2.75	0.12	0.30	0.06	0.54	0.07
FLD17	FLD17.2	74.72	3.16	13.02	0.65	2.94	0.22	3.49	0.14	2.91	0.13	2.62	0.12	0.34	0.06	0.52	0.07
FLD17	FLD17.2	75.40	3.18	13.55	0.68	3.01	0.22	3.40	0.14	3.06	0.13	2.79	0.12	0.23	0.05	0.59	0.08
FLD17	FLD17.2	75.74	3.20	13.81	0.69	3.04	0.23	3.53	0.14	3.10	0.13	2.75	0.12	0.31	0.06	0.57	0.07
FLD17	FLD17.2	76.05	3.21	13.76	0.69	3.01	0.22	3.41	0.14	3.38	0.14	2.89	0.13	0.30	0.06	0.65	0.08
FLD17	FLD17.2	76.82	3.24	13.40	0.67	3.10	0.23	3.53	0.14	2.91	0.13	2.67	0.12	0.29	0.06	0.58	0.08
FLD17	FLD17.2	77.26	3.26	13.42	0.67	3.03	0.22	3.40	0.14	2.71	0.12	2.72	0.12	0.31	0.06	0.59	0.08
FLD17	FLD17.2	76.11	3.21	13.36	0.67	3.04	0.23	3.49	0.14	2.75	0.12	2.74	0.12	0.28	0.06	0.57	0.07
FLD17	FLD17.2	76.25	3.22	13.24	0.66	3.04	0.23	3.40	0.14	3.02	0.13	2.76	0.12	0.36	0.06	0.57	0.07
FLD17	FLD17.2	75.00	3.17	13.63	0.68	3.02	0.22	3.43	0.14	3.06	0.13	2.70	0.12	0.28	0.05	0.56	0.07
FLD17	FLD17.2	75.22	3.18	13.53	0.68	3.12	0.23	3.58	0.14	3.10	0.13	2.65	0.12	0.28	0.05	0.58	0.08
FLD17	FLD17.2	77.11	3.25	13.19	0.66	3.02	0.22	3.51	0.14	3.01	0.13	2.73	0.12	0.25	0.05	0.59	0.08
FLD17	FLD17.2	76.43	3.23	12.72	0.64	2.92	0.22	3.47	0.14	2.68	0.12	2.75	0.12	0.27	0.05	0.53	0.07
FLD17	FLD17.2	77.13	3.25	12.76	0.64	3.07	0.23	3.54	0.14	3.03	0.13	2.78	0.12	0.24	0.05	0.57	0.08
FLD18	FLD18.1	73.63	3.11	13.22	0.66	3.00	0.22	3.93	0.15	2.76	0.12	2.81	0.12	0.31	0.06	0.50	0.07
FLD18	FLD18.1	74.09	3.13	15.19	0.75	2.92	0.22	3.37	0.14	3.10	0.13	2.90	0.13	0.32	0.06	0.83	0.09
FLD18	FLD18.1	72.48	3.06	13.22	0.66	3.03	0.23	3.84	0.15	2.75	0.12	2.88	0.13	0.31	0.06	0.55	0.07
FLD18	FLD18.1	73.82	3.12	13.58	0.68	3.02	0.22	3.56	0.14	2.72	0.12	2.80	0.12	0.32	0.06	0.83	0.09
FLD18	FLD18.1	74.70	3.15	13.75	0.69	2.34	0.18	3.89	0.15	2.66	0.12	2.77	0.12	0.28	0.06	0.85	0.09
FLD18	FLD18.2	72.07	3.05	13.72	0.69	2.36	0.18	3.92	0.15	1.49	0.08	2.24	0.11	0.32	0.06	0.37	0.06
FLD18	FLD18.2	73.35	3.10	13.84	0.69	2.33	0.18	3.69	0.15	1.54	0.08	2.19	0.11	0.29	0.06	0.40	0.07
FLD18	FLD18.2	75.52	3.19	14.42	0.72	2.35	0.18	3.58	0.14	1.38	0.08	2.46	0.11	0.36	0.06	0.45	0.07
FLD18	FLD18.2	74.25	3.14	13.57	0.68	2.84	0.21	3.67	0.15	1.49	0.08	2.80	0.12	0.31	0.06	0.58	0.08
FLD18	FLD18.2	73.83	3.12	13.87	0.69	3.23	0.24	3.99	0.16	1.61	0.09	2.53	0.12	0.36	0.06	0.59	0.08
FLD18	FLD18.2	75.03	3.17	12.69	0.64	3.59	0.26	4.06	0.16	1.79	0.09	2.72	0.12	0.33	0.06	0.66	0.08
FLD18	FLD18.2	74.08	3.13	14.03	0.70	3.73	0.27	4.16	0.16	1.67	0.09	2.48	0.11	0.35	0.06	0.53	0.07
FLD18	FLD18.2	72.05	3.04	13.67	0.68	2.92	0.22	3.77	0.15	1.60	0.09	2.71	0.12	0.34	0.06	0.62	0.08
FLD18	FLD18.2	73.30	3.10	13.39	0.67	2.87	0.22	3.93	0.15	1.50	0.08	2.29	0.11	0.35	0.06	0.57	0.07
FLD18	FLD18.2	74.49	3.15	13.73	0.69	2.96	0.22	3.62	0.14	1.65	0.09	2.72	0.12	0.28	0.05	0.62	0.08
FLD18	FLD18.2	73.48	3.10	14.28	0.71	3.23	0.24	3.82	0.15	1.75	0.09	2.55	0.12	0.31	0.06	0.62	0.08
FLD18	FLD18.2	75.05	3.17	13.61	0.68	2.89	0.22	3.52	0.14	1.55	0.09	2.85	0.13	0.36	0.06	0.59	0.08
FLD18	FLD18.2	74.68	3.15	13.91	0.69	2.06	0.16	3.97	0.15	2.65	0.12	2.87	0.13	0.34	0.06	0.86	0.09
FLD18	FLD18.2	75.39	3.18	13.42	0.67	1.75	0.15	3.83	0.15	2.32	0.11	3.31	0.14	0.29	0.06	0.92	0.09
FLD18	FLD18.2	75.79	3.20	13.76	0.69	1.70	0.14	3.88	0.15	1.83	0.09	2.55	0.12	0.32	0.06	0.79	0.09
FLD18	FLD18.2	77.20	3.26	14.61	0.73	1.62	0.14	3.85	0.15	1.38	0.08	2.39	0.11	0.31	0.06	0.79	0.09
FLD18	FLD18.2	76.08	3.21	13.69	0.68	2.09	0.17	4.20	0.16	1.85	0.09	2.72	0.12	0.32	0.06	0.83	0.09
FLD18	FLD18.2	76.93	3.25	14.62	0.73	1.96	0.16	3.86	0.15	1.49	0.08	2.63	0.12	0.31	0.06	0.83	0.09
FLD18	FLD18.2	75.26	3.18	13.99	0.70	1.52	0.13	3.66	0.15	1.55	0.09	2.84	0.13	0.34	0.06	0.82	0.09
FLD18	FLD18.2	75.68	3.19	14.49	0.72	1.78	0.15	3.91	0.15	1.62	0.09	2.59	0.12	0.39	0.06	0.80	0.09
FLD18	FLD18.2	74.90	3.16	14.66	0.73	1.77	0.15	3.83	0.15	1.76	0.09	2.72	0.12	0.32	0.06	0.83	0.09

FLD18	FLD18.2	75.04	3.17	13.78	0.69	1.46	0.13	3.71	0.15	1.63	0.09	2.74	0.12	0.34	0.06	0.81	0.09
FLD18	FLD18.2	75.55	3.19	13.84	0.69	1.53	0.13	3.74	0.15	1.69	0.09	2.54	0.12	0.32	0.06	0.82	0.09
FLD18	FLD18.2	76.94	3.25	14.29	0.71	1.70	0.14	3.85	0.15	1.79	0.09	2.57	0.12	0.34	0.06	0.84	0.09
FLD18	FLD18.2	72.91	3.08	14.95	0.74	2.41	0.19	3.97	0.15	2.87	0.12	2.80	0.12	0.29	0.06	0.81	0.09
FLD18	FLD18.2	76.92	3.25	13.90	0.69	2.08	0.17	4.20	0.16	1.27	0.08	2.13	0.10	0.29	0.06	0.71	0.08
FLD18	FLD18.2	74.63	3.15	14.47	0.72	1.67	0.14	3.86	0.15	1.41	0.08	2.68	0.12	0.34	0.06	0.80	0.09
FLD18	FLD18.2	75.26	3.18	14.36	0.72	1.59	0.14	3.76	0.15	1.68	0.09	2.74	0.12	0.32	0.06	0.82	0.09
FLD18	FLD18.3	72.41	3.06	13.42	0.67	2.53	0.19	3.33	0.14	2.31	0.11	2.81	0.12	0.36	0.06	0.54	0.07
FLD18	FLD18.3	74.22	3.13	13.72	0.69	2.53	0.19	3.31	0.13	2.63	0.12	2.85	0.13	0.37	0.06	0.55	0.07
FLD18	FLD18.3	73.92	3.12	13.85	0.69	2.62	0.20	3.28	0.13	2.28	0.11	2.89	0.13	0.36	0.06	0.61	0.08
FLD18	FLD18.3	73.72	3.11	14.09	0.70	2.64	0.20	3.18	0.13	2.24	0.11	2.86	0.13	0.28	0.06	0.59	0.08
FLD18	FLD18.3	77.13	3.26	14.04	0.70	2.57	0.20	3.09	0.13	2.33	0.11	2.81	0.12	0.32	0.06	0.63	0.08
FLD18	FLD18.3	75.64	3.19	13.35	0.67	2.67	0.20	3.30	0.13	2.30	0.11	2.83	0.13	0.26	0.05	0.57	0.07
FLD18	FLD18.3	73.22	3.09	13.73	0.69	2.63	0.20	3.25	0.13	2.54	0.11	2.56	0.12	0.37	0.06	0.50	0.07
FLD18	FLD18.3	75.33	3.18	13.70	0.68	2.52	0.19	3.14	0.13	2.55	0.12	2.85	0.13	0.31	0.06	0.58	0.08
FLD18	FLD18.3	73.86	3.12	13.84	0.69	2.94	0.22	3.45	0.14	2.45	0.11	2.65	0.12	0.36	0.06	0.51	0.07
FLD18	FLD18.4	75.63	3.19	12.64	0.64	3.65	0.26	4.17	0.16	2.30	0.11	2.59	0.12	0.27	0.05	0.57	0.07
FLD18	FLD18.4	70.40	2.98	14.22	0.71	3.69	0.27	4.19	0.16	2.72	0.12	2.65	0.12	0.35	0.06	0.56	0.07
FLD18	FLD18.4	72.74	3.07	13.95	0.70	3.87	0.28	4.18	0.16	2.42	0.11	2.65	0.12	0.20	0.05	0.59	0.08
FLD18	FLD18.4	73.13	3.09	13.91	0.69	3.01	0.22	3.47	0.14	2.72	0.12	2.83	0.13	0.34	0.06	0.58	0.08
FLD18	FLD18.4	74.20	3.13	13.46	0.67	3.30	0.24	3.69	0.15	2.45	0.11	2.60	0.12	0.30	0.06	0.54	0.07
FLD18	FLD18.4	73.61	3.11	14.53	0.72	3.18	0.23	3.65	0.15	2.31	0.11	2.63	0.12	0.32	0.06	0.57	0.07
FLD18	FLD18.4	73.10	3.09	14.44	0.72	2.66	0.20	3.22	0.13	2.72	0.12	2.81	0.12	0.33	0.06	0.60	0.08
FLD18	FLD18.4	73.91	3.12	14.41	0.72	2.90	0.22	3.39	0.14	2.32	0.11	2.68	0.12	0.30	0.06	0.60	0.08
FLD18	FLD18.4	74.30	3.14	14.54	0.72	2.87	0.22	3.29	0.13	2.20	0.10	2.87	0.13	0.37	0.06	0.64	0.08
FLD18	FLD18.4	75.11	3.17	14.74	0.73	2.76	0.21	3.08	0.13	2.36	0.11	2.91	0.13	0.38	0.06	0.64	0.08
FLD18	FLD18.4	72.18	3.05	14.57	0.73	3.07	0.23	3.56	0.14	2.26	0.11	2.80	0.12	0.37	0.06	0.59	0.08
FLD18	FLD18.4	72.93	3.08	14.48	0.72	2.60	0.20	3.16	0.13	2.23	0.11	2.98	0.13	0.34	0.06	0.65	0.08
FLD18	FLD18.4	73.46	3.10	14.31	0.71	2.97	0.22	3.43	0.14	2.41	0.11	2.67	0.12	0.43	0.06	0.60	0.08
FLD18	FLD18.4	73.64	3.11	13.47	0.67	3.17	0.23	3.75	0.15	2.73	0.12	2.82	0.12	0.28	0.06	0.57	0.07
FLD18	FLD18.4	73.35	3.10	14.68	0.73	2.67	0.20	3.19	0.13	2.26	0.11	2.87	0.13	0.37	0.06	0.69	0.08
FLD18	FLD18.4	74.49	3.15	13.77	0.69	3.04	0.23	3.60	0.14	2.82	0.12	2.81	0.12	0.31	0.06	0.61	0.08
FLD18	FLD18.4	74.56	3.15	13.50	0.68	2.95	0.22	3.45	0.14	2.79	0.12	2.96	0.13	0.33	0.06	0.63	0.08
FLD18	FLD18.4	73.44	3.10	13.56	0.68	2.93	0.22	3.39	0.14	2.94	0.13	2.83	0.13	0.30	0.06	0.62	0.08
FLD18	FLD18.4	72.66	3.07	13.37	0.67	2.75	0.21	3.26	0.13	2.55	0.12	2.86	0.13	0.33	0.06	0.57	0.07
FLD18	FLD18.4	74.34	3.14	13.63	0.68	3.09	0.23	3.46	0.14	2.74	0.12	2.89	0.13	0.29	0.06	0.58	0.08
FLD18	FLD18.4	74.46	3.14	13.70	0.68	3.20	0.24	3.62	0.14	2.90	0.13	2.72	0.12	0.34	0.06	0.61	0.08
FLD18	FLD18.4	73.20	3.09	13.31	0.67	3.18	0.23	3.66	0.15	2.84	0.12	2.77	0.12	0.34	0.06	0.54	0.07
FLD18	FLD18.4	72.89	3.08	13.33	0.67	3.78	0.27	4.19	0.16	2.67	0.12	2.52	0.12	0.32	0.06	0.54	0.07
FLD21	FLD21.L	71.20	3.01	13.19	0.66	2.32	0.18	2.96	0.12	3.99	0.16	2.73	0.12	0.24	0.05	0.60	0.08
FLD21	FLD21.L	75.36	3.18	14.55	0.72	2.44	0.19	2.90	0.12	4.20	0.17	2.63	0.12	0.33	0.06	0.63	0.08
FLD21	FLD21.L	73.88	3.12	13.72	0.69	2.42	0.19	2.96	0.12	4.04	0.16	2.65	0.12	0.28	0.05	0.55	0.07
FLD21	FLD21.L	72.52	3.06	14.00	0.70	2.42	0.19	2.71	0.12	4.00	0.16	2.63	0.12	0.24	0.05	0.64	0.08
FLD21	FLD21.L	74.95	3.16	14.26	0.71	2.43	0.19	2.67	0.12	4.02	0.16	2.50	0.11	0.27	0.05	0.61	0.08
FLD21	FLD21.L	72.83	3.08	14.16	0.71	2.49	0.19	2.82	0.12	4.14	0.16	2.75	0.12	0.22	0.05	0.62	0.08
FLD21	FLD21.L	75.44	3.18	14.07	0.70	2.52	0.19	2.87	0.12	3.92	0.16	2.65	0.12	0.17	0.05	0.66	0.08

FLD21	FLD21.L	73.99	3.13	14.20	0.71	2.64	0.20	3.00	0.13	3.90	0.16	2.68	0.12	0.21	0.05	0.61	0.08
FLD21	FLD21.1	76.66	3.24	13.26	0.66	2.98	0.22	3.53	0.14	3.10	0.13	2.71	0.12	0.35	0.06	0.68	0.08
FLD21	FLD21.1	76.65	3.24	13.03	0.65	2.76	0.21	3.39	0.14	2.93	0.13	2.49	0.11	0.24	0.05	0.60	0.08
FLD21	FLD21.1	76.49	3.23	13.17	0.66	3.01	0.22	3.63	0.14	3.02	0.13	2.61	0.12	0.35	0.06	0.63	0.08
FLD21	FLD21.1	75.35	3.18	12.83	0.64	2.48	0.19	3.39	0.14	3.00	0.13	2.63	0.12	0.36	0.06	0.69	0.08
FLD21	FLD21.1	78.48	3.31	13.05	0.65	2.24	0.18	2.92	0.12	3.06	0.13	2.93	0.13	0.19	0.05	0.65	0.08
FLD21	FLD21.1	75.07	3.17	13.87	0.69	2.55	0.20	3.12	0.13	3.52	0.14	2.93	0.13	0.31	0.06	0.73	0.08
FLD21	FLD21.1	74.77	3.16	13.16	0.66	2.85	0.21	3.33	0.14	2.94	0.13	2.46	0.11	0.29	0.06	0.63	0.08
FLD21	FLD21.1	76.52	3.23	13.33	0.67	2.74	0.21	3.38	0.14	3.08	0.13	2.91	0.13	0.36	0.06	0.76	0.08
FLD21	FLD21.1	77.25	3.26	13.49	0.67	2.99	0.22	3.16	0.13	2.84	0.12	2.54	0.12	0.36	0.06	0.64	0.08
FLD21	FLD21.1	76.93	3.25	13.36	0.67	2.90	0.22	3.38	0.14	3.11	0.13	2.90	0.13	0.25	0.05	0.68	0.08
FLD23	FLD23.1.2	75.39	3.18	14.04	0.70	1.95	0.16	3.86	0.15	2.11	0.10	2.71	0.12	0.37	0.06	0.60	0.08
FLD23	FLD23.1.2	76.27	3.22	13.70	0.68	1.89	0.15	3.76	0.15	2.39	0.11	2.67	0.12	0.30	0.06	0.55	0.07
FLD23	FLD23.1.2	75.67	3.19	14.16	0.71	2.04	0.16	3.72	0.15	2.36	0.11	2.79	0.12	0.32	0.06	0.59	0.08
FLD23	FLD23.1.1	76.20	3.22	14.16	0.71	1.88	0.15	3.66	0.15	2.64	0.12	2.57	0.12	0.34	0.06	0.56	0.07
FLD23	FLD23.1.1	74.47	3.14	13.88	0.69	1.83	0.15	3.73	0.15	2.62	0.12	2.65	0.12	0.35	0.06	0.59	0.08
FLD23	FLD23.1.1	75.49	3.19	14.07	0.70	2.15	0.17	3.73	0.15	2.47	0.11	2.71	0.12	0.32	0.06	0.58	0.08
FLD23	FLD23.1.3	75.33	3.18	13.93	0.70	2.21	0.17	3.80	0.15	2.33	0.11	2.79	0.12	0.31	0.06	0.60	0.08
FLD23	FLD23.1.3	74.75	3.16	14.37	0.72	2.18	0.17	3.84	0.15	2.34	0.11	2.83	0.13	0.37	0.06	0.58	0.08
FLD23	FLD23.1.3	79.33	3.35	13.88	0.69	1.79	0.15	3.59	0.14	1.83	0.09	2.57	0.12	0.33	0.06	0.65	0.08
FLD23	FLD23.2.1	77.39	3.27	14.15	0.71	1.95	0.16	3.80	0.15	2.23	0.11	2.64	0.12	0.36	0.06	0.58	0.08
FLD23	FLD23.2.1	76.67	3.24	14.36	0.72	1.72	0.14	3.72	0.15	2.50	0.11	2.67	0.12	0.29	0.06	0.63	0.08
FLD23	FLD23.2.2	76.39	3.22	14.30	0.71	2.22	0.17	3.77	0.15	2.33	0.11	2.66	0.12	0.35	0.06	0.59	0.08
FLD23	FLD23.2.2	77.23	3.26	14.36	0.72	1.58	0.14	3.76	0.15	2.24	0.11	2.63	0.12	0.37	0.06	0.59	0.08
FLD23	FLD23.2.2	76.62	3.23	14.38	0.72	2.17	0.17	3.77	0.15	2.43	0.11	2.78	0.12	0.34	0.06	0.66	0.08
FLD23	FLD23.2.2	74.46	3.14	13.61	0.68	2.34	0.18	3.72	0.15	2.50	0.11	2.76	0.12	0.31	0.06	0.57	0.07
FLD23	FLD23.3.1	73.56	3.11	13.80	0.69	2.10	0.17	3.76	0.15	2.48	0.11	2.72	0.12	0.37	0.06	0.63	0.08
FLD23	FLD23.3.1	75.01	3.17	13.98	0.70	2.46	0.19	3.69	0.15	2.22	0.11	2.67	0.12	0.32	0.06	0.60	0.08
FLD23	FLD23.3.1	75.43	3.18	14.27	0.71	2.58	0.20	3.70	0.15	2.32	0.11	2.72	0.12	0.35	0.06	0.63	0.08
FLD23	FLD23.3.1	74.98	3.17	14.22	0.71	2.53	0.19	3.77	0.15	2.22	0.11	2.70	0.12	0.29	0.06	0.61	0.08
FLD23	FLD23.3.2	74.34	3.14	14.01	0.70	2.58	0.20	4.03	0.16	2.43	0.11	2.75	0.12	0.30	0.06	0.62	0.08
FLD23	FLD23.3.2	75.62	3.19	13.12	0.66	2.60	0.20	3.95	0.15	2.07	0.10	2.66	0.12	0.30	0.06	0.55	0.07
FLD23	FLD23.4.1	74.88	3.16	13.79	0.69	2.72	0.21	3.86	0.15	2.19	0.10	2.62	0.12	0.36	0.06	0.62	0.08
FLD23	FLD23.4.1	74.55	3.15	13.79	0.69	2.69	0.20	3.73	0.15	2.18	0.10	2.63	0.12	0.29	0.06	0.59	0.08
FLD23	FLD23.4.1	73.89	3.12	13.77	0.69	2.61	0.20	3.64	0.14	2.33	0.11	2.61	0.12	0.32	0.06	0.62	0.08
FLD23	FLD23.4.1	75.38	3.18	13.89	0.69	2.84	0.21	3.85	0.15	2.25	0.11	2.63	0.12	0.29	0.06	0.62	0.08
FLD23	FLD23.4.1	75.24	3.18	13.68	0.68	3.01	0.22	4.03	0.16	2.26	0.11	2.58	0.12	0.30	0.06	0.60	0.08
FLD23	FLD23.4.2	74.16	3.13	14.35	0.71	3.20	0.24	4.12	0.16	2.32	0.11	2.76	0.12	0.35	0.06	0.64	0.08
FLD23	FLD23.4.2	74.57	3.15	13.21	0.66	2.99	0.22	4.00	0.16	2.33	0.11	2.62	0.12	0.30	0.06	0.59	0.08
FLD23	FLD23.4.2	73.92	3.12	13.97	0.70	3.11	0.23	3.98	0.16	2.09	0.10	2.68	0.12	0.31	0.06	0.60	0.08
FLD23	FLD23.4.2	73.02	3.08	13.76	0.69	2.94	0.22	3.94	0.15	1.99	0.10	2.79	0.12	0.32	0.06	0.59	0.08
FLD23	FLD23.4.2	73.65	3.11	14.12	0.70	3.03	0.22	3.95	0.15	2.40	0.11	2.77	0.12	0.36	0.06	0.73	0.08
FLD23	FLD23.4.2	75.17	3.17	13.02	0.65	2.84	0.21	3.94	0.15	1.90	0.10	2.49	0.11	0.32	0.06	0.56	0.07
FLD23	FLD23.5.1	73.22	3.09	13.98	0.70	2.71	0.20	3.83	0.15	2.61	0.12	2.64	0.12	0.29	0.06	0.53	0.07
FLD23	FLD23.5.1	74.35	3.14	13.47	0.67	2.93	0.22	3.84	0.15	2.24	0.11	2.62	0.12	0.35	0.06	0.60	0.08
FLD23	FLD23.5.1	73.95	3.12	13.75	0.69	2.87	0.22	3.78	0.15	2.39	0.11	2.62	0.12	0.29	0.06	0.61	0.08

FLD23	FLD23.5.1	73.87	3.12	13.51	0.68	2.72	0.21	3.69	0.15	2.31	0.11	2.44	0.11	0.27	0.05	0.49	0.07
FLD23	FLD23.L	73.69	3.11	13.17	0.66	1.96	0.16	3.34	0.14	3.04	0.13	2.57	0.12	0.26	0.05	0.55	0.07
FLD23	FLD23.L	72.94	3.08	13.55	0.68	1.80	0.15	2.86	0.12	3.61	0.15	2.71	0.12	0.27	0.05	0.58	0.08
FLD23	FLD23.L	72.38	3.06	12.81	0.64	2.25	0.18	3.55	0.14	2.69	0.12	2.62	0.12	0.28	0.06	0.53	0.07
FLD23	FLD23.L	73.17	3.09	12.39	0.62	2.12	0.17	3.44	0.14	2.66	0.12	2.52	0.12	0.29	0.06	0.56	0.07
FLD23	FLD23.L	73.53	3.11	12.84	0.65	2.15	0.17	3.50	0.14	2.99	0.13	2.62	0.12	0.29	0.06	0.56	0.07
FLD23	FLD23.L	73.79	3.12	13.02	0.65	2.14	0.17	3.50	0.14	2.81	0.12	2.60	0.12	0.28	0.06	0.57	0.07
FLD23	FLD23.L	73.50	3.10	12.93	0.65	1.94	0.16	3.35	0.14	2.93	0.13	2.64	0.12	0.27	0.05	0.54	0.07
FLD23	FLD23.L	73.61	3.11	12.93	0.65	2.07	0.17	3.34	0.14	3.06	0.13	2.60	0.12	0.29	0.06	0.52	0.07
FLD4.3	FLD4.3.1	74.05	3.13	12.17	0.61	1.98	0.16	3.81	0.15	1.12	0.07	3.06	0.13	0.44	0.06	0.54	0.07
FLD4.3	FLD4.3.1	78.18	3.30	11.57	0.59	1.67	0.14	3.82	0.15	0.96	0.07	2.88	0.13	0.36	0.06	0.53	0.07
FLD4.3	FLD4.3.1	76.78	3.24	12.12	0.61	1.67	0.14	3.91	0.15	1.04	0.07	2.83	0.12	0.35	0.06	0.55	0.07
FLD4.3	FLD4.3.2	77.07	3.25	9.99	0.51	1.83	0.15	3.50	0.14	1.23	0.08	2.84	0.13	0.31	0.06	0.49	0.07
FLD4.3	FLD4.3.2	78.73	3.32	10.30	0.53	1.53	0.13	3.62	0.14	1.20	0.07	2.73	0.12	0.29	0.06	0.47	0.07
FLD4.3	FLD4.3.2	78.33	3.30	10.99	0.56	1.55	0.13	3.57	0.14	1.37	0.08	2.69	0.12	0.28	0.06	0.50	0.07
FLD4.3	FLD4.3.3	79.24	3.34	10.20	0.52	1.85	0.15	3.52	0.14	1.06	0.07	2.75	0.12	0.25	0.05	0.43	0.07
FLD4.3	FLD4.3.3	78.30	3.30	10.00	0.51	1.54	0.13	3.62	0.14	0.91	0.07	2.67	0.12	0.29	0.06	0.39	0.07
FLD4.3	FLD4.3.3	78.67	3.32	10.73	0.55	1.55	0.13	3.67	0.15	1.04	0.07	2.86	0.13	0.32	0.06	0.44	0.07
FLD4.3	FLD4.3.UA	71.57	3.02	14.28	0.71	1.83	0.15	3.70	0.15	1.83	0.09	3.05	0.13	0.37	0.06	0.97	0.10
FLD4.3	FLD4.3.UA	72.39	3.06	14.45	0.72	1.81	0.15	3.65	0.15	1.85	0.09	2.92	0.13	0.34	0.06	1.03	0.10
FLD4.3	FLD4.3.UA	72.52	3.06	14.55	0.72	1.76	0.15	3.70	0.15	1.80	0.09	3.03	0.13	0.40	0.06	1.00	0.10
FLD4.3	FLD4.3.UA	73.51	3.11	12.48	0.63	1.80	0.15	3.34	0.14	1.66	0.09	2.65	0.12	0.35	0.06	0.61	0.08
FLD4.3	FLD4.3.4	74.11	3.13	12.81	0.64	2.89	0.22	3.81	0.15	1.29	0.08	3.25	0.14	0.49	0.06	1.05	0.10
FLD4.3	FLD4.3.4	74.71	3.15	13.92	0.69	2.82	0.21	3.89	0.15	1.24	0.08	2.81	0.12	0.47	0.06	1.07	0.10
FLD4.3	FLD4.3.4	75.16	3.17	14.58	0.73	3.21	0.24	3.87	0.15	1.29	0.08	2.96	0.13	0.50	0.06	1.12	0.10
FLD4.3	FLD4.3.4	75.51	3.19	13.94	0.70	3.15	0.23	3.82	0.15	1.32	0.08	3.08	0.13	0.43	0.06	1.12	0.10
FLD4.3	FLD4.3.5	71.04	3.00	16.36	0.81	3.42	0.25	3.92	0.15	1.86	0.09	3.04	0.13	0.54	0.06	1.08	0.10
FLD4.3	FLD4.3.5	71.98	3.04	15.62	0.77	2.98	0.22	3.91	0.15	1.69	0.09	3.02	0.13	0.54	0.06	1.04	0.10
FLD4.4	FLD4.4.1	70.85	2.99	17.00	0.84	2.14	0.17	2.72	0.12	2.13	0.10	3.17	0.14	0.35	0.06	0.79	0.09
FLD4.4	FLD4.4.1	71.10	3.01	17.19	0.85	2.18	0.17	2.68	0.12	2.32	0.11	3.15	0.13	0.38	0.06	0.74	0.08
FLD4.4	FLD4.4.1	72.58	3.07	17.92	0.88	2.21	0.17	2.66	0.11	2.25	0.11	3.18	0.14	0.35	0.06	0.75	0.08
FLD4.4	FLD4.4.1	72.28	3.05	16.88	0.83	2.17	0.17	2.68	0.12	2.20	0.10	3.19	0.14	0.40	0.06	0.76	0.08
FLD4.4	FLD4.4.1	71.84	3.04	16.82	0.83	2.07	0.17	2.65	0.11	2.24	0.11	3.35	0.14	0.37	0.06	0.71	0.08
FLD4.4	FLD4.4.1	71.42	3.02	16.44	0.81	2.01	0.16	2.59	0.11	2.22	0.11	3.07	0.13	0.38	0.06	0.77	0.09
FLD4.4	FLD4.4.1	71.22	3.01	16.80	0.83	2.05	0.16	2.53	0.11	2.16	0.10	3.16	0.14	0.38	0.06	0.75	0.08
FLD4.4	FLD4.4.1	71.39	3.02	16.38	0.81	2.11	0.17	2.77	0.12	2.17	0.10	3.15	0.13	0.46	0.06	0.74	0.08
FLD4.4	FLD4.4.1	72.29	3.05	17.41	0.86	2.09	0.17	2.62	0.11	2.38	0.11	3.13	0.13	0.39	0.06	0.73	0.08
FLD4.4	FLD4.4.1	89.27	3.76	6.63	0.36	1.13	0.11	1.71	0.09	0.74	0.06	1.64	0.09	0.08	0.05	0.34	0.06
FLD4.4	FLD4.4.1	72.09	3.05	16.98	0.84	2.05	0.16	2.61	0.11	2.27	0.11	3.18	0.14	0.43	0.06	0.76	0.08
FLD4.4	FLD4.4.1	69.18	2.93	16.94	0.83	2.02	0.16	2.75	0.12	2.41	0.11	3.30	0.14	0.44	0.06	0.79	0.09
FLD4.4	FLD4.4.1	72.43	3.06	17.39	0.86	2.05	0.16	2.64	0.11	2.36	0.11	2.97	0.13	0.39	0.06	0.76	0.08
FLD4.4	FLD4.4.1	71.66	3.03	16.78	0.83	2.06	0.16	2.71	0.12	2.32	0.11	3.16	0.14	0.44	0.06	0.72	0.08
FLD4.4	FLD4.4.1	72.38	3.06	16.79	0.83	2.14	0.17	2.60	0.11	2.12	0.10	3.20	0.14	0.34	0.06	0.76	0.08
FLD4.4	FLD4.4.1	70.81	2.99	17.26	0.85	2.11	0.17	2.66	0.11	2.30	0.11	3.25	0.14	0.38	0.06	0.73	0.08
FLD4.4	FLD4.4.1	71.09	3.01	17.02	0.84	2.09	0.17	2.60	0.11	2.29	0.11	3.21	0.14	0.33	0.06	0.72	0.08
FLD4.4	FLD4.4.1	69.60	2.94	17.12	0.84	2.04	0.16	2.76	0.12	2.33	0.11	3.50	0.15	0.45	0.06	0.69	0.08

FLD4.4	FLD4.4.1	72.03	3.04	16.97	0.84	2.07	0.17	2.58	0.11	2.21	0.11	3.13	0.13	0.38	0.06	0.73	0.08
FLD4.4	FLD4.4.2	71.22	3.01	14.80	0.74	2.38	0.18	3.02	0.13	2.11	0.10	3.19	0.14	0.30	0.06	0.73	0.08
FLD4.4	FLD4.4.2	71.08	3.00	15.14	0.75	2.48	0.19	3.06	0.13	2.22	0.11	3.28	0.14	0.41	0.06	0.75	0.08
FLD4.4	FLD4.4.2	70.66	2.99	16.69	0.82	2.30	0.18	2.69	0.12	2.31	0.11	3.16	0.14	0.42	0.06	0.81	0.09
FLD4.4	FLD4.4.2	69.41	2.94	16.52	0.82	2.32	0.18	2.77	0.12	2.39	0.11	3.12	0.13	0.40	0.06	0.75	0.08
FLD4.4	FLD4.4.2	69.93	2.96	17.36	0.85	2.48	0.19	2.91	0.12	2.43	0.11	3.55	0.15	0.39	0.06	0.76	0.09
FLD4.4	FLD4.4.2	66.81	2.83	18.90	0.93	2.32	0.18	2.58	0.11	2.78	0.12	3.52	0.15	0.46	0.06	0.83	0.09
FLD4.4	FLD4.4.2	68.62	2.90	17.46	0.86	2.35	0.18	2.89	0.12	2.48	0.11	3.27	0.14	0.45	0.06	0.84	0.09
FLD4.4	FLD4.4.2	68.77	2.91	17.11	0.84	2.24	0.18	2.74	0.12	2.45	0.11	3.18	0.14	0.43	0.06	0.75	0.08
FLD4.4	FLD4.4.2	71.06	3.00	17.97	0.88	2.42	0.19	2.83	0.12	2.45	0.11	3.19	0.14	0.49	0.06	0.89	0.09
FLD4.4	FLD4.4.2	70.74	2.99	16.50	0.81	2.41	0.19	2.99	0.12	2.23	0.11	3.19	0.14	0.36	0.06	0.79	0.09
FLD4.4	FLD4.4.2	70.51	2.98	16.18	0.80	2.47	0.19	3.06	0.13	2.36	0.11	3.27	0.14	0.48	0.06	0.78	0.09
FLD4.4	FLD4.4.2	69.26	2.93	18.88	0.92	2.36	0.18	2.54	0.11	2.70	0.12	3.14	0.13	0.47	0.06	0.85	0.09
U1B	U1B.L	69.89	2.96	15.50	0.77	2.45	0.19	3.64	0.14	1.70	0.09	3.64	0.15	0.54	0.06	0.77	0.09
U1B	U1B.L	68.52	2.90	15.30	0.76	2.42	0.19	3.58	0.14	1.78	0.09	3.28	0.14	0.52	0.06	0.77	0.09
U1B	U1B.L	71.38	3.02	15.92	0.79	2.50	0.19	3.57	0.14	1.58	0.09	3.37	0.14	0.51	0.06	0.88	0.09
U1B	U1B.L	69.28	2.93	15.53	0.77	2.44	0.19	3.73	0.15	1.59	0.09	3.16	0.14	0.52	0.06	0.87	0.09
U1B	U1B.L	69.48	2.94	15.89	0.79	2.34	0.18	3.60	0.14	1.68	0.09	3.38	0.14	0.54	0.06	0.91	0.09
U1B	U1B.L	69.33	2.93	15.58	0.77	2.53	0.19	3.73	0.15	1.75	0.09	3.35	0.14	0.48	0.06	0.79	0.09
U1B	U1B.L	70.10	2.96	16.04	0.79	2.60	0.20	3.61	0.14	1.63	0.09	3.33	0.14	0.52	0.06	0.91	0.09
U1B	U1B.L	71.32	3.01	16.13	0.80	2.53	0.19	3.72	0.15	1.68	0.09	3.39	0.14	0.51	0.06	0.91	0.09
U1B	U1B.L	71.70	3.03	16.00	0.79	2.39	0.19	3.51	0.14	1.55	0.09	3.18	0.14	0.44	0.06	0.89	0.09
U1B	U1B.L	75.30	3.18	15.13	0.75	2.18	0.17	3.53	0.14	1.45	0.08	3.15	0.13	0.49	0.06	0.84	0.09
U1B	U1B.L	78.23	3.30	13.12	0.66	1.96	0.16	3.51	0.14	1.14	0.07	2.66	0.12	0.36	0.06	0.65	0.08
U1B	U1B.L	70.52	2.98	15.36	0.76	2.43	0.19	3.69	0.15	1.62	0.09	3.38	0.14	0.52	0.06	0.78	0.09
U1B	U1B.L	73.34	3.10	15.86	0.78	2.40	0.19	3.61	0.14	1.50	0.08	3.34	0.14	0.43	0.06	0.81	0.09
U1B	U1B.L	72.52	3.06	15.80	0.78	2.28	0.18	3.63	0.14	1.57	0.09	3.19	0.14	0.47	0.06	0.87	0.09
U1B	U1B.L	70.13	2.97	15.82	0.78	2.29	0.18	3.58	0.14	1.62	0.09	3.32	0.14	0.49	0.06	0.87	0.09
U1B	U1B.L	71.32	3.01	16.03	0.79	2.44	0.19	3.46	0.14	1.62	0.09	3.16	0.14	0.47	0.06	0.90	0.09
U1B	U1B.L	69.24	2.93	15.42	0.76	2.30	0.18	3.66	0.15	1.67	0.09	3.25	0.14	0.44	0.06	0.78	0.09
U1B	U1B.L	69.70	2.95	15.50	0.77	2.39	0.19	3.79	0.15	1.76	0.09	3.37	0.14	0.48	0.06	0.79	0.09
U1B	U1B.L	73.33	3.10	15.81	0.78	2.42	0.19	3.52	0.14	1.50	0.08	3.28	0.14	0.38	0.06	0.82	0.09
U1B	U1B.L	71.37	3.02	15.68	0.78	2.36	0.18	3.71	0.15	1.70	0.09	3.24	0.14	0.48	0.06	0.79	0.09
U1B	U1B.L	71.09	3.00	15.73	0.78	2.50	0.19	3.67	0.15	1.69	0.09	3.31	0.14	0.53	0.06	0.83	0.09
U1B	U1B.L	71.88	3.04	16.06	0.79	2.50	0.19	3.63	0.14	1.59	0.09	3.30	0.14	0.51	0.06	0.84	0.09
U1B	U1B.L	72.71	3.07	16.45	0.81	2.58	0.20	3.36	0.14	1.61	0.09	3.15	0.13	0.53	0.06	0.92	0.09
U1B	U1B.L	70.44	2.98	15.32	0.76	2.59	0.20	3.75	0.15	1.78	0.09	3.21	0.14	0.52	0.06	0.81	0.09
U1B	U1B.L	73.74	3.11	14.94	0.74	2.25	0.18	3.55	0.14	1.48	0.08	3.06	0.13	0.38	0.06	0.86	0.09
U1B	U1B.2	71.67	3.03	12.81	0.64	4.50	0.32	4.68	0.18	0.98	0.07	2.44	0.11	0.31	0.06	0.37	0.06
U1B	U1B.2	71.79	3.03	13.39	0.67	4.06	0.29	4.59	0.17	0.90	0.07	2.40	0.11	0.34	0.06	0.48	0.07
U1B	U1B.2	71.96	3.04	13.48	0.67	1.93	0.16	4.78	0.18	0.85	0.06	2.49	0.11	0.31	0.06	0.45	0.07
U1B	U1B.2	72.72	3.07	13.40	0.67	4.06	0.29	4.66	0.18	0.83	0.06	2.42	0.11	0.33	0.06	0.47	0.07
U1B	U1B.2	73.73	3.11	13.29	0.67	5.24	0.36	4.88	0.18	0.77	0.06	2.26	0.11	0.36	0.06	0.37	0.06
U1B	U1B.2	73.27	3.10	13.07	0.66	4.45	0.31	5.10	0.19	0.87	0.06	2.32	0.11	0.32	0.06	0.46	0.07
U1B	U1B.2	74.29	3.14	9.83	0.51	3.45	0.25	4.11	0.16	1.48	0.08	3.72	0.15	0.26	0.05	0.53	0.07
U1B	U1B.2	72.27	3.05	10.43	0.53	4.08	0.29	4.26	0.16	1.51	0.08	3.63	0.15	0.25	0.05	0.49	0.07

U1B	U1B.2	75.48	3.19	10.05	0.52	3.95	0.28	4.16	0.16	1.32	0.08	3.34	0.14	0.32	0.06	0.50	0.07
U3	U3.1	69.87	2.95	13.66	0.68	2.19	0.17	3.13	0.13	3.43	0.14	2.84	0.13	0.36	0.06	0.55	0.07
U3	U3.1	72.14	3.05	14.36	0.72	2.43	0.19	3.21	0.13	3.57	0.15	2.80	0.12	0.33	0.06	0.56	0.07
U3	U3.1	74.22	3.13	12.86	0.65	2.70	0.20	3.27	0.13	3.04	0.13	2.76	0.12	0.29	0.06	0.50	0.07
U3	U3.1	73.80	3.12	14.88	0.74	2.34	0.18	3.24	0.13	3.50	0.14	3.03	0.13	0.31	0.06	0.74	0.08
U3	U3.1	72.65	3.07	14.25	0.71	2.23	0.18	3.17	0.13	3.41	0.14	2.96	0.13	0.34	0.06	0.73	0.08
U3	U3.1	75.21	3.18	13.40	0.67	2.51	0.19	3.40	0.14	3.07	0.13	2.98	0.13	0.27	0.05	0.67	0.08
U3	U3.1	75.12	3.17	13.37	0.67	2.38	0.18	3.32	0.13	3.14	0.13	3.01	0.13	0.28	0.05	0.72	0.08
U3	U3.2	74.90	3.16	12.20	0.62	2.28	0.18	3.71	0.15	2.57	0.12	2.98	0.13	0.27	0.05	0.55	0.07
U3	U3.2	72.31	3.06	12.86	0.65	2.40	0.19	3.69	0.15	2.73	0.12	2.85	0.13	0.29	0.06	0.51	0.07
U3	U3.2	73.35	3.10	12.15	0.61	2.30	0.18	3.74	0.15	2.67	0.12	2.87	0.13	0.35	0.06	0.49	0.07
U3	U3.2	75.87	3.20	12.84	0.65	2.37	0.18	3.67	0.15	2.54	0.12	3.24	0.14	0.21	0.05	0.72	0.08
U3	U3.2	75.64	3.19	13.63	0.68	2.30	0.18	3.70	0.15	2.67	0.12	3.14	0.13	0.28	0.05	0.70	0.08
U3	U3.2	75.22	3.18	13.77	0.69	2.59	0.20	3.76	0.15	2.59	0.12	3.04	0.13	0.31	0.06	0.75	0.08
U4	U4.1	75.78	3.20	14.21	0.71	2.72	0.21	3.30	0.13	2.34	0.11	3.04	0.13	0.23	0.05	0.66	0.08
U4	U4.1	73.88	3.12	13.38	0.67	2.47	0.19	3.37	0.14	2.30	0.11	2.85	0.13	0.25	0.05	0.58	0.08
U4	U4.1	73.24	3.09	13.92	0.70	2.65	0.20	3.35	0.14	2.47	0.11	3.03	0.13	0.35	0.06	0.71	0.08
U4	U4.1	72.72	3.07	13.41	0.67	2.46	0.19	3.38	0.14	2.39	0.11	3.03	0.13	0.21	0.05	0.61	0.08
U4	U4.1	75.57	3.19	13.73	0.69	2.54	0.19	3.29	0.13	2.25	0.11	2.93	0.13	0.24	0.05	0.66	0.08
U4	U4.1	73.39	3.10	13.84	0.69	2.44	0.19	3.38	0.14	2.34	0.11	2.91	0.13	0.29	0.06	0.65	0.08
U4	U4.1	76.84	3.24	13.91	0.69	2.51	0.19	3.34	0.14	2.18	0.10	2.83	0.12	0.20	0.05	0.66	0.08
U4	U4.1	75.40	3.18	14.54	0.72	2.34	0.18	3.20	0.13	2.36	0.11	2.94	0.13	0.33	0.06	0.62	0.08
U4	U4.1	74.15	3.13	13.88	0.69	2.10	0.17	3.25	0.13	2.47	0.11	2.94	0.13	0.35	0.06	0.65	0.08
U4	U4.1	73.93	3.12	13.87	0.69	1.76	0.15	2.97	0.12	2.45	0.11	2.81	0.12	0.32	0.06	0.65	0.08
U4	U4.1	74.48	3.15	13.98	0.70	1.87	0.15	3.21	0.13	2.52	0.11	2.96	0.13	0.33	0.06	0.59	0.08
U4	U4.1	75.92	3.21	13.36	0.67	1.84	0.15	3.23	0.13	2.29	0.11	2.82	0.12	0.27	0.05	0.65	0.08
U4	U4.1	72.65	3.07	13.28	0.67	2.03	0.16	3.15	0.13	2.31	0.11	2.69	0.12	0.29	0.06	0.56	0.07
U4	U4.2	75.13	3.17	12.93	0.65	2.88	0.22	3.33	0.14	2.61	0.12	2.68	0.12	0.27	0.05	0.52	0.07
U4	U4.2	71.89	3.04	12.85	0.65	2.87	0.21	3.45	0.14	2.84	0.12	2.98	0.13	0.29	0.06	0.58	0.08
U4	U4.2	75.89	3.20	12.38	0.62	2.74	0.21	3.34	0.14	2.32	0.11	2.59	0.12	0.19	0.05	0.60	0.08
U4	U4.2	73.48	3.10	12.98	0.65	2.84	0.21	3.41	0.14	2.70	0.12	2.84	0.13	0.34	0.06	0.58	0.08
U4	U4.2	75.61	3.19	12.05	0.61	3.06	0.23	3.76	0.15	1.78	0.09	2.64	0.12	0.28	0.05	0.49	0.07
U4	U4.2	71.56	3.02	13.40	0.67	3.48	0.25	3.83	0.15	1.84	0.09	3.44	0.14	0.35	0.06	0.52	0.07
U4	U4.2	74.52	3.15	12.40	0.62	3.32	0.24	3.82	0.15	1.70	0.09	3.01	0.13	0.21	0.05	0.45	0.07
U4	U4.2	78.16	3.30	12.42	0.63	3.11	0.23	3.49	0.14	2.19	0.10	2.42	0.11	0.23	0.05	0.51	0.07
AE.C	C3	74.64	3.15	11.74	0.59	3.43	0.25	5.36	0.20	1.60	0.09	2.23	0.11	0.25	0.05	0.47	0.07
AE.C	C3	74.26	3.14	10.67	0.54	5.44	0.37	5.39	0.20	1.81	0.09	2.25	0.11	0.25	0.05	0.51	0.07
AE.C	C3	73.53	3.11	11.85	0.60	5.55	0.38	5.52	0.20	1.63	0.09	2.29	0.11	0.22	0.05	0.46	0.07
AE.C	C3	71.60	3.03	10.90	0.56	5.58	0.38	5.41	0.20	1.82	0.09	2.37	0.11	0.26	0.05	0.45	0.07
AE.C	C4	73.24	3.09	12.81	0.64	4.71	0.33	4.38	0.17	1.00	0.07	2.24	0.11	0.22	0.05	0.39	0.07
AE.C	C4	71.50	3.02	12.33	0.62	4.62	0.32	4.39	0.17	1.23	0.08	2.70	0.12	0.40	0.06	0.44	0.07
AE.C	C4	70.93	3.00	13.10	0.66	4.70	0.33	4.37	0.17	2.36	0.11	2.81	0.12	0.41	0.06	0.73	0.08
AE.C	C4	68.98	2.92	13.68	0.68	5.26	0.36	4.68	0.18	2.03	0.10	2.88	0.13	0.36	0.06	0.66	0.08
AE.C	C4	75.21	3.18	11.78	0.60	4.26	0.30	4.21	0.16	0.99	0.07	2.25	0.11	0.23	0.05	0.35	0.06
AE.C	C4	72.20	3.05	11.96	0.60	4.40	0.31	4.37	0.17	2.34	0.11	2.79	0.12	0.40	0.06	0.77	0.09
AE.C	C4	73.41	3.10	11.62	0.59	4.37	0.31	4.40	0.17	1.02	0.07	2.08	0.10	0.26	0.05	0.31	0.06

AE.C	C4	70.31	2.97	12.63	0.64	4.58	0.32	4.38	0.17	2.33	0.11	2.82	0.12	0.32	0.06	0.69	0.08
AE.C	C4	70.84	2.99	11.66	0.59	4.56	0.32	4.57	0.17	2.09	0.10	2.74	0.12	0.48	0.06	0.75	0.08
U3	U3.3	75.10	3.17	13.18	0.66	3.18	0.23	3.59	0.14	3.03	0.13	2.83	0.12	0.33	0.06	0.90	0.09
U3	U3.3	74.60	3.15	13.51	0.68	3.40	0.25	3.68	0.15	2.92	0.13	2.75	0.12	0.34	0.06	0.94	0.09
U3	U3.3	74.54	3.15	13.57	0.68	3.28	0.24	3.63	0.14	2.94	0.13	2.75	0.12	0.32	0.06	0.92	0.09
U3	U3.3	74.57	3.15	13.41	0.67	3.47	0.25	3.77	0.15	2.57	0.12	2.64	0.12	0.29	0.06	0.91	0.09
U3	U3.3	74.09	3.13	13.17	0.66	3.30	0.24	3.87	0.15	2.71	0.12	2.71	0.12	0.32	0.06	0.87	0.09
U3	U3.3	73.39	3.10	13.19	0.66	3.22	0.24	3.72	0.15	2.94	0.13	2.83	0.13	0.33	0.06	0.89	0.09
U3	U3.3	74.93	3.16	13.63	0.68	3.42	0.25	3.80	0.15	2.86	0.12	2.74	0.12	0.33	0.06	0.93	0.09
U3	U3.3	75.54	3.19	13.72	0.69	3.45	0.25	3.59	0.14	2.82	0.12	2.80	0.12	0.34	0.06	0.95	0.09
U3	U3.3	74.09	3.13	13.37	0.67	3.33	0.24	3.79	0.15	3.01	0.13	2.70	0.12	0.32	0.06	0.91	0.09
U3	U3.3	74.93	3.16	13.46	0.67	3.24	0.24	3.56	0.14	2.91	0.13	2.77	0.12	0.32	0.06	0.92	0.09
U3	U3.3	74.23	3.14	13.44	0.67	3.28	0.24	3.61	0.14	3.03	0.13	2.74	0.12	0.34	0.06	0.92	0.09
U3	U3.3	74.80	3.16	13.51	0.68	3.33	0.24	3.57	0.14	2.82	0.12	2.75	0.12	0.30	0.06	0.96	0.10
U3	U3.3	73.79	3.12	13.31	0.67	3.33	0.24	3.79	0.15	2.77	0.12	2.67	0.12	0.34	0.06	0.89	0.09
U3	U3.4	76.07	3.21	13.90	0.69	3.40	0.25	3.81	0.15	2.69	0.12	2.81	0.12	0.33	0.06	0.89	0.09
U3	U3.4	74.97	3.17	14.14	0.70	3.30	0.24	3.84	0.15	2.51	0.11	2.76	0.12	0.33	0.06	0.86	0.09
U3	U3.4	73.89	3.12	13.31	0.67	3.01	0.22	3.89	0.15	2.51	0.11	2.89	0.13	0.34	0.06	0.87	0.09
U3	U3.4	75.80	3.20	12.55	0.63	2.93	0.22	3.70	0.15	2.57	0.12	3.03	0.13	0.28	0.05	0.86	0.09
U3	U3.4	76.09	3.21	13.74	0.69	3.23	0.24	3.74	0.15	2.71	0.12	2.90	0.13	0.36	0.06	0.86	0.09
U3	U3.4	74.24	3.14	13.42	0.67	3.26	0.24	3.84	0.15	2.82	0.12	2.89	0.13	0.37	0.06	0.83	0.09
U3	U3.5	73.51	3.11	13.30	0.67	3.31	0.24	3.82	0.15	2.73	0.12	2.78	0.12	0.29	0.06	0.87	0.09
U3	U3.5	75.21	3.18	13.61	0.68	3.23	0.24	3.75	0.15	2.72	0.12	2.70	0.12	0.28	0.06	0.92	0.09
U3	U3.5	74.62	3.15	13.66	0.68	3.20	0.24	3.67	0.15	2.65	0.12	2.67	0.12	0.31	0.06	0.87	0.09
U3	U3.5	73.10	3.09	13.40	0.67	3.18	0.23	3.83	0.15	2.63	0.12	2.79	0.12	0.30	0.06	0.87	0.09
U3	U3.5	75.28	3.18	13.93	0.70	3.19	0.23	3.80	0.15	2.69	0.12	2.77	0.12	0.35	0.06	0.87	0.09
U3	U3.5	74.04	3.13	13.65	0.68	3.26	0.24	3.79	0.15	2.66	0.12	2.75	0.12	0.34	0.06	0.88	0.09
U3	U3.5	73.08	3.09	13.82	0.69	3.24	0.24	3.86	0.15	2.63	0.12	2.81	0.12	0.31	0.06	0.89	0.09
U4	U4.3	76.22	3.22	13.79	0.69	2.04	0.16	3.26	0.13	2.54	0.12	2.72	0.12	0.31	0.06	0.81	0.09
U4	U4.3	74.42	3.14	13.42	0.67	1.92	0.16	3.31	0.13	2.57	0.12	2.72	0.12	0.30	0.06	0.74	0.08
U4	U4.3	74.53	3.15	13.43	0.67	2.03	0.16	3.46	0.14	2.78	0.12	2.79	0.12	0.26	0.05	0.72	0.08
U4	U4.3	76.25	3.22	13.43	0.67	2.12	0.17	3.35	0.14	2.48	0.11	2.74	0.12	0.29	0.06	0.74	0.08
U4	U4.3	74.17	3.13	13.47	0.67	2.06	0.16	3.54	0.14	2.81	0.12	2.79	0.12	0.34	0.06	0.72	0.08
U4	U4.3	77.71	3.28	13.76	0.69	2.10	0.17	3.37	0.14	2.46	0.11	2.76	0.12	0.28	0.05	0.79	0.09
U4	U4.3	77.35	3.26	13.76	0.69	1.99	0.16	3.24	0.13	2.57	0.12	2.63	0.12	0.28	0.06	0.80	0.09
U4	U4.3	77.89	3.29	13.85	0.69	2.05	0.16	3.03	0.13	2.64	0.12	2.80	0.12	0.25	0.05	0.84	0.09
U4	U4.3	77.63	3.28	14.04	0.70	2.13	0.17	3.23	0.13	2.80	0.12	2.70	0.12	0.28	0.06	0.81	0.09
U4	U4.3	77.48	3.27	13.64	0.68	2.01	0.16	3.20	0.13	2.73	0.12	2.66	0.12	0.28	0.06	0.78	0.09
U4	U4.3	77.20	3.26	13.77	0.69	2.02	0.16	3.09	0.13	2.57	0.12	2.61	0.12	0.28	0.05	0.83	0.09
U4	U4.3	77.23	3.26	13.74	0.69	2.06	0.17	3.23	0.13	2.82	0.12	2.75	0.12	0.31	0.06	0.80	0.09
U4	U4.3	76.34	3.22	13.74	0.69	2.07	0.17	3.24	0.13	2.86	0.12	2.67	0.12	0.24	0.05	0.78	0.09
U4	U4.3	76.37	3.22	13.84	0.69	2.05	0.16	3.17	0.13	2.80	0.12	2.74	0.12	0.28	0.06	0.80	0.09
U4	U4.3	77.89	3.29	13.82	0.69	2.01	0.16	3.12	0.13	2.73	0.12	2.67	0.12	0.28	0.06	0.81	0.09
U4	U4.3	78.53	3.31	13.85	0.69	2.19	0.17	3.32	0.13	2.39	0.11	2.64	0.12	0.29	0.06	0.79	0.09
U4	U4.3	73.15	3.09	12.72	0.64	2.24	0.18	3.66	0.15	2.45	0.11	2.59	0.12	0.26	0.05	0.66	0.08
U4	U4.3	75.47	3.19	13.72	0.69	2.58	0.20	3.53	0.14	2.17	0.10	2.88	0.13	0.27	0.05	0.76	0.08

U4	U4.3	76.68	3.24	13.48	0.67	2.49	0.19	3.60	0.14	2.27	0.11	2.73	0.12	0.26	0.05	0.76	0.08
U4	U4.3	76.51	3.23	13.61	0.68	2.40	0.19	3.39	0.14	2.46	0.11	2.74	0.12	0.25	0.05	0.77	0.09
U4	U4.3	77.64	3.28	13.67	0.68	2.58	0.20	3.45	0.14	2.22	0.11	2.68	0.12	0.26	0.05	0.75	0.08
U4	U4.3	76.65	3.24	13.71	0.69	2.32	0.18	3.38	0.14	2.54	0.12	2.66	0.12	0.24	0.05	0.77	0.09
U4	U4.3	75.84	3.20	13.20	0.66	2.30	0.18	3.45	0.14	2.38	0.11	2.68	0.12	0.23	0.05	0.70	0.08
U4	U4.3	74.71	3.15	12.51	0.63	2.25	0.18	3.67	0.15	2.28	0.11	2.69	0.12	0.29	0.06	0.67	0.08
U4	U4.3	76.57	3.23	13.21	0.66	2.25	0.18	3.52	0.14	2.29	0.11	2.86	0.13	0.27	0.05	0.77	0.09
U4	U4.3	77.46	3.27	13.57	0.68	2.31	0.18	3.41	0.14	2.32	0.11	2.71	0.12	0.27	0.05	0.77	0.09
U4	U4.3	76.19	3.22	13.50	0.68	2.41	0.19	3.56	0.14	2.35	0.11	2.70	0.12	0.27	0.05	0.70	0.08
U4	U4.3	77.94	3.29	13.71	0.69	2.19	0.17	3.35	0.14	2.37	0.11	2.64	0.12	0.27	0.05	0.76	0.08
U4	U4.3	73.27	3.10	13.07	0.66	2.24	0.18	3.56	0.14	2.43	0.11	2.77	0.12	0.30	0.06	0.69	0.08
U4	U4.4	69.01	2.92	17.28	0.85	3.35	0.24	3.33	0.14	3.46	0.14	3.04	0.13	0.35	0.06	0.90	0.09
U4	U4.4	70.25	2.97	17.84	0.88	3.21	0.24	3.01	0.13	3.48	0.14	2.93	0.13	0.41	0.06	0.95	0.09
U4	U4.4	78.86	3.33	12.58	0.63	2.57	0.20	3.01	0.13	2.29	0.11	2.29	0.11	0.22	0.05	0.71	0.08
U4	U4.4	72.36	3.06	15.29	0.76	3.08	0.23	3.27	0.13	2.81	0.12	2.68	0.12	0.32	0.06	0.84	0.09
U4	U4.4	73.31	3.10	15.81	0.78	2.91	0.22	2.92	0.12	2.88	0.13	2.90	0.13	0.31	0.06	0.84	0.09
U4	U4.4	73.22	3.09	15.39	0.76	2.86	0.21	3.11	0.13	3.01	0.13	2.86	0.13	0.29	0.06	0.82	0.09
U4	U4.4	74.55	3.15	15.63	0.77	3.17	0.23	3.16	0.13	2.61	0.12	2.81	0.12	0.34	0.06	0.90	0.09
U4	U4.4	74.01	3.13	15.33	0.76	3.02	0.22	3.11	0.13	2.94	0.13	2.83	0.13	0.34	0.06	0.83	0.09
U4	U4.4	74.44	3.14	13.64	0.68	3.10	0.23	3.56	0.14	2.23	0.11	2.92	0.13	0.34	0.06	0.80	0.09
U4	U4.5	76.13	3.21	14.31	0.71	3.51	0.25	3.91	0.15	2.01	0.10	2.79	0.12	0.33	0.06	0.81	0.09
U4	U4.5	73.12	3.09	13.56	0.68	3.31	0.24	3.72	0.15	1.85	0.09	2.92	0.13	0.27	0.05	0.74	0.08
U4	U4.5	74.54	3.15	14.07	0.70	3.48	0.25	4.04	0.16	2.13	0.10	2.79	0.12	0.34	0.06	0.75	0.08
U4	U4.5	72.69	3.07	14.13	0.70	3.61	0.26	3.94	0.15	2.28	0.11	2.90	0.13	0.32	0.06	0.76	0.08
U4	U4.6	74.57	3.15	14.60	0.73	2.91	0.22	3.30	0.13	2.01	0.10	2.89	0.13	0.34	0.06	0.87	0.09
U4	U4.6	76.30	3.22	13.24	0.66	3.01	0.22	3.57	0.14	1.88	0.10	2.92	0.13	0.35	0.06	0.80	0.09
U4	U4.6	75.45	3.19	14.21	0.71	2.95	0.22	3.45	0.14	1.95	0.10	3.00	0.13	0.34	0.06	0.84	0.09
U4	U4.6	72.74	3.07	15.17	0.75	2.76	0.21	3.27	0.13	2.36	0.11	2.90	0.13	0.39	0.06	0.87	0.09
U4	U4.6	73.02	3.08	16.13	0.80	2.83	0.21	3.21	0.13	2.43	0.11	3.03	0.13	0.36	0.06	0.90	0.09
U4	U4.7	77.13	3.25	14.05	0.70	2.56	0.20	3.06	0.13	2.54	0.11	2.96	0.13	0.28	0.05	0.76	0.09
U4	U4.7	76.26	3.22	13.89	0.69	2.57	0.20	3.03	0.13	2.65	0.12	2.81	0.12	0.28	0.05	0.75	0.08
U4	U4.7	75.83	3.20	14.47	0.72	2.61	0.20	3.02	0.13	2.72	0.12	2.83	0.12	0.33	0.06	0.80	0.09
U4	U4.7	75.88	3.20	15.09	0.75	2.58	0.20	2.98	0.12	2.65	0.12	2.86	0.13	0.28	0.05	0.78	0.09
U4	U4.7	76.22	3.22	13.79	0.69	2.64	0.20	3.14	0.13	2.55	0.12	2.81	0.12	0.29	0.06	0.76	0.09
U4	U4.7	75.71	3.20	13.85	0.69	2.67	0.20	3.20	0.13	2.55	0.12	2.81	0.12	0.30	0.06	0.76	0.08
U4	U4.7	74.68	3.15	13.92	0.69	2.58	0.20	3.39	0.14	2.06	0.10	3.07	0.13	0.31	0.06	0.80	0.09
U4	U4.7	76.38	3.22	14.19	0.71	2.74	0.21	3.16	0.13	2.62	0.12	2.95	0.13	0.29	0.06	0.79	0.09
U4	U4.7	76.68	3.24	13.95	0.70	2.64	0.20	3.28	0.13	2.09	0.10	3.04	0.13	0.32	0.06	0.80	0.09
U4	U4.7	75.99	3.21	14.36	0.72	2.45	0.19	2.99	0.12	2.87	0.12	2.84	0.13	0.28	0.06	0.75	0.08
U4	U4.7	76.71	3.24	14.16	0.71	2.70	0.20	3.07	0.13	2.53	0.11	2.89	0.13	0.27	0.05	0.79	0.09
U4	U4.7	75.04	3.17	13.91	0.69	2.54	0.19	3.21	0.13	2.75	0.12	2.96	0.13	0.28	0.06	0.74	0.08

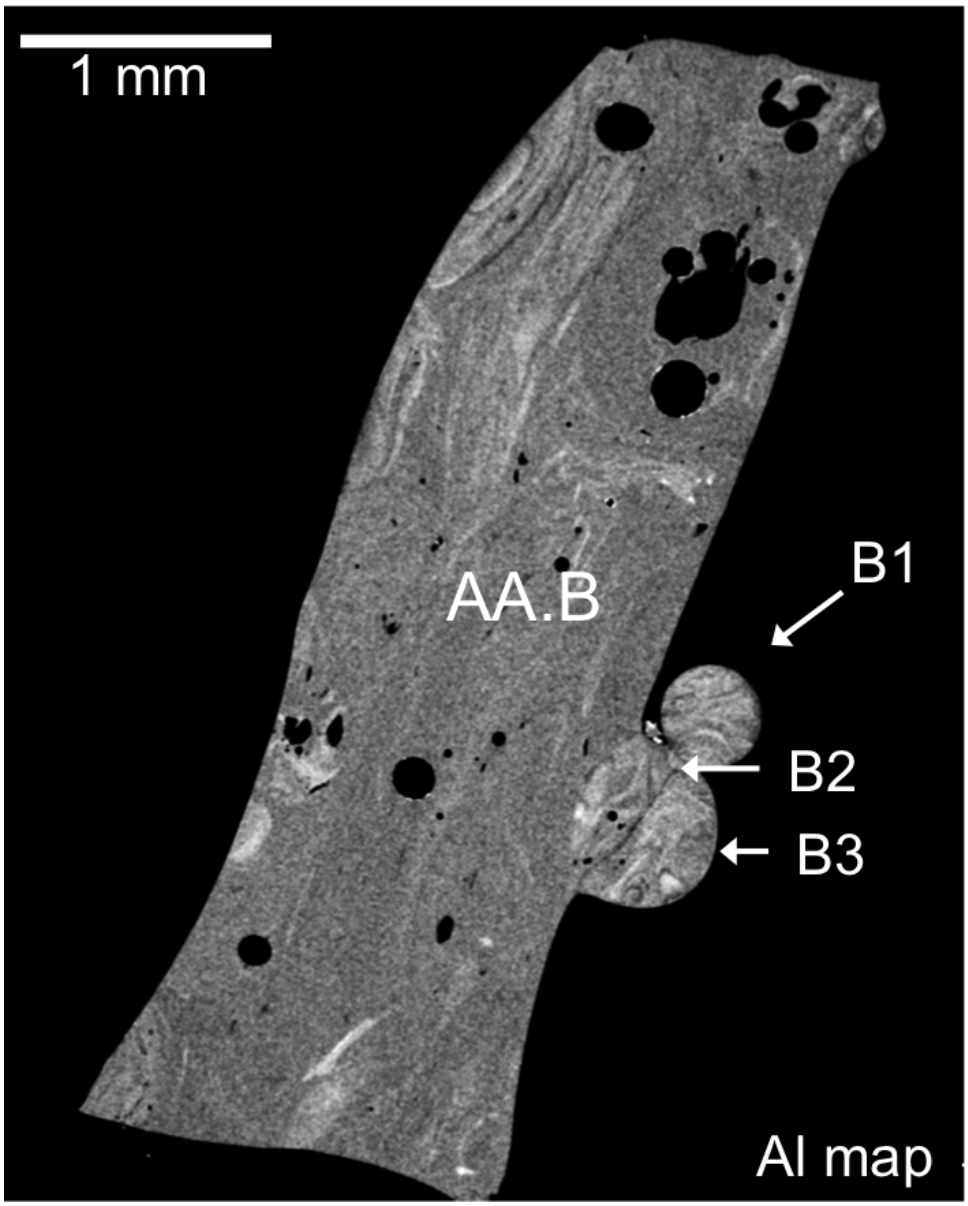

Figure C.1: Al compositional map of sample AA.B showing the agglomerates characterized in the sample. Agglomerates B1, B2, and B3 have CaMgFe interfaces. B1 and B3 are exterior agglomerates, while B2 is a surface agglomerate within agglomerate B3. All were characterized for their U isotopic (from [67]) and major element compositions.

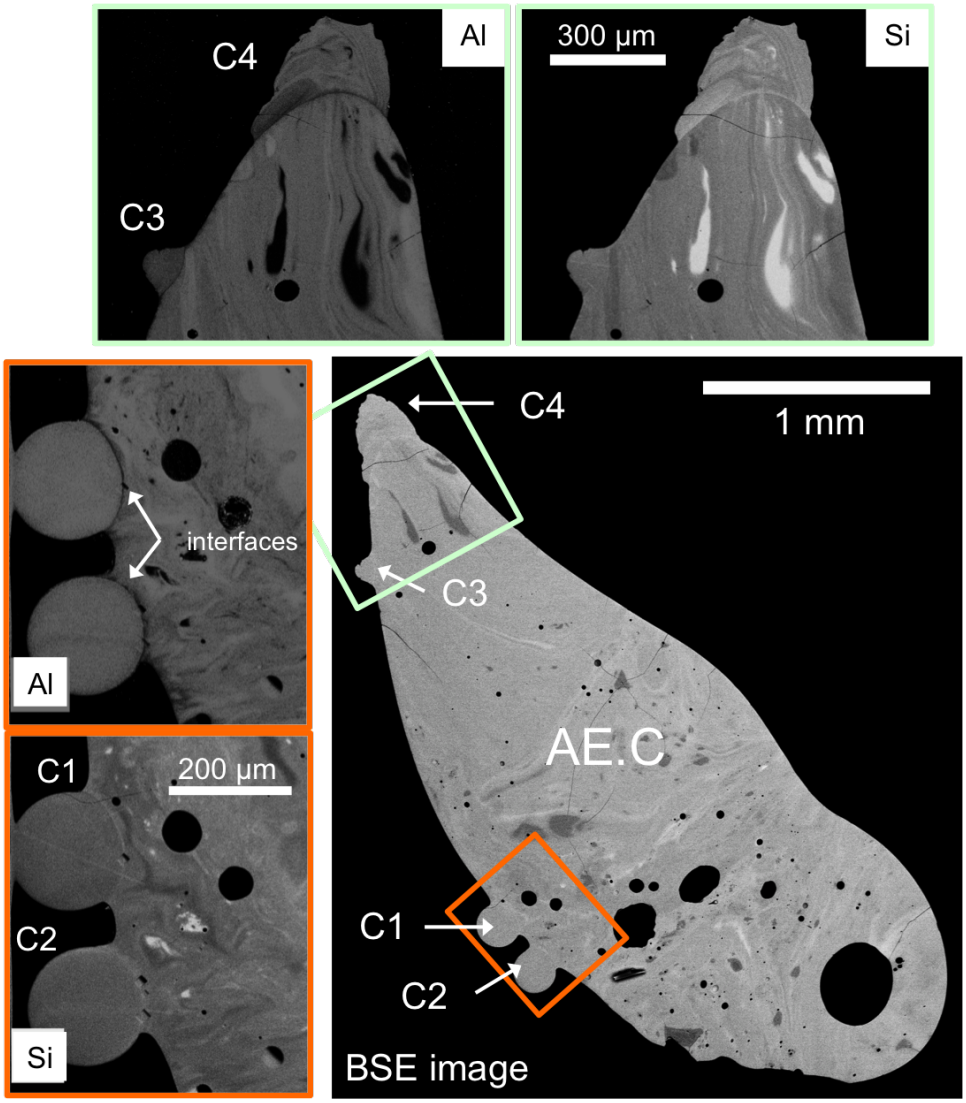

Figure C.2: Si and Al Compositional maps showing the agglomerates characterized in sample AE.C (shown with a BSE image). C1 and C2 were characterized for both their U isotopic (from obtained from [67]) and major element compositions. Agglomerates C3 and C4 were characterized for their major element compositions. All are exterior agglomerates.

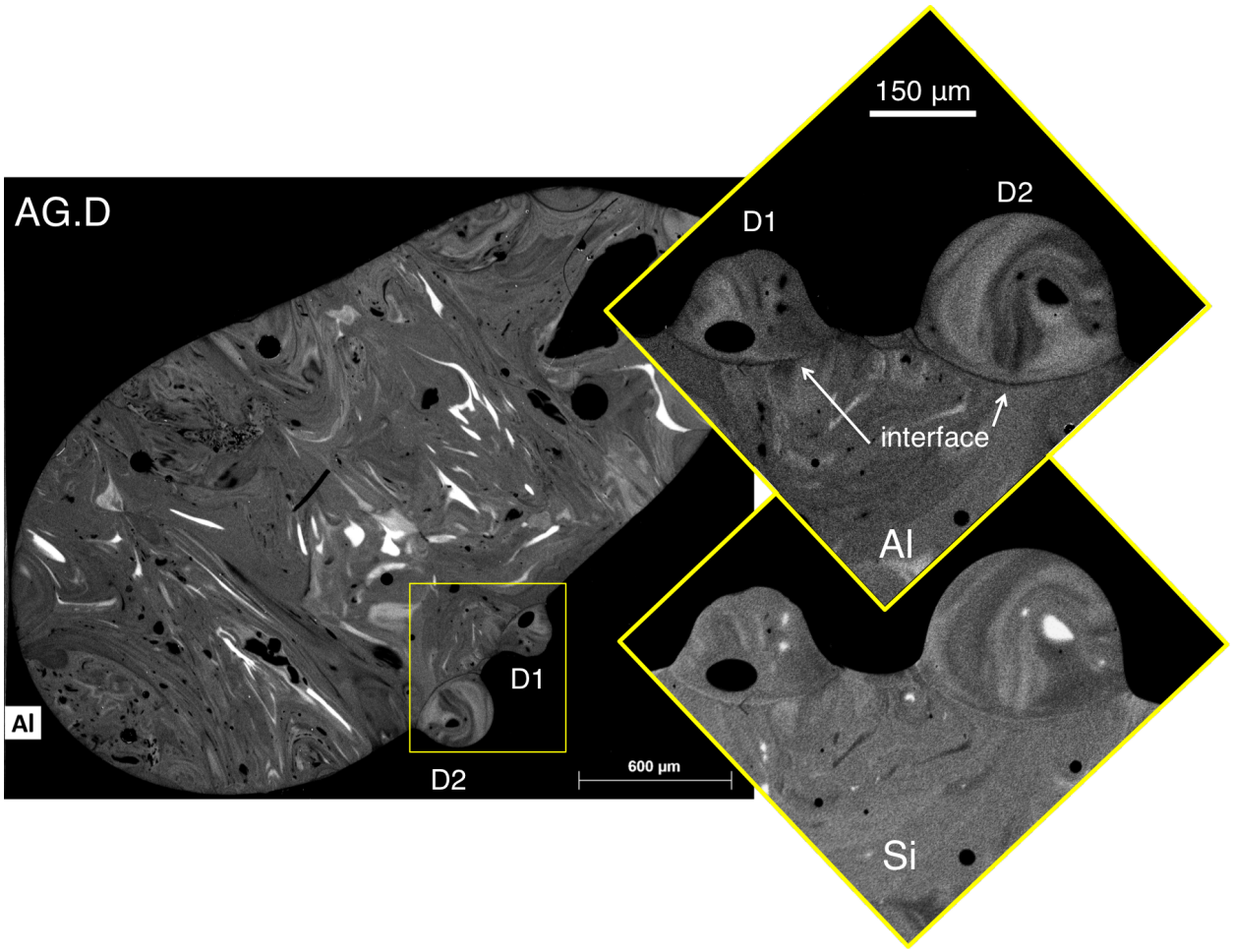

Figure C.3: Compositional maps showing the agglomerates characterized in sample AG.D. Both D1 and D2 (exterior agglomerates with CaMgFe interfaces) were characterized for both their U isotopic and major element compositions.

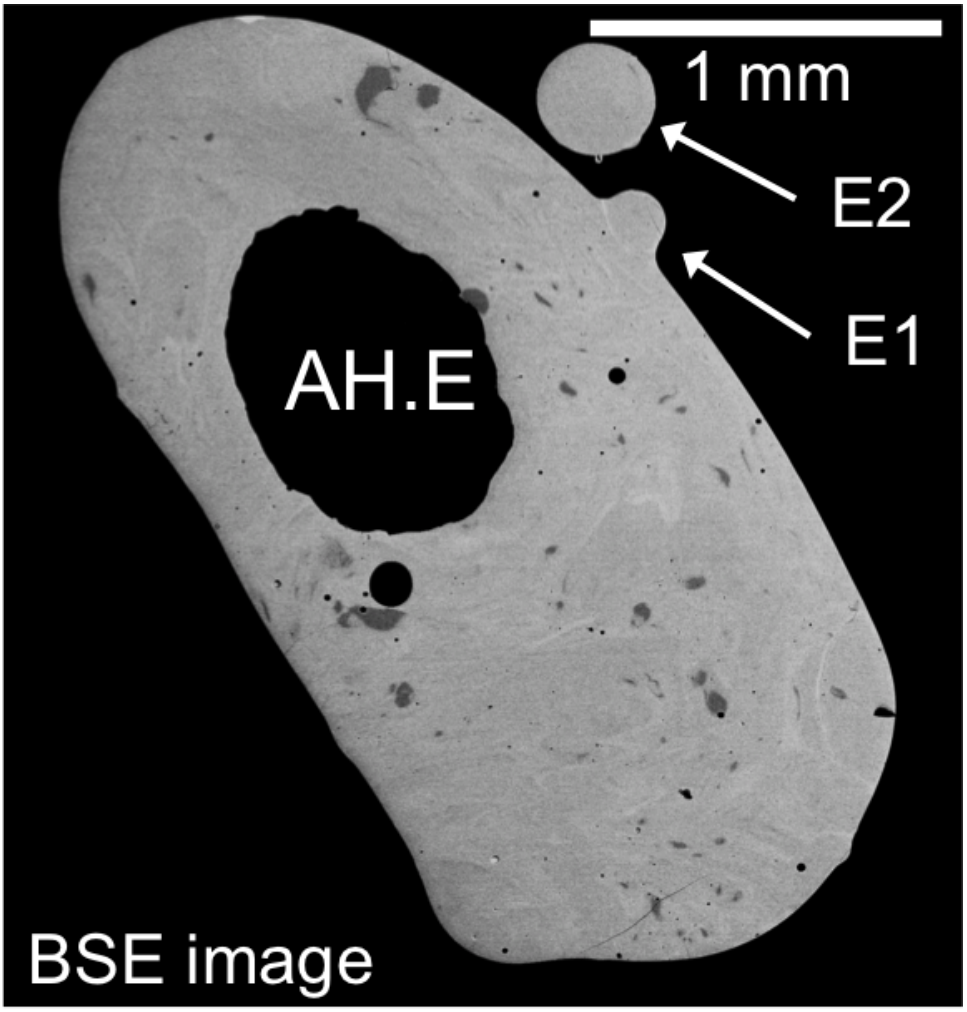

Figure C.4: BSE image of sample AH.E showing the agglomerates characterized in the sample. Both E1 and E2 are exterior agglomerates. E1 (CaMgFe interface) was characterized for both its U isotopic (from [67]) and major element compositions and E2 (indeterminate interface) was characterized for its major element composition.

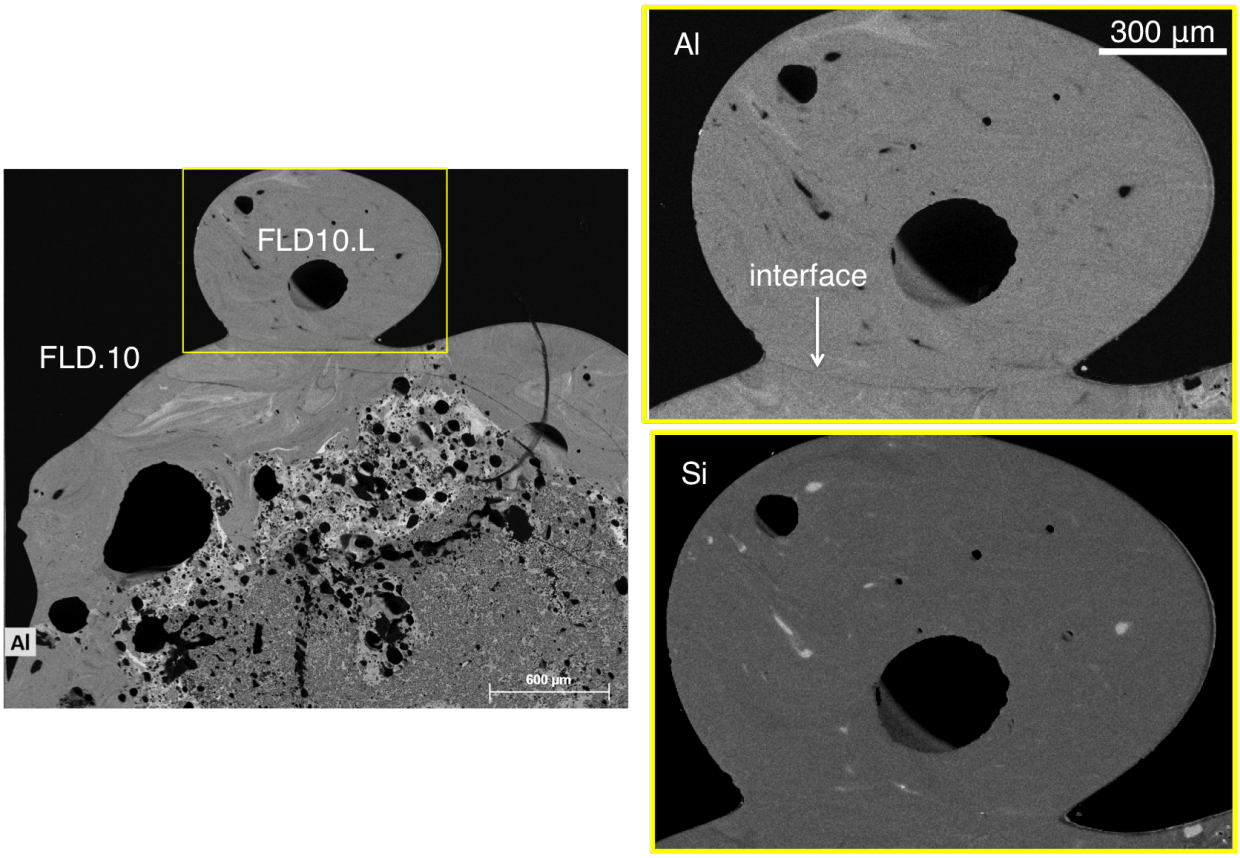

Figure C.5: Compositional maps showing the agglomerate characterized in sample FLD10. FLD10.L (exterior agglomerate) was characterized for both its U isotopic and major element compositions.

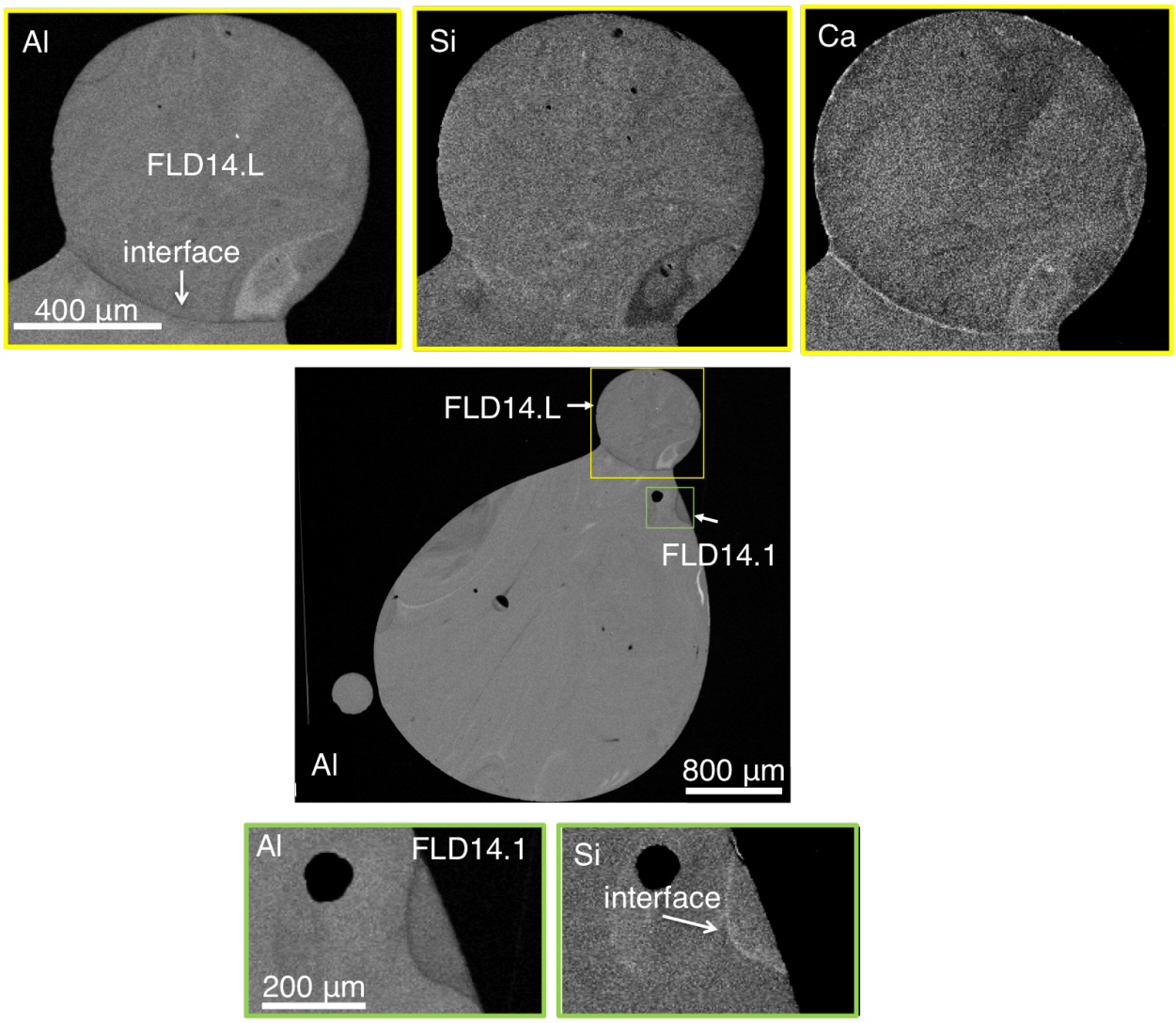

Figure C.6: Compositional maps showing the agglomerates characterized in sample FLD14. Both FLD14.L (CaMgFe interface) and FLD14.1 (Si interface) were characterized for their U isotopic and major compositions.

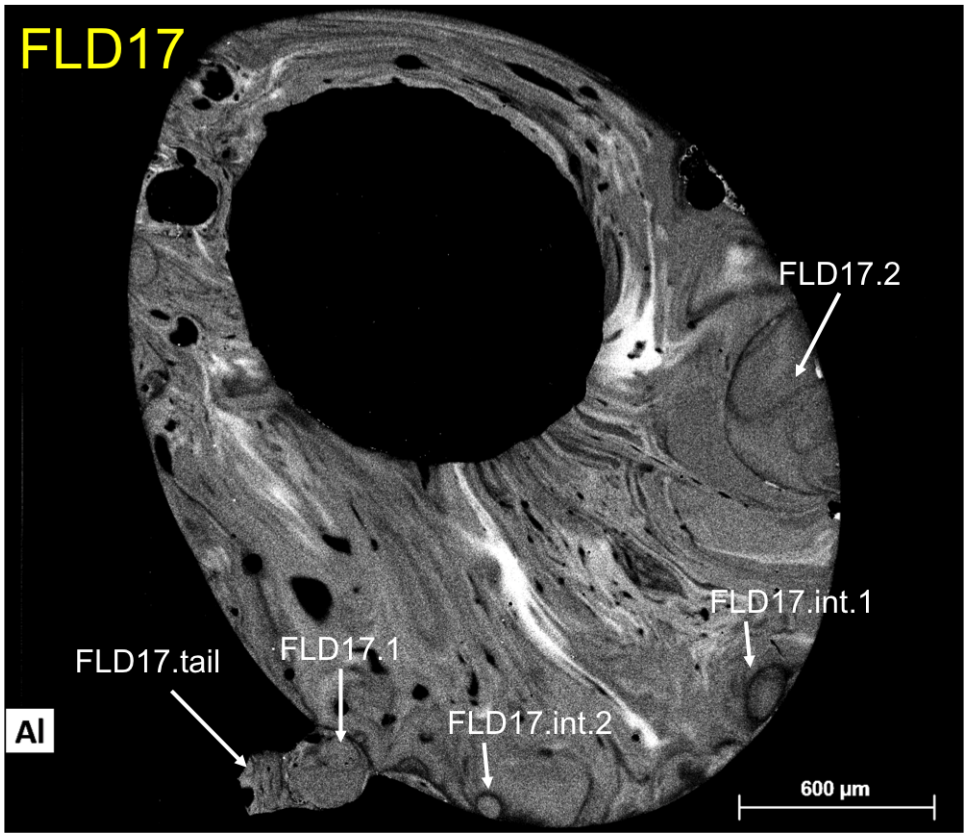

Figure C.7: Compositional maps showing the agglomerates characterized in sample FLD17. FLD17.int.2 was characterized for both its U isotopic and major element compositions. All other agglomerates were characterized for their major element compositions.

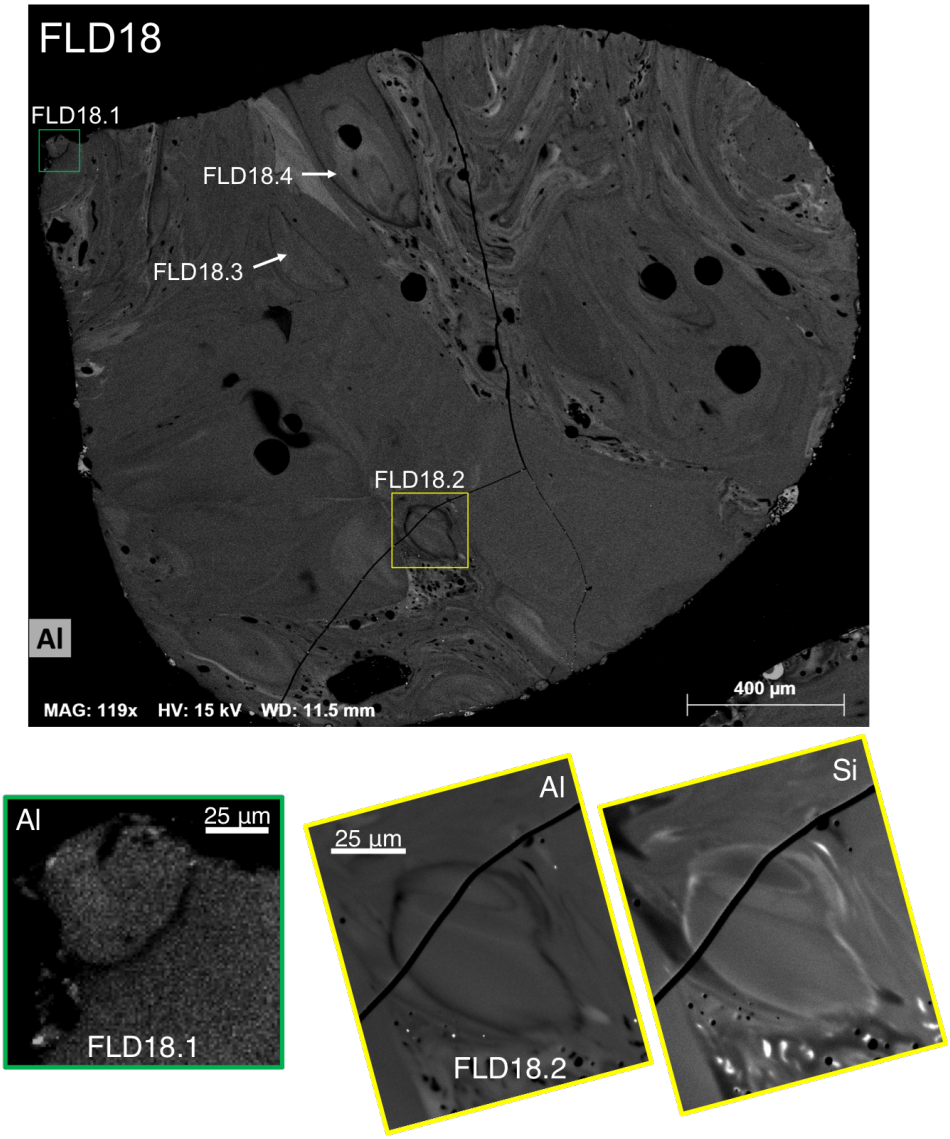

Figure C.8: Compositional maps showing the agglomerates characterized in sample FLD18. FLD18.1 and FLD18.2 were characterized for both their U isotopic and major element compositions FLD18.1 has a CaMgFe interface and FLD18.2 has a Si interface. FLD18.3 and FLD18.4 were characterized for their major element compositions.

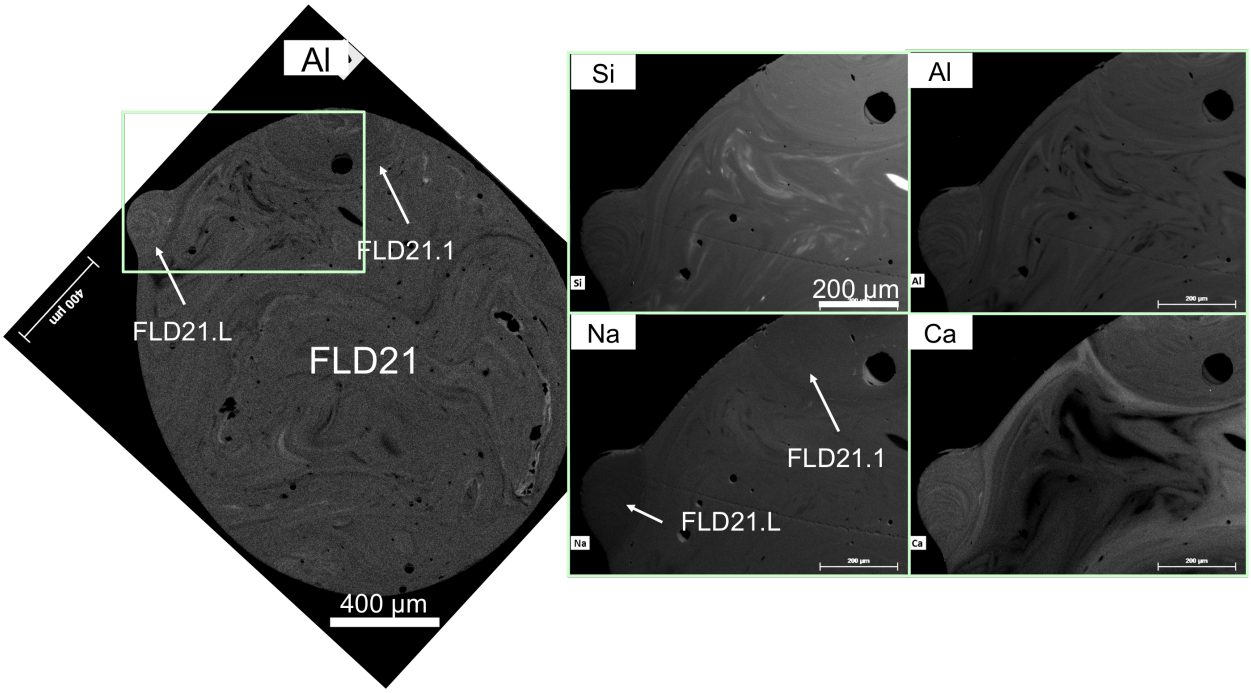

Figure C.9: Compositional maps showing the agglomerates characterized in sample FLD21.

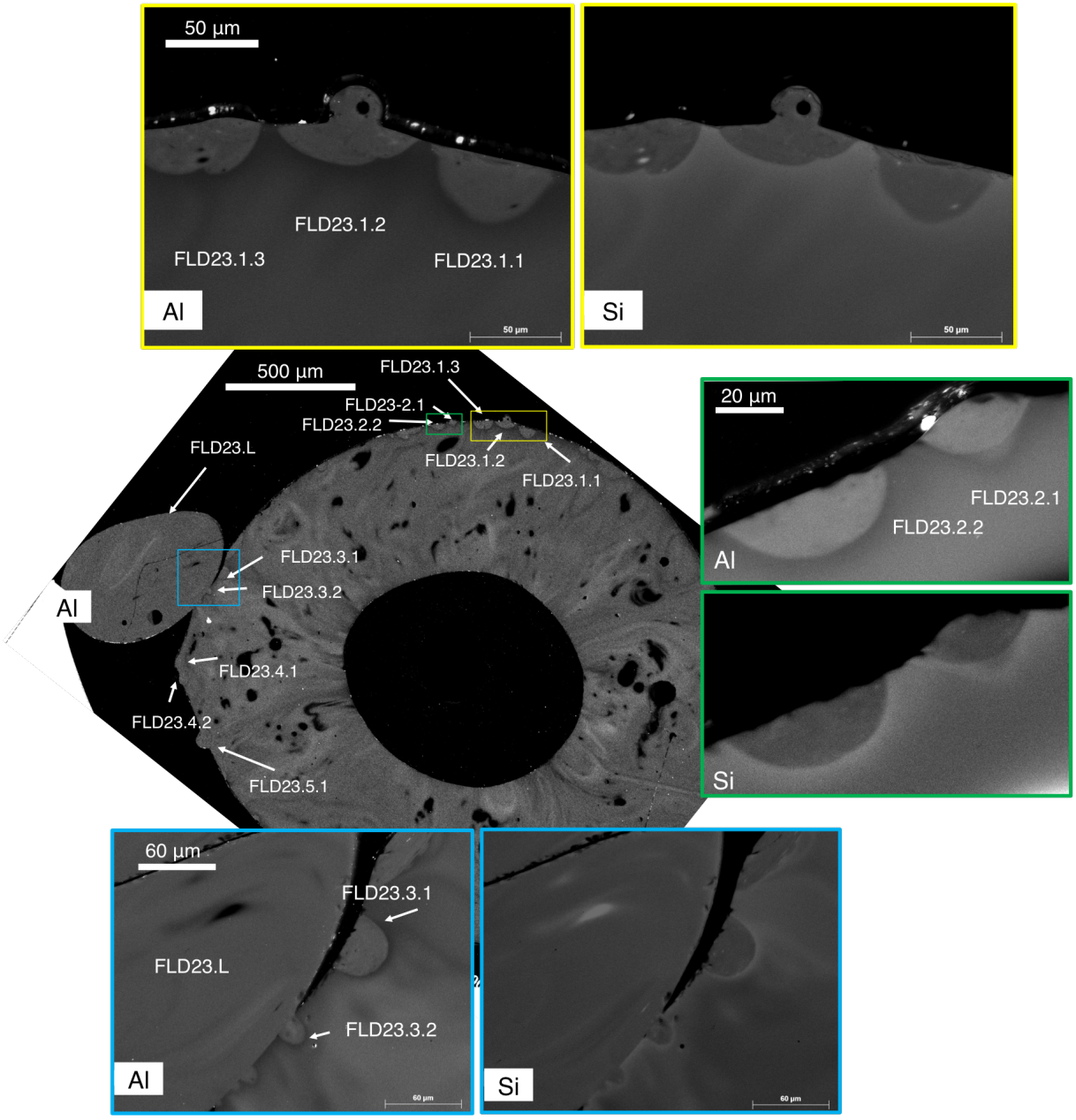

Figure C.10: Compositional maps showing the agglomerates characterized in sample FLD23. FLD23.1.1–FLD23.5.1 are surface agglomerates and FLD23.L is an exterior agglomerate. All were characterized for both major element and U isotopic composition. All agglomerates have Si interfaces.

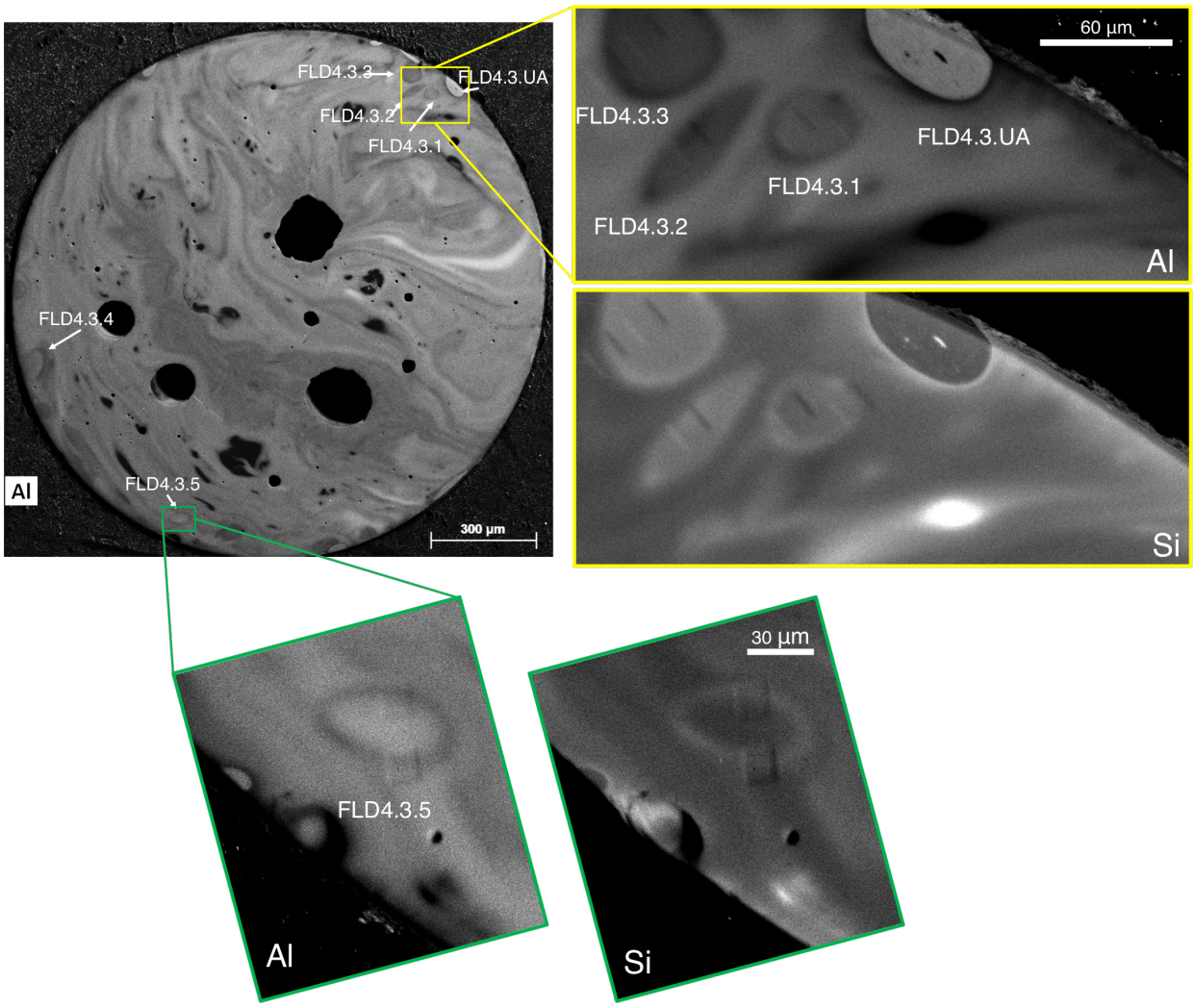

Figure C.11: Compositional maps showing the agglomerates characterized in sample FLD4.3. Agglomerates FLD4.3.1, FLD4.3.2, FLD4.3.3, and FLD4.3.5 are interior agglomerates and were characterized for both their major element and U isotopic composition. FLD4.3.UA and FLD4.3.4 are surface agglomerates and were characterized for their major element composition. All agglomerates have Si interfaces.

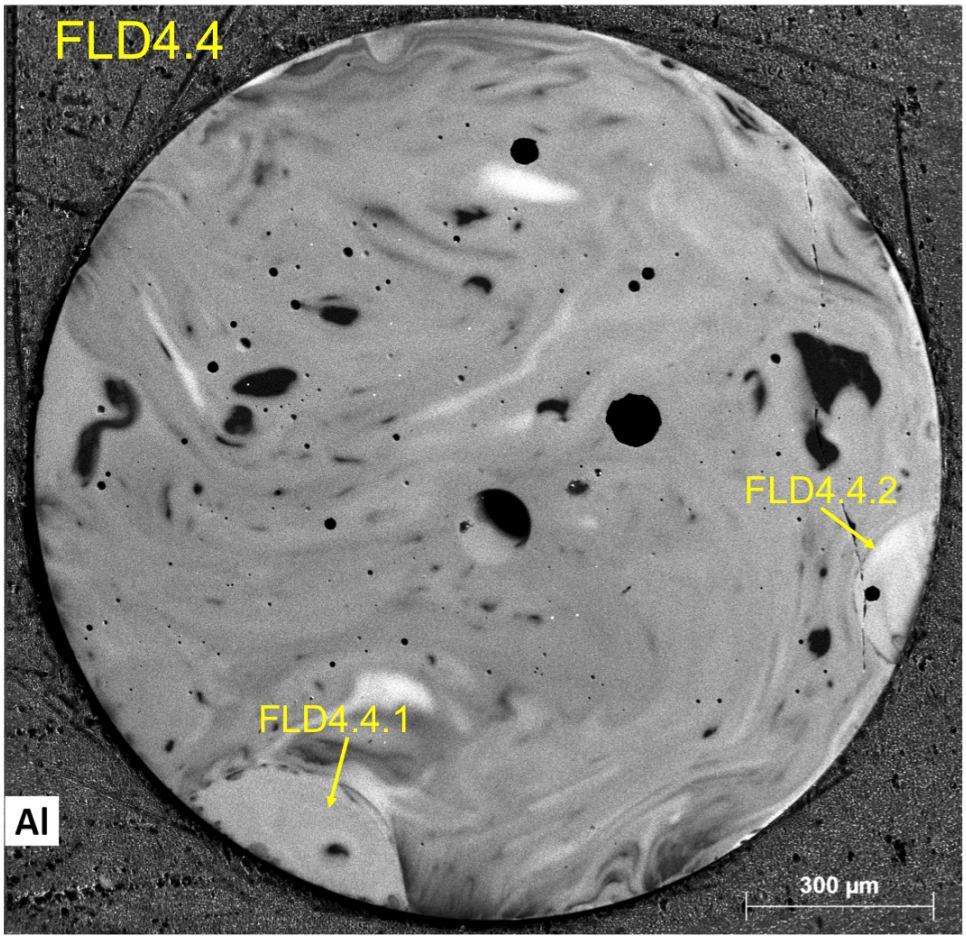

Figure C.12: Al compositional map showing the agglomerates characterized in sample FLD4.4. Both FLD4.4.1 and FLD4.4.2 were characterized for their major element compositions. Both agglomerates have Si interfaces.

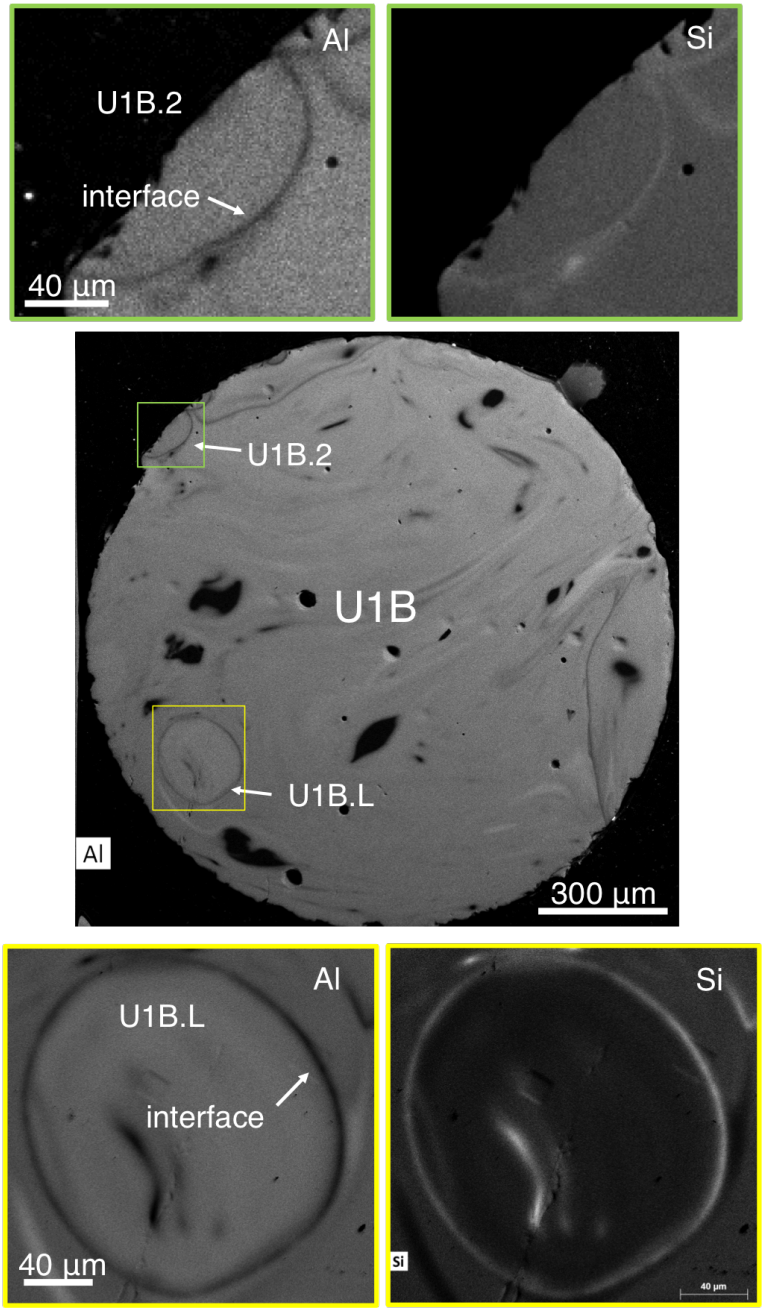

Figure C.13: Compositional maps showing the agglomerates characterized in sample U1B. Both U1B.L (interior agglomerate) and U1B.2 (surface agglomerate) were characterized for both their U isotopic and major element compositions. Both agglomerates have Si interfaces.

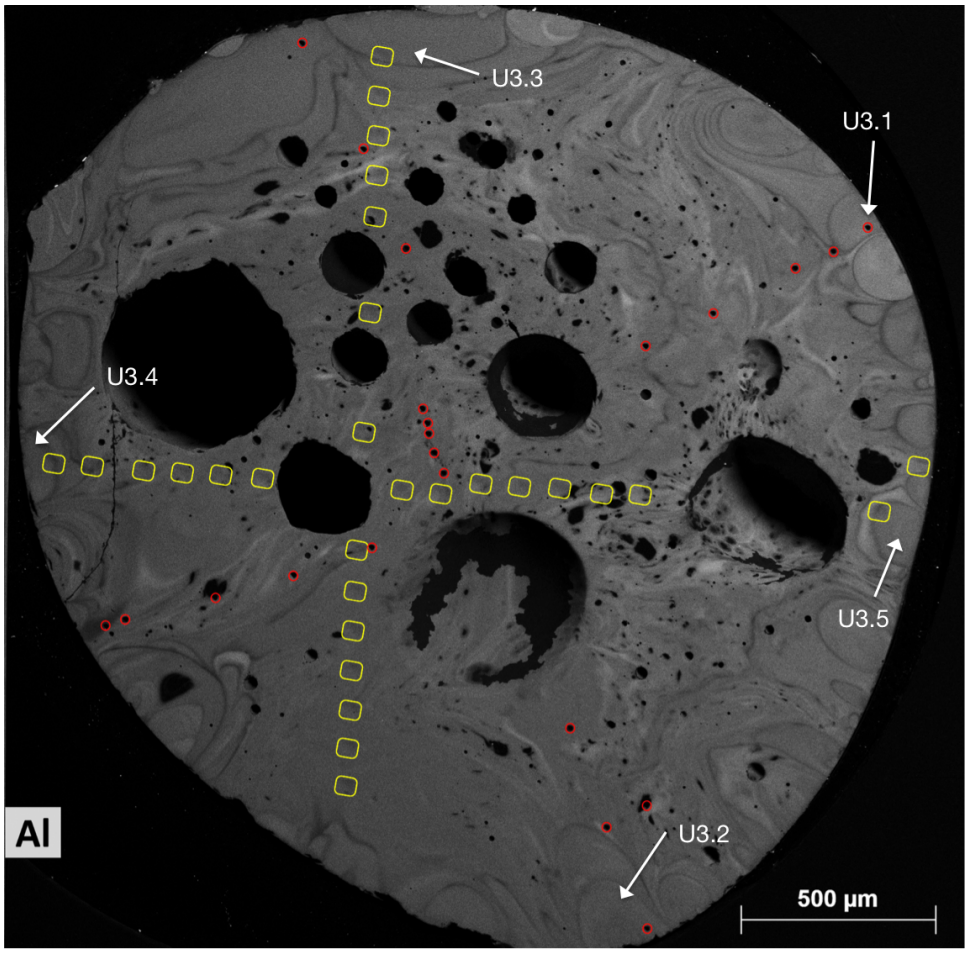

Figure C.14: Al compositional map showing the agglomerates characterized in sample U3. All labeled agglomerates were characterized for both their major element and U isotopic compositions. However, only SIMS analyses in agglomerates U3.1 and U3.2 were fully located in the agglomerate. SIMS analyses in U3.3–U3.5 sampled the agglomerate, the compositional interface, and the host object and represent a mixture of the U isotopic compositions from these three regions. Red circles show the SIMS analyses conducted using the IMS-3f at LLNL in a 2012 analytical campaign and yellow squares show the locations of SIMS analyses conducted using the IMS-1280 at LANL in a 2012-2013 analytical campaign (both discussed further in [60]). The SIMS analyses are labeled in Appendix F.

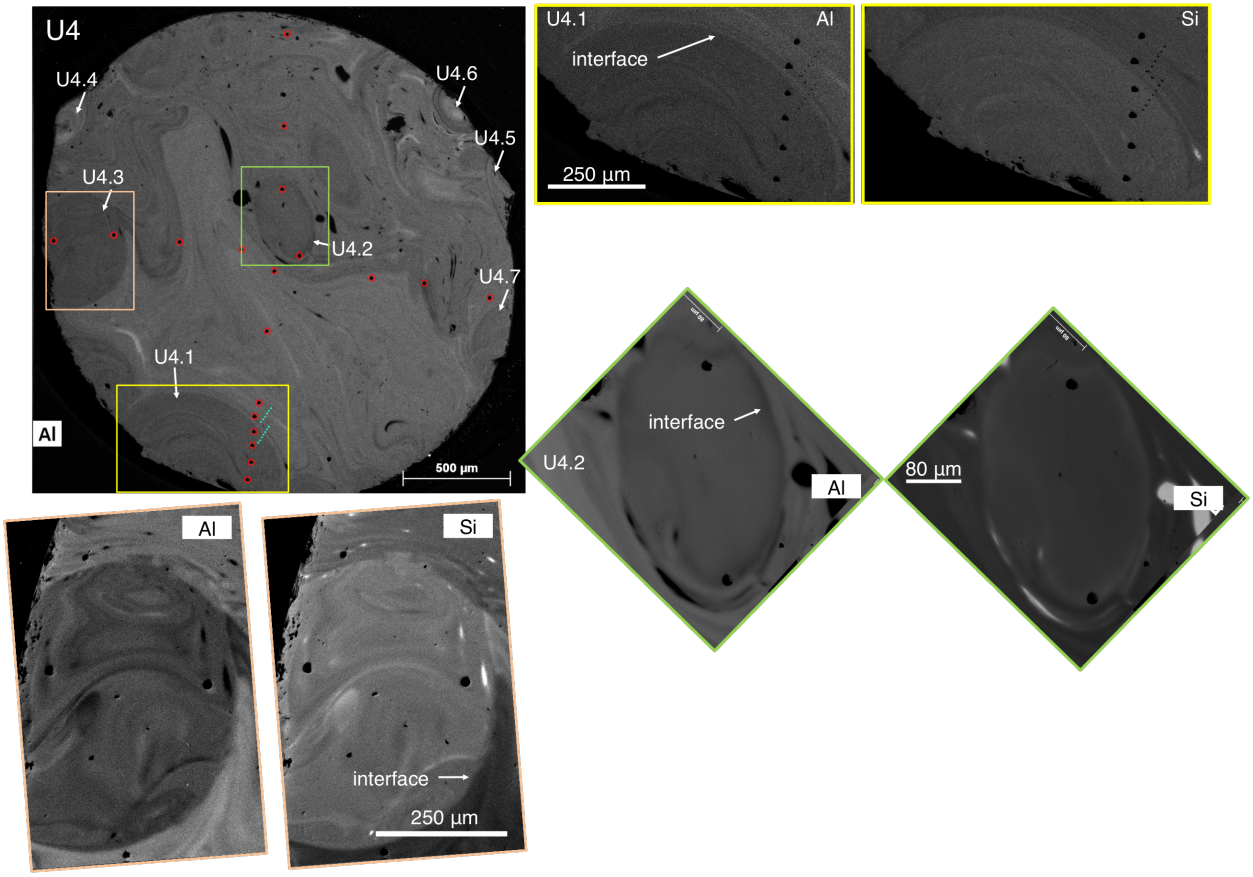

Figure C.15: Compositional maps showing the agglomerates characterized in sample U4. U4.1 (surface), U4.2 (interior), and U4.3 (surface) were characterized for both their U isotopic and major element compositions. Agglomerates U4.4–U4.7 were charactered for their major element compositions. Red circles in the full map of sample U4 show the SIMS analyses conducted using the IMS-3f in a 2012 analytical campaign (discussed further in [60] and labeled in Appendix F).

Appendix D

EDS analyses of unmelted soil and unmelted/partially-melted regions in sample FLD10

Table D.1: Major element compositions (as wt.% oxides) of unmelted soil collected proximate to ground zero analyzed with EDS rasters. Analyses were targeted and not collected in a grid-based pattern, unlike the host and agglomerate EDS analyses. Analytical procedure is detailed in Chapter 4. Uncertainties are calculated as detailed in Chapter 6.

SiO_2	1σ	Al_2O_3	1σ	Na_2O	1σ	K_2O	1σ	CaO	1σ	FeO	1σ	TiO_2	1σ	MgO	1σ
97.85	4.11	0.56	0.08	0.03	0.04	0.03	0.03	0.03	0.04	0.07	0.04	0.03	0.05	0.03	0.05
76.97	3.25	12.28	0.62	5.00	0.35	4.66	0.18	0.03	0.04	2.96	0.13	0.07	0.05	0.03	0.05
83.80	3.53	9.76	0.50	3.74	0.27	3.61	0.14	0.03	0.04	1.76	0.09	0.03	0.05	0.12	0.05
77.43	3.27	9.68	0.50	4.55	0.32	3.79	0.15	0.03	0.04	3.94	0.16	0.33	0.06	0.03	0.05
77.95	3.29	11.29	0.57	4.60	0.32	4.27	0.16	0.03	0.04	2.70	0.12	0.03	0.05	0.03	0.05
67.43	2.85	19.94	0.97	5.94	0.41	7.14	0.25	0.84	0.06	1.58	0.09	0.56	0.06	0.06	0.05
66.75	2.83	22.02	1.07	5.35	0.37	7.54	0.26	0.69	0.06	0.23	0.04	0.03	0.05	0.27	0.06
66.92	2.83	22.30	1.08	5.31	0.37	7.39	0.26	0.86	0.06	0.30	0.05	0.07	0.05	0.25	0.06
62.63	2.65	25.10	1.21	7.62	0.51	1.83	0.09	5.64	0.21	0.42	0.05	0.14	0.05	0.27	0.06
60.03	2.55	25.73	1.24	7.23	0.49	1.31	0.07	6.78	0.24	0.33	0.05	0.10	0.05	0.03	0.05
61.08	2.59	24.53	1.19	7.51	0.50	1.80	0.09	5.51	0.20	0.36	0.05	0.13	0.05	0.22	0.06
60.57	2.57	25.11	1.21	7.84	0.52	0.92	0.06	6.11	0.22	0.45	0.05	0.16	0.05	0.03	0.05
65.99	2.79	20.17	0.98	7.19	0.48	5.23	0.19	1.13	0.07	0.85	0.06	0.14	0.05	0.30	0.06
58.77	2.49	26.30	1.27	6.99	0.47	1.00	0.06	7.50	0.26	0.39	0.05	0.16	0.05	0.24	0.06
59.97	2.54	25.90	1.25	7.00	0.47	1.14	0.07	6.91	0.25	0.44	0.05	0.15	0.05	0.27	0.06
99.89	4.20	0.50	0.07	0.03	0.04	0.03	0.03	0.05	0.04	0.03	0.04	0.03	0.05	0.03	0.05
59.36	2.52	25.00	1.21	7.19	0.48	1.44	0.08	6.68	0.24	0.31	0.05	0.09	0.05	0.21	0.06
66.12	2.80	19.11	0.93	5.40	0.37	7.28	0.26	0.82	0.06	2.35	0.11	0.52	0.06	0.33	0.06
66.76	2.83	18.91	0.93	5.59	0.38	6.89	0.24	1.02	0.07	1.84	0.09	0.56	0.06	0.30	0.06
100.81	4.24	1.08	0.10	0.09	0.04	0.13	0.04	0.05	0.04	0.14	0.04	0.03	0.05	0.03	0.05
65.43	2.77	20.92	1.02	6.63	0.45	5.64	0.21	1.26	0.08	0.61	0.06	0.62	0.07	0.03	0.05
66.42	2.81	19.59	0.96	5.83	0.40	6.87	0.24	0.98	0.07	1.33	0.08	0.61	0.07	0.13	0.05
66.39	2.81	18.45	0.90	5.50	0.38	6.49	0.23	0.94	0.07	1.76	0.09	0.62	0.07	0.16	0.05
61.41	2.60	24.45	1.18	7.51	0.50	1.82	0.09	5.43	0.20	0.39	0.05	0.05	0.05	0.23	0.06
62.28	2.64	22.65	1.10	7.21	0.48	2.77	0.12	4.10	0.16	0.90	0.07	0.17	0.05	0.11	0.05
67.34	2.85	19.77	0.97	5.69	0.39	7.29	0.26	0.82	0.06	1.83	0.09	0.51	0.06	0.11	0.05
66.28	2.81	19.08	0.93	5.36	0.37	7.62	0.27	1.21	0.08	2.03	0.10	0.54	0.06	0.43	0.07
61.86	2.62	18.14	0.89	5.25	0.36	5.73	0.21	1.65	0.09	2.40	0.11	0.54	0.06	0.77	0.09
67.94	2.87	19.93	0.97	5.68	0.39	7.59	0.27	0.77	0.06	1.38	0.08	0.57	0.06	0.03	0.05
64.96	2.75	19.30	0.94	6.15	0.42	6.33	0.23	0.85	0.06	1.42	0.08	0.68	0.07	0.07	0.05

65.80	2.79	19.32	0.94	6.41	0.43	5.70	0.21	0.98	0.07	2.35	0.11	0.60	0.07	0.15	0.05
61.08	2.59	24.80	1.20	7.39	0.49	1.73	0.09	5.58	0.21	0.37	0.05	0.11	0.05	0.24	0.06
59.45	2.52	23.77	1.15	7.45	0.50	1.65	0.08	5.58	0.21	0.40	0.05	0.19	0.05	0.03	0.05
101.47	4.26	0.56	0.08	0.03	0.04	0.03	0.03	0.03	0.04	0.03	0.04	0.03	0.05	0.03	0.05
101.09	4.25	0.56	0.08	0.03	0.04	0.03	0.03	0.03	0.04	0.03	0.04	0.03	0.05	0.03	0.05
83.10	3.50	10.13	0.52	3.61	0.26	4.18	0.16	0.03	0.04	1.55	0.09	0.03	0.05	0.11	0.05
78.40	3.31	12.84	0.64	4.77	0.33	5.26	0.19	0.03	0.04	1.84	0.09	0.03	0.05	0.03	0.05
83.96	3.54	10.05	0.52	3.83	0.27	3.78	0.15	0.12	0.04	1.43	0.08	0.05	0.05	0.16	0.05
89.44	3.76	5.89	0.32	2.59	0.20	2.19	0.10	0.03	0.04	0.90	0.07	0.03	0.05	0.14	0.05
75.45	3.19	14.27	0.71	5.44	0.37	5.48	0.20	0.03	0.04	2.11	0.10	0.06	0.05	0.14	0.05
78.98	3.33	12.29	0.62	5.13	0.36	4.43	0.17	0.03	0.04	1.92	0.10	0.03	0.05	0.18	0.05
76.73	3.24	13.71	0.68	5.06	0.35	5.41	0.20	0.05	0.04	1.99	0.10	0.03	0.05	0.03	0.05
78.80	3.32	8.84	0.46	4.60	0.32	3.21	0.13	0.81	0.06	4.99	0.19	0.09	0.05	0.03	0.05
81.27	3.43	11.09	0.56	4.35	0.31	4.44	0.17	0.09	0.04	2.10	0.10	0.03	0.05	0.13	0.05
77.47	3.27	13.05	0.65	5.19	0.36	4.81	0.18	0.12	0.04	2.40	0.11	0.03	0.05	0.03	0.05
71.43	3.02	16.17	0.80	6.08	0.41	5.94	0.22	0.03	0.04	2.68	0.12	0.03	0.05	0.17	0.05
82.57	3.48	9.91	0.51	3.75	0.27	3.81	0.15	0.11	0.04	1.55	0.09	0.03	0.05	0.11	0.05
84.19	3.55	8.18	0.43	3.24	0.24	3.01	0.13	0.07	0.04	1.45	0.08	0.03	0.05	0.18	0.05
77.74	3.28	13.19	0.66	4.69	0.33	5.50	0.20	0.03	0.04	2.06	0.10	0.03	0.05	0.03	0.05
83.68	3.53	10.22	0.52	3.62	0.26	4.29	0.16	0.03	0.04	1.69	0.09	0.06	0.05	0.09	0.05
84.03	3.54	9.69	0.50	3.45	0.25	4.03	0.16	0.05	0.04	1.55	0.09	0.03	0.05	0.15	0.05
75.84	3.20	12.19	0.61	4.16	0.30	4.40	0.17	0.05	0.04	3.07	0.13	0.03	0.05	0.03	0.05
83.94	3.54	10.16	0.52	3.83	0.27	3.99	0.16	0.03	0.04	1.51	0.08	0.03	0.05	0.14	0.05
59.99	2.55	25.68	1.24	7.16	0.48	1.34	0.07	6.61	0.24	0.39	0.05	0.12	0.05	0.03	0.05
59.63	2.53	24.80	1.20	7.27	0.49	1.61	0.08	6.14	0.22	0.53	0.05	0.19	0.05	0.22	0.06
61.31	2.60	25.33	1.22	7.41	0.50	1.60	0.08	5.94	0.22	0.34	0.05	0.13	0.05	0.22	0.06
59.44	2.52	26.42	1.27	6.94	0.47	1.15	0.07	7.59	0.27	0.43	0.05	0.11	0.05	0.27	0.06
64.70	2.74	21.20	1.03	5.02	0.35	7.56	0.26	0.84	0.06	0.24	0.05	1.13	0.08	0.22	0.06
66.82	2.83	21.26	1.03	4.97	0.34	8.24	0.29	0.62	0.06	0.35	0.05	0.80	0.07	0.21	0.06
60.53	2.57	24.87	1.20	7.24	0.49	1.62	0.08	6.09	0.22	0.52	0.05	0.20	0.05	0.03	0.05
56.65	2.41	28.81	1.38	5.95	0.41	0.61	0.05	9.67	0.33	0.47	0.05	0.10	0.05	0.33	0.06
72.23	3.05	14.63	0.73	3.18	0.23	7.22	0.25	0.60	0.06	1.08	0.07	0.28	0.05	0.24	0.06
67.96	2.88	17.49	0.86	5.21	0.36	6.31	0.23	0.86	0.06	0.68	0.06	0.15	0.05	0.31	0.06
51.45	2.19	1.78	0.13	5.46	0.38	0.83	0.06	9.88	0.34	26.72	0.86	0.71	0.07	0.13	0.05
74.87	3.16	12.53	0.63	3.82	0.27	4.37	0.17	0.37	0.05	0.57	0.06	0.07	0.05	0.03	0.05
76.64	3.23	12.86	0.65	3.81	0.27	4.34	0.17	0.35	0.05	0.59	0.06	0.10	0.05	0.03	0.05
95.36	4.01	1.48	0.12	0.03	0.04	0.15	0.04	0.59	0.06	0.25	0.05	0.03	0.05	0.17	0.05
80.60	3.40	12.10	0.61	3.11	0.23	5.02	0.19	0.22	0.04	0.40	0.05	0.03	0.05	0.03	0.05
75.59	3.19	13.17	0.66	3.26	0.24	4.64	0.18	1.19	0.07	1.17	0.07	0.22	0.05	0.16	0.05
74.49	3.15	12.56	0.63	3.31	0.24	4.73	0.18	0.42	0.05	0.73	0.06	0.11	0.05	0.24	0.06
76.03	3.21	12.80	0.64	4.01	0.29	4.23	0.16	0.28	0.05	1.12	0.07	0.03	0.05	0.25	0.06
71.69	3.03	11.61	0.59	3.11	0.23	4.43	0.17	1.37	0.08	4.49	0.18	0.18	0.05	0.29	0.06
74.02	3.13	14.56	0.72	3.40	0.25	5.71	0.21	0.62	0.06	1.30	0.08	0.57	0.06	0.17	0.05
68.02	2.88	19.89	0.97	5.04	0.35	8.94	0.31	0.11	0.04	0.34	0.05	0.09	0.05	0.03	0.05
77.66	3.28	13.10	0.66	3.37	0.25	4.67	0.18	0.32	0.05	0.69	0.06	0.07	0.05	0.03	0.05
74.61	3.15	11.49	0.58	4.62	0.32	4.42	0.17	0.03	0.04	2.97	0.13	0.03	0.05	0.16	0.05
74.16	3.13	13.81	0.69	5.46	0.38	4.71	0.18	0.08	0.04	1.69	0.09	0.07	0.05	0.03	0.05
78.83	3.33	11.51	0.58	4.60	0.32	4.08	0.16	0.03	0.04	1.45	0.08	0.05	0.05	0.21	0.06
77.67	3.28	10.52	0.54	4.42	0.31	3.59	0.14	0.15	0.04	3.67	0.15	0.38	0.06	0.03	0.05
82.60	3.48	10.90	0.56	4.05	0.29	3.82	0.15	0.09	0.04	1.65	0.09	0.03	0.05	0.22	0.06
76.24	3.22	11.30	0.57	4.51	0.32	4.24	0.16	0.07	0.04	2.91	0.13	0.19	0.05	0.03	0.05
77.61	3.27	11.68	0.59	4.61	0.32	4.48	0.17	0.05	0.04	1.60	0.09	0.03	0.05	0.03	0.05
77.70	3.28	14.03	0.70	5.10	0.35	5.12	0.19	0.07	0.04	0.63	0.06	0.03	0.05	0.03	0.05
76.33	3.22	12.30	0.62	4.82	0.34	4.43	0.17	0.07	0.04	1.76	0.09	0.03	0.05	0.06	0.05
61.89	2.62	10.01	0.51	7.36	0.49	4.29	0.16	2.04	0.10	11.67	0.40	0.32	0.06	0.13	0.05
77.90	3.29	12.81	0.64	5.02	0.35	4.74	0.18	0.07	0.04	1.85	0.09	0.03	0.05	0.03	0.05
81.02	3.42	11.76	0.59	4.24	0.30	4.48	0.17	0.07	0.04	1.84	0.09	0.03	0.05	0.34	0.06
77.85	3.28	10.69	0.55	3.82	0.27	3.94	0.15	0.08	0.04	3.26	0.14	0.29	0.06	0.07	0.05
71.61	3.03	15.46	0.77	5.81	0.40	6.10	0.22	0.05	0.04	2.36	0.11	0.03	0.05	0.26	0.06
87.30	3.68	8.72	0.45	3.94	0.28	2.33	0.10	0.03	0.04	1.21	0.07	0.03	0.05	0.03	0.05
76.38	3.22	14.41	0.72	4.88	0.34	5.78	0.21	0.13	0.04	1.59	0.09	0.03	0.05	0.03	0.05
68.16	2.88	19.06	0.93	8.03	0.53	5.34	0.20	0.03	0.04	1.12	0.07	0.12	0.05	0.26	0.06

83.55	3.52	10.46	0.53	3.59	0.26	4.22	0.16	0.03	0.04	1.66	0.09	0.03	0.05	0.03	0.05
79.93	3.37	12.09	0.61	4.78	0.33	4.32	0.17	0.03	0.04	1.74	0.09	0.03	0.05	0.03	0.05
78.56	3.31	12.93	0.65	4.99	0.35	4.79	0.18	0.03	0.04	1.85	0.09	0.05	0.05	0.03	0.05
84.52	3.56	9.23	0.48	3.58	0.26	3.37	0.14	0.03	0.04	1.51	0.08	0.03	0.05	0.03	0.05
96.70	4.07	3.72	0.22	1.22	0.11	1.13	0.07	0.03	0.04	1.14	0.07	0.03	0.05	0.03	0.05
81.43	3.43	11.84	0.60	4.19	0.30	4.46	0.17	0.05	0.04	0.59	0.06	0.03	0.05	0.03	0.05
67.98	2.88	17.15	0.84	7.19	0.48	6.70	0.24	0.03	0.04	3.73	0.15	0.06	0.05	0.29	0.06
71.77	3.03	16.46	0.81	6.24	0.42	6.40	0.23	0.03	0.04	2.47	0.11	0.03	0.05	0.30	0.06
82.34	3.47	10.58	0.54	3.81	0.27	4.18	0.16	0.08	0.04	1.84	0.09	0.03	0.05	0.03	0.05
69.58	2.94	17.27	0.85	6.73	0.45	6.61	0.24	0.03	0.04	2.24	0.11	0.03	0.05	0.33	0.06
83.62	3.52	9.04	0.47	3.54	0.26	3.19	0.13	0.03	0.04	1.50	0.08	0.03	0.05	0.03	0.05
84.96	3.58	8.58	0.45	3.54	0.26	3.01	0.13	0.03	0.04	1.40	0.08	0.03	0.05	0.03	0.05
76.24	3.22	10.62	0.54	4.11	0.29	4.38	0.17	0.03	0.04	1.98	0.10	0.03	0.05	0.07	0.05
84.80	3.57	7.96	0.42	3.04	0.23	3.03	0.13	0.03	0.04	1.39	0.08	0.07	0.05	0.03	0.05
60.58	2.57	12.55	0.63	7.80	0.52	3.83	0.15	3.15	0.13	10.88	0.37	0.25	0.05	0.08	0.05
73.84	3.12	16.09	0.80	6.02	0.41	6.03	0.22	0.03	0.04	1.42	0.08	0.03	0.05	0.03	0.05
70.00	2.96	17.34	0.85	5.72	0.39	6.84	0.24	0.10	0.04	2.88	0.13	0.07	0.05	0.05	0.05
69.45	2.94	19.54	0.95	7.89	0.53	5.93	0.21	0.03	0.04	0.80	0.06	0.07	0.05	0.28	0.06
72.84	3.08	15.81	0.78	6.02	0.41	6.04	0.22	0.03	0.04	2.15	0.10	0.03	0.05	0.03	0.05
69.49	2.94	17.01	0.84	6.05	0.41	6.92	0.25	0.06	0.04	2.79	0.12	0.03	0.05	0.27	0.06
73.95	3.12	13.71	0.69	4.08	0.29	4.19	0.16	0.17	0.04	2.76	0.12	0.12	0.05	0.27	0.06
97.75	4.11	0.37	0.07	0.03	0.04	0.03	0.03	0.17	0.04	0.05	0.04	0.03	0.05	0.11	0.05
100.19	4.21	0.41	0.07	0.06	0.04	0.03	0.03	0.32	0.05	0.07	0.04	0.03	0.05	0.15	0.05
96.63	4.06	0.36	0.07	0.03	0.04	0.03	0.03	0.26	0.05	0.03	0.04	0.03	0.05	0.07	0.05
98.07	4.12	0.32	0.07	0.03	0.04	0.03	0.03	0.35	0.05	0.03	0.04	0.03	0.05	0.07	0.05
95.54	4.02	0.70	0.08	0.03	0.04	0.03	0.03	0.51	0.05	0.11	0.04	0.03	0.05	0.14	0.05
96.81	4.07	0.43	0.07	0.12	0.04	0.03	0.03	0.33	0.05	0.03	0.04	0.03	0.05	0.12	0.05
99.70	4.19	0.48	0.07	0.16	0.05	0.03	0.03	0.32	0.05	0.03	0.04	0.03	0.05	0.03	0.05
97.72	4.11	0.47	0.07	0.11	0.04	0.03	0.03	0.37	0.05	0.07	0.04	0.03	0.05	0.08	0.05
99.78	4.19	0.38	0.07	0.03	0.04	0.03	0.03	0.59	0.06	0.03	0.04	0.03	0.05	0.03	0.05
94.73	3.98	0.90	0.09	0.03	0.04	0.03	0.03	0.34	0.05	0.26	0.05	0.06	0.05	0.07	0.05
68.47	2.90	17.48	0.86	7.24	0.49	6.21	0.22	0.03	0.04	1.99	0.10	0.03	0.05	0.25	0.06
96.87	4.07	0.39	0.07	0.03	0.04	0.03	0.03	0.24	0.05	0.08	0.04	0.03	0.05	0.11	0.05
79.54	3.35	11.37	0.58	3.93	0.28	4.28	0.16	0.05	0.04	1.96	0.10	0.03	0.05	0.03	0.05
60.61	2.57	25.45	1.23	8.84	0.58	0.23	0.04	4.77	0.18	0.76	0.06	0.09	0.05	0.39	0.07
79.66	3.36	11.57	0.59	4.38	0.31	4.46	0.17	0.03	0.04	1.28	0.08	0.03	0.05	0.03	0.05
67.97	2.88	15.38	0.76	5.33	0.37	5.01	0.19	0.09	0.04	2.69	0.12	0.03	0.05	0.13	0.05
100.76	4.23	0.32	0.07	0.03	0.04	0.03	0.03	0.23	0.05	0.03	0.04	0.03	0.05	0.06	0.05
101.78	4.28	0.46	0.07	0.03	0.04	0.03	0.03	0.25	0.05	0.08	0.04	0.03	0.05	0.03	0.05
95.74	4.03	0.39	0.07	0.03	0.04	0.03	0.03	0.41	0.05	0.03	0.04	0.03	0.05	0.30	0.06
63.73	2.70	19.90	0.97	4.25	0.30	8.49	0.29	0.35	0.05	0.19	0.04	0.40	0.06	0.26	0.06
64.74	2.74	20.21	0.99	4.35	0.31	8.38	0.29	0.32	0.05	0.11	0.04	0.49	0.06	0.29	0.06
99.21	4.17	0.38	0.07	0.15	0.05	0.03	0.03	0.23	0.05	0.05	0.04	0.03	0.05	0.28	0.06
99.88	4.20	0.40	0.07	0.03	0.04	0.03	0.03	0.17	0.04	0.03	0.04	0.03	0.05	0.07	0.05
95.17	4.00	0.45	0.07	0.09	0.04	0.03	0.03	0.28	0.05	0.15	0.04	0.03	0.05	0.06	0.05
97.23	4.09	3.29	0.20	0.32	0.06	0.51	0.05	0.28	0.05	1.25	0.08	0.08	0.05	0.76	0.08
76.12	3.21	12.92	0.65	1.31	0.12	2.27	0.10	0.39	0.05	3.35	0.14	0.41	0.06	2.35	0.17
96.03	4.04	0.36	0.07	0.03	0.04	0.03	0.03	0.47	0.05	0.03	0.04	0.03	0.05	0.03	0.05
63.92	2.71	20.08	0.98	4.35	0.31	8.24	0.29	0.39	0.05	0.17	0.04	0.49	0.06	0.26	0.06
95.78	4.03	0.35	0.07	0.13	0.05	0.03	0.03	0.38	0.05	0.03	0.04	0.03	0.05	0.03	0.05
65.27	2.76	12.20	0.62	6.56	0.44	5.13	0.19	0.22	0.05	8.43	0.30	0.32	0.06	0.03	0.05
81.26	3.43	11.17	0.57	4.30	0.30	4.22	0.16	0.03	0.04	2.17	0.10	0.03	0.05	0.18	0.05
82.80	3.49	10.16	0.52	3.63	0.26	3.54	0.14	0.08	0.04	1.61	0.09	0.09	0.05	0.25	0.06
77.99	3.29	11.37	0.58	4.40	0.31	4.16	0.16	0.07	0.04	1.69	0.09	0.06	0.05	0.21	0.06
98.23	4.13	0.61	0.08	0.07	0.04	0.09	0.04	0.21	0.04	0.05	0.04	0.03	0.05	0.09	0.05
97.70	4.11	0.48	0.07	0.03	0.04	0.03	0.03	0.18	0.04	0.18	0.04	0.03	0.05	0.05	0.05
75.98	3.21	11.99	0.61	5.18	0.36	4.68	0.18	0.09	0.04	3.78	0.15	0.13	0.05	0.19	0.05
77.32	3.26	13.19	0.66	5.09	0.35	5.00	0.19	0.14	0.04	1.71	0.09	0.03	0.05	0.11	0.05
70.63	2.99	14.64	0.73	5.93	0.40	5.09	0.19	0.10	0.04	2.90	0.13	0.10	0.05	0.05	0.05
98.34	4.13	0.50	0.07	0.03	0.04	0.03	0.03	0.19	0.04	0.26	0.05	0.03	0.05	0.03	0.05
55.35	2.35	28.56	1.37	5.33	0.37	0.64	0.05	7.36	0.26	0.68	0.06	0.03	0.05	0.34	0.06
61.81	2.62	25.51	1.23	6.89	0.46	1.91	0.09	4.95	0.19	0.54	0.05	0.09	0.05	0.34	0.06

60.43	2.56	25.42	1.23	6.61	0.45	1.82	0.09	5.26	0.20	0.59	0.06	0.12	0.05	0.30	0.06
55.07	2.34	28.24	1.36	5.25	0.36	0.77	0.06	7.34	0.26	0.59	0.06	0.08	0.05	0.33	0.06
56.30	2.39	28.19	1.36	5.61	0.38	0.70	0.05	7.13	0.25	0.68	0.06	0.09	0.05	0.03	0.05
58.32	2.48	27.00	1.30	6.13	0.42	1.17	0.07	6.25	0.23	0.68	0.06	0.13	0.05	0.39	0.07
57.40	2.44	29.40	1.41	5.59	0.38	0.67	0.05	7.39	0.26	0.69	0.06	0.10	0.05	0.37	0.06
56.27	2.39	28.07	1.35	5.56	0.38	0.75	0.06	7.13	0.25	0.67	0.06	0.11	0.05	0.34	0.06
92.86	3.91	4.68	0.27	1.16	0.11	1.74	0.09	0.03	0.04	0.13	0.04	0.10	0.05	0.09	0.05
60.76	2.58	5.93	0.32	1.54	0.13	0.69	0.05	9.66	0.33	10.43	0.36	0.57	0.06	9.33	0.54
56.12	2.38	2.98	0.19	0.68	0.08	0.11	0.04	12.52	0.42	12.00	0.41	0.43	0.06	17.72	0.98
54.09	2.30	3.51	0.21	0.65	0.08	0.03	0.03	12.17	0.41	12.93	0.44	0.84	0.07	18.06	1.00
57.86	2.46	27.69	1.33	5.94	0.41	0.98	0.06	6.77	0.24	0.64	0.06	0.07	0.05	0.35	0.06
57.81	2.45	27.71	1.33	5.88	0.40	1.00	0.06	6.98	0.25	0.55	0.05	0.06	0.05	0.34	0.06
59.47	2.52	26.12	1.26	6.37	0.43	1.44	0.08	5.85	0.21	0.53	0.05	0.07	0.05	0.33	0.06
62.84	2.66	21.99	1.07	5.08	0.35	5.87	0.21	2.88	0.13	0.66	0.06	0.39	0.06	0.31	0.06
59.86	2.54	24.53	1.19	6.30	0.43	2.25	0.10	5.03	0.19	0.75	0.06	0.11	0.05	0.16	0.05
56.34	2.39	28.01	1.35	5.68	0.39	0.82	0.06	7.15	0.25	0.63	0.06	0.03	0.05	0.03	0.05
96.09	4.04	3.80	0.23	1.19	0.11	1.22	0.07	0.03	0.04	0.22	0.04	0.03	0.05	0.18	0.05
67.37	2.85	17.00	0.84	4.06	0.29	7.48	0.26	0.68	0.06	0.70	0.06	0.62	0.07	0.12	0.05
66.47	2.81	20.25	0.99	4.88	0.34	8.24	0.29	0.68	0.06	0.39	0.05	0.33	0.06	0.29	0.06
63.16	2.68	24.32	1.18	6.58	0.44	3.25	0.13	4.15	0.16	0.69	0.06	0.17	0.05	0.03	0.05
57.95	2.46	27.43	1.32	6.09	0.41	0.75	0.06	6.60	0.24	0.80	0.06	0.11	0.05	0.38	0.07
59.15	2.51	26.15	1.26	6.28	0.43	1.42	0.08	5.85	0.22	0.68	0.06	0.14	0.05	0.34	0.06
57.62	2.45	27.27	1.31	5.62	0.39	1.42	0.08	6.56	0.24	0.79	0.06	0.11	0.05	0.37	0.06
59.70	2.53	26.12	1.26	6.48	0.44	1.44	0.08	5.90	0.22	0.61	0.06	0.09	0.05	0.32	0.06
59.77	2.54	27.68	1.33	6.31	0.43	1.13	0.07	6.34	0.23	0.61	0.06	0.11	0.05	0.35	0.06
61.15	2.59	16.63	0.82	3.93	0.28	5.31	0.20	2.92	0.13	3.76	0.15	0.80	0.07	1.98	0.15
75.63	3.19	11.88	0.60	3.55	0.26	3.96	0.15	0.85	0.06	3.02	0.13	0.24	0.05	0.53	0.07
75.61	3.19	11.71	0.59	4.23	0.30	4.72	0.18	0.41	0.05	2.70	0.12	0.18	0.05	0.13	0.05
77.25	3.26	10.71	0.55	3.79	0.27	4.08	0.16	0.59	0.06	2.86	0.13	0.18	0.05	0.23	0.06
75.29	3.18	13.19	0.66	3.21	0.24	4.51	0.17	0.68	0.06	2.11	0.10	0.27	0.05	0.51	0.07
76.66	3.24	12.26	0.62	3.69	0.27	4.93	0.18	0.62	0.06	1.39	0.08	0.14	0.05	0.15	0.05
72.99	3.08	11.71	0.59	3.05	0.23	4.89	0.18	5.55	0.21	1.09	0.07	0.21	0.05	0.38	0.07
75.80	3.20	11.71	0.59	4.23	0.30	4.72	0.18	0.41	0.05	2.70	0.12	0.18	0.05	0.13	0.05
77.44	3.27	10.71	0.55	3.79	0.27	4.08	0.16	0.59	0.06	2.86	0.13	0.18	0.05	0.23	0.06
75.85	3.20	11.88	0.60	3.55	0.26	3.96	0.15	0.85	0.06	3.02	0.13	0.24	0.05	0.53	0.07
73.02	3.08	11.71	0.59	3.05	0.23	4.89	0.18	5.55	0.21	1.09	0.07	0.21	0.05	0.38	0.07
75.44	3.19	13.19	0.66	3.21	0.24	4.51	0.17	0.68	0.06	2.11	0.10	0.27	0.05	0.51	0.07
76.73	3.24	12.26	0.62	3.69	0.27	4.93	0.18	0.62	0.06	1.39	0.08	0.14	0.05	0.15	0.05

Table D.2: Major element compositions (as wt.% oxides) of unmelted/partially melted regions in sample FLD10 measured using EDS rasters. Data were collected in a grid-based pattern like the host and agglomerate EDS analyses. Analytical procedure is detailed in Chapter 4. Uncertainties are calculated as detailed in Chapter 6.

SiO_2	1σ	Al_2O_3	1σ	Na_2O	1σ	K_2O	1σ	CaO	1σ	FeO	1σ	TiO_2	1σ	MgO	1σ
71.96	3.04	12.79	0.64	3.42	0.25	4.60	0.17	0.98	0.07	4.83	0.19	0.31	0.06	0.47	0.07
90.97	3.83	3.97	0.23	1.04	0.10	1.34	0.07	0.07	0.04	1.14	0.07	0.03	0.05	0.11	0.05
75.87	3.20	12.81	0.64	3.02	0.22	4.69	0.18	0.74	0.06	0.99	0.07	0.12	0.05	0.09	0.05
92.21	3.88	3.70	0.22	1.16	0.11	1.37	0.08	0.55	0.05	0.97	0.07	0.20	0.05	0.32	0.06
65.15	2.76	14.04	0.70	3.84	0.28	4.43	0.17	1.79	0.09	8.45	0.30	1.47	0.09	1.19	0.11
67.25	2.85	13.16	0.66	3.52	0.26	4.62	0.17	3.11	0.13	2.57	0.12	3.23	0.15	0.61	0.08
63.37	2.69	20.76	1.01	4.69	0.33	4.54	0.17	2.18	0.10	3.04	0.13	0.45	0.06	0.97	0.10
64.06	2.71	18.31	0.90	4.21	0.30	4.64	0.18	2.57	0.12	3.97	0.16	0.51	0.06	1.21	0.11
72.69	3.07	12.40	0.62	3.52	0.26	4.31	0.17	1.15	0.07	3.36	0.14	0.90	0.07	0.59	0.08
64.14	2.72	18.91	0.93	4.46	0.31	4.71	0.18	1.10	0.07	2.76	0.12	0.61	0.07	1.15	0.11
69.90	2.96	16.54	0.82	3.95	0.28	4.85	0.18	1.51	0.08	1.86	0.10	0.19	0.05	0.03	0.05
72.68	3.07	13.22	0.66	3.15	0.23	3.71	0.15	2.60	0.12	2.46	0.11	0.32	0.06	0.50	0.07
81.44	3.43	10.94	0.56	4.19	0.30	3.92	0.15	0.03	0.04	1.62	0.09	0.03	0.05	0.22	0.06
81.61	3.44	10.50	0.54	3.64	0.26	3.56	0.14	0.03	0.04	1.37	0.08	0.03	0.05	0.16	0.05
72.13	3.05	13.16	0.66	3.64	0.26	4.31	0.17	1.44	0.08	4.07	0.16	0.44	0.06	0.21	0.06

80.47	3.39	9.16	0.47	2.35	0.18	3.47	0.14	0.49	0.05	2.34	0.11	0.30	0.06	0.46	0.07
78.05	3.29	12.63	0.64	4.77	0.33	4.54	0.17	0.03	0.04	1.80	0.09	0.10	0.05	0.16	0.05
71.70	3.03	13.59	0.68	5.55	0.38	5.25	0.19	0.31	0.05	3.87	0.16	0.13	0.05	0.10	0.05
79.13	3.34	12.29	0.62	4.72	0.33	4.28	0.16	0.12	0.04	2.06	0.10	0.10	0.05	0.03	0.05
67.53	2.86	15.03	0.75	4.39	0.31	4.64	0.18	1.24	0.08	3.26	0.14	0.21	0.05	0.35	0.06
75.08	3.17	12.93	0.65	3.41	0.25	4.58	0.17	0.72	0.06	0.96	0.07	0.15	0.05	0.49	0.07
80.54	3.40	12.46	0.63	4.58	0.32	4.40	0.17	0.03	0.04	1.59	0.09	0.03	0.05	0.23	0.06
74.60	3.15	9.26	0.48	4.30	0.30	4.18	0.16	1.15	0.07	5.40	0.20	0.19	0.05	0.20	0.06
75.36	3.18	13.71	0.69	5.52	0.38	4.81	0.18	0.03	0.04	2.56	0.12	0.14	0.05	0.13	0.05
76.91	3.25	12.92	0.65	4.68	0.33	4.83	0.18	0.03	0.04	2.01	0.10	0.06	0.05	0.03	0.05
63.43	2.69	17.81	0.87	3.71	0.27	3.87	0.15	4.07	0.16	3.70	0.15	0.42	0.06	1.48	0.12
78.10	3.30	11.10	0.56	4.35	0.31	4.35	0.17	0.03	0.04	2.81	0.12	0.08	0.05	0.17	0.05
80.46	3.39	11.84	0.60	4.25	0.30	4.28	0.16	0.03	0.04	1.66	0.09	0.03	0.05	0.20	0.06
68.35	2.89	13.23	0.66	5.20	0.36	5.33	0.20	0.33	0.05	5.04	0.19	2.87	0.14	0.31	0.06
70.66	2.99	13.33	0.67	3.11	0.23	4.39	0.17	2.08	0.10	4.73	0.18	0.31	0.06	1.13	0.10
72.60	3.07	15.43	0.76	5.83	0.40	5.34	0.20	0.07	0.04	2.87	0.13	0.06	0.05	0.21	0.06
65.37	2.77	19.65	0.96	5.87	0.40	6.01	0.22	1.20	0.07	0.35	0.05	0.03	0.05	0.03	0.05
77.42	3.27	11.39	0.58	4.21	0.30	4.50	0.17	0.71	0.06	4.29	0.17	0.23	0.05	0.14	0.05
69.39	2.93	15.38	0.76	4.09	0.29	4.06	0.16	1.67	0.09	3.41	0.14	0.46	0.06	0.89	0.09
76.01	3.21	10.22	0.52	2.90	0.22	5.21	0.19	0.27	0.05	3.71	0.15	0.15	0.05	0.09	0.05
67.90	2.87	15.78	0.78	4.34	0.31	4.81	0.18	1.58	0.09	3.97	0.16	0.67	0.07	0.78	0.09
67.90	2.87	16.99	0.84	3.96	0.28	4.57	0.17	1.59	0.09	3.43	0.14	0.53	0.06	1.04	0.10
73.27	3.10	15.19	0.75	3.45	0.25	4.73	0.18	0.98	0.07	1.81	0.09	0.18	0.05	0.38	0.06
70.26	2.97	16.85	0.83	4.23	0.30	4.81	0.18	1.31	0.08	2.95	0.13	0.41	0.06	0.74	0.08
73.79	3.12	14.54	0.72	3.24	0.24	4.73	0.18	1.11	0.07	2.24	0.11	0.27	0.05	0.59	0.08
85.30	3.59	7.71	0.41	2.86	0.21	2.78	0.12	0.03	0.04	1.02	0.07	0.05	0.05	0.16	0.05
67.77	2.87	16.44	0.81	5.47	0.38	5.20	0.19	1.32	0.08	3.56	0.15	0.19	0.05	0.22	0.06
75.09	3.17	10.51	0.54	3.54	0.26	4.52	0.17	0.08	0.04	2.39	0.11	0.08	0.05	0.03	0.05
64.23	2.72	19.99	0.98	3.61	0.26	3.42	0.14	2.95	0.13	3.49	0.15	0.63	0.07	1.25	0.11
86.54	3.64	7.55	0.40	2.87	0.22	2.95	0.12	0.11	0.04	1.73	0.09	0.30	0.06	0.12	0.05
70.63	2.99	14.46	0.72	3.48	0.25	4.49	0.17	1.11	0.07	2.47	0.11	0.27	0.05	0.68	0.08
73.71	3.11	14.76	0.73	5.40	0.37	5.09	0.19	0.44	0.05	2.10	0.10	0.03	0.05	0.09	0.05
79.10	3.34	10.94	0.56	4.08	0.29	3.97	0.15	0.03	0.04	1.62	0.09	0.11	0.05	0.03	0.05
64.68	2.74	11.72	0.59	6.36	0.43	5.14	0.19	2.32	0.11	8.81	0.31	0.70	0.07	0.33	0.06
81.72	3.45	10.20	0.52	3.80	0.27	3.74	0.15	0.03	0.04	1.45	0.08	0.08	0.05	0.03	0.05
67.20	2.84	6.22	0.34	5.33	0.37	4.72	0.18	1.43	0.08	12.54	0.43	1.29	0.09	0.17	0.05
80.54	3.40	11.83	0.60	4.51	0.32	4.08	0.16	0.03	0.04	1.67	0.09	0.03	0.05	0.22	0.06
80.26	3.38	12.58	0.63	4.69	0.33	4.35	0.17	0.03	0.04	1.86	0.09	0.05	0.05	0.17	0.05
78.51	3.31	11.77	0.60	4.45	0.31	4.36	0.17	0.03	0.04	1.79	0.09	0.09	0.05	0.03	0.05
78.41	3.31	11.51	0.58	5.07	0.35	4.21	0.16	0.43	0.05	3.98	0.16	0.09	0.05	0.18	0.05
85.69	3.61	9.55	0.49	3.66	0.26	3.18	0.13	0.03	0.04	1.37	0.08	0.05	0.05	0.14	0.05
67.76	2.87	16.63	0.82	6.55	0.44	6.08	0.22	0.03	0.04	2.77	0.12	0.03	0.05	0.17	0.05
71.47	3.02	9.88	0.51	4.28	0.30	4.21	0.16	2.18	0.10	6.73	0.25	0.36	0.06	0.03	0.05
83.06	3.50	10.94	0.56	3.99	0.28	3.97	0.15	0.03	0.04	1.48	0.08	0.03	0.05	0.17	0.05
81.03	3.42	11.58	0.59	4.38	0.31	4.25	0.16	0.03	0.04	1.71	0.09	0.03	0.05	0.03	0.05
82.89	3.49	9.65	0.50	3.70	0.27	3.64	0.14	0.03	0.04	1.45	0.08	0.03	0.05	0.17	0.05
69.02	2.92	14.94	0.74	3.61	0.26	4.22	0.16	1.73	0.09	3.81	0.16	0.50	0.06	0.97	0.10
88.70	3.73	7.12	0.38	2.77	0.21	2.68	0.12	0.03	0.04	1.05	0.07	0.03	0.05	0.05	0.05
78.83	3.33	12.69	0.64	4.94	0.34	4.66	0.18	0.03	0.04	1.90	0.10	0.03	0.05	0.03	0.05
77.21	3.26	12.98	0.65	5.06	0.35	4.73	0.18	0.03	0.04	1.88	0.10	0.03	0.05	0.03	0.05
76.82	3.24	12.48	0.63	4.81	0.34	4.50	0.17	0.03	0.04	1.69	0.09	0.06	0.05	0.03	0.05
73.40	3.10	13.99	0.70	5.48	0.38	4.83	0.18	0.03	0.04	2.09	0.10	0.08	0.05	0.05	0.05
85.09	3.58	8.45	0.44	3.17	0.23	3.17	0.13	0.20	0.04	2.01	0.10	0.10	0.05	0.16	0.05
79.93	3.37	9.92	0.51	3.81	0.27	3.66	0.15	0.09	0.04	1.70	0.09	0.03	0.05	0.03	0.05
64.08	2.71	11.94	0.60	6.54	0.44	5.24	0.19	1.53	0.08	9.32	0.33	0.60	0.07	0.13	0.05
84.58	3.56	8.24	0.43	3.24	0.24	3.15	0.13	0.08	0.04	1.31	0.08	0.05	0.05	0.19	0.05
61.63	2.61	10.58	0.54	5.99	0.41	5.03	0.19	1.29	0.08	9.33	0.33	2.80	0.13	0.97	0.10
65.64	2.78	5.62	0.31	3.22	0.24	3.41	0.14	0.42	0.05	16.11	0.54	5.82	0.23	0.89	0.09
98.30	4.13	0.33	0.07	0.03	0.04	0.03	0.03	0.03	0.04	0.13	0.04	0.03	0.05	0.03	0.05
74.01	3.13	11.73	0.59	5.82	0.40	4.71	0.18	0.72	0.06	6.48	0.24	0.32	0.06	0.09	0.05
77.34	3.26	13.13	0.66	5.22	0.36	4.66	0.18	0.03	0.04	1.82	0.09	0.03	0.05	0.23	0.06
81.59	3.44	9.77	0.50	3.69	0.27	3.67	0.15	0.03	0.04	1.59	0.09	0.08	0.05	0.08	0.05

75.64	3.19	12.85	0.65	4.79	0.33	4.77	0.18	0.03	0.04	1.87	0.10	0.03	0.05	0.15	0.05
72.45	3.06	11.19	0.57	4.91	0.34	4.65	0.18	0.03	0.04	4.14	0.17	0.13	0.05	0.09	0.05
67.50	2.86	11.42	0.58	6.04	0.41	5.03	0.19	0.36	0.05	11.20	0.38	0.74	0.07	0.91	0.09
80.04	3.38	10.95	0.56	4.30	0.30	4.08	0.16	0.03	0.04	1.53	0.08	0.03	0.05	0.03	0.05
76.08	3.21	11.46	0.58	4.74	0.33	4.46	0.17	0.10	0.04	2.45	0.11	0.08	0.05	0.16	0.05
78.42	3.31	11.47	0.58	4.63	0.32	4.33	0.17	0.03	0.04	1.73	0.09	0.03	0.05	0.17	0.05
71.04	3.00	14.39	0.72	6.07	0.41	5.13	0.19	0.10	0.04	3.43	0.14	0.23	0.05	0.26	0.06
77.19	3.26	12.38	0.62	4.93	0.34	4.61	0.17	0.03	0.04	2.23	0.11	0.03	0.05	0.10	0.05
78.71	3.32	12.99	0.65	5.21	0.36	4.56	0.17	0.03	0.04	2.15	0.10	0.06	0.05	0.28	0.06
73.19	3.09	13.13	0.66	5.33	0.37	4.93	0.18	0.35	0.05	3.02	0.13	0.13	0.05	0.17	0.05
73.55	3.11	9.91	0.51	5.54	0.38	4.75	0.18	0.62	0.06	7.80	0.28	0.41	0.06	0.03	0.05
73.56	3.11	12.23	0.62	5.62	0.39	4.77	0.18	0.80	0.06	4.81	0.19	0.34	0.06	0.10	0.05
78.29	3.30	12.63	0.64	4.77	0.33	4.42	0.17	0.06	0.04	1.88	0.10	0.17	0.05	0.26	0.06
63.51	2.69	11.51	0.58	6.49	0.44	5.19	0.19	1.80	0.09	9.91	0.34	0.35	0.06	0.03	0.05
77.22	3.26	12.69	0.64	5.00	0.35	4.54	0.17	0.41	0.05	2.50	0.11	0.03	0.05	0.15	0.05
80.66	3.40	10.10	0.52	4.16	0.30	3.98	0.16	0.19	0.04	2.42	0.11	0.35	0.06	0.16	0.05
77.79	3.28	11.17	0.57	4.43	0.31	4.42	0.17	0.03	0.04	2.80	0.12	0.64	0.07	0.03	0.05
81.40	3.43	9.47	0.49	3.57	0.26	3.71	0.15	0.14	0.04	1.76	0.09	0.06	0.05	0.07	0.05
74.97	3.17	13.37	0.67	5.50	0.38	5.04	0.19	0.03	0.04	3.11	0.13	0.28	0.05	0.21	0.06
64.19	2.72	14.27	0.71	5.75	0.39	5.57	0.20	0.43	0.05	3.44	0.14	2.52	0.13	0.44	0.07
87.15	3.67	8.47	0.44	2.96	0.22	3.06	0.13	0.03	0.04	1.48	0.08	0.06	0.05	0.15	0.05
89.08	3.75	5.58	0.31	1.92	0.16	2.20	0.10	0.03	0.04	1.04	0.07	0.03	0.05	0.08	0.05
74.94	3.16	15.25	0.76	5.74	0.39	5.04	0.19	0.03	0.04	2.00	0.10	0.05	0.05	0.26	0.06
76.33	3.22	13.71	0.68	5.16	0.36	4.83	0.18	0.08	0.04	1.97	0.10	0.03	0.05	0.05	0.05
79.83	3.37	11.52	0.58	4.27	0.30	4.39	0.17	0.03	0.04	1.65	0.09	0.03	0.05	0.16	0.05
71.13	3.01	13.72	0.69	6.00	0.41	5.13	0.19	0.76	0.06	4.38	0.17	0.12	0.05	0.25	0.06
70.30	2.97	10.93	0.56	5.20	0.36	4.82	0.18	1.11	0.07	6.12	0.23	0.31	0.06	0.07	0.05
64.40	2.73	12.10	0.61	6.67	0.45	5.34	0.20	1.77	0.09	9.22	0.32	0.45	0.06	0.18	0.05
78.37	3.31	11.97	0.60	4.59	0.32	4.48	0.17	0.03	0.04	1.93	0.10	0.05	0.05	0.19	0.05
77.96	3.29	11.35	0.58	4.46	0.31	4.32	0.17	0.03	0.04	2.39	0.11	0.03	0.05	0.16	0.05
72.95	3.08	15.00	0.74	6.03	0.41	5.35	0.20	0.25	0.05	3.18	0.14	0.10	0.05	0.05	0.05
78.54	3.31	11.77	0.60	4.49	0.32	4.28	0.16	0.03	0.04	1.52	0.08	0.03	0.05	0.15	0.05
78.55	3.31	11.91	0.60	4.48	0.31	4.25	0.16	0.10	0.04	1.77	0.09	0.03	0.05	0.14	0.05
76.46	3.23	12.65	0.64	4.64	0.32	4.66	0.18	0.28	0.05	2.64	0.12	0.10	0.05	0.18	0.05
79.63	3.36	9.70	0.50	3.73	0.27	3.85	0.15	0.09	0.04	1.51	0.08	0.05	0.05	0.03	0.05
74.35	3.14	13.40	0.67	5.01	0.35	4.82	0.18	0.06	0.04	2.16	0.10	0.07	0.05	0.14	0.05
77.72	3.28	11.84	0.60	4.69	0.33	4.48	0.17	0.03	0.04	2.48	0.11	0.03	0.05	0.10	0.05
77.91	3.29	11.73	0.59	4.63	0.32	4.43	0.17	0.03	0.04	2.12	0.10	0.03	0.05	0.03	0.05
81.01	3.42	12.12	0.61	4.50	0.32	4.20	0.16	0.03	0.04	1.65	0.09	0.03	0.05	0.20	0.06
77.98	3.29	11.43	0.58	4.37	0.31	4.26	0.16	0.03	0.04	1.53	0.08	0.03	0.05	0.03	0.05
72.54	3.06	16.30	0.80	6.34	0.43	5.43	0.20	0.29	0.05	2.56	0.12	0.03	0.05	0.25	0.06
65.79	2.79	15.81	0.78	6.95	0.47	5.56	0.20	0.67	0.06	3.39	0.14	0.08	0.05	0.50	0.07
76.43	3.23	13.47	0.67	5.03	0.35	4.75	0.18	0.03	0.04	2.03	0.10	0.03	0.05	0.09	0.05
95.87	4.03	0.29	0.06	0.10	0.04	0.03	0.03	0.06	0.04	0.08	0.04	0.03	0.05	0.13	0.05
79.86	3.37	11.19	0.57	4.27	0.30	4.05	0.16	0.03	0.04	1.83	0.09	0.07	0.05	0.03	0.05
78.24	3.30	11.71	0.59	4.51	0.32	4.47	0.17	0.03	0.04	1.70	0.09	0.03	0.05	0.03	0.05
79.65	3.36	11.91	0.60	4.93	0.34	4.45	0.17	0.03	0.04	2.11	0.10	0.10	0.05	0.03	0.05
61.66	2.61	8.88	0.46	6.40	0.43	4.86	0.18	3.57	0.15	13.93	0.47	0.81	0.07	0.18	0.05
67.84	2.87	15.60	0.77	6.61	0.45	5.59	0.20	0.70	0.06	4.41	0.17	0.15	0.05	0.18	0.05
78.69	3.32	11.01	0.56	4.59	0.32	4.30	0.17	0.07	0.04	2.40	0.11	0.15	0.05	0.21	0.06
95.91	4.03	0.29	0.06	0.12	0.05	0.03	0.03	0.11	0.04	0.07	0.04	0.03	0.05	0.03	0.05
73.29	3.10	13.91	0.69	5.68	0.39	4.87	0.18	0.27	0.05	2.99	0.13	0.08	0.05	0.44	0.07
77.57	3.27	9.83	0.51	4.73	0.33	4.14	0.16	0.82	0.06	4.95	0.19	0.28	0.05	0.19	0.05
78.22	3.30	9.89	0.51	4.05	0.29	3.86	0.15	0.03	0.04	1.93	0.10	0.13	0.05	0.13	0.05
73.99	3.12	15.05	0.75	6.10	0.42	5.29	0.20	0.03	0.04	2.08	0.10	0.06	0.05	0.23	0.06
101.43	4.26	0.31	0.07	0.11	0.04	0.06	0.04	0.03	0.04	0.09	0.04	0.03	0.05	0.03	0.05
65.64	2.78	16.64	0.82	7.81	0.52	5.69	0.21	0.07	0.04	2.14	0.10	0.03	0.05	0.05	0.05
78.49	3.31	13.47	0.67	5.22	0.36	4.65	0.18	0.03	0.04	1.86	0.10	0.05	0.05	0.24	0.06
98.89	4.16	0.28	0.06	0.05	0.04	0.03	0.03	0.03	0.04	0.03	0.04	0.03	0.05	0.03	0.05
76.54	3.23	12.17	0.61	4.82	0.34	4.35	0.17	0.06	0.04	1.95	0.10	0.03	0.05	0.21	0.06
88.94	3.74	6.46	0.35	2.39	0.19	2.36	0.11	0.03	0.04	0.86	0.06	0.03	0.05	0.15	0.05
76.99	3.25	12.02	0.61	4.72	0.33	4.29	0.16	0.03	0.04	1.75	0.09	0.14	0.05	0.08	0.05

65.68	2.78	16.51	0.81	6.27	0.43	5.43	0.20	0.53	0.05	2.11	0.10	0.12	0.05	0.16	0.05
83.01	3.50	7.06	0.38	3.07	0.23	2.84	0.12	0.03	0.04	1.74	0.09	0.11	0.05	0.23	0.06
84.30	3.55	8.91	0.46	3.54	0.26	3.14	0.13	0.03	0.04	1.25	0.08	0.06	0.05	0.03	0.05
78.81	3.32	9.24	0.48	3.46	0.25	3.74	0.15	0.03	0.04	1.28	0.08	0.03	0.05	0.12	0.05
76.54	3.23	10.45	0.53	4.09	0.29	3.95	0.15	0.03	0.04	1.46	0.08	0.07	0.05	0.03	0.05
68.60	2.90	15.00	0.74	5.68	0.39	5.18	0.19	0.33	0.05	3.07	0.13	0.74	0.07	0.24	0.06
70.66	2.99	14.96	0.74	5.70	0.39	5.20	0.19	0.10	0.04	2.31	0.11	0.06	0.05	0.22	0.06
73.01	3.08	12.87	0.65	5.00	0.35	4.56	0.17	0.03	0.04	2.09	0.10	0.10	0.05	0.05	0.05
78.59	3.32	9.89	0.51	3.98	0.28	3.78	0.15	0.03	0.04	1.89	0.10	0.03	0.05	0.20	0.06
76.58	3.23	11.25	0.57	4.13	0.29	4.07	0.16	0.03	0.04	1.63	0.09	0.07	0.05	0.03	0.05
68.98	2.92	13.80	0.69	5.52	0.38	5.16	0.19	0.03	0.04	3.10	0.13	0.06	0.05	0.03	0.05
81.98	3.46	8.26	0.43	2.94	0.22	3.27	0.13	0.03	0.04	1.25	0.08	0.03	0.05	0.03	0.05
77.65	3.28	11.39	0.58	4.34	0.31	4.07	0.16	0.07	0.04	1.82	0.09	0.03	0.05	0.25	0.06
74.82	3.16	13.23	0.66	4.99	0.35	4.60	0.17	0.03	0.04	1.84	0.09	0.03	0.05	0.22	0.06
72.12	3.05	10.88	0.55	4.88	0.34	4.36	0.17	0.06	0.04	3.87	0.16	0.20	0.05	0.61	0.08
75.89	3.20	11.99	0.61	4.52	0.32	4.48	0.17	0.03	0.04	1.56	0.09	0.03	0.05	0.03	0.05
85.81	3.61	9.26	0.48	3.43	0.25	3.23	0.13	0.03	0.04	1.17	0.07	0.03	0.05	0.21	0.06
82.86	3.49	8.58	0.45	3.31	0.24	3.12	0.13	0.03	0.04	1.36	0.08	0.03	0.05	0.03	0.05
74.90	3.16	11.40	0.58	5.05	0.35	4.45	0.17	0.03	0.04	3.92	0.16	0.15	0.05	0.18	0.05
72.64	3.07	13.29	0.67	5.38	0.37	4.88	0.18	0.03	0.04	3.17	0.14	0.03	0.05	0.19	0.05
73.53	3.11	12.08	0.61	4.74	0.33	4.41	0.17	0.03	0.04	3.27	0.14	0.03	0.05	0.26	0.06
78.25	3.30	12.56	0.63	4.68	0.33	4.51	0.17	0.06	0.04	1.65	0.09	0.03	0.05	0.21	0.06
77.87	3.29	11.22	0.57	4.01	0.29	4.14	0.16	0.03	0.04	1.39	0.08	0.07	0.05	0.18	0.05
70.33	2.97	11.86	0.60	4.91	0.34	4.75	0.18	0.03	0.04	4.23	0.17	0.49	0.06	0.43	0.07
80.34	3.39	9.60	0.50	3.46	0.25	3.72	0.15	0.03	0.04	1.30	0.08	0.03	0.05	0.13	0.05
68.86	2.91	13.69	0.68	4.87	0.34	4.77	0.18	0.60	0.06	2.76	0.12	0.43	0.06	0.15	0.05

Appendix E

BCR-1 Data tables

Table E.1: Same spot variation of fallout and BCR-1. Shown in Figure 4.7.

Raster Sequence	Na (wt.%)	1σ	Na (wt.%)	1σ	K (wt.%)	1σ	K (wt.%)	1σ
1	1.95	0.15	2.49	0.18	3.16	0.12	1.50	0.07
2	1.79	0.14	2.52	0.18	3.11	0.12	1.44	0.07
3	1.71	0.13	2.50	0.18	3.15	0.12	1.49	0.07

Table E.3: 90 measurements of the major element composition of the glass standard BCR-1 using EDS raster analyses (raster diameter ≈10 μm). Data are presented here as oxide wt.%. Data are used in Figure 4.4 to show the deviations between EDS, EPMA, and literature values of BCR-1 and summarized in Table 4.3 to highlight the spot-to-spot precision of the EDS analyses.

SiO_2	1σ	Al_2O_3	1σ	Na_2O	1σ	K_2O	1σ	CaO	1σ	FeO	1σ	TiO_2	1σ	MgO	1σ
54.61	2.32	13.76	0.69	3.33	0.24	1.73	0.09	7.74	0.27	11.16	0.38	2.58	0.13	3.49	0.23
55.79	2.37	14.21	0.71	3.42	0.25	1.72	0.09	7.47	0.26	11.71	0.40	2.64	0.13	3.74	0.24
57.16	2.43	14.52	0.72	3.54	0.26	1.69	0.08	7.45	0.26	11.33	0.39	2.58	0.13	3.93	0.25
56.80	2.41	14.40	0.72	3.52	0.26	1.72	0.09	7.55	0.27	10.92	0.38	2.55	0.13	3.81	0.25
55.82	2.37	14.19	0.71	3.41	0.25	1.76	0.09	7.64	0.27	11.15	0.38	2.55	0.13	3.74	0.24
55.30	2.35	13.96	0.70	3.42	0.25	1.77	0.09	7.59	0.27	10.97	0.38	2.58	0.13	3.48	0.23
56.06	2.38	14.07	0.70	3.52	0.26	1.74	0.09	7.62	0.27	11.08	0.38	2.55	0.13	3.54	0.23
55.56	2.36	13.94	0.70	3.46	0.25	1.73	0.09	7.72	0.27	11.10	0.38	2.46	0.12	3.60	0.23
56.27	2.39	14.22	0.71	3.53	0.26	1.70	0.09	7.54	0.27	11.15	0.38	2.49	0.12	3.63	0.24
56.28	2.39	14.32	0.71	3.47	0.25	1.68	0.08	7.46	0.26	10.86	0.37	2.57	0.13	3.78	0.24
55.82	2.37	14.02	0.70	3.50	0.25	1.74	0.09	7.70	0.27	11.19	0.38	2.67	0.13	3.51	0.23
55.94	2.38	14.23	0.71	3.45	0.25	1.77	0.09	7.55	0.27	10.97	0.38	2.64	0.13	3.78	0.24
56.33	2.39	14.24	0.71	3.46	0.25	1.79	0.09	7.74	0.27	11.07	0.38	2.61	0.13	3.56	0.23
57.02	2.42	14.54	0.72	3.50	0.25	1.72	0.09	7.54	0.27	10.94	0.38	2.57	0.13	3.86	0.25
56.81	2.41	14.56	0.72	3.44	0.25	1.72	0.09	7.67	0.27	10.99	0.38	2.56	0.13	3.87	0.25
56.24	2.39	14.41	0.72	3.49	0.25	1.73	0.09	7.45	0.26	11.72	0.40	2.52	0.13	3.76	0.24
56.43	2.40	14.37	0.72	3.45	0.25	1.69	0.09	7.48	0.26	10.84	0.37	2.42	0.12	3.80	0.25
56.01	2.38	14.14	0.70	3.47	0.25	1.75	0.09	7.58	0.27	11.10	0.38	2.47	0.12	3.58	0.23
56.18	2.39	14.35	0.71	3.50	0.25	1.75	0.09	7.54	0.27	11.12	0.38	2.49	0.13	3.75	0.24
55.01	2.34	13.90	0.69	3.42	0.25	1.83	0.09	7.85	0.28	10.91	0.37	2.67	0.13	3.48	0.23
55.75	2.37	14.07	0.70	3.45	0.25	1.74	0.09	7.53	0.27	10.98	0.38	2.65	0.13	3.57	0.23
56.52	2.40	14.24	0.71	3.51	0.25	1.72	0.09	7.47	0.26	11.98	0.41	2.54	0.13	3.61	0.23
55.73	2.37	14.00	0.70	3.46	0.25	1.78	0.09	7.66	0.27	10.93	0.38	2.57	0.13	3.52	0.23
56.33	2.39	14.19	0.71	3.56	0.26	1.72	0.09	7.64	0.27	11.10	0.38	2.49	0.12	3.59	0.23

55.37	2.35	13.97	0.70	3.50	0.25	1.79	0.09	7.72	0.27	11.12	0.38	2.59	0.13	3.48	0.23
58.08	2.47	14.82	0.74	3.57	0.26	1.68	0.08	7.34	0.26	11.05	0.38	2.49	0.12	3.91	0.25
54.47	2.32	13.72	0.69	3.35	0.24	1.79	0.09	7.74	0.27	11.04	0.38	2.62	0.13	3.45	0.23
55.13	2.34	13.83	0.69	3.42	0.25	1.75	0.09	7.52	0.27	11.73	0.40	2.45	0.12	3.43	0.23
57.54	2.44	14.68	0.73	3.52	0.26	1.72	0.09	7.50	0.26	10.99	0.38	2.53	0.13	3.84	0.25
56.43	2.40	14.15	0.71	3.43	0.25	1.78	0.09	7.77	0.27	10.36	0.36	2.57	0.13	3.58	0.23
57.54	2.44	14.52	0.72	3.54	0.26	1.74	0.09	7.43	0.26	10.80	0.37	2.46	0.12	3.86	0.25
56.65	2.41	14.30	0.71	3.54	0.26	1.69	0.08	7.37	0.26	11.03	0.38	2.51	0.13	3.54	0.23
54.84	2.33	13.86	0.69	3.35	0.24	1.79	0.09	7.69	0.27	10.64	0.37	2.63	0.13	3.48	0.23
55.88	2.38	14.15	0.71	3.42	0.25	1.68	0.08	7.48	0.26	10.79	0.37	2.53	0.13	3.45	0.23
56.53	2.40	14.27	0.71	3.48	0.25	1.71	0.09	7.41	0.26	10.98	0.38	2.52	0.13	3.52	0.23
55.64	2.36	13.86	0.69	3.47	0.25	1.81	0.09	7.56	0.27	10.65	0.37	2.46	0.12	3.50	0.23
56.00	2.38	14.09	0.70	3.51	0.25	1.76	0.09	7.58	0.27	10.74	0.37	2.52	0.13	3.50	0.23
56.38	2.40	14.20	0.71	3.55	0.26	1.74	0.09	7.58	0.27	11.01	0.38	2.52	0.13	3.57	0.23
56.01	2.38	14.20	0.71	3.50	0.25	1.71	0.09	7.54	0.27	10.64	0.37	2.49	0.12	3.59	0.23
56.12	2.38	14.04	0.70	3.51	0.25	1.80	0.09	7.56	0.27	11.28	0.39	2.62	0.13	3.57	0.23
55.02	2.34	13.85	0.69	3.41	0.25	1.73	0.09	7.59	0.27	11.24	0.39	2.57	0.13	3.51	0.23
56.87	2.42	14.25	0.71	3.54	0.26	1.78	0.09	7.70	0.27	10.97	0.38	2.56	0.13	3.60	0.23
54.60	2.32	13.92	0.69	3.36	0.25	1.79	0.09	7.64	0.27	11.02	0.38	2.60	0.13	3.42	0.23
56.67	2.41	14.28	0.71	3.55	0.26	1.69	0.08	7.43	0.26	10.68	0.37	2.41	0.12	3.61	0.24
55.05	2.34	13.91	0.69	3.37	0.25	1.75	0.09	7.57	0.27	10.99	0.38	2.55	0.13	3.49	0.23
56.27	2.39	14.06	0.70	3.51	0.25	1.73	0.09	7.46	0.26	11.09	0.38	2.51	0.13	3.44	0.23
57.31	2.43	14.46	0.72	3.59	0.26	1.74	0.09	7.53	0.27	11.26	0.39	2.61	0.13	3.65	0.24
55.93	2.38	14.00	0.70	3.45	0.25	1.75	0.09	7.54	0.27	11.16	0.38	2.56	0.13	3.55	0.23
56.68	2.41	14.22	0.71	3.55	0.26	1.68	0.08	7.47	0.26	10.87	0.37	2.60	0.13	3.56	0.23
57.44	2.44	14.50	0.72	3.60	0.26	1.71	0.09	7.53	0.27	10.88	0.37	2.49	0.12	3.60	0.23
54.80	2.33	13.67	0.68	3.40	0.25	1.79	0.09	7.83	0.27	10.59	0.37	2.51	0.13	3.43	0.23
56.06	2.38	14.14	0.71	3.52	0.26	1.74	0.09	7.60	0.27	11.17	0.38	2.70	0.13	3.51	0.23
56.41	2.40	14.31	0.71	3.51	0.25	1.64	0.08	7.56	0.27	11.04	0.38	2.52	0.13	3.51	0.23
55.93	2.38	14.08	0.70	3.43	0.25	1.71	0.09	7.53	0.27	11.27	0.39	2.56	0.13	3.53	0.23
56.03	2.38	14.04	0.70	3.44	0.25	1.65	0.08	7.52	0.27	10.58	0.36	2.38	0.12	3.52	0.23
56.49	2.40	14.28	0.71	3.51	0.25	1.65	0.08	7.43	0.26	10.89	0.37	2.36	0.12	3.59	0.23
54.34	2.31	13.72	0.69	3.30	0.24	1.74	0.09	7.67	0.27	10.83	0.37	2.56	0.13	3.41	0.22
57.44	2.44	14.31	0.71	3.56	0.26	1.62	0.08	7.26	0.26	10.67	0.37	2.61	0.13	3.51	0.23
55.81	2.37	14.15	0.71	3.55	0.26	1.71	0.09	7.68	0.27	11.04	0.38	2.41	0.12	3.53	0.23
57.08	2.42	14.13	0.70	3.61	0.26	1.65	0.08	7.37	0.26	10.90	0.37	2.42	0.12	3.56	0.23
56.04	2.38	14.01	0.70	3.52	0.26	1.87	0.09	8.00	0.28	10.79	0.37	2.65	0.13	3.50	0.23
54.34	2.31	13.81	0.69	3.36	0.25	1.75	0.09	7.66	0.27	11.12	0.38	2.56	0.13	3.40	0.22
56.23	2.39	14.08	0.70	3.47	0.25	1.79	0.09	7.53	0.27	11.29	0.39	2.45	0.12	3.51	0.23
56.47	2.40	14.19	0.71	3.59	0.26	1.80	0.09	7.67	0.27	11.09	0.38	2.48	0.12	3.50	0.23
55.06	2.34	13.74	0.69	3.33	0.24	1.82	0.09	7.80	0.27	10.83	0.37	2.49	0.12	3.48	0.23
52.80	2.25	13.36	0.67	3.27	0.24	1.81	0.09	7.81	0.27	10.73	0.37	2.43	0.12	3.35	0.22
56.47	2.40	14.23	0.71	3.53	0.26	1.73	0.09	7.37	0.26	11.09	0.38	2.48	0.12	3.58	0.23
54.89	2.33	13.80	0.69	3.38	0.25	1.69	0.08	7.49	0.26	10.94	0.38	2.53	0.13	3.42	0.22
55.79	2.37	13.97	0.70	3.43	0.25	1.76	0.09	7.51	0.26	11.11	0.38	2.54	0.13	3.58	0.23
57.01	2.42	14.34	0.71	3.57	0.26	1.72	0.09	7.71	0.27	10.60	0.37	2.64	0.13	3.64	0.24
56.03	2.38	14.08	0.70	3.52	0.26	1.71	0.09	7.67	0.27	11.24	0.39	2.47	0.12	3.48	0.23
56.31	2.39	14.00	0.70	3.45	0.25	1.65	0.08	7.48	0.26	11.03	0.38	2.43	0.12	3.60	0.23
56.42	2.40	14.10	0.70	3.51	0.25	1.69	0.08	7.55	0.27	10.82	0.37	2.54	0.13	3.52	0.23
56.72	2.41	14.29	0.71	3.58	0.26	1.71	0.09	7.39	0.26	10.77	0.37	2.52	0.13	3.54	0.23
55.87	2.37	13.95	0.70	3.48	0.25	1.65	0.08	7.54	0.27	10.94	0.38	2.34	0.12	3.52	0.23
55.47	2.36	13.90	0.69	3.50	0.25	1.71	0.09	7.58	0.27	11.12	0.38	2.43	0.12	3.49	0.23
56.83	2.41	14.30	0.71	3.62	0.26	1.71	0.09	7.40	0.26	11.21	0.38	2.43	0.12	3.55	0.23
55.38	2.35	14.07	0.70	3.44	0.25	1.63	0.08	7.41	0.26	10.59	0.37	2.40	0.12	3.53	0.23
56.15	2.39	14.06	0.70	3.55	0.26	1.70	0.09	7.33	0.26	11.29	0.39	2.46	0.12	3.54	0.23
55.43	2.36	13.88	0.69	3.40	0.25	1.70	0.09	7.70	0.27	10.83	0.37	2.54	0.13	3.47	0.23
55.66	2.37	14.06	0.70	3.39	0.25	1.73	0.09	7.64	0.27	10.93	0.38	2.73	0.13	3.55	0.23
55.28	2.35	13.85	0.69	3.47	0.25	1.78	0.09	7.69	0.27	10.78	0.37	2.55	0.13	3.42	0.23
56.21	2.39	14.04	0.70	3.51	0.25	1.74	0.09	7.74	0.27	11.12	0.38	2.57	0.13	3.52	0.23
56.79	2.41	14.28	0.71	3.39	0.25	1.70	0.09	7.57	0.27	10.72	0.37	2.46	0.12	3.52	0.23
56.12	2.38	14.08	0.70	3.43	0.25	1.77	0.09	7.46	0.26	10.71	0.37	2.56	0.13	3.54	0.23
56.05	2.38	14.12	0.70	3.48	0.25	1.72	0.09	7.39	0.26	10.92	0.38	2.52	0.13	3.58	0.23

54.95	2.34	13.88	0.69	3.43	0.25	1.76	0.09	7.56	0.27	11.32	0.39	2.43	0.12	3.44	0.23
55.93	2.38	13.95	0.70	3.43	0.25	1.74	0.09	7.58	0.27	10.71	0.37	2.47	0.12	3.42	0.22
56.63	2.41	14.33	0.71	3.53	0.26	1.74	0.09	7.69	0.27	10.86	0.37	2.48	0.12	3.52	0.23
56.32	2.39	14.12	0.70	3.51	0.25	1.76	0.09	7.70	0.27	11.07	0.38	2.57	0.13	3.49	0.23

Table E.2: Volatilization of Na and K compositions in BCR-1 based on EDS raster diameters. Raster diameters of < 1 μm are "spot" analyses. Raster diameters were measured after the analyses using ImageJ [86]. Data are plotted in Figure 4.5.

Raster diameter (μm)	Na (wt.%)	1σ	K (wt.%)	1σ
<1	1.78	0.14	1.31	0.07
<1	1.76	0.14	1.27	0.07
<1	1.76	0.14	1.28	0.07
<1	1.80	0.14	1.32	0.07
3.25	2.49	0.18	1.47	0.07
2.97	2.43	0.18	1.46	0.07
3.04	2.45	0.18	1.42	0.07
2.83	2.46	0.18	1.43	0.07
8.34	2.46	0.18	1.49	0.07
9.83	2.51	0.18	1.45	0.07
8.77	2.46	0.18	1.47	0.07
10.96	2.47	0.18	1.47	0.07
13.08	2.53	0.18	1.43	0.07
13.22	2.49	0.18	1.48	0.07
13.15	2.50	0.18	1.45	0.07
13.01	2.51	0.18	1.49	0.07
17.68	2.57	0.19	1.44	0.07
16.48	2.48	0.18	1.43	0.07
18.17	2.51	0.18	1.47	0.07
18.88	2.47	0.18	1.45	0.07

Appendix F

U isotope Analyses

F.1 Standards Measurements

Table F.1: $^{235}U/^{238}U$ measurements of U-bearing glass standards used to correct the analytical data for fractionation and instrumental bias. These data were used to generate Figure 5.6. The rows in bold refer to the mean of the individual standards measurements for that analytical campaign. Due to possible contamination during the fabrication process, the ICP-MS measured values of the $^{235}U/^{238}U$ ratio are used instead of the certified values of the U dopant. The samples analyzed during each of these analytical campaigns is listed in Table 5.1. The operating conditions for each of the analytical campaigns is listed in Table 5.4.

Analytical Session	SIMS Instrument	Standard	$^{235}U/^{238}U$	2σ	ICP-MS $^{235}U/^{238}U$	ICP-MS 2σ	Fractionation Factor	Fractionation Factor 2σ
Jan 2017	**NanoSIMS**	**CAS-53-500**	**1.126**	**0.006**	**1.125**	**0.0004**	**0.999**	**0.005**
			1.136	0.008				
			1.133	0.008				
			1.127	0.008				
			1.123	0.007				
			1.137	0.009				
			1.125	0.013				
			1.105	0.012				
			1.127	0.005				
			1.125	0.004				

Analytical Session	SIMS Instrument	Standard	$^{235}U/^{238}U$	2σ	ICP-MS $^{235}U/^{238}U$	ICP-MS 2σ	Fractionation Factor	Fractionation Factor 2σ
Jan 2017	**NanoSIMS**	**U500**	**0.958**	**0.005**	**0.962**	**0.001**	**1.004**	**0.005**
			0.964	0.004				
			0.962	0.003				
			0.958	0.003				
			0.963	0.003				
			0.961	0.004				
			0.945	0.006				
			0.955	0.011				

Analytical Session	SIMS Instrument	Standard	$^{235}U/^{238}U$	2σ	ICP-MS $^{235}U/^{238}U$	ICP-MS 2σ	Fractionation Factor	Fractionation Factor 2σ
Aug 2016	**NanoSIMS**	**U500**	**0.944**	**0.006**	**0.962**	**0.001**	**1.019**	**0.006**
			0.946	0.017				
			0.951	0.020				
			0.939	0.021				
			0.954	0.019				

			0.945	0.019				
			0.949	0.016				
			0.931	0.021				
			0.934	0.019				
			0.932	0.020				
			0.936	0.020				
			0.962	0.022				
			0.957	0.021				
			0.935	0.021				

Analytical Session	SIMS Instrument	Standard	$^{235}U/^{238}U$	2σ	ICP-MS $^{235}U/^{238}U$	ICP-MS 2σ	Fractionation Factor	Fractionation Factor 2σ
April 2015	**IMS-1280**	**U500**	**0.976**	**0.002**	**0.962**	**0.001**	**0.986**	**0.002**
			0.974	0.002				
			0.976	0.002				
			0.976	0.002				
			0.978	0.002				
			0.976	0.002				
			0.972	0.002				
			0.978	0.003				

Analytical Session	SIMS Instrument	Standard	$^{235}U/^{238}U$	2σ	ICP-MS $^{235}U/^{238}U$	ICP-MS 2σ	Fractionation Factor	Fractionation Factor 2σ
March 2015	**IMS-1280**	**U500**	**0.973**	**0.001**	**0.962**	**0.001**	**0.988**	**0.001**
			0.973	0.003				
			0.972	0.003				
			0.974	0.003				
			0.972	0.003				
			0.971	0.003				
			0.972	0.003				
			0.973	0.002				
			0.973	0.003				
			0.973	0.002				
			0.974	0.003				
			0.976	0.002				
			0.974	0.003				
			0.974	0.002				
			0.974	0.002				
			0.972	0.002				
			0.973	0.003				
			0.976	0.003				
			0.972	0.003				
			0.971	0.003				
			0.974	0.003				
			0.975	0.003				
			0.974	0.003				
			0.973	0.003				
			0.974	0.003				
			0.973	0.003				
			0.973	0.003				
			0.971	0.003				
			0.976	0.003				
			0.970	0.003				

Analytical Session	SIMS Instrument	Standard	$^{235}U/^{238}U$	2σ	ICP-MS $^{235}U/^{238}U$	ICP-MS 2σ	Fractionation Factor	Fractionation Factor 2σ
2012	**IMS-3f**	**U500**	**0.966**	**0.003**	**0.962**	**0.001**	0.**996**	**0.003**
			0.974	0.014				
			0.955	0.011				
			0.965	0.008				
			0.961	0.010				
			0.967	0.008				

0.955	0.009
0.968	0.011
0.960	0.014
0.975	0.009
0.970	0.011
0.968	0.009
0.970	0.012
0.968	0.007
0.969	0.014
0.971	0.017
0.959	0.013
0.974	0.013
0.965	0.019
0.957	0.011
0.956	0.023
0.979	0.012
0.969	0.007
0.955	0.009

F.2 $^{235}U/^{238}U$ Measurements

Table F.2: Fractionation-corrected SIMS measurements of the $^{235}U/^{238}U$ ratios in fallout. These data are used to generate Figures 5.17, 5.18, 5.20, 5.22, 5.24, 5.26 and Tables 5.9, 5.10, 5.11 in Chapter 5. "Sampled interface?" refers to whether the SIMS analytical crater sampled the agglomerate, the interface, and an insignificant portion of the host. These measurements are always included when calculating the agglomerates mean or median U isotope composition. "Sampled host?" refers to whether the SIMS analytical crater sampled the agglomerate, the interface, and significantly sampled the host. They are only included when calculated agglomerate compositions when noted (such as in Table 5.10). Both measurements are shown as blue triangles in Figure 5.24.

Sample	Object	Location	$^{235}U/^{238}U$	2σ	Sampled interface?	Sampled host?	Analytical Campaign	Run Name
AA.B	Agglomerate	B1	6.358	2.551	-	-	Weisz (2016)	N/A
AA.B	Agglomerate	B2	4.560	1.375	-	-	Weisz (2016)	N/A
AE.C	Host	Host	5.729	0.679	-	-	Weisz (2016)	N/A
AE.C	Agglomerate	C1	6.557	0.882	-	-	Weisz (2016)	N/A
AE.C	Agglomerate	C2	6.230	1.510	-	-	Weisz (2016)	N/A
AG.D	Host	Host	6.273	1.249	-	-	Weisz (2016)	N/A
AG.D	Agglomerate	D2	6.120	1.598	-	-	Weisz (2016)	N/A
AH.E	Host	Host	7.683	3.588	-	-	Weisz (2016)	N/A
AH.E	Agglomerate	E1	7.417	1.171	-	-	Weisz (2016)	N/A
FLD10	Host	Host	6.603	0.183	-	-	NanoSIMS (2017)	FLD10-NS17-1
FLD10	Host	Host	7.238	0.236	-	-	NanoSIMS (2017)	FLD10-NS17-2
FLD10	Host	Host	6.554	0.178	-	-	NanoSIMS (2017)	FLD10-NS17-3
FLD10	Host	Host	7.691	0.218	-	-	NanoSIMS (2017)	FLD10-NS17-4
FLD10	Host	Host	6.088	0.170	-	-	NanoSIMS (2017)	FLD10-NS17-5
FLD10	Host	Host	7.650	0.248	-	-	NanoSIMS (2017)	FLD10-NS17-9
FLD10	Host	Host	5.301	0.138	-	-	NanoSIMS (2017)	FLD10-NS17-10
FLD10	Host	Host	7.143	0.163	-	-	NanoSIMS (2017)	FLD10-NS17-11
FLD10	Host	Host	7.539	0.198	-	-	NanoSIMS (2017)	FLD10-NS17-12
FLD10	Host	Host	7.983	0.166	-	-	NanoSIMS (2017)	FLD10-NS17-13
FLD10	Agglomerate	FLD10.L	5.902	0.136	-	-	NanoSIMS (2017)	FLD10-NS17-6
FLD10	Agglomerate	FLD10.L	7.509	0.207	-	-	NanoSIMS (2017)	FLD10-NS17-7
FLD10	Agglomerate	FLD10.L	8.859	0.302	X	X	NanoSIMS (2017)	FLD10-NS17-8
FLD14	Host	Host	3.718	0.097	-	-	NanoSIMS (2017)	FLD14-NS17-3
FLD14	Host	Host	4.042	0.121	-	-	NanoSIMS (2017)	FLD14-NS17-4
FLD14	Host	Host	4.577	0.104	-	-	NanoSIMS (2017)	FLD14-NS17-5
FLD14	Host	Host	4.553	0.128	-	-	NanoSIMS (2017)	FLD14-NS17-6

FLD14	Host	Host	4.633	0.112	-	-	NanoSIMS (2017)	FLD14-NS17-7
FLD14	Host	Host	5.082	0.124	-	-	NanoSIMS (2017)	FLD14-NS17-8
FLD14	Host	Host	5.307	0.132	-	-	NanoSIMS (2017)	FLD14-NS17-9
FLD14	Host	Host	4.431	0.141	-	-	NanoSIMS (2017)	FLD14-NS17-11
FLD14	Host	Host	4.935	0.141	-	-	NanoSIMS (2017)	FLD14-NS17-12
FLD14	Host	Host	5.258	0.128	-	-	NanoSIMS (2017)	FLD14-NS17-13
FLD14	Host	Host	5.292	0.129	-	-	NanoSIMS (2017)	FLD14-NS17-14
FLD14	Agglomerate	FLD14.L	3.683	0.086	-	-	NanoSIMS (2017)	FLD14-NS17-1
FLD14	Agglomerate	FLD14.L	4.019	0.108	X	-	NanoSIMS (2017)	FLD14-NS17-2
FLD14	Agglomerate	FLD14.1	4.411	0.100	X	-	NanoSIMS (2017)	FLD14-NS17-10
FLD15	Host	Host	3.280	0.032	-	-	IMS-1280 (2015)	FLD15-IMS1280-1
FLD15	Host	Host	3.591	0.036	-	-	IMS-1280 (2015)	FLD15-IMS1280-2
FLD15	Host	Host	3.784	0.038	-	-	IMS-1280 (2015)	FLD15-IMS1280-3
FLD15	Host	Host	3.322	0.032	-	-	IMS-1280 (2015)	FLD15-IMS1280-4
FLD15	Host	Host	3.586	0.040	-	-	IMS-1280 (2015)	FLD15-IMS1280-5
FLD15	Host	Host	3.388	0.035	-	-	IMS-1280 (2015)	FLD15-IMS1280-6
FLD15	Host	Host	3.697	0.033	-	-	IMS-1280 (2015)	FLD15-IMS1280-7
FLD15	Host	Host	3.792	0.036	-	-	IMS-1280 (2015)	FLD15-IMS1280-8
FLD15	Host	Host	2.848	0.024	-	-	IMS-1280 (2015)	FLD15-IMS1280-9
FLD15	Host	Host	4.165	0.035	-	-	IMS-1280 (2015)	FLD15-IMS1280-10
FLD15	Host	Host	3.864	0.033	-	-	IMS-1280 (2015)	FLD15-IMS1280-11
FLD15	Host	Host	3.256	0.033	-	-	IMS-1280 (2015)	FLD15-IMS1280-12
FLD15	Host	Host	3.189	0.026	-	-	IMS-1280 (2015)	FLD15-IMS1280-13
FLD15	Host	Host	3.527	0.029	-	-	IMS-1280 (2015)	FLD15-IMS1280-14
FLD15	Host	Host	4.417	0.043	-	-	IMS-1280 (2015)	FLD15-IMS1280-15
FLD16	Host	Host	7.271	0.071	-	-	IMS-1280 (2015)	FLD16-IMS1280-1
FLD16	Host	Host	6.603	0.055	-	-	IMS-1280 (2015)	FLD16-IMS1280-2
FLD16	Host	Host	5.866	0.049	-	-	IMS-1280 (2015)	FLD16-IMS1280-3
FLD16	Host	Host	5.656	0.054	-	-	IMS-1280 (2015)	FLD16-IMS1280-4
FLD16	Host	Host	6.398	0.061	-	-	IMS-1280 (2015)	FLD16-IMS1280-5
FLD16	Host	Host	1.413	0.008	-	-	IMS-1280 (2015)	FLD16-IMS1280-6
FLD16	Host	Host	8.697	0.089	-	-	IMS-1280 (2015)	FLD16-IMS1280-7
FLD16	Host	Host	6.061	0.060	-	-	IMS-1280 (2015)	FLD16-IMS1280-8
FLD16	Host	Host	1.580	0.008	-	-	IMS-1280 (2015)	FLD16-IMS1280-9
FLD16	Host	Host	5.609	0.059	-	-	IMS-1280 (2015)	FLD16-IMS1280-10
FLD16	Host	Host	2.356	0.034	-	-	IMS-1280 (2015)	FLD16-IMS1280-11
FLD16	Host	Host	6.218	0.067	-	-	IMS-1280 (2015)	FLD16-IMS1280-12
FLD16	Host	Host	4.823	0.051	-	-	IMS-1280 (2015)	FLD16-IMS1280-13
FLD16	Host	Host	7.103	0.084	-	-	IMS-1280 (2015)	FLD16-IMS1280-14
FLD16	Host	Host	6.057	0.059	-	-	IMS-1280 (2015)	FLD16-IMS1280-15
FLD16	Host	Host	5.464	0.046	-	-	IMS-1280 (2015)	FLD16-IMS1280-16
FLD16	Host	Host	5.864	0.048	-	-	IMS-1280 (2015)	FLD16-IMS1280-17
FLD16	Host	Host	5.300	0.046	-	-	IMS-1280 (2015)	FLD16-IMS1280-18
FLD16	Host	Host	5.518	0.051	-	-	IMS-1280 (2015)	FLD16-IMS1280-19
FLD16	Host	Host	5.357	0.044	-	-	IMS-1280 (2015)	FLD16-IMS1280-20
FLD16	Host	Host	4.173	0.035	-	-	IMS-1280 (2015)	FLD16-IMS1280-21
FLD16	Host	Host	4.047	0.033	-	-	IMS-1280 (2015)	FLD16-IMS1280-22
FLD16	Host	Host	6.339	0.065	-	-	IMS-1280 (2015)	FLD16-IMS1280-23
FLD16	Host	Host	5.506	0.052	-	-	IMS-1280 (2015)	FLD16-IMS1280-24
FLD16	Host	Host	6.888	0.079	-	-	IMS-1280 (2015)	FLD16-IMS1280-25
FLD16	Host	Host	6.358	0.070	-	-	IMS-1280 (2015)	FLD16-IMS1280-26
FLD16	Host	Host	5.290	0.055	-	-	IMS-1280 (2015)	FLD16-IMS1280-27
FLD16	Host	Host	5.794	0.065	-	-	IMS-1280 (2015)	FLD16-IMS1280-28
FLD16	Host	Host	5.296	0.051	-	-	IMS-1280 (2015)	FLD16-IMS1280-29
FLD16	Host	Host	4.726	0.061	-	-	IMS-1280 (2015)	FLD16-IMS1280-30
FLD16	Host	Host	5.307	0.053	-	-	IMS-1280 (2015)	FLD16-IMS1280-31
FLD16	Host	Host	6.390	0.090	-	-	IMS-1280 (2015)	FLD16-IMS1280-32
FLD16	Host	Host	7.415	0.077	-	-	IMS-1280 (2015)	FLD16-IMS1280-33
FLD16	Host	Host	6.095	0.075	-	-	IMS-1280 (2015)	FLD16-IMS1280-34
FLD16	Host	Host	5.543	0.041	-	-	IMS-1280 (2015)	FLD16-IMS1280-35
FLD16	Host	Host	5.108	0.057	-	-	IMS-1280 (2015)	FLD16-IMS1280-36
FLD17	Host	Host	4.592	0.092	-	-	NanoSIMS (2017)	FLD17-NS17-1

FLD17	Host	Host	4.854	0.183	-	-	NanoSIMS (2017)	FLD17-NS17-5
FLD17	Agglomerate	FLD17.int.2	3.913	0.089	-	-	NanoSIMS (2017)	FLD17-NS17-2
FLD17	Agglomerate	FLD17.int.2	4.180	0.113	X	X	NanoSIMS (2017)	FLD17-NS17-3
FLD17	Agglomerate	FLD17.int.2	5.109	0.126	X	X	NanoSIMS (2017)	FLD17-NS17-4
FLD18	Host	Host	4.833	0.039	-	-	IMS-1280 (2015)	FLD18-IMS1280-1
FLD18	Host	Host	4.424	0.041	-	-	IMS-1280 (2015)	FLD18-IMS1280-2
FLD18	Host	Host	4.817	0.039	-	-	IMS-1280 (2015)	FLD18-IMS1280-3
FLD18	Host	Host	3.053	0.029	-	-	IMS-1280 (2015)	FLD18-IMS1280-4
FLD18	Host	Host	4.193	0.039	-	-	IMS-1280 (2015)	FLD18-IMS1280-5
FLD18	Host	Host	4.659	0.037	-	-	IMS-1280 (2015)	FLD18-IMS1280-6
FLD18	Host	Host	4.756	0.040	-	-	IMS-1280 (2015)	FLD18-IMS1280-7
FLD18	Host	Host	4.392	0.036	-	-	IMS-1280 (2015)	FLD18-IMS1280-8
FLD18	Host	Host	4.546	0.036	-	-	IMS-1280 (2015)	FLD18-IMS1280-9
FLD18	Host	Host	4.565	0.037	-	-	IMS-1280 (2015)	FLD18-IMS1280-10
FLD18	Agglomerate	FLD18.1	3.858	0.114	X	-	NanoSIMS (2017)	FLD18-NS17-1
FLD18	Agglomerate	FLD18.2	8.191	0.403	-	-	NanoSIMS (2016)	FLD18-NS16-1
FLD20	Host	Host	2.504	0.025	-	-	IMS-1280 (2015)	FLD20-IMS1280-1
FLD20	Host	Host	5.395	0.049	-	-	IMS-1280 (2015)	FLD20-IMS1280-2
FLD20	Host	Host	3.541	0.030	-	-	IMS-1280 (2015)	FLD20-IMS1280-3
FLD20	Host	Host	4.601	0.042	-	-	IMS-1280 (2015)	FLD20-IMS1280-4
FLD20	Host	Host	4.586	0.036	-	-	IMS-1280 (2015)	FLD20-IMS1280-5
FLD23	Host	Host	4.864	0.460	-	-	NanoSIMS (2016)	FLD23-NS16-16
FLD23	Host	Host	5.087	0.158	-	-	NanoSIMS (2016)	FLD23-NS16-10
FLD23	Host	Host	4.393	0.134	-	-	NanoSIMS (2016)	FLD23-NS16-6
FLD23	Host	Host	4.705	0.138	-	-	NanoSIMS (2016)	FLD23-NS16-9
FLD23	Agglomerate	FLD23.L	3.793	0.082	-	-	NanoSIMS (2017)	FLD23-NS17-1
FLD23	Agglomerate	FLD23.L	4.332	0.110	X	X	NanoSIMS (2017)	FLD23-NS17-2
FLD23	Agglomerate	FLD23.3.1	4.306	0.120	-	-	NanoSIMS (2016)	FLD23-NS16-11
FLD23	Agglomerate	FLD23.3.2	4.666	0.139	-	-	NanoSIMS (2016)	FLD23-NS16-12
FLD23	Agglomerate	FLD23.4.1	4.674	0.152	-	-	NanoSIMS (2016)	FLD23-NS16-13
FLD23	Agglomerate	FLD23.4.2	4.781	0.152	-	-	NanoSIMS (2016)	FLD23-NS16-14
FLD23	Agglomerate	FLD23.5.1	4.326	0.133	-	-	NanoSIMS (2016)	FLD23-NS16-15
FLD23	Agglomerate	FLD23.1.1	4.424	0.127	-	-	NanoSIMS (2016)	FLD23-NS16-1
FLD23	Agglomerate	FLD23.1.2	4.435	0.138	-	-	NanoSIMS (2016)	FLD23-NS16-2
FLD23	Agglomerate	FLD23.1.2	4.426	0.140	-	-	NanoSIMS (2016)	FLD23-NS16-3
FLD23	Agglomerate	FLD23.1.3	4.004	0.119	-	-	NanoSIMS (2016)	FLD23-NS16-4
FLD23	Agglomerate	FLD23.1.3	4.511	0.141	-	-	NanoSIMS (2016)	FLD23-NS16-5
FLD23	Agglomerate	FLD23.2.1	4.315	0.134	-	-	NanoSIMS (2016)	FLD23-NS16-7
FLD23	Agglomerate	FLD23.2.2	4.279	0.135	-	-	NanoSIMS (2016)	FLD23-NS16-8
FLD4.3	Host	Host	7.176	0.311	-	-	NanoSIMS (2017)	FLD43-NS17-5
FLD4.3	Agglomerate	FLD4.3.1	9.872	0.765	X	X	NanoSIMS (2017)	FLD43-NS17-1
FLD4.3	Agglomerate	FLD4.3.2	9.760	0.311	-	-	NanoSIMS (2017)	FLD43-NS17-2
FLD4.3	Agglomerate	FLD4.3.3	10.535	0.326	-	-	NanoSIMS (2017)	FLD43-NS17-3
FLD4.3	Agglomerate	FLD4.3.3	8.498	0.251	X	X	NanoSIMS (2017)	FLD43-NS17-4
FLD4.3	Agglomerate	FLD4.3.5	8.135	0.379	X	X	NanoSIMS (2017)	FLD43-NS17-6
U1A	Host	Host	3.850	0.064	-	-	IMS-1280 (2012)	U1A-LANL-1
U1A	Host	Host	3.084	0.051	-	-	IMS-1280 (2012)	U1A-LANL-2
U1A	Host	Host	3.519	0.074	-	-	IMS-1280 (2012)	U1A-LANL-3
U1B	Unknown	Unknown	6.576	0.129	Unknown	Unknown	IMS-3f (2012)	U1B-LLNL-1
U1B	Unknown	Unknown	7.215	0.151	Unknown	Unknown	IMS-3f (2012)	U1B-LLNL-2
U1B	Unknown	Unknown	7.185	0.166	Unknown	Unknown	IMS-3f (2012)	U1B-LLNL-3
U1B	Unknown	Unknown	7.967	0.119	Unknown	Unknown	IMS-3f (2012)	U1B-LLNL-4
U1B	Unknown	Unknown	7.421	0.134	Unknown	Unknown	IMS-3f (2012)	U1B-LLNL-5
U1B	Unknown	Unknown	7.326	0.110	Unknown	Unknown	IMS-3f (2012)	U1B-LLNL-6
U1B	Unknown	Unknown	7.081	0.095	Unknown	Unknown	IMS-3f (2012)	U1B-LLNL-7
U1B	Unknown	Unknown	7.718	0.107	Unknown	Unknown	IMS-3f (2012)	U1B-LLNL-8
U1B	Unknown	Unknown	8.025	0.104	Unknown	Unknown	IMS-3f (2012)	U1B-LLNL-9
U1B	Unknown	Unknown	6.676	0.083	Unknown	Unknown	IMS-3f (2012)	U1B-LLNL-10
U1B	Unknown	Unknown	6.768	0.098	Unknown	Unknown	IMS-3f (2012)	U1B-LLNL-11
U1B	Unknown	Unknown	6.867	0.091	Unknown	Unknown	IMS-3f (2012)	U1B-LLNL-12
U1B	Unknown	Unknown	6.354	0.049	Unknown	Unknown	IMS-3f (2012)	U1B-LLNL-13
U1B	Unknown	Unknown	7.070	0.127	Unknown	Unknown	IMS-3f (2012)	U1B-LLNL-14

U1B	Unknown	Unknown	6.772	0.152	Unknown	Unknown	IMS-3f (2012)	U1B-LLNL-15
U1B	Unknown	Unknown	6.575	0.119	Unknown	Unknown	IMS-3f (2012)	U1B-LLNL-16
U1B	Unknown	Unknown	7.059	0.146	Unknown	Unknown	IMS-3f (2012)	U1B-LLNL-17
U1B	Unknown	Unknown	11.843	0.219	Unknown	Unknown	IMS-3f (2012)	U1B-LLNL-18
U1B	Unknown	Unknown	8.162	0.133	Unknown	Unknown	IMS-3f (2012)	U1B-LLNL-19
U1B	Host	Host	7.609	0.103	-	-	IMS-1280 (2012)	U1B-LANL-1
U1B	Host	Host	7.339	0.092	-	-	IMS-1280 (2012)	U1B-LANL-2
U1B	Host	Host	6.142	0.081	-	-	IMS-1280 (2012)	U1B-LANL-3
U1B	Host	Host	7.172	0.091	-	-	IMS-1280 (2012)	U1B-LANL-4
U1B	Host	Host	7.264	0.093	-	-	IMS-1280 (2012)	U1B-LANL-5
U1B	Host	Host	8.637	0.120	-	-	IMS-1280 (2012)	U1B-LANL-6
U1B	Host	Host	7.121	0.098	-	-	IMS-1280 (2012)	U1B-LANL-7
U1B	Host	Host	6.284	0.090	-	-	IMS-1280 (2012)	U1B-LANL-8
U1B	Host	Host	7.052	0.244	-	-	IMS-1280 (2012)	U1B-LANL-9
U1B	Host	Host	7.248	0.097	-	-	IMS-1280 (2012)	U1B-LANL-10
U1B	Host	Host	7.451	0.099	-	-	IMS-1280 (2012)	U1B-LANL-11
U1B	Host	Host	6.085	0.106	-	-	IMS-1280 (2012)	U1B-LANL-12
U1B	Agglomerate	U1B.L	8.427	0.222	-	-	NanoSIMS (2017)	U1B-NS17-1
U1B	Agglomerate	U1B.L	8.214	0.269	X	X	NanoSIMS (2017)	U1B-NS17-2
U1B	Agglomerate	U1B.L	8.027	0.417	-	-	NanoSIMS (2016)	U1B-NS16-1
U1B	Agglomerate	U1B.2	6.800	0.412	-	-	NanoSIMS (2016)	U1B-NS16-2
U2	Host	Host	3.372	0.043	-	-	IMS-1280 (2012)	U2-LANL-1
U2	Host	Host	3.841	0.055	-	-	IMS-1280 (2012)	U2-LANL-2
U2	Host	Host	2.178	0.076	-	-	IMS-1280 (2012)	U2-LANL-3
U2	Host	Host	1.220	0.011	-	-	IMS-1280 (2012)	U2-LANL-4
U2	Host	Host	3.187	0.029	-	-	IMS-1280 (2012)	U2-LANL-5
U2	Host	Host	3.086	0.025	-	-	IMS-1280 (2012)	U2-LANL-6
U2	Host	Host	1.576	0.019	-	-	IMS-1280 (2012)	U2-LANL-7
U2	Host	Host	2.595	0.085	-	-	IMS-1280 (2012)	U2-LANL-8
U2	Host	Host	2.953	0.035	-	-	IMS-1280 (2012)	U2-LANL-9
U2	Host	Host	0.607	0.011	-	-	IMS-1280 (2012)	U2-LANL-10
U2	Host	Host	0.838	0.031	-	-	IMS-1280 (2012)	U2-LANL-11
U2	Host	Host	2.341	0.043	-	-	IMS-1280 (2012)	U2-LANL-12
U2	Host	Host	5.716	0.055	-	-	IMS-1280 (2012)	U2-LANL-13
U2	Host	Host	2.631	0.029	-	-	IMS-1280 (2012)	U2-LANL-14
U2	Host	Host	4.599	0.043	-	-	IMS-1280 (2012)	U2-LANL-15
U2	Host	Host	5.006	0.049	-	-	IMS-1280 (2012)	U2-LANL-16
U2	Host	Host	4.295	0.042	-	-	IMS-1280 (2012)	U2-LANL-17
U2	Host	Host	0.044	0.003	-	-	IMS-1280 (2012)	U2-LANL-18
U2	Host	Host	2.767	0.026	-	-	IMS-1280 (2012)	U2-LANL-19
U2	Host	Host	0.076	0.002	-	-	IMS-1280 (2012)	U2-LANL-20
U2	Host	Host	0.110	0.002	-	-	IMS-1280 (2012)	U2-LANL-21
U2	Host	Host	0.165	0.004	-	-	IMS-1280 (2012)	U2-LANL-22
U2	Host	Host	1.232	0.011	-	-	IMS-1280 (2012)	U2-LANL-23
U2	Host	Host	3.887	0.039	-	-	IMS-1280 (2012)	U2-LANL-24
U2	Host	Host	0.745	0.010	-	-	IMS-1280 (2012)	U2-LANL-25
U2	Host	Host	1.164	0.019	-	-	IMS-1280 (2012)	U2-LANL-26
U2	Host	Host	4.447	0.037	-	-	IMS-1280 (2012)	U2-LANL-27
U2	Host	Host	3.008	0.024	-	-	IMS-1280 (2012)	U2-LANL-28
U2	Host	Host	3.344	0.027	-	-	IMS-1280 (2012)	U2-LANL-29
U2	Host	Host	0.192	0.003	-	-	IMS-1280 (2012)	U2-LANL-30
U2	Host	Host	0.301	0.005	-	-	IMS-1280 (2012)	U2-LANL-31
U2	Host	Host	0.052	0.002	-	-	IMS-1280 (2012)	U2-LANL-32
U2	Host	Host	0.034	0.002	-	-	IMS-1280 (2012)	U2-LANL-33
U2	Host	Host	0.126	0.002	-	-	IMS-1280 (2012)	U2-LANL-34
U2	Host	Host	0.288	0.004	-	-	IMS-1280 (2012)	U2-LANL-35
U2	Host	Host	5.133	0.043	-	-	IMS-1280 (2012)	U2-LANL-36
U2	Host	Host	1.039	0.026	-	-	IMS-1280 (2012)	U2-LANL-37
U2	Host	Host	2.340	0.023	-	-	IMS-1280 (2012)	U2-LANL-38
U2	Host	Host	2.390	0.038	-	-	IMS-1280 (2012)	U2-LANL-39
U2	Host	Host	4.474	0.046	-	-	IMS-1280 (2012)	U2-LANL-40
U2	Host	Host	5.132	0.039	-	-	IMS-1280 (2012)	U2-LANL-41

U2	Host	Host	5.225	0.040	-	-	IMS-1280 (2012)	U2-LANL-42
U2	Host	Host	4.962	0.036	-	-	IMS-1280 (2012)	U2-LANL-43
U2	Host	Host	5.972	0.061	-	-	IMS-1280 (2012)	U2-LANL-44
U2	Host	Host	5.420	0.054	-	-	IMS-1280 (2012)	U2-LANL-45
U2	Host	Host	0.913	0.011	-	-	IMS-1280 (2012)	U2-LANL-46
U2	Host	Host	1.389	0.024	-	-	IMS-1280 (2012)	U2-LANL-47
U2	Host	Host	0.234	0.011	-	-	IMS-3f (2012)	U2-LLNL-1
U2	Host	Host	0.315	0.015	-	-	IMS-3f (2012)	U2-LLNL-2
U2	Host	Host	0.350	0.014	-	-	IMS-3f (2012)	U2-LLNL-3
U2	Host	Host	7.410	0.240	-	-	IMS-3f (2012)	U2-LLNL-4
U2	Host	Host	3.760	0.150	-	-	IMS-3f (2012)	U2-LLNL-5
U2	Host	Host	2.850	0.100	-	-	IMS-3f (2012)	U2-LLNL-6
U2	Host	Host	2.830	0.120	-	-	IMS-3f (2012)	U2-LLNL-7
U2	Host	Host	4.130	0.180	-	-	IMS-3f (2012)	U2-LLNL-8
U2	Host	Host	1.470	0.090	-	-	IMS-3f (2012)	U2-LLNL-9
U2	Host	Host	0.110	0.005	-	-	IMS-3f (2012)	U2-LLNL-10
U2	Host	Host	4.710	0.140	-	-	IMS-3f (2012)	U2-LLNL-11
U2	Host	Host	3.740	0.150	-	-	IMS-3f (2012)	U2-LLNL-12
U2	Host	Host	2.120	0.030	-	-	IMS-3f (2012)	U2-LLNL-13
U2	Host	Host	4.690	0.180	-	-	IMS-3f (2012)	U2-LLNL-14
U2	Host	Host	5.010	0.140	-	-	IMS-3f (2012)	U2-LLNL-15
U2	Host	Host	2.710	0.130	-	-	IMS-3f (2012)	U2-LLNL-16
U2	Host	Host	0.020	0.002	-	-	IMS-3f (2012)	U2-LLNL-17
U2	Host	Host	2.810	0.100	-	-	IMS-3f (2012)	U2-LLNL-18
U2	Host	Host	0.200	0.010	-	-	IMS-3f (2012)	U2-LLNL-19
U2	Host	Host	1.010	0.040	-	-	IMS-3f (2012)	U2-LLNL-20
U3	Unknown	Unknown	3.779	0.038	Unknown	Unknown	IMS-1280 (2012)	U3-LANL-12
U3	Unknown	Unknown	4.713	0.064	Unknown	Unknown	IMS-1280 (2012)	U3-LANL-15
U3	Unknown	Unknown	6.780	0.180	Unknown	Unknown	IMS-3f (2012)	U3-LLNL-10
U3	Unknown	Unknown	6.110	0.190	Unknown	Unknown	IMS-3f (2012)	U3-LLNL-13
U3	Unknown	Unknown	4.320	0.140	Unknown	Unknown	IMS-3f (2012)	U3-LLNL-22
U3	Host	Host	3.236	0.076	-	-	IMS-1280 (2012)	U3-LANL-1
U3	Host	Host	2.180	0.034	-	-	IMS-1280 (2012)	U3-LANL-2
U3	Host	Host	3.118	0.039	-	-	IMS-1280 (2012)	U3-LANL-3
U3	Host	Host	3.768	0.047	-	-	IMS-1280 (2012)	U3-LANL-4
U3	Host	Host	3.838	0.043	-	-	IMS-1280 (2012)	U3-LANL-5
U3	Host	Host	3.898	0.048	-	-	IMS-1280 (2012)	U3-LANL-6
U3	Host	Host	3.662	0.029	-	-	IMS-1280 (2012)	U3-LANL-7
U3	Host	Host	1.133	0.012	-	-	IMS-1280 (2012)	U3-LANL-8
U3	Host	Host	2.047	0.020	-	-	IMS-1280 (2012)	U3-LANL-9
U3	Host	Host	2.923	0.026	-	-	IMS-1280 (2012)	U3-LANL-10
U3	Host	Host	4.030	0.040	-	-	IMS-1280 (2012)	U3-LANL-11
U3	Host	Host	3.834	0.042	-	-	IMS-1280 (2012)	U3-LANL-16
U3	Host	Host	2.517	0.029	-	-	IMS-1280 (2012)	U3-LANL-17
U3	Host	Host	3.208	0.033	-	-	IMS-1280 (2012)	U3-LANL-18
U3	Host	Host	4.629	0.046	-	-	IMS-1280 (2012)	U3-LANL-19
U3	Host	Host	4.520	0.052	-	-	IMS-1280 (2012)	U3-LANL-20
U3	Host	Host	1.103	0.019	-	-	IMS-1280 (2012)	U3-LANL-21
U3	Host	Host	0.522	0.008	-	-	IMS-1280 (2012)	U3-LANL-22
U3	Host	Host	4.121	0.042	-	-	IMS-1280 (2012)	U3-LANL-23
U3	Host	Host	4.034	0.039	-	-	IMS-1280 (2012)	U3-LANL-24
U3	Host	Host	5.317	0.054	-	-	IMS-1280 (2012)	U3-LANL-25
U3	Host	Host	6.565	0.058	-	-	IMS-1280 (2012)	U3-LANL-26
U3	Host	Host	5.152	0.053	-	-	IMS-1280 (2012)	U3-LANL-28
U3	Host	Host	5.450	0.110	-	-	IMS-3f (2012)	U3-LLNL-1
U3	Host	Host	4.390	0.120	-	-	IMS-3f (2012)	U3-LLNL-2
U3	Host	Host	5.480	0.110	-	-	IMS-3f (2012)	U3-LLNL-3
U3	Host	Host	4.280	0.100	-	-	IMS-3f (2012)	U3-LLNL-4
U3	Host	Host	3.970	0.110	-	-	IMS-3f (2012)	U3-LLNL-5
U3	Host	Host	1.910	0.080	-	-	IMS-3f (2012)	U3-LLNL-6
U3	Host	Host	3.160	0.090	-	-	IMS-3f (2012)	U3-LLNL-7
U3	Host	Host	4.090	0.100	-	-	IMS-3f (2012)	U3-LLNL-8

U3	Host	Host	4.320	0.100	-	-	IMS-3f (2012)	U3-LLNL-9
U3	Host	Host	4.470	0.120	-	-	IMS-3f (2012)	U3-LLNL-14
U3	Host	Host	3.080	0.060	-	-	IMS-3f (2012)	U3-LLNL-15
U3	Host	Host	0.410	0.030	-	-	IMS-3f (2012)	U3-LLNL-16
U3	Host	Host	1.150	0.030	-	-	IMS-3f (2012)	U3-LLNL-17
U3	Host	Host	0.240	0.010	-	-	IMS-3f (2012)	U3-LLNL-18
U3	Host	Host	0.900	0.060	-	-	IMS-3f (2012)	U3-LLNL-19
U3	Host	Host	2.630	0.080	-	-	IMS-3f (2012)	U3-LLNL-20
U3	Host	Host	3.040	0.080	-	-	IMS-3f (2012)	U3-LLNL-21
U3	Agglomerate	U3.3	4.585	0.045	X	X	IMS-1280 (2012)	U3-LANL-13
U3	Agglomerate	U3.4	5.712	0.073	X	X	IMS-1280 (2012)	U3-LANL-14
U3	Agglomerate	U3.5	4.414	0.053	X	X	IMS-1280 (2012)	U3-LANL-27
U3	Agglomerate	U3.1	4.900	0.110	-	-	IMS-3f (2012)	U3-LLNL-11
U3	Agglomerate	U3.2	4.470	0.110	-	-	IMS-3f (2012)	U3-LLNL-12
U4	Unknown	Unknown	4.708	0.070	Unknown	Unknown	IMS-1280 (2012)	U4-LANL-1
U4	Unknown	Unknown	4.596	0.066	Unknown	Unknown	IMS-1280 (2012)	U4-LANL-2
U4	Unknown	Unknown	4.635	0.063	Unknown	Unknown	IMS-1280 (2012)	U4-LANL-3
U4	Unknown	Unknown	3.935	0.067	Unknown	Unknown	IMS-1280 (2012)	U4-LANL-4
U4	Unknown	Unknown	3.811	0.061	Unknown	Unknown	IMS-1280 (2012)	U4-LANL-5
U4	Unknown	Unknown	3.075	0.038	Unknown	Unknown	IMS-1280 (2012)	U4-LANL-6
U4	Unknown	Unknown	3.218	0.034	Unknown	Unknown	IMS-1280 (2012)	U4-LANL-7
U4	Unknown	Unknown	3.953	0.049	Unknown	Unknown	IMS-1280 (2012)	U4-LANL-8
U4	Unknown	Unknown	4.204	0.052	Unknown	Unknown	IMS-1280 (2012)	U4-LANL-9
U4	Unknown	Unknown	3.869	0.047	Unknown	Unknown	IMS-1280 (2012)	U4-LANL-10
U4	Unknown	Unknown	5.225	0.066	Unknown	Unknown	IMS-1280 (2012)	U4-LANL-11
U4	Unknown	Unknown	4.737	0.068	Unknown	Unknown	IMS-1280 (2012)	U4-LANL-12
U4	Unknown	Unknown	5.237	0.064	Unknown	Unknown	IMS-1280 (2012)	U4-LANL-13
U4	Unknown	Unknown	5.150	0.066	Unknown	Unknown	IMS-1280 (2012)	U4-LANL-14
U4	Unknown	Unknown	5.164	0.070	Unknown	Unknown	IMS-1280 (2012)	U4-LANL-15
U4	Unknown	Unknown	5.344	0.069	Unknown	Unknown	IMS-1280 (2012)	U4-LANL-16
U4	Host	Host	1.900	0.050	-	-	IMS-3f (2012)	U4-LLNL-5
U4	Host	Host	3.920	0.080	-	-	IMS-3f (2012)	U4-LLNL-6
U4	Host	Host	2.960	0.060	-	-	IMS-3f (2012)	U4-LLNL-7
U4	Host	Host	2.940	0.060	-	-	IMS-3f (2012)	U4-LLNL-8
U4	Host	Host	5.100	0.120	-	-	IMS-3f (2012)	U4-LLNL-10
U4	Host	Host	5.430	0.120	-	-	IMS-3f (2012)	U4-LLNL-11
U4	Host	Host	4.670	0.100	-	-	IMS-3f (2012)	U4-LLNL-14
U4	Host	Host	3.050	0.080	-	-	IMS-3f (2012)	U4-LLNL-15
U4	Host	Host	2.460	0.070	-	-	IMS-3f (2012)	U4-LLNL-17
U4	Host	Host	3.310	0.080	-	-	IMS-3f (2012)	U4-LLNL-18
U4	Host	Host	2.110	0.050	-	-	IMS-3f (2012)	U4-LLNL-19
U4	Agglomerate	U4.1	5.890	0.140	-	-	IMS-3f (2012)	U4-LLNL-1
U4	Agglomerate	U4.1	6.240	0.120	-	-	IMS-3f (2012)	U4-LLNL-2
U4	Agglomerate	U4.1	5.710	0.110	-	-	IMS-3f (2012)	U4-LLNL-3
U4	Agglomerate	U4.1	6.090	0.110	-	-	IMS-3f (2012)	U4-LLNL-4
U4	Agglomerate	U4.2	4.320	0.120	-	-	IMS-3f (2012)	U4-LLNL-9
U4	Agglomerate	U4.3	5.860	0.130	-	-	IMS-3f (2012)	U4-LLNL-12
U4	Agglomerate	U4.3	5.160	0.140	-	-	IMS-3f (2012)	U4-LLNL-13
U4	Agglomerate	U4.2	5.850	0.150	-	-	IMS-3f (2012)	U4-LLNL-16

F.3 Minor U Isotope Ratio Measurements

Table F.3: Fractionation-corrected SIMS measurements of the $^{235}U/^{238}U$, $^{234}U/^{238}U$, and $^{236}U/^{238}U$ ratios in fallout. All measurements that included the minor isotopes of U were collected using LANL's IMS-1280 and include a total of 172 measurements, approximately 53% of all measurements collected in this study. While all the measurements below include $^{234}U/^{238}U$, only a subset also include the $^{236}U/^{238}U$ ratio. The three agglomerates for for which the minor the isotope ratio was measured (U3.3, U3.4, and U3.5), were measurements that overlapped the compositional interface and also significantly sampled the host object in addition to the agglomerate.

Sample	Session	Run Name	Location	$^{235}U/^{238}U$	2σ	$^{234}U/^{238}U$	2σ	$^{236}U/^{238}U$	2σ
FLD15	IMS-1280 (2015)	FLD15-IMS1280-1	Host	3.280	0.032	3.69E-02	1.89E-03	-	-
FLD15	IMS-1280 (2015)	FLD15-IMS1280-2	Host	3.591	0.036	3.99E-02	1.80E-03	-	-
FLD15	IMS-1280 (2015)	FLD15-IMS1280-3	Host	3.784	0.038	4.11E-02	1.81E-03	-	-
FLD15	IMS-1280 (2015)	FLD15-IMS1280-4	Host	3.322	0.032	3.71E-02	1.63E-03	-	-
FLD15	IMS-1280 (2015)	FLD15-IMS1280-5	Host	3.586	0.040	3.83E-02	1.80E-03	-	-
FLD15	IMS-1280 (2015)	FLD15-IMS1280-6	Host	3.388	0.035	3.60E-02	1.95E-03	-	-
FLD15	IMS-1280 (2015)	FLD15-IMS1280-7	Host	3.697	0.033	4.03E-02	1.61E-03	-	-
FLD15	IMS-1280 (2015)	FLD15-IMS1280-8	Host	3.792	0.036	4.07E-02	1.61E-03	-	-
FLD15	IMS-1280 (2015)	FLD15-IMS1280-9	Host	2.848	0.024	3.15E-02	1.47E-03	-	-
FLD15	IMS-1280 (2015)	FLD15-IMS1280-10	Host	4.165	0.035	4.45E-02	1.68E-03	-	-
FLD15	IMS-1280 (2015)	FLD15-IMS1280-11	Host	3.864	0.033	4.17E-02	1.56E-03	-	-
FLD15	IMS-1280 (2015)	FLD15-IMS1280-12	Host	3.256	0.033	3.54E-02	1.42E-03	-	-
FLD15	IMS-1280 (2015)	FLD15-IMS1280-13	Host	3.189	0.026	3.35E-02	1.28E-03	-	-
FLD15	IMS-1280 (2015)	FLD15-IMS1280-14	Host	3.527	0.029	3.82E-02	1.38E-03	-	-
FLD15	IMS-1280 (2015)	FLD15-IMS1280-15	Host	4.417	0.043	4.83E-02	1.91E-03	-	-
FLD16	IMS-1280 (2015)	FLD16-IMS1280-1	Host	7.271	0.071	7.99E-02	2.31E-03	-	-
FLD16	IMS-1280 (2015)	FLD16-IMS1280-2	Host	6.603	0.055	7.03E-02	2.21E-03	-	-
FLD16	IMS-1280 (2015)	FLD16-IMS1280-3	Host	5.866	0.049	6.30E-02	1.96E-03	-	-
FLD16	IMS-1280 (2015)	FLD16-IMS1280-4	Host	5.656	0.054	6.11E-02	2.30E-03	-	-
FLD16	IMS-1280 (2015)	FLD16-IMS1280-5	Host	6.398	0.061	6.73E-02	2.37E-03	-	-
FLD16	IMS-1280 (2015)	FLD16-IMS1280-6	Host	1.413	0.008	1.55E-02	5.78E-04	-	-
FLD16	IMS-1280 (2015)	FLD16-IMS1280-7	Host	8.697	0.089	9.25E-02	2.77E-03	-	-
FLD16	IMS-1280 (2015)	FLD16-IMS1280-8	Host	6.061	0.060	6.29E-02	2.32E-03	-	-
FLD16	IMS-1280 (2015)	FLD16-IMS1280-9	Host	1.580	0.008	1.71E-02	4.95E-04	-	-
FLD16	IMS-1280 (2015)	FLD16-IMS1280-10	Host	5.609	0.059	5.97E-02	2.55E-03	-	-
FLD16	IMS-1280 (2015)	FLD16-IMS1280-11	Host	2.356	0.034	2.43E-02	1.91E-03	-	-
FLD16	IMS-1280 (2015)	FLD16-IMS1280-12	Host	6.218	0.067	6.63E-02	2.48E-03	-	-
FLD16	IMS-1280 (2015)	FLD16-IMS1280-13	Host	4.823	0.051	5.25E-02	2.07E-03	-	-
FLD16	IMS-1280 (2015)	FLD16-IMS1280-14	Host	7.103	0.084	7.57E-02	3.04E-03	-	-
FLD16	IMS-1280 (2015)	FLD16-IMS1280-15	Host	6.057	0.059	6.57E-02	2.42E-03	-	-
FLD16	IMS-1280 (2015)	FLD16-IMS1280-16	Host	5.464	0.046	5.95E-02	1.75E-03	-	-
FLD16	IMS-1280 (2015)	FLD16-IMS1280-17	Host	5.864	0.048	6.31E-02	2.27E-03	-	-
FLD16	IMS-1280 (2015)	FLD16-IMS1280-18	Host	5.300	0.046	5.80E-02	1.96E-03	-	-
FLD16	IMS-1280 (2015)	FLD16-IMS1280-19	Host	5.518	0.051	6.05E-02	2.14E-03	-	-
FLD16	IMS-1280 (2015)	FLD16-IMS1280-20	Host	5.357	0.044	5.97E-02	1.99E-03	-	-
FLD16	IMS-1280 (2015)	FLD16-IMS1280-21	Host	4.173	0.035	4.53E-02	1.63E-03	-	-
FLD16	IMS-1280 (2015)	FLD16-IMS1280-22	Host	4.047	0.033	4.45E-02	1.38E-03	-	-
FLD16	IMS-1280 (2015)	FLD16-IMS1280-23	Host	6.339	0.065	7.10E-02	3.03E-03	-	-
FLD16	IMS-1280 (2015)	FLD16-IMS1280-24	Host	5.506	0.052	5.87E-02	2.04E-03	-	-
FLD16	IMS-1280 (2015)	FLD16-IMS1280-25	Host	6.888	0.079	7.80E-02	3.38E-03	-	-

FLD16	IMS-1280 (2015)	FLD16-IMS1280-26	Host	6.358	0.070	6.72E-02	3.07E-03	-	-
FLD16	IMS-1280 (2015)	FLD16-IMS1280-27	Host	5.290	0.055	5.77E-02	3.01E-03	-	-
FLD16	IMS-1280 (2015)	FLD16-IMS1280-28	Host	5.794	0.065	6.24E-02	2.82E-03	-	-
FLD16	IMS-1280 (2015)	FLD16-IMS1280-29	Host	5.296	0.051	5.76E-02	2.36E-03	-	-
FLD16	IMS-1280 (2015)	FLD16-IMS1280-30	Host	4.726	0.061	5.13E-02	2.17E-03	-	-
FLD16	IMS-1280 (2015)	FLD16-IMS1280-31	Host	5.307	0.053	5.70E-02	2.22E-03	-	-
FLD16	IMS-1280 (2015)	FLD16-IMS1280-32	Host	6.390	0.090	7.07E-02	3.54E-03	-	-
FLD16	IMS-1280 (2015)	FLD16-IMS1280-33	Host	7.415	0.077	7.96E-02	2.84E-03	-	-
FLD16	IMS-1280 (2015)	FLD16-IMS1280-34	Host	6.095	0.075	6.76E-02	2.98E-03	-	-
FLD16	IMS-1280 (2015)	FLD16-IMS1280-35	Host	5.543	0.041	6.22E-02	1.71E-03	-	-
FLD16	IMS-1280 (2015)	FLD16-IMS1280-36	Host	5.108	0.057	5.43E-02	2.90E-03	-	-
FLD18	IMS-1280 (2015)	FLD18-IMS1280-1	Host	4.833	0.039	5.02E-02	1.93E-03	-	-
FLD18	IMS-1280 (2015)	FLD18-IMS1280-2	Host	4.424	0.041	4.75E-02	1.96E-03	-	-
FLD18	IMS-1280 (2015)	FLD18-IMS1280-3	Host	4.817	0.039	5.02E-02	1.67E-03	-	-
FLD18	IMS-1280 (2015)	FLD18-IMS1280-4	Host	3.053	0.029	3.30E-02	1.33E-03	-	-
FLD18	IMS-1280 (2015)	FLD18-IMS1280-5	Host	4.193	0.039	4.56E-02	1.81E-03	-	-
FLD18	IMS-1280 (2015)	FLD18-IMS1280-6	Host	4.659	0.037	4.93E-02	1.60E-03	-	-
FLD18	IMS-1280 (2015)	FLD18-IMS1280-7	Host	4.756	0.040	5.02E-02	1.77E-03	-	-
FLD18	IMS-1280 (2015)	FLD18-IMS1280-8	Host	4.392	0.036	4.70E-02	1.61E-03	-	-
FLD18	IMS-1280 (2015)	FLD18-IMS1280-9	Host	4.546	0.036	4.94E-02	2.01E-03	-	-
FLD18	IMS-1280 (2015)	FLD18-IMS1280-10	Host	4.565	0.037	4.96E-02	2.09E-03	-	-
FLD20	IMS-1280 (2015)	FLD20-IMS1280-1	Host	2.504	0.025	2.69E-02	1.16E-03	-	-
FLD20	IMS-1280 (2015)	FLD20-IMS1280-2	Host	5.395	0.049	5.85E-02	1.80E-03	-	-
FLD20	IMS-1280 (2015)	FLD20-IMS1280-3	Host	3.541	0.030	3.74E-02	1.50E-03	-	-
FLD20	IMS-1280 (2015)	FLD20-IMS1280-4	Host	4.601	0.042	5.05E-02	1.80E-03	-	-
FLD20	IMS-1280 (2015)	FLD20-IMS1280-5	Host	4.586	0.036	4.93E-02	1.61E-03	-	-
U1A	IMS-1280 (2012)	U1A-LANL-1	Host	3.850	0.064	4.16E-02	1.79E-03	1.82E-02	1.11E-03
U1A	IMS-1280 (2012)	U1A-LANL-2	Host	3.084	0.051	3.29E-02	1.69E-03	1.54E-02	1.10E-03
U1A	IMS-1280 (2012)	U1A-LANL-3	Host	3.519	0.074	3.84E-02	2.89E-03	1.89E-02	1.51E-03
U1B	IMS-1280 (2012)	U1B-LANL-1	Host	7.609	0.103	8.36E-02	2.50E-03	3.56E-02	1.71E-03
U1B	IMS-1280 (2012)	U1B-LANL-2	Host	7.339	0.092	7.95E-02	2.30E-03	3.48E-02	1.41E-03
U1B	IMS-1280 (2012)	U1B-LANL-3	Host	6.142	0.081	6.74E-02	2.10E-03	3.00E-02	1.31E-03
U1B	IMS-1280 (2012)	U1B-LANL-4	Host	7.172	0.091	7.67E-02	2.49E-03	3.44E-02	1.41E-03
U1B	IMS-1280 (2012)	U1B-LANL-5	Host	7.264	0.093	7.85E-02	2.30E-03	3.57E-02	1.51E-03
U1B	IMS-1280 (2012)	U1B-LANL-6	Host	8.637	0.120	9.40E-02	2.89E-03	4.20E-02	1.72E-03
U1B	IMS-1280 (2012)	U1B-LANL-7	Host	7.121	0.098	7.60E-02	2.30E-03	3.55E-02	1.51E-03
U1B	IMS-1280 (2012)	U1B-LANL-8	Host	6.284	0.090	6.64E-02	2.79E-03	3.00E-02	1.41E-03
U1B	IMS-1280 (2012)	U1B-LANL-9	Host	7.052	0.244	7.92E-02	6.27E-03	3.26E-02	3.21E-03
U1B	IMS-1280 (2012)	U1B-LANL-10	Host	7.248	0.097	7.76E-02	2.89E-03	3.51E-02	1.61E-03
U1B	IMS-1280 (2012)	U1B-LANL-11	Host	7.451	0.099	7.99E-02	2.69E-03	3.59E-02	1.51E-03
U1B	IMS-1280 (2012)	U1B-LANL-12	Host	6.085	0.106	6.49E-02	2.69E-03	2.91E-02	1.51E-03
U2	IMS-1280 (2012)	U2-LANL-1	Host	3.372	0.043	3.60E-02	1.58E-03	1.75E-02	9.54E-04
U2	IMS-1280 (2012)	U2-LANL-2	Host	3.841	0.055	4.16E-02	1.42E-03	1.97E-02	9.15E-04
U2	IMS-1280 (2012)	U2-LANL-3	Host	2.178	0.076	2.39E-02	1.13E-03	1.13E-02	6.11E-04
U2	IMS-1280 (2012)	U2-LANL-4	Host	1.220	0.011	1.31E-02	4.76E-04	6.15E-03	3.30E-04
U2	IMS-1280 (2012)	U2-LANL-5	Host	3.187	0.029	3.46E-02	8.83E-04	1.64E-02	6.85E-04
U2	IMS-1280 (2012)	U2-LANL-6	Host	3.086	0.025	3.36E-02	7.92E-04	1.56E-02	5.61E-04
U2	IMS-1280 (2012)	U2-LANL-7	Host	1.576	0.019	1.74E-02	6.22E-04	7.95E-03	4.07E-04

U2	IMS-1280 (2012)	U2-LANL-8	Host	2.595	0.085	2.82E-02	1.16E-03	1.31E-02	4.56E-04
U2	IMS-1280 (2012)	U2-LANL-9	Host	2.953	0.035	3.18E-02	8.28E-04	1.50E-02	5.29E-04
U2	IMS-1280 (2012)	U2-LANL-10	Host	0.607	0.011	7.13E-03	3.49E-04	3.11E-03	2.56E-04
U2	IMS-1280 (2012)	U2-LANL-11	Host	0.838	0.031	9.50E-03	5.15E-04	4.39E-03	2.73E-04
U2	IMS-1280 (2012)	U2-LANL-12	Host	2.341	0.043	2.56E-02	8.24E-04	1.19E-02	5.55E-04
U2	IMS-1280 (2012)	U2-LANL-13	Host	5.716	0.055	6.25E-02	1.21E-03	2.80E-02	8.03E-04
U2	IMS-1280 (2012)	U2-LANL-14	Host	2.631	0.029	2.89E-02	9.20E-04	1.30E-02	6.97E-04
U2	IMS-1280 (2012)	U2-LANL-15	Host	4.599	0.043	4.88E-02	1.06E-03	2.23E-02	7.01E-04
U2	IMS-1280 (2012)	U2-LANL-16	Host	5.006	0.049	5.44E-02	1.32E-03	2.46E-02	7.41E-04
U2	IMS-1280 (2012)	U2-LANL-17	Host	4.295	0.042	4.68E-02	1.18E-03	2.11E-02	7.73E-04
U2	IMS-1280 (2012)	U2-LANL-18	Host	0.044	0.003	5.47E-04	1.44E-04	2.14E-04	9.07E-05
U2	IMS-1280 (2012)	U2-LANL-19	Host	2.767	0.026	2.97E-02	6.57E-04	1.33E-02	4.32E-04
U2	IMS-1280 (2012)	U2-LANL-20	Host	0.076	0.002	8.09E-04	1.60E-04	3.81E-04	1.04E-04
U2	IMS-1280 (2012)	U2-LANL-21	Host	0.110	0.002	1.32E-03	1.49E-04	5.58E-04	9.34E-05
U2	IMS-1280 (2012)	U2-LANL-22	Host	0.165	0.004	1.71E-03	1.80E-04	8.03E-04	1.29E-04
U2	IMS-1280 (2012)	U2-LANL-23	Host	1.232	0.011	1.29E-02	4.73E-04	6.24E-03	3.52E-04
U2	IMS-1280 (2012)	U2-LANL-24	Host	3.887	0.039	4.27E-02	1.22E-03	1.93E-02	7.64E-04
U2	IMS-1280 (2012)	U2-LANL-25	Host	0.745	0.010	7.83E-03	3.95E-04	3.61E-03	2.66E-04
U2	IMS-1280 (2012)	U2-LANL-26	Host	1.164	0.019	1.26E-02	6.42E-04	5.47E-03	3.85E-04
U2	IMS-1280 (2012)	U2-LANL-27	Host	4.447	0.037	4.79E-02	1.08E-03	2.12E-02	8.21E-04
U2	IMS-1280 (2012)	U2-LANL-28	Host	3.008	0.024	3.28E-02	7.94E-04	1.46E-02	6.59E-04
U2	IMS-1280 (2012)	U2-LANL-29	Host	3.344	0.027	3.60E-02	8.88E-04	1.65E-02	5.74E-04
U2	IMS-1280 (2012)	U2-LANL-30	Host	0.192	0.003	2.02E-03	1.84E-04	9.79E-04	1.27E-04
U2	IMS-1280 (2012)	U2-LANL-31	Host	0.301	0.005	3.32E-03	2.52E-04	1.58E-03	1.64E-04
U2	IMS-1280 (2012)	U2-LANL-32	Host	0.052	0.002	5.17E-04	1.21E-04	2.21E-04	8.15E-05
U2	IMS-1280 (2012)	U2-LANL-33	Host	0.034	0.002	3.44E-04	7.71E-05	1.70E-04	4.85E-05
U2	IMS-1280 (2012)	U2-LANL-34	Host	0.126	0.002	1.31E-03	1.16E-04	6.08E-04	7.37E-05
U2	IMS-1280 (2012)	U2-LANL-35	Host	0.288	0.004	2.93E-03	2.18E-04	1.46E-03	1.41E-04
U2	IMS-1280 (2012)	U2-LANL-36	Host	5.133	0.043	5.53E-02	1.17E-03	2.48E-02	8.21E-04
U2	IMS-1280 (2012)	U2-LANL-37	Host	1.039	0.026	1.10E-02	4.10E-04	4.83E-03	3.35E-04
U2	IMS-1280 (2012)	U2-LANL-38	Host	2.340	0.023	2.56E-02	7.10E-04	1.11E-02	4.41E-04
U2	IMS-1280 (2012)	U2-LANL-39	Host	2.390	0.038	2.53E-02	7.91E-04	1.17E-02	4.96E-04
U2	IMS-1280 (2012)	U2-LANL-40	Host	4.474	0.046	4.76E-02	1.04E-03	2.15E-02	6.65E-04
U2	IMS-1280 (2012)	U2-LANL-41	Host	5.132	0.039	5.46E-02	1.10E-03	2.39E-02	6.92E-04
U2	IMS-1280 (2012)	U2-LANL-42	Host	5.225	0.040	5.66E-02	1.30E-03	2.50E-02	7.65E-04
U2	IMS-1280 (2012)	U2-LANL-43	Host	4.962	0.036	5.32E-02	9.53E-04	2.35E-02	6.26E-04
U2	IMS-1280 (2012)	U2-LANL-44	Host	5.972	0.061	6.47E-02	1.62E-03	2.88E-02	1.11E-03
U2	IMS-1280 (2012)	U2-LANL-45	Host	5.420	0.054	5.86E-02	1.49E-03	2.61E-02	1.12E-03
U2	IMS-1280 (2012)	U2-LANL-46	Host	0.913	0.011	9.85E-03	4.17E-04	4.38E-03	3.17E-04
U2	IMS-1280 (2012)	U2-LANL-47	Host	1.389	0.024	1.63E-02	6.56E-04	7.01E-03	4.34E-04
U3	IMS-1280 (2012)	U3-LANL-12	Unknown	3.779	0.038	3.99E-02	1.16E-03	1.79E-02	7.61E-04
U3	IMS-1280 (2012)	U3-LANL-15	Unknown	4.713	0.064	5.01E-02	1.57E-03	2.29E-02	1.03E-03
U3	IMS-1280 (2012)	U3-LANL-1	Host	3.236	0.076	3.43E-02	2.27E-03	1.58E-02	1.49E-03
U3	IMS-1280 (2012)	U3-LANL-2	Host	2.180	0.034	2.42E-02	1.16E-03	1.10E-02	8.17E-04
U3	IMS-1280 (2012)	U3-LANL-3	Host	3.118	0.039	3.37E-02	1.24E-03	1.44E-02	8.13E-04
U3	IMS-1280 (2012)	U3-LANL-4	Host	3.768	0.047	4.03E-02	1.34E-03	1.77E-02	9.29E-04
U3	IMS-1280 (2012)	U3-LANL-5	Host	3.838	0.043	4.23E-02	1.45E-03	1.81E-02	9.81E-04
U3	IMS-1280 (2012)	U3-LANL-6	Host	3.898	0.048	4.25E-02	1.52E-03	1.96E-02	8.63E-04

U3	IMS-1280 (2012)	U3-LANL-7	Host	3.662	0.029	4.01E-02	9.12E-04	1.78E-02	6.23E-04
U3	IMS-1280 (2012)	U3-LANL-8	Host	1.133	0.012	1.27E-02	5.51E-04	5.46E-03	3.76E-04
U3	IMS-1280 (2012)	U3-LANL-9	Host	2.047	0.020	2.21E-02	7.18E-04	1.00E-02	4.56E-04
U3	IMS-1280 (2012)	U3-LANL-10	Host	2.923	0.026	3.16E-02	8.03E-04	1.41E-02	5.28E-04
U3	IMS-1280 (2012)	U3-LANL-11	Host	4.030	0.040	4.30E-02	1.01E-03	1.97E-02	7.01E-04
U3	IMS-1280 (2012)	U3-LANL-16	Host	3.834	0.042	4.13E-02	1.56E-03	1.85E-02	8.45E-04
U3	IMS-1280 (2012)	U3-LANL-17	Host	2.517	0.029	2.71E-02	9.44E-04	1.27E-02	6.35E-04
U3	IMS-1280 (2012)	U3-LANL-18	Host	3.208	0.033	3.44E-02	1.07E-03	1.53E-02	7.06E-04
U3	IMS-1280 (2012)	U3-LANL-19	Host	4.629	0.046	5.06E-02	1.46E-03	2.31E-02	8.73E-04
U3	IMS-1280 (2012)	U3-LANL-20	Host	4.520	0.052	4.83E-02	1.35E-03	2.23E-02	8.82E-04
U3	IMS-1280 (2012)	U3-LANL-21	Host	1.103	0.019	1.18E-02	6.43E-04	5.36E-03	4.11E-04
U3	IMS-1280 (2012)	U3-LANL-22	Host	0.522	0.008	5.51E-03	3.91E-04	2.48E-03	2.67E-04
U3	IMS-1280 (2012)	U3-LANL-23	Host	4.121	0.042	4.42E-02	1.32E-03	2.02E-02	9.26E-04
U3	IMS-1280 (2012)	U3-LANL-24	Host	4.034	0.039	4.34E-02	1.25E-03	1.96E-02	7.52E-04
U3	IMS-1280 (2012)	U3-LANL-25	Host	5.317	0.054	5.76E-02	1.49E-03	2.60E-02	8.81E-04
U3	IMS-1280 (2012)	U3-LANL-26	Host	6.565	0.058	7.08E-02	1.44E-03	3.21E-02	9.88E-04
U3	IMS-1280 (2012)	U3-LANL-28	Host	5.152	0.053	5.72E-02	1.36E-03	2.47E-02	8.65E-04
U3	IMS-1280 (2012)	U3-LANL-13	U3.3	4.585	0.045	4.95E-02	1.30E-03	2.31E-02	8.62E-04
U3	IMS-1280 (2012)	U3-LANL-14	U3.4	5.712	0.073	6.13E-02	2.07E-03	2.85E-02	1.23E-03
U3	IMS-1280 (2012)	U3-LANL-27	U3.5	4.414	0.053	4.77E-02	1.34E-03	2.18E-02	8.83E-04
U4	IMS-1280 (2012)	U4-LANL-1	Unknown	4.708	0.070	4.91E-02	2.85E-03	2.30E-02	1.59E-03
U4	IMS-1280 (2012)	U4-LANL-2	Unknown	4.596	0.066	5.23E-02	2.45E-03	2.37E-02	1.64E-03
U4	IMS-1280 (2012)	U4-LANL-3	Unknown	4.635	0.063	4.96E-02	2.65E-03	2.35E-02	1.61E-03
U4	IMS-1280 (2012)	U4-LANL-4	Unknown	3.935	0.067	4.30E-02	2.39E-03	2.16E-02	1.61E-03
U4	IMS-1280 (2012)	U4-LANL-5	Unknown	3.811	0.061	4.16E-02	2.20E-03	1.80E-02	1.36E-03
U4	IMS-1280 (2012)	U4-LANL-6	Unknown	3.075	0.038	3.32E-02	1.69E-03	1.54E-02	1.21E-03
U4	IMS-1280 (2012)	U4-LANL-7	Unknown	3.218	0.034	3.44E-02	1.79E-03	1.57E-02	1.16E-03
U4	IMS-1280 (2012)	U4-LANL-8	Unknown	3.953	0.049	4.43E-02	2.21E-03	1.98E-02	1.50E-03
U4	IMS-1280 (2012)	U4-LANL-9	Unknown	4.204	0.052	4.61E-02	2.19E-03	2.04E-02	1.46E-03
U4	IMS-1280 (2012)	U4-LANL-10	Unknown	3.869	0.047	4.23E-02	2.35E-03	1.97E-02	1.49E-03
U4	IMS-1280 (2012)	U4-LANL-11	Unknown	5.225	0.066	5.65E-02	2.62E-03	2.55E-02	1.75E-03
U4	IMS-1280 (2012)	U4-LANL-12	Unknown	4.737	0.068	4.91E-02	2.40E-03	2.34E-02	1.65E-03
U4	IMS-1280 (2012)	U4-LANL-13	Unknown	5.237	0.064	5.88E-02	2.77E-03	2.43E-02	1.77E-03
U4	IMS-1280 (2012)	U4-LANL-14	Unknown	5.150	0.066	5.65E-02	3.01E-03	2.55E-02	1.85E-03
U4	IMS-1280 (2012)	U4-LANL-15	Unknown	5.164	0.070	5.57E-02	3.26E-03	2.43E-02	1.96E-03
U4	IMS-1280 (2012)	U4-LANL-16	Unknown	5.344	0.069	5.93E-02	3.19E-03	2.68E-02	1.98E-03

F.4 Location of SIMS Analyses

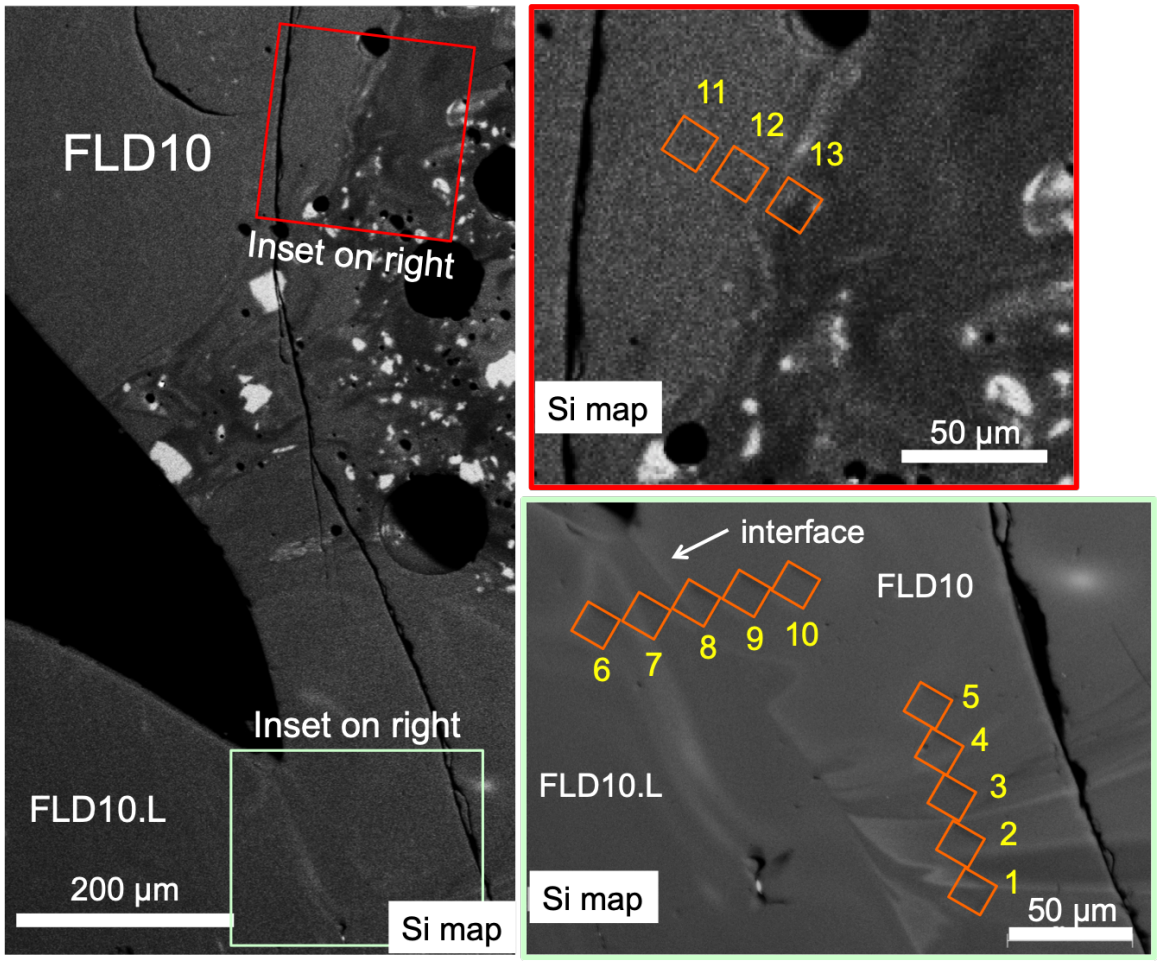

Figure F.1: Si compositional map showing the location of the SIMS analyses in agglomerate FLD10.L (Analyses FLD10-NS17-6 to FLD10-NS17-8) and the host FLD10 during a 2017 analytical campaign with a CAMECA NanoSIMS. $^{235}U/^{238}U$, $U/^{30}Si$, and $U/^{42}Ca$ ratios were measured. The SIMS analyses craters have dimensions 15×15 μm.

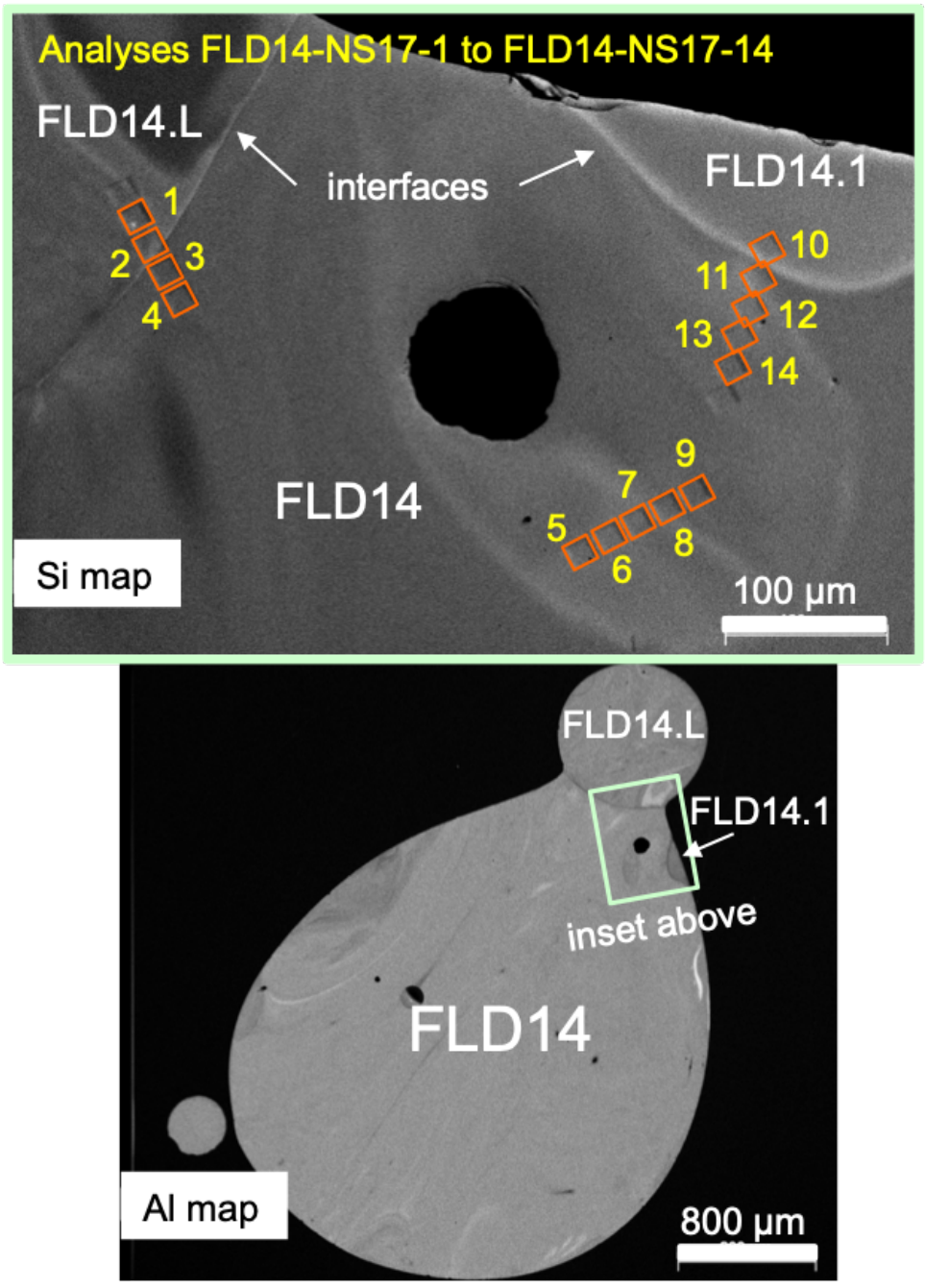

Figure F.2: Si compositional map showing the location of the SIMS analyses in agglomerates FLD14.L (Analyses FLD14-NS17-1 and FLD14-NS17-2) and FLD14.1 (Analysis FLD14-NS17-10) and the host FLD14 during a 2017 analytical campaign with a CAMECA NanoSIMS. $^{235}U/^{238}U$, $U/^{30}Si$, and $U/^{42}Ca$ ratios were measured. The SIMS analyses craters are square and have dimensions 15×15 μm.

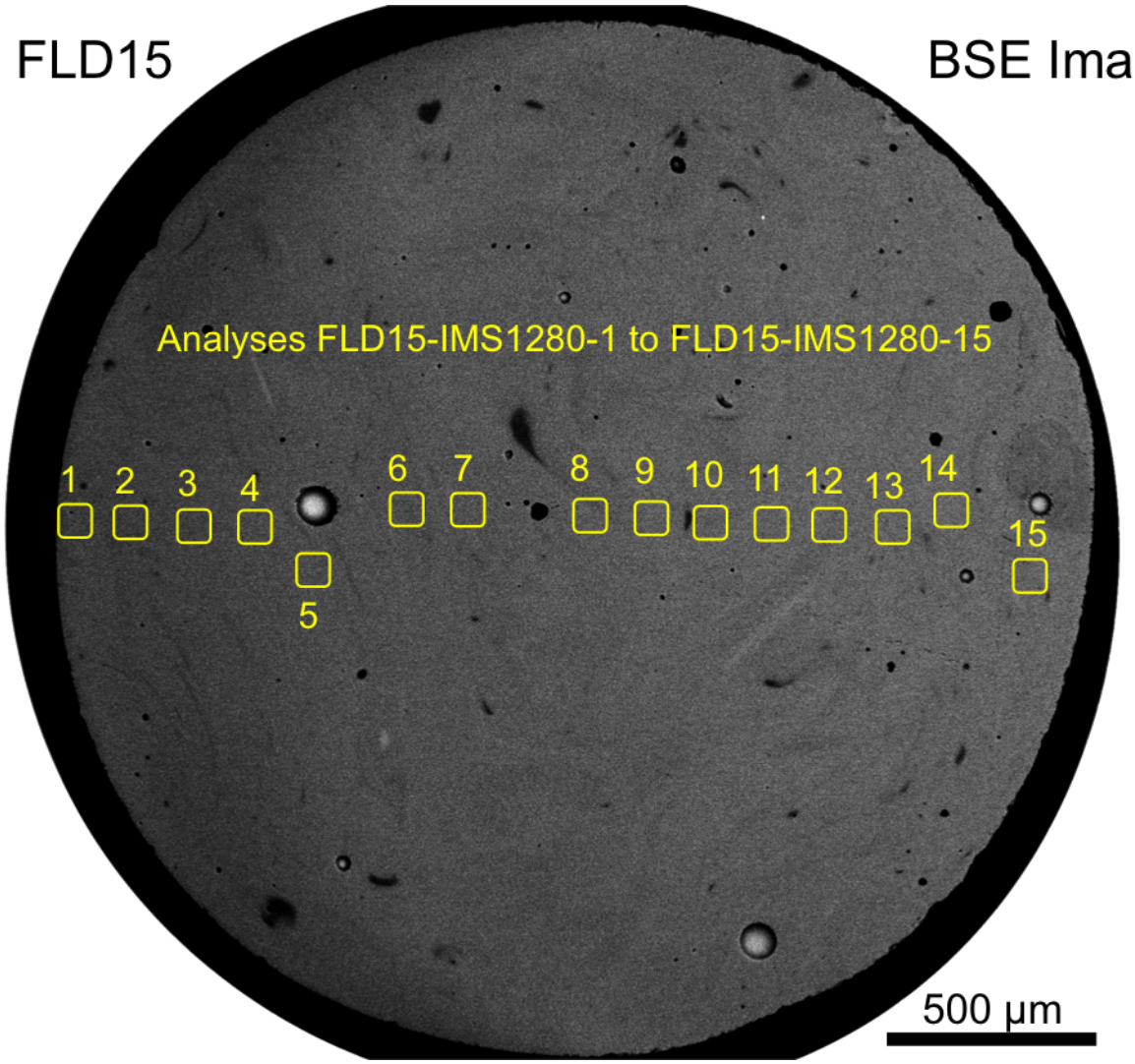

Figure F.3: Location of the SIMS analyses in sample FLD15 conducted during a 2015 analytical campaign at LANL with a CAMECA IMS-1280. $^{235}U/^{238}U$ and $^{234}U/^{238}U$ ratios were measured. The SIMS analyses craters are square rasters with dimensions $\sim$30 μm $\times$ $\sim$30 μm.

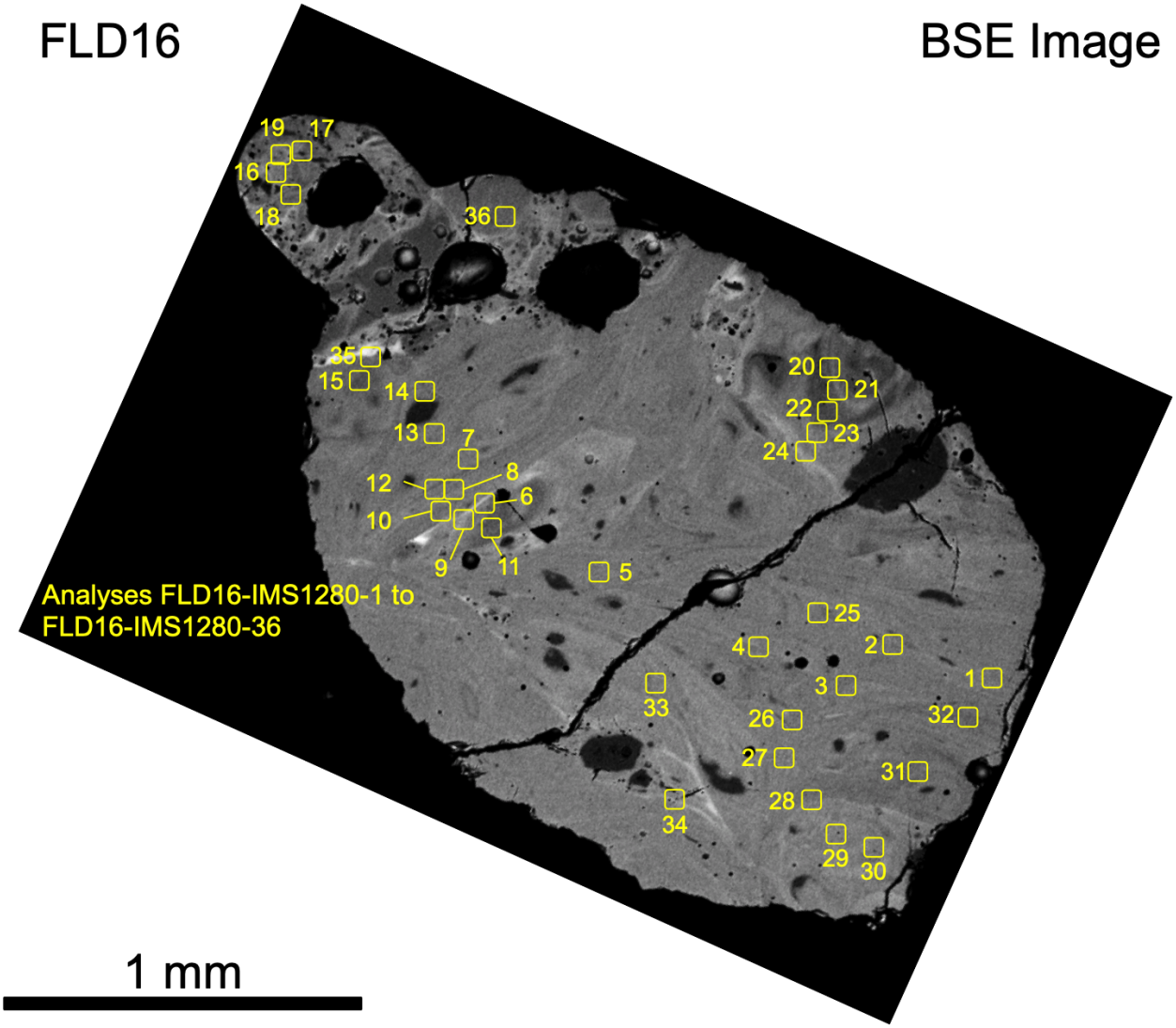

Figure F.4: Location of the SIMS analyses in sample FLD16 conducted during a 2015 analytical campaign at LANL with a CAMECA IMS-1280. $^{235}U/^{238}U$ and $^{234}U/^{238}U$ ratios were measured. The SIMS analyses craters are square rasters with dimensions $\sim$30 μm $\times$ $\sim$30 μm.

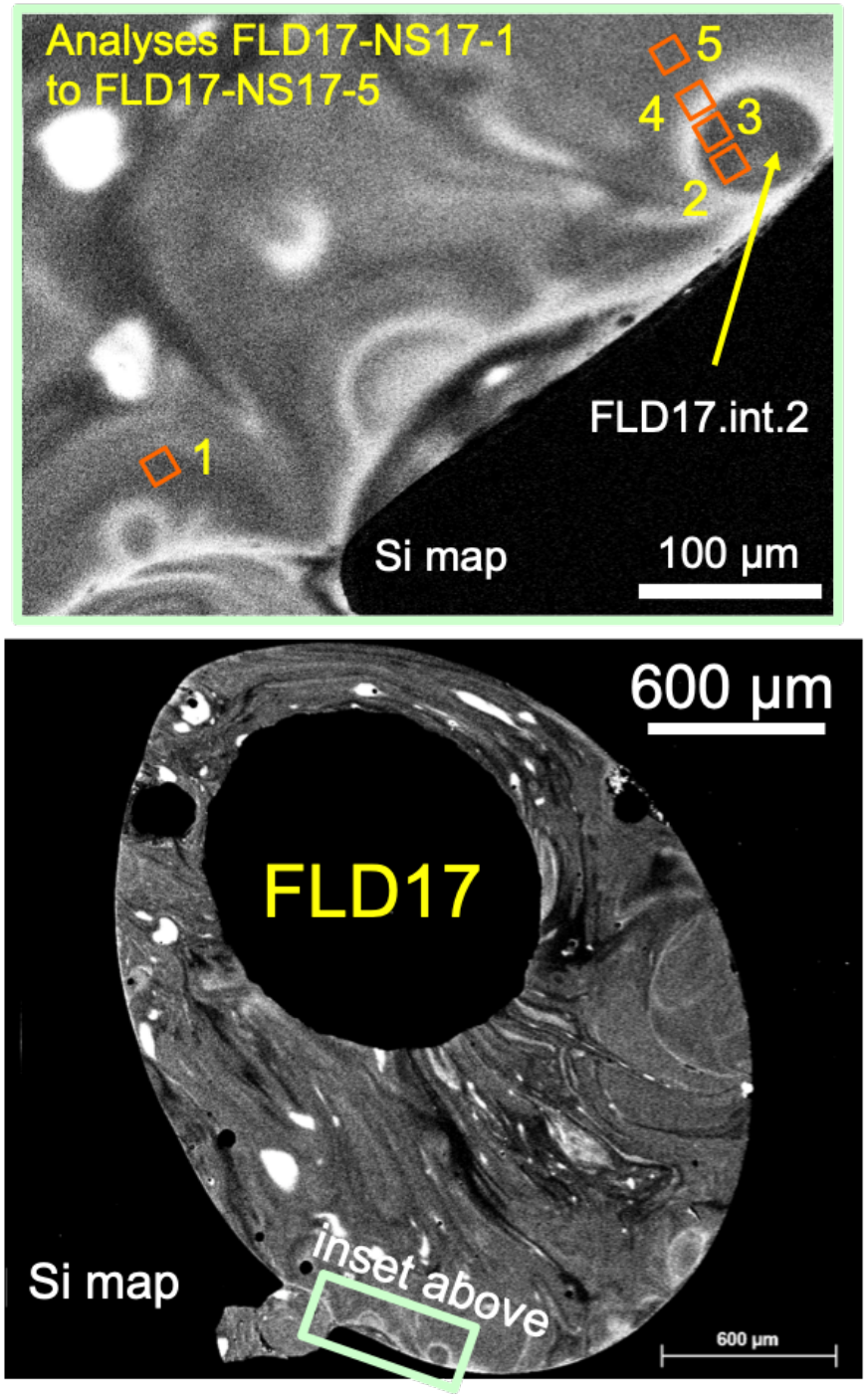

Figure F.5: Si compositional maps showing the location of the SIMS analyses in agglomerates FLD17.int.2 (Analyses FLD17-NS17-2, FLD17-NS17-3, and FLD17-NS17-4) and the host FLD17 (Analyses FLD17-NS17-1 and FLD17-NS17-5) during a 2017 analytical campaign with a CAMECA NanoSIMS. $^{235}U/^{238}U$, $U/^{30}Si$, and $U/^{42}Ca$ ratios were measured. The SIMS analyses craters for all analyses within the agglomerates are square and have dimensions 15×15 μm.

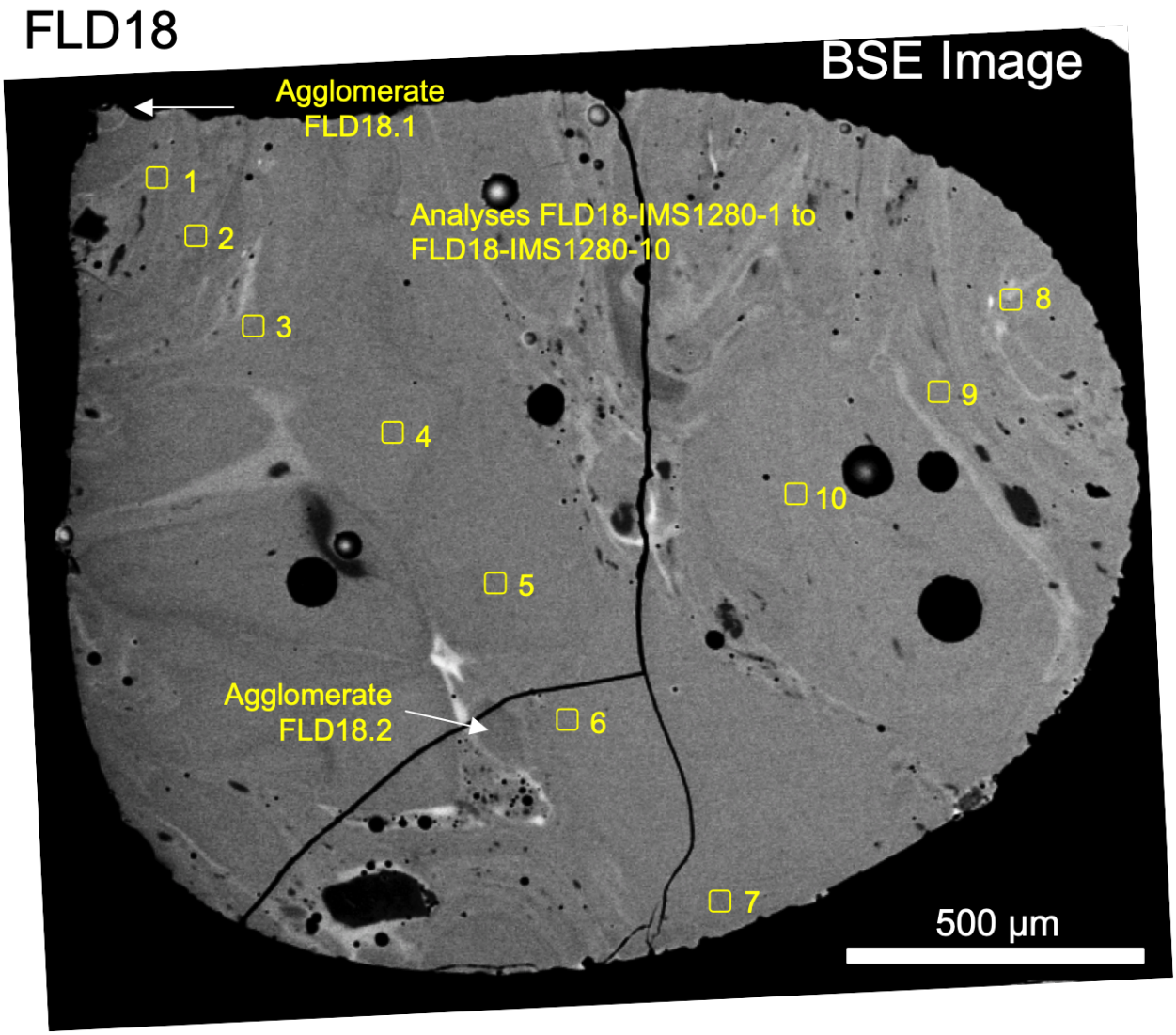

Figure F.6: Location of the SIMS analyses in sample FLD18 conducted during a 2015 analytical campaign at LANL with a CAMECA IMS-1280. $^{235}U/^{238}U$ and $^{234}U/^{238}U$ ratios were measured. The SIMS analyses craters are square rasters with dimensions$\sim$30 μm $\times$ $\sim$30 μm. The SIMS analyses within FLD18.1 and FLD18.2 are shown below.

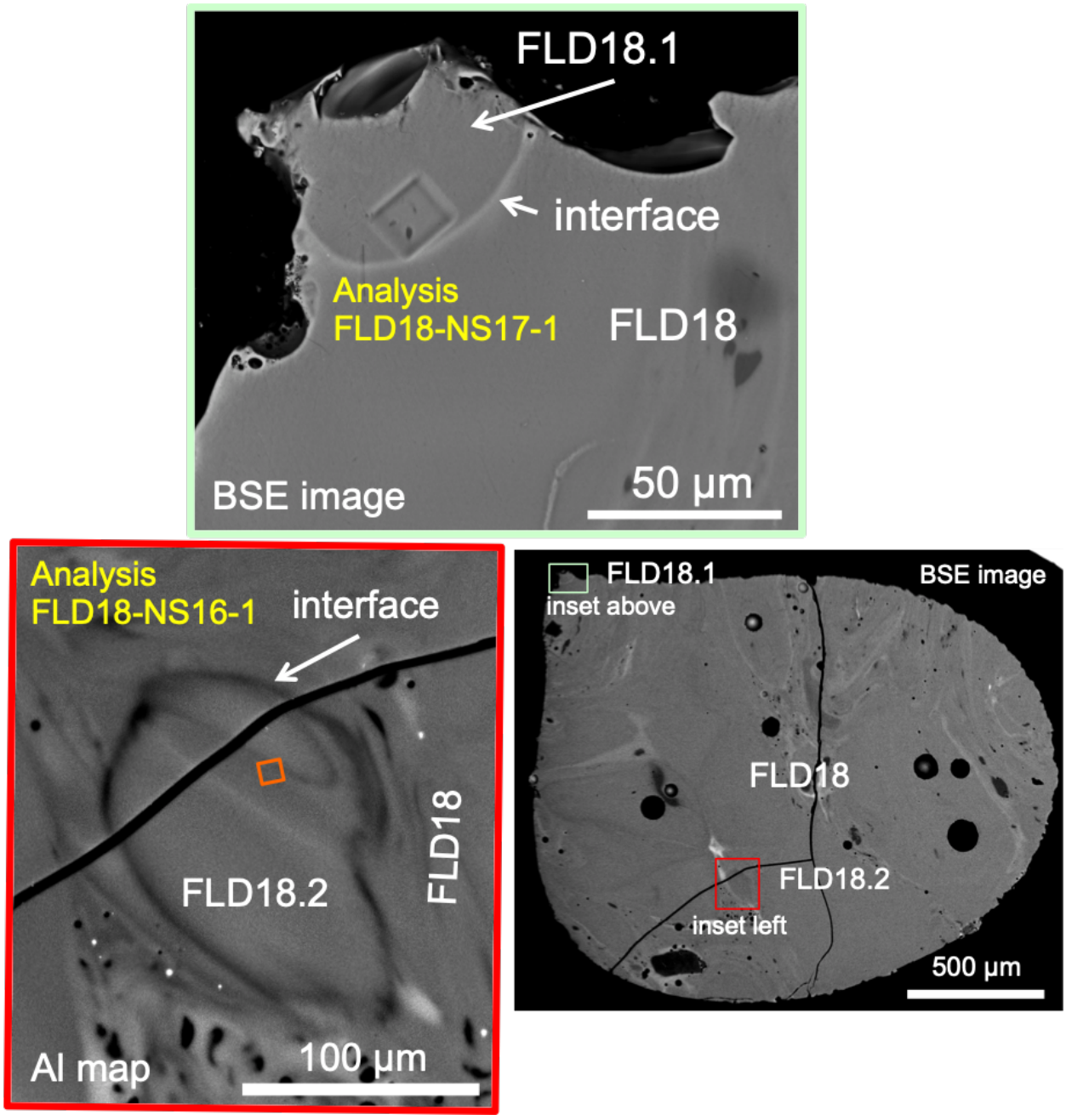

Figure F.7: Location of the SIMS analyses in agglomerates FLD18.2 (interior agglomerate) and FLD18.1 (exterior agglomerate) associated with the host FLD18 during 2016 and 2017 NanoSIMS analytical campaigns, respectively. The inset of showing FLD18.1 is a BSE image while the inset showing FLD18.2 is an Al compositional map to better highlight the compositional interface. $^{235}U/^{238}U$, $U/^{30}Si$, and $U/^{42}Ca$ ratios were measured. The SIMS analyses craters are square rasters with dimensions 15×15 μm.

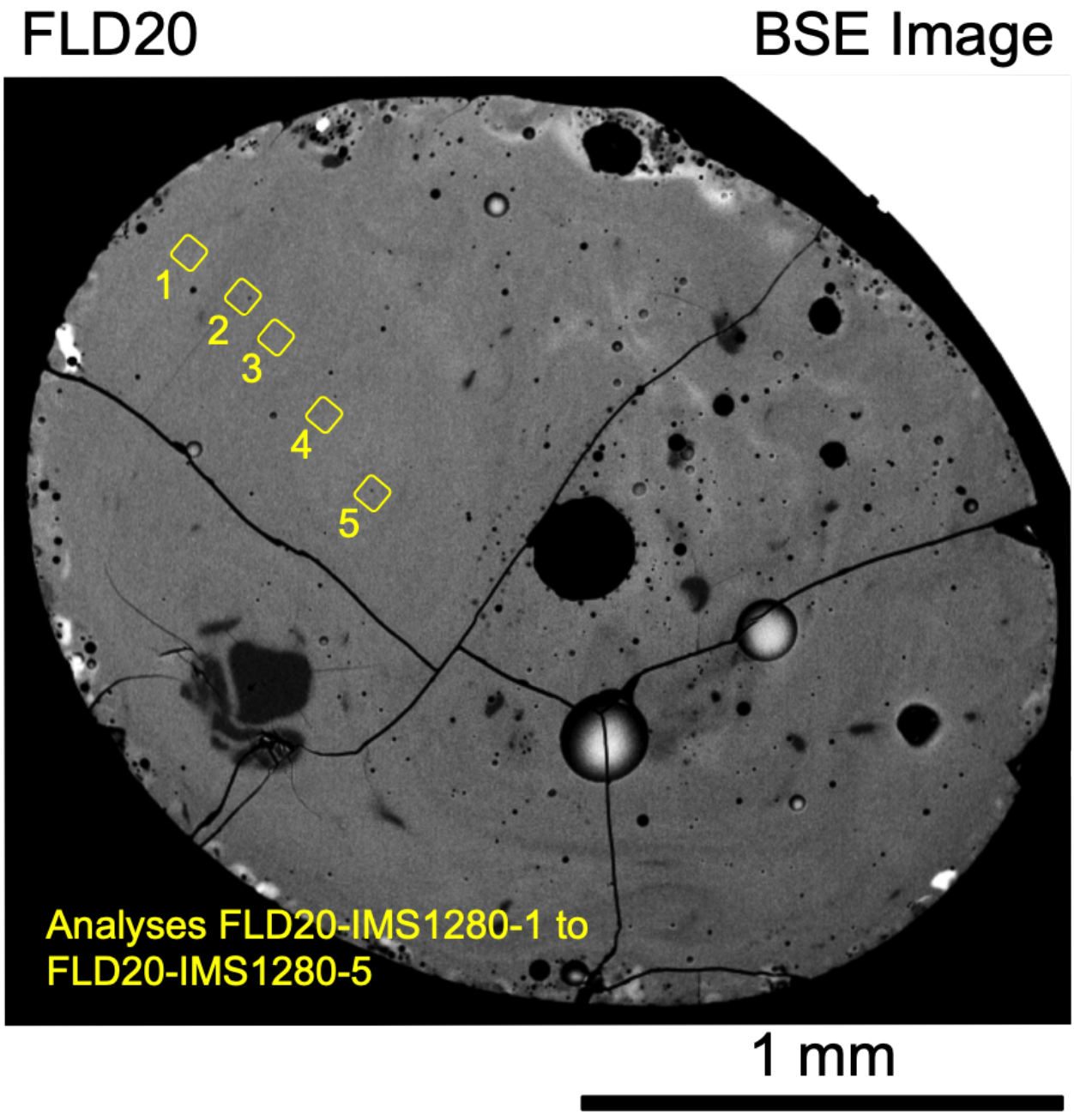

Figure F.8: Location of the SIMS analyses in sample FLD20 conducted during a 2015 analytical campaign at LANL with a CAMECA IMS-1280. $^{235}U/^{238}U$ and $^{234}U/^{238}U$ ratios were measured. The SIMS analyses craters are square rasters with dimensions $\sim$30 μm $\times$ $\sim$30 μm.

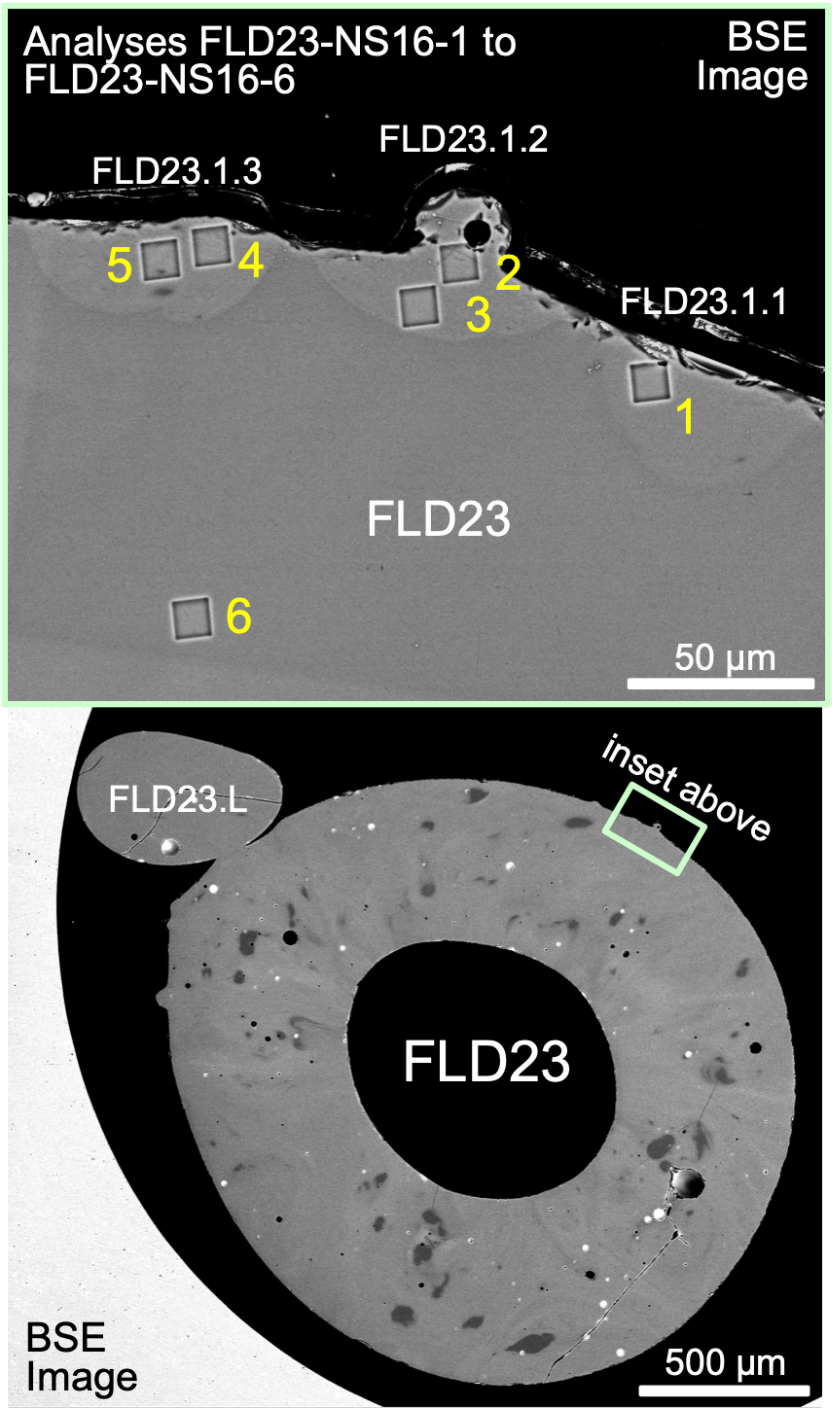

Figure F.9: Location of the SIMS analyses in agglomerates FLD23.1.1, FLD23.1.2, FLD23.1.3, and one analysis in host FLD23 conducted during a 2016 analytical campaign with a CAMECA NanoSIMS. $^{235}U/^{238}U$, $U/^{30}Si$, and $U/^{42}Ca$ ratios were measured. The SIMS analyses craters are square rasters with dimensions 15×15 μm.

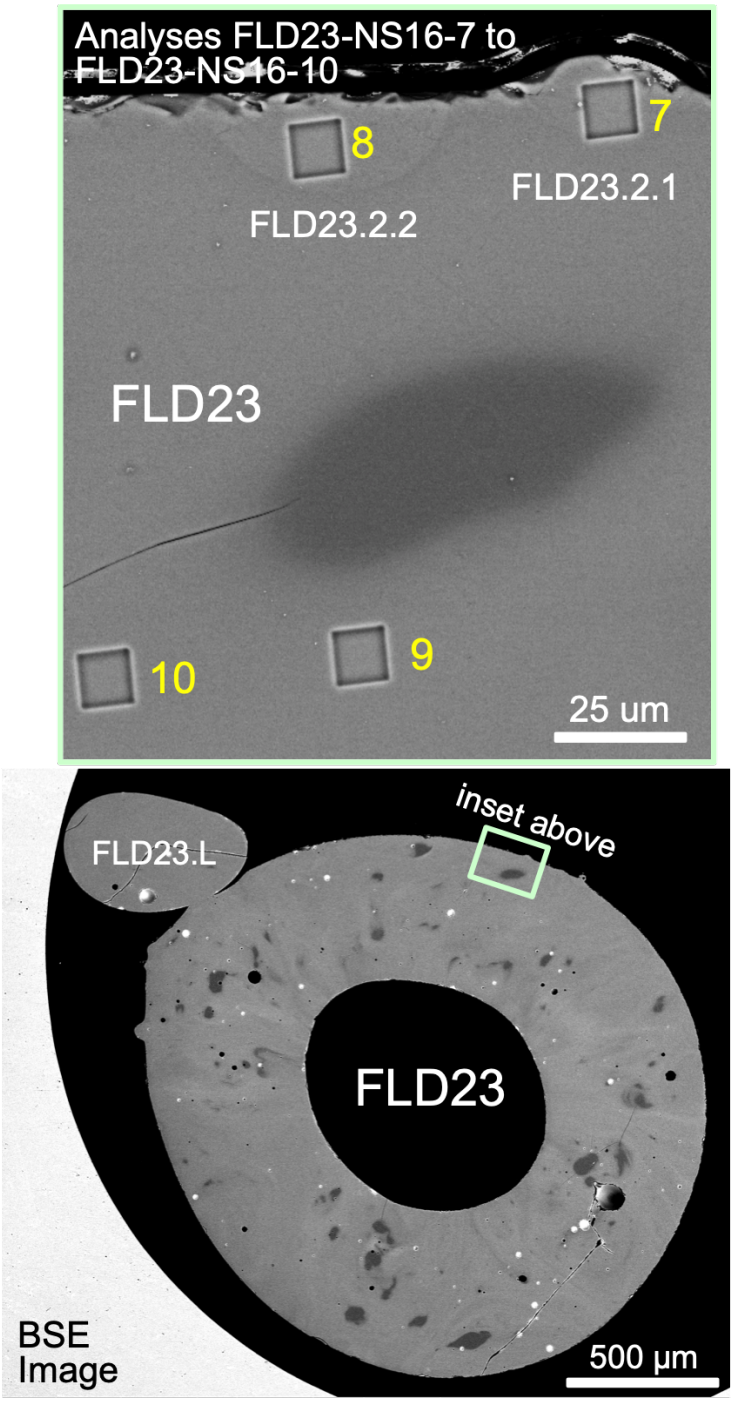

Figure F.10: BSE image showing the location of the SIMS analyses in agglomerates FLD23.2.1, FLD23.1.2, and two analyses in host FLD23 conducted during a 2016 analytical campaign with a CAMECA NanoSIMS. $^{235}U/^{238}U$, $U/^{30}Si$, and $U/^{42}Ca$ ratios were measured. The SIMS analyses craters are square rasters with dimensions 15×15 μm.

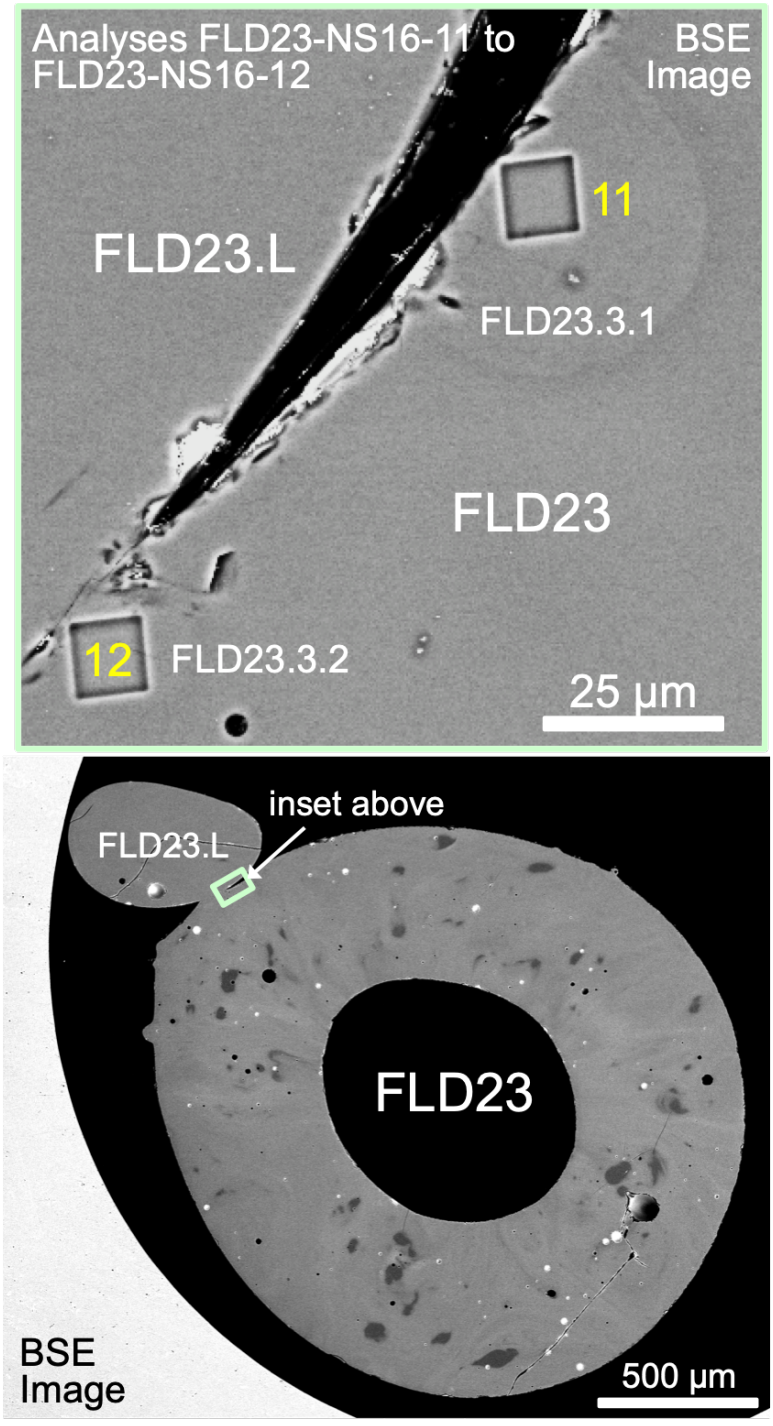

Figure F.11: BSE image showing the location of the SIMS analyses in agglomerates FLD23.3.1 and FLD23.3.2 during a 2016 analytical campaign with a CAMECA NanoSIMS. $^{235}U/^{238}U$, $U/^{30}Si$, and $U/^{42}Ca$ ratios were measured. The SIMS analyses craters are square rasters with dimensions 15×15 μm.

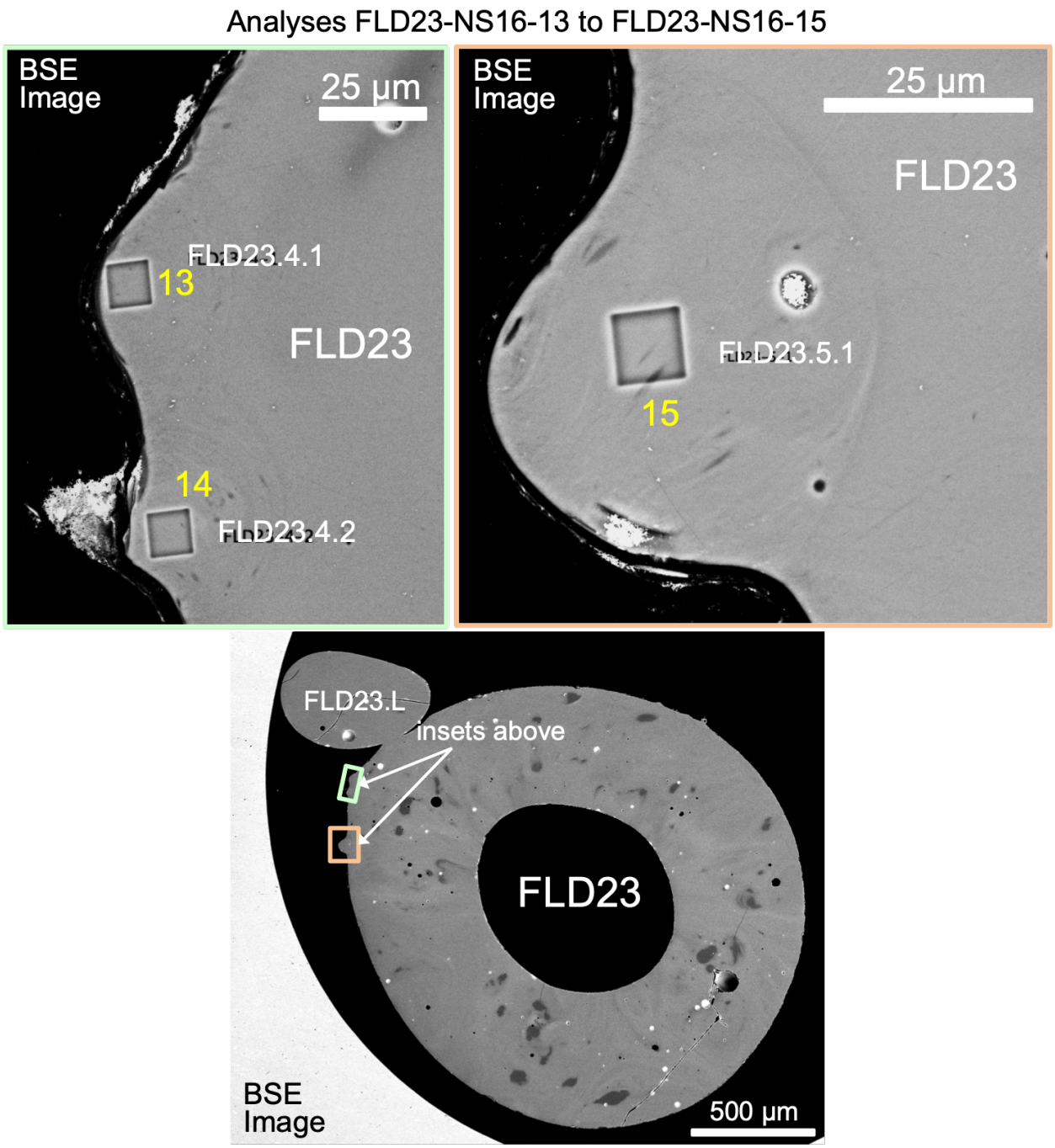

Figure F.12: BSE image showing the location of the SIMS analyses in agglomerates FLD23.4.1, FLD23.4.2, and FLD23.5.1 during a 2016 analytical campaign with a CAMECA NanoSIMS. $^{235}U/^{238}U$, $U/^{30}Si$, and $U/^{42}Ca$ ratios were measured. The SIMS analyses craters are square rasters with dimensions 15×15 μm.

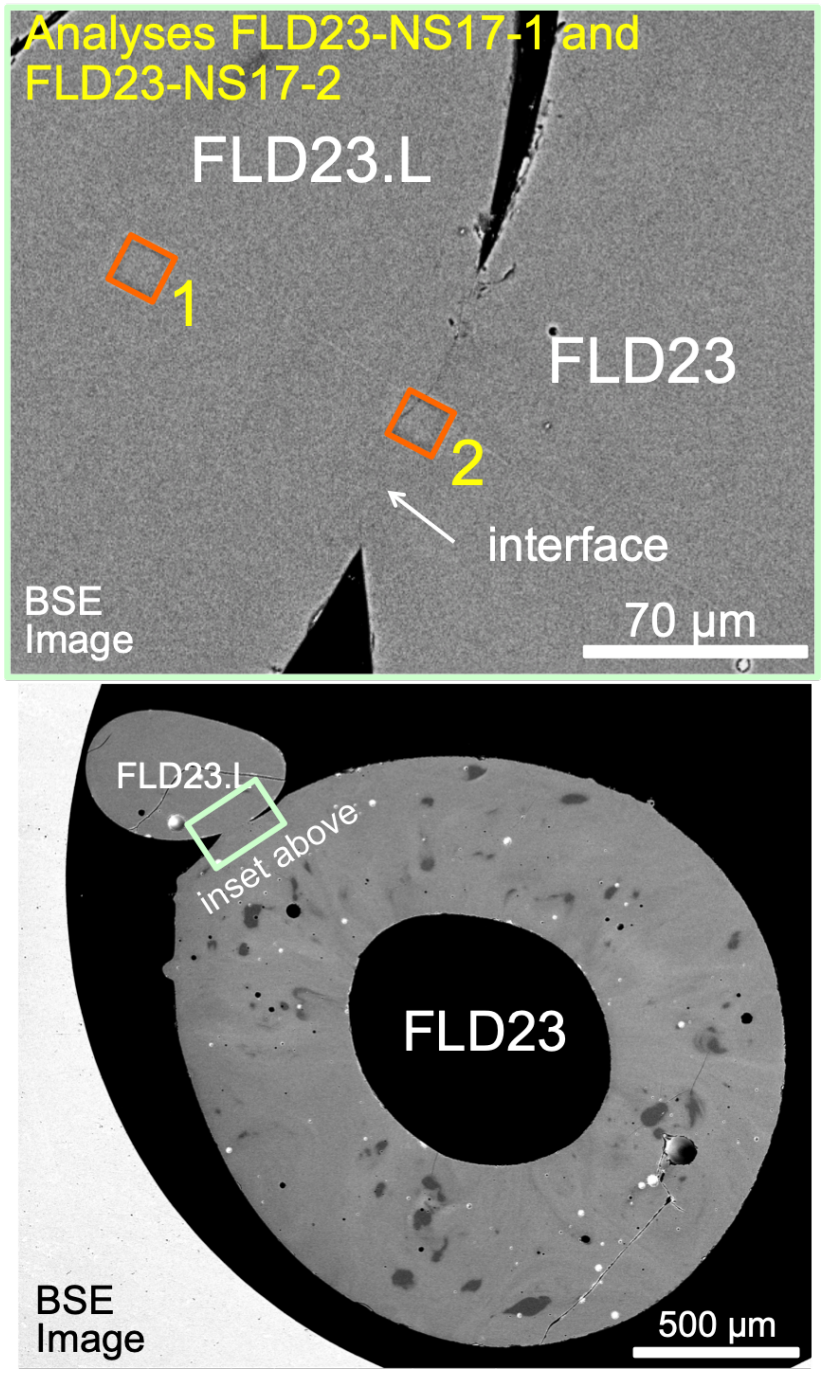

Figure F.13: BSE image showing the location of the SIMS analyses in agglomerate FLD23.L during a 2017 analytical campaign with a CAMECA NanoSIMS. One analysis was performed within the agglomerate and one analysis overlapped the interface between FLD23.L and FLD23. $^{235}U/^{238}U$, $U/^{30}Si$, and $U/^{42}Ca$ ratios were measured. The SIMS analyses craters are square rasters with dimensions 15×15 μm.

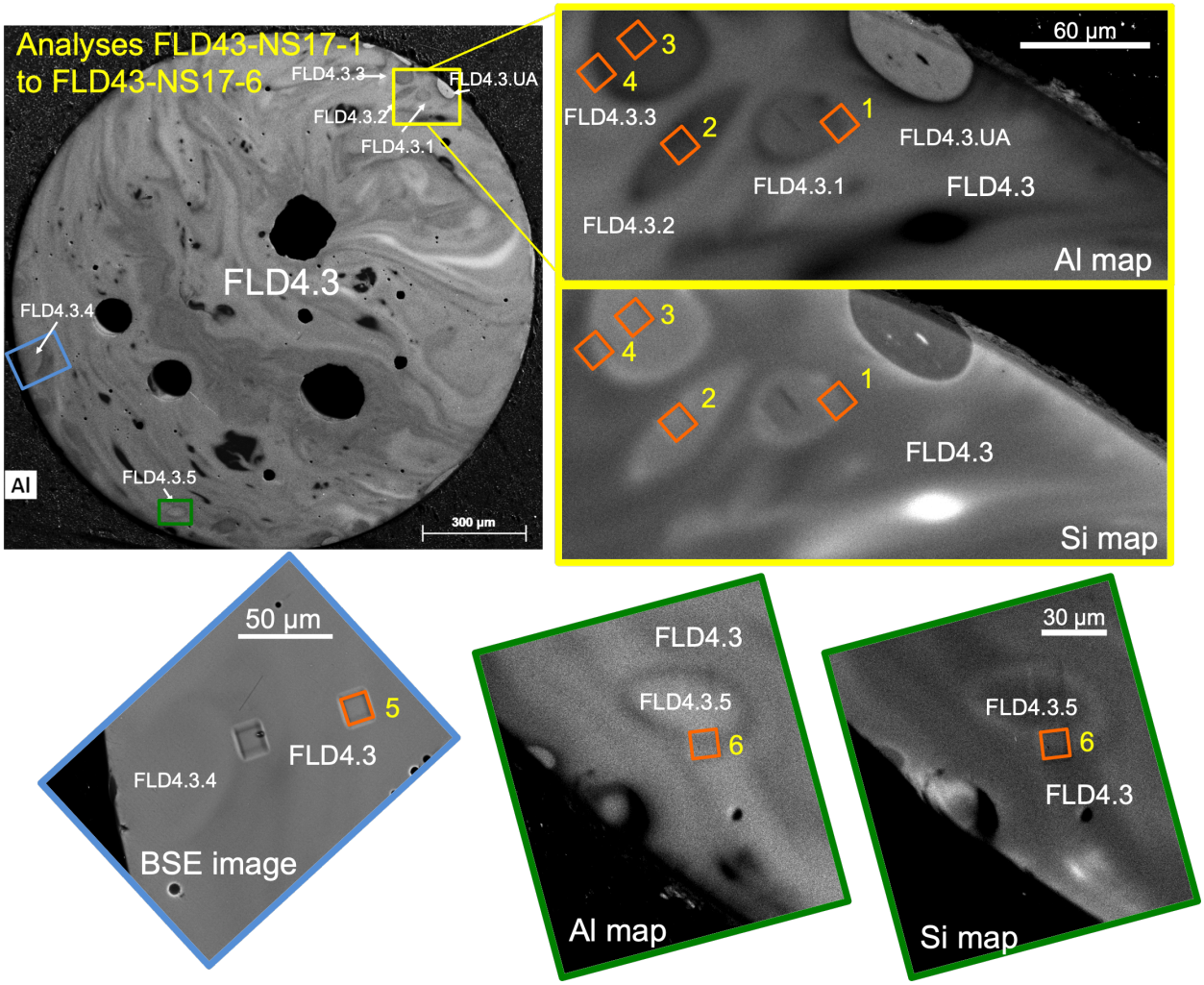

Figure F.14: Locations of the SIMS analyses in agglomerates FLD4.3.1 (analysis FLD43-NS17-1), FLD4.3.2 (analysis FLD43-NS17-2), FLD4.3.3 (analyses FLD43-NS17-3 and FLD43-NS17-4), FLD4.3.5 (analysis FLD43-NS17-6), and the host FLD4.3 (analysis FLD43-NS17-5) during a 2017 analytical campaign with a CAMECA NanoSIMS. $^{235}U/^{238}U$, $U/^{30}Si$, and $U/^{42}Ca$ ratios were measured. The SIMS analyses craters are square rasters with dimensions 15×15 μm.

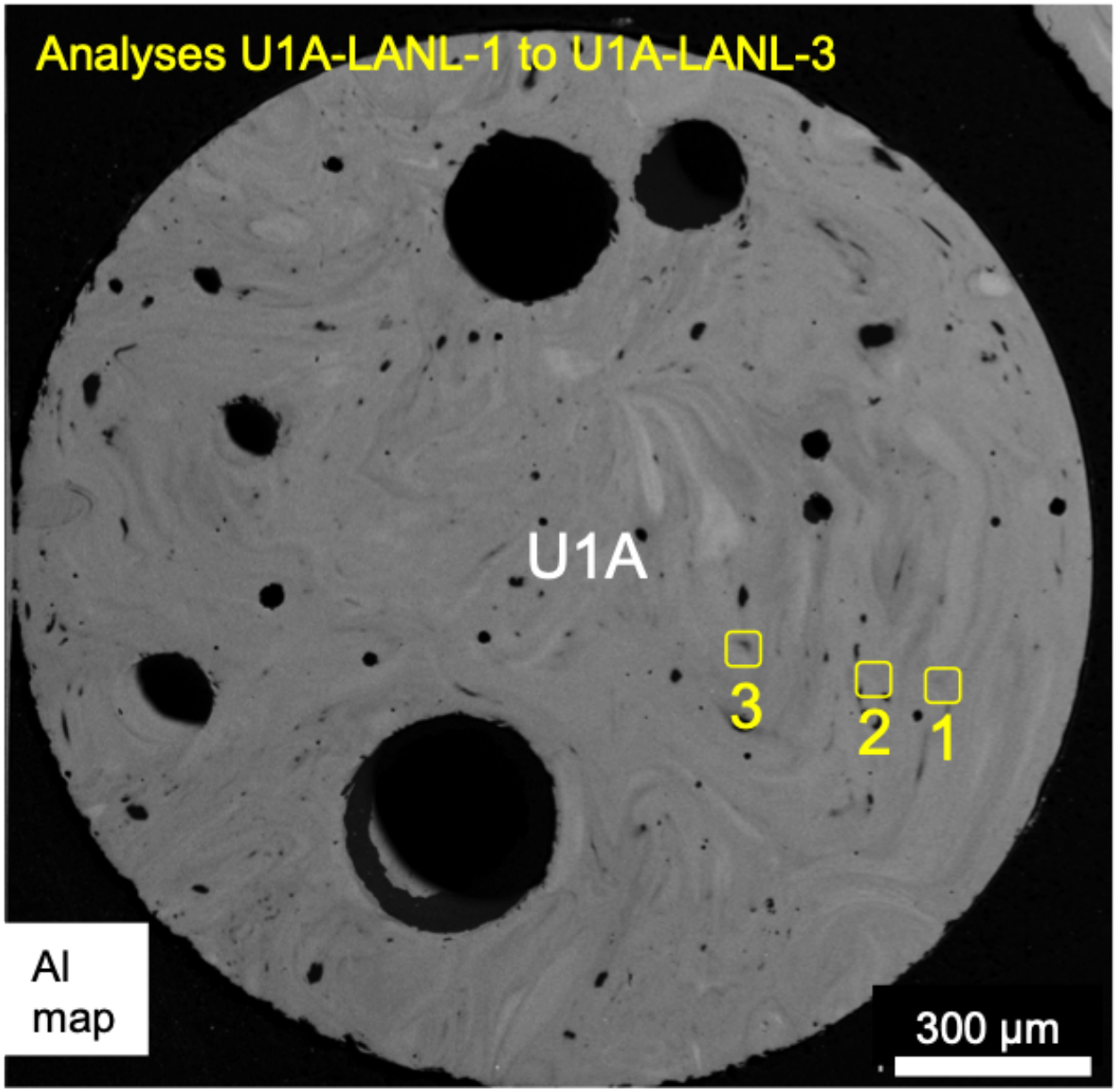

Figure F.15: Al compositional map showing the location of the SIMS analyses in the host of sample U1A conducted during a 2015 analytical campaign at LANL with a CAMECA IMS-1280. $^{235}U/^{238}U$, $^{234}U/^{238}U$, and $^{236}U/^{238}U$ ratios were measured. The SIMS analyses craters are square rasters with dimensions ~30 μm × ~30 μm.

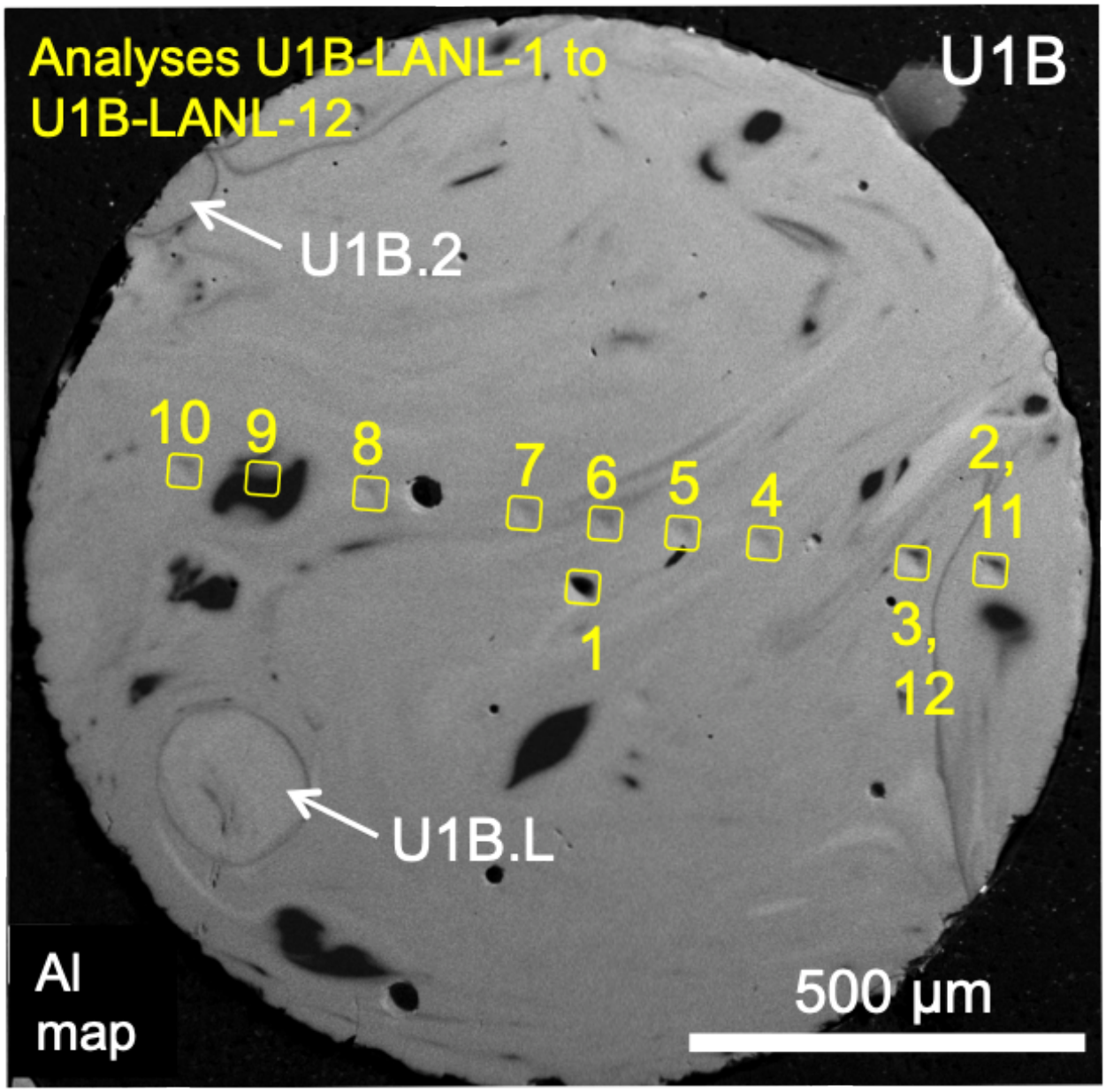

Figure F.16: Al compositional map showing the location of the SIMS analyses in the host of sample U1B conducted during a 2015 analytical campaign at LANL with a CAMECA IMS-1280. Analyses U1B-LANL-2 and U1B-LANL-11 and analyses U1B-LANL-3 and U1B-LANL-12 were performed in the same location. $^{235}U/^{238}U$, $^{234}U/^{238}U$, and $^{236}U/^{238}U$ ratios were measured. The SIMS analyses craters are square rasters with dimensions $\sim$30 μm $\times$ $\sim$30 μm. Analyses performed in U1B.L and U1B.2 are shown below.

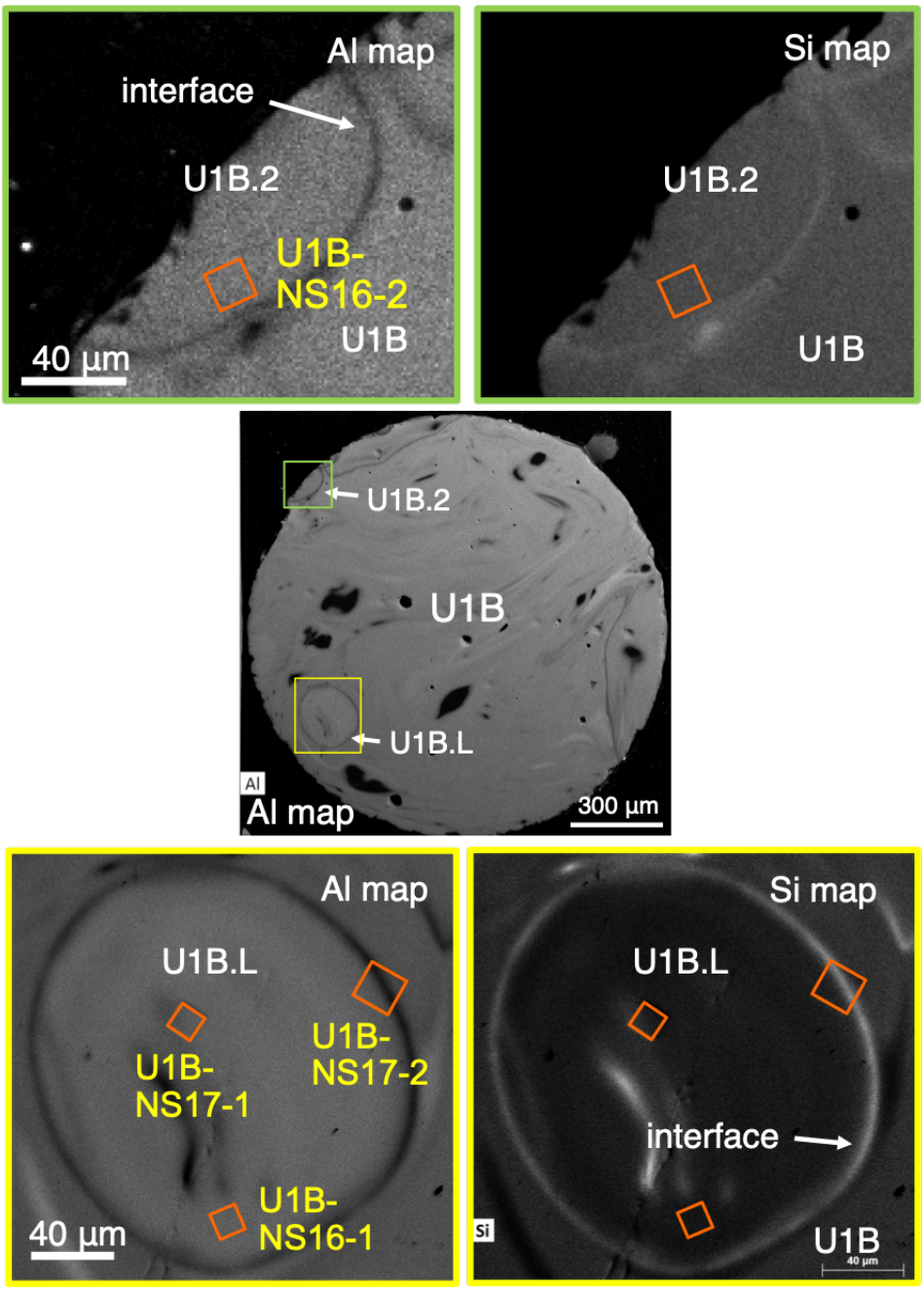

Figure F.17: Al and Si compositional maps showing the location of the SIMS analyses in agglomerates U1B.2 and U1B.L during 2016 and 2017 analytical campaigns with a CAMECA NanoSIMS. $^{235}U/^{238}U$, $U/^{30}Si$, and $U/^{42}Ca$ ratios were measured. The SIMS analyses craters for all analyses within the agglomerates are square and have dimensions 15×15 μm. The NanoSIMS analysis over the interface of U1B.L (U1B-NS17-2) is square and has dimensions 20×20 μm.

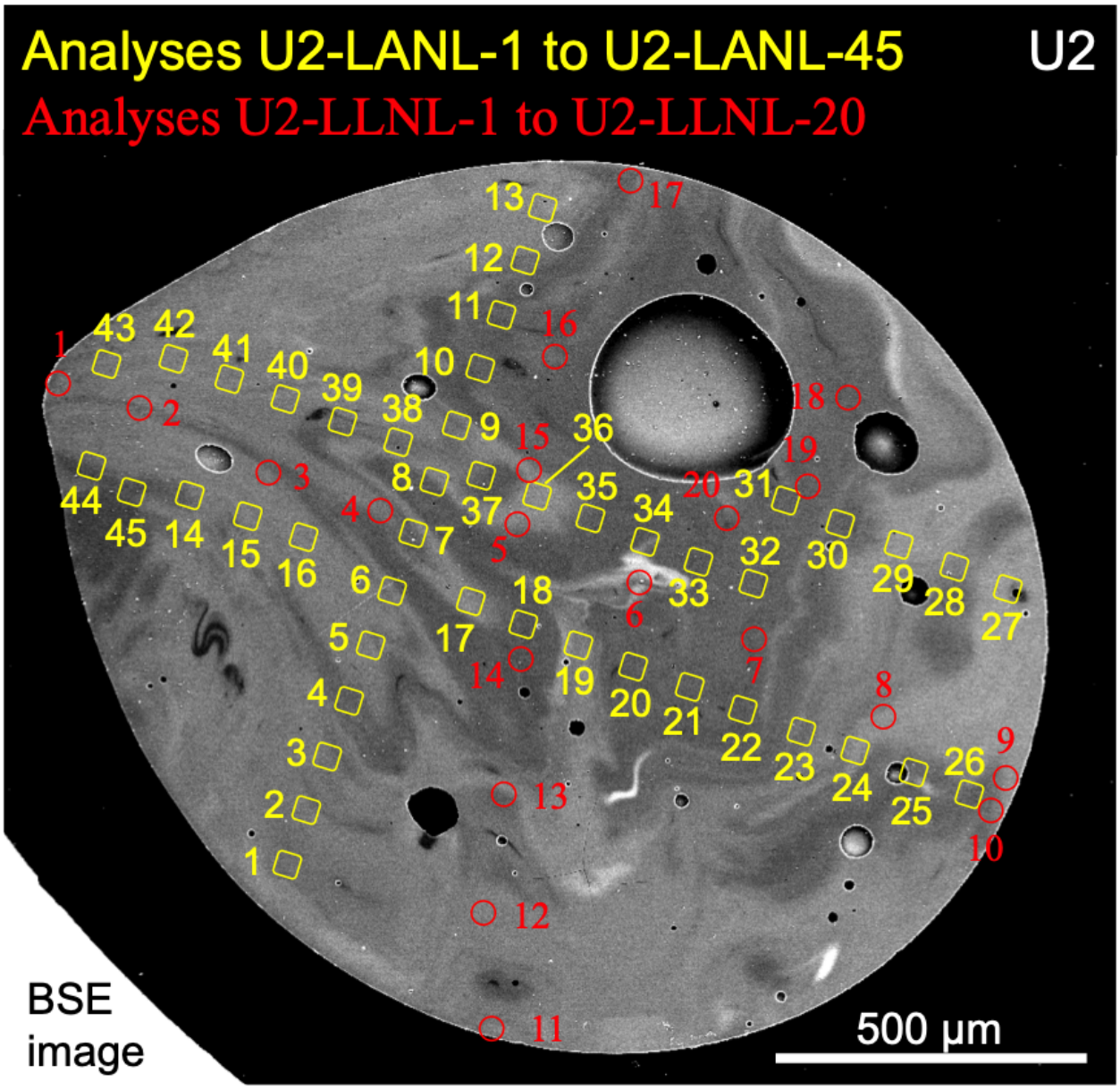

Figure F.18: BSE image showing the location of the SIMS analyses in the host of sample U2 conducted during a 2012 analytical campaign at LLNL with a CAMECA IMS-3f (analyses denoted with red circles, marked with serif numbers) and a 2013 analytical campaign at LANL with a CAMECA IMS-1280 (analyses denoted with yellow squares and marked with sans-serif numbers). $^{235}U/^{238}U$ were measured for both analytical campaigns and $^{234}U/^{238}U$ and $^{236}U/^{238}U$ ratios were measured during the IMS-1280 analyses. The IMS-3f analytical craters are approximately circular with diameters ∼15-30 μm and the IMS-1280 analytical craters are square rasters with dimensions ∼30 μm × ∼30 μm.

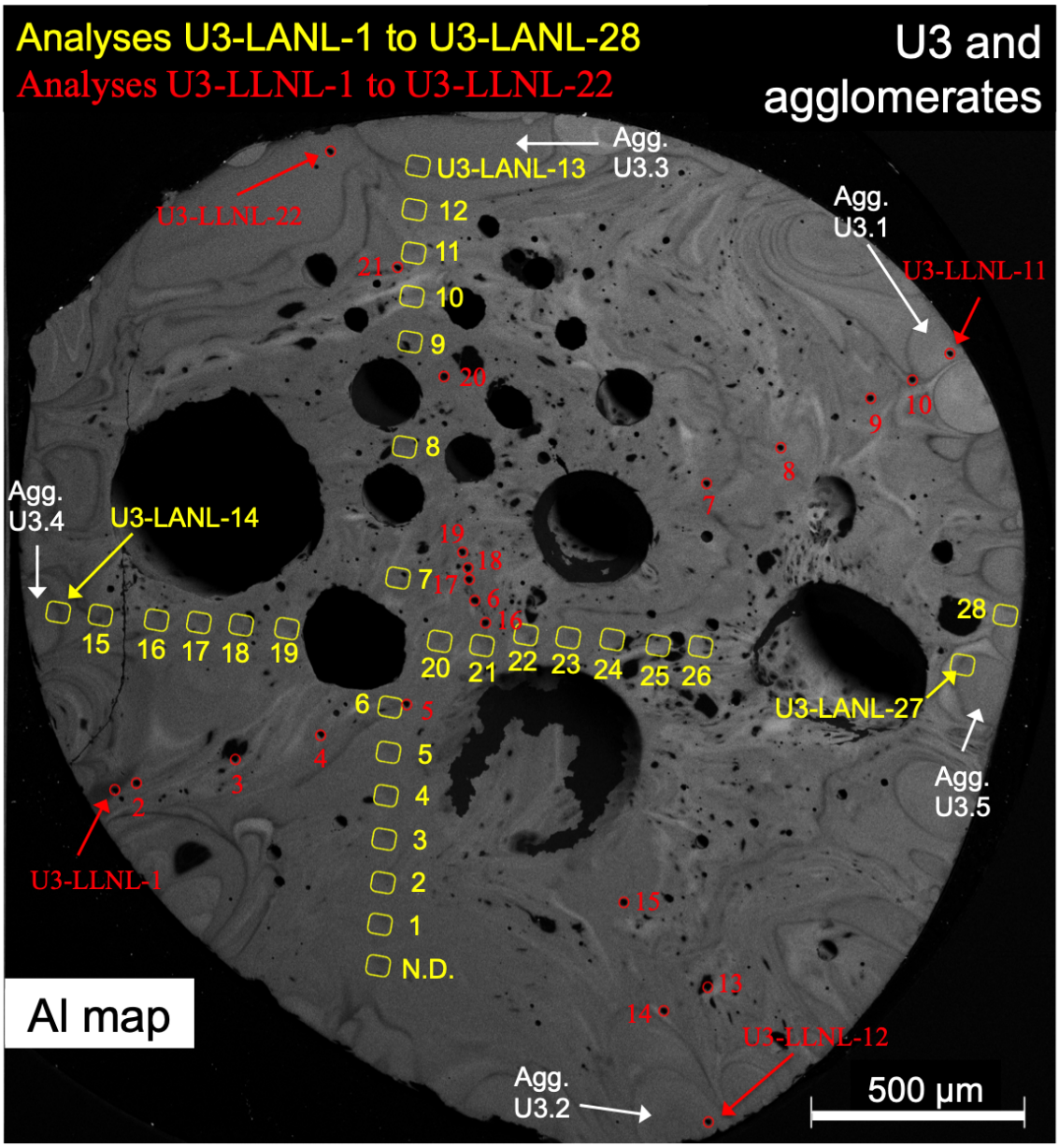

Figure F.19: Al compositional map showing the location of the SIMS analyses in the host and associated agglomerates of sample U3 conducted during a 2012 analytical campaign at LLNL with a CAMECA IMS-3f (analyses denoted with red circles, marked with serif numbers) and a 2013 analytical campaign at LANL with a CAMECA IMS-1280 (analyses denoted with yellow squares and marked with sans-serif numbers). Agglomerates are marked in white. $^{235}U/^{238}U$ and $U/^{30}Si$ ratios were measured during the IMS-3f analyses in 2012 and $^{235}U/^{238}U$, $^{234}U/^{238}U$, and $^{236}U/^{238}U$ ratios were measured during the IMS-1280 analyses. The IMS-3f analytical craters are approximately circular with diameters ∼15-30 μm and the IMS-1280 analytical craters are square rasters with dimensions ∼30 μm × ∼30 μm. The analysis marked "N.D." denotes that no data was collected.

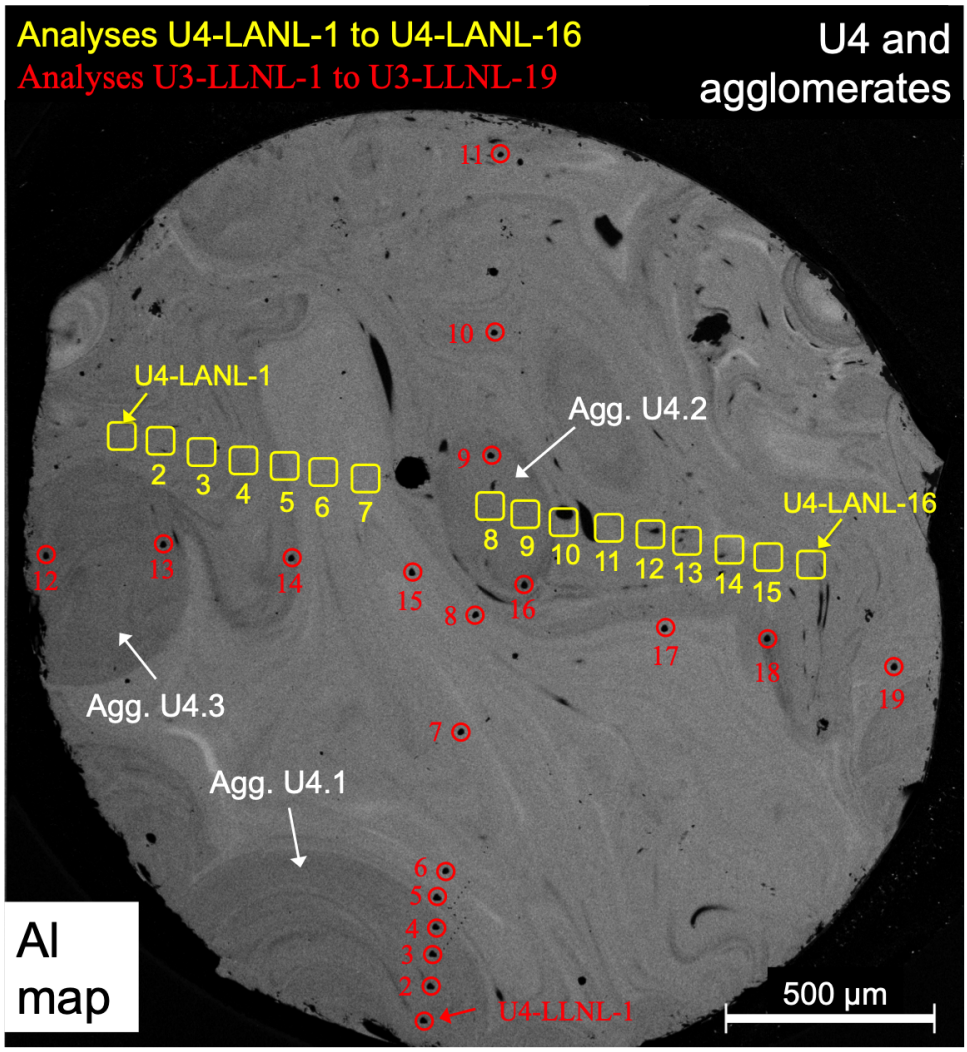

Figure F.20: Al compositional map showing the location of the SIMS analyses in host U4 and its associated agglomerates characterized with SIMS conducted during a 2012 analytical campaign at LLNL with a CAMECA IMS-3f (analyses denoted with red circles, marked with serif numbers) and a 2013 analytical campaign at LANL with a CAMECA IMS-1280 (analyses denoted with yellow squares and marked with sans-serif numbers). Agglomerates characterized with SIMS are marked in white. $^{235}U/^{238}U$ and $U/^{30}Si$ ratios were measured during the IMS-3f analyses in 2012 and $^{235}U/^{238}U$, $^{234}U/^{238}U$, and $^{236}U/^{238}U$ ratios were measured during the IMS-1280 analyses. The IMS-3f analytical craters are approximately circular with diameters ~15-30 μm and the IMS-1280 analytical craters are square rasters with dimensions ~30 μm × ~30 μm. The location of the IMS-1280 analytical craters are approximate as they were too shallow to located by SEM after the SIMS analysis due to the short analytical times (these regions were analyzed using the multi-collector mode of the IMS-1280).

Appendix G

Combined major element U isotope analyses

Table G.1: Compositions of SIMS analytical craters and the U isotope ratios measured in those craters. EDS measurements were conducted between 1–4 rasters per SIMS analytical crater. For single EDS rasters, the uncertainties of the EDS composition is calculated as discussed in Chapter 6. For multiple EDS rasters, the data are the mean of the compositions and the uncertainties are the standard deviation of those measurements. Na_2O compositions are included in this table but should be disregarded, following the discussion and results in Chapter 5. Compositions and U isotope ratios for samples AA.B, AE.C, AG.D, and AH.E are extracted from the electronic annex of Weisz et al. (2016) and detailed in Chapter 5.

Sample	Location	Interface	$^{235}U/^{238}U$	2σ	SiO_2	1σ	Al_2O_3	1σ	Na_2O	1σ	K_2O	1σ	CaO	1σ	FeO	1σ	TiO_2	1σ	MgO	1σ
AA.B	B1	-	6.36	2.55	73.98	0.26	12.11	0.15	1.46	0.01	4.36	0.02	1.72	0.03	2.23	0.04	0.30	0.00	0.52	0.02
AA.B	B2	-	4.56	1.38	72.47	0.43	13.05	0.07	2.19	0.01	4.57	0.05	2.61	0.17	1.89	0.07	0.26	0.01	0.39	0.01
AE.C	C1	-	6.56	0.88	73.39	0.58	10.95	0.24	1.56	0.03	4.94	0.07	2.16	0.08	2.85	0.12	0.27	0.01	0.53	0.03
AE.C	Host	-	5.73	0.68	72.39	1.10	11.19	0.63	1.50	0.03	4.91	0.07	2.03	0.06	3.10	0.04	0.23	0.03	0.77	0.02
AE.C	C2	-	6.23	1.51	77.28	0.05	10.46	0.38	1.44	0.01	4.56	0.27	1.25	0.08	2.38	0.09	0.22	0.01	0.39	0.04
AG.D	D2	-	6.12	1.60	69.66	0.55	15.66	0.60	1.21	0.02	4.34	0.13	1.62	0.13	3.33	0.12	0.41	0.02	0.77	0.04
AG.D	Host	-	6.27	1.25	70.80	0.41	14.49	0.35	1.21	0.03	4.33	0.09	1.85	0.17	3.25	0.20	0.31	0.02	0.54	0.05
AH.E	E1	-	7.42	1.17	70.69	0.72	13.52	0.13	2.66	0.02	5.71	0.03	1.29	0.13	2.42	0.08	0.30	0.01	0.56	0.03
AH.E	Host	-	7.68	3.59	75.94	0.45	9.73	0.33	2.12	0.00	5.14	0.02	1.02	0.10	2.33	0.05	0.22	0.01	0.30	0.01
FLD10	FLD10.L	-	5.90	0.14	74.78	1.65	12.95	0.28	2.13	0.11	3.58	0.06	2.57	0.04	3.01	0.06	0.34	0.01	0.59	0.01
FLD10	FLD10.L	-	7.51	0.21	75.97	0.16	12.99	0.07	2.05	0.04	3.56	0.02	2.44	0.03	3.01	0.04	0.33	0.03	0.59	0.03
FLD10	FLD10.L	X	8.86	0.30	75.49	0.92	13.47	0.26	2.03	0.01	3.67	0.04	2.37	0.00	2.91	0.01	0.31	0.01	0.68	0.14
FLD10	Host	-	7.65	0.25	73.74	1.46	13.54	0.28	2.05	0.03	3.77	0.01	2.26	0.03	3.01	0.04	0.34	0.02	0.57	0.02
FLD10	Host	-	5.30	0.14	73.88	0.69	13.29	0.16	1.99	0.02	3.75	0.03	2.13	0.02	3.00	0.00	0.34	0.01	0.52	0.02
FLD10	Host	-	7.54	0.20	74.54	0.81	13.12	0.26	2.54	0.10	3.75	0.03	2.49	0.03	2.91	0.08	0.31	0.01	0.64	0.13
FLD10	Host	-	7.14	0.16	74.26	0.71	12.94	0.13	2.75	0.10	4.00	0.06	2.47	0.02	2.98	0.02	0.24	0.01	0.59	0.01
FLD10	Host	-	7.98	0.17	67.78	0.09	15.02	0.10	2.76	0.07	4.29	0.04	1.87	0.03	3.76	0.01	0.50	0.02	0.86	0.09
FLD14	FLD14.L	-	3.68	0.09	76.03	0.52	12.97	0.06	2.86	0.05	3.78	0.03	3.01	0.05	2.53	0.02	0.27	0.01	0.45	0.02
FLD14	FLD14.L	X	4.02	0.11	75.36	0.31	11.82	0.08	3.10	0.06	3.96	0.03	3.49	0.03	2.78	0.05	0.25	0.02	0.46	0.01
FLD14	Host	-	3.72	0.10	73.60	1.28	13.91	0.25	2.52	0.02	3.57	0.05	3.49	0.03	2.81	0.05	0.32	0.02	0.52	0.01
FLD14	Host	-	4.04	0.12	73.59	0.50	14.22	0.12	2.47	0.07	3.38	0.04	3.51	0.02	2.82	0.04	0.33	0.01	0.50	0.00
FLD14	Host	-	4.58	0.10	75.34	0.50	12.98	0.06	2.40	0.05	3.32	0.04	2.98	0.03	2.77	0.01	0.31	0.03	0.48	0.00
FLD14	Host	-	4.55	0.13	76.40	1.14	13.07	0.21	2.41	0.03	3.40	0.02	3.00	0.03	2.79	0.05	0.28	0.03	0.47	0.04
FLD14	Host	-	4.63	0.11	75.73	0.84	13.30	0.25	2.67	0.07	3.44	0.05	2.92	0.04	2.91	0.02	0.27	0.01	0.59	0.14
FLD14	Host	-	5.08	0.12	74.29	0.98	13.43	0.18	2.61	0.09	3.55	0.03	2.48	0.03	2.95	0.06	0.36	0.01	0.50	0.00
FLD14	Host	-	5.31	0.13	73.26	0.22	13.97	0.10	2.60	0.07	3.58	0.02	2.38	0.03	3.13	0.02	0.37	0.02	0.55	0.01
FLD14	FLD14.1	X	4.41	0.10	75.39	0.22	11.61	0.03	2.90	0.08	3.82	0.02	3.32	0.04	2.88	0.05	0.27	0.03	0.51	0.01
FLD14	Host	-	4.93	0.14	74.90	0.86	12.93	0.17	2.44	0.06	3.75	0.03	2.13	0.04	2.85	0.04	0.31	0.02	0.46	0.02
FLD14	Host	-	5.26	0.13	72.56	0.47	13.17	0.09	2.28	0.07	3.67	0.01	2.18	0.02	3.10	0.01	0.37	0.03	0.51	0.02
FLD14	Host	-	5.29	0.13	73.36	0.70	13.96	0.28	2.37	0.13	3.67	0.04	2.13	0.05	3.26	0.06	0.37	0.01	0.72	0.13
FLD15	Host	-	3.28	0.03	72.46	1.00	12.80	0.19	2.99	0.06	3.67	0.02	3.48	0.03	2.90	0.03	0.30	0.02	0.57	0.01
FLD15	Host	-	3.59	0.04	72.87	0.45	12.43	0.08	2.90	0.03	3.75	0.01	3.17	0.06	2.82	0.02	0.28	0.02	0.55	0.02
FLD15	Host	-	3.78	0.04	71.93	1.00	12.51	0.16	2.91	0.07	3.75	0.03	3.35	0.04	2.83	0.04	0.31	0.02	0.55	0.00
FLD15	Host	-	3.32	0.03	72.14	1.11	12.89	0.16	3.10	0.08	3.74	0.03	3.74	0.03	2.79	0.03	0.33	0.04	0.59	0.01
FLD15	Host	-	3.59	0.04	72.96	0.35	12.88	0.06	3.10	0.04	3.75	0.04	3.46	0.06	2.85	0.03	0.31	0.01	0.57	0.01
FLD15	Host	-	3.39	0.04	72.25	0.82	12.34	0.14	2.94	0.03	3.81	0.06	2.75	0.04	2.77	0.04	0.30	0.02	0.46	0.01
FLD15	Host	-	3.70	0.03	71.16	1.04	12.36	0.19	2.80	0.05	3.80	0.03	3.14	0.08	2.82	0.04	0.31	0.01	0.50	0.01
FLD15	Host	-	3.79	0.04	72.00	0.94	12.82	0.18	2.96	0.06	3.79	0.04	3.19	0.07	2.73	0.06	0.31	0.02	0.53	0.02
FLD15	Host	-	2.85	0.02	71.57	0.84	12.71	0.19	2.70	0.04	3.80	0.04	3.59	0.04	2.73	0.05	0.31	0.02	0.52	0.01

FLD15	Host	-	4.17	0.03	73.51	0.13	12.22	0.05	2.66	0.02	3.75	0.03	3.18	0.02	2.86	0.05	0.29	0.01	0.54	0.01
FLD15	Host	-	3.86	0.03	72.14	0.92	12.56	0.19	2.80	0.07	3.81	0.01	3.30	0.01	2.81	0.02	0.31	0.02	0.52	0.03
FLD15	Host	-	3.26	0.03	71.95	0.12	12.18	0.01	2.86	0.02	3.86	0.01	2.97	0.03	2.83	0.07	0.27	0.02	0.44	0.02
FLD15	Host	-	3.19	0.03	72.34	0.94	12.75	0.14	3.00	0.06	3.72	0.02	3.54	0.04	2.81	0.08	0.30	0.00	0.55	0.01
FLD15	Host	-	3.53	0.03	72.02	0.60	12.85	0.07	2.94	0.03	3.78	0.03	3.42	0.03	2.85	0.04	0.31	0.00	0.54	0.01
FLD15	Host	-	4.42	0.04	71.02	0.84	13.28	0.16	2.89	0.06	3.57	0.00	3.13	0.03	2.83	0.05	0.32	0.01	0.50	0.04
FLD16	Host	-	6.22	0.07	71.01	3.00	15.30	0.77	1.48	0.11	3.70	0.15	1.35	0.05	3.55	0.18	0.56	0.16	0.90	0.13
FLD16	Host	-	4.82	0.05	72.80	3.08	13.86	0.70	2.00	0.15	3.90	0.16	2.55	0.10	3.06	0.16	0.30	0.08	0.71	0.10
FLD16	Host	-	7.10	0.08	71.07	3.01	17.55	0.88	2.73	0.20	4.54	0.18	1.42	0.06	2.45	0.12	0.34	0.09	0.59	0.08
FLD16	Host	-	6.06	0.06	73.89	3.13	14.17	0.71	1.96	0.15	3.77	0.15	1.27	0.05	2.80	0.14	0.40	0.11	0.61	0.09
FLD16	Host	-	5.30	0.05	69.90	2.96	15.22	0.76	2.41	0.18	4.70	0.19	1.79	0.07	3.18	0.16	0.40	0.11	0.88	0.13
FLD16	Host	-	5.52	0.05	69.81	2.95	15.92	0.80	2.89	0.22	5.02	0.20	1.85	0.07	3.69	0.19	0.43	0.12	0.80	0.11
FLD16	Host	-	5.36	0.04	78.58	3.32	13.36	0.67	2.20	0.16	4.70	0.19	1.03	0.04	2.00	0.10	0.41	0.11	0.65	0.09
FLD16	Host	-	4.17	0.04	79.16	3.35	13.71	0.69	2.46	0.18	4.93	0.20	0.97	0.04	1.71	0.09	0.25	0.07	0.59	0.08
FLD16	Host	-	4.05	0.03	76.47	3.23	13.22	0.66	2.56	0.19	5.11	0.20	1.02	0.04	1.57	0.08	0.17	0.05	0.48	0.07
FLD16	Host	-	6.34	0.06	74.98	3.17	13.14	0.66	2.66	0.20	4.86	0.19	1.49	0.06	3.02	0.15	0.26	0.07	0.53	0.08
FLD16	Host	-	5.51	0.05	74.99	3.17	13.52	0.68	2.48	0.18	4.50	0.18	1.47	0.06	3.43	0.17	0.43	0.12	0.83	0.12
FLD16	Host	-	5.54	0.04	62.41	2.64	13.47	0.68	3.08	0.23	2.84	0.11	12.08	0.48	3.77	0.19	0.38	0.11	1.05	0.15
FLD16	Host	-	5.11	0.06	73.91	3.13	13.00	0.65	2.40	0.18	4.28	0.17	1.78	0.07	2.74	0.14	0.34	0.09	0.55	0.08
FLD16	Host	-	8.70	0.09	70.68	1.04	17.42	2.09	2.08	0.16	3.97	0.56	1.54	0.03	3.40	0.34	0.62	0.14	0.88	0.13
FLD16	Host	-	6.06	0.06	72.46	3.06	15.81	0.79	1.53	0.11	3.68	0.15	1.56	0.06	3.40	0.17	0.49	0.14	1.04	0.15
FLD16	Host	-	1.58	0.01	67.87	2.87	16.99	0.85	2.43	0.18	4.71	0.19	2.38	0.10	3.16	0.16	0.33	0.09	0.72	0.10
FLD16	Host	-	5.61	0.06	74.50	3.15	13.64	0.68	1.59	0.12	3.90	0.16	1.67	0.07	3.11	0.16	0.34	0.09	0.67	0.10
FLD17	Host	-	4.59	0.09	74.14	1.50	12.91	0.27	3.79	0.01	4.20	0.06	2.25	0.05	2.89	0.02	0.27	0.02	0.50	0.03
FLD17	FLD17.int.1	-	3.91	0.09	74.35	0.48	13.62	0.11	4.12	0.12	3.98	0.06	3.03	0.05	2.68	0.03	0.34	0.00	0.55	0.01
FLD17	FLD17.int.1	X	4.18	0.11	75.45	1.03	12.81	0.20	3.79	0.06	3.87	0.03	2.85	0.01	2.86	0.03	0.30	0.01	0.57	0.02
FLD17	FLD17.int.1	X	5.11	0.13	76.50	0.58	12.31	0.12	3.69	0.07	3.85	0.02	2.46	0.01	2.90	0.05	0.31	0.01	0.58	0.01
FLD17	Host	-	4.85	0.18	73.40	1.34	13.50	0.30	3.84	0.16	3.93	0.02	2.42	0.01	2.90	0.04	0.35	0.01	0.68	0.15
FLD18	Host	-	4.83	0.04	74.52	0.81	14.16	0.15	2.97	0.03	3.94	0.01	2.23	0.02	3.35	0.05	0.34	0.02	0.89	0.02
FLD18	FLD18.2	-	8.19	0.40	78.09	0.70	13.67	0.11	1.77	0.01	3.92	0.08	1.42	0.03	2.41	0.06	0.29	0.04	0.77	0.03
FLD18	Host	-	4.42	0.04	76.16	1.09	13.73	0.14	2.86	0.06	3.67	0.02	2.72	0.01	3.03	0.08	0.32	0.01	0.91	0.02
FLD18	Host	-	4.82	0.04	72.54	3.07	13.06	0.66	1.85	0.14	3.38	0.14	2.30	0.09	2.45	0.12	0.33	0.09	0.45	0.06
FLD18	Host	-	3.05	0.03	73.28	3.10	13.26	0.67	1.74	0.13	3.17	0.13	2.95	0.12	2.32	0.12	0.17	0.05	0.43	0.06
FLD18	Host	-	4.19	0.04	73.44	3.11	12.83	0.64	1.59	0.12	3.06	0.12	2.53	0.10	2.43	0.12	0.06	0.02	0.31	0.04
FLD18	Host	-	4.76	0.04	73.40	3.10	13.99	0.70	1.71	0.13	3.04	0.12	2.85	0.11	2.30	0.12	0.29	0.08	0.43	0.06
FLD18	Host	-	4.55	0.04	73.25	3.10	14.34	0.72	2.42	0.18	3.80	0.15	1.69	0.07	2.75	0.14	0.22	0.06	0.57	0.08
FLD18	Host	-	4.57	0.04	75.03	3.17	13.81	0.69	2.41	0.18	3.48	0.14	2.18	0.09	2.67	0.14	0.17	0.05	0.53	0.07
FLD18	FLD18.1	X	3.86	0.11	76.00	0.48	13.34	0.19	3.81	0.11	3.83	0.04	2.27	0.01	2.92	0.01	0.32	0.01	0.72	0.14
FLD20	Host	-	2.50	0.02	75.40	0.57	13.55	0.10	2.99	0.04	3.78	0.02	3.22	0.02	2.66	0.03	0.31	0.02	0.88	0.02
FLD20	Host	-	5.40	0.05	74.33	1.21	14.53	0.19	2.72	0.08	3.70	0.06	3.00	0.05	2.57	0.04	0.35	0.04	0.95	0.01
FLD20	Host	-	3.54	0.03	76.78	0.25	13.60	0.05	2.77	0.05	3.69	0.02	2.95	0.02	2.76	0.01	0.33	0.02	0.90	0.02
FLD20	Host	-	4.60	0.04	76.36	0.69	13.61	0.10	2.91	0.05	3.61	0.06	3.31	0.06	2.66	0.05	0.29	0.02	0.89	0.00
FLD20	Host	-	4.59	0.04	77.05	3.26	12.42	0.62	2.82	0.21	3.56	0.14	3.74	0.15	2.66	0.13	0.29	0.08	0.89	0.13
FLD23	FLD23.3.1	-	4.31	0.12	72.28	3.06	13.38	0.67	2.76	0.21	3.39	0.14	2.25	0.09	2.73	0.14	0.27	0.07	0.45	0.06
FLD23	FLD23.3.2	-	4.67	0.14	74.25	3.14	12.88	0.65	2.36	0.18	3.88	0.16	2.12	0.08	2.85	0.14	0.27	0.08	0.45	0.06
FLD23	FLD23.4.1	-	4.67	0.15	72.93	3.09	13.02	0.65	2.79	0.21	3.56	0.14	2.27	0.09	2.47	0.13	0.21	0.06	0.38	0.05
FLD23	FLD23.4.2	-	4.78	0.15	71.78	3.04	13.60	0.68	3.17	0.24	3.73	0.15	1.87	0.07	2.83	0.14	0.46	0.13	0.52	0.07
FLD23	FLD23.5.1	-	4.33	0.13	73.78	3.12	13.49	0.68	2.92	0.22	3.57	0.14	2.17	0.09	2.74	0.14	0.27	0.07	0.55	0.08

FLD23	Host	-	4.86	0.46	75.39	3.19	11.68	0.59	2.76	0.21	3.68	0.15	2.06	0.08	2.33	0.12	0.21	0.06	0.46	0.07
FLD23	FLD23.1.1	-	4.42	0.13	76.79	3.25	14.07	0.71	1.99	0.15	3.55	0.14	2.54	0.10	2.41	0.12	0.32	0.09	0.42	0.06
FLD23	Host	-	5.09	0.16	76.35	3.23	13.24	0.66	2.91	0.22	3.62	0.14	1.89	0.08	2.37	0.12	0.26	0.07	0.44	0.06
FLD23	FLD23.1.2.1	-	4.43	0.14	76.40	3.23	13.97	0.70	1.45	0.11	3.66	0.15	2.44	0.10	2.53	0.13	0.19	0.05	0.43	0.06
FLD23	FLD23.1.2.2	-	4.43	0.14	75.36	3.19	13.97	0.70	1.60	0.12	3.60	0.14	2.25	0.09	2.67	0.14	0.29	0.08	0.47	0.07
FLD23	FLD23.1.3.1	-	4.00	0.12	75.82	3.21	14.18	0.71	1.69	0.13	3.94	0.16	2.33	0.09	3.06	0.16	0.30	0.08	0.38	0.05
FLD23	FLD23.1.3.2	-	4.51	0.14	77.42	3.27	14.20	0.71	1.54	0.12	3.67	0.15	1.94	0.08	2.52	0.13	0.44	0.12	0.43	0.06
FLD23	Host	-	4.39	0.13	75.31	3.19	13.68	0.69	2.23	0.17	3.68	0.15	2.09	0.08	2.76	0.14	0.35	0.10	0.48	0.07
FLD23	FLD23.2.2	-	4.28	0.14	73.98	3.13	13.47	0.68	2.74	0.20	3.34	0.13	2.17	0.09	2.63	0.13	0.42	0.11	0.38	0.05
FLD23	Host	-	4.70	0.14	73.20	3.10	13.30	0.67	2.83	0.21	3.84	0.15	2.19	0.09	2.72	0.14	0.33	0.09	0.47	0.07
FLD23	FLD23.L	-	3.79	0.08	75.23	1.17	13.27	0.32	3.95	0.02	3.53	0.05	2.98	0.04	2.95	0.05	0.32	0.01	0.68	0.15
FLD23	FLD23.L	X	4.33	0.11	76.55	1.05	12.68	0.31	4.07	0.05	3.65	0.04	2.63	0.01	2.87	0.04	0.30	0.00	0.65	0.16
FLD4.3	FLD43.1	-	9.87	0.77	75.48	0.46	12.02	0.07	1.97	0.05	3.84	0.03	1.00	0.02	3.20	0.07	0.37	0.04	0.48	0.01
FLD4.3	FLD43.2	X	9.76	0.31	78.40	0.95	10.18	0.14	1.83	0.04	3.46	0.04	1.20	0.02	2.81	0.05	0.30	0.01	0.47	0.01
FLD4.3	FLD43.3	-	10.54	0.33	78.60	0.88	10.11	0.14	1.85	0.08	3.55	0.02	1.06	0.01	2.85	0.07	0.27	0.02	0.43	0.01
FLD4.3	FLD43.3	X	8.50	0.25	77.83	1.36	11.46	0.35	1.84	0.03	3.63	0.02	1.27	0.01	3.05	0.04	0.31	0.00	0.65	0.15
FLD4.3	Host	-	7.18	0.31	71.72	0.34	13.96	0.08	3.54	0.11	3.95	0.01	1.85	0.01	3.43	0.06	0.40	0.02	0.71	0.01
FLD4.3	FLD43.5	X	8.13	0.38	72.48	0.74	14.77	0.28	3.81	0.11	3.89	0.00	2.00	0.02	3.19	0.02	0.48	0.03	0.96	0.15
U1A	Host	-	3.85	0.06	73.24	1.27	14.10	0.29	3.56	0.05	3.41	0.02	1.91	0.15	2.86	0.13	0.29	0.01	0.80	0.03
U1A	Host	-	3.08	0.05	72.53	0.17	14.11	0.40	1.56	0.26	3.43	0.05	1.94	0.04	2.83	0.03	0.30	0.01	0.77	0.03
U1A	Host	-	3.52	0.07	73.10	0.85	14.39	0.19	1.61	0.11	3.51	0.08	1.75	0.07	3.03	0.08	0.35	0.02	0.82	0.04
U1B	Host	-	7.34	0.09	74.12	1.78	13.58	0.57	1.22	0.06	3.46	0.07	1.31	0.08	2.93	0.07	0.28	0.01	0.48	0.02
U1B	Host	-	7.17	0.09	71.43	0.48	14.24	0.02	1.33	0.06	3.47	0.02	1.90	0.04	2.84	0.08	0.40	0.01	0.48	0.06
U1B	U1B.L	-	8.03	0.42	68.77	2.91	14.81	0.74	2.67	0.21	3.67	0.15	1.69	0.09	3.17	0.14	0.52	0.07	0.76	0.09
U1B	U1B.2	-	6.80	0.41	71.31	2.91	12.61	0.74	4.14	0.21	4.91	0.15	1.06	0.09	2.52	0.14	0.25	0.07	0.46	0.09
U1B	U1B.L	-	8.43	0.22	72.49	0.42	15.52	0.10	2.25	0.06	3.38	0.01	1.46	0.02	3.37	0.05	0.46	0.01	1.11	0.02
U1B	U1B.L	X	8.21	0.27	73.70	1.12	12.93	0.17	2.17	0.06	3.47	0.01	1.44	0.02	3.27	0.05	0.38	0.01	0.64	0.01
U1B	Host	-	6.28	0.09	73.38	0.68	15.17	0.05	2.83	0.17	3.66	0.05	1.32	0.00	3.51	0.10	0.34	0.01	0.56	0.01
U1B	Host	-	7.25	0.10	73.50	0.88	14.33	0.23	2.56	0.16	3.50	0.04	1.37	0.02	3.36	0.04	0.36	0.03	0.57	0.02
U2	Host	-	5.97	0.06	76.69	3.24	13.92	0.70	3.91	0.29	4.64	0.19	1.12	0.04	1.88	0.10	0.16	0.04	0.37	0.05
U2	Host	-	5.42	0.05	76.77	3.25	13.00	0.65	3.95	0.29	4.88	0.20	0.82	0.03	1.64	0.08	0.15	0.04	0.31	0.04
U2	Host	-	3.84	0.05	72.84	3.08	12.57	0.63	3.03	0.23	4.03	0.16	1.92	0.08	2.85	0.14	0.35	0.10	0.55	0.08
U2	Host	-	2.63	0.03	75.52	3.19	13.80	0.69	3.68	0.27	4.21	0.17	1.69	0.07	2.47	0.13	0.32	0.09	0.56	0.08
U2	Host	-	2.18	0.08	75.44	3.19	13.43	0.67	3.30	0.25	4.41	0.18	1.35	0.05	2.13	0.11	0.15	0.04	0.44	0.06
U2	Host	-	4.60	0.04	71.36	3.02	13.82	0.69	3.46	0.26	4.01	0.16	2.05	0.08	2.93	0.15	0.33	0.09	0.68	0.10
U2	Host	-	1.22	0.01	78.39	3.32	14.08	0.71	3.16	0.24	4.66	0.19	1.29	0.05	1.81	0.09	0.30	0.08	0.30	0.04
U2	Host	-	0.17	0.00	77.29	3.27	13.93	0.70	3.79	0.28	5.32	0.21	0.32	0.01	0.92	0.05	0.15	0.04	0.04	0.01
U2	Host	-	2.34	0.04	73.49	3.11	12.50	0.63	3.38	0.25	4.53	0.18	1.43	0.06	2.17	0.11	0.27	0.07	0.40	0.06
U2	Host	-	3.89	0.04	73.43	3.11	12.80	0.64	3.55	0.26	4.42	0.18	1.78	0.07	2.42	0.12	0.26	0.07	0.45	0.06
U2	Host	-	5.72	0.05	75.60	3.20	12.93	0.65	3.66	0.27	4.37	0.17	1.72	0.07	3.27	0.17	0.38	0.10	0.75	0.11
U2	Host	-	0.75	0.01	75.24	3.18	13.57	0.68	4.00	0.30	4.83	0.19	0.92	0.04	1.41	0.07	0.23	0.06	0.27	0.04
U2	Host	-	1.16	0.02	76.41	3.23	13.72	0.69	4.07	0.30	4.88	0.20	0.93	0.04	1.28	0.06	0.12	0.03	0.25	0.04
U2	Host	-	3.01	0.02	73.59	3.11	13.48	0.68	3.66	0.27	4.42	0.18	1.56	0.06	2.40	0.12	0.34	0.09	0.47	0.07
U2	Host	-	3.34	0.03	72.42	3.06	13.39	0.67	3.71	0.28	4.38	0.18	2.01	0.08	2.82	0.14	0.32	0.09	0.55	0.08
U2	Host	-	0.19	0.00	77.86	3.29	14.28	0.72	4.11	0.31	5.27	0.21	0.32	0.01	1.14	0.06	0.18	0.05	0.13	0.02
U2	Host	-	0.30	0.00	77.72	3.29	14.43	0.72	4.04	0.30	5.22	0.21	0.27	0.01	1.00	0.05	0.12	0.03	0.09	0.01
U2	Host	-	0.05	0.00	77.09	3.26	14.46	0.73	4.09	0.30	5.55	0.22	0.25	0.01	0.97	0.05	0.27	0.08	0.10	0.01
U2	Host	-	0.03	0.00	80.15	3.39	13.28	0.67	3.87	0.29	4.98	0.20	0.07	0.00	0.79	0.04	0.17	0.05	0.05	0.01

U2	Host	-	0.29	0.00	75.81	3.21	13.24	0.66	3.72	0.28	5.16	0.21	0.42	0.02	1.32	0.07	0.17	0.05	0.09	0.01
U2	Host	-	5.13	0.04	72.09	3.05	12.81	0.64	3.47	0.26	4.47	0.18	2.30	0.09	2.91	0.15	0.40	0.11	0.59	0.08
U2	Host	-	1.04	0.03	76.21	3.22	13.61	0.68	3.54	0.26	4.57	0.18	0.98	0.04	1.32	0.07	0.27	0.07	0.24	0.03
U2	Host	-	2.34	0.02	75.63	3.20	12.48	0.63	3.33	0.25	4.33	0.17	1.50	0.06	2.22	0.11	0.29	0.08	0.48	0.07
U2	Host	-	2.39	0.04	77.33	0.45	12.33	0.07	3.20	0.06	4.13	0.02	1.32	0.05	2.12	0.02	0.29	0.03	0.49	0.04
U2	Host	-	4.47	0.05	73.62	3.11	13.42	0.67	3.37	0.25	4.05	0.16	2.06	0.08	2.71	0.14	0.31	0.09	0.69	0.10
U2	Host	-	5.13	0.04	73.91	3.13	13.49	0.68	3.49	0.26	4.17	0.17	1.70	0.07	3.13	0.16	0.31	0.09	0.66	0.09
U2	Host	-	5.23	0.04	70.85	3.00	13.63	0.68	3.69	0.28	4.39	0.18	1.72	0.07	2.99	0.15	0.36	0.10	0.67	0.10
U2	Host	-	3.19	0.03	72.56	3.07	13.58	0.68	2.99	0.22	4.24	0.17	2.18	0.09	2.64	0.13	0.33	0.09	0.65	0.09
U2	Host	-	3.09	0.02	75.36	3.19	12.33	0.62	3.16	0.24	4.39	0.18	1.70	0.07	2.49	0.13	0.29	0.08	0.48	0.07
U2	Host	-	1.58	0.02	77.35	3.27	13.09	0.66	3.14	0.23	4.64	0.19	1.16	0.05	1.88	0.10	0.18	0.05	0.34	0.05
U2	Host	-	2.60	0.08	75.86	3.21	13.16	0.66	3.41	0.25	4.65	0.19	1.54	0.06	2.17	0.11	0.30	0.08	0.41	0.06
U2	Host	-	2.95	0.03	76.56	3.24	12.14	0.61	3.30	0.25	4.42	0.18	1.53	0.06	2.31	0.12	0.33	0.09	0.46	0.06
U2	Host	-	0.61	0.01	78.03	0.66	14.24	0.11	3.96	0.03	5.16	0.05	0.53	0.03	1.21	0.01	0.20	0.03	0.16	0.03
U2	Host	-	3.37	0.04	75.24	3.18	11.07	0.56	3.23	0.24	3.93	0.16	1.78	0.07	2.59	0.13	0.26	0.07	0.55	0.08
U2	Host	-	2.12	0.03	74.71	0.92	13.59	0.37	3.57	0.31	5.19	0.09	1.04	0.31	1.53	0.16	0.22	0.03	0.30	0.06
U2	Host	-	4.69	0.18	72.90	1.89	13.28	0.19	3.79	0.30	4.57	0.03	1.99	0.14	2.89	0.18	0.36	0.05	0.73	0.07
U2	Host	-	5.01	0.14	71.60	0.61	13.78	0.15	3.46	0.16	4.29	0.05	2.00	0.03	2.93	0.03	0.37	0.03	0.70	0.02
U2	Host	-	2.71	0.13	74.70	2.17	12.93	0.50	3.89	0.14	4.94	0.09	1.42	0.22	2.02	0.44	0.27	0.02	0.46	0.15
U2	Host	-	0.32	0.02	76.67	1.04	13.86	0.48	4.10	0.32	5.55	0.24	0.35	0.06	0.99	0.13	0.15	0.03	0.07	0.02
U2	Host	-	3.76	0.15	74.12	1.37	12.93	0.49	3.22	0.15	4.29	0.05	1.61	0.11	2.93	0.15	0.33	0.03	0.63	0.03
U2	Host	-	0.35	0.01	75.85	0.94	13.47	0.46	3.87	0.16	5.54	0.18	0.52	0.28	1.28	0.30	0.18	0.00	0.18	0.12
U2	Host	-	2.85	0.10	74.10	0.23	13.49	0.10	3.28	0.14	4.32	0.04	1.68	0.04	2.52	0.22	0.35	0.02	0.60	0.05
U2	Host	-	2.85	0.10	73.22	1.24	13.40	0.33	3.36	0.12	4.29	0.06	1.70	0.05	2.80	0.27	0.34	0.01	0.62	0.05
U2	Host	-	2.83	0.12	74.33	1.35	13.91	0.23	3.45	0.11	4.80	0.10	1.27	0.21	1.93	0.28	0.28	0.06	0.43	0.07
U2	Host	-	4.13	0.18	73.67	1.16	13.26	0.15	3.65	0.04	4.87	0.22	1.42	0.42	2.13	0.54	0.31	0.03	0.40	0.15
U2	Host	-	1.47	0.09	77.24	0.54	14.13	0.23	3.90	0.15	5.50	0.13	0.43	0.13	1.12	0.16	0.17	0.04	0.19	0.07
U2	Host	-	4.71	0.14	75.22	1.88	12.77	0.29	3.47	0.04	4.44	0.04	1.82	0.24	2.42	0.20	0.28	0.04	0.51	0.05
U2	Host	-	3.74	0.15	74.48	1.30	13.09	0.56	3.25	0.05	4.72	0.13	1.73	0.34	2.11	0.46	0.26	0.06	0.43	0.12
U3	Host	-	3.24	0.08	72.14	1.04	13.18	0.20	2.67	0.06	3.69	0.03	2.87	0.01	2.92	0.04	0.35	0.02	0.79	0.01
U3	Host	-	2.18	0.03	72.74	1.13	13.15	0.18	2.68	0.02	3.68	0.13	2.58	0.07	2.85	0.03	0.30	0.01	0.81	0.02
U3	Host	-	3.12	0.04	72.09	0.41	12.96	0.13	2.67	0.07	3.65	0.02	2.75	0.02	2.84	0.03	0.33	0.01	0.71	0.13
U3	Host	-	3.77	0.05	72.99	0.77	13.10	0.14	2.77	0.09	3.66	0.05	2.85	0.02	2.77	0.00	0.30	0.01	0.76	0.02
U3	Host	-	3.84	0.04	72.95	1.08	13.28	0.36	2.72	0.07	3.64	0.04	2.93	0.12	2.85	0.03	0.33	0.01	0.73	0.15
U3	Host	-	3.90	0.05	73.60	0.19	12.85	0.05	2.44	0.06	3.62	0.03	3.05	0.04	2.86	0.01	0.32	0.04	0.74	0.01
U3	Host	-	1.13	0.01	71.66	0.32	12.93	0.04	2.80	0.05	3.96	0.00	3.33	0.02	3.64	0.00	0.49	0.03	0.90	0.01
U3	Host	-	2.05	0.02	71.88	1.19	13.21	0.25	2.68	0.08	3.90	0.04	3.54	0.03	4.15	0.07	0.51	0.02	0.86	0.04
U3	Host	-	2.92	0.03	70.65	0.35	14.07	0.08	3.42	0.09	4.14	0.04	2.49	0.02	2.95	0.02	0.34	0.01	0.77	0.02
U3	Host	-	4.03	0.04	71.96	1.21	13.64	0.24	2.82	0.08	3.90	0.08	2.55	0.04	3.03	0.06	0.37	0.02	0.79	0.03
U3	U3.3	X	4.58	0.04	71.87	0.45	12.60	0.06	3.10	0.10	3.72	0.05	3.00	0.03	2.71	0.04	0.31	0.00	0.80	0.00
U3	U3.4	X	5.71	0.07	75.77	0.69	12.30	0.17	2.48	0.08	3.76	0.03	2.94	0.01	2.86	0.01	0.31	0.02	0.76	0.02
U3	Host	-	4.71	0.06	73.01	0.84	12.44	0.12	2.50	0.07	3.78	0.01	2.56	0.02	2.88	0.05	0.30	0.01	0.71	0.01
U3	Host	-	3.83	0.04	71.85	0.51	13.85	0.07	2.74	0.03	3.93	0.01	2.42	0.04	2.99	0.02	0.32	0.03	0.81	0.01
U3	Host	-	2.52	0.03	71.04	0.38	14.01	0.10	2.68	0.09	3.86	0.02	3.16	0.01	2.99	0.03	0.38	0.04	0.91	0.01
U3	Host	-	3.21	0.03	69.81	0.24	13.44	0.11	2.79	0.05	3.86	0.07	3.16	0.06	2.95	0.08	0.32	0.01	0.91	0.01
U3	Host	-	4.63	0.05	70.74	0.44	14.03	0.04	2.76	0.05	3.97	0.10	2.64	0.05	3.06	0.03	0.39	0.01	0.89	0.00
U3	Host	-	4.52	0.05	73.74	0.50	13.68	0.14	2.24	0.08	3.69	0.02	2.61	0.03	2.87	0.03	0.35	0.01	0.81	0.02
U3	Host	-	1.10	0.02	73.82	0.69	13.21	0.11	2.43	0.07	3.92	0.03	2.30	0.03	2.94	0.03	0.31	0.03	0.73	0.02

U3	Host	-	0.52	0.01	74.62	0.79	13.12	0.29	2.46	0.05	3.95	0.07	2.08	0.09	2.73	0.06	0.25	0.01	0.80	0.03
U3	Host	-	4.12	0.04	73.94	1.28	13.28	0.25	2.36	0.02	3.79	0.09	2.58	0.07	2.75	0.02	0.33	0.02	0.78	0.03
U3	Host	-	4.03	0.04	71.86	0.46	13.32	0.09	2.50	0.02	3.92	0.05	2.34	0.04	2.94	0.02	0.32	0.01	0.81	0.02
U3	Host	-	5.32	0.05	73.42	0.23	14.23	0.20	2.83	0.04	4.05	0.05	1.43	0.03	2.53	0.03	0.27	0.01	0.77	0.01
U3	Host	-	6.57	0.06	74.45	0.83	13.56	0.41	2.70	0.12	3.99	0.03	1.38	0.02	2.82	0.04	0.40	0.03	0.88	0.03
U3	U3.5	X	4.41	0.05	75.94	1.68	12.64	0.36	2.93	0.09	3.72	0.03	2.83	0.03	2.85	0.04	0.32	0.02	0.80	0.04
U3	Host	-	5.15	0.05	72.16	1.09	14.24	0.23	3.31	0.08	3.94	0.06	2.31	0.03	2.90	0.08	0.41	0.02	0.91	0.04
U3	Host	-	5.45	0.11	57.92	1.37	7.87	0.26	2.05	0.14	1.26	0.09	25.04	0.99	3.55	0.06	0.20	0.03	1.05	0.02
U3	U3.1	-	4.90	0.11	74.20	1.05	13.97	0.63	2.36	0.10	3.28	0.09	3.28	0.18	3.00	0.03	0.30	0.03	0.72	0.03
U3	U3.2	-	4.47	0.11	75.58	0.27	13.41	0.41	2.42	0.12	3.71	0.04	2.60	0.06	3.14	0.08	0.27	0.04	0.72	0.02
U3	Host	-	4.48	0.12	72.10	1.04	13.35	0.28	2.85	0.16	3.72	0.03	3.17	0.12	2.84	0.08	0.29	0.05	0.66	0.01
U3	Host	-	3.08	0.06	74.02	1.49	13.36	0.37	2.80	0.08	3.77	0.06	2.36	0.09	3.03	0.06	0.31	0.04	0.70	0.02
U3	Host	-	0.41	0.03	73.82	1.61	13.12	0.33	2.92	0.11	3.89	0.11	2.34	0.16	3.11	0.15	0.31	0.02	0.64	0.05
U3	Host	-	1.15	0.03	73.55	0.77	13.14	0.57	2.92	0.16	3.92	0.04	2.42	0.16	3.13	0.08	0.26	0.04	0.77	0.14
U3	Host	-	0.24	0.01	72.32	1.09	13.64	0.29	3.08	0.03	4.02	0.12	2.56	0.08	3.27	0.02	0.32	0.01	0.91	0.08
U3	Host	-	0.90	0.06	73.73	0.86	13.31	0.53	3.19	0.15	4.06	0.05	2.56	0.15	3.02	0.07	0.33	0.01	0.77	0.08
U3	Host	-	4.39	0.12	72.33	0.58	13.27	0.09	3.10	0.06	3.68	0.09	2.95	0.26	2.70	0.15	0.23	0.04	0.61	0.06
U3	Host	-	2.63	0.08	71.15	0.66	12.65	0.12	3.14	0.05	3.89	0.05	3.20	0.05	3.85	0.37	0.41	0.05	0.74	0.03
U3	Host	-	3.04	0.08	71.68	1.77	13.55	0.67	3.50	0.20	4.04	0.14	2.33	0.36	2.90	0.17	0.29	0.02	0.68	0.03
U3	Host	-	4.28	0.10	73.25	1.50	13.60	0.33	2.90	0.09	3.68	0.07	2.68	0.29	3.12	0.02	0.33	0.02	0.72	0.02
U3	Host	-	3.97	0.11	73.03	1.25	13.19	0.30	2.90	0.20	3.62	0.04	2.89	0.12	2.87	0.05	0.26	0.06	0.69	0.02
U3	Host	-	1.91	0.08	75.71	3.81	12.46	1.16	2.73	0.19	3.79	0.12	2.03	0.59	2.95	0.45	0.25	0.07	0.52	0.16
U3	Host	-	3.16	0.09	73.20	0.68	13.23	0.61	2.36	0.12	3.77	0.07	2.89	0.17	2.93	0.14	0.28	0.02	0.69	0.04
U3	Host	-	4.09	0.10	73.30	0.53	13.92	0.44	2.55	0.06	3.52	0.13	3.30	0.32	2.86	0.09	0.27	0.01	0.77	0.05
U3	Host	-	4.32	0.10	73.85	0.38	12.86	0.10	2.45	0.09	3.74	0.06	2.55	0.09	2.90	0.05	0.28	0.03	0.67	0.02
U4	U4.1	-	5.89	0.14	73.91	1.16	13.73	0.35	2.57	0.11	3.35	0.03	2.37	0.06	2.99	0.08	0.26	0.05	0.64	0.05
U4	Host	-	5.10	0.12	73.52	0.96	13.81	0.35	3.30	0.10	3.83	0.04	1.88	0.05	3.13	0.09	0.32	0.02	0.70	0.01
U4	Host	-	5.43	0.12	71.21	2.35	13.33	0.28	3.16	0.03	3.84	0.09	1.92	0.05	3.22	0.14	0.29	0.05	0.65	0.03
U4	U4.3	-	5.86	0.13	75.53	1.40	12.85	0.18	3.22	0.03	3.55	0.03	2.25	0.07	2.76	0.01	0.26	0.04	0.56	0.02
U4	U4.3	-	5.16	0.14	74.56	1.73	12.91	0.11	2.86	0.09	3.44	0.05	2.41	0.09	2.83	0.04	0.29	0.01	0.52	0.02
U4	Host	-	4.67	0.10	72.43	1.97	13.74	0.27	2.88	0.09	3.46	0.03	2.84	0.23	2.86	0.08	0.28	0.02	0.66	0.03
U4	Host	-	3.05	0.08	69.01	2.02	14.98	0.39	2.83	0.08	3.40	0.03	3.52	0.01	3.00	0.02	0.32	0.02	0.63	0.03
U4	U4.2	-	5.85	0.15	74.96	2.37	12.57	0.50	3.24	0.17	3.73	0.14	1.88	0.19	2.88	0.39	0.27	0.05	0.49	0.03
U4	Host	-	2.46	0.07	71.94	0.71	15.20	0.17	3.14	0.05	3.47	0.09	3.40	0.13	2.88	0.09	0.29	0.01	0.66	0.04
U4	Host	-	2.11	0.05	74.06	1.15	14.21	0.18	2.41	0.06	2.90	0.03	3.05	0.10	2.95	0.04	0.24	0.03	0.56	0.02
U4	U4.1	-	6.24	0.12	73.96	2.58	13.75	0.15	2.50	0.04	3.33	0.04	2.31	0.11	2.89	0.04	0.27	0.06	0.65	0.01
U4	U4.1	-	5.71	0.11	72.28	2.60	13.69	0.59	2.22	0.12	3.26	0.04	2.37	0.06	2.96	0.02	0.33	0.02	0.61	0.03
U4	U4.1	-	6.09	0.11	74.25	1.17	13.62	0.31	1.87	0.10	3.14	0.10	2.39	0.09	2.82	0.09	0.30	0.02	0.61	0.04
U4	Host	-	1.90	0.05	69.41	2.72	14.91	0.42	2.52	0.14	3.28	0.05	3.55	0.14	2.89	0.08	0.31	0.03	0.61	0.03
U4	Host	-	3.92	0.08	68.16	1.68	15.31	0.46	2.63	0.11	3.29	0.09	3.74	0.11	2.91	0.11	0.27	0.06	0.62	0.01
U4	Host	-	2.96	0.06	70.23	1.73	15.33	0.30	2.83	0.07	3.34	0.09	3.66	0.05	2.85	0.05	0.29	0.07	0.62	0.03
U4	Host	-	2.94	0.06	72.22	0.77	15.13	0.22	3.12	0.08	3.50	0.07	3.19	0.22	2.95	0.10	0.34	0.02	0.66	0.02
U4	U4.2	-	4.32	0.12	74.10	1.54	12.78	0.24	2.83	0.06	3.39	0.05	2.62	0.19	2.77	0.15	0.27	0.05	0.57	0.03
U4	U4.1	-	5.97	0.30	75.20	3.18	13.24	0.66	2.25	0.17	3.11	0.12	2.31	0.09	2.67	0.14	0.36	0.10	0.46	0.07
U4	U4.1	-	6.60	0.33	73.39	3.10	12.96	0.65	2.25	0.17	3.15	0.13	2.36	0.09	2.76	0.14	0.25	0.07	0.40	0.06
U4	U4.1	-	6.36	0.32	73.61	3.11	13.47	0.68	2.32	0.17	3.05	0.12	2.50	0.10	2.83	0.14	0.28	0.08	0.46	0.07
U4	Host	-	3.02	0.15	75.10	3.18	13.67	0.69	2.30	0.17	3.10	0.12	2.73	0.11	2.77	0.14	0.36	0.10	0.44	0.06
U4	Host	-	3.28	0.16	75.49	3.19	13.75	0.69	2.37	0.18	3.09	0.12	2.54	0.10	2.73	0.14	0.31	0.09	0.47	0.07

U4	Host	-	3.20	0.16	72.19	3.05	13.09	0.66	2.18	0.16	3.15	0.13	2.50	0.10	2.82	0.14	0.31	0.09	0.40	0.06
U4	Host	-	3.23	0.16	72.54	3.07	13.21	0.66	2.27	0.17	3.21	0.13	2.56	0.10	2.66	0.13	0.35	0.10	0.44	0.06
U4	Host	-	2.64	0.13	74.69	3.16	13.72	0.69	2.36	0.18	3.19	0.13	2.55	0.10	2.78	0.14	0.32	0.09	0.41	0.06
U4	Host	-	2.82	0.14	73.08	3.09	13.36	0.67	2.17	0.16	3.18	0.13	2.40	0.10	2.80	0.14	0.38	0.11	0.50	0.07
U4	Host	-	2.13	0.11	74.69	3.16	13.36	0.67	2.19	0.16	3.13	0.13	2.40	0.10	2.66	0.14	0.31	0.09	0.46	0.07
U4	Host	-	2.34	0.12	77.02	3.26	13.44	0.67	2.34	0.17	3.10	0.12	2.26	0.09	2.57	0.13	0.30	0.08	0.53	0.08

Appendix H

PCA

H.1 The PCA model

As discussed in Section 6.2, the PCA model is generated using the grid-based EDS analyses across 37 hosts ($n = 3,698$). Prior to generating the model, the data (tabulated in Appendix B) are imputed, mean centered, and scaled so each major element oxide has a variance of 1. The variance explained by each PC is tabulated in Appendix 6.5.

Table H.1: Means subtracted from each major element oxide and scaling factors so each major element oxide has unit variance prior to generating the PCA model.

	Mean (wt.%)	Scaling Factor
SiO_2	73.77	4.12
Al_2O_3	13.59	2.16
Na_2O	3.26	0.70
K_2O	3.80	0.70
CaO	2.12	0.99
FeO	2.77	0.76
TiO_2	0.32	0.17
MgO	0.60	0.26

H.2 Deviations between EDS only and combined EDS/SIMS datasets

Table H.2: Loadings of the principal components. Although the loadings for all PCs are listed, only the first 5 are retained.

	PC1	PC2	PC3	PC4	PC5	PC6	PC7	PC8
SiO_2	-0.506	0.032	-0.138	0.136	-0.139	0.235	0.073	0.791
Al_2O_3	0.438	-0.071	0.397	-0.382	-0.074	-0.383	0.327	0.490
Na_2O	0.332	-0.445	-0.098	0.516	0.078	0.306	0.562	-0.004
K_2O	0.333	-0.496	0.087	-0.087	-0.094	0.355	-0.672	0.204
CaO	0.147	0.488	0.504	0.166	0.519	0.416	-0.064	0.107
FeO	0.366	0.217	-0.493	0.371	0.306	-0.433	-0.276	0.284
TiO_2	0.305	0.284	-0.545	-0.532	-0.002	0.457	0.190	0.027
MgO	0.285	0.430	0.111	0.335	-0.773	0.089	-0.058	-0.030

Table H.3: Percent deviation of the composition of each major element oxide from EDS rasters collected around SIMS craters relative to the EDS rasters collected across entire objects in a grid-based pattern. Na_2O is excluded, as discussed in Chapter 5

					Deviation of composition from EDS rasters collected around SIMS craters from compositions of EDS rasters collected across entire objects (%)													
Sample	Object	EDS Count	U/EDS Count	Equiv. d (μm)	SiO_2	1σ	Al_2O_3	1σ	K_2O	1σ	CaO	1σ	FeO	1σ	TiO_2	1σ	MgO	1σ
AE.C	Host	188	1	2224	-1.7	-7.4	-15.7	-20.9	20.6	17.4	41.1	60.4	12.8	19.6	-24.3	-45.9	39.6	47.4
AG.D	Host	127	1	2410	-5.9	-6.9	7.4	20.7	22.5	21.7	-3.2	-38.3	21.3	26.4	-2.8	-30.9	-12.2	-31.3
AH.E	Host	55	1	2298	1.0	2.8	-28.9	-9.2	37.2	5.6	-16.6	-41.0	-23.3	-7.5	-37.4	-21.8	-61.0	-27.8
AA.B	B1	43	1	384	0.1	2.2	-11.8	-5.7	21.1	7.7	-29.7	-14.8	-15.2	-8.2	1.6	24.3	-31.9	-11.5
AA.B	B2	4	1	70	-0.2	-2.4	-4.1	-4.5	9.1	2.5	9.7	13.1	-22.2	-5.6	5.7	27.2	-49.2	-15.4
AE.C	C1	12	1	200	0.1	2.1	-22.8	-6.3	20.0	13.2	1.3	13.2	4.7	7.8	-12.5	-21.5	-14.4	-9.6
AE.C	C2	14	1	207	1.1	1.1	-20.5	-7.7	41.5	11.0	-53.3	-9.2	-10.0	-7.2	-16.5	-25.0	-32.7	-13.3
AG.D	D2	19	1	283	-5.3	-9.4	13.3	29.2	23.9	27.9	-10.1	-37.9	21.4	28.7	11.6	38.1	8.7	30.3
AH.E	E1	9	1	178	-3.6	-3.2	-1.5	-4.0	25.7	12.5	17.0	21.8	-7.4	-10.3	-5.3	-16.4	-22.7	-9.6
FLD10	Host	343	5	4404	-2.3	-12.9	8.8	33.0	-1.5	-30.2	67.7	124.7	12.0	77.0	15.4	189.4	70.0	122.8
FLD10	FLD10.L	30	2	1089	2.0	2.9	-1.1	-2.8	-1.0	-4.6	10.2	12.1	7.0	4.6	2.7	16.4	20.1	8.7
FLD14	Host	89	10	2886	-1.1	-2.8	-5.0	-6.0	5.4	7.6	-18.7	-21.2	6.2	10.4	31.8	36.0	-12.6	-20.0
FLD14	FLD14.1	7	1	157	3.0	2.8	-4.7	-2.4	-9.0	-3.3	13.3	7.9	16.5	4.1	1.8	16.8	-15.7	-28.2
FLD14	FLD14.L	75	2	856	2.0	2.7	-9.7	-10.5	12.8	8.3	-0.5	-18.9	0.5	10.0	-10.4	-18.1	-33.5	-21.4
FLD15	Host	144	15	2452	-1.7	-2.5	-2.1	-5.3	0.3	4.9	4.7	17.2	2.8	6.0	0.5	16.5	-4.1	-16.6
FLD16	Host	75	18	2155	-1.8	-10.3	4.4	23.4	8.0	23.7	35.4	181.5	1.1	38.1	3.9	60.9	15.7	50.9
FLD17	Host	39	2	2352	-0.5	-3.6	-3.1	-12.9	2.1	14.1	0.1	29.4	6.7	12.5	11.6	39.8	-3.5	-38.8
FLD17	FLD17.int.2	6	1	111	-3.4	-2.1	7.1	5.7	7.5	2.4	55.5	7.7	-0.8	-4.0	15.8	9.1	-1.1	-7.4
FLD18	Host	90	10	1824	-0.8	-7.2	1.2	15.0	-9.6	-21.7	1.9	42.9	-0.7	-29.3	-12.0	-70.6	-22.9	-52.4
FLD18	FLD18.1	5	1	60	3.1	1.8	-3.3	-7.3	3.0	7.7	-18.8	-6.6	3.0	2.3	2.7	7.5	1.5	43.6
FLD18	FLD18.2	28	1	124	4.3	2.8	-2.2	-4.3	1.7	6.5	-16.8	-22.8	-8.0	-11.7	-10.9	-18.7	9.9	25.7
FLD20	Host	105	5	2287	2.2	7.9	3.8	22.5	-2.6	-19.5	7.2	33.7	-0.4	-20.7	-4.1	-33.2	32.3	21.3
FLD23	Host	47	4	1926	0.1	12.0	13.2	36.6	4.7	28.2	7.0	42.7	6.9	37.8	7.7	55.5	-7.9	-33.7
FLD23	FLD23.1.1	3	1	46	1.9	5.5	0.2	6.0	-4.3	-5.0	-1.5	-8.1	-8.7	-6.9	-5.5	-21.4	-27.6	-14.4
FLD23	FLD23.1.2	3	2	47	0.1	1.6	0.0	1.7	-3.9	-3.2	2.5	12.6	-4.5	-5.9	-27.7	-32.3	-22.7	-8.6
FLD23	FLD23.1.3	3	2	47	0.2	4.7	0.9	2.0	1.6	8.6	-1.4	-26.3	2.2	19.2	9.1	38.6	-34.1	-11.7
FLD23	FLD23.2.2	4	1	31	-2.9	-5.7	-4.9	-7.4	-11.1	-4.3	-8.5	-9.2	-3.0	-7.1	22.0	24.9	-37.7	-17.6
FLD23	FLD23.3.1	4	1	40	-3.3	-5.2	-4.9	-6.3	-9.2	-4.8	-2.4	-9.9	0.9	5.4	-18.7	-27.2	-27.8	-13.4
FLD23	FLD23.3.2	2	1	17	-1.0	-5.4	-5.1	-9.4	-2.9	-5.3	-5.5	-16.1	5.2	7.1	-10.2	-18.1	-23.3	-19.8
FLD23	FLD23.4.1	5	1	42	-2.5	-4.9	-5.5	-5.3	-6.8	-7.6	1.4	7.6	-5.5	-5.1	-33.1	-25.9	-37.4	-13.2
FLD23	FLD23.4.2	6	1	43	-3.1	-5.1	-1.0	-8.8	-6.5	-5.4	-13.8	-13.9	5.3	8.9	43.6	25.9	-16.1	-21.6
FLD23	FLD23.5.1	4	1	60	-0.1	-4.9	-1.3	-6.7	-5.8	-5.5	-9.0	-11.2	6.2	8.4	-9.7	-29.2	-2.4	-23.3
FLD23	FLD23.L	8	1	498	2.6	2.2	2.4	5.0	5.1	8.0	0.2	11.5	13.2	4.2	12.6	8.3	23.9	31.7
FLD4.3	Host	55	1	1470	0.0	3.8	-0.8	-11.6	-1.4	-5.2	9.1	37.2	10.3	10.5	5.7	25.8	-13.6	-27.8
FLD4.3	FLD4.3.2	3	1	41	0.5	2.3	-2.4	-6.2	-3.0	-2.8	-5.3	-9.0	2.3	4.7	2.2	6.6	-1.9	-5.0
FLD4.3	FLD4.3.3	3	1	53	-0.2	-1.7	-2.0	-5.1	-1.6	-2.6	5.4	8.8	3.2	6.2	-5.1	-19.1	2.8	8.6
U1A	Host	60	3	1584	0.2	3.8	5.3	8.5	2.0	8.8	0.7	21.5	0.8	11.0	1.2	23.0	73.5	19.8
U1B	Host	60	8	1339	-1.1	-7.6	2.8	18.3	3.4	13.1	4.2	33.4	5.8	19.9	0.1	29.4	-11.3	-24.6

U1B	U1B.2	9	1	84	-2.3	-5.9	3.4	18.2	7.3	11.4	-0.1	-34.5	-9.4	-25.8	-20.5	-28.3	0.9	27.0
U1B	U1B.L	25	2	195	-1.1	-6.7	-2.7	-7.2	-2.5	-8.4	-1.9	-18.5	0.4	9.7	1.9	19.0	11.9	37.5
U2	Host	67	48	1539	2.3	5.7	1.4	12.0	1.8	18.2	-7.1	-96.1	-5.1	-67.5	-4.5	-63.1	-13.6	-89.9
U3	Host	72	39	2369	-1.4	-6.3	-0.5	-12.7	-0.0	-16.6	16.6	153.4	3.0	20.8	-3.0	-34.2	9.3	28.9
U3	U3.1	7	1	134	1.2	4.0	1.1	9.6	1.0	5.6	-0.9	-12.0	2.9	4.8	-3.6	-19.6	12.0	19.9
U3	U3.2	6	1	191	1.4	2.3	3.9	8.5	-0.1	-1.9	-1.1	-5.0	4.0	7.9	-6.2	-31.4	16.5	22.0
U4	Host	74	18	2230	1.5	5.4	-2.1	-12.5	-6.9	-12.9	-3.3	-48.3	-0.6	-10.9	-9.5	-23.4	-12.0	-23.7
U4	U4.1	13	8	553	-1.3	-3.4	-2.6	-5.0	-2.1	-6.8	1.0	7.0	-2.5	-7.3	6.7	32.4	-16.0	-22.8
U4	U4.2	7	2	335	1.3	2.4	-1.3	-2.9	9.1	9.7	-17.6	-22.6	6.4	8.5	-4.5	-21.5	30.4	23.5
U4	U4.3	29	2	465	-1.8	-2.8	-5.0	-2.8	3.8	7.6	-7.4	-12.7	3.0	4.5	-0.1	-15.9	-29.6	-10.2

Appendix I

MDS and Euclidean Distance Data

I.1 MDS plots

Table I.1: MDS coordinates of the EDS grid data set of hosts and EDS measurements of agglomerates where each object's composition is determined by its median composition (derived from data in Appendices B and C and excluding MgO, as discussed in the text). The resulting MDS plot is shown in Figure 7.4. Each coordinate pair refers to the mean coordinates from 500 non-metric MDS models of 500 randomly-generated UP matrices (Fig. 7.3). Uncertainties to refer to 2 standard deviation about these values.

Type	Sample	Agglomerate	Attachment Location	MDS1	1σ	MDS2	1σ
Agglomerate	AA.B	B1	Exterior	-0.53	0.05	-0.41	0.06
Agglomerate	AA.B	B2	Surface	-0.72	0.17	-0.56	0.14
Agglomerate	AA.B	B3	Exterior	-0.66	0.05	-0.38	0.06
Agglomerate	AE.C	C1	Exterior	-0.83	0.10	-0.07	0.07
Agglomerate	AE.C	C2	Exterior	-0.26	0.09	-0.55	0.10
Agglomerate	AE.C	C3	Exterior	-2.36	0.21	0.13	0.13
Agglomerate	AE.C	C4	Exterior	-1.33	0.14	0.10	0.10
Agglomerate	AG.D	D1	Exterior	-0.99	0.11	0.34	0.08
Agglomerate	AG.D	D2	Exterior	-0.25	0.07	0.21	0.07
Agglomerate	AH.E	E1	Exterior	-1.11	0.13	0.66	0.10
Agglomerate	AH.E	E2	Exterior	-0.10	0.08	-0.11	0.07
Agglomerate	FLD10	FLD10.L	Exterior	-0.10	0.04	-0.02	0.04
Agglomerate	FLD14	FLD14.1	Surface	-0.35	0.14	-0.73	0.12
Agglomerate	FLD14	FLD14.L	Exterior	0.03	0.05	-0.65	0.04
Agglomerate	FLD17	FLD17.1	Exterior	-0.25	0.09	-0.21	0.08
Agglomerate	FLD17	FLD17.2	Surface	-0.02	0.06	-0.48	0.06
Agglomerate	FLD17	FLD17.int.1	Interior	-0.20	0.10	0.01	0.06
Agglomerate	FLD17	FLD17.int.2	Interior	0.18	0.13	-0.63	0.11
Agglomerate	FLD17	FLD17.tail	Exterior	-0.44	0.10	-0.32	0.08
Agglomerate	FLD18	FLD18.1	Exterior	0.07	0.10	-0.35	0.08
Agglomerate	FLD18	FLD18.2	Interior	0.72	0.10	0.29	0.06
Agglomerate	FLD18	FLD18.3	Interior	0.33	0.07	-0.14	0.06
Agglomerate	FLD18	FLD18.4	Surface	0.02	0.05	-0.22	0.04
Agglomerate	FLD21	FLD21.1	Surface	0.19	0.09	-0.55	0.06
Agglomerate	FLD21	FLD21.L	Surface	0.54	0.13	-1.15	0.12
Agglomerate	FLD23	FLD23.1.1	Surface	1.05	0.18	-0.16	0.13
Agglomerate	FLD23	FLD23.1.2	Surface	0.96	0.16	0.01	0.11
Agglomerate	FLD23	FLD23.1.3	Surface	0.83	0.16	0.05	0.10
Agglomerate	FLD23	FLD23.2.1	Surface	1.17	0.17	-0.05	0.14
Agglomerate	FLD23	FLD23.2.2	Surface	0.79	0.14	-0.02	0.09
Agglomerate	FLD23	FLD23.3.1	Surface	0.41	0.11	-0.05	0.08

Agglomerate	FLD23	FLD23.3.2	Surface	0.26	0.15	-0.02	0.10
Agglomerate	FLD23	FLD23.4.1	Surface	0.09	0.11	-0.09	0.08
Agglomerate	FLD23	FLD23.4.2	Surface	-0.10	0.09	-0.03	0.06
Agglomerate	FLD23	FLD23.5.1	Surface	0.03	0.12	-0.16	0.09
Agglomerate	FLD23	FLD23.L	Exterior	0.72	0.11	-0.46	0.09
Agglomerate	FLD4.3	FLD4.3.1	Interior	1.12	0.22	1.24	0.14
Agglomerate	FLD4.3	FLD4.3.2	Interior	1.24	0.21	0.95	0.14
Agglomerate	FLD4.3	FLD4.3.3	Interior	1.10	0.24	1.35	0.15
Agglomerate	FLD4.3	FLD4.3.4	Surface	0.16	0.13	0.85	0.13
Agglomerate	FLD4.3	FLD4.3.5	Interior	0.35	0.18	0.78	0.19
Agglomerate	FLD4.3	FLD4.3.UA	Surface	1.26	0.15	0.24	0.10
Agglomerate	FLD4.4	FLD4.4.1	Surface	1.66	0.13	-0.29	0.13
Agglomerate	FLD4.4	FLD4.4.2	Surface	1.44	0.13	-0.33	0.14
Agglomerate	U1B	U1B.2	Surface	-1.31	0.16	1.05	0.12
Agglomerate	U1B	U1B.L	Interior	0.93	0.10	0.63	0.08
Agglomerate	U3	U3.1	Surface	0.63	0.12	-0.60	0.08
Agglomerate	U3	U3.2	Surface	0.51	0.10	-0.33	0.12
Agglomerate	U3	U3.3	Surface	-0.20	0.07	-0.63	0.07
Agglomerate	U3	U3.4	Surface	-0.08	0.09	-0.42	0.07
Agglomerate	U3	U3.5	Surface	-0.16	0.09	-0.48	0.08
Agglomerate	U4	U4.1	Surface	0.58	0.10	-0.24	0.09
Agglomerate	U4	U4.2	Interior	-0.04	0.12	-0.30	0.09
Agglomerate	U4	U4.3	Surface	0.66	0.07	-0.41	0.07
Agglomerate	U4	U4.4	Surface	0.29	0.09	-0.70	0.09
Agglomerate	U4	U4.5	Surface	-0.33	0.10	-0.08	0.06
Agglomerate	U4	U4.6	Surface	0.28	0.12	-0.06	0.12
Agglomerate	U4	U4.7	Surface	0.42	0.07	-0.47	0.08
Host	AA.B	-	-	-0.59	0.04	-0.02	0.04
Host	AE.C	-	-	-0.75	0.06	0.46	0.05
Host	AG.D	-	-	-0.02	0.02	0.03	0.02
Host	AH.E	-	-	-0.40	0.06	0.64	0.06
Host	CC	-	-	-0.26	0.03	-0.01	0.03
Host	CD	-	-	-0.08	0.03	0.24	0.03
Host	FLD10	-	-	-0.85	0.08	0.83	0.07
Host	FLD11	-	-	-0.17	0.03	-0.31	0.03
Host	FLD12	-	-	-0.32	0.03	0.27	0.03
Host	FLD13	-	-	0.04	0.05	-0.68	0.05
Host	FLD14	-	-	0.10	0.07	-0.80	0.07
Host	FLD15	-	-	-0.28	0.04	-0.50	0.04
Host	FLD16	-	-	-0.04	0.04	0.42	0.04
Host	FLD17	-	-	-0.30	0.06	-0.20	0.04
Host	FLD18	-	-	-0.09	0.03	-0.20	0.03
Host	FLD20	-	-	-0.17	0.05	-0.55	0.04
Host	FLD21	-	-	-0.02	0.06	-0.73	0.05
Host	FLD23	-	-	0.35	0.05	0.02	0.05
Host	FLD25	-	-	-2.53	0.17	-1.20	0.17
Host	FLD3.1	-	-	0.25	0.04	0.35	0.04
Host	FLD3.2	-	-	0.43	0.15	1.98	0.13
Host	FLD3.3	-	-	0.26	0.04	0.24	0.03
Host	FLD4.1	-	-	0.15	0.03	-0.16	0.02
Host	FLD4.2	-	-	0.49	0.06	0.44	0.06
Host	FLD4.3	-	-	-0.13	0.04	0.31	0.04
Host	FLD4.4	-	-	0.45	0.05	-0.12	0.04
Host	FLD5.1	-	-	0.05	0.05	0.42	0.06
Host	FLD5.2	-	-	-0.34	0.06	0.53	0.06
Host	FLD5.3	-	-	-1.53	0.20	1.75	0.15
Host	FLD5.4	-	-	-0.39	0.06	0.44	0.06
Host	FLD5.5	-	-	-0.03	0.10	0.75	0.08
Host	FLD9	-	-	-0.20	0.02	0.10	0.02
Host	U1A	-	-	-0.30	0.05	0.26	0.04
Host	U1B	-	-	-0.49	0.06	0.58	0.05
Host	U2	-	-	-0.76	0.07	0.31	0.06

Host	U3	-	-	0.04	0.04	-0.32	0.03
Host	U4	-	-	0.18	0.04	-0.37	0.03

Table I.2: MDS coordinates of the agglomerates and hosts characterized with both SIMS analyses and EDS rasters within/around the SIMS analysis craters. Each object's composition is determined by its median composition (derived from data in Appendix G, excluding MgO, as discussed in the text). The resulting MDS plot is shown in the top left plot of Figure 7.6. Each coordinate pair refers to the mean coordinates from 500 non-metric MDS models of 500 randomly-generated UP matrices (Fig. 7.3). Uncertainties to refer to 2 standard deviation about these values.

Type	Sample	Agglomerate	MDS1	1σ	MDS2	1σ
Agglomerate	AA.B	B1	-0.60	0.40	-0.68	0.18
Agglomerate	AA.B	B2	1.73	0.41	-1.33	0.34
Agglomerate	AE.C	C1	-0.63	0.20	-0.75	0.18
Agglomerate	AE.C	C2	-1.30	0.40	-1.64	0.23
Agglomerate	AG.D	D2	-1.24	0.32	0.81	0.38
Agglomerate	AH.E	E1	-1.30	0.35	-1.23	0.22
Agglomerate	FLD10	FLD10.L	-0.16	0.06	0.39	0.12
Agglomerate	FLD14	FLD14.1	1.24	0.12	0.06	0.30
Agglomerate	FLD14	FLD14.L	1.30	0.09	-0.19	0.17
Agglomerate	FLD17	FLD17.int.1	1.47	0.11	0.44	0.17
Agglomerate	FLD18	FLD18.1	1.00	0.18	0.33	0.19
Agglomerate	FLD18	FLD18.2	-1.26	0.14	-0.38	0.32
Agglomerate	FLD23	FLD23.1.1	0.81	0.27	-0.18	1.11
Agglomerate	FLD23	FLD23.1.2	0.41	0.19	-1.17	0.53
Agglomerate	FLD23	FLD23.1.3	0.01	0.18	-0.10	0.94
Agglomerate	FLD23	FLD23.2.2	0.48	0.25	0.88	1.00
Agglomerate	FLD23	FLD23.3.1	0.60	0.20	-0.21	0.68
Agglomerate	FLD23	FLD23.3.2	0.18	0.22	-0.33	0.56
Agglomerate	FLD23	FLD23.4.1	0.70	0.25	-0.92	0.73
Agglomerate	FLD23	FLD23.4.2	0.23	0.26	1.24	0.82
Agglomerate	FLD23	FLD23.5.1	0.69	0.23	-0.18	0.53
Agglomerate	FLD23	FLD23.L	1.39	0.25	0.48	0.21
Agglomerate	FLD4.3	FLD4.3.2	-2.64	0.13	0.19	0.21
Agglomerate	FLD4.3	FLD4.3.3	-3.24	0.16	-0.05	0.26
Agglomerate	U1B	U1B.2	-1.10	0.34	-1.31	0.66
Agglomerate	U1B	U1B.L	-1.20	0.17	1.69	0.23
Agglomerate	U3	U3.1	0.96	0.17	0.40	0.30
Agglomerate	U3	U3.2	0.74	0.15	-0.14	0.37
Agglomerate	U4	U4.1	0.04	0.07	0.24	0.13
Agglomerate	U4	U4.2	0.43	0.17	-0.06	0.30
Agglomerate	U4	U4.3	0.39	0.07	0.07	0.13
Interface	FLD10	FLD10.L	-0.92	0.16	0.55	0.27
Interface	FLD17	FLD17.int.1	0.90	0.08	0.27	0.15
Interface	FLD23	FLD23.L	1.12	0.23	0.35	0.22
Interface	FLD4.3	FLD4.3.1	-3.05	0.19	0.57	0.25
Interface	FLD4.3	FLD4.3.3	-1.90	0.17	0.23	0.15
Interface	FLD4.3	FLD4.3.5	-0.49	0.24	1.87	0.25
Interface	U1B	U1B.L	-1.53	0.12	0.79	0.14
Interface	U3	U3.3	1.36	0.12	0.58	0.18
Interface	U3	U3.4	0.73	0.11	0.47	0.24
Interface	U3	U3.5	1.14	0.12	0.47	0.21
Host	AE.C	-	-0.30	0.22	-1.20	0.48
Host	AG.D	-	-1.21	0.39	-0.28	0.29
Host	AH.E	-	-2.20	0.77	-1.74	0.31
Host	FLD10	-	-0.54	0.07	0.40	0.12
Host	FLD14	-	0.48	0.07	0.30	0.08
Host	FLD15	-	1.34	0.08	0.23	0.14

Host	FLD16	-	-0.41	0.10	0.26	0.27
Host	FLD17	-	0.69	0.11	0.20	0.14
Host	FLD18	-	0.50	0.10	-0.35	0.21
Host	FLD20	-	1.48	0.13	0.48	0.22
Host	FLD23	-	0.36	0.13	-0.23	0.28
Host	FLD4.3	-	-0.56	0.11	0.99	0.14
Host	U1A	-	0.49	0.13	-0.02	0.38
Host	U1B	-	-1.38	0.12	0.38	0.18
Host	U2	-	1.19	0.25	-1.45	0.25
Host	U3	-	1.04	0.07	0.28	0.11
Host	U4	-	1.35	0.10	0.03	0.22

I.2 Euclidean distances and distance percentiles

Table I.3: Euclidean distances and distance percentiles of agglomerates from *their* host objects for the major element only data (as shown in Figure 7.8). Euclidean distances and distance percentiles correspond to mean values from 500 randomly generated UP matrices and the 2σ uncertainties correspond to 2 standard deviations about this mean value.

Sample	Agglomerate	Location	Euclidean Distance	2σ	Distance Percentile	2σ
AA.B	B1	Exterior	0.62	0.09	5.64	4.10
AA.B	B2	Surface	0.91	0.34	28.94	31.18
AA.B	B3	Exterior	0.55	0.08	2.88	2.77
AE.C	C1	Exterior	0.76	0.17	10.27	6.81
AE.C	C2	Exterior	1.49	0.19	49.46	10.10
AE.C	C3	Exterior	1.91	0.33	77.09	15.17
AE.C	C4	Exterior	0.97	0.28	20.57	12.31
AG.D	D1	Exterior	1.31	0.22	78.13	8.51
AG.D	D2	Exterior	0.55	0.18	15.13	15.14
AH.E	E1	Exterior	1.07	0.25	23.47	13.46
AH.E	E2	Exterior	1.05	0.17	21.95	7.18
FLD10	FLD10.L	Exterior	1.44	0.17	28.33	7.28
FLD14	FLD14.1	Surface	1.18	0.25	43.48	17.52
FLD14	FLD14.L	Exterior	0.54	0.18	3.87	3.18
FLD17	FLD17.1	Exterior	0.44	0.21	5.07	10.96
FLD17	FLD17.2	Surface	0.62	0.14	15.99	11.34
FLD17	FLD17.int.1	Interior	0.52	0.23	9.02	14.76
FLD17	FLD17.int.2	Interior	0.96	0.27	46.83	21.69
FLD17	FLD17.tail	Exterior	0.47	0.26	6.44	13.69
FLD18	FLD18.1	Exterior	0.49	0.29	14.07	20.83
FLD18	FLD18.2	Interior	1.31	0.22	75.28	9.53
FLD18	FLD18.3	Interior	0.75	0.21	37.00	18.92
FLD18	FLD18.4	Surface	0.38	0.14	5.71	7.97
FLD21	FLD21.1	Surface	0.54	0.27	7.29	10.34
FLD21	FLD21.L	Surface	0.95	0.21	33.66	16.04
FLD23	FLD23.1.1	Surface	0.96	0.36	36.61	36.93
FLD23	FLD23.1.2	Surface	0.88	0.34	25.75	34.04
FLD23	FLD23.1.3	Surface	0.79	0.37	19.46	29.99
FLD23	FLD23.2.1	Surface	1.08	0.38	45.92	37.17
FLD23	FLD23.2.2	Surface	0.72	0.30	13.78	22.42
FLD23	FLD23.3.1	Surface	0.55	0.26	4.68	9.65
FLD23	FLD23.3.2	Surface	0.48	0.37	4.44	18.56
FLD23	FLD23.4.1	Surface	0.61	0.25	5.90	10.87
FLD23	FLD23.4.2	Surface	0.69	0.24	10.29	14.09
FLD23	FLD23.5.1	Surface	0.69	0.28	9.91	17.39

FLD23	FLD23.L	Exterior	0.83	0.19	20.74	19.11
FLD4.3	FLD4.3.1	Interior	1.89	0.36	90.65	7.11
FLD4.3	FLD4.3.2	Interior	1.92	0.36	91.08	6.33
FLD4.3	FLD4.3.3	Interior	2.05	0.34	93.84	5.24
FLD4.3	FLD4.3.4	Surface	0.84	0.31	25.50	24.58
FLD4.3	FLD4.3.5	Interior	1.03	0.39	38.70	29.63
FLD4.3	FLD4.3.UA	Surface	1.70	0.31	85.69	10.05
FLD4.4	FLD4.4.1	Surface	1.50	0.19	78.73	8.23
FLD4.4	FLD4.4.2	Surface	1.26	0.20	64.16	15.51
U1B	U1B.2	Surface	1.45	0.23	51.03	16.49
U1B	U1B.L	Interior	1.73	0.20	70.74	9.74
U3	U3.1	Surface	0.93	0.23	46.61	18.07
U3	U3.2	Surface	0.82	0.29	35.93	23.50
U3	U3.3	Surface	0.58	0.15	15.48	14.35
U3	U3.4	Surface	0.39	0.20	4.57	9.92
U3	U3.5	Surface	0.49	0.23	11.32	18.41
U4	U4.1	Surface	0.86	0.23	36.55	19.47
U4	U4.2	Interior	0.65	0.28	15.60	21.04
U4	U4.3	Surface	0.95	0.17	45.54	13.57
U4	U4.4	Surface	0.65	0.20	17.30	17.07
U4	U4.5	Surface	0.92	0.23	43.42	19.02
U4	U4.6	Surface	0.71	0.18	22.12	16.55
U4	U4.7	Surface	0.68	0.19	19.26	17.33

Table I.4: Euclidean distances and distance percentiles of agglomerates from *their* host objects for the combined major element/U isotopic data (as shown in Figure 7.9). Euclidean distances and distance percentiles correspond to mean values from 500 randomly generated UP matrices and the 2σ uncertainties correspond to 2 standard deviations about this mean value. Measurements in FLD4.3.1, FLD4.3.5, U3.3, U3.4, U3.5 consisted of single SIMS analyses that significantly sampled the host in addition to the interface and the agglomerate. While their Euclidean distances were calculated and are shown here, they are excluded from Figure 7.9 and distance percentile calculations to avoid biasing the dataset.

Sample	Agglomerate	Location	Euclidean Distance	2σ	Distance Percentile	2σ
AE.C	C1	Exterior	1.27	0.94	3.03	5.47
AE.C	C2	Exterior	2.14	0.58	17.00	25.09
AG.D	D2	Exterior	1.47	0.66	16.48	27.33
AH.E	E1	Exterior	2.38	0.66	8.51	8.54
FLD10	FLD10.L	Exterior	0.52	0.21	2.13	0.19
FLD14	FLD14.1	Surface	1.26	0.40	45.44	12.62
FLD14	FLD14.L	Exterior	1.37	0.29	48.23	10.05
FLD17	FLD17.int.1	Interior	0.70	0.21	29.82	14.36
FLD18	FLD18.1	Exterior	1.07	0.47	14.36	15.23
FLD18	FLD18.2	Interior	2.58	0.39	82.41	7.21
FLD23	FLD23.1.1	Surface	1.36	0.86	32.12	40.83
FLD23	FLD23.1.2	Surface	1.28	1.22	32.87	54.60
FLD23	FLD23.1.3	Surface	1.10	0.76	18.24	35.44
FLD23	FLD23.2.2	Surface	1.65	1.17	50.15	48.58
FLD23	FLD23.3.1	Surface	1.27	1.02	26.93	42.02
FLD23	FLD23.3.2	Surface	1.24	1.12	26.10	44.91
FLD23	FLD23.4.1	Surface	1.57	1.81	38.06	65.06
FLD23	FLD23.4.2	Surface	1.95	1.18	63.74	45.71
FLD23	FLD23.5.1	Surface	1.18	1.02	25.74	47.50
FLD23	FLD23.L	Exterior	1.30	0.39	36.76	13.96
FLD4.3	FLD4.3.1	Interior	2.39	0.32	N/A	N/A
FLD4.3	FLD4.3.2	Interior	2.21	0.21	51.54	17.77
FLD4.3	FLD4.3.3	Interior	2.14	0.28	80.49	15.20
FLD4.3	FLD4.3.5	Interior	1.42	0.50	N/A	N/A

U1B	U1B.2	Surface	2.30	1.33	43.23	43.87
U1B	U1B.L	Interior	1.44	0.35	11.36	12.12
U3	U3.1	Surface	1.08	0.31	31.71	17.49
U3	U3.2	Surface	1.20	1.06	30.58	40.63
U3	U3.3	Surface	0.87	0.18	N/A	N/A
U3	U3.4	Surface	1.19	0.15	N/A	N/A
U3	U3.5	Surface	0.70	0.27	N/A	N/A
U4	U4.1	Surface	1.68	0.13	47.49	7.66
U4	U4.2	Interior	1.64	0.63	42.92	18.27
U4	U4.3	Surface	1.53	0.20	42.29	9.80

Appendix J

Interface Scans using EDS Maps

Interface scans conducted using quantified EDS compositional maps. Method and technique are discussed in Chapter 8. Plots are centered at $x = 0$ based either on the location of the interface peak, which is identified by the SiO_2 maximum (for Si interfaces) or FeO maximum for CaMgFe interfaces (or the CaO maximum when noted). Peak points are highlighted in yellow. The peak points for Si interfaces are the points within 2σ of the SiO_2 maximum (shown with the shaded grey box outlined in blue). Similarly, the peak points for the CaMgFe interfaces are the points within 2σ of the FeO maximum (or the CaO maximum when noted). **All traverses start in the agglomerate, traverse the interface, and end in the host** (except the traverse across agglomerate B2, which starts in agglomerate B2 and ends in agglomerate B3).

J.1 Exterior Agglomerates

Agglomerate B2

Table J.1: Major element compositions (as wt.% oxides) from a line traverse across the interface of surface agglomerate B2 (from surface agglomerate B2 to exterior agglomerate B3) extracted from quantified EDS compositional maps. The EDS compositional maps were collected at a resolution of 3.9 pixels/μm. The smoothing width for this traverse was 75 pixels (19.0 μm) wide. This is a CaMgFe interface and has been centered at $x = 0$ based on its FeO maximum. Peak points within 2σ of the FeO maximum are highlighted in yellow. Uncertainties are 2SEOM.

Pt.	Position (μm)	SiO_2	2σ	Al_2O_3	2σ	Na_2O	2σ	K_2O	2σ	CaO	2σ	FeO	2σ	TiO_2	2σ	MgO	2σ
1	-6.35	74.26	0.29	12.70	0.19	3.19	0.13	4.50	0.12	2.17	0.11	2.34	0.17	0.41	0.07	0.43	0.05
2	-6.09	74.07	0.29	12.90	0.19	3.13	0.12	4.46	0.12	2.26	0.11	2.39	0.17	0.39	0.06	0.40	0.05
3	-5.84	74.22	0.29	12.65	0.19	3.18	0.13	4.58	0.12	2.18	0.11	2.34	0.17	0.44	0.07	0.40	0.05
4	-5.58	74.08	0.29	12.54	0.19	3.14	0.12	4.68	0.13	2.27	0.11	2.41	0.18	0.43	0.07	0.45	0.06
5	-5.33	74.04	0.29	12.82	0.19	3.09	0.12	4.46	0.12	2.19	0.11	2.44	0.18	0.46	0.07	0.50	0.06
6	-5.08	74.08	0.29	12.69	0.19	3.14	0.12	4.56	0.12	2.37	0.11	2.41	0.18	0.35	0.06	0.40	0.05
7	-4.82	74.19	0.29	12.65	0.19	3.10	0.12	4.45	0.12	2.28	0.11	2.42	0.18	0.46	0.07	0.46	0.06
8	-4.57	73.98	0.29	12.47	0.19	3.16	0.12	4.60	0.12	2.32	0.11	2.47	0.18	0.52	0.08	0.48	0.06
9	-4.31	74.04	0.29	12.33	0.18	3.16	0.12	4.60	0.12	2.41	0.12	2.56	0.19	0.46	0.07	0.45	0.06

10	-4.06	74.30	0.29	12.35	0.18	3.01	0.12	4.59	0.12	2.45	0.12	2.44	0.18	0.44	0.07	0.42	0.05
11	-3.81	74.30	0.29	12.41	0.18	3.06	0.12	4.54	0.12	2.57	0.12	2.36	0.17	0.34	0.06	0.43	0.05
12	-3.55	74.15	0.29	12.34	0.18	2.98	0.12	4.67	0.13	2.60	0.13	2.38	0.17	0.40	0.06	0.47	0.06
13	-3.30	74.24	0.29	12.51	0.19	3.12	0.12	4.44	0.12	2.43	0.12	2.42	0.18	0.38	0.06	0.47	0.06
14	-3.05	74.61	0.30	12.33	0.18	3.04	0.12	4.30	0.12	2.43	0.12	2.39	0.17	0.47	0.08	0.42	0.05
15	-2.79	74.74	0.30	12.18	0.18	3.04	0.12	4.35	0.12	2.48	0.12	2.38	0.17	0.40	0.06	0.42	0.05
16	-2.54	74.54	0.30	12.08	0.18	3.07	0.12	4.37	0.12	2.65	0.13	2.34	0.17	0.50	0.08	0.45	0.06
17	-2.28	74.53	0.30	11.85	0.18	3.03	0.12	4.45	0.12	2.79	0.14	2.43	0.18	0.46	0.07	0.45	0.06
18	-2.03	74.49	0.30	11.79	0.18	2.92	0.12	4.51	0.12	2.68	0.13	2.77	0.20	0.41	0.07	0.43	0.05
19	-1.78	74.85	0.30	11.76	0.17	2.95	0.12	4.32	0.12	2.51	0.12	2.66	0.20	0.41	0.07	0.54	0.07
20	-1.52	74.39	0.29	11.62	0.17	2.98	0.12	4.45	0.12	2.78	0.13	2.86	0.21	0.43	0.07	0.50	0.06
21	-1.27	74.20	0.29	11.52	0.17	2.94	0.12	4.58	0.12	2.93	0.14	2.89	0.21	0.49	0.08	0.46	0.06
22	-1.02	74.75	0.30	11.43	0.17	2.87	0.11	4.40	0.12	2.87	0.14	2.73	0.20	0.45	0.07	0.50	0.06
23	-0.76	74.80	0.30	11.40	0.17	2.89	0.11	4.21	0.11	2.82	0.14	2.92	0.21	0.44	0.07	0.51	0.06
24	-0.51	74.88	0.30	11.27	0.17	2.88	0.11	4.28	0.11	3.04	0.15	2.75	0.20	0.41	0.07	0.50	0.06
25	-0.25	74.91	0.30	11.06	0.16	2.91	0.11	4.27	0.11	2.89	0.14	3.09	0.23	0.36	0.06	0.52	0.07
26	0.00	74.99	0.30	10.89	0.16	2.89	0.11	4.21	0.11	2.82	0.14	3.24	0.24	0.45	0.07	0.50	0.06
27	0.25	75.46	0.30	10.88	0.16	2.84	0.11	4.26	0.11	2.65	0.13	3.03	0.22	0.40	0.07	0.47	0.06
28	0.51	75.79	0.30	10.81	0.16	2.83	0.11	4.17	0.11	2.55	0.12	2.94	0.22	0.35	0.06	0.56	0.07
29	0.76	75.99	0.30	10.78	0.16	2.78	0.11	4.18	0.11	2.57	0.12	2.86	0.21	0.27	0.04	0.54	0.07
30	1.02	76.65	0.30	10.46	0.16	2.77	0.11	4.12	0.11	2.55	0.12	2.51	0.18	0.43	0.07	0.51	0.06
31	1.27	76.81	0.30	10.41	0.15	2.80	0.11	4.13	0.11	2.44	0.12	2.60	0.19	0.33	0.05	0.47	0.06
32	1.52	76.84	0.30	10.43	0.15	2.74	0.11	4.35	0.12	2.18	0.11	2.58	0.19	0.46	0.07	0.44	0.05
33	1.78	76.64	0.30	10.56	0.16	2.77	0.11	4.45	0.12	2.24	0.11	2.50	0.18	0.39	0.06	0.44	0.06
34	2.03	77.07	0.31	10.45	0.16	2.59	0.10	4.51	0.12	2.16	0.10	2.45	0.18	0.37	0.06	0.39	0.05
35	2.28	77.19	0.31	10.39	0.15	2.60	0.10	4.40	0.12	2.22	0.11	2.45	0.18	0.36	0.06	0.38	0.05
36	2.54	76.74	0.30	10.82	0.16	2.71	0.11	4.47	0.12	2.11	0.10	2.32	0.17	0.41	0.07	0.41	0.05
37	2.79	76.67	0.30	10.88	0.16	2.78	0.11	4.45	0.12	2.02	0.10	2.38	0.17	0.40	0.06	0.42	0.05
38	3.05	76.90	0.30	10.91	0.16	2.79	0.11	4.45	0.12	2.01	0.10	2.20	0.16	0.34	0.05	0.40	0.05
39	3.30	76.77	0.30	10.85	0.16	2.79	0.11	4.49	0.12	2.05	0.10	2.22	0.16	0.36	0.06	0.47	0.06
40	3.55	76.68	0.30	11.00	0.16	2.77	0.11	4.53	0.12	2.00	0.10	2.18	0.16	0.38	0.06	0.45	0.06
41	3.81	76.71	0.30	11.07	0.16	2.79	0.11	4.39	0.12	2.00	0.10	2.29	0.17	0.34	0.06	0.41	0.05
42	4.06	76.55	0.30	11.08	0.16	2.83	0.11	4.48	0.12	1.86	0.09	2.41	0.18	0.41	0.07	0.38	0.05
43	4.31	76.02	0.30	11.29	0.17	2.92	0.12	4.55	0.12	2.05	0.10	2.32	0.17	0.44	0.07	0.42	0.05
44	4.57	76.02	0.30	11.15	0.17	2.94	0.12	4.58	0.12	2.02	0.10	2.40	0.18	0.48	0.08	0.41	0.05
45	4.82	76.31	0.30	11.18	0.17	2.80	0.11	4.46	0.12	1.98	0.10	2.44	0.18	0.37	0.06	0.47	0.06
46	5.08	76.27	0.30	11.40	0.17	2.76	0.11	4.28	0.12	2.07	0.10	2.37	0.17	0.43	0.07	0.41	0.05
47	5.33	75.88	0.30	11.42	0.17	2.84	0.11	4.33	0.12	2.09	0.10	2.56	0.19	0.43	0.07	0.44	0.06
48	5.58	76.14	0.30	11.36	0.17	2.84	0.11	4.47	0.12	1.93	0.09	2.53	0.19	0.30	0.05	0.42	0.05
49	5.84	75.56	0.30	11.60	0.17	3.03	0.12	4.48	0.12	2.03	0.10	2.49	0.18	0.36	0.06	0.47	0.06
50	6.09	75.59	0.30	11.60	0.17	2.85	0.11	4.50	0.12	2.18	0.11	2.47	0.18	0.37	0.06	0.44	0.06
51	6.35	75.90	0.30	11.52	0.17	2.71	0.11	4.49	0.12	2.06	0.10	2.45	0.18	0.45	0.07	0.43	0.05
52	6.60	75.70	0.30	11.67	0.17	2.89	0.11	4.39	0.12	1.97	0.10	2.52	0.18	0.41	0.07	0.45	0.06
53	6.85	75.88	0.30	11.58	0.17	2.88	0.11	4.42	0.12	1.96	0.09	2.45	0.18	0.37	0.06	0.46	0.06
54	7.11	75.75	0.30	11.44	0.17	2.86	0.11	4.47	0.12	2.04	0.10	2.61	0.19	0.41	0.07	0.42	0.05
55	7.36	75.91	0.30	11.62	0.17	2.87	0.11	4.43	0.12	1.97	0.10	2.43	0.18	0.36	0.06	0.41	0.05
56	7.61	75.74	0.30	11.60	0.17	2.99	0.12	4.36	0.12	1.96	0.09	2.47	0.18	0.40	0.06	0.48	0.06
57	7.87	75.36	0.30	11.79	0.17	2.95	0.12	4.54	0.12	2.07	0.10	2.46	0.18	0.37	0.06	0.46	0.06
58	8.12	75.33	0.30	11.83	0.18	2.93	0.12	4.47	0.12	2.01	0.10	2.53	0.19	0.44	0.07	0.46	0.06
59	8.38	75.13	0.30	11.85	0.18	2.92	0.12	4.39	0.12	2.12	0.10	2.65	0.19	0.43	0.07	0.51	0.06
60	8.63	75.46	0.30	11.68	0.17	2.90	0.11	4.49	0.12	2.01	0.10	2.56	0.19	0.41	0.07	0.48	0.06
61	8.88	75.47	0.30	11.85	0.18	2.92	0.12	4.36	0.12	2.09	0.10	2.53	0.19	0.36	0.06	0.42	0.05
62	9.14	75.51	0.30	11.85	0.18	2.95	0.12	4.38	0.12	1.96	0.10	2.57	0.19	0.40	0.07	0.38	0.05
63	9.39	75.48	0.30	11.84	0.18	2.91	0.12	4.22	0.11	2.11	0.10	2.61	0.19	0.38	0.06	0.46	0.06
64	9.64	75.39	0.30	11.91	0.18	2.93	0.12	4.36	0.12	2.16	0.10	2.44	0.18	0.41	0.07	0.40	0.05
65	9.90	75.37	0.30	11.84	0.18	2.95	0.12	4.43	0.12	2.06	0.10	2.55	0.19	0.39	0.06	0.41	0.05
66	10.15	75.09	0.30	11.82	0.18	2.81	0.11	4.46	0.12	2.11	0.10	2.71	0.20	0.54	0.09	0.46	0.06
67	10.41	75.13	0.30	11.77	0.17	2.85	0.11	4.41	0.12	2.16	0.10	2.75	0.20	0.50	0.08	0.43	0.05
68	10.66	75.27	0.30	11.72	0.17	2.76	0.11	4.53	0.12	2.22	0.11	2.77	0.20	0.35	0.06	0.37	0.05
69	10.91	75.19	0.30	12.18	0.18	2.81	0.11	4.28	0.11	2.03	0.10	2.62	0.19	0.39	0.06	0.50	0.06
70	11.17	75.18	0.30	12.00	0.18	2.81	0.11	4.41	0.12	2.11	0.10	2.53	0.19	0.47	0.08	0.48	0.06

Agglomerate C1

Table J.2: Major element compositions (as wt.% oxides) from a line traverse across the interface of exterior agglomerate C1 (from agglomerate C1 to host AE.C) extracted from quantified EDS compositional maps. The EDS compositional maps were collected at a resolution of 7.4 pixels/μm. The smoothing width for this traverse was 100 pixels (13.6 μm) wide. This is a CaMgFe interface and has been centered at $x = 0$ based on the FeO maximum. Peak points within 2σ of the FeO maximum are highlighted in yellow. Uncertainties are 2SEOM.

Pt.	Position (μm)	SiO_2	2σ	Al_2O_3	2σ	Na_2O	2σ	K_2O	2σ	CaO	2σ	FeO	2σ	TiO_2	2σ	MgO	2σ
1	-10.75	71.67	0.20	13.47	0.16	3.91	0.08	5.67	0.14	1.62	0.08	2.74	0.15	0.43	0.06	0.50	0.05
2	-10.61	71.66	0.20	13.43	0.16	3.93	0.08	5.68	0.14	1.65	0.08	2.75	0.15	0.43	0.06	0.47	0.05
3	-10.48	71.94	0.20	13.63	0.16	3.92	0.08	5.53	0.13	1.55	0.07	2.43	0.13	0.50	0.06	0.51	0.05
4	-10.34	71.88	0.20	13.51	0.16	3.89	0.08	5.56	0.13	1.58	0.07	2.57	0.14	0.45	0.06	0.56	0.05
5	-10.20	71.80	0.20	13.42	0.16	3.89	0.08	5.64	0.14	1.59	0.07	2.64	0.14	0.49	0.06	0.54	0.05
6	-10.07	72.05	0.20	13.49	0.16	3.84	0.08	5.59	0.13	1.52	0.07	2.62	0.14	0.38	0.05	0.51	0.05
7	-9.93	71.67	0.20	13.51	0.16	3.94	0.08	5.56	0.13	1.68	0.08	2.67	0.14	0.47	0.06	0.50	0.05
8	-9.80	71.40	0.20	13.38	0.16	4.00	0.08	5.67	0.14	1.74	0.08	2.83	0.15	0.47	0.06	0.51	0.05
9	-9.66	71.68	0.20	13.31	0.16	4.06	0.08	5.66	0.14	1.65	0.08	2.60	0.14	0.49	0.06	0.55	0.05
10	-9.52	71.93	0.20	13.34	0.16	3.94	0.08	5.63	0.14	1.60	0.08	2.54	0.14	0.49	0.06	0.54	0.05
11	-9.39	71.82	0.20	13.27	0.16	3.93	0.08	5.70	0.14	1.68	0.08	2.66	0.14	0.42	0.05	0.52	0.05
12	-9.25	72.07	0.20	13.30	0.16	3.83	0.08	5.60	0.13	1.56	0.07	2.72	0.14	0.41	0.05	0.52	0.05
13	-9.12	72.04	0.20	13.32	0.16	3.91	0.08	5.68	0.14	1.62	0.08	2.51	0.13	0.39	0.05	0.53	0.05
14	-8.98	71.97	0.20	13.23	0.16	3.98	0.08	5.76	0.14	1.68	0.08	2.50	0.13	0.42	0.05	0.46	0.05
15	-8.84	71.72	0.20	13.20	0.16	3.95	0.08	5.73	0.14	1.71	0.08	2.67	0.14	0.52	0.07	0.51	0.05
16	-8.71	71.61	0.20	13.32	0.16	3.97	0.08	5.73	0.14	1.69	0.08	2.54	0.14	0.55	0.07	0.60	0.06
17	-8.57	71.82	0.20	13.33	0.16	3.96	0.08	5.64	0.14	1.59	0.07	2.64	0.14	0.48	0.06	0.55	0.05
18	-8.44	71.77	0.20	13.28	0.16	4.00	0.08	5.71	0.14	1.67	0.08	2.61	0.14	0.45	0.06	0.50	0.05
19	-8.30	72.00	0.20	13.10	0.16	4.02	0.08	5.67	0.14	1.60	0.08	2.58	0.14	0.46	0.06	0.57	0.06
20	-8.16	71.70	0.20	13.32	0.16	4.02	0.08	5.70	0.14	1.63	0.08	2.64	0.14	0.42	0.05	0.57	0.06
21	-8.03	71.94	0.20	13.33	0.16	3.94	0.08	5.67	0.14	1.64	0.08	2.55	0.14	0.40	0.05	0.53	0.05
22	-7.89	71.80	0.20	13.10	0.16	4.12	0.08	5.69	0.14	1.69	0.08	2.66	0.14	0.44	0.06	0.50	0.05
23	-7.76	71.65	0.20	13.13	0.16	4.06	0.08	5.64	0.14	1.71	0.08	2.82	0.15	0.44	0.06	0.56	0.05
24	-7.62	71.76	0.20	13.14	0.16	4.17	0.08	5.64	0.14	1.58	0.07	2.71	0.14	0.42	0.05	0.59	0.06
25	-7.48	71.82	0.20	12.94	0.15	4.08	0.08	5.73	0.14	1.66	0.08	2.76	0.15	0.47	0.06	0.54	0.05
26	-7.35	71.72	0.20	13.17	0.16	3.96	0.08	5.68	0.14	1.64	0.08	2.81	0.15	0.45	0.06	0.56	0.06
27	-7.21	71.88	0.20	13.14	0.16	4.08	0.08	5.65	0.14	1.61	0.08	2.64	0.14	0.40	0.05	0.59	0.06
28	-7.07	71.85	0.20	13.06	0.16	4.07	0.08	5.67	0.14	1.59	0.07	2.75	0.15	0.39	0.05	0.62	0.06
29	-6.94	72.12	0.20	12.95	0.15	4.03	0.08	5.72	0.14	1.54	0.07	2.66	0.14	0.43	0.06	0.54	0.05
30	-6.80	72.18	0.20	12.90	0.15	4.06	0.08	5.78	0.14	1.61	0.08	2.57	0.14	0.41	0.05	0.48	0.05
31	-6.67	72.09	0.20	12.74	0.15	4.08	0.08	5.85	0.14	1.65	0.08	2.64	0.14	0.44	0.06	0.51	0.05
32	-6.53	71.61	0.20	12.91	0.15	4.11	0.08	5.80	0.14	1.76	0.08	2.74	0.15	0.49	0.06	0.58	0.06
33	-6.39	71.99	0.20	12.82	0.15	3.99	0.08	5.77	0.14	1.66	0.08	2.80	0.15	0.44	0.06	0.53	0.05
34	-6.26	72.18	0.20	12.83	0.15	4.08	0.08	5.60	0.13	1.63	0.08	2.71	0.14	0.45	0.06	0.52	0.05
35	-6.12	72.19	0.20	12.55	0.15	4.02	0.08	5.85	0.14	1.79	0.08	2.68	0.14	0.43	0.06	0.50	0.05
36	-5.99	71.81	0.20	12.61	0.15	4.17	0.08	5.87	0.14	1.79	0.08	2.75	0.15	0.47	0.06	0.52	0.05
37	-5.85	72.25	0.20	12.64	0.15	4.08	0.08	5.82	0.14	1.60	0.08	2.63	0.14	0.48	0.06	0.50	0.05
38	-5.71	72.15	0.20	12.57	0.15	4.12	0.08	5.83	0.14	1.62	0.08	2.72	0.15	0.45	0.06	0.53	0.05
39	-5.58	71.88	0.20	12.50	0.15	4.15	0.08	5.97	0.14	1.70	0.08	2.72	0.14	0.56	0.07	0.52	0.05
40	-5.44	71.97	0.20	12.40	0.15	4.16	0.08	5.98	0.14	1.78	0.08	2.75	0.15	0.49	0.06	0.48	0.05
41	-5.31	72.19	0.20	12.67	0.15	4.19	0.08	5.64	0.14	1.63	0.08	2.71	0.14	0.45	0.06	0.54	0.05
42	-5.17	72.22	0.20	12.48	0.15	4.11	0.08	5.81	0.14	1.66	0.08	2.67	0.14	0.49	0.06	0.55	0.05
43	-5.03	72.25	0.20	12.41	0.15	4.20	0.08	5.84	0.14	1.61	0.08	2.72	0.15	0.41	0.05	0.56	0.06
44	-4.90	72.12	0.20	12.31	0.15	4.35	0.09	5.85	0.14	1.69	0.08	2.73	0.15	0.37	0.05	0.58	0.06
45	-4.76	72.20	0.20	12.26	0.15	4.31	0.09	5.84	0.14	1.63	0.08	2.84	0.15	0.41	0.05	0.50	0.05
46	-4.63	72.38	0.20	12.22	0.15	4.32	0.09	5.81	0.14	1.55	0.07	2.76	0.15	0.44	0.06	0.52	0.05
47	-4.49	72.23	0.20	12.39	0.15	4.30	0.09	5.69	0.14	1.57	0.07	2.88	0.15	0.38	0.05	0.56	0.05
48	-4.35	72.11	0.20	12.29	0.15	4.42	0.09	5.75	0.14	1.67	0.08	2.75	0.15	0.45	0.06	0.55	0.05
49	-4.22	72.35	0.20	12.19	0.14	4.40	0.09	5.82	0.14	1.56	0.07	2.71	0.14	0.43	0.06	0.52	0.05
50	-4.08	72.19	0.20	12.15	0.14	4.44	0.09	5.90	0.14	1.60	0.08	2.77	0.15	0.44	0.06	0.52	0.05

51	-3.95	72.14	0.20	11.95	0.14	4.40	0.09	5.92	0.14	1.64	0.08	2.96	0.16	0.44	0.06	0.55	0.05
52	-3.81	72.30	0.20	12.12	0.14	4.33	0.09	5.87	0.14	1.62	0.08	2.85	0.15	0.37	0.05	0.55	0.05
53	-3.67	72.50	0.21	12.08	0.14	4.37	0.09	5.77	0.14	1.64	0.08	2.67	0.14	0.41	0.05	0.57	0.06
54	-3.54	72.51	0.21	12.15	0.14	4.43	0.09	5.76	0.14	1.54	0.07	2.66	0.14	0.39	0.05	0.56	0.06
55	-3.40	72.34	0.20	11.99	0.14	4.48	0.09	5.77	0.14	1.60	0.08	2.85	0.15	0.42	0.05	0.55	0.05
56	-3.27	72.26	0.20	11.79	0.14	4.41	0.09	6.08	0.15	1.60	0.08	2.94	0.16	0.40	0.05	0.53	0.05
57	-3.13	72.39	0.20	11.82	0.14	4.45	0.09	5.94	0.14	1.54	0.07	2.86	0.15	0.41	0.05	0.59	0.06
58	-2.99	72.25	0.20	11.83	0.14	4.63	0.09	5.81	0.14	1.63	0.08	2.88	0.15	0.41	0.05	0.56	0.06
59	-2.86	72.54	0.21	11.76	0.14	4.47	0.09	5.87	0.14	1.62	0.08	2.76	0.15	0.39	0.05	0.59	0.06
60	-2.72	72.12	0.20	11.61	0.14	4.51	0.09	6.12	0.15	1.64	0.08	3.07	0.16	0.39	0.05	0.55	0.05
61	-2.59	72.25	0.20	11.61	0.14	4.66	0.09	5.96	0.14	1.62	0.08	2.87	0.15	0.43	0.06	0.59	0.06
62	-2.45	72.36	0.20	11.59	0.14	4.64	0.09	6.04	0.15	1.62	0.08	2.82	0.15	0.38	0.05	0.55	0.05
63	-2.31	72.44	0.20	11.67	0.14	4.65	0.09	6.01	0.14	1.49	0.07	2.81	0.15	0.39	0.05	0.54	0.05
64	-2.18	72.39	0.20	11.38	0.14	4.76	0.10	5.94	0.14	1.57	0.07	2.94	0.16	0.46	0.06	0.55	0.05
65	-2.04	72.22	0.20	11.24	0.13	4.71	0.09	6.06	0.15	1.71	0.08	3.02	0.16	0.44	0.06	0.60	0.06
66	-1.90	72.34	0.20	11.29	0.13	4.74	0.10	6.08	0.15	1.64	0.08	2.90	0.15	0.43	0.06	0.57	0.06
67	-1.77	72.02	0.20	11.39	0.14	4.90	0.10	5.99	0.14	1.63	0.08	3.10	0.17	0.42	0.05	0.56	0.05
68	-1.63	72.19	0.20	11.43	0.14	4.98	0.10	5.87	0.14	1.58	0.07	2.96	0.16	0.38	0.05	0.61	0.06
69	-1.50	72.28	0.20	11.34	0.13	4.94	0.10	5.89	0.14	1.58	0.07	2.98	0.16	0.39	0.05	0.60	0.06
70	-1.36	72.08	0.20	11.04	0.13	4.94	0.10	6.01	0.14	1.69	0.08	3.28	0.17	0.40	0.05	0.56	0.05
71	-1.22	72.43	0.20	11.09	0.13	5.00	0.10	5.93	0.14	1.60	0.07	3.01	0.16	0.41	0.05	0.53	0.05
72	-1.09	72.92	0.21	10.90	0.13	4.82	0.10	5.84	0.14	1.66	0.08	2.92	0.16	0.39	0.05	0.55	0.05
73	-0.95	72.72	0.21	10.66	0.13	4.86	0.10	6.02	0.14	1.72	0.08	3.13	0.17	0.42	0.05	0.48	0.05
74	-0.82	72.61	0.21	10.61	0.13	5.02	0.10	5.81	0.14	1.86	0.09	3.12	0.17	0.42	0.05	0.56	0.06
75	-0.68	73.05	0.21	10.30	0.12	5.02	0.10	5.65	0.14	1.85	0.09	3.23	0.17	0.40	0.05	0.50	0.05
76	-0.54	73.12	0.21	9.84	0.12	4.95	0.10	5.71	0.14	1.98	0.09	3.42	0.18	0.51	0.07	0.47	0.05
77	-0.41	73.44	0.21	9.46	0.11	5.01	0.10	5.56	0.13	2.13	0.10	3.54	0.19	0.37	0.05	0.49	0.05
78	-0.27	73.73	0.21	8.82	0.10	4.96	0.10	5.53	0.13	2.22	0.10	3.80	0.20	0.40	0.05	0.53	0.05
79	-0.14	73.94	0.21	8.23	0.10	5.06	0.10	5.36	0.13	2.37	0.11	4.08	0.22	0.39	0.05	0.56	0.06
80	0.00	74.27	0.21	7.95	0.09	4.95	0.10	5.18	0.12	2.48	0.12	4.14	0.22	0.43	0.06	0.59	0.06
81	0.14	74.74	0.21	7.75	0.09	4.95	0.10	5.21	0.13	2.54	0.12	3.91	0.21	0.37	0.05	0.52	0.05
82	0.27	74.87	0.21	7.92	0.09	4.87	0.10	5.32	0.13	2.42	0.11	3.76	0.20	0.34	0.04	0.50	0.05
83	0.41	75.28	0.21	8.00	0.09	4.79	0.10	5.47	0.13	2.14	0.10	3.54	0.19	0.31	0.04	0.47	0.05
84	0.54	75.32	0.21	8.19	0.10	4.77	0.10	5.49	0.13	2.11	0.10	3.35	0.18	0.34	0.04	0.45	0.04
85	0.68	75.51	0.21	8.32	0.10	5.01	0.10	5.35	0.13	1.99	0.09	3.06	0.16	0.31	0.04	0.45	0.04
86	0.82	75.74	0.21	8.52	0.10	4.91	0.10	5.48	0.13	1.87	0.09	2.76	0.15	0.29	0.04	0.43	0.04
87	0.95	75.46	0.21	8.68	0.10	5.04	0.10	5.46	0.13	1.83	0.09	2.78	0.15	0.33	0.04	0.41	0.04
88	1.09	75.54	0.21	8.57	0.10	4.98	0.10	5.53	0.13	1.87	0.09	2.81	0.15	0.27	0.04	0.42	0.04
89	1.22	75.36	0.21	8.66	0.10	4.94	0.10	5.62	0.13	1.86	0.09	2.83	0.15	0.32	0.04	0.42	0.04
90	1.36	75.54	0.21	8.81	0.10	5.09	0.10	5.45	0.13	1.67	0.08	2.68	0.14	0.31	0.04	0.45	0.04
91	1.50	75.16	0.21	8.77	0.10	5.19	0.10	5.55	0.13	1.77	0.08	2.74	0.15	0.36	0.05	0.45	0.04
92	1.63	75.09	0.21	8.72	0.10	5.13	0.10	5.74	0.14	1.76	0.08	2.71	0.14	0.37	0.05	0.48	0.05
93	1.77	75.02	0.21	8.91	0.11	5.29	0.11	5.53	0.13	1.69	0.08	2.77	0.15	0.36	0.05	0.43	0.04
94	1.90	75.03	0.21	8.81	0.10	5.21	0.10	5.56	0.13	1.69	0.08	2.85	0.15	0.42	0.05	0.44	0.04
95	2.04	74.73	0.21	8.90	0.11	5.33	0.11	5.68	0.14	1.65	0.08	2.91	0.16	0.35	0.05	0.46	0.05
96	2.18	74.97	0.21	8.76	0.10	5.20	0.10	5.79	0.14	1.75	0.08	2.78	0.15	0.30	0.04	0.46	0.04
97	2.31	74.75	0.21	8.73	0.10	5.31	0.11	5.88	0.14	1.72	0.08	2.85	0.15	0.32	0.04	0.44	0.04
98	2.45	74.75	0.21	9.02	0.11	5.35	0.11	5.54	0.13	1.66	0.08	2.88	0.15	0.33	0.04	0.48	0.05
99	2.58	74.75	0.21	9.07	0.11	5.48	0.11	5.59	0.13	1.67	0.08	2.69	0.14	0.28	0.04	0.48	0.05
100	2.72	74.51	0.21	9.05	0.11	5.40	0.11	5.59	0.13	1.71	0.08	2.96	0.16	0.27	0.04	0.51	0.05
101	2.86	74.47	0.21	8.98	0.11	5.45	0.11	5.58	0.13	1.64	0.08	3.13	0.17	0.28	0.04	0.48	0.05
102	2.99	74.11	0.21	9.14	0.11	5.49	0.11	5.66	0.14	1.64	0.08	3.10	0.17	0.36	0.05	0.49	0.05
103	3.13	74.40	0.21	9.19	0.11	5.44	0.11	5.55	0.13	1.65	0.08	2.97	0.16	0.29	0.04	0.51	0.05
104	3.27	74.16	0.21	9.15	0.11	5.47	0.11	5.78	0.14	1.55	0.07	2.97	0.16	0.39	0.05	0.52	0.05
105	3.40	74.22	0.21	9.29	0.11	5.44	0.11	5.72	0.14	1.69	0.08	2.80	0.15	0.39	0.05	0.45	0.04
106	3.54	74.00	0.21	9.44	0.11	5.53	0.11	5.68	0.14	1.68	0.08	2.86	0.15	0.34	0.04	0.47	0.05
107	3.67	74.03	0.21	9.33	0.11	5.52	0.11	5.74	0.14	1.65	0.08	2.89	0.15	0.37	0.05	0.47	0.05
108	3.81	74.11	0.21	9.28	0.11	5.42	0.11	5.73	0.14	1.66	0.08	2.89	0.15	0.41	0.05	0.50	0.05
109	3.95	74.07	0.21	9.36	0.11	5.52	0.11	5.70	0.14	1.66	0.08	2.81	0.15	0.40	0.05	0.49	0.05
110	4.08	74.17	0.21	9.41	0.11	5.43	0.11	5.79	0.14	1.62	0.08	2.73	0.15	0.36	0.05	0.49	0.05
111	4.22	73.88	0.21	9.31	0.11	5.52	0.11	5.86	0.14	1.60	0.08	2.88	0.15	0.46	0.06	0.49	0.05
112	4.35	73.84	0.21	9.53	0.11	5.54	0.11	5.71	0.14	1.65	0.08	2.87	0.15	0.38	0.05	0.48	0.05

113	4.49	73.69	0.21	9.51	0.11	5.49	0.11	5.77	0.14	1.68	0.08	3.00	0.16	0.36	0.05	0.49	0.05
114	4.63	73.77	0.21	9.64	0.11	5.58	0.11	5.75	0.14	1.55	0.07	2.86	0.15	0.36	0.05	0.49	0.05
115	4.76	74.15	0.21	9.47	0.11	5.49	0.11	5.82	0.14	1.54	0.07	2.72	0.14	0.34	0.04	0.47	0.05
116	4.90	73.95	0.21	9.58	0.11	5.54	0.11	5.73	0.14	1.53	0.07	2.78	0.15	0.40	0.05	0.50	0.05
117	5.03	73.83	0.21	9.56	0.11	5.62	0.11	5.67	0.14	1.53	0.07	2.87	0.15	0.39	0.05	0.52	0.05
118	5.17	73.86	0.21	9.68	0.11	5.51	0.11	5.72	0.14	1.50	0.07	2.85	0.15	0.36	0.05	0.51	0.05
119	5.31	73.95	0.21	9.69	0.12	5.45	0.11	5.80	0.14	1.59	0.07	2.74	0.15	0.33	0.04	0.45	0.04
120	5.44	73.84	0.21	9.67	0.11	5.40	0.11	5.80	0.14	1.57	0.07	2.83	0.15	0.35	0.05	0.53	0.05
121	5.58	74.00	0.21	9.65	0.11	5.38	0.11	5.78	0.14	1.54	0.07	2.83	0.15	0.30	0.04	0.52	0.05
122	5.71	74.01	0.21	9.62	0.11	5.30	0.11	5.79	0.14	1.54	0.07	2.90	0.15	0.34	0.04	0.51	0.05
123	5.85	73.60	0.21	9.71	0.12	5.42	0.11	5.81	0.14	1.58	0.07	3.00	0.16	0.37	0.05	0.50	0.05
124	5.99	73.82	0.21	9.68	0.11	5.38	0.11	5.86	0.14	1.52	0.07	2.97	0.16	0.30	0.04	0.46	0.04
125	6.12	73.76	0.21	9.67	0.11	5.54	0.11	5.84	0.14	1.51	0.07	2.89	0.15	0.39	0.05	0.40	0.04
126	6.26	73.94	0.21	9.79	0.12	5.42	0.11	5.81	0.14	1.39	0.07	2.86	0.15	0.33	0.04	0.46	0.04
127	6.39	73.87	0.21	9.79	0.12	5.43	0.11	5.69	0.14	1.46	0.07	3.01	0.16	0.31	0.04	0.45	0.04
128	6.53	74.08	0.21	9.75	0.12	5.39	0.11	5.64	0.14	1.50	0.07	2.86	0.15	0.31	0.04	0.47	0.05
129	6.67	73.94	0.21	9.65	0.11	5.50	0.11	5.73	0.14	1.52	0.07	2.87	0.15	0.34	0.04	0.46	0.05
130	6.80	73.64	0.21	9.62	0.11	5.37	0.11	5.96	0.14	1.57	0.07	3.00	0.16	0.38	0.05	0.46	0.05
131	6.94	73.88	0.21	9.68	0.11	5.38	0.11	5.88	0.14	1.54	0.07	2.83	0.15	0.33	0.04	0.48	0.05
132	7.07	74.10	0.21	9.82	0.12	5.35	0.11	5.79	0.14	1.45	0.07	2.63	0.14	0.38	0.05	0.48	0.05
133	7.21	74.12	0.21	9.86	0.12	5.40	0.11	5.62	0.13	1.32	0.06	2.80	0.15	0.39	0.05	0.50	0.05
134	7.35	74.11	0.21	9.82	0.12	5.31	0.11	5.79	0.14	1.45	0.07	2.72	0.14	0.37	0.05	0.43	0.04
135	7.48	74.09	0.21	9.75	0.12	5.32	0.11	5.80	0.14	1.42	0.07	2.75	0.15	0.42	0.06	0.43	0.04
136	7.62	74.02	0.21	9.77	0.12	5.30	0.11	5.90	0.14	1.45	0.07	2.66	0.14	0.42	0.05	0.49	0.05
137	7.76	74.09	0.21	9.86	0.12	5.26	0.11	5.74	0.14	1.42	0.07	2.74	0.15	0.37	0.05	0.51	0.05
138	7.89	73.89	0.21	9.80	0.12	5.23	0.10	5.97	0.14	1.41	0.07	2.88	0.15	0.34	0.04	0.48	0.05
139	8.03	73.92	0.21	9.87	0.12	5.21	0.10	5.81	0.14	1.43	0.07	2.86	0.15	0.43	0.06	0.47	0.05
140	8.16	73.75	0.21	9.94	0.12	5.34	0.11	5.85	0.14	1.40	0.07	2.86	0.15	0.38	0.05	0.48	0.05
141	8.30	73.92	0.21	9.78	0.12	5.13	0.10	5.95	0.14	1.46	0.07	2.90	0.15	0.37	0.05	0.48	0.05
142	8.44	73.85	0.21	9.91	0.12	5.23	0.10	5.86	0.14	1.36	0.06	2.86	0.15	0.44	0.06	0.48	0.05
143	8.57	74.31	0.21	9.88	0.12	5.12	0.10	5.88	0.14	1.36	0.06	2.66	0.14	0.35	0.05	0.45	0.04
144	8.71	74.03	0.21	9.86	0.12	5.20	0.10	5.91	0.14	1.32	0.06	2.94	0.16	0.36	0.05	0.40	0.04
145	8.84	74.24	0.21	9.91	0.12	5.17	0.10	5.92	0.14	1.35	0.06	2.68	0.14	0.31	0.04	0.42	0.04
146	8.98	74.18	0.21	10.00	0.12	5.07	0.10	5.94	0.14	1.29	0.06	2.72	0.14	0.37	0.05	0.44	0.04
147	9.12	74.03	0.21	10.06	0.12	5.16	0.10	5.81	0.14	1.33	0.06	2.82	0.15	0.35	0.05	0.45	0.04
148	9.25	74.01	0.21	10.06	0.12	5.05	0.10	5.91	0.14	1.37	0.06	2.76	0.15	0.39	0.05	0.46	0.05
149	9.39	74.05	0.21	10.02	0.12	5.09	0.10	5.91	0.14	1.34	0.06	2.77	0.15	0.41	0.05	0.40	0.04
150	9.52	73.95	0.21	10.12	0.12	5.18	0.10	5.93	0.14	1.34	0.06	2.63	0.14	0.40	0.05	0.44	0.04
151	9.66	73.83	0.21	10.11	0.12	5.11	0.10	5.97	0.14	1.33	0.06	2.75	0.15	0.46	0.06	0.43	0.04
152	9.80	74.01	0.21	10.17	0.12	5.10	0.10	5.88	0.14	1.20	0.06	2.80	0.15	0.41	0.05	0.42	0.04
153	9.93	73.95	0.21	10.20	0.12	5.03	0.10	6.00	0.14	1.30	0.06	2.70	0.14	0.37	0.05	0.45	0.04
154	10.07	74.12	0.21	10.22	0.12	4.95	0.10	5.91	0.14	1.25	0.06	2.72	0.15	0.38	0.05	0.46	0.04
155	10.20	73.88	0.21	10.40	0.12	5.04	0.10	5.90	0.14	1.34	0.06	2.60	0.14	0.41	0.05	0.43	0.04
156	10.34	73.58	0.21	10.26	0.12	5.05	0.10	5.96	0.14	1.32	0.06	2.87	0.15	0.49	0.06	0.48	0.05
157	10.48	73.67	0.21	10.29	0.12	5.08	0.10	5.96	0.14	1.23	0.06	2.87	0.15	0.49	0.06	0.43	0.04

Agglomerate C2

Table J.3: Major element compositions (as wt.% oxides) from a line traverse across the interface of exterior agglomerate C2 (from agglomerate C2 to host AE.C) extracted from quantified EDS compositional maps. The EDS compositional maps were collected at a resolution of 9.9 pixels/μm. The smoothing width for this traverse was 100 pixels (10.1 μm) wide. This is a CaMgFe interface and has been centered at $x = 0$ based on the **CaO** maximum across the interface due to significantly different FeO compositions in the host and the agglomerate that render the interface difficult to find. (The CaO maximum from this traverse occurs in the agglomerate, but the interface is centered at $x = 0$.) Peak points within 2σ of the CaO maximum are highlighted in yellow. Uncertainties are 2SEOM.

Pt.	Position (μm)	SiO_2	2σ	Al_2O_3	2σ	Na_2O	2σ	K_2O	2σ	CaO	2σ	FeO	2σ	TiO_2	2σ	MgO	2σ
1	-10.00	78.14	0.20	11.25	0.12	1.57	0.07	3.56	0.08	2.07	0.08	2.60	0.12	0.34	0.06	0.47	0.04
2	-9.90	77.97	0.20	11.31	0.13	1.61	0.07	3.65	0.08	2.06	0.08	2.58	0.12	0.37	0.06	0.46	0.04
3	-9.80	78.02	0.20	11.27	0.12	1.56	0.07	3.67	0.08	2.09	0.09	2.46	0.12	0.44	0.07	0.49	0.04
4	-9.70	77.82	0.20	11.26	0.12	1.53	0.06	3.63	0.08	2.18	0.09	2.67	0.13	0.45	0.07	0.46	0.04
5	-9.60	77.99	0.20	11.18	0.12	1.52	0.06	3.61	0.08	2.26	0.09	2.62	0.13	0.40	0.07	0.42	0.04
6	-9.49	78.04	0.20	11.18	0.12	1.56	0.07	3.62	0.08	2.08	0.08	2.69	0.13	0.38	0.06	0.45	0.04
7	-9.39	77.95	0.20	11.09	0.12	1.59	0.07	3.60	0.08	2.16	0.09	2.77	0.13	0.40	0.07	0.44	0.04
8	-9.29	78.14	0.20	11.19	0.12	1.53	0.06	3.54	0.08	2.08	0.08	2.64	0.13	0.42	0.07	0.46	0.04
9	-9.19	78.13	0.20	11.14	0.12	1.51	0.06	3.59	0.08	2.15	0.09	2.64	0.13	0.34	0.06	0.48	0.04
10	-9.09	78.11	0.20	11.04	0.12	1.53	0.06	3.61	0.08	2.21	0.09	2.73	0.13	0.39	0.06	0.40	0.04
11	-8.99	78.44	0.20	10.95	0.12	1.60	0.07	3.61	0.08	2.08	0.08	2.53	0.12	0.36	0.06	0.41	0.04
12	-8.89	78.26	0.20	11.06	0.12	1.57	0.07	3.61	0.08	1.99	0.08	2.66	0.13	0.40	0.07	0.45	0.04
13	-8.79	78.23	0.20	11.02	0.12	1.50	0.06	3.60	0.08	2.10	0.09	2.75	0.13	0.34	0.06	0.45	0.04
14	-8.69	78.24	0.20	11.00	0.12	1.54	0.06	3.66	0.08	2.05	0.08	2.73	0.13	0.36	0.06	0.42	0.04
15	-8.59	78.26	0.20	11.05	0.12	1.47	0.06	3.63	0.08	1.98	0.08	2.72	0.13	0.43	0.07	0.45	0.04
16	-8.48	78.26	0.20	11.14	0.12	1.54	0.06	3.65	0.08	1.99	0.08	2.57	0.12	0.39	0.06	0.46	0.04
17	-8.38	78.32	0.20	11.07	0.12	1.57	0.07	3.55	0.08	1.94	0.08	2.71	0.13	0.38	0.06	0.46	0.04
18	-8.28	78.47	0.20	11.03	0.12	1.56	0.07	3.56	0.08	2.01	0.08	2.54	0.12	0.35	0.06	0.48	0.04
19	-8.18	78.73	0.20	10.98	0.12	1.51	0.06	3.66	0.08	1.94	0.08	2.43	0.12	0.33	0.05	0.43	0.04
20	-8.08	78.49	0.20	11.02	0.12	1.51	0.06	3.71	0.08	2.06	0.08	2.44	0.12	0.34	0.06	0.43	0.04
21	-7.98	78.46	0.20	10.91	0.12	1.53	0.06	3.64	0.08	1.95	0.08	2.65	0.13	0.39	0.06	0.47	0.04
22	-7.88	78.67	0.20	10.79	0.12	1.55	0.07	3.72	0.08	1.91	0.08	2.53	0.12	0.40	0.07	0.44	0.04
23	-7.78	78.59	0.20	10.84	0.12	1.59	0.07	3.69	0.08	1.88	0.08	2.55	0.12	0.40	0.07	0.46	0.04
24	-7.68	78.65	0.20	10.94	0.12	1.57	0.07	3.61	0.08	1.86	0.08	2.57	0.12	0.35	0.06	0.45	0.04
25	-7.58	78.62	0.20	10.74	0.12	1.58	0.07	3.68	0.08	1.94	0.08	2.65	0.13	0.37	0.06	0.43	0.04
26	-7.47	78.67	0.20	10.70	0.12	1.54	0.06	3.72	0.08	2.01	0.08	2.58	0.12	0.35	0.06	0.42	0.04
27	-7.37	78.57	0.20	10.75	0.12	1.49	0.06	3.77	0.08	1.98	0.08	2.63	0.13	0.39	0.07	0.42	0.04
28	-7.27	78.77	0.20	10.77	0.12	1.51	0.06	3.76	0.08	1.91	0.08	2.50	0.12	0.32	0.05	0.45	0.04
29	-7.17	78.61	0.20	10.78	0.12	1.50	0.06	3.82	0.08	1.96	0.08	2.57	0.12	0.32	0.05	0.44	0.04
30	-7.07	78.73	0.20	10.74	0.12	1.48	0.06	3.80	0.08	1.88	0.08	2.53	0.12	0.33	0.06	0.50	0.04
31	-6.97	78.76	0.20	10.68	0.12	1.62	0.07	3.75	0.08	1.79	0.07	2.59	0.12	0.33	0.05	0.49	0.04
32	-6.87	78.92	0.20	10.59	0.12	1.57	0.07	3.72	0.08	1.87	0.08	2.47	0.12	0.36	0.06	0.50	0.05
33	-6.77	78.86	0.20	10.69	0.12	1.56	0.07	3.74	0.08	1.77	0.07	2.52	0.12	0.35	0.06	0.51	0.05
34	-6.67	78.84	0.20	10.72	0.12	1.55	0.07	3.66	0.08	1.69	0.07	2.69	0.13	0.41	0.07	0.43	0.04
35	-6.57	79.13	0.20	10.48	0.12	1.52	0.06	3.79	0.08	1.70	0.07	2.55	0.12	0.42	0.07	0.42	0.04
36	-6.46	79.14	0.20	10.65	0.12	1.52	0.06	3.72	0.08	1.77	0.07	2.38	0.11	0.33	0.05	0.48	0.04
37	-6.36	78.90	0.20	10.52	0.12	1.55	0.06	3.79	0.08	1.79	0.07	2.62	0.13	0.41	0.07	0.44	0.04
38	-6.26	79.05	0.20	10.41	0.12	1.56	0.07	3.84	0.08	1.71	0.07	2.58	0.12	0.44	0.07	0.42	0.04
39	-6.16	78.93	0.20	10.49	0.12	1.58	0.07	3.80	0.08	1.68	0.07	2.65	0.13	0.44	0.07	0.43	0.04
40	-6.06	78.96	0.20	10.61	0.12	1.52	0.06	3.81	0.08	1.66	0.07	2.65	0.13	0.39	0.07	0.40	0.04
41	-5.96	79.13	0.20	10.45	0.12	1.56	0.07	3.88	0.08	1.66	0.07	2.54	0.12	0.38	0.06	0.41	0.04
42	-5.86	79.42	0.21	10.43	0.12	1.60	0.07	3.79	0.08	1.64	0.07	2.38	0.11	0.36	0.06	0.39	0.03
43	-5.76	79.26	0.20	10.51	0.12	1.61	0.07	3.74	0.08	1.61	0.07	2.43	0.12	0.40	0.07	0.44	0.04
44	-5.66	79.36	0.21	10.42	0.12	1.61	0.07	3.84	0.08	1.47	0.06	2.50	0.12	0.34	0.06	0.46	0.04
45	-5.56	79.26	0.20	10.38	0.11	1.60	0.07	3.86	0.08	1.60	0.06	2.53	0.12	0.34	0.06	0.43	0.04
46	-5.45	79.35	0.21	10.53	0.12	1.60	0.07	3.87	0.08	1.57	0.06	2.24	0.11	0.36	0.06	0.47	0.04
47	-5.35	79.36	0.21	10.45	0.12	1.59	0.07	3.85	0.08	1.50	0.06	2.35	0.11	0.42	0.07	0.47	0.04
48	-5.25	79.44	0.21	10.38	0.12	1.69	0.07	3.86	0.08	1.43	0.06	2.39	0.11	0.37	0.06	0.44	0.04

49	-5.15	79.59	0.21	10.40	0.12	1.60	0.07	3.89	0.08	1.41	0.06	2.34	0.11	0.35	0.06	0.41	0.04
50	-5.05	79.55	0.21	10.46	0.12	1.53	0.06	3.90	0.08	1.41	0.06	2.34	0.11	0.35	0.06	0.45	0.04
51	-4.95	79.43	0.21	10.35	0.11	1.55	0.07	4.00	0.09	1.38	0.06	2.50	0.12	0.39	0.06	0.40	0.04
52	-4.85	79.62	0.21	10.32	0.11	1.64	0.07	3.96	0.08	1.41	0.06	2.31	0.11	0.36	0.06	0.40	0.04
53	-4.75	79.54	0.21	10.36	0.11	1.63	0.07	4.03	0.09	1.39	0.06	2.23	0.11	0.36	0.06	0.46	0.04
54	-4.65	79.65	0.21	10.37	0.11	1.63	0.07	4.02	0.09	1.33	0.05	2.22	0.11	0.33	0.05	0.45	0.04
55	-4.55	79.76	0.21	10.29	0.11	1.65	0.07	4.09	0.09	1.26	0.05	2.14	0.10	0.37	0.06	0.44	0.04
56	-4.44	79.33	0.21	10.29	0.11	1.60	0.07	4.09	0.09	1.25	0.05	2.62	0.13	0.39	0.06	0.43	0.04
57	-4.34	79.59	0.21	10.33	0.11	1.66	0.07	4.03	0.09	1.23	0.05	2.30	0.11	0.40	0.07	0.45	0.04
58	-4.24	79.73	0.21	10.24	0.11	1.66	0.07	3.97	0.08	1.23	0.05	2.39	0.11	0.36	0.06	0.42	0.04
59	-4.14	79.58	0.21	10.26	0.11	1.73	0.07	4.12	0.09	1.25	0.05	2.30	0.11	0.34	0.06	0.43	0.04
60	-4.04	79.53	0.21	10.14	0.11	1.72	0.07	4.26	0.09	1.22	0.05	2.36	0.11	0.40	0.07	0.37	0.03
61	-3.94	79.56	0.21	10.15	0.11	1.74	0.07	4.29	0.09	1.16	0.05	2.31	0.11	0.38	0.06	0.42	0.04
62	-3.84	79.50	0.21	10.25	0.11	1.77	0.07	4.18	0.09	1.13	0.05	2.33	0.11	0.40	0.07	0.43	0.04
63	-3.74	79.60	0.21	10.30	0.11	1.84	0.08	4.22	0.09	0.99	0.04	2.28	0.11	0.38	0.06	0.38	0.03
64	-3.64	79.64	0.21	10.20	0.11	1.89	0.08	4.20	0.09	1.00	0.04	2.32	0.11	0.35	0.06	0.40	0.04
65	-3.54	79.85	0.21	10.15	0.11	1.84	0.08	4.24	0.09	0.96	0.04	2.23	0.11	0.32	0.05	0.40	0.04
66	-3.43	79.66	0.21	10.02	0.11	1.88	0.08	4.43	0.09	0.95	0.04	2.32	0.11	0.33	0.05	0.40	0.04
67	-3.33	79.70	0.21	10.14	0.11	1.89	0.08	4.45	0.09	0.98	0.04	2.18	0.10	0.31	0.05	0.36	0.03
68	-3.23	79.76	0.21	10.16	0.11	1.87	0.08	4.39	0.09	0.96	0.04	2.10	0.10	0.39	0.07	0.37	0.03
69	-3.13	79.78	0.21	10.08	0.11	1.89	0.08	4.43	0.09	0.89	0.04	2.14	0.10	0.38	0.06	0.41	0.04
70	-3.03	79.50	0.21	10.20	0.11	1.93	0.08	4.49	0.10	0.87	0.04	2.20	0.11	0.44	0.07	0.38	0.03
71	-2.93	79.65	0.21	10.09	0.11	1.91	0.08	4.59	0.10	0.92	0.04	2.18	0.10	0.30	0.05	0.35	0.03
72	-2.83	79.89	0.21	10.04	0.11	1.86	0.08	4.67	0.10	0.86	0.03	2.07	0.10	0.28	0.05	0.34	0.03
73	-2.73	79.49	0.21	10.15	0.11	2.02	0.09	4.65	0.10	0.82	0.03	2.08	0.10	0.40	0.07	0.39	0.04
74	-2.63	79.46	0.21	10.13	0.11	2.11	0.09	4.78	0.10	0.77	0.03	2.06	0.10	0.31	0.05	0.38	0.03
75	-2.53	79.56	0.21	9.97	0.11	2.05	0.09	4.79	0.10	0.80	0.03	2.08	0.10	0.37	0.06	0.38	0.03
76	-2.42	79.45	0.21	10.04	0.11	2.10	0.09	4.75	0.10	0.84	0.03	2.07	0.10	0.40	0.07	0.34	0.03
77	-2.32	79.47	0.21	10.00	0.11	2.18	0.09	4.85	0.10	0.78	0.03	2.05	0.10	0.34	0.06	0.33	0.03
78	-2.22	79.33	0.21	9.89	0.11	2.30	0.10	4.88	0.10	0.86	0.03	1.97	0.09	0.41	0.07	0.36	0.03
79	-2.12	79.46	0.21	9.80	0.11	2.31	0.10	4.94	0.11	0.80	0.03	2.00	0.10	0.37	0.06	0.33	0.03
80	-2.02	79.32	0.21	9.94	0.11	2.42	0.10	4.86	0.10	0.85	0.03	1.94	0.09	0.32	0.05	0.34	0.03
81	-1.92	79.27	0.20	9.82	0.11	2.42	0.10	4.92	0.10	0.87	0.04	1.98	0.09	0.32	0.05	0.40	0.04
82	-1.82	79.30	0.20	9.86	0.11	2.43	0.10	4.94	0.11	0.91	0.04	1.88	0.09	0.30	0.05	0.37	0.03
83	-1.72	79.16	0.20	9.75	0.11	2.49	0.10	5.05	0.11	0.95	0.04	1.93	0.09	0.37	0.06	0.30	0.03
84	-1.62	79.17	0.20	9.82	0.11	2.52	0.11	4.97	0.11	0.92	0.04	1.97	0.09	0.30	0.05	0.34	0.03
85	-1.52	78.95	0.20	9.79	0.11	2.55	0.11	4.93	0.11	1.03	0.04	2.08	0.10	0.35	0.06	0.32	0.03
86	-1.41	78.93	0.20	9.56	0.11	2.70	0.11	4.93	0.10	1.07	0.04	2.19	0.11	0.32	0.05	0.31	0.03
87	-1.31	78.97	0.20	9.32	0.10	2.66	0.11	4.96	0.11	1.11	0.04	2.31	0.11	0.33	0.06	0.34	0.03
88	-1.21	78.89	0.20	9.27	0.10	2.72	0.11	4.84	0.10	1.20	0.05	2.31	0.11	0.40	0.07	0.37	0.03
89	-1.11	78.90	0.20	9.08	0.10	2.82	0.12	4.82	0.10	1.20	0.05	2.44	0.12	0.36	0.06	0.37	0.03
90	-1.01	79.02	0.20	8.93	0.10	2.79	0.12	4.88	0.10	1.30	0.05	2.39	0.11	0.33	0.05	0.37	0.03
91	-0.91	79.00	0.20	8.86	0.10	2.86	0.12	4.80	0.10	1.37	0.06	2.42	0.12	0.35	0.06	0.35	0.03
92	-0.81	78.87	0.20	8.69	0.10	2.91	0.12	4.78	0.10	1.40	0.06	2.67	0.13	0.33	0.05	0.35	0.03
93	-0.71	78.76	0.20	8.53	0.09	2.98	0.13	4.83	0.10	1.54	0.06	2.67	0.13	0.31	0.05	0.37	0.03
94	-0.61	78.79	0.20	8.37	0.09	2.99	0.13	4.84	0.10	1.64	0.07	2.64	0.13	0.33	0.06	0.39	0.03
95	-0.51	78.45	0.20	8.35	0.09	3.00	0.13	4.85	0.10	1.65	0.07	2.95	0.14	0.36	0.06	0.39	0.04
96	-0.40	78.31	0.20	8.21	0.09	3.04	0.13	4.88	0.10	1.69	0.07	3.09	0.15	0.37	0.06	0.40	0.04
97	-0.30	78.51	0.20	8.27	0.09	3.13	0.13	4.78	0.10	1.67	0.07	2.94	0.14	0.34	0.06	0.35	0.03
98	-0.20	78.58	0.20	8.33	0.09	3.15	0.13	4.74	0.10	1.61	0.07	2.95	0.14	0.28	0.05	0.36	0.03
99	-0.10	78.51	0.20	8.36	0.09	3.23	0.14	4.72	0.10	1.60	0.06	2.87	0.14	0.30	0.05	0.41	0.04
100	0.00	78.42	0.20	8.14	0.09	3.20	0.13	4.91	0.10	1.62	0.07	3.02	0.14	0.31	0.05	0.38	0.03
101	0.10	78.04	0.20	8.31	0.09	3.20	0.13	4.95	0.11	1.67	0.07	3.08	0.15	0.32	0.05	0.41	0.04
102	0.20	78.09	0.20	8.18	0.09	3.24	0.14	5.02	0.11	1.68	0.07	3.09	0.15	0.35	0.06	0.36	0.03
103	0.30	78.09	0.20	8.32	0.09	3.35	0.14	4.96	0.11	1.62	0.07	3.08	0.15	0.27	0.04	0.32	0.03
104	0.40	78.03	0.20	8.27	0.09	3.41	0.14	4.95	0.11	1.57	0.06	3.05	0.15	0.35	0.06	0.37	0.03
105	0.51	77.74	0.20	8.28	0.09	3.43	0.14	4.94	0.11	1.62	0.07	3.28	0.16	0.30	0.05	0.40	0.04
106	0.61	77.47	0.20	8.36	0.09	3.49	0.15	5.06	0.11	1.64	0.07	3.22	0.15	0.34	0.06	0.42	0.04
107	0.71	77.63	0.20	8.37	0.09	3.43	0.14	5.18	0.11	1.58	0.06	3.07	0.15	0.34	0.06	0.40	0.04
108	0.81	77.60	0.20	8.54	0.09	3.42	0.14	5.11	0.11	1.51	0.06	3.04	0.15	0.43	0.07	0.35	0.03
109	0.91	77.30	0.20	8.73	0.10	3.62	0.15	4.98	0.11	1.45	0.06	3.17	0.15	0.34	0.06	0.39	0.04
110	1.01	77.07	0.20	8.72	0.10	3.57	0.15	5.14	0.11	1.48	0.06	3.33	0.16	0.34	0.06	0.35	0.03

111	1.11	77.01	0.20	8.75	0.10	3.50	0.15	5.29	0.11	1.41	0.06	3.34	0.16	0.35	0.06	0.35	0.03
112	1.21	76.88	0.20	8.79	0.10	3.66	0.15	5.26	0.11	1.35	0.05	3.32	0.16	0.33	0.06	0.41	0.04
113	1.31	76.99	0.20	8.83	0.10	3.68	0.15	5.20	0.11	1.37	0.06	3.20	0.15	0.33	0.06	0.40	0.04
114	1.41	77.07	0.20	8.94	0.10	3.73	0.16	5.18	0.11	1.36	0.06	2.99	0.14	0.37	0.06	0.35	0.03
115	1.52	76.96	0.20	8.98	0.10	3.71	0.16	5.31	0.11	1.33	0.05	3.01	0.14	0.32	0.05	0.37	0.03
116	1.62	76.59	0.20	8.94	0.10	3.74	0.16	5.46	0.12	1.33	0.05	3.29	0.16	0.29	0.05	0.35	0.03
117	1.72	76.75	0.20	8.97	0.10	3.71	0.16	5.51	0.12	1.33	0.05	3.07	0.15	0.33	0.06	0.33	0.03
118	1.82	76.54	0.20	9.21	0.10	3.81	0.16	5.45	0.12	1.22	0.05	3.03	0.15	0.38	0.06	0.37	0.03
119	1.92	76.28	0.20	9.27	0.10	3.82	0.16	5.42	0.12	1.20	0.05	3.23	0.15	0.39	0.07	0.38	0.03
120	2.02	76.37	0.20	9.29	0.10	3.88	0.16	5.41	0.12	1.23	0.05	3.16	0.15	0.34	0.06	0.33	0.03
121	2.12	76.21	0.20	9.40	0.10	3.90	0.16	5.49	0.12	1.12	0.05	3.16	0.15	0.34	0.06	0.37	0.03
122	2.22	76.20	0.20	9.46	0.10	3.91	0.16	5.47	0.12	1.14	0.05	3.06	0.15	0.39	0.07	0.37	0.03
123	2.32	75.99	0.20	9.52	0.11	3.91	0.16	5.61	0.12	1.14	0.05	3.19	0.15	0.32	0.05	0.32	0.03
124	2.42	75.82	0.20	9.53	0.11	3.93	0.17	5.59	0.12	1.11	0.05	3.27	0.16	0.38	0.06	0.36	0.03
125	2.53	76.03	0.20	9.56	0.11	3.96	0.17	5.50	0.12	0.98	0.04	3.23	0.15	0.38	0.06	0.36	0.03
126	2.63	76.10	0.20	9.67	0.11	3.94	0.17	5.54	0.12	0.98	0.04	3.02	0.14	0.38	0.06	0.37	0.03
127	2.73	75.92	0.20	9.68	0.11	4.03	0.17	5.56	0.12	1.03	0.04	3.11	0.15	0.30	0.05	0.38	0.03
128	2.83	75.88	0.20	9.79	0.11	4.04	0.17	5.54	0.12	0.96	0.04	3.09	0.15	0.30	0.05	0.39	0.04
129	2.93	75.61	0.20	9.72	0.11	4.01	0.17	5.61	0.12	1.01	0.04	3.31	0.16	0.35	0.06	0.37	0.03
130	3.03	75.62	0.20	9.65	0.11	4.10	0.17	5.68	0.12	0.98	0.04	3.23	0.16	0.33	0.06	0.40	0.04
131	3.13	75.80	0.20	9.70	0.11	4.08	0.17	5.67	0.12	0.97	0.04	3.09	0.15	0.34	0.06	0.35	0.03
132	3.23	75.45	0.20	9.77	0.11	4.15	0.17	5.71	0.12	0.95	0.04	3.24	0.16	0.35	0.06	0.37	0.03
133	3.33	75.88	0.20	9.83	0.11	4.01	0.17	5.64	0.12	0.91	0.04	2.96	0.14	0.35	0.06	0.43	0.04
134	3.43	75.49	0.20	9.63	0.11	4.04	0.17	5.86	0.12	0.94	0.04	3.25	0.16	0.40	0.07	0.38	0.03
135	3.54	75.27	0.19	9.77	0.11	4.14	0.17	5.78	0.12	0.99	0.04	3.29	0.16	0.36	0.06	0.41	0.04
136	3.64	75.40	0.19	9.84	0.11	4.16	0.17	5.72	0.12	0.94	0.04	3.18	0.15	0.36	0.06	0.38	0.03
137	3.74	75.21	0.19	9.72	0.11	4.16	0.17	5.86	0.12	0.91	0.04	3.42	0.16	0.36	0.06	0.37	0.03
138	3.84	75.43	0.19	9.81	0.11	4.14	0.17	5.73	0.12	0.93	0.04	3.17	0.15	0.39	0.06	0.40	0.04
139	3.94	75.51	0.20	9.93	0.11	4.16	0.17	5.60	0.12	0.88	0.04	3.10	0.15	0.37	0.06	0.45	0.04
140	4.04	75.59	0.20	9.80	0.11	4.07	0.17	5.72	0.12	0.91	0.04	3.14	0.15	0.41	0.07	0.37	0.03
141	4.14	75.52	0.20	9.84	0.11	4.14	0.17	5.73	0.12	0.86	0.04	3.15	0.15	0.37	0.06	0.39	0.03
142	4.24	75.39	0.19	9.80	0.11	4.15	0.17	5.82	0.12	0.85	0.03	3.30	0.16	0.32	0.05	0.37	0.03
143	4.34	75.21	0.19	9.88	0.11	4.18	0.18	5.76	0.12	0.83	0.03	3.43	0.16	0.32	0.05	0.40	0.04
144	4.44	75.16	0.19	9.89	0.11	4.26	0.18	5.76	0.12	0.81	0.03	3.35	0.16	0.35	0.06	0.42	0.04
145	4.55	75.28	0.19	9.85	0.11	4.22	0.18	5.71	0.12	0.78	0.03	3.35	0.16	0.40	0.07	0.40	0.04
146	4.65	74.98	0.19	9.87	0.11	4.31	0.18	5.78	0.12	0.83	0.03	3.37	0.16	0.45	0.07	0.41	0.04
147	4.75	74.96	0.19	10.03	0.11	4.29	0.18	5.75	0.12	0.83	0.03	3.38	0.16	0.36	0.06	0.40	0.04
148	4.85	75.38	0.19	9.89	0.11	4.23	0.18	5.71	0.12	0.82	0.03	3.25	0.16	0.30	0.05	0.41	0.04
149	4.95	75.13	0.19	10.11	0.11	4.30	0.18	5.68	0.12	0.77	0.03	3.20	0.15	0.39	0.06	0.43	0.04
150	5.05	75.16	0.19	10.03	0.11	4.28	0.18	5.67	0.12	0.76	0.03	3.32	0.16	0.38	0.06	0.40	0.04
151	5.15	75.20	0.19	9.90	0.11	4.26	0.18	5.66	0.12	0.75	0.03	3.46	0.17	0.37	0.06	0.41	0.04
152	5.25	74.94	0.19	10.01	0.11	4.28	0.18	5.73	0.12	0.78	0.03	3.39	0.16	0.40	0.07	0.45	0.04
153	5.35	75.06	0.19	9.88	0.11	4.31	0.18	5.84	0.12	0.80	0.03	3.31	0.16	0.40	0.07	0.40	0.04
154	5.45	74.99	0.19	9.94	0.11	4.35	0.18	5.85	0.12	0.77	0.03	3.31	0.16	0.38	0.06	0.41	0.04
155	5.56	75.18	0.19	10.08	0.11	4.31	0.18	5.75	0.12	0.70	0.03	3.17	0.15	0.38	0.06	0.44	0.04
156	5.66	75.43	0.19	9.99	0.11	4.19	0.18	5.72	0.12	0.77	0.03	3.16	0.15	0.35	0.06	0.39	0.03
157	5.76	75.17	0.19	9.97	0.11	4.31	0.18	5.74	0.12	0.77	0.03	3.21	0.15	0.40	0.07	0.43	0.04
158	5.86	75.33	0.19	9.94	0.11	4.33	0.18	5.72	0.12	0.71	0.03	3.20	0.15	0.34	0.06	0.42	0.04
159	5.96	75.21	0.19	10.00	0.11	4.26	0.18	5.81	0.12	0.75	0.03	3.20	0.15	0.34	0.06	0.43	0.04
160	6.06	75.19	0.19	9.98	0.11	4.28	0.18	5.82	0.12	0.68	0.03	3.32	0.16	0.36	0.06	0.36	0.03
161	6.16	74.95	0.19	10.05	0.11	4.34	0.18	5.78	0.12	0.70	0.03	3.42	0.16	0.37	0.06	0.39	0.04
162	6.26	75.02	0.19	9.96	0.11	4.26	0.18	5.84	0.12	0.73	0.03	3.39	0.16	0.39	0.07	0.40	0.04
163	6.36	74.78	0.19	9.90	0.11	4.37	0.18	5.91	0.13	0.80	0.03	3.40	0.16	0.43	0.07	0.40	0.04
164	6.46	75.08	0.19	9.98	0.11	4.30	0.18	5.85	0.12	0.79	0.03	3.14	0.15	0.41	0.07	0.44	0.04
165	6.57	74.91	0.19	10.02	0.11	4.31	0.18	5.78	0.12	0.77	0.03	3.43	0.16	0.37	0.06	0.42	0.04
166	6.67	74.99	0.19	10.08	0.11	4.34	0.18	5.76	0.12	0.69	0.03	3.28	0.16	0.38	0.06	0.47	0.04
167	6.77	75.19	0.19	10.00	0.11	4.33	0.18	5.78	0.12	0.64	0.03	3.23	0.16	0.38	0.06	0.43	0.04
168	6.87	75.06	0.19	10.24	0.11	4.32	0.18	5.71	0.12	0.67	0.03	3.26	0.16	0.30	0.05	0.44	0.04
169	6.97	75.08	0.19	10.08	0.11	4.35	0.18	5.76	0.12	0.70	0.03	3.33	0.16	0.33	0.05	0.38	0.03
170	7.07	74.86	0.19	10.04	0.11	4.36	0.18	5.95	0.13	0.71	0.03	3.33	0.16	0.36	0.06	0.39	0.03
171	7.17	75.14	0.19	10.11	0.11	4.32	0.18	5.80	0.12	0.66	0.03	3.23	0.15	0.34	0.06	0.39	0.03
172	7.27	74.89	0.19	10.14	0.11	4.29	0.18	5.85	0.12	0.69	0.03	3.35	0.16	0.43	0.07	0.37	0.03

173	7.37	74.78	0.19	10.09	0.11	4.35	0.18	5.98	0.13	0.78	0.03	3.24	0.16	0.42	0.07	0.35	0.03
174	7.47	74.84	0.19	10.11	0.11	4.35	0.18	5.91	0.13	0.75	0.03	3.27	0.16	0.38	0.06	0.39	0.04
175	7.58	74.89	0.19	10.12	0.11	4.31	0.18	5.89	0.13	0.70	0.03	3.29	0.16	0.42	0.07	0.38	0.03
176	7.68	75.04	0.19	10.21	0.11	4.22	0.18	5.87	0.13	0.64	0.03	3.16	0.15	0.40	0.07	0.45	0.04
177	7.78	75.02	0.19	10.16	0.11	4.35	0.18	5.76	0.12	0.69	0.03	3.18	0.15	0.38	0.06	0.45	0.04
178	7.88	74.87	0.19	10.28	0.11	4.38	0.18	5.86	0.12	0.67	0.03	3.09	0.15	0.39	0.06	0.46	0.04
179	7.98	74.95	0.19	10.17	0.11	4.35	0.18	5.88	0.13	0.64	0.03	3.22	0.15	0.38	0.06	0.42	0.04
180	8.08	74.84	0.19	10.09	0.11	4.31	0.18	5.87	0.12	0.63	0.03	3.45	0.17	0.42	0.07	0.40	0.04
181	8.18	75.00	0.19	10.12	0.11	4.28	0.18	5.82	0.12	0.65	0.03	3.32	0.16	0.41	0.07	0.39	0.03
182	8.28	74.64	0.19	10.10	0.11	4.27	0.18	5.99	0.13	0.73	0.03	3.42	0.16	0.43	0.07	0.43	0.04
183	8.38	74.92	0.19	10.20	0.11	4.30	0.18	5.80	0.12	0.70	0.03	3.33	0.16	0.33	0.06	0.42	0.04
184	8.48	74.87	0.19	10.14	0.11	4.25	0.18	5.91	0.13	0.74	0.03	3.42	0.16	0.30	0.05	0.37	0.03
185	8.59	74.87	0.19	10.19	0.11	4.25	0.18	5.94	0.13	0.70	0.03	3.22	0.15	0.46	0.08	0.39	0.03
186	8.69	74.94	0.19	10.10	0.11	4.28	0.18	5.86	0.12	0.66	0.03	3.29	0.16	0.44	0.07	0.43	0.04
187	8.79	74.91	0.19	10.13	0.11	4.29	0.18	5.92	0.13	0.63	0.03	3.27	0.16	0.40	0.07	0.44	0.04
188	8.89	75.06	0.19	10.14	0.11	4.27	0.18	5.89	0.13	0.63	0.03	3.28	0.16	0.35	0.06	0.38	0.03
189	8.99	74.84	0.19	10.20	0.11	4.38	0.18	5.90	0.13	0.64	0.03	3.29	0.16	0.35	0.06	0.39	0.04
190	9.09	74.77	0.19	10.27	0.11	4.28	0.18	5.97	0.13	0.66	0.03	3.31	0.16	0.30	0.05	0.44	0.04
191	9.19	74.76	0.19	10.24	0.11	4.24	0.18	6.00	0.13	0.63	0.03	3.37	0.16	0.34	0.06	0.41	0.04
192	9.29	74.67	0.19	10.29	0.11	4.34	0.18	5.95	0.13	0.62	0.03	3.32	0.16	0.40	0.07	0.40	0.04

Agglomerate D1

Table J.4: Major element compositions (as wt.% oxides) from a line traverse across the interface of exterior agglomerate D1 (from agglomerate D1 to host AG.D) extracted from quantified EDS compositional maps. The EDS compositional maps were collected at a resolution of 4.1 pixels/μm. The smoothing width for this traverse was 125 pixels (30.8 μm) wide. This is a CaMgFe interface and has been centered at $x = 0$ based on the FeO maximum. Peak points within 2σ of the FeO maximum are highlighted in yellow. Uncertainties are 2SEOM.

Pt.	Position (μm)	SiO_2	2σ	Al_2O_3	2σ	Na_2O	2σ	K_2O	2σ	CaO	2σ	FeO	2σ	TiO_2	2σ	MgO	2σ
1	-12.56	74.06	0.17	12.77	0.10	2.71	0.08	4.38	0.07	1.90	0.05	3.24	0.13	0.32	0.04	0.62	0.03
2	-12.32	73.94	0.17	12.75	0.10	2.75	0.08	4.42	0.07	1.91	0.05	3.24	0.13	0.38	0.04	0.61	0.03
3	-12.07	73.79	0.17	12.80	0.10	2.74	0.08	4.49	0.07	1.95	0.06	3.23	0.13	0.37	0.04	0.62	0.03
4	-11.82	73.92	0.17	12.87	0.10	2.71	0.08	4.36	0.07	1.93	0.06	3.21	0.12	0.36	0.04	0.64	0.04
5	-11.58	74.09	0.17	12.80	0.10	2.73	0.08	4.41	0.07	1.92	0.06	3.06	0.12	0.36	0.04	0.64	0.03
6	-11.33	74.00	0.17	12.83	0.10	2.71	0.08	4.43	0.07	1.99	0.06	3.11	0.12	0.32	0.04	0.59	0.03
7	-11.08	73.98	0.17	12.80	0.10	2.70	0.08	4.35	0.07	1.98	0.06	3.20	0.12	0.36	0.04	0.62	0.03
8	-10.84	73.93	0.17	12.78	0.10	2.71	0.08	4.43	0.07	1.93	0.06	3.27	0.13	0.33	0.04	0.61	0.03
9	-10.59	74.20	0.17	12.67	0.10	2.69	0.08	4.36	0.07	1.93	0.06	3.22	0.13	0.34	0.04	0.59	0.03
10	-10.34	74.04	0.17	12.67	0.10	2.77	0.08	4.37	0.07	1.93	0.06	3.31	0.13	0.32	0.04	0.59	0.03
11	-10.10	74.05	0.17	12.80	0.10	2.73	0.08	4.33	0.07	1.87	0.05	3.27	0.13	0.37	0.04	0.58	0.03
12	-9.85	73.88	0.17	12.76	0.10	2.73	0.08	4.46	0.07	2.01	0.06	3.19	0.12	0.36	0.04	0.61	0.03
13	-9.61	74.07	0.17	12.67	0.10	2.70	0.08	4.46	0.07	1.98	0.06	3.16	0.12	0.35	0.04	0.61	0.03
14	-9.36	74.12	0.17	12.65	0.10	2.71	0.08	4.47	0.07	1.92	0.06	3.22	0.13	0.32	0.04	0.60	0.03
15	-9.11	74.16	0.17	12.63	0.10	2.72	0.08	4.42	0.07	1.87	0.05	3.26	0.13	0.31	0.04	0.63	0.03
16	-8.87	74.11	0.17	12.68	0.10	2.72	0.08	4.27	0.07	1.88	0.05	3.30	0.13	0.38	0.04	0.65	0.04
17	-8.62	74.16	0.17	12.59	0.10	2.70	0.08	4.33	0.07	1.88	0.05	3.35	0.13	0.37	0.04	0.62	0.03
18	-8.37	74.24	0.17	12.62	0.10	2.68	0.08	4.31	0.07	1.90	0.05	3.26	0.13	0.37	0.04	0.62	0.03
19	-8.13	74.37	0.17	12.60	0.10	2.68	0.08	4.31	0.07	1.85	0.05	3.27	0.13	0.31	0.04	0.61	0.03
20	-7.88	74.39	0.17	12.57	0.10	2.69	0.08	4.33	0.07	1.83	0.05	3.30	0.13	0.29	0.03	0.60	0.03
21	-7.64	74.37	0.17	12.62	0.10	2.64	0.07	4.29	0.07	1.84	0.05	3.29	0.13	0.31	0.04	0.63	0.03
22	-7.39	74.33	0.17	12.60	0.10	2.67	0.08	4.27	0.07	1.86	0.05	3.29	0.13	0.33	0.04	0.66	0.04
23	-7.14	74.35	0.17	12.54	0.10	2.67	0.08	4.29	0.07	1.87	0.05	3.28	0.13	0.34	0.04	0.65	0.04
24	-6.90	74.53	0.17	12.45	0.10	2.69	0.08	4.27	0.07	1.80	0.05	3.27	0.13	0.36	0.04	0.63	0.03
25	-6.65	74.35	0.17	12.47	0.10	2.73	0.08	4.31	0.07	1.83	0.05	3.35	0.13	0.32	0.04	0.64	0.03
26	-6.40	74.51	0.17	12.42	0.10	2.65	0.08	4.34	0.07	1.87	0.05	3.24	0.13	0.32	0.04	0.63	0.03
27	-6.16	74.71	0.17	12.43	0.10	2.67	0.08	4.22	0.07	1.85	0.05	3.14	0.12	0.35	0.04	0.64	0.03
28	-5.91	74.31	0.17	12.39	0.10	2.66	0.08	4.38	0.07	1.87	0.05	3.39	0.13	0.37	0.04	0.63	0.03
29	-5.67	74.40	0.17	12.39	0.10	2.65	0.08	4.34	0.07	1.83	0.05	3.43	0.13	0.34	0.04	0.63	0.03
30	-5.42	74.50	0.17	12.39	0.10	2.69	0.08	4.31	0.07	1.83	0.05	3.37	0.13	0.29	0.03	0.62	0.03
31	-5.17	74.58	0.17	12.32	0.10	2.64	0.07	4.28	0.07	1.83	0.05	3.38	0.13	0.31	0.04	0.64	0.04
32	-4.93	74.81	0.17	12.23	0.09	2.67	0.08	4.26	0.07	1.82	0.05	3.27	0.13	0.31	0.04	0.62	0.03
33	-4.68	74.68	0.17	12.24	0.10	2.69	0.08	4.27	0.07	1.78	0.05	3.37	0.13	0.33	0.04	0.64	0.04
34	-4.43	74.78	0.17	12.24	0.10	2.65	0.08	4.26	0.07	1.78	0.05	3.30	0.13	0.31	0.04	0.68	0.04
35	-4.19	74.88	0.18	12.24	0.10	2.64	0.07	4.28	0.07	1.76	0.05	3.21	0.12	0.35	0.04	0.64	0.03
36	-3.94	74.86	0.18	12.21	0.09	2.62	0.07	4.26	0.07	1.70	0.05	3.35	0.13	0.33	0.04	0.66	0.04
37	-3.69	74.85	0.17	12.16	0.09	2.59	0.07	4.26	0.07	1.72	0.05	3.39	0.13	0.35	0.04	0.67	0.04
38	-3.45	74.80	0.17	12.02	0.09	2.59	0.07	4.30	0.07	1.74	0.05	3.51	0.14	0.37	0.04	0.66	0.04
39	-3.20	75.08	0.18	12.06	0.09	2.59	0.07	4.25	0.07	1.68	0.05	3.38	0.13	0.29	0.03	0.66	0.04
40	-2.96	75.21	0.18	12.10	0.09	2.54	0.07	4.25	0.07	1.62	0.05	3.29	0.13	0.31	0.04	0.68	0.04
41	-2.71	75.05	0.18	12.07	0.09	2.58	0.07	4.27	0.07	1.57	0.05	3.45	0.13	0.32	0.04	0.69	0.04
42	-2.46	75.14	0.18	12.11	0.09	2.52	0.07	4.19	0.07	1.56	0.04	3.45	0.13	0.34	0.04	0.69	0.04
43	-2.22	75.17	0.18	12.16	0.09	2.50	0.07	4.24	0.07	1.53	0.04	3.42	0.13	0.32	0.04	0.66	0.04
44	-1.97	75.05	0.18	12.07	0.09	2.54	0.07	4.26	0.07	1.56	0.04	3.50	0.14	0.29	0.03	0.72	0.04
45	-1.72	74.93	0.18	12.11	0.09	2.49	0.07	4.25	0.07	1.66	0.05	3.53	0.14	0.31	0.04	0.72	0.04
46	-1.48	74.67	0.17	12.17	0.09	2.45	0.07	4.28	0.07	1.62	0.05	3.83	0.15	0.29	0.03	0.71	0.04
47	-1.23	74.01	0.17	12.27	0.10	2.54	0.07	4.33	0.07	1.80	0.05	3.99	0.16	0.35	0.04	0.71	0.04
48	-0.99	73.51	0.17	12.35	0.10	2.60	0.07	4.30	0.07	1.94	0.06	4.21	0.16	0.35	0.04	0.75	0.04
49	-0.74	72.93	0.17	12.63	0.10	2.62	0.07	4.26	0.07	2.10	0.06	4.38	0.17	0.36	0.04	0.73	0.04
50	-0.49	72.48	0.17	12.84	0.10	2.66	0.08	4.26	0.07	2.26	0.06	4.39	0.17	0.34	0.04	0.77	0.04

51	-0.25	72.02	0.17	13.03	0.10	2.71	0.08	4.26	0.07	2.32	0.07	4.51	0.18	0.35	0.04	0.80	0.04
52	0.00	71.66	0.17	13.09	0.10	2.74	0.08	4.25	0.07	2.44	0.07	4.64	0.18	0.35	0.04	0.82	0.05
53	0.25	71.62	0.17	13.31	0.10	2.74	0.08	4.23	0.07	2.37	0.07	4.48	0.17	0.37	0.04	0.87	0.05
54	0.49	71.44	0.17	13.34	0.10	2.80	0.08	4.28	0.07	2.36	0.07	4.58	0.18	0.35	0.04	0.85	0.05
55	0.74	71.50	0.17	13.40	0.10	2.76	0.08	4.27	0.07	2.30	0.07	4.53	0.18	0.38	0.04	0.85	0.05
56	0.99	71.73	0.17	13.31	0.10	2.75	0.08	4.24	0.07	2.25	0.06	4.48	0.17	0.41	0.05	0.81	0.04
57	1.23	71.94	0.17	13.32	0.10	2.76	0.08	4.36	0.07	2.18	0.06	4.28	0.17	0.36	0.04	0.80	0.04
58	1.48	72.15	0.17	13.27	0.10	2.74	0.08	4.32	0.07	2.09	0.06	4.29	0.17	0.33	0.04	0.80	0.04
59	1.72	72.54	0.17	13.18	0.10	2.73	0.08	4.33	0.07	2.04	0.06	4.04	0.16	0.36	0.04	0.78	0.04
60	1.97	72.90	0.17	13.12	0.10	2.69	0.08	4.32	0.07	1.92	0.06	3.91	0.15	0.38	0.04	0.76	0.04
61	2.22	73.32	0.17	13.11	0.10	2.67	0.08	4.28	0.07	1.79	0.05	3.78	0.15	0.32	0.04	0.72	0.04
62	2.46	73.53	0.17	13.05	0.10	2.63	0.07	4.34	0.07	1.76	0.05	3.66	0.14	0.33	0.04	0.70	0.04
63	2.71	73.69	0.17	13.03	0.10	2.60	0.07	4.29	0.07	1.66	0.05	3.62	0.14	0.40	0.05	0.71	0.04
64	2.96	73.91	0.17	12.97	0.10	2.59	0.07	4.30	0.07	1.63	0.05	3.61	0.14	0.31	0.04	0.67	0.04
65	3.20	74.23	0.17	12.93	0.10	2.58	0.07	4.33	0.07	1.54	0.04	3.36	0.13	0.34	0.04	0.69	0.04
66	3.45	74.35	0.17	12.79	0.10	2.61	0.07	4.38	0.07	1.54	0.04	3.32	0.13	0.35	0.04	0.65	0.04
67	3.69	74.50	0.17	12.89	0.10	2.61	0.07	4.37	0.07	1.46	0.04	3.19	0.12	0.36	0.04	0.62	0.03
68	3.94	74.54	0.17	12.82	0.10	2.57	0.07	4.44	0.07	1.47	0.04	3.19	0.12	0.35	0.04	0.61	0.03
69	4.19	74.69	0.17	12.80	0.10	2.58	0.07	4.40	0.07	1.40	0.04	3.16	0.12	0.37	0.04	0.60	0.03
70	4.43	74.84	0.17	12.79	0.10	2.59	0.07	4.42	0.07	1.36	0.04	3.08	0.12	0.36	0.04	0.57	0.03
71	4.68	75.02	0.18	12.70	0.10	2.56	0.07	4.45	0.07	1.34	0.04	2.99	0.12	0.39	0.05	0.56	0.03
72	4.93	74.98	0.18	12.72	0.10	2.61	0.07	4.48	0.07	1.34	0.04	2.98	0.12	0.34	0.04	0.55	0.03
73	5.17	75.05	0.18	12.76	0.10	2.63	0.07	4.42	0.07	1.28	0.04	2.92	0.11	0.36	0.04	0.57	0.03
74	5.42	75.26	0.18	12.75	0.10	2.58	0.07	4.35	0.07	1.26	0.04	2.94	0.11	0.33	0.04	0.53	0.03
75	5.67	75.30	0.18	12.76	0.10	2.53	0.07	4.34	0.07	1.23	0.04	2.94	0.11	0.36	0.04	0.55	0.03
76	5.91	75.37	0.18	12.77	0.10	2.52	0.07	4.40	0.07	1.22	0.04	2.79	0.11	0.37	0.04	0.55	0.03
77	6.16	75.30	0.18	12.83	0.10	2.58	0.07	4.40	0.07	1.21	0.03	2.77	0.11	0.34	0.04	0.57	0.03
78	6.40	75.37	0.18	12.75	0.10	2.57	0.07	4.44	0.07	1.19	0.03	2.78	0.11	0.34	0.04	0.56	0.03
79	6.65	75.56	0.18	12.62	0.10	2.50	0.07	4.41	0.07	1.22	0.04	2.80	0.11	0.36	0.04	0.53	0.03
80	6.90	75.59	0.18	12.65	0.10	2.58	0.07	4.33	0.07	1.16	0.03	2.81	0.11	0.34	0.04	0.53	0.03
81	7.14	75.73	0.18	12.67	0.10	2.59	0.07	4.36	0.07	1.13	0.03	2.66	0.10	0.34	0.04	0.52	0.03
82	7.39	75.61	0.18	12.71	0.10	2.58	0.07	4.36	0.07	1.13	0.03	2.74	0.11	0.35	0.04	0.51	0.03
83	7.64	75.68	0.18	12.53	0.10	2.57	0.07	4.37	0.07	1.12	0.03	2.88	0.11	0.35	0.04	0.50	0.03
84	7.88	75.65	0.18	12.50	0.10	2.61	0.07	4.38	0.07	1.10	0.03	2.87	0.11	0.38	0.04	0.51	0.03
85	8.13	75.83	0.18	12.52	0.10	2.58	0.07	4.40	0.07	1.11	0.03	2.71	0.11	0.34	0.04	0.52	0.03
86	8.37	75.85	0.18	12.49	0.10	2.47	0.07	4.46	0.07	1.09	0.03	2.79	0.11	0.32	0.04	0.53	0.03
87	8.62	75.98	0.18	12.52	0.10	2.49	0.07	4.38	0.07	1.02	0.03	2.74	0.11	0.37	0.04	0.50	0.03
88	8.87	76.22	0.18	12.49	0.10	2.48	0.07	4.38	0.07	1.02	0.03	2.58	0.10	0.34	0.04	0.50	0.03
89	9.11	76.12	0.18	12.48	0.10	2.50	0.07	4.38	0.07	1.00	0.03	2.66	0.10	0.37	0.04	0.49	0.03
90	9.36	76.17	0.18	12.44	0.10	2.53	0.07	4.38	0.07	1.00	0.03	2.68	0.10	0.33	0.04	0.48	0.03
91	9.61	76.29	0.18	12.44	0.10	2.50	0.07	4.34	0.07	0.98	0.03	2.62	0.10	0.35	0.04	0.47	0.03
92	9.85	76.32	0.18	12.48	0.10	2.42	0.07	4.34	0.07	1.01	0.03	2.60	0.10	0.33	0.04	0.52	0.03
93	10.10	76.24	0.18	12.48	0.10	2.44	0.07	4.35	0.07	1.02	0.03	2.66	0.10	0.33	0.04	0.48	0.03
94	10.34	76.08	0.18	12.48	0.10	2.53	0.07	4.35	0.07	0.96	0.03	2.73	0.11	0.37	0.04	0.51	0.03
95	10.59	76.33	0.18	12.51	0.10	2.46	0.07	4.33	0.07	0.93	0.03	2.63	0.10	0.34	0.04	0.48	0.03
96	10.84	76.14	0.18	12.48	0.10	2.45	0.07	4.40	0.07	0.98	0.03	2.71	0.11	0.36	0.04	0.48	0.03
97	11.08	76.19	0.18	12.46	0.10	2.49	0.07	4.31	0.07	0.99	0.03	2.69	0.10	0.37	0.04	0.51	0.03
98	11.33	76.33	0.18	12.47	0.10	2.50	0.07	4.32	0.07	0.90	0.03	2.66	0.10	0.32	0.04	0.50	0.03
99	11.58	76.33	0.18	12.56	0.10	2.42	0.07	4.31	0.07	0.94	0.03	2.64	0.10	0.30	0.04	0.49	0.03
100	11.82	76.26	0.18	12.55	0.10	2.40	0.07	4.31	0.07	0.94	0.03	2.72	0.11	0.33	0.04	0.50	0.03
101	12.07	76.20	0.18	12.50	0.10	2.44	0.07	4.31	0.07	0.98	0.03	2.75	0.11	0.34	0.04	0.48	0.03
102	12.32	76.36	0.18	12.54	0.10	2.44	0.07	4.33	0.07	0.91	0.03	2.61	0.10	0.34	0.04	0.48	0.03
103	12.56	76.15	0.18	12.44	0.10	2.40	0.07	4.42	0.07	0.98	0.03	2.76	0.11	0.36	0.04	0.50	0.03

Agglomerate D2

Table J.5: Major element compositions (as wt.% oxides) from a line traverse across the interface of exterior agglomerate D2 (from agglomerate D2 to host AG.D) extracted from quantified EDS compositional maps. The EDS compositional maps were collected at a resolution of 4.1 pixels/μm. The smoothing width for this traverse was 125 pixels (30.8 μm) wide. This is a CaMgFe interface and has been centered at $x = 0$ based on the FeO maximum. Peak points within 2σ of the FeO maximum are highlighted in yellow. Uncertainties are 2SEOM.

Pt.	Position (μm)	SiO_2	2σ	Al_2O_3	2σ	Na_2O	2σ	K_2O	2σ	CaO	2σ	FeO	2σ	TiO_2	2σ	MgO	2σ
1	-16.75	74.37	0.17	12.93	0.10	2.43	0.07	4.19	0.07	2.19	0.06	2.95	0.11	0.34	0.04	0.60	0.03
2	-16.50	74.41	0.17	12.89	0.10	2.38	0.07	4.22	0.07	2.29	0.07	2.88	0.11	0.35	0.04	0.57	0.03
3	-16.26	74.17	0.17	12.89	0.10	2.48	0.07	4.26	0.07	2.29	0.07	2.96	0.12	0.36	0.04	0.58	0.03
4	-16.01	74.20	0.17	12.96	0.10	2.50	0.07	4.25	0.07	2.28	0.07	2.85	0.11	0.34	0.04	0.62	0.03
5	-15.76	74.19	0.17	12.98	0.10	2.48	0.07	4.25	0.07	2.27	0.07	2.84	0.11	0.35	0.04	0.63	0.03
6	-15.52	74.28	0.17	12.97	0.10	2.43	0.07	4.26	0.07	2.24	0.06	2.86	0.11	0.34	0.04	0.61	0.03
7	-15.27	74.04	0.17	12.96	0.10	2.48	0.07	4.29	0.07	2.31	0.07	3.01	0.12	0.31	0.04	0.60	0.03
8	-15.02	74.07	0.17	13.12	0.10	2.47	0.07	4.18	0.07	2.34	0.07	2.83	0.11	0.35	0.04	0.63	0.03
9	-14.78	74.14	0.17	13.14	0.10	2.46	0.07	4.22	0.07	2.36	0.07	2.74	0.11	0.35	0.04	0.60	0.03
10	-14.53	74.12	0.17	13.07	0.10	2.49	0.07	4.24	0.07	2.31	0.07	2.79	0.11	0.34	0.04	0.64	0.03
11	-14.29	74.03	0.17	13.03	0.10	2.49	0.07	4.27	0.07	2.35	0.07	2.87	0.11	0.36	0.04	0.61	0.03
12	-14.04	73.77	0.17	13.07	0.10	2.52	0.07	4.27	0.07	2.35	0.07	3.03	0.12	0.36	0.04	0.64	0.03
13	-13.79	73.86	0.17	13.15	0.10	2.50	0.07	4.30	0.07	2.33	0.07	2.89	0.11	0.36	0.04	0.61	0.03
14	-13.55	73.63	0.17	13.20	0.10	2.53	0.07	4.31	0.07	2.34	0.07	3.00	0.12	0.36	0.04	0.62	0.03
15	-13.30	73.58	0.17	13.18	0.10	2.57	0.07	4.30	0.07	2.35	0.07	3.06	0.12	0.31	0.04	0.66	0.04
16	-13.05	73.65	0.17	13.09	0.10	2.52	0.07	4.37	0.07	2.44	0.07	2.97	0.12	0.36	0.04	0.61	0.03
17	-12.81	73.73	0.17	13.12	0.10	2.55	0.07	4.31	0.07	2.37	0.07	2.94	0.11	0.33	0.04	0.65	0.04
18	-12.56	73.71	0.17	13.07	0.10	2.53	0.07	4.40	0.07	2.46	0.07	2.90	0.11	0.32	0.04	0.61	0.03
19	-12.32	73.58	0.17	13.16	0.10	2.56	0.07	4.32	0.07	2.43	0.07	2.98	0.12	0.34	0.04	0.63	0.03
20	-12.07	73.51	0.17	13.29	0.10	2.62	0.07	4.27	0.07	2.38	0.07	2.95	0.11	0.32	0.04	0.65	0.04
21	-11.82	73.55	0.17	13.25	0.10	2.62	0.07	4.33	0.07	2.42	0.07	2.89	0.11	0.30	0.03	0.63	0.03
22	-11.58	73.62	0.17	13.30	0.10	2.63	0.07	4.28	0.07	2.32	0.07	2.94	0.11	0.30	0.04	0.62	0.03
23	-11.33	73.51	0.17	13.30	0.10	2.67	0.08	4.31	0.07	2.38	0.07	2.85	0.11	0.32	0.04	0.66	0.04
24	-11.08	73.36	0.17	13.36	0.10	2.66	0.08	4.34	0.07	2.41	0.07	2.89	0.11	0.35	0.04	0.64	0.03
25	-10.84	73.40	0.17	13.36	0.10	2.67	0.08	4.36	0.07	2.34	0.07	2.89	0.11	0.34	0.04	0.63	0.03
26	-10.59	73.30	0.17	13.35	0.10	2.61	0.07	4.39	0.07	2.38	0.07	3.00	0.12	0.31	0.04	0.66	0.04
27	-10.34	73.32	0.17	13.31	0.10	2.63	0.07	4.36	0.07	2.41	0.07	3.01	0.12	0.32	0.04	0.65	0.04
28	-10.10	73.26	0.17	13.38	0.10	2.62	0.07	4.42	0.07	2.43	0.07	2.91	0.11	0.34	0.04	0.64	0.03
29	-9.85	73.10	0.17	13.37	0.10	2.68	0.08	4.44	0.07	2.41	0.07	3.01	0.12	0.34	0.04	0.64	0.04
30	-9.61	73.20	0.17	13.24	0.10	2.61	0.07	4.45	0.07	2.45	0.07	3.07	0.12	0.34	0.04	0.64	0.03
31	-9.36	73.17	0.17	13.26	0.10	2.61	0.07	4.51	0.07	2.45	0.07	3.06	0.12	0.33	0.04	0.62	0.03
32	-9.11	73.18	0.17	13.31	0.10	2.61	0.07	4.52	0.07	2.42	0.07	2.96	0.12	0.34	0.04	0.65	0.04
33	-8.87	73.15	0.17	13.29	0.10	2.64	0.07	4.58	0.08	2.44	0.07	2.96	0.12	0.31	0.04	0.62	0.03
34	-8.62	73.14	0.17	13.33	0.10	2.65	0.07	4.51	0.07	2.38	0.07	2.96	0.12	0.38	0.04	0.65	0.04
35	-8.37	73.22	0.17	13.31	0.10	2.70	0.08	4.53	0.07	2.37	0.07	2.91	0.11	0.33	0.04	0.63	0.03
36	-8.13	73.26	0.17	13.36	0.10	2.69	0.08	4.49	0.07	2.36	0.07	2.89	0.11	0.35	0.04	0.61	0.03
37	-7.88	73.12	0.17	13.41	0.10	2.72	0.08	4.46	0.07	2.32	0.07	2.98	0.12	0.37	0.04	0.62	0.03
38	-7.64	73.32	0.17	13.30	0.10	2.74	0.08	4.54	0.07	2.31	0.07	2.80	0.11	0.34	0.04	0.64	0.03
39	-7.39	73.15	0.17	13.31	0.10	2.76	0.08	4.64	0.08	2.36	0.07	2.81	0.11	0.34	0.04	0.64	0.03
40	-7.14	73.11	0.17	13.28	0.10	2.79	0.08	4.64	0.08	2.36	0.07	2.84	0.11	0.35	0.04	0.61	0.03
41	-6.90	73.14	0.17	13.29	0.10	2.76	0.08	4.63	0.08	2.40	0.07	2.86	0.11	0.34	0.04	0.59	0.03
42	-6.65	73.16	0.17	13.31	0.10	2.84	0.08	4.58	0.08	2.34	0.07	2.89	0.11	0.30	0.03	0.59	0.03
43	-6.40	73.04	0.17	13.18	0.10	2.79	0.08	4.74	0.08	2.41	0.07	2.89	0.11	0.39	0.04	0.57	0.03
44	-6.16	72.96	0.17	13.36	0.10	2.86	0.08	4.70	0.08	2.30	0.07	2.91	0.11	0.33	0.04	0.58	0.03
45	-5.91	73.10	0.17	13.23	0.10	2.84	0.08	4.73	0.08	2.26	0.06	2.89	0.11	0.38	0.04	0.57	0.03
46	-5.67	73.20	0.17	13.26	0.10	2.85	0.08	4.77	0.08	2.25	0.06	2.72	0.11	0.36	0.04	0.59	0.03
47	-5.42	73.22	0.17	13.35	0.10	2.87	0.08	4.69	0.08	2.17	0.06	2.76	0.11	0.35	0.04	0.60	0.03
48	-5.17	72.98	0.17	13.31	0.10	2.90	0.08	4.82	0.08	2.23	0.06	2.83	0.11	0.33	0.04	0.61	0.03
49	-4.93	73.09	0.17	13.32	0.10	2.88	0.08	4.77	0.08	2.23	0.06	2.77	0.11	0.36	0.04	0.58	0.03
50	-4.68	73.11	0.17	13.30	0.10	2.97	0.08	4.81	0.08	2.19	0.06	2.73	0.11	0.33	0.04	0.56	0.03

51	-4.43	73.09	0.17	13.29	0.10	2.97	0.08	4.88	0.08	2.15	0.06	2.69	0.10	0.36	0.04	0.57	0.03
52	-4.19	73.25	0.17	13.22	0.10	3.05	0.09	4.83	0.08	2.13	0.06	2.59	0.10	0.34	0.04	0.58	0.03
53	-3.94	73.22	0.17	13.19	0.10	3.02	0.09	4.83	0.08	2.10	0.06	2.68	0.10	0.35	0.04	0.59	0.03
54	-3.69	73.25	0.17	13.11	0.10	2.97	0.08	4.89	0.08	2.13	0.06	2.72	0.11	0.36	0.04	0.56	0.03
55	-3.45	73.32	0.17	12.97	0.10	3.01	0.09	4.96	0.08	2.15	0.06	2.70	0.11	0.31	0.04	0.57	0.03
56	-3.20	73.41	0.17	12.70	0.10	3.08	0.09	5.14	0.08	2.13	0.06	2.67	0.10	0.35	0.04	0.52	0.03
57	-2.96	73.79	0.17	12.78	0.10	3.08	0.09	4.96	0.08	1.98	0.06	2.48	0.10	0.36	0.04	0.57	0.03
58	-2.71	74.17	0.17	12.59	0.10	3.04	0.09	4.90	0.08	1.93	0.06	2.50	0.10	0.35	0.04	0.52	0.03
59	-2.46	74.47	0.17	12.37	0.10	3.04	0.09	4.83	0.08	1.87	0.05	2.59	0.10	0.32	0.04	0.52	0.03
60	-2.22	74.69	0.17	12.08	0.09	3.01	0.09	4.85	0.08	1.83	0.05	2.67	0.10	0.34	0.04	0.54	0.03
61	-1.97	74.90	0.18	11.71	0.09	3.02	0.09	4.92	0.08	1.85	0.05	2.73	0.11	0.32	0.04	0.55	0.03
62	-1.72	75.33	0.18	11.20	0.09	2.99	0.08	4.86	0.08	1.89	0.05	2.86	0.11	0.32	0.04	0.54	0.03
63	-1.48	75.56	0.18	10.83	0.08	3.01	0.09	4.80	0.08	1.97	0.06	2.97	0.12	0.31	0.04	0.55	0.03
64	-1.23	75.63	0.18	10.49	0.08	2.95	0.08	4.83	0.08	1.96	0.06	3.33	0.13	0.28	0.03	0.54	0.03
65	-0.99	75.52	0.18	10.33	0.08	3.01	0.09	4.75	0.08	2.07	0.06	3.44	0.13	0.27	0.03	0.60	0.03
66	-0.74	75.17	0.18	10.26	0.08	3.08	0.09	4.73	0.08	2.17	0.06	3.68	0.14	0.28	0.03	0.63	0.03
67	-0.49	74.42	0.17	10.40	0.08	3.22	0.09	4.70	0.08	2.31	0.07	3.88	0.15	0.33	0.04	0.74	0.04
68	-0.25	73.48	0.17	10.66	0.08	3.29	0.09	4.87	0.08	2.55	0.07	4.09	0.16	0.38	0.04	0.69	0.04
69	0.00	72.73	0.17	11.17	0.09	3.51	0.10	4.83	0.08	2.60	0.07	4.10	0.16	0.33	0.04	0.74	0.04
70	0.25	72.14	0.17	11.53	0.09	3.61	0.10	4.88	0.08	2.70	0.08	4.06	0.16	0.32	0.04	0.76	0.04
71	0.49	71.68	0.17	11.74	0.09	3.71	0.11	5.04	0.08	2.74	0.08	4.00	0.16	0.34	0.04	0.76	0.04
72	0.74	71.41	0.17	11.92	0.09	3.80	0.11	5.03	0.08	2.80	0.08	3.95	0.15	0.32	0.04	0.76	0.04
73	0.99	71.45	0.17	12.00	0.09	3.82	0.11	5.00	0.08	2.76	0.08	3.91	0.15	0.32	0.04	0.74	0.04
74	1.23	71.55	0.17	11.92	0.09	3.87	0.11	5.06	0.08	2.73	0.08	3.85	0.15	0.30	0.03	0.73	0.04
75	1.48	71.84	0.17	11.96	0.09	3.88	0.11	4.99	0.08	2.63	0.08	3.67	0.14	0.30	0.04	0.72	0.04
76	1.72	71.85	0.17	12.03	0.09	3.94	0.11	5.08	0.08	2.54	0.07	3.50	0.14	0.30	0.03	0.77	0.04
77	1.97	71.76	0.17	12.04	0.09	3.91	0.11	5.16	0.08	2.60	0.07	3.46	0.13	0.34	0.04	0.73	0.04
78	2.22	71.76	0.17	12.11	0.09	3.97	0.11	5.21	0.09	2.55	0.07	3.37	0.13	0.34	0.04	0.69	0.04
79	2.46	71.80	0.17	12.20	0.09	3.97	0.11	5.13	0.08	2.51	0.07	3.30	0.13	0.37	0.04	0.73	0.04
80	2.71	72.04	0.17	12.22	0.09	3.98	0.11	5.14	0.08	2.51	0.07	3.11	0.12	0.33	0.04	0.67	0.04
81	2.96	71.98	0.17	12.28	0.10	4.06	0.11	5.07	0.08	2.49	0.07	3.12	0.12	0.31	0.04	0.68	0.04
82	3.20	72.11	0.17	12.18	0.09	4.09	0.12	5.11	0.08	2.48	0.07	3.06	0.12	0.29	0.03	0.68	0.04
83	3.45	72.02	0.17	12.15	0.09	4.11	0.12	5.13	0.08	2.42	0.07	3.16	0.12	0.34	0.04	0.66	0.04
84	3.69	71.92	0.17	12.25	0.10	4.10	0.12	5.21	0.09	2.37	0.07	3.10	0.12	0.38	0.04	0.67	0.04
85	3.94	71.95	0.17	12.22	0.09	4.12	0.12	5.23	0.09	2.39	0.07	3.05	0.12	0.35	0.04	0.69	0.04
86	4.19	72.16	0.17	12.17	0.09	4.23	0.12	5.17	0.08	2.33	0.07	3.00	0.12	0.30	0.03	0.64	0.04
87	4.43	72.13	0.17	12.07	0.09	4.15	0.12	5.26	0.09	2.34	0.07	3.07	0.12	0.33	0.04	0.63	0.03
88	4.68	72.19	0.17	12.08	0.09	4.16	0.12	5.25	0.09	2.25	0.06	3.09	0.12	0.35	0.04	0.62	0.03
89	4.93	72.22	0.17	12.18	0.09	4.17	0.12	5.19	0.09	2.25	0.06	3.02	0.12	0.31	0.04	0.65	0.04
90	5.17	72.39	0.17	12.12	0.09	4.19	0.12	5.15	0.08	2.20	0.06	3.01	0.12	0.33	0.04	0.61	0.03
91	5.42	72.37	0.17	12.08	0.09	4.09	0.12	5.30	0.09	2.22	0.06	3.01	0.12	0.32	0.04	0.60	0.03
92	5.66	72.44	0.17	12.10	0.09	4.09	0.12	5.22	0.09	2.17	0.06	3.05	0.12	0.30	0.03	0.62	0.03
93	5.91	72.62	0.17	12.00	0.09	4.07	0.12	5.25	0.09	2.06	0.06	3.05	0.12	0.34	0.04	0.62	0.03
94	6.16	72.73	0.17	12.06	0.09	3.98	0.11	5.19	0.09	2.09	0.06	3.01	0.12	0.35	0.04	0.59	0.03
95	6.40	72.82	0.17	11.98	0.09	4.00	0.11	5.25	0.09	2.07	0.06	3.03	0.12	0.29	0.03	0.58	0.03
96	6.65	72.96	0.17	11.94	0.09	4.05	0.11	5.26	0.09	1.96	0.06	2.94	0.11	0.30	0.04	0.58	0.03
97	6.90	72.97	0.17	12.01	0.09	4.04	0.11	5.21	0.09	1.90	0.05	2.95	0.11	0.34	0.04	0.57	0.03
98	7.14	73.21	0.17	12.00	0.09	3.97	0.11	5.19	0.09	1.82	0.05	2.89	0.11	0.29	0.03	0.63	0.03
99	7.39	73.42	0.17	12.01	0.09	3.90	0.11	5.16	0.08	1.75	0.05	2.87	0.11	0.31	0.04	0.59	0.03
100	7.64	73.50	0.17	11.96	0.09	3.87	0.11	5.25	0.09	1.73	0.05	2.80	0.11	0.31	0.04	0.59	0.03
101	7.88	73.61	0.17	11.98	0.09	3.80	0.11	5.29	0.09	1.64	0.05	2.75	0.11	0.35	0.04	0.58	0.03
102	8.13	73.68	0.17	12.05	0.09	3.79	0.11	5.15	0.08	1.58	0.05	2.86	0.11	0.34	0.04	0.56	0.03
103	8.37	73.58	0.17	12.21	0.09	3.80	0.11	5.18	0.08	1.54	0.04	2.79	0.11	0.33	0.04	0.58	0.03
104	8.62	73.51	0.17	12.20	0.09	3.70	0.10	5.24	0.09	1.56	0.04	2.86	0.11	0.39	0.04	0.55	0.03
105	8.87	73.58	0.17	12.25	0.10	3.69	0.10	5.23	0.09	1.52	0.04	2.80	0.11	0.39	0.04	0.54	0.03
106	9.11	73.59	0.17	12.41	0.10	3.57	0.10	5.32	0.09	1.45	0.04	2.76	0.11	0.36	0.04	0.54	0.03
107	9.36	73.80	0.17	12.36	0.10	3.41	0.10	5.42	0.09	1.43	0.04	2.72	0.11	0.35	0.04	0.53	0.03
108	9.61	73.82	0.17	12.52	0.10	3.50	0.10	5.28	0.09	1.34	0.04	2.64	0.10	0.34	0.04	0.54	0.03
109	9.85	73.84	0.17	12.57	0.10	3.55	0.10	5.27	0.09	1.23	0.04	2.64	0.10	0.35	0.04	0.55	0.03
110	10.10	73.79	0.17	12.62	0.10	3.54	0.10	5.35	0.09	1.26	0.04	2.61	0.10	0.32	0.04	0.50	0.03
111	10.34	73.83	0.17	12.76	0.10	3.48	0.10	5.30	0.09	1.24	0.04	2.57	0.10	0.35	0.04	0.47	0.03
112	10.59	73.84	0.17	12.78	0.10	3.40	0.10	5.28	0.09	1.19	0.03	2.66	0.10	0.36	0.04	0.49	0.03

113	10.84	73.98	0.17	12.83	0.10	3.32	0.09	5.26	0.09	1.14	0.03	2.63	0.10	0.36	0.04	0.48	0.03
114	11.08	73.87	0.17	12.96	0.10	3.28	0.09	5.37	0.09	1.18	0.03	2.52	0.10	0.32	0.04	0.48	0.03
115	11.33	73.88	0.17	12.90	0.10	3.25	0.09	5.38	0.09	1.11	0.03	2.66	0.10	0.32	0.04	0.49	0.03
116	11.58	74.06	0.17	12.93	0.10	3.23	0.09	5.31	0.09	1.08	0.03	2.60	0.10	0.32	0.04	0.48	0.03
117	11.82	74.01	0.17	13.01	0.10	3.25	0.09	5.33	0.09	1.07	0.03	2.50	0.10	0.34	0.04	0.48	0.03
118	12.07	73.94	0.17	13.01	0.10	3.18	0.09	5.34	0.09	1.06	0.03	2.66	0.10	0.35	0.04	0.47	0.03
119	12.32	73.95	0.17	13.11	0.10	3.19	0.09	5.33	0.09	1.06	0.03	2.54	0.10	0.32	0.04	0.50	0.03
120	12.56	74.00	0.17	13.13	0.10	3.16	0.09	5.24	0.09	1.01	0.03	2.60	0.10	0.35	0.04	0.52	0.03
121	12.81	74.07	0.17	13.15	0.10	3.14	0.09	5.22	0.09	1.02	0.03	2.58	0.10	0.34	0.04	0.48	0.03
122	13.05	73.93	0.17	13.29	0.10	3.10	0.09	5.30	0.09	1.03	0.03	2.51	0.10	0.36	0.04	0.48	0.03
123	13.30	74.11	0.17	13.34	0.10	3.07	0.09	5.18	0.09	1.02	0.03	2.47	0.10	0.33	0.04	0.49	0.03
124	13.55	73.94	0.17	13.38	0.10	3.05	0.09	5.10	0.08	1.00	0.03	2.72	0.11	0.32	0.04	0.49	0.03
125	13.79	74.05	0.17	13.43	0.10	3.01	0.09	5.10	0.08	1.01	0.03	2.54	0.10	0.37	0.04	0.49	0.03
126	14.04	74.01	0.17	13.50	0.10	2.98	0.08	5.10	0.08	1.04	0.03	2.51	0.10	0.38	0.04	0.48	0.03
127	14.29	73.88	0.17	13.45	0.10	2.94	0.08	5.16	0.08	1.03	0.03	2.65	0.10	0.39	0.04	0.50	0.03
128	14.53	73.84	0.17	13.39	0.10	2.97	0.08	5.18	0.09	1.09	0.03	2.66	0.10	0.38	0.04	0.48	0.03
129	14.78	73.87	0.17	13.52	0.10	2.93	0.08	5.09	0.08	1.06	0.03	2.69	0.10	0.36	0.04	0.48	0.03
130	15.02	73.94	0.17	13.61	0.11	2.90	0.08	5.04	0.08	1.07	0.03	2.62	0.10	0.32	0.04	0.50	0.03
131	15.27	73.86	0.17	13.59	0.11	2.85	0.08	5.08	0.08	1.11	0.03	2.68	0.10	0.34	0.04	0.50	0.03
132	15.52	73.85	0.17	13.60	0.11	2.83	0.08	5.10	0.08	1.05	0.03	2.71	0.11	0.37	0.04	0.48	0.03
133	15.76	73.82	0.17	13.63	0.11	2.88	0.08	5.05	0.08	1.10	0.03	2.71	0.11	0.32	0.04	0.49	0.03
134	16.01	73.66	0.17	13.64	0.11	2.88	0.08	5.06	0.08	1.14	0.03	2.77	0.11	0.32	0.04	0.52	0.03
135	16.26	73.63	0.17	13.74	0.11	2.81	0.08	5.05	0.08	1.16	0.03	2.77	0.11	0.33	0.04	0.51	0.03
136	16.50	73.73	0.17	13.81	0.11	2.76	0.08	5.04	0.08	1.13	0.03	2.73	0.11	0.31	0.04	0.49	0.03
137	16.75	73.85	0.17	13.65	0.11	2.78	0.08	5.06	0.08	1.19	0.03	2.64	0.10	0.31	0.04	0.51	0.03
138	17.00	73.82	0.17	13.76	0.11	2.75	0.08	4.94	0.08	1.16	0.03	2.72	0.11	0.34	0.04	0.50	0.03
139	17.24	73.91	0.17	13.81	0.11	2.63	0.07	4.89	0.08	1.15	0.03	2.73	0.11	0.35	0.04	0.54	0.03
140	17.49	73.63	0.17	13.90	0.11	2.71	0.08	4.92	0.08	1.16	0.03	2.78	0.11	0.36	0.04	0.54	0.03
141	17.73	73.60	0.17	13.98	0.11	2.73	0.08	4.84	0.08	1.16	0.03	2.81	0.11	0.36	0.04	0.52	0.03

Agglomerate E1

Table J.6: Major element compositions (as wt.% oxides) from a line traverse across the interface of exterior agglomerate E1 (from agglomerate E1 to host AH.E) extracted from quantified EDS compositional maps. The EDS compositional maps were collected at a resolution of 4.8 pixels/μm. The smoothing width for this traverse was 100 pixels (21.1 μm) wide. This is a CaMgFe interface and has been centered at $x = 0$ based on the CaO maximum, due to anomalous behavior of FeO at the interface. Peak points within 2σ of the CaO maximum are highlighted in yellow. Uncertainties are 2SEOM.

Pt.	Position (μm)	SiO_2	2σ	Al_2O_3	2σ	Na_2O	2σ	K_2O	2σ	CaO	2σ	FeO	2σ	TiO_2	2σ	MgO	2σ
1	-28.73	72.48	0.27	13.37	0.18	3.70	0.12	6.28	0.14	0.73	0.04	2.57	0.14	0.41	0.07	0.47	0.06
2	-28.52	72.41	0.27	13.44	0.18	3.67	0.12	6.28	0.14	0.72	0.04	2.49	0.13	0.44	0.07	0.54	0.06
3	-28.31	72.52	0.27	13.36	0.18	3.68	0.12	6.36	0.14	0.76	0.05	2.41	0.13	0.41	0.07	0.49	0.06
4	-28.10	72.49	0.27	13.35	0.18	3.69	0.12	6.41	0.15	0.76	0.05	2.41	0.13	0.41	0.07	0.48	0.06
5	-27.89	72.57	0.27	13.40	0.18	3.66	0.11	6.30	0.14	0.74	0.05	2.48	0.13	0.42	0.07	0.43	0.05
6	-27.68	72.42	0.27	13.26	0.18	3.78	0.12	6.47	0.15	0.79	0.05	2.37	0.13	0.44	0.08	0.46	0.06
7	-27.46	72.50	0.27	13.35	0.18	3.82	0.12	6.43	0.15	0.78	0.05	2.21	0.12	0.43	0.07	0.47	0.06
8	-27.25	72.35	0.27	13.26	0.18	3.79	0.12	6.46	0.15	0.77	0.05	2.41	0.13	0.45	0.08	0.51	0.06
9	-27.04	72.49	0.27	13.22	0.17	3.83	0.12	6.44	0.15	0.75	0.05	2.28	0.12	0.48	0.08	0.52	0.06
10	-26.83	72.36	0.27	13.31	0.18	3.81	0.12	6.37	0.14	0.74	0.05	2.45	0.13	0.45	0.08	0.51	0.06
11	-26.62	72.18	0.27	13.32	0.18	3.83	0.12	6.40	0.14	0.79	0.05	2.45	0.13	0.47	0.08	0.54	0.07
12	-26.41	72.21	0.27	13.24	0.18	3.85	0.12	6.44	0.15	0.84	0.05	2.43	0.13	0.46	0.08	0.52	0.06
13	-26.20	72.28	0.27	13.27	0.18	3.80	0.12	6.52	0.15	0.81	0.05	2.39	0.13	0.46	0.08	0.47	0.06
14	-25.99	72.33	0.27	13.36	0.18	3.90	0.12	6.42	0.15	0.77	0.05	2.32	0.12	0.41	0.07	0.48	0.06
15	-25.77	72.14	0.27	13.30	0.18	3.91	0.12	6.47	0.15	0.78	0.05	2.52	0.13	0.42	0.07	0.48	0.06
16	-25.56	72.22	0.27	13.35	0.18	3.95	0.12	6.38	0.14	0.78	0.05	2.38	0.13	0.44	0.08	0.49	0.06
17	-25.35	72.37	0.27	13.21	0.17	3.89	0.12	6.47	0.15	0.82	0.05	2.32	0.12	0.46	0.08	0.46	0.06
18	-25.14	72.14	0.27	13.29	0.18	4.04	0.13	6.55	0.15	0.78	0.05	2.32	0.12	0.39	0.07	0.48	0.06
19	-24.93	72.02	0.27	13.11	0.17	4.06	0.13	6.68	0.15	0.90	0.05	2.34	0.12	0.41	0.07	0.48	0.06
20	-24.72	72.05	0.27	13.11	0.17	4.03	0.13	6.62	0.15	0.91	0.06	2.38	0.13	0.41	0.07	0.49	0.06
21	-24.51	71.92	0.27	13.17	0.17	4.08	0.13	6.49	0.15	0.87	0.05	2.48	0.13	0.51	0.09	0.49	0.06
22	-24.30	72.08	0.27	13.24	0.18	4.05	0.13	6.44	0.15	0.86	0.05	2.41	0.13	0.43	0.07	0.48	0.06
23	-24.08	72.10	0.27	13.00	0.17	4.02	0.13	6.67	0.15	0.86	0.05	2.47	0.13	0.39	0.07	0.48	0.06
24	-23.87	71.85	0.27	13.20	0.17	4.17	0.13	6.56	0.15	0.87	0.05	2.36	0.13	0.45	0.08	0.54	0.06
25	-23.66	71.89	0.27	13.10	0.17	4.22	0.13	6.47	0.15	0.90	0.05	2.38	0.13	0.45	0.08	0.59	0.07
26	-23.45	71.94	0.27	12.90	0.17	4.21	0.13	6.65	0.15	0.92	0.06	2.46	0.13	0.39	0.07	0.52	0.06
27	-23.24	71.86	0.27	12.86	0.17	4.22	0.13	6.61	0.15	0.91	0.06	2.60	0.14	0.45	0.08	0.49	0.06
28	-23.03	71.79	0.27	13.05	0.17	4.29	0.13	6.54	0.15	0.88	0.05	2.54	0.14	0.41	0.07	0.49	0.06
29	-22.82	71.62	0.27	13.09	0.17	4.36	0.14	6.52	0.15	0.93	0.06	2.56	0.14	0.40	0.07	0.53	0.06
30	-22.61	71.90	0.27	12.85	0.17	4.36	0.14	6.55	0.15	0.87	0.05	2.51	0.13	0.40	0.07	0.56	0.07
31	-22.39	71.82	0.27	12.93	0.17	4.34	0.14	6.53	0.15	0.94	0.06	2.48	0.13	0.40	0.07	0.56	0.07
32	-22.18	71.61	0.27	12.83	0.17	4.38	0.14	6.60	0.15	0.97	0.06	2.66	0.14	0.44	0.08	0.51	0.06
33	-21.97	71.74	0.27	12.87	0.17	4.38	0.14	6.61	0.15	0.94	0.06	2.48	0.13	0.48	0.08	0.51	0.06
34	-21.76	71.70	0.27	12.89	0.17	4.46	0.14	6.53	0.15	0.98	0.06	2.48	0.13	0.44	0.08	0.52	0.06
35	-21.55	71.45	0.27	12.72	0.17	4.62	0.15	6.59	0.15	0.98	0.06	2.69	0.14	0.44	0.08	0.51	0.06
36	-21.34	71.50	0.27	12.76	0.17	4.55	0.14	6.55	0.15	0.98	0.06	2.74	0.15	0.38	0.07	0.52	0.06
37	-21.13	71.45	0.27	12.71	0.17	4.66	0.15	6.70	0.15	1.03	0.06	2.53	0.13	0.41	0.07	0.51	0.06
38	-20.92	71.83	0.27	12.56	0.17	4.56	0.14	6.64	0.15	1.04	0.06	2.41	0.13	0.51	0.09	0.45	0.05
39	-20.70	71.63	0.27	12.54	0.17	4.72	0.15	6.60	0.15	0.98	0.06	2.56	0.14	0.47	0.08	0.49	0.06
40	-20.49	71.56	0.27	12.61	0.17	4.77	0.15	6.56	0.15	1.00	0.06	2.61	0.14	0.37	0.06	0.52	0.06
41	-20.28	71.76	0.27	12.45	0.16	4.69	0.15	6.57	0.15	1.00	0.06	2.60	0.14	0.43	0.07	0.51	0.06
42	-20.07	71.69	0.27	12.35	0.16	4.77	0.15	6.59	0.15	1.06	0.06	2.59	0.14	0.42	0.07	0.53	0.06
43	-19.86	71.75	0.27	12.19	0.16	4.65	0.15	6.71	0.15	1.13	0.07	2.58	0.14	0.46	0.08	0.52	0.06
44	-19.65	71.57	0.27	12.21	0.16	4.94	0.16	6.60	0.15	1.12	0.07	2.58	0.14	0.41	0.07	0.57	0.07
45	-19.44	71.84	0.27	12.25	0.16	4.89	0.15	6.54	0.15	1.10	0.07	2.49	0.13	0.41	0.07	0.47	0.06
46	-19.23	71.76	0.27	12.08	0.16	4.82	0.15	6.69	0.15	1.22	0.07	2.47	0.13	0.44	0.07	0.53	0.06
47	-19.01	71.36	0.27	12.20	0.16	5.13	0.16	6.57	0.15	1.21	0.07	2.59	0.14	0.40	0.07	0.54	0.07
48	-18.80	71.50	0.27	12.15	0.16	5.04	0.16	6.41	0.15	1.19	0.07	2.73	0.15	0.43	0.07	0.55	0.07
49	-18.59	71.60	0.27	11.87	0.16	5.15	0.16	6.59	0.15	1.28	0.08	2.64	0.14	0.35	0.06	0.52	0.06
50	-18.38	71.96	0.27	11.75	0.16	5.11	0.16	6.54	0.15	1.27	0.08	2.51	0.13	0.33	0.06	0.53	0.06

51	-18.17	72.12	0.27	11.61	0.15	5.12	0.16	6.46	0.15	1.26	0.08	2.47	0.13	0.37	0.06	0.60	0.07
52	-17.96	71.75	0.27	11.51	0.15	5.17	0.16	6.39	0.14	1.36	0.08	2.81	0.15	0.38	0.07	0.62	0.07
53	-17.75	72.26	0.27	11.33	0.15	5.33	0.17	6.19	0.14	1.33	0.08	2.56	0.14	0.39	0.07	0.61	0.07
54	-17.54	72.59	0.27	11.09	0.15	5.24	0.16	6.25	0.14	1.32	0.08	2.53	0.13	0.37	0.06	0.60	0.07
55	-17.32	72.84	0.28	10.93	0.14	5.06	0.16	6.29	0.14	1.29	0.08	2.64	0.14	0.35	0.06	0.61	0.07
56	-17.11	72.85	0.28	10.76	0.14	5.12	0.16	6.35	0.14	1.38	0.08	2.61	0.14	0.37	0.06	0.58	0.07
57	-16.90	72.93	0.28	10.54	0.14	5.21	0.16	6.33	0.14	1.38	0.08	2.66	0.14	0.41	0.07	0.55	0.07
58	-16.69	73.26	0.28	10.52	0.14	5.24	0.16	6.31	0.14	1.28	0.08	2.48	0.13	0.40	0.07	0.51	0.06
59	-16.48	73.44	0.28	10.26	0.14	5.12	0.16	6.35	0.14	1.33	0.08	2.55	0.14	0.42	0.07	0.53	0.06
60	-16.27	73.86	0.28	10.43	0.14	5.13	0.16	6.24	0.14	1.20	0.07	2.23	0.12	0.38	0.07	0.53	0.06
61	-16.06	73.84	0.28	10.54	0.14	5.18	0.16	6.23	0.14	1.13	0.07	2.19	0.12	0.39	0.07	0.49	0.06
62	-15.85	73.79	0.28	10.48	0.14	5.21	0.16	6.36	0.14	1.11	0.07	2.18	0.12	0.42	0.07	0.44	0.05
63	-15.63	73.76	0.28	10.81	0.14	5.10	0.16	6.43	0.15	1.07	0.07	1.97	0.10	0.39	0.07	0.47	0.06
64	-15.42	73.61	0.28	10.87	0.14	5.21	0.16	6.36	0.14	1.05	0.06	2.01	0.11	0.42	0.07	0.47	0.06
65	-15.21	73.65	0.28	10.95	0.14	5.21	0.16	6.44	0.15	0.96	0.06	1.98	0.11	0.43	0.07	0.38	0.05
66	-15.00	73.34	0.28	11.15	0.15	5.33	0.17	6.53	0.15	0.95	0.06	1.97	0.10	0.36	0.06	0.36	0.04
67	-14.79	73.38	0.28	11.22	0.15	5.29	0.17	6.59	0.15	0.87	0.05	1.91	0.10	0.40	0.07	0.34	0.04
68	-14.58	73.13	0.28	11.28	0.15	5.39	0.17	6.51	0.15	0.90	0.05	1.97	0.10	0.40	0.07	0.40	0.05
69	-14.37	73.08	0.28	11.42	0.15	5.27	0.17	6.63	0.15	0.86	0.05	2.01	0.11	0.36	0.06	0.36	0.04
70	-14.15	73.04	0.28	11.51	0.15	5.39	0.17	6.64	0.15	0.78	0.05	1.89	0.10	0.38	0.06	0.37	0.04
71	-13.94	72.92	0.28	11.72	0.15	5.47	0.17	6.58	0.15	0.73	0.04	1.82	0.10	0.38	0.07	0.38	0.05
72	-13.73	72.84	0.28	11.71	0.15	5.55	0.17	6.64	0.15	0.76	0.05	1.70	0.09	0.39	0.07	0.40	0.05
73	-13.52	72.77	0.27	11.64	0.15	5.57	0.18	6.70	0.15	0.76	0.05	1.81	0.10	0.41	0.07	0.34	0.04
74	-13.31	72.73	0.27	11.70	0.15	5.53	0.17	6.59	0.15	0.77	0.05	1.87	0.10	0.38	0.07	0.42	0.05
75	-13.10	72.80	0.28	11.64	0.15	5.65	0.18	6.64	0.15	0.69	0.04	1.81	0.10	0.39	0.07	0.38	0.05
76	-12.89	72.65	0.27	11.79	0.16	5.71	0.18	6.58	0.15	0.70	0.04	1.82	0.10	0.36	0.06	0.38	0.05
77	-12.68	72.51	0.27	11.85	0.16	5.74	0.18	6.63	0.15	0.68	0.04	1.81	0.10	0.43	0.07	0.35	0.04
78	-12.46	72.54	0.27	11.80	0.16	5.70	0.18	6.68	0.15	0.72	0.04	1.80	0.10	0.39	0.07	0.36	0.04
79	-12.25	72.49	0.27	11.80	0.16	5.75	0.18	6.68	0.15	0.70	0.04	1.89	0.10	0.37	0.06	0.33	0.04
80	-12.04	72.52	0.27	11.68	0.15	5.81	0.18	6.67	0.15	0.70	0.04	1.88	0.10	0.39	0.07	0.36	0.04
81	-11.83	72.62	0.27	11.69	0.15	5.79	0.18	6.68	0.15	0.68	0.04	1.81	0.10	0.37	0.06	0.36	0.04
82	-11.62	72.84	0.28	11.63	0.15	5.73	0.18	6.65	0.15	0.66	0.04	1.74	0.09	0.39	0.07	0.35	0.04
83	-11.41	72.98	0.28	11.55	0.15	5.79	0.18	6.54	0.15	0.67	0.04	1.75	0.09	0.37	0.06	0.35	0.04
84	-11.20	72.88	0.28	11.36	0.15	5.86	0.18	6.67	0.15	0.69	0.04	1.85	0.10	0.37	0.06	0.32	0.04
85	-10.99	72.84	0.28	11.43	0.15	5.89	0.19	6.52	0.15	0.73	0.04	1.83	0.10	0.39	0.07	0.35	0.04
86	-10.77	73.04	0.28	11.22	0.15	5.82	0.18	6.67	0.15	0.71	0.04	1.82	0.10	0.40	0.07	0.32	0.04
87	-10.56	73.45	0.28	11.07	0.15	5.77	0.18	6.48	0.15	0.71	0.04	1.72	0.09	0.46	0.08	0.34	0.04
88	-10.35	73.62	0.28	10.88	0.14	5.78	0.18	6.38	0.14	0.72	0.04	1.78	0.09	0.47	0.08	0.36	0.04
89	-10.14	73.73	0.28	10.76	0.14	5.74	0.18	6.42	0.15	0.78	0.05	1.75	0.09	0.44	0.08	0.38	0.05
90	-9.93	73.71	0.28	10.54	0.14	5.79	0.18	6.38	0.14	0.85	0.05	1.91	0.10	0.41	0.07	0.40	0.05
91	-9.72	73.96	0.28	10.38	0.14	5.77	0.18	6.34	0.14	0.78	0.05	2.04	0.11	0.37	0.06	0.37	0.04
92	-9.51	74.20	0.28	10.16	0.13	5.77	0.18	6.35	0.14	0.80	0.05	2.01	0.11	0.29	0.05	0.41	0.05
93	-9.30	74.43	0.28	9.87	0.13	5.62	0.18	6.31	0.14	0.83	0.05	2.12	0.11	0.39	0.07	0.42	0.05
94	-9.08	74.64	0.28	9.76	0.13	5.68	0.18	6.12	0.14	0.87	0.05	2.07	0.11	0.43	0.07	0.43	0.05
95	-8.87	74.66	0.28	9.56	0.13	5.79	0.18	6.14	0.14	0.87	0.05	2.18	0.12	0.37	0.06	0.42	0.05
96	-8.66	74.97	0.28	9.36	0.12	5.84	0.18	5.98	0.14	0.95	0.06	2.11	0.11	0.36	0.06	0.42	0.05
97	-8.45	75.09	0.28	9.19	0.12	5.76	0.18	6.06	0.14	0.98	0.06	2.19	0.12	0.34	0.06	0.39	0.05
98	-8.24	75.34	0.28	8.87	0.12	5.73	0.18	5.97	0.14	0.91	0.06	2.33	0.12	0.42	0.07	0.43	0.05
99	-8.03	75.24	0.28	8.83	0.12	5.81	0.18	5.97	0.14	0.92	0.06	2.40	0.13	0.38	0.07	0.44	0.05
100	-7.82	75.48	0.29	8.70	0.12	5.62	0.18	5.99	0.14	0.98	0.06	2.42	0.13	0.39	0.07	0.41	0.05
101	-7.61	75.69	0.29	8.65	0.11	5.56	0.17	5.98	0.14	0.99	0.06	2.43	0.13	0.30	0.05	0.40	0.05
102	-7.39	75.49	0.29	8.80	0.12	5.89	0.18	5.94	0.13	0.95	0.06	2.20	0.12	0.32	0.05	0.40	0.05
103	-7.18	75.48	0.29	9.08	0.12	5.72	0.18	5.91	0.13	0.91	0.06	2.13	0.11	0.38	0.07	0.39	0.05
104	-6.97	75.40	0.28	9.42	0.12	5.50	0.17	6.01	0.14	0.82	0.05	2.17	0.12	0.37	0.06	0.31	0.04
105	-6.76	75.06	0.28	9.70	0.13	5.59	0.18	6.12	0.14	0.74	0.05	2.08	0.11	0.35	0.06	0.34	0.04
106	-6.55	74.82	0.28	9.94	0.13	5.60	0.18	6.28	0.14	0.75	0.05	1.95	0.10	0.34	0.06	0.33	0.04
107	-6.34	74.69	0.28	10.30	0.14	5.61	0.18	6.30	0.14	0.68	0.04	1.75	0.09	0.37	0.06	0.30	0.04
108	-6.13	74.39	0.28	10.50	0.14	5.58	0.18	6.26	0.14	0.67	0.04	1.87	0.10	0.43	0.07	0.30	0.04
109	-5.92	74.29	0.28	10.63	0.14	5.59	0.18	6.28	0.14	0.70	0.04	1.80	0.10	0.44	0.08	0.26	0.03
110	-5.70	74.24	0.28	10.74	0.14	5.54	0.17	6.35	0.14	0.69	0.04	1.81	0.10	0.39	0.07	0.24	0.03
111	-5.49	74.04	0.28	10.93	0.14	5.62	0.18	6.29	0.14	0.62	0.04	1.84	0.10	0.38	0.07	0.28	0.03
112	-5.28	73.92	0.28	10.87	0.14	5.69	0.18	6.35	0.14	0.64	0.04	1.83	0.10	0.37	0.06	0.32	0.04

113	-5.07	73.78	0.28	11.10	0.15	5.56	0.17	6.38	0.14	0.62	0.04	1.86	0.10	0.39	0.07	0.31	0.04
114	-4.86	73.78	0.28	11.08	0.15	5.46	0.17	6.37	0.14	0.67	0.04	2.00	0.11	0.41	0.07	0.24	0.03
115	-4.65	73.89	0.28	11.02	0.15	5.43	0.17	6.39	0.14	0.70	0.04	1.93	0.10	0.36	0.06	0.28	0.03
116	-4.44	73.96	0.28	10.99	0.15	5.35	0.17	6.48	0.15	0.69	0.04	1.84	0.10	0.39	0.07	0.30	0.04
117	-4.23	74.08	0.28	10.99	0.15	5.40	0.17	6.33	0.14	0.59	0.04	1.92	0.10	0.39	0.07	0.30	0.04
118	-4.01	73.98	0.28	10.95	0.14	5.40	0.17	6.36	0.14	0.67	0.04	1.92	0.10	0.41	0.07	0.31	0.04
119	-3.80	74.07	0.28	10.97	0.15	5.34	0.17	6.34	0.14	0.67	0.04	1.91	0.10	0.41	0.07	0.28	0.03
120	-3.59	74.20	0.28	10.88	0.14	5.31	0.17	6.41	0.15	0.75	0.05	1.82	0.10	0.38	0.07	0.26	0.03
121	-3.38	74.40	0.28	10.58	0.14	5.12	0.16	6.45	0.15	0.88	0.05	1.97	0.10	0.34	0.06	0.28	0.03
122	-3.17	74.68	0.28	10.56	0.14	5.11	0.16	6.22	0.14	0.82	0.05	1.97	0.10	0.34	0.06	0.31	0.04
123	-2.96	74.86	0.28	10.46	0.14	5.07	0.16	6.04	0.14	0.87	0.05	1.98	0.11	0.45	0.08	0.28	0.03
124	-2.75	74.84	0.28	10.34	0.14	5.12	0.16	6.04	0.14	1.00	0.06	1.92	0.10	0.43	0.07	0.31	0.04
125	-2.54	75.07	0.28	10.12	0.13	4.98	0.16	6.09	0.14	1.02	0.06	2.00	0.11	0.39	0.07	0.33	0.04
126	-2.32	75.56	0.29	9.78	0.13	4.87	0.15	5.96	0.13	1.01	0.06	2.07	0.11	0.38	0.06	0.37	0.04
127	-2.11	75.91	0.29	9.59	0.13	4.75	0.15	5.92	0.13	1.11	0.07	2.10	0.11	0.29	0.05	0.33	0.04
128	-1.90	75.98	0.29	9.51	0.13	4.71	0.15	5.83	0.13	1.14	0.07	2.08	0.11	0.37	0.06	0.38	0.05
129	-1.69	75.98	0.29	9.29	0.12	4.64	0.15	5.86	0.13	1.15	0.07	2.33	0.12	0.34	0.06	0.41	0.05
130	-1.48	75.96	0.29	9.02	0.12	4.55	0.14	5.84	0.13	1.32	0.08	2.48	0.13	0.43	0.07	0.41	0.05
131	-1.27	76.26	0.29	8.89	0.12	4.50	0.14	5.82	0.13	1.34	0.08	2.41	0.13	0.41	0.07	0.38	0.05
132	-1.06	76.32	0.29	8.77	0.12	4.50	0.14	5.72	0.13	1.43	0.09	2.48	0.13	0.34	0.06	0.43	0.05
133	-0.85	76.28	0.29	8.80	0.12	4.54	0.14	5.64	0.13	1.36	0.08	2.51	0.13	0.41	0.07	0.45	0.05
134	-0.63	76.10	0.29	8.76	0.12	4.44	0.14	5.73	0.13	1.46	0.09	2.80	0.15	0.31	0.05	0.40	0.05
135	-0.42	75.98	0.29	8.83	0.12	4.44	0.14	5.59	0.13	1.46	0.09	2.96	0.16	0.32	0.06	0.42	0.05
136	-0.21	76.06	0.29	8.88	0.12	4.32	0.14	5.58	0.13	1.40	0.09	2.94	0.16	0.36	0.06	0.46	0.06
137	0.00	75.87	0.29	8.82	0.12	4.35	0.14	5.80	0.13	1.56	0.10	2.82	0.15	0.35	0.06	0.44	0.05
138	0.21	75.66	0.29	8.94	0.12	4.41	0.14	5.79	0.13	1.54	0.09	2.83	0.15	0.35	0.06	0.47	0.06
139	0.42	75.34	0.28	9.41	0.12	4.33	0.14	5.69	0.13	1.50	0.09	2.88	0.15	0.38	0.07	0.47	0.06
140	0.63	75.22	0.28	9.65	0.13	4.22	0.13	5.68	0.13	1.47	0.09	2.91	0.15	0.36	0.06	0.50	0.06
141	0.85	74.60	0.28	9.89	0.13	4.21	0.13	5.77	0.13	1.44	0.09	3.27	0.17	0.37	0.06	0.46	0.05
142	1.06	74.43	0.28	10.42	0.14	4.34	0.14	5.86	0.13	1.34	0.08	2.76	0.15	0.37	0.06	0.47	0.06
143	1.27	74.46	0.28	10.70	0.14	4.29	0.13	5.84	0.13	1.33	0.08	2.57	0.14	0.36	0.06	0.44	0.05
144	1.48	74.29	0.28	10.83	0.14	4.17	0.13	5.91	0.13	1.32	0.08	2.62	0.14	0.43	0.07	0.43	0.05
145	1.69	74.29	0.28	11.15	0.15	4.09	0.13	5.97	0.14	1.22	0.07	2.54	0.14	0.31	0.05	0.42	0.05
146	1.90	74.10	0.28	11.51	0.15	4.09	0.13	6.10	0.14	1.15	0.07	2.30	0.12	0.29	0.05	0.46	0.06
147	2.11	74.02	0.28	11.86	0.16	4.06	0.13	6.09	0.14	1.07	0.07	2.12	0.11	0.35	0.06	0.42	0.05
148	2.32	73.94	0.28	11.85	0.16	4.01	0.13	6.17	0.14	1.04	0.06	2.19	0.12	0.34	0.06	0.46	0.05
149	2.54	73.87	0.28	12.12	0.16	3.95	0.12	6.13	0.14	1.02	0.06	2.13	0.11	0.37	0.06	0.41	0.05
150	2.75	74.10	0.28	12.20	0.16	3.84	0.12	6.17	0.14	0.93	0.06	2.04	0.11	0.36	0.06	0.37	0.04
151	2.96	74.06	0.28	12.29	0.16	3.77	0.12	6.21	0.14	0.91	0.06	2.00	0.11	0.36	0.06	0.40	0.05
152	3.17	73.76	0.28	12.45	0.16	3.75	0.12	6.15	0.14	0.92	0.06	2.20	0.12	0.32	0.06	0.44	0.05
153	3.38	73.88	0.28	12.60	0.17	3.71	0.12	6.14	0.14	0.90	0.05	2.05	0.11	0.29	0.05	0.44	0.05
154	3.59	74.00	0.28	12.61	0.17	3.56	0.11	6.16	0.14	0.89	0.05	2.06	0.11	0.33	0.06	0.40	0.05
155	3.80	74.07	0.28	12.70	0.17	3.55	0.11	6.05	0.14	0.83	0.05	2.07	0.11	0.33	0.06	0.39	0.05
156	4.01	74.05	0.28	12.76	0.17	3.55	0.11	5.98	0.14	0.82	0.05	2.08	0.11	0.33	0.06	0.42	0.05
157	4.23	74.17	0.28	12.67	0.17	3.37	0.11	5.98	0.14	0.84	0.05	2.18	0.12	0.37	0.06	0.42	0.05
158	4.44	74.34	0.28	12.65	0.17	3.32	0.10	6.16	0.14	0.76	0.05	2.08	0.11	0.31	0.05	0.38	0.05
159	4.65	74.16	0.28	12.81	0.17	3.38	0.11	6.07	0.14	0.83	0.05	2.01	0.11	0.33	0.06	0.41	0.05
160	4.86	74.28	0.28	12.87	0.17	3.32	0.10	5.96	0.13	0.89	0.05	1.97	0.10	0.35	0.06	0.37	0.04
161	5.07	73.96	0.28	12.91	0.17	3.31	0.10	6.02	0.14	0.90	0.06	2.06	0.11	0.39	0.07	0.45	0.05
162	5.28	73.94	0.28	12.89	0.17	3.24	0.10	6.04	0.14	0.85	0.05	2.25	0.12	0.36	0.06	0.42	0.05
163	5.49	74.14	0.28	12.98	0.17	3.10	0.10	6.05	0.14	0.92	0.06	2.00	0.11	0.43	0.07	0.38	0.05
164	5.70	74.17	0.28	13.08	0.17	3.16	0.10	5.87	0.13	0.95	0.06	2.02	0.11	0.36	0.06	0.38	0.05
165	5.92	74.11	0.28	12.95	0.17	3.08	0.10	5.98	0.14	0.93	0.06	2.18	0.12	0.39	0.07	0.38	0.05
166	6.13	74.10	0.28	13.08	0.17	3.15	0.10	5.80	0.13	0.97	0.06	2.13	0.11	0.37	0.06	0.40	0.05
167	6.34	74.23	0.28	13.09	0.17	3.13	0.10	5.70	0.13	0.94	0.06	2.14	0.11	0.37	0.06	0.41	0.05
168	6.55	74.24	0.28	13.25	0.18	3.01	0.09	5.60	0.13	0.94	0.06	2.12	0.11	0.37	0.06	0.45	0.05
169	6.76	73.98	0.28	13.38	0.18	3.07	0.10	5.71	0.13	0.98	0.06	2.14	0.11	0.30	0.05	0.44	0.05
170	6.97	73.89	0.28	13.49	0.18	3.05	0.10	5.55	0.13	1.03	0.06	2.19	0.12	0.34	0.06	0.47	0.06
171	7.18	73.78	0.28	13.40	0.18	3.05	0.10	5.69	0.13	1.06	0.06	2.29	0.12	0.32	0.05	0.42	0.05
172	7.39	73.99	0.28	13.39	0.18	3.03	0.10	5.49	0.12	0.99	0.06	2.35	0.12	0.34	0.06	0.42	0.05
173	7.61	73.99	0.28	13.43	0.18	3.00	0.09	5.53	0.13	0.95	0.06	2.30	0.12	0.38	0.06	0.41	0.05
174	7.82	74.01	0.28	13.48	0.18	2.91	0.09	5.52	0.13	1.03	0.06	2.24	0.12	0.38	0.06	0.43	0.05

175	8.03	73.95	0.28	13.49	0.18	2.96	0.09	5.52	0.12	1.13	0.07	2.20	0.12	0.33	0.06	0.42	0.05
176	8.24	73.85	0.28	13.32	0.18	2.98	0.09	5.53	0.13	1.10	0.07	2.48	0.13	0.34	0.06	0.40	0.05
177	8.45	74.19	0.28	13.32	0.18	2.88	0.09	5.46	0.12	1.15	0.07	2.25	0.12	0.34	0.06	0.40	0.05
178	8.66	74.18	0.28	13.18	0.17	2.95	0.09	5.45	0.12	1.09	0.07	2.37	0.13	0.34	0.06	0.43	0.05
179	8.87	73.87	0.28	13.49	0.18	2.95	0.09	5.43	0.12	1.12	0.07	2.33	0.12	0.39	0.07	0.43	0.05
180	9.08	73.91	0.28	13.38	0.18	2.97	0.09	5.40	0.12	1.17	0.07	2.35	0.13	0.39	0.07	0.43	0.05
181	9.30	73.96	0.28	13.52	0.18	2.93	0.09	5.26	0.12	1.19	0.07	2.30	0.12	0.35	0.06	0.49	0.06
182	9.51	74.10	0.28	13.34	0.18	2.97	0.09	5.34	0.12	1.14	0.07	2.32	0.12	0.35	0.06	0.43	0.05
183	9.72	74.04	0.28	13.49	0.18	2.91	0.09	5.33	0.12	1.17	0.07	2.28	0.12	0.34	0.06	0.45	0.05
184	9.93	74.13	0.28	13.40	0.18	2.80	0.09	5.30	0.12	1.14	0.07	2.36	0.13	0.39	0.07	0.48	0.06
185	10.14	74.21	0.28	13.36	0.18	2.83	0.09	5.23	0.12	1.13	0.07	2.44	0.13	0.38	0.07	0.42	0.05
186	10.35	73.91	0.28	13.47	0.18	2.81	0.09	5.30	0.12	1.27	0.08	2.46	0.13	0.35	0.06	0.42	0.05
187	10.56	73.90	0.28	13.42	0.18	2.93	0.09	5.35	0.12	1.20	0.07	2.32	0.12	0.41	0.07	0.47	0.06
188	10.77	74.06	0.28	13.57	0.18	2.93	0.09	5.18	0.12	1.20	0.07	2.26	0.12	0.32	0.06	0.48	0.06
189	10.99	74.20	0.28	13.37	0.18	2.90	0.09	5.11	0.12	1.18	0.07	2.42	0.13	0.34	0.06	0.48	0.06

Agglomerate FLD10.L

Table J.7: Major element compositions (as wt.% oxides) from a line traverse across the interface of exterior agglomerate FLD10.L (from agglomerate FLD10.L to host FLD10) extracted from quantified EDS compositional maps. The EDS compositional maps were collected at a resolution of 6.3 pixels/μm. The smoothing width for this traverse was 125 pixels (19.8 μm) wide. This is a double-layered CaMgFe and Si interface, but has been centered at $x = 0$ based on the FeO maximum. Peak points within 2σ of the FeO maximum are highlighted in yellow. Uncertainties are 2SEOM.

Pt.	Position (μm)	SiO_2	2σ	Al_2O_3	2σ	Na_2O	2σ	K_2O	2σ	CaO	2σ	FeO	2σ	TiO_2	2σ	MgO	2σ
1	-8.73	74.99	0.12	13.58	0.05	0.73	0.03	3.92	0.04	2.60	0.05	3.07	0.10	0.38	0.04	0.53	0.03
2	-8.57	74.85	0.12	13.59	0.05	0.73	0.03	3.93	0.04	2.60	0.05	3.18	0.10	0.37	0.04	0.54	0.03
3	-8.41	74.96	0.12	13.50	0.05	0.70	0.03	3.94	0.04	2.67	0.05	3.08	0.10	0.36	0.04	0.54	0.03
4	-8.25	74.87	0.12	13.48	0.05	0.71	0.03	3.99	0.04	2.68	0.05	3.15	0.10	0.34	0.04	0.57	0.03
5	-8.10	74.85	0.12	13.51	0.05	0.74	0.03	4.00	0.04	2.62	0.05	3.16	0.10	0.36	0.04	0.55	0.03
6	-7.94	74.91	0.12	13.52	0.05	0.69	0.03	3.98	0.04	2.64	0.05	3.16	0.10	0.33	0.03	0.54	0.03
7	-7.78	74.97	0.12	13.52	0.05	0.68	0.03	3.92	0.04	2.62	0.05	3.17	0.10	0.37	0.04	0.53	0.03
8	-7.62	74.94	0.12	13.52	0.05	0.68	0.03	3.94	0.04	2.63	0.05	3.22	0.10	0.31	0.03	0.54	0.03
9	-7.46	74.89	0.12	13.54	0.05	0.67	0.03	3.96	0.04	2.66	0.05	3.23	0.10	0.33	0.03	0.53	0.03
10	-7.30	74.85	0.12	13.49	0.05	0.72	0.03	3.94	0.04	2.61	0.05	3.23	0.10	0.41	0.04	0.53	0.03
11	-7.14	74.97	0.12	13.56	0.05	0.66	0.03	3.96	0.04	2.60	0.05	3.13	0.10	0.40	0.04	0.53	0.03
12	-6.98	75.01	0.12	13.49	0.05	0.67	0.03	3.96	0.04	2.64	0.05	3.16	0.10	0.41	0.04	0.52	0.03
13	-6.83	74.95	0.12	13.44	0.05	0.67	0.03	4.00	0.04	2.65	0.05	3.21	0.10	0.36	0.04	0.54	0.03
14	-6.67	74.77	0.12	13.50	0.05	0.70	0.03	4.00	0.04	2.62	0.05	3.31	0.11	0.36	0.04	0.53	0.03
15	-6.51	74.99	0.12	13.49	0.05	0.70	0.03	3.97	0.04	2.65	0.05	3.10	0.10	0.39	0.04	0.54	0.03
16	-6.35	74.97	0.12	13.50	0.05	0.68	0.03	3.94	0.04	2.61	0.05	3.24	0.10	0.35	0.04	0.53	0.03
17	-6.19	74.97	0.12	13.53	0.05	0.69	0.03	3.95	0.04	2.60	0.05	3.15	0.10	0.34	0.04	0.54	0.03
18	-6.03	74.85	0.12	13.52	0.05	0.70	0.03	3.93	0.04	2.63	0.05	3.21	0.10	0.41	0.04	0.53	0.03
19	-5.87	74.94	0.12	13.51	0.05	0.70	0.03	3.97	0.04	2.64	0.05	3.15	0.10	0.33	0.03	0.54	0.03
20	-5.71	74.92	0.12	13.44	0.05	0.67	0.03	3.99	0.04	2.63	0.05	3.27	0.10	0.36	0.04	0.55	0.03
21	-5.56	74.91	0.12	13.44	0.05	0.65	0.03	3.98	0.04	2.63	0.05	3.28	0.10	0.36	0.04	0.53	0.03
22	-5.40	74.99	0.12	13.41	0.05	0.69	0.03	3.94	0.04	2.55	0.05	3.24	0.10	0.38	0.04	0.58	0.04
23	-5.24	75.00	0.12	13.41	0.05	0.68	0.03	3.95	0.04	2.68	0.05	3.14	0.10	0.37	0.04	0.56	0.03
24	-5.08	74.98	0.12	13.41	0.05	0.64	0.03	3.98	0.04	2.67	0.05	3.19	0.10	0.38	0.04	0.54	0.03
25	-4.92	75.03	0.12	13.55	0.05	0.63	0.03	3.96	0.04	2.59	0.05	3.11	0.10	0.35	0.04	0.56	0.03
26	-4.76	75.07	0.12	13.50	0.05	0.63	0.03	3.93	0.04	2.57	0.05	3.21	0.10	0.36	0.04	0.54	0.03
27	-4.60	74.97	0.12	13.38	0.05	0.72	0.03	3.96	0.04	2.62	0.05	3.20	0.10	0.39	0.04	0.53	0.03
28	-4.44	74.99	0.12	13.34	0.05	0.68	0.03	3.99	0.04	2.65	0.05	3.19	0.10	0.39	0.04	0.54	0.03
29	-4.29	74.96	0.12	13.31	0.05	0.66	0.03	3.95	0.04	2.68	0.05	3.24	0.10	0.42	0.04	0.57	0.03
30	-4.13	74.99	0.12	13.34	0.05	0.68	0.03	4.00	0.04	2.60	0.05	3.24	0.10	0.39	0.04	0.55	0.03
31	-3.97	75.11	0.12	13.43	0.05	0.66	0.03	3.95	0.04	2.57	0.05	3.14	0.10	0.36	0.04	0.55	0.03
32	-3.81	75.03	0.12	13.44	0.05	0.65	0.03	3.92	0.04	2.60	0.05	3.18	0.10	0.36	0.04	0.58	0.04
33	-3.65	74.95	0.12	13.42	0.05	0.62	0.03	3.96	0.04	2.64	0.05	3.27	0.10	0.38	0.04	0.55	0.03
34	-3.49	75.05	0.12	13.38	0.05	0.65	0.03	3.96	0.04	2.66	0.05	3.26	0.10	0.32	0.03	0.53	0.03
35	-3.33	75.11	0.12	13.37	0.05	0.65	0.03	3.93	0.04	2.65	0.05	3.18	0.10	0.36	0.04	0.58	0.04
36	-3.17	75.05	0.12	13.37	0.05	0.63	0.03	3.99	0.04	2.68	0.05	3.19	0.10	0.34	0.04	0.56	0.03
37	-3.02	75.08	0.12	13.37	0.05	0.64	0.03	4.02	0.04	2.65	0.05	3.16	0.10	0.33	0.03	0.55	0.03
38	-2.86	75.04	0.12	13.31	0.05	0.63	0.03	3.98	0.04	2.59	0.05	3.31	0.11	0.36	0.04	0.56	0.03
39	-2.70	75.13	0.12	13.32	0.05	0.58	0.03	3.97	0.04	2.63	0.05	3.20	0.10	0.39	0.04	0.57	0.03
40	-2.54	75.03	0.12	13.28	0.05	0.64	0.03	3.96	0.04	2.56	0.05	3.37	0.11	0.40	0.04	0.55	0.03
41	-2.38	75.05	0.12	13.31	0.05	0.66	0.03	3.98	0.04	2.50	0.05	3.33	0.11	0.40	0.04	0.55	0.03
42	-2.22	75.17	0.12	13.25	0.05	0.62	0.03	4.01	0.04	2.60	0.05	3.25	0.10	0.35	0.04	0.52	0.03
43	-2.06	75.04	0.12	13.24	0.05	0.63	0.03	4.00	0.04	2.62	0.05	3.32	0.11	0.40	0.04	0.55	0.03
44	-1.90	75.05	0.12	13.23	0.05	0.66	0.03	3.98	0.04	2.55	0.05	3.35	0.11	0.39	0.04	0.57	0.03
45	-1.75	75.19	0.12	13.23	0.05	0.63	0.03	3.99	0.04	2.48	0.05	3.32	0.11	0.39	0.04	0.54	0.03
46	-1.59	75.12	0.12	13.17	0.05	0.63	0.03	3.96	0.04	2.55	0.05	3.46	0.11	0.35	0.04	0.54	0.03
47	-1.43	75.10	0.12	13.14	0.05	0.62	0.03	3.98	0.04	2.54	0.05	3.50	0.11	0.33	0.03	0.57	0.03
48	-1.27	75.27	0.12	13.07	0.05	0.58	0.03	3.93	0.04	2.55	0.05	3.44	0.11	0.35	0.04	0.59	0.04
49	-1.11	75.13	0.12	13.06	0.05	0.58	0.03	3.98	0.04	2.53	0.05	3.56	0.11	0.38	0.04	0.55	0.03
50	-0.95	75.18	0.12	13.04	0.05	0.58	0.03	3.98	0.04	2.54	0.05	3.57	0.11	0.37	0.04	0.52	0.03

51	-0.79	74.99	0.12	13.03	0.05	0.60	0.03	3.92	0.04	2.53	0.05	3.78	0.12	0.37	0.04	0.54	0.03
52	-0.63	74.95	0.12	12.95	0.05	0.61	0.03	3.95	0.04	2.53	0.05	3.84	0.12	0.36	0.04	0.57	0.03
53	-0.48	74.81	0.12	12.92	0.05	0.58	0.03	3.91	0.04	2.59	0.05	4.03	0.13	0.40	0.04	0.55	0.03
54	-0.32	74.84	0.12	12.83	0.05	0.58	0.03	3.90	0.04	2.58	0.05	4.12	0.13	0.40	0.04	0.58	0.04
55	-0.16	74.93	0.12	12.84	0.05	0.55	0.02	3.93	0.04	2.50	0.05	4.08	0.13	0.38	0.04	0.61	0.04
56	0.00	74.97	0.12	12.73	0.05	0.53	0.02	3.91	0.04	2.54	0.05	4.16	0.13	0.35	0.04	0.59	0.04
57	0.16	75.25	0.12	12.54	0.05	0.55	0.02	3.91	0.04	2.47	0.05	4.14	0.13	0.37	0.04	0.58	0.04
58	0.32	75.45	0.13	12.47	0.05	0.53	0.02	3.93	0.04	2.42	0.05	4.05	0.13	0.39	0.04	0.56	0.03
59	0.48	75.69	0.13	12.30	0.05	0.53	0.02	3.94	0.04	2.36	0.04	4.08	0.13	0.37	0.04	0.53	0.03
60	0.63	75.97	0.13	12.14	0.05	0.52	0.02	3.92	0.04	2.25	0.04	4.03	0.13	0.41	0.04	0.55	0.03
61	0.79	76.39	0.13	12.09	0.05	0.51	0.02	3.91	0.04	2.12	0.04	3.82	0.12	0.42	0.04	0.53	0.03
62	0.95	76.69	0.13	12.03	0.05	0.53	0.02	3.94	0.04	2.04	0.04	3.69	0.12	0.37	0.04	0.51	0.03
63	1.11	77.13	0.13	11.98	0.05	0.52	0.02	3.92	0.04	1.94	0.04	3.49	0.11	0.34	0.04	0.47	0.03
64	1.27	77.41	0.13	11.93	0.05	0.51	0.02	3.95	0.04	1.88	0.04	3.32	0.11	0.35	0.04	0.46	0.03
65	1.43	77.40	0.13	11.98	0.05	0.50	0.02	3.97	0.04	1.88	0.04	3.20	0.10	0.38	0.04	0.44	0.03
66	1.59	77.74	0.13	12.03	0.05	0.52	0.02	3.93	0.04	1.77	0.03	3.00	0.10	0.33	0.03	0.49	0.03
67	1.75	77.67	0.13	12.04	0.05	0.52	0.02	3.98	0.04	1.77	0.03	3.00	0.10	0.34	0.03	0.46	0.03
68	1.90	77.70	0.13	12.05	0.05	0.50	0.02	3.97	0.04	1.79	0.03	3.00	0.10	0.31	0.03	0.47	0.03
69	2.06	77.79	0.13	12.03	0.05	0.48	0.02	3.94	0.04	1.67	0.03	3.06	0.10	0.36	0.04	0.47	0.03
70	2.22	77.83	0.13	12.08	0.05	0.51	0.02	4.01	0.04	1.66	0.03	2.87	0.09	0.37	0.04	0.48	0.03
71	2.38	77.91	0.13	12.13	0.05	0.49	0.02	4.02	0.04	1.68	0.03	2.79	0.09	0.31	0.03	0.44	0.03
72	2.54	77.81	0.13	12.16	0.05	0.51	0.02	4.03	0.04	1.76	0.03	2.71	0.09	0.35	0.04	0.48	0.03
73	2.70	77.98	0.13	12.10	0.05	0.54	0.02	4.02	0.04	1.68	0.03	2.68	0.09	0.37	0.04	0.46	0.03
74	2.86	77.96	0.13	12.15	0.05	0.52	0.02	3.98	0.04	1.67	0.03	2.73	0.09	0.36	0.04	0.42	0.03
75	3.02	77.94	0.13	12.26	0.05	0.52	0.02	4.01	0.04	1.68	0.03	2.58	0.08	0.37	0.04	0.45	0.03
76	3.17	77.89	0.13	12.33	0.05	0.49	0.02	4.01	0.04	1.69	0.03	2.58	0.08	0.31	0.03	0.47	0.03
77	3.33	77.86	0.13	12.32	0.05	0.52	0.02	3.99	0.04	1.64	0.03	2.61	0.08	0.40	0.04	0.43	0.03
78	3.49	77.77	0.13	12.34	0.05	0.54	0.02	3.96	0.04	1.61	0.03	2.68	0.09	0.40	0.04	0.44	0.03
79	3.65	77.75	0.13	12.32	0.05	0.54	0.02	4.01	0.04	1.70	0.03	2.65	0.08	0.35	0.04	0.46	0.03
80	3.81	77.74	0.13	12.41	0.05	0.56	0.03	3.99	0.04	1.69	0.03	2.64	0.08	0.33	0.03	0.44	0.03
81	3.97	77.71	0.13	12.50	0.05	0.53	0.02	4.00	0.04	1.72	0.03	2.58	0.08	0.33	0.03	0.45	0.03
82	4.13	77.64	0.13	12.47	0.05	0.54	0.02	3.96	0.04	1.71	0.03	2.67	0.09	0.34	0.04	0.46	0.03
83	4.29	77.61	0.13	12.45	0.05	0.54	0.02	3.99	0.04	1.69	0.03	2.67	0.09	0.32	0.03	0.48	0.03
84	4.44	77.66	0.13	12.42	0.05	0.56	0.03	3.95	0.04	1.71	0.03	2.72	0.09	0.33	0.03	0.43	0.03
85	4.60	77.51	0.13	12.47	0.05	0.54	0.02	3.98	0.04	1.76	0.03	2.70	0.09	0.37	0.04	0.47	0.03
86	4.76	77.64	0.13	12.50	0.05	0.55	0.03	3.95	0.04	1.68	0.03	2.65	0.08	0.34	0.03	0.48	0.03
87	4.92	77.63	0.13	12.51	0.05	0.54	0.02	3.92	0.04	1.66	0.03	2.74	0.09	0.34	0.03	0.47	0.03
88	5.08	77.41	0.13	12.56	0.05	0.53	0.02	3.93	0.04	1.72	0.03	2.80	0.09	0.35	0.04	0.46	0.03
89	5.24	77.48	0.13	12.59	0.05	0.52	0.02	3.95	0.04	1.68	0.03	2.78	0.09	0.34	0.04	0.47	0.03
90	5.40	77.54	0.13	12.63	0.05	0.54	0.02	3.90	0.04	1.68	0.03	2.70	0.09	0.33	0.03	0.47	0.03
91	5.56	77.29	0.13	12.63	0.05	0.56	0.03	3.92	0.04	1.73	0.03	2.74	0.09	0.38	0.04	0.51	0.03
92	5.71	77.22	0.13	12.68	0.05	0.56	0.03	3.96	0.04	1.74	0.03	2.81	0.09	0.33	0.03	0.49	0.03
93	5.87	77.36	0.13	12.65	0.05	0.56	0.03	3.93	0.04	1.75	0.03	2.77	0.09	0.32	0.03	0.50	0.03
94	6.03	77.18	0.13	12.67	0.05	0.56	0.03	3.91	0.04	1.79	0.03	2.85	0.09	0.37	0.04	0.48	0.03
95	6.19	77.26	0.13	12.68	0.05	0.52	0.02	3.95	0.04	1.81	0.03	2.75	0.09	0.39	0.04	0.46	0.03
96	6.35	77.06	0.13	12.70	0.05	0.55	0.02	3.97	0.04	1.83	0.03	2.85	0.09	0.35	0.04	0.47	0.03
97	6.51	77.03	0.13	12.78	0.05	0.54	0.02	3.98	0.04	1.78	0.03	2.88	0.09	0.35	0.04	0.48	0.03
98	6.67	76.98	0.13	12.76	0.05	0.54	0.02	3.98	0.04	1.90	0.04	2.78	0.09	0.39	0.04	0.46	0.03
99	6.83	76.98	0.13	12.77	0.05	0.54	0.02	3.97	0.04	1.84	0.04	2.81	0.09	0.37	0.04	0.50	0.03
100	6.98	77.01	0.13	12.81	0.05	0.52	0.02	3.95	0.04	1.85	0.04	2.74	0.09	0.38	0.04	0.51	0.03
101	7.14	76.92	0.13	12.80	0.05	0.55	0.03	3.96	0.04	1.84	0.03	2.83	0.09	0.36	0.04	0.51	0.03
102	7.30	76.81	0.13	12.76	0.05	0.54	0.02	3.96	0.04	1.83	0.03	3.04	0.10	0.32	0.03	0.51	0.03
103	7.46	76.68	0.13	12.77	0.05	0.55	0.02	3.96	0.04	1.84	0.04	3.06	0.10	0.41	0.04	0.52	0.03
104	7.62	76.83	0.13	12.78	0.05	0.52	0.02	3.91	0.04	1.86	0.04	3.00	0.10	0.39	0.04	0.49	0.03
105	7.78	76.82	0.13	12.77	0.05	0.55	0.02	3.93	0.04	1.85	0.04	2.97	0.10	0.41	0.04	0.49	0.03
106	7.94	76.78	0.13	12.83	0.05	0.55	0.02	3.94	0.04	1.83	0.03	2.99	0.10	0.37	0.04	0.50	0.03
107	8.10	76.83	0.13	12.87	0.05	0.56	0.03	3.92	0.04	1.76	0.03	3.02	0.10	0.37	0.04	0.48	0.03
108	8.25	76.63	0.13	12.85	0.05	0.57	0.03	3.90	0.04	1.84	0.04	3.09	0.10	0.39	0.04	0.52	0.03
109	8.41	76.55	0.13	12.89	0.05	0.59	0.03	3.93	0.04	1.90	0.04	3.06	0.10	0.37	0.04	0.52	0.03
110	8.57	76.62	0.13	12.90	0.05	0.54	0.02	3.86	0.04	1.91	0.04	3.08	0.10	0.35	0.04	0.53	0.03
111	8.73	76.49	0.13	12.87	0.05	0.57	0.03	3.91	0.04	1.93	0.04	3.14	0.10	0.33	0.03	0.53	0.03
112	8.89	76.57	0.13	12.91	0.05	0.56	0.03	3.90	0.04	1.89	0.04	3.10	0.10	0.35	0.04	0.53	0.03

113	9.05	76.60	0.13	12.82	0.05	0.55	0.03	3.88	0.04	1.91	0.04	3.20	0.10	0.34	0.04	0.51	0.03
114	9.21	76.47	0.13	12.90	0.05	0.59	0.03	3.89	0.04	1.96	0.04	3.08	0.10	0.37	0.04	0.52	0.03
115	9.37	76.30	0.13	12.98	0.05	0.56	0.03	3.91	0.04	1.96	0.04	3.13	0.10	0.38	0.04	0.53	0.03
116	9.52	76.34	0.13	12.92	0.05	0.58	0.03	3.92	0.04	1.94	0.04	3.23	0.10	0.35	0.04	0.52	0.03
117	9.68	76.48	0.13	12.97	0.05	0.57	0.03	3.92	0.04	1.92	0.04	3.08	0.10	0.34	0.04	0.52	0.03
118	9.84	76.36	0.13	13.05	0.05	0.57	0.03	3.90	0.04	1.90	0.04	3.14	0.10	0.33	0.03	0.53	0.03
119	10.00	76.25	0.13	13.05	0.05	0.59	0.03	3.91	0.04	1.98	0.04	3.18	0.10	0.34	0.04	0.50	0.03
120	10.16	76.26	0.13	13.04	0.05	0.56	0.03	3.91	0.04	1.99	0.04	3.18	0.10	0.32	0.03	0.50	0.03

Agglomerate FLD14.L

Table J.8: Major element compositions (as wt.% oxides) from a line traverse across the interface of exterior agglomerate FLD14.L (from agglomerate FLD14.L to host FLD14) extracted from quantified EDS compositional maps. The EDS compositional maps were collected at a resolution of 2.5 pixels/μm. The smoothing width for this traverse was 150 pixels (60.5 μm) wide. This is a CaMgFe interface and has been centered at $x = 0$ based on the FeO maximum. Peak points within 2σ of the FeO maximum are highlighted in yellow. Uncertainties are 2SEOM.

Pt.	Position (μm)	SiO_2	2σ	Al_2O_3	2σ	Na_2O	2σ	K_2O	2σ	CaO	2σ	FeO	2σ	TiO_2	2σ	MgO	2σ
1	-33.47	75.15	0.30	12.25	0.18	2.36	0.11	3.91	0.13	2.97	0.14	2.54	0.18	0.40	0.08	0.42	0.05
2	-33.06	75.24	0.30	12.16	0.18	2.31	0.11	4.00	0.13	2.92	0.14	2.55	0.18	0.41	0.08	0.42	0.05
3	-32.66	75.30	0.30	12.15	0.18	2.36	0.11	3.92	0.13	2.90	0.14	2.52	0.18	0.44	0.09	0.41	0.05
4	-32.26	75.20	0.30	12.05	0.18	2.39	0.11	4.04	0.13	2.95	0.14	2.49	0.18	0.43	0.08	0.45	0.06
5	-31.85	75.26	0.30	11.99	0.18	2.38	0.11	4.05	0.13	2.92	0.14	2.60	0.19	0.34	0.07	0.46	0.06
6	-31.45	75.23	0.30	12.04	0.18	2.34	0.11	3.96	0.13	2.96	0.14	2.63	0.19	0.41	0.08	0.42	0.05
7	-31.05	75.17	0.30	12.05	0.18	2.34	0.11	3.94	0.13	2.92	0.14	2.68	0.19	0.47	0.09	0.42	0.05
8	-30.65	75.36	0.30	11.97	0.18	2.38	0.11	3.88	0.13	2.81	0.14	2.70	0.19	0.48	0.09	0.41	0.05
9	-30.24	75.32	0.30	11.98	0.18	2.36	0.11	3.99	0.13	2.79	0.14	2.70	0.19	0.45	0.09	0.40	0.05
10	-29.84	75.38	0.30	11.94	0.18	2.43	0.12	3.96	0.13	2.75	0.13	2.72	0.19	0.44	0.09	0.37	0.05
11	-29.44	75.49	0.30	11.92	0.18	2.37	0.11	4.00	0.13	2.76	0.14	2.68	0.19	0.36	0.07	0.42	0.05
12	-29.03	75.47	0.30	12.04	0.18	2.32	0.11	3.98	0.13	2.79	0.14	2.59	0.19	0.41	0.08	0.40	0.05
13	-28.63	75.61	0.30	11.94	0.18	2.40	0.11	3.91	0.13	2.61	0.13	2.68	0.19	0.42	0.08	0.42	0.05
14	-28.23	75.40	0.30	11.95	0.18	2.41	0.11	3.99	0.13	2.75	0.13	2.65	0.19	0.43	0.08	0.41	0.05
15	-27.82	75.47	0.30	12.02	0.18	2.41	0.11	4.03	0.13	2.69	0.13	2.56	0.18	0.41	0.08	0.41	0.05
16	-27.42	75.53	0.30	12.07	0.18	2.41	0.11	4.03	0.13	2.68	0.13	2.46	0.18	0.41	0.08	0.42	0.05
17	-27.02	75.52	0.30	11.91	0.18	2.44	0.12	3.91	0.13	2.63	0.13	2.75	0.20	0.42	0.08	0.42	0.05
18	-26.61	75.44	0.30	11.87	0.18	2.37	0.11	4.01	0.13	2.72	0.13	2.65	0.19	0.51	0.10	0.44	0.06
19	-26.21	75.48	0.30	11.91	0.18	2.42	0.11	4.08	0.13	2.69	0.13	2.56	0.18	0.40	0.08	0.47	0.06
20	-25.81	75.61	0.30	11.79	0.17	2.41	0.11	4.08	0.13	2.66	0.13	2.64	0.19	0.38	0.07	0.42	0.05
21	-25.40	75.77	0.30	11.80	0.17	2.43	0.12	4.04	0.13	2.63	0.13	2.52	0.18	0.38	0.07	0.45	0.06
22	-25.00	75.77	0.30	11.86	0.18	2.47	0.12	4.06	0.13	2.64	0.13	2.44	0.17	0.36	0.07	0.38	0.05
23	-24.60	75.77	0.30	11.82	0.18	2.44	0.12	4.05	0.13	2.59	0.13	2.54	0.18	0.39	0.08	0.41	0.05
24	-24.19	75.82	0.30	11.68	0.17	2.36	0.11	4.09	0.13	2.68	0.13	2.62	0.19	0.38	0.08	0.37	0.05
25	-23.79	75.74	0.30	11.75	0.17	2.43	0.12	4.15	0.13	2.58	0.13	2.59	0.19	0.36	0.07	0.39	0.05
26	-23.39	75.74	0.30	11.84	0.18	2.39	0.11	4.05	0.13	2.56	0.12	2.63	0.19	0.34	0.07	0.45	0.06
27	-22.98	75.67	0.30	11.85	0.18	2.43	0.12	4.10	0.13	2.55	0.12	2.58	0.18	0.36	0.07	0.44	0.06
28	-22.58	75.93	0.30	11.72	0.17	2.46	0.12	4.11	0.13	2.50	0.12	2.51	0.18	0.38	0.08	0.39	0.05
29	-22.18	76.15	0.30	11.69	0.17	2.39	0.11	4.14	0.13	2.46	0.12	2.42	0.17	0.42	0.08	0.33	0.04
30	-21.77	76.07	0.30	11.64	0.17	2.45	0.12	4.10	0.13	2.48	0.12	2.47	0.18	0.42	0.08	0.37	0.05
31	-21.37	76.12	0.30	11.71	0.17	2.45	0.12	4.10	0.13	2.42	0.12	2.39	0.17	0.42	0.08	0.39	0.05
32	-20.97	75.98	0.30	11.66	0.17	2.41	0.11	4.20	0.14	2.49	0.12	2.51	0.18	0.36	0.07	0.39	0.05
33	-20.56	76.02	0.30	11.62	0.17	2.47	0.12	4.19	0.14	2.43	0.12	2.50	0.18	0.39	0.08	0.38	0.05
34	-20.16	76.18	0.30	11.57	0.17	2.51	0.12	4.18	0.14	2.36	0.12	2.39	0.17	0.41	0.08	0.38	0.05
35	-19.76	76.23	0.30	11.57	0.17	2.47	0.12	4.20	0.14	2.35	0.11	2.38	0.17	0.42	0.08	0.37	0.05
36	-19.35	76.01	0.30	11.66	0.17	2.50	0.12	4.16	0.14	2.30	0.11	2.60	0.19	0.40	0.08	0.37	0.05
37	-18.95	76.05	0.30	11.50	0.17	2.33	0.11	4.25	0.14	2.39	0.12	2.64	0.19	0.43	0.09	0.41	0.05
38	-18.55	76.14	0.30	11.49	0.17	2.54	0.12	4.23	0.14	2.34	0.11	2.41	0.17	0.39	0.08	0.45	0.06
39	-18.15	76.21	0.30	11.64	0.17	2.59	0.12	4.10	0.13	2.27	0.11	2.35	0.17	0.42	0.08	0.43	0.06
40	-17.74	76.00	0.30	11.52	0.17	2.58	0.12	4.28	0.14	2.26	0.11	2.52	0.18	0.42	0.08	0.41	0.05
41	-17.34	76.21	0.30	11.56	0.17	2.52	0.12	4.28	0.14	2.22	0.11	2.42	0.17	0.38	0.08	0.41	0.05
42	-16.94	76.12	0.30	11.41	0.17	2.57	0.12	4.35	0.14	2.27	0.11	2.51	0.18	0.38	0.07	0.39	0.05
43	-16.53	76.31	0.30	11.44	0.17	2.59	0.12	4.25	0.14	2.25	0.11	2.37	0.17	0.38	0.07	0.40	0.05
44	-16.13	76.35	0.30	11.46	0.17	2.56	0.12	4.33	0.14	2.30	0.11	2.27	0.16	0.35	0.07	0.37	0.05
45	-15.73	76.38	0.30	11.42	0.17	2.52	0.12	4.36	0.14	2.28	0.11	2.36	0.17	0.32	0.06	0.36	0.05
46	-15.32	76.39	0.30	11.29	0.17	2.58	0.12	4.38	0.14	2.32	0.11	2.31	0.17	0.33	0.07	0.39	0.05
47	-14.92	76.25	0.30	11.33	0.17	2.68	0.13	4.32	0.14	2.24	0.11	2.39	0.17	0.38	0.08	0.41	0.05
48	-14.52	76.53	0.30	11.30	0.17	2.60	0.12	4.26	0.14	2.17	0.11	2.32	0.17	0.42	0.08	0.40	0.05
49	-14.11	76.44	0.30	11.25	0.17	2.65	0.13	4.37	0.14	2.27	0.11	2.25	0.16	0.42	0.08	0.36	0.05
50	-13.71	76.58	0.30	11.29	0.17	2.58	0.12	4.34	0.14	2.13	0.10	2.27	0.16	0.42	0.08	0.39	0.05

51	-13.31	76.38	0.30	11.28	0.17	2.71	0.13	4.29	0.14	2.20	0.11	2.34	0.17	0.41	0.08	0.40	0.05
52	-12.90	76.26	0.30	11.18	0.17	2.65	0.13	4.41	0.14	2.22	0.11	2.43	0.17	0.44	0.09	0.41	0.05
53	-12.50	76.46	0.30	11.16	0.17	2.62	0.12	4.46	0.14	2.15	0.11	2.35	0.17	0.43	0.08	0.37	0.05
54	-12.10	76.42	0.30	11.11	0.16	2.65	0.13	4.43	0.14	2.27	0.11	2.35	0.17	0.39	0.08	0.38	0.05
55	-11.69	76.57	0.30	11.15	0.17	2.70	0.13	4.38	0.14	2.18	0.11	2.27	0.16	0.38	0.08	0.38	0.05
56	-11.29	76.64	0.30	11.06	0.16	2.73	0.13	4.35	0.14	2.20	0.11	2.25	0.16	0.40	0.08	0.37	0.05
57	-10.89	76.47	0.30	11.02	0.16	2.74	0.13	4.41	0.14	2.33	0.11	2.27	0.16	0.37	0.07	0.38	0.05
58	-10.48	76.62	0.30	10.94	0.16	2.71	0.13	4.37	0.14	2.35	0.11	2.22	0.16	0.42	0.08	0.36	0.05
59	-10.08	76.88	0.30	10.92	0.16	2.72	0.13	4.29	0.14	2.30	0.11	2.16	0.15	0.38	0.08	0.35	0.05
60	-9.68	76.44	0.30	11.08	0.16	2.82	0.13	4.39	0.14	2.37	0.12	2.17	0.15	0.37	0.07	0.37	0.05
61	-9.27	76.39	0.30	11.00	0.16	2.74	0.13	4.43	0.14	2.42	0.12	2.26	0.16	0.36	0.07	0.39	0.05
62	-8.87	76.48	0.30	10.84	0.16	2.74	0.13	4.53	0.15	2.45	0.12	2.19	0.16	0.37	0.07	0.40	0.05
63	-8.47	76.29	0.30	10.86	0.16	2.82	0.13	4.54	0.15	2.51	0.12	2.29	0.16	0.33	0.06	0.35	0.05
64	-8.06	76.19	0.30	10.82	0.16	2.85	0.14	4.46	0.14	2.62	0.13	2.34	0.17	0.36	0.07	0.35	0.05
65	-7.66	76.32	0.30	10.83	0.16	2.78	0.13	4.38	0.14	2.64	0.13	2.27	0.16	0.39	0.08	0.39	0.05
66	-7.26	76.31	0.30	10.62	0.16	2.80	0.13	4.43	0.14	2.78	0.14	2.30	0.16	0.39	0.08	0.37	0.05
67	-6.85	76.12	0.30	10.71	0.16	2.80	0.13	4.42	0.14	2.92	0.14	2.28	0.16	0.38	0.07	0.37	0.05
68	-6.45	76.03	0.30	10.71	0.16	2.78	0.13	4.30	0.14	3.13	0.15	2.32	0.17	0.36	0.07	0.37	0.05
69	-6.05	75.95	0.30	10.60	0.16	2.80	0.13	4.38	0.14	3.20	0.16	2.34	0.17	0.36	0.07	0.37	0.05
70	-5.65	75.55	0.30	10.55	0.16	2.81	0.13	4.39	0.14	3.42	0.17	2.51	0.18	0.40	0.08	0.38	0.05
71	-5.24	75.36	0.30	10.62	0.16	2.82	0.13	4.37	0.14	3.61	0.18	2.44	0.17	0.39	0.08	0.39	0.05
72	-4.84	75.09	0.30	10.50	0.16	2.82	0.13	4.45	0.14	3.79	0.19	2.54	0.18	0.44	0.09	0.38	0.05
73	-4.44	74.98	0.29	10.38	0.15	2.77	0.13	4.42	0.14	4.07	0.20	2.61	0.19	0.38	0.07	0.40	0.05
74	-4.03	75.04	0.30	10.38	0.15	2.76	0.13	4.29	0.14	4.06	0.20	2.65	0.19	0.38	0.08	0.43	0.06
75	-3.63	75.04	0.30	10.21	0.15	2.69	0.13	4.25	0.14	4.17	0.20	2.83	0.20	0.41	0.08	0.38	0.05
76	-3.23	74.60	0.29	10.27	0.15	2.77	0.13	4.31	0.14	4.32	0.21	2.96	0.21	0.35	0.07	0.42	0.05
77	-2.82	74.58	0.29	10.08	0.15	2.73	0.13	4.29	0.14	4.50	0.22	2.96	0.21	0.39	0.08	0.48	0.06
78	-2.42	74.58	0.29	9.98	0.15	2.70	0.13	4.18	0.14	4.57	0.22	3.10	0.22	0.40	0.08	0.48	0.06
79	-2.02	74.46	0.29	9.79	0.15	2.66	0.13	4.18	0.14	4.68	0.23	3.34	0.24	0.42	0.08	0.47	0.06
80	-1.61	74.82	0.29	9.55	0.14	2.68	0.13	4.13	0.13	4.58	0.22	3.36	0.24	0.35	0.07	0.52	0.07
81	-1.21	74.95	0.29	9.36	0.14	2.57	0.12	4.12	0.13	4.65	0.23	3.46	0.25	0.40	0.08	0.49	0.06
82	-0.81	75.26	0.30	9.32	0.14	2.60	0.12	4.02	0.13	4.50	0.22	3.44	0.25	0.41	0.08	0.45	0.06
83	-0.40	75.16	0.30	9.40	0.14	2.57	0.12	4.01	0.13	4.40	0.21	3.59	0.26	0.36	0.07	0.52	0.07
84	0.00	75.36	0.30	9.31	0.14	2.47	0.12	4.05	0.13	4.32	0.21	3.63	0.26	0.38	0.08	0.48	0.06
85	0.40	75.49	0.30	9.59	0.14	2.47	0.12	4.02	0.13	4.12	0.20	3.38	0.24	0.45	0.09	0.49	0.06
86	0.81	75.50	0.30	9.78	0.15	2.49	0.12	4.05	0.13	3.97	0.19	3.40	0.24	0.37	0.07	0.44	0.06
87	1.21	75.74	0.30	10.00	0.15	2.44	0.12	4.14	0.13	3.77	0.18	3.10	0.22	0.37	0.07	0.45	0.06
88	1.61	75.66	0.30	10.41	0.15	2.42	0.12	4.18	0.14	3.65	0.18	2.89	0.21	0.36	0.07	0.43	0.06
89	2.02	75.33	0.30	10.76	0.16	2.54	0.12	4.24	0.14	3.43	0.17	2.85	0.20	0.43	0.08	0.43	0.06
90	2.42	75.21	0.30	11.12	0.16	2.49	0.12	4.28	0.14	3.29	0.16	2.74	0.20	0.40	0.08	0.47	0.06
91	2.82	75.21	0.30	11.42	0.17	2.50	0.12	4.28	0.14	3.08	0.15	2.68	0.19	0.39	0.08	0.44	0.06
92	3.23	75.10	0.30	11.68	0.17	2.54	0.12	4.27	0.14	2.95	0.14	2.64	0.19	0.41	0.08	0.43	0.05
93	3.63	74.92	0.29	11.76	0.17	2.56	0.12	4.28	0.14	2.98	0.15	2.62	0.19	0.44	0.09	0.44	0.06
94	4.03	74.84	0.29	12.02	0.18	2.60	0.12	4.31	0.14	2.83	0.14	2.59	0.19	0.37	0.07	0.45	0.06
95	4.44	74.61	0.29	12.32	0.18	2.61	0.12	4.18	0.14	2.79	0.14	2.59	0.18	0.43	0.09	0.48	0.06
96	4.84	74.53	0.29	12.28	0.18	2.52	0.12	4.31	0.14	2.87	0.14	2.57	0.18	0.42	0.08	0.48	0.06
97	5.24	74.48	0.29	12.34	0.18	2.54	0.12	4.29	0.14	2.92	0.14	2.58	0.18	0.41	0.08	0.45	0.06
98	5.65	74.32	0.29	12.50	0.19	2.50	0.12	4.27	0.14	2.90	0.14	2.68	0.19	0.39	0.08	0.44	0.06
99	6.05	74.31	0.29	12.48	0.18	2.52	0.12	4.16	0.14	2.98	0.15	2.62	0.19	0.49	0.10	0.43	0.06
100	6.45	74.27	0.29	12.61	0.19	2.50	0.12	4.12	0.13	2.95	0.14	2.59	0.18	0.46	0.09	0.50	0.06
101	6.85	74.33	0.29	12.58	0.19	2.51	0.12	4.12	0.13	2.96	0.14	2.54	0.18	0.44	0.09	0.52	0.07
102	7.26	74.28	0.29	12.61	0.19	2.45	0.12	4.14	0.13	2.99	0.15	2.58	0.18	0.45	0.09	0.49	0.06
103	7.66	74.25	0.29	12.44	0.18	2.44	0.12	4.07	0.13	3.18	0.16	2.72	0.19	0.48	0.09	0.43	0.05
104	8.06	74.21	0.29	12.58	0.19	2.39	0.11	4.02	0.13	3.15	0.15	2.78	0.20	0.41	0.08	0.46	0.06
105	8.47	74.33	0.29	12.64	0.19	2.36	0.11	4.06	0.13	3.17	0.15	2.61	0.19	0.35	0.07	0.47	0.06
106	8.87	74.07	0.29	12.53	0.19	2.45	0.12	4.05	0.13	3.19	0.16	2.83	0.20	0.41	0.08	0.46	0.06
107	9.27	74.05	0.29	12.70	0.19	2.43	0.12	4.04	0.13	3.09	0.15	2.82	0.20	0.45	0.09	0.42	0.05
108	9.68	74.17	0.29	12.79	0.19	2.42	0.11	3.99	0.13	3.06	0.15	2.64	0.19	0.46	0.09	0.48	0.06
109	10.08	74.17	0.29	12.77	0.19	2.41	0.11	3.94	0.13	3.15	0.15	2.64	0.19	0.41	0.08	0.51	0.06
110	10.48	74.13	0.29	12.65	0.19	2.41	0.11	4.04	0.13	3.25	0.16	2.66	0.19	0.41	0.08	0.45	0.06
111	10.89	74.34	0.29	12.69	0.19	2.36	0.11	3.90	0.13	3.16	0.15	2.63	0.19	0.45	0.09	0.47	0.06
112	11.29	74.30	0.29	12.60	0.19	2.29	0.11	4.00	0.13	3.17	0.16	2.69	0.19	0.44	0.09	0.50	0.06

113	11.69	74.13	0.29	12.78	0.19	2.31	0.11	3.93	0.13	3.28	0.16	2.62	0.19	0.43	0.09	0.53	0.07
114	12.10	74.13	0.29	12.75	0.19	2.39	0.11	3.88	0.13	3.19	0.16	2.72	0.19	0.46	0.09	0.48	0.06
115	12.50	74.31	0.29	12.65	0.19	2.31	0.11	3.93	0.13	3.27	0.16	2.62	0.19	0.45	0.09	0.46	0.06
116	12.90	74.46	0.29	12.73	0.19	2.24	0.11	3.91	0.13	3.17	0.16	2.56	0.18	0.47	0.09	0.45	0.06
117	13.31	74.33	0.29	12.79	0.19	2.28	0.11	3.90	0.13	3.20	0.16	2.62	0.19	0.45	0.09	0.42	0.05
118	13.71	74.08	0.29	12.77	0.19	2.27	0.11	3.96	0.13	3.30	0.16	2.68	0.19	0.46	0.09	0.48	0.06
119	14.11	74.11	0.29	12.76	0.19	2.26	0.11	3.93	0.13	3.32	0.16	2.75	0.20	0.39	0.08	0.48	0.06
120	14.52	74.46	0.29	12.73	0.19	2.22	0.11	3.87	0.13	3.28	0.16	2.58	0.18	0.38	0.07	0.48	0.06
121	14.92	74.13	0.29	12.73	0.19	2.27	0.11	3.91	0.13	3.28	0.16	2.74	0.20	0.42	0.08	0.50	0.06
122	15.32	74.49	0.29	12.70	0.19	2.22	0.11	3.85	0.13	3.23	0.16	2.62	0.19	0.43	0.09	0.46	0.06
123	15.73	74.33	0.29	12.70	0.19	2.19	0.10	3.98	0.13	3.34	0.16	2.66	0.19	0.38	0.07	0.41	0.05
124	16.13	74.22	0.29	12.69	0.19	2.21	0.10	3.84	0.12	3.41	0.17	2.70	0.19	0.44	0.09	0.48	0.06
125	16.53	74.38	0.29	12.65	0.19	2.17	0.10	3.80	0.12	3.30	0.16	2.80	0.20	0.45	0.09	0.45	0.06
126	16.94	74.22	0.29	12.71	0.19	2.16	0.10	3.93	0.13	3.35	0.16	2.70	0.19	0.46	0.09	0.45	0.06
127	17.34	74.20	0.29	12.67	0.19	2.24	0.11	3.96	0.13	3.46	0.17	2.60	0.19	0.42	0.08	0.45	0.06
128	17.74	74.27	0.29	12.79	0.19	2.29	0.11	3.83	0.12	3.34	0.16	2.57	0.18	0.42	0.08	0.48	0.06
129	18.15	74.28	0.29	12.82	0.19	2.14	0.10	3.85	0.13	3.26	0.16	2.69	0.19	0.50	0.10	0.47	0.06
130	18.55	74.35	0.29	12.75	0.19	2.22	0.11	3.84	0.12	3.30	0.16	2.56	0.18	0.51	0.10	0.47	0.06
131	18.95	74.42	0.29	12.78	0.19	2.22	0.11	3.76	0.12	3.30	0.16	2.60	0.19	0.44	0.09	0.47	0.06
132	19.35	74.34	0.29	12.75	0.19	2.20	0.10	3.92	0.13	3.29	0.16	2.62	0.19	0.40	0.08	0.48	0.06
133	19.76	74.20	0.29	12.80	0.19	2.25	0.11	3.81	0.12	3.37	0.16	2.75	0.20	0.38	0.08	0.44	0.06
134	20.16	74.30	0.29	12.79	0.19	2.24	0.11	3.78	0.12	3.28	0.16	2.71	0.19	0.41	0.08	0.48	0.06
135	20.56	74.32	0.29	12.79	0.19	2.16	0.10	3.75	0.12	3.32	0.16	2.71	0.19	0.45	0.09	0.48	0.06
136	20.97	74.15	0.29	12.84	0.19	2.15	0.10	3.80	0.12	3.28	0.16	2.85	0.20	0.44	0.09	0.49	0.06
137	21.37	74.35	0.29	12.78	0.19	2.12	0.10	3.86	0.13	3.28	0.16	2.70	0.19	0.41	0.08	0.50	0.06
138	21.77	74.14	0.29	12.87	0.19	2.20	0.10	3.84	0.12	3.27	0.16	2.78	0.20	0.41	0.08	0.50	0.06
139	22.18	74.11	0.29	12.91	0.19	2.21	0.11	3.76	0.12	3.29	0.16	2.80	0.20	0.42	0.08	0.49	0.06
140	22.58	74.10	0.29	12.80	0.19	2.26	0.11	3.77	0.12	3.30	0.16	2.78	0.20	0.49	0.10	0.50	0.06
141	22.98	74.08	0.29	12.82	0.19	2.28	0.11	3.73	0.12	3.33	0.16	2.84	0.20	0.40	0.08	0.50	0.06
142	23.39	74.17	0.29	12.85	0.19	2.22	0.11	3.77	0.12	3.40	0.17	2.72	0.19	0.40	0.08	0.46	0.06
143	23.79	74.29	0.29	12.90	0.19	2.14	0.10	3.76	0.12	3.31	0.16	2.69	0.19	0.42	0.08	0.48	0.06
144	24.19	74.17	0.29	12.86	0.19	2.20	0.10	3.77	0.12	3.28	0.16	2.83	0.20	0.43	0.08	0.47	0.06
145	24.60	74.03	0.29	12.87	0.19	2.17	0.10	3.82	0.12	3.39	0.17	2.85	0.20	0.42	0.08	0.46	0.06
146	25.00	74.00	0.29	12.83	0.19	2.22	0.11	3.85	0.13	3.38	0.16	2.73	0.20	0.48	0.10	0.50	0.06
147	25.40	74.23	0.29	12.77	0.19	2.18	0.10	3.80	0.12	3.33	0.16	2.79	0.20	0.43	0.08	0.46	0.06
148	25.81	74.14	0.29	12.98	0.19	2.15	0.10	3.68	0.12	3.38	0.17	2.69	0.19	0.45	0.09	0.53	0.07
149	26.21	74.12	0.29	12.90	0.19	2.19	0.10	3.77	0.12	3.37	0.16	2.71	0.19	0.45	0.09	0.49	0.06
150	26.61	74.21	0.29	12.93	0.19	2.14	0.10	3.73	0.12	3.38	0.17	2.72	0.19	0.43	0.08	0.46	0.06
151	27.02	74.31	0.29	12.88	0.19	2.09	0.10	3.72	0.12	3.37	0.16	2.66	0.19	0.47	0.09	0.51	0.07
152	27.42	74.21	0.29	12.75	0.19	2.18	0.10	3.80	0.12	3.47	0.17	2.67	0.19	0.43	0.09	0.49	0.06
153	27.82	74.16	0.29	12.78	0.19	2.24	0.11	3.77	0.12	3.38	0.17	2.75	0.20	0.44	0.09	0.48	0.06
154	28.23	74.25	0.29	12.89	0.19	2.24	0.11	3.73	0.12	3.38	0.17	2.68	0.19	0.40	0.08	0.44	0.06
155	28.63	74.41	0.29	12.95	0.19	2.23	0.11	3.73	0.12	3.38	0.17	2.45	0.17	0.39	0.08	0.46	0.06
156	29.03	74.23	0.29	12.97	0.19	2.18	0.10	3.72	0.12	3.38	0.17	2.63	0.19	0.40	0.08	0.50	0.06
157	29.44	74.16	0.29	12.89	0.19	2.16	0.10	3.76	0.12	3.40	0.17	2.71	0.19	0.44	0.09	0.47	0.06
158	29.84	74.47	0.29	12.93	0.19	2.16	0.10	3.69	0.12	3.27	0.16	2.63	0.19	0.39	0.08	0.47	0.06
159	30.24	74.20	0.29	12.92	0.19	2.20	0.10	3.73	0.12	3.30	0.16	2.72	0.19	0.43	0.09	0.48	0.06

Agglomerate FLD18.1

Table J.9: Major element compositions (as wt.% oxides) from a line traverse across the interface of exterior agglomerate FLD18.1 (from agglomerate FLD18.1 to host FLD18) extracted from quantified EDS compositional maps. The EDS compositional maps were collected at a resolution of 11.5 pixels/μm. The smoothing width for this traverse was 175 pixels (15.2 μm) wide. This is a CaMgFe interface and has been centered at $x = 0$ based on the FeO maximum. Peak points within 2σ of the FeO maximum are highlighted in yellow. Uncertainties are 2SEOM.

Pt.	Position (μm)	SiO_2	2σ	Al_2O_3	2σ	Na_2O	2σ	K_2O	2σ	CaO	2σ	FeO	2σ	TiO_2	2σ	MgO	2σ
1	-5.83	74.10	0.20	13.18	0.11	2.25	0.07	4.33	0.08	1.94	0.08	2.71	0.14	0.51	0.06	0.58	0.06
2	-5.74	74.08	0.20	13.12	0.11	2.23	0.07	4.40	0.08	1.97	0.09	2.66	0.14	0.54	0.07	0.59	0.06
3	-5.65	74.16	0.20	13.06	0.11	2.30	0.07	4.43	0.08	1.86	0.08	2.74	0.15	0.52	0.06	0.58	0.06
4	-5.56	74.13	0.20	13.08	0.11	2.27	0.07	4.41	0.08	1.87	0.08	2.68	0.14	0.55	0.07	0.61	0.07
5	-5.48	74.19	0.20	13.08	0.11	2.25	0.07	4.40	0.08	1.85	0.08	2.77	0.15	0.48	0.06	0.59	0.06
6	-5.39	74.10	0.20	13.16	0.11	2.20	0.07	4.40	0.08	1.82	0.08	2.85	0.15	0.49	0.06	0.57	0.06
7	-5.30	73.92	0.20	13.22	0.11	2.29	0.07	4.44	0.08	1.86	0.08	2.77	0.15	0.55	0.07	0.56	0.06
8	-5.22	74.15	0.20	13.11	0.11	2.29	0.07	4.46	0.09	1.85	0.08	2.67	0.14	0.50	0.06	0.54	0.06
9	-5.13	74.19	0.20	13.01	0.11	2.31	0.07	4.44	0.08	1.89	0.08	2.69	0.14	0.54	0.07	0.54	0.06
10	-5.04	74.25	0.20	13.03	0.11	2.31	0.07	4.49	0.09	1.79	0.08	2.67	0.14	0.51	0.06	0.55	0.06
11	-4.96	74.14	0.20	13.05	0.11	2.34	0.07	4.54	0.09	1.71	0.07	2.74	0.14	0.50	0.06	0.61	0.07
12	-4.87	74.10	0.20	13.08	0.11	2.33	0.07	4.58	0.09	1.72	0.08	2.64	0.14	0.52	0.06	0.61	0.07
13	-4.78	73.93	0.20	13.21	0.11	2.35	0.07	4.58	0.09	1.69	0.07	2.70	0.14	0.53	0.06	0.57	0.06
14	-4.70	74.09	0.20	13.18	0.11	2.39	0.07	4.49	0.09	1.68	0.07	2.64	0.14	0.53	0.06	0.61	0.07
15	-4.61	74.20	0.20	13.06	0.11	2.44	0.08	4.52	0.09	1.67	0.07	2.66	0.14	0.49	0.06	0.58	0.06
16	-4.52	74.10	0.20	13.04	0.11	2.34	0.07	4.65	0.09	1.72	0.08	2.70	0.14	0.52	0.06	0.53	0.06
17	-4.43	74.09	0.20	13.07	0.11	2.37	0.07	4.61	0.09	1.65	0.07	2.72	0.14	0.48	0.06	0.61	0.07
18	-4.35	74.27	0.20	13.07	0.11	2.45	0.08	4.57	0.09	1.60	0.07	2.56	0.14	0.50	0.06	0.56	0.06
19	-4.26	73.99	0.20	13.10	0.11	2.38	0.07	4.62	0.09	1.75	0.08	2.74	0.14	0.49	0.06	0.56	0.06
20	-4.17	73.97	0.20	13.11	0.11	2.41	0.07	4.69	0.09	1.63	0.07	2.76	0.15	0.48	0.06	0.55	0.06
21	-4.09	73.91	0.20	13.12	0.11	2.40	0.07	4.67	0.09	1.62	0.07	2.76	0.15	0.48	0.06	0.58	0.06
22	-4.00	73.95	0.20	13.20	0.11	2.44	0.08	4.74	0.09	1.59	0.07	2.63	0.14	0.50	0.06	0.60	0.06
23	-3.91	73.95	0.20	13.09	0.11	2.51	0.08	4.78	0.09	1.46	0.06	2.76	0.15	0.51	0.06	0.57	0.06
24	-3.83	74.07	0.20	13.04	0.11	2.40	0.07	4.76	0.09	1.60	0.07	2.62	0.14	0.51	0.06	0.59	0.06
25	-3.74	74.05	0.20	13.09	0.11	2.54	0.08	4.66	0.09	1.58	0.07	2.58	0.14	0.51	0.06	0.57	0.06
26	-3.65	74.17	0.20	13.12	0.11	2.45	0.08	4.77	0.09	1.54	0.07	2.47	0.13	0.52	0.06	0.58	0.06
27	-3.56	73.99	0.20	13.08	0.11	2.45	0.08	4.91	0.09	1.54	0.07	2.57	0.14	0.50	0.06	0.59	0.06
28	-3.48	74.02	0.20	13.06	0.11	2.59	0.08	4.82	0.09	1.57	0.07	2.51	0.13	0.52	0.06	0.58	0.06
29	-3.39	74.07	0.20	13.08	0.11	2.65	0.08	4.76	0.09	1.50	0.07	2.48	0.13	0.48	0.06	0.56	0.06
30	-3.30	73.99	0.20	13.10	0.11	2.53	0.08	4.81	0.09	1.54	0.07	2.61	0.14	0.54	0.07	0.48	0.05
31	-3.22	74.03	0.20	13.10	0.11	2.53	0.08	4.80	0.09	1.53	0.07	2.57	0.14	0.54	0.07	0.50	0.05
32	-3.13	73.96	0.20	13.11	0.11	2.52	0.08	4.87	0.09	1.54	0.07	2.56	0.14	0.47	0.06	0.52	0.06
33	-3.04	74.23	0.20	13.02	0.11	2.57	0.08	4.91	0.09	1.47	0.06	2.36	0.12	0.52	0.06	0.50	0.05
34	-2.96	74.30	0.20	12.95	0.11	2.62	0.08	4.88	0.09	1.47	0.06	2.37	0.13	0.51	0.06	0.50	0.05
35	-2.87	74.05	0.20	12.95	0.11	2.61	0.08	4.86	0.09	1.47	0.06	2.57	0.14	0.54	0.07	0.58	0.06
36	-2.78	73.83	0.20	12.95	0.11	2.64	0.08	5.00	0.10	1.57	0.07	2.60	0.14	0.52	0.06	0.51	0.06
37	-2.70	74.03	0.20	12.95	0.11	2.64	0.08	4.86	0.09	1.64	0.07	2.49	0.13	0.51	0.06	0.52	0.06
38	-2.61	74.15	0.20	12.88	0.11	2.67	0.08	4.89	0.09	1.53	0.07	2.44	0.13	0.50	0.06	0.55	0.06
39	-2.52	73.94	0.20	12.87	0.11	2.74	0.08	5.02	0.10	1.52	0.07	2.51	0.13	0.51	0.06	0.52	0.06
40	-2.43	73.93	0.20	12.91	0.11	2.80	0.09	5.01	0.10	1.59	0.07	2.34	0.12	0.54	0.07	0.48	0.05
41	-2.35	74.06	0.20	12.90	0.11	2.79	0.09	4.98	0.10	1.70	0.07	2.24	0.12	0.49	0.06	0.42	0.05
42	-2.26	73.82	0.20	12.85	0.11	2.79	0.09	5.08	0.10	1.76	0.08	2.30	0.12	0.47	0.06	0.46	0.05
43	-2.17	73.85	0.20	12.85	0.11	2.82	0.09	4.97	0.09	1.82	0.08	2.35	0.12	0.46	0.06	0.49	0.05
44	-2.09	73.81	0.20	12.82	0.11	2.90	0.09	4.95	0.09	1.88	0.08	2.28	0.12	0.51	0.06	0.48	0.05
45	-2.00	73.66	0.20	12.67	0.11	3.01	0.09	4.91	0.09	1.93	0.08	2.49	0.13	0.48	0.06	0.50	0.05
46	-1.91	73.33	0.20	12.81	0.11	3.08	0.09	5.03	0.10	1.98	0.09	2.40	0.13	0.55	0.07	0.47	0.05
47	-1.83	73.62	0.20	12.59	0.11	3.07	0.09	4.86	0.09	2.09	0.09	2.39	0.13	0.50	0.06	0.49	0.05
48	-1.74	73.34	0.20	12.53	0.11	3.16	0.10	4.86	0.09	2.26	0.10	2.41	0.13	0.46	0.06	0.51	0.06
49	-1.65	73.05	0.20	12.48	0.11	3.19	0.10	4.84	0.09	2.46	0.11	2.54	0.13	0.49	0.06	0.52	0.06
50	-1.56	73.14	0.20	12.24	0.10	3.10	0.10	4.77	0.09	2.54	0.11	2.73	0.14	0.52	0.06	0.55	0.06

51	-1.48	73.23	0.20	12.04	0.10	3.12	0.10	4.76	0.09	2.67	0.12	2.73	0.14	0.53	0.06	0.56	0.06
52	-1.39	73.12	0.20	11.81	0.10	3.21	0.10	4.69	0.09	2.89	0.13	2.81	0.15	0.51	0.06	0.57	0.06
53	-1.30	73.03	0.20	11.83	0.10	3.21	0.10	4.70	0.09	2.90	0.13	2.93	0.15	0.50	0.06	0.52	0.06
54	-1.22	72.84	0.20	11.48	0.10	3.32	0.10	4.68	0.09	3.22	0.14	3.12	0.16	0.49	0.06	0.50	0.05
55	-1.13	72.74	0.20	11.23	0.09	3.32	0.10	4.55	0.09	3.47	0.15	3.21	0.17	0.51	0.06	0.57	0.06
56	-1.04	72.69	0.20	10.92	0.09	3.25	0.10	4.61	0.09	3.76	0.16	3.29	0.17	0.49	0.06	0.63	0.07
57	-0.96	72.77	0.20	10.75	0.09	3.24	0.10	4.59	0.09	3.88	0.17	3.30	0.17	0.53	0.06	0.61	0.07
58	-0.87	73.10	0.20	10.42	0.09	3.16	0.10	4.39	0.08	3.94	0.17	3.54	0.19	0.46	0.06	0.62	0.07
59	-0.78	72.98	0.20	10.12	0.09	3.10	0.10	4.30	0.08	4.17	0.18	3.75	0.20	0.51	0.06	0.63	0.07
60	-0.70	72.80	0.20	9.90	0.08	3.19	0.10	4.28	0.08	4.39	0.19	3.95	0.21	0.50	0.06	0.63	0.07
61	-0.61	72.91	0.20	9.62	0.08	3.19	0.10	4.24	0.08	4.59	0.20	3.85	0.20	0.46	0.06	0.69	0.08
62	-0.52	72.73	0.20	9.40	0.08	3.27	0.10	4.24	0.08	4.72	0.21	4.11	0.22	0.41	0.05	0.69	0.07
63	-0.43	72.78	0.20	9.26	0.08	3.19	0.10	4.20	0.08	4.92	0.21	4.09	0.22	0.48	0.06	0.64	0.07
64	-0.35	72.48	0.20	9.14	0.08	3.26	0.10	4.17	0.08	5.01	0.22	4.29	0.23	0.54	0.07	0.69	0.08
65	-0.26	72.64	0.20	9.04	0.08	3.23	0.10	4.05	0.08	5.07	0.22	4.33	0.23	0.48	0.06	0.71	0.08
66	-0.17	72.90	0.20	8.81	0.07	3.24	0.10	4.08	0.08	5.12	0.22	4.18	0.22	0.48	0.06	0.77	0.08
67	-0.09	72.84	0.20	8.83	0.07	3.39	0.10	3.99	0.08	5.17	0.23	4.18	0.22	0.44	0.05	0.72	0.08
68	0.00	72.66	0.20	8.73	0.07	3.33	0.10	4.06	0.08	5.10	0.22	4.39	0.23	0.49	0.06	0.79	0.09
69	0.09	72.70	0.20	8.84	0.07	3.33	0.10	4.10	0.08	5.28	0.23	4.22	0.22	0.42	0.05	0.71	0.08
70	0.17	72.94	0.20	8.82	0.07	3.33	0.10	4.01	0.08	5.13	0.22	4.16	0.22	0.47	0.06	0.72	0.08
71	0.26	72.82	0.20	8.95	0.08	3.33	0.10	4.08	0.08	5.18	0.23	4.05	0.21	0.45	0.05	0.73	0.08
72	0.35	72.70	0.20	8.86	0.07	3.31	0.10	4.13	0.08	5.26	0.23	4.17	0.22	0.49	0.06	0.67	0.07
73	0.44	72.76	0.20	8.93	0.08	3.38	0.10	4.09	0.08	5.11	0.22	4.15	0.22	0.46	0.06	0.69	0.08
74	0.52	72.79	0.20	9.07	0.08	3.38	0.10	4.17	0.08	5.05	0.22	3.94	0.21	0.50	0.06	0.68	0.07
75	0.61	72.93	0.20	9.04	0.08	3.34	0.10	4.21	0.08	5.11	0.22	3.83	0.20	0.47	0.06	0.65	0.07
76	0.70	72.75	0.20	9.20	0.08	3.30	0.10	4.18	0.08	5.01	0.22	3.90	0.21	0.50	0.06	0.68	0.07
77	0.78	72.43	0.20	9.39	0.08	3.36	0.10	4.27	0.08	5.07	0.22	3.90	0.21	0.48	0.06	0.67	0.07
78	0.87	72.53	0.20	9.60	0.08	3.37	0.10	4.28	0.08	4.99	0.22	3.70	0.20	0.50	0.06	0.58	0.06
79	0.96	72.40	0.20	9.66	0.08	3.53	0.11	4.20	0.08	4.93	0.22	3.69	0.20	0.51	0.06	0.67	0.07
80	1.04	72.30	0.20	9.76	0.08	3.48	0.11	4.34	0.08	4.94	0.22	3.58	0.19	0.52	0.06	0.61	0.07
81	1.13	72.29	0.20	9.92	0.08	3.50	0.11	4.37	0.08	4.89	0.21	3.51	0.19	0.47	0.06	0.60	0.07
82	1.22	72.14	0.20	10.00	0.08	3.67	0.11	4.37	0.08	4.75	0.21	3.58	0.19	0.47	0.06	0.60	0.07
83	1.30	72.30	0.20	10.22	0.09	3.60	0.11	4.41	0.08	4.64	0.20	3.24	0.17	0.54	0.07	0.61	0.07
84	1.39	72.56	0.20	10.16	0.09	3.60	0.11	4.39	0.08	4.68	0.20	3.11	0.16	0.48	0.06	0.60	0.07
85	1.48	72.38	0.20	10.24	0.09	3.68	0.11	4.34	0.08	4.55	0.20	3.30	0.17	0.45	0.05	0.62	0.07
86	1.57	72.18	0.20	10.33	0.09	3.70	0.11	4.44	0.08	4.57	0.20	3.19	0.17	0.45	0.05	0.63	0.07
87	1.65	72.21	0.20	10.45	0.09	3.65	0.11	4.44	0.08	4.57	0.20	3.03	0.16	0.54	0.07	0.65	0.07
88	1.74	72.30	0.20	10.63	0.09	3.59	0.11	4.44	0.08	4.42	0.19	3.15	0.17	0.52	0.06	0.57	0.06
89	1.83	72.54	0.20	10.62	0.09	3.61	0.11	4.49	0.09	4.27	0.19	2.98	0.16	0.52	0.06	0.58	0.06
90	1.91	72.38	0.20	10.72	0.09	3.73	0.11	4.54	0.09	4.24	0.19	2.95	0.16	0.47	0.06	0.54	0.06
91	2.00	72.21	0.20	10.72	0.09	3.79	0.12	4.54	0.09	4.27	0.19	3.04	0.16	0.50	0.06	0.54	0.06
92	2.09	72.35	0.20	10.80	0.09	3.66	0.11	4.46	0.09	4.20	0.18	3.07	0.16	0.48	0.06	0.60	0.07
93	2.17	72.33	0.20	11.00	0.09	3.61	0.11	4.53	0.09	4.20	0.18	2.85	0.15	0.52	0.06	0.57	0.06
94	2.26	72.22	0.20	11.06	0.09	3.65	0.11	4.66	0.09	4.32	0.19	2.71	0.14	0.46	0.06	0.51	0.06
95	2.35	72.50	0.20	11.10	0.09	3.71	0.11	4.51	0.09	3.91	0.17	2.85	0.15	0.46	0.06	0.55	0.06
96	2.43	72.33	0.20	10.96	0.09	3.75	0.12	4.60	0.09	4.11	0.18	2.82	0.15	0.49	0.06	0.56	0.06
97	2.52	72.21	0.20	11.09	0.09	3.70	0.11	4.70	0.09	4.07	0.18	2.74	0.15	0.48	0.06	0.58	0.06
98	2.61	72.48	0.20	11.07	0.09	3.66	0.11	4.68	0.09	3.93	0.17	2.70	0.14	0.53	0.06	0.54	0.06
99	2.70	72.31	0.20	11.23	0.09	3.66	0.11	4.71	0.09	3.90	0.17	2.72	0.14	0.52	0.06	0.55	0.06
100	2.78	72.44	0.20	11.29	0.10	3.81	0.12	4.66	0.09	3.79	0.17	2.57	0.14	0.48	0.06	0.52	0.06
101	2.87	72.65	0.20	11.27	0.10	3.76	0.12	4.66	0.09	3.69	0.16	2.58	0.14	0.50	0.06	0.52	0.06
102	2.96	72.64	0.20	11.22	0.09	3.81	0.12	4.68	0.09	3.64	0.16	2.64	0.14	0.52	0.06	0.55	0.06
103	3.04	72.55	0.20	11.26	0.10	3.70	0.11	4.74	0.09	3.64	0.16	2.70	0.14	0.50	0.06	0.49	0.05
104	3.13	72.63	0.20	11.46	0.10	3.69	0.11	4.70	0.09	3.54	0.15	2.68	0.14	0.41	0.05	0.49	0.05
105	3.22	72.66	0.20	11.50	0.10	3.78	0.12	4.66	0.09	3.49	0.15	2.57	0.14	0.49	0.06	0.46	0.05
106	3.30	72.79	0.20	11.39	0.10	3.78	0.12	4.79	0.09	3.43	0.15	2.42	0.13	0.48	0.06	0.51	0.06
107	3.39	72.84	0.20	11.51	0.10	3.70	0.11	4.67	0.09	3.40	0.15	2.54	0.13	0.50	0.06	0.47	0.05
108	3.48	73.08	0.20	11.59	0.10	3.70	0.11	4.67	0.09	3.15	0.14	2.45	0.13	0.48	0.06	0.48	0.05
109	3.57	73.07	0.20	11.53	0.10	3.67	0.11	4.75	0.09	3.11	0.14	2.51	0.13	0.51	0.06	0.49	0.05
110	3.65	72.97	0.20	11.57	0.10	3.73	0.11	4.80	0.09	3.20	0.14	2.40	0.13	0.45	0.05	0.47	0.05
111	3.74	73.25	0.20	11.55	0.10	3.60	0.11	4.68	0.09	3.08	0.13	2.48	0.13	0.50	0.06	0.48	0.05
112	3.83	73.17	0.20	11.58	0.10	3.56	0.11	4.75	0.09	3.08	0.13	2.59	0.14	0.45	0.05	0.50	0.05

113	3.91	73.02	0.20	11.70	0.10	3.64	0.11	4.82	0.09	2.98	0.13	2.45	0.13	0.55	0.07	0.48	0.05
114	4.00	73.24	0.20	11.72	0.10	3.65	0.11	4.75	0.09	3.00	0.13	2.29	0.12	0.52	0.06	0.50	0.05
115	4.09	73.33	0.20	11.68	0.10	3.63	0.11	4.84	0.09	2.82	0.12	2.32	0.12	0.47	0.06	0.49	0.05
116	4.17	73.21	0.20	11.82	0.10	3.61	0.11	4.91	0.09	2.85	0.12	2.29	0.12	0.50	0.06	0.43	0.05
117	4.26	73.48	0.20	11.79	0.10	3.56	0.11	4.96	0.09	2.68	0.12	2.29	0.12	0.47	0.06	0.46	0.05
118	4.35	73.23	0.20	11.93	0.10	3.70	0.11	4.87	0.09	2.69	0.12	2.28	0.12	0.43	0.05	0.46	0.05
119	4.43	73.29	0.20	11.89	0.10	3.56	0.11	4.90	0.09	2.62	0.11	2.34	0.12	0.48	0.06	0.50	0.05
120	4.52	73.45	0.20	11.87	0.10	3.69	0.11	4.89	0.09	2.55	0.11	2.28	0.12	0.49	0.06	0.47	0.05
121	4.61	73.62	0.20	11.88	0.10	3.64	0.11	4.91	0.09	2.48	0.11	2.22	0.12	0.41	0.05	0.46	0.05
122	4.70	73.53	0.20	11.86	0.10	3.60	0.11	4.89	0.09	2.47	0.11	2.34	0.12	0.48	0.06	0.47	0.05
123	4.78	73.41	0.20	11.91	0.10	3.59	0.11	4.85	0.09	2.50	0.11	2.39	0.13	0.46	0.06	0.45	0.05
124	4.87	73.53	0.20	12.00	0.10	3.68	0.11	4.80	0.09	2.42	0.11	2.30	0.12	0.43	0.05	0.43	0.05
125	4.96	73.43	0.20	12.09	0.10	3.63	0.11	4.90	0.09	2.39	0.10	2.28	0.12	0.47	0.06	0.45	0.05
126	5.04	73.56	0.20	12.01	0.10	3.59	0.11	4.98	0.10	2.32	0.10	2.26	0.12	0.44	0.05	0.43	0.05
127	5.13	73.68	0.20	12.08	0.10	3.48	0.11	4.89	0.09	2.31	0.10	2.20	0.12	0.55	0.07	0.47	0.05
128	5.22	73.55	0.20	12.02	0.10	3.52	0.11	4.96	0.09	2.21	0.10	2.37	0.13	0.51	0.06	0.45	0.05
129	5.30	73.62	0.20	11.97	0.10	3.50	0.11	4.96	0.09	2.25	0.10	2.42	0.13	0.46	0.06	0.43	0.05
130	5.39	73.58	0.20	12.06	0.10	3.48	0.11	5.01	0.10	2.19	0.10	2.39	0.13	0.48	0.06	0.46	0.05
131	5.48	73.86	0.20	12.12	0.10	3.44	0.11	4.97	0.09	2.05	0.09	2.25	0.12	0.47	0.06	0.47	0.05
132	5.57	73.79	0.20	12.18	0.10	3.41	0.10	4.89	0.09	2.08	0.09	2.25	0.12	0.46	0.06	0.53	0.06
133	5.65	73.73	0.20	12.15	0.10	3.42	0.11	4.93	0.09	2.02	0.09	2.35	0.12	0.47	0.06	0.51	0.06
134	5.74	73.89	0.20	12.17	0.10	3.37	0.10	4.95	0.09	1.99	0.09	2.20	0.12	0.50	0.06	0.45	0.05
135	5.83	73.96	0.20	12.09	0.10	3.39	0.10	4.96	0.09	2.02	0.09	2.21	0.12	0.50	0.06	0.47	0.05
136	5.91	73.86	0.20	12.22	0.10	3.32	0.10	4.99	0.10	2.03	0.09	2.19	0.12	0.49	0.06	0.48	0.05
137	6.00	73.91	0.20	12.23	0.10	3.39	0.10	4.94	0.09	1.93	0.08	2.15	0.11	0.53	0.06	0.45	0.05
138	6.09	73.81	0.20	12.27	0.10	3.46	0.11	5.00	0.10	1.87	0.08	2.33	0.12	0.43	0.05	0.47	0.05
139	6.17	73.81	0.20	12.24	0.10	3.39	0.10	5.00	0.10	1.93	0.08	2.25	0.12	0.49	0.06	0.49	0.05
140	6.26	74.05	0.20	12.18	0.10	3.26	0.10	4.99	0.10	1.83	0.08	2.28	0.12	0.52	0.06	0.50	0.05
141	6.35	73.86	0.20	12.37	0.10	3.29	0.10	5.04	0.10	1.84	0.08	2.29	0.12	0.48	0.06	0.47	0.05
142	6.43	73.79	0.20	12.43	0.11	3.28	0.10	4.97	0.09	1.90	0.08	2.28	0.12	0.51	0.06	0.45	0.05
143	6.52	73.92	0.20	12.35	0.10	3.32	0.10	4.98	0.10	1.83	0.08	2.24	0.12	0.48	0.06	0.44	0.05
144	6.61	73.86	0.20	12.38	0.10	3.30	0.10	5.01	0.10	1.82	0.08	2.29	0.12	0.47	0.06	0.46	0.05
145	6.70	73.97	0.20	12.27	0.10	3.28	0.10	4.96	0.09	1.80	0.08	2.31	0.12	0.48	0.06	0.49	0.05
146	6.78	74.04	0.20	12.27	0.10	3.28	0.10	5.06	0.10	1.81	0.08	2.25	0.12	0.45	0.05	0.47	0.05
147	6.87	74.03	0.20	12.33	0.10	3.19	0.10	5.04	0.10	1.74	0.08	2.30	0.12	0.48	0.06	0.49	0.05
148	6.96	74.11	0.20	12.47	0.11	3.11	0.10	5.04	0.10	1.67	0.07	2.29	0.12	0.50	0.06	0.47	0.05
149	7.04	74.29	0.20	12.26	0.10	3.16	0.10	4.99	0.10	1.73	0.08	2.19	0.12	0.52	0.06	0.51	0.06
150	7.13	74.13	0.20	12.32	0.10	3.18	0.10	4.90	0.09	1.75	0.08	2.32	0.12	0.52	0.06	0.52	0.06
151	7.22	74.02	0.20	12.41	0.10	3.11	0.10	4.86	0.09	1.78	0.08	2.51	0.13	0.45	0.05	0.48	0.05
152	7.30	74.13	0.20	12.56	0.11	3.10	0.10	4.97	0.09	1.70	0.07	2.26	0.12	0.46	0.06	0.48	0.05
153	7.39	74.15	0.20	12.46	0.11	3.16	0.10	4.96	0.09	1.71	0.07	2.31	0.12	0.49	0.06	0.44	0.05
154	7.48	74.20	0.20	12.27	0.10	3.07	0.09	5.08	0.10	1.75	0.08	2.31	0.12	0.51	0.06	0.40	0.04
155	7.57	74.40	0.20	12.56	0.11	2.96	0.09	4.89	0.09	1.70	0.07	2.25	0.12	0.48	0.06	0.43	0.05
156	7.65	74.13	0.20	12.55	0.11	2.94	0.09	4.95	0.09	1.66	0.07	2.28	0.12	0.57	0.07	0.50	0.05
157	7.74	74.22	0.20	12.38	0.10	3.00	0.09	5.02	0.10	1.61	0.07	2.34	0.12	0.52	0.06	0.49	0.05
158	7.83	74.26	0.20	12.52	0.11	3.06	0.09	5.04	0.10	1.64	0.07	2.15	0.11	0.50	0.06	0.47	0.05
159	7.91	74.23	0.20	12.51	0.11	3.02	0.09	4.98	0.10	1.67	0.07	2.34	0.12	0.46	0.06	0.46	0.05
160	8.00	74.36	0.20	12.54	0.11	2.97	0.09	4.88	0.09	1.61	0.07	2.40	0.13	0.45	0.05	0.45	0.05
161	8.09	74.36	0.20	12.39	0.10	3.08	0.09	4.94	0.09	1.58	0.07	2.30	0.12	0.54	0.07	0.48	0.05
162	8.17	74.27	0.20	12.50	0.11	2.95	0.09	4.92	0.09	1.62	0.07	2.31	0.12	0.56	0.07	0.45	0.05
163	8.26	74.29	0.20	12.67	0.11	2.93	0.09	4.90	0.09	1.50	0.07	2.37	0.13	0.48	0.06	0.47	0.05

Agglomerate FLD23.L

Table J.10: Major element compositions (as wt.% oxides) from a line traverse across the interface of agglomerate FLD23.L (from agglomerate FLD23.L to host FLD23) extracted from quantified EDS compositional maps. This is an exterior agglomerate with an Si interface and has been centered at $x = 0$ based on the SiO_2 maximum. Peak points within 2σ of the SiO_2 maximum are highlighted in yellow. Uncertainties are 2SEOM.

Pt.	Position (μm)	SiO_2	2σ	Al_2O_3	2σ	Na_2O	2σ	K_2O	2σ	CaO	2σ	FeO	2σ	TiO_2	2σ	MgO	2σ
1	-16.16	74.27	0.23	12.84	0.13	3.20	0.09	3.61	0.10	2.47	0.11	2.64	0.18	0.45	0.08	0.52	0.05
2	-15.90	74.18	0.23	12.94	0.13	3.18	0.09	3.57	0.10	2.45	0.11	2.72	0.19	0.44	0.08	0.53	0.05
3	-15.63	74.41	0.23	12.85	0.13	3.18	0.09	3.42	0.09	2.33	0.10	2.91	0.20	0.39	0.07	0.51	0.05
4	-15.36	74.02	0.23	12.90	0.13	3.15	0.09	3.54	0.10	2.46	0.11	2.91	0.20	0.48	0.08	0.53	0.05
5	-15.09	73.98	0.23	12.79	0.12	3.11	0.09	3.66	0.10	2.50	0.11	2.92	0.20	0.51	0.09	0.52	0.05
6	-14.82	73.88	0.23	12.77	0.12	3.25	0.09	3.58	0.10	2.55	0.11	2.93	0.20	0.46	0.08	0.59	0.06
7	-14.55	73.95	0.23	12.88	0.13	3.31	0.10	3.45	0.09	2.49	0.11	2.84	0.19	0.45	0.08	0.62	0.06
8	-14.28	73.99	0.23	12.88	0.13	3.36	0.10	3.52	0.10	2.61	0.11	2.66	0.18	0.41	0.07	0.57	0.05
9	-14.01	73.87	0.23	12.75	0.12	3.30	0.10	3.54	0.10	2.71	0.12	2.79	0.19	0.46	0.08	0.58	0.05
10	-13.74	73.75	0.23	12.68	0.12	3.28	0.09	3.55	0.10	2.72	0.12	3.00	0.20	0.47	0.08	0.57	0.05
11	-13.47	73.42	0.22	12.95	0.13	3.19	0.09	3.65	0.10	2.72	0.12	3.03	0.21	0.48	0.08	0.56	0.05
12	-13.20	73.90	0.23	12.88	0.13	3.25	0.09	3.47	0.09	2.69	0.12	2.83	0.19	0.43	0.07	0.55	0.05
13	-12.93	73.89	0.23	12.94	0.13	3.28	0.09	3.48	0.09	2.72	0.12	2.70	0.18	0.45	0.08	0.54	0.05
14	-12.66	73.55	0.22	12.85	0.13	3.30	0.10	3.57	0.10	2.69	0.12	3.02	0.21	0.45	0.08	0.56	0.05
15	-12.39	73.53	0.22	12.85	0.13	3.21	0.09	3.48	0.09	2.86	0.13	3.01	0.20	0.48	0.08	0.59	0.06
16	-12.12	73.30	0.22	12.77	0.12	3.24	0.09	3.53	0.10	2.84	0.12	3.20	0.22	0.50	0.09	0.62	0.06
17	-11.85	73.43	0.22	12.83	0.13	3.29	0.09	3.60	0.10	2.76	0.12	3.00	0.20	0.54	0.09	0.57	0.05
18	-11.58	73.70	0.23	12.95	0.13	3.27	0.09	3.54	0.10	2.70	0.12	2.72	0.19	0.46	0.08	0.66	0.06
19	-11.32	73.73	0.23	12.94	0.13	3.21	0.09	3.52	0.10	2.69	0.12	2.86	0.19	0.41	0.07	0.64	0.06
20	-11.05	73.75	0.23	12.86	0.13	3.23	0.09	3.52	0.10	2.73	0.12	2.84	0.19	0.45	0.08	0.62	0.06
21	-10.78	73.58	0.22	12.80	0.12	3.24	0.09	3.61	0.10	2.74	0.12	2.87	0.20	0.50	0.09	0.65	0.06
22	-10.51	73.73	0.23	12.75	0.12	3.27	0.09	3.51	0.10	2.62	0.11	3.01	0.21	0.46	0.08	0.65	0.06
23	-10.24	74.00	0.23	12.80	0.12	3.23	0.09	3.48	0.09	2.65	0.12	2.83	0.19	0.45	0.08	0.57	0.05
24	-9.97	73.92	0.23	12.81	0.12	3.25	0.09	3.46	0.09	2.74	0.12	2.78	0.19	0.46	0.08	0.58	0.05
25	-9.70	73.81	0.23	12.76	0.12	3.31	0.10	3.47	0.09	2.75	0.12	2.93	0.20	0.42	0.07	0.55	0.05
26	-9.43	73.75	0.23	12.74	0.12	3.26	0.09	3.51	0.09	2.77	0.12	2.91	0.20	0.41	0.07	0.64	0.06
27	-9.16	73.87	0.23	12.85	0.13	3.25	0.09	3.57	0.10	2.65	0.12	2.78	0.19	0.44	0.08	0.59	0.06
28	-8.89	73.76	0.23	12.81	0.13	3.31	0.10	3.53	0.10	2.80	0.12	2.78	0.19	0.43	0.08	0.58	0.05
29	-8.62	73.76	0.23	12.88	0.13	3.31	0.10	3.51	0.10	2.79	0.12	2.70	0.18	0.47	0.08	0.58	0.05
30	-8.35	73.78	0.23	12.84	0.13	3.11	0.09	3.52	0.10	2.75	0.12	3.04	0.21	0.41	0.07	0.55	0.05
31	-8.08	73.74	0.23	12.83	0.13	3.24	0.09	3.56	0.10	2.75	0.12	2.79	0.19	0.47	0.08	0.62	0.06
32	-7.81	73.57	0.22	12.84	0.13	3.23	0.09	3.56	0.10	2.93	0.13	2.78	0.19	0.47	0.08	0.61	0.06
33	-7.54	73.57	0.22	12.91	0.13	3.28	0.09	3.56	0.10	2.87	0.13	2.73	0.19	0.47	0.08	0.61	0.06
34	-7.27	73.74	0.23	12.82	0.13	3.26	0.09	3.55	0.10	2.72	0.12	2.91	0.20	0.46	0.08	0.55	0.05
35	-7.01	73.99	0.23	12.75	0.12	3.25	0.09	3.61	0.10	2.67	0.12	2.64	0.18	0.50	0.09	0.59	0.06
36	-6.74	73.70	0.23	12.90	0.13	3.38	0.10	3.50	0.09	2.74	0.12	2.73	0.19	0.44	0.08	0.62	0.06
37	-6.47	73.52	0.22	12.76	0.12	3.41	0.10	3.58	0.10	2.72	0.12	2.92	0.20	0.44	0.08	0.66	0.06
38	-6.20	73.88	0.23	12.69	0.12	3.39	0.10	3.50	0.09	2.71	0.12	2.83	0.19	0.42	0.07	0.57	0.05
39	-5.93	73.52	0.22	12.82	0.13	3.42	0.10	3.57	0.10	2.77	0.12	2.81	0.19	0.46	0.08	0.63	0.06
40	-5.66	73.52	0.22	12.86	0.13	3.49	0.10	3.54	0.10	2.79	0.12	2.74	0.19	0.47	0.08	0.59	0.06
41	-5.39	73.52	0.22	12.84	0.13	3.37	0.10	3.54	0.10	2.78	0.12	2.91	0.20	0.39	0.07	0.64	0.06
42	-5.12	73.51	0.22	12.79	0.12	3.43	0.10	3.55	0.10	2.72	0.12	2.95	0.20	0.41	0.07	0.65	0.06
43	-4.85	73.57	0.22	12.93	0.13	3.32	0.10	3.53	0.10	2.65	0.12	2.86	0.19	0.55	0.10	0.59	0.06
44	-4.58	73.62	0.23	12.84	0.13	3.43	0.10	3.65	0.10	2.56	0.11	2.82	0.19	0.48	0.08	0.60	0.06
45	-4.31	73.64	0.23	12.78	0.12	3.47	0.10	3.59	0.10	2.58	0.11	2.79	0.19	0.51	0.09	0.64	0.06
46	-4.04	74.03	0.23	12.83	0.13	3.31	0.10	3.50	0.09	2.46	0.11	2.68	0.18	0.56	0.10	0.63	0.06
47	-3.77	74.15	0.23	12.91	0.13	3.29	0.10	3.61	0.10	2.46	0.11	2.54	0.17	0.51	0.09	0.53	0.05
48	-3.50	73.92	0.23	12.87	0.13	3.26	0.09	3.57	0.10	2.59	0.11	2.72	0.19	0.52	0.09	0.55	0.05
49	-3.23	73.83	0.23	12.89	0.13	3.39	0.10	3.64	0.10	2.52	0.11	2.68	0.18	0.44	0.08	0.61	0.06
50	-2.96	73.98	0.23	12.85	0.13	3.24	0.09	3.67	0.10	2.48	0.11	2.67	0.18	0.45	0.08	0.66	0.06
51	-2.69	74.27	0.23	12.83	0.13	3.27	0.09	3.74	0.10	2.32	0.10	2.44	0.17	0.56	0.10	0.57	0.05

52	-2.43	74.46	0.23	12.84	0.13	3.12	0.09	3.61	0.10	2.18	0.10	2.69	0.18	0.51	0.09	0.59	0.05
53	-2.16	74.43	0.23	12.62	0.12	3.14	0.09	3.73	0.10	2.22	0.10	2.77	0.19	0.53	0.09	0.57	0.05
54	-1.89	74.92	0.23	12.38	0.12	3.01	0.09	3.65	0.10	2.22	0.10	2.90	0.20	0.40	0.07	0.53	0.05
55	-1.62	75.62	0.23	11.82	0.12	2.83	0.08	3.66	0.10	2.14	0.09	2.91	0.20	0.49	0.09	0.55	0.05
56	-1.35	77.34	0.24	10.69	0.10	2.74	0.08	3.62	0.10	1.84	0.08	2.84	0.19	0.44	0.08	0.49	0.05
57	-1.08	78.58	0.24	10.16	0.10	2.64	0.08	3.62	0.10	1.59	0.07	2.57	0.18	0.36	0.06	0.47	0.04
58	-0.81	79.15	0.24	9.90	0.10	2.71	0.08	3.41	0.09	1.47	0.06	2.54	0.17	0.38	0.07	0.44	0.04
59	-0.54	79.15	0.24	9.57	0.09	2.79	0.08	3.57	0.10	1.56	0.07	2.53	0.17	0.35	0.06	0.47	0.04
60	-0.27	79.14	0.24	9.62	0.09	2.93	0.08	3.51	0.10	1.46	0.06	2.52	0.17	0.36	0.06	0.46	0.04
61	0.00	79.22	0.24	9.69	0.09	2.93	0.08	3.59	0.10	1.32	0.06	2.36	0.16	0.41	0.07	0.47	0.04
62	0.27	78.84	0.24	9.60	0.09	3.02	0.09	3.75	0.10	1.43	0.06	2.47	0.17	0.39	0.07	0.49	0.05
63	0.54	78.96	0.24	9.65	0.09	2.99	0.09	3.81	0.10	1.53	0.07	2.19	0.15	0.41	0.07	0.46	0.04
64	0.81	78.51	0.24	9.75	0.10	3.02	0.09	3.85	0.10	1.47	0.06	2.49	0.17	0.45	0.08	0.46	0.04
65	1.08	78.45	0.24	9.83	0.10	3.00	0.09	3.75	0.10	1.41	0.06	2.60	0.18	0.41	0.07	0.54	0.05
66	1.35	78.08	0.24	10.06	0.10	3.07	0.09	3.76	0.10	1.35	0.06	2.66	0.18	0.45	0.08	0.58	0.05
67	1.62	78.16	0.24	9.96	0.10	3.08	0.09	3.72	0.10	1.53	0.07	2.55	0.17	0.46	0.08	0.54	0.05
68	1.89	77.82	0.24	10.29	0.10	3.09	0.09	3.81	0.10	1.56	0.07	2.49	0.17	0.41	0.07	0.53	0.05
69	2.15	77.57	0.24	10.23	0.10	3.28	0.09	3.73	0.10	1.55	0.07	2.64	0.18	0.41	0.07	0.60	0.06
70	2.42	77.43	0.24	10.41	0.10	3.31	0.10	3.77	0.10	1.53	0.07	2.60	0.18	0.40	0.07	0.55	0.05
71	2.69	76.97	0.24	10.43	0.10	3.28	0.09	3.86	0.10	1.60	0.07	2.91	0.20	0.40	0.07	0.55	0.05
72	2.96	77.03	0.24	10.58	0.10	3.24	0.09	3.88	0.11	1.62	0.07	2.66	0.18	0.50	0.09	0.49	0.05
73	3.23	77.00	0.24	10.61	0.10	3.26	0.09	3.98	0.11	1.64	0.07	2.52	0.17	0.49	0.09	0.50	0.05
74	3.50	76.75	0.23	10.62	0.10	3.27	0.09	3.94	0.11	1.69	0.07	2.74	0.19	0.47	0.08	0.53	0.05
75	3.77	76.75	0.23	10.72	0.10	3.38	0.10	3.87	0.10	1.60	0.07	2.72	0.19	0.43	0.08	0.53	0.05
76	4.04	76.71	0.23	10.83	0.11	3.34	0.10	3.90	0.11	1.69	0.07	2.62	0.18	0.37	0.06	0.55	0.05
77	4.31	76.28	0.23	10.89	0.11	3.49	0.10	3.88	0.10	1.66	0.07	2.80	0.19	0.45	0.08	0.54	0.05
78	4.58	76.08	0.23	10.83	0.11	3.54	0.10	3.94	0.11	1.61	0.07	2.90	0.20	0.53	0.09	0.57	0.05
79	4.85	75.95	0.23	10.97	0.11	3.58	0.10	3.86	0.10	1.74	0.08	2.91	0.20	0.44	0.08	0.55	0.05
80	5.12	76.15	0.23	11.03	0.11	3.49	0.10	3.88	0.11	1.83	0.08	2.65	0.18	0.43	0.07	0.54	0.05
81	5.39	75.63	0.23	11.06	0.11	3.59	0.10	4.08	0.11	1.88	0.08	2.77	0.19	0.45	0.08	0.53	0.05
82	5.66	75.69	0.23	11.19	0.11	3.56	0.10	4.00	0.11	1.78	0.08	2.88	0.20	0.38	0.07	0.52	0.05
83	5.93	75.60	0.23	11.27	0.11	3.57	0.10	4.04	0.11	1.82	0.08	2.82	0.19	0.37	0.07	0.51	0.05
84	6.20	75.40	0.23	11.38	0.11	3.66	0.11	3.89	0.11	1.87	0.08	2.77	0.19	0.44	0.08	0.58	0.05
85	6.46	75.49	0.23	11.37	0.11	3.69	0.11	3.91	0.11	1.86	0.08	2.66	0.18	0.45	0.08	0.56	0.05
86	6.73	75.22	0.23	11.34	0.11	3.66	0.11	3.96	0.11	1.92	0.08	2.89	0.20	0.42	0.07	0.59	0.05
87	7.00	75.30	0.23	11.40	0.11	3.63	0.10	4.04	0.11	1.87	0.08	2.75	0.19	0.46	0.08	0.56	0.05
88	7.27	75.32	0.23	11.56	0.11	3.53	0.10	4.07	0.11	1.88	0.08	2.64	0.18	0.42	0.07	0.58	0.05
89	7.54	75.00	0.23	11.53	0.11	3.64	0.11	3.96	0.11	1.88	0.08	2.88	0.20	0.49	0.09	0.61	0.06
90	7.81	75.14	0.23	11.54	0.11	3.66	0.11	3.94	0.11	1.85	0.08	2.77	0.19	0.52	0.09	0.59	0.05
91	8.08	74.92	0.23	11.70	0.11	3.64	0.11	4.01	0.11	2.01	0.09	2.72	0.19	0.39	0.07	0.61	0.06
92	8.35	74.89	0.23	11.68	0.11	3.60	0.10	4.02	0.11	2.06	0.09	2.82	0.19	0.40	0.07	0.53	0.05
93	8.62	74.91	0.23	11.61	0.11	3.60	0.10	4.06	0.11	1.98	0.09	2.73	0.19	0.52	0.09	0.60	0.06
94	8.89	74.94	0.23	11.65	0.11	3.62	0.10	4.00	0.11	1.93	0.08	2.83	0.19	0.49	0.09	0.54	0.05
95	9.16	74.50	0.23	11.70	0.11	3.60	0.10	4.07	0.11	2.05	0.09	3.01	0.21	0.48	0.08	0.59	0.06
96	9.43	74.47	0.23	11.66	0.11	3.68	0.11	4.10	0.11	2.03	0.09	3.01	0.20	0.49	0.09	0.57	0.05
97	9.70	74.55	0.23	11.72	0.11	3.64	0.11	4.02	0.11	2.00	0.09	3.02	0.21	0.49	0.09	0.55	0.05
98	9.97	74.62	0.23	11.79	0.12	3.68	0.11	4.08	0.11	2.02	0.09	2.85	0.19	0.40	0.07	0.56	0.05
99	10.24	74.68	0.23	11.79	0.12	3.79	0.11	3.99	0.11	2.04	0.09	2.72	0.19	0.45	0.08	0.55	0.05
100	10.51	74.34	0.23	11.92	0.12	3.77	0.11	4.06	0.11	1.99	0.09	2.94	0.20	0.40	0.07	0.59	0.05
101	10.78	74.37	0.23	11.82	0.12	3.78	0.11	4.10	0.11	2.00	0.09	2.92	0.20	0.43	0.08	0.58	0.05
102	11.04	74.59	0.23	11.79	0.12	3.79	0.11	4.01	0.11	1.96	0.09	2.76	0.19	0.50	0.09	0.61	0.06
103	11.31	74.48	0.23	11.91	0.12	3.64	0.11	4.01	0.11	2.00	0.09	2.96	0.20	0.42	0.07	0.59	0.06
104	11.58	74.54	0.23	11.96	0.12	3.71	0.11	4.00	0.11	1.95	0.09	2.87	0.20	0.38	0.07	0.59	0.05
105	11.85	74.59	0.23	11.92	0.12	3.69	0.11	4.08	0.11	1.97	0.09	2.81	0.19	0.36	0.06	0.58	0.05
106	12.12	74.17	0.23	11.97	0.12	3.74	0.11	4.08	0.11	2.08	0.09	2.91	0.20	0.47	0.08	0.58	0.05
107	12.39	74.20	0.23	11.95	0.12	3.87	0.11	4.05	0.11	2.01	0.09	2.88	0.20	0.46	0.08	0.57	0.05
108	12.66	74.27	0.23	12.05	0.12	3.74	0.11	4.13	0.11	2.02	0.09	2.74	0.19	0.46	0.08	0.59	0.05
109	12.93	74.09	0.23	12.24	0.12	3.93	0.11	3.96	0.11	1.95	0.09	2.74	0.19	0.52	0.09	0.58	0.05
110	13.20	74.21	0.23	12.09	0.12	3.86	0.11	4.01	0.11	2.02	0.09	2.78	0.19	0.45	0.08	0.58	0.05
111	13.47	73.91	0.23	12.07	0.12	3.84	0.11	4.07	0.11	2.10	0.09	2.92	0.20	0.52	0.09	0.57	0.05
112	13.74	74.02	0.23	12.19	0.12	3.77	0.11	4.11	0.11	1.97	0.09	2.95	0.20	0.43	0.08	0.58	0.05
113	14.01	73.93	0.23	12.15	0.12	3.68	0.11	4.13	0.11	2.07	0.09	2.95	0.20	0.49	0.09	0.60	0.06

114	14.28	73.87	0.23	12.03	0.12	3.80	0.11	4.19	0.11	2.05	0.09	2.91	0.20	0.53	0.09	0.62	0.06
115	14.55	73.84	0.23	12.22	0.12	3.86	0.11	4.14	0.11	2.02	0.09	2.81	0.19	0.51	0.09	0.60	0.06
116	14.82	73.81	0.23	12.14	0.12	3.72	0.11	4.19	0.11	2.16	0.09	2.95	0.20	0.43	0.08	0.60	0.06
117	15.09	73.93	0.23	12.21	0.12	3.77	0.11	4.05	0.11	2.14	0.09	2.88	0.20	0.43	0.08	0.59	0.06
118	15.35	73.97	0.23	12.14	0.12	3.73	0.11	4.08	0.11	2.01	0.09	3.01	0.21	0.46	0.08	0.59	0.06
119	15.62	74.01	0.23	12.20	0.12	3.83	0.11	4.07	0.11	1.99	0.09	2.94	0.20	0.38	0.07	0.58	0.05
120	15.89	74.06	0.23	12.19	0.12	3.83	0.11	4.03	0.11	1.97	0.09	2.86	0.19	0.45	0.08	0.60	0.06
121	16.16	74.07	0.23	12.24	0.12	3.89	0.11	4.11	0.11	2.00	0.09	2.59	0.18	0.50	0.09	0.61	0.06
122	16.43	73.80	0.23	12.22	0.12	3.88	0.11	4.12	0.11	1.98	0.09	3.00	0.20	0.51	0.09	0.50	0.05
123	16.70	73.65	0.23	12.31	0.12	3.85	0.11	4.14	0.11	2.11	0.09	2.86	0.19	0.49	0.09	0.58	0.05
124	16.97	73.69	0.23	12.23	0.12	3.88	0.11	4.09	0.11	2.09	0.09	2.84	0.19	0.55	0.10	0.64	0.06
125	17.24	73.76	0.23	12.24	0.12	3.86	0.11	4.16	0.11	2.17	0.10	2.81	0.19	0.41	0.07	0.60	0.06
126	17.51	73.69	0.23	12.04	0.12	3.86	0.11	4.21	0.11	2.07	0.09	3.07	0.21	0.50	0.09	0.56	0.05
127	17.78	73.59	0.22	12.18	0.12	3.85	0.11	4.24	0.11	2.18	0.10	2.89	0.20	0.48	0.08	0.58	0.05
128	18.05	73.65	0.23	12.31	0.12	3.86	0.11	4.14	0.11	2.07	0.09	2.82	0.19	0.56	0.10	0.58	0.05
129	18.32	73.76	0.23	12.26	0.12	3.91	0.11	4.14	0.11	2.14	0.09	2.70	0.18	0.49	0.09	0.61	0.06
130	18.59	73.86	0.23	12.22	0.12	3.89	0.11	4.10	0.11	2.16	0.09	2.80	0.19	0.40	0.07	0.58	0.05
131	18.86	73.80	0.23	12.43	0.12	3.81	0.11	4.17	0.11	2.13	0.09	2.60	0.18	0.45	0.08	0.62	0.06
132	19.13	73.77	0.23	12.40	0.12	3.85	0.11	4.07	0.11	2.13	0.09	2.68	0.18	0.48	0.08	0.62	0.06
133	19.40	73.68	0.23	12.20	0.12	3.95	0.11	4.14	0.11	2.17	0.10	2.78	0.19	0.46	0.08	0.61	0.06
134	19.67	73.46	0.22	12.28	0.12	4.00	0.12	4.15	0.11	2.19	0.10	2.81	0.19	0.52	0.09	0.58	0.05
135	19.93	73.59	0.22	12.38	0.12	3.86	0.11	4.16	0.11	2.06	0.09	2.76	0.19	0.54	0.10	0.64	0.06
136	20.20	73.98	0.23	12.27	0.12	3.86	0.11	4.09	0.11	2.05	0.09	2.67	0.18	0.52	0.09	0.56	0.05
137	20.47	73.64	0.23	12.24	0.12	3.84	0.11	4.16	0.11	2.22	0.10	2.84	0.19	0.49	0.09	0.57	0.05
138	20.74	73.52	0.22	12.21	0.12	3.93	0.11	4.18	0.11	2.24	0.10	2.80	0.19	0.54	0.09	0.59	0.06

J.2 Surface Agglomerates

Agglomerate FLD4.3.UA

Table J.11: Major element compositions (as wt.% oxides) from a line traverse across the interface of surface agglomerate FLD4.3.UA (from agglomerate FLD4.3.UA to host FLD4.3) extracted from quantified EDS compositional maps. The EDS compositional maps were collected at a resolution of 3.5 pixels/μm. The smoothing width for this traverse was 50 pixels (14.4 μm) wide. This is a Si interface and has been centered at $x = 0$ based on the SiO_2 maximum. Peak points within 2σ of the SiO_2 maximum are highlighted in yellow. Uncertainties are 2SEOM.

Pt.	Position (μm)	SiO_2	2σ	Al_2O_3	2σ	Na_2O	2σ	K_2O	2σ	CaO	2σ	FeO	2σ	TiO_2	2σ	MgO	2σ
1	-8.33	75.14	0.24	14.13	0.21	1.32	0.09	4.12	0.10	1.35	0.09	2.89	0.21	0.35	0.06	0.69	0.07
2	-8.04	75.16	0.24	13.75	0.20	1.30	0.09	4.16	0.10	1.36	0.09	3.22	0.23	0.53	0.09	0.52	0.05
3	-7.75	75.61	0.24	13.71	0.20	1.23	0.09	4.08	0.10	1.33	0.08	2.89	0.21	0.54	0.09	0.61	0.06
4	-7.46	75.27	0.24	13.97	0.21	1.31	0.09	4.16	0.10	1.38	0.09	2.81	0.20	0.46	0.07	0.64	0.07
5	-7.18	75.39	0.24	13.98	0.21	1.24	0.09	4.11	0.10	1.34	0.09	2.97	0.21	0.41	0.07	0.57	0.06
6	-6.89	74.99	0.24	13.96	0.21	1.34	0.09	4.16	0.10	1.39	0.09	3.08	0.22	0.47	0.07	0.62	0.06
7	-6.60	75.24	0.24	14.04	0.21	1.24	0.09	4.12	0.10	1.35	0.09	2.89	0.21	0.45	0.07	0.67	0.07
8	-6.32	75.21	0.24	13.91	0.21	1.24	0.09	4.09	0.10	1.50	0.10	2.92	0.21	0.48	0.08	0.65	0.07
9	-6.03	75.42	0.24	13.91	0.21	1.24	0.09	4.13	0.10	1.26	0.08	2.98	0.22	0.36	0.06	0.69	0.07
10	-5.74	74.93	0.24	14.01	0.21	1.33	0.09	4.12	0.10	1.37	0.09	3.24	0.23	0.40	0.06	0.60	0.06
11	-5.45	74.87	0.24	14.30	0.21	1.44	0.10	4.07	0.10	1.28	0.08	3.01	0.22	0.36	0.06	0.66	0.07
12	-5.17	75.03	0.24	14.08	0.21	1.31	0.09	4.07	0.10	1.32	0.08	3.12	0.23	0.52	0.08	0.54	0.06
13	-4.88	75.08	0.24	13.84	0.20	1.26	0.09	4.27	0.10	1.43	0.09	3.13	0.23	0.40	0.06	0.58	0.06
14	-4.59	74.78	0.24	14.06	0.21	1.30	0.09	4.14	0.10	1.33	0.08	3.27	0.24	0.46	0.07	0.64	0.07
15	-4.31	75.00	0.24	13.90	0.21	1.34	0.09	4.04	0.10	1.35	0.09	3.15	0.23	0.52	0.08	0.69	0.07
16	-4.02	75.55	0.24	13.74	0.20	1.26	0.09	4.08	0.10	1.33	0.08	2.96	0.21	0.49	0.08	0.59	0.06
17	-3.73	75.45	0.24	13.85	0.20	1.27	0.09	4.05	0.10	1.22	0.08	3.14	0.23	0.36	0.06	0.67	0.07
18	-3.45	75.44	0.24	13.44	0.20	1.32	0.09	4.14	0.10	1.36	0.09	3.28	0.24	0.44	0.07	0.58	0.06
19	-3.16	75.90	0.24	13.23	0.20	1.24	0.09	4.04	0.10	1.26	0.08	3.29	0.24	0.41	0.07	0.63	0.07
20	-2.87	75.83	0.24	13.06	0.19	1.18	0.08	4.30	0.10	1.36	0.09	3.21	0.23	0.44	0.07	0.60	0.06
21	-2.58	75.93	0.24	13.11	0.19	1.34	0.09	4.26	0.10	1.28	0.08	3.12	0.23	0.44	0.07	0.53	0.06
22	-2.30	76.49	0.24	12.87	0.19	1.24	0.09	4.20	0.10	1.22	0.08	3.07	0.22	0.42	0.07	0.49	0.05
23	-2.01	76.45	0.24	12.81	0.19	1.22	0.09	4.05	0.10	1.29	0.08	3.17	0.23	0.43	0.07	0.57	0.06
24	-1.72	77.13	0.24	12.13	0.18	1.11	0.08	4.05	0.10	1.27	0.08	3.36	0.24	0.42	0.07	0.54	0.06
25	-1.44	78.06	0.25	11.60	0.17	1.08	0.08	3.85	0.09	1.03	0.07	3.38	0.25	0.45	0.07	0.55	0.06
26	-1.15	79.26	0.25	10.65	0.16	1.07	0.08	3.74	0.09	0.91	0.06	3.35	0.24	0.51	0.08	0.51	0.05
27	-0.86	81.49	0.26	9.08	0.13	0.91	0.06	3.70	0.09	0.68	0.04	3.22	0.23	0.51	0.08	0.41	0.04
28	-0.57	84.12	0.26	7.74	0.11	0.85	0.06	3.36	0.08	0.43	0.03	2.71	0.20	0.44	0.07	0.35	0.04
29	-0.29	85.92	0.27	6.52	0.10	0.71	0.05	3.16	0.07	0.29	0.02	2.65	0.19	0.44	0.07	0.31	0.03
30	0.00	86.30	0.27	6.15	0.09	0.58	0.04	3.21	0.08	0.30	0.02	2.80	0.20	0.40	0.06	0.27	0.03
31	0.29	86.07	0.27	6.32	0.09	0.65	0.05	3.11	0.07	0.28	0.02	2.90	0.21	0.40	0.06	0.27	0.03
32	0.57	86.18	0.27	6.41	0.09	0.68	0.05	3.15	0.07	0.25	0.02	2.71	0.20	0.36	0.06	0.26	0.03
33	0.86	86.00	0.27	6.45	0.10	0.69	0.05	3.21	0.08	0.28	0.02	2.78	0.20	0.34	0.05	0.25	0.03
34	1.15	85.99	0.27	6.54	0.10	0.66	0.05	3.19	0.08	0.24	0.02	2.80	0.20	0.33	0.05	0.24	0.03
35	1.44	85.53	0.27	6.66	0.10	0.70	0.05	3.45	0.08	0.28	0.02	2.86	0.21	0.27	0.04	0.25	0.03
36	1.72	84.89	0.27	6.83	0.10	0.71	0.05	3.38	0.08	0.28	0.02	3.21	0.23	0.40	0.06	0.30	0.03
37	2.01	84.42	0.27	7.00	0.10	0.66	0.05	3.67	0.09	0.31	0.02	3.35	0.24	0.34	0.05	0.25	0.03
38	2.30	84.06	0.26	7.33	0.11	0.72	0.05	3.64	0.09	0.25	0.02	3.30	0.24	0.42	0.07	0.27	0.03
39	2.58	83.94	0.26	7.43	0.11	0.70	0.05	3.80	0.09	0.27	0.02	3.28	0.24	0.33	0.05	0.25	0.03
40	2.87	83.48	0.26	7.66	0.11	0.68	0.05	3.79	0.09	0.37	0.02	3.34	0.24	0.41	0.06	0.26	0.03
41	3.16	83.18	0.26	7.77	0.12	0.72	0.05	3.88	0.09	0.34	0.02	3.39	0.25	0.44	0.07	0.29	0.03
42	3.44	83.01	0.26	8.00	0.12	0.79	0.06	3.89	0.09	0.31	0.02	3.29	0.24	0.43	0.07	0.28	0.03
43	3.73	82.66	0.26	8.18	0.12	0.81	0.06	3.86	0.09	0.34	0.02	3.39	0.25	0.47	0.07	0.29	0.03
44	4.02	82.16	0.26	8.42	0.12	0.88	0.06	4.03	0.10	0.36	0.02	3.45	0.25	0.42	0.07	0.28	0.03
45	4.31	82.04	0.26	8.83	0.13	0.91	0.06	3.95	0.09	0.39	0.02	3.23	0.23	0.35	0.06	0.30	0.03
46	4.59	81.73	0.26	8.93	0.13	1.01	0.07	3.98	0.09	0.38	0.02	3.27	0.24	0.42	0.07	0.29	0.03
47	4.88	81.34	0.26	9.18	0.14	0.98	0.07	3.95	0.09	0.44	0.03	3.44	0.25	0.41	0.07	0.27	0.03

48	5.17	81.21	0.26	9.40	0.14	1.01	0.07	4.09	0.10	0.36	0.02	3.19	0.23	0.40	0.06	0.34	0.04
49	5.45	80.93	0.25	9.53	0.14	0.99	0.07	4.25	0.10	0.46	0.03	3.10	0.22	0.40	0.06	0.35	0.04
50	5.74	80.15	0.25	9.80	0.15	1.06	0.07	4.39	0.10	0.46	0.03	3.53	0.26	0.32	0.05	0.29	0.03
51	6.03	79.79	0.25	10.05	0.15	1.13	0.08	4.17	0.10	0.46	0.03	3.61	0.26	0.47	0.08	0.30	0.03
52	6.32	79.71	0.25	10.23	0.15	1.08	0.08	4.29	0.10	0.45	0.03	3.53	0.26	0.37	0.06	0.34	0.04
53	6.60	79.54	0.25	10.09	0.15	1.02	0.07	4.34	0.10	0.60	0.04	3.55	0.26	0.48	0.08	0.38	0.04
54	6.89	79.40	0.25	10.22	0.15	1.04	0.07	4.53	0.11	0.55	0.04	3.51	0.25	0.46	0.07	0.28	0.03
55	7.18	79.26	0.25	10.45	0.15	1.13	0.08	4.47	0.11	0.51	0.03	3.51	0.25	0.40	0.06	0.26	0.03
56	7.46	79.27	0.25	10.65	0.16	1.10	0.08	4.35	0.10	0.49	0.03	3.47	0.25	0.36	0.06	0.31	0.03
57	7.75	78.74	0.25	10.84	0.16	1.09	0.08	4.44	0.10	0.51	0.03	3.55	0.26	0.47	0.08	0.35	0.04
58	8.04	78.71	0.25	10.98	0.16	1.19	0.08	4.33	0.10	0.56	0.04	3.43	0.25	0.43	0.07	0.38	0.04
59	8.33	78.69	0.25	11.01	0.16	1.26	0.09	4.43	0.10	0.58	0.04	3.18	0.23	0.48	0.08	0.35	0.04
60	8.61	78.72	0.25	11.06	0.16	1.19	0.08	4.50	0.11	0.55	0.04	3.25	0.24	0.39	0.06	0.33	0.03
61	8.90	78.65	0.25	11.08	0.16	1.23	0.09	4.45	0.11	0.59	0.04	3.38	0.24	0.30	0.05	0.33	0.03
62	9.19	78.42	0.25	11.20	0.17	1.18	0.08	4.47	0.11	0.60	0.04	3.37	0.24	0.37	0.06	0.37	0.04
63	9.47	77.99	0.25	11.14	0.16	1.19	0.08	4.63	0.11	0.59	0.04	3.67	0.27	0.44	0.07	0.34	0.04
64	9.76	77.99	0.25	11.27	0.17	1.22	0.09	4.40	0.10	0.65	0.04	3.59	0.26	0.47	0.08	0.40	0.04
65	10.05	77.89	0.24	11.62	0.17	1.20	0.08	4.45	0.11	0.66	0.04	3.32	0.24	0.38	0.06	0.48	0.05
66	10.33	78.00	0.25	11.46	0.17	1.16	0.08	4.44	0.10	0.76	0.05	3.34	0.24	0.43	0.07	0.42	0.04
67	10.62	77.80	0.24	11.41	0.17	1.20	0.08	4.59	0.11	0.70	0.04	3.55	0.26	0.42	0.07	0.33	0.03
68	10.91	77.58	0.24	11.52	0.17	1.21	0.09	4.57	0.11	0.71	0.05	3.73	0.27	0.37	0.06	0.30	0.03
69	11.20	77.49	0.24	11.75	0.17	1.19	0.08	4.61	0.11	0.60	0.04	3.51	0.25	0.53	0.08	0.32	0.03
70	11.48	77.67	0.24	11.75	0.17	1.27	0.09	4.58	0.11	0.71	0.05	3.13	0.23	0.56	0.09	0.33	0.03

Agglomerate FLD14.1

Table J.12: Major element compositions (as wt.% oxides) from a line traverse across the interface of surface agglomerate FLD14.1 (from agglomerate FLD14.1 to host FLD14) extracted from quantified EDS compositional maps. The EDS compositional maps were collected at a resolution of 5.8 pixels/μm. The smoothing width for this traverse was 250 pixels (42.6 μm) wide. This is a Si interface and has been centered at $x = 0$ based on the SiO_2 maximum. Peak points within 2σ of the SiO_2 maximum are highlighted in yellow. Uncertainties are 2SEOM.

Pt.	Position (μm)	SiO_2	2σ	Al_2O_3	2σ	Na_2O	2σ	K_2O	2σ	CaO	2σ	FeO	2σ	TiO_2	2σ	MgO	2σ
1	-28.12	75.50	0.16	11.57	0.09	2.00	0.05	4.62	0.07	2.82	0.09	2.64	0.10	0.42	0.04	0.43	0.03
2	-27.95	75.61	0.16	11.60	0.09	2.02	0.05	4.58	0.07	2.76	0.09	2.54	0.10	0.42	0.04	0.46	0.03
3	-27.78	75.58	0.16	11.52	0.09	2.06	0.05	4.57	0.07	2.77	0.09	2.62	0.10	0.42	0.04	0.46	0.03
4	-27.61	75.49	0.16	11.55	0.09	2.10	0.05	4.53	0.07	2.71	0.09	2.71	0.11	0.41	0.04	0.49	0.03
5	-27.44	75.41	0.16	11.60	0.09	2.07	0.05	4.61	0.07	2.79	0.09	2.68	0.11	0.37	0.04	0.47	0.03
6	-27.27	75.41	0.16	11.61	0.09	2.13	0.05	4.55	0.07	2.77	0.09	2.63	0.10	0.42	0.04	0.47	0.03
7	-27.10	75.25	0.15	11.67	0.09	2.08	0.05	4.58	0.07	2.76	0.09	2.73	0.11	0.45	0.04	0.47	0.03
8	-26.93	75.42	0.16	11.62	0.09	2.08	0.05	4.59	0.07	2.82	0.09	2.59	0.10	0.41	0.04	0.47	0.03
9	-26.76	75.52	0.16	11.61	0.09	2.01	0.05	4.62	0.07	2.73	0.09	2.61	0.10	0.44	0.04	0.47	0.03
10	-26.59	75.65	0.16	11.48	0.09	2.01	0.05	4.63	0.07	2.75	0.09	2.57	0.10	0.46	0.04	0.44	0.03
11	-26.42	75.53	0.16	11.53	0.09	2.03	0.05	4.63	0.07	2.77	0.09	2.63	0.10	0.44	0.04	0.45	0.03
12	-26.25	75.57	0.16	11.51	0.09	1.99	0.05	4.64	0.07	2.75	0.09	2.65	0.10	0.44	0.04	0.45	0.03
13	-26.08	75.67	0.16	11.55	0.09	1.99	0.05	4.59	0.07	2.69	0.09	2.57	0.10	0.47	0.04	0.46	0.03
14	-25.91	75.51	0.16	11.56	0.09	2.04	0.05	4.52	0.07	2.75	0.09	2.69	0.11	0.44	0.04	0.49	0.03
15	-25.74	75.58	0.16	11.49	0.09	1.99	0.05	4.63	0.07	2.75	0.09	2.62	0.10	0.46	0.04	0.48	0.03
16	-25.57	75.69	0.16	11.54	0.09	2.02	0.05	4.55	0.07	2.72	0.09	2.57	0.10	0.44	0.04	0.47	0.03
17	-25.40	75.54	0.16	11.59	0.09	2.01	0.05	4.61	0.07	2.70	0.09	2.59	0.10	0.46	0.04	0.49	0.03
18	-25.23	75.45	0.16	11.62	0.09	2.00	0.05	4.60	0.07	2.80	0.09	2.56	0.10	0.48	0.05	0.48	0.03
19	-25.05	75.67	0.16	11.65	0.09	2.02	0.05	4.48	0.07	2.76	0.09	2.50	0.10	0.46	0.04	0.45	0.03
20	-24.89	75.59	0.16	11.53	0.09	2.02	0.05	4.63	0.07	2.79	0.09	2.60	0.10	0.40	0.04	0.45	0.03
21	-24.71	75.49	0.16	11.59	0.09	2.02	0.05	4.53	0.07	2.82	0.09	2.65	0.10	0.44	0.04	0.45	0.03
22	-24.54	75.48	0.16	11.59	0.09	1.96	0.04	4.54	0.07	2.89	0.09	2.66	0.10	0.45	0.04	0.43	0.03
23	-24.37	75.58	0.16	11.49	0.09	1.95	0.04	4.59	0.07	2.87	0.09	2.65	0.10	0.42	0.04	0.45	0.03
24	-24.20	75.50	0.16	11.61	0.09	1.98	0.05	4.59	0.07	2.86	0.09	2.60	0.10	0.36	0.03	0.49	0.03
25	-24.03	75.82	0.16	11.64	0.09	1.99	0.05	4.53	0.07	2.72	0.09	2.39	0.09	0.42	0.04	0.48	0.03
26	-23.86	75.62	0.16	11.61	0.09	1.90	0.04	4.61	0.07	2.88	0.09	2.55	0.10	0.41	0.04	0.42	0.03
27	-23.69	75.62	0.16	11.53	0.09	1.99	0.05	4.61	0.07	2.78	0.09	2.64	0.10	0.39	0.04	0.44	0.03
28	-23.52	75.56	0.16	11.54	0.09	2.02	0.05	4.61	0.07	2.82	0.09	2.59	0.10	0.43	0.04	0.43	0.03
29	-23.35	75.74	0.16	11.59	0.09	1.99	0.05	4.52	0.07	2.83	0.09	2.45	0.10	0.42	0.04	0.46	0.03
30	-23.18	75.60	0.16	11.57	0.09	1.95	0.04	4.53	0.07	2.89	0.09	2.56	0.10	0.45	0.04	0.46	0.03
31	-23.01	75.61	0.16	11.48	0.09	1.90	0.04	4.60	0.07	2.87	0.09	2.66	0.10	0.44	0.04	0.44	0.03
32	-22.84	75.49	0.16	11.56	0.09	1.94	0.04	4.62	0.07	2.89	0.09	2.59	0.10	0.43	0.04	0.47	0.03
33	-22.67	75.58	0.16	11.52	0.09	1.98	0.05	4.53	0.07	2.82	0.09	2.63	0.10	0.44	0.04	0.49	0.03
34	-22.50	75.70	0.16	11.38	0.09	2.00	0.05	4.56	0.07	2.92	0.09	2.57	0.10	0.41	0.04	0.45	0.03
35	-22.33	75.52	0.16	11.49	0.09	1.98	0.05	4.59	0.07	2.93	0.09	2.61	0.10	0.43	0.04	0.45	0.03
36	-22.16	75.49	0.16	11.61	0.09	1.96	0.04	4.55	0.07	2.88	0.09	2.60	0.10	0.41	0.04	0.50	0.03
37	-21.99	75.56	0.16	11.47	0.09	1.90	0.04	4.58	0.07	2.95	0.09	2.70	0.11	0.39	0.04	0.44	0.03
38	-21.82	75.50	0.16	11.43	0.09	1.91	0.04	4.61	0.07	2.97	0.09	2.71	0.11	0.42	0.04	0.45	0.03
39	-21.65	75.46	0.16	11.50	0.09	1.92	0.04	4.58	0.07	2.96	0.09	2.68	0.11	0.44	0.04	0.45	0.03
40	-21.48	75.61	0.16	11.58	0.09	1.96	0.04	4.50	0.07	2.83	0.09	2.58	0.10	0.46	0.04	0.47	0.03
41	-21.30	75.71	0.16	11.50	0.09	2.00	0.05	4.48	0.07	2.89	0.09	2.53	0.10	0.43	0.04	0.47	0.03
42	-21.14	75.68	0.16	11.47	0.09	1.99	0.05	4.47	0.07	2.84	0.09	2.68	0.11	0.44	0.04	0.42	0.03
43	-20.96	75.69	0.16	11.42	0.09	1.99	0.05	4.49	0.07	2.85	0.09	2.67	0.10	0.41	0.04	0.48	0.03
44	-20.79	75.48	0.16	11.45	0.09	1.99	0.05	4.56	0.07	2.93	0.09	2.66	0.10	0.42	0.04	0.51	0.04
45	-20.62	75.59	0.16	11.50	0.09	1.96	0.04	4.48	0.07	2.98	0.09	2.60	0.10	0.45	0.04	0.43	0.03
46	-20.45	75.49	0.16	11.43	0.09	2.01	0.05	4.57	0.07	2.98	0.09	2.65	0.10	0.45	0.04	0.42	0.03
47	-20.28	75.39	0.16	11.45	0.09	1.99	0.05	4.58	0.07	2.93	0.09	2.75	0.11	0.47	0.04	0.44	0.03
48	-20.11	75.58	0.16	11.50	0.09	1.96	0.04	4.52	0.07	2.97	0.09	2.62	0.10	0.42	0.04	0.43	0.03
49	-19.94	75.62	0.16	11.49	0.09	1.97	0.04	4.51	0.07	2.97	0.09	2.60	0.10	0.38	0.04	0.46	0.03
50	-19.77	75.58	0.16	11.48	0.09	1.97	0.04	4.60	0.07	2.96	0.09	2.54	0.10	0.43	0.04	0.44	0.03

51	-19.60	75.58	0.16	11.44	0.09	1.98	0.05	4.54	0.07	2.95	0.09	2.65	0.10	0.43	0.04	0.44	0.03
52	-19.43	75.57	0.16	11.40	0.09	1.93	0.04	4.47	0.07	3.03	0.10	2.69	0.11	0.42	0.04	0.49	0.03
53	-19.26	75.58	0.16	11.39	0.09	2.01	0.05	4.55	0.07	2.92	0.09	2.65	0.10	0.45	0.04	0.46	0.03
54	-19.09	75.88	0.16	11.38	0.09	1.94	0.04	4.50	0.07	2.92	0.09	2.57	0.10	0.33	0.03	0.48	0.03
55	-18.92	75.59	0.16	11.39	0.09	1.98	0.04	4.53	0.07	2.98	0.09	2.66	0.10	0.43	0.04	0.44	0.03
56	-18.75	75.54	0.16	11.41	0.09	2.02	0.05	4.47	0.07	2.96	0.09	2.66	0.10	0.47	0.04	0.46	0.03
57	-18.58	75.58	0.16	11.52	0.09	1.98	0.05	4.54	0.07	2.86	0.09	2.64	0.10	0.42	0.04	0.46	0.03
58	-18.41	75.81	0.16	11.34	0.09	1.89	0.04	4.54	0.07	2.91	0.09	2.67	0.10	0.39	0.04	0.46	0.03
59	-18.24	75.60	0.16	11.37	0.09	1.90	0.04	4.58	0.07	2.97	0.09	2.66	0.10	0.44	0.04	0.48	0.03
60	-18.07	75.53	0.16	11.34	0.09	1.93	0.04	4.55	0.07	3.01	0.10	2.76	0.11	0.42	0.04	0.46	0.03
61	-17.90	75.61	0.16	11.42	0.09	1.93	0.04	4.46	0.07	2.99	0.09	2.69	0.11	0.41	0.04	0.50	0.03
62	-17.73	75.70	0.16	11.35	0.09	1.92	0.04	4.53	0.07	3.00	0.09	2.64	0.10	0.42	0.04	0.45	0.03
63	-17.55	75.60	0.16	11.31	0.09	1.89	0.04	4.52	0.07	3.01	0.10	2.74	0.11	0.46	0.04	0.46	0.03
64	-17.39	75.74	0.16	11.48	0.09	1.95	0.04	4.49	0.07	2.95	0.09	2.49	0.10	0.44	0.04	0.46	0.03
65	-17.22	75.42	0.16	11.37	0.09	1.98	0.04	4.47	0.07	3.12	0.10	2.75	0.11	0.43	0.04	0.46	0.03
66	-17.04	75.53	0.16	11.37	0.09	1.94	0.04	4.48	0.07	3.13	0.10	2.69	0.11	0.40	0.04	0.47	0.03
67	-16.87	75.78	0.16	11.38	0.09	1.95	0.04	4.48	0.07	2.99	0.09	2.55	0.10	0.42	0.04	0.44	0.03
68	-16.70	75.59	0.16	11.42	0.09	1.93	0.04	4.44	0.07	3.13	0.10	2.58	0.10	0.44	0.04	0.47	0.03
69	-16.53	75.62	0.16	11.32	0.09	1.98	0.04	4.52	0.07	3.09	0.10	2.59	0.10	0.41	0.04	0.49	0.03
70	-16.36	75.62	0.16	11.33	0.09	2.00	0.05	4.55	0.07	3.08	0.10	2.54	0.10	0.40	0.04	0.47	0.03
71	-16.19	75.66	0.16	11.39	0.09	1.97	0.04	4.51	0.07	3.06	0.10	2.51	0.10	0.42	0.04	0.47	0.03
72	-16.02	75.52	0.16	11.30	0.09	1.97	0.04	4.51	0.07	3.03	0.10	2.70	0.11	0.44	0.04	0.52	0.04
73	-15.85	75.43	0.16	11.36	0.09	1.92	0.04	4.47	0.07	3.14	0.10	2.74	0.11	0.44	0.04	0.49	0.03
74	-15.68	75.48	0.16	11.36	0.09	1.89	0.04	4.45	0.07	3.06	0.10	2.80	0.11	0.49	0.05	0.48	0.03
75	-15.51	75.65	0.16	11.37	0.09	1.96	0.04	4.46	0.07	3.03	0.10	2.68	0.11	0.41	0.04	0.45	0.03
76	-15.34	75.63	0.16	11.34	0.09	1.92	0.04	4.48	0.07	3.04	0.10	2.75	0.11	0.37	0.04	0.46	0.03
77	-15.17	75.69	0.16	11.28	0.09	1.92	0.04	4.52	0.07	3.05	0.10	2.66	0.10	0.41	0.04	0.48	0.03
78	-15.00	75.63	0.16	11.27	0.09	1.90	0.04	4.50	0.07	3.05	0.10	2.77	0.11	0.42	0.04	0.45	0.03
79	-14.83	75.58	0.16	11.35	0.09	1.97	0.04	4.41	0.07	3.08	0.10	2.71	0.11	0.45	0.04	0.46	0.03
80	-14.66	75.61	0.16	11.23	0.09	1.91	0.04	4.45	0.07	3.07	0.10	2.82	0.11	0.47	0.04	0.44	0.03
81	-14.49	75.61	0.16	11.20	0.09	1.91	0.04	4.47	0.07	3.09	0.10	2.73	0.11	0.49	0.05	0.50	0.03
82	-14.32	75.70	0.16	11.21	0.09	1.90	0.04	4.47	0.07	3.14	0.10	2.67	0.10	0.42	0.04	0.49	0.03
83	-14.15	75.68	0.16	11.24	0.09	1.83	0.04	4.52	0.07	3.20	0.10	2.66	0.10	0.42	0.04	0.45	0.03
84	-13.98	75.83	0.16	11.22	0.09	1.88	0.04	4.41	0.07	3.09	0.10	2.70	0.11	0.38	0.04	0.48	0.03
85	-13.81	75.91	0.16	11.23	0.09	1.88	0.04	4.40	0.07	3.07	0.10	2.59	0.10	0.42	0.04	0.51	0.04
86	-13.64	75.86	0.16	11.31	0.09	1.92	0.04	4.38	0.07	3.01	0.10	2.57	0.10	0.43	0.04	0.52	0.04
87	-13.47	75.79	0.16	11.31	0.09	1.92	0.04	4.37	0.07	3.09	0.10	2.61	0.10	0.41	0.04	0.50	0.03
88	-13.29	75.78	0.16	11.12	0.09	1.94	0.04	4.47	0.07	3.08	0.10	2.75	0.11	0.42	0.04	0.44	0.03
89	-13.12	75.69	0.16	11.14	0.09	1.91	0.04	4.47	0.07	3.09	0.10	2.76	0.11	0.46	0.04	0.48	0.03
90	-12.95	75.78	0.16	11.17	0.09	1.90	0.04	4.42	0.07	3.05	0.10	2.78	0.11	0.40	0.04	0.49	0.03
91	-12.78	75.76	0.16	11.14	0.09	1.92	0.04	4.42	0.07	3.12	0.10	2.72	0.11	0.44	0.04	0.49	0.03
92	-12.61	75.92	0.16	11.20	0.09	1.85	0.04	4.37	0.07	3.09	0.10	2.64	0.10	0.42	0.04	0.51	0.04
93	-12.44	75.82	0.16	11.13	0.09	1.85	0.04	4.44	0.07	3.13	0.10	2.72	0.11	0.43	0.04	0.49	0.03
94	-12.27	75.88	0.16	11.09	0.09	1.84	0.04	4.45	0.07	3.12	0.10	2.71	0.11	0.41	0.04	0.50	0.03
95	-12.10	75.85	0.16	11.06	0.09	1.87	0.04	4.40	0.07	3.23	0.10	2.67	0.10	0.45	0.04	0.47	0.03
96	-11.93	75.86	0.16	11.03	0.09	1.86	0.04	4.44	0.07	3.16	0.10	2.76	0.11	0.42	0.04	0.47	0.03
97	-11.76	76.01	0.16	10.98	0.09	1.89	0.04	4.36	0.07	3.10	0.10	2.78	0.11	0.40	0.04	0.48	0.03
98	-11.59	75.91	0.16	11.01	0.09	1.84	0.04	4.40	0.07	3.13	0.10	2.83	0.11	0.39	0.04	0.47	0.03
99	-11.42	75.54	0.16	11.08	0.09	1.90	0.04	4.44	0.07	3.22	0.10	2.87	0.11	0.41	0.04	0.53	0.04
100	-11.25	75.85	0.16	11.07	0.09	1.88	0.04	4.38	0.07	3.13	0.10	2.77	0.11	0.43	0.04	0.49	0.03
101	-11.08	76.15	0.16	11.06	0.09	1.84	0.04	4.32	0.06	3.01	0.10	2.77	0.11	0.40	0.04	0.47	0.03
102	-10.91	76.16	0.16	10.98	0.09	1.84	0.04	4.38	0.07	3.07	0.10	2.72	0.11	0.37	0.03	0.49	0.03
103	-10.74	75.98	0.16	11.02	0.09	1.87	0.04	4.38	0.07	3.15	0.10	2.73	0.11	0.39	0.04	0.49	0.03
104	-10.57	75.85	0.16	10.99	0.09	1.87	0.04	4.42	0.07	3.17	0.10	2.79	0.11	0.42	0.04	0.49	0.03
105	-10.40	76.17	0.16	10.98	0.09	1.82	0.04	4.38	0.07	3.05	0.10	2.68	0.11	0.42	0.04	0.48	0.03
106	-10.23	76.11	0.16	10.94	0.09	1.82	0.04	4.38	0.07	3.10	0.10	2.71	0.11	0.46	0.04	0.47	0.03
107	-10.06	76.12	0.16	10.85	0.09	1.79	0.04	4.31	0.06	3.13	0.10	2.87	0.11	0.45	0.04	0.47	0.03
108	-9.89	76.05	0.16	10.87	0.09	1.84	0.04	4.34	0.06	3.14	0.10	2.85	0.11	0.42	0.04	0.50	0.03
109	-9.71	76.05	0.16	10.92	0.09	1.86	0.04	4.28	0.06	3.12	0.10	2.86	0.11	0.42	0.04	0.49	0.03
110	-9.55	76.10	0.16	10.83	0.09	1.78	0.04	4.38	0.07	3.22	0.10	2.74	0.11	0.43	0.04	0.51	0.04
111	-9.37	76.10	0.16	10.80	0.09	1.75	0.04	4.41	0.07	3.17	0.10	2.93	0.11	0.37	0.03	0.47	0.03
112	-9.20	76.08	0.16	10.80	0.09	1.79	0.04	4.42	0.07	3.11	0.10	2.92	0.11	0.38	0.04	0.50	0.03

113	-9.03	76.08	0.16	10.77	0.09	1.77	0.04	4.44	0.07	3.18	0.10	2.86	0.11	0.42	0.04	0.48	0.03
114	-8.86	76.28	0.16	10.70	0.08	1.77	0.04	4.35	0.06	3.14	0.10	2.89	0.11	0.39	0.04	0.49	0.03
115	-8.69	76.11	0.16	10.73	0.09	1.75	0.04	4.36	0.07	3.16	0.10	3.02	0.12	0.41	0.04	0.46	0.03
116	-8.52	76.34	0.16	10.69	0.08	1.78	0.04	4.35	0.06	3.14	0.10	2.85	0.11	0.37	0.04	0.48	0.03
117	-8.35	76.27	0.16	10.78	0.09	1.79	0.04	4.28	0.06	3.12	0.10	2.85	0.11	0.42	0.04	0.50	0.03
118	-8.18	76.28	0.16	10.64	0.08	1.79	0.04	4.38	0.07	3.14	0.10	2.83	0.11	0.41	0.04	0.52	0.04
119	-8.01	76.42	0.16	10.71	0.09	1.75	0.04	4.27	0.06	3.01	0.10	2.90	0.11	0.43	0.04	0.50	0.03
120	-7.84	76.42	0.16	10.68	0.08	1.73	0.04	4.30	0.06	3.01	0.10	2.90	0.11	0.44	0.04	0.51	0.04
121	-7.67	76.61	0.16	10.65	0.08	1.73	0.04	4.31	0.06	2.97	0.09	2.82	0.11	0.41	0.04	0.51	0.04
122	-7.50	76.67	0.16	10.65	0.08	1.81	0.04	4.25	0.06	2.92	0.09	2.85	0.11	0.36	0.03	0.49	0.03
123	-7.33	76.35	0.16	10.68	0.08	1.81	0.04	4.26	0.06	3.07	0.10	2.94	0.12	0.40	0.04	0.48	0.03
124	-7.16	76.48	0.16	10.54	0.08	1.74	0.04	4.31	0.06	3.14	0.10	2.93	0.11	0.39	0.04	0.47	0.03
125	-6.99	76.59	0.16	10.52	0.08	1.66	0.04	4.32	0.06	3.04	0.10	2.99	0.12	0.41	0.04	0.46	0.03
126	-6.82	76.69	0.16	10.49	0.08	1.71	0.04	4.27	0.06	2.98	0.09	2.92	0.11	0.43	0.04	0.50	0.03
127	-6.65	76.66	0.16	10.51	0.08	1.69	0.04	4.33	0.06	3.06	0.10	2.80	0.11	0.44	0.04	0.50	0.03
128	-6.48	76.71	0.16	10.46	0.08	1.70	0.04	4.30	0.06	3.09	0.10	2.85	0.11	0.40	0.04	0.49	0.03
129	-6.31	76.78	0.16	10.35	0.08	1.74	0.04	4.25	0.06	3.08	0.10	2.90	0.11	0.40	0.04	0.51	0.04
130	-6.14	76.81	0.16	10.38	0.08	1.72	0.04	4.29	0.06	3.00	0.09	2.90	0.11	0.37	0.04	0.53	0.04
131	-5.96	76.83	0.16	10.34	0.08	1.71	0.04	4.25	0.06	3.06	0.10	2.94	0.12	0.42	0.04	0.46	0.03
132	-5.80	76.96	0.16	10.28	0.08	1.68	0.04	4.25	0.06	3.02	0.10	2.88	0.11	0.43	0.04	0.49	0.03
133	-5.62	77.19	0.16	10.19	0.08	1.62	0.04	4.23	0.06	2.93	0.09	2.92	0.11	0.40	0.04	0.51	0.04
134	-5.45	77.23	0.16	10.29	0.08	1.64	0.04	4.17	0.06	2.89	0.09	2.89	0.11	0.39	0.04	0.48	0.03
135	-5.28	77.25	0.16	10.22	0.08	1.62	0.04	4.27	0.06	2.84	0.09	2.92	0.11	0.38	0.04	0.50	0.03
136	-5.11	77.16	0.16	10.17	0.08	1.63	0.04	4.26	0.06	2.99	0.09	2.94	0.12	0.35	0.03	0.51	0.04
137	-4.94	77.25	0.16	10.13	0.08	1.68	0.04	4.22	0.06	2.99	0.09	2.84	0.11	0.38	0.04	0.51	0.04
138	-4.77	77.40	0.16	10.17	0.08	1.67	0.04	4.15	0.06	2.90	0.09	2.80	0.11	0.42	0.04	0.49	0.03
139	-4.60	77.45	0.16	10.09	0.08	1.67	0.04	4.19	0.06	2.89	0.09	2.78	0.11	0.46	0.04	0.47	0.03
140	-4.43	77.40	0.16	10.08	0.08	1.61	0.04	4.19	0.06	2.85	0.09	2.94	0.12	0.44	0.04	0.48	0.03
141	-4.26	77.44	0.16	10.05	0.08	1.63	0.04	4.11	0.06	2.82	0.09	3.03	0.12	0.42	0.04	0.51	0.03
142	-4.09	77.63	0.16	10.01	0.08	1.68	0.04	4.10	0.06	2.76	0.09	2.92	0.11	0.38	0.04	0.54	0.04
143	-3.92	77.62	0.16	9.95	0.08	1.62	0.04	4.18	0.06	2.83	0.09	2.93	0.11	0.38	0.04	0.49	0.03
144	-3.75	77.52	0.16	9.95	0.08	1.55	0.04	4.20	0.06	2.92	0.09	2.96	0.12	0.41	0.04	0.48	0.03
145	-3.58	77.67	0.16	9.90	0.08	1.53	0.03	4.23	0.06	2.90	0.09	2.90	0.11	0.41	0.04	0.46	0.03
146	-3.41	77.53	0.16	9.88	0.08	1.55	0.04	4.21	0.06	2.88	0.09	3.01	0.12	0.43	0.04	0.52	0.04
147	-3.24	77.73	0.16	9.78	0.08	1.57	0.04	4.24	0.06	2.80	0.09	2.95	0.12	0.42	0.04	0.50	0.03
148	-3.07	77.87	0.16	9.69	0.08	1.52	0.03	4.16	0.06	2.75	0.09	3.07	0.12	0.43	0.04	0.50	0.03
149	-2.90	77.97	0.16	9.72	0.08	1.54	0.04	4.13	0.06	2.72	0.09	2.99	0.12	0.42	0.04	0.50	0.03
150	-2.73	78.12	0.16	9.71	0.08	1.53	0.03	4.10	0.06	2.70	0.09	2.92	0.11	0.41	0.04	0.53	0.04
151	-2.56	78.27	0.16	9.66	0.08	1.53	0.03	4.09	0.06	2.67	0.08	2.90	0.11	0.39	0.04	0.49	0.03
152	-2.39	78.18	0.16	9.74	0.08	1.58	0.04	4.05	0.06	2.61	0.08	2.92	0.11	0.40	0.04	0.52	0.04
153	-2.21	78.22	0.16	9.61	0.08	1.55	0.04	4.13	0.06	2.64	0.08	2.93	0.12	0.41	0.04	0.50	0.03
154	-2.05	78.50	0.16	9.62	0.08	1.52	0.03	4.10	0.06	2.60	0.08	2.76	0.11	0.39	0.04	0.50	0.03
155	-1.87	78.62	0.16	9.52	0.08	1.52	0.03	4.04	0.06	2.56	0.08	2.86	0.11	0.38	0.04	0.50	0.03
156	-1.70	78.60	0.16	9.51	0.08	1.49	0.03	4.01	0.06	2.54	0.08	2.99	0.12	0.36	0.03	0.50	0.03
157	-1.53	78.85	0.16	9.45	0.08	1.47	0.03	4.03	0.06	2.49	0.08	2.84	0.11	0.35	0.03	0.51	0.04
158	-1.36	78.84	0.16	9.41	0.07	1.44	0.03	3.99	0.06	2.52	0.08	2.87	0.11	0.45	0.04	0.49	0.03
159	-1.19	78.78	0.16	9.30	0.07	1.50	0.03	4.05	0.06	2.39	0.08	3.07	0.12	0.44	0.04	0.47	0.03
160	-1.02	78.92	0.16	9.32	0.07	1.47	0.03	3.98	0.06	2.42	0.08	2.94	0.12	0.45	0.04	0.49	0.03
161	-0.85	79.05	0.16	9.33	0.07	1.45	0.03	4.02	0.06	2.40	0.08	2.84	0.11	0.40	0.04	0.51	0.04
162	-0.68	78.98	0.16	9.35	0.07	1.47	0.03	4.01	0.06	2.36	0.07	2.88	0.11	0.42	0.04	0.52	0.04
163	-0.51	79.00	0.16	9.37	0.07	1.39	0.03	4.08	0.06	2.33	0.07	2.90	0.11	0.42	0.04	0.51	0.03
164	-0.34	79.12	0.16	9.25	0.07	1.40	0.03	4.07	0.06	2.41	0.08	2.88	0.11	0.36	0.03	0.50	0.03
165	-0.17	79.03	0.16	9.24	0.07	1.45	0.03	4.05	0.06	2.44	0.08	2.88	0.11	0.41	0.04	0.52	0.04
166	0.00	79.33	0.16	9.25	0.07	1.43	0.03	3.96	0.06	2.27	0.07	2.85	0.11	0.41	0.04	0.50	0.03
167	0.17	79.33	0.16	9.30	0.07	1.37	0.03	3.98	0.06	2.26	0.07	2.88	0.11	0.41	0.04	0.47	0.03
168	0.34	79.27	0.16	9.27	0.07	1.42	0.03	3.99	0.06	2.27	0.07	2.87	0.11	0.40	0.04	0.51	0.03
169	0.51	79.27	0.16	9.28	0.07	1.47	0.03	3.97	0.06	2.25	0.07	2.88	0.11	0.40	0.04	0.47	0.03
170	0.68	79.20	0.16	9.41	0.07	1.41	0.03	3.96	0.06	2.23	0.07	2.88	0.11	0.40	0.04	0.50	0.03
171	0.85	79.19	0.16	9.43	0.07	1.40	0.03	3.96	0.06	2.26	0.07	2.93	0.11	0.36	0.03	0.48	0.03
172	1.02	79.18	0.16	9.40	0.07	1.42	0.03	4.02	0.06	2.30	0.07	2.82	0.11	0.39	0.04	0.46	0.03
173	1.19	79.06	0.16	9.49	0.08	1.48	0.03	4.03	0.06	2.25	0.07	2.86	0.11	0.35	0.03	0.48	0.03
174	1.36	78.93	0.16	9.58	0.08	1.44	0.03	4.01	0.06	2.26	0.07	2.94	0.12	0.36	0.03	0.48	0.03

175	1.53	78.97	0.16	9.54	0.08	1.48	0.03	3.98	0.06	2.29	0.07	2.91	0.11	0.38	0.04	0.44	0.03
176	1.70	78.82	0.16	9.63	0.08	1.49	0.03	4.04	0.06	2.25	0.07	2.97	0.12	0.37	0.04	0.42	0.03
177	1.88	78.68	0.16	9.78	0.08	1.44	0.03	4.08	0.06	2.25	0.07	2.88	0.11	0.40	0.04	0.48	0.03
178	2.05	78.43	0.16	9.94	0.08	1.47	0.03	4.13	0.06	2.26	0.07	2.86	0.11	0.40	0.04	0.52	0.04
179	2.22	78.37	0.16	10.04	0.08	1.48	0.03	4.10	0.06	2.26	0.07	2.86	0.11	0.40	0.04	0.49	0.03
180	2.39	77.99	0.16	10.05	0.08	1.52	0.03	4.17	0.06	2.47	0.08	2.86	0.11	0.43	0.04	0.51	0.04
181	2.56	77.88	0.16	10.13	0.08	1.52	0.03	4.16	0.06	2.49	0.08	2.92	0.11	0.39	0.04	0.50	0.03
182	2.73	77.83	0.16	10.34	0.08	1.53	0.03	4.04	0.06	2.43	0.08	2.95	0.12	0.38	0.04	0.50	0.03
183	2.90	77.58	0.16	10.36	0.08	1.51	0.03	4.18	0.06	2.47	0.08	3.03	0.12	0.39	0.04	0.47	0.03
184	3.07	77.54	0.16	10.60	0.08	1.52	0.03	4.10	0.06	2.41	0.08	2.90	0.11	0.42	0.04	0.51	0.04
185	3.24	77.31	0.16	10.68	0.08	1.55	0.04	4.13	0.06	2.52	0.08	2.92	0.11	0.41	0.04	0.48	0.03
186	3.41	77.03	0.16	10.74	0.09	1.56	0.04	4.17	0.06	2.57	0.08	3.01	0.12	0.42	0.04	0.49	0.03
187	3.58	76.85	0.16	10.97	0.09	1.64	0.04	4.17	0.06	2.58	0.08	2.91	0.11	0.40	0.04	0.49	0.03
188	3.75	76.62	0.16	10.99	0.09	1.64	0.04	4.28	0.06	2.71	0.09	2.88	0.11	0.42	0.04	0.47	0.03
189	3.92	76.56	0.16	11.13	0.09	1.64	0.04	4.28	0.06	2.63	0.08	2.87	0.11	0.41	0.04	0.47	0.03
190	4.09	76.45	0.16	11.21	0.09	1.65	0.04	4.29	0.06	2.65	0.08	2.89	0.11	0.38	0.04	0.48	0.03
191	4.26	76.21	0.16	11.43	0.09	1.68	0.04	4.20	0.06	2.67	0.08	2.89	0.11	0.44	0.04	0.49	0.03
192	4.43	76.03	0.16	11.45	0.09	1.71	0.04	4.21	0.06	2.70	0.09	2.98	0.12	0.41	0.04	0.51	0.03
193	4.60	75.81	0.16	11.44	0.09	1.72	0.04	4.33	0.06	2.75	0.09	3.03	0.12	0.41	0.04	0.52	0.04
194	4.77	75.78	0.16	11.55	0.09	1.66	0.04	4.27	0.06	2.81	0.09	2.99	0.12	0.42	0.04	0.52	0.04
195	4.94	75.63	0.16	11.68	0.09	1.69	0.04	4.32	0.06	2.82	0.09	2.96	0.12	0.43	0.04	0.47	0.03
196	5.11	75.62	0.16	11.86	0.09	1.73	0.04	4.26	0.06	2.70	0.09	2.94	0.12	0.41	0.04	0.47	0.03
197	5.28	75.45	0.16	11.81	0.09	1.72	0.04	4.35	0.06	2.79	0.09	2.95	0.12	0.42	0.04	0.50	0.03
198	5.46	75.47	0.16	11.98	0.10	1.68	0.04	4.33	0.06	2.78	0.09	2.84	0.11	0.41	0.04	0.52	0.04
199	5.62	75.33	0.15	11.95	0.09	1.73	0.04	4.31	0.06	2.85	0.09	2.92	0.11	0.43	0.04	0.48	0.03
200	5.80	75.16	0.15	12.05	0.10	1.81	0.04	4.31	0.06	2.79	0.09	2.98	0.12	0.41	0.04	0.50	0.03
201	5.97	75.23	0.15	12.01	0.10	1.74	0.04	4.33	0.06	2.84	0.09	2.95	0.12	0.44	0.04	0.47	0.03
202	6.14	75.03	0.15	12.15	0.10	1.75	0.04	4.35	0.06	2.85	0.09	2.93	0.11	0.44	0.04	0.50	0.03
203	6.31	75.12	0.15	12.20	0.10	1.72	0.04	4.29	0.06	2.85	0.09	2.87	0.11	0.44	0.04	0.50	0.03
204	6.48	75.13	0.15	12.21	0.10	1.70	0.04	4.35	0.06	2.83	0.09	2.87	0.11	0.43	0.04	0.49	0.03
205	6.65	75.21	0.15	12.12	0.10	1.73	0.04	4.35	0.06	2.73	0.09	2.91	0.11	0.47	0.04	0.47	0.03
206	6.82	75.23	0.15	12.18	0.10	1.77	0.04	4.37	0.07	2.80	0.09	2.80	0.11	0.42	0.04	0.45	0.03
207	6.99	75.15	0.15	12.17	0.10	1.74	0.04	4.36	0.07	2.83	0.09	2.86	0.11	0.44	0.04	0.46	0.03
208	7.16	75.10	0.15	12.23	0.10	1.71	0.04	4.33	0.06	2.84	0.09	2.86	0.11	0.47	0.04	0.46	0.03
209	7.33	75.07	0.15	12.21	0.10	1.77	0.04	4.34	0.06	2.84	0.09	2.88	0.11	0.47	0.04	0.43	0.03
210	7.50	74.98	0.15	12.38	0.10	1.80	0.04	4.36	0.07	2.70	0.09	2.85	0.11	0.47	0.04	0.46	0.03
211	7.67	75.04	0.15	12.28	0.10	1.76	0.04	4.39	0.07	2.71	0.09	2.91	0.11	0.43	0.04	0.49	0.03
212	7.84	75.15	0.15	12.27	0.10	1.78	0.04	4.37	0.07	2.69	0.08	2.82	0.11	0.43	0.04	0.49	0.03
213	8.01	75.27	0.15	12.25	0.10	1.71	0.04	4.35	0.06	2.73	0.09	2.77	0.11	0.44	0.04	0.47	0.03
214	8.18	75.34	0.15	12.28	0.10	1.74	0.04	4.33	0.06	2.64	0.08	2.76	0.11	0.42	0.04	0.47	0.03
215	8.35	75.27	0.15	12.33	0.10	1.75	0.04	4.35	0.06	2.63	0.08	2.73	0.11	0.45	0.04	0.47	0.03
216	8.52	75.24	0.15	12.34	0.10	1.70	0.04	4.34	0.06	2.59	0.08	2.89	0.11	0.41	0.04	0.49	0.03
217	8.69	75.08	0.15	12.33	0.10	1.75	0.04	4.42	0.07	2.69	0.09	2.84	0.11	0.44	0.04	0.45	0.03
218	8.86	75.25	0.15	12.30	0.10	1.75	0.04	4.39	0.07	2.60	0.08	2.85	0.11	0.42	0.04	0.45	0.03
219	9.03	75.37	0.16	12.42	0.10	1.70	0.04	4.36	0.07	2.52	0.08	2.69	0.11	0.45	0.04	0.49	0.03
220	9.20	75.27	0.15	12.40	0.10	1.73	0.04	4.39	0.07	2.51	0.08	2.76	0.11	0.47	0.04	0.46	0.03
221	9.37	75.34	0.15	12.40	0.10	1.73	0.04	4.34	0.06	2.51	0.08	2.79	0.11	0.44	0.04	0.45	0.03
222	9.54	75.37	0.16	12.51	0.10	1.69	0.04	4.33	0.06	2.48	0.08	2.71	0.11	0.44	0.04	0.47	0.03
223	9.72	75.43	0.16	12.44	0.10	1.73	0.04	4.40	0.07	2.46	0.08	2.69	0.11	0.39	0.04	0.46	0.03
224	9.89	75.47	0.16	12.45	0.10	1.74	0.04	4.37	0.07	2.49	0.08	2.61	0.10	0.45	0.04	0.42	0.03
225	10.06	75.41	0.16	12.51	0.10	1.76	0.04	4.31	0.06	2.41	0.08	2.69	0.11	0.46	0.04	0.46	0.03
226	10.23	75.39	0.16	12.44	0.10	1.72	0.04	4.38	0.07	2.42	0.08	2.75	0.11	0.44	0.04	0.46	0.03
227	10.40	75.36	0.15	12.44	0.10	1.76	0.04	4.33	0.06	2.41	0.08	2.76	0.11	0.46	0.04	0.48	0.03
228	10.57	75.39	0.16	12.42	0.10	1.72	0.04	4.31	0.06	2.43	0.08	2.80	0.11	0.46	0.04	0.47	0.03
229	10.74	75.66	0.16	12.46	0.10	1.67	0.04	4.35	0.07	2.32	0.07	2.64	0.10	0.44	0.04	0.45	0.03
230	10.91	75.46	0.16	12.35	0.10	1.75	0.04	4.44	0.07	2.36	0.07	2.71	0.11	0.45	0.04	0.46	0.03
231	11.08	75.35	0.15	12.44	0.10	1.76	0.04	4.39	0.07	2.38	0.08	2.81	0.11	0.42	0.04	0.45	0.03
232	11.25	75.67	0.16	12.51	0.10	1.66	0.04	4.30	0.06	2.32	0.07	2.63	0.10	0.43	0.04	0.47	0.03
233	11.42	75.60	0.16	12.57	0.10	1.68	0.04	4.29	0.06	2.26	0.07	2.70	0.11	0.43	0.04	0.47	0.03
234	11.59	75.61	0.16	12.53	0.10	1.73	0.04	4.36	0.07	2.28	0.07	2.65	0.10	0.40	0.04	0.44	0.03
235	11.76	75.78	0.16	12.42	0.10	1.72	0.04	4.35	0.06	2.26	0.07	2.67	0.10	0.39	0.04	0.42	0.03
236	11.93	75.61	0.16	12.46	0.10	1.73	0.04	4.36	0.07	2.25	0.07	2.72	0.11	0.43	0.04	0.44	0.03

237	12.10	75.56	0.16	12.53	0.10	1.70	0.04	4.34	0.06	2.15	0.07	2.84	0.11	0.44	0.04	0.44	0.03
238	12.27	75.75	0.16	12.49	0.10	1.65	0.04	4.39	0.07	2.19	0.07	2.65	0.10	0.43	0.04	0.45	0.03
239	12.44	75.57	0.16	12.47	0.10	1.70	0.04	4.44	0.07	2.17	0.07	2.75	0.11	0.43	0.04	0.47	0.03
240	12.61	75.67	0.16	12.49	0.10	1.67	0.04	4.41	0.07	2.17	0.07	2.73	0.11	0.43	0.04	0.44	0.03
241	12.78	75.49	0.16	12.42	0.10	1.69	0.04	4.44	0.07	2.21	0.07	2.81	0.11	0.48	0.05	0.46	0.03
242	12.95	75.63	0.16	12.44	0.10	1.72	0.04	4.37	0.07	2.16	0.07	2.81	0.11	0.43	0.04	0.45	0.03
243	13.12	75.72	0.16	12.40	0.10	1.70	0.04	4.34	0.06	2.12	0.07	2.80	0.11	0.48	0.05	0.43	0.03
244	13.29	75.74	0.16	12.47	0.10	1.66	0.04	4.42	0.07	2.20	0.07	2.65	0.10	0.45	0.04	0.40	0.03
245	13.47	75.88	0.16	12.55	0.10	1.64	0.04	4.37	0.07	2.14	0.07	2.63	0.10	0.37	0.04	0.41	0.03
246	13.64	75.67	0.16	12.59	0.10	1.73	0.04	4.38	0.07	2.16	0.07	2.57	0.10	0.44	0.04	0.46	0.03
247	13.81	75.79	0.16	12.50	0.10	1.70	0.04	4.39	0.07	2.10	0.07	2.67	0.10	0.44	0.04	0.42	0.03
248	13.98	75.65	0.16	12.45	0.10	1.68	0.04	4.41	0.07	2.12	0.07	2.82	0.11	0.45	0.04	0.42	0.03
249	14.15	75.85	0.16	12.43	0.10	1.66	0.04	4.40	0.07	2.16	0.07	2.62	0.10	0.46	0.04	0.42	0.03
250	14.32	75.87	0.16	12.44	0.10	1.66	0.04	4.43	0.07	2.12	0.07	2.64	0.10	0.42	0.04	0.43	0.03
251	14.49	75.95	0.16	12.42	0.10	1.60	0.04	4.36	0.07	2.08	0.07	2.72	0.11	0.44	0.04	0.43	0.03
252	14.66	75.91	0.16	12.42	0.10	1.66	0.04	4.35	0.06	2.04	0.06	2.69	0.11	0.50	0.05	0.42	0.03
253	14.83	76.09	0.16	12.47	0.10	1.65	0.04	4.32	0.06	2.01	0.06	2.59	0.10	0.47	0.04	0.39	0.03
254	15.00	75.87	0.16	12.50	0.10	1.65	0.04	4.38	0.07	1.97	0.06	2.75	0.11	0.44	0.04	0.44	0.03
255	15.17	75.87	0.16	12.43	0.10	1.67	0.04	4.33	0.06	2.02	0.06	2.77	0.11	0.48	0.05	0.43	0.03
256	15.34	75.86	0.16	12.39	0.10	1.64	0.04	4.47	0.07	2.01	0.06	2.79	0.11	0.44	0.04	0.41	0.03
257	15.51	76.01	0.16	12.35	0.10	1.63	0.04	4.40	0.07	1.98	0.06	2.73	0.11	0.50	0.05	0.40	0.03
258	15.68	76.15	0.16	12.42	0.10	1.61	0.04	4.38	0.07	2.00	0.06	2.57	0.10	0.44	0.04	0.42	0.03
259	15.85	76.00	0.16	12.48	0.10	1.59	0.04	4.41	0.07	1.96	0.06	2.74	0.11	0.42	0.04	0.42	0.03
260	16.02	76.18	0.16	12.49	0.10	1.60	0.04	4.32	0.06	1.95	0.06	2.59	0.10	0.40	0.04	0.46	0.03
261	16.19	76.26	0.16	12.41	0.10	1.59	0.04	4.37	0.07	1.86	0.06	2.66	0.10	0.40	0.04	0.45	0.03
262	16.36	76.29	0.16	12.45	0.10	1.61	0.04	4.30	0.06	1.88	0.06	2.59	0.10	0.42	0.04	0.46	0.03
263	16.53	76.13	0.16	12.53	0.10	1.63	0.04	4.35	0.06	1.82	0.06	2.68	0.11	0.44	0.04	0.43	0.03
264	16.70	76.12	0.16	12.50	0.10	1.55	0.04	4.35	0.06	1.89	0.06	2.71	0.11	0.46	0.04	0.42	0.03
265	16.87	76.25	0.16	12.31	0.10	1.54	0.04	4.40	0.07	1.89	0.06	2.72	0.11	0.46	0.04	0.43	0.03
266	17.04	76.38	0.16	12.30	0.10	1.56	0.04	4.44	0.07	1.81	0.06	2.70	0.11	0.40	0.04	0.41	0.03
267	17.21	76.41	0.16	12.30	0.10	1.57	0.04	4.36	0.07	1.83	0.06	2.67	0.10	0.41	0.04	0.44	0.03
268	17.39	76.36	0.16	12.30	0.10	1.56	0.04	4.36	0.07	1.81	0.06	2.74	0.11	0.42	0.04	0.44	0.03
269	17.56	76.43	0.16	12.30	0.10	1.57	0.04	4.37	0.07	1.80	0.06	2.68	0.11	0.47	0.04	0.40	0.03
270	17.73	76.34	0.16	12.21	0.10	1.55	0.04	4.39	0.07	1.84	0.06	2.75	0.11	0.49	0.05	0.43	0.03
271	17.90	76.44	0.16	12.16	0.10	1.56	0.04	4.39	0.07	1.89	0.06	2.71	0.11	0.44	0.04	0.41	0.03
272	18.07	76.60	0.16	12.25	0.10	1.53	0.03	4.35	0.06	1.80	0.06	2.63	0.10	0.42	0.04	0.43	0.03
273	18.24	76.41	0.16	12.25	0.10	1.54	0.04	4.36	0.07	1.78	0.06	2.71	0.11	0.49	0.05	0.45	0.03
274	18.41	76.41	0.16	12.28	0.10	1.56	0.04	4.36	0.07	1.76	0.06	2.72	0.11	0.46	0.04	0.44	0.03
275	18.58	76.48	0.16	12.29	0.10	1.60	0.04	4.32	0.06	1.82	0.06	2.57	0.10	0.48	0.05	0.43	0.03
276	18.75	76.69	0.16	12.26	0.10	1.54	0.03	4.32	0.06	1.72	0.05	2.61	0.10	0.44	0.04	0.42	0.03
277	18.92	76.47	0.16	12.31	0.10	1.52	0.03	4.37	0.07	1.75	0.06	2.68	0.11	0.46	0.04	0.43	0.03
278	19.09	76.63	0.16	12.28	0.10	1.49	0.03	4.32	0.06	1.66	0.05	2.66	0.10	0.54	0.05	0.42	0.03
279	19.26	76.55	0.16	12.24	0.10	1.51	0.03	4.29	0.06	1.73	0.05	2.74	0.11	0.50	0.05	0.44	0.03
280	19.43	76.67	0.16	12.27	0.10	1.53	0.03	4.31	0.06	1.68	0.05	2.66	0.10	0.46	0.04	0.43	0.03
281	19.60	76.66	0.16	12.29	0.10	1.49	0.03	4.32	0.06	1.67	0.05	2.67	0.10	0.46	0.04	0.44	0.03
282	19.77	76.62	0.16	12.26	0.10	1.55	0.04	4.38	0.07	1.66	0.05	2.67	0.10	0.48	0.05	0.40	0.03
283	19.94	76.66	0.16	12.23	0.10	1.51	0.03	4.30	0.06	1.65	0.05	2.75	0.11	0.49	0.05	0.40	0.03
284	20.11	76.69	0.16	12.23	0.10	1.51	0.03	4.31	0.06	1.69	0.05	2.70	0.11	0.46	0.04	0.42	0.03
285	20.28	76.71	0.16	12.23	0.10	1.47	0.03	4.28	0.06	1.66	0.05	2.75	0.11	0.48	0.05	0.42	0.03
286	20.45	76.71	0.16	12.23	0.10	1.53	0.03	4.28	0.06	1.66	0.05	2.72	0.11	0.47	0.04	0.40	0.03
287	20.62	76.60	0.16	12.25	0.10	1.51	0.03	4.30	0.06	1.63	0.05	2.81	0.11	0.50	0.05	0.40	0.03
288	20.79	76.76	0.16	12.25	0.10	1.50	0.03	4.33	0.06	1.65	0.05	2.66	0.10	0.46	0.04	0.41	0.03
289	20.96	76.66	0.16	12.26	0.10	1.48	0.03	4.28	0.06	1.71	0.05	2.69	0.11	0.47	0.04	0.45	0.03
290	21.14	76.66	0.16	12.24	0.10	1.46	0.03	4.35	0.06	1.66	0.05	2.71	0.11	0.47	0.04	0.44	0.03
291	21.31	76.68	0.16	12.16	0.10	1.43	0.03	4.44	0.07	1.73	0.05	2.68	0.11	0.46	0.04	0.42	0.03
292	21.48	76.59	0.16	12.24	0.10	1.44	0.03	4.42	0.07	1.76	0.06	2.67	0.10	0.47	0.04	0.41	0.03
293	21.65	76.51	0.16	12.22	0.10	1.42	0.03	4.38	0.07	1.70	0.05	2.80	0.11	0.55	0.05	0.41	0.03
294	21.82	76.56	0.16	12.20	0.10	1.48	0.03	4.40	0.07	1.63	0.05	2.80	0.11	0.51	0.05	0.43	0.03
295	21.99	76.56	0.16	12.37	0.10	1.47	0.03	4.39	0.07	1.67	0.05	2.66	0.10	0.45	0.04	0.44	0.03
296	22.16	76.68	0.16	12.31	0.10	1.44	0.03	4.29	0.06	1.64	0.05	2.76	0.11	0.46	0.04	0.42	0.03
297	22.33	76.62	0.16	12.36	0.10	1.47	0.03	4.27	0.06	1.67	0.05	2.69	0.11	0.46	0.04	0.46	0.03
298	22.50	76.67	0.16	12.29	0.10	1.43	0.03	4.31	0.06	1.59	0.05	2.72	0.11	0.54	0.05	0.46	0.03

299	22.67	76.64	0.16	12.28	0.10	1.49	0.03	4.35	0.06	1.60	0.05	2.67	0.10	0.50	0.05	0.47	0.03
300	22.84	76.56	0.16	12.35	0.10	1.45	0.03	4.27	0.06	1.72	0.05	2.71	0.11	0.52	0.05	0.41	0.03
301	23.01	76.63	0.16	12.39	0.10	1.47	0.03	4.19	0.06	1.59	0.05	2.82	0.11	0.50	0.05	0.43	0.03
302	23.18	76.61	0.16	12.38	0.10	1.50	0.03	4.21	0.06	1.53	0.05	2.82	0.11	0.50	0.05	0.45	0.03
303	23.35	76.46	0.16	12.44	0.10	1.44	0.03	4.27	0.06	1.63	0.05	2.83	0.11	0.50	0.05	0.43	0.03
304	23.52	76.45	0.16	12.43	0.10	1.45	0.03	4.33	0.06	1.63	0.05	2.79	0.11	0.47	0.04	0.45	0.03
305	23.69	76.53	0.16	12.41	0.10	1.45	0.03	4.31	0.06	1.62	0.05	2.78	0.11	0.46	0.04	0.43	0.03
306	23.86	76.35	0.16	12.33	0.10	1.49	0.03	4.37	0.07	1.69	0.05	2.86	0.11	0.51	0.05	0.41	0.03
307	24.03	76.51	0.16	12.37	0.10	1.45	0.03	4.38	0.07	1.59	0.05	2.76	0.11	0.50	0.05	0.43	0.03
308	24.20	76.65	0.16	12.40	0.10	1.42	0.03	4.23	0.06	1.53	0.05	2.79	0.11	0.53	0.05	0.45	0.03
309	24.37	76.44	0.16	12.40	0.10	1.48	0.03	4.31	0.06	1.64	0.05	2.83	0.11	0.48	0.05	0.42	0.03
310	24.54	76.53	0.16	12.44	0.10	1.47	0.03	4.23	0.06	1.57	0.05	2.79	0.11	0.50	0.05	0.46	0.03
311	24.71	76.51	0.16	12.47	0.10	1.43	0.03	4.27	0.06	1.59	0.05	2.84	0.11	0.48	0.05	0.42	0.03
312	24.89	76.59	0.16	12.46	0.10	1.48	0.03	4.24	0.06	1.60	0.05	2.75	0.11	0.48	0.05	0.41	0.03
313	25.06	76.43	0.16	12.53	0.10	1.42	0.03	4.25	0.06	1.60	0.05	2.81	0.11	0.51	0.05	0.44	0.03
314	25.23	76.46	0.16	12.49	0.10	1.49	0.03	4.26	0.06	1.61	0.05	2.82	0.11	0.45	0.04	0.42	0.03
315	25.40	76.28	0.16	12.42	0.10	1.47	0.03	4.32	0.06	1.64	0.05	2.95	0.12	0.46	0.04	0.45	0.03
316	25.57	76.33	0.16	12.41	0.10	1.41	0.03	4.36	0.07	1.65	0.05	2.88	0.11	0.51	0.05	0.45	0.03
317	25.74	76.41	0.16	12.46	0.10	1.46	0.03	4.25	0.06	1.61	0.05	2.93	0.11	0.44	0.04	0.44	0.03
318	25.91	76.42	0.16	12.50	0.10	1.41	0.03	4.25	0.06	1.63	0.05	2.88	0.11	0.48	0.05	0.43	0.03
319	26.08	76.56	0.16	12.49	0.10	1.41	0.03	4.20	0.06	1.59	0.05	2.79	0.11	0.49	0.05	0.46	0.03
320	26.25	76.44	0.16	12.54	0.10	1.42	0.03	4.25	0.06	1.61	0.05	2.78	0.11	0.54	0.05	0.44	0.03
321	26.42	76.30	0.16	12.53	0.10	1.47	0.03	4.28	0.06	1.58	0.05	2.88	0.11	0.52	0.05	0.45	0.03
322	26.59	76.44	0.16	12.49	0.10	1.46	0.03	4.29	0.06	1.61	0.05	2.84	0.11	0.44	0.04	0.43	0.03
323	26.76	76.46	0.16	12.55	0.10	1.49	0.03	4.23	0.06	1.55	0.05	2.81	0.11	0.45	0.04	0.46	0.03
324	26.93	76.33	0.16	12.43	0.10	1.42	0.03	4.24	0.06	1.62	0.05	2.97	0.12	0.55	0.05	0.43	0.03
325	27.10	76.36	0.16	12.49	0.10	1.42	0.03	4.33	0.06	1.61	0.05	2.84	0.11	0.51	0.05	0.44	0.03
326	27.27	76.40	0.16	12.51	0.10	1.44	0.03	4.22	0.06	1.61	0.05	2.85	0.11	0.46	0.04	0.50	0.03
327	27.44	76.46	0.16	12.61	0.10	1.41	0.03	4.22	0.06	1.65	0.05	2.67	0.10	0.48	0.05	0.50	0.03
328	27.61	76.29	0.16	12.55	0.10	1.39	0.03	4.30	0.06	1.64	0.05	2.91	0.11	0.47	0.04	0.44	0.03
329	27.78	76.29	0.16	12.66	0.10	1.38	0.03	4.25	0.06	1.59	0.05	2.92	0.11	0.45	0.04	0.46	0.03
330	27.95	76.34	0.16	12.59	0.10	1.42	0.03	4.26	0.06	1.58	0.05	2.86	0.11	0.49	0.05	0.47	0.03
331	28.12	76.34	0.16	12.53	0.10	1.39	0.03	4.34	0.06	1.62	0.05	2.84	0.11	0.50	0.05	0.46	0.03
332	28.29	76.44	0.16	12.57	0.10	1.32	0.03	4.31	0.06	1.59	0.05	2.87	0.11	0.43	0.04	0.46	0.03
333	28.46	76.29	0.16	12.64	0.10	1.36	0.03	4.26	0.06	1.60	0.05	2.89	0.11	0.49	0.05	0.47	0.03
334	28.64	76.38	0.16	12.59	0.10	1.39	0.03	4.22	0.06	1.63	0.05	2.86	0.11	0.50	0.05	0.44	0.03
335	28.81	76.35	0.16	12.67	0.10	1.40	0.03	4.21	0.06	1.58	0.05	2.85	0.11	0.49	0.05	0.43	0.03
336	28.98	76.34	0.16	12.60	0.10	1.43	0.03	4.19	0.06	1.55	0.05	2.97	0.12	0.44	0.04	0.48	0.03
337	29.15	76.37	0.16	12.49	0.10	1.40	0.03	4.26	0.06	1.59	0.05	2.96	0.12	0.47	0.04	0.45	0.03
338	29.32	76.37	0.16	12.67	0.10	1.40	0.03	4.19	0.06	1.61	0.05	2.89	0.11	0.42	0.04	0.46	0.03
339	29.49	76.23	0.16	12.71	0.10	1.45	0.03	4.21	0.06	1.55	0.05	2.93	0.12	0.45	0.04	0.47	0.03
340	29.66	76.15	0.16	12.76	0.10	1.44	0.03	4.21	0.06	1.57	0.05	2.92	0.11	0.49	0.05	0.47	0.03
341	29.83	76.24	0.16	12.62	0.10	1.43	0.03	4.22	0.06	1.60	0.05	2.93	0.11	0.52	0.05	0.44	0.03
342	30.00	76.27	0.16	12.59	0.10	1.40	0.03	4.28	0.06	1.58	0.05	2.96	0.12	0.48	0.05	0.45	0.03
343	30.17	76.32	0.16	12.63	0.10	1.43	0.03	4.19	0.06	1.55	0.05	2.93	0.12	0.44	0.04	0.51	0.04
344	30.34	76.20	0.16	12.63	0.10	1.35	0.03	4.23	0.06	1.69	0.05	2.91	0.11	0.53	0.05	0.45	0.03
345	30.51	76.18	0.16	12.57	0.10	1.42	0.03	4.22	0.06	1.66	0.05	2.98	0.12	0.49	0.05	0.48	0.03
346	30.68	76.21	0.16	12.61	0.10	1.40	0.03	4.24	0.06	1.60	0.05	2.98	0.12	0.47	0.04	0.49	0.03
347	30.85	76.25	0.16	12.61	0.10	1.43	0.03	4.25	0.06	1.60	0.05	2.97	0.12	0.41	0.04	0.47	0.03
348	31.02	76.34	0.16	12.64	0.10	1.42	0.03	4.20	0.06	1.59	0.05	2.91	0.11	0.45	0.04	0.45	0.03
349	31.19	76.26	0.16	12.69	0.10	1.39	0.03	4.25	0.06	1.62	0.05	2.89	0.11	0.47	0.04	0.44	0.03
350	31.36	76.31	0.16	12.67	0.10	1.41	0.03	4.25	0.06	1.54	0.05	2.89	0.11	0.48	0.05	0.45	0.03
351	31.53	76.32	0.16	12.62	0.10	1.41	0.03	4.26	0.06	1.60	0.05	2.87	0.11	0.48	0.05	0.44	0.03
352	31.70	76.34	0.16	12.48	0.10	1.41	0.03	4.25	0.06	1.62	0.05	2.97	0.12	0.50	0.05	0.43	0.03
353	31.87	76.15	0.16	12.76	0.10	1.45	0.03	4.16	0.06	1.59	0.05	2.93	0.12	0.50	0.05	0.47	0.03
354	32.04	76.37	0.16	12.69	0.10	1.38	0.03	4.19	0.06	1.58	0.05	2.84	0.11	0.50	0.05	0.46	0.03
355	32.21	76.21	0.16	12.70	0.10	1.42	0.03	4.22	0.06	1.64	0.05	2.92	0.11	0.46	0.04	0.43	0.03

Agglomerate FLD23.1.1

Table J.13: Major element compositions (as wt.% oxides) from a line traverse across the interface of surface agglomerate FLD23.1.1 (from agglomerate FLD23.1.1 to host FLD23) extracted from quantified EDS compositional maps. The EDS compositional maps were collected at a resolution of 4.7 pixels/μm. The smoothing width for this traverse was 125 pixels (26.4 μm) wide. This is a Si interface and has been centered at $x = 0$ based on the SiO_2 maximum. Peak points within 2σ of the SiO_2 maximum are highlighted in yellow. Uncertainties are 2SEOM.

Pt.	Position (μm)	SiO_2	2σ	Al_2O_3	2σ	Na_2O	2σ	K_2O	2σ	CaO	2σ	FeO	2σ	TiO_2	2σ	MgO	2σ
1	-13.95	73.81	0.21	12.86	0.13	3.16	0.09	4.08	0.10	2.29	0.10	2.86	0.15	0.39	0.06	0.56	0.04
2	-13.73	73.69	0.21	12.93	0.14	3.28	0.09	4.04	0.10	2.20	0.09	2.88	0.16	0.43	0.06	0.54	0.04
3	-13.52	73.53	0.21	12.93	0.14	3.28	0.09	4.07	0.10	2.35	0.10	2.82	0.15	0.40	0.06	0.62	0.05
4	-13.31	73.67	0.21	12.88	0.13	3.27	0.09	4.08	0.10	2.33	0.10	2.81	0.15	0.40	0.06	0.56	0.04
5	-13.10	73.82	0.21	12.81	0.13	3.17	0.09	4.06	0.10	2.32	0.10	2.84	0.15	0.42	0.06	0.56	0.04
6	-12.89	73.66	0.21	12.91	0.14	3.18	0.09	4.09	0.10	2.38	0.10	2.87	0.16	0.37	0.05	0.54	0.04
7	-12.68	73.86	0.21	12.76	0.13	3.11	0.09	4.21	0.10	2.25	0.09	2.91	0.16	0.37	0.05	0.53	0.04
8	-12.47	73.94	0.21	12.76	0.13	3.10	0.09	4.14	0.10	2.27	0.10	2.87	0.16	0.38	0.05	0.55	0.04
9	-12.26	73.60	0.21	12.83	0.13	3.15	0.09	4.19	0.10	2.31	0.10	3.01	0.16	0.42	0.06	0.50	0.04
10	-12.04	73.77	0.21	12.88	0.13	3.16	0.09	4.12	0.10	2.34	0.10	2.76	0.15	0.45	0.06	0.53	0.04
11	-11.83	73.77	0.21	13.09	0.14	3.20	0.09	4.04	0.10	2.18	0.09	2.73	0.15	0.42	0.06	0.58	0.05
12	-11.62	73.85	0.21	12.99	0.14	3.09	0.09	4.03	0.10	2.26	0.10	2.85	0.15	0.39	0.06	0.54	0.04
13	-11.41	73.82	0.21	12.86	0.13	3.09	0.09	4.06	0.10	2.39	0.10	2.87	0.16	0.38	0.05	0.52	0.04
14	-11.20	73.77	0.21	12.93	0.14	3.18	0.09	4.05	0.10	2.25	0.09	2.82	0.15	0.46	0.07	0.54	0.04
15	-10.99	73.76	0.21	12.78	0.13	3.14	0.09	4.16	0.10	2.34	0.10	2.81	0.15	0.45	0.07	0.56	0.04
16	-10.78	73.81	0.21	12.90	0.14	3.19	0.09	4.11	0.10	2.27	0.10	2.77	0.15	0.37	0.05	0.57	0.05
17	-10.56	73.71	0.21	12.83	0.13	3.24	0.09	4.16	0.10	2.25	0.09	2.88	0.16	0.39	0.06	0.55	0.04
18	-10.35	73.98	0.21	12.67	0.13	3.16	0.09	4.08	0.10	2.17	0.09	3.01	0.16	0.41	0.06	0.53	0.04
19	-10.14	73.92	0.21	12.74	0.13	3.17	0.09	4.03	0.10	2.21	0.09	2.90	0.16	0.46	0.07	0.57	0.05
20	-9.93	73.93	0.21	12.83	0.13	3.19	0.09	4.00	0.10	2.16	0.09	2.92	0.16	0.39	0.06	0.59	0.05
21	-9.72	73.96	0.21	12.77	0.13	3.10	0.09	4.08	0.10	2.23	0.09	2.94	0.16	0.41	0.06	0.51	0.04
22	-9.51	74.08	0.21	12.68	0.13	3.15	0.09	4.06	0.10	2.25	0.09	2.77	0.15	0.45	0.07	0.55	0.04
23	-9.30	73.99	0.21	12.76	0.13	3.08	0.09	4.13	0.10	2.26	0.10	2.81	0.15	0.43	0.06	0.55	0.04
24	-9.09	73.70	0.21	12.82	0.13	3.10	0.09	4.13	0.10	2.40	0.10	2.84	0.15	0.46	0.07	0.55	0.04
25	-8.87	74.03	0.21	12.76	0.13	3.09	0.09	4.05	0.10	2.31	0.10	2.78	0.15	0.43	0.06	0.54	0.04
26	-8.66	73.89	0.21	12.92	0.14	3.17	0.09	4.05	0.10	2.29	0.10	2.72	0.15	0.39	0.06	0.57	0.04
27	-8.45	74.06	0.21	12.91	0.14	3.11	0.09	4.02	0.10	2.22	0.09	2.74	0.15	0.36	0.05	0.58	0.05
28	-8.24	73.90	0.21	12.93	0.14	3.16	0.09	4.03	0.10	2.28	0.10	2.71	0.15	0.39	0.06	0.60	0.05
29	-8.03	73.95	0.21	12.87	0.13	3.18	0.09	4.02	0.10	2.24	0.09	2.75	0.15	0.43	0.06	0.55	0.04
30	-7.82	73.99	0.21	12.78	0.13	3.15	0.09	4.07	0.10	2.26	0.10	2.82	0.15	0.42	0.06	0.51	0.04
31	-7.61	73.72	0.21	12.92	0.14	3.19	0.09	4.15	0.10	2.20	0.09	2.85	0.15	0.38	0.06	0.59	0.05
32	-7.40	73.68	0.21	12.83	0.13	3.14	0.09	4.17	0.10	2.35	0.10	2.85	0.15	0.42	0.06	0.56	0.04
33	-7.18	73.70	0.21	12.80	0.13	3.16	0.09	4.19	0.10	2.32	0.10	2.85	0.15	0.38	0.06	0.60	0.05
34	-6.97	73.65	0.21	12.88	0.13	3.20	0.09	4.14	0.10	2.38	0.10	2.83	0.15	0.36	0.05	0.57	0.04
35	-6.76	73.53	0.21	13.02	0.14	3.19	0.09	4.08	0.10	2.36	0.10	2.81	0.15	0.39	0.06	0.61	0.05
36	-6.55	73.52	0.21	12.87	0.13	3.22	0.09	4.11	0.10	2.35	0.10	2.89	0.16	0.45	0.07	0.58	0.05
37	-6.34	73.64	0.21	12.76	0.13	3.17	0.09	4.10	0.10	2.32	0.10	2.97	0.16	0.45	0.06	0.59	0.05
38	-6.13	73.62	0.21	12.71	0.13	3.26	0.09	4.05	0.10	2.34	0.10	3.04	0.16	0.41	0.06	0.58	0.05
39	-5.92	73.85	0.21	12.68	0.13	3.25	0.09	4.08	0.10	2.32	0.10	2.82	0.15	0.43	0.06	0.57	0.04
40	-5.71	73.71	0.21	12.77	0.13	3.24	0.09	4.11	0.10	2.34	0.10	2.87	0.16	0.38	0.05	0.59	0.05
41	-5.49	73.65	0.21	12.70	0.13	3.20	0.09	4.16	0.10	2.42	0.10	2.86	0.15	0.47	0.07	0.54	0.04
42	-5.28	74.01	0.21	12.68	0.13	3.19	0.09	4.12	0.10	2.29	0.10	2.75	0.15	0.43	0.06	0.54	0.04
43	-5.07	74.00	0.21	12.71	0.13	3.21	0.09	4.08	0.10	2.23	0.09	2.74	0.15	0.45	0.06	0.59	0.05
44	-4.86	73.98	0.21	12.63	0.13	3.11	0.09	4.10	0.10	2.25	0.09	2.92	0.16	0.45	0.06	0.56	0.04
45	-4.65	74.27	0.21	12.49	0.13	3.05	0.09	4.12	0.10	2.21	0.09	2.89	0.16	0.41	0.06	0.55	0.04
46	-4.44	74.57	0.21	12.43	0.13	3.10	0.09	4.04	0.10	2.16	0.09	2.80	0.15	0.37	0.05	0.52	0.04
47	-4.23	74.58	0.21	12.29	0.13	3.08	0.09	4.11	0.10	2.22	0.09	2.77	0.15	0.37	0.05	0.58	0.05
48	-4.02	74.87	0.21	12.17	0.13	3.00	0.09	4.01	0.10	2.19	0.09	2.76	0.15	0.40	0.06	0.60	0.05
49	-3.80	74.95	0.21	11.93	0.12	2.92	0.08	4.11	0.10	2.23	0.09	2.86	0.15	0.47	0.07	0.53	0.04
50	-3.59	75.11	0.21	11.98	0.13	2.92	0.08	4.04	0.10	2.19	0.09	2.78	0.15	0.42	0.06	0.57	0.04

51	-3.38	75.53	0.21	11.76	0.12	2.85	0.08	4.11	0.10	2.10	0.09	2.74	0.15	0.36	0.05	0.55	0.04
52	-3.17	75.86	0.21	11.59	0.12	2.82	0.08	4.08	0.10	2.02	0.09	2.67	0.14	0.43	0.06	0.53	0.04
53	-2.96	76.17	0.21	11.47	0.12	2.76	0.08	4.05	0.10	1.94	0.08	2.68	0.15	0.40	0.06	0.53	0.04
54	-2.75	76.44	0.22	11.11	0.12	2.71	0.08	4.12	0.10	1.88	0.08	2.80	0.15	0.41	0.06	0.53	0.04
55	-2.54	76.94	0.22	10.99	0.12	2.68	0.08	4.01	0.10	1.81	0.08	2.66	0.14	0.37	0.05	0.53	0.04
56	-2.32	77.30	0.22	10.81	0.11	2.59	0.07	3.96	0.10	1.73	0.07	2.77	0.15	0.36	0.05	0.48	0.04
57	-2.11	77.51	0.22	10.50	0.11	2.60	0.07	4.03	0.10	1.74	0.07	2.70	0.15	0.42	0.06	0.50	0.04
58	-1.90	77.83	0.22	10.32	0.11	2.54	0.07	3.96	0.10	1.69	0.07	2.76	0.15	0.40	0.06	0.50	0.04
59	-1.69	78.10	0.22	10.15	0.11	2.50	0.07	3.99	0.10	1.61	0.07	2.72	0.15	0.44	0.06	0.50	0.04
60	-1.48	78.37	0.22	9.98	0.10	2.48	0.07	3.90	0.10	1.63	0.07	2.62	0.14	0.50	0.07	0.51	0.04
61	-1.27	78.47	0.22	9.97	0.10	2.45	0.07	3.86	0.09	1.54	0.07	2.80	0.15	0.40	0.06	0.51	0.04
62	-1.06	78.67	0.22	9.83	0.10	2.42	0.07	3.78	0.09	1.52	0.06	2.85	0.15	0.41	0.06	0.52	0.04
63	-0.85	78.96	0.22	9.66	0.10	2.49	0.07	3.71	0.09	1.55	0.07	2.77	0.15	0.35	0.05	0.51	0.04
64	-0.63	79.05	0.22	9.58	0.10	2.42	0.07	3.78	0.09	1.56	0.07	2.71	0.15	0.38	0.05	0.52	0.04
65	-0.42	79.24	0.22	9.47	0.10	2.41	0.07	3.77	0.09	1.54	0.06	2.71	0.15	0.37	0.05	0.49	0.04
66	-0.21	79.36	0.22	9.49	0.10	2.38	0.07	3.73	0.09	1.48	0.06	2.73	0.15	0.40	0.06	0.45	0.04
67	0.00	79.49	0.22	9.35	0.10	2.42	0.07	3.72	0.09	1.43	0.06	2.75	0.15	0.37	0.05	0.47	0.04
68	0.21	79.16	0.22	9.35	0.10	2.42	0.07	3.70	0.09	1.55	0.07	2.92	0.16	0.41	0.06	0.49	0.04
69	0.42	79.24	0.22	9.30	0.10	2.50	0.07	3.75	0.09	1.47	0.06	2.83	0.15	0.38	0.06	0.53	0.04
70	0.63	79.27	0.22	9.40	0.10	2.48	0.07	3.78	0.09	1.49	0.06	2.70	0.15	0.36	0.05	0.50	0.04
71	0.84	79.32	0.22	9.41	0.10	2.40	0.07	3.73	0.09	1.51	0.06	2.77	0.15	0.39	0.06	0.46	0.04
72	1.06	79.10	0.22	9.39	0.10	2.50	0.07	3.73	0.09	1.53	0.06	2.83	0.15	0.31	0.04	0.60	0.05
73	1.27	79.14	0.22	9.41	0.10	2.44	0.07	3.69	0.09	1.57	0.07	2.82	0.15	0.36	0.05	0.57	0.05
74	1.48	78.97	0.22	9.45	0.10	2.42	0.07	3.74	0.09	1.63	0.07	2.86	0.15	0.38	0.06	0.53	0.04
75	1.69	78.81	0.22	9.47	0.10	2.45	0.07	3.83	0.09	1.64	0.07	2.84	0.15	0.43	0.06	0.53	0.04
76	1.90	78.91	0.22	9.47	0.10	2.55	0.07	3.79	0.09	1.60	0.07	2.75	0.15	0.39	0.06	0.53	0.04
77	2.11	78.79	0.22	9.40	0.10	2.60	0.07	3.84	0.09	1.63	0.07	2.84	0.15	0.37	0.05	0.54	0.04
78	2.32	78.83	0.22	9.44	0.10	2.58	0.07	3.81	0.09	1.72	0.07	2.78	0.15	0.33	0.05	0.52	0.04
79	2.54	78.58	0.22	9.66	0.10	2.56	0.07	3.80	0.09	1.70	0.07	2.80	0.15	0.35	0.05	0.54	0.04
80	2.75	78.46	0.22	9.64	0.10	2.62	0.08	3.84	0.09	1.74	0.07	2.81	0.15	0.37	0.05	0.51	0.04
81	2.96	78.47	0.22	9.66	0.10	2.60	0.07	3.80	0.09	1.73	0.07	2.87	0.15	0.41	0.06	0.47	0.04
82	3.17	78.31	0.22	9.67	0.10	2.68	0.08	3.88	0.10	1.75	0.07	2.83	0.15	0.37	0.05	0.51	0.04
83	3.38	78.31	0.22	9.85	0.10	2.67	0.08	3.83	0.09	1.65	0.07	2.77	0.15	0.33	0.05	0.59	0.05
84	3.59	78.20	0.22	9.90	0.10	2.66	0.08	3.81	0.09	1.74	0.07	2.84	0.15	0.31	0.04	0.54	0.04
85	3.80	78.27	0.22	9.89	0.10	2.64	0.08	3.75	0.09	1.70	0.07	2.85	0.15	0.37	0.05	0.52	0.04
86	4.01	78.01	0.22	9.83	0.10	2.71	0.08	3.89	0.10	1.66	0.07	2.93	0.16	0.44	0.06	0.52	0.04
87	4.23	77.85	0.22	9.94	0.10	2.74	0.08	3.91	0.10	1.66	0.07	2.95	0.16	0.45	0.06	0.50	0.04
88	4.44	77.83	0.22	9.84	0.10	2.73	0.08	3.93	0.10	1.74	0.07	2.94	0.16	0.46	0.07	0.53	0.04
89	4.65	77.99	0.22	9.91	0.10	2.75	0.08	3.87	0.10	1.68	0.07	2.78	0.15	0.47	0.07	0.56	0.04
90	4.86	77.81	0.22	9.98	0.10	2.75	0.08	3.94	0.10	1.67	0.07	2.92	0.16	0.39	0.06	0.54	0.04
91	5.07	77.46	0.22	10.14	0.11	2.72	0.08	3.92	0.10	1.81	0.08	2.95	0.16	0.43	0.06	0.56	0.04
92	5.28	77.65	0.22	10.19	0.11	2.74	0.08	3.92	0.10	1.76	0.07	2.78	0.15	0.39	0.06	0.57	0.05
93	5.49	77.41	0.22	10.07	0.11	2.82	0.08	3.90	0.10	1.87	0.08	2.90	0.16	0.48	0.07	0.54	0.04
94	5.70	77.49	0.22	10.10	0.11	2.78	0.08	3.90	0.10	1.83	0.08	3.01	0.16	0.40	0.06	0.50	0.04
95	5.92	77.53	0.22	10.18	0.11	2.71	0.08	3.97	0.10	1.85	0.08	2.84	0.15	0.37	0.05	0.55	0.04
96	6.13	77.49	0.22	10.17	0.11	2.85	0.08	3.88	0.10	1.85	0.08	2.84	0.15	0.38	0.05	0.55	0.04
97	6.34	77.29	0.22	10.33	0.11	2.88	0.08	3.89	0.10	1.88	0.08	2.80	0.15	0.39	0.06	0.54	0.04
98	6.55	77.25	0.22	10.17	0.11	2.88	0.08	3.98	0.10	1.84	0.08	2.89	0.16	0.42	0.06	0.57	0.04
99	6.76	77.26	0.22	10.27	0.11	2.87	0.08	3.96	0.10	1.80	0.08	2.96	0.16	0.37	0.05	0.52	0.04
100	6.97	77.35	0.22	10.26	0.11	2.78	0.08	3.94	0.10	1.80	0.08	2.97	0.16	0.38	0.05	0.52	0.04
101	7.18	77.12	0.22	10.48	0.11	2.79	0.08	3.99	0.10	1.77	0.07	2.97	0.16	0.35	0.05	0.54	0.04
102	7.39	77.14	0.22	10.53	0.11	2.79	0.08	4.04	0.10	1.86	0.08	2.76	0.15	0.36	0.05	0.51	0.04
103	7.61	77.04	0.22	10.51	0.11	2.88	0.08	3.87	0.10	1.84	0.08	2.92	0.16	0.39	0.06	0.55	0.04
104	7.82	76.95	0.22	10.52	0.11	2.85	0.08	3.92	0.10	1.83	0.08	2.99	0.16	0.44	0.06	0.49	0.04
105	8.03	76.91	0.22	10.47	0.11	2.84	0.08	4.03	0.10	1.89	0.08	2.89	0.16	0.42	0.06	0.53	0.04
106	8.24	76.96	0.22	10.46	0.11	2.79	0.08	4.05	0.10	1.84	0.08	2.98	0.16	0.41	0.06	0.52	0.04
107	8.45	76.78	0.22	10.55	0.11	2.89	0.08	4.02	0.10	1.93	0.08	2.93	0.16	0.36	0.05	0.56	0.04
108	8.66	76.79	0.22	10.67	0.11	2.90	0.08	3.96	0.10	1.84	0.08	2.89	0.16	0.36	0.05	0.58	0.05
109	8.87	76.66	0.22	10.70	0.11	2.91	0.08	3.99	0.10	1.92	0.08	2.87	0.16	0.38	0.05	0.57	0.04
110	9.09	76.77	0.22	10.71	0.11	2.88	0.08	4.05	0.10	1.85	0.08	2.86	0.15	0.36	0.05	0.53	0.04
111	9.30	76.81	0.22	10.66	0.11	2.83	0.08	4.11	0.10	1.87	0.08	2.75	0.15	0.46	0.07	0.53	0.04
112	9.51	76.59	0.22	10.71	0.11	2.88	0.08	4.13	0.10	1.85	0.08	2.92	0.16	0.40	0.06	0.51	0.04

113	9.72	76.64	0.22	10.73	0.11	2.90	0.08	4.04	0.10	1.85	0.08	2.90	0.16	0.41	0.06	0.53	0.04
114	9.93	76.58	0.22	10.87	0.11	2.92	0.08	4.07	0.10	1.88	0.08	2.78	0.15	0.37	0.05	0.53	0.04
115	10.14	76.71	0.22	10.81	0.11	2.88	0.08	4.01	0.10	1.88	0.08	2.84	0.15	0.37	0.05	0.50	0.04
116	10.35	76.35	0.21	10.86	0.11	2.92	0.08	4.05	0.10	1.95	0.08	2.95	0.16	0.38	0.05	0.54	0.04
117	10.56	76.64	0.22	10.92	0.11	2.86	0.08	3.99	0.10	1.86	0.08	2.83	0.15	0.35	0.05	0.55	0.04
118	10.77	76.34	0.21	10.91	0.11	2.85	0.08	4.06	0.10	1.98	0.08	2.88	0.16	0.41	0.06	0.58	0.05
119	10.99	76.38	0.21	10.87	0.11	2.96	0.08	4.04	0.10	1.99	0.08	2.78	0.15	0.40	0.06	0.57	0.05
120	11.20	76.31	0.21	10.75	0.11	3.01	0.09	4.08	0.10	2.00	0.08	2.93	0.16	0.40	0.06	0.53	0.04
121	11.41	76.25	0.21	10.69	0.11	3.05	0.09	4.14	0.10	1.96	0.08	2.98	0.16	0.43	0.06	0.49	0.04
122	11.62	76.34	0.21	10.72	0.11	2.98	0.09	4.19	0.10	1.92	0.08	2.92	0.16	0.45	0.06	0.48	0.04
123	11.83	76.31	0.21	10.92	0.11	2.98	0.09	4.10	0.10	1.98	0.08	2.80	0.15	0.40	0.06	0.51	0.04
124	12.04	76.12	0.21	10.94	0.11	3.11	0.09	4.09	0.10	2.01	0.08	2.83	0.15	0.38	0.05	0.53	0.04
125	12.25	76.22	0.21	10.92	0.11	3.07	0.09	4.04	0.10	1.97	0.08	2.82	0.15	0.41	0.06	0.55	0.04
126	12.46	76.26	0.21	10.89	0.11	3.00	0.09	4.06	0.10	1.93	0.08	2.89	0.16	0.42	0.06	0.56	0.04
127	12.68	76.07	0.21	11.08	0.12	3.00	0.09	4.13	0.10	1.96	0.08	2.79	0.15	0.41	0.06	0.57	0.04
128	12.89	75.76	0.21	10.97	0.11	3.05	0.09	4.16	0.10	2.02	0.09	3.09	0.17	0.42	0.06	0.54	0.04
129	13.10	75.86	0.21	11.12	0.12	3.07	0.09	4.12	0.10	1.95	0.08	2.96	0.16	0.39	0.06	0.52	0.04
130	13.31	76.26	0.21	11.00	0.12	2.99	0.09	4.11	0.10	1.94	0.08	2.79	0.15	0.36	0.05	0.54	0.04
131	13.52	76.20	0.21	11.06	0.12	3.04	0.09	4.05	0.10	1.94	0.08	2.77	0.15	0.39	0.06	0.54	0.04
132	13.73	76.03	0.21	11.14	0.12	3.10	0.09	4.06	0.10	1.89	0.08	2.82	0.15	0.44	0.06	0.53	0.04
133	13.94	76.09	0.21	10.97	0.11	3.08	0.09	4.08	0.10	1.96	0.08	2.94	0.16	0.34	0.05	0.53	0.04
134	14.16	76.02	0.21	11.10	0.12	3.06	0.09	4.17	0.10	1.91	0.08	2.84	0.15	0.42	0.06	0.49	0.04
135	14.37	75.89	0.21	11.12	0.12	3.06	0.09	4.22	0.10	1.92	0.08	2.75	0.15	0.49	0.07	0.56	0.04
136	14.58	75.93	0.21	11.06	0.12	3.08	0.09	4.16	0.10	2.01	0.08	2.82	0.15	0.45	0.06	0.50	0.04
137	14.79	75.96	0.21	11.19	0.12	3.06	0.09	4.06	0.10	1.94	0.08	2.89	0.16	0.40	0.06	0.52	0.04
138	15.00	75.92	0.21	11.17	0.12	3.09	0.09	4.06	0.10	1.97	0.08	2.89	0.16	0.40	0.06	0.51	0.04
139	15.21	75.75	0.21	11.19	0.12	3.16	0.09	4.13	0.10	1.98	0.08	2.83	0.15	0.43	0.06	0.52	0.04
140	15.42	75.89	0.21	11.15	0.12	3.11	0.09	4.14	0.10	1.97	0.08	2.83	0.15	0.38	0.05	0.53	0.04
141	15.63	75.87	0.21	11.16	0.12	3.10	0.09	4.24	0.10	1.95	0.08	2.77	0.15	0.37	0.05	0.53	0.04
142	15.85	75.79	0.21	11.33	0.12	3.19	0.09	4.13	0.10	1.89	0.08	2.73	0.15	0.39	0.06	0.55	0.04
143	16.06	76.00	0.21	11.26	0.12	3.13	0.09	4.09	0.10	1.86	0.08	2.79	0.15	0.36	0.05	0.51	0.04
144	16.27	75.65	0.21	11.28	0.12	3.18	0.09	4.15	0.10	1.92	0.08	2.88	0.16	0.43	0.06	0.52	0.04
145	16.48	75.67	0.21	11.26	0.12	3.20	0.09	4.18	0.10	1.89	0.08	2.80	0.15	0.45	0.07	0.54	0.04
146	16.69	75.86	0.21	11.16	0.12	3.16	0.09	4.19	0.10	1.86	0.08	2.90	0.16	0.35	0.05	0.52	0.04
147	16.90	75.77	0.21	11.33	0.12	3.20	0.09	4.16	0.10	1.91	0.08	2.76	0.15	0.34	0.05	0.53	0.04
148	17.11	75.65	0.21	11.34	0.12	3.24	0.09	4.15	0.10	1.94	0.08	2.79	0.15	0.38	0.05	0.52	0.04
149	17.32	75.64	0.21	11.22	0.12	3.14	0.09	4.30	0.11	1.99	0.08	2.84	0.15	0.35	0.05	0.51	0.04
150	17.54	75.63	0.21	11.28	0.12	3.15	0.09	4.16	0.10	1.91	0.08	2.94	0.16	0.38	0.06	0.55	0.04
151	17.75	75.62	0.21	11.20	0.12	3.13	0.09	4.19	0.10	1.96	0.08	2.94	0.16	0.41	0.06	0.55	0.04
152	17.96	75.56	0.21	11.32	0.12	3.09	0.09	4.20	0.10	1.92	0.08	2.95	0.16	0.45	0.06	0.51	0.04
153	18.17	75.56	0.21	11.40	0.12	3.26	0.09	4.13	0.10	1.91	0.08	2.81	0.15	0.40	0.06	0.54	0.04
154	18.38	75.51	0.21	11.44	0.12	3.28	0.09	4.22	0.10	1.88	0.08	2.75	0.15	0.37	0.05	0.54	0.04
155	18.59	75.69	0.21	11.47	0.12	3.23	0.09	4.21	0.10	1.89	0.08	2.58	0.14	0.39	0.06	0.55	0.04
156	18.80	75.57	0.21	11.43	0.12	3.18	0.09	4.21	0.10	2.01	0.08	2.71	0.15	0.36	0.05	0.53	0.04
157	19.02	75.60	0.21	11.44	0.12	3.22	0.09	4.19	0.10	1.97	0.08	2.71	0.15	0.36	0.05	0.52	0.04
158	19.23	75.47	0.21	11.42	0.12	3.29	0.09	4.20	0.10	1.93	0.08	2.73	0.15	0.46	0.07	0.50	0.04
159	19.44	75.45	0.21	11.56	0.12	3.25	0.09	4.14	0.10	1.92	0.08	2.78	0.15	0.40	0.06	0.49	0.04
160	19.65	75.67	0.21	11.47	0.12	3.27	0.09	4.13	0.10	1.90	0.08	2.72	0.15	0.36	0.05	0.48	0.04
161	19.86	75.53	0.21	11.28	0.12	3.33	0.10	4.22	0.10	1.89	0.08	2.81	0.15	0.38	0.05	0.55	0.04
162	20.07	75.83	0.21	11.38	0.12	3.19	0.09	4.08	0.10	1.81	0.08	2.79	0.15	0.41	0.06	0.52	0.04
163	20.28	75.54	0.21	11.49	0.12	3.24	0.09	4.08	0.10	1.92	0.08	2.83	0.15	0.39	0.06	0.52	0.04
164	20.49	75.42	0.21	11.47	0.12	3.19	0.09	4.21	0.10	1.96	0.08	2.74	0.15	0.43	0.06	0.57	0.04
165	20.70	75.72	0.21	11.49	0.12	3.24	0.09	4.15	0.10	1.83	0.08	2.70	0.15	0.36	0.05	0.51	0.04
166	20.92	75.39	0.21	11.48	0.12	3.24	0.09	4.21	0.10	1.94	0.08	2.80	0.15	0.40	0.06	0.53	0.04

Agglomerate FLD23.1.2

Table J.14: Major element compositions (as wt.% oxides) from a line traverse across the interface of surface agglomerate FLD23.1.2 (from agglomerate FLD23.1.2 to host FLD23) extracted from quantified EDS compositional maps. The EDS compositional maps were collected at a resolution of 4.7 pixels/μm. The smoothing width for this traverse was 125 pixels (26.4 μm) wide. This is an Si interface and has been centered at $x = 0$ based on the SiO_2 maximum. Peak points within 2σ of the SiO_2 maximum are highlighted in yellow. Uncertainties are 2SEOM.

Pt.	Position (μm)	SiO_2	2σ	Al_2O_3	2σ	Na_2O	2σ	K_2O	2σ	CaO	2σ	FeO	2σ	TiO_2	2σ	MgO	2σ
1	-14.37	74.61	0.21	12.82	0.13	2.83	0.08	4.08	0.10	1.92	0.08	2.74	0.15	0.41	0.06	0.59	0.05
2	-14.16	74.55	0.21	12.58	0.13	2.89	0.08	4.10	0.10	2.02	0.09	2.80	0.15	0.47	0.07	0.58	0.05
3	-13.94	74.56	0.21	12.69	0.13	2.80	0.08	4.03	0.10	1.99	0.08	2.85	0.15	0.48	0.07	0.60	0.05
4	-13.73	74.59	0.21	12.81	0.13	2.86	0.08	4.06	0.10	2.01	0.08	2.66	0.14	0.43	0.06	0.59	0.05
5	-13.52	74.32	0.21	12.83	0.13	2.90	0.08	4.11	0.10	2.08	0.09	2.67	0.14	0.46	0.07	0.62	0.05
6	-13.31	74.45	0.21	12.92	0.14	2.87	0.08	3.93	0.10	2.00	0.08	2.77	0.15	0.40	0.06	0.65	0.05
7	-13.10	74.46	0.21	12.86	0.13	2.86	0.08	3.97	0.10	2.04	0.09	2.78	0.15	0.41	0.06	0.62	0.05
8	-12.89	74.13	0.21	12.83	0.13	2.81	0.08	4.06	0.10	2.09	0.09	3.08	0.17	0.43	0.06	0.58	0.05
9	-12.68	74.19	0.21	12.87	0.13	2.89	0.08	4.10	0.10	2.05	0.09	2.89	0.16	0.41	0.06	0.58	0.05
10	-12.47	74.16	0.21	12.97	0.14	2.81	0.08	3.95	0.10	2.11	0.09	2.92	0.16	0.42	0.06	0.66	0.05
11	-12.25	74.11	0.21	13.01	0.14	2.74	0.08	4.04	0.10	2.18	0.09	2.85	0.15	0.43	0.06	0.64	0.05
12	-12.04	74.10	0.21	12.89	0.14	2.78	0.08	4.02	0.10	2.20	0.09	2.94	0.16	0.46	0.07	0.60	0.05
13	-11.83	73.82	0.21	13.00	0.14	2.75	0.08	4.06	0.10	2.20	0.09	3.08	0.17	0.48	0.07	0.62	0.05
14	-11.62	73.93	0.21	13.09	0.14	2.83	0.08	3.94	0.10	2.16	0.09	3.00	0.16	0.36	0.05	0.69	0.05
15	-11.41	73.75	0.21	13.03	0.14	2.83	0.08	4.07	0.10	2.18	0.09	3.06	0.17	0.44	0.06	0.65	0.05
16	-11.20	73.99	0.21	13.09	0.14	2.80	0.08	4.03	0.10	2.10	0.09	2.91	0.16	0.45	0.06	0.64	0.05
17	-10.99	74.01	0.21	13.13	0.14	2.80	0.08	3.97	0.10	2.15	0.09	2.93	0.16	0.38	0.06	0.63	0.05
18	-10.78	73.93	0.21	13.07	0.14	2.85	0.08	3.98	0.10	2.12	0.09	3.01	0.16	0.44	0.06	0.60	0.05
19	-10.56	73.92	0.21	13.14	0.14	2.78	0.08	3.98	0.10	2.09	0.09	2.92	0.16	0.49	0.07	0.69	0.05
20	-10.35	73.85	0.21	13.05	0.14	2.83	0.08	4.07	0.10	2.17	0.09	2.99	0.16	0.43	0.06	0.59	0.05
21	-10.14	74.03	0.21	13.08	0.14	2.86	0.08	4.01	0.10	2.00	0.08	2.94	0.16	0.47	0.07	0.61	0.05
22	-9.93	73.97	0.21	13.09	0.14	2.80	0.08	4.05	0.10	2.02	0.09	2.97	0.16	0.43	0.06	0.66	0.05
23	-9.72	74.07	0.21	13.02	0.14	2.82	0.08	4.08	0.10	2.09	0.09	2.90	0.16	0.45	0.06	0.58	0.05
24	-9.51	74.11	0.21	12.91	0.14	2.82	0.08	4.11	0.10	2.07	0.09	3.01	0.16	0.41	0.06	0.56	0.04
25	-9.30	74.03	0.21	13.05	0.14	2.80	0.08	4.11	0.10	1.99	0.08	2.99	0.16	0.38	0.06	0.66	0.05
26	-9.09	74.18	0.21	12.99	0.14	2.79	0.08	4.11	0.10	1.97	0.08	2.93	0.16	0.39	0.06	0.64	0.05
27	-8.87	74.07	0.21	12.94	0.14	2.75	0.08	4.19	0.10	2.13	0.09	2.91	0.16	0.43	0.06	0.59	0.05
28	-8.66	74.36	0.21	12.91	0.14	2.71	0.08	4.09	0.10	1.96	0.08	2.98	0.16	0.41	0.06	0.58	0.05
29	-8.45	74.30	0.21	12.88	0.13	2.77	0.08	4.14	0.10	2.00	0.08	2.93	0.16	0.36	0.05	0.63	0.05
30	-8.24	74.56	0.21	12.94	0.14	2.77	0.08	4.11	0.10	1.92	0.08	2.70	0.15	0.41	0.06	0.60	0.05
31	-8.03	74.64	0.21	12.79	0.13	2.69	0.08	4.22	0.10	1.89	0.08	2.76	0.15	0.44	0.06	0.58	0.05
32	-7.82	74.31	0.21	12.97	0.14	2.81	0.08	4.11	0.10	1.85	0.08	2.87	0.16	0.46	0.07	0.63	0.05
33	-7.61	74.57	0.21	13.10	0.14	2.83	0.08	4.05	0.10	1.80	0.08	2.71	0.15	0.34	0.05	0.61	0.05
34	-7.40	74.51	0.21	12.97	0.14	2.73	0.08	4.15	0.10	1.87	0.08	2.77	0.15	0.38	0.05	0.62	0.05
35	-7.18	74.51	0.21	12.86	0.13	2.72	0.08	4.18	0.10	1.82	0.08	2.86	0.15	0.48	0.07	0.56	0.04
36	-6.97	74.77	0.21	13.01	0.14	2.75	0.08	4.01	0.10	1.82	0.08	2.65	0.14	0.39	0.06	0.61	0.05
37	-6.76	74.54	0.21	13.07	0.14	2.77	0.08	4.03	0.10	1.85	0.08	2.73	0.15	0.42	0.06	0.58	0.05
38	-6.55	74.41	0.21	13.06	0.14	2.79	0.08	4.09	0.10	1.89	0.08	2.76	0.15	0.42	0.06	0.58	0.05
39	-6.34	74.28	0.21	13.01	0.14	2.80	0.08	4.24	0.10	1.91	0.08	2.79	0.15	0.42	0.06	0.55	0.04
40	-6.13	74.48	0.21	13.07	0.14	2.79	0.08	4.08	0.10	1.85	0.08	2.77	0.15	0.37	0.05	0.60	0.05
41	-5.92	74.49	0.21	13.08	0.14	2.72	0.08	4.12	0.10	1.86	0.08	2.75	0.15	0.35	0.05	0.63	0.05
42	-5.70	74.07	0.21	13.05	0.14	2.86	0.08	4.22	0.10	1.97	0.08	2.84	0.15	0.41	0.06	0.58	0.05
43	-5.49	74.25	0.21	13.09	0.14	2.85	0.08	4.16	0.10	1.93	0.08	2.73	0.15	0.43	0.06	0.55	0.04
44	-5.28	74.30	0.21	13.20	0.14	2.82	0.08	4.13	0.10	1.87	0.08	2.71	0.15	0.41	0.06	0.55	0.04
45	-5.07	74.10	0.21	13.26	0.14	2.85	0.08	4.12	0.10	1.92	0.08	2.74	0.15	0.42	0.06	0.59	0.05
46	-4.86	74.15	0.21	13.12	0.14	2.77	0.08	4.15	0.10	1.98	0.08	2.75	0.15	0.47	0.07	0.61	0.05
47	-4.65	74.22	0.21	13.03	0.14	2.83	0.08	4.25	0.10	1.96	0.08	2.70	0.15	0.41	0.06	0.61	0.05
48	-4.44	74.20	0.21	13.16	0.14	2.83	0.08	4.08	0.10	1.91	0.08	2.77	0.15	0.43	0.06	0.63	0.05
49	-4.23	73.98	0.21	13.20	0.14	2.86	0.08	4.16	0.10	2.00	0.08	2.79	0.15	0.41	0.06	0.60	0.05
50	-4.01	74.01	0.21	13.26	0.14	2.84	0.08	4.22	0.10	1.98	0.08	2.68	0.15	0.43	0.06	0.58	0.05

51	-3.80	73.92	0.21	13.25	0.14	2.80	0.08	4.20	0.10	2.00	0.08	2.80	0.15	0.42	0.06	0.61	0.05
52	-3.59	74.06	0.21	13.22	0.14	2.82	0.08	4.17	0.10	1.97	0.08	2.76	0.15	0.40	0.06	0.61	0.05
53	-3.38	74.20	0.21	13.18	0.14	2.82	0.08	4.12	0.10	1.99	0.08	2.75	0.15	0.38	0.05	0.56	0.04
54	-3.17	74.32	0.21	12.90	0.14	2.74	0.08	4.10	0.10	2.00	0.08	2.88	0.16	0.48	0.07	0.58	0.05
55	-2.96	74.14	0.21	12.82	0.13	2.76	0.08	4.21	0.10	1.95	0.08	3.13	0.17	0.42	0.06	0.55	0.04
56	-2.75	74.20	0.21	12.70	0.13	2.79	0.08	4.32	0.11	2.17	0.09	2.86	0.15	0.43	0.06	0.53	0.04
57	-2.54	74.56	0.21	12.75	0.13	2.69	0.08	4.13	0.10	2.00	0.08	2.92	0.16	0.38	0.05	0.57	0.05
58	-2.32	74.77	0.21	12.56	0.13	2.72	0.08	4.01	0.10	1.94	0.08	2.92	0.16	0.44	0.06	0.64	0.05
59	-2.11	75.10	0.21	12.32	0.13	2.69	0.08	4.04	0.10	1.87	0.08	2.96	0.16	0.49	0.07	0.55	0.04
60	-1.90	75.34	0.21	12.15	0.13	2.59	0.07	4.02	0.10	1.95	0.08	2.96	0.16	0.43	0.06	0.57	0.04
61	-1.69	75.77	0.21	11.80	0.12	2.53	0.07	4.00	0.10	1.87	0.08	3.02	0.16	0.46	0.07	0.54	0.04
62	-1.48	76.77	0.22	11.36	0.12	2.44	0.07	3.92	0.10	1.65	0.07	2.89	0.16	0.38	0.05	0.58	0.05
63	-1.27	77.61	0.22	11.06	0.12	2.30	0.07	3.83	0.09	1.55	0.07	2.71	0.15	0.37	0.05	0.58	0.05
64	-1.06	78.53	0.22	10.36	0.11	2.22	0.06	3.79	0.09	1.41	0.06	2.83	0.15	0.32	0.05	0.54	0.04
65	-0.85	79.57	0.22	9.78	0.10	2.12	0.06	3.75	0.09	1.27	0.05	2.63	0.14	0.37	0.05	0.51	0.04
66	-0.63	80.23	0.23	9.48	0.10	2.03	0.06	3.76	0.09	1.13	0.05	2.49	0.13	0.36	0.05	0.51	0.04
67	-0.42	80.76	0.23	9.11	0.10	2.00	0.06	3.75	0.09	1.16	0.05	2.49	0.13	0.28	0.04	0.45	0.04
68	-0.21	80.97	0.23	8.89	0.09	2.00	0.06	3.68	0.09	1.18	0.05	2.53	0.14	0.29	0.04	0.45	0.04
69	0.00	81.01	0.23	8.80	0.09	2.01	0.06	3.62	0.09	1.18	0.05	2.56	0.14	0.33	0.05	0.48	0.04
70	0.21	80.93	0.23	8.72	0.09	2.04	0.06	3.73	0.09	1.24	0.05	2.56	0.14	0.34	0.05	0.46	0.04
71	0.42	80.84	0.23	8.63	0.09	2.04	0.06	3.73	0.09	1.30	0.05	2.67	0.14	0.35	0.05	0.45	0.04
72	0.63	80.77	0.23	8.77	0.09	2.08	0.06	3.64	0.09	1.34	0.06	2.57	0.14	0.38	0.06	0.45	0.04
73	0.84	80.41	0.23	8.83	0.09	2.18	0.06	3.63	0.09	1.40	0.06	2.64	0.14	0.40	0.06	0.50	0.04
74	1.06	80.45	0.23	8.76	0.09	2.18	0.06	3.69	0.09	1.37	0.06	2.67	0.14	0.37	0.05	0.50	0.04
75	1.27	80.56	0.23	8.81	0.09	2.10	0.06	3.69	0.09	1.41	0.06	2.66	0.14	0.30	0.04	0.47	0.04
76	1.48	80.29	0.23	8.83	0.09	2.18	0.06	3.74	0.09	1.41	0.06	2.73	0.15	0.35	0.05	0.47	0.04
77	1.69	80.31	0.23	8.90	0.09	2.12	0.06	3.67	0.09	1.49	0.06	2.75	0.15	0.32	0.05	0.46	0.04
78	1.90	80.10	0.23	9.00	0.09	2.18	0.06	3.68	0.09	1.54	0.06	2.64	0.14	0.36	0.05	0.50	0.04
79	2.11	80.06	0.23	8.96	0.09	2.19	0.06	3.69	0.09	1.49	0.06	2.75	0.15	0.38	0.05	0.48	0.04
80	2.32	80.02	0.23	8.97	0.09	2.23	0.06	3.75	0.09	1.54	0.06	2.71	0.15	0.32	0.05	0.44	0.03
81	2.54	79.76	0.22	9.11	0.10	2.26	0.06	3.78	0.09	1.54	0.07	2.76	0.15	0.34	0.05	0.46	0.04
82	2.75	79.94	0.22	9.06	0.09	2.26	0.06	3.69	0.09	1.52	0.06	2.62	0.14	0.36	0.05	0.53	0.04
83	2.96	79.66	0.22	9.11	0.10	2.38	0.07	3.76	0.09	1.57	0.07	2.64	0.14	0.35	0.05	0.53	0.04
84	3.17	79.64	0.22	9.21	0.10	2.38	0.07	3.71	0.09	1.56	0.07	2.60	0.14	0.39	0.06	0.50	0.04
85	3.38	79.46	0.22	9.21	0.10	2.34	0.07	3.80	0.09	1.63	0.07	2.68	0.15	0.35	0.05	0.52	0.04
86	3.59	79.25	0.22	9.32	0.10	2.35	0.07	3.79	0.09	1.65	0.07	2.83	0.15	0.34	0.05	0.48	0.04
87	3.80	79.27	0.22	9.26	0.10	2.40	0.07	3.83	0.09	1.59	0.07	2.82	0.15	0.36	0.05	0.47	0.04
88	4.02	79.26	0.22	9.32	0.10	2.35	0.07	3.77	0.09	1.59	0.07	2.78	0.15	0.38	0.06	0.54	0.04
89	4.23	79.24	0.22	9.35	0.10	2.45	0.07	3.83	0.09	1.65	0.07	2.64	0.14	0.32	0.05	0.52	0.04
90	4.44	79.06	0.22	9.42	0.10	2.43	0.07	3.81	0.09	1.65	0.07	2.77	0.15	0.37	0.05	0.50	0.04
91	4.65	78.78	0.22	9.57	0.10	2.48	0.07	3.82	0.09	1.61	0.07	2.85	0.15	0.37	0.05	0.52	0.04
92	4.86	78.97	0.22	9.45	0.10	2.47	0.07	3.85	0.09	1.64	0.07	2.78	0.15	0.35	0.05	0.49	0.04
93	5.07	78.86	0.22	9.51	0.10	2.46	0.07	3.85	0.09	1.68	0.07	2.76	0.15	0.39	0.06	0.49	0.04
94	5.28	78.84	0.22	9.51	0.10	2.45	0.07	3.84	0.09	1.64	0.07	2.86	0.15	0.36	0.05	0.50	0.04
95	5.49	78.82	0.22	9.68	0.10	2.43	0.07	3.79	0.09	1.61	0.07	2.80	0.15	0.34	0.05	0.52	0.04
96	5.70	78.65	0.22	9.71	0.10	2.50	0.07	3.84	0.09	1.69	0.07	2.73	0.15	0.39	0.06	0.49	0.04
97	5.92	78.53	0.22	9.81	0.10	2.55	0.07	3.82	0.09	1.67	0.07	2.71	0.15	0.38	0.05	0.54	0.04
98	6.13	78.42	0.22	9.84	0.10	2.47	0.07	3.87	0.10	1.73	0.07	2.77	0.15	0.39	0.06	0.51	0.04
99	6.34	78.32	0.22	9.85	0.10	2.52	0.07	3.87	0.10	1.74	0.07	2.83	0.15	0.39	0.06	0.49	0.04
100	6.55	78.27	0.22	9.90	0.10	2.58	0.07	3.91	0.10	1.69	0.07	2.73	0.15	0.39	0.06	0.53	0.04
101	6.76	78.24	0.22	9.89	0.10	2.61	0.07	3.90	0.10	1.70	0.07	2.68	0.14	0.46	0.07	0.53	0.04
102	6.97	78.19	0.22	9.90	0.10	2.61	0.07	3.88	0.10	1.77	0.07	2.75	0.15	0.42	0.06	0.49	0.04
103	7.18	78.22	0.22	9.83	0.10	2.57	0.07	3.89	0.10	1.72	0.07	2.90	0.16	0.38	0.05	0.49	0.04
104	7.39	78.05	0.22	9.90	0.10	2.61	0.07	4.05	0.10	1.70	0.07	2.79	0.15	0.41	0.06	0.49	0.04
105	7.61	78.00	0.22	9.98	0.10	2.67	0.08	3.93	0.10	1.76	0.07	2.75	0.15	0.40	0.06	0.51	0.04
106	7.82	77.93	0.22	9.95	0.10	2.64	0.08	3.93	0.10	1.78	0.07	2.85	0.15	0.40	0.06	0.52	0.04
107	8.03	77.92	0.22	10.14	0.11	2.65	0.08	3.86	0.09	1.69	0.07	2.82	0.15	0.39	0.06	0.53	0.04
108	8.24	77.94	0.22	10.11	0.11	2.62	0.08	3.93	0.10	1.68	0.07	2.75	0.15	0.45	0.07	0.51	0.04
109	8.45	77.79	0.22	10.19	0.11	2.73	0.08	3.84	0.09	1.70	0.07	2.87	0.16	0.40	0.06	0.47	0.04
110	8.66	77.79	0.22	10.24	0.11	2.66	0.08	3.87	0.10	1.65	0.07	2.95	0.16	0.38	0.05	0.46	0.04
111	8.87	77.95	0.22	10.28	0.11	2.70	0.08	3.83	0.09	1.67	0.07	2.71	0.15	0.32	0.05	0.54	0.04
112	9.09	77.79	0.22	10.25	0.11	2.63	0.08	3.93	0.10	1.76	0.07	2.77	0.15	0.34	0.05	0.54	0.04

113	9.30	77.88	0.22	10.16	0.11	2.58	0.07	4.00	0.10	1.77	0.07	2.76	0.15	0.33	0.05	0.52	0.04
114	9.51	77.47	0.22	10.27	0.11	2.68	0.08	3.93	0.10	1.77	0.07	2.89	0.16	0.42	0.06	0.56	0.04
115	9.72	77.61	0.22	10.32	0.11	2.70	0.08	4.01	0.10	1.72	0.07	2.77	0.15	0.37	0.05	0.48	0.04
116	9.93	77.44	0.22	10.34	0.11	2.71	0.08	4.03	0.10	1.75	0.07	2.85	0.15	0.37	0.05	0.51	0.04
117	10.14	77.39	0.22	10.39	0.11	2.69	0.08	4.01	0.10	1.73	0.07	2.89	0.16	0.37	0.05	0.53	0.04
118	10.35	77.31	0.22	10.26	0.11	2.72	0.08	4.09	0.10	1.80	0.08	2.93	0.16	0.38	0.05	0.51	0.04
119	10.56	77.40	0.22	10.42	0.11	2.71	0.08	4.12	0.10	1.74	0.07	2.67	0.14	0.39	0.06	0.54	0.04
120	10.78	77.25	0.22	10.46	0.11	2.74	0.08	4.13	0.10	1.79	0.08	2.80	0.15	0.34	0.05	0.50	0.04
121	10.99	77.16	0.22	10.42	0.11	2.73	0.08	4.06	0.10	1.88	0.08	2.89	0.16	0.37	0.05	0.50	0.04
122	11.20	77.10	0.22	10.49	0.11	2.72	0.08	4.03	0.10	1.89	0.08	2.83	0.15	0.43	0.06	0.51	0.04
123	11.41	77.10	0.22	10.56	0.11	2.71	0.08	4.02	0.10	1.79	0.08	2.89	0.16	0.41	0.06	0.52	0.04
124	11.62	77.27	0.22	10.56	0.11	2.69	0.08	4.05	0.10	1.85	0.08	2.71	0.15	0.39	0.06	0.48	0.04
125	11.83	77.10	0.22	10.62	0.11	2.76	0.08	4.01	0.10	1.82	0.08	2.81	0.15	0.36	0.05	0.52	0.04
126	12.04	76.96	0.22	10.69	0.11	2.78	0.08	4.01	0.10	1.83	0.08	2.84	0.15	0.36	0.05	0.54	0.04
127	12.25	77.19	0.22	10.59	0.11	2.73	0.08	4.04	0.10	1.75	0.07	2.82	0.15	0.40	0.06	0.48	0.04
128	12.47	77.03	0.22	10.57	0.11	2.86	0.08	4.05	0.10	1.77	0.07	2.82	0.15	0.42	0.06	0.48	0.04
129	12.68	77.11	0.22	10.62	0.11	2.81	0.08	4.04	0.10	1.77	0.07	2.78	0.15	0.37	0.05	0.51	0.04
130	12.89	77.06	0.22	10.71	0.11	2.79	0.08	4.09	0.10	1.77	0.07	2.73	0.15	0.37	0.05	0.49	0.04
131	13.10	77.07	0.22	10.67	0.11	2.75	0.08	4.06	0.10	1.74	0.07	2.86	0.15	0.35	0.05	0.50	0.04
132	13.31	76.87	0.22	10.77	0.11	2.79	0.08	4.07	0.10	1.89	0.08	2.68	0.15	0.39	0.06	0.53	0.04
133	13.52	76.80	0.22	10.92	0.11	2.85	0.08	4.05	0.10	1.85	0.08	2.65	0.14	0.34	0.05	0.56	0.04
134	13.73	76.59	0.22	10.91	0.11	2.86	0.08	4.05	0.10	1.86	0.08	2.82	0.15	0.37	0.05	0.54	0.04
135	13.95	76.76	0.22	10.75	0.11	2.79	0.08	4.16	0.10	1.85	0.08	2.79	0.15	0.34	0.05	0.55	0.04
136	14.16	76.57	0.22	10.96	0.11	2.79	0.08	4.11	0.10	1.87	0.08	2.79	0.15	0.41	0.06	0.50	0.04
137	14.37	76.77	0.22	10.78	0.11	2.81	0.08	4.12	0.10	1.77	0.07	2.90	0.16	0.35	0.05	0.51	0.04
138	14.58	76.72	0.22	10.79	0.11	2.93	0.08	4.07	0.10	1.78	0.08	2.79	0.15	0.42	0.06	0.49	0.04
139	14.79	76.50	0.22	10.86	0.11	2.97	0.09	4.05	0.10	1.77	0.07	2.87	0.16	0.46	0.07	0.53	0.04
140	15.00	76.41	0.21	10.98	0.12	2.82	0.08	4.08	0.10	1.92	0.08	2.88	0.16	0.42	0.06	0.50	0.04
141	15.21	76.48	0.22	11.02	0.12	2.83	0.08	4.13	0.10	1.87	0.08	2.81	0.15	0.34	0.05	0.51	0.04
142	15.42	76.56	0.22	10.90	0.11	2.85	0.08	4.21	0.10	1.90	0.08	2.79	0.15	0.35	0.05	0.45	0.04
143	15.63	76.68	0.22	10.78	0.11	2.85	0.08	4.09	0.10	1.84	0.08	2.89	0.16	0.37	0.05	0.49	0.04
144	15.85	76.69	0.22	10.89	0.11	2.94	0.08	4.10	0.10	1.82	0.08	2.73	0.15	0.36	0.05	0.46	0.04
145	16.06	76.49	0.22	10.95	0.11	2.99	0.09	4.07	0.10	1.85	0.08	2.76	0.15	0.37	0.05	0.52	0.04
146	16.27	76.64	0.22	11.06	0.12	2.90	0.08	4.05	0.10	1.83	0.08	2.64	0.14	0.40	0.06	0.48	0.04

Agglomerate FLD23.1.3

Table J.15: Major element compositions (as wt.% oxides) from a line traverse across the interface of surface agglomerate FLD23.1.3 (from agglomerate FLD23.1.3 to host FLD23) extracted from quantified EDS compositional maps. The EDS compositional maps were collected at a resolution of 4.7 pixels/μm. The smoothing width for this traverse was 100 pixels (21.1 μm) wide. This is an Si interface and has been centered at $x = 0$ based on the SiO_2 maximum. Peak points within 2σ of the SiO_2 maximum are highlighted in yellow. Uncertainties are 2SEOM.

Pt.	Position (μm)	SiO_2	2σ	Al_2O_3	2σ	Na_2O	2σ	K_2O	2σ	CaO	2σ	FeO	2σ	TiO_2	2σ	MgO	2σ
1	-13.31	74.02	0.23	12.89	0.14	3.03	0.10	4.18	0.11	1.86	0.09	2.98	0.18	0.46	0.07	0.57	0.05
2	-13.10	74.07	0.23	12.94	0.14	3.09	0.10	4.12	0.11	1.83	0.08	2.88	0.17	0.45	0.07	0.61	0.05
3	-12.89	74.08	0.23	12.93	0.14	3.09	0.10	4.17	0.11	1.82	0.08	2.84	0.17	0.45	0.07	0.60	0.05
4	-12.68	74.21	0.23	12.94	0.14	3.13	0.10	4.01	0.11	1.80	0.08	2.92	0.18	0.40	0.06	0.59	0.05
5	-12.47	74.03	0.23	12.88	0.14	3.14	0.10	4.10	0.11	1.92	0.09	2.93	0.18	0.39	0.06	0.62	0.05
6	-12.25	74.16	0.23	12.86	0.14	3.04	0.10	4.13	0.11	1.89	0.09	2.94	0.18	0.42	0.06	0.57	0.05
7	-12.04	74.37	0.23	12.99	0.14	2.98	0.10	4.06	0.11	1.80	0.08	2.79	0.17	0.43	0.07	0.58	0.05
8	-11.83	74.47	0.23	12.84	0.14	2.90	0.09	4.20	0.11	1.80	0.08	2.92	0.18	0.33	0.05	0.55	0.05
9	-11.62	74.53	0.23	12.82	0.14	2.98	0.10	4.07	0.11	1.88	0.09	2.80	0.17	0.35	0.05	0.57	0.05
10	-11.41	74.15	0.23	12.86	0.14	3.03	0.10	4.13	0.11	1.91	0.09	2.89	0.17	0.41	0.06	0.62	0.05
11	-11.20	74.22	0.23	12.67	0.14	2.94	0.09	4.18	0.11	2.01	0.09	2.98	0.18	0.40	0.06	0.61	0.05
12	-10.99	74.18	0.23	12.78	0.14	3.00	0.10	4.16	0.11	1.91	0.09	2.93	0.18	0.44	0.07	0.59	0.05
13	-10.78	74.23	0.23	12.91	0.14	2.92	0.09	4.13	0.11	1.93	0.09	2.86	0.17	0.40	0.06	0.63	0.05
14	-10.56	74.16	0.23	12.98	0.14	2.95	0.09	4.14	0.11	1.93	0.09	2.82	0.17	0.37	0.06	0.65	0.05
15	-10.35	74.29	0.23	12.95	0.14	2.91	0.09	4.06	0.11	1.91	0.09	2.89	0.17	0.42	0.06	0.58	0.05
16	-10.14	74.30	0.23	12.96	0.14	2.81	0.09	4.06	0.11	1.83	0.08	3.07	0.18	0.40	0.06	0.57	0.05
17	-9.93	74.34	0.23	12.80	0.14	2.87	0.09	4.08	0.11	1.84	0.09	3.05	0.18	0.42	0.07	0.59	0.05
18	-9.72	74.35	0.23	12.76	0.14	2.81	0.09	4.13	0.11	1.84	0.09	3.10	0.19	0.42	0.07	0.59	0.05
19	-9.51	74.33	0.23	12.78	0.14	2.87	0.09	4.18	0.11	1.77	0.08	3.02	0.18	0.46	0.07	0.59	0.05
20	-9.30	74.50	0.23	12.78	0.14	2.79	0.09	4.07	0.11	1.76	0.08	3.04	0.18	0.46	0.07	0.60	0.05
21	-9.09	74.38	0.23	12.78	0.14	2.79	0.09	4.11	0.11	1.84	0.09	3.03	0.18	0.45	0.07	0.62	0.05
22	-8.87	74.63	0.23	12.86	0.14	2.83	0.09	4.17	0.11	1.79	0.08	2.75	0.17	0.39	0.06	0.59	0.05
23	-8.66	74.72	0.23	12.75	0.14	2.88	0.09	4.17	0.11	1.79	0.08	2.77	0.17	0.36	0.06	0.57	0.05
24	-8.45	74.49	0.23	12.86	0.14	2.88	0.09	4.18	0.11	1.84	0.09	2.78	0.17	0.42	0.06	0.57	0.05
25	-8.24	74.43	0.23	12.80	0.14	2.86	0.09	4.12	0.11	1.91	0.09	2.90	0.17	0.42	0.06	0.56	0.05
26	-8.03	74.51	0.23	12.87	0.14	2.83	0.09	4.19	0.11	1.90	0.09	2.75	0.17	0.39	0.06	0.57	0.05
27	-7.82	74.50	0.23	12.96	0.14	2.77	0.09	4.18	0.11	1.85	0.09	2.82	0.17	0.34	0.05	0.58	0.05
28	-7.61	74.16	0.23	13.10	0.15	2.74	0.09	4.20	0.11	1.88	0.09	2.86	0.17	0.43	0.07	0.62	0.05
29	-7.39	74.19	0.23	13.05	0.14	2.74	0.09	4.09	0.11	1.92	0.09	3.01	0.18	0.40	0.06	0.60	0.05
30	-7.18	73.95	0.23	13.18	0.15	2.85	0.09	4.16	0.11	1.89	0.09	2.94	0.18	0.44	0.07	0.60	0.05
31	-6.97	73.89	0.23	13.18	0.15	2.86	0.09	4.09	0.11	1.93	0.09	3.04	0.18	0.41	0.06	0.61	0.05
32	-6.76	74.05	0.23	13.18	0.15	2.84	0.09	4.12	0.11	1.91	0.09	2.84	0.17	0.45	0.07	0.61	0.05
33	-6.55	73.80	0.23	13.24	0.15	2.86	0.09	4.09	0.11	1.94	0.09	2.89	0.17	0.53	0.08	0.65	0.05
34	-6.34	73.71	0.23	13.30	0.15	2.80	0.09	4.25	0.12	2.00	0.09	2.93	0.18	0.41	0.06	0.60	0.05
35	-6.13	73.79	0.23	13.34	0.15	2.84	0.09	4.13	0.11	1.97	0.09	2.87	0.17	0.47	0.07	0.60	0.05
36	-5.92	73.60	0.23	13.42	0.15	2.81	0.09	4.13	0.11	1.99	0.09	3.03	0.18	0.41	0.06	0.62	0.05
37	-5.71	73.24	0.23	13.49	0.15	2.85	0.09	4.15	0.11	2.07	0.10	3.15	0.19	0.41	0.06	0.64	0.05
38	-5.49	73.32	0.23	13.42	0.15	2.97	0.10	4.19	0.11	2.06	0.10	2.92	0.18	0.51	0.08	0.60	0.05
39	-5.28	73.40	0.23	13.54	0.15	2.87	0.09	4.23	0.12	2.10	0.10	2.79	0.17	0.47	0.07	0.60	0.05
40	-5.07	73.44	0.23	13.51	0.15	2.91	0.09	4.21	0.11	1.95	0.09	2.99	0.18	0.44	0.07	0.55	0.05
41	-4.86	73.32	0.23	13.51	0.15	2.89	0.09	4.15	0.11	2.05	0.10	3.08	0.19	0.42	0.06	0.58	0.05
42	-4.65	73.43	0.23	13.52	0.15	2.90	0.09	4.18	0.11	2.01	0.09	2.92	0.18	0.42	0.07	0.61	0.05
43	-4.44	73.24	0.23	13.49	0.15	2.91	0.09	4.20	0.11	2.15	0.10	2.95	0.18	0.47	0.07	0.59	0.05
44	-4.23	73.07	0.23	13.55	0.15	2.90	0.09	4.27	0.12	2.14	0.10	3.02	0.18	0.49	0.08	0.56	0.05
45	-4.02	73.35	0.23	13.53	0.15	2.97	0.10	4.13	0.11	2.09	0.10	2.97	0.18	0.41	0.06	0.55	0.05
46	-3.80	73.28	0.23	13.45	0.15	2.89	0.09	4.18	0.11	2.17	0.10	2.95	0.18	0.48	0.07	0.61	0.05
47	-3.59	73.41	0.23	13.22	0.15	2.84	0.09	4.29	0.12	2.09	0.10	3.06	0.18	0.49	0.08	0.59	0.05
48	-3.38	73.54	0.23	13.17	0.15	2.91	0.09	4.20	0.11	2.05	0.10	3.06	0.18	0.45	0.07	0.61	0.05
49	-3.17	73.78	0.23	12.95	0.14	2.78	0.09	4.27	0.12	2.02	0.09	3.13	0.19	0.47	0.07	0.60	0.05
50	-2.96	74.01	0.23	12.90	0.14	2.75	0.09	4.21	0.11	2.02	0.09	3.09	0.19	0.43	0.07	0.60	0.05

51	-2.75	74.19	0.23	12.78	0.14	2.76	0.09	4.11	0.11	2.06	0.10	3.10	0.19	0.37	0.06	0.63	0.05
52	-2.54	74.71	0.23	12.80	0.14	2.70	0.09	3.97	0.11	1.91	0.09	2.86	0.17	0.42	0.06	0.63	0.05
53	-2.32	74.98	0.23	12.58	0.14	2.69	0.09	3.99	0.11	1.87	0.09	2.88	0.17	0.40	0.06	0.62	0.05
54	-2.11	75.82	0.24	12.06	0.13	2.56	0.08	4.03	0.11	1.75	0.08	2.79	0.17	0.41	0.06	0.57	0.05
55	-1.90	76.25	0.24	11.79	0.13	2.53	0.08	3.99	0.11	1.71	0.08	2.78	0.17	0.39	0.06	0.56	0.05
56	-1.69	76.98	0.24	11.46	0.13	2.48	0.08	3.93	0.11	1.54	0.07	2.65	0.16	0.43	0.07	0.52	0.04
57	-1.48	77.62	0.24	11.07	0.12	2.40	0.08	3.92	0.11	1.44	0.07	2.71	0.16	0.30	0.05	0.55	0.05
58	-1.27	78.09	0.24	10.63	0.12	2.29	0.07	4.00	0.11	1.41	0.07	2.67	0.16	0.37	0.06	0.54	0.04
59	-1.06	79.02	0.25	10.27	0.11	2.20	0.07	3.86	0.11	1.23	0.06	2.48	0.15	0.41	0.06	0.53	0.04
60	-0.85	79.66	0.25	9.86	0.11	2.09	0.07	3.79	0.10	1.09	0.05	2.66	0.16	0.39	0.06	0.45	0.04
61	-0.63	80.27	0.25	9.41	0.10	2.04	0.07	3.91	0.11	1.06	0.05	2.48	0.15	0.36	0.06	0.46	0.04
62	-0.42	80.45	0.25	9.12	0.10	2.03	0.07	3.95	0.11	1.08	0.05	2.57	0.15	0.33	0.05	0.48	0.04
63	-0.21	80.69	0.25	9.05	0.10	2.00	0.06	3.72	0.10	1.12	0.05	2.63	0.16	0.35	0.05	0.44	0.04
64	0.00	80.96	0.25	9.00	0.10	1.94	0.06	3.66	0.10	1.09	0.05	2.52	0.15	0.37	0.06	0.45	0.04
65	0.21	80.90	0.25	8.97	0.10	1.95	0.06	3.66	0.10	1.16	0.05	2.57	0.15	0.34	0.05	0.44	0.04
66	0.42	80.92	0.25	8.97	0.10	1.90	0.06	3.69	0.10	1.15	0.05	2.50	0.15	0.37	0.06	0.49	0.04
67	0.63	80.63	0.25	8.98	0.10	1.97	0.06	3.62	0.10	1.20	0.06	2.73	0.16	0.38	0.06	0.48	0.04
68	0.85	80.79	0.25	8.94	0.10	2.01	0.06	3.65	0.10	1.23	0.06	2.53	0.15	0.39	0.06	0.45	0.04
69	1.06	80.49	0.25	9.04	0.10	2.00	0.06	3.76	0.10	1.27	0.06	2.62	0.16	0.34	0.05	0.48	0.04
70	1.27	80.47	0.25	9.10	0.10	1.98	0.06	3.80	0.10	1.28	0.06	2.49	0.15	0.36	0.06	0.51	0.04
71	1.48	80.30	0.25	9.12	0.10	2.04	0.07	3.81	0.10	1.33	0.06	2.58	0.16	0.32	0.05	0.49	0.04
72	1.69	80.25	0.25	9.05	0.10	2.11	0.07	3.75	0.10	1.37	0.06	2.60	0.16	0.33	0.05	0.54	0.04
73	1.90	80.08	0.25	9.16	0.10	2.09	0.07	3.69	0.10	1.32	0.06	2.78	0.17	0.36	0.06	0.51	0.04
74	2.11	79.81	0.25	9.31	0.10	2.17	0.07	3.82	0.10	1.35	0.06	2.66	0.16	0.38	0.06	0.49	0.04
75	2.32	79.79	0.25	9.43	0.10	2.11	0.07	3.77	0.10	1.40	0.06	2.63	0.16	0.37	0.06	0.50	0.04
76	2.54	79.79	0.25	9.42	0.10	2.02	0.06	3.83	0.10	1.32	0.06	2.74	0.16	0.42	0.07	0.46	0.04
77	2.75	79.47	0.25	9.43	0.10	2.13	0.07	3.72	0.10	1.43	0.07	2.89	0.17	0.39	0.06	0.53	0.04
78	2.96	79.40	0.25	9.44	0.10	2.16	0.07	3.80	0.10	1.41	0.07	2.84	0.17	0.47	0.07	0.49	0.04
79	3.17	79.31	0.25	9.52	0.11	2.22	0.07	3.84	0.10	1.54	0.07	2.66	0.16	0.40	0.06	0.50	0.04
80	3.38	79.29	0.25	9.55	0.11	2.28	0.07	3.81	0.10	1.46	0.07	2.72	0.16	0.35	0.05	0.54	0.04
81	3.59	79.23	0.25	9.61	0.11	2.25	0.07	3.83	0.10	1.48	0.07	2.69	0.16	0.40	0.06	0.51	0.04
82	3.80	79.01	0.25	9.60	0.11	2.28	0.07	3.87	0.11	1.58	0.07	2.77	0.17	0.38	0.06	0.49	0.04
83	4.01	79.12	0.25	9.72	0.11	2.29	0.07	3.84	0.10	1.52	0.07	2.61	0.16	0.36	0.06	0.54	0.05
84	4.23	78.93	0.25	9.82	0.11	2.25	0.07	3.82	0.10	1.56	0.07	2.71	0.16	0.38	0.06	0.52	0.04
85	4.44	78.72	0.25	9.75	0.11	2.31	0.07	3.88	0.11	1.62	0.07	2.84	0.17	0.40	0.06	0.49	0.04
86	4.65	78.77	0.25	9.91	0.11	2.36	0.08	3.81	0.10	1.61	0.07	2.69	0.16	0.36	0.06	0.48	0.04
87	4.86	78.74	0.25	10.00	0.11	2.31	0.07	3.80	0.10	1.58	0.07	2.68	0.16	0.34	0.05	0.54	0.05
88	5.07	78.75	0.25	9.88	0.11	2.27	0.07	3.89	0.11	1.63	0.08	2.76	0.17	0.30	0.05	0.52	0.04
89	5.28	78.50	0.25	10.02	0.11	2.38	0.08	3.86	0.11	1.61	0.07	2.70	0.16	0.37	0.06	0.55	0.05
90	5.49	78.50	0.25	9.88	0.11	2.36	0.08	4.04	0.11	1.54	0.07	2.82	0.17	0.39	0.06	0.48	0.04
91	5.70	78.34	0.24	10.02	0.11	2.46	0.08	4.02	0.11	1.58	0.07	2.71	0.16	0.38	0.06	0.49	0.04
92	5.92	78.41	0.24	10.03	0.11	2.44	0.08	3.91	0.11	1.57	0.07	2.73	0.16	0.38	0.06	0.53	0.04
93	6.13	78.17	0.24	10.03	0.11	2.48	0.08	3.99	0.11	1.62	0.08	2.75	0.17	0.39	0.06	0.56	0.05
94	6.34	78.14	0.24	10.09	0.11	2.54	0.08	3.99	0.11	1.67	0.08	2.72	0.16	0.34	0.05	0.51	0.04
95	6.55	78.15	0.24	10.12	0.11	2.48	0.08	3.98	0.11	1.67	0.08	2.76	0.17	0.32	0.05	0.52	0.04
96	6.76	78.23	0.24	10.19	0.11	2.44	0.08	4.00	0.11	1.60	0.07	2.63	0.16	0.37	0.06	0.54	0.04
97	6.97	78.42	0.24	10.11	0.11	2.40	0.08	3.93	0.11	1.60	0.07	2.69	0.16	0.36	0.06	0.48	0.04
98	7.18	78.20	0.24	10.28	0.11	2.51	0.08	3.88	0.11	1.53	0.07	2.69	0.16	0.40	0.06	0.52	0.04
99	7.39	78.15	0.24	10.30	0.11	2.56	0.08	3.87	0.11	1.60	0.07	2.65	0.16	0.37	0.06	0.49	0.04
100	7.61	77.94	0.24	10.46	0.12	2.51	0.08	3.94	0.11	1.61	0.07	2.66	0.16	0.41	0.06	0.48	0.04
101	7.82	77.84	0.24	10.36	0.11	2.54	0.08	4.00	0.11	1.62	0.08	2.74	0.16	0.38	0.06	0.52	0.04
102	8.03	77.85	0.24	10.30	0.11	2.45	0.08	4.03	0.11	1.66	0.08	2.80	0.17	0.41	0.06	0.51	0.04
103	8.24	77.88	0.24	10.28	0.11	2.47	0.08	4.00	0.11	1.73	0.08	2.77	0.17	0.41	0.06	0.45	0.04
104	8.45	77.78	0.24	10.34	0.11	2.51	0.08	4.05	0.11	1.73	0.08	2.73	0.16	0.40	0.06	0.46	0.04
105	8.66	77.80	0.24	10.41	0.12	2.58	0.08	3.90	0.11	1.70	0.08	2.73	0.16	0.40	0.06	0.48	0.04
106	8.87	77.79	0.24	10.44	0.12	2.59	0.08	3.85	0.11	1.69	0.08	2.76	0.17	0.39	0.06	0.49	0.04
107	9.09	77.45	0.24	10.53	0.12	2.61	0.08	3.95	0.11	1.75	0.08	2.77	0.17	0.42	0.07	0.52	0.04
108	9.30	77.40	0.24	10.45	0.12	2.61	0.08	4.14	0.11	1.76	0.08	2.69	0.16	0.42	0.07	0.53	0.04
109	9.51	77.61	0.24	10.48	0.12	2.63	0.08	4.02	0.11	1.74	0.08	2.67	0.16	0.36	0.06	0.48	0.04
110	9.72	77.88	0.24	10.47	0.12	2.60	0.08	3.95	0.11	1.65	0.08	2.61	0.16	0.36	0.06	0.48	0.04
111	9.93	77.61	0.24	10.53	0.12	2.61	0.08	3.92	0.11	1.66	0.08	2.76	0.17	0.41	0.06	0.51	0.04
112	10.14	77.55	0.24	10.56	0.12	2.63	0.08	4.01	0.11	1.73	0.08	2.71	0.16	0.33	0.05	0.48	0.04

113	10.35	77.39	0.24	10.66	0.12	2.63	0.08	4.01	0.11	1.74	0.08	2.63	0.16	0.41	0.06	0.52	0.04
114	10.56	77.53	0.24	10.51	0.12	2.56	0.08	4.04	0.11	1.67	0.08	2.71	0.16	0.44	0.07	0.54	0.04
115	10.77	77.50	0.24	10.65	0.12	2.68	0.09	3.99	0.11	1.71	0.08	2.64	0.16	0.35	0.05	0.48	0.04
116	10.99	77.13	0.24	10.61	0.12	2.63	0.08	4.11	0.11	1.77	0.08	2.86	0.17	0.44	0.07	0.45	0.04
117	11.20	77.11	0.24	10.76	0.12	2.68	0.09	4.09	0.11	1.73	0.08	2.76	0.17	0.38	0.06	0.50	0.04
118	11.41	77.11	0.24	10.73	0.12	2.69	0.09	4.06	0.11	1.77	0.08	2.77	0.17	0.36	0.06	0.52	0.04
119	11.62	77.21	0.24	10.56	0.12	2.74	0.09	4.08	0.11	1.72	0.08	2.73	0.16	0.44	0.07	0.52	0.04
120	11.83	77.06	0.24	10.59	0.12	2.77	0.09	4.09	0.11	1.75	0.08	2.82	0.17	0.44	0.07	0.48	0.04
121	12.04	76.89	0.24	10.80	0.12	2.76	0.09	4.18	0.11	1.76	0.08	2.76	0.17	0.35	0.05	0.51	0.04
122	12.25	76.87	0.24	10.84	0.12	2.69	0.09	4.08	0.11	1.81	0.08	2.82	0.17	0.33	0.05	0.55	0.05
123	12.46	76.97	0.24	10.89	0.12	2.69	0.09	3.99	0.11	1.69	0.08	2.88	0.17	0.33	0.05	0.55	0.05
124	12.68	76.73	0.24	10.84	0.12	2.78	0.09	4.17	0.11	1.76	0.08	2.82	0.17	0.40	0.06	0.50	0.04
125	12.89	76.83	0.24	10.88	0.12	2.83	0.09	4.10	0.11	1.80	0.08	2.71	0.16	0.37	0.06	0.49	0.04
126	13.10	76.77	0.24	10.97	0.12	2.84	0.09	4.01	0.11	1.73	0.08	2.84	0.17	0.31	0.05	0.52	0.04
127	13.31	76.97	0.24	10.87	0.12	2.71	0.09	4.07	0.11	1.77	0.08	2.76	0.17	0.40	0.06	0.45	0.04

Agglomerate FLD23.2.1

Table J.16: Major element compositions (as wt.% oxides) from a line traverse across the interface of surface agglomerate FLD23.2.1 (from agglomerate FLD23.2.1 to host FLD23) extracted from quantified EDS compositional maps. The EDS compositional maps were collected at a resolution of 7.4 pixels/μm. The smoothing width for this traverse was 100 pixels (13.5 μm) wide. This is an Si interface and has been centered at $x = 0$ based on the SiO_2 maximum. Peak points within 2σ of the SiO_2 maximum are highlighted in yellow. Uncertainties are 2SEOM.

Pt.	Position (μm)	SiO_2	2σ	Al_2O_3	2σ	Na_2O	2σ	K_2O	2σ	CaO	2σ	FeO	2σ	TiO_2	2σ	MgO	2σ
1	-4.32	73.16	0.28	13.52	0.14	3.00	0.12	3.95	0.09	2.27	0.11	3.02	0.20	0.46	0.08	0.63	0.08
2	-4.19	73.36	0.28	13.41	0.14	2.94	0.12	3.90	0.09	2.15	0.11	3.12	0.21	0.50	0.09	0.62	0.08
3	-4.05	73.74	0.28	13.50	0.14	2.94	0.12	3.85	0.09	2.21	0.11	2.76	0.18	0.43	0.08	0.57	0.08
4	-3.92	73.47	0.28	13.40	0.14	3.00	0.12	3.90	0.09	2.25	0.11	2.85	0.19	0.50	0.09	0.63	0.08
5	-3.78	73.41	0.28	13.38	0.14	3.07	0.12	3.87	0.09	2.16	0.11	3.01	0.20	0.46	0.08	0.64	0.09
6	-3.65	73.46	0.28	13.42	0.14	2.95	0.12	3.91	0.09	2.18	0.11	3.01	0.20	0.40	0.07	0.67	0.09
7	-3.51	73.83	0.28	13.22	0.14	2.83	0.12	3.96	0.09	2.15	0.11	3.00	0.20	0.42	0.08	0.57	0.08
8	-3.38	73.70	0.28	13.26	0.14	2.93	0.12	3.86	0.09	2.20	0.11	3.00	0.20	0.46	0.08	0.58	0.08
9	-3.24	73.39	0.28	13.31	0.14	3.00	0.12	3.85	0.09	2.15	0.11	3.09	0.20	0.60	0.11	0.60	0.08
10	-3.11	73.36	0.28	13.41	0.14	2.89	0.12	3.89	0.09	2.24	0.11	3.02	0.20	0.50	0.09	0.70	0.09
11	-2.97	73.57	0.28	13.23	0.14	2.90	0.12	3.81	0.09	2.18	0.11	3.15	0.21	0.56	0.10	0.59	0.08
12	-2.84	73.60	0.28	13.16	0.14	2.99	0.12	3.92	0.09	2.06	0.10	3.10	0.21	0.54	0.10	0.63	0.08
13	-2.70	73.77	0.28	13.25	0.14	2.98	0.12	3.84	0.09	2.14	0.11	2.89	0.19	0.54	0.10	0.59	0.08
14	-2.57	73.95	0.28	13.01	0.13	2.94	0.12	3.79	0.09	2.15	0.11	2.88	0.19	0.58	0.11	0.69	0.09
15	-2.43	74.01	0.28	13.00	0.13	2.95	0.12	3.96	0.09	2.18	0.11	2.76	0.18	0.50	0.09	0.63	0.08
16	-2.30	74.04	0.28	12.79	0.13	2.91	0.12	3.92	0.09	2.12	0.11	3.05	0.20	0.55	0.10	0.63	0.08
17	-2.16	74.09	0.28	12.99	0.13	2.83	0.12	3.96	0.09	2.22	0.11	2.80	0.19	0.49	0.09	0.62	0.08
18	-2.03	74.34	0.28	12.98	0.13	2.81	0.11	3.92	0.09	2.07	0.10	2.74	0.18	0.54	0.10	0.60	0.08
19	-1.89	74.36	0.28	12.89	0.13	2.92	0.12	3.90	0.09	2.03	0.10	2.76	0.18	0.55	0.10	0.59	0.08
20	-1.76	74.63	0.28	12.63	0.13	2.88	0.12	3.89	0.09	2.00	0.10	2.81	0.19	0.52	0.10	0.64	0.09
21	-1.62	75.13	0.28	12.53	0.13	2.77	0.11	3.77	0.09	1.96	0.10	2.81	0.19	0.41	0.07	0.61	0.08
22	-1.49	75.41	0.28	12.31	0.13	2.73	0.11	3.90	0.09	1.85	0.09	2.76	0.18	0.46	0.08	0.57	0.08
23	-1.35	75.28	0.28	12.22	0.13	2.78	0.11	3.77	0.09	1.97	0.10	2.90	0.19	0.50	0.09	0.58	0.08
24	-1.22	75.62	0.29	12.01	0.12	2.74	0.11	3.83	0.09	1.89	0.09	2.89	0.19	0.45	0.08	0.58	0.08
25	-1.08	76.02	0.29	11.85	0.12	2.59	0.11	3.75	0.09	1.84	0.09	2.92	0.19	0.45	0.08	0.56	0.07
26	-0.95	76.44	0.29	11.61	0.12	2.58	0.11	3.77	0.09	1.79	0.09	2.83	0.19	0.45	0.08	0.53	0.07
27	-0.81	76.80	0.29	11.38	0.12	2.58	0.11	3.62	0.09	1.83	0.09	2.88	0.19	0.35	0.06	0.55	0.07
28	-0.67	77.13	0.29	11.13	0.12	2.55	0.10	3.72	0.09	1.74	0.09	2.80	0.19	0.40	0.07	0.54	0.07
29	-0.54	77.40	0.29	11.07	0.11	2.42	0.10	3.75	0.09	1.70	0.09	2.69	0.18	0.42	0.08	0.55	0.07
30	-0.40	77.67	0.29	10.77	0.11	2.50	0.10	3.78	0.09	1.70	0.09	2.66	0.18	0.42	0.08	0.51	0.07
31	-0.27	77.84	0.29	10.60	0.11	2.48	0.10	3.71	0.09	1.61	0.08	2.78	0.18	0.42	0.08	0.56	0.07
32	-0.13	77.85	0.29	10.62	0.11	2.44	0.10	3.76	0.09	1.60	0.08	2.74	0.18	0.46	0.08	0.53	0.07
33	0.00	78.13	0.30	10.52	0.11	2.33	0.09	3.75	0.09	1.64	0.08	2.60	0.17	0.51	0.09	0.52	0.07
34	0.13	77.75	0.29	10.54	0.11	2.50	0.10	3.72	0.09	1.72	0.09	2.75	0.18	0.43	0.08	0.60	0.08
35	0.27	77.89	0.29	10.58	0.11	2.44	0.10	3.67	0.09	1.78	0.09	2.59	0.17	0.43	0.08	0.61	0.08
36	0.41	77.95	0.29	10.52	0.11	2.38	0.10	3.81	0.09	1.84	0.09	2.59	0.17	0.38	0.07	0.52	0.07
37	0.54	77.76	0.29	10.38	0.11	2.44	0.10	3.82	0.09	1.81	0.09	2.87	0.19	0.38	0.07	0.54	0.07
38	0.68	77.89	0.29	10.45	0.11	2.38	0.10	3.79	0.09	1.77	0.09	2.74	0.18	0.43	0.08	0.55	0.07
39	0.81	77.65	0.29	10.55	0.11	2.43	0.10	3.73	0.09	1.84	0.09	2.82	0.19	0.37	0.07	0.61	0.08
40	0.95	77.64	0.29	10.62	0.11	2.46	0.10	3.71	0.09	1.79	0.09	2.70	0.18	0.46	0.08	0.64	0.09
41	1.08	77.86	0.29	10.53	0.11	2.40	0.10	3.71	0.09	1.86	0.09	2.68	0.18	0.39	0.07	0.57	0.08
42	1.22	77.86	0.29	10.49	0.11	2.38	0.10	3.83	0.09	1.89	0.09	2.62	0.17	0.35	0.06	0.57	0.08
43	1.35	77.50	0.29	10.55	0.11	2.38	0.10	3.83	0.09	1.92	0.10	2.82	0.19	0.37	0.07	0.63	0.08
44	1.49	77.66	0.29	10.58	0.11	2.44	0.10	3.68	0.09	1.83	0.09	2.81	0.19	0.46	0.08	0.53	0.07
45	1.62	77.59	0.29	10.69	0.11	2.38	0.10	3.77	0.09	1.89	0.09	2.72	0.18	0.43	0.08	0.53	0.07
46	1.76	77.67	0.29	10.59	0.11	2.42	0.10	3.72	0.09	1.86	0.09	2.79	0.18	0.37	0.07	0.58	0.08
47	1.89	77.36	0.29	10.60	0.11	2.37	0.10	3.71	0.09	1.87	0.09	3.03	0.20	0.47	0.09	0.59	0.08
48	2.03	77.64	0.29	10.76	0.11	2.44	0.10	3.80	0.09	1.90	0.10	2.56	0.17	0.37	0.07	0.54	0.07
49	2.16	77.67	0.29	10.64	0.11	2.46	0.10	3.80	0.09	1.93	0.10	2.67	0.18	0.29	0.05	0.55	0.07
50	2.30	77.29	0.29	10.66	0.11	2.44	0.10	3.83	0.09	1.93	0.10	2.86	0.19	0.44	0.08	0.54	0.07

51	2.43	77.41	0.29	10.73	0.11	2.42	0.10	3.79	0.09	1.91	0.10	2.85	0.19	0.35	0.06	0.54	0.07
52	2.57	77.30	0.29	10.70	0.11	2.47	0.10	3.70	0.09	1.90	0.10	2.86	0.19	0.46	0.08	0.61	0.08
53	2.70	77.26	0.29	10.72	0.11	2.51	0.10	3.68	0.09	1.92	0.10	2.88	0.19	0.49	0.09	0.54	0.07
54	2.84	77.15	0.29	10.82	0.11	2.36	0.10	3.76	0.09	2.04	0.10	2.90	0.19	0.45	0.08	0.52	0.07
55	2.97	77.11	0.29	11.03	0.11	2.41	0.10	3.71	0.09	1.90	0.10	2.89	0.19	0.39	0.07	0.56	0.07
56	3.11	77.14	0.29	10.86	0.11	2.43	0.10	3.81	0.09	1.91	0.10	2.84	0.19	0.43	0.08	0.58	0.08
57	3.24	76.96	0.29	10.96	0.11	2.45	0.10	3.78	0.09	1.96	0.10	2.98	0.20	0.37	0.07	0.53	0.07
58	3.38	76.97	0.29	10.89	0.11	2.47	0.10	3.70	0.09	2.05	0.10	2.89	0.19	0.48	0.09	0.55	0.07
59	3.51	76.79	0.29	11.04	0.11	2.50	0.10	3.72	0.09	2.03	0.10	2.94	0.19	0.44	0.08	0.55	0.07
60	3.65	77.03	0.29	10.98	0.11	2.39	0.10	3.75	0.09	2.03	0.10	2.88	0.19	0.43	0.08	0.51	0.07
61	3.78	76.65	0.29	10.97	0.11	2.46	0.10	3.81	0.09	2.14	0.11	2.95	0.20	0.46	0.08	0.56	0.08
62	3.92	76.68	0.29	11.07	0.11	2.40	0.10	3.81	0.09	2.01	0.10	3.02	0.20	0.44	0.08	0.57	0.08
63	4.05	76.50	0.29	11.11	0.11	2.48	0.10	3.79	0.09	2.05	0.10	3.06	0.20	0.42	0.08	0.58	0.08
64	4.19	76.37	0.29	11.11	0.11	2.52	0.10	3.77	0.09	2.18	0.11	3.09	0.20	0.45	0.08	0.51	0.07
65	4.32	76.51	0.29	11.21	0.12	2.48	0.10	3.76	0.09	2.10	0.11	2.92	0.19	0.39	0.07	0.63	0.08
66	4.46	76.29	0.29	11.23	0.12	2.56	0.10	3.86	0.09	2.16	0.11	2.89	0.19	0.43	0.08	0.59	0.08
67	4.60	76.22	0.29	11.34	0.12	2.48	0.10	3.75	0.09	2.06	0.10	3.11	0.21	0.38	0.07	0.66	0.09
68	4.73	76.65	0.29	11.33	0.12	2.43	0.10	3.74	0.09	2.11	0.11	2.75	0.18	0.43	0.08	0.56	0.08
69	4.87	76.38	0.29	11.34	0.12	2.43	0.10	3.78	0.09	2.10	0.11	2.89	0.19	0.47	0.09	0.60	0.08
70	5.00	76.06	0.29	11.31	0.12	2.53	0.10	3.84	0.09	2.17	0.11	3.04	0.20	0.43	0.08	0.62	0.08
71	5.13	76.06	0.29	11.39	0.12	2.59	0.11	3.75	0.09	2.21	0.11	2.99	0.20	0.44	0.08	0.58	0.08
72	5.27	76.01	0.29	11.44	0.12	2.50	0.10	3.91	0.09	2.28	0.11	2.94	0.19	0.38	0.07	0.54	0.07
73	5.41	75.93	0.29	11.47	0.12	2.50	0.10	3.78	0.09	2.16	0.11	3.21	0.21	0.42	0.08	0.53	0.07
74	5.54	75.97	0.29	11.50	0.12	2.51	0.10	3.85	0.09	2.22	0.11	2.90	0.19	0.46	0.08	0.59	0.08
75	5.68	75.92	0.29	11.52	0.12	2.53	0.10	3.90	0.09	2.20	0.11	2.91	0.19	0.42	0.08	0.60	0.08
76	5.81	75.71	0.29	11.70	0.12	2.51	0.10	3.76	0.09	2.27	0.11	2.84	0.19	0.52	0.10	0.67	0.09
77	5.95	75.62	0.29	11.61	0.12	2.55	0.10	3.88	0.09	2.20	0.11	3.04	0.20	0.49	0.09	0.62	0.08
78	6.08	75.80	0.29	11.57	0.12	2.55	0.10	3.86	0.09	2.22	0.11	3.05	0.20	0.40	0.07	0.55	0.07
79	6.22	75.56	0.29	11.59	0.12	2.70	0.11	3.89	0.09	2.34	0.12	2.93	0.19	0.44	0.08	0.56	0.08
80	6.35	75.51	0.29	11.73	0.12	2.62	0.11	3.93	0.09	2.29	0.11	2.92	0.19	0.43	0.08	0.57	0.08
81	6.49	75.65	0.29	11.70	0.12	2.71	0.11	3.88	0.09	2.22	0.11	2.80	0.19	0.42	0.08	0.62	0.08
82	6.62	75.28	0.28	11.79	0.12	2.62	0.11	3.99	0.09	2.40	0.12	2.86	0.19	0.48	0.09	0.58	0.08
83	6.76	75.24	0.28	11.74	0.12	2.61	0.11	3.86	0.09	2.38	0.12	3.08	0.20	0.53	0.10	0.56	0.07
84	6.89	75.50	0.29	11.73	0.12	2.63	0.11	3.86	0.09	2.27	0.11	3.05	0.20	0.38	0.07	0.58	0.08
85	7.03	75.40	0.28	11.89	0.12	2.61	0.11	3.81	0.09	2.22	0.11	3.13	0.21	0.41	0.08	0.53	0.07
86	7.16	75.34	0.28	11.91	0.12	2.67	0.11	3.80	0.09	2.24	0.11	2.98	0.20	0.47	0.09	0.59	0.08
87	7.30	75.52	0.29	12.02	0.12	2.55	0.10	3.82	0.09	2.20	0.11	2.87	0.19	0.45	0.08	0.58	0.08
88	7.43	75.61	0.29	11.97	0.12	2.55	0.10	3.81	0.09	2.13	0.11	2.93	0.19	0.45	0.08	0.55	0.07
89	7.57	75.40	0.28	11.95	0.12	2.60	0.11	3.91	0.09	2.22	0.11	2.90	0.19	0.42	0.08	0.61	0.08
90	7.70	75.27	0.28	11.96	0.12	2.62	0.11	3.95	0.09	2.32	0.12	2.88	0.19	0.43	0.08	0.57	0.08
91	7.84	75.21	0.28	12.12	0.13	2.66	0.11	3.84	0.09	2.17	0.11	3.02	0.20	0.39	0.07	0.60	0.08
92	7.97	75.45	0.29	12.08	0.12	2.54	0.10	3.89	0.09	2.21	0.11	2.82	0.19	0.40	0.07	0.62	0.08
93	8.11	75.37	0.28	11.92	0.12	2.47	0.10	3.90	0.09	2.23	0.11	3.07	0.20	0.45	0.08	0.60	0.08
94	8.24	75.16	0.28	11.96	0.12	2.62	0.11	3.87	0.09	2.33	0.12	2.98	0.20	0.43	0.08	0.65	0.09
95	8.38	75.11	0.28	11.96	0.12	2.65	0.11	3.95	0.09	2.27	0.11	3.04	0.20	0.47	0.09	0.56	0.08
96	8.51	75.10	0.28	12.00	0.12	2.56	0.10	3.94	0.09	2.30	0.12	3.05	0.20	0.48	0.09	0.57	0.08
97	8.65	75.12	0.28	12.08	0.12	2.51	0.10	3.92	0.09	2.35	0.12	3.01	0.20	0.45	0.08	0.57	0.08
98	8.78	75.06	0.28	12.16	0.13	2.57	0.10	3.93	0.09	2.29	0.11	2.96	0.20	0.49	0.09	0.54	0.07
99	8.92	74.91	0.28	12.14	0.13	2.67	0.11	3.97	0.09	2.37	0.12	2.83	0.19	0.50	0.09	0.62	0.08
100	9.05	75.08	0.28	12.04	0.12	2.57	0.10	3.91	0.09	2.34	0.12	2.97	0.20	0.47	0.09	0.62	0.08
101	9.19	75.22	0.28	11.96	0.12	2.56	0.10	3.90	0.09	2.28	0.11	3.04	0.20	0.51	0.09	0.52	0.07
102	9.32	75.06	0.28	12.19	0.13	2.51	0.10	3.87	0.09	2.31	0.12	2.93	0.19	0.49	0.09	0.64	0.09
103	9.46	75.11	0.28	12.29	0.13	2.45	0.10	3.94	0.09	2.31	0.12	2.87	0.19	0.42	0.08	0.62	0.08
104	9.60	74.96	0.28	12.11	0.13	2.54	0.10	3.97	0.09	2.34	0.12	3.07	0.20	0.45	0.08	0.56	0.07
105	9.73	74.93	0.28	12.20	0.13	2.60	0.11	4.02	0.09	2.27	0.11	2.86	0.19	0.57	0.10	0.55	0.07
106	9.87	74.81	0.28	12.26	0.13	2.62	0.11	3.89	0.09	2.37	0.12	3.05	0.20	0.44	0.08	0.56	0.07
107	10.00	75.06	0.28	12.29	0.13	2.61	0.11	3.87	0.09	2.27	0.11	2.92	0.19	0.39	0.07	0.60	0.08
108	10.13	74.98	0.28	12.19	0.13	2.65	0.11	3.90	0.09	2.21	0.11	3.06	0.20	0.45	0.08	0.57	0.08
109	10.27	74.99	0.28	12.12	0.13	2.57	0.10	3.90	0.09	2.28	0.11	3.07	0.20	0.50	0.09	0.56	0.08
110	10.41	75.12	0.28	12.26	0.13	2.57	0.10	3.81	0.09	2.26	0.11	2.97	0.20	0.45	0.08	0.57	0.08
111	10.54	75.02	0.28	12.28	0.13	2.64	0.11	3.84	0.09	2.33	0.12	2.91	0.19	0.42	0.08	0.55	0.07
112	10.68	75.04	0.28	12.20	0.13	2.65	0.11	3.93	0.09	2.29	0.11	2.84	0.19	0.48	0.09	0.57	0.08

113	10.81	75.11	0.28	12.18	0.13	2.63	0.11	3.87	0.09	2.23	0.11	2.94	0.19	0.46	0.08	0.59	0.08
114	10.95	74.65	0.28	12.42	0.13	2.59	0.11	3.99	0.09	2.40	0.12	2.93	0.19	0.45	0.08	0.56	0.08
115	11.08	74.77	0.28	12.38	0.13	2.57	0.10	3.99	0.09	2.36	0.12	2.92	0.19	0.40	0.07	0.61	0.08
116	11.22	74.81	0.28	12.33	0.13	2.59	0.11	4.00	0.09	2.35	0.12	2.89	0.19	0.42	0.08	0.60	0.08
117	11.35	74.84	0.28	12.30	0.13	2.58	0.11	4.01	0.09	2.31	0.12	2.94	0.20	0.46	0.08	0.55	0.07
118	11.49	74.95	0.28	12.31	0.13	2.64	0.11	3.97	0.09	2.29	0.11	2.79	0.18	0.39	0.07	0.65	0.09
119	11.62	75.07	0.28	12.43	0.13	2.62	0.11	3.88	0.09	2.23	0.11	2.78	0.18	0.41	0.07	0.59	0.08
120	11.76	74.99	0.28	12.38	0.13	2.62	0.11	3.96	0.09	2.25	0.11	2.75	0.18	0.46	0.08	0.60	0.08
121	11.89	74.87	0.28	12.42	0.13	2.61	0.11	3.98	0.09	2.23	0.11	2.80	0.19	0.48	0.09	0.62	0.08
122	12.03	75.00	0.28	12.32	0.13	2.63	0.11	3.94	0.09	2.29	0.11	2.76	0.18	0.44	0.08	0.61	0.08
123	12.16	74.83	0.28	12.40	0.13	2.59	0.11	3.98	0.09	2.38	0.12	2.85	0.19	0.39	0.07	0.58	0.08
124	12.30	74.91	0.28	12.38	0.13	2.54	0.10	3.94	0.09	2.34	0.12	2.82	0.19	0.51	0.09	0.56	0.08
125	12.43	74.60	0.28	12.45	0.13	2.65	0.11	4.01	0.09	2.33	0.12	2.78	0.18	0.57	0.10	0.62	0.08
126	12.57	74.60	0.28	12.51	0.13	2.62	0.11	4.03	0.10	2.33	0.12	2.87	0.19	0.46	0.08	0.59	0.08
127	12.70	74.76	0.28	12.46	0.13	2.63	0.11	3.97	0.09	2.17	0.11	2.99	0.20	0.44	0.08	0.57	0.08
128	12.84	74.63	0.28	12.34	0.13	2.72	0.11	3.92	0.09	2.28	0.11	3.01	0.20	0.47	0.09	0.62	0.08
129	12.97	74.62	0.28	12.30	0.13	2.65	0.11	3.93	0.09	2.41	0.12	2.97	0.20	0.48	0.09	0.65	0.09
130	13.11	74.72	0.28	12.39	0.13	2.62	0.11	3.88	0.09	2.34	0.12	2.92	0.19	0.53	0.10	0.60	0.08
131	13.24	74.57	0.28	12.51	0.13	2.77	0.11	3.95	0.09	2.38	0.12	2.83	0.19	0.43	0.08	0.56	0.07
132	13.38	74.56	0.28	12.54	0.13	2.66	0.11	4.03	0.10	2.32	0.12	2.81	0.19	0.47	0.09	0.62	0.08
133	13.51	74.81	0.28	12.56	0.13	2.67	0.11	3.91	0.09	2.23	0.11	2.72	0.18	0.50	0.09	0.60	0.08
134	13.65	74.76	0.28	12.54	0.13	2.64	0.11	3.93	0.09	2.34	0.12	2.77	0.18	0.47	0.09	0.54	0.07
135	13.78	74.55	0.28	12.54	0.13	2.55	0.10	3.96	0.09	2.33	0.12	3.05	0.20	0.47	0.09	0.54	0.07
136	13.92	74.80	0.28	12.53	0.13	2.63	0.11	3.89	0.09	2.26	0.11	2.87	0.19	0.46	0.08	0.55	0.07

Agglomerate FLD23.2.2

Table J.17: Major element compositions (as wt.% oxides) from a line traverse across the interface of surface agglomerate FLD23.2.2 (from agglomerate FLD23.2.2 to host FLD23) extracted from quantified EDS compositional maps. The EDS compositional maps were collected at a resolution of 7.4 pixels/μm. The smoothing width for this traverse was 125 pixels (16.9 μm) wide. This is an Si interface and has been centered at $x = 0$ based on the SiO_2 maximum. Peak points within 2σ of the SiO_2 maximum are highlighted in yellow. Uncertainties are 2SEOM.

Pt.	Position (μm)	SiO_2	2σ	Al_2O_3	2σ	Na_2O	2σ	K_2O	2σ	CaO	2σ	FeO	2σ	TiO_2	2σ	MgO	2σ
1	-8.38	73.81	0.19	13.50	0.12	2.79	0.10	3.88	0.07	1.98	0.08	2.94	0.15	0.50	0.07	0.60	0.05
2	-8.24	73.67	0.19	13.47	0.12	2.80	0.10	3.91	0.07	2.02	0.08	3.08	0.16	0.48	0.07	0.58	0.05
3	-8.11	73.63	0.19	13.46	0.12	2.78	0.10	3.89	0.07	2.07	0.08	3.01	0.15	0.52	0.07	0.65	0.05
4	-7.97	74.06	0.19	13.47	0.12	2.72	0.09	3.94	0.07	1.95	0.08	2.79	0.14	0.50	0.07	0.59	0.05
5	-7.84	73.95	0.19	13.41	0.12	2.80	0.10	3.91	0.07	1.96	0.08	2.88	0.15	0.47	0.07	0.62	0.05
6	-7.70	73.98	0.19	13.42	0.12	2.75	0.10	3.90	0.07	1.93	0.08	2.84	0.15	0.52	0.07	0.66	0.05
7	-7.57	73.83	0.19	13.42	0.12	2.83	0.10	3.90	0.07	1.99	0.08	2.82	0.14	0.50	0.07	0.71	0.06
8	-7.43	74.02	0.19	13.44	0.12	2.82	0.10	3.86	0.07	1.96	0.08	2.80	0.14	0.46	0.06	0.65	0.05
9	-7.30	74.04	0.19	13.60	0.13	2.77	0.10	3.84	0.07	1.95	0.08	2.76	0.14	0.44	0.06	0.59	0.05
10	-7.16	73.89	0.19	13.47	0.12	2.80	0.10	3.92	0.07	1.96	0.08	2.85	0.15	0.53	0.07	0.58	0.05
11	-7.03	73.85	0.19	13.49	0.12	2.83	0.10	3.89	0.07	1.94	0.08	3.00	0.15	0.40	0.06	0.60	0.05
12	-6.89	73.92	0.19	13.50	0.12	2.78	0.10	3.88	0.07	1.90	0.08	2.88	0.15	0.45	0.06	0.68	0.06
13	-6.76	73.99	0.19	13.49	0.12	2.77	0.10	3.89	0.07	1.92	0.08	2.87	0.15	0.46	0.06	0.59	0.05
14	-6.62	74.10	0.19	13.56	0.12	2.77	0.10	3.93	0.07	1.97	0.08	2.67	0.14	0.45	0.06	0.56	0.05
15	-6.49	74.02	0.19	13.53	0.12	2.71	0.09	3.90	0.07	2.01	0.08	2.70	0.14	0.50	0.07	0.63	0.05
16	-6.35	74.19	0.19	13.41	0.12	2.71	0.09	3.94	0.07	1.97	0.08	2.61	0.13	0.52	0.07	0.65	0.05
17	-6.22	74.15	0.19	13.38	0.12	2.69	0.09	3.96	0.07	1.90	0.08	2.84	0.15	0.48	0.07	0.61	0.05
18	-6.08	73.96	0.19	13.48	0.12	2.72	0.10	3.95	0.07	1.94	0.08	2.84	0.15	0.49	0.07	0.63	0.05
19	-5.95	74.02	0.19	13.55	0.12	2.76	0.10	3.83	0.07	1.98	0.08	2.77	0.14	0.46	0.06	0.62	0.05
20	-5.81	74.08	0.19	13.52	0.12	2.68	0.09	3.92	0.07	1.92	0.08	2.92	0.15	0.41	0.06	0.56	0.05
21	-5.68	74.17	0.19	13.32	0.12	2.82	0.10	3.85	0.07	1.86	0.08	2.95	0.15	0.47	0.06	0.57	0.05
22	-5.54	74.14	0.19	13.37	0.12	2.78	0.10	3.95	0.07	1.92	0.08	2.78	0.14	0.45	0.06	0.62	0.05
23	-5.41	74.01	0.19	13.36	0.12	2.80	0.10	3.95	0.07	1.99	0.08	2.80	0.14	0.45	0.06	0.64	0.05
24	-5.27	74.13	0.19	13.38	0.12	2.75	0.10	3.92	0.07	2.04	0.08	2.72	0.14	0.45	0.06	0.63	0.05
25	-5.13	74.22	0.19	13.26	0.12	2.84	0.10	3.88	0.07	2.02	0.08	2.72	0.14	0.47	0.06	0.59	0.05
26	-5.00	74.15	0.19	13.39	0.12	2.78	0.10	3.79	0.07	1.99	0.08	2.93	0.15	0.41	0.06	0.56	0.05
27	-4.86	74.15	0.19	13.38	0.12	2.74	0.10	3.85	0.07	2.01	0.08	2.82	0.14	0.46	0.06	0.58	0.05
28	-4.73	74.12	0.19	13.32	0.12	2.77	0.10	3.90	0.07	1.98	0.08	2.80	0.14	0.50	0.07	0.62	0.05
29	-4.59	74.25	0.19	13.23	0.12	2.65	0.09	3.90	0.07	2.00	0.08	2.81	0.14	0.51	0.07	0.65	0.05
30	-4.46	74.27	0.19	13.27	0.12	2.57	0.09	3.96	0.07	2.05	0.08	2.87	0.15	0.42	0.06	0.59	0.05
31	-4.32	74.50	0.20	13.29	0.12	2.62	0.09	3.83	0.07	1.91	0.08	2.79	0.14	0.46	0.06	0.60	0.05
32	-4.19	74.24	0.19	13.31	0.12	2.67	0.09	3.93	0.07	1.98	0.08	2.80	0.14	0.46	0.06	0.61	0.05
33	-4.05	74.27	0.19	13.19	0.12	2.64	0.09	3.93	0.07	2.01	0.08	2.93	0.15	0.44	0.06	0.60	0.05
34	-3.92	74.47	0.20	13.22	0.12	2.56	0.09	3.97	0.07	1.98	0.08	2.79	0.14	0.44	0.06	0.56	0.05
35	-3.78	74.35	0.19	13.19	0.12	2.68	0.09	3.95	0.07	1.95	0.08	2.84	0.14	0.49	0.07	0.55	0.05
36	-3.65	74.43	0.20	13.24	0.12	2.59	0.09	3.88	0.07	2.02	0.08	2.78	0.14	0.48	0.07	0.59	0.05
37	-3.51	74.34	0.19	13.11	0.12	2.51	0.09	3.84	0.07	2.03	0.08	2.99	0.15	0.57	0.08	0.60	0.05
38	-3.38	74.61	0.20	13.09	0.12	2.54	0.09	3.87	0.07	2.05	0.08	2.74	0.14	0.56	0.08	0.56	0.05
39	-3.24	74.65	0.20	13.15	0.12	2.61	0.09	3.90	0.07	1.99	0.08	2.71	0.14	0.47	0.07	0.51	0.04
40	-3.11	74.77	0.20	13.11	0.12	2.54	0.09	3.87	0.07	1.97	0.08	2.76	0.14	0.44	0.06	0.53	0.04
41	-2.97	74.77	0.20	12.96	0.12	2.59	0.09	3.92	0.07	2.02	0.08	2.67	0.14	0.49	0.07	0.57	0.05
42	-2.84	74.94	0.20	12.88	0.12	2.56	0.09	3.81	0.07	2.10	0.09	2.69	0.14	0.47	0.07	0.55	0.05
43	-2.70	75.08	0.20	12.80	0.12	2.59	0.09	3.84	0.07	2.00	0.08	2.69	0.14	0.48	0.07	0.53	0.04
44	-2.57	75.15	0.20	12.64	0.12	2.60	0.09	3.80	0.07	1.96	0.08	2.76	0.14	0.44	0.06	0.64	0.05
45	-2.43	75.22	0.20	12.55	0.12	2.55	0.09	3.91	0.07	1.96	0.08	2.82	0.14	0.39	0.05	0.60	0.05
46	-2.30	75.13	0.20	12.48	0.12	2.57	0.09	3.89	0.07	2.07	0.09	2.81	0.14	0.43	0.06	0.62	0.05
47	-2.16	75.45	0.20	12.43	0.11	2.45	0.09	3.82	0.07	1.99	0.08	2.84	0.15	0.46	0.06	0.57	0.05
48	-2.03	75.93	0.20	12.30	0.11	2.42	0.08	3.75	0.07	1.92	0.08	2.73	0.14	0.40	0.06	0.55	0.05
49	-1.89	75.86	0.20	12.25	0.11	2.44	0.09	3.75	0.07	1.94	0.08	2.75	0.14	0.43	0.06	0.58	0.05
50	-1.76	75.93	0.20	12.21	0.11	2.40	0.08	3.79	0.07	1.94	0.08	2.76	0.14	0.38	0.05	0.59	0.05

51	-1.62	75.95	0.20	12.03	0.11	2.37	0.08	3.77	0.07	2.00	0.08	2.86	0.15	0.45	0.06	0.56	0.05
52	-1.49	76.38	0.20	11.83	0.11	2.31	0.08	3.73	0.07	1.95	0.08	2.79	0.14	0.45	0.06	0.56	0.05
53	-1.35	76.67	0.20	11.59	0.11	2.34	0.08	3.76	0.07	1.90	0.08	2.75	0.14	0.43	0.06	0.56	0.05
54	-1.22	76.79	0.20	11.42	0.11	2.32	0.08	3.78	0.07	1.89	0.08	2.71	0.14	0.47	0.07	0.61	0.05
55	-1.08	77.09	0.20	11.30	0.10	2.25	0.08	3.74	0.07	1.78	0.07	2.83	0.14	0.44	0.06	0.56	0.05
56	-0.95	77.43	0.20	11.03	0.10	2.28	0.08	3.64	0.07	1.76	0.07	2.83	0.14	0.45	0.06	0.57	0.05
57	-0.81	77.87	0.20	10.81	0.10	2.27	0.08	3.67	0.07	1.72	0.07	2.68	0.14	0.44	0.06	0.53	0.04
58	-0.67	78.17	0.20	10.55	0.10	2.25	0.08	3.68	0.07	1.67	0.07	2.73	0.14	0.39	0.05	0.56	0.05
59	-0.54	78.71	0.21	10.32	0.10	2.14	0.07	3.64	0.07	1.61	0.07	2.64	0.14	0.41	0.06	0.54	0.04
60	-0.41	79.03	0.21	10.10	0.09	2.09	0.07	3.59	0.07	1.57	0.06	2.67	0.14	0.40	0.06	0.54	0.04
61	-0.27	79.00	0.21	10.01	0.09	2.07	0.07	3.65	0.07	1.59	0.07	2.74	0.14	0.38	0.05	0.56	0.05
62	-0.13	79.47	0.21	9.81	0.09	2.08	0.07	3.59	0.07	1.60	0.07	2.56	0.13	0.40	0.06	0.49	0.04
63	0.00	79.51	0.21	9.76	0.09	2.05	0.07	3.52	0.06	1.52	0.06	2.62	0.13	0.48	0.07	0.53	0.04
64	0.14	79.44	0.21	9.67	0.09	2.02	0.07	3.54	0.07	1.56	0.06	2.78	0.14	0.44	0.06	0.56	0.05
65	0.27	79.37	0.21	9.68	0.09	2.01	0.07	3.59	0.07	1.57	0.06	2.73	0.14	0.49	0.07	0.56	0.05
66	0.41	79.24	0.21	9.75	0.09	2.07	0.07	3.51	0.06	1.61	0.07	2.77	0.14	0.52	0.07	0.53	0.04
67	0.54	79.38	0.21	9.67	0.09	2.05	0.07	3.47	0.06	1.62	0.07	2.81	0.14	0.42	0.06	0.58	0.05
68	0.68	79.41	0.21	9.76	0.09	2.05	0.07	3.51	0.06	1.59	0.07	2.75	0.14	0.41	0.06	0.53	0.04
69	0.81	79.35	0.21	9.74	0.09	2.03	0.07	3.56	0.07	1.68	0.07	2.69	0.14	0.41	0.06	0.55	0.05
70	0.95	79.11	0.21	9.75	0.09	2.10	0.07	3.52	0.06	1.80	0.07	2.87	0.15	0.34	0.05	0.52	0.04
71	1.08	78.98	0.21	9.84	0.09	1.99	0.07	3.59	0.07	1.77	0.07	2.82	0.14	0.45	0.06	0.56	0.05
72	1.22	78.98	0.21	9.65	0.09	2.10	0.07	3.57	0.07	1.84	0.08	2.88	0.15	0.39	0.05	0.58	0.05
73	1.35	78.97	0.21	9.76	0.09	2.22	0.08	3.62	0.07	1.86	0.08	2.66	0.14	0.39	0.05	0.52	0.04
74	1.49	78.95	0.21	9.88	0.09	2.17	0.08	3.59	0.07	1.82	0.07	2.71	0.14	0.35	0.05	0.52	0.04
75	1.62	78.55	0.21	9.99	0.09	2.20	0.08	3.57	0.07	1.80	0.07	2.86	0.15	0.43	0.06	0.59	0.05
76	1.76	78.46	0.21	10.05	0.09	2.26	0.08	3.58	0.07	1.91	0.08	2.71	0.14	0.45	0.06	0.59	0.05
77	1.89	78.46	0.21	9.95	0.09	2.20	0.08	3.58	0.07	1.97	0.08	2.87	0.15	0.39	0.05	0.58	0.05
78	2.03	78.32	0.21	10.04	0.09	2.18	0.08	3.61	0.07	1.97	0.08	2.86	0.15	0.41	0.06	0.61	0.05
79	2.16	78.49	0.21	10.18	0.09	2.12	0.07	3.58	0.07	1.92	0.08	2.80	0.14	0.35	0.05	0.54	0.04
80	2.30	78.06	0.20	10.26	0.09	2.22	0.08	3.58	0.07	2.07	0.09	2.80	0.14	0.40	0.06	0.62	0.05
81	2.43	77.89	0.20	10.29	0.09	2.16	0.08	3.60	0.07	2.07	0.09	2.92	0.15	0.47	0.06	0.60	0.05
82	2.57	77.82	0.20	10.43	0.10	2.22	0.08	3.65	0.07	2.06	0.08	2.81	0.14	0.44	0.06	0.56	0.05
83	2.70	78.00	0.20	10.31	0.09	2.20	0.08	3.66	0.07	1.96	0.08	2.86	0.15	0.44	0.06	0.57	0.05
84	2.84	77.93	0.20	10.37	0.10	2.21	0.08	3.60	0.07	2.04	0.08	2.86	0.15	0.41	0.06	0.59	0.05
85	2.97	77.81	0.20	10.41	0.10	2.25	0.08	3.71	0.07	2.02	0.08	2.85	0.15	0.42	0.06	0.53	0.04
86	3.11	77.61	0.20	10.42	0.10	2.26	0.08	3.72	0.07	2.00	0.08	3.01	0.15	0.45	0.06	0.53	0.04
87	3.24	77.77	0.20	10.47	0.10	2.31	0.08	3.59	0.07	2.05	0.08	2.77	0.14	0.51	0.07	0.54	0.04
88	3.38	77.52	0.20	10.55	0.10	2.34	0.08	3.63	0.07	2.12	0.09	2.84	0.15	0.45	0.06	0.55	0.05
89	3.51	77.42	0.20	10.63	0.10	2.40	0.08	3.54	0.07	2.13	0.09	2.83	0.14	0.48	0.07	0.59	0.05
90	3.65	77.40	0.20	10.66	0.10	2.32	0.08	3.70	0.07	2.10	0.09	2.82	0.14	0.43	0.06	0.57	0.05
91	3.78	77.32	0.20	10.49	0.10	2.36	0.08	3.67	0.07	2.08	0.09	3.11	0.16	0.41	0.06	0.54	0.05
92	3.92	77.28	0.20	10.61	0.10	2.31	0.08	3.74	0.07	2.15	0.09	2.93	0.15	0.42	0.06	0.56	0.05
93	4.05	77.31	0.20	10.72	0.10	2.35	0.08	3.61	0.07	2.19	0.09	2.80	0.14	0.43	0.06	0.58	0.05
94	4.19	77.02	0.20	10.83	0.10	2.34	0.08	3.69	0.07	2.25	0.09	2.89	0.15	0.39	0.05	0.57	0.05
95	4.32	77.08	0.20	10.90	0.10	2.36	0.08	3.63	0.07	2.19	0.09	2.83	0.14	0.44	0.06	0.57	0.05
96	4.46	77.07	0.20	10.77	0.10	2.40	0.08	3.66	0.07	2.18	0.09	2.88	0.15	0.50	0.07	0.54	0.04
97	4.60	76.70	0.20	10.90	0.10	2.36	0.08	3.74	0.07	2.17	0.09	3.06	0.16	0.48	0.07	0.58	0.05
98	4.73	76.83	0.20	10.99	0.10	2.30	0.08	3.75	0.07	2.21	0.09	2.92	0.15	0.41	0.06	0.59	0.05
99	4.87	76.63	0.20	10.96	0.10	2.35	0.08	3.71	0.07	2.27	0.09	3.06	0.16	0.47	0.07	0.55	0.05
100	5.00	76.53	0.20	11.11	0.10	2.36	0.08	3.82	0.07	2.29	0.09	2.88	0.15	0.45	0.06	0.56	0.05
101	5.14	76.56	0.20	11.14	0.10	2.26	0.08	3.79	0.07	2.29	0.09	2.97	0.15	0.41	0.06	0.59	0.05
102	5.27	76.45	0.20	11.28	0.10	2.29	0.08	3.75	0.07	2.32	0.10	2.98	0.15	0.39	0.05	0.54	0.04
103	5.41	76.16	0.20	11.26	0.10	2.38	0.08	3.83	0.07	2.27	0.09	3.03	0.16	0.46	0.06	0.61	0.05
104	5.54	76.16	0.20	11.14	0.10	2.35	0.08	3.79	0.07	2.37	0.10	3.09	0.16	0.45	0.06	0.63	0.05
105	5.68	76.24	0.20	11.24	0.10	2.43	0.09	3.73	0.07	2.37	0.10	2.94	0.15	0.44	0.06	0.59	0.05
106	5.81	76.31	0.20	11.38	0.10	2.44	0.09	3.71	0.07	2.35	0.10	2.87	0.15	0.40	0.06	0.54	0.04
107	5.95	76.22	0.20	11.35	0.10	2.46	0.09	3.68	0.07	2.31	0.10	2.88	0.15	0.51	0.07	0.59	0.05
108	6.08	76.00	0.20	11.37	0.10	2.43	0.09	3.70	0.07	2.38	0.10	3.10	0.16	0.42	0.06	0.59	0.05
109	6.22	75.89	0.20	11.49	0.11	2.45	0.09	3.75	0.07	2.38	0.10	3.04	0.16	0.43	0.06	0.57	0.05
110	6.35	76.10	0.20	11.45	0.11	2.45	0.09	3.81	0.07	2.30	0.09	2.95	0.15	0.37	0.05	0.58	0.05
111	6.49	75.71	0.20	11.45	0.11	2.47	0.09	3.91	0.07	2.46	0.10	2.93	0.15	0.50	0.07	0.59	0.05
112	6.62	75.76	0.20	11.59	0.11	2.39	0.08	3.81	0.07	2.39	0.10	2.96	0.15	0.49	0.07	0.60	0.05

113	6.76	75.89	0.20	11.56	0.11	2.45	0.09	3.75	0.07	2.36	0.10	2.98	0.15	0.37	0.05	0.63	0.05
114	6.89	75.51	0.20	11.62	0.11	2.43	0.08	3.87	0.07	2.44	0.10	3.14	0.16	0.39	0.05	0.60	0.05
115	7.03	75.54	0.20	11.76	0.11	2.44	0.09	3.88	0.07	2.42	0.10	2.99	0.15	0.43	0.06	0.53	0.04
116	7.16	75.36	0.20	11.78	0.11	2.48	0.09	3.81	0.07	2.46	0.10	3.08	0.16	0.42	0.06	0.60	0.05
117	7.30	75.49	0.20	11.79	0.11	2.39	0.08	3.78	0.07	2.48	0.10	3.00	0.15	0.45	0.06	0.63	0.05
118	7.43	75.54	0.20	11.73	0.11	2.48	0.09	3.84	0.07	2.41	0.10	2.97	0.15	0.44	0.06	0.59	0.05
119	7.57	75.46	0.20	11.89	0.11	2.48	0.09	3.77	0.07	2.39	0.10	2.98	0.15	0.47	0.07	0.55	0.05
120	7.70	75.57	0.20	11.83	0.11	2.43	0.09	3.83	0.07	2.39	0.10	2.95	0.15	0.39	0.05	0.61	0.05
121	7.84	75.30	0.20	11.90	0.11	2.47	0.09	3.87	0.07	2.49	0.10	2.97	0.15	0.45	0.06	0.55	0.05
122	7.97	75.28	0.20	11.91	0.11	2.43	0.09	3.77	0.07	2.52	0.10	3.01	0.15	0.51	0.07	0.56	0.05
123	8.11	75.30	0.20	12.04	0.11	2.45	0.09	3.81	0.07	2.41	0.10	2.96	0.15	0.45	0.06	0.59	0.05
124	8.24	75.15	0.20	12.01	0.11	2.46	0.09	3.91	0.07	2.54	0.10	2.95	0.15	0.41	0.06	0.57	0.05
125	8.38	75.27	0.20	12.02	0.11	2.45	0.09	3.85	0.07	2.41	0.10	2.95	0.15	0.43	0.06	0.61	0.05
126	8.51	75.13	0.20	12.08	0.11	2.45	0.09	3.83	0.07	2.52	0.10	3.02	0.15	0.40	0.06	0.57	0.05
127	8.65	75.41	0.20	12.05	0.11	2.41	0.08	3.75	0.07	2.36	0.10	2.93	0.15	0.47	0.07	0.62	0.05
128	8.78	75.20	0.20	12.12	0.11	2.48	0.09	3.87	0.07	2.36	0.10	2.93	0.15	0.45	0.06	0.59	0.05

Agglomerate FLD23.3.1

Table J.18: Major element compositions (as wt.% oxides) from a line traverse across the interface of surface agglomerate FLD23.3.1 (from agglomerate FLD23.3.1 to host FLD23) extracted from quantified EDS compositional maps. The EDS compositional maps were collected at a resolution of 3.7 pixels/μm. The smoothing width for this traverse was 90 pixels (24.2 μm) wide. This is an Si interface and has been centered at $x = 0$ based on the SiO_2 maximum. Peak points within 2σ of the SiO_2 maximum are highlighted in yellow. Uncertainties are 2SEOM.

Pt.	Position (μm)	SiO_2	2σ	Al_2O_3	2σ	Na_2O	2σ	K_2O	2σ	CaO	2σ	FeO	2σ	TiO_2	2σ	MgO	2σ
1	-9.70	73.48	0.22	13.42	0.13	3.34	0.10	3.84	0.10	1.94	0.09	2.91	0.20	0.49	0.09	0.58	0.05
2	-9.43	73.49	0.22	13.38	0.13	3.36	0.10	3.84	0.10	1.95	0.09	2.91	0.20	0.47	0.08	0.60	0.06
3	-9.16	73.60	0.22	13.30	0.13	3.27	0.09	3.81	0.10	1.99	0.09	2.84	0.19	0.51	0.09	0.68	0.06
4	-8.89	73.77	0.23	13.38	0.13	3.29	0.10	3.85	0.10	1.94	0.08	2.66	0.18	0.43	0.07	0.68	0.06
5	-8.62	73.69	0.23	13.38	0.13	3.22	0.09	3.80	0.10	1.90	0.08	2.78	0.19	0.60	0.11	0.63	0.06
6	-8.35	73.54	0.22	13.45	0.13	3.21	0.09	3.80	0.10	2.07	0.09	2.80	0.19	0.52	0.09	0.62	0.06
7	-8.08	73.43	0.22	13.38	0.13	3.28	0.09	3.85	0.10	2.00	0.09	2.84	0.19	0.55	0.10	0.68	0.06
8	-7.81	73.58	0.22	13.27	0.13	3.29	0.10	3.93	0.11	1.92	0.08	2.81	0.19	0.54	0.09	0.66	0.06
9	-7.54	73.74	0.23	13.30	0.13	3.23	0.09	3.84	0.10	1.87	0.08	2.89	0.20	0.50	0.09	0.62	0.06
10	-7.27	73.33	0.22	13.45	0.13	3.22	0.09	3.93	0.11	1.97	0.09	2.94	0.20	0.56	0.10	0.60	0.06
11	-7.00	73.44	0.22	13.32	0.13	3.29	0.10	3.99	0.11	2.01	0.09	2.89	0.20	0.49	0.09	0.56	0.05
12	-6.74	73.74	0.23	13.15	0.13	3.36	0.10	3.87	0.10	2.01	0.09	2.81	0.19	0.48	0.08	0.59	0.06
13	-6.46	73.88	0.23	13.09	0.13	3.29	0.10	3.85	0.10	2.00	0.09	2.78	0.19	0.48	0.08	0.63	0.06
14	-6.20	73.84	0.23	13.09	0.13	3.30	0.10	3.86	0.10	1.90	0.08	2.97	0.20	0.45	0.08	0.59	0.06
15	-5.93	73.81	0.23	13.04	0.13	3.32	0.10	3.89	0.11	1.89	0.08	2.97	0.20	0.50	0.09	0.58	0.05
16	-5.66	73.83	0.23	13.10	0.13	3.33	0.10	3.86	0.10	1.91	0.08	2.82	0.19	0.58	0.10	0.57	0.05
17	-5.39	74.01	0.23	12.97	0.13	3.21	0.09	3.99	0.11	1.97	0.09	2.79	0.19	0.46	0.08	0.59	0.06
18	-5.12	73.94	0.23	12.88	0.13	3.33	0.10	3.90	0.11	2.00	0.09	2.83	0.19	0.49	0.09	0.62	0.06
19	-4.85	74.00	0.23	12.91	0.13	3.33	0.10	3.81	0.10	1.95	0.09	2.92	0.20	0.48	0.08	0.59	0.06
20	-4.58	74.15	0.23	12.94	0.13	3.32	0.10	3.78	0.10	1.93	0.08	2.81	0.19	0.48	0.08	0.59	0.06
21	-4.31	73.94	0.23	13.07	0.13	3.29	0.10	3.81	0.10	1.96	0.09	2.82	0.19	0.49	0.09	0.61	0.06
22	-4.04	73.94	0.23	13.05	0.13	3.40	0.10	3.94	0.11	1.91	0.08	2.70	0.18	0.44	0.08	0.63	0.06
23	-3.77	74.33	0.23	12.71	0.12	3.31	0.10	3.98	0.11	1.90	0.08	2.73	0.19	0.46	0.08	0.58	0.05
24	-3.50	74.65	0.23	12.42	0.12	3.32	0.10	3.91	0.11	1.85	0.08	2.80	0.19	0.52	0.09	0.53	0.05
25	-3.23	75.07	0.23	12.37	0.12	3.16	0.09	3.86	0.10	1.80	0.08	2.77	0.19	0.45	0.08	0.53	0.05
26	-2.96	75.30	0.23	12.16	0.12	3.19	0.09	3.98	0.11	1.75	0.08	2.67	0.18	0.41	0.07	0.54	0.05
27	-2.69	75.23	0.23	12.15	0.12	3.14	0.09	3.98	0.11	1.76	0.08	2.83	0.19	0.37	0.07	0.52	0.05
28	-2.42	75.39	0.23	12.03	0.12	3.17	0.09	3.96	0.11	1.68	0.07	2.76	0.19	0.46	0.08	0.55	0.05
29	-2.16	75.91	0.23	11.92	0.12	3.11	0.09	3.77	0.10	1.72	0.08	2.50	0.17	0.52	0.09	0.56	0.05
30	-1.89	75.97	0.23	11.61	0.11	3.05	0.09	3.89	0.11	1.72	0.08	2.77	0.19	0.44	0.08	0.56	0.05
31	-1.62	76.56	0.23	11.40	0.11	2.98	0.09	3.77	0.10	1.68	0.07	2.63	0.18	0.42	0.07	0.55	0.05
32	-1.35	76.78	0.23	11.22	0.11	3.01	0.09	3.80	0.10	1.60	0.07	2.66	0.18	0.42	0.07	0.50	0.05
33	-1.08	77.24	0.24	10.89	0.11	3.03	0.09	3.77	0.10	1.53	0.07	2.67	0.18	0.33	0.06	0.54	0.05
34	-0.81	77.39	0.24	10.75	0.10	2.95	0.09	3.80	0.10	1.48	0.06	2.63	0.18	0.43	0.07	0.58	0.05
35	-0.54	77.72	0.24	10.47	0.10	2.89	0.08	3.85	0.10	1.52	0.07	2.56	0.17	0.44	0.08	0.55	0.05
36	-0.27	78.02	0.24	10.34	0.10	2.92	0.08	3.77	0.10	1.40	0.06	2.64	0.18	0.36	0.06	0.54	0.05
37	0.00	78.32	0.24	10.25	0.10	2.85	0.08	3.65	0.10	1.40	0.06	2.59	0.18	0.45	0.08	0.49	0.05
38	0.27	78.26	0.24	10.07	0.10	2.86	0.08	3.75	0.10	1.55	0.07	2.52	0.17	0.44	0.08	0.55	0.05
39	0.54	78.10	0.24	10.10	0.10	3.01	0.09	3.79	0.10	1.46	0.06	2.63	0.18	0.42	0.07	0.49	0.05
40	0.81	77.48	0.24	10.22	0.10	3.13	0.09	3.77	0.10	1.55	0.07	2.84	0.19	0.44	0.08	0.56	0.05
41	1.08	77.36	0.24	10.27	0.10	3.16	0.09	3.86	0.10	1.61	0.07	2.67	0.18	0.43	0.08	0.64	0.06
42	1.35	77.55	0.24	10.34	0.10	3.10	0.09	3.86	0.10	1.60	0.07	2.55	0.17	0.40	0.07	0.58	0.05
43	1.62	77.18	0.24	10.53	0.10	3.23	0.09	3.89	0.11	1.54	0.07	2.72	0.19	0.40	0.07	0.51	0.05
44	1.89	76.51	0.23	10.80	0.11	3.28	0.09	3.86	0.10	1.66	0.07	2.90	0.20	0.45	0.08	0.54	0.05
45	2.15	76.38	0.23	10.93	0.11	3.29	0.09	3.82	0.10	1.72	0.08	2.79	0.19	0.45	0.08	0.62	0.06
46	2.42	76.16	0.23	11.05	0.11	3.34	0.10	3.86	0.10	1.74	0.08	2.81	0.19	0.50	0.09	0.55	0.05
47	2.69	75.89	0.23	11.07	0.11	3.44	0.10	3.91	0.11	1.68	0.07	2.95	0.20	0.43	0.08	0.62	0.06
48	2.96	75.75	0.23	11.25	0.11	3.43	0.10	3.99	0.11	1.84	0.08	2.75	0.19	0.40	0.07	0.59	0.06
49	3.23	75.51	0.23	11.43	0.11	3.46	0.10	3.98	0.11	1.92	0.08	2.73	0.19	0.41	0.07	0.56	0.05
50	3.50	75.04	0.23	11.60	0.11	3.57	0.10	3.98	0.11	1.91	0.08	2.87	0.20	0.41	0.07	0.62	0.06

51	3.77	74.78	0.23	11.65	0.11	3.61	0.10	3.98	0.11	1.97	0.09	2.90	0.20	0.52	0.09	0.61	0.06
52	4.04	74.44	0.23	11.83	0.12	3.67	0.11	4.14	0.11	2.05	0.09	2.79	0.19	0.43	0.08	0.65	0.06
53	4.31	74.44	0.23	11.92	0.12	3.66	0.11	4.11	0.11	2.11	0.09	2.74	0.19	0.42	0.07	0.60	0.06
54	4.58	74.18	0.23	12.16	0.12	3.70	0.11	3.89	0.11	2.12	0.09	2.89	0.20	0.45	0.08	0.61	0.06
55	4.85	73.72	0.23	12.27	0.12	3.74	0.11	4.03	0.11	2.23	0.10	2.94	0.20	0.47	0.08	0.58	0.05
56	5.12	73.75	0.23	12.28	0.12	3.69	0.11	4.05	0.11	2.26	0.10	2.85	0.19	0.42	0.07	0.69	0.06
57	5.39	73.47	0.22	12.45	0.12	3.79	0.11	4.04	0.11	2.24	0.10	2.98	0.20	0.43	0.08	0.61	0.06
58	5.66	73.31	0.22	12.51	0.12	3.86	0.11	4.04	0.11	2.20	0.10	2.98	0.20	0.48	0.08	0.61	0.06
59	5.93	73.16	0.22	12.58	0.12	3.88	0.11	4.05	0.11	2.17	0.10	3.03	0.21	0.49	0.09	0.64	0.06
60	6.20	73.10	0.22	12.73	0.12	3.89	0.11	4.04	0.11	2.21	0.10	2.94	0.20	0.43	0.07	0.65	0.06
61	6.47	72.96	0.22	12.81	0.12	4.01	0.12	4.08	0.11	2.20	0.10	2.86	0.20	0.48	0.08	0.60	0.06
62	6.73	72.97	0.22	12.83	0.13	3.95	0.11	4.16	0.11	2.28	0.10	2.79	0.19	0.43	0.08	0.59	0.06
63	7.00	72.89	0.22	12.82	0.13	3.99	0.12	4.05	0.11	2.33	0.10	2.88	0.20	0.45	0.08	0.60	0.06
64	7.27	72.36	0.22	13.06	0.13	4.01	0.12	4.19	0.11	2.26	0.10	3.02	0.21	0.48	0.08	0.62	0.06
65	7.54	72.35	0.22	12.96	0.13	3.96	0.11	4.12	0.11	2.36	0.10	3.15	0.21	0.48	0.08	0.63	0.06
66	7.81	72.09	0.22	12.93	0.13	3.97	0.11	4.12	0.11	2.55	0.11	3.22	0.22	0.49	0.09	0.62	0.06
67	8.08	72.17	0.22	13.18	0.13	3.96	0.11	4.17	0.11	2.37	0.10	2.98	0.20	0.54	0.10	0.63	0.06
68	8.35	72.01	0.22	13.25	0.13	4.13	0.12	4.11	0.11	2.35	0.10	3.04	0.21	0.43	0.08	0.68	0.06
69	8.62	71.98	0.22	13.24	0.13	4.07	0.12	4.17	0.11	2.42	0.11	3.08	0.21	0.45	0.08	0.61	0.06
70	8.89	72.17	0.22	13.19	0.13	4.11	0.12	4.15	0.11	2.35	0.10	2.97	0.20	0.46	0.08	0.61	0.06
71	9.16	72.34	0.22	13.16	0.13	3.99	0.12	4.15	0.11	2.30	0.10	3.02	0.21	0.44	0.08	0.60	0.06
72	9.43	71.84	0.22	13.25	0.13	4.10	0.12	4.20	0.11	2.41	0.11	2.98	0.20	0.61	0.11	0.62	0.06
73	9.70	72.05	0.22	13.35	0.13	4.08	0.12	4.19	0.11	2.25	0.10	2.98	0.20	0.44	0.08	0.64	0.06
74	9.97	71.89	0.22	13.34	0.13	4.10	0.12	4.20	0.11	2.35	0.10	2.96	0.20	0.50	0.09	0.66	0.06
75	10.24	71.83	0.22	13.24	0.13	4.22	0.12	4.18	0.11	2.43	0.11	3.00	0.20	0.50	0.09	0.60	0.06
76	10.51	71.89	0.22	13.12	0.13	4.27	0.12	4.11	0.11	2.38	0.10	3.10	0.21	0.52	0.09	0.62	0.06
77	10.78	72.18	0.22	13.18	0.13	4.24	0.12	4.16	0.11	2.35	0.10	2.81	0.19	0.48	0.08	0.59	0.06
78	11.05	72.00	0.22	13.30	0.13	4.24	0.12	4.19	0.11	2.19	0.10	2.92	0.20	0.51	0.09	0.64	0.06
79	11.32	72.04	0.22	13.29	0.13	4.17	0.12	4.16	0.11	2.26	0.10	2.98	0.20	0.49	0.09	0.61	0.06
80	11.58	71.73	0.22	13.31	0.13	4.18	0.12	4.15	0.11	2.40	0.11	3.12	0.21	0.52	0.09	0.60	0.06
81	11.85	71.99	0.22	13.29	0.13	4.17	0.12	4.12	0.11	2.32	0.10	3.18	0.22	0.42	0.07	0.51	0.05
82	12.12	72.11	0.22	13.28	0.13	4.22	0.12	4.14	0.11	2.22	0.10	2.98	0.20	0.50	0.09	0.55	0.05
83	12.39	71.88	0.22	13.28	0.13	4.30	0.12	4.20	0.11	2.27	0.10	3.08	0.21	0.37	0.06	0.61	0.06
84	12.66	71.47	0.22	13.27	0.13	4.23	0.12	4.25	0.11	2.43	0.11	2.96	0.20	0.43	0.08	0.60	0.06

Agglomerate FLD23.3.2

Table J.19: Major element compositions (as wt.% oxides) from a line traverse across the interface of surface agglomerate FLD23.3.2 (from agglomerate FLD23.3.2 to host FLD23) extracted from quantified EDS compositional maps. The EDS compositional maps were collected at a resolution of 3.7 pixels/μm. The smoothing width for this traverse was 50 pixels (13.5 μm) wide. This is an Si interface and has been centered at $x = 0$ based on the SiO_2 maximum. Peak points within 2σ of the SiO_2 maximum are highlighted in yellow. Uncertainties are 2SEOM.

Pt.	Position (μm)	SiO_2	2σ	Al_2O_3	2σ	Na_2O	2σ	K_2O	2σ	CaO	2σ	FeO	2σ	TiO_2	2σ	MgO	2σ
1	-9.43	73.45	0.49	13.19	0.26	3.53	0.13	4.08	0.12	1.96	0.11	2.70	0.21	0.48	0.10	0.61	0.09
2	-9.16	73.31	0.49	13.08	0.25	3.57	0.13	4.10	0.13	2.01	0.11	2.75	0.22	0.53	0.11	0.65	0.10
3	-8.89	73.46	0.49	12.98	0.25	3.53	0.13	4.09	0.12	1.97	0.11	2.82	0.22	0.53	0.11	0.63	0.09
4	-8.62	73.52	0.49	13.16	0.25	3.40	0.12	4.09	0.12	1.97	0.11	2.87	0.22	0.41	0.08	0.58	0.09
5	-8.35	73.51	0.49	13.04	0.25	3.47	0.13	4.17	0.13	2.06	0.11	2.71	0.21	0.41	0.08	0.62	0.09
6	-8.08	73.38	0.49	13.01	0.25	3.65	0.13	4.22	0.13	1.91	0.10	2.81	0.22	0.44	0.09	0.56	0.08
7	-7.81	73.44	0.49	13.01	0.25	3.60	0.13	4.22	0.13	1.92	0.10	2.82	0.22	0.41	0.08	0.58	0.09
8	-7.54	73.36	0.49	12.94	0.25	3.55	0.13	4.18	0.13	1.89	0.10	2.87	0.22	0.55	0.11	0.65	0.10
9	-7.27	73.07	0.49	13.04	0.25	3.54	0.13	4.24	0.13	2.00	0.11	2.89	0.23	0.51	0.10	0.70	0.11
10	-7.00	73.50	0.49	13.08	0.25	3.60	0.13	4.12	0.13	1.89	0.10	2.81	0.22	0.51	0.10	0.49	0.07
11	-6.74	73.33	0.49	12.94	0.25	3.75	0.14	4.16	0.13	1.90	0.10	2.88	0.23	0.54	0.11	0.50	0.08
12	-6.47	73.16	0.49	12.84	0.25	3.71	0.13	4.21	0.13	1.96	0.11	2.93	0.23	0.57	0.11	0.63	0.09
13	-6.20	73.04	0.49	12.94	0.25	3.75	0.14	4.29	0.13	1.99	0.11	2.82	0.22	0.54	0.11	0.63	0.09
14	-5.93	73.08	0.49	12.97	0.25	3.81	0.14	4.06	0.12	2.09	0.11	2.95	0.23	0.45	0.09	0.59	0.09
15	-5.66	72.95	0.48	12.87	0.25	3.74	0.13	4.11	0.13	2.08	0.11	3.08	0.24	0.53	0.11	0.64	0.10
16	-5.39	73.00	0.48	12.67	0.25	3.82	0.14	4.18	0.13	2.14	0.12	3.03	0.24	0.49	0.10	0.68	0.10
17	-5.12	72.72	0.48	12.83	0.25	3.88	0.14	4.25	0.13	2.02	0.11	3.06	0.24	0.55	0.11	0.69	0.10
18	-4.85	73.00	0.48	12.66	0.25	3.82	0.14	4.29	0.13	1.92	0.10	3.15	0.25	0.47	0.09	0.69	0.10
19	-4.58	73.35	0.49	12.80	0.25	3.92	0.14	4.08	0.12	1.91	0.10	2.73	0.21	0.51	0.10	0.69	0.10
20	-4.31	73.32	0.49	12.61	0.24	3.88	0.14	3.98	0.12	2.05	0.11	3.05	0.24	0.44	0.09	0.67	0.10
21	-4.04	73.39	0.49	12.75	0.25	3.84	0.14	4.13	0.13	1.94	0.10	2.96	0.23	0.37	0.07	0.62	0.09
22	-3.77	73.84	0.49	12.70	0.25	3.66	0.13	4.01	0.12	1.91	0.10	2.69	0.21	0.48	0.10	0.71	0.11
23	-3.50	73.75	0.49	12.73	0.25	3.83	0.14	4.05	0.12	2.03	0.11	2.63	0.21	0.38	0.08	0.59	0.09
24	-3.23	73.64	0.49	12.61	0.24	3.87	0.14	3.99	0.12	1.94	0.10	2.91	0.23	0.46	0.09	0.58	0.09
25	-2.96	73.63	0.49	12.52	0.24	3.82	0.14	4.13	0.13	1.94	0.10	2.89	0.23	0.54	0.11	0.53	0.08
26	-2.69	73.58	0.49	12.49	0.24	3.82	0.14	4.13	0.13	1.98	0.11	2.74	0.21	0.55	0.11	0.71	0.11
27	-2.43	74.14	0.49	12.39	0.24	3.75	0.14	4.17	0.13	1.80	0.10	2.61	0.20	0.50	0.10	0.63	0.09
28	-2.16	74.12	0.49	12.13	0.23	3.81	0.14	4.20	0.13	1.89	0.10	2.77	0.22	0.51	0.10	0.59	0.09
29	-1.89	74.11	0.49	12.13	0.23	3.86	0.14	4.12	0.13	1.74	0.09	3.04	0.24	0.39	0.08	0.61	0.09
30	-1.62	74.61	0.50	11.77	0.23	3.76	0.14	4.14	0.13	1.72	0.09	2.98	0.23	0.41	0.08	0.62	0.09
31	-1.35	75.21	0.50	11.35	0.22	3.69	0.13	4.04	0.12	1.67	0.09	2.91	0.23	0.50	0.10	0.62	0.09
32	-1.08	75.78	0.50	10.96	0.21	3.59	0.13	4.11	0.13	1.68	0.09	2.86	0.22	0.44	0.09	0.59	0.09
33	-0.81	76.11	0.51	10.99	0.21	3.38	0.12	4.16	0.13	1.69	0.09	2.65	0.21	0.47	0.09	0.56	0.08
34	-0.54	76.46	0.51	10.99	0.21	3.31	0.12	4.00	0.12	1.50	0.08	2.53	0.20	0.56	0.11	0.64	0.10
35	-0.27	76.83	0.51	10.74	0.21	3.27	0.12	3.96	0.12	1.61	0.09	2.58	0.20	0.40	0.08	0.62	0.09
36	0.00	77.00	0.51	10.65	0.21	3.25	0.12	4.03	0.12	1.70	0.09	2.48	0.19	0.37	0.07	0.51	0.08
37	0.27	76.88	0.51	10.65	0.21	3.37	0.12	3.96	0.12	1.60	0.09	2.67	0.21	0.39	0.08	0.48	0.07
38	0.54	76.42	0.51	10.67	0.21	3.47	0.13	4.03	0.12	1.60	0.09	2.81	0.22	0.44	0.09	0.55	0.08
39	0.81	76.76	0.51	10.51	0.20	3.49	0.13	3.82	0.12	1.54	0.08	2.90	0.23	0.46	0.09	0.53	0.08
40	1.08	76.57	0.51	10.60	0.21	3.35	0.12	3.88	0.12	1.67	0.09	3.02	0.24	0.37	0.07	0.55	0.08
41	1.35	76.58	0.51	10.59	0.20	3.32	0.12	3.97	0.12	1.74	0.09	2.83	0.22	0.34	0.07	0.64	0.10
42	1.62	76.64	0.51	10.82	0.21	3.34	0.12	3.85	0.12	1.65	0.09	2.67	0.21	0.42	0.08	0.61	0.09
43	1.89	76.53	0.51	10.78	0.21	3.44	0.12	3.93	0.12	1.83	0.10	2.52	0.20	0.39	0.08	0.58	0.09
44	2.15	75.87	0.50	10.96	0.21	3.54	0.13	3.86	0.12	1.74	0.09	2.92	0.23	0.46	0.09	0.64	0.10
45	2.42	75.63	0.50	11.16	0.22	3.63	0.13	3.96	0.12	1.78	0.10	2.80	0.22	0.42	0.08	0.61	0.09
46	2.69	75.63	0.50	11.09	0.21	3.56	0.13	4.07	0.12	1.86	0.10	2.83	0.22	0.42	0.08	0.54	0.08
47	2.96	75.49	0.50	11.14	0.22	3.49	0.13	4.05	0.12	1.84	0.10	2.85	0.22	0.57	0.11	0.57	0.09
48	3.23	75.32	0.50	11.36	0.22	3.43	0.12	4.13	0.13	1.93	0.10	2.76	0.22	0.47	0.09	0.60	0.09
49	3.50	75.25	0.50	11.44	0.22	3.49	0.13	4.12	0.13	1.87	0.10	2.71	0.21	0.47	0.09	0.64	0.10
50	3.77	75.18	0.50	11.39	0.22	3.62	0.13	3.97	0.12	1.94	0.10	2.96	0.23	0.45	0.09	0.50	0.08

51	4.04	74.88	0.50	11.51	0.22	3.73	0.13	4.09	0.12	1.94	0.10	2.83	0.22	0.60	0.12	0.43	0.06
52	4.31	74.73	0.50	11.82	0.23	3.68	0.13	4.15	0.13	1.98	0.11	2.62	0.21	0.46	0.09	0.57	0.09
53	4.58	74.75	0.50	11.73	0.23	3.72	0.13	4.06	0.12	1.95	0.11	2.76	0.22	0.40	0.08	0.64	0.10
54	4.85	74.71	0.50	11.78	0.23	3.71	0.13	4.08	0.12	1.99	0.11	2.69	0.21	0.38	0.08	0.65	0.10
55	5.12	74.59	0.50	11.80	0.23	3.82	0.14	4.06	0.12	2.00	0.11	2.66	0.21	0.44	0.09	0.64	0.10
56	5.39	74.14	0.49	11.98	0.23	3.78	0.14	4.03	0.12	2.14	0.12	2.89	0.23	0.44	0.09	0.59	0.09
57	5.66	74.38	0.49	12.03	0.23	3.69	0.13	4.04	0.12	1.95	0.11	2.83	0.22	0.41	0.08	0.66	0.10
58	5.93	73.89	0.49	11.94	0.23	3.80	0.14	4.11	0.13	2.13	0.11	2.97	0.23	0.52	0.10	0.63	0.09
59	6.20	73.54	0.49	11.92	0.23	3.76	0.14	4.18	0.13	2.06	0.11	3.23	0.25	0.65	0.13	0.65	0.10
60	6.46	73.86	0.49	12.16	0.24	3.92	0.14	4.10	0.13	2.14	0.12	2.71	0.21	0.42	0.08	0.70	0.11
61	6.74	73.81	0.49	12.07	0.23	3.92	0.14	4.03	0.12	2.08	0.11	2.78	0.22	0.65	0.13	0.66	0.10
62	7.00	73.68	0.49	12.09	0.23	4.00	0.14	3.91	0.12	2.16	0.12	3.09	0.24	0.42	0.08	0.65	0.10
63	7.27	73.98	0.49	12.01	0.23	3.83	0.14	4.00	0.12	2.21	0.12	2.92	0.23	0.40	0.08	0.65	0.10
64	7.54	74.01	0.49	12.07	0.23	3.77	0.14	4.19	0.13	2.13	0.11	2.79	0.22	0.46	0.09	0.59	0.09
65	7.81	73.56	0.49	12.20	0.24	3.81	0.14	4.14	0.13	2.15	0.12	2.98	0.23	0.53	0.11	0.63	0.09
66	8.08	73.84	0.49	12.23	0.24	3.91	0.14	4.09	0.12	2.13	0.11	2.72	0.21	0.48	0.10	0.60	0.09
67	8.35	74.11	0.49	12.28	0.24	3.89	0.14	4.09	0.12	2.00	0.11	2.61	0.20	0.40	0.08	0.62	0.09
68	8.62	74.12	0.49	12.23	0.24	3.76	0.14	4.09	0.12	2.05	0.11	2.72	0.21	0.46	0.09	0.57	0.09
69	8.89	74.01	0.49	12.40	0.24	3.80	0.14	4.07	0.12	2.03	0.11	2.64	0.21	0.51	0.10	0.53	0.08
70	9.16	74.11	0.49	12.10	0.23	3.94	0.14	4.03	0.12	2.16	0.12	2.66	0.21	0.50	0.10	0.50	0.08
71	9.43	73.86	0.49	12.15	0.24	3.86	0.14	4.08	0.12	2.04	0.11	3.00	0.23	0.48	0.10	0.53	0.08
72	9.70	73.77	0.49	12.35	0.24	3.83	0.14	4.08	0.12	2.09	0.11	2.81	0.22	0.55	0.11	0.53	0.08
73	9.97	74.00	0.49	12.35	0.24	3.79	0.14	4.14	0.13	2.09	0.11	2.59	0.20	0.51	0.10	0.53	0.08
74	10.24	73.79	0.49	12.29	0.24	3.71	0.13	4.05	0.12	2.22	0.12	2.77	0.22	0.47	0.09	0.71	0.11
75	10.51	73.53	0.49	12.39	0.24	3.91	0.14	4.08	0.12	2.12	0.11	2.79	0.22	0.52	0.10	0.65	0.10
76	10.78	73.63	0.49	12.20	0.24	3.99	0.14	4.15	0.13	2.11	0.11	2.82	0.22	0.46	0.09	0.64	0.10
77	11.04	73.64	0.49	12.26	0.24	3.95	0.14	4.11	0.13	2.24	0.12	2.71	0.21	0.46	0.09	0.64	0.10
78	11.31	73.92	0.49	12.25	0.24	3.86	0.14	4.10	0.13	2.25	0.12	2.55	0.20	0.45	0.09	0.62	0.09
79	11.58	73.49	0.49	12.32	0.24	4.01	0.14	4.19	0.13	2.19	0.12	2.69	0.21	0.47	0.09	0.63	0.09
80	11.85	73.70	0.49	12.37	0.24	4.03	0.15	4.15	0.13	2.18	0.12	2.48	0.19	0.50	0.10	0.58	0.09
81	12.12	73.48	0.49	12.42	0.24	3.88	0.14	4.08	0.12	2.03	0.11	3.01	0.24	0.46	0.09	0.65	0.10
82	12.39	73.71	0.49	12.26	0.24	3.91	0.14	4.21	0.13	2.09	0.11	2.80	0.22	0.45	0.09	0.56	0.08
83	12.66	73.40	0.49	12.48	0.24	3.75	0.14	4.12	0.13	2.17	0.12	2.88	0.23	0.61	0.12	0.60	0.09
84	12.93	73.71	0.49	12.19	0.24	4.01	0.14	4.08	0.12	2.20	0.12	2.80	0.22	0.46	0.09	0.57	0.09
85	13.20	73.41	0.49	12.36	0.24	3.97	0.14	4.30	0.13	2.18	0.12	2.73	0.21	0.43	0.09	0.63	0.10
86	13.47	73.86	0.49	12.51	0.24	3.76	0.14	4.07	0.12	2.06	0.11	2.68	0.21	0.45	0.09	0.60	0.09
87	13.74	73.64	0.49	12.40	0.24	3.88	0.14	4.01	0.12	2.10	0.11	2.81	0.22	0.48	0.10	0.68	0.10
88	14.01	73.30	0.49	12.38	0.24	4.05	0.15	4.17	0.13	2.21	0.12	2.87	0.22	0.49	0.10	0.54	0.08
89	14.28	73.20	0.49	12.41	0.24	4.03	0.15	4.27	0.13	2.16	0.12	2.96	0.23	0.45	0.09	0.51	0.08
90	14.55	73.84	0.49	12.68	0.25	4.02	0.15	3.94	0.12	2.04	0.11	2.61	0.20	0.44	0.09	0.44	0.07
91	14.82	73.47	0.49	12.57	0.24	4.05	0.15	4.17	0.13	2.05	0.11	2.73	0.21	0.46	0.09	0.51	0.08
92	15.09	73.17	0.49	12.71	0.25	4.11	0.15	4.11	0.13	2.24	0.12	2.75	0.22	0.37	0.07	0.53	0.08
93	15.35	73.52	0.49	12.30	0.24	4.05	0.15	4.27	0.13	2.26	0.12	2.46	0.19	0.49	0.10	0.64	0.10
94	15.62	73.75	0.49	12.57	0.24	4.04	0.15	4.06	0.12	2.08	0.11	2.36	0.18	0.48	0.10	0.66	0.10
95	15.89	73.45	0.49	12.52	0.24	3.99	0.14	4.05	0.12	2.05	0.11	2.90	0.23	0.41	0.08	0.62	0.09
96	16.16	73.04	0.49	12.68	0.25	4.00	0.14	4.09	0.12	2.18	0.12	3.01	0.24	0.47	0.09	0.52	0.08
97	16.43	73.05	0.49	12.49	0.24	4.01	0.14	4.17	0.13	2.23	0.12	2.97	0.23	0.47	0.09	0.61	0.09
98	16.70	73.51	0.49	12.51	0.24	4.00	0.14	4.18	0.13	2.05	0.11	2.68	0.21	0.49	0.10	0.58	0.09
99	16.97	73.51	0.49	12.73	0.25	3.88	0.14	4.04	0.12	2.19	0.12	2.54	0.20	0.53	0.11	0.58	0.09
100	17.24	72.99	0.48	12.90	0.25	3.86	0.14	4.07	0.12	2.25	0.12	2.65	0.21	0.67	0.13	0.62	0.09
101	17.51	73.24	0.49	12.66	0.25	3.86	0.14	4.12	0.13	2.28	0.12	2.77	0.22	0.46	0.09	0.61	0.09

Agglomerate FLD23.4.1

Table J.20: Major element compositions (as wt.% oxides) from a line traverse across the interface of surface agglomerate FLD23.4.1 (from agglomerate FLD23.4.1 to host FLD23) extracted from quantified EDS compositional maps. The EDS compositional maps were collected at a resolution of 6.0 pixels/μm. The smoothing width for this traverse was 75 pixels (12.5 μm) wide. This is an Si interface and has been centered at $x = 0$ based on the SiO_2 maximum. Peak points within 2σ of the SiO_2 maximum are highlighted in yellow. Uncertainties are 2SEOM.

Pt.	Position (μm)	SiO_2	2σ	Al_2O_3	2σ	Na_2O	2σ	K_2O	2σ	CaO	2σ	FeO	2σ	TiO_2	2σ	MgO	2σ
1	-7.81	73.94	0.30	13.29	0.12	2.94	0.11	3.86	0.07	1.82	0.09	3.02	0.20	0.47	0.08	0.65	0.06
2	-7.64	73.79	0.30	13.24	0.12	2.88	0.11	3.87	0.07	1.82	0.09	3.15	0.21	0.50	0.09	0.75	0.07
3	-7.48	73.82	0.30	13.35	0.12	3.06	0.11	3.91	0.07	1.88	0.09	2.87	0.19	0.48	0.08	0.63	0.06
4	-7.31	73.69	0.30	13.50	0.12	3.10	0.11	3.96	0.07	1.83	0.09	2.83	0.19	0.46	0.08	0.63	0.06
5	-7.14	73.55	0.30	13.35	0.12	3.15	0.12	3.88	0.07	1.85	0.09	3.07	0.21	0.45	0.08	0.69	0.06
6	-6.98	73.79	0.30	13.41	0.12	3.00	0.11	3.93	0.07	1.88	0.09	2.86	0.19	0.42	0.07	0.70	0.06
7	-6.81	73.76	0.30	13.52	0.12	3.00	0.11	3.93	0.07	1.81	0.09	2.88	0.20	0.36	0.06	0.74	0.07
8	-6.65	73.88	0.30	13.46	0.12	3.04	0.11	3.86	0.07	1.86	0.09	2.89	0.20	0.37	0.07	0.62	0.06
9	-6.48	73.60	0.30	13.44	0.12	3.10	0.11	3.87	0.07	1.81	0.09	3.00	0.20	0.52	0.09	0.66	0.06
10	-6.31	73.80	0.30	13.43	0.12	3.04	0.11	3.86	0.07	1.80	0.09	2.91	0.20	0.49	0.09	0.66	0.06
11	-6.15	73.72	0.30	13.40	0.12	3.09	0.11	3.92	0.07	1.71	0.08	3.00	0.20	0.48	0.08	0.68	0.06
12	-5.98	73.93	0.30	13.38	0.12	3.11	0.11	3.95	0.07	1.74	0.09	2.82	0.19	0.46	0.08	0.60	0.05
13	-5.81	73.75	0.30	13.52	0.12	3.08	0.11	3.87	0.07	1.79	0.09	2.88	0.20	0.49	0.08	0.62	0.05
14	-5.65	73.98	0.30	13.38	0.12	3.08	0.11	3.87	0.07	1.83	0.09	2.74	0.19	0.53	0.09	0.60	0.05
15	-5.48	73.72	0.30	13.32	0.12	3.14	0.12	3.92	0.07	1.83	0.09	2.97	0.20	0.51	0.09	0.60	0.05
16	-5.32	73.87	0.30	13.48	0.12	2.98	0.11	3.93	0.07	1.81	0.09	2.82	0.19	0.45	0.08	0.65	0.06
17	-5.15	73.80	0.30	13.56	0.12	3.01	0.11	3.95	0.07	1.75	0.09	2.83	0.19	0.45	0.08	0.65	0.06
18	-4.98	73.92	0.30	13.38	0.12	3.06	0.11	4.00	0.08	1.78	0.09	2.77	0.19	0.43	0.07	0.66	0.06
19	-4.82	73.77	0.30	13.47	0.12	2.99	0.11	4.01	0.08	1.84	0.09	2.85	0.19	0.41	0.07	0.66	0.06
20	-4.65	73.47	0.30	13.72	0.12	2.98	0.11	4.00	0.07	1.96	0.10	2.86	0.19	0.37	0.06	0.63	0.06
21	-4.49	73.45	0.30	13.64	0.12	3.06	0.11	4.08	0.08	1.92	0.09	2.92	0.20	0.37	0.06	0.56	0.05
22	-4.32	73.53	0.30	13.71	0.12	3.20	0.12	3.97	0.07	1.82	0.09	2.73	0.18	0.40	0.07	0.64	0.06
23	-4.15	73.70	0.30	13.65	0.12	3.07	0.11	4.01	0.08	1.81	0.09	2.69	0.18	0.43	0.08	0.65	0.06
24	-3.99	73.36	0.30	13.81	0.13	3.03	0.11	4.12	0.08	1.89	0.09	2.64	0.18	0.48	0.08	0.67	0.06
25	-3.82	73.35	0.30	13.76	0.12	3.15	0.12	4.07	0.08	1.89	0.09	2.71	0.18	0.46	0.08	0.62	0.05
26	-3.66	73.39	0.30	13.69	0.12	3.12	0.11	4.00	0.07	1.82	0.09	2.83	0.19	0.49	0.09	0.66	0.06
27	-3.49	73.43	0.30	13.77	0.12	3.11	0.11	3.91	0.07	1.86	0.09	2.92	0.20	0.42	0.07	0.58	0.05
28	-3.32	73.63	0.30	13.73	0.12	3.09	0.11	3.93	0.07	1.77	0.09	2.82	0.19	0.46	0.08	0.57	0.05
29	-3.16	73.62	0.30	13.63	0.12	3.07	0.11	4.07	0.08	1.82	0.09	2.64	0.18	0.45	0.08	0.70	0.06
30	-2.99	73.66	0.30	13.59	0.12	3.08	0.11	4.06	0.08	1.76	0.09	2.77	0.19	0.44	0.08	0.65	0.06
31	-2.82	73.68	0.30	13.77	0.12	3.03	0.11	4.00	0.08	1.70	0.08	2.76	0.19	0.43	0.07	0.63	0.06
32	-2.66	73.35	0.30	13.82	0.13	3.05	0.11	4.02	0.08	1.82	0.09	2.83	0.19	0.43	0.07	0.68	0.06
33	-2.49	73.45	0.30	13.65	0.12	3.10	0.11	4.06	0.08	1.79	0.09	2.77	0.19	0.49	0.08	0.68	0.06
34	-2.33	73.81	0.30	13.49	0.12	3.01	0.11	4.00	0.07	1.69	0.08	2.86	0.19	0.49	0.08	0.65	0.06
35	-2.16	73.59	0.30	13.53	0.12	2.97	0.11	4.05	0.08	1.86	0.09	2.92	0.20	0.40	0.07	0.67	0.06
36	-1.99	73.72	0.30	13.33	0.12	3.01	0.11	4.04	0.08	1.75	0.09	3.00	0.20	0.44	0.08	0.71	0.06
37	-1.83	73.98	0.30	13.36	0.12	3.01	0.11	4.04	0.08	1.60	0.08	2.94	0.20	0.43	0.08	0.63	0.06
38	-1.66	74.27	0.30	13.34	0.12	2.85	0.10	3.92	0.07	1.65	0.08	2.86	0.19	0.41	0.07	0.69	0.06
39	-1.50	74.59	0.30	13.13	0.12	2.81	0.10	3.99	0.07	1.67	0.08	2.72	0.18	0.45	0.08	0.64	0.06
40	-1.33	74.72	0.30	13.00	0.12	2.89	0.11	3.99	0.07	1.59	0.08	2.77	0.19	0.43	0.07	0.62	0.05
41	-1.16	74.70	0.30	12.85	0.12	2.89	0.11	4.07	0.08	1.64	0.08	2.82	0.19	0.43	0.07	0.60	0.05
42	-1.00	75.00	0.30	12.79	0.12	2.77	0.10	3.99	0.07	1.66	0.08	2.71	0.18	0.44	0.08	0.64	0.06
43	-0.83	74.75	0.30	12.69	0.12	2.86	0.11	4.07	0.08	1.68	0.08	2.79	0.19	0.50	0.09	0.65	0.06
44	-0.66	75.14	0.30	12.67	0.11	2.79	0.10	3.99	0.07	1.67	0.08	2.64	0.18	0.52	0.09	0.58	0.05
45	-0.50	75.01	0.30	12.71	0.12	2.82	0.10	3.94	0.07	1.63	0.08	2.82	0.19	0.48	0.08	0.60	0.05
46	-0.33	75.05	0.30	12.53	0.11	2.78	0.10	3.99	0.07	1.71	0.08	2.84	0.19	0.50	0.09	0.60	0.05
47	-0.17	75.19	0.30	12.42	0.11	2.76	0.10	4.08	0.08	1.76	0.09	2.69	0.18	0.46	0.08	0.63	0.06
48	0.00	75.43	0.30	12.34	0.11	2.91	0.11	4.04	0.08	1.67	0.08	2.61	0.18	0.46	0.08	0.53	0.05
49	0.17	75.42	0.30	12.45	0.11	2.67	0.10	3.99	0.07	1.60	0.08	2.79	0.19	0.52	0.09	0.57	0.05
50	0.33	75.24	0.30	12.39	0.11	2.69	0.10	4.04	0.08	1.77	0.09	2.74	0.19	0.45	0.08	0.68	0.06

51	0.50	75.28	0.30	12.37	0.11	2.72	0.10	4.09	0.08	1.77	0.09	2.67	0.18	0.48	0.08	0.64	0.06
52	0.66	75.16	0.30	12.45	0.11	2.82	0.10	4.01	0.08	1.73	0.08	2.72	0.18	0.49	0.09	0.61	0.05
53	0.83	74.70	0.30	12.54	0.11	2.77	0.10	4.01	0.08	1.83	0.09	2.93	0.20	0.59	0.10	0.64	0.06
54	1.00	74.57	0.30	12.67	0.11	2.84	0.10	3.95	0.07	1.87	0.09	2.89	0.20	0.57	0.10	0.64	0.06
55	1.16	74.42	0.30	12.73	0.12	2.87	0.11	4.06	0.08	1.85	0.09	2.98	0.20	0.49	0.08	0.60	0.05
56	1.33	74.60	0.30	12.70	0.12	2.78	0.10	4.00	0.07	1.91	0.09	2.91	0.20	0.50	0.09	0.61	0.05
57	1.50	74.39	0.30	12.65	0.11	2.91	0.11	4.02	0.08	1.92	0.09	2.93	0.20	0.51	0.09	0.68	0.06
58	1.66	74.53	0.30	12.67	0.11	2.84	0.10	3.98	0.07	2.02	0.10	2.81	0.19	0.50	0.09	0.66	0.06
59	1.83	74.48	0.30	12.84	0.12	2.80	0.10	3.95	0.07	2.04	0.10	2.72	0.18	0.48	0.08	0.69	0.06
60	1.99	74.18	0.30	12.74	0.12	2.90	0.11	4.03	0.08	2.05	0.10	2.94	0.20	0.44	0.08	0.71	0.06
61	2.16	73.97	0.30	12.86	0.12	2.94	0.11	4.08	0.08	2.08	0.10	2.99	0.20	0.42	0.07	0.65	0.06
62	2.33	73.96	0.30	12.95	0.12	2.95	0.11	3.94	0.07	2.12	0.10	3.01	0.20	0.45	0.08	0.62	0.05
63	2.49	73.74	0.30	13.01	0.12	2.94	0.11	4.11	0.08	2.09	0.10	2.97	0.20	0.44	0.08	0.69	0.06
64	2.66	73.92	0.30	12.99	0.12	2.82	0.10	4.05	0.08	1.95	0.10	3.09	0.21	0.47	0.08	0.70	0.06
65	2.82	73.79	0.30	13.04	0.12	2.90	0.11	4.07	0.08	1.93	0.09	2.99	0.20	0.60	0.10	0.67	0.06
66	2.99	73.82	0.30	12.98	0.12	2.77	0.10	4.06	0.08	2.14	0.10	2.99	0.20	0.51	0.09	0.73	0.06
67	3.16	74.03	0.30	13.03	0.12	2.88	0.11	4.00	0.08	2.05	0.10	2.83	0.19	0.53	0.09	0.64	0.06
68	3.32	74.34	0.30	12.93	0.12	2.83	0.10	4.03	0.08	2.05	0.10	2.73	0.19	0.47	0.08	0.62	0.05
69	3.49	73.85	0.30	13.11	0.12	2.79	0.10	4.06	0.08	2.20	0.11	2.74	0.19	0.55	0.10	0.69	0.06
70	3.65	73.47	0.30	13.03	0.12	2.87	0.11	4.15	0.08	2.18	0.11	3.09	0.21	0.55	0.10	0.65	0.06
71	3.82	73.82	0.30	13.02	0.12	2.94	0.11	4.02	0.08	2.17	0.11	2.86	0.19	0.51	0.09	0.67	0.06
72	3.99	73.84	0.30	13.05	0.12	2.84	0.10	3.98	0.07	2.17	0.11	2.93	0.20	0.52	0.09	0.66	0.06
73	4.15	73.76	0.30	13.02	0.12	2.81	0.10	4.16	0.08	2.12	0.10	3.07	0.21	0.45	0.08	0.61	0.05
74	4.32	73.45	0.30	13.02	0.12	2.92	0.11	4.15	0.08	2.23	0.11	3.06	0.21	0.48	0.08	0.68	0.06
75	4.49	73.46	0.30	13.13	0.12	2.84	0.10	4.14	0.08	2.25	0.11	2.95	0.20	0.57	0.10	0.66	0.06
76	4.65	73.83	0.30	13.07	0.12	2.87	0.11	4.04	0.08	2.04	0.10	3.02	0.20	0.50	0.09	0.63	0.06
77	4.82	73.46	0.30	13.13	0.12	3.00	0.11	4.14	0.08	2.07	0.10	3.10	0.21	0.49	0.08	0.61	0.05
78	4.98	73.35	0.30	13.02	0.12	2.96	0.11	4.14	0.08	2.19	0.11	3.18	0.22	0.55	0.10	0.61	0.05
79	5.15	73.46	0.30	13.23	0.12	3.00	0.11	4.07	0.08	2.17	0.11	2.93	0.20	0.46	0.08	0.68	0.06
80	5.32	73.32	0.30	13.28	0.12	2.93	0.11	4.04	0.08	2.12	0.10	3.15	0.21	0.53	0.09	0.64	0.06
81	5.48	73.24	0.30	13.18	0.12	2.96	0.11	4.17	0.08	2.21	0.11	3.19	0.22	0.48	0.08	0.58	0.05
82	5.65	73.69	0.30	13.08	0.12	2.92	0.11	4.15	0.08	2.15	0.11	2.85	0.19	0.45	0.08	0.71	0.06
83	5.81	73.55	0.30	13.12	0.12	2.85	0.10	4.09	0.08	2.13	0.10	3.13	0.21	0.49	0.08	0.65	0.06
84	5.98	73.48	0.30	13.20	0.12	2.89	0.11	4.11	0.08	2.20	0.11	2.98	0.20	0.48	0.08	0.64	0.06
85	6.15	73.57	0.30	13.11	0.12	2.80	0.10	4.15	0.08	2.18	0.11	3.00	0.20	0.50	0.09	0.68	0.06
86	6.31	73.55	0.30	13.15	0.12	2.97	0.11	4.16	0.08	2.13	0.10	2.96	0.20	0.46	0.08	0.61	0.05
87	6.48	73.53	0.30	13.13	0.12	2.89	0.11	4.03	0.08	2.16	0.11	3.03	0.21	0.56	0.10	0.67	0.06
88	6.65	73.52	0.30	13.12	0.12	2.86	0.10	4.12	0.08	2.13	0.10	3.09	0.21	0.53	0.09	0.63	0.06
89	6.81	73.26	0.30	13.00	0.12	2.92	0.11	4.26	0.08	2.30	0.11	3.07	0.21	0.53	0.09	0.66	0.06

Agglomerate FLD23.4.2

Table J.21: Major element compositions (as wt.% oxides) from a line traverse across the interface of surface agglomerate FLD23.4.2 (from agglomerate FLD23.4.2 to host FLD23) extracted from quantified EDS compositional maps. The EDS compositional maps were collected at a resolution of 6.0 pixels/μm. The smoothing width for this traverse was 75 pixels (12.5 μm) wide. This is an Si interface and has been centered at $x = 0$ based on the SiO_2 maximum. Peak points within 2σ of the SiO_2 maximum are highlighted in yellow. Uncertainties are 2SEOM.

Pt.	Position (μm)	SiO_2	2σ	Al_2O_3	2σ	Na_2O	2σ	K_2O	2σ	CaO	2σ	FeO	2σ	TiO_2	2σ	MgO	2σ
1	-10.47	72.49	0.29	13.89	0.13	3.06	0.11	4.27	0.08	1.67	0.08	3.40	0.23	0.51	0.09	0.71	0.06
2	-10.30	72.37	0.29	13.84	0.13	3.09	0.11	4.32	0.08	1.84	0.09	3.31	0.22	0.56	0.10	0.66	0.06
3	-10.13	72.65	0.29	13.75	0.12	3.02	0.11	4.34	0.08	1.70	0.08	3.29	0.22	0.54	0.09	0.70	0.06
4	-9.97	72.69	0.29	13.82	0.13	3.06	0.11	4.16	0.08	1.69	0.08	3.40	0.23	0.50	0.09	0.68	0.06
5	-9.80	72.27	0.29	13.82	0.13	3.13	0.11	4.19	0.08	1.73	0.09	3.66	0.25	0.50	0.09	0.69	0.06
6	-9.64	72.23	0.29	14.02	0.13	3.10	0.11	4.25	0.08	1.78	0.09	3.40	0.23	0.59	0.10	0.63	0.06
7	-9.47	72.51	0.29	13.95	0.13	3.10	0.11	4.26	0.08	1.80	0.09	3.25	0.22	0.47	0.08	0.67	0.06
8	-9.30	72.54	0.29	13.91	0.13	3.08	0.11	4.28	0.08	1.84	0.09	3.17	0.21	0.47	0.08	0.70	0.06
9	-9.14	72.95	0.29	13.84	0.13	3.02	0.11	4.23	0.08	1.71	0.08	3.15	0.21	0.46	0.08	0.64	0.06
10	-8.97	72.74	0.29	13.84	0.13	3.05	0.11	4.33	0.08	1.72	0.08	3.25	0.22	0.45	0.08	0.62	0.05
11	-8.81	73.02	0.30	13.64	0.12	3.07	0.11	4.27	0.08	1.74	0.09	3.07	0.21	0.52	0.09	0.66	0.06
12	-8.64	73.05	0.30	13.64	0.12	3.07	0.11	4.32	0.08	1.80	0.09	3.08	0.21	0.43	0.08	0.60	0.05
13	-8.47	73.52	0.30	13.59	0.12	3.04	0.11	4.31	0.08	1.66	0.08	2.85	0.19	0.48	0.08	0.56	0.05
14	-8.31	73.74	0.30	13.37	0.12	3.00	0.11	4.21	0.08	1.68	0.08	2.99	0.20	0.39	0.07	0.62	0.05
15	-8.14	73.65	0.30	13.31	0.12	3.07	0.11	4.25	0.08	1.66	0.08	2.98	0.20	0.43	0.07	0.65	0.06
16	-7.97	73.69	0.30	13.23	0.12	2.98	0.11	4.29	0.08	1.77	0.09	3.01	0.20	0.44	0.08	0.58	0.05
17	-7.81	73.69	0.30	13.18	0.12	3.01	0.11	4.23	0.08	1.84	0.09	2.98	0.20	0.54	0.09	0.52	0.05
18	-7.64	73.90	0.30	13.20	0.12	3.16	0.12	4.20	0.08	1.70	0.08	2.79	0.19	0.45	0.08	0.60	0.05
19	-7.48	74.06	0.30	13.21	0.12	3.03	0.11	4.26	0.08	1.76	0.09	2.66	0.18	0.46	0.08	0.55	0.05
20	-7.31	74.01	0.30	13.07	0.12	3.10	0.11	4.29	0.08	1.77	0.09	2.72	0.18	0.46	0.08	0.58	0.05
21	-7.14	73.87	0.30	12.96	0.12	3.18	0.12	4.17	0.08	1.92	0.09	2.88	0.20	0.46	0.08	0.56	0.05
22	-6.98	73.66	0.30	13.02	0.12	3.18	0.12	4.27	0.08	1.83	0.09	3.04	0.21	0.41	0.07	0.59	0.05
23	-6.81	73.66	0.30	13.21	0.12	3.16	0.12	4.20	0.08	2.01	0.10	2.76	0.19	0.46	0.08	0.54	0.05
24	-6.65	73.80	0.30	13.15	0.12	3.09	0.11	4.20	0.08	1.95	0.10	2.77	0.19	0.45	0.08	0.59	0.05
25	-6.48	73.78	0.30	13.02	0.12	3.08	0.11	4.27	0.08	1.98	0.10	2.95	0.20	0.38	0.07	0.54	0.05
26	-6.31	73.91	0.30	12.96	0.12	3.08	0.11	4.31	0.08	2.03	0.10	2.82	0.19	0.34	0.06	0.55	0.05
27	-6.15	73.80	0.30	13.06	0.12	3.05	0.11	4.33	0.08	2.22	0.11	2.60	0.18	0.35	0.06	0.60	0.05
28	-5.98	73.60	0.30	13.11	0.12	3.05	0.11	4.30	0.08	2.28	0.11	2.67	0.18	0.41	0.07	0.57	0.05
29	-5.81	73.22	0.30	13.07	0.12	3.12	0.11	4.25	0.08	2.29	0.11	3.09	0.21	0.37	0.06	0.59	0.05
30	-5.65	73.15	0.30	13.07	0.12	3.13	0.11	4.15	0.08	2.38	0.12	3.04	0.21	0.48	0.08	0.61	0.05
31	-5.48	73.42	0.30	12.96	0.12	3.09	0.11	4.09	0.08	2.38	0.12	3.00	0.20	0.48	0.08	0.59	0.05
32	-5.32	73.50	0.30	12.86	0.12	3.03	0.11	4.24	0.08	2.47	0.12	2.86	0.19	0.43	0.08	0.60	0.05
33	-5.15	73.50	0.30	12.88	0.12	3.12	0.11	4.25	0.08	2.44	0.12	2.82	0.19	0.43	0.08	0.57	0.05
34	-4.98	73.66	0.30	12.69	0.12	3.15	0.12	4.13	0.08	2.38	0.12	2.92	0.20	0.46	0.08	0.62	0.05
35	-4.82	73.84	0.30	12.72	0.12	3.02	0.11	4.11	0.08	2.43	0.12	2.74	0.19	0.52	0.09	0.63	0.06
36	-4.65	73.87	0.30	12.79	0.12	3.10	0.11	4.07	0.08	2.31	0.11	2.82	0.19	0.42	0.07	0.63	0.06
37	-4.49	73.92	0.30	12.63	0.11	3.03	0.11	4.04	0.08	2.42	0.12	2.87	0.19	0.46	0.08	0.63	0.06
38	-4.32	73.83	0.30	12.69	0.12	3.08	0.11	4.09	0.08	2.50	0.12	2.75	0.19	0.47	0.08	0.60	0.05
39	-4.15	73.83	0.30	12.68	0.12	3.10	0.11	4.14	0.08	2.43	0.12	2.78	0.19	0.41	0.07	0.63	0.06
40	-3.99	73.81	0.30	12.66	0.11	3.04	0.11	4.10	0.08	2.40	0.12	2.92	0.20	0.41	0.07	0.66	0.06
41	-3.82	73.51	0.30	12.97	0.12	3.01	0.11	4.13	0.08	2.55	0.13	2.68	0.18	0.49	0.09	0.65	0.06
42	-3.66	73.38	0.30	13.03	0.12	3.00	0.11	4.18	0.08	2.66	0.13	2.67	0.18	0.42	0.07	0.65	0.06
43	-3.49	73.57	0.30	12.93	0.12	3.15	0.12	4.22	0.08	2.53	0.12	2.52	0.17	0.42	0.07	0.66	0.06
44	-3.32	73.49	0.30	12.95	0.12	3.12	0.11	4.14	0.08	2.67	0.13	2.67	0.18	0.32	0.06	0.64	0.06
45	-3.16	73.14	0.30	13.05	0.12	3.08	0.11	4.14	0.08	2.66	0.13	2.89	0.20	0.39	0.07	0.65	0.06
46	-2.99	73.45	0.30	13.00	0.12	3.02	0.11	4.13	0.08	2.59	0.13	2.79	0.19	0.43	0.07	0.59	0.05
47	-2.82	73.46	0.30	12.96	0.12	3.11	0.11	4.13	0.08	2.66	0.13	2.70	0.18	0.40	0.07	0.59	0.05
48	-2.66	73.56	0.30	12.93	0.12	3.07	0.11	4.15	0.08	2.54	0.12	2.73	0.19	0.38	0.07	0.64	0.06
49	-2.49	73.53	0.30	12.91	0.12	2.98	0.11	4.14	0.08	2.46	0.12	2.88	0.20	0.47	0.08	0.62	0.05
50	-2.33	73.83	0.30	12.76	0.12	2.95	0.11	4.23	0.08	2.47	0.12	2.69	0.18	0.41	0.07	0.66	0.06

51	-2.16	74.08	0.30	12.75	0.12	3.00	0.11	4.15	0.08	2.23	0.11	2.77	0.19	0.40	0.07	0.62	0.05
52	-1.99	74.00	0.30	12.67	0.11	2.96	0.11	4.20	0.08	2.25	0.11	2.91	0.20	0.44	0.08	0.57	0.05
53	-1.83	74.17	0.30	12.61	0.11	2.89	0.11	4.18	0.08	2.26	0.11	2.92	0.20	0.40	0.07	0.58	0.05
54	-1.66	74.17	0.30	12.63	0.11	2.91	0.11	4.18	0.08	2.22	0.11	2.90	0.20	0.40	0.07	0.59	0.05
55	-1.50	74.26	0.30	12.65	0.11	2.86	0.10	4.19	0.08	2.15	0.11	2.83	0.19	0.45	0.08	0.60	0.05
56	-1.33	74.11	0.30	12.59	0.11	2.79	0.10	4.15	0.08	2.09	0.10	3.12	0.21	0.49	0.08	0.66	0.06
57	-1.16	74.59	0.30	12.35	0.11	2.76	0.10	4.21	0.08	1.97	0.10	3.04	0.21	0.45	0.08	0.64	0.06
58	-1.00	74.99	0.30	12.20	0.11	2.80	0.10	4.19	0.08	2.02	0.10	2.86	0.19	0.34	0.06	0.60	0.05
59	-0.83	75.37	0.30	12.14	0.11	2.75	0.10	4.17	0.08	1.96	0.10	2.63	0.18	0.41	0.07	0.58	0.05
60	-0.66	75.34	0.30	11.95	0.11	2.79	0.10	4.14	0.08	1.93	0.09	2.91	0.20	0.34	0.06	0.59	0.05
61	-0.50	75.67	0.31	11.86	0.11	2.65	0.10	4.13	0.08	1.84	0.09	2.92	0.20	0.42	0.07	0.51	0.04
62	-0.33	76.09	0.31	11.63	0.11	2.63	0.10	4.10	0.08	1.70	0.08	2.95	0.20	0.35	0.06	0.55	0.05
63	-0.17	76.03	0.31	11.64	0.11	2.59	0.09	4.09	0.08	1.71	0.08	2.97	0.20	0.37	0.06	0.61	0.05
64	0.00	76.13	0.31	11.58	0.10	2.70	0.10	4.12	0.08	1.64	0.08	2.81	0.19	0.43	0.07	0.61	0.05
65	0.17	76.03	0.31	11.46	0.10	2.71	0.10	4.13	0.08	1.66	0.08	3.04	0.21	0.42	0.07	0.56	0.05
66	0.33	76.09	0.31	11.68	0.11	2.60	0.10	4.10	0.08	1.60	0.08	3.00	0.20	0.39	0.07	0.52	0.05
67	0.50	75.83	0.31	11.74	0.11	2.63	0.10	4.19	0.08	1.79	0.09	2.78	0.19	0.47	0.08	0.57	0.05
68	0.66	75.78	0.31	11.87	0.11	2.65	0.10	4.24	0.08	1.81	0.09	2.64	0.18	0.46	0.08	0.54	0.05
69	0.83	75.53	0.31	12.00	0.11	2.71	0.10	4.12	0.08	1.76	0.09	2.86	0.19	0.40	0.07	0.61	0.05
70	1.00	75.31	0.30	12.16	0.11	2.69	0.10	4.12	0.08	1.75	0.09	2.97	0.20	0.39	0.07	0.60	0.05
71	1.16	74.92	0.30	12.37	0.11	2.70	0.10	4.18	0.08	1.86	0.09	2.87	0.19	0.46	0.08	0.63	0.06
72	1.33	74.86	0.30	12.35	0.11	2.68	0.10	4.18	0.08	1.75	0.09	3.13	0.21	0.42	0.07	0.62	0.05
73	1.50	74.58	0.30	12.34	0.11	2.84	0.10	4.24	0.08	1.82	0.09	3.13	0.21	0.49	0.09	0.55	0.05
74	1.66	74.72	0.30	12.42	0.11	2.78	0.10	4.20	0.08	1.90	0.09	3.00	0.20	0.39	0.07	0.59	0.05
75	1.83	74.81	0.30	12.46	0.11	2.79	0.10	4.14	0.08	1.92	0.09	2.90	0.20	0.38	0.07	0.60	0.05
76	1.99	74.69	0.30	12.56	0.11	2.75	0.10	4.12	0.08	1.89	0.09	3.02	0.20	0.39	0.07	0.59	0.05
77	2.16	74.50	0.30	12.64	0.11	2.76	0.10	4.14	0.08	1.87	0.09	3.06	0.21	0.38	0.07	0.65	0.06
78	2.33	74.28	0.30	12.54	0.11	2.87	0.11	4.22	0.08	1.90	0.09	3.10	0.21	0.44	0.08	0.64	0.06
79	2.49	74.43	0.30	12.47	0.11	2.94	0.11	4.15	0.08	1.87	0.09	2.99	0.20	0.49	0.08	0.67	0.06
80	2.66	74.57	0.30	12.69	0.12	2.82	0.10	4.12	0.08	1.87	0.09	2.94	0.20	0.44	0.08	0.55	0.05
81	2.82	74.30	0.30	12.72	0.12	2.79	0.10	4.19	0.08	1.99	0.10	3.01	0.20	0.40	0.07	0.60	0.05
82	2.99	74.38	0.30	12.71	0.12	2.82	0.10	4.19	0.08	1.89	0.09	3.01	0.20	0.43	0.07	0.57	0.05
83	3.16	74.29	0.30	12.63	0.11	2.82	0.10	4.21	0.08	1.86	0.09	3.04	0.21	0.50	0.09	0.64	0.06
84	3.32	74.21	0.30	12.82	0.12	2.72	0.10	4.19	0.08	2.01	0.10	2.97	0.20	0.46	0.08	0.62	0.05
85	3.49	74.30	0.30	12.70	0.12	2.71	0.10	4.26	0.08	1.91	0.09	3.06	0.21	0.45	0.08	0.62	0.05
86	3.66	74.21	0.30	12.82	0.12	2.76	0.10	4.21	0.08	1.88	0.09	2.94	0.20	0.51	0.09	0.66	0.06
87	3.82	74.29	0.30	12.79	0.12	2.81	0.10	4.22	0.08	1.86	0.09	3.06	0.21	0.35	0.06	0.61	0.05
88	3.99	74.44	0.30	12.83	0.12	2.83	0.10	4.14	0.08	1.80	0.09	2.88	0.20	0.49	0.09	0.58	0.05
89	4.15	74.24	0.30	12.92	0.12	2.84	0.10	4.13	0.08	1.81	0.09	2.96	0.20	0.51	0.09	0.59	0.05
90	4.32	74.24	0.30	12.94	0.12	2.80	0.10	4.09	0.08	1.84	0.09	2.98	0.20	0.43	0.08	0.67	0.06
91	4.49	74.13	0.30	12.84	0.12	2.83	0.10	4.13	0.08	1.96	0.10	3.04	0.21	0.46	0.08	0.63	0.06
92	4.65	74.19	0.30	12.78	0.12	2.89	0.11	4.13	0.08	1.87	0.09	3.12	0.21	0.38	0.07	0.64	0.06
93	4.82	74.17	0.30	12.80	0.12	2.84	0.10	4.14	0.08	1.88	0.09	3.13	0.21	0.41	0.07	0.62	0.05
94	4.98	74.25	0.30	12.81	0.12	2.79	0.10	4.17	0.08	1.80	0.09	3.07	0.21	0.50	0.09	0.62	0.05
95	5.15	74.26	0.30	12.84	0.12	2.82	0.10	4.20	0.08	1.90	0.09	2.92	0.20	0.47	0.08	0.60	0.05
96	5.32	74.34	0.30	12.87	0.12	2.80	0.10	4.10	0.08	1.92	0.09	2.94	0.20	0.42	0.07	0.61	0.05
97	5.48	74.34	0.30	12.91	0.12	2.76	0.10	4.19	0.08	2.00	0.10	2.75	0.19	0.42	0.07	0.64	0.06
98	5.65	74.11	0.30	12.96	0.12	2.71	0.10	4.19	0.08	1.93	0.09	2.89	0.20	0.55	0.10	0.66	0.06
99	5.81	74.19	0.30	12.68	0.12	2.85	0.10	4.17	0.08	1.88	0.09	3.15	0.21	0.45	0.08	0.62	0.05
100	5.98	74.18	0.30	12.96	0.12	2.74	0.10	4.16	0.08	1.90	0.09	3.11	0.21	0.38	0.07	0.56	0.05
101	6.15	74.12	0.30	12.96	0.12	2.72	0.10	4.18	0.08	1.90	0.09	2.99	0.20	0.53	0.09	0.58	0.05
102	6.31	74.13	0.30	12.89	0.12	2.76	0.10	4.25	0.08	1.90	0.09	2.96	0.20	0.49	0.09	0.62	0.06
103	6.48	74.12	0.30	12.95	0.12	2.83	0.10	4.24	0.08	1.93	0.09	2.86	0.19	0.49	0.09	0.57	0.05
104	6.65	74.03	0.30	12.93	0.12	2.86	0.10	4.19	0.08	2.06	0.10	2.90	0.20	0.47	0.08	0.56	0.05
105	6.81	73.67	0.30	13.00	0.12	2.89	0.11	4.28	0.08	1.98	0.10	3.10	0.21	0.45	0.08	0.62	0.05
106	6.98	74.00	0.30	12.96	0.12	2.81	0.10	4.16	0.08	1.91	0.09	2.99	0.20	0.54	0.09	0.62	0.05
107	7.14	73.89	0.30	13.07	0.12	2.80	0.10	4.17	0.08	1.98	0.10	3.01	0.20	0.45	0.08	0.64	0.06
108	7.31	73.84	0.30	13.00	0.12	2.87	0.11	4.16	0.08	1.89	0.09	3.16	0.21	0.43	0.07	0.65	0.06
109	7.48	73.76	0.30	13.03	0.12	2.88	0.11	4.14	0.08	1.92	0.09	3.10	0.21	0.49	0.08	0.69	0.06
110	7.64	73.80	0.30	13.09	0.12	2.96	0.11	4.23	0.08	1.86	0.09	2.87	0.19	0.53	0.09	0.66	0.06
111	7.81	73.82	0.30	13.13	0.12	2.99	0.11	4.19	0.08	1.90	0.09	2.98	0.20	0.40	0.07	0.59	0.05
112	7.97	73.99	0.30	13.12	0.12	2.79	0.10	4.20	0.08	2.00	0.10	2.83	0.19	0.44	0.08	0.63	0.06

113	8.14	73.88	0.30	13.14	0.12	2.82	0.10	4.18	0.08	1.94	0.10	3.07	0.21	0.43	0.08	0.54	0.05
114	-10.47	73.86	0.30	13.22	0.12	3.05	0.11	3.77	0.07	1.81	0.09	3.17	0.21	0.45	0.08	0.67	0.06

Agglomerate FLD23.5.1

Table J.22: Major element compositions (as wt.% oxides) from a line traverse across the interface of surface agglomerate FLD23.5.1 (from agglomerate FLD23.5.1 to host FLD23) extracted from quantified EDS compositional maps. The EDS compositional maps were collected at a resolution of 6.0 pixels/μm. The smoothing width for this traverse was 100 pixels (16.6 μm) wide. This is an Si interface and has been centered at $x = 0$ based on the SiO_2 maximum. Peak points within 2σ of the SiO_2 maximum are highlighted in yellow. Uncertainties are 2SEOM.

Pt.	Position (μm)	SiO_2	2σ	Al_2O_3	2σ	Na_2O	2σ	K_2O	2σ	CaO	2σ	FeO	2σ	TiO_2	2σ	MgO	2σ
1	-9.97	74.50	0.25	12.96	0.10	2.35	0.07	3.75	0.06	2.57	0.11	2.84	0.16	0.45	0.07	0.59	0.05
2	-9.80	74.63	0.25	13.00	0.10	2.34	0.07	3.79	0.07	2.53	0.11	2.74	0.16	0.42	0.06	0.55	0.04
3	-9.64	74.39	0.25	12.89	0.10	2.36	0.07	3.92	0.07	2.61	0.11	2.86	0.16	0.39	0.06	0.58	0.04
4	-9.47	74.35	0.25	12.88	0.10	2.34	0.07	3.86	0.07	2.63	0.11	2.89	0.16	0.39	0.06	0.65	0.05
5	-9.30	74.44	0.25	12.95	0.10	2.38	0.07	3.78	0.06	2.57	0.11	2.86	0.16	0.41	0.06	0.61	0.05
6	-9.14	74.36	0.25	12.96	0.10	2.39	0.07	3.79	0.07	2.56	0.11	2.99	0.17	0.37	0.06	0.58	0.04
7	-8.97	74.38	0.25	12.90	0.10	2.29	0.07	3.92	0.07	2.65	0.11	2.92	0.17	0.42	0.06	0.52	0.04
8	-8.81	74.66	0.25	12.84	0.10	2.37	0.07	3.80	0.07	2.51	0.11	2.77	0.16	0.47	0.07	0.58	0.04
9	-8.64	74.57	0.25	12.94	0.10	2.42	0.08	3.81	0.07	2.53	0.11	2.72	0.15	0.45	0.07	0.56	0.04
10	-8.47	74.43	0.25	12.85	0.10	2.34	0.07	3.76	0.06	2.66	0.11	2.95	0.17	0.48	0.07	0.53	0.04
11	-8.31	74.51	0.25	12.78	0.10	2.33	0.07	3.88	0.07	2.64	0.11	2.87	0.16	0.41	0.06	0.57	0.04
12	-8.14	74.57	0.25	12.89	0.10	2.38	0.07	3.83	0.07	2.49	0.11	2.88	0.16	0.38	0.06	0.59	0.05
13	-7.97	74.71	0.25	12.80	0.10	2.32	0.07	3.86	0.07	2.50	0.11	2.85	0.16	0.44	0.07	0.53	0.04
14	-7.81	74.63	0.25	12.80	0.10	2.34	0.07	3.80	0.07	2.60	0.11	2.82	0.16	0.46	0.07	0.55	0.04
15	-7.64	74.46	0.25	12.83	0.10	2.40	0.08	3.81	0.07	2.57	0.11	2.90	0.16	0.47	0.07	0.56	0.04
16	-7.48	74.35	0.25	12.90	0.10	2.35	0.07	3.88	0.07	2.69	0.11	2.78	0.16	0.49	0.07	0.56	0.04
17	-7.31	74.41	0.25	13.00	0.10	2.37	0.07	3.77	0.06	2.66	0.11	2.81	0.16	0.44	0.07	0.55	0.04
18	-7.14	74.68	0.25	12.88	0.10	2.38	0.07	3.79	0.07	2.58	0.11	2.75	0.16	0.39	0.06	0.55	0.04
19	-6.98	74.65	0.25	12.83	0.10	2.36	0.07	3.74	0.06	2.58	0.11	2.90	0.17	0.42	0.06	0.53	0.04
20	-6.81	74.60	0.25	12.85	0.10	2.27	0.07	3.81	0.07	2.62	0.11	2.84	0.16	0.43	0.06	0.58	0.04
21	-6.65	74.65	0.25	12.92	0.10	2.32	0.07	3.86	0.07	2.57	0.11	2.73	0.16	0.38	0.06	0.57	0.04
22	-6.48	74.67	0.25	12.88	0.10	2.33	0.07	3.85	0.07	2.54	0.11	2.71	0.15	0.44	0.07	0.58	0.04
23	-6.31	74.35	0.25	12.90	0.10	2.42	0.08	3.81	0.07	2.63	0.11	2.85	0.16	0.44	0.07	0.60	0.05
24	-6.15	74.45	0.25	12.95	0.10	2.36	0.07	3.86	0.07	2.60	0.11	2.80	0.16	0.37	0.06	0.61	0.05
25	-5.98	74.40	0.25	12.99	0.10	2.39	0.07	3.86	0.07	2.56	0.11	2.83	0.16	0.43	0.07	0.54	0.04
26	-5.81	74.54	0.25	12.81	0.10	2.38	0.07	3.83	0.07	2.64	0.11	2.80	0.16	0.47	0.07	0.54	0.04
27	-5.65	74.38	0.25	12.98	0.10	2.33	0.07	3.89	0.07	2.59	0.11	2.83	0.16	0.46	0.07	0.55	0.04
28	-5.48	74.52	0.25	12.96	0.10	2.34	0.07	3.92	0.07	2.58	0.11	2.75	0.16	0.40	0.06	0.53	0.04
29	-5.32	74.43	0.25	12.89	0.10	2.35	0.07	3.93	0.07	2.63	0.11	2.78	0.16	0.44	0.07	0.54	0.04
30	-5.15	74.69	0.25	13.00	0.10	2.33	0.07	3.97	0.07	2.50	0.11	2.59	0.15	0.37	0.06	0.55	0.04
31	-4.98	74.54	0.25	12.95	0.10	2.33	0.07	3.91	0.07	2.52	0.11	2.73	0.16	0.40	0.06	0.61	0.05
32	-4.82	74.65	0.25	13.06	0.11	2.33	0.07	3.91	0.07	2.48	0.11	2.59	0.15	0.35	0.05	0.63	0.05
33	-4.65	74.51	0.25	13.06	0.11	2.41	0.08	3.97	0.07	2.51	0.11	2.63	0.15	0.34	0.05	0.57	0.04
34	-4.49	74.12	0.25	12.97	0.10	2.40	0.08	4.01	0.07	2.68	0.11	2.87	0.16	0.39	0.06	0.55	0.04
35	-4.32	74.26	0.25	13.05	0.11	2.45	0.08	3.87	0.07	2.63	0.11	2.77	0.16	0.43	0.06	0.53	0.04
36	-4.15	74.41	0.25	13.02	0.10	2.36	0.07	3.90	0.07	2.58	0.11	2.71	0.15	0.42	0.06	0.60	0.05
37	-3.99	74.34	0.25	12.97	0.10	2.46	0.08	3.95	0.07	2.54	0.11	2.73	0.16	0.44	0.07	0.55	0.04
38	-3.82	74.33	0.25	13.01	0.10	2.43	0.08	3.98	0.07	2.49	0.11	2.69	0.15	0.53	0.08	0.54	0.04
39	-3.66	74.51	0.25	13.17	0.11	2.44	0.08	3.90	0.07	2.43	0.10	2.56	0.15	0.43	0.06	0.57	0.04
40	-3.49	74.31	0.25	13.23	0.11	2.46	0.08	3.96	0.07	2.50	0.11	2.54	0.14	0.45	0.07	0.56	0.04
41	-3.32	74.29	0.25	13.25	0.11	2.44	0.08	4.01	0.07	2.46	0.10	2.60	0.15	0.40	0.06	0.55	0.04
42	-3.16	74.20	0.25	13.21	0.11	2.43	0.08	4.02	0.07	2.52	0.11	2.69	0.15	0.40	0.06	0.54	0.04
43	-2.99	74.29	0.25	13.20	0.11	2.39	0.07	3.97	0.07	2.43	0.10	2.78	0.16	0.45	0.07	0.51	0.04
44	-2.82	74.38	0.25	13.21	0.11	2.42	0.08	3.99	0.07	2.40	0.10	2.60	0.15	0.44	0.07	0.57	0.04
45	-2.66	74.02	0.25	13.37	0.11	2.43	0.08	3.98	0.07	2.43	0.10	2.67	0.15	0.54	0.08	0.55	0.04
46	-2.49	74.14	0.25	13.32	0.11	2.55	0.08	3.94	0.07	2.38	0.10	2.59	0.15	0.53	0.08	0.54	0.04
47	-2.33	74.19	0.25	13.22	0.11	2.47	0.08	4.11	0.07	2.53	0.11	2.52	0.14	0.43	0.07	0.53	0.04
48	-2.16	74.06	0.25	13.25	0.11	2.35	0.07	4.10	0.07	2.55	0.11	2.64	0.15	0.50	0.08	0.54	0.04
49	-1.99	74.18	0.25	13.28	0.11	2.41	0.08	4.04	0.07	2.52	0.11	2.54	0.14	0.46	0.07	0.57	0.04
50	-1.83	74.19	0.25	13.21	0.11	2.47	0.08	3.95	0.07	2.44	0.10	2.76	0.16	0.45	0.07	0.53	0.04

51	-1.66	74.23	0.25	13.29	0.11	2.43	0.08	4.00	0.07	2.44	0.10	2.69	0.15	0.40	0.06	0.52	0.04
52	-1.50	74.34	0.25	13.26	0.11	2.40	0.08	4.03	0.07	2.40	0.10	2.58	0.15	0.43	0.07	0.56	0.04
53	-1.33	74.63	0.25	13.16	0.11	2.36	0.07	4.07	0.07	2.34	0.10	2.58	0.15	0.38	0.06	0.48	0.04
54	-1.16	74.72	0.25	12.87	0.10	2.32	0.07	4.07	0.07	2.27	0.10	2.78	0.16	0.48	0.07	0.49	0.04
55	-1.00	74.89	0.25	12.78	0.10	2.36	0.07	4.06	0.07	2.26	0.10	2.73	0.16	0.41	0.06	0.50	0.04
56	-0.83	75.51	0.25	12.46	0.10	2.28	0.07	4.05	0.07	2.05	0.09	2.73	0.16	0.44	0.07	0.47	0.04
57	-0.66	75.97	0.25	12.21	0.10	2.21	0.07	3.97	0.07	1.92	0.08	2.81	0.16	0.40	0.06	0.51	0.04
58	-0.50	76.60	0.25	11.94	0.10	2.17	0.07	3.90	0.07	1.82	0.08	2.66	0.15	0.40	0.06	0.50	0.04
59	-0.33	76.84	0.26	11.60	0.09	2.11	0.07	3.98	0.07	1.79	0.08	2.78	0.16	0.43	0.07	0.47	0.04
60	-0.17	76.99	0.26	11.37	0.09	2.14	0.07	3.93	0.07	1.73	0.07	2.78	0.16	0.46	0.07	0.59	0.05
61	0.00	77.63	0.26	11.24	0.09	2.02	0.06	3.89	0.07	1.67	0.07	2.62	0.15	0.42	0.06	0.51	0.04
62	0.17	77.46	0.26	11.16	0.09	2.13	0.07	3.92	0.07	1.66	0.07	2.75	0.16	0.40	0.06	0.52	0.04
63	0.33	77.16	0.26	11.26	0.09	2.12	0.07	4.00	0.07	1.72	0.07	2.72	0.15	0.46	0.07	0.56	0.04
64	0.50	77.19	0.26	11.28	0.09	2.18	0.07	4.02	0.07	1.63	0.07	2.65	0.15	0.49	0.07	0.55	0.04
65	0.66	76.97	0.26	11.39	0.09	2.22	0.07	3.99	0.07	1.75	0.07	2.66	0.15	0.43	0.07	0.59	0.05
66	0.83	76.83	0.26	11.64	0.09	2.13	0.07	3.95	0.07	1.74	0.07	2.72	0.15	0.45	0.07	0.55	0.04
67	1.00	76.44	0.25	11.83	0.10	2.24	0.07	4.06	0.07	1.80	0.08	2.61	0.15	0.44	0.07	0.57	0.04
68	1.16	76.44	0.25	11.81	0.10	2.22	0.07	4.01	0.07	1.82	0.08	2.70	0.15	0.42	0.06	0.58	0.04
69	1.33	75.81	0.25	11.92	0.10	2.31	0.07	4.09	0.07	1.93	0.08	2.89	0.16	0.46	0.07	0.60	0.05
70	1.50	75.66	0.25	11.98	0.10	2.30	0.07	4.13	0.07	1.99	0.09	2.78	0.16	0.53	0.08	0.62	0.05
71	1.66	75.39	0.25	12.13	0.10	2.34	0.07	4.10	0.07	2.01	0.09	2.96	0.17	0.44	0.07	0.63	0.05
72	1.83	75.13	0.25	12.38	0.10	2.34	0.07	4.13	0.07	2.06	0.09	2.94	0.17	0.46	0.07	0.56	0.04
73	1.99	74.94	0.25	12.43	0.10	2.48	0.08	4.11	0.07	2.07	0.09	2.85	0.16	0.45	0.07	0.65	0.05
74	2.16	74.80	0.25	12.51	0.10	2.46	0.08	4.14	0.07	2.19	0.09	2.81	0.16	0.42	0.06	0.67	0.05
75	2.33	74.77	0.25	12.62	0.10	2.46	0.08	4.11	0.07	2.16	0.09	2.76	0.16	0.48	0.07	0.63	0.05
76	2.49	74.40	0.25	12.72	0.10	2.48	0.08	4.11	0.07	2.19	0.09	2.95	0.17	0.50	0.08	0.64	0.05
77	2.66	74.20	0.25	12.90	0.10	2.49	0.08	4.15	0.07	2.15	0.09	2.99	0.17	0.50	0.08	0.61	0.05
78	2.82	74.10	0.25	12.90	0.10	2.41	0.08	4.13	0.07	2.32	0.10	3.00	0.17	0.54	0.08	0.61	0.05
79	2.99	74.02	0.25	13.09	0.11	2.50	0.08	4.07	0.07	2.32	0.10	2.91	0.17	0.47	0.07	0.62	0.05
80	3.16	73.85	0.25	13.04	0.10	2.46	0.08	4.16	0.07	2.34	0.10	3.02	0.17	0.48	0.07	0.65	0.05
81	3.32	73.65	0.24	13.05	0.11	2.64	0.08	4.16	0.07	2.29	0.10	3.12	0.18	0.46	0.07	0.64	0.05
82	3.49	73.61	0.24	13.16	0.11	2.58	0.08	4.20	0.07	2.36	0.10	3.00	0.17	0.43	0.06	0.66	0.05
83	3.65	73.51	0.24	13.19	0.11	2.49	0.08	4.14	0.07	2.41	0.10	3.15	0.18	0.49	0.07	0.62	0.05
84	3.82	73.53	0.24	13.27	0.11	2.61	0.08	4.24	0.07	2.32	0.10	2.86	0.16	0.53	0.08	0.64	0.05
85	3.99	73.33	0.24	13.34	0.11	2.60	0.08	4.17	0.07	2.48	0.11	2.96	0.17	0.47	0.07	0.65	0.05
86	4.15	73.33	0.24	13.46	0.11	2.56	0.08	4.22	0.07	2.39	0.10	2.96	0.17	0.41	0.06	0.66	0.05
87	4.32	73.25	0.24	13.34	0.11	2.56	0.08	4.29	0.07	2.40	0.10	3.05	0.17	0.46	0.07	0.65	0.05
88	4.49	73.10	0.24	13.35	0.11	2.58	0.08	4.25	0.07	2.41	0.10	3.16	0.18	0.48	0.07	0.67	0.05
89	4.65	72.86	0.24	13.46	0.11	2.58	0.08	4.27	0.07	2.48	0.11	3.17	0.18	0.48	0.07	0.69	0.05
90	4.82	72.85	0.24	13.53	0.11	2.63	0.08	4.20	0.07	2.44	0.10	3.11	0.18	0.56	0.09	0.69	0.05
91	4.98	73.05	0.24	13.56	0.11	2.57	0.08	4.24	0.07	2.45	0.10	3.02	0.17	0.43	0.07	0.68	0.05
92	5.15	73.08	0.24	13.44	0.11	2.60	0.08	4.37	0.08	2.46	0.10	2.97	0.17	0.41	0.06	0.67	0.05
93	5.32	72.89	0.24	13.46	0.11	2.60	0.08	4.25	0.07	2.45	0.10	3.20	0.18	0.50	0.08	0.65	0.05
94	5.48	72.98	0.24	13.49	0.11	2.67	0.08	4.21	0.07	2.45	0.10	3.03	0.17	0.53	0.08	0.66	0.05
95	5.65	73.08	0.24	13.62	0.11	2.60	0.08	4.20	0.07	2.36	0.10	3.03	0.17	0.42	0.06	0.69	0.05
96	5.81	73.05	0.24	13.56	0.11	2.63	0.08	4.19	0.07	2.43	0.10	3.04	0.17	0.47	0.07	0.63	0.05
97	5.98	72.65	0.24	13.65	0.11	2.64	0.08	4.28	0.07	2.54	0.11	3.07	0.17	0.49	0.07	0.68	0.05
98	6.15	72.91	0.24	13.50	0.11	2.66	0.08	4.22	0.07	2.50	0.11	3.05	0.17	0.48	0.07	0.68	0.05
99	6.31	72.92	0.24	13.58	0.11	2.67	0.08	4.24	0.07	2.39	0.10	3.04	0.17	0.48	0.07	0.67	0.05
100	6.48	72.97	0.24	13.50	0.11	2.67	0.08	4.23	0.07	2.48	0.11	3.06	0.17	0.46	0.07	0.64	0.05
101	6.65	72.81	0.24	13.56	0.11	2.72	0.09	4.29	0.07	2.44	0.10	3.01	0.17	0.50	0.08	0.67	0.05
102	6.81	72.90	0.24	13.54	0.11	2.78	0.09	4.27	0.07	2.48	0.11	2.87	0.16	0.52	0.08	0.66	0.05
103	6.98	72.81	0.24	13.57	0.11	2.67	0.08	4.22	0.07	2.41	0.10	3.21	0.18	0.46	0.07	0.65	0.05
104	7.14	72.81	0.24	13.51	0.11	2.58	0.08	4.28	0.07	2.57	0.11	3.10	0.18	0.49	0.07	0.67	0.05
105	7.31	72.79	0.24	13.50	0.11	2.62	0.08	4.28	0.07	2.42	0.10	3.20	0.18	0.52	0.08	0.67	0.05
106	7.48	72.95	0.24	13.54	0.11	2.59	0.08	4.31	0.07	2.47	0.11	3.02	0.17	0.47	0.07	0.65	0.05
107	7.64	72.89	0.24	13.54	0.11	2.69	0.08	4.30	0.07	2.42	0.10	3.04	0.17	0.44	0.07	0.67	0.05
108	7.81	72.91	0.24	13.54	0.11	2.73	0.09	4.24	0.07	2.41	0.10	3.04	0.17	0.47	0.07	0.65	0.05
109	7.97	72.59	0.24	13.59	0.11	2.61	0.08	4.31	0.07	2.37	0.10	3.28	0.19	0.53	0.08	0.72	0.06
110	8.14	72.97	0.24	13.50	0.11	2.60	0.08	4.22	0.07	2.37	0.10	3.18	0.18	0.46	0.07	0.70	0.05
111	8.31	72.91	0.24	13.56	0.11	2.65	0.08	4.22	0.07	2.43	0.10	3.09	0.18	0.44	0.07	0.69	0.05
112	8.47	72.88	0.24	13.51	0.11	2.65	0.08	4.35	0.07	2.46	0.10	3.09	0.18	0.40	0.06	0.67	0.05

113	8.64	72.90	0.24	13.61	0.11	2.62	0.08	4.32	0.07	2.47	0.11	2.97	0.17	0.46	0.07	0.65	0.05
114	8.81	72.79	0.24	13.59	0.11	2.64	0.08	4.31	0.07	2.36	0.10	3.19	0.18	0.42	0.06	0.69	0.05
115	8.97	73.01	0.24	13.40	0.11	2.67	0.08	4.36	0.07	2.32	0.10	3.03	0.17	0.49	0.07	0.72	0.06
116	9.14	72.68	0.24	13.53	0.11	2.62	0.08	4.45	0.08	2.37	0.10	3.16	0.18	0.48	0.07	0.70	0.05
117	9.30	73.09	0.24	13.44	0.11	2.70	0.08	4.33	0.07	2.20	0.09	3.09	0.18	0.43	0.06	0.73	0.06
118	9.47	72.99	0.24	13.45	0.11	2.69	0.08	4.26	0.07	2.32	0.10	3.18	0.18	0.43	0.07	0.68	0.05
119	9.64	73.21	0.24	13.50	0.11	2.68	0.08	4.25	0.07	2.32	0.10	2.93	0.17	0.46	0.07	0.66	0.05
120	9.80	73.08	0.24	13.59	0.11	2.65	0.08	4.22	0.07	2.37	0.10	2.97	0.17	0.47	0.07	0.66	0.05
121	9.97	72.99	0.24	13.49	0.11	2.63	0.08	4.32	0.07	2.35	0.10	3.08	0.18	0.43	0.07	0.72	0.06
122	10.13	73.02	0.24	13.40	0.11	2.68	0.08	4.25	0.07	2.27	0.10	3.31	0.19	0.42	0.06	0.64	0.05
123	10.30	72.99	0.24	13.53	0.11	2.59	0.08	4.39	0.08	2.33	0.10	3.08	0.17	0.43	0.07	0.67	0.05
124	10.47	73.01	0.24	13.49	0.11	2.61	0.08	4.37	0.08	2.38	0.10	2.96	0.17	0.48	0.07	0.70	0.05
125	10.63	73.11	0.24	13.44	0.11	2.64	0.08	4.28	0.07	2.31	0.10	3.04	0.17	0.48	0.07	0.70	0.05

Agglomerate U1B.2

Table J.23: Major element compositions (as wt.% oxides) from a line traverse across the interface of surface agglomerate U1B.2 (from agglomerate U1B.2 to host U1B) extracted from quantified EDS compositional maps. The EDS compositional maps were collected at a resolution of 7.15 pixels/μm. The smoothing width for this traverse was 125 pixels (17.5 μm) wide. This is a Si interface and has been centered at $x = 0$ based on the SiO_2 maximum. Peak points within 2σ of the SiO_2 maximum are highlighted in yellow. Uncertainties are 2SEOM.

Pt.	Position (μm)	SiO_2	2σ	Al_2O_3	2σ	Na_2O	2σ	K_2O	2σ	CaO	2σ	FeO	2σ	TiO_2	2σ	MgO	2σ
1	-8.39	76.95	0.16	13.43	0.06	3.17	0.05	5.26	0.04	0.77	0.04	2.90	0.09	0.39	0.04	0.51	0.03
2	-8.25	77.11	0.16	13.40	0.06	3.13	0.05	5.26	0.04	0.80	0.04	2.95	0.09	0.37	0.04	0.51	0.03
3	-8.11	77.12	0.16	13.40	0.06	3.19	0.05	5.26	0.04	0.79	0.04	2.99	0.09	0.37	0.04	0.47	0.03
4	-7.97	77.05	0.16	13.43	0.06	3.12	0.05	5.23	0.04	0.76	0.04	2.98	0.09	0.38	0.04	0.50	0.03
5	-7.83	76.83	0.16	13.36	0.06	3.12	0.05	5.23	0.04	0.81	0.04	3.09	0.09	0.40	0.04	0.50	0.03
6	-7.69	76.86	0.16	13.36	0.06	3.20	0.05	5.26	0.04	0.85	0.04	3.02	0.09	0.41	0.04	0.47	0.03
7	-7.55	76.92	0.16	13.36	0.06	3.17	0.05	5.24	0.04	0.85	0.04	3.04	0.09	0.40	0.04	0.48	0.03
8	-7.41	76.86	0.16	13.43	0.06	3.15	0.05	5.22	0.04	0.85	0.04	3.12	0.09	0.38	0.04	0.48	0.03
9	-7.27	76.75	0.16	13.39	0.06	3.14	0.05	5.24	0.04	0.88	0.04	3.12	0.09	0.34	0.04	0.47	0.03
10	-7.13	76.80	0.16	13.47	0.06	3.17	0.05	5.22	0.04	0.87	0.04	3.12	0.09	0.37	0.04	0.46	0.03
11	-6.99	76.76	0.16	13.41	0.06	3.20	0.05	5.18	0.04	0.87	0.04	3.26	0.10	0.42	0.04	0.48	0.03
12	-6.85	76.83	0.16	13.36	0.06	3.13	0.05	5.19	0.04	0.88	0.04	3.27	0.10	0.35	0.04	0.50	0.03
13	-6.71	76.79	0.16	13.38	0.06	3.12	0.05	5.18	0.04	0.86	0.04	3.27	0.10	0.39	0.04	0.51	0.03
14	-6.57	76.91	0.16	13.39	0.06	3.10	0.05	5.19	0.04	0.91	0.04	3.23	0.10	0.36	0.04	0.49	0.03
15	-6.43	76.89	0.16	13.40	0.06	3.14	0.05	5.16	0.04	0.91	0.04	3.18	0.10	0.39	0.04	0.53	0.03
16	-6.29	76.76	0.16	13.40	0.06	3.06	0.05	5.15	0.04	0.92	0.05	3.32	0.10	0.40	0.04	0.51	0.03
17	-6.15	76.84	0.16	13.36	0.06	3.08	0.05	5.19	0.04	0.96	0.05	3.39	0.10	0.37	0.04	0.51	0.03
18	-6.01	76.86	0.16	13.40	0.06	3.16	0.05	5.14	0.04	0.99	0.05	3.29	0.10	0.35	0.04	0.50	0.03
19	-5.87	76.79	0.16	13.39	0.06	3.12	0.05	5.11	0.04	0.95	0.05	3.38	0.10	0.38	0.04	0.52	0.03
20	-5.73	76.63	0.16	13.35	0.06	3.07	0.05	5.17	0.04	0.97	0.05	3.41	0.10	0.34	0.03	0.53	0.03
21	-5.59	76.55	0.16	13.32	0.06	3.05	0.05	5.13	0.04	1.01	0.05	3.53	0.11	0.33	0.03	0.50	0.03
22	-5.45	76.64	0.16	13.33	0.06	3.05	0.05	5.14	0.04	1.02	0.05	3.54	0.11	0.37	0.04	0.50	0.03
23	-5.31	76.45	0.16	13.35	0.06	3.05	0.05	5.21	0.04	1.02	0.05	3.48	0.10	0.36	0.04	0.52	0.03
24	-5.17	76.59	0.16	13.28	0.06	3.06	0.05	5.13	0.04	1.02	0.05	3.61	0.11	0.38	0.04	0.52	0.03
25	-5.04	76.52	0.16	13.32	0.06	3.07	0.05	5.10	0.04	1.02	0.05	3.59	0.11	0.37	0.04	0.52	0.03
26	-4.90	76.41	0.16	13.26	0.06	3.09	0.05	5.13	0.04	1.03	0.05	3.58	0.11	0.35	0.04	0.52	0.03
27	-4.76	76.34	0.16	13.28	0.06	3.04	0.05	5.07	0.04	1.12	0.06	3.76	0.11	0.34	0.03	0.50	0.03
28	-4.62	76.34	0.16	13.16	0.06	3.04	0.05	5.07	0.04	1.12	0.06	3.83	0.11	0.38	0.04	0.54	0.03
29	-4.48	76.26	0.16	13.19	0.06	3.07	0.05	5.02	0.04	1.07	0.05	3.90	0.12	0.36	0.04	0.53	0.03
30	-4.34	76.40	0.16	13.11	0.06	2.98	0.05	5.03	0.04	1.12	0.06	3.94	0.12	0.34	0.03	0.57	0.03
31	-4.20	76.35	0.16	13.11	0.06	3.00	0.05	5.08	0.04	1.15	0.06	3.94	0.12	0.38	0.04	0.57	0.03
32	-4.06	76.38	0.16	13.04	0.06	3.01	0.05	5.05	0.04	1.14	0.06	3.91	0.12	0.38	0.04	0.58	0.03
33	-3.92	76.43	0.16	12.96	0.06	2.97	0.05	5.00	0.04	1.17	0.06	3.99	0.12	0.39	0.04	0.55	0.03
34	-3.78	76.63	0.16	12.98	0.06	2.94	0.05	5.01	0.04	1.17	0.06	3.96	0.12	0.33	0.03	0.56	0.03
35	-3.64	76.57	0.16	12.85	0.06	2.92	0.04	4.97	0.04	1.16	0.06	4.05	0.12	0.36	0.04	0.54	0.03
36	-3.50	76.69	0.16	12.76	0.06	2.89	0.04	4.97	0.04	1.14	0.06	4.09	0.12	0.33	0.03	0.56	0.03
37	-3.36	76.74	0.16	12.65	0.06	2.83	0.04	4.98	0.04	1.15	0.06	4.14	0.12	0.33	0.03	0.57	0.03
38	-3.22	76.95	0.16	12.57	0.06	2.87	0.04	4.90	0.04	1.16	0.06	4.10	0.12	0.33	0.03	0.61	0.03
39	-3.08	77.02	0.16	12.44	0.06	2.86	0.04	4.92	0.04	1.15	0.06	4.10	0.12	0.36	0.04	0.59	0.03
40	-2.94	77.40	0.16	12.19	0.06	2.79	0.04	4.88	0.04	1.17	0.06	4.21	0.13	0.32	0.03	0.57	0.03
41	-2.80	77.37	0.16	12.07	0.06	2.79	0.04	4.91	0.04	1.15	0.06	4.27	0.13	0.36	0.04	0.58	0.03
42	-2.66	77.75	0.16	11.93	0.06	2.68	0.04	4.83	0.04	1.12	0.06	4.27	0.13	0.38	0.04	0.59	0.03
43	-2.52	78.03	0.16	11.75	0.06	2.68	0.04	4.77	0.04	1.11	0.05	4.35	0.13	0.31	0.03	0.59	0.03
44	-2.38	78.04	0.16	11.55	0.05	2.67	0.04	4.72	0.04	1.13	0.06	4.48	0.13	0.32	0.03	0.60	0.03
45	-2.24	78.57	0.16	11.32	0.05	2.59	0.04	4.70	0.04	1.10	0.05	4.46	0.13	0.31	0.03	0.59	0.03
46	-2.10	79.08	0.16	11.08	0.05	2.50	0.04	4.66	0.04	1.08	0.05	4.46	0.13	0.34	0.04	0.61	0.03
47	-1.96	79.18	0.16	10.87	0.05	2.47	0.04	4.61	0.04	1.10	0.05	4.43	0.13	0.34	0.04	0.62	0.04
48	-1.82	79.60	0.16	10.66	0.05	2.45	0.04	4.56	0.04	1.04	0.05	4.46	0.13	0.38	0.04	0.60	0.03
49	-1.68	79.85	0.16	10.45	0.05	2.40	0.04	4.50	0.03	1.01	0.05	4.50	0.13	0.33	0.03	0.59	0.03
50	-1.54	80.31	0.16	10.14	0.05	2.36	0.04	4.45	0.03	1.06	0.05	4.54	0.14	0.32	0.03	0.64	0.04

51	-1.40	80.67	0.16	10.01	0.05	2.31	0.04	4.39	0.03	0.99	0.05	4.53	0.14	0.33	0.03	0.60	0.03
52	-1.26	81.01	0.16	9.80	0.05	2.27	0.03	4.37	0.03	0.98	0.05	4.61	0.14	0.31	0.03	0.59	0.03
53	-1.12	80.96	0.16	9.62	0.05	2.29	0.04	4.34	0.03	0.96	0.05	4.67	0.14	0.33	0.03	0.64	0.04
54	-0.98	81.54	0.17	9.50	0.04	2.24	0.03	4.27	0.03	0.96	0.05	4.57	0.14	0.33	0.03	0.62	0.03
55	-0.84	81.40	0.17	9.40	0.04	2.23	0.03	4.26	0.03	0.98	0.05	4.57	0.14	0.37	0.04	0.61	0.03
56	-0.70	81.65	0.17	9.34	0.04	2.17	0.03	4.27	0.03	0.97	0.05	4.52	0.14	0.31	0.03	0.61	0.03
57	-0.56	81.70	0.17	9.30	0.04	2.21	0.03	4.29	0.03	0.92	0.05	4.51	0.14	0.33	0.03	0.62	0.03
58	-0.42	81.77	0.17	9.30	0.04	2.19	0.03	4.25	0.03	0.92	0.05	4.55	0.14	0.33	0.03	0.63	0.04
59	-0.28	81.72	0.17	9.30	0.04	2.23	0.03	4.25	0.03	0.96	0.05	4.47	0.13	0.32	0.03	0.63	0.04
60	-0.14	81.68	0.17	9.39	0.04	2.23	0.03	4.29	0.03	0.93	0.05	4.49	0.13	0.31	0.03	0.59	0.03
61	0.00	81.85	0.17	9.50	0.04	2.22	0.03	4.32	0.03	0.93	0.05	4.40	0.13	0.31	0.03	0.59	0.03
62	0.14	81.74	0.17	9.66	0.05	2.22	0.03	4.31	0.03	0.96	0.05	4.31	0.13	0.28	0.03	0.59	0.03
63	0.28	81.40	0.17	9.80	0.05	2.25	0.03	4.39	0.03	0.97	0.05	4.24	0.13	0.34	0.03	0.58	0.03
64	0.42	81.11	0.17	9.98	0.05	2.28	0.03	4.37	0.03	0.98	0.05	4.35	0.13	0.32	0.03	0.56	0.03
65	0.56	81.11	0.17	10.22	0.05	2.31	0.04	4.37	0.03	0.99	0.05	4.31	0.13	0.36	0.04	0.54	0.03
66	0.70	80.83	0.16	10.41	0.05	2.31	0.04	4.42	0.03	1.00	0.05	4.18	0.13	0.36	0.04	0.58	0.03
67	0.84	80.61	0.16	10.56	0.05	2.37	0.04	4.48	0.03	1.01	0.05	3.99	0.12	0.30	0.03	0.60	0.03
68	0.98	80.42	0.16	10.73	0.05	2.39	0.04	4.49	0.03	1.05	0.05	4.08	0.12	0.31	0.03	0.57	0.03
69	1.12	80.20	0.16	11.01	0.05	2.40	0.04	4.49	0.03	1.02	0.05	4.02	0.12	0.34	0.03	0.58	0.03
70	1.26	80.04	0.16	11.24	0.05	2.42	0.04	4.54	0.03	1.04	0.05	3.91	0.12	0.32	0.03	0.54	0.03
71	1.40	79.75	0.16	11.38	0.05	2.43	0.04	4.60	0.04	1.06	0.05	3.92	0.12	0.31	0.03	0.55	0.03
72	1.54	79.60	0.16	11.53	0.05	2.45	0.04	4.55	0.04	1.03	0.05	3.94	0.12	0.33	0.03	0.56	0.03
73	1.68	79.45	0.16	11.72	0.06	2.46	0.04	4.60	0.04	1.05	0.05	3.93	0.12	0.32	0.03	0.55	0.03
74	1.82	79.03	0.16	11.88	0.06	2.55	0.04	4.70	0.04	1.08	0.05	3.84	0.11	0.34	0.03	0.52	0.03
75	1.96	78.69	0.16	12.07	0.06	2.59	0.04	4.70	0.04	1.13	0.06	3.88	0.12	0.35	0.04	0.54	0.03
76	2.10	78.71	0.16	12.21	0.06	2.54	0.04	4.74	0.04	1.13	0.06	3.76	0.11	0.33	0.03	0.55	0.03
77	2.24	78.65	0.16	12.34	0.06	2.53	0.04	4.68	0.04	1.06	0.05	3.83	0.11	0.42	0.04	0.56	0.03
78	2.38	78.40	0.16	12.48	0.06	2.55	0.04	4.68	0.04	1.11	0.05	3.77	0.11	0.38	0.04	0.54	0.03
79	2.52	78.37	0.16	12.64	0.06	2.54	0.04	4.73	0.04	1.11	0.05	3.61	0.11	0.38	0.04	0.53	0.03
80	2.66	78.12	0.16	12.78	0.06	2.56	0.04	4.75	0.04	1.10	0.05	3.69	0.11	0.37	0.04	0.51	0.03
81	2.80	78.18	0.16	12.91	0.06	2.60	0.04	4.71	0.04	1.12	0.06	3.68	0.11	0.35	0.04	0.53	0.03
82	2.94	77.75	0.16	13.07	0.06	2.62	0.04	4.74	0.04	1.13	0.06	3.70	0.11	0.36	0.04	0.55	0.03
83	3.08	77.56	0.16	13.14	0.06	2.61	0.04	4.78	0.04	1.13	0.06	3.72	0.11	0.37	0.04	0.55	0.03
84	3.22	77.41	0.16	13.21	0.06	2.65	0.04	4.77	0.04	1.13	0.06	3.70	0.11	0.39	0.04	0.54	0.03
85	3.36	77.41	0.16	13.27	0.06	2.66	0.04	4.76	0.04	1.15	0.06	3.64	0.11	0.38	0.04	0.53	0.03
86	3.50	77.26	0.16	13.38	0.06	2.63	0.04	4.80	0.04	1.16	0.06	3.62	0.11	0.38	0.04	0.54	0.03
87	3.64	77.06	0.16	13.48	0.06	2.64	0.04	4.84	0.04	1.21	0.06	3.70	0.11	0.35	0.04	0.50	0.03
88	3.78	77.01	0.16	13.56	0.06	2.69	0.04	4.80	0.04	1.16	0.06	3.69	0.11	0.37	0.04	0.54	0.03
89	3.92	76.98	0.16	13.67	0.06	2.72	0.04	4.80	0.04	1.16	0.06	3.73	0.11	0.39	0.04	0.54	0.03
90	4.06	76.88	0.16	13.76	0.06	2.66	0.04	4.82	0.04	1.19	0.06	3.67	0.11	0.39	0.04	0.51	0.03
91	4.20	76.73	0.16	13.84	0.07	2.67	0.04	4.80	0.04	1.22	0.06	3.49	0.10	0.41	0.04	0.54	0.03
92	4.34	76.72	0.16	13.95	0.07	2.70	0.04	4.81	0.04	1.20	0.06	3.52	0.11	0.41	0.04	0.56	0.03
93	4.48	76.77	0.16	13.96	0.07	2.70	0.04	4.81	0.04	1.16	0.06	3.66	0.11	0.41	0.04	0.52	0.03
94	4.62	76.78	0.16	14.09	0.07	2.71	0.04	4.80	0.04	1.16	0.06	3.53	0.11	0.38	0.04	0.53	0.03
95	4.76	76.59	0.16	14.05	0.07	2.71	0.04	4.78	0.04	1.17	0.06	3.65	0.11	0.39	0.04	0.53	0.03
96	4.90	76.64	0.16	14.11	0.07	2.67	0.04	4.73	0.04	1.18	0.06	3.66	0.11	0.40	0.04	0.56	0.03
97	5.04	76.55	0.16	14.18	0.07	2.64	0.04	4.79	0.04	1.18	0.06	3.57	0.11	0.41	0.04	0.52	0.03
98	5.17	76.49	0.16	14.14	0.07	2.69	0.04	4.84	0.04	1.15	0.06	3.74	0.11	0.45	0.05	0.53	0.03
99	5.31	76.13	0.16	14.15	0.07	2.70	0.04	4.83	0.04	1.22	0.06	3.67	0.11	0.43	0.04	0.56	0.03
100	5.45	76.31	0.16	14.27	0.07	2.71	0.04	4.80	0.04	1.15	0.06	3.64	0.11	0.39	0.04	0.56	0.03
101	5.59	76.32	0.16	14.40	0.07	2.69	0.04	4.81	0.04	1.19	0.06	3.63	0.11	0.36	0.04	0.54	0.03
102	5.73	76.57	0.16	14.38	0.07	2.68	0.04	4.76	0.04	1.14	0.06	3.66	0.11	0.40	0.04	0.56	0.03

Agglomerate U3.1

Table J.24: Major element compositions (as wt.% oxides) from a line traverse across the interface of agglomerate U3.1 (from agglomerate U3.1 to host U3) extracted from quantified EDS compositional maps. The EDS compositional maps were collected at a resolution of 3.3 pixels/μm. The smoothing width for this traverse was 150 pixels (45.1 μm) wide. This is an Si interface and has been centered at $x = 0$ based on the SiO_2 maximum. Peak points within 2σ of the SiO_2 maximum are highlighted in yellow. Uncertainties are 2SEOM.

Pt.	Position (μm)	SiO_2	2σ	Al_2O_3	2σ	Na_2O	2σ	K_2O	2σ	CaO	2σ	FeO	2σ	TiO_2	2σ	MgO	2σ
1	-29.47	73.53	0.24	13.49	0.12	2.22	0.09	3.04	0.10	3.36	0.13	2.90	0.19	0.49	0.07	0.66	0.06
2	-29.17	73.57	0.24	13.45	0.12	2.26	0.09	2.99	0.10	3.40	0.14	2.91	0.19	0.45	0.06	0.62	0.06
3	-28.87	73.63	0.24	13.38	0.12	2.25	0.09	3.09	0.10	3.33	0.13	2.83	0.19	0.52	0.07	0.62	0.06
4	-28.57	73.24	0.24	13.64	0.13	2.20	0.09	3.16	0.10	3.42	0.14	2.85	0.19	0.54	0.07	0.64	0.06
5	-28.27	73.47	0.24	13.58	0.13	2.24	0.09	2.98	0.10	3.34	0.13	2.87	0.19	0.55	0.08	0.62	0.06
6	-27.97	73.59	0.24	13.65	0.13	2.24	0.09	3.08	0.10	3.28	0.13	2.70	0.18	0.53	0.07	0.59	0.06
7	-27.67	73.68	0.24	13.53	0.12	2.19	0.09	3.01	0.10	3.40	0.14	2.82	0.19	0.45	0.06	0.58	0.06
8	-27.37	73.52	0.24	13.65	0.13	2.19	0.09	3.10	0.10	3.40	0.14	2.72	0.18	0.43	0.06	0.60	0.06
9	-27.07	73.77	0.24	13.56	0.13	2.13	0.08	3.04	0.10	3.43	0.14	2.67	0.18	0.44	0.06	0.60	0.06
10	-26.77	73.45	0.24	13.56	0.13	2.12	0.08	3.00	0.10	3.33	0.13	3.02	0.20	0.45	0.06	0.64	0.06
11	-26.47	73.45	0.24	13.54	0.12	2.23	0.09	3.15	0.10	3.23	0.13	2.89	0.19	0.47	0.07	0.68	0.07
12	-26.17	73.33	0.24	13.56	0.13	2.17	0.09	3.13	0.10	3.43	0.14	2.89	0.19	0.50	0.07	0.62	0.06
13	-25.87	73.63	0.24	13.45	0.12	2.25	0.09	3.09	0.10	3.31	0.13	2.77	0.18	0.49	0.07	0.63	0.06
14	-25.56	73.50	0.24	13.49	0.12	2.33	0.09	3.12	0.10	3.22	0.13	2.79	0.18	0.51	0.07	0.68	0.07
15	-25.26	73.62	0.24	13.57	0.13	2.27	0.09	3.08	0.10	3.19	0.13	2.77	0.18	0.51	0.07	0.63	0.06
16	-24.96	73.43	0.24	13.56	0.13	2.22	0.09	3.10	0.10	3.32	0.13	2.87	0.19	0.48	0.07	0.64	0.06
17	-24.66	73.60	0.24	13.49	0.12	2.29	0.09	3.21	0.11	3.29	0.13	2.74	0.18	0.45	0.06	0.65	0.06
18	-24.36	73.18	0.24	13.72	0.13	2.29	0.09	3.13	0.10	3.38	0.13	2.77	0.18	0.48	0.07	0.65	0.06
19	-24.06	73.27	0.24	13.48	0.12	2.33	0.09	3.15	0.10	3.35	0.13	2.83	0.19	0.46	0.06	0.64	0.06
20	-23.76	73.75	0.24	13.37	0.12	2.30	0.09	3.08	0.10	3.38	0.13	2.71	0.18	0.46	0.06	0.61	0.06
21	-23.46	73.41	0.24	13.49	0.12	2.24	0.09	3.13	0.10	3.35	0.13	2.84	0.19	0.51	0.07	0.67	0.06
22	-23.16	73.45	0.24	13.55	0.12	2.19	0.09	3.07	0.10	3.27	0.13	2.87	0.19	0.57	0.08	0.67	0.06
23	-22.86	73.47	0.24	13.54	0.12	2.28	0.09	3.19	0.11	3.27	0.13	2.79	0.18	0.51	0.07	0.64	0.06
24	-22.56	73.34	0.24	13.62	0.13	2.30	0.09	3.14	0.10	3.31	0.13	2.87	0.19	0.49	0.07	0.59	0.06
25	-22.26	73.44	0.24	13.54	0.12	2.28	0.09	3.02	0.10	3.42	0.14	2.90	0.19	0.47	0.07	0.64	0.06
26	-21.95	73.39	0.24	13.57	0.13	2.29	0.09	3.12	0.10	3.43	0.14	2.75	0.18	0.49	0.07	0.66	0.06
27	-21.65	73.31	0.24	13.52	0.12	2.31	0.09	3.16	0.10	3.52	0.14	2.63	0.17	0.54	0.07	0.63	0.06
28	-21.35	73.44	0.24	13.55	0.12	2.27	0.09	3.08	0.10	3.34	0.13	2.77	0.18	0.50	0.07	0.66	0.06
29	-21.05	73.31	0.24	13.59	0.13	2.24	0.09	3.12	0.10	3.42	0.14	2.85	0.19	0.48	0.07	0.62	0.06
30	-20.75	73.36	0.24	13.59	0.13	2.31	0.09	3.15	0.10	3.39	0.13	2.74	0.18	0.48	0.07	0.60	0.06
31	-20.45	73.24	0.24	13.57	0.13	2.35	0.09	3.22	0.11	3.36	0.13	2.77	0.18	0.51	0.07	0.63	0.06
32	-20.15	73.37	0.24	13.55	0.12	2.26	0.09	3.21	0.11	3.40	0.14	2.77	0.18	0.46	0.06	0.63	0.06
33	-19.85	73.24	0.24	13.64	0.13	2.36	0.09	3.15	0.10	3.45	0.14	2.72	0.18	0.43	0.06	0.66	0.06
34	-19.55	73.25	0.24	13.56	0.13	2.30	0.09	3.23	0.11	3.37	0.13	2.79	0.18	0.45	0.06	0.67	0.06
35	-19.25	73.15	0.24	13.56	0.13	2.31	0.09	3.20	0.11	3.45	0.14	2.85	0.19	0.48	0.07	0.65	0.06
36	-18.95	73.26	0.24	13.56	0.13	2.37	0.09	3.18	0.10	3.36	0.13	2.76	0.18	0.49	0.07	0.64	0.06
37	-18.65	73.33	0.24	13.55	0.12	2.32	0.09	3.22	0.11	3.32	0.13	2.73	0.18	0.52	0.07	0.62	0.06
38	-18.35	73.14	0.24	13.56	0.13	2.35	0.09	3.19	0.11	3.42	0.14	2.79	0.18	0.51	0.07	0.61	0.06
39	-18.05	73.29	0.24	13.61	0.13	2.38	0.09	3.10	0.10	3.50	0.14	2.72	0.18	0.48	0.07	0.59	0.06
40	-17.75	73.13	0.24	13.65	0.13	2.30	0.09	3.25	0.11	3.39	0.13	2.89	0.19	0.51	0.07	0.61	0.06
41	-17.44	73.22	0.24	13.72	0.13	2.25	0.09	3.21	0.11	3.32	0.13	2.84	0.19	0.51	0.07	0.65	0.06
42	-17.14	73.23	0.24	13.75	0.13	2.28	0.09	3.25	0.11	3.22	0.13	2.74	0.18	0.53	0.07	0.61	0.06
43	-16.84	73.21	0.24	13.66	0.13	2.24	0.09	3.19	0.11	3.51	0.14	2.69	0.18	0.47	0.06	0.65	0.06
44	-16.54	73.22	0.24	13.52	0.12	2.22	0.09	3.20	0.11	3.56	0.14	2.79	0.18	0.54	0.07	0.59	0.06
45	-16.24	72.97	0.24	13.66	0.13	2.28	0.09	3.29	0.11	3.49	0.14	2.79	0.18	0.52	0.07	0.61	0.06
46	-15.94	73.15	0.24	13.53	0.12	2.37	0.09	3.23	0.11	3.46	0.14	2.82	0.19	0.46	0.06	0.58	0.06
47	-15.64	72.93	0.24	13.61	0.13	2.32	0.09	3.19	0.11	3.51	0.14	2.91	0.19	0.49	0.07	0.63	0.06
48	-15.34	73.03	0.24	13.65	0.13	2.31	0.09	3.29	0.11	3.46	0.14	2.85	0.19	0.43	0.06	0.60	0.06
49	-15.04	73.30	0.24	13.58	0.13	2.21	0.09	3.28	0.11	3.45	0.14	2.78	0.18	0.45	0.06	0.63	0.06
50	-14.74	72.99	0.24	13.60	0.13	2.29	0.09	3.36	0.11	3.34	0.13	2.96	0.20	0.42	0.06	0.65	0.06

51	-14.44	73.30	0.24	13.47	0.12	2.27	0.09	3.27	0.11	3.45	0.14	2.74	0.18	0.47	0.06	0.63	0.06
52	-14.14	73.35	0.24	13.65	0.13	2.22	0.09	3.22	0.11	3.40	0.14	2.67	0.18	0.50	0.07	0.63	0.06
53	-13.84	73.17	0.24	13.56	0.12	2.21	0.09	3.21	0.11	3.26	0.13	3.08	0.20	0.52	0.07	0.67	0.06
54	-13.53	73.13	0.24	13.43	0.12	2.28	0.09	3.32	0.11	3.50	0.14	2.86	0.19	0.49	0.07	0.64	0.06
55	-13.23	73.17	0.24	13.47	0.12	2.28	0.09	3.24	0.11	3.50	0.14	2.95	0.20	0.45	0.06	0.64	0.06
56	-12.93	72.96	0.24	13.50	0.12	2.28	0.09	3.30	0.11	3.44	0.14	3.00	0.20	0.50	0.07	0.63	0.06
57	-12.63	73.34	0.24	13.45	0.12	2.34	0.09	3.21	0.11	3.44	0.14	2.75	0.18	0.45	0.06	0.64	0.06
58	-12.33	73.38	0.24	13.46	0.12	2.23	0.09	3.26	0.11	3.44	0.14	2.74	0.18	0.50	0.07	0.59	0.06
59	-12.03	73.29	0.24	13.43	0.12	2.26	0.09	3.32	0.11	3.40	0.14	2.84	0.19	0.53	0.07	0.59	0.06
60	-11.73	73.64	0.24	13.33	0.12	2.26	0.09	3.24	0.11	3.28	0.13	2.80	0.19	0.48	0.07	0.63	0.06
61	-11.43	73.61	0.24	13.37	0.12	2.31	0.09	3.33	0.11	3.29	0.13	2.68	0.18	0.48	0.07	0.64	0.06
62	-11.13	73.58	0.24	13.37	0.12	2.32	0.09	3.35	0.11	3.30	0.13	2.65	0.18	0.43	0.06	0.61	0.06
63	-10.83	73.76	0.24	13.26	0.12	2.32	0.09	3.24	0.11	3.31	0.13	2.75	0.18	0.46	0.06	0.59	0.06
64	-10.53	73.84	0.24	13.25	0.12	2.31	0.09	3.22	0.11	3.29	0.13	2.72	0.18	0.46	0.06	0.61	0.06
65	-10.23	73.79	0.24	13.20	0.12	2.36	0.09	3.24	0.11	3.23	0.13	2.84	0.19	0.48	0.07	0.56	0.05
66	-9.93	73.85	0.24	13.28	0.12	2.26	0.09	3.20	0.11	3.17	0.13	2.83	0.19	0.45	0.06	0.61	0.06
67	-9.62	73.85	0.24	13.21	0.12	2.28	0.09	3.22	0.11	3.28	0.13	2.72	0.18	0.46	0.06	0.61	0.06
68	-9.32	73.74	0.24	13.09	0.12	2.33	0.09	3.32	0.11	3.26	0.13	2.78	0.18	0.48	0.07	0.63	0.06
69	-9.02	73.68	0.24	13.08	0.12	2.23	0.09	3.37	0.11	3.22	0.13	2.94	0.19	0.52	0.07	0.59	0.06
70	-8.72	73.81	0.24	13.01	0.12	2.29	0.09	3.34	0.11	3.17	0.13	2.88	0.19	0.52	0.07	0.61	0.06
71	-8.42	73.98	0.24	12.86	0.12	2.22	0.09	3.30	0.11	3.25	0.13	2.89	0.19	0.45	0.06	0.68	0.07
72	-8.12	74.16	0.24	12.83	0.12	2.26	0.09	3.26	0.11	3.18	0.13	2.82	0.19	0.53	0.07	0.60	0.06
73	-7.82	74.13	0.24	12.82	0.12	2.24	0.09	3.29	0.11	3.21	0.13	2.91	0.19	0.46	0.06	0.57	0.06
74	-7.52	74.43	0.24	12.81	0.12	2.25	0.09	3.26	0.11	3.14	0.12	2.72	0.18	0.51	0.07	0.56	0.05
75	-7.22	74.37	0.24	12.73	0.12	2.25	0.09	3.26	0.11	3.14	0.12	2.81	0.19	0.46	0.06	0.62	0.06
76	-6.92	74.60	0.24	12.68	0.12	2.25	0.09	3.32	0.11	2.99	0.12	2.75	0.18	0.46	0.06	0.57	0.05
77	-6.62	74.76	0.24	12.43	0.11	2.21	0.09	3.26	0.11	3.07	0.12	2.81	0.19	0.45	0.06	0.64	0.06
78	-6.32	75.01	0.24	12.38	0.11	2.21	0.09	3.27	0.11	2.89	0.12	2.79	0.18	0.49	0.07	0.59	0.06
79	-6.02	74.72	0.24	12.44	0.11	2.19	0.09	3.29	0.11	3.07	0.12	2.90	0.19	0.48	0.07	0.58	0.06
80	-5.71	74.83	0.24	12.33	0.11	2.17	0.09	3.36	0.11	3.00	0.12	3.02	0.20	0.40	0.06	0.59	0.06
81	-5.41	75.26	0.25	12.26	0.11	2.21	0.09	3.28	0.11	2.88	0.11	2.83	0.19	0.38	0.05	0.59	0.06
82	-5.11	75.39	0.25	12.22	0.11	2.13	0.08	3.25	0.11	2.86	0.11	2.72	0.18	0.46	0.06	0.60	0.06
83	-4.81	75.15	0.25	12.09	0.11	2.23	0.09	3.29	0.11	2.81	0.11	3.00	0.20	0.51	0.07	0.58	0.06
84	-4.51	75.24	0.25	12.12	0.11	2.12	0.08	3.31	0.11	2.76	0.11	2.94	0.19	0.52	0.07	0.61	0.06
85	-4.21	75.54	0.25	12.07	0.11	2.00	0.08	3.25	0.11	2.69	0.11	2.91	0.19	0.53	0.07	0.63	0.06
86	-3.91	75.62	0.25	11.91	0.11	2.06	0.08	3.25	0.11	2.74	0.11	2.99	0.20	0.43	0.06	0.59	0.06
87	-3.61	75.62	0.25	11.79	0.11	2.18	0.09	3.23	0.11	2.71	0.11	3.07	0.20	0.41	0.06	0.63	0.06
88	-3.31	75.65	0.25	11.84	0.11	2.20	0.09	3.25	0.11	2.67	0.11	3.09	0.20	0.38	0.05	0.59	0.06
89	-3.01	75.98	0.25	11.70	0.11	2.11	0.08	3.35	0.11	2.65	0.11	2.87	0.19	0.39	0.05	0.63	0.06
90	-2.71	76.18	0.25	11.58	0.11	2.17	0.09	3.27	0.11	2.62	0.10	2.80	0.19	0.43	0.06	0.64	0.06
91	-2.41	75.99	0.25	11.50	0.11	2.17	0.09	3.34	0.11	2.55	0.10	2.91	0.19	0.51	0.07	0.62	0.06
92	-2.11	75.79	0.25	11.62	0.11	2.09	0.08	3.46	0.11	2.66	0.11	2.95	0.19	0.43	0.06	0.60	0.06
93	-1.80	76.12	0.25	11.54	0.11	2.18	0.09	3.26	0.11	2.56	0.10	2.96	0.20	0.40	0.06	0.60	0.06
94	-1.50	76.02	0.25	11.57	0.11	2.13	0.08	3.27	0.11	2.56	0.10	3.01	0.20	0.49	0.07	0.57	0.05
95	-1.20	76.17	0.25	11.40	0.11	2.05	0.08	3.26	0.11	2.59	0.10	2.95	0.20	0.50	0.07	0.66	0.06
96	-0.90	76.37	0.25	11.29	0.10	2.05	0.08	3.24	0.11	2.62	0.10	3.05	0.20	0.46	0.06	0.62	0.06
97	-0.60	76.42	0.25	11.27	0.10	2.09	0.08	3.35	0.11	2.50	0.10	3.08	0.20	0.36	0.05	0.60	0.06
98	-0.30	76.42	0.25	11.32	0.10	2.09	0.08	3.32	0.11	2.53	0.10	2.96	0.20	0.45	0.06	0.60	0.06
99	0.00	76.62	0.25	11.22	0.10	2.10	0.08	3.34	0.11	2.38	0.09	2.91	0.19	0.49	0.07	0.60	0.06
100	0.30	76.29	0.25	11.37	0.10	2.06	0.08	3.38	0.11	2.55	0.10	2.98	0.20	0.41	0.06	0.63	0.06
101	0.60	76.34	0.25	11.43	0.11	2.09	0.08	3.31	0.11	2.49	0.10	2.96	0.20	0.43	0.06	0.60	0.06
102	0.90	76.35	0.25	11.30	0.10	2.09	0.08	3.35	0.11	2.50	0.10	3.05	0.20	0.39	0.05	0.64	0.06
103	1.20	75.98	0.25	11.47	0.11	2.16	0.09	3.38	0.11	2.56	0.10	3.04	0.20	0.44	0.06	0.64	0.06
104	1.50	75.80	0.25	11.57	0.11	2.09	0.08	3.44	0.11	2.59	0.10	3.02	0.20	0.50	0.07	0.61	0.06
105	1.80	75.55	0.25	11.59	0.11	2.11	0.08	3.40	0.11	2.65	0.11	3.20	0.21	0.44	0.06	0.68	0.07
106	2.11	75.70	0.25	11.74	0.11	2.18	0.09	3.31	0.11	2.58	0.10	2.99	0.20	0.45	0.06	0.70	0.07
107	2.41	75.31	0.25	11.76	0.11	2.20	0.09	3.41	0.11	2.59	0.10	3.05	0.20	0.55	0.08	0.71	0.07
108	2.71	75.32	0.25	11.86	0.11	2.11	0.08	3.40	0.11	2.66	0.11	3.17	0.21	0.45	0.06	0.66	0.06
109	3.01	74.85	0.24	12.13	0.11	2.17	0.09	3.51	0.12	2.70	0.11	3.17	0.21	0.44	0.06	0.63	0.06
110	3.31	74.90	0.24	12.21	0.11	2.25	0.09	3.42	0.11	2.68	0.11	2.96	0.20	0.54	0.07	0.65	0.06
111	3.61	74.64	0.24	12.24	0.11	2.28	0.09	3.37	0.11	2.64	0.11	3.25	0.22	0.47	0.07	0.69	0.07
112	3.91	74.52	0.24	12.30	0.11	2.27	0.09	3.37	0.11	2.80	0.11	3.23	0.21	0.44	0.06	0.71	0.07

113	4.21	73.98	0.24	12.59	0.12	2.24	0.09	3.42	0.11	2.95	0.12	3.25	0.21	0.56	0.08	0.69	0.07
114	4.51	74.01	0.24	12.63	0.12	2.23	0.09	3.42	0.11	2.87	0.11	3.35	0.22	0.49	0.07	0.67	0.06
115	4.81	73.92	0.24	12.60	0.12	2.33	0.09	3.60	0.12	2.89	0.12	3.16	0.21	0.48	0.07	0.66	0.06
116	5.11	73.92	0.24	12.67	0.12	2.36	0.09	3.50	0.12	2.91	0.12	3.07	0.20	0.50	0.07	0.73	0.07
117	5.41	73.86	0.24	12.80	0.12	2.33	0.09	3.52	0.12	3.00	0.12	2.97	0.20	0.50	0.07	0.70	0.07
118	5.71	73.91	0.24	12.83	0.12	2.43	0.10	3.43	0.11	2.92	0.12	2.98	0.20	0.50	0.07	0.65	0.06
119	6.01	73.80	0.24	12.89	0.12	2.39	0.09	3.45	0.11	2.89	0.12	3.03	0.20	0.49	0.07	0.68	0.07
120	6.32	73.59	0.24	13.07	0.12	2.39	0.09	3.48	0.11	2.85	0.11	3.11	0.21	0.51	0.07	0.67	0.06
121	6.62	73.62	0.24	13.03	0.12	2.45	0.10	3.49	0.12	2.84	0.11	3.06	0.20	0.49	0.07	0.68	0.07
122	6.92	73.37	0.24	13.12	0.12	2.39	0.09	3.57	0.12	2.90	0.12	3.07	0.20	0.51	0.07	0.67	0.06
123	7.22	73.46	0.24	13.15	0.12	2.44	0.10	3.54	0.12	2.89	0.11	3.05	0.20	0.47	0.06	0.68	0.07
124	7.52	73.33	0.24	13.11	0.12	2.44	0.10	3.59	0.12	2.83	0.11	3.17	0.21	0.46	0.06	0.73	0.07
125	7.82	73.50	0.24	13.21	0.12	2.38	0.09	3.59	0.12	2.82	0.11	3.03	0.20	0.46	0.06	0.66	0.06
126	8.12	73.52	0.24	13.32	0.12	2.33	0.09	3.46	0.11	2.80	0.11	3.03	0.20	0.53	0.07	0.67	0.06
127	8.42	73.48	0.24	13.28	0.12	2.39	0.09	3.54	0.12	2.86	0.11	2.88	0.19	0.47	0.06	0.69	0.07
128	8.72	73.35	0.24	13.25	0.12	2.45	0.10	3.64	0.12	2.89	0.12	2.98	0.20	0.42	0.06	0.63	0.06
129	9.02	73.41	0.24	13.36	0.12	2.39	0.09	3.62	0.12	2.71	0.11	3.02	0.20	0.53	0.07	0.63	0.06
130	9.32	73.26	0.24	13.43	0.12	2.48	0.10	3.53	0.12	2.74	0.11	3.02	0.20	0.56	0.08	0.62	0.06
131	9.62	73.17	0.24	13.28	0.12	2.54	0.10	3.62	0.12	2.83	0.11	3.02	0.20	0.49	0.07	0.65	0.06
132	9.92	73.33	0.24	13.39	0.12	2.34	0.09	3.61	0.12	2.73	0.11	3.08	0.20	0.48	0.07	0.69	0.07
133	10.22	73.25	0.24	13.30	0.12	2.35	0.09	3.58	0.12	2.73	0.11	3.21	0.21	0.57	0.08	0.63	0.06
134	10.53	73.50	0.24	13.33	0.12	2.40	0.10	3.66	0.12	2.67	0.11	2.97	0.20	0.46	0.06	0.65	0.06
135	10.83	73.55	0.24	13.36	0.12	2.43	0.10	3.67	0.12	2.69	0.11	2.86	0.19	0.45	0.06	0.61	0.06
136	11.13	73.42	0.24	13.44	0.12	2.36	0.09	3.75	0.12	2.75	0.11	2.87	0.19	0.46	0.06	0.59	0.06
137	11.43	73.43	0.24	13.29	0.12	2.36	0.09	3.65	0.12	2.69	0.11	3.06	0.20	0.46	0.06	0.66	0.06
138	11.73	73.51	0.24	13.28	0.12	2.42	0.10	3.70	0.12	2.65	0.11	2.96	0.20	0.47	0.07	0.65	0.06
139	12.03	73.43	0.24	13.34	0.12	2.39	0.09	3.66	0.12	2.61	0.10	3.07	0.20	0.49	0.07	0.63	0.06
140	12.33	73.76	0.24	13.26	0.12	2.38	0.09	3.70	0.12	2.58	0.10	2.92	0.19	0.44	0.06	0.63	0.06
141	12.63	73.65	0.24	13.28	0.12	2.45	0.10	3.82	0.13	2.55	0.10	2.80	0.19	0.43	0.06	0.64	0.06
142	12.93	73.80	0.24	13.37	0.12	2.51	0.10	3.70	0.12	2.62	0.10	2.65	0.18	0.41	0.06	0.64	0.06
143	13.23	73.61	0.24	13.50	0.12	2.51	0.10	3.62	0.12	2.55	0.10	2.73	0.18	0.52	0.07	0.65	0.06
144	13.53	73.91	0.24	13.30	0.12	2.38	0.09	3.69	0.12	2.48	0.10	2.74	0.18	0.54	0.07	0.62	0.06
145	13.83	73.81	0.24	13.20	0.12	2.35	0.09	3.67	0.12	2.44	0.10	2.97	0.20	0.50	0.07	0.67	0.06
146	14.14	73.67	0.24	13.21	0.12	2.45	0.10	3.69	0.12	2.42	0.10	2.99	0.20	0.55	0.08	0.62	0.06
147	14.44	73.95	0.24	13.28	0.12	2.43	0.10	3.72	0.12	2.37	0.09	2.77	0.18	0.54	0.07	0.65	0.06
148	14.74	74.08	0.24	13.19	0.12	2.46	0.10	3.65	0.12	2.33	0.09	2.78	0.18	0.51	0.07	0.66	0.06
149	15.04	74.09	0.24	13.18	0.12	2.45	0.10	3.66	0.12	2.33	0.09	2.83	0.19	0.51	0.07	0.61	0.06
150	15.34	73.95	0.24	13.27	0.12	2.43	0.10	3.64	0.12	2.40	0.10	2.89	0.19	0.44	0.06	0.63	0.06
151	15.64	73.85	0.24	13.36	0.12	2.45	0.10	3.63	0.12	2.34	0.09	2.83	0.19	0.50	0.07	0.62	0.06
152	15.94	74.17	0.24	13.21	0.12	2.43	0.10	3.73	0.12	2.32	0.09	2.65	0.18	0.55	0.08	0.61	0.06
153	16.24	73.96	0.24	13.17	0.12	2.45	0.10	3.78	0.12	2.36	0.09	2.72	0.18	0.55	0.08	0.69	0.07
154	16.54	74.27	0.24	13.26	0.12	2.46	0.10	3.60	0.12	2.34	0.09	2.62	0.17	0.47	0.07	0.60	0.06
155	16.84	74.12	0.24	13.36	0.12	2.47	0.10	3.70	0.12	2.30	0.09	2.67	0.18	0.45	0.06	0.58	0.06
156	17.14	74.32	0.24	13.27	0.12	2.38	0.09	3.81	0.13	2.22	0.09	2.62	0.17	0.42	0.06	0.60	0.06
157	17.44	74.24	0.24	13.26	0.12	2.44	0.10	3.72	0.12	2.24	0.09	2.71	0.18	0.43	0.06	0.65	0.06
158	17.74	73.95	0.24	13.25	0.12	2.45	0.10	3.73	0.12	2.24	0.09	2.99	0.20	0.44	0.06	0.60	0.06
159	18.04	74.03	0.24	13.30	0.12	2.46	0.10	3.65	0.12	2.32	0.09	2.84	0.19	0.45	0.06	0.57	0.05
160	18.35	73.93	0.24	13.28	0.12	2.55	0.10	3.79	0.12	2.31	0.09	2.66	0.18	0.47	0.07	0.62	0.06
161	18.65	73.95	0.24	13.44	0.12	2.47	0.10	3.70	0.12	2.24	0.09	2.65	0.18	0.49	0.07	0.63	0.06
162	18.95	74.10	0.24	13.34	0.12	2.45	0.10	3.77	0.12	2.27	0.09	2.63	0.17	0.51	0.07	0.58	0.06
163	19.25	74.06	0.24	13.20	0.12	2.42	0.10	3.72	0.12	2.30	0.09	2.82	0.19	0.52	0.07	0.64	0.06
164	19.55	73.90	0.24	13.33	0.12	2.43	0.10	3.73	0.12	2.35	0.09	2.80	0.19	0.51	0.07	0.60	0.06
165	19.85	74.11	0.24	13.37	0.12	2.47	0.10	3.72	0.12	2.26	0.09	2.63	0.17	0.45	0.06	0.62	0.06
166	20.15	73.92	0.24	13.31	0.12	2.44	0.10	3.78	0.12	2.32	0.09	2.77	0.18	0.52	0.07	0.58	0.06
167	20.45	73.94	0.24	13.31	0.12	2.44	0.10	3.79	0.13	2.29	0.09	2.73	0.18	0.49	0.07	0.62	0.06
168	20.75	73.91	0.24	13.46	0.12	2.43	0.10	3.75	0.12	2.38	0.09	2.65	0.18	0.44	0.06	0.66	0.06
169	21.05	73.93	0.24	13.38	0.12	2.47	0.10	3.72	0.12	2.21	0.09	2.82	0.19	0.51	0.07	0.65	0.06
170	21.35	73.87	0.24	13.40	0.12	2.49	0.10	3.77	0.12	2.22	0.09	2.79	0.18	0.51	0.07	0.60	0.06
171	21.65	73.81	0.24	13.44	0.12	2.55	0.10	3.83	0.13	2.27	0.09	2.68	0.18	0.52	0.07	0.55	0.05
172	21.96	73.80	0.24	13.45	0.12	2.42	0.10	3.76	0.12	2.23	0.09	2.81	0.19	0.52	0.07	0.64	0.06
173	22.25	73.89	0.24	13.41	0.12	2.47	0.10	3.69	0.12	2.24	0.09	2.79	0.18	0.46	0.06	0.68	0.07
174	22.56	73.95	0.24	13.43	0.12	2.51	0.10	3.78	0.12	2.24	0.09	2.61	0.17	0.44	0.06	0.66	0.06

175	22.86	73.87	0.24	13.31	0.12	2.54	0.10	3.74	0.12	2.27	0.09	2.86	0.19	0.44	0.06	0.60	0.06
176	23.16	73.86	0.24	13.33	0.12	2.45	0.10	3.69	0.12	2.34	0.09	2.84	0.19	0.49	0.07	0.66	0.06
177	23.46	73.82	0.24	13.46	0.12	2.41	0.10	3.80	0.13	2.32	0.09	2.74	0.18	0.54	0.07	0.56	0.05
178	23.76	73.81	0.24	13.44	0.12	2.41	0.10	3.77	0.12	2.25	0.09	2.83	0.19	0.49	0.07	0.64	0.06
179	24.06	73.76	0.24	13.38	0.12	2.47	0.10	3.77	0.12	2.32	0.09	2.87	0.19	0.47	0.06	0.61	0.06
180	24.36	73.91	0.24	13.29	0.12	2.48	0.10	3.78	0.12	2.42	0.10	2.72	0.18	0.50	0.07	0.59	0.06
181	24.66	73.83	0.24	13.42	0.12	2.56	0.10	3.78	0.12	2.32	0.09	2.63	0.17	0.48	0.07	0.57	0.06
182	24.96	73.87	0.24	13.36	0.12	2.47	0.10	3.78	0.12	2.17	0.09	2.83	0.19	0.45	0.06	0.65	0.06
183	25.26	73.92	0.24	13.43	0.12	2.44	0.10	3.78	0.12	2.17	0.09	2.81	0.19	0.48	0.07	0.61	0.06
184	25.56	73.82	0.24	13.43	0.12	2.45	0.10	3.79	0.12	2.18	0.09	2.82	0.19	0.54	0.08	0.59	0.06
185	25.86	73.93	0.24	13.34	0.12	2.40	0.09	3.77	0.12	2.30	0.09	2.86	0.19	0.51	0.07	0.57	0.05
186	26.17	73.73	0.24	13.35	0.12	2.51	0.10	3.77	0.12	2.36	0.09	2.85	0.19	0.50	0.07	0.61	0.06
187	26.47	73.76	0.24	13.32	0.12	2.50	0.10	3.81	0.13	2.28	0.09	2.87	0.19	0.45	0.06	0.62	0.06
188	26.77	73.68	0.24	13.40	0.12	2.55	0.10	3.79	0.13	2.27	0.09	2.82	0.19	0.44	0.06	0.61	0.06
189	27.07	73.64	0.24	13.35	0.12	2.52	0.10	3.79	0.12	2.28	0.09	2.94	0.19	0.53	0.07	0.59	0.06
190	27.37	73.79	0.24	13.29	0.12	2.44	0.10	3.83	0.13	2.35	0.09	2.81	0.19	0.45	0.06	0.61	0.06
191	27.67	73.82	0.24	13.37	0.12	2.49	0.10	3.81	0.13	2.28	0.09	2.75	0.18	0.47	0.06	0.62	0.06

Agglomerate U4.1

Table J.25: Major element compositions (as wt.% oxides) from a line traverse across the interface of surface agglomerate U4.1 (from agglomerate U4.1 to host U4) extracted from quantified EDS compositional maps. The EDS compositional maps were collected at a resolution of 6.5 pixels/μm. The smoothing width for this traverse was 200 pixels (30.9 μm) wide. This is a Si interface and has been centered at $x = 0$ based on the SiO_2 maximum. Peak points within 2σ of the SiO_2 maximum are highlighted in yellow. Uncertainties are 2SEOM. However, there is no significant enrichment at the interface, so $x = 0$ may not correspond to the exact location of the interface.

Pt.	Position (μm)	SiO_2	2σ	Al_2O_3	2σ	Na_2O	2σ	K_2O	2σ	CaO	2σ	FeO	2σ	TiO_2	2σ	MgO	2σ
1	-18.84	74.74	0.15	13.56	0.09	1.55	0.05	3.26	0.06	2.44	0.06	2.95	0.10	0.55	0.05	0.58	0.04
2	-18.69	75.12	0.15	13.61	0.09	1.49	0.05	3.17	0.06	2.46	0.06	2.77	0.10	0.46	0.04	0.60	0.04
3	-18.53	75.09	0.15	13.59	0.09	1.51	0.05	3.14	0.06	2.49	0.07	2.74	0.09	0.45	0.04	0.61	0.04
4	-18.38	75.19	0.15	13.50	0.08	1.55	0.05	3.13	0.06	2.46	0.06	2.72	0.09	0.47	0.05	0.57	0.04
5	-18.22	74.79	0.15	13.53	0.08	1.59	0.05	3.17	0.06	2.52	0.07	2.95	0.10	0.51	0.05	0.55	0.04
6	-18.07	74.84	0.15	13.51	0.08	1.58	0.05	3.14	0.06	2.50	0.07	2.97	0.10	0.44	0.04	0.62	0.04
7	-17.91	74.88	0.15	13.63	0.09	1.54	0.05	3.05	0.06	2.51	0.07	2.95	0.10	0.48	0.05	0.60	0.04
8	-17.76	74.87	0.15	13.53	0.08	1.54	0.05	3.12	0.06	2.50	0.07	3.03	0.10	0.48	0.05	0.55	0.04
9	-17.61	74.91	0.15	13.64	0.09	1.53	0.05	3.11	0.06	2.48	0.06	2.85	0.10	0.51	0.05	0.59	0.04
10	-17.45	74.98	0.15	13.53	0.08	1.52	0.05	3.22	0.06	2.47	0.06	2.85	0.10	0.49	0.05	0.57	0.04
11	-17.30	74.78	0.15	13.57	0.09	1.49	0.05	3.21	0.06	2.54	0.07	2.92	0.10	0.49	0.05	0.62	0.04
12	-17.14	74.89	0.15	13.69	0.09	1.56	0.05	3.12	0.06	2.49	0.07	2.80	0.10	0.47	0.05	0.61	0.04
13	-16.99	74.63	0.15	13.74	0.09	1.58	0.05	3.13	0.06	2.58	0.07	2.87	0.10	0.50	0.05	0.59	0.04
14	-16.83	74.54	0.15	13.64	0.09	1.54	0.05	3.18	0.06	2.55	0.07	3.07	0.11	0.46	0.04	0.61	0.04
15	-16.68	74.66	0.15	13.65	0.09	1.63	0.05	3.17	0.06	2.53	0.07	2.95	0.10	0.49	0.05	0.56	0.04
16	-16.52	74.73	0.15	13.65	0.09	1.62	0.05	3.19	0.06	2.52	0.07	2.96	0.10	0.47	0.05	0.53	0.04
17	-16.37	74.69	0.15	13.63	0.09	1.56	0.05	3.19	0.06	2.54	0.07	2.91	0.10	0.51	0.05	0.57	0.04
18	-16.22	74.69	0.15	13.78	0.09	1.52	0.05	3.09	0.06	2.48	0.06	2.96	0.10	0.50	0.05	0.59	0.04
19	-16.06	74.61	0.15	13.80	0.09	1.49	0.05	3.08	0.06	2.44	0.06	3.06	0.11	0.51	0.05	0.56	0.04
20	-15.91	74.76	0.15	13.74	0.09	1.51	0.05	3.17	0.06	2.46	0.06	2.86	0.10	0.49	0.05	0.58	0.04
21	-15.75	74.80	0.15	13.66	0.09	1.56	0.05	3.14	0.06	2.62	0.07	2.76	0.10	0.50	0.05	0.57	0.04
22	-15.60	74.67	0.15	13.66	0.09	1.57	0.05	3.18	0.06	2.56	0.07	2.92	0.10	0.49	0.05	0.58	0.04
23	-15.44	74.68	0.15	13.68	0.09	1.56	0.05	3.12	0.06	2.54	0.07	2.99	0.10	0.52	0.05	0.54	0.04
24	-15.29	74.68	0.15	13.73	0.09	1.50	0.05	3.15	0.06	2.55	0.07	2.99	0.10	0.51	0.05	0.54	0.04
25	-15.13	74.57	0.15	13.72	0.09	1.52	0.05	3.16	0.06	2.55	0.07	3.02	0.10	0.47	0.05	0.60	0.04
26	-14.98	74.70	0.15	13.64	0.09	1.59	0.05	3.17	0.06	2.58	0.07	2.90	0.10	0.52	0.05	0.58	0.04
27	-14.83	74.74	0.15	13.65	0.09	1.52	0.05	3.14	0.06	2.58	0.07	2.89	0.10	0.47	0.05	0.58	0.04
28	-14.67	74.72	0.15	13.52	0.08	1.57	0.05	3.11	0.06	2.55	0.07	2.98	0.10	0.55	0.05	0.58	0.04
29	-14.52	74.57	0.15	13.63	0.09	1.54	0.05	3.14	0.06	2.56	0.07	2.98	0.10	0.56	0.05	0.62	0.04
30	-14.36	74.76	0.15	13.75	0.09	1.56	0.05	3.10	0.06	2.50	0.07	2.80	0.10	0.55	0.05	0.60	0.04
31	-14.21	74.62	0.15	13.86	0.09	1.56	0.05	3.10	0.06	2.46	0.06	2.95	0.10	0.51	0.05	0.57	0.04
32	-14.05	74.91	0.15	13.67	0.09	1.55	0.05	3.13	0.06	2.46	0.06	2.92	0.10	0.45	0.04	0.55	0.04
33	-13.90	74.90	0.15	13.57	0.09	1.55	0.05	3.16	0.06	2.57	0.07	2.89	0.10	0.44	0.04	0.55	0.04
34	-13.74	74.84	0.15	13.71	0.09	1.55	0.05	3.09	0.06	2.41	0.06	2.97	0.10	0.53	0.05	0.53	0.04
35	-13.59	74.88	0.15	13.63	0.09	1.55	0.05	3.14	0.06	2.46	0.06	2.96	0.10	0.48	0.05	0.52	0.04
36	-13.44	74.98	0.15	13.59	0.09	1.62	0.05	3.11	0.06	2.44	0.06	2.89	0.10	0.50	0.05	0.52	0.04
37	-13.28	74.81	0.15	13.68	0.09	1.52	0.05	3.19	0.06	2.47	0.06	2.82	0.10	0.56	0.05	0.56	0.04
38	-13.13	74.74	0.15	13.73	0.09	1.48	0.05	3.12	0.06	2.48	0.06	3.01	0.10	0.49	0.05	0.51	0.03
39	-12.97	74.73	0.15	13.66	0.09	1.52	0.05	3.19	0.06	2.44	0.06	2.99	0.10	0.48	0.05	0.56	0.04
40	-12.82	74.82	0.15	13.57	0.09	1.57	0.05	3.25	0.06	2.37	0.06	2.98	0.10	0.49	0.05	0.54	0.04
41	-12.66	74.97	0.15	13.54	0.08	1.56	0.05	3.21	0.06	2.42	0.06	2.88	0.10	0.48	0.05	0.56	0.04
42	-12.51	74.88	0.15	13.64	0.09	1.55	0.05	3.06	0.06	2.41	0.06	2.97	0.10	0.53	0.05	0.57	0.04
43	-12.36	74.85	0.15	13.53	0.08	1.53	0.05	3.12	0.06	2.52	0.07	3.01	0.10	0.46	0.04	0.54	0.04
44	-12.20	74.98	0.15	13.61	0.09	1.47	0.05	3.18	0.06	2.48	0.06	2.85	0.10	0.47	0.05	0.57	0.04
45	-12.05	75.04	0.15	13.63	0.09	1.51	0.05	3.19	0.06	2.37	0.06	2.83	0.10	0.42	0.04	0.63	0.04
46	-11.89	74.99	0.15	13.56	0.09	1.49	0.05	3.14	0.06	2.42	0.06	2.88	0.10	0.56	0.05	0.58	0.04
47	-11.74	74.95	0.15	13.49	0.08	1.51	0.05	3.16	0.06	2.41	0.06	2.97	0.10	0.57	0.06	0.57	0.04
48	-11.58	74.97	0.15	13.60	0.09	1.49	0.05	3.25	0.06	2.41	0.06	2.91	0.10	0.45	0.04	0.56	0.04
49	-11.43	75.05	0.15	13.52	0.08	1.47	0.05	3.19	0.06	2.41	0.06	2.97	0.10	0.49	0.05	0.58	0.04

50	-11.27	75.14	0.15	13.53	0.08	1.50	0.05	3.15	0.06	2.42	0.06	2.91	0.10	0.45	0.04	0.56	0.04
51	-11.12	75.04	0.15	13.52	0.08	1.61	0.05	3.15	0.06	2.31	0.06	3.03	0.10	0.45	0.04	0.52	0.04
52	-10.97	75.03	0.15	13.51	0.08	1.53	0.05	3.21	0.06	2.37	0.06	3.00	0.10	0.50	0.05	0.50	0.03
53	-10.81	75.10	0.15	13.50	0.08	1.50	0.05	3.14	0.06	2.43	0.06	2.94	0.10	0.46	0.04	0.56	0.04
54	-10.66	75.26	0.15	13.51	0.08	1.49	0.05	3.09	0.06	2.38	0.06	2.89	0.10	0.45	0.04	0.56	0.04
55	-10.50	75.30	0.15	13.52	0.08	1.46	0.05	3.05	0.06	2.43	0.06	2.81	0.10	0.47	0.05	0.51	0.03
56	-10.35	75.22	0.15	13.51	0.08	1.48	0.05	3.11	0.06	2.42	0.06	2.87	0.10	0.49	0.05	0.53	0.04
57	-10.19	75.28	0.15	13.44	0.08	1.44	0.05	3.20	0.06	2.40	0.06	2.82	0.10	0.45	0.04	0.55	0.04
58	-10.04	74.99	0.15	13.51	0.08	1.57	0.05	3.21	0.06	2.35	0.06	2.92	0.10	0.53	0.05	0.56	0.04
59	-9.88	75.06	0.15	13.51	0.08	1.51	0.05	3.24	0.06	2.36	0.06	2.87	0.10	0.54	0.05	0.56	0.04
60	-9.73	75.01	0.15	13.35	0.08	1.51	0.05	3.17	0.06	2.45	0.06	3.06	0.11	0.51	0.05	0.56	0.04
61	-9.58	75.21	0.15	13.49	0.08	1.47	0.05	3.18	0.06	2.40	0.06	2.85	0.10	0.48	0.05	0.57	0.04
62	-9.42	75.20	0.15	13.54	0.08	1.49	0.05	3.17	0.06	2.31	0.06	2.85	0.10	0.43	0.04	0.60	0.04
63	-9.27	75.41	0.15	13.46	0.08	1.49	0.05	3.17	0.06	2.34	0.06	2.75	0.10	0.46	0.04	0.53	0.04
64	-9.11	75.19	0.15	13.43	0.08	1.48	0.05	3.19	0.06	2.36	0.06	2.96	0.10	0.48	0.05	0.53	0.04
65	-8.96	75.24	0.15	13.50	0.08	1.51	0.05	3.19	0.06	2.19	0.06	2.94	0.10	0.52	0.05	0.57	0.04
66	-8.80	75.36	0.15	13.39	0.08	1.47	0.05	3.09	0.06	2.28	0.06	2.96	0.10	0.52	0.05	0.55	0.04
67	-8.65	75.20	0.15	13.35	0.08	1.50	0.05	3.17	0.06	2.34	0.06	2.97	0.10	0.49	0.05	0.60	0.04
68	-8.49	75.08	0.15	13.40	0.08	1.47	0.05	3.25	0.06	2.28	0.06	2.98	0.10	0.55	0.05	0.61	0.04
69	-8.34	75.23	0.15	13.36	0.08	1.44	0.04	3.30	0.06	2.33	0.06	2.91	0.10	0.50	0.05	0.55	0.04
70	-8.19	75.37	0.15	13.39	0.08	1.48	0.05	3.20	0.06	2.39	0.06	2.84	0.10	0.42	0.04	0.55	0.04
71	-8.03	75.37	0.15	13.38	0.08	1.53	0.05	3.15	0.06	2.39	0.06	2.90	0.10	0.45	0.04	0.51	0.04
72	-7.88	75.28	0.15	13.35	0.08	1.54	0.05	3.15	0.06	2.31	0.06	2.96	0.10	0.49	0.05	0.55	0.04
73	-7.72	75.37	0.15	13.38	0.08	1.47	0.05	3.13	0.06	2.28	0.06	3.00	0.10	0.46	0.05	0.56	0.04
74	-7.57	75.35	0.15	13.45	0.08	1.44	0.04	3.21	0.06	2.29	0.06	2.85	0.10	0.44	0.04	0.60	0.04
75	-7.41	75.16	0.15	13.52	0.08	1.51	0.05	3.13	0.06	2.33	0.06	2.92	0.10	0.51	0.05	0.57	0.04
76	-7.26	75.16	0.15	13.48	0.08	1.45	0.05	3.28	0.06	2.32	0.06	2.83	0.10	0.50	0.05	0.58	0.04
77	-7.10	75.39	0.15	13.43	0.08	1.50	0.05	3.29	0.06	2.23	0.06	2.79	0.10	0.49	0.05	0.54	0.04
78	-6.95	75.20	0.15	13.52	0.08	1.50	0.05	3.24	0.06	2.27	0.06	2.87	0.10	0.48	0.05	0.57	0.04
79	-6.80	75.30	0.15	13.53	0.08	1.42	0.04	3.22	0.06	2.26	0.06	2.82	0.10	0.48	0.05	0.56	0.04
80	-6.64	75.37	0.15	13.48	0.08	1.46	0.05	3.12	0.06	2.30	0.06	2.89	0.10	0.54	0.05	0.52	0.04
81	-6.49	75.25	0.15	13.47	0.08	1.46	0.05	3.20	0.06	2.30	0.06	2.94	0.10	0.47	0.05	0.53	0.04
82	-6.33	75.15	0.15	13.41	0.08	1.43	0.04	3.27	0.06	2.30	0.06	3.01	0.10	0.51	0.05	0.55	0.04
83	-6.18	75.21	0.15	13.45	0.08	1.44	0.04	3.30	0.06	2.27	0.06	2.88	0.10	0.51	0.05	0.59	0.04
84	-6.02	75.31	0.15	13.42	0.08	1.48	0.05	3.25	0.06	2.25	0.06	2.83	0.10	0.50	0.05	0.54	0.04
85	-5.87	75.41	0.15	13.45	0.08	1.51	0.05	3.16	0.06	2.24	0.06	2.81	0.10	0.47	0.05	0.53	0.04
86	-5.71	75.31	0.15	13.44	0.08	1.55	0.05	3.27	0.06	2.21	0.06	2.76	0.10	0.51	0.05	0.52	0.04
87	-5.56	75.30	0.15	13.48	0.08	1.50	0.05	3.22	0.06	2.16	0.06	2.92	0.10	0.50	0.05	0.58	0.04
88	-5.41	75.18	0.15	13.39	0.08	1.49	0.05	3.21	0.06	2.30	0.06	2.96	0.10	0.55	0.05	0.55	0.04
89	-5.25	75.26	0.15	13.48	0.08	1.45	0.05	3.23	0.06	2.30	0.06	2.85	0.10	0.52	0.05	0.55	0.04
90	-5.10	75.15	0.15	13.48	0.08	1.48	0.05	3.18	0.06	2.26	0.06	2.88	0.10	0.61	0.06	0.58	0.04
91	-4.94	75.49	0.15	13.42	0.08	1.45	0.05	3.33	0.06	2.23	0.06	2.66	0.09	0.52	0.05	0.54	0.04
92	-4.79	75.46	0.15	13.49	0.08	1.48	0.05	3.25	0.06	2.17	0.06	2.71	0.09	0.54	0.05	0.55	0.04
93	-4.63	75.42	0.15	13.42	0.08	1.53	0.05	3.28	0.06	2.16	0.06	2.78	0.10	0.49	0.05	0.58	0.04
94	-4.48	75.34	0.15	13.38	0.08	1.46	0.05	3.35	0.06	2.23	0.06	2.72	0.09	0.51	0.05	0.63	0.04
95	-4.32	75.44	0.15	13.50	0.08	1.49	0.05	3.31	0.06	2.24	0.06	2.63	0.09	0.44	0.04	0.58	0.04
96	-4.17	75.33	0.15	13.52	0.08	1.49	0.05	3.27	0.06	2.26	0.06	2.65	0.09	0.47	0.05	0.56	0.04
97	-4.02	75.29	0.15	13.48	0.08	1.54	0.05	3.30	0.06	2.24	0.06	2.71	0.09	0.49	0.05	0.56	0.04
98	-3.86	75.40	0.15	13.48	0.08	1.52	0.05	3.27	0.06	2.25	0.06	2.64	0.09	0.55	0.05	0.54	0.04
99	-3.71	75.48	0.15	13.52	0.08	1.48	0.05	3.25	0.06	2.18	0.06	2.60	0.09	0.56	0.05	0.55	0.04
100	-3.55	75.31	0.15	13.52	0.08	1.48	0.05	3.29	0.06	2.23	0.06	2.68	0.09	0.50	0.05	0.57	0.04
101	-3.40	75.46	0.15	13.51	0.08	1.43	0.04	3.26	0.06	2.18	0.06	2.76	0.10	0.46	0.05	0.53	0.04
102	-3.24	75.39	0.15	13.51	0.08	1.49	0.05	3.22	0.06	2.15	0.06	2.89	0.10	0.50	0.05	0.55	0.04
103	-3.09	75.32	0.15	13.55	0.08	1.54	0.05	3.21	0.06	2.19	0.06	2.75	0.10	0.51	0.05	0.55	0.04
104	-2.93	75.43	0.15	13.41	0.08	1.49	0.05	3.30	0.06	2.25	0.06	2.62	0.09	0.54	0.05	0.56	0.04
105	-2.78	75.31	0.15	13.48	0.08	1.47	0.05	3.34	0.06	2.22	0.06	2.73	0.09	0.54	0.05	0.52	0.04
106	-2.63	75.55	0.15	13.45	0.08	1.52	0.05	3.39	0.06	2.14	0.06	2.60	0.09	0.50	0.05	0.50	0.03
107	-2.47	75.57	0.15	13.53	0.08	1.47	0.05	3.28	0.06	2.21	0.06	2.58	0.09	0.49	0.05	0.52	0.04
108	-2.32	75.43	0.15	13.54	0.08	1.49	0.05	3.29	0.06	2.15	0.06	2.70	0.09	0.48	0.05	0.57	0.04
109	-2.16	75.38	0.15	13.46	0.08	1.44	0.04	3.24	0.06	2.21	0.06	2.78	0.10	0.53	0.05	0.56	0.04
110	-2.01	75.56	0.15	13.49	0.08	1.46	0.05	3.28	0.06	2.19	0.06	2.69	0.09	0.48	0.05	0.52	0.04
111	-1.85	75.57	0.15	13.47	0.08	1.49	0.05	3.25	0.06	2.22	0.06	2.65	0.09	0.49	0.05	0.53	0.04

112	-1.70	75.48	0.15	13.49	0.08	1.48	0.05	3.24	0.06	2.27	0.06	2.68	0.09	0.49	0.05	0.54	0.04
113	-1.54	75.58	0.15	13.47	0.08	1.51	0.05	3.25	0.06	2.23	0.06	2.59	0.09	0.50	0.05	0.52	0.04
114	-1.39	75.49	0.15	13.56	0.09	1.49	0.05	3.38	0.06	2.06	0.05	2.59	0.09	0.51	0.05	0.56	0.04
115	-1.24	75.40	0.15	13.49	0.08	1.41	0.04	3.33	0.06	2.18	0.06	2.72	0.09	0.54	0.05	0.58	0.04
116	-1.08	75.33	0.15	13.47	0.08	1.46	0.05	3.32	0.06	2.17	0.06	2.77	0.10	0.54	0.05	0.55	0.04
117	-0.93	75.51	0.15	13.42	0.08	1.48	0.05	3.29	0.06	2.19	0.06	2.56	0.09	0.52	0.05	0.62	0.04
118	-0.77	75.48	0.15	13.48	0.08	1.52	0.05	3.29	0.06	2.16	0.06	2.65	0.09	0.50	0.05	0.54	0.04
119	-0.62	75.48	0.15	13.52	0.08	1.52	0.05	3.35	0.06	2.15	0.06	2.60	0.09	0.48	0.05	0.54	0.04
120	-0.46	75.48	0.15	13.49	0.08	1.53	0.05	3.31	0.06	2.15	0.06	2.58	0.09	0.52	0.05	0.55	0.04
121	-0.31	75.41	0.15	13.50	0.08	1.53	0.05	3.42	0.06	2.21	0.06	2.50	0.09	0.47	0.05	0.53	0.04
122	-0.15	75.68	0.15	13.46	0.08	1.53	0.05	3.36	0.06	2.12	0.06	2.52	0.09	0.48	0.05	0.51	0.04
123	0.00	75.80	0.15	13.42	0.08	1.51	0.05	3.32	0.06	2.11	0.06	2.54	0.09	0.45	0.04	0.49	0.03
124	0.15	75.63	0.15	13.48	0.08	1.50	0.05	3.33	0.06	2.16	0.06	2.60	0.09	0.42	0.04	0.53	0.04
125	0.31	75.55	0.15	13.51	0.08	1.53	0.05	3.28	0.06	2.17	0.06	2.58	0.09	0.47	0.05	0.52	0.04
126	0.46	75.73	0.15	13.42	0.08	1.51	0.05	3.32	0.06	2.17	0.06	2.49	0.09	0.47	0.05	0.55	0.04
127	0.62	75.51	0.15	13.50	0.08	1.51	0.05	3.34	0.06	2.14	0.06	2.60	0.09	0.53	0.05	0.49	0.03
128	0.77	75.49	0.15	13.53	0.08	1.45	0.05	3.33	0.06	2.18	0.06	2.61	0.09	0.47	0.05	0.55	0.04
129	0.93	75.56	0.15	13.56	0.09	1.49	0.05	3.38	0.06	2.15	0.06	2.49	0.09	0.48	0.05	0.53	0.04
130	1.08	75.44	0.15	13.49	0.08	1.53	0.05	3.38	0.06	2.22	0.06	2.53	0.09	0.46	0.05	0.53	0.04
131	1.24	75.49	0.15	13.43	0.08	1.52	0.05	3.32	0.06	2.22	0.06	2.65	0.09	0.50	0.05	0.52	0.04
132	1.39	75.56	0.15	13.53	0.08	1.52	0.05	3.34	0.06	2.22	0.06	2.46	0.09	0.48	0.05	0.53	0.04
133	1.54	75.41	0.15	13.61	0.09	1.55	0.05	3.32	0.06	2.17	0.06	2.52	0.09	0.49	0.05	0.57	0.04
134	1.70	75.45	0.15	13.61	0.09	1.52	0.05	3.30	0.06	2.20	0.06	2.52	0.09	0.56	0.05	0.52	0.04
135	1.85	75.62	0.15	13.56	0.09	1.53	0.05	3.42	0.06	2.19	0.06	2.42	0.08	0.46	0.04	0.51	0.03
136	2.01	75.39	0.15	13.63	0.09	1.54	0.05	3.41	0.06	2.20	0.06	2.43	0.08	0.52	0.05	0.53	0.04
137	2.16	75.43	0.15	13.62	0.09	1.53	0.05	3.39	0.06	2.17	0.06	2.46	0.09	0.53	0.05	0.52	0.04
138	2.32	75.33	0.15	13.62	0.09	1.57	0.05	3.28	0.06	2.32	0.06	2.44	0.08	0.52	0.05	0.55	0.04
139	2.47	75.12	0.15	13.73	0.09	1.60	0.05	3.32	0.06	2.29	0.06	2.55	0.09	0.49	0.05	0.52	0.04
140	2.62	75.26	0.15	13.62	0.09	1.57	0.05	3.38	0.06	2.34	0.06	2.54	0.09	0.47	0.05	0.48	0.03
141	2.78	74.91	0.15	13.69	0.09	1.63	0.05	3.41	0.06	2.36	0.06	2.59	0.09	0.52	0.05	0.55	0.04
142	2.93	75.17	0.15	13.71	0.09	1.60	0.05	3.30	0.06	2.29	0.06	2.52	0.09	0.52	0.05	0.53	0.04
143	3.09	75.18	0.15	13.69	0.09	1.57	0.05	3.31	0.06	2.32	0.06	2.49	0.09	0.53	0.05	0.52	0.04
144	3.24	74.83	0.15	13.80	0.09	1.62	0.05	3.45	0.06	2.31	0.06	2.50	0.09	0.53	0.05	0.55	0.04
145	3.40	74.79	0.15	13.72	0.09	1.66	0.05	3.45	0.06	2.32	0.06	2.63	0.09	0.51	0.05	0.54	0.04
146	3.55	74.82	0.15	13.73	0.09	1.60	0.05	3.36	0.06	2.42	0.06	2.59	0.09	0.53	0.05	0.56	0.04
147	3.71	74.60	0.15	13.85	0.09	1.72	0.05	3.38	0.06	2.48	0.06	2.55	0.09	0.51	0.05	0.53	0.04
148	3.86	74.42	0.15	13.84	0.09	1.72	0.05	3.45	0.06	2.47	0.06	2.67	0.09	0.57	0.06	0.48	0.03
149	4.02	74.57	0.15	13.95	0.09	1.63	0.05	3.40	0.06	2.47	0.06	2.60	0.09	0.51	0.05	0.50	0.03
150	4.17	74.59	0.15	14.05	0.09	1.56	0.05	3.38	0.06	2.48	0.06	2.56	0.09	0.52	0.05	0.51	0.03
151	4.32	74.59	0.15	14.00	0.09	1.61	0.05	3.28	0.06	2.50	0.07	2.57	0.09	0.51	0.05	0.57	0.04
152	4.48	74.50	0.15	13.92	0.09	1.63	0.05	3.40	0.06	2.53	0.07	2.57	0.09	0.53	0.05	0.55	0.04
153	4.63	74.50	0.15	13.99	0.09	1.66	0.05	3.31	0.06	2.49	0.07	2.68	0.09	0.49	0.05	0.51	0.03
154	4.79	74.56	0.15	14.02	0.09	1.64	0.05	3.33	0.06	2.53	0.07	2.61	0.09	0.47	0.05	0.49	0.03
155	4.94	74.49	0.15	14.04	0.09	1.61	0.05	3.33	0.06	2.51	0.07	2.69	0.09	0.48	0.05	0.50	0.03
156	5.10	74.17	0.15	14.07	0.09	1.65	0.05	3.32	0.06	2.60	0.07	2.75	0.10	0.53	0.05	0.51	0.03
157	5.25	74.18	0.15	14.12	0.09	1.70	0.05	3.30	0.06	2.65	0.07	2.72	0.09	0.45	0.04	0.51	0.03
158	5.41	74.16	0.15	14.09	0.09	1.69	0.05	3.31	0.06	2.67	0.07	2.71	0.09	0.48	0.05	0.52	0.04
159	5.56	74.07	0.15	14.10	0.09	1.66	0.05	3.36	0.06	2.71	0.07	2.70	0.09	0.55	0.05	0.49	0.03
160	5.71	73.93	0.15	14.15	0.09	1.73	0.05	3.32	0.06	2.70	0.07	2.75	0.10	0.51	0.05	0.50	0.03
161	5.87	73.62	0.15	14.24	0.09	1.73	0.05	3.31	0.06	2.71	0.07	2.95	0.10	0.53	0.05	0.56	0.04
162	6.02	73.64	0.15	14.23	0.09	1.71	0.05	3.32	0.06	2.77	0.07	2.91	0.10	0.52	0.05	0.57	0.04
163	6.18	73.77	0.15	14.30	0.09	1.70	0.05	3.28	0.06	2.76	0.07	2.75	0.10	0.54	0.05	0.58	0.04
164	6.33	73.56	0.15	14.48	0.09	1.72	0.05	3.33	0.06	2.78	0.07	2.69	0.09	0.47	0.05	0.61	0.04
165	6.49	73.39	0.15	14.41	0.09	1.75	0.05	3.35	0.06	2.83	0.07	2.77	0.10	0.54	0.05	0.59	0.04
166	6.64	73.11	0.15	14.47	0.09	1.78	0.06	3.32	0.06	3.04	0.08	2.80	0.10	0.47	0.05	0.60	0.04
167	6.80	73.13	0.15	14.55	0.09	1.78	0.06	3.32	0.06	2.99	0.08	2.75	0.10	0.46	0.04	0.57	0.04
168	6.95	73.09	0.15	14.46	0.09	1.78	0.06	3.36	0.06	2.93	0.08	2.90	0.10	0.51	0.05	0.53	0.04
169	7.10	72.90	0.15	14.58	0.09	1.78	0.06	3.40	0.06	2.97	0.08	2.90	0.10	0.49	0.05	0.59	0.04
170	7.26	72.86	0.15	14.68	0.09	1.86	0.06	3.30	0.06	3.01	0.08	2.79	0.10	0.52	0.05	0.61	0.04
171	7.41	72.66	0.15	14.75	0.09	1.83	0.06	3.33	0.06	3.11	0.08	2.86	0.10	0.56	0.05	0.54	0.04
172	7.57	72.58	0.15	14.80	0.09	1.74	0.05	3.34	0.06	3.22	0.08	2.89	0.10	0.53	0.05	0.54	0.04
173	7.72	72.41	0.14	14.90	0.09	1.84	0.06	3.35	0.06	3.14	0.08	2.91	0.10	0.51	0.05	0.58	0.04

174	7.88	72.25	0.14	14.89	0.09	1.92	0.06	3.29	0.06	3.24	0.08	2.90	0.10	0.52	0.05	0.60	0.04
175	8.03	72.46	0.14	14.84	0.09	1.89	0.06	3.22	0.06	3.19	0.08	2.95	0.10	0.49	0.05	0.60	0.04
176	8.19	72.22	0.14	14.96	0.09	1.86	0.06	3.28	0.06	3.25	0.08	3.04	0.11	0.49	0.05	0.54	0.04
177	8.34	72.24	0.14	15.06	0.09	1.83	0.06	3.18	0.06	3.21	0.08	2.99	0.10	0.57	0.06	0.54	0.04
178	8.49	72.04	0.14	15.10	0.09	1.84	0.06	3.23	0.06	3.21	0.08	3.07	0.11	0.54	0.05	0.57	0.04
179	8.65	71.85	0.14	15.09	0.09	1.81	0.06	3.27	0.06	3.29	0.09	3.07	0.11	0.54	0.05	0.62	0.04
180	8.80	71.86	0.14	15.10	0.09	1.89	0.06	3.23	0.06	3.37	0.09	3.02	0.10	0.54	0.05	0.60	0.04
181	8.96	71.95	0.14	15.10	0.09	1.91	0.06	3.27	0.06	3.30	0.09	2.98	0.10	0.54	0.05	0.60	0.04
182	9.11	72.10	0.14	15.04	0.09	1.93	0.06	3.30	0.06	3.25	0.08	2.95	0.10	0.58	0.06	0.54	0.04
183	9.27	71.95	0.14	15.00	0.09	1.81	0.06	3.29	0.06	3.35	0.09	3.12	0.11	0.56	0.05	0.57	0.04
184	9.42	71.86	0.14	15.16	0.10	1.82	0.06	3.25	0.06	3.43	0.09	3.00	0.10	0.51	0.05	0.61	0.04
185	9.58	71.91	0.14	15.12	0.09	1.86	0.06	3.26	0.06	3.43	0.09	2.87	0.10	0.49	0.05	0.65	0.04
186	9.73	71.91	0.14	15.05	0.09	1.92	0.06	3.24	0.06	3.47	0.09	2.88	0.10	0.53	0.05	0.63	0.04
187	9.88	71.86	0.14	15.13	0.09	1.93	0.06	3.24	0.06	3.33	0.09	2.95	0.10	0.55	0.05	0.59	0.04
188	10.04	71.71	0.14	14.97	0.09	1.90	0.06	3.29	0.06	3.50	0.09	3.12	0.11	0.49	0.05	0.63	0.04
189	10.19	71.88	0.14	15.08	0.09	1.90	0.06	3.16	0.06	3.38	0.09	3.14	0.11	0.53	0.05	0.58	0.04
190	10.35	71.75	0.14	15.08	0.09	1.95	0.06	3.25	0.06	3.40	0.09	3.05	0.11	0.52	0.05	0.62	0.04
191	10.50	71.88	0.14	14.97	0.09	1.87	0.06	3.38	0.06	3.45	0.09	2.93	0.10	0.55	0.05	0.62	0.04
192	10.66	71.90	0.14	15.01	0.09	1.86	0.06	3.29	0.06	3.45	0.09	2.99	0.10	0.52	0.05	0.57	0.04
193	10.81	71.88	0.14	15.06	0.09	1.86	0.06	3.23	0.06	3.43	0.09	2.96	0.10	0.53	0.05	0.62	0.04
194	10.96	71.88	0.14	15.01	0.09	1.93	0.06	3.27	0.06	3.42	0.09	2.93	0.10	0.51	0.05	0.64	0.04
195	11.12	71.90	0.14	15.07	0.09	1.90	0.06	3.31	0.06	3.39	0.09	2.97	0.10	0.51	0.05	0.59	0.04
196	11.27	71.96	0.14	14.99	0.09	1.88	0.06	3.36	0.06	3.39	0.09	2.94	0.10	0.52	0.05	0.57	0.04
197	11.43	71.80	0.14	14.99	0.09	1.92	0.06	3.28	0.06	3.50	0.09	3.02	0.10	0.47	0.05	0.64	0.04
198	11.58	71.61	0.14	14.95	0.09	1.85	0.06	3.33	0.06	3.56	0.09	3.07	0.11	0.53	0.05	0.68	0.05
199	11.74	71.74	0.14	15.01	0.09	1.88	0.06	3.38	0.06	3.49	0.09	2.97	0.10	0.50	0.05	0.60	0.04
200	11.89	71.93	0.14	14.86	0.09	1.91	0.06	3.33	0.06	3.45	0.09	3.05	0.11	0.49	0.05	0.60	0.04
201	12.05	71.93	0.14	15.00	0.09	1.86	0.06	3.31	0.06	3.47	0.09	2.98	0.10	0.50	0.05	0.58	0.04
202	12.20	71.90	0.14	15.06	0.09	1.85	0.06	3.28	0.06	3.48	0.09	2.95	0.10	0.51	0.05	0.59	0.04
203	12.36	72.08	0.14	15.16	0.10	1.86	0.06	3.30	0.06	3.37	0.09	2.76	0.10	0.49	0.05	0.57	0.04
204	12.51	72.05	0.14	14.96	0.09	1.87	0.06	3.29	0.06	3.48	0.09	2.89	0.10	0.53	0.05	0.56	0.04
205	12.66	71.96	0.14	14.90	0.09	1.84	0.06	3.29	0.06	3.54	0.09	3.07	0.11	0.47	0.05	0.59	0.04
206	12.82	72.11	0.14	14.90	0.09	1.94	0.06	3.30	0.06	3.39	0.09	2.91	0.10	0.52	0.05	0.59	0.04
207	12.97	72.06	0.14	14.75	0.09	1.92	0.06	3.36	0.06	3.46	0.09	2.97	0.10	0.50	0.05	0.64	0.04
208	13.13	71.99	0.14	14.84	0.09	1.91	0.06	3.33	0.06	3.38	0.09	3.02	0.10	0.58	0.06	0.57	0.04
209	13.28	72.10	0.14	14.82	0.09	1.92	0.06	3.32	0.06	3.41	0.09	2.94	0.10	0.52	0.05	0.55	0.04
210	13.44	72.38	0.14	14.83	0.09	1.89	0.06	3.29	0.06	3.36	0.09	2.87	0.10	0.45	0.04	0.56	0.04
211	13.59	72.32	0.14	14.77	0.09	1.87	0.06	3.29	0.06	3.38	0.09	2.95	0.10	0.49	0.05	0.58	0.04
212	13.75	72.29	0.14	14.84	0.09	1.93	0.06	3.28	0.06	3.42	0.09	2.80	0.10	0.47	0.05	0.61	0.04
213	13.90	72.21	0.14	14.74	0.09	1.90	0.06	3.25	0.06	3.37	0.09	3.04	0.11	0.52	0.05	0.60	0.04
214	14.05	72.27	0.14	14.71	0.09	1.91	0.06	3.29	0.06	3.43	0.09	2.92	0.10	0.51	0.05	0.59	0.04
215	14.21	72.28	0.14	14.73	0.09	1.89	0.06	3.29	0.06	3.40	0.09	2.90	0.10	0.51	0.05	0.62	0.04
216	14.36	72.40	0.14	14.75	0.09	1.86	0.06	3.30	0.06	3.37	0.09	2.86	0.10	0.52	0.05	0.64	0.04
217	14.52	72.34	0.14	14.64	0.09	1.91	0.06	3.37	0.06	3.41	0.09	2.88	0.10	0.51	0.05	0.59	0.04
218	14.67	72.35	0.14	14.72	0.09	1.85	0.06	3.38	0.06	3.37	0.09	2.91	0.10	0.50	0.05	0.58	0.04
219	14.83	72.65	0.15	14.61	0.09	1.82	0.06	3.23	0.06	3.20	0.08	2.95	0.10	0.59	0.06	0.63	0.04
220	14.98	72.18	0.14	14.64	0.09	1.85	0.06	3.30	0.06	3.49	0.09	3.01	0.10	0.50	0.05	0.63	0.04
221	15.13	72.34	0.14	14.66	0.09	1.87	0.06	3.27	0.06	3.47	0.09	2.88	0.10	0.52	0.05	0.58	0.04
222	15.29	72.43	0.14	14.71	0.09	1.79	0.06	3.38	0.06	3.41	0.09	2.87	0.10	0.47	0.05	0.59	0.04
223	15.44	72.32	0.14	14.60	0.09	1.89	0.06	3.30	0.06	3.45	0.09	2.89	0.10	0.50	0.05	0.61	0.04
224	15.60	72.36	0.14	14.48	0.09	1.88	0.06	3.32	0.06	3.52	0.09	2.92	0.10	0.51	0.05	0.65	0.04
225	15.75	72.38	0.14	14.62	0.09	1.89	0.06	3.29	0.06	3.36	0.09	2.96	0.10	0.52	0.05	0.59	0.04
226	15.91	72.48	0.14	14.61	0.09	1.90	0.06	3.28	0.06	3.48	0.09	2.76	0.10	0.52	0.05	0.58	0.04
227	16.06	72.56	0.15	14.54	0.09	1.84	0.06	3.28	0.06	3.42	0.09	2.93	0.10	0.51	0.05	0.56	0.04
228	16.22	72.60	0.15	14.51	0.09	1.89	0.06	3.22	0.06	3.42	0.09	2.90	0.10	0.52	0.05	0.58	0.04
229	16.37	72.72	0.15	14.39	0.09	1.88	0.06	3.19	0.06	3.40	0.09	2.96	0.10	0.50	0.05	0.56	0.04
230	16.52	72.68	0.15	14.27	0.09	1.95	0.06	3.35	0.06	3.32	0.09	2.96	0.10	0.51	0.05	0.56	0.04
231	16.68	72.79	0.15	14.41	0.09	1.83	0.06	3.36	0.06	3.40	0.09	2.81	0.10	0.46	0.05	0.58	0.04
232	16.83	72.66	0.15	14.42	0.09	1.82	0.06	3.39	0.06	3.42	0.09	2.88	0.10	0.49	0.05	0.59	0.04
233	16.99	72.49	0.14	14.33	0.09	1.83	0.06	3.40	0.06	3.40	0.09	3.06	0.11	0.51	0.05	0.61	0.04
234	17.14	72.66	0.15	14.38	0.09	1.85	0.06	3.33	0.06	3.41	0.09	2.96	0.10	0.44	0.04	0.60	0.04
235	17.30	72.67	0.15	14.53	0.09	1.87	0.06	3.31	0.06	3.40	0.09	2.75	0.10	0.44	0.04	0.64	0.04

236	17.45	72.76	0.15	14.40	0.09	1.89	0.06	3.40	0.06	3.33	0.09	2.68	0.09	0.49	0.05	0.59	0.04
237	17.61	72.87	0.15	14.41	0.09	1.91	0.06	3.35	0.06	3.33	0.09	2.64	0.09	0.51	0.05	0.59	0.04
238	17.76	72.87	0.15	14.41	0.09	1.85	0.06	3.28	0.06	3.32	0.09	2.83	0.10	0.52	0.05	0.60	0.04
239	17.91	72.91	0.15	14.32	0.09	1.77	0.06	3.33	0.06	3.41	0.09	2.85	0.10	0.49	0.05	0.55	0.04
240	18.07	72.77	0.15	14.30	0.09	1.80	0.06	3.27	0.06	3.43	0.09	2.98	0.10	0.50	0.05	0.59	0.04
241	18.22	72.66	0.15	14.36	0.09	1.88	0.06	3.28	0.06	3.39	0.09	3.03	0.10	0.46	0.05	0.55	0.04
242	18.38	72.69	0.15	14.32	0.09	1.85	0.06	3.24	0.06	3.39	0.09	3.08	0.11	0.48	0.05	0.57	0.04
243	18.53	72.82	0.15	14.27	0.09	1.85	0.06	3.27	0.06	3.39	0.09	2.96	0.10	0.48	0.05	0.57	0.04
244	18.69	72.81	0.15	14.15	0.09	1.89	0.06	3.31	0.06	3.46	0.09	2.90	0.10	0.52	0.05	0.58	0.04

J.3 Interior Agglomerates

Agglomerate FLD4.3.1

Table J.26: Major element compositions (as wt.% oxides) from a line traverse across the interface of agglomerate FLD4.3.1 (from agglomerate FLD4.3.1 to host FLD4.3) extracted from quantified EDS compositional maps. The EDS compositional maps were collected at a resolution of 3.5 pixels/μm. The smoothing width for this traverse was 50 pixels (14.4 μm) wide. This is a Si interface and has been centered at $x = 0$ based on the SiO_2 maximum. Peak points within 2σ of the SiO_2 maximum are highlighted in yellow. Uncertainties are 2SEOM.

Pt.	Position (μm)	SiO_2	2σ	Al_2O_3	2σ	Na_2O	2σ	K_2O	2σ	CaO	2σ	FeO	2σ	TiO_2	2σ	MgO	2σ
1	-6.32	77.76	0.24	11.87	0.18	1.26	0.09	4.33	0.10	0.75	0.05	2.93	0.21	0.52	0.08	0.57	0.06
2	-6.03	78.00	0.25	11.70	0.17	1.26	0.09	4.30	0.10	0.80	0.05	2.93	0.21	0.46	0.07	0.55	0.06
3	-5.74	77.81	0.24	12.06	0.18	1.29	0.09	4.11	0.10	0.79	0.05	2.94	0.21	0.39	0.06	0.60	0.06
4	-5.45	77.29	0.24	12.05	0.18	1.26	0.09	4.37	0.10	0.84	0.05	3.12	0.23	0.51	0.08	0.55	0.06
5	-5.17	77.34	0.24	11.90	0.18	1.24	0.09	4.29	0.10	0.91	0.06	3.19	0.23	0.54	0.09	0.58	0.06
6	-4.88	77.41	0.24	11.79	0.17	1.28	0.09	4.44	0.10	0.89	0.06	3.04	0.22	0.56	0.09	0.58	0.06
7	-4.59	77.62	0.24	11.94	0.18	1.20	0.08	4.40	0.10	0.84	0.05	2.89	0.21	0.53	0.08	0.59	0.06
8	-4.31	77.64	0.24	11.75	0.17	1.21	0.08	4.44	0.10	0.79	0.05	3.16	0.23	0.49	0.08	0.52	0.05
9	-4.02	77.90	0.24	11.76	0.17	1.22	0.09	4.28	0.10	0.78	0.05	3.05	0.22	0.48	0.08	0.54	0.06
10	-3.73	77.82	0.24	11.79	0.17	1.23	0.09	4.27	0.10	0.77	0.05	3.03	0.22	0.55	0.09	0.54	0.06
11	-3.45	77.87	0.24	11.65	0.17	1.25	0.09	4.38	0.10	0.73	0.05	2.94	0.21	0.63	0.10	0.55	0.06
12	-3.16	78.02	0.25	11.59	0.17	1.19	0.08	4.47	0.11	0.72	0.05	3.01	0.22	0.53	0.08	0.48	0.05
13	-2.87	78.07	0.25	11.57	0.17	1.16	0.08	4.39	0.10	0.76	0.05	3.04	0.22	0.56	0.09	0.46	0.05
14	-2.58	78.30	0.25	11.26	0.17	1.11	0.08	4.46	0.11	0.84	0.05	2.99	0.22	0.56	0.09	0.47	0.05
15	-2.30	78.25	0.25	11.42	0.17	1.09	0.08	4.41	0.10	0.79	0.05	2.93	0.21	0.58	0.09	0.52	0.05
16	-2.01	78.15	0.25	11.42	0.17	1.18	0.08	4.42	0.10	0.80	0.05	2.94	0.21	0.55	0.09	0.52	0.05
17	-1.72	78.16	0.25	11.20	0.17	1.18	0.08	4.52	0.11	0.83	0.05	3.04	0.22	0.54	0.09	0.53	0.06
18	-1.44	78.38	0.25	11.29	0.17	1.20	0.08	4.28	0.10	0.78	0.05	3.03	0.22	0.49	0.08	0.55	0.06
19	-1.15	79.02	0.25	11.11	0.16	1.10	0.08	4.26	0.10	0.68	0.04	2.88	0.21	0.47	0.08	0.48	0.05
20	-0.86	78.74	0.25	11.24	0.17	1.09	0.08	4.27	0.10	0.76	0.05	2.85	0.21	0.56	0.09	0.48	0.05
21	-0.57	78.53	0.25	11.17	0.17	1.13	0.08	4.36	0.10	0.78	0.05	3.01	0.22	0.52	0.08	0.50	0.05
22	-0.29	78.90	0.25	11.34	0.17	1.16	0.08	4.28	0.10	0.68	0.04	2.66	0.19	0.49	0.08	0.49	0.05
23	0.00	79.05	0.25	11.13	0.16	1.05	0.07	4.34	0.10	0.80	0.05	2.78	0.20	0.45	0.07	0.40	0.04
24	0.29	78.87	0.25	11.00	0.16	0.98	0.07	4.33	0.10	0.72	0.05	3.18	0.23	0.41	0.07	0.50	0.05
25	0.57	78.94	0.25	11.02	0.16	1.05	0.07	4.36	0.10	0.70	0.04	3.02	0.22	0.43	0.07	0.48	0.05
26	0.86	78.48	0.25	11.25	0.17	1.11	0.08	4.35	0.10	0.79	0.05	3.01	0.22	0.51	0.08	0.52	0.05
27	1.15	78.55	0.25	11.19	0.17	1.08	0.08	4.45	0.11	0.80	0.05	2.91	0.21	0.54	0.09	0.48	0.05
28	1.44	78.55	0.25	11.24	0.17	1.12	0.08	4.44	0.10	0.77	0.05	2.97	0.22	0.46	0.07	0.45	0.05
29	1.72	78.41	0.25	11.37	0.17	1.20	0.08	4.29	0.10	0.74	0.05	3.08	0.22	0.42	0.07	0.48	0.05
30	2.01	78.24	0.25	11.43	0.17	1.16	0.08	4.38	0.10	0.78	0.05	3.10	0.23	0.42	0.07	0.47	0.05
31	2.30	77.95	0.25	11.61	0.17	1.19	0.08	4.42	0.10	0.90	0.06	2.95	0.21	0.51	0.08	0.47	0.05
32	2.58	77.73	0.24	11.74	0.17	1.16	0.08	4.51	0.11	0.84	0.05	3.06	0.22	0.44	0.07	0.51	0.05
33	2.87	77.25	0.24	11.99	0.18	1.15	0.08	4.39	0.10	0.77	0.05	3.44	0.25	0.49	0.08	0.52	0.05
34	3.16	77.12	0.24	12.28	0.18	1.16	0.08	4.44	0.10	0.94	0.06	3.00	0.22	0.55	0.09	0.51	0.05
35	3.44	77.17	0.24	12.30	0.18	1.24	0.09	4.53	0.11	0.90	0.06	2.88	0.21	0.53	0.09	0.44	0.05
36	3.73	76.88	0.24	12.55	0.19	1.27	0.09	4.46	0.11	0.93	0.06	2.96	0.21	0.45	0.07	0.50	0.05
37	4.02	76.73	0.24	12.75	0.19	1.24	0.09	4.45	0.11	0.94	0.06	2.94	0.21	0.52	0.08	0.43	0.04
38	4.31	76.51	0.24	12.90	0.19	1.26	0.09	4.48	0.11	0.91	0.06	3.01	0.22	0.41	0.06	0.52	0.05
39	4.59	76.05	0.24	12.81	0.19	1.29	0.09	4.57	0.11	1.07	0.07	3.26	0.24	0.47	0.08	0.47	0.05
40	4.88	75.60	0.24	13.07	0.19	1.26	0.09	4.61	0.11	1.01	0.06	3.33	0.24	0.58	0.09	0.53	0.06
41	5.17	75.66	0.24	13.29	0.20	1.35	0.09	4.42	0.10	0.97	0.06	3.25	0.24	0.47	0.07	0.60	0.06
42	5.45	75.61	0.24	13.49	0.20	1.24	0.09	4.48	0.11	0.98	0.06	3.15	0.23	0.46	0.07	0.59	0.06
43	5.74	75.43	0.24	13.22	0.20	1.29	0.09	4.76	0.11	1.02	0.07	3.25	0.24	0.51	0.08	0.50	0.05
44	6.03	75.26	0.24	13.52	0.20	1.37	0.10	4.68	0.11	0.94	0.06	3.34	0.24	0.39	0.06	0.50	0.05
45	6.32	74.60	0.23	13.71	0.20	1.39	0.10	4.63	0.11	1.04	0.07	3.59	0.26	0.50	0.08	0.54	0.06
46	6.60	74.81	0.24	14.00	0.21	1.43	0.10	4.50	0.11	1.07	0.07	3.14	0.23	0.53	0.08	0.53	0.05
47	6.89	74.81	0.24	13.93	0.21	1.39	0.10	4.57	0.11	1.05	0.07	3.26	0.24	0.54	0.09	0.46	0.05

48	7.18	74.36	0.23	14.04	0.21	1.42	0.10	4.57	0.11	1.13	0.07	3.56	0.26	0.48	0.08	0.43	0.05
49	7.46	74.53	0.23	14.09	0.21	1.38	0.10	4.52	0.11	1.16	0.07	3.44	0.25	0.40	0.06	0.49	0.05
50	7.75	74.23	0.23	14.22	0.21	1.42	0.10	4.58	0.11	1.15	0.07	3.46	0.25	0.47	0.08	0.46	0.05
51	8.04	74.36	0.23	14.22	0.21	1.36	0.10	4.52	0.11	1.13	0.07	3.40	0.25	0.52	0.08	0.48	0.05
52	8.33	73.75	0.23	14.40	0.21	1.39	0.10	4.63	0.11	1.15	0.07	3.57	0.26	0.53	0.08	0.59	0.06
53	8.61	73.76	0.23	14.27	0.21	1.48	0.10	4.69	0.11	1.22	0.08	3.55	0.26	0.50	0.08	0.53	0.05
54	8.90	73.59	0.23	14.25	0.21	1.46	0.10	4.53	0.11	1.22	0.08	3.92	0.28	0.52	0.08	0.51	0.05
55	9.19	73.59	0.23	14.42	0.21	1.47	0.10	4.56	0.11	1.22	0.08	3.76	0.27	0.46	0.07	0.53	0.06
56	9.47	73.85	0.23	14.46	0.21	1.46	0.10	4.58	0.11	1.13	0.07	3.51	0.25	0.45	0.07	0.57	0.06
57	9.76	73.84	0.23	14.40	0.21	1.34	0.09	4.69	0.11	1.25	0.08	3.46	0.25	0.45	0.07	0.56	0.06
58	10.05	73.63	0.23	14.31	0.21	1.44	0.10	4.67	0.11	1.28	0.08	3.68	0.27	0.50	0.08	0.49	0.05
59	10.33	73.67	0.23	14.39	0.21	1.39	0.10	4.64	0.11	1.27	0.08	3.74	0.27	0.45	0.07	0.45	0.05
60	10.62	73.56	0.23	14.61	0.22	1.33	0.09	4.70	0.11	1.26	0.08	3.53	0.26	0.52	0.08	0.49	0.05
61	10.91	73.67	0.23	14.59	0.22	1.37	0.10	4.70	0.11	1.24	0.08	3.44	0.25	0.46	0.07	0.53	0.06
62	11.20	73.46	0.23	14.70	0.22	1.36	0.10	4.56	0.11	1.30	0.08	3.61	0.26	0.56	0.09	0.45	0.05
63	11.48	73.35	0.23	14.61	0.22	1.48	0.10	4.57	0.11	1.30	0.08	3.79	0.27	0.41	0.07	0.49	0.05
64	11.77	74.04	0.23	14.84	0.22	1.43	0.10	4.37	0.10	1.14	0.07	3.23	0.23	0.43	0.07	0.52	0.05
65	12.06	73.87	0.23	14.94	0.22	1.42	0.10	4.47	0.11	1.18	0.08	3.08	0.22	0.49	0.08	0.55	0.06
66	12.34	73.67	0.23	14.72	0.22	1.47	0.10	4.56	0.11	1.26	0.08	3.37	0.24	0.47	0.07	0.48	0.05
67	12.63	73.53	0.23	14.85	0.22	1.45	0.10	4.50	0.11	1.27	0.08	3.44	0.25	0.45	0.07	0.51	0.05
68	12.92	73.66	0.23	14.72	0.22	1.43	0.10	4.60	0.11	1.19	0.08	3.45	0.25	0.43	0.07	0.52	0.05
69	13.21	73.62	0.23	14.63	0.22	1.44	0.10	4.53	0.11	1.29	0.08	3.55	0.26	0.42	0.07	0.50	0.05
70	13.49	74.00	0.23	14.41	0.21	1.45	0.10	4.58	0.11	1.30	0.08	3.27	0.24	0.50	0.08	0.48	0.05
71	13.78	74.00	0.23	14.59	0.22	1.37	0.10	4.56	0.11	1.20	0.08	3.38	0.25	0.41	0.07	0.48	0.05
72	14.07	73.87	0.23	14.73	0.22	1.39	0.10	4.48	0.11	1.19	0.08	3.27	0.24	0.51	0.08	0.55	0.06
73	14.35	73.82	0.23	14.53	0.22	1.38	0.10	4.53	0.11	1.30	0.08	3.37	0.24	0.48	0.08	0.58	0.06
74	14.64	73.87	0.23	14.30	0.21	1.34	0.09	4.52	0.11	1.35	0.09	3.55	0.26	0.55	0.09	0.53	0.05

Agglomerate FLD4.3.3

Table J.27: Major element compositions (as wt.% oxides) from a line traverse across the interface of agglomerate FLD4.3.3 (from agglomerate FLD4.3.3 to host FLD4.3) extracted from quantified EDS compositional maps. The EDS compositional maps were collected at a resolution of 3.5 pixels/μm. The smoothing width for this traverse was 50 pixels (14.4 μm) wide. This is a Si interface and has been centered at $x = 0$ based on the SiO_2 maximum. Peak points within 2σ of the FeO maximum are highlighted in yellow. Uncertainties are 2SEOM.

Pt.	Position (μm)	SiO_2	2σ	Al_2O_3	2σ	Na_2O	2σ	K_2O	2σ	CaO	2σ	FeO	2σ	TiO_2	2σ	MgO	2σ
1	-8.04	80.30	0.25	9.92	0.15	0.95	0.07	4.21	0.10	0.88	0.06	2.87	0.21	0.37	0.06	0.50	0.05
2	-7.75	80.54	0.25	9.90	0.15	0.94	0.07	3.98	0.09	0.87	0.06	2.89	0.21	0.44	0.07	0.44	0.05
3	-7.46	80.48	0.25	10.01	0.15	0.99	0.07	3.97	0.09	0.88	0.06	2.76	0.20	0.39	0.06	0.52	0.05
4	-7.18	80.66	0.25	9.94	0.15	1.02	0.07	3.94	0.09	0.82	0.05	2.73	0.20	0.39	0.06	0.49	0.05
5	-6.89	80.14	0.25	9.95	0.15	1.00	0.07	3.99	0.09	0.82	0.05	3.12	0.23	0.48	0.08	0.50	0.05
6	-6.60	80.40	0.25	9.81	0.15	0.97	0.07	4.05	0.10	0.88	0.06	2.96	0.21	0.43	0.07	0.50	0.05
7	-6.32	80.51	0.25	9.87	0.15	0.98	0.07	4.06	0.10	0.77	0.05	2.97	0.22	0.39	0.06	0.44	0.05
8	-6.03	80.82	0.25	9.83	0.15	0.96	0.07	4.06	0.10	0.76	0.05	2.73	0.20	0.43	0.07	0.40	0.04
9	-5.74	80.86	0.25	9.81	0.15	0.98	0.07	3.98	0.09	0.84	0.05	2.63	0.19	0.46	0.07	0.43	0.05
10	-5.45	81.22	0.26	9.64	0.14	1.01	0.07	3.93	0.09	0.86	0.05	2.45	0.18	0.46	0.07	0.43	0.04
11	-5.17	80.90	0.25	9.67	0.14	0.97	0.07	3.98	0.09	0.86	0.05	2.76	0.20	0.43	0.07	0.42	0.04
12	-4.88	80.73	0.25	9.62	0.14	0.94	0.07	4.09	0.10	0.94	0.06	2.82	0.20	0.44	0.07	0.43	0.04
13	-4.59	80.88	0.25	9.67	0.14	0.99	0.07	4.04	0.10	0.91	0.06	2.71	0.20	0.35	0.06	0.45	0.05
14	-4.31	81.04	0.25	9.59	0.14	0.96	0.07	3.93	0.09	0.82	0.05	2.77	0.20	0.46	0.07	0.42	0.04
15	-4.02	81.18	0.26	9.49	0.14	0.94	0.07	3.90	0.09	0.84	0.05	2.77	0.20	0.47	0.07	0.41	0.04
16	-3.73	80.96	0.25	9.50	0.14	0.98	0.07	3.92	0.09	0.82	0.05	2.88	0.21	0.46	0.07	0.47	0.05
17	-3.44	81.22	0.26	9.31	0.14	0.94	0.07	4.07	0.10	0.85	0.05	2.74	0.20	0.48	0.08	0.39	0.04
18	-3.16	81.40	0.26	9.23	0.14	0.92	0.06	3.94	0.09	0.81	0.05	2.85	0.21	0.41	0.06	0.44	0.05
19	-2.87	81.43	0.26	9.20	0.14	0.87	0.06	4.03	0.10	0.86	0.06	2.76	0.20	0.41	0.06	0.44	0.05
20	-2.58	81.51	0.26	9.24	0.14	1.00	0.07	3.76	0.09	0.82	0.05	2.82	0.20	0.41	0.07	0.44	0.05
21	-2.30	81.40	0.26	9.31	0.14	0.95	0.07	3.79	0.09	0.76	0.05	2.82	0.20	0.47	0.07	0.50	0.05
22	-2.01	81.48	0.26	9.11	0.13	0.98	0.07	3.91	0.09	0.82	0.05	2.78	0.20	0.45	0.07	0.47	0.05
23	-1.72	81.71	0.26	8.98	0.13	0.87	0.06	3.88	0.09	0.74	0.05	2.88	0.21	0.45	0.07	0.49	0.05
24	-1.44	81.78	0.26	8.95	0.13	0.81	0.06	3.79	0.09	0.82	0.05	2.82	0.20	0.55	0.09	0.48	0.05
25	-1.15	82.15	0.26	8.80	0.13	0.89	0.06	3.73	0.09	0.71	0.05	2.84	0.21	0.43	0.07	0.45	0.05
26	-0.86	82.24	0.26	8.56	0.13	0.88	0.06	3.94	0.09	0.78	0.05	2.73	0.20	0.45	0.07	0.42	0.04
27	-0.57	82.00	0.26	8.53	0.13	0.96	0.07	3.82	0.09	0.82	0.05	2.89	0.21	0.51	0.08	0.47	0.05
28	-0.29	82.39	0.26	8.53	0.13	0.94	0.07	3.91	0.09	0.69	0.04	2.69	0.19	0.40	0.06	0.46	0.05
29	0.00	82.55	0.26	8.49	0.13	0.84	0.06	3.79	0.09	0.68	0.04	2.80	0.20	0.45	0.07	0.41	0.04
30	0.29	82.49	0.26	8.59	0.13	0.84	0.06	3.81	0.09	0.71	0.05	2.79	0.20	0.37	0.06	0.39	0.04
31	0.57	82.45	0.26	8.56	0.13	0.90	0.06	3.75	0.09	0.75	0.05	2.77	0.20	0.37	0.06	0.45	0.05
32	0.86	82.25	0.26	8.68	0.13	0.97	0.07	3.73	0.09	0.73	0.05	2.70	0.20	0.45	0.07	0.48	0.05
33	1.15	82.48	0.26	8.66	0.13	0.90	0.06	3.72	0.09	0.75	0.05	2.62	0.19	0.38	0.06	0.48	0.05
34	1.44	82.28	0.26	8.86	0.13	0.82	0.06	3.79	0.09	0.73	0.05	2.53	0.18	0.49	0.08	0.50	0.05
35	1.72	82.28	0.26	8.78	0.13	0.86	0.06	3.84	0.09	0.76	0.05	2.54	0.18	0.51	0.08	0.44	0.05
36	2.01	81.78	0.26	8.95	0.13	0.94	0.07	3.86	0.09	0.86	0.05	2.83	0.20	0.32	0.05	0.46	0.05
37	2.30	81.57	0.26	9.21	0.14	0.94	0.07	3.85	0.09	0.79	0.05	2.70	0.20	0.38	0.06	0.56	0.06
38	2.58	81.51	0.26	9.17	0.14	0.95	0.07	3.99	0.09	0.83	0.05	2.60	0.19	0.46	0.07	0.48	0.05
39	2.87	80.95	0.25	9.52	0.14	1.02	0.07	4.01	0.09	0.86	0.05	2.66	0.19	0.51	0.08	0.47	0.05
40	3.16	80.74	0.25	9.83	0.15	1.01	0.07	3.98	0.09	0.90	0.06	2.64	0.19	0.43	0.07	0.46	0.05
41	3.45	80.48	0.25	9.99	0.15	0.96	0.07	3.98	0.09	0.92	0.06	2.71	0.20	0.47	0.08	0.48	0.05
42	3.73	80.36	0.25	10.20	0.15	1.04	0.07	3.84	0.09	0.88	0.06	2.68	0.19	0.46	0.07	0.55	0.06
43	4.02	79.78	0.25	10.58	0.16	1.04	0.07	3.95	0.09	1.02	0.06	2.69	0.19	0.47	0.07	0.48	0.05
44	4.31	79.41	0.25	10.59	0.16	1.12	0.08	4.15	0.10	1.02	0.06	2.79	0.20	0.42	0.07	0.50	0.05
45	4.59	79.06	0.25	10.73	0.16	1.07	0.08	4.13	0.10	1.15	0.07	2.89	0.21	0.43	0.07	0.56	0.06
46	4.88	78.78	0.25	11.19	0.17	1.11	0.08	4.10	0.10	1.08	0.07	2.85	0.21	0.41	0.07	0.48	0.05
47	5.17	78.22	0.25	11.34	0.17	1.12	0.08	4.37	0.10	1.19	0.08	2.75	0.20	0.48	0.08	0.52	0.05
48	5.45	77.84	0.24	11.48	0.17	1.14	0.08	4.33	0.10	1.18	0.08	3.00	0.22	0.49	0.08	0.54	0.06
49	5.74	77.69	0.24	11.84	0.18	1.20	0.08	4.20	0.10	1.26	0.08	2.83	0.21	0.40	0.06	0.58	0.06
50	6.03	77.30	0.24	11.96	0.18	1.23	0.09	4.25	0.10	1.33	0.08	2.96	0.21	0.43	0.07	0.55	0.06

51	6.32	77.00	0.24	12.28	0.18	1.34	0.09	4.10	0.10	1.32	0.08	2.96	0.21	0.41	0.07	0.59	0.06
52	6.60	76.83	0.24	12.38	0.18	1.21	0.08	4.25	0.10	1.45	0.09	2.84	0.21	0.54	0.09	0.50	0.05
53	6.89	76.63	0.24	12.42	0.18	1.20	0.08	4.28	0.10	1.47	0.09	3.00	0.22	0.48	0.08	0.50	0.05
54	7.18	76.21	0.24	12.61	0.19	1.25	0.09	4.15	0.10	1.40	0.09	3.33	0.24	0.47	0.08	0.58	0.06
55	7.46	76.06	0.24	12.72	0.19	1.23	0.09	4.29	0.10	1.45	0.09	3.25	0.24	0.49	0.08	0.53	0.06
56	7.75	76.05	0.24	12.93	0.19	1.35	0.09	4.28	0.10	1.49	0.09	2.86	0.21	0.51	0.08	0.52	0.05
57	8.04	75.85	0.24	12.91	0.19	1.37	0.10	4.25	0.10	1.59	0.10	2.97	0.22	0.46	0.07	0.60	0.06
58	8.33	75.49	0.24	13.11	0.19	1.38	0.10	4.16	0.10	1.48	0.09	3.25	0.24	0.44	0.07	0.69	0.07
59	8.61	75.41	0.24	13.11	0.19	1.30	0.09	4.37	0.10	1.60	0.10	3.11	0.23	0.48	0.08	0.62	0.07
60	8.90	75.32	0.24	13.43	0.20	1.35	0.09	4.42	0.10	1.60	0.10	2.87	0.21	0.44	0.07	0.57	0.06
61	9.19	75.04	0.24	13.50	0.20	1.35	0.10	4.29	0.10	1.62	0.10	3.20	0.23	0.42	0.07	0.57	0.06

Agglomerate FLD4.3.5

Table J.28: Major element compositions (as wt.% oxides) from a line traverse across the interface of interior agglomerate FLD4.3.5 (from agglomerate FLD4.3.5 to host FLD4.3) extracted from quantified EDS compositional maps. The EDS compositional maps were collected at a resolution of 3.8 pixels/μm. The smoothing width for this traverse was 100 pixels (26 μm) wide. This is an Si interface and has been centered at $x = 0$ based on the SiO_2 maximum. Peak points within 2σ of the SiO_2 maximum are highlighted in yellow. Uncertainties are 2SEOM.

Pt.	Position (μm)	SiO_2	2σ	Al_2O_3	2σ	Na_2O	2σ	K_2O	2σ	CaO	2σ	FeO	2σ	TiO_2	2σ	MgO	2σ
1	-13.02	71.03	0.30	15.69	0.17	2.52	0.12	4.01	0.16	1.67	0.13	3.08	0.26	0.67	0.09	0.83	0.09
2	-12.76	70.87	0.30	15.74	0.17	2.52	0.12	3.92	0.15	1.61	0.12	3.39	0.28	0.62	0.08	0.83	0.09
3	-12.50	70.99	0.30	15.65	0.17	2.57	0.12	3.90	0.15	1.61	0.12	3.13	0.26	0.86	0.12	0.83	0.09
4	-12.24	71.15	0.30	15.53	0.17	2.54	0.12	3.96	0.16	1.73	0.13	2.85	0.24	0.94	0.13	0.86	0.09
5	-11.98	70.64	0.30	15.72	0.17	2.51	0.12	4.01	0.16	1.75	0.13	3.24	0.27	0.80	0.11	0.88	0.09
6	-11.72	70.58	0.29	15.74	0.17	2.59	0.12	4.14	0.16	1.67	0.13	3.26	0.27	0.85	0.12	0.76	0.08
7	-11.46	70.85	0.30	15.97	0.18	2.52	0.12	3.99	0.16	1.61	0.12	2.93	0.24	0.84	0.11	0.83	0.09
8	-11.20	70.97	0.30	15.82	0.17	2.50	0.12	4.00	0.16	1.68	0.13	3.09	0.26	0.70	0.09	0.74	0.08
9	-10.94	71.24	0.30	15.89	0.17	2.50	0.12	3.97	0.16	1.57	0.12	2.88	0.24	0.74	0.10	0.77	0.08
10	-10.68	70.98	0.30	15.70	0.17	2.63	0.13	3.91	0.15	1.67	0.13	2.94	0.25	0.97	0.13	0.79	0.08
11	-10.42	71.04	0.30	15.85	0.17	2.64	0.13	3.90	0.15	1.76	0.13	2.87	0.24	0.70	0.09	0.77	0.08
12	-10.16	70.80	0.30	15.83	0.17	2.64	0.13	4.08	0.16	1.70	0.13	2.87	0.24	0.72	0.10	0.81	0.09
13	-9.90	70.86	0.30	15.58	0.17	2.59	0.12	4.11	0.16	1.70	0.13	3.00	0.25	0.77	0.10	0.80	0.09
14	-9.64	70.80	0.30	15.64	0.17	2.72	0.13	4.05	0.16	1.75	0.13	3.01	0.25	0.75	0.10	0.75	0.08
15	-9.38	70.48	0.29	15.78	0.17	2.64	0.13	4.08	0.16	1.76	0.13	3.29	0.27	0.74	0.10	0.79	0.08
16	-9.12	71.11	0.30	15.67	0.17	2.49	0.12	3.83	0.15	1.79	0.13	3.13	0.26	0.73	0.10	0.80	0.08
17	-8.85	70.58	0.29	15.63	0.17	2.67	0.13	4.16	0.16	1.68	0.13	3.17	0.26	0.75	0.10	0.86	0.09
18	-8.59	70.65	0.30	15.60	0.17	2.63	0.13	4.11	0.16	1.61	0.12	3.32	0.28	0.80	0.11	0.89	0.09
19	-8.33	70.65	0.30	15.60	0.17	2.71	0.13	4.05	0.16	1.53	0.11	3.28	0.27	0.79	0.11	0.94	0.10
20	-8.07	70.75	0.30	15.67	0.17	2.65	0.13	4.00	0.16	1.58	0.12	3.34	0.28	0.73	0.10	0.84	0.09
21	-7.81	71.03	0.30	15.42	0.17	2.67	0.13	3.92	0.15	1.74	0.13	3.20	0.27	0.76	0.10	0.77	0.08
22	-7.55	71.09	0.30	15.49	0.17	2.55	0.12	3.90	0.15	1.80	0.13	3.12	0.26	0.78	0.11	0.84	0.09
23	-7.29	71.32	0.30	15.55	0.17	2.44	0.12	3.98	0.16	1.67	0.13	3.03	0.25	0.70	0.09	0.86	0.09
24	-7.03	71.34	0.30	15.50	0.17	2.58	0.12	4.02	0.16	1.74	0.13	2.87	0.24	0.66	0.09	0.85	0.09
25	-6.77	71.04	0.30	15.32	0.17	2.69	0.13	3.93	0.15	1.66	0.12	3.24	0.27	0.83	0.11	0.77	0.08
26	-6.51	71.16	0.30	15.24	0.17	2.66	0.13	3.93	0.15	1.76	0.13	3.26	0.27	0.63	0.09	0.80	0.08
27	-6.25	71.43	0.30	15.34	0.17	2.55	0.12	4.00	0.16	1.68	0.13	3.22	0.27	0.58	0.08	0.77	0.08
28	-5.99	71.62	0.30	15.04	0.16	2.53	0.12	4.11	0.16	1.79	0.13	3.05	0.25	0.69	0.09	0.80	0.08
29	-5.73	71.78	0.30	14.96	0.16	2.47	0.12	4.09	0.16	1.64	0.12	3.06	0.26	0.79	0.11	0.75	0.08
30	-5.47	71.89	0.30	14.92	0.16	2.47	0.12	4.07	0.16	1.65	0.12	3.07	0.26	0.70	0.09	0.76	0.08
31	-5.21	72.04	0.30	14.88	0.16	2.55	0.12	3.90	0.15	1.71	0.13	3.12	0.26	0.66	0.09	0.74	0.08
32	-4.95	72.06	0.30	14.79	0.16	2.48	0.12	3.96	0.16	1.66	0.12	3.11	0.26	0.66	0.09	0.79	0.08
33	-4.69	72.27	0.30	14.79	0.16	2.31	0.11	4.04	0.16	1.55	0.12	2.96	0.25	0.73	0.10	0.90	0.10
34	-4.43	72.07	0.30	14.72	0.16	2.58	0.12	3.96	0.16	1.56	0.12	3.16	0.26	0.70	0.09	0.83	0.09
35	-4.17	72.19	0.30	14.52	0.16	2.63	0.13	3.80	0.15	1.47	0.11	3.26	0.27	0.84	0.11	0.84	0.09
36	-3.91	72.63	0.30	14.38	0.16	2.44	0.12	4.04	0.16	1.51	0.11	2.98	0.25	0.73	0.10	0.78	0.08
37	-3.65	73.03	0.30	14.24	0.16	2.52	0.12	4.02	0.16	1.44	0.11	2.81	0.23	0.72	0.10	0.76	0.08
38	-3.39	73.18	0.31	14.03	0.15	2.62	0.13	4.13	0.16	1.40	0.11	2.87	0.24	0.68	0.09	0.68	0.07
39	-3.12	73.43	0.31	13.93	0.15	2.46	0.12	3.89	0.15	1.46	0.11	2.96	0.25	0.65	0.09	0.77	0.08
40	-2.87	73.29	0.31	13.72	0.15	2.51	0.12	3.98	0.16	1.43	0.11	3.09	0.26	0.70	0.09	0.72	0.08
41	-2.60	74.17	0.31	13.58	0.15	2.31	0.11	3.89	0.15	1.46	0.11	2.83	0.24	0.66	0.09	0.66	0.07
42	-2.34	74.22	0.31	13.48	0.15	2.29	0.11	4.02	0.16	1.39	0.10	2.79	0.23	0.57	0.08	0.71	0.08
43	-2.08	73.96	0.31	13.58	0.15	2.28	0.11	3.97	0.16	1.45	0.11	3.02	0.25	0.61	0.08	0.69	0.07
44	-1.82	74.21	0.31	13.34	0.15	2.37	0.11	3.88	0.15	1.38	0.10	3.11	0.26	0.66	0.09	0.63	0.07
45	-1.56	74.10	0.31	13.25	0.15	2.27	0.11	3.92	0.15	1.41	0.11	3.18	0.26	0.64	0.09	0.73	0.08
46	-1.30	74.75	0.31	13.26	0.15	2.43	0.12	3.88	0.15	1.26	0.09	2.75	0.23	0.54	0.07	0.60	0.06
47	-1.04	74.56	0.31	13.27	0.15	2.37	0.11	3.95	0.16	1.33	0.10	2.66	0.22	0.66	0.09	0.70	0.07
48	-0.78	74.63	0.31	13.05	0.14	2.26	0.11	4.01	0.16	1.39	0.10	2.78	0.23	0.70	0.09	0.75	0.08
49	-0.52	74.71	0.31	12.87	0.14	2.39	0.11	4.06	0.16	1.23	0.09	2.96	0.25	0.63	0.09	0.70	0.07
50	-0.26	74.95	0.31	12.78	0.14	2.37	0.11	3.89	0.15	1.29	0.10	2.87	0.24	0.69	0.09	0.68	0.07

51	0.00	75.29	0.31	12.76	0.14	2.29	0.11	3.97	0.16	1.32	0.10	2.70	0.23	0.63	0.08	0.65	0.07
52	0.26	75.19	0.31	12.69	0.14	2.35	0.11	3.86	0.15	1.31	0.10	2.87	0.24	0.58	0.08	0.66	0.07
53	0.52	75.15	0.31	12.64	0.14	2.27	0.11	3.81	0.15	1.40	0.10	2.86	0.24	0.72	0.10	0.67	0.07
54	0.78	75.02	0.31	12.71	0.14	2.34	0.11	3.93	0.15	1.36	0.10	2.82	0.23	0.66	0.09	0.69	0.07
55	1.04	75.14	0.31	12.55	0.14	2.19	0.11	4.11	0.16	1.43	0.11	2.82	0.23	0.65	0.09	0.77	0.08
56	1.30	74.77	0.31	12.84	0.14	2.36	0.11	4.03	0.16	1.43	0.11	2.71	0.23	0.62	0.08	0.75	0.08
57	1.56	74.72	0.31	12.90	0.14	2.40	0.12	3.99	0.16	1.47	0.11	2.81	0.23	0.53	0.07	0.73	0.08
58	1.82	75.17	0.31	12.97	0.14	2.27	0.11	3.77	0.15	1.39	0.10	2.72	0.23	0.59	0.08	0.71	0.08
59	2.08	74.82	0.31	13.05	0.14	2.27	0.11	3.82	0.15	1.36	0.10	2.84	0.24	0.61	0.08	0.76	0.08
60	2.34	74.41	0.31	12.99	0.14	2.39	0.11	3.76	0.15	1.42	0.11	3.21	0.27	0.66	0.09	0.74	0.08
61	2.60	74.26	0.31	12.90	0.14	2.37	0.11	3.86	0.15	1.44	0.11	3.21	0.27	0.75	0.10	0.73	0.08
62	2.86	74.23	0.31	13.12	0.14	2.28	0.11	3.88	0.15	1.44	0.11	3.21	0.27	0.65	0.09	0.75	0.08
63	3.12	74.24	0.31	13.16	0.14	2.33	0.11	3.88	0.15	1.53	0.11	3.05	0.25	0.69	0.09	0.66	0.07
64	3.38	73.76	0.31	13.24	0.15	2.43	0.12	4.01	0.16	1.58	0.12	3.24	0.27	0.64	0.09	0.70	0.07
65	3.65	73.44	0.31	13.31	0.15	2.51	0.12	4.03	0.16	1.62	0.12	3.25	0.27	0.58	0.08	0.76	0.08
66	3.91	73.57	0.31	13.38	0.15	2.46	0.12	3.98	0.16	1.69	0.13	3.11	0.26	0.61	0.08	0.73	0.08
67	4.17	73.96	0.31	13.49	0.15	2.40	0.12	3.71	0.15	1.62	0.12	2.95	0.25	0.62	0.08	0.72	0.08
68	4.43	73.82	0.31	13.64	0.15	2.39	0.11	3.78	0.15	1.59	0.12	2.98	0.25	0.59	0.08	0.72	0.08
69	4.69	73.78	0.31	13.66	0.15	2.29	0.11	3.82	0.15	1.45	0.11	3.07	0.26	0.63	0.09	0.76	0.08
70	4.95	73.23	0.31	13.56	0.15	2.48	0.12	4.04	0.16	1.67	0.13	3.09	0.26	0.66	0.09	0.75	0.08
71	5.21	73.05	0.31	13.56	0.15	2.55	0.12	4.07	0.16	1.74	0.13	3.13	0.26	0.71	0.10	0.73	0.08
72	5.47	73.53	0.31	13.56	0.15	2.55	0.12	3.93	0.15	1.72	0.13	2.81	0.23	0.60	0.08	0.79	0.08
73	5.73	73.53	0.31	13.63	0.15	2.56	0.12	3.86	0.15	1.67	0.13	2.96	0.25	0.64	0.09	0.70	0.07
74	5.99	73.23	0.31	13.72	0.15	2.28	0.11	3.95	0.16	1.66	0.12	3.37	0.28	0.65	0.09	0.77	0.08
75	6.25	72.76	0.30	13.96	0.15	2.45	0.12	3.89	0.15	1.82	0.14	3.19	0.27	0.63	0.09	0.79	0.08
76	6.51	72.97	0.30	14.06	0.15	2.46	0.12	3.86	0.15	1.87	0.14	2.91	0.24	0.59	0.08	0.80	0.08
77	6.77	72.75	0.30	13.85	0.15	2.52	0.12	3.91	0.15	1.87	0.14	3.07	0.26	0.70	0.10	0.84	0.09
78	7.03	72.63	0.30	14.08	0.15	2.63	0.13	3.76	0.15	1.82	0.14	3.22	0.27	0.62	0.08	0.74	0.08
79	7.29	72.62	0.30	14.07	0.15	2.66	0.13	3.83	0.15	1.80	0.13	3.20	0.27	0.56	0.08	0.71	0.08
80	7.55	72.46	0.30	14.05	0.15	2.67	0.13	4.07	0.16	1.86	0.14	3.02	0.25	0.55	0.07	0.86	0.09
81	7.81	72.64	0.30	14.10	0.15	2.47	0.12	4.07	0.16	1.68	0.13	3.24	0.27	0.54	0.07	0.78	0.08
82	8.07	72.34	0.30	14.10	0.15	2.56	0.12	3.91	0.15	1.71	0.13	3.45	0.29	0.72	0.10	0.77	0.08
83	8.33	72.25	0.30	14.11	0.15	2.49	0.12	3.97	0.16	1.78	0.13	3.46	0.29	0.60	0.08	0.79	0.08
84	8.59	72.06	0.30	14.13	0.15	2.68	0.13	3.99	0.16	1.78	0.13	3.41	0.28	0.64	0.09	0.88	0.09
85	8.85	72.33	0.30	14.18	0.16	2.67	0.13	3.89	0.15	1.76	0.13	3.26	0.27	0.71	0.10	0.85	0.09
86	9.11	72.40	0.30	14.20	0.16	2.73	0.13	3.82	0.15	1.75	0.13	3.21	0.27	0.73	0.10	0.79	0.08
87	9.38	72.25	0.30	14.13	0.15	2.60	0.12	4.01	0.16	1.85	0.14	3.16	0.26	0.66	0.09	0.84	0.09
88	9.63	72.63	0.30	13.89	0.15	2.48	0.12	3.91	0.15	1.96	0.15	3.23	0.27	0.66	0.09	0.77	0.08
89	9.90	72.69	0.30	13.93	0.15	2.65	0.13	3.92	0.15	1.83	0.14	3.15	0.26	0.54	0.07	0.79	0.08
90	10.16	72.42	0.30	14.30	0.16	2.59	0.12	3.90	0.15	1.82	0.14	3.19	0.27	0.61	0.08	0.75	0.08
91	10.42	72.36	0.30	14.10	0.15	2.59	0.12	3.91	0.15	1.92	0.14	3.32	0.28	0.61	0.08	0.80	0.09
92	10.68	72.69	0.30	14.03	0.15	2.47	0.12	3.96	0.16	1.80	0.14	3.21	0.27	0.63	0.08	0.84	0.09

Agglomerate FLD17.int.2

Table J.29: Major element compositions (as wt.% oxides) from a line traverse across the interface of interior agglomerate FLD17.int.2 (from agglomerate FLD17.int.2 to host FLD17) extracted from quantified EDS compositional maps. This is a CaMgFe interface and has been centered at $x = 0$ based on the SiO_2 maximum. Peak points within 2σ of the SiO_2 maximum are highlighted in yellow. Uncertainties are 2SEOM.

Pt.	Position (μm)	SiO_2	2σ	Al_2O_3	2σ	Na_2O	2σ	K_2O	2σ	CaO	2σ	FeO	2σ	TiO_2	2σ	MgO	2σ
1	-21.35	73.42	0.29	13.14	0.16	2.89	0.12	3.80	0.14	2.68	0.13	2.77	0.20	0.65	0.09	0.65	0.08
2	-21.11	73.78	0.29	13.09	0.16	2.98	0.12	3.75	0.14	2.43	0.12	2.63	0.19	0.70	0.10	0.64	0.08
3	-20.88	73.81	0.29	13.10	0.16	3.06	0.13	3.82	0.14	2.55	0.13	2.46	0.18	0.59	0.09	0.61	0.07
4	-20.65	73.76	0.29	13.22	0.16	2.97	0.12	3.73	0.14	2.60	0.13	2.42	0.18	0.67	0.10	0.63	0.08
5	-20.42	73.49	0.29	13.11	0.16	2.84	0.12	3.91	0.14	2.72	0.13	2.68	0.20	0.66	0.10	0.58	0.07
6	-20.19	73.79	0.29	13.01	0.16	2.75	0.11	3.87	0.14	2.51	0.12	2.71	0.20	0.71	0.10	0.65	0.08
7	-19.95	73.71	0.29	13.11	0.16	2.82	0.12	3.87	0.14	2.53	0.12	2.61	0.19	0.74	0.11	0.61	0.07
8	-19.72	73.99	0.29	13.00	0.16	2.89	0.12	3.64	0.13	2.67	0.13	2.59	0.19	0.60	0.09	0.63	0.08
9	-19.49	73.66	0.29	13.22	0.16	2.88	0.12	3.81	0.14	2.53	0.12	2.69	0.20	0.59	0.09	0.62	0.07
10	-19.26	73.59	0.29	13.19	0.16	2.93	0.12	3.76	0.14	2.54	0.13	2.73	0.20	0.62	0.09	0.62	0.07
11	-19.03	73.37	0.29	13.20	0.16	2.98	0.12	3.84	0.14	2.71	0.13	2.63	0.19	0.63	0.09	0.65	0.08
12	-18.79	73.46	0.29	13.06	0.16	2.93	0.12	3.86	0.14	2.75	0.14	2.73	0.20	0.60	0.09	0.61	0.07
13	-18.56	73.46	0.29	13.11	0.16	2.90	0.12	3.86	0.14	2.74	0.13	2.64	0.19	0.69	0.10	0.59	0.07
14	-18.33	73.36	0.29	13.10	0.16	2.97	0.12	3.83	0.14	2.70	0.13	2.83	0.21	0.60	0.09	0.63	0.08
15	-18.10	73.36	0.29	13.32	0.16	2.87	0.12	3.87	0.14	2.60	0.13	2.78	0.20	0.56	0.08	0.64	0.08
16	-17.87	73.68	0.29	13.03	0.16	2.92	0.12	3.84	0.14	2.53	0.12	2.87	0.21	0.52	0.08	0.61	0.07
17	-17.63	73.59	0.29	12.98	0.16	2.78	0.12	3.89	0.14	2.69	0.13	2.76	0.20	0.61	0.09	0.70	0.09
18	-17.40	73.54	0.29	13.21	0.16	2.88	0.12	3.78	0.14	2.68	0.13	2.56	0.19	0.65	0.10	0.68	0.08
19	-17.17	73.61	0.29	13.06	0.16	2.76	0.12	3.88	0.14	2.74	0.14	2.63	0.19	0.63	0.09	0.68	0.08
20	-16.94	73.55	0.29	13.14	0.16	2.89	0.12	3.77	0.14	2.79	0.14	2.53	0.19	0.63	0.09	0.71	0.09
21	-16.71	73.65	0.29	13.10	0.16	2.89	0.12	3.78	0.14	2.70	0.13	2.60	0.19	0.65	0.09	0.63	0.08
22	-16.47	73.63	0.29	13.01	0.16	2.90	0.12	3.81	0.14	2.67	0.13	2.67	0.20	0.59	0.09	0.71	0.09
23	-16.24	73.66	0.29	13.28	0.16	2.85	0.12	3.98	0.15	2.55	0.13	2.50	0.18	0.51	0.08	0.66	0.08
24	-16.01	73.70	0.29	13.17	0.16	2.71	0.11	3.80	0.14	2.71	0.13	2.73	0.20	0.57	0.08	0.62	0.08
25	-15.78	73.58	0.29	13.32	0.16	2.74	0.11	3.71	0.14	2.63	0.13	2.84	0.21	0.56	0.08	0.62	0.07
26	-15.55	73.99	0.29	13.28	0.16	2.71	0.11	3.68	0.13	2.64	0.13	2.61	0.19	0.50	0.07	0.58	0.07
27	-15.31	73.43	0.29	13.25	0.16	2.89	0.12	3.80	0.14	2.76	0.14	2.63	0.19	0.62	0.09	0.62	0.08
28	-15.08	73.60	0.29	13.04	0.16	2.72	0.11	3.92	0.14	2.75	0.14	2.57	0.19	0.68	0.10	0.72	0.09
29	-14.85	73.96	0.29	12.87	0.16	2.78	0.12	3.81	0.14	2.70	0.13	2.66	0.19	0.62	0.09	0.60	0.07
30	-14.62	73.42	0.29	13.11	0.16	2.81	0.12	3.92	0.14	2.58	0.13	2.90	0.21	0.64	0.09	0.61	0.07
31	-14.38	73.28	0.29	12.92	0.16	2.84	0.12	3.80	0.14	2.66	0.13	3.13	0.23	0.67	0.10	0.69	0.08
32	-14.15	73.64	0.29	12.99	0.16	2.78	0.12	3.75	0.14	2.73	0.13	2.84	0.21	0.54	0.08	0.73	0.09
33	-13.92	73.51	0.29	13.05	0.16	2.82	0.12	3.95	0.14	2.69	0.13	2.74	0.20	0.52	0.08	0.72	0.09
34	-13.69	73.54	0.29	13.15	0.16	2.85	0.12	3.92	0.14	2.46	0.12	2.77	0.20	0.69	0.10	0.61	0.07
35	-13.46	73.79	0.29	13.03	0.16	2.73	0.11	3.87	0.14	2.70	0.13	2.59	0.19	0.60	0.09	0.68	0.08
36	-13.22	73.51	0.29	13.09	0.16	2.81	0.12	3.83	0.14	2.77	0.14	2.68	0.20	0.65	0.09	0.66	0.08
37	-12.99	73.59	0.29	12.86	0.15	2.91	0.12	3.73	0.14	2.69	0.13	2.93	0.21	0.64	0.09	0.65	0.08
38	-12.76	73.58	0.29	13.02	0.16	2.97	0.12	3.90	0.14	2.60	0.13	2.73	0.20	0.63	0.09	0.56	0.07
39	-12.53	73.75	0.29	12.81	0.15	2.75	0.11	3.98	0.15	2.73	0.13	2.76	0.20	0.64	0.09	0.60	0.07
40	-12.30	73.89	0.29	12.75	0.15	2.71	0.11	3.98	0.15	2.80	0.14	2.68	0.20	0.57	0.08	0.63	0.08
41	-12.06	74.16	0.29	12.64	0.15	2.82	0.12	3.82	0.14	2.68	0.13	2.49	0.18	0.71	0.10	0.68	0.08
42	-11.83	73.85	0.29	12.89	0.16	2.93	0.12	3.77	0.14	2.58	0.13	2.62	0.19	0.70	0.10	0.64	0.08
43	-11.60	73.96	0.29	13.02	0.16	2.72	0.11	3.67	0.13	2.63	0.13	2.74	0.20	0.63	0.09	0.64	0.08
44	-11.37	74.05	0.29	12.84	0.15	2.64	0.11	3.81	0.14	2.71	0.13	2.71	0.20	0.63	0.09	0.62	0.07
45	-11.14	74.32	0.29	12.69	0.15	2.50	0.10	3.83	0.14	2.59	0.13	2.70	0.20	0.74	0.11	0.63	0.08
46	-10.90	74.36	0.29	12.52	0.15	2.66	0.11	3.81	0.14	2.70	0.13	2.67	0.20	0.66	0.10	0.61	0.07
47	-10.67	74.09	0.29	12.67	0.15	2.66	0.11	3.78	0.14	2.60	0.13	2.90	0.21	0.64	0.09	0.65	0.08
48	-10.44	74.09	0.29	12.68	0.15	2.68	0.11	3.75	0.14	2.70	0.13	2.85	0.21	0.64	0.09	0.61	0.07
49	-10.21	74.55	0.29	12.45	0.15	2.72	0.11	3.68	0.13	2.73	0.13	2.69	0.20	0.63	0.09	0.56	0.07
50	-9.98	74.61	0.29	12.44	0.15	2.52	0.11	3.83	0.14	2.73	0.13	2.80	0.20	0.55	0.08	0.52	0.06
51	-9.74	74.66	0.29	12.41	0.15	2.65	0.11	3.84	0.14	2.63	0.13	2.69	0.20	0.52	0.08	0.60	0.07
52	-9.51	74.73	0.29	12.36	0.15	2.53	0.11	3.79	0.14	2.59	0.13	2.68	0.20	0.72	0.10	0.60	0.07
53	-9.28	74.68	0.29	12.35	0.15	2.69	0.11	3.73	0.14	2.54	0.13	2.83	0.21	0.65	0.09	0.53	0.06

54	-9.05	74.73	0.29	12.29	0.15	2.63	0.11	3.82	0.14	2.52	0.12	2.79	0.20	0.63	0.09	0.59	0.07
55	-8.82	74.92	0.29	12.25	0.15	2.74	0.11	3.70	0.14	2.47	0.12	2.80	0.20	0.59	0.09	0.54	0.07
56	-8.59	75.26	0.29	12.05	0.15	2.65	0.11	3.66	0.13	2.35	0.12	2.84	0.21	0.58	0.08	0.62	0.07
57	-8.35	75.00	0.29	11.96	0.14	2.52	0.11	3.92	0.14	2.41	0.12	2.96	0.22	0.59	0.09	0.64	0.08
58	-8.12	75.06	0.29	12.06	0.15	2.56	0.11	3.92	0.14	2.35	0.12	2.76	0.20	0.59	0.09	0.69	0.08
59	-7.89	75.33	0.29	11.82	0.14	2.60	0.11	3.78	0.14	2.44	0.12	2.77	0.20	0.64	0.09	0.63	0.08
60	-7.66	75.00	0.29	11.95	0.14	2.55	0.11	3.83	0.14	2.44	0.12	2.99	0.22	0.60	0.09	0.64	0.08
61	-7.43	75.46	0.30	11.70	0.14	2.50	0.10	3.74	0.14	2.46	0.12	3.03	0.22	0.57	0.08	0.55	0.07
62	-7.19	75.92	0.30	11.57	0.14	2.48	0.10	3.76	0.14	2.34	0.12	2.64	0.19	0.62	0.09	0.67	0.08
63	-6.96	76.12	0.30	11.49	0.14	2.60	0.11	3.66	0.13	2.19	0.11	2.75	0.20	0.55	0.08	0.64	0.08
64	-6.73	76.15	0.30	11.55	0.14	2.69	0.11	3.51	0.13	2.22	0.11	2.71	0.20	0.47	0.07	0.69	0.08
65	-6.50	76.36	0.30	11.48	0.14	2.53	0.11	3.64	0.13	2.13	0.10	2.66	0.19	0.53	0.08	0.67	0.08
66	-6.27	76.60	0.30	11.40	0.14	2.45	0.10	3.51	0.13	2.17	0.11	2.65	0.19	0.63	0.09	0.59	0.07
67	-6.03	76.61	0.30	11.07	0.13	2.48	0.10	3.65	0.13	2.18	0.11	2.85	0.21	0.58	0.08	0.59	0.07
68	-5.80	76.82	0.30	11.03	0.13	2.29	0.10	3.59	0.13	2.29	0.11	2.68	0.20	0.68	0.10	0.61	0.07
69	-5.57	77.07	0.30	10.85	0.13	2.38	0.10	3.76	0.14	2.07	0.10	2.59	0.19	0.60	0.09	0.69	0.08
70	-5.34	77.01	0.30	10.74	0.13	2.38	0.10	3.76	0.14	2.12	0.10	2.72	0.20	0.64	0.09	0.64	0.08
71	-5.11	77.30	0.30	10.69	0.13	2.26	0.09	3.71	0.14	2.04	0.10	2.80	0.20	0.53	0.08	0.66	0.08
72	-4.87	77.37	0.30	10.61	0.13	2.36	0.10	3.67	0.13	2.09	0.10	2.63	0.19	0.60	0.09	0.67	0.08
73	-4.64	77.43	0.30	10.75	0.13	2.27	0.09	3.57	0.13	1.98	0.10	2.70	0.20	0.68	0.10	0.63	0.08
74	-4.41	77.60	0.30	10.62	0.13	2.32	0.10	3.70	0.14	1.85	0.09	2.65	0.19	0.62	0.09	0.64	0.08
75	-4.18	77.77	0.30	10.32	0.12	2.28	0.10	3.63	0.13	1.90	0.09	2.73	0.20	0.73	0.11	0.63	0.08
76	-3.95	78.03	0.31	10.21	0.12	2.35	0.10	3.63	0.13	1.95	0.10	2.69	0.20	0.54	0.08	0.60	0.07
77	-3.71	78.24	0.31	10.24	0.12	2.22	0.09	3.73	0.14	1.89	0.09	2.54	0.19	0.50	0.07	0.64	0.08
78	-3.48	78.13	0.31	10.20	0.12	2.28	0.10	3.63	0.13	1.83	0.09	2.70	0.20	0.59	0.09	0.64	0.08
79	-3.25	78.16	0.31	10.07	0.12	2.28	0.10	3.52	0.13	2.02	0.10	2.67	0.20	0.55	0.08	0.73	0.09
80	-3.02	78.28	0.31	10.31	0.12	2.11	0.09	3.50	0.13	1.94	0.10	2.64	0.19	0.61	0.09	0.62	0.07
81	-2.79	78.51	0.31	10.13	0.12	2.26	0.09	3.43	0.13	1.76	0.09	2.70	0.20	0.59	0.09	0.62	0.07
82	-2.55	78.05	0.31	9.95	0.12	2.26	0.09	3.45	0.13	1.91	0.09	3.12	0.23	0.58	0.09	0.68	0.08
83	-2.32	78.56	0.31	10.13	0.12	2.28	0.10	3.45	0.13	1.87	0.09	2.69	0.20	0.44	0.06	0.58	0.07
84	-2.09	78.71	0.31	10.08	0.12	2.20	0.09	3.56	0.13	1.88	0.09	2.45	0.18	0.57	0.08	0.54	0.07
85	-1.86	78.44	0.31	10.02	0.12	2.30	0.10	3.48	0.13	1.87	0.09	2.62	0.19	0.64	0.09	0.62	0.07
86	-1.62	78.60	0.31	9.82	0.12	2.18	0.09	3.53	0.13	1.97	0.10	2.61	0.19	0.72	0.10	0.56	0.07
87	-1.39	78.60	0.31	10.03	0.12	2.14	0.09	3.53	0.13	1.87	0.09	2.56	0.19	0.60	0.09	0.66	0.08
88	-1.16	78.65	0.31	10.03	0.12	2.16	0.09	3.40	0.12	1.88	0.09	2.56	0.19	0.67	0.10	0.65	0.08
89	-0.93	78.55	0.31	10.08	0.12	2.20	0.09	3.43	0.13	1.90	0.09	2.71	0.20	0.49	0.07	0.64	0.08
90	-0.70	78.44	0.31	10.04	0.12	2.28	0.10	3.56	0.13	1.91	0.09	2.54	0.19	0.57	0.08	0.66	0.08
91	-0.46	78.28	0.31	9.99	0.12	2.34	0.10	3.69	0.14	1.92	0.09	2.52	0.18	0.60	0.09	0.67	0.08
92	-0.23	78.61	0.31	10.11	0.12	2.21	0.09	3.54	0.13	1.81	0.09	2.48	0.18	0.63	0.09	0.61	0.07
93	0.00	78.86	0.31	10.03	0.12	2.22	0.09	3.35	0.12	1.87	0.09	2.43	0.18	0.64	0.09	0.61	0.07
94	0.23	78.59	0.31	9.87	0.12	2.36	0.10	3.54	0.13	1.84	0.09	2.66	0.19	0.58	0.09	0.56	0.07
95	0.46	78.63	0.31	10.08	0.12	2.33	0.10	3.55	0.13	1.78	0.09	2.58	0.19	0.54	0.08	0.52	0.06
96	0.70	78.40	0.31	10.09	0.12	2.21	0.09	3.46	0.13	1.83	0.09	2.70	0.20	0.65	0.10	0.65	0.08
97	0.93	78.05	0.31	10.10	0.12	2.29	0.10	3.50	0.13	1.89	0.09	3.00	0.22	0.55	0.08	0.62	0.07
98	1.16	77.98	0.31	10.20	0.12	2.31	0.10	3.65	0.13	1.89	0.09	2.76	0.20	0.54	0.08	0.67	0.08
99	1.39	77.79	0.30	10.19	0.12	2.34	0.10	3.63	0.13	2.01	0.10	2.81	0.21	0.63	0.09	0.61	0.07
100	1.62	78.00	0.31	10.20	0.12	2.29	0.10	3.45	0.13	1.93	0.10	2.86	0.21	0.61	0.09	0.66	0.08
101	1.86	78.06	0.31	10.26	0.12	2.27	0.09	3.56	0.13	1.89	0.09	2.80	0.20	0.56	0.08	0.60	0.07
102	2.09	77.89	0.30	10.33	0.12	2.34	0.10	3.49	0.13	2.02	0.10	2.69	0.20	0.56	0.08	0.67	0.08
103	2.32	77.98	0.31	10.38	0.13	2.36	0.10	3.49	0.13	1.96	0.10	2.54	0.19	0.61	0.09	0.68	0.08
104	2.55	78.15	0.31	10.55	0.13	2.24	0.09	3.51	0.13	1.88	0.09	2.52	0.18	0.53	0.08	0.62	0.07
105	2.78	78.01	0.31	10.50	0.13	2.31	0.10	3.54	0.13	1.93	0.10	2.58	0.19	0.57	0.08	0.56	0.07
106	3.02	77.75	0.30	10.53	0.13	2.31	0.10	3.65	0.13	1.87	0.09	2.77	0.20	0.56	0.08	0.55	0.07
107	3.25	77.44	0.30	10.58	0.13	2.51	0.10	3.61	0.13	1.96	0.10	2.74	0.20	0.64	0.09	0.53	0.06
108	3.48	77.73	0.30	10.55	0.13	2.39	0.10	3.64	0.13	1.98	0.10	2.67	0.20	0.54	0.08	0.51	0.06
109	3.71	77.54	0.30	10.56	0.13	2.37	0.10	3.73	0.14	1.97	0.10	2.67	0.20	0.59	0.09	0.57	0.07
110	3.94	77.39	0.30	10.83	0.13	2.28	0.10	3.58	0.13	2.10	0.10	2.62	0.19	0.59	0.09	0.61	0.07
111	4.18	77.14	0.30	10.81	0.13	2.33	0.10	3.73	0.14	1.99	0.10	2.73	0.20	0.64	0.09	0.62	0.08
112	4.41	77.60	0.30	10.80	0.13	2.37	0.10	3.54	0.13	1.93	0.09	2.62	0.19	0.54	0.08	0.61	0.07
113	4.64	77.50	0.30	10.89	0.13	2.28	0.10	3.54	0.13	1.90	0.09	2.72	0.20	0.55	0.08	0.61	0.07
114	4.87	77.16	0.30	10.92	0.13	2.33	0.10	3.58	0.13	2.08	0.10	2.76	0.20	0.56	0.08	0.61	0.07
115	5.10	77.14	0.30	10.86	0.13	2.35	0.10	3.67	0.13	2.05	0.10	2.72	0.20	0.59	0.09	0.61	0.07

116	5.34	77.05	0.30	10.76	0.13	2.44	0.10	3.90	0.14	2.02	0.10	2.66	0.19	0.62	0.09	0.54	0.06
117	5.57	77.05	0.30	10.94	0.13	2.43	0.10	3.72	0.14	2.08	0.10	2.63	0.19	0.56	0.08	0.59	0.07
118	5.80	76.73	0.30	11.14	0.13	2.37	0.10	3.68	0.13	1.96	0.10	2.82	0.21	0.61	0.09	0.68	0.08
119	6.03	77.05	0.30	10.91	0.13	2.39	0.10	3.72	0.14	1.97	0.10	2.73	0.20	0.56	0.08	0.67	0.08
120	6.26	77.31	0.30	10.90	0.13	2.47	0.10	3.65	0.13	1.89	0.09	2.66	0.19	0.54	0.08	0.58	0.07
121	6.50	76.53	0.30	11.12	0.13	2.58	0.11	3.62	0.13	2.00	0.10	2.94	0.21	0.60	0.09	0.62	0.07
122	6.73	76.56	0.30	11.19	0.13	2.50	0.10	3.65	0.13	1.87	0.09	2.99	0.22	0.67	0.10	0.57	0.07
123	6.96	76.91	0.30	11.20	0.13	2.50	0.10	3.64	0.13	1.89	0.09	2.62	0.19	0.66	0.10	0.59	0.07
124	7.19	77.11	0.30	11.35	0.14	2.37	0.10	3.75	0.14	1.96	0.10	2.22	0.16	0.56	0.08	0.68	0.08
125	7.42	77.05	0.30	11.20	0.13	2.48	0.10	3.69	0.14	2.08	0.10	2.39	0.17	0.54	0.08	0.58	0.07
126	7.66	76.46	0.30	11.49	0.14	2.55	0.11	3.63	0.13	2.05	0.10	2.52	0.18	0.63	0.09	0.67	0.08
127	7.89	76.06	0.30	11.50	0.14	2.55	0.11	3.87	0.14	1.97	0.10	2.82	0.21	0.62	0.09	0.62	0.07
128	8.12	76.17	0.30	11.47	0.14	2.52	0.11	3.63	0.13	2.12	0.10	2.83	0.21	0.62	0.09	0.64	0.08
129	8.35	75.96	0.30	11.13	0.13	2.67	0.11	3.80	0.14	2.06	0.10	2.99	0.22	0.64	0.09	0.74	0.09
130	8.58	76.49	0.30	11.31	0.14	2.50	0.10	3.70	0.14	1.97	0.10	2.79	0.20	0.65	0.10	0.59	0.07
131	8.82	76.19	0.30	11.37	0.14	2.41	0.10	3.84	0.14	2.08	0.10	2.91	0.21	0.54	0.08	0.66	0.08
132	9.05	76.04	0.30	11.43	0.14	2.57	0.11	3.76	0.14	2.05	0.10	2.83	0.21	0.63	0.09	0.68	0.08
133	9.28	75.80	0.30	11.69	0.14	2.64	0.11	3.76	0.14	2.06	0.10	2.79	0.20	0.57	0.08	0.69	0.08
134	9.51	75.82	0.30	11.61	0.14	2.59	0.11	3.83	0.14	1.96	0.10	2.87	0.21	0.64	0.09	0.68	0.08
135	9.74	76.06	0.30	11.46	0.14	2.69	0.11	3.73	0.14	2.08	0.10	2.83	0.21	0.54	0.08	0.61	0.07
136	9.98	76.15	0.30	11.74	0.14	2.56	0.11	3.67	0.13	1.90	0.09	2.82	0.21	0.57	0.08	0.59	0.07
137	10.21	76.33	0.30	11.58	0.14	2.48	0.10	3.73	0.14	1.84	0.09	2.76	0.20	0.60	0.09	0.67	0.08
138	10.44	76.36	0.30	11.57	0.14	2.61	0.11	3.62	0.13	1.93	0.09	2.66	0.19	0.61	0.09	0.65	0.08
139	10.67	76.06	0.30	11.63	0.14	2.56	0.11	3.67	0.13	2.08	0.10	2.80	0.20	0.57	0.08	0.63	0.08
140	10.90	75.73	0.30	11.79	0.14	2.66	0.11	3.81	0.14	2.05	0.10	2.71	0.20	0.69	0.10	0.55	0.07
141	11.14	76.29	0.30	11.73	0.14	2.44	0.10	3.61	0.13	2.06	0.10	2.61	0.19	0.64	0.09	0.62	0.07
142	11.37	75.74	0.30	11.86	0.14	2.54	0.11	3.77	0.14	2.10	0.10	2.73	0.20	0.65	0.09	0.62	0.07
143	11.60	75.77	0.30	11.70	0.14	2.60	0.11	3.77	0.14	2.16	0.11	2.79	0.20	0.59	0.09	0.62	0.08
144	11.83	76.09	0.30	11.84	0.14	2.53	0.11	3.55	0.13	2.07	0.10	2.68	0.20	0.60	0.09	0.64	0.08
145	12.07	76.11	0.30	11.77	0.14	2.47	0.10	3.67	0.13	2.06	0.10	2.54	0.19	0.70	0.10	0.69	0.08
146	12.30	75.70	0.30	11.84	0.14	2.71	0.11	3.84	0.14	2.08	0.10	2.60	0.19	0.61	0.09	0.62	0.07
147	12.53	75.55	0.30	11.99	0.14	2.54	0.11	3.78	0.14	2.05	0.10	2.94	0.22	0.49	0.07	0.66	0.08
148	12.76	76.03	0.30	11.98	0.14	2.38	0.10	3.56	0.13	1.97	0.10	2.83	0.21	0.57	0.08	0.69	0.08
149	12.99	76.00	0.30	11.88	0.14	2.49	0.10	3.78	0.14	1.97	0.10	2.62	0.19	0.59	0.09	0.68	0.08
150	13.22	75.57	0.30	11.93	0.14	2.72	0.11	3.74	0.14	2.01	0.10	2.85	0.21	0.53	0.08	0.64	0.08
151	13.46	75.90	0.30	11.89	0.14	2.64	0.11	3.88	0.14	2.04	0.10	2.47	0.18	0.54	0.08	0.65	0.08
152	13.69	75.63	0.30	12.05	0.15	2.69	0.11	3.77	0.14	2.08	0.10	2.54	0.19	0.56	0.08	0.68	0.08
153	13.92	75.48	0.30	12.09	0.15	2.70	0.11	3.78	0.14	2.06	0.10	2.67	0.20	0.58	0.09	0.65	0.08
154	14.15	75.35	0.29	12.25	0.15	2.68	0.11	3.74	0.14	2.19	0.11	2.65	0.19	0.58	0.09	0.57	0.07
155	14.39	75.22	0.29	12.18	0.15	2.68	0.11	3.78	0.14	2.11	0.10	2.80	0.21	0.64	0.09	0.59	0.07
156	14.62	75.51	0.30	11.94	0.14	2.66	0.11	3.86	0.14	2.11	0.10	2.67	0.20	0.62	0.09	0.63	0.08
157	14.85	75.60	0.30	12.07	0.15	2.65	0.11	3.84	0.14	2.08	0.10	2.60	0.19	0.51	0.08	0.64	0.08
158	15.08	75.10	0.29	12.18	0.15	2.75	0.11	3.74	0.14	2.21	0.11	2.80	0.20	0.54	0.08	0.69	0.08
159	15.31	75.38	0.30	12.21	0.15	2.74	0.11	3.83	0.14	2.04	0.10	2.55	0.19	0.50	0.07	0.74	0.09
160	15.54	75.37	0.30	12.26	0.15	2.63	0.11	3.78	0.14	2.05	0.10	2.65	0.19	0.58	0.08	0.68	0.08
161	15.78	75.56	0.30	12.34	0.15	2.61	0.11	3.74	0.14	2.09	0.10	2.49	0.18	0.59	0.09	0.59	0.07
162	16.01	75.48	0.30	12.17	0.15	2.56	0.11	3.81	0.14	2.03	0.10	2.65	0.19	0.64	0.09	0.66	0.08
163	16.24	74.96	0.29	12.37	0.15	2.60	0.11	3.83	0.14	2.07	0.10	2.90	0.21	0.58	0.09	0.69	0.08
164	16.47	75.07	0.29	12.30	0.15	2.69	0.11	3.87	0.14	1.99	0.10	2.74	0.20	0.63	0.09	0.71	0.09
165	16.71	74.85	0.29	12.35	0.15	2.54	0.11	3.92	0.14	2.17	0.11	2.78	0.20	0.73	0.11	0.66	0.08
166	16.94	74.92	0.29	12.36	0.15	2.66	0.11	3.79	0.14	2.06	0.10	2.89	0.21	0.60	0.09	0.71	0.09
167	17.17	74.95	0.29	12.34	0.15	2.67	0.11	3.89	0.14	2.16	0.11	2.72	0.20	0.65	0.10	0.62	0.07
168	17.40	75.18	0.29	12.30	0.15	2.66	0.11	3.74	0.14	2.09	0.10	2.83	0.21	0.53	0.08	0.66	0.08
169	17.63	75.15	0.29	12.50	0.15	2.75	0.11	3.79	0.14	2.00	0.10	2.63	0.19	0.50	0.07	0.67	0.08
170	17.86	75.19	0.29	12.32	0.15	2.84	0.12	3.80	0.14	2.13	0.11	2.59	0.19	0.48	0.07	0.64	0.08

Agglomerate FLD18.2

Table J.30: Major element compositions (as wt.% oxides) from a line traverse across the interface of interior agglomerate FLD18.2 (from agglomerate FLD18.2 to host FLD18) extracted from quantified EDS compositional maps. The EDS compositional maps were collected at a resolution of 4.8 pixels/μm. The smoothing width for this traverse was 125 pixels (26 μm) wide. The EDS compositional maps were collected at a resolution of 4.3 pixels/μm. The smoothing width for this traverse was 125 pixels (29 μm) wide. This is an Si interface and has been centered at $x = 0$ based on the SiO_2 maximum. Peak points within 2σ of the SiO_2 maximum are highlighted in yellow. Uncertainties are 2SEOM.

Pt.	Position (μm)	SiO_2	2σ	Al_2O_3	2σ	Na_2O	2σ	K_2O	2σ	CaO	2σ	FeO	2σ	TiO_2	2σ	MgO	2σ
1	-10.79	74.85	0.22	13.50	0.15	2.04	0.07	3.96	0.09	1.81	0.08	2.81	0.16	0.50	0.08	0.54	0.05
2	-10.58	74.77	0.22	13.57	0.15	2.11	0.08	3.94	0.09	1.83	0.08	2.71	0.16	0.47	0.07	0.60	0.06
3	-10.37	74.69	0.22	13.63	0.15	2.05	0.07	3.90	0.09	1.82	0.08	2.76	0.16	0.56	0.09	0.59	0.05
4	-10.17	74.93	0.22	13.60	0.15	2.06	0.07	3.87	0.09	1.85	0.08	2.60	0.15	0.51	0.08	0.57	0.05
5	-9.96	74.63	0.22	13.53	0.15	2.08	0.07	3.87	0.09	1.79	0.08	3.04	0.17	0.53	0.08	0.54	0.05
6	-9.75	74.62	0.22	13.60	0.15	2.07	0.07	3.95	0.09	1.79	0.08	2.87	0.16	0.44	0.07	0.65	0.06
7	-9.54	74.69	0.22	13.46	0.15	2.05	0.07	4.00	0.09	1.88	0.08	2.80	0.16	0.52	0.08	0.59	0.05
8	-9.34	74.56	0.22	13.35	0.14	2.09	0.07	3.99	0.09	1.85	0.08	2.90	0.17	0.67	0.10	0.58	0.05
9	-9.13	74.69	0.22	13.54	0.15	2.07	0.07	3.85	0.09	1.79	0.08	2.94	0.17	0.57	0.09	0.56	0.05
10	-8.92	74.92	0.22	13.44	0.14	2.07	0.07	3.87	0.09	1.81	0.08	2.79	0.16	0.52	0.08	0.58	0.05
11	-8.71	74.89	0.22	13.39	0.14	2.11	0.08	3.84	0.09	1.83	0.08	2.77	0.16	0.59	0.09	0.57	0.05
12	-8.51	74.75	0.22	13.38	0.14	2.13	0.08	3.98	0.09	1.85	0.08	2.83	0.16	0.52	0.08	0.55	0.05
13	-8.30	74.84	0.22	13.35	0.14	2.06	0.07	3.90	0.09	1.86	0.08	2.84	0.16	0.53	0.08	0.62	0.06
14	-8.09	74.94	0.22	13.40	0.14	1.97	0.07	3.95	0.09	1.85	0.08	2.81	0.16	0.50	0.08	0.59	0.05
15	-7.88	74.73	0.22	13.36	0.14	2.11	0.08	3.96	0.09	1.97	0.08	2.79	0.16	0.46	0.07	0.60	0.06
16	-7.68	74.94	0.22	13.32	0.14	2.10	0.08	3.74	0.09	1.90	0.08	2.84	0.16	0.52	0.08	0.64	0.06
17	-7.47	74.87	0.22	13.30	0.14	2.05	0.07	3.88	0.09	1.84	0.08	2.92	0.17	0.50	0.08	0.65	0.06
18	-7.26	74.78	0.22	13.23	0.14	2.07	0.07	4.00	0.09	1.90	0.08	2.89	0.17	0.54	0.08	0.60	0.06
19	-7.05	74.89	0.22	13.23	0.14	2.03	0.07	3.90	0.09	1.91	0.08	2.90	0.17	0.51	0.08	0.64	0.06
20	-6.85	74.76	0.22	13.20	0.14	2.01	0.07	3.90	0.09	1.90	0.08	3.02	0.17	0.58	0.09	0.62	0.06
21	-6.64	74.80	0.22	13.10	0.14	2.07	0.07	3.90	0.09	2.05	0.09	3.00	0.17	0.51	0.08	0.58	0.05
22	-6.43	74.78	0.22	13.12	0.14	2.07	0.07	3.84	0.09	1.97	0.08	3.13	0.18	0.50	0.08	0.59	0.05
23	-6.22	74.64	0.22	13.06	0.14	2.01	0.07	3.91	0.09	2.05	0.09	3.24	0.19	0.48	0.07	0.61	0.06
24	-6.02	74.83	0.22	13.05	0.14	2.03	0.07	3.86	0.09	1.97	0.08	3.15	0.18	0.48	0.07	0.64	0.06
25	-5.81	74.71	0.22	13.02	0.14	2.09	0.07	3.85	0.09	1.93	0.08	3.35	0.19	0.53	0.08	0.52	0.05
26	-5.60	74.67	0.22	13.00	0.14	2.06	0.07	3.83	0.09	1.98	0.09	3.29	0.19	0.56	0.09	0.61	0.06
27	-5.39	74.71	0.22	12.86	0.14	2.06	0.07	3.80	0.09	2.01	0.09	3.35	0.19	0.60	0.09	0.62	0.06
28	-5.19	74.82	0.22	12.98	0.14	2.06	0.07	3.67	0.08	2.04	0.09	3.32	0.19	0.48	0.07	0.63	0.06
29	-4.98	75.01	0.22	12.89	0.14	1.97	0.07	3.73	0.09	2.07	0.09	3.26	0.19	0.42	0.06	0.66	0.06
30	-4.77	75.18	0.22	12.85	0.14	1.94	0.07	3.81	0.09	1.97	0.08	3.10	0.18	0.53	0.08	0.62	0.06
31	-4.56	74.80	0.22	12.75	0.14	1.93	0.07	3.75	0.09	2.01	0.09	3.55	0.20	0.51	0.08	0.72	0.07
32	-4.36	74.84	0.22	12.61	0.14	1.88	0.07	3.81	0.09	2.01	0.09	3.68	0.21	0.49	0.08	0.67	0.06
33	-4.15	74.85	0.22	12.54	0.14	1.99	0.07	3.82	0.09	1.95	0.08	3.71	0.21	0.50	0.08	0.64	0.06
34	-3.94	75.06	0.22	12.47	0.13	2.00	0.07	3.77	0.09	1.94	0.08	3.67	0.21	0.48	0.07	0.62	0.06
35	-3.73	75.39	0.22	12.48	0.13	1.84	0.07	3.80	0.09	1.93	0.08	3.38	0.19	0.48	0.07	0.70	0.06
36	-3.53	75.60	0.22	12.19	0.13	1.83	0.07	3.73	0.09	1.97	0.08	3.43	0.20	0.54	0.08	0.70	0.06
37	-3.32	75.53	0.22	11.96	0.13	1.91	0.07	3.78	0.09	2.02	0.09	3.67	0.21	0.49	0.08	0.64	0.06
38	-3.11	75.93	0.22	11.86	0.13	1.77	0.06	3.77	0.09	1.90	0.08	3.59	0.21	0.52	0.08	0.66	0.06
39	-2.90	76.30	0.22	11.80	0.13	1.71	0.06	3.71	0.08	1.86	0.08	3.46	0.20	0.55	0.09	0.61	0.06
40	-2.70	76.65	0.22	11.57	0.12	1.72	0.06	3.68	0.08	1.81	0.08	3.51	0.20	0.44	0.07	0.62	0.06
41	-2.49	76.94	0.22	11.26	0.12	1.75	0.06	3.64	0.08	1.76	0.08	3.52	0.20	0.50	0.08	0.64	0.06
42	-2.28	77.16	0.22	11.00	0.12	1.75	0.06	3.60	0.08	1.77	0.08	3.54	0.20	0.53	0.08	0.65	0.06
43	-2.07	77.44	0.22	10.76	0.12	1.69	0.06	3.64	0.08	1.65	0.07	3.69	0.21	0.51	0.08	0.62	0.06
44	-1.87	78.01	0.23	10.49	0.11	1.61	0.06	3.64	0.08	1.62	0.07	3.54	0.20	0.51	0.08	0.59	0.05
45	-1.66	78.48	0.23	10.22	0.11	1.62	0.06	3.62	0.08	1.52	0.07	3.40	0.19	0.52	0.08	0.62	0.06
46	-1.45	78.89	0.23	10.01	0.11	1.68	0.06	3.45	0.08	1.43	0.06	3.51	0.20	0.45	0.07	0.57	0.05
47	-1.24	79.22	0.23	9.78	0.11	1.53	0.05	3.46	0.08	1.37	0.06	3.60	0.21	0.42	0.07	0.62	0.06
48	-1.04	79.56	0.23	9.60	0.10	1.51	0.05	3.57	0.08	1.38	0.06	3.38	0.19	0.42	0.07	0.58	0.05
49	-0.83	80.12	0.23	9.42	0.10	1.43	0.05	3.35	0.08	1.33	0.06	3.34	0.19	0.48	0.07	0.53	0.05

50	-0.62	80.12	0.23	9.23	0.10	1.34	0.05	3.35	0.08	1.36	0.06	3.50	0.20	0.53	0.08	0.56	0.05
51	-0.42	79.98	0.23	9.11	0.10	1.39	0.05	3.46	0.08	1.38	0.06	3.55	0.20	0.54	0.08	0.58	0.05
52	-0.21	80.29	0.23	9.10	0.10	1.46	0.05	3.51	0.08	1.32	0.06	3.27	0.19	0.46	0.07	0.60	0.06
53	0.00	80.36	0.23	9.09	0.10	1.43	0.05	3.48	0.08	1.25	0.05	3.32	0.19	0.46	0.07	0.61	0.06
54	0.21	79.97	0.23	9.23	0.10	1.44	0.05	3.49	0.08	1.25	0.05	3.56	0.20	0.44	0.07	0.61	0.06
55	0.41	79.87	0.23	9.41	0.10	1.49	0.05	3.44	0.08	1.33	0.06	3.46	0.20	0.49	0.08	0.49	0.05
56	0.62	79.33	0.23	9.67	0.10	1.54	0.06	3.56	0.08	1.43	0.06	3.42	0.20	0.52	0.08	0.53	0.05
57	0.83	78.87	0.23	9.87	0.11	1.64	0.06	3.58	0.08	1.47	0.06	3.51	0.20	0.45	0.07	0.62	0.06
58	1.04	78.18	0.23	10.12	0.11	1.69	0.06	3.66	0.08	1.55	0.07	3.72	0.21	0.45	0.07	0.63	0.06
59	1.24	77.89	0.23	10.50	0.11	1.64	0.06	3.65	0.08	1.49	0.06	3.78	0.22	0.46	0.07	0.59	0.05
60	1.45	77.37	0.22	10.75	0.12	1.74	0.06	3.67	0.08	1.62	0.07	3.80	0.22	0.39	0.06	0.65	0.06
61	1.66	76.94	0.22	11.07	0.12	1.79	0.06	3.74	0.09	1.68	0.07	3.58	0.21	0.50	0.08	0.70	0.06
62	1.87	76.79	0.22	11.23	0.12	1.87	0.07	3.75	0.09	1.72	0.07	3.52	0.20	0.50	0.08	0.63	0.06
63	2.07	76.12	0.22	11.49	0.12	1.92	0.07	3.78	0.09	1.83	0.08	3.66	0.21	0.54	0.08	0.66	0.06
64	2.28	75.84	0.22	11.71	0.13	1.90	0.07	3.77	0.09	1.90	0.08	3.70	0.21	0.51	0.08	0.66	0.06
65	2.49	75.59	0.22	11.88	0.13	1.86	0.07	3.82	0.09	1.96	0.08	3.81	0.22	0.48	0.07	0.60	0.06
66	2.70	75.26	0.22	12.17	0.13	1.90	0.07	3.81	0.09	1.99	0.09	3.70	0.21	0.52	0.08	0.65	0.06
67	2.90	74.97	0.22	12.24	0.13	2.05	0.07	3.82	0.09	2.08	0.09	3.74	0.21	0.44	0.07	0.67	0.06
68	3.11	74.97	0.22	12.40	0.13	1.96	0.07	3.78	0.09	2.09	0.09	3.63	0.21	0.51	0.08	0.66	0.06
69	3.32	75.02	0.22	12.52	0.14	1.94	0.07	3.76	0.09	2.08	0.09	3.43	0.20	0.55	0.09	0.70	0.06
70	3.53	74.53	0.22	12.60	0.14	2.03	0.07	3.92	0.09	2.11	0.09	3.62	0.21	0.50	0.08	0.69	0.06
71	3.73	74.56	0.22	12.79	0.14	2.05	0.07	3.94	0.09	2.11	0.09	3.37	0.19	0.48	0.07	0.69	0.06
72	3.94	74.28	0.22	12.84	0.14	2.10	0.08	3.91	0.09	2.19	0.09	3.44	0.20	0.54	0.08	0.69	0.06
73	4.15	74.01	0.21	12.98	0.14	2.15	0.08	3.93	0.09	2.23	0.10	3.52	0.20	0.56	0.09	0.64	0.06
74	4.36	74.33	0.22	13.10	0.14	2.06	0.07	3.91	0.09	2.18	0.09	3.33	0.19	0.48	0.07	0.62	0.06
75	4.56	74.28	0.22	12.98	0.14	2.06	0.07	3.92	0.09	2.10	0.09	3.52	0.20	0.49	0.08	0.65	0.06
76	4.77	74.30	0.22	13.07	0.14	2.08	0.07	3.90	0.09	2.21	0.09	3.36	0.19	0.48	0.07	0.61	0.06
77	4.98	74.24	0.22	13.10	0.14	2.06	0.07	3.96	0.09	2.20	0.09	3.27	0.19	0.52	0.08	0.67	0.06
78	5.19	74.02	0.21	13.20	0.14	2.09	0.07	3.91	0.09	2.10	0.09	3.43	0.20	0.58	0.09	0.67	0.06
79	5.39	74.05	0.21	13.32	0.14	2.04	0.07	3.96	0.09	2.13	0.09	3.32	0.19	0.53	0.08	0.65	0.06
80	5.60	73.96	0.21	13.25	0.14	2.11	0.08	3.90	0.09	2.24	0.10	3.42	0.20	0.52	0.08	0.59	0.05
81	5.81	73.94	0.21	13.27	0.14	2.19	0.08	3.84	0.09	2.28	0.10	3.39	0.19	0.47	0.07	0.64	0.06
82	6.02	74.01	0.21	13.29	0.14	2.16	0.08	3.96	0.09	2.14	0.09	3.30	0.19	0.47	0.07	0.67	0.06
83	6.22	74.12	0.22	13.20	0.14	2.22	0.08	4.06	0.09	2.14	0.09	3.17	0.18	0.46	0.07	0.63	0.06
84	6.43	74.11	0.22	13.30	0.14	2.28	0.08	3.89	0.09	2.09	0.09	3.17	0.18	0.49	0.08	0.67	0.06
85	6.64	74.51	0.22	13.32	0.14	2.16	0.08	3.89	0.09	1.98	0.09	3.02	0.17	0.49	0.08	0.63	0.06
86	6.85	74.49	0.22	13.15	0.14	2.18	0.08	4.03	0.09	1.96	0.08	3.01	0.17	0.55	0.09	0.62	0.06
87	7.05	74.53	0.22	13.21	0.14	2.08	0.07	4.02	0.09	2.02	0.09	3.07	0.18	0.50	0.08	0.57	0.05
88	7.26	74.45	0.22	13.39	0.14	2.07	0.07	3.98	0.09	2.02	0.09	3.06	0.18	0.48	0.07	0.54	0.05
89	7.47	74.39	0.22	13.17	0.14	2.09	0.07	4.06	0.09	2.01	0.09	3.15	0.18	0.53	0.08	0.61	0.06
90	7.68	74.11	0.22	13.36	0.14	2.13	0.08	4.01	0.09	2.03	0.09	3.23	0.18	0.53	0.08	0.61	0.06
91	7.88	74.31	0.22	13.38	0.14	2.20	0.08	4.01	0.09	2.01	0.09	3.04	0.17	0.48	0.07	0.57	0.05
92	8.09	74.52	0.22	13.23	0.14	2.15	0.08	3.99	0.09	2.01	0.09	2.98	0.17	0.51	0.08	0.60	0.06
93	8.30	74.58	0.22	13.30	0.14	2.11	0.08	3.95	0.09	1.90	0.08	2.95	0.17	0.55	0.09	0.66	0.06
94	8.51	74.33	0.22	13.19	0.14	2.09	0.07	4.03	0.09	1.98	0.09	3.16	0.18	0.58	0.09	0.63	0.06
95	8.71	74.48	0.22	13.23	0.14	2.07	0.07	4.00	0.09	1.96	0.08	3.12	0.18	0.56	0.09	0.58	0.05
96	8.92	74.69	0.22	13.11	0.14	2.11	0.08	3.94	0.09	2.04	0.09	2.99	0.17	0.53	0.08	0.59	0.05
97	9.13	74.43	0.22	13.20	0.14	2.12	0.08	4.10	0.09	1.93	0.08	3.01	0.17	0.55	0.09	0.66	0.06
98	9.34	74.65	0.22	13.20	0.14	2.17	0.08	4.08	0.09	1.87	0.08	2.84	0.16	0.56	0.09	0.62	0.06
99	9.54	74.53	0.22	13.19	0.14	2.13	0.08	3.99	0.09	2.04	0.09	2.94	0.17	0.52	0.08	0.65	0.06
100	9.75	74.57	0.22	13.14	0.14	2.22	0.08	3.97	0.09	1.98	0.09	2.98	0.17	0.55	0.09	0.60	0.05
101	9.96	74.61	0.22	13.19	0.14	2.12	0.08	4.03	0.09	1.89	0.08	3.06	0.18	0.51	0.08	0.60	0.05
102	10.17	74.91	0.22	13.17	0.14	2.08	0.07	4.01	0.09	1.83	0.08	2.81	0.16	0.55	0.08	0.64	0.06
103	10.37	74.54	0.22	13.25	0.14	2.15	0.08	4.01	0.09	1.89	0.08	3.00	0.17	0.56	0.09	0.61	0.06
104	10.58	74.69	0.22	13.07	0.14	2.18	0.08	3.93	0.09	1.95	0.08	3.07	0.18	0.56	0.09	0.55	0.05
105	10.79	74.90	0.22	12.99	0.14	2.07	0.07	4.01	0.09	1.89	0.08	2.97	0.17	0.52	0.08	0.65	0.06
106	11.00	74.73	0.22	13.08	0.14	2.20	0.08	4.08	0.09	1.95	0.08	2.81	0.16	0.53	0.08	0.62	0.06
107	11.20	74.97	0.22	13.14	0.14	2.12	0.08	4.13	0.09	1.84	0.08	2.69	0.15	0.54	0.08	0.57	0.05
108	11.41	74.84	0.22	13.11	0.14	2.17	0.08	4.01	0.09	1.91	0.08	2.91	0.17	0.48	0.07	0.58	0.05
109	11.62	74.74	0.22	13.12	0.14	2.11	0.08	4.02	0.09	1.89	0.08	3.03	0.17	0.51	0.08	0.58	0.05
110	11.83	74.73	0.22	13.10	0.14	2.13	0.08	4.09	0.09	1.89	0.08	2.88	0.17	0.56	0.09	0.61	0.06

Agglomerate U1B.L

Table J.31: Major element compositions (as wt.% oxides) from a line traverse across the interface of interior agglomerate U1B.L (from agglomerate U1B.L to host U1B) extracted from quantified EDS compositional maps. The EDS compositional maps were collected at a resolution of 8.1 pixels/μm. The smoothing width for this traverse was 250 pixels (19.8 μm) wide. This is an Si interface and has been centered at $x = 0$ based on the SiO_2 maximum. Peak points within 2σ of the SiO_2 maximum are highlighted in yellow. Uncertainties are 2SEOM.

Pt.	Position (μm)	SiO_2	2σ	Al_2O_3	2σ	Na_2O	2σ	K_2O	2σ	CaO	2σ	FeO	2σ	TiO_2	2σ	MgO	2σ
1	-17.33	71.56	0.23	15.33	0.14	3.06	0.10	3.50	0.11	1.56	0.08	3.38	0.18	0.73	0.07	0.87	0.07
2	-17.20	71.72	0.24	15.35	0.14	2.99	0.10	3.47	0.11	1.58	0.09	3.30	0.18	0.77	0.07	0.83	0.06
3	-17.08	71.53	0.23	15.44	0.15	2.99	0.10	3.42	0.11	1.53	0.08	3.48	0.19	0.75	0.07	0.85	0.06
4	-16.96	71.55	0.23	15.33	0.14	2.99	0.10	3.54	0.11	1.58	0.09	3.38	0.18	0.79	0.08	0.84	0.06
5	-16.83	71.84	0.24	15.28	0.14	2.91	0.09	3.54	0.11	1.50	0.08	3.41	0.19	0.71	0.07	0.82	0.06
6	-16.71	71.82	0.24	15.12	0.14	3.07	0.10	3.58	0.12	1.53	0.08	3.34	0.18	0.73	0.07	0.81	0.06
7	-16.58	71.80	0.24	15.30	0.14	2.98	0.10	3.58	0.12	1.49	0.08	3.33	0.18	0.73	0.07	0.79	0.06
8	-16.46	71.65	0.23	15.34	0.14	3.03	0.10	3.48	0.11	1.53	0.08	3.30	0.18	0.81	0.08	0.85	0.06
9	-16.34	71.47	0.23	15.40	0.15	2.93	0.10	3.53	0.11	1.48	0.08	3.45	0.19	0.84	0.08	0.90	0.07
10	-16.21	71.78	0.24	15.27	0.14	3.02	0.10	3.48	0.11	1.50	0.08	3.28	0.18	0.84	0.08	0.84	0.06
11	-16.09	71.54	0.23	15.26	0.14	3.05	0.10	3.42	0.11	1.53	0.08	3.51	0.19	0.81	0.08	0.87	0.07
12	-15.97	71.62	0.23	15.30	0.14	3.11	0.10	3.43	0.11	1.42	0.08	3.38	0.18	0.85	0.08	0.89	0.07
13	-15.84	71.93	0.24	15.23	0.14	3.09	0.10	3.51	0.11	1.53	0.08	3.20	0.17	0.74	0.07	0.78	0.06
14	-15.72	71.71	0.23	15.51	0.15	2.97	0.10	3.54	0.11	1.52	0.08	3.20	0.17	0.74	0.07	0.81	0.06
15	-15.59	71.75	0.24	15.31	0.14	3.00	0.10	3.61	0.12	1.50	0.08	3.32	0.18	0.65	0.06	0.85	0.06
16	-15.47	71.74	0.24	15.23	0.14	2.98	0.10	3.48	0.11	1.59	0.09	3.31	0.18	0.80	0.08	0.87	0.07
17	-15.35	71.79	0.24	15.17	0.14	2.99	0.10	3.56	0.12	1.60	0.09	3.20	0.17	0.84	0.08	0.85	0.06
18	-15.22	71.70	0.23	15.30	0.14	2.95	0.10	3.47	0.11	1.61	0.09	3.25	0.18	0.81	0.08	0.89	0.07
19	-15.10	71.61	0.23	15.40	0.15	3.00	0.10	3.56	0.12	1.47	0.08	3.35	0.18	0.76	0.07	0.84	0.06
20	-14.98	71.82	0.24	15.30	0.14	2.94	0.10	3.42	0.11	1.52	0.08	3.47	0.19	0.74	0.07	0.79	0.06
21	-14.85	71.50	0.23	15.40	0.15	3.00	0.10	3.42	0.11	1.57	0.09	3.41	0.19	0.81	0.08	0.89	0.07
22	-14.73	71.95	0.24	15.24	0.14	2.95	0.10	3.47	0.11	1.53	0.08	3.20	0.18	0.80	0.08	0.86	0.06
23	-14.60	71.63	0.23	15.35	0.14	3.00	0.10	3.50	0.11	1.64	0.09	3.20	0.17	0.87	0.08	0.83	0.06
24	-14.48	71.74	0.24	15.26	0.14	3.00	0.10	3.40	0.11	1.49	0.08	3.46	0.19	0.76	0.07	0.87	0.07
25	-14.36	71.80	0.24	15.31	0.14	2.94	0.10	3.40	0.11	1.49	0.08	3.39	0.19	0.80	0.08	0.86	0.07
26	-14.23	71.54	0.23	15.24	0.14	3.01	0.10	3.49	0.11	1.56	0.08	3.41	0.19	0.86	0.08	0.89	0.07
27	-14.11	71.69	0.23	15.17	0.14	3.00	0.10	3.56	0.12	1.60	0.09	3.34	0.18	0.77	0.07	0.86	0.06
28	-13.99	71.66	0.23	15.19	0.14	3.01	0.10	3.49	0.11	1.60	0.09	3.30	0.18	0.88	0.08	0.86	0.07
29	-13.86	71.77	0.24	15.13	0.14	2.97	0.10	3.53	0.11	1.64	0.09	3.37	0.18	0.75	0.07	0.84	0.06
30	-13.74	71.78	0.24	15.10	0.14	3.01	0.10	3.47	0.11	1.50	0.08	3.40	0.19	0.81	0.08	0.94	0.07
31	-13.61	71.44	0.23	15.18	0.14	2.97	0.10	3.56	0.12	1.63	0.09	3.42	0.19	0.81	0.08	0.98	0.07
32	-13.49	71.66	0.23	15.24	0.14	2.94	0.10	3.57	0.12	1.59	0.09	3.40	0.19	0.72	0.07	0.89	0.07
33	-13.37	71.26	0.23	15.27	0.14	2.99	0.10	3.54	0.11	1.66	0.09	3.55	0.19	0.82	0.08	0.91	0.07
34	-13.24	71.67	0.23	15.28	0.14	3.01	0.10	3.58	0.12	1.51	0.08	3.27	0.18	0.80	0.08	0.88	0.07
35	-13.12	72.13	0.24	15.20	0.14	2.99	0.10	3.42	0.11	1.56	0.08	3.21	0.18	0.68	0.07	0.81	0.06
36	-13.00	71.75	0.24	15.27	0.14	3.03	0.10	3.55	0.12	1.51	0.08	3.41	0.19	0.64	0.06	0.83	0.06
37	-12.87	71.81	0.24	15.15	0.14	2.99	0.10	3.59	0.12	1.49	0.08	3.37	0.18	0.76	0.07	0.85	0.06
38	-12.75	71.93	0.24	15.17	0.14	2.99	0.10	3.44	0.11	1.53	0.08	3.33	0.18	0.75	0.07	0.87	0.07
39	-12.62	71.89	0.24	15.35	0.14	2.87	0.09	3.43	0.11	1.61	0.09	3.11	0.17	0.81	0.08	0.94	0.07
40	-12.50	71.53	0.23	15.24	0.14	2.94	0.10	3.50	0.11	1.56	0.08	3.47	0.19	0.83	0.08	0.92	0.07
41	-12.38	71.23	0.23	15.28	0.14	3.13	0.10	3.52	0.11	1.62	0.09	3.61	0.20	0.76	0.07	0.84	0.06
42	-12.25	71.62	0.23	15.37	0.14	3.07	0.10	3.50	0.11	1.63	0.09	3.28	0.18	0.72	0.07	0.81	0.06
43	-12.13	71.66	0.23	15.31	0.14	3.01	0.10	3.52	0.11	1.57	0.09	3.27	0.18	0.76	0.07	0.89	0.07
44	-12.01	71.83	0.24	15.29	0.14	2.95	0.10	3.40	0.11	1.47	0.08	3.32	0.18	0.84	0.08	0.90	0.07
45	-11.88	71.89	0.24	15.25	0.14	3.11	0.10	3.44	0.11	1.52	0.08	3.17	0.17	0.77	0.07	0.84	0.06
46	-11.76	71.66	0.23	15.36	0.14	2.96	0.10	3.44	0.11	1.54	0.08	3.40	0.19	0.76	0.07	0.88	0.07
47	-11.63	71.65	0.23	15.16	0.14	2.98	0.10	3.48	0.11	1.64	0.09	3.34	0.18	0.82	0.08	0.92	0.07
48	-11.51	71.43	0.23	15.28	0.14	3.04	0.10	3.47	0.11	1.59	0.09	3.49	0.19	0.86	0.08	0.84	0.06
49	-11.39	71.52	0.23	15.20	0.14	2.99	0.10	3.36	0.11	1.62	0.09	3.53	0.19	0.94	0.09	0.83	0.06
50	-11.26	71.89	0.24	15.04	0.14	2.98	0.10	3.38	0.11	1.58	0.09	3.43	0.19	0.87	0.08	0.85	0.06

51	-11.14	71.50	0.23	15.22	0.14	3.02	0.10	3.44	0.11	1.54	0.08	3.63	0.20	0.78	0.08	0.86	0.06
52	-11.02	71.49	0.23	15.30	0.14	3.04	0.10	3.51	0.11	1.57	0.09	3.54	0.19	0.73	0.07	0.83	0.06
53	-10.89	71.68	0.23	15.21	0.14	2.96	0.10	3.64	0.12	1.65	0.09	3.32	0.18	0.72	0.07	0.81	0.06
54	-10.77	71.68	0.23	15.33	0.14	3.04	0.10	3.50	0.11	1.60	0.09	3.35	0.18	0.71	0.07	0.78	0.06
55	-10.64	71.43	0.23	15.34	0.14	2.97	0.10	3.43	0.11	1.60	0.09	3.61	0.20	0.70	0.07	0.92	0.07
56	-10.52	71.67	0.23	15.17	0.14	3.03	0.10	3.44	0.11	1.65	0.09	3.35	0.18	0.82	0.08	0.87	0.07
57	-10.40	71.75	0.24	15.02	0.14	3.16	0.10	3.54	0.11	1.54	0.08	3.39	0.19	0.74	0.07	0.85	0.06
58	-10.27	71.72	0.24	15.10	0.14	3.01	0.10	3.50	0.11	1.67	0.09	3.40	0.19	0.82	0.08	0.79	0.06
59	-10.15	71.70	0.23	15.21	0.14	3.00	0.10	3.49	0.11	1.62	0.09	3.37	0.18	0.78	0.08	0.82	0.06
60	-10.03	71.75	0.24	15.16	0.14	3.02	0.10	3.46	0.11	1.67	0.09	3.26	0.18	0.79	0.08	0.89	0.07
61	-9.90	71.62	0.23	15.15	0.14	3.06	0.10	3.61	0.12	1.60	0.09	3.38	0.18	0.75	0.07	0.82	0.06
62	-9.78	71.48	0.23	15.23	0.14	2.93	0.10	3.56	0.12	1.62	0.09	3.54	0.19	0.76	0.07	0.88	0.07
63	-9.65	71.61	0.23	15.31	0.14	3.04	0.10	3.47	0.11	1.61	0.09	3.43	0.19	0.74	0.07	0.78	0.06
64	-9.53	71.74	0.24	15.19	0.14	3.07	0.10	3.55	0.11	1.58	0.09	3.29	0.18	0.80	0.08	0.79	0.06
65	-9.41	71.64	0.23	15.05	0.14	3.10	0.10	3.39	0.11	1.70	0.09	3.42	0.19	0.79	0.08	0.91	0.07
66	-9.28	71.61	0.23	15.03	0.14	3.05	0.10	3.43	0.11	1.60	0.09	3.60	0.20	0.77	0.07	0.89	0.07
67	-9.16	71.44	0.23	15.20	0.14	3.00	0.10	3.51	0.11	1.58	0.09	3.55	0.19	0.88	0.08	0.84	0.06
68	-9.04	71.50	0.23	15.18	0.14	3.04	0.10	3.35	0.11	1.69	0.09	3.59	0.20	0.78	0.08	0.86	0.07
69	-8.91	71.33	0.23	15.23	0.14	2.98	0.10	3.39	0.11	1.61	0.09	3.68	0.20	0.78	0.08	1.00	0.08
70	-8.79	71.56	0.23	15.17	0.14	3.03	0.10	3.49	0.11	1.68	0.09	3.36	0.18	0.85	0.08	0.86	0.07
71	-8.66	71.71	0.23	15.30	0.14	2.95	0.10	3.45	0.11	1.64	0.09	3.37	0.18	0.78	0.08	0.80	0.06
72	-8.54	71.68	0.23	15.23	0.14	2.83	0.09	3.48	0.11	1.65	0.09	3.55	0.19	0.70	0.07	0.87	0.07
73	-8.42	71.54	0.23	15.12	0.14	2.95	0.10	3.40	0.11	1.82	0.10	3.46	0.19	0.86	0.08	0.86	0.06
74	-8.29	72.06	0.24	14.97	0.14	2.96	0.10	3.44	0.11	1.67	0.09	3.33	0.18	0.72	0.07	0.85	0.06
75	-8.17	71.68	0.23	15.18	0.14	3.00	0.10	3.41	0.11	1.60	0.09	3.47	0.19	0.78	0.08	0.86	0.07
76	-8.05	71.71	0.23	15.10	0.14	2.89	0.09	3.59	0.12	1.61	0.09	3.41	0.19	0.77	0.07	0.91	0.07
77	-7.92	71.72	0.24	15.03	0.14	2.99	0.10	3.54	0.11	1.58	0.09	3.54	0.19	0.74	0.07	0.86	0.06
78	-7.80	71.70	0.23	15.11	0.14	3.09	0.10	3.56	0.12	1.51	0.08	3.43	0.19	0.79	0.08	0.82	0.06
79	-7.67	71.57	0.23	15.18	0.14	3.04	0.10	3.42	0.11	1.66	0.09	3.52	0.19	0.75	0.07	0.87	0.07
80	-7.55	71.50	0.23	14.92	0.14	2.99	0.10	3.59	0.12	1.63	0.09	3.65	0.20	0.82	0.08	0.90	0.07
81	-7.43	71.59	0.23	14.94	0.14	3.12	0.10	3.50	0.11	1.58	0.09	3.60	0.20	0.76	0.07	0.90	0.07
82	-7.30	71.70	0.23	14.92	0.14	2.99	0.10	3.49	0.11	1.61	0.09	3.59	0.20	0.80	0.08	0.91	0.07
83	-7.18	72.06	0.24	14.91	0.14	3.03	0.10	3.46	0.11	1.64	0.09	3.30	0.18	0.77	0.07	0.83	0.06
84	-7.06	71.82	0.24	15.13	0.14	2.97	0.10	3.52	0.11	1.58	0.09	3.43	0.19	0.73	0.07	0.80	0.06
85	-6.93	71.54	0.23	15.06	0.14	2.99	0.10	3.56	0.12	1.66	0.09	3.55	0.19	0.80	0.08	0.84	0.06
86	-6.81	71.72	0.24	15.00	0.14	3.08	0.10	3.51	0.11	1.64	0.09	3.45	0.19	0.76	0.07	0.83	0.06
87	-6.68	71.77	0.24	14.97	0.14	2.99	0.10	3.41	0.11	1.65	0.09	3.62	0.20	0.75	0.07	0.85	0.06
88	-6.56	72.04	0.24	14.88	0.14	2.99	0.10	3.55	0.11	1.60	0.09	3.35	0.18	0.76	0.07	0.83	0.06
89	-6.44	72.06	0.24	14.88	0.14	2.94	0.10	3.41	0.11	1.57	0.09	3.56	0.19	0.71	0.07	0.86	0.07
90	-6.31	71.83	0.24	14.99	0.14	2.97	0.10	3.38	0.11	1.59	0.09	3.62	0.20	0.74	0.07	0.88	0.07
91	-6.19	71.76	0.24	14.92	0.14	2.98	0.10	3.55	0.12	1.61	0.09	3.59	0.20	0.75	0.07	0.83	0.06
92	-6.07	72.03	0.24	14.84	0.14	3.00	0.10	3.39	0.11	1.61	0.09	3.58	0.20	0.73	0.07	0.82	0.06
93	-5.94	72.09	0.24	14.81	0.14	2.92	0.10	3.45	0.11	1.58	0.09	3.52	0.19	0.78	0.08	0.84	0.06
94	-5.82	72.25	0.24	14.75	0.14	3.02	0.10	3.42	0.11	1.58	0.09	3.36	0.18	0.78	0.08	0.82	0.06
95	-5.69	72.11	0.24	14.73	0.14	3.05	0.10	3.42	0.11	1.60	0.09	3.38	0.18	0.84	0.08	0.87	0.07
96	-5.57	71.99	0.24	14.77	0.14	3.08	0.10	3.52	0.11	1.61	0.09	3.42	0.19	0.76	0.07	0.85	0.06
97	-5.45	72.17	0.24	14.66	0.14	2.92	0.09	3.51	0.11	1.59	0.09	3.65	0.20	0.71	0.07	0.79	0.06
98	-5.32	72.47	0.24	14.50	0.14	2.99	0.10	3.36	0.11	1.56	0.08	3.49	0.19	0.79	0.08	0.83	0.06
99	-5.20	72.50	0.24	14.52	0.14	2.98	0.10	3.47	0.11	1.54	0.08	3.47	0.19	0.74	0.07	0.77	0.06
100	-5.08	72.50	0.24	14.37	0.14	3.02	0.10	3.47	0.11	1.49	0.08	3.59	0.20	0.74	0.07	0.84	0.06
101	-4.95	72.36	0.24	14.33	0.13	3.00	0.10	3.42	0.11	1.61	0.09	3.63	0.20	0.80	0.08	0.85	0.06
102	-4.83	72.64	0.24	14.31	0.13	2.91	0.09	3.48	0.11	1.53	0.08	3.65	0.20	0.71	0.07	0.78	0.06
103	-4.70	73.09	0.24	14.24	0.13	2.96	0.10	3.43	0.11	1.55	0.08	3.23	0.18	0.72	0.07	0.78	0.06
104	-4.58	72.75	0.24	14.22	0.13	2.94	0.10	3.48	0.11	1.55	0.08	3.48	0.19	0.77	0.07	0.80	0.06
105	-4.46	72.94	0.24	14.24	0.13	2.87	0.09	3.44	0.11	1.47	0.08	3.41	0.19	0.76	0.07	0.86	0.07
106	-4.33	72.99	0.24	14.17	0.13	2.88	0.09	3.49	0.11	1.48	0.08	3.42	0.19	0.68	0.07	0.89	0.07
107	-4.21	72.77	0.24	13.96	0.13	2.90	0.09	3.55	0.11	1.53	0.08	3.72	0.20	0.71	0.07	0.86	0.07
108	-4.08	73.19	0.24	13.96	0.13	2.93	0.10	3.53	0.11	1.50	0.08	3.39	0.19	0.67	0.06	0.83	0.06
109	-3.96	73.35	0.24	14.01	0.13	2.90	0.09	3.42	0.11	1.46	0.08	3.40	0.19	0.63	0.06	0.83	0.06
110	-3.84	73.31	0.24	14.05	0.13	2.97	0.10	3.46	0.11	1.40	0.08	3.23	0.18	0.77	0.07	0.81	0.06
111	-3.71	73.38	0.24	13.94	0.13	2.91	0.09	3.45	0.11	1.37	0.07	3.37	0.18	0.76	0.07	0.83	0.06
112	-3.59	73.81	0.24	13.85	0.13	2.90	0.09	3.39	0.11	1.36	0.07	3.18	0.17	0.65	0.06	0.85	0.06

113	-3.47	73.71	0.24	13.67	0.13	2.97	0.10	3.41	0.11	1.36	0.07	3.37	0.18	0.68	0.07	0.82	0.06
114	-3.34	73.64	0.24	13.51	0.13	2.93	0.10	3.41	0.11	1.42	0.08	3.66	0.20	0.72	0.07	0.73	0.06
115	-3.22	73.80	0.24	13.40	0.13	2.92	0.10	3.44	0.11	1.47	0.08	3.54	0.19	0.67	0.06	0.76	0.06
116	-3.09	73.92	0.24	13.35	0.13	2.93	0.10	3.41	0.11	1.46	0.08	3.54	0.19	0.65	0.06	0.75	0.06
117	-2.97	74.16	0.24	13.28	0.13	2.89	0.09	3.44	0.11	1.45	0.08	3.36	0.18	0.67	0.06	0.74	0.06
118	-2.85	74.43	0.24	13.22	0.12	2.83	0.09	3.49	0.11	1.51	0.08	3.07	0.17	0.70	0.07	0.74	0.06
119	-2.72	74.53	0.24	13.12	0.12	2.79	0.09	3.42	0.11	1.31	0.07	3.30	0.18	0.71	0.07	0.84	0.06
120	-2.60	75.14	0.25	13.00	0.12	2.73	0.09	3.31	0.11	1.28	0.07	2.98	0.16	0.71	0.07	0.85	0.06
121	-2.48	75.12	0.25	12.84	0.12	2.71	0.09	3.45	0.11	1.34	0.07	3.08	0.17	0.72	0.07	0.75	0.06
122	-2.35	75.22	0.25	12.73	0.12	2.68	0.09	3.33	0.11	1.41	0.08	3.19	0.17	0.73	0.07	0.70	0.05
123	-2.23	75.25	0.25	12.66	0.12	2.74	0.09	3.51	0.11	1.21	0.07	3.20	0.17	0.73	0.07	0.70	0.05
124	-2.10	75.40	0.25	12.80	0.12	2.75	0.09	3.33	0.11	1.26	0.07	3.08	0.17	0.69	0.07	0.69	0.05
125	-1.98	75.53	0.25	12.41	0.12	2.68	0.09	3.49	0.11	1.33	0.07	3.23	0.18	0.62	0.06	0.70	0.05
126	-1.86	75.50	0.25	12.49	0.12	2.67	0.09	3.35	0.11	1.28	0.07	3.30	0.18	0.71	0.07	0.70	0.05
127	-1.73	75.76	0.25	12.32	0.12	2.63	0.09	3.41	0.11	1.26	0.07	3.21	0.18	0.72	0.07	0.68	0.05
128	-1.61	76.12	0.25	12.13	0.11	2.71	0.09	3.36	0.11	1.21	0.07	3.06	0.17	0.70	0.07	0.70	0.05
129	-1.49	76.26	0.25	12.22	0.12	2.69	0.09	3.42	0.11	1.21	0.07	2.79	0.15	0.70	0.07	0.72	0.05
130	-1.36	76.43	0.25	12.22	0.12	2.63	0.09	3.36	0.11	1.06	0.06	2.89	0.16	0.68	0.07	0.73	0.06
131	-1.24	76.53	0.25	11.94	0.11	2.59	0.08	3.40	0.11	1.19	0.06	2.99	0.16	0.67	0.06	0.70	0.05
132	-1.11	76.80	0.25	11.73	0.11	2.58	0.08	3.38	0.11	1.13	0.06	3.04	0.17	0.64	0.06	0.70	0.05
133	-0.99	76.99	0.25	11.70	0.11	2.62	0.09	3.43	0.11	1.05	0.06	2.90	0.16	0.64	0.06	0.68	0.05
134	-0.87	77.05	0.25	11.68	0.11	2.58	0.08	3.36	0.11	1.09	0.06	2.92	0.16	0.64	0.06	0.68	0.05
135	-0.74	77.15	0.25	11.53	0.11	2.57	0.08	3.35	0.11	1.16	0.06	2.88	0.16	0.66	0.06	0.69	0.05
136	-0.62	77.34	0.25	11.51	0.11	2.65	0.09	3.32	0.11	0.99	0.05	2.88	0.16	0.65	0.06	0.66	0.05
137	-0.50	77.49	0.25	11.35	0.11	2.46	0.08	3.40	0.11	1.06	0.06	3.02	0.17	0.58	0.06	0.64	0.05
138	-0.37	77.69	0.25	11.11	0.10	2.60	0.08	3.40	0.11	0.98	0.05	2.92	0.16	0.62	0.06	0.68	0.05
139	-0.25	77.82	0.26	11.08	0.10	2.51	0.08	3.43	0.11	1.08	0.06	2.82	0.15	0.63	0.06	0.63	0.05
140	-0.12	77.88	0.26	11.00	0.10	2.51	0.08	3.35	0.11	0.98	0.05	2.92	0.16	0.75	0.07	0.60	0.05
141	0.00	78.43	0.26	10.92	0.10	2.52	0.08	3.29	0.11	0.96	0.05	2.64	0.14	0.65	0.06	0.58	0.04
142	0.12	78.18	0.26	10.91	0.10	2.47	0.08	3.28	0.11	0.93	0.05	2.94	0.16	0.64	0.06	0.65	0.05
143	0.25	78.14	0.26	10.93	0.10	2.52	0.08	3.25	0.11	0.90	0.05	2.92	0.16	0.73	0.07	0.63	0.05
144	0.37	78.31	0.26	10.96	0.10	2.43	0.08	3.22	0.10	0.86	0.05	2.88	0.16	0.68	0.07	0.65	0.05
145	0.49	78.27	0.26	11.01	0.10	2.47	0.08	3.19	0.10	0.98	0.05	2.81	0.15	0.62	0.06	0.65	0.05
146	0.62	78.34	0.26	10.86	0.10	2.42	0.08	3.25	0.11	1.05	0.06	2.77	0.15	0.65	0.06	0.66	0.05
147	0.74	78.36	0.26	10.84	0.10	2.50	0.08	3.27	0.11	0.93	0.05	2.74	0.15	0.67	0.06	0.67	0.05
148	0.87	78.25	0.26	10.96	0.10	2.49	0.08	3.39	0.11	0.95	0.05	2.70	0.15	0.63	0.06	0.64	0.05
149	0.99	78.20	0.26	10.92	0.10	2.62	0.09	3.37	0.11	1.01	0.05	2.63	0.14	0.64	0.06	0.61	0.05
150	1.11	78.09	0.26	11.12	0.10	2.50	0.08	3.35	0.11	0.97	0.05	2.69	0.15	0.67	0.06	0.62	0.05
151	1.24	77.83	0.26	11.19	0.11	2.49	0.08	3.32	0.11	1.02	0.06	2.86	0.16	0.70	0.07	0.59	0.04
152	1.36	77.65	0.25	11.34	0.11	2.42	0.08	3.35	0.11	1.04	0.06	2.90	0.16	0.67	0.06	0.63	0.05
153	1.48	77.38	0.25	11.41	0.11	2.45	0.08	3.42	0.11	0.97	0.05	2.94	0.16	0.73	0.07	0.71	0.05
154	1.61	77.49	0.25	11.35	0.11	2.50	0.08	3.35	0.11	1.07	0.06	2.99	0.16	0.57	0.05	0.69	0.05
155	1.73	77.11	0.25	11.50	0.11	2.61	0.08	3.46	0.11	1.06	0.06	2.96	0.16	0.65	0.06	0.65	0.05
156	1.86	76.97	0.25	11.66	0.11	2.62	0.09	3.51	0.11	0.92	0.05	3.01	0.16	0.61	0.06	0.72	0.05
157	1.98	76.75	0.25	11.85	0.11	2.59	0.08	3.51	0.11	1.01	0.05	2.99	0.16	0.64	0.06	0.66	0.05
158	2.10	76.63	0.25	11.83	0.11	2.59	0.08	3.42	0.11	1.05	0.06	3.08	0.17	0.67	0.06	0.73	0.06
159	2.23	76.63	0.25	11.88	0.11	2.61	0.08	3.43	0.11	1.06	0.06	3.08	0.17	0.62	0.06	0.69	0.05
160	2.35	76.37	0.25	12.26	0.12	2.60	0.08	3.31	0.11	1.11	0.06	3.07	0.17	0.63	0.06	0.66	0.05
161	2.47	76.23	0.25	12.20	0.11	2.66	0.09	3.35	0.11	1.19	0.06	2.99	0.16	0.74	0.07	0.64	0.05
162	2.60	75.92	0.25	12.26	0.12	2.81	0.09	3.40	0.11	1.22	0.07	3.10	0.17	0.61	0.06	0.67	0.05
163	2.72	75.79	0.25	12.32	0.12	2.70	0.09	3.52	0.11	1.11	0.06	3.17	0.17	0.69	0.07	0.70	0.05
164	2.85	75.56	0.25	12.61	0.12	2.67	0.09	3.53	0.11	1.16	0.06	3.04	0.17	0.72	0.07	0.71	0.05
165	2.97	75.57	0.25	12.81	0.12	2.60	0.08	3.50	0.11	1.20	0.06	3.04	0.17	0.58	0.06	0.71	0.05
166	3.09	75.52	0.25	12.77	0.12	2.80	0.09	3.50	0.11	1.21	0.07	2.86	0.16	0.62	0.06	0.71	0.05
167	3.22	75.27	0.25	12.86	0.12	2.76	0.09	3.46	0.11	1.15	0.06	3.16	0.17	0.66	0.06	0.68	0.05
168	3.34	75.05	0.25	12.95	0.12	2.75	0.09	3.44	0.11	1.29	0.07	3.18	0.17	0.68	0.07	0.66	0.05
169	3.46	74.74	0.24	13.16	0.12	2.92	0.10	3.41	0.11	1.24	0.07	3.17	0.17	0.67	0.06	0.68	0.05
170	3.59	74.56	0.24	13.06	0.12	2.89	0.09	3.44	0.11	1.29	0.07	3.30	0.18	0.76	0.07	0.69	0.05
171	3.71	74.60	0.24	13.22	0.12	2.83	0.09	3.55	0.11	1.33	0.07	3.09	0.17	0.71	0.07	0.67	0.05
172	3.84	74.65	0.24	13.05	0.12	2.90	0.09	3.55	0.12	1.27	0.07	3.18	0.17	0.73	0.07	0.67	0.05
173	3.96	74.53	0.24	13.26	0.12	2.96	0.10	3.53	0.11	1.35	0.07	2.97	0.16	0.67	0.06	0.74	0.06
174	4.08	74.35	0.24	13.27	0.13	2.87	0.09	3.52	0.11	1.34	0.07	3.24	0.18	0.67	0.06	0.73	0.06

175	4.21	74.25	0.24	13.41	0.13	2.91	0.09	3.49	0.11	1.30	0.07	3.24	0.18	0.64	0.06	0.75	0.06
176	4.33	73.92	0.24	13.58	0.13	3.00	0.10	3.55	0.11	1.35	0.07	3.10	0.17	0.82	0.08	0.68	0.05
177	4.45	73.91	0.24	13.54	0.13	3.03	0.10	3.42	0.11	1.34	0.07	3.25	0.18	0.75	0.07	0.76	0.06
178	4.58	74.10	0.24	13.69	0.13	2.85	0.09	3.56	0.12	1.28	0.07	3.17	0.17	0.69	0.07	0.66	0.05
179	4.70	73.93	0.24	13.74	0.13	2.95	0.10	3.49	0.11	1.42	0.08	3.10	0.17	0.66	0.06	0.71	0.05
180	4.83	73.86	0.24	13.66	0.13	2.98	0.10	3.52	0.11	1.37	0.07	3.10	0.17	0.76	0.07	0.75	0.06
181	4.95	74.08	0.24	13.57	0.13	2.94	0.10	3.45	0.11	1.40	0.08	3.18	0.17	0.69	0.07	0.70	0.05
182	5.07	73.94	0.24	13.72	0.13	2.92	0.09	3.37	0.11	1.38	0.07	3.35	0.18	0.61	0.06	0.72	0.05
183	5.20	74.13	0.24	13.68	0.13	2.89	0.09	3.48	0.11	1.33	0.07	3.11	0.17	0.73	0.07	0.65	0.05
184	5.32	73.98	0.24	13.82	0.13	2.77	0.09	3.52	0.11	1.24	0.07	3.26	0.18	0.70	0.07	0.72	0.05
185	5.44	73.65	0.24	13.86	0.13	2.98	0.10	3.62	0.12	1.33	0.07	3.11	0.17	0.71	0.07	0.72	0.05
186	5.57	73.67	0.24	13.88	0.13	3.03	0.10	3.59	0.12	1.36	0.07	3.14	0.17	0.64	0.06	0.69	0.05
187	5.69	73.53	0.24	13.94	0.13	2.99	0.10	3.56	0.12	1.46	0.08	3.12	0.17	0.69	0.07	0.72	0.05
188	5.82	73.55	0.24	13.90	0.13	3.01	0.10	3.54	0.11	1.39	0.08	3.18	0.17	0.74	0.07	0.70	0.05
189	5.94	73.69	0.24	13.91	0.13	2.94	0.10	3.39	0.11	1.42	0.08	3.21	0.18	0.76	0.07	0.67	0.05
190	6.06	73.40	0.24	13.95	0.13	2.93	0.10	3.43	0.11	1.41	0.08	3.44	0.19	0.71	0.07	0.72	0.05
191	6.19	73.42	0.24	13.97	0.13	3.10	0.10	3.44	0.11	1.41	0.08	3.24	0.18	0.74	0.07	0.68	0.05
192	6.31	73.61	0.24	13.95	0.13	2.93	0.10	3.45	0.11	1.39	0.08	3.23	0.18	0.80	0.08	0.64	0.05
193	6.43	73.48	0.24	13.98	0.13	2.96	0.10	3.50	0.11	1.37	0.07	3.29	0.18	0.75	0.07	0.67	0.05
194	6.56	73.61	0.24	14.07	0.13	2.88	0.09	3.49	0.11	1.35	0.07	3.23	0.18	0.72	0.07	0.64	0.05
195	6.68	73.74	0.24	14.02	0.13	2.92	0.10	3.48	0.11	1.29	0.07	3.13	0.17	0.72	0.07	0.69	0.05
196	6.81	73.48	0.24	14.04	0.13	2.88	0.09	3.56	0.12	1.39	0.08	3.24	0.18	0.66	0.06	0.75	0.06
197	6.93	73.62	0.24	13.98	0.13	2.96	0.10	3.56	0.12	1.28	0.07	3.15	0.17	0.71	0.07	0.74	0.06
198	7.05	73.64	0.24	13.97	0.13	2.93	0.10	3.56	0.12	1.27	0.07	3.16	0.17	0.75	0.07	0.72	0.05
199	7.18	73.25	0.24	14.05	0.13	2.90	0.09	3.65	0.12	1.37	0.07	3.32	0.18	0.75	0.07	0.70	0.05
200	7.30	73.31	0.24	14.15	0.13	2.86	0.09	3.52	0.11	1.45	0.08	3.22	0.18	0.75	0.07	0.73	0.05
201	7.42	73.41	0.24	14.15	0.13	2.87	0.09	3.48	0.11	1.32	0.07	3.31	0.18	0.77	0.07	0.69	0.05
202	7.55	73.37	0.24	14.04	0.13	2.94	0.10	3.54	0.11	1.40	0.08	3.30	0.18	0.73	0.07	0.68	0.05
203	7.67	73.56	0.24	14.09	0.13	2.99	0.10	3.53	0.11	1.44	0.08	2.99	0.16	0.73	0.07	0.66	0.05
204	7.80	73.40	0.24	14.24	0.13	2.90	0.09	3.49	0.11	1.36	0.07	3.19	0.17	0.78	0.08	0.64	0.05
205	7.92	73.11	0.24	14.22	0.13	2.96	0.10	3.61	0.12	1.28	0.07	3.38	0.18	0.73	0.07	0.70	0.05
206	8.04	73.47	0.24	14.06	0.13	3.00	0.10	3.59	0.12	1.29	0.07	3.25	0.18	0.69	0.07	0.64	0.05
207	8.17	73.45	0.24	14.18	0.13	2.98	0.10	3.59	0.12	1.38	0.07	2.99	0.16	0.69	0.07	0.73	0.06
208	8.29	73.21	0.24	14.13	0.13	2.99	0.10	3.57	0.12	1.44	0.08	3.21	0.18	0.73	0.07	0.72	0.05
209	8.42	73.47	0.24	14.00	0.13	2.91	0.09	3.72	0.12	1.39	0.08	3.15	0.17	0.67	0.06	0.69	0.05
210	8.54	73.38	0.24	14.13	0.13	2.90	0.09	3.54	0.11	1.41	0.08	3.25	0.18	0.70	0.07	0.70	0.05
211	8.66	73.51	0.24	14.15	0.13	2.94	0.10	3.49	0.11	1.48	0.08	3.04	0.17	0.68	0.07	0.72	0.05
212	8.79	73.63	0.24	14.11	0.13	3.04	0.10	3.46	0.11	1.30	0.07	2.97	0.16	0.76	0.07	0.73	0.05
213	8.91	73.45	0.24	14.27	0.13	3.02	0.10	3.54	0.11	1.36	0.07	3.01	0.16	0.71	0.07	0.66	0.05
214	9.03	73.53	0.24	14.12	0.13	3.08	0.10	3.45	0.11	1.39	0.08	3.08	0.17	0.68	0.07	0.68	0.05
215	9.16	73.41	0.24	14.11	0.13	2.95	0.10	3.53	0.11	1.35	0.07	3.25	0.18	0.76	0.07	0.64	0.05
216	9.28	73.66	0.24	14.10	0.13	3.00	0.10	3.52	0.11	1.29	0.07	2.99	0.16	0.76	0.07	0.68	0.05
217	9.41	73.46	0.24	14.01	0.13	2.97	0.10	3.54	0.11	1.36	0.07	3.22	0.18	0.69	0.07	0.74	0.06
218	9.53	73.43	0.24	14.13	0.13	2.94	0.10	3.49	0.11	1.33	0.07	3.34	0.18	0.68	0.07	0.65	0.05
219	9.65	73.58	0.24	14.00	0.13	2.97	0.10	3.51	0.11	1.39	0.08	3.24	0.18	0.66	0.06	0.66	0.05
220	9.78	73.59	0.24	13.98	0.13	3.03	0.10	3.58	0.12	1.38	0.07	2.98	0.16	0.74	0.07	0.72	0.05
221	9.90	73.27	0.24	14.11	0.13	3.02	0.10	3.56	0.12	1.37	0.07	3.28	0.18	0.70	0.07	0.70	0.05
222	10.02	73.22	0.24	14.15	0.13	3.08	0.10	3.45	0.11	1.29	0.07	3.38	0.18	0.76	0.07	0.68	0.05
223	10.15	73.28	0.24	14.19	0.13	2.97	0.10	3.56	0.12	1.37	0.07	3.19	0.17	0.74	0.07	0.68	0.05
224	10.27	73.64	0.24	14.07	0.13	3.00	0.10	3.54	0.11	1.35	0.07	2.97	0.16	0.70	0.07	0.73	0.06
225	10.40	73.48	0.24	14.12	0.13	2.96	0.10	3.54	0.11	1.36	0.07	3.08	0.17	0.75	0.07	0.70	0.05
226	10.52	73.34	0.24	14.08	0.13	2.91	0.09	3.70	0.12	1.33	0.07	3.24	0.18	0.74	0.07	0.67	0.05
227	10.64	73.59	0.24	14.16	0.13	2.90	0.09	3.50	0.11	1.37	0.07	3.12	0.17	0.70	0.07	0.65	0.05
228	10.77	73.44	0.24	14.20	0.13	2.96	0.10	3.51	0.11	1.38	0.07	3.03	0.17	0.73	0.07	0.75	0.06
229	10.89	73.31	0.24	14.13	0.13	2.94	0.10	3.60	0.12	1.35	0.07	3.26	0.18	0.70	0.07	0.70	0.05
230	11.01	73.40	0.24	14.06	0.13	2.95	0.10	3.69	0.12	1.26	0.07	3.30	0.18	0.64	0.06	0.69	0.05
231	11.14	73.61	0.24	14.17	0.13	2.87	0.09	3.62	0.12	1.26	0.07	3.14	0.17	0.66	0.06	0.68	0.05
232	11.26	73.43	0.24	14.15	0.13	2.96	0.10	3.55	0.11	1.28	0.07	3.25	0.18	0.68	0.07	0.69	0.05
233	11.39	73.46	0.24	14.09	0.13	2.93	0.10	3.54	0.11	1.35	0.07	3.20	0.17	0.75	0.07	0.69	0.05
234	11.51	73.44	0.24	14.13	0.13	2.96	0.10	3.53	0.11	1.39	0.08	3.11	0.17	0.71	0.07	0.73	0.06
235	11.63	73.25	0.24	14.13	0.13	2.97	0.10	3.63	0.12	1.29	0.07	3.32	0.18	0.70	0.07	0.70	0.05
236	11.76	73.48	0.24	14.09	0.13	3.06	0.10	3.67	0.12	1.30	0.07	3.07	0.17	0.64	0.06	0.69	0.05

237	11.88	73.36	0.24	14.23	0.13	2.91	0.09	3.62	0.12	1.36	0.07	3.17	0.17	0.62	0.06	0.73	0.05
238	12.00	73.28	0.24	13.99	0.13	3.07	0.10	3.46	0.11	1.33	0.07	3.34	0.18	0.83	0.08	0.70	0.05
239	12.13	73.87	0.24	14.04	0.13	3.00	0.10	3.53	0.11	1.28	0.07	2.88	0.16	0.71	0.07	0.69	0.05
240	12.25	73.38	0.24	14.18	0.13	3.03	0.10	3.60	0.12	1.34	0.07	3.10	0.17	0.70	0.07	0.67	0.05
241	12.38	73.38	0.24	14.17	0.13	3.04	0.10	3.59	0.12	1.41	0.08	3.02	0.17	0.71	0.07	0.66	0.05
242	12.50	73.33	0.24	14.11	0.13	2.99	0.10	3.63	0.12	1.31	0.07	3.16	0.17	0.75	0.07	0.71	0.05
243	12.62	73.37	0.24	14.16	0.13	2.84	0.09	3.57	0.12	1.31	0.07	3.30	0.18	0.74	0.07	0.71	0.05
244	12.75	73.49	0.24	14.06	0.13	2.85	0.09	3.52	0.11	1.35	0.07	3.29	0.18	0.72	0.07	0.71	0.05
245	12.87	73.39	0.24	14.17	0.13	2.87	0.09	3.56	0.12	1.33	0.07	3.27	0.18	0.72	0.07	0.68	0.05
246	12.99	73.65	0.24	14.14	0.13	2.94	0.10	3.56	0.12	1.23	0.07	3.05	0.17	0.74	0.07	0.70	0.05
247	13.12	73.79	0.24	14.12	0.13	2.86	0.09	3.54	0.11	1.24	0.07	3.03	0.17	0.69	0.07	0.73	0.05
248	13.24	73.70	0.24	14.15	0.13	2.90	0.09	3.48	0.11	1.27	0.07	3.12	0.17	0.68	0.07	0.71	0.05
249	13.37	73.46	0.24	14.13	0.13	2.97	0.10	3.52	0.11	1.35	0.07	3.23	0.18	0.67	0.06	0.67	0.05
250	13.49	73.63	0.24	14.16	0.13	2.88	0.09	3.59	0.12	1.28	0.07	3.16	0.17	0.66	0.06	0.65	0.05
251	13.61	73.66	0.24	14.27	0.13	3.03	0.10	3.53	0.11	1.24	0.07	3.05	0.17	0.60	0.06	0.62	0.05
252	13.74	73.44	0.24	14.22	0.13	3.05	0.10	3.61	0.12	1.27	0.07	3.12	0.17	0.67	0.06	0.63	0.05
253	13.86	73.43	0.24	14.23	0.13	2.98	0.10	3.66	0.12	1.26	0.07	3.16	0.17	0.62	0.06	0.64	0.05
254	13.98	73.76	0.24	14.17	0.13	2.81	0.09	3.50	0.11	1.31	0.07	3.08	0.17	0.74	0.07	0.64	0.05
255	14.11	73.75	0.24	14.21	0.13	2.94	0.10	3.35	0.11	1.16	0.06	3.22	0.18	0.71	0.07	0.66	0.05
256	14.23	73.60	0.24	14.26	0.13	2.90	0.09	3.48	0.11	1.25	0.07	3.22	0.18	0.69	0.07	0.60	0.05
257	14.36	73.44	0.24	14.27	0.13	2.95	0.10	3.57	0.12	1.24	0.07	3.12	0.17	0.73	0.07	0.67	0.05
258	14.48	73.51	0.24	14.19	0.13	2.95	0.10	3.58	0.12	1.27	0.07	3.17	0.17	0.62	0.06	0.70	0.05
259	14.60	73.34	0.24	14.18	0.13	3.04	0.10	3.50	0.11	1.30	0.07	3.22	0.18	0.73	0.07	0.70	0.05
260	14.73	73.31	0.24	14.14	0.13	2.92	0.10	3.62	0.12	1.33	0.07	3.29	0.18	0.71	0.07	0.68	0.05
261	14.85	73.34	0.24	14.23	0.13	2.89	0.09	3.56	0.12	1.42	0.08	3.23	0.18	0.63	0.06	0.69	0.05
262	14.97	73.36	0.24	14.14	0.13	3.05	0.10	3.44	0.11	1.42	0.08	3.15	0.17	0.76	0.07	0.68	0.05
263	15.10	73.50	0.24	14.22	0.13	2.94	0.10	3.53	0.11	1.37	0.07	3.05	0.17	0.73	0.07	0.66	0.05
264	15.22	73.38	0.24	14.18	0.13	3.00	0.10	3.60	0.12	1.37	0.07	3.07	0.17	0.73	0.07	0.66	0.05
265	15.35	73.28	0.24	14.27	0.13	3.02	0.10	3.63	0.12	1.26	0.07	3.15	0.17	0.75	0.07	0.64	0.05
266	15.47	73.63	0.24	14.15	0.13	2.99	0.10	3.55	0.12	1.22	0.07	3.00	0.16	0.71	0.07	0.74	0.06
267	15.59	73.70	0.24	14.12	0.13	2.96	0.10	3.58	0.12	1.19	0.06	3.07	0.17	0.72	0.07	0.66	0.05
268	15.72	73.44	0.24	14.21	0.13	3.10	0.10	3.55	0.11	1.24	0.07	3.10	0.17	0.70	0.07	0.66	0.05
269	15.84	73.53	0.24	14.16	0.13	3.01	0.10	3.53	0.11	1.36	0.07	3.09	0.17	0.69	0.07	0.63	0.05
270	15.96	73.86	0.24	14.12	0.13	2.96	0.10	3.50	0.11	1.34	0.07	2.89	0.16	0.69	0.07	0.63	0.05
271	16.09	73.72	0.24	14.21	0.13	2.92	0.10	3.53	0.11	1.25	0.07	3.05	0.17	0.70	0.07	0.61	0.05
272	16.21	73.62	0.24	14.21	0.13	2.91	0.09	3.52	0.11	1.24	0.07	3.08	0.17	0.77	0.07	0.64	0.05
273	16.34	73.49	0.24	14.25	0.13	2.98	0.10	3.46	0.11	1.19	0.06	3.19	0.17	0.75	0.07	0.70	0.05
274	16.46	73.31	0.24	14.25	0.13	2.95	0.10	3.44	0.11	1.30	0.07	3.26	0.18	0.76	0.07	0.72	0.05
275	16.58	73.46	0.24	14.18	0.13	2.88	0.09	3.46	0.11	1.33	0.07	3.24	0.18	0.72	0.07	0.72	0.05
276	16.71	73.62	0.24	14.26	0.13	2.89	0.09	3.67	0.12	1.25	0.07	3.04	0.17	0.60	0.06	0.67	0.05
277	16.83	73.59	0.24	14.16	0.13	2.93	0.10	3.56	0.12	1.32	0.07	3.02	0.17	0.69	0.07	0.72	0.05
278	16.95	73.40	0.24	14.17	0.13	3.07	0.10	3.50	0.11	1.31	0.07	3.20	0.18	0.65	0.06	0.69	0.05
279	17.08	73.47	0.24	14.28	0.13	2.85	0.09	3.57	0.12	1.32	0.07	3.16	0.17	0.67	0.06	0.69	0.05
280	17.20	73.53	0.24	14.18	0.13	3.04	0.10	3.66	0.12	1.18	0.06	3.06	0.17	0.67	0.06	0.68	0.05
281	17.33	73.72	0.24	13.96	0.13	3.01	0.10	3.56	0.12	1.26	0.07	3.07	0.17	0.74	0.07	0.68	0.05
282	17.45	73.80	0.24	14.26	0.13	2.88	0.09	3.54	0.11	1.17	0.06	3.00	0.16	0.70	0.07	0.66	0.05
283	17.57	73.55	0.24	14.10	0.13	3.03	0.10	3.52	0.11	1.26	0.07	3.14	0.17	0.69	0.07	0.73	0.05
284	17.70	73.40	0.24	14.22	0.13	3.04	0.10	3.57	0.12	1.27	0.07	3.11	0.17	0.74	0.07	0.67	0.05
285	17.82	73.69	0.24	14.34	0.14	2.97	0.10	3.44	0.11	1.35	0.07	2.95	0.16	0.66	0.06	0.60	0.05
286	17.94	73.60	0.24	14.27	0.13	2.90	0.09	3.41	0.11	1.36	0.07	3.17	0.17	0.65	0.06	0.63	0.05
287	18.07	73.62	0.24	14.20	0.13	2.90	0.09	3.60	0.12	1.34	0.07	2.92	0.16	0.75	0.07	0.68	0.05
288	18.19	73.43	0.24	14.28	0.13	2.98	0.10	3.54	0.11	1.27	0.07	3.16	0.17	0.66	0.06	0.67	0.05
289	18.32	73.45	0.24	14.25	0.13	2.95	0.10	3.49	0.11	1.31	0.07	3.21	0.18	0.65	0.06	0.68	0.05
290	18.44	73.56	0.24	14.21	0.13	2.90	0.09	3.49	0.11	1.35	0.07	3.15	0.17	0.70	0.07	0.64	0.05
291	18.56	73.39	0.24	14.36	0.14	2.95	0.10	3.55	0.11	1.26	0.07	3.10	0.17	0.74	0.07	0.64	0.05
292	18.69	73.64	0.24	14.36	0.14	2.89	0.09	3.54	0.11	1.31	0.07	2.90	0.16	0.71	0.07	0.65	0.05
293	18.81	73.56	0.24	14.07	0.13	2.93	0.10	3.62	0.12	1.36	0.07	3.27	0.18	0.57	0.06	0.61	0.05
294	18.93	73.33	0.24	14.19	0.13	2.97	0.10	3.60	0.12	1.27	0.07	3.22	0.18	0.76	0.07	0.67	0.05
295	19.06	73.45	0.24	14.15	0.13	2.98	0.10	3.55	0.11	1.36	0.07	3.11	0.17	0.73	0.07	0.67	0.05
296	19.18	73.62	0.24	14.07	0.13	3.02	0.10	3.49	0.11	1.26	0.07	3.25	0.18	0.65	0.06	0.63	0.05
297	19.31	73.53	0.24	14.05	0.13	3.05	0.10	3.51	0.11	1.27	0.07	3.18	0.17	0.76	0.07	0.66	0.05

Agglomerate U4.2

Table J.32: Major element compositions (as wt.% oxides) from a line traverse across the interface of interior agglomerate U4.2 (from agglomerate U4.2 to host U4) extracted from quantified EDS compositional maps. The EDS compositional maps were collected at a resolution of 3.4 pixels/μm. The smoothing width for this traverse was 225 pixels (65.5 μm) wide. This is an Si interface and has been centered at $x = 0$ based on the SiO_2 maximum. Peak points within 2σ of the SiO_2 maximum are highlighted in yellow. Uncertainties are 2SEOM.

Pt.	Position (μm)	SiO_2	2σ	Al_2O_3	2σ	Na_2O	2σ	K_2O	2σ	CaO	2σ	FeO	2σ	TiO_2	2σ	MgO	2σ
1	-27.38	75.55	0.14	12.70	0.06	2.16	0.04	3.33	0.04	2.15	0.06	2.90	0.09	0.38	0.04	0.52	0.03
2	-27.09	75.67	0.14	12.62	0.06	2.13	0.04	3.36	0.04	2.14	0.06	2.90	0.09	0.38	0.04	0.48	0.03
3	-26.80	75.60	0.14	12.75	0.06	2.13	0.04	3.33	0.04	2.08	0.06	2.94	0.09	0.41	0.04	0.46	0.02
4	-26.51	75.80	0.14	12.70	0.06	2.10	0.04	3.31	0.04	2.11	0.06	2.78	0.08	0.42	0.04	0.50	0.03
5	-26.22	75.76	0.14	12.70	0.06	2.11	0.04	3.28	0.04	2.09	0.06	2.92	0.09	0.42	0.04	0.45	0.02
6	-25.93	75.64	0.14	12.65	0.06	2.12	0.04	3.31	0.04	2.19	0.07	2.89	0.09	0.41	0.04	0.46	0.02
7	-25.63	75.56	0.14	12.67	0.06	2.08	0.04	3.35	0.04	2.17	0.07	2.95	0.09	0.40	0.04	0.47	0.02
8	-25.34	75.87	0.14	12.68	0.06	2.11	0.04	3.30	0.04	2.11	0.06	2.78	0.08	0.39	0.04	0.48	0.03
9	-25.05	75.88	0.14	12.71	0.06	2.11	0.04	3.30	0.04	2.10	0.06	2.73	0.08	0.41	0.04	0.48	0.03
10	-24.76	75.87	0.14	12.64	0.06	2.10	0.04	3.27	0.04	2.09	0.06	2.83	0.08	0.43	0.04	0.48	0.03
11	-24.47	75.76	0.14	12.65	0.06	2.11	0.04	3.32	0.04	2.12	0.06	2.82	0.08	0.41	0.04	0.49	0.03
12	-24.18	75.71	0.14	12.68	0.06	2.13	0.04	3.32	0.04	2.09	0.06	2.88	0.09	0.42	0.04	0.45	0.02
13	-23.89	75.83	0.14	12.50	0.06	2.15	0.04	3.34	0.04	2.13	0.06	2.86	0.09	0.47	0.05	0.46	0.02
14	-23.59	75.69	0.14	12.58	0.06	2.15	0.04	3.34	0.04	2.17	0.07	2.89	0.09	0.41	0.04	0.49	0.03
15	-23.30	75.61	0.14	12.61	0.06	2.15	0.04	3.30	0.04	2.20	0.07	2.91	0.09	0.44	0.04	0.50	0.03
16	-23.01	75.71	0.14	12.52	0.06	2.14	0.04	3.32	0.04	2.13	0.06	2.97	0.09	0.42	0.04	0.47	0.03
17	-22.72	75.82	0.14	12.56	0.06	2.10	0.04	3.31	0.04	2.14	0.06	2.84	0.09	0.45	0.04	0.48	0.03
18	-22.43	75.83	0.14	12.59	0.06	2.11	0.04	3.33	0.04	2.15	0.06	2.77	0.08	0.41	0.04	0.48	0.03
19	-22.14	75.83	0.14	12.58	0.06	2.17	0.04	3.29	0.04	2.12	0.06	2.83	0.08	0.39	0.04	0.47	0.03
20	-21.85	75.94	0.14	12.53	0.06	2.11	0.04	3.29	0.04	2.08	0.06	2.86	0.09	0.39	0.04	0.48	0.03
21	-21.55	75.90	0.14	12.52	0.06	2.06	0.04	3.32	0.04	2.06	0.06	2.91	0.09	0.45	0.04	0.50	0.03
22	-21.26	75.84	0.14	12.52	0.06	2.11	0.04	3.27	0.04	2.09	0.06	2.99	0.09	0.38	0.04	0.49	0.03
23	-20.97	76.01	0.14	12.56	0.06	2.06	0.04	3.32	0.04	2.05	0.06	2.81	0.08	0.44	0.04	0.49	0.03
24	-20.68	75.84	0.14	12.51	0.06	2.13	0.04	3.31	0.04	2.06	0.06	2.97	0.09	0.43	0.04	0.45	0.02
25	-20.39	75.93	0.14	12.55	0.06	2.12	0.04	3.35	0.04	2.10	0.06	2.75	0.08	0.40	0.04	0.47	0.02
26	-20.10	76.03	0.14	12.51	0.06	2.09	0.04	3.36	0.04	2.03	0.06	2.84	0.09	0.37	0.04	0.47	0.03
27	-19.81	75.95	0.14	12.52	0.06	2.12	0.04	3.36	0.04	2.07	0.06	2.87	0.09	0.40	0.04	0.45	0.02
28	-19.52	75.95	0.14	12.56	0.06	2.12	0.04	3.37	0.04	2.08	0.06	2.82	0.08	0.38	0.04	0.43	0.02
29	-19.23	75.87	0.14	12.46	0.06	2.16	0.04	3.38	0.05	2.07	0.06	2.88	0.09	0.41	0.04	0.46	0.02
30	-18.93	75.95	0.14	12.47	0.06	2.06	0.04	3.39	0.05	2.09	0.06	2.85	0.09	0.38	0.04	0.47	0.02
31	-18.64	76.06	0.14	12.49	0.06	2.05	0.04	3.35	0.04	2.03	0.06	2.85	0.09	0.37	0.04	0.46	0.02
32	-18.35	76.09	0.14	12.47	0.06	2.04	0.04	3.38	0.04	2.04	0.06	2.88	0.09	0.38	0.04	0.43	0.02
33	-18.06	76.09	0.14	12.43	0.06	2.00	0.04	3.39	0.05	2.05	0.06	2.83	0.08	0.43	0.04	0.51	0.03
34	-17.77	76.14	0.14	12.45	0.06	2.09	0.04	3.37	0.04	1.98	0.06	2.81	0.08	0.40	0.04	0.50	0.03
35	-17.48	76.19	0.14	12.34	0.06	2.09	0.04	3.32	0.04	2.00	0.06	2.86	0.09	0.40	0.04	0.49	0.03
36	-17.19	76.11	0.14	12.39	0.06	2.08	0.04	3.34	0.04	2.00	0.06	2.88	0.09	0.43	0.04	0.50	0.03
37	-16.89	76.18	0.14	12.40	0.06	2.11	0.04	3.32	0.04	2.00	0.06	2.85	0.09	0.38	0.04	0.48	0.03
38	-16.60	76.17	0.14	12.40	0.06	2.13	0.04	3.33	0.04	2.00	0.06	2.81	0.08	0.39	0.04	0.47	0.02
39	-16.31	76.23	0.14	12.36	0.06	2.13	0.04	3.32	0.04	1.95	0.06	2.88	0.09	0.39	0.04	0.47	0.02
40	-16.02	76.31	0.14	12.39	0.06	2.11	0.04	3.31	0.04	1.89	0.06	2.83	0.08	0.40	0.04	0.48	0.03
41	-15.73	76.26	0.14	12.37	0.06	2.17	0.04	3.29	0.04	1.89	0.06	2.80	0.08	0.41	0.04	0.48	0.03
42	-15.44	76.37	0.14	12.30	0.06	2.11	0.04	3.35	0.04	1.89	0.06	2.80	0.08	0.39	0.04	0.48	0.03
43	-15.15	76.33	0.14	12.33	0.06	2.11	0.04	3.36	0.04	1.95	0.06	2.77	0.08	0.40	0.04	0.44	0.02
44	-14.86	76.34	0.14	12.31	0.06	2.13	0.04	3.32	0.04	1.97	0.06	2.75	0.08	0.44	0.04	0.44	0.02
45	-14.56	76.47	0.14	12.29	0.06	2.02	0.04	3.32	0.04	1.90	0.06	2.86	0.09	0.41	0.04	0.45	0.02
46	-14.27	76.52	0.14	12.20	0.06	2.06	0.04	3.31	0.04	1.86	0.06	2.85	0.09	0.43	0.04	0.49	0.03
47	-13.98	76.47	0.14	12.25	0.06	2.06	0.04	3.31	0.04	1.84	0.06	2.89	0.09	0.43	0.04	0.48	0.03
48	-13.69	76.41	0.14	12.29	0.06	2.09	0.04	3.35	0.04	1.87	0.06	2.75	0.08	0.45	0.04	0.46	0.02
49	-13.40	76.50	0.14	12.29	0.06	2.06	0.04	3.33	0.04	1.85	0.06	2.80	0.08	0.38	0.04	0.48	0.03
50	-13.11	76.61	0.14	12.22	0.06	2.07	0.04	3.31	0.04	1.88	0.06	2.79	0.08	0.38	0.04	0.46	0.02

51	-12.82	76.58	0.14	12.15	0.06	2.10	0.04	3.34	0.04	1.87	0.06	2.79	0.08	0.43	0.04	0.44	0.02
52	-12.53	76.65	0.14	12.14	0.06	2.09	0.04	3.30	0.04	1.82	0.05	2.82	0.08	0.41	0.04	0.45	0.02
53	-12.23	76.73	0.14	12.16	0.06	2.08	0.04	3.30	0.04	1.76	0.05	2.74	0.08	0.41	0.04	0.47	0.03
54	-11.94	76.74	0.14	12.14	0.06	2.03	0.04	3.30	0.04	1.78	0.05	2.83	0.09	0.42	0.04	0.48	0.03
55	-11.65	76.75	0.14	12.11	0.06	2.08	0.04	3.32	0.04	1.77	0.05	2.75	0.08	0.43	0.04	0.48	0.03
56	-11.36	76.72	0.14	12.09	0.06	2.13	0.04	3.35	0.04	1.79	0.05	2.76	0.08	0.42	0.04	0.48	0.03
57	-11.07	76.82	0.14	12.14	0.06	2.07	0.04	3.33	0.04	1.75	0.05	2.79	0.08	0.38	0.04	0.45	0.02
58	-10.78	76.72	0.14	12.09	0.06	2.10	0.04	3.31	0.04	1.84	0.06	2.81	0.08	0.43	0.04	0.46	0.02
59	-10.49	76.88	0.14	11.98	0.06	2.11	0.04	3.33	0.04	1.80	0.05	2.69	0.08	0.40	0.04	0.47	0.03
60	-10.20	76.92	0.14	12.02	0.06	2.09	0.04	3.32	0.04	1.73	0.05	2.75	0.08	0.36	0.03	0.45	0.02
61	-9.90	77.04	0.14	12.06	0.06	2.06	0.04	3.28	0.04	1.72	0.05	2.72	0.08	0.38	0.04	0.47	0.03
62	-9.61	77.12	0.14	11.98	0.06	2.04	0.04	3.27	0.04	1.73	0.05	2.71	0.08	0.40	0.04	0.47	0.03
63	-9.32	77.06	0.14	11.94	0.05	2.08	0.04	3.30	0.04	1.76	0.05	2.76	0.08	0.38	0.04	0.44	0.02
64	-9.03	77.11	0.14	11.92	0.05	2.05	0.04	3.28	0.04	1.72	0.05	2.77	0.08	0.40	0.04	0.45	0.02
65	-8.74	77.06	0.14	11.96	0.06	2.03	0.04	3.35	0.04	1.68	0.05	2.80	0.08	0.37	0.04	0.49	0.03
66	-8.45	76.97	0.14	11.95	0.05	2.01	0.04	3.38	0.05	1.68	0.05	2.82	0.08	0.43	0.04	0.45	0.02
67	-8.16	77.05	0.14	11.94	0.05	2.04	0.04	3.28	0.04	1.69	0.05	2.77	0.08	0.44	0.04	0.48	0.03
68	-7.87	77.34	0.14	11.88	0.05	2.02	0.04	3.29	0.04	1.70	0.05	2.65	0.08	0.39	0.04	0.45	0.02
69	-7.57	77.30	0.14	11.86	0.05	2.04	0.04	3.30	0.04	1.62	0.05	2.70	0.08	0.40	0.04	0.45	0.02
70	-7.28	77.24	0.14	11.92	0.05	2.03	0.04	3.34	0.04	1.56	0.05	2.71	0.08	0.40	0.04	0.44	0.02
71	-6.99	77.38	0.14	11.85	0.05	2.05	0.04	3.28	0.04	1.61	0.05	2.68	0.08	0.38	0.04	0.48	0.03
72	-6.70	77.36	0.14	11.82	0.05	1.99	0.04	3.33	0.04	1.63	0.05	2.75	0.08	0.37	0.04	0.47	0.02
73	-6.41	77.31	0.14	11.83	0.05	2.08	0.04	3.34	0.04	1.55	0.05	2.80	0.08	0.35	0.03	0.44	0.02
74	-6.12	77.31	0.14	11.85	0.05	2.05	0.04	3.34	0.04	1.56	0.05	2.73	0.08	0.42	0.04	0.45	0.02
75	-5.83	77.40	0.14	11.71	0.05	2.02	0.04	3.34	0.04	1.59	0.05	2.77	0.08	0.42	0.04	0.45	0.02
76	-5.53	77.36	0.14	11.76	0.05	2.04	0.04	3.35	0.04	1.60	0.05	2.78	0.08	0.38	0.04	0.44	0.02
77	-5.24	77.62	0.14	11.71	0.05	2.03	0.04	3.33	0.04	1.56	0.05	2.59	0.08	0.39	0.04	0.47	0.03
78	-4.95	77.58	0.14	11.73	0.05	2.01	0.04	3.31	0.04	1.53	0.05	2.70	0.08	0.42	0.04	0.45	0.02
79	-4.66	77.57	0.14	11.68	0.05	2.01	0.04	3.31	0.04	1.51	0.05	2.76	0.08	0.42	0.04	0.46	0.02
80	-4.37	77.46	0.14	11.75	0.05	2.03	0.04	3.35	0.04	1.53	0.05	2.70	0.08	0.42	0.04	0.46	0.02
81	-4.08	77.61	0.14	11.79	0.05	1.99	0.04	3.34	0.04	1.47	0.04	2.62	0.08	0.46	0.04	0.45	0.02
82	-3.79	77.66	0.14	11.64	0.05	1.97	0.04	3.41	0.05	1.51	0.05	2.70	0.08	0.38	0.04	0.44	0.02
83	-3.50	77.73	0.14	11.67	0.05	2.02	0.04	3.35	0.04	1.45	0.04	2.69	0.08	0.36	0.04	0.46	0.02
84	-3.20	77.69	0.14	11.63	0.05	2.01	0.04	3.35	0.04	1.44	0.04	2.72	0.08	0.38	0.04	0.46	0.02
85	-2.91	77.76	0.14	11.57	0.05	1.99	0.04	3.34	0.04	1.45	0.04	2.73	0.08	0.41	0.04	0.45	0.02
86	-2.62	78.00	0.14	11.53	0.05	1.96	0.04	3.33	0.04	1.38	0.04	2.68	0.08	0.41	0.04	0.44	0.02
87	-2.33	77.89	0.14	11.56	0.05	1.99	0.04	3.36	0.04	1.40	0.04	2.64	0.08	0.40	0.04	0.46	0.02
88	-2.04	77.80	0.14	11.54	0.05	2.00	0.04	3.33	0.04	1.39	0.04	2.81	0.08	0.40	0.04	0.45	0.02
89	-1.75	77.73	0.14	11.56	0.05	1.97	0.04	3.41	0.05	1.39	0.04	2.76	0.08	0.40	0.04	0.45	0.02
90	-1.46	77.90	0.14	11.54	0.05	1.95	0.04	3.40	0.05	1.35	0.04	2.67	0.08	0.40	0.04	0.47	0.02
91	-1.16	78.01	0.14	11.56	0.05	1.99	0.04	3.33	0.04	1.35	0.04	2.63	0.08	0.38	0.04	0.46	0.02
92	-0.87	78.04	0.14	11.49	0.05	2.01	0.04	3.32	0.04	1.33	0.04	2.68	0.08	0.39	0.04	0.48	0.03
93	-0.58	78.06	0.14	11.49	0.05	2.00	0.04	3.35	0.04	1.33	0.04	2.63	0.08	0.45	0.04	0.43	0.02
94	-0.29	78.04	0.14	11.44	0.05	1.99	0.04	3.41	0.05	1.35	0.04	2.64	0.08	0.40	0.04	0.44	0.02
95	0.00	78.12	0.14	11.46	0.05	1.95	0.04	3.37	0.04	1.32	0.04	2.63	0.08	0.41	0.04	0.45	0.02
96	0.29	77.95	0.14	11.52	0.05	1.99	0.04	3.37	0.04	1.35	0.04	2.70	0.08	0.38	0.04	0.47	0.02
97	0.58	77.94	0.14	11.47	0.05	2.01	0.04	3.38	0.05	1.30	0.04	2.71	0.08	0.40	0.04	0.51	0.03
98	0.87	77.95	0.14	11.47	0.05	1.99	0.04	3.37	0.04	1.31	0.04	2.76	0.08	0.41	0.04	0.46	0.02
99	1.16	77.99	0.14	11.52	0.05	1.97	0.04	3.36	0.04	1.32	0.04	2.74	0.08	0.40	0.04	0.44	0.02
100	1.46	77.87	0.14	11.57	0.05	1.97	0.04	3.34	0.04	1.31	0.04	2.79	0.08	0.39	0.04	0.45	0.02
101	1.75	77.98	0.14	11.59	0.05	2.02	0.04	3.38	0.05	1.27	0.04	2.60	0.08	0.40	0.04	0.41	0.02
102	2.04	77.88	0.14	11.63	0.05	1.98	0.04	3.43	0.05	1.31	0.04	2.64	0.08	0.38	0.04	0.44	0.02
103	2.33	77.76	0.14	11.65	0.05	2.00	0.04	3.40	0.05	1.29	0.04	2.71	0.08	0.46	0.05	0.44	0.02
104	2.62	77.67	0.14	11.69	0.05	1.99	0.04	3.44	0.05	1.28	0.04	2.71	0.08	0.47	0.05	0.42	0.02
105	2.91	77.54	0.14	11.72	0.05	2.06	0.04	3.41	0.05	1.32	0.04	2.76	0.08	0.41	0.04	0.45	0.02
106	3.20	77.61	0.14	11.66	0.05	2.02	0.04	3.41	0.05	1.33	0.04	2.75	0.08	0.44	0.04	0.45	0.02
107	3.50	77.49	0.14	11.75	0.05	2.04	0.04	3.46	0.05	1.32	0.04	2.77	0.08	0.42	0.04	0.46	0.02
108	3.79	77.48	0.14	11.80	0.05	2.03	0.04	3.45	0.05	1.32	0.04	2.74	0.08	0.44	0.04	0.48	0.03
109	4.08	77.63	0.14	11.83	0.05	2.00	0.04	3.43	0.05	1.26	0.04	2.63	0.08	0.42	0.04	0.48	0.03
110	4.37	77.28	0.14	11.92	0.05	2.09	0.04	3.49	0.05	1.34	0.04	2.70	0.08	0.40	0.04	0.51	0.03
111	4.66	77.14	0.14	11.96	0.06	2.11	0.04	3.42	0.05	1.36	0.04	2.81	0.08	0.44	0.04	0.46	0.02
112	4.95	77.09	0.14	12.04	0.06	2.12	0.04	3.46	0.05	1.38	0.04	2.77	0.08	0.41	0.04	0.47	0.02

113	5.24	76.83	0.14	12.14	0.06	2.10	0.04	3.42	0.05	1.39	0.04	2.92	0.09	0.38	0.04	0.49	0.03
114	5.53	76.73	0.14	12.18	0.06	2.13	0.04	3.49	0.05	1.39	0.04	2.88	0.09	0.38	0.04	0.49	0.03
115	5.83	76.64	0.14	12.30	0.06	2.12	0.04	3.45	0.05	1.40	0.04	2.94	0.09	0.39	0.04	0.50	0.03
116	6.12	76.71	0.14	12.33	0.06	2.07	0.04	3.47	0.05	1.39	0.04	2.79	0.08	0.43	0.04	0.51	0.03
117	6.41	76.50	0.14	12.39	0.06	2.09	0.04	3.46	0.05	1.43	0.04	2.89	0.09	0.46	0.04	0.52	0.03
118	6.70	76.32	0.14	12.49	0.06	2.11	0.04	3.47	0.05	1.48	0.04	2.88	0.09	0.46	0.04	0.51	0.03
119	6.99	76.25	0.14	12.52	0.06	2.13	0.04	3.48	0.05	1.47	0.04	2.90	0.09	0.43	0.04	0.53	0.03
120	7.28	76.16	0.14	12.60	0.06	2.16	0.04	3.49	0.05	1.44	0.04	2.91	0.09	0.44	0.04	0.53	0.03
121	7.57	76.02	0.14	12.69	0.06	2.18	0.04	3.49	0.05	1.47	0.04	2.94	0.09	0.42	0.04	0.51	0.03
122	7.87	75.87	0.14	12.68	0.06	2.15	0.04	3.53	0.05	1.48	0.04	3.08	0.09	0.39	0.04	0.53	0.03
123	8.16	75.82	0.14	12.75	0.06	2.17	0.04	3.52	0.05	1.51	0.05	3.01	0.09	0.38	0.04	0.55	0.03
124	8.45	75.66	0.14	12.83	0.06	2.15	0.04	3.54	0.05	1.57	0.05	3.00	0.09	0.42	0.04	0.54	0.03
125	8.74	75.59	0.14	12.87	0.06	2.16	0.04	3.53	0.05	1.54	0.05	3.02	0.09	0.45	0.04	0.54	0.03
126	9.03	75.52	0.14	12.88	0.06	2.16	0.04	3.55	0.05	1.60	0.05	2.98	0.09	0.46	0.05	0.54	0.03
127	9.32	75.29	0.14	13.01	0.06	2.21	0.04	3.51	0.05	1.56	0.05	3.13	0.09	0.46	0.05	0.55	0.03
128	9.61	75.32	0.14	13.05	0.06	2.19	0.04	3.54	0.05	1.58	0.05	3.04	0.09	0.42	0.04	0.55	0.03
129	9.90	75.11	0.14	13.13	0.06	2.18	0.04	3.56	0.05	1.58	0.05	3.10	0.09	0.47	0.05	0.51	0.03
130	10.20	75.20	0.14	13.13	0.06	2.18	0.04	3.54	0.05	1.59	0.05	3.14	0.09	0.41	0.04	0.51	0.03
131	10.49	75.15	0.14	13.20	0.06	2.16	0.04	3.54	0.05	1.59	0.05	3.08	0.09	0.44	0.04	0.54	0.03
132	10.78	74.94	0.14	13.28	0.06	2.21	0.04	3.54	0.05	1.60	0.05	3.10	0.09	0.45	0.04	0.58	0.03
133	11.07	74.85	0.14	13.30	0.06	2.24	0.04	3.55	0.05	1.62	0.05	3.09	0.09	0.48	0.05	0.55	0.03
134	11.36	74.79	0.14	13.38	0.06	2.25	0.04	3.54	0.05	1.64	0.05	3.07	0.09	0.45	0.04	0.54	0.03
135	11.65	74.76	0.14	13.38	0.06	2.20	0.04	3.53	0.05	1.63	0.05	3.21	0.10	0.43	0.04	0.57	0.03
136	11.94	74.69	0.14	13.43	0.06	2.24	0.04	3.55	0.05	1.67	0.05	3.08	0.09	0.43	0.04	0.57	0.03
137	12.23	74.67	0.14	13.42	0.06	2.22	0.04	3.55	0.05	1.71	0.05	3.15	0.09	0.44	0.04	0.57	0.03
138	12.53	74.63	0.14	13.46	0.06	2.21	0.04	3.55	0.05	1.70	0.05	3.08	0.09	0.44	0.04	0.57	0.03
139	12.82	74.37	0.14	13.46	0.06	2.26	0.04	3.56	0.05	1.68	0.05	3.28	0.10	0.51	0.05	0.56	0.03
140	13.11	74.57	0.14	13.51	0.06	2.22	0.04	3.55	0.05	1.63	0.05	3.15	0.09	0.49	0.05	0.58	0.03
141	13.40	74.52	0.14	13.50	0.06	2.23	0.04	3.58	0.05	1.65	0.05	3.13	0.09	0.49	0.05	0.58	0.03
142	13.69	74.61	0.14	13.49	0.06	2.21	0.04	3.57	0.05	1.60	0.05	3.16	0.09	0.49	0.05	0.58	0.03
143	13.98	74.55	0.14	13.52	0.06	2.21	0.04	3.58	0.05	1.60	0.05	3.22	0.10	0.47	0.05	0.53	0.03
144	14.27	74.53	0.14	13.48	0.06	2.22	0.04	3.55	0.05	1.65	0.05	3.27	0.10	0.46	0.05	0.55	0.03
145	14.56	74.27	0.14	13.49	0.06	2.27	0.04	3.59	0.05	1.67	0.05	3.30	0.10	0.48	0.05	0.61	0.03
146	14.86	74.25	0.14	13.54	0.06	2.25	0.04	3.62	0.05	1.70	0.05	3.24	0.10	0.52	0.05	0.59	0.03
147	15.15	74.21	0.14	13.58	0.06	2.25	0.04	3.64	0.05	1.63	0.05	3.24	0.10	0.52	0.05	0.61	0.03
148	15.44	74.27	0.14	13.56	0.06	2.24	0.04	3.64	0.05	1.65	0.05	3.25	0.10	0.47	0.05	0.58	0.03
149	15.73	74.38	0.14	13.56	0.06	2.27	0.04	3.63	0.05	1.66	0.05	3.20	0.10	0.47	0.05	0.56	0.03
150	16.02	74.41	0.14	13.55	0.06	2.27	0.04	3.62	0.05	1.65	0.05	3.18	0.10	0.47	0.05	0.59	0.03
151	16.31	74.36	0.14	13.62	0.06	2.22	0.04	3.66	0.05	1.61	0.05	3.18	0.10	0.45	0.04	0.59	0.03
152	16.60	74.39	0.14	13.60	0.06	2.24	0.04	3.59	0.05	1.60	0.05	3.20	0.10	0.45	0.04	0.61	0.03
153	16.90	74.33	0.14	13.62	0.06	2.26	0.04	3.61	0.05	1.60	0.05	3.22	0.10	0.47	0.05	0.59	0.03
154	17.19	74.26	0.14	13.63	0.06	2.27	0.04	3.67	0.05	1.62	0.05	3.22	0.10	0.43	0.04	0.59	0.03
155	17.48	74.27	0.14	13.60	0.06	2.27	0.04	3.61	0.05	1.58	0.05	3.30	0.10	0.44	0.04	0.58	0.03
156	17.77	74.29	0.14	13.57	0.06	2.25	0.04	3.63	0.05	1.65	0.05	3.33	0.10	0.45	0.04	0.56	0.03
157	18.06	74.26	0.14	13.61	0.06	2.24	0.04	3.67	0.05	1.66	0.05	3.21	0.10	0.47	0.05	0.57	0.03
158	18.35	74.32	0.14	13.64	0.06	2.24	0.04	3.59	0.05	1.61	0.05	3.19	0.10	0.48	0.05	0.60	0.03
159	18.64	74.29	0.14	13.65	0.06	2.20	0.04	3.62	0.05	1.59	0.05	3.26	0.10	0.49	0.05	0.59	0.03
160	18.93	74.22	0.14	13.68	0.06	2.29	0.04	3.60	0.05	1.60	0.05	3.25	0.10	0.49	0.05	0.59	0.03
161	19.23	74.15	0.14	13.68	0.06	2.21	0.04	3.66	0.05	1.59	0.05	3.35	0.10	0.49	0.05	0.57	0.03
162	19.52	74.06	0.14	13.63	0.06	2.23	0.04	3.70	0.05	1.63	0.05	3.35	0.10	0.48	0.05	0.61	0.03
163	19.81	74.31	0.14	13.64	0.06	2.26	0.04	3.60	0.05	1.57	0.05	3.25	0.10	0.45	0.04	0.60	0.03
164	20.10	74.22	0.14	13.70	0.06	2.26	0.04	3.57	0.05	1.60	0.05	3.31	0.10	0.45	0.04	0.58	0.03
165	20.39	74.33	0.14	13.66	0.06	2.33	0.05	3.65	0.05	1.58	0.05	3.14	0.09	0.44	0.04	0.59	0.03
166	20.68	74.39	0.14	13.69	0.06	2.27	0.04	3.64	0.05	1.56	0.05	3.13	0.09	0.50	0.05	0.57	0.03
167	20.97	74.40	0.14	13.62	0.06	2.26	0.04	3.61	0.05	1.59	0.05	3.16	0.09	0.50	0.05	0.61	0.03
168	21.27	74.27	0.14	13.66	0.06	2.24	0.04	3.65	0.05	1.62	0.05	3.22	0.10	0.47	0.05	0.60	0.03
169	21.56	74.22	0.14	13.55	0.06	2.23	0.04	3.69	0.05	1.58	0.05	3.31	0.10	0.49	0.05	0.62	0.03
170	21.85	74.26	0.14	13.58	0.06	2.24	0.04	3.69	0.05	1.60	0.05	3.26	0.10	0.51	0.05	0.58	0.03
171	22.14	74.28	0.14	13.64	0.06	2.28	0.04	3.64	0.05	1.56	0.05	3.22	0.10	0.50	0.05	0.57	0.03
172	22.43	74.34	0.14	13.62	0.06	2.29	0.04	3.64	0.05	1.57	0.05	3.13	0.09	0.51	0.05	0.59	0.03

Appendix K

NanoSIMS interface scans

$^{235}U/^{238}U$, $(^{235}U + ^{238}U)/^{30}Si$, $(^{235}U + ^{238}U)/^{42}Ca$ ratios of traverses across compositional interfaces extracted using from NanoSIMS isotope ratio raster images using L'Image SIMS image processing software. Ratios have been corrected for fractionation. Despite the observed enrichment of SiO_2 at Si interfaces and near some CaMgFe interfaces, the relative enrichment in SiO_2 is usually <10% (as discussed in Chapter 8), so the $U/^{30}Si$ ratio serves as a proxy for the change in U concentration at the interface. Included interfaces are U1B.L (an interior agglomerate with a Si interface), FLD14.L (an exterior agglomerate with a CaMgFe interface), FLD23.L (an exterior agglomerate with a Si interface), FLD4.3.3 (an interior agglomerate with a Si interface), and FLD10.L (a double-layered interface with overlaying CaMgFe and Si interfaces). Peak points are highlighted in yellow. How linear traverses across interfaces using NanoSIMS isotope ratio images are extracted and processed are discussed in Chapter 9.

U1B.L

Table K.1: Isotope ratios of a linear traverse across the Si interface U1B.L (beginning in U1B.L and ending in the host U1B) extracted from NanoSIMS rasters using L'image. The location of the interface is highlighted in yellow and was identified by visual inspection and the location of the U/^{42}Ca maximum (caused by a depletion in Ca and invariability in the ^{235}U/^{238}U ratio across the interface). Uncertainties are 2σ.

Index	Position (μm)	^{235}U/^{238}U	2σ	U/^{30}Si	2σ	U/^{42}Ca	2σ
1	0.00	8.06	0.44	1.99E-04	5.80E-05	6.47E-02	3.80E-03
2	1.09	7.43	0.37	1.98E-04	5.77E-05	6.72E-02	3.92E-03
3	2.18	8.91	0.50	1.91E-04	5.57E-05	6.93E-02	4.06E-03
4	3.27	8.95	0.57	1.78E-04	5.22E-05	6.75E-02	4.03E-03
5	4.36	8.22	0.50	1.68E-04	4.90E-05	6.74E-02	4.02E-03
6	5.45	7.64	0.44	1.68E-04	4.91E-05	7.21E-02	4.29E-03
7	6.54	7.10	0.46	1.50E-04	4.38E-05	7.15E-02	4.36E-03
8	7.63	9.02	0.63	1.42E-04	4.14E-05	7.72E-02	4.69E-03
9	8.72	9.42	0.68	1.23E-04	3.59E-05	8.10E-02	4.92E-03
10	9.81	8.63	0.65	1.17E-04	3.43E-05	9.77E-02	6.05E-03
11	10.90	8.19	0.58	1.14E-04	3.35E-05	1.15E-01	7.09E-03
12	11.99	8.13	0.53	1.20E-04	3.50E-05	1.27E-01	7.67E-03
13	13.08	8.54	0.61	1.12E-04	3.27E-05	1.09E-01	6.70E-03
14	14.17	6.83	0.46	1.10E-04	3.21E-05	9.18E-02	5.68E-03
15	15.26	6.86	0.41	1.17E-04	3.42E-05	8.27E-02	4.99E-03
16	16.35	7.48	0.47	1.15E-04	3.36E-05	7.20E-02	4.35E-03
17	17.44	6.03	0.35	1.19E-04	3.48E-05	6.75E-02	4.09E-03
18	18.53	7.62	0.44	1.12E-04	3.28E-05	5.98E-02	3.55E-03
19	19.61	7.38	0.47	1.06E-04	3.10E-05	5.42E-02	3.29E-03

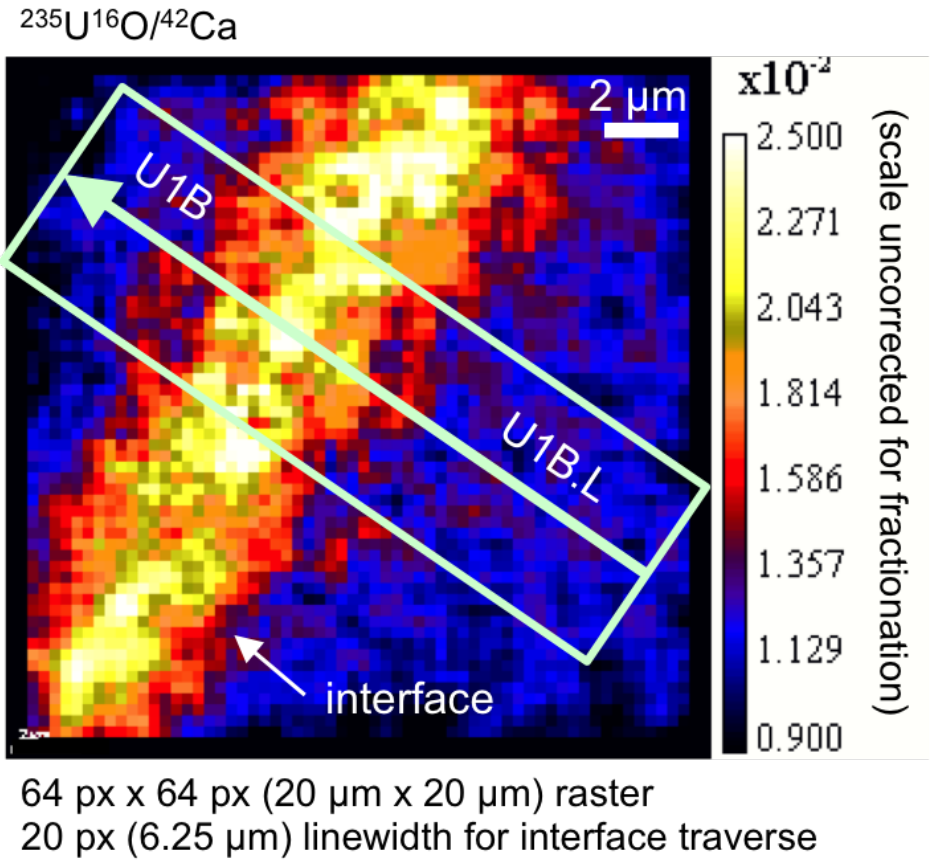

Figure K.1: Location and smoothing width of the linear traverse across the Si interface of U1B.L (interior agglomerate) extracted from NanoSIMS raster analyses (shown overlaid with the $^{235}U^{16}O/^{42}Ca$ isotope ratio image). The dimensions of the NanoSIMS raster are 20 μm $\times$ 20 μm with a resolution of 64 px $\times$ 64 px. The extracted traverse has a smoothing width of 20 pixels (6.25 μm) wide and begins in U1B.L (bottom right of the image), traverses the interface, and ends in the host U1B.L (top left of the image).

FLD14.L

Table K.2: Isotope ratios of a linear traverse across the CaMgFe interface of FLD14.L (beginning in FLD14.L and ending in the host FLD14) extracted from NanoSIMS rasters using L'image. The location of the interface is highlighted in yellow and was identified by visual inspection and the location of the $^{235}U/^{238}U$, $U/^{30}Si$, and $U/^{42}Ca$ maxima, which are coincident. Uncertainties are 2σ.

Index	Position (μm)	$^{235}U/^{238}U$	2σ	$U/^{30}Si$	2σ	$U/^{42}Ca$	2σ
1	0.00	3.01	0.28	1.03E-04	1.71E-05	2.38E-02	2.22E-03
2	0.79	2.94	0.24	1.27E-04	2.07E-05	2.91E-02	2.61E-03
3	1.57	4.54	0.48	1.14E-04	1.88E-05	2.53E-02	2.31E-03
4	2.36	3.98	0.39	1.20E-04	1.97E-05	2.50E-02	2.27E-03
5	3.15	3.75	0.37	1.11E-04	1.83E-05	2.13E-02	1.96E-03
6	3.94	4.60	0.46	1.19E-04	1.94E-05	2.07E-02	1.84E-03
7	4.72	4.45	0.43	1.17E-04	1.90E-05	1.82E-02	1.62E-03
8	5.51	4.76	0.36	1.71E-04	2.71E-05	2.37E-02	1.93E-03
9	6.30	4.84	0.30	2.36E-04	3.71E-05	3.09E-02	2.43E-03
10	7.08	5.49	0.34	2.56E-04	4.01E-05	3.18E-02	2.46E-03
11	7.87	5.41	0.43	1.86E-04	2.96E-05	2.02E-02	1.64E-03
12	8.66	4.59	0.44	9.82E-05	1.60E-05	1.07E-02	9.47E-04

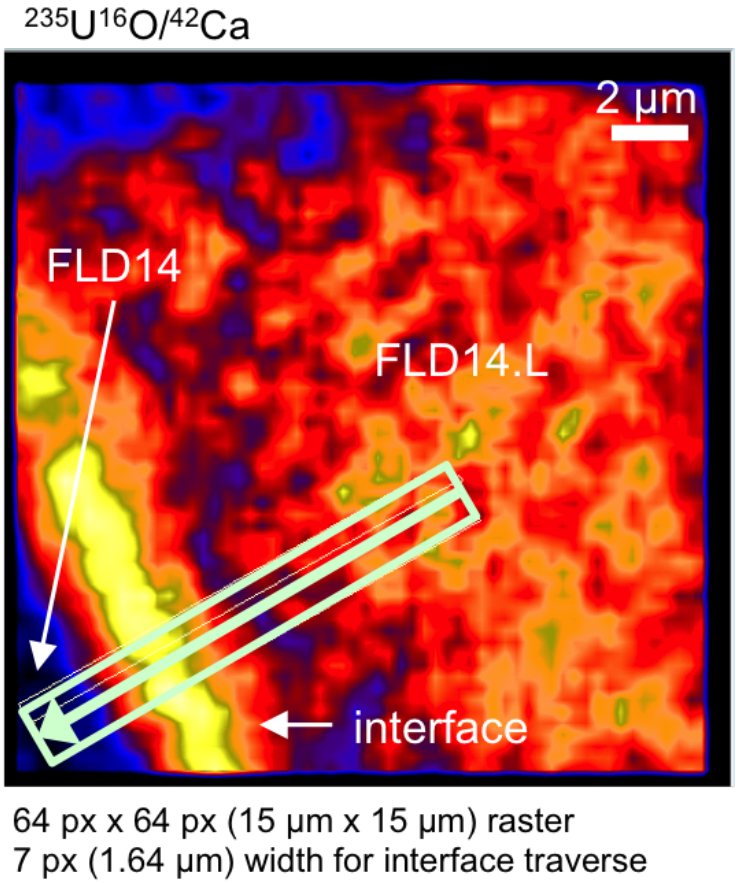

Figure K.2: Location and smoothing width of the linear traverse across the CaMgFe interface of FLD14.L (exterior agglomerate) extracted from NanoSIMS raster analyses (shown overlaid with the $^{235}U^{16}O/^{42}Ca$ isotope ratio image). The dimensions of the NanoSIMS raster are 15 μm × 15 μm with a resolution of 64 px × 64 px. The extracted traverse has a smoothing width of 7 pixels (1.65 μm) wide and begins in FLD14.L (right side of the image), traverses the interface, and ends in the host FLD14 (bottom left corner of the image).

FLD23.L

Table K.3: Isotope ratios of a linear traverse across the Si interface of FLD23.L (beginning in FLD23.L and ending in the host FLD23) extracted from NanoSIMS rasters using L'image. The location of the interface is highlighted in yellow and was identified by visual inspection and the location of the U/^{30}Si minimum (which is approximately coincident with the U/^{42}Ca minimum). Uncertainties are 2σ.

Index	Position (μm)	^{235}U/^{238}U	2σ	U/^{30}Si	2σ	U/^{42}Ca	2σ
1	0.00	3.70	0.16	1.29E-04	3.76E-05	2.00E-02	1.19E-03
2	0.69	4.01	0.17	1.46E-04	4.26E-05	2.17E-02	1.28E-03
3	1.38	3.90	0.15	1.65E-04	4.82E-05	2.42E-02	1.41E-03
4	2.07	3.62	0.14	1.60E-04	4.68E-05	2.30E-02	1.35E-03
5	2.76	3.72	0.14	1.62E-04	4.73E-05	2.31E-02	1.35E-03
6	3.45	3.67	0.14	1.69E-04	4.94E-05	2.44E-02	1.42E-03
7	4.14	4.05	0.16	1.58E-04	4.62E-05	2.33E-02	1.36E-03
8	4.84	3.28	0.13	1.38E-04	4.03E-05	2.12E-02	1.25E-03
9	5.53	4.04	0.19	1.14E-04	3.34E-05	1.91E-02	1.14E-03
10	6.22	3.59	0.18	8.82E-05	2.58E-05	1.64E-02	1.00E-03
11	6.91	4.60	0.26	7.68E-05	2.25E-05	1.63E-02	1.01E-03
12	7.60	5.51	0.34	7.07E-05	2.07E-05	1.71E-02	1.06E-03
13	8.29	4.76	0.25	7.49E-05	2.19E-05	2.28E-02	1.38E-03
14	8.98	5.90	0.32	8.57E-05	2.51E-05	2.60E-02	1.55E-03
15	9.67	7.03	0.35	9.98E-05	2.92E-05	3.35E-02	1.96E-03
16	10.36	5.79	0.25	1.35E-04	3.96E-05	3.63E-02	2.11E-03
17	11.05	5.97	0.25	1.48E-04	4.32E-05	3.73E-02	2.14E-03
18	11.74	5.88	0.24	1.71E-04	5.01E-05	3.97E-02	2.28E-03
19	12.43	5.84	0.23	1.72E-04	5.01E-05	3.89E-02	2.24E-03

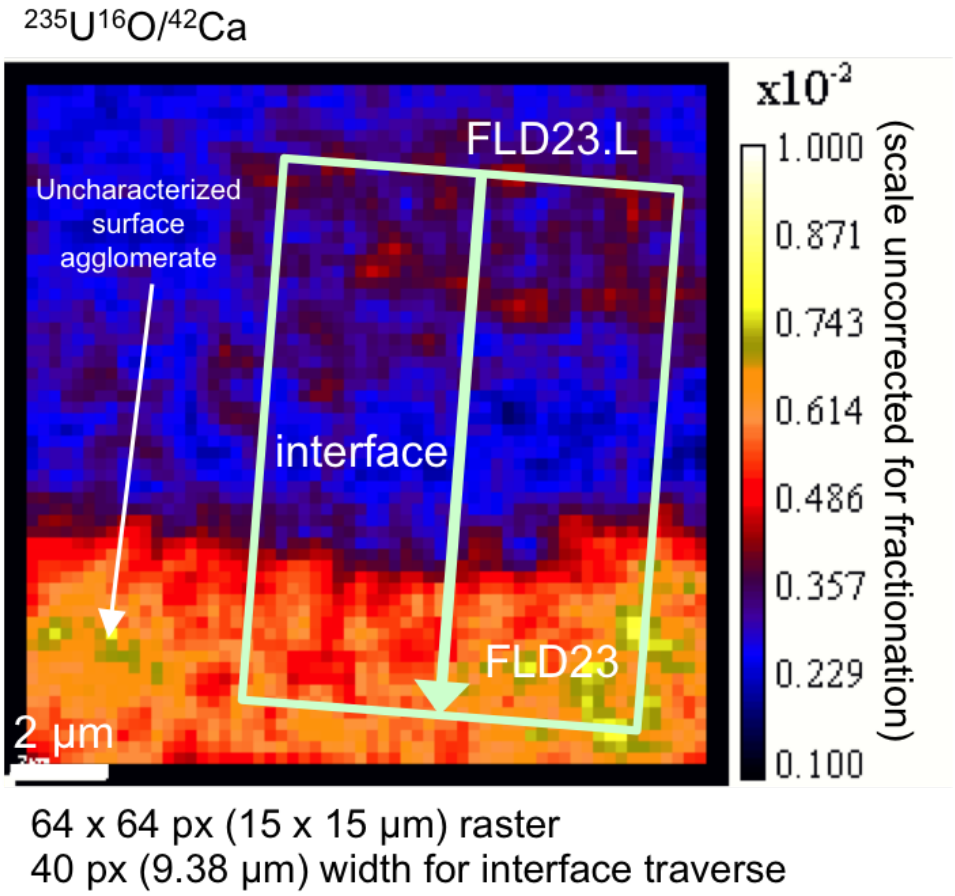

Figure K.3: Location and smoothing width of the linear traverse across the Si interface of FLD23.L extracted from NanoSIMS raster analyses (shown overlaid with the $^{235}U^{16}O/^{42}Ca$ isotope ratio image). The dimensions of the NanoSIMS raster are 15 μm × 15 μm with a resolution of 64 px × 64 px. The extracted traverse has a smoothing width of 40 pixels (∼9.38 μm) wide and begins in FLD23.L (top of the image), traverses the interface, and ends in the host FLD23 (bottom of image). There is an uncharacterized surface agglomerate visible in the bottom left of the image.

FLD4.3.3

Table K.4: Isotope ratios of a linear traverse across the Si interface of FLD4.3.3 (beginning in FLD4.3.3 and ending in the host FLD4.3) extracted from NanoSIMS rasters using L'image. The location of the interface is highlighted in yellow and was identified by visual inspection and the location of the U/^{42}Ca maximum, due to the slight depletion of Ca at the interface. Uncertainties are 2σ.

Index	Position (μm)	^{235}U/^{238}U	2σ	U/^{30}Si	2σ	U/^{42}Ca	2σ
1	0.00	10.08	0.76	1.83E-04	5.36E-05	1.03E-01	6.30E-03
2	0.97	9.79	0.71	2.08E-04	6.08E-05	1.16E-01	7.03E-03
3	1.95	9.46	0.67	2.18E-04	6.39E-05	1.21E-01	7.33E-03
4	2.92	9.17	0.67	2.08E-04	6.10E-05	1.16E-01	7.10E-03
5	3.89	10.16	0.79	2.04E-04	5.98E-05	1.14E-01	6.98E-03
6	4.87	7.97	0.57	2.04E-04	5.96E-05	1.09E-01	6.74E-03
7	5.84	9.20	0.68	2.17E-04	6.35E-05	1.11E-01	6.81E-03
8	6.81	9.37	0.72	2.03E-04	5.94E-05	9.83E-02	6.07E-03
9	7.79	7.89	0.58	1.97E-04	5.76E-05	8.74E-02	5.44E-03
10	8.76	8.26	0.62	1.98E-04	5.81E-05	8.16E-02	5.06E-03
11	9.73	7.09	0.51	1.91E-04	5.60E-05	7.34E-02	4.58E-03
12	10.71	9.34	0.74	1.87E-04	5.47E-05	6.71E-02	4.17E-03
13	11.68	6.45	0.44	1.91E-04	5.61E-05	6.54E-02	4.07E-03
14	12.65	6.85	0.46	1.94E-04	5.67E-05	6.40E-02	3.96E-03
15	13.62	6.59	0.44	1.86E-04	5.45E-05	5.94E-02	3.68E-03

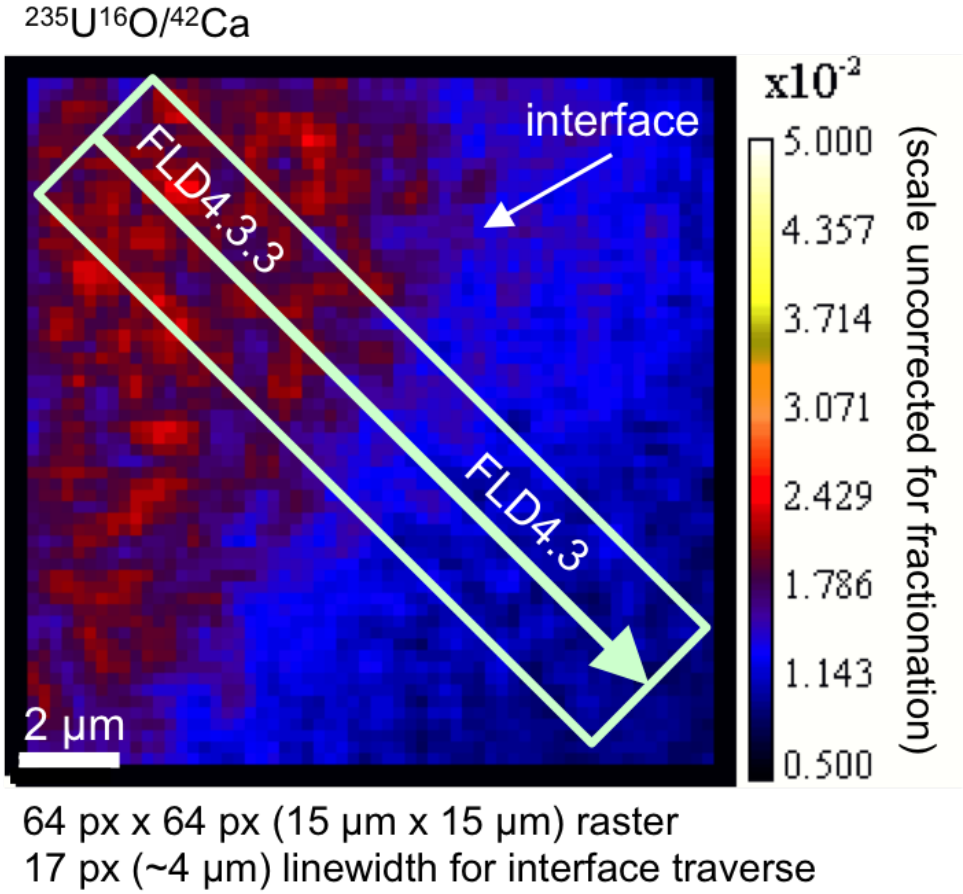

Figure K.4: Location and smoothing width of the linear traverse across the Si interface of FLD4.3.3 extracted from NanoSIMS raster analyses (shown overlaid with the $^{235}U^{16}O/^{42}Ca$ isotope ratio image). The dimensions of the NanoSIMS raster are 15 μm $\times$ 15 μm with a resolution of 64 px $\times$ 64 px. The extracted traverse has a smoothing width of 17 pixels ($\sim$4 μm) wide and begins in FLD4.3.3 (top left of the image), traverses the interface, and ends in the host FLD4.3 (bottom right of the image).

FLD10.L

Table K.5: Isotope ratios of a linear traverse across the double-layered CaMgFe and Si interface of FLD10.L (beginning in CaMgFe interface and ending in the host FLD10.L) extracted from NanoSIMS rasters using L'image. The location of the interfaces are highlighted in yellow and was identified by visual inspection and the location of the U/^{30}Si maximum (for the CaMgFe interface, which appears first) and minimum (for the Si interface). Uncertainties are 2σ.

Index	Position (μm)	^{235}U/^{238}U	2σ	U/^{30}Si	2σ	U/^{42}Ca	2σ
1	0.00	7.95	0.41	1.49E-04	2.31E-05	3.17E-02	2.35E-03
2	0.71	7.77	0.39	1.55E-04	2.41E-05	3.33E-02	2.46E-03
3	1.43	7.81	0.40	1.46E-04	2.26E-05	3.18E-02	2.35E-03
4	2.14	9.17	0.51	1.39E-04	2.16E-05	3.05E-02	2.26E-03
5	2.85	8.79	0.52	1.20E-04	1.87E-05	2.70E-02	2.02E-03
6	3.57	8.69	0.54	1.09E-04	1.70E-05	2.57E-02	1.92E-03
7	4.28	8.70	0.59	8.90E-05	1.39E-05	2.26E-02	1.71E-03
8	4.99	8.27	0.53	9.19E-05	1.43E-05	2.52E-02	1.90E-03
9	5.71	9.25	0.59	1.02E-04	1.59E-05	2.88E-02	2.16E-03
10	6.42	9.83	0.59	1.24E-04	1.93E-05	3.44E-02	2.55E-03
11	7.13	8.93	0.50	1.28E-04	1.98E-05	3.41E-02	2.53E-03
12	7.85	8.53	0.47	1.27E-04	1.98E-05	3.32E-02	2.46E-03
13	8.56	9.20	0.53	1.21E-04	1.88E-05	3.06E-02	2.27E-03
14	9.27	8.79	0.46	1.35E-04	2.10E-05	3.34E-02	2.46E-03

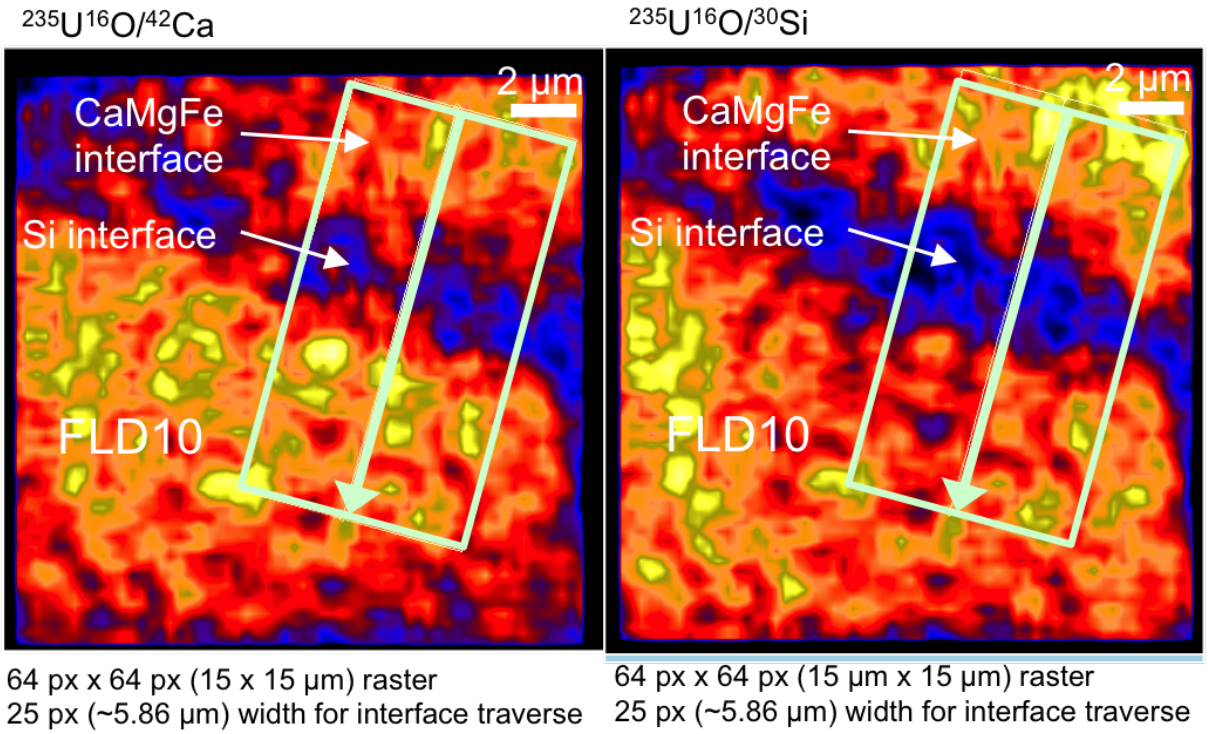

Figure K.5: Location and smoothing width of the linear traverse across the CaMgFe and Si interface of FLD10.L extracted from NanoSIMS raster analyses (shown overlaid with the $^{235}U^{16}O/^{42}Ca$ and $^{235}U^{16}O/^{30}Si$ isotope ratio images). The dimensions of the NanoSIMS raster are 15 μm × 15 μm with a resolution of 64 px × 64 px. The extracted traverse has a smoothing width of 25 pixels (~5.86 μm) wide and begins in the CaMgFe interface (top right of the image), traverses the Si interface, and ends in the host FLD10 (bottom left of the image).